



GRID
2018

PROCEEDINGS

9TH INTERNATIONAL SYMPOSIUM ON
GRAPHIC ENGINEERING AND DESIGN

UNIVERSITY OF NOVI SAD
FACULTY OF TECHNICAL SCIENCES
DEPARTMENT OF GRAPHIC ENGINEERING AND DESIGN



University of Novi Sad
Faculty of Technical Sciences
DEPARTMENT OF GRAPHIC
ENGINEERING AND DESIGN

GRID
2018

9TH INTERNATIONAL SYMPOSIUM
GRAPHIC ENGINEERING AND DESIGN

www.grid.uns.ac.rs/symposium/enpocetna.html

Proceedings – The Ninth International Symposium GRID 2018

EDITION:

INTERNATIONAL SYMPOSIUM ON GRAPHIC ENGINEERING AND DESIGN

PUBLISHER:

UNIVERSITY OF NOVI SAD
FACULTY OF TECHNICAL SCIENCES
DEPARTMENT OF GRAPHIC ENGINEERING AND DESIGN
21000 Novi Sad, Trg Dositeja Obradovića 6

EDITORIAL COMMITTEE:

PhD Nemanja Kašiković
PhD Dragoljub Novaković
PhD Živko Pavlović
PhD Sandra Dedijer

TECHNICAL SECRETARY:

MSc Stefan Đurđević

EDITOR:

PhD Nemanja Kašiković

LAYOUT AND PRODUCTION:

GRID team

PRINT:

Grafički centar GRID, Trg Dositeja Obradovića 6, Novi Sad

CIRCULATION:

150 copies

CIP - Каталогизacija у публикацији
Библиотека Матице српске, Нови Сад

655(082)
7.05:655(082)

INTERNATIONAL Symposium on Graphic Engineering and Design GRID (9 ; 2018 ; Novi Sad)

Proceedings [Elektronski izvor] / 9th International Symposium on Graphic Engineering and Design GRID 2018, November 8-10th, 2018, Novi Sad ; [editor Nemanja Kašiković]. - Novi Sad : Faculty of Technical Sciences, Department of Graphic Engineering and Design, 2018. - (International Symposium on Graphic Engineering and Design GRID, ISSN 2620-1437)

Način dostupa (URL): http://www.grid.uns.ac.rs/symposium/download/2018/proceedings_grid_2018.pdf. - Opis zasnovan na stanju na dan 2.11.2018. - Nasl. s naslovnog ekrana. - Bibliografija uz svaki rad. - Registar.

ISBN 978-86-6022-115-7

a) Графичка индустрија - Зборници b) Графички дизајн - Зборници
COBISS.SR-ID 326435847



GRID
2018

PROCEEDINGS

9TH INTERNATIONAL SYMPOSIUM ON
GRAPHIC ENGINEERING AND DESIGN

UNIVERSITY OF NOVI SAD
FACULTY OF TECHNICAL SCIENCES
DEPARTMENT OF GRAPHIC ENGINEERING AND DESIGN

SCIENTIFIC COMMITTEE

Dragoljub Novaković, University of Novi Sad, Faculty of Technical Sciences, Novi Sad, **(president)** (SRB)
Wolfgang Faigle, Stuttgart Media University, Stuttgart (DEU)
Thomas Hoffman-Walbeck, Stuttgart Media University, Stuttgart (DEU)
Lidija Mandić, University of Zagreb, Faculty of Graphic Arts, Zagreb (HRV)
Igor Majnarić, University of Zagreb, Faculty of Graphic Arts, Zagreb (HRV)
Sanja Mahović Poljaček, University of Zagreb, Faculty of Graphic Arts, Zagreb (HRV)
Diana Gregor – Svetec, University of Ljubljana, Faculty of Natural Sciences and Engineering, Ljubljana (SVN)
Aleš Hladnik, University of Ljubljana, Faculty of Natural Sciences and Engineering, Ljubljana (SVN)
Tadeja Muck, University of Ljubljana, Faculty of Natural Sciences and Engineering, Ljubljana (SVN)
Raša Urbas, University of Ljubljana, Faculty of Natural Sciences and Engineering, Ljubljana (SVN)
Urška Stanković Elesini, University of Ljubljana, Faculty of Natural Sciences and Engineering, Ljubljana (SVN)
Tomáš Syrový, University of Pardubice, Faculty of Chemical Technology, Pardubice (CZE)
Michal Veselý, Brno University of Technology, Faculty of Chemistry, Brno (CZE)
Petr Nemec, University of Pardubice, Faculty of Chemical Technology, Pardubice (CZE)
Michal Ceppan, Slovak University of Technology in Bratislava,
Faculty of Chemical and Food Technology, Bratislava (SVK)
Joanna Ewa Izdebska, Warsaw University of Technology, Faculty of Production Engineering, Warsaw (POL)
Thomas Sabu, Mahatma Gandhi University, School of Chemical Sciences, Kottayam (IND)
Csaba Horváth, Obuda University, Faculty of Light Industry and Environmental Engineering, Budapest (HUN)
Rozália Szentgyörgyvölgyi, Obuda University,
Faculty of Light Industry and Environmental Engineering, Budapest (HUN)
Ákos Borbély, Obuda University, Faculty of Light Industry and Environmental Engineering, Budapest (HUN)
Rafael Huertas, University of Granada, Faculty of Science, Granada (ESP)
Anastasios Politis, Technological Educational Institute of Athens, Athens (GRC)
Slobodan Nedeljković, University of Novi Sad, Academy of Arts, Novi Sad (SRB)
Boško Ševo, University of Novi Sad, Academy of Arts, Novi Sad (SRB)
Branko Milosavljević, University of Novi Sad, Faculty of Technical Sciences, Novi Sad (SRB)
Iskren Spiridonov, University of Chemical Technology and Metallurgy, Sofia (BGR)
Miloš Sorak, University of Banja Luka, Faculty of Technology, Banja Luka (BIH)
Mladen Stančić, University of Banja Luka, Faculty of Technology, Banja Luka (BIH)
Miljana Prica, University of Novi Sad, Faculty of Technical Sciences, Novi Sad (SRB)
Nemanja Kašiković, University of Novi Sad, Faculty of Technical Sciences, Novi Sad (SRB)
Gojko Vladić, University of Novi Sad, Faculty of Technical Sciences, Novi Sad (SRB)
Živko Pavlović, University of Novi Sad, Faculty of Technical Sciences, Novi Sad (SRB)
Jonas Malinauskas, Vilnius College of Technologies and Design, Vilnius (LTU)
Roberto Pašić, St. Clement of Ohrid University of Bitola, Bitola (MKD)
Vladan Končar, Ecole Nationale Supérieure des Arts et Industries Textiles, Roubaix (FRA)
Arif Özcan, Marmara University, School of Applied Sciences, Printing Technologies, Istanbul (TUR)
Catarina Silva, Polytechnic Institute of Cávado and Ave, Barcelos (POR)
Tim C. Claypole, Swansea University, Welsh Centre for Printing and Coating, Swansea (GBR)
Alexandra Pekarovicova, Western Michigan University,
Department of Chemical and Paper Engineering, Kalamazoo (USA)

ORGANIZATIONAL COMMITTEE

Dragoljub Novaković, University of Novi Sad, Faculty of Technical Sciences, Novi Sad (SRB)
Živko Pavlović, University of Novi Sad, Faculty of Technical Sciences, Novi Sad (SRB)
Miljana Prica, University of Novi Sad, Faculty of Technical Sciences, Novi Sad (SRB)
Nemanja Kašiković, University of Novi Sad, Faculty of Technical Sciences, Novi Sad (SRB)
Sandra Dedijer, University of Novi Sad, Faculty of Technical Sciences, Novi Sad (SRB)
Gojko Vladić, University of Novi Sad, Faculty of Technical Sciences, Novi Sad (SRB)
Magdolna Pál, University of Novi Sad, Faculty of Technical Sciences, Novi Sad (SRB)
Uroš Nedeljković, University of Novi Sad, Faculty of Technical Sciences, Novi Sad (SRB)

Željko Zeljković, University of Novi Sad, Faculty of Technical Sciences, Novi Sad (SRB)
Ivan Pinčjer, University of Novi Sad, Faculty of Technical Sciences, Novi Sad (SRB)
Neda Milić, University of Novi Sad, Faculty of Technical Sciences, Novi Sad (SRB)
Ivana Tomić, University of Novi Sad, Faculty of Technical Sciences, Novi Sad (SRB)
Ivana Jurić, University of Novi Sad, Faculty of Technical Sciences, Novi Sad (SRB)
Vladimir Dimovski, University of Novi Sad, Faculty of Technical Sciences, Novi Sad (SRB)
Bojan Banjanin, University of Novi Sad, Faculty of Technical Sciences, Novi Sad (SRB)
Irma Puškarević, University of Novi Sad, Faculty of Technical Sciences, Novi Sad (SRB)
Rastko Milošević, University of Novi Sad, Faculty of Technical Sciences, Novi Sad (SRB)
Stefan Đurđević, University of Novi Sad, Faculty of Technical Sciences, Novi Sad (SRB)
Darko Avramović, University of Novi Sad, Faculty of Technical Sciences, Novi Sad (SRB)
Jelena Vladušić, University of Novi Sad, Faculty of Technical Sciences, Novi Sad (SRB)
Savka Adamović, University of Novi Sad, Faculty of Technical Sciences, Novi Sad (SRB)
Vladimir Zorić, University of Novi Sad, Faculty of Technical Sciences, Novi Sad (SRB)
Jelena Novaković, University of Novi Sad, Faculty of Technical Sciences, Novi Sad (SRB)
Jelena Vasić, University of Novi Sad, Faculty of Technical Sciences, Novi Sad (SRB)
Vesna Kecić, University of Novi Sad, Faculty of Technical Sciences, Novi Sad (SRB)
Saša Petrović, University of Novi Sad, Faculty of Technical Sciences, Novi Sad (SRB)
Gordana Delić, University of Novi Sad, Faculty of Technical Sciences, Novi Sad (SRB)
Goran Jureša, University of Novi Sad, Faculty of Technical Sciences, Novi Sad (SRB)
Dunja Branovački, University of Novi Sad, Faculty of Technical Sciences, Novi Sad (SRB)
Predrag Ubović, University of Novi Sad, Faculty of Technical Sciences, Novi Sad (SRB)
Ana Lilić, University of Novi Sad, Faculty of Technical Sciences, Novi Sad (SRB)
Nada Miketić, University of Novi Sad, Faculty of Technical Sciences, Novi Sad (SRB)

CHAIR OF ORGANIZATIONAL COMMITTEE

Nemanja Kašiković, Faculty of Technical Sciences, Novi Sad (SRB)

TECHNICAL SECRETARY

Stefan Đurđević, Faculty of Technical Sciences, Novi Sad (SRB)

REVIEWING COMMITTEE

Tomislav Cigula, University of Zagreb, Faculty of Graphic Arts, Zagreb (HRV)
Igor Majnarić, University of Zagreb, Faculty of Graphic Arts, Zagreb (HRV)
Sanja Mahović Poljaček, University of Zagreb, Faculty of Graphic Arts, Zagreb (HRV)
Csaba Horváth, Obuda University, Faculty of Light Industry and Environmental Engineering, Budapest (HUN)
László Koltai, Obuda University, Faculty of Light Industry and Environmental Engineering, Budapest (HUN)
Erzsébet Novotny, Obuda University, Faculty of Light Industry and Environmental Engineering, Budapest (HUN)
Raša Urbas, Faculty of Natural Sciences and Engineering, Ljubljana (SVN)
Klementina Možina, University of Ljubljana, Faculty of Natural Sciences and Engineering, Ljubljana (SVN)
Dragoljub Novaković, University of Novi Sad, Faculty of Technical Sciences, Novi Sad (SRB)
Iskren Spiridonov, University of Chemical Technology and Metallurgy, Sofia (BGR)
Rafael Huertas, University of Granada, Faculty of Science, Granada (ESP)
Ondrej Panak, University of Pardubice, Faculty of Chemical Technology, Pardubice (CZE)
Markéta Držková, University of Pardubice, Faculty of Chemical Technology, Pardubice (CZE)
Bohumil Jašůrek, University of Pardubice, Faculty of Chemical Technology, Pardubice (CZE)
Petr Dzik, Brno University of Technology, Faculty of Chemistry, Brno (CZE)
Viera Jančovičová, Slovak University of Technology in Bratislava, Faculty of Chemical and Food Technology, Bratislava (SVK)

Pavol Gemeiner, Slovak University of Technology in Bratislava,
Faculty of Chemical and Food Technology, Bratislava (SVK)
Miljana Prica, University of Novi Sad, Faculty of Technical Sciences, Novi Sad (SRB)
Sandra Dedijer, University of Novi Sad, Faculty of Technical Sciences, Novi Sad (SRB)
Živko Pavlović, University of Novi Sad, Faculty of Technical Sciences, Novi Sad (SRB)
Nemanja Kašiković, University of Novi Sad, Faculty of Technical Sciences, Novi Sad (SRB)
Magdolna Pál, University of Novi Sad, Faculty of Technical Sciences, Novi Sad (SRB)
Darko Avramović, University of Novi Sad, Faculty of Technical Sciences, Novi Sad (SRB)
Gajko Vladić, University of Novi Sad, Faculty of Technical Sciences, Novi Sad (SRB)
Uroš Nedeljković, University of Novi Sad, Faculty of Technical Sciences, Novi Sad (SRB)
Ivan Pinčjer, University of Novi Sad, Faculty of Technical Sciences, Novi Sad (SRB)
Mladen Stančić, University of Banja Luka, Faculty of Technology, Banja Luka (BIH)
Thomas Hoffman-Walbeck, Stuttgart Media University, Stuttgart (DEU)
Joanna Ewa Izdebska, Warsaw University of Technology, Faculty of Production Engineering, Warsaw (POL)
Anastasios Politis, Technological Educational Institute of Athens, Athens (GRC)
Thomas Sabu, Mahatma Gandhi University, School of Chemical Sciences, Kottayam (IND)
Jonas Malinauskas, Vilnius College of Technologies and Design, Vilnius (LTU)
Roberto Pašić, St. Clement of Ohrid University of Bitola, Bitola (MKD)
Vladan Končar, Ecole Nationale Supérieure des Arts et Industries Textiles, Roubaix (FRA)
Arif Özcan, Marmara University, School of Applied Sciences, Printing Technologies, Istanbul (TUR)
Catarina Silva, Polytechnic Institute of Cávado and Ave, Barcelos (POR)
Tim C. Claypole, Swansea University, Welsh Centre for Printing and Coating, Swansea (GBR)
Alexandra Pekarovicova, Western Michigan University,
Department of Chemical and Paper Engineering, Kalamazoo (USA)

WITH SUPPORT OF:

Ministry of Education, Science and Technological Development, Republic of Serbia

Provincial Secretariat for Higher Education and Scientific Research,
Vojvodina, Republic of Serbia

Faculty of Technical Sciences, Novi Sad, Republic of Serbia

CO – ORGANISER:

University of Zagreb, Faculty of Graphic Arts, Zagreb, Croatia

Óbuda University, Institute of Media Technology, Budapest, Hungary

University of Ljubljana, Faculty of Natural Sciences and Engineering, Ljubljana, Slovenia

EQUIPMENT AND MATERIAL DONORS:

Alfa Digital, Belgrade, Serbia

Centropapir, Sremski Karlovci, Serbia

Diginet, Zrenjanin, Serbia

Flint Group, Germany

Fortuna Digital, Belgrade, Serbia

Futura, Novi Sad, Serbia

GrafikNET, Croatia

Pre-Print, Serbia

Rotografika, Subotica, Serbia

TABLE OF CONTENTS

FOREWORD	17
----------------	----

INTRODUCTORY INVITED LECTURES

1. Končar V.: SMART TEXTILES AND THEIR APPLICATIONS – VISUAL PERCEPTIONS	19
2. Politis A.: INNOVATIONS IN THE GRAPHIC ARTS, MEDIA AND PACKAGING FIELDS	29

PRINTING ADDED VALUE

3. Adamović S., Pinčjer I., Adamović D., Zorić V., Đurđević S.: THE IMPACT OF DIGITAL PRINTING MACHINES ON INDOOR AIR QUALITY	39
4. Cigula T., Tomašegović T., Hudika T., Donevski D.: INFLUENCE OF THE INK AND SUBSTRATE PROPERTIES ON THE INK TRANSFER IN LITHOGRAPHY.	45
5. Jurič I., Novaković D., Tomić I., Lilić A., Zeljković Ž.: DIFFERENCE BETWEEN USING COLOURIMETRIC VALUES ($L^*a^*b^*$) OR OPTICAL DENSITY FOR RANDOM PRINT NONUNIFORMITY QUANTIFICATION	51
6. Karlovits I., Lavrič G.: INFLUENCE OF PLASMA TREATMENT ON PROPERTIES OF WAXED PAPERS	55
7. Panák O., Kailová N., Držková M.: COMPARISON OF COLOUR REPRODUCTION BY PENTAX K10D DIGITAL CAMERA EMPLOYING POLYNOMIAL MODELS AND ICC BASED COLOUR MANAGEMENT TOOLS.	61
8. Spiridonov I., Shterev K., Bozhkova T.: FUTURE DEVELOPMENT OF SECURITY PRINTING AND RFID MARKS.	71
9. Tomić I., Huertas R., Gómez-Robledo L., Dedijer S., Jurič I.: APPLICABILITY OF STANDARD GREY SCALE FOR REPORTING PERCEIVED COLOR DIFFERENCE OF PRINTS ENHANCED WITH PEARLESCENT PIGMENTS	77
10. Vukoje M., Kulčar R., Itrić K., Rožić M.: SPECTROSCOPIC EVALUATION OF THERMOCHROMIC PRINTED CARDBOARD BIODEGRADATION.	87

PAPER AS A SUBSTRATE

11. Lavrič G., Pleša T., Mendizza A., Ropret M., Karlovits I., Gregor-Svetec D.: PRINTABILITY CHARACTERISTICS OF PAPER MADE FROM A JAPANESE KNOTWEED	99
12. Özden Ö., Sönmez S.: THE EFFECT OF BEATING ON THE DYEING OF CELLULOSE	103
13. Petković G., Pasanec Preprotić S., Vukoje M.: THE QUALITY ASSESSMENT OF BOOKBINDING STRENGTH FOR POLYVINYL ACETATE ADHESIVE (PVAc) AND NANO-MODIFIED PVAc ADHESIVES	109
14. Plazonić I., Malnar L., Džimbeg-Malčić V., Barbarić-Mikočević Ž., Bates I.: CHANGES IN THE OPTICAL PROPERTIES OF HEMP OFFICE PAPERS DUE TO ACCELERATED AGEING	121

15. Sesli Y., Ozomay Z., Arman Kandirmaz E., Ozcan A.:
THE INVESTIGATION OF USING ZIRCONIUM OXIDE
MICROSPHERES IN PAPER COATING. 129
16. Tóth B., Koltai L.; Böröcz P.:
QUALITY PERFORMANCE TESTING FOR BASE PAPER OF
CORRUGATED PAPERBOARD BY DSC METHOD 135

GRAPHIC MATERIALS AND PROCESSES EFFICIENCY

17. Golob M.:
UV ENERGY CURING OF DIELECTRIC LAYER FOR
SCREEN PRINTED CAPACITIVE CHEMICAL SENSORS 143
18. Hudika T., Tomašegović T., Cigula T., Poljičak A.:
ANALYSIS OF THE INTERACTIONS IN THE
"VARNISH – PHOTOPOLYMER" SYSTEM 151
19. Kecić V., Prica M., Kerkez Đ., Lužanin O., Bečelić-Tomin M.,
Tomašević Pilipović D., Leovac Mačarak A.:
DEFINITIVE SCREENING DESIGN FOR THE OPTIMIZATION OF FLEXOGRAPHIC
WATER-BASED CYAN DYE REMOVAL FROM AQUEOUS SOLUTION BY
nZVI-INDUCED FENTON PROCESS 161
20. Kerkez Đ., Bečelić-Tomin M., Kulić A., Tomašević Pilipović D.,
Leovac Mačarak A., Dalmacija B., Prica M.:
TREATMENT OF WASTEWATER CONTAINING DYE MIXTURE
USING PYRITE CINDER IN HETEROGENEOUS FENTON PROCESS. 169
21. Kulić A., Bečelić-Tomin M., Kerkez Đ., Pucar Milidrag G., Kecić V., Prica M.:
EXAMINATION OF THE APPLICATION POSSIBILITIES OF
WASTE RED MUD IN TREATMENT OF COLORED EFFLUENT. 175
22. Milošević R., Kašiković N., Pavlović Ž., Stančić M., Urbas R.:
CHARACTERIZATION OF COATED PRINTS WITH FRAGRANCED MICROCAPSULES. 181
23. Ozcan A., Arman Kandirmaz E.:
POLY[(VINYL ALCOHOL) - (STEARIC ACID)] SYNTHESIS
AND USE IN LAVENDER OIL CAPSULATION 189
24. Pál M., Dedijer S., Pavlović Ž., Banjanin B., Vasić J.:
STATISTICAL ANALYSIS OF ADHESIVE LAYER THICKNESS`
DISTRIBUTION ON PERFECT BOUNDED BROCHURES 197
25. Stančić M., Ružičić B., Vujčić Đ., Grujić D.:
DEPENDENCE OF THERMAL CONDUCTIVITY AND HEAT RETENTION
ABILITY OF FABRICS FROM DIGITAL PRINT PARAMETERS 205
26. Vališ J., Jašúrek B.; Brunová Z.:
INHIBITION OF PREMATURE POLYMERIZATION OF
CATIONICALLY CURABLE SYSTEMS BY TRIETHANOLAMINE. 213
27. Żółtek-Tryznowska Z., Cichy Ł.:
GLYCEROL DERIVATIVES AS A MODERN PLASTICIZERS FOR STARCH FILMS. 217

PACKAGING ADDED VALUE

28. Banjanin B., Vladić G., Pál M., Dimovski V., Adamović S., Deliđ G.:
PRODUCTION FACTORS INFLUENCING MECHANICAL AND
PHYSICAL PROPERTIES OF FDM PRINTED EMBOSsing DIES. 225

29.	Bota J., Jamnicki Hanzer S., Banić D., Brozović M.: COMPRESSION RESISTANCE OF SMALL PAPERBOARD PACKAGING SHAPES.	237
30.	Delić G., Vladić G., Banjanin B., Vasić J.: THE INFLUENCE OF THE TYPE OF A BEVERAGE ON ITS PACKAGING SHAPE.	243
31.	Kavčič U., Pleša T.: THE INFLUENCE OF PRINTING PROPERTIES OF SCREEN PRINTED ELECTRODES ON SENSITIVITY MEASURED WITH CYCLIC VOLTAMMETRY.	253
32.	Kovačević D., Brozović M.: NOTICEABILITY AND RECALL OF VISUAL ELEMENTS ON PACKAGING.	261
33.	Rastovac M., Dolić J., Pibernik J., Mandić L.: USER-CENTERED APPROACH TO PRODUCT DESIGN FOR PEOPLE WITH VISUAL IMPAIRMENTS.	267
34.	Vrabič Brodnjak U., Todorova D.: CHITOSAN AND RICE STARCH FILMS AS PACKAGING MATERIALS.	275
35.	Vukić N., Erceg T., Teofilović V., Nikolić Lj., Cakić S., Simendić B., Ristić I.: THE USE OF THE GREEN CHEMISTRY CONCEPT IN THE SYNTHESIS OF PACKAGING MATERIAL BASED ON POLYLACTIDE.	281

PRINTING QUALITY

36.	Boeva R., Spiridonov I., Yordanov S., Bozhkova T., Ivanov Z.: INVESTIGATION OF COLOR REPRODUCTION ACCURACY OF DIFFERENT INK JET AND ELECTROPHOTOGRAPHICAL PRINTING SYSTEMS.	291
37.	Boeva R., Spiridonov I., Ivanova Y.: INVESTIGATION OF UV ARTIFICIAL AGEING OF OPTICAL CHARACTERISTICS OF PRINTED IMAGES.	303
38.	Dedijer S., Tomić I., Pál M., Jurič I., Pavlović Ž., Milić N.: REPEATABILITY AND REPRODUCTION ACCURACY IN ELECTROPHOTOGRAPHY FOR COLOR DIFFERENCE EVALUATIONS.	313
39.	Horvath C., Görgényi-Tóth P.: STUDY OF COLOUR CHANGE IN THE COURSE OF DRYING ON PRINTS CREATED USING OFFSET PRINTING TECHNOLOGY.	323
40.	Jašurek B., Vališ J., Hozmanová M.: INFLUENCE OF PRINTING SPEED AND RADIATION DOSE ON THE CURING OF UV INKS AND VARNISHES.	333
41.	Lilić A., Kašiković N., Miketić N.: RUBBING FASTNESS OF GREEN INK PRINTED ON TEXTILE USING SCREEN PRINTING TRANSFER TECHNIQUE.	341
42.	Szentgyörgyvölgyi R., Novotny E., Weimert M.: DETERMINING AND SELECTING SCREEN PRINTING FORM PARAMETERS FOR PRINTING ON PAPER AND TEXTILE.	347
43.	Tomašegović T., Cigula T., Huzjak J., Prša M.: LS FITTING OF THE MATERIAL PROPERTIES INFLUENCING THE PRINT QUALITY IN FLEXOGRAPHIC REPRODUCTION SYSTEM.	357
44.	Vasić J., Kašiković N., Đurđević M.: IMPACT OF TYPE OF INK AND SUBSTRATE ON COLORIMETRIC VALUES OF INKJET PRINTS.	365

EDUCATION

45. Ahtik J., Kočevar T. N.:
A NOVEL APPROACH TO GRAPHIC COMMUNICATION EDUCATION 375
46. Jevtić M., Muck D., Gabrijelčič Tomc H.:
IMPLEMENTATION OF CAPACITIVE TOUCH SENSORS ON
ARTWORKS FOR AUGMENTATION OF USER EXPERIENCE
OF BLIND AND VISUALLY IMPAIRED USERS. 383
47. Kočevar T. N., Škerjanc A., Porok A., Jurca T., Pivar M., Gabrijelčič Tomc H.:
DETERMINING THE FRAMEWORK FOR ŽIŽKA MONUMENT 3D REPRODUCTION 389
48. Prokai P., Horvath C.:
NEW INITIATIVE TO EDUCATE THE "POSTPRESS: BINDING, FINISHING
AND MAILING" AS OBLIGATORY COURSE-UNIT AT ÓBUDA UNIVERSITY. 397
49. Purg P.:
HOW TO MASTER MODULAR REALITIES IN ART, SCIENCE AND TECHNOLOGY —
WITH NEW ELECTRONIC MEDIA, AND FOR A BETTER FUTURE OF WORK 405
50. Šafranč J., Katić M.:
DEFINITION IN SCIENTIFIC AND TECHNICAL DISCOURSE 411
51. Vladić G., Novaković D., Delić G., Milošević R., Đurđević S.:
USING MODERN INFORMATION TECHNOLOGY TO ENRICH THE
PRESENTATION OF RESULTS IN SCIENTIFIC PUBLICATIONS. 421

NOVEL TECHNOLOGIES

52. Bushati J., Leshi V., Strica D.:
THE MODELING OF FACIAL RECOGNITION PROCESS IN PROSPECTIVE OF
SIMULATION TECHNIQUES (A methodical elaboration through
the built-in modules of Matlab) 429
53. Đurđević S., Novaković D., Adamović S., Boadu F., Rodríguez Lezaca A., Zeljković Ž.:
DEVELOPING AUGMENTED REALITY APP FOR SMART PACKAGING 435
54. Hoffmann-Walbeck T.:
PDF METADATA AND ITS CONVERSION TO XJDF 445
55. Konygina T., Minaeva O., Ermakov A.:
EVOLUTION OF GRAPHIC DESIGN AS AN WORLDSKILLS
INTERNATIONAL COMPETENCE IN RUSSIA 455
56. Selimović A., Hladnik A.:
CONTENT-AWARE IMAGE COMPRESSION WITH
CONVOLUTIONAL NEURAL NETWORKS 459
57. Škerjanc A., Abram T., Knific Košir A., Brajković R., Fon Ž.,
Žvab Rožič P., Gabrijelčič Tomc H.:
DESIGNING THE EDUCATIVE APP FOR THE
DETERMINATION OF TYPICAL SLOVENIA ROCKS 469
58. Trochoutsos C., Politis A.:
DEVELOPMENTS IN DIGITAL PRINT STANDARDIZATION 475
59. Urbas R., Kuščer A., Ferati M., Stankovič Elesini U.:
ACCESSIBILITY OF SLOVENIA'S MUSEUMS FOR BLIND AND VISUALLY IMPAIRED 489

DESIGN

60. Beris Y.:
EFFECTS OF DIGITAL PRINTING APPLICATIONS ON CONTEMPORARY ART 499
61. Heđa M., Valdec D., Hajdek K., Miljković P.:
INFLUENCE OF BEER LABEL DESIGN ON MAKING DECISION
ABOUT CHOOSING AND BUYING PRODUCT 509
62. Lakićević M., Kordić D.:
GEOMETRIC STYLE IN DESIGN OF URBAN LANDSCAPES 519
63. Malinauskas J.:
EVOLUTION OF GESTALT PRINCIPLES IN CONTEMPORARY GRAPHIC DESIGN 525
64. Miketić N., Pinčjer I., Lilić A.:
INTEGRATION OF THE VISUAL ELEMENTS OF ART AND
PERSONALITY FACTORS IN PROCESS OF CHARACTER DESIGN 533
65. Plahuta E., Pušnik N.:
REDESIGN OF KOZJANSKO REGIONAL PARK VISUAL IDENTITY THROUGH
AN EYE TRACKING ANALYSIS OF THE CURRENT AND NEW SOLUTION 541
66. Stankovič Elesini U., Armič T., Urbas R.:
SCENTED CORPORATE VISUAL IDENTITY 551

DIGITAL MEDIA

67. Franken G., Pangerc M., Možina K.:
LCD DISPLAY LEGIBILITY INFLUENCED BY TYPEFACES AND COLOUR CONTRASTS ... 561
68. Hladnik A., Saksida P.:
COMPRESSED SENSING AND SOME IMAGE PROCESSING APPLICATIONS. 567
69. Molek I., Javoršek D.:
GRADATION, COLOUR RANGE AND COLORIMETRIC ACCURACY OF
DIGITAL PROJECTOR JVC DLA-RS 15 573
70. Pinčjer I., Milić N., Puškarević I., Miketić N.:
CONVERSION OF VIRTUAL REALITY INTO A MIXED REALITY 583
71. Šišić A., Mandić L., Agić A., Poljičak A.:
THE IMPLEMENTATION OF GAMIFICATION IN MOBILE APPLICATION 591
72. Weingerl P., Javoršek D.:
WEB-BASED APPLICATION FOR INTERACTIVE SELECTION
OF IMAGE PROMINENT COLOURS 597

TYPOGRAPHY

73. Puškarević I., Nedeljković U., Pušnik N.:
CHARACTERIZATION OF LETTERFORM COMPLEXITY 605

AUTHOR INDEX 612

Foreword

Dear readers,

It is my great pleasure to introduce You the research papers of the Ninth Symposium on Graphic Engineering and Design. With this proceeding we continue the works of previous symposiums which have been held biennial since year 2002.


We're delighted that this international symposium has again a great number of the papers and participants coming from many countries.

The papers include the achievements of researches in the field of technology and scientific areas relevant to graphic technology and graphic design. Through the work of the symposium GRID we continued significant scientific cooperation with educational institutions all over the Europe, especially with the neighbouring countries in the region. With them we are continuing good cooperation which is the driving force for the creation and display of new developments, both individual and common.

I want to thank everyone who participated with their paper and presentation in the symposium. Your contribution is significant for the improvement of the Symposium on Graphic Engineering and Design GRID 18. The research achievements here presented are also valuable to the scientific and professional community and are highly appreciated.

Editor

SMART TEXTILES AND THEIR APPLICATIONS - VISUAL PERCEPTIONS

Vladan Koncar 

University of Lille, ENSAIT - GEMTEX, Roubaix, France

Abstract: *Smart textiles, encompassing electronics combined with textiles also called textronics, have a very promising realm in science and technology nowadays because of commercial viability and public interests. Smart textiles play a significant role as well in the European textile sector and assist the textile industry in its transformation into a competitive knowledge driven industry. These kinds of textiles combine knowledge from many disciplines with the specific requirements of textile. Numerous materials and systems are available together with devices for sensing and actuation, but they are not compatible with a textile or with the textile production processes. They could be transformed into a textile compatible structure or even in a full textile structure.*

Smart textiles can be defined as textiles that are able to sense and respond to changes in their environment. They may be divided into two classes: passive and active smart textiles. Passive smart textiles have the ability to change their properties according to an environmental stimulation. Shape memory materials, hydrophobic or hydrophilic textiles etc. make part of this category.

Active smart textiles are fitted with sensors and actuators, in order to connect internal parameters to the transmitted message. They are able to detect different signals from the environment (temperature, light intensity, pollution...), to decide how to react and finally to act using various textile based, flexible or miniaturized actuators (textile displays, micro vibrating devices, LED, OLED...). The "decision" can be taken locally in case of embedded electronic devices (textile electronics) to smart textile structures or remotely in case the smart textile is wirelessly connected to clouds containing data base, servers with artificial intelligence software etc. and may be a part of Internet of Things (IoT) concept. This presentation focuses on smart textiles actuators used as active and passive flexible displays.

Key words: actuators, textile displays, smart textiles

1. INTRODUCTION

Two different approaches relative to the development of textile flexible displays are presented in this study. The first one, also called active display, is based on the weaving of optical fibers and the second one (passive displays) uses electrochromic compounds within textile structures.

Upon the first approach, flexible displays can be created on textiles by producing a screen matrix using the texture of the fabric during the weaving process. A small electronic device that is integrated into the system controls the Light Emitting Diodes (LEDs) or even Diode lasers that illuminate groups of fibers. Each group provides light to one pixel on the matrix.

These displays are very thin and ultra lightweight—two characteristics that could enable many innovative applications. Although initially developed for clothing, the displays could be used to exhibit information or designs in cars, portable electronic devices and even houses and buildings. Indeed, research on the design and development of flexible displays based on processed optical fibers has opened up new frontiers in fashion, public safety, automotive equipment and home decoration.

The second approach involves materials that can undergo a reversible color change, upon the application of an external stimulus, are technically known as chromic materials. Research into the application of such species has been extensive due to the ability of color change to effectively convey important information, i.e. traffic lights, advertisement billboards etc. (Mortimer et al, 2006; Somani et al, 2003; Tehrani et al, 2006). Materials that display chromic properties are classified by the type of stimuli that induces their color change. For example, photochromics and thermochromics see a change in color when there is a change in light, or a change in heat, respectively. Both thermo and photochromic materials have current applications within textile fields. Photochromics, when applied to textiles have been used in solar protection through the monitoring and notification of UV radiation levels (Shanmugasundaram, 2008). In addition, for added interest within fashion and interior furnishings, wallpapers treated with thermochromics, when heated by nearby radiators, 'grow' flower buds across a vine (Sierra, 2008). Photochromic products include pillow covers which reveal a motif when exposed to sunlight. When the heat or sunlight is removed, the flowers and motif disappears correspondingly.

On the other hand, an electrochromic compound is one in which a reversible change in color occurs when an electrical voltage is applied. Many materials express electrochromic properties, including metal oxides, the Prussian family, rare earth phthalocyanines and conducting polymer systems. Products that harness the fascinating spectroelectrochemical properties of electrochromic materials, currently available on the market, are predominantly rigid in their form and include the glass windows of buildings and cars which can darken reversibly (Sage Electrochromics, 2012; Gentex Corporation, 2012). Other proposed applications include re-usable price labels, camouflage materials and controllable light reflective or light-transmissive displays for optical information and storage (Mortimer et al, 2006), (Rosseinsky et al, 2001; Silver, 1989). In this study, 5 generations of electrochromic displays realized in GEMTEX laboratory are presented.

2. FLEXIBLE TEXTILE DISPLAYS

2.1 Active textile displays based on optical fibers weaving

Weaving Optical Fibers

Poly(methyl methacrylate) (PMMA) optical fibers possess a rigidity and fragility that make them different from most traditional textile fiber threads and filaments. With regard to section diameter, a good compromise must be reached: A diameter that is too large can cause inflexibility, while a too-small diameter induces a low shear resistance and loss of light intensity.

We used fibers with a diameter of 0.5 mm to make the first prototypes. We have also conducted tests on fibers with a diameter of 0.25 mm, but further developments in the process of weaving are still required to ensure sufficient fabric resistance in bending.

Weaving takes place on a traditional two-dimensional loom. The optical fibers can be woven or placed as warp or weft yarns, in addition to other kinds of yarns. Therefore, it is theoretically possible to obtain an optical fiber X-Y network. However, this would present several disadvantages:

- The grid (and, hence, the resolution) would not be very dense and the fabric would be extremely rigid because of the relatively high radius of curvature of optical fibers.
- Constituting an optical fiber chain is very long and very expensive.
- The resolution would be tiny.

It is also possible that a three-dimensional structure in weaving would not bring any significant advantages. Thus, our initial plan was to develop a fabric comprising optical fibers for wefts and polyester in warp. Other natural, artificial or synthetic yarns could also have been used to constitute the warp yarns. The choice of warp yarns must be chosen with the aim of achieving good flexibility in the fabric, fine titration and an improved capacity to diffuse and reflect the light emitted by optical fibers for better legibility of information. An example of an optical fiber fabric display (OFFD) weaved structure is shown in Figure 1. Different textile finishing methods are being tested—either in pasting or in coating—to guarantee grid stability and flame resistance and to enable optimal light emission intensity and contrast.

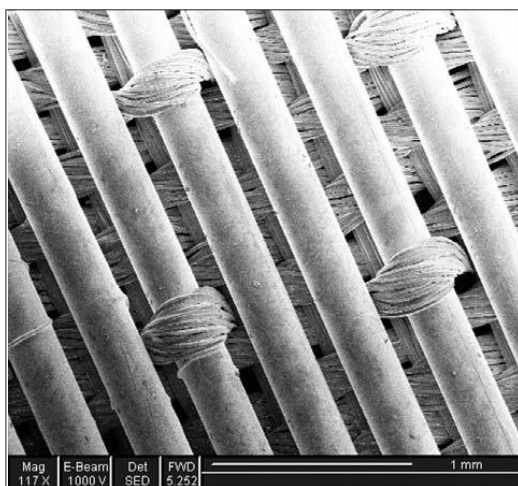


Figure 1: Scanning electron microscope picture of OFFD structure (a two-layer basic-velour fabric)

2.2 Display Matrix Design

The screen for fabric displays comprises a number of surface units, or pixels; each one can be illuminated by a light source emitted from one side of the fabric by one or several PMMA optical fibers with discrete index variation. The pixels are directly formed on optical fibers while transversely forming a spout of light on the fabric. The process consists of generating micro-perforations that reach into the core of the fiber (Fig. 2). The remainder of the optical fiber, which did not receive any specific processing, conveys the light without being visible on the surface.

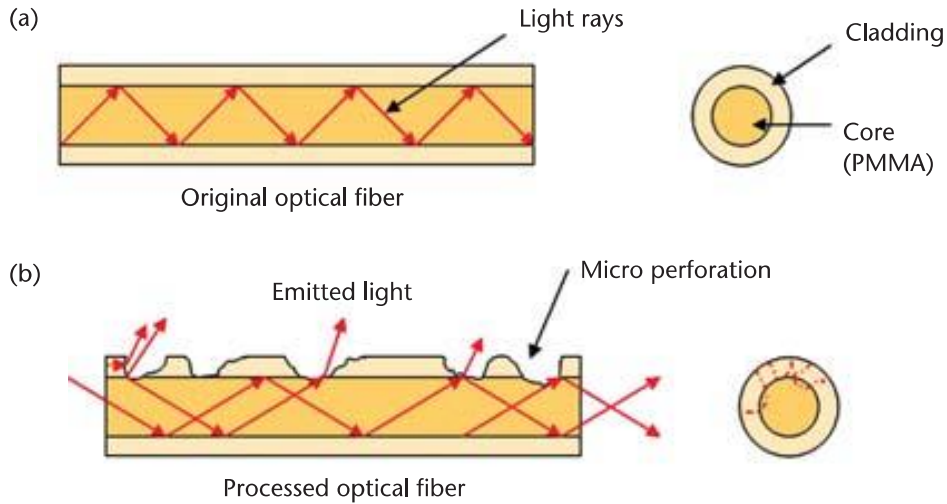


Figure 2: Principle of lateral light emission. a) Original optical fiber, b) processed optical fiber

Two processing techniques have been developed for optical fibers. The first is a mechanical treatment by the projection of micro particles with different velocities on the optical fiber's cladding. The result is presented in Fig. 3. The second technique uses different chemical solvents to make these micro perforations; this method seems to produce a better final result. (A chemically processed cladding surface is shown in Fig. 4). Finally, Fig. 5 shows the chemically processed fiber obtained by a scanning electron microscope.

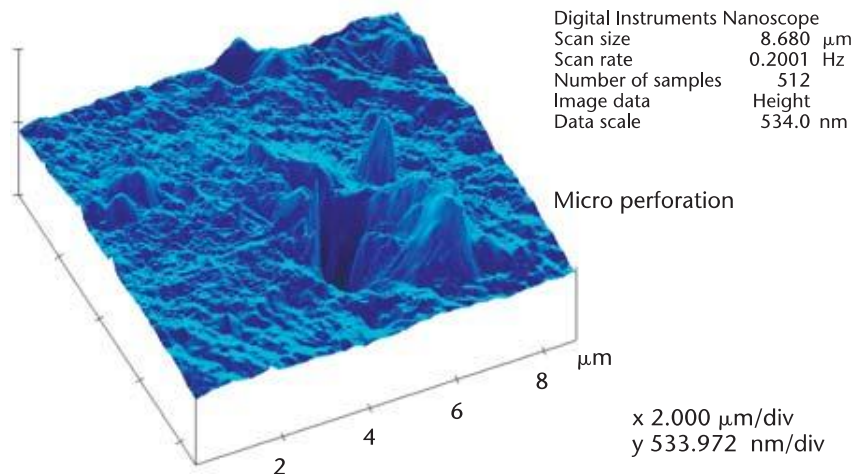


Figure 3: Micro perforation obtained by mechanical treatment (particle projected on the cladding of optical fiber).
Picture obtained by nanoscope

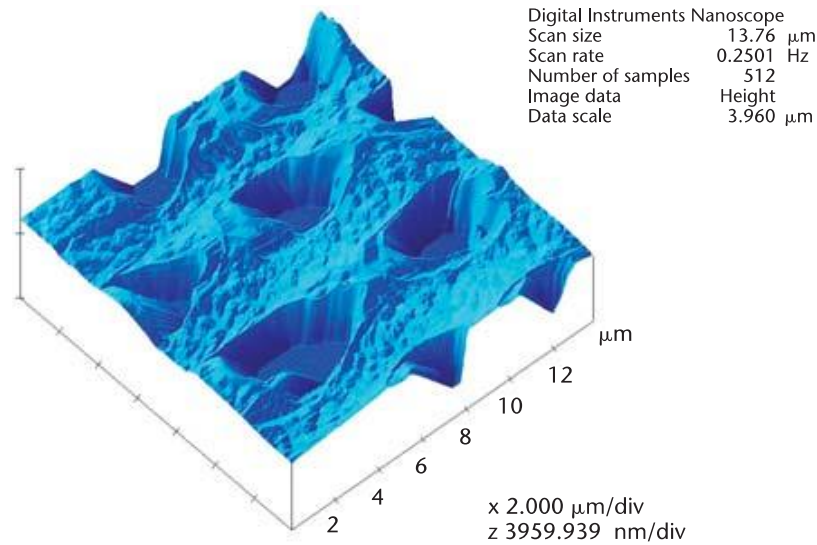


Figure 4: Micro perforation obtained by chemical treatment (solvent action on the cladding of optical fiber). Picture obtained by nanoscope

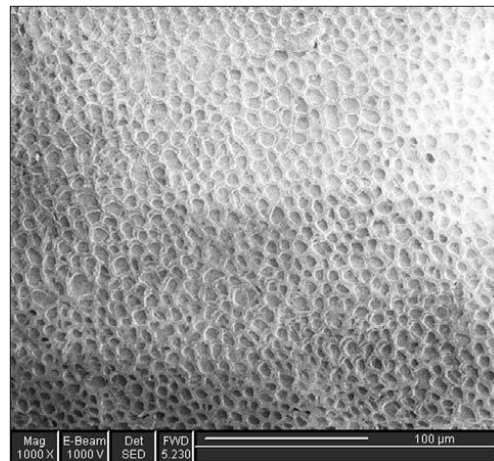


Figure 5: Micro perforation obtained by chemical treatment (solvent action on the cladding of optical fiber). Picture obtained by scanning electron microscope

There are three methods that are used to light ON and OFF static patterns on the fabric (texts, logos and scanned pictures), which we adapted to develop our own technique. A basic fabric is used in the first method. The lighting zone to be processed, which is composed of optical fibers, is delimited by a stencil key. The picture remains static—with eventual color changes—but can offer quite a high resolution. In the second method, the zone to be lit is formed during weaving on a Jacquard loom before being processed. The remaining, inactive fabric is composed of the floating fibers on the back of the fabric. A third method uses a two-layer adapted basic-velour fabric that makes optical fibers as visible as possible, but with sufficient consistency of fabric structure. Prior to the weaving process, the optical fibers are chemically treated, enabling the specific dynamic lighting zones to be created. We modified these techniques by creating specific weaving armor and an adapted lighting control in order to generate variable information on the same fabric zone. We developed a matrix that makes it possible to display a great deal of basic information, such as texts, logos or other patterns, in a static or dynamic way. Because a fabric display can only be produced by columns made of a single optical fiber or group of fibers, we had to create lines artificially. Similar to the process that would be used with two superimposed patterns to be lightened on the same column, this involves alternating two consecutive weft fibers—one for the first pattern, and the other for the second. Each is processed on a precise section in order to re-emit light at a specific place.

The principle is the same for three superimposed patterns, except that one fiber is taken out of three for each pattern. When the weaving is sufficiently tight, a visual impression is given of full, enlightened zones. Warp yarns will be able to help diffuse the light toward the dark zones between lightened segments. The number of rows to be produced seems limited by the technique, insofar as, on the same unit zone, more dark zones are produced than lightened ones. The appreciation of the definition will then be based on the size of the pixels and the screen, in addition to the distance from which people watch the screen.

Various light sources can be used to feed the matrix. The choice mainly depends on the number of fibers connected to each source and the level of power consumption. For the first prototypes, we used high luminous LEDs that are 3 mm in diameter. LED technology has many advantages, as diodes can be easily driven by electronics under low voltages (2V to 4V, depending on the color). Therefore, many “light effects” can be generated on the display, such as flashing or varying the intensity of the light, providing all kinds of animated movies.

The very first OFFD, has been displayed on a jacket. It comprises a screen matrix specially designed to display on one line three 60 mm x 60 mm alphanumeric characters, each made up of three rows and three columns using 0.5 mm diameter optical fibers and a 7 fibers/cm width density. Each pixel is composed of four fiber segments and is controlled by one LED located in the lining of the cloth, on one side of the OFFD. The color of the pixels is determined by the corresponding LEDs.

OFFDs offer another possibility: Although the definition is limited by the number of rows, it is possible to repeat on fabric the same line of characters or patterns in the direction imposed by optical fibers. The fixed or animated pattern reproduction can be used for purely decorative applications; for example, to create a mural tapestry adapting its colors to the clothes worn by the occupants of a room.

Optical fiber screens provide access to simple and animated visual information, such as texts or pictograms. It is possible to download, create or exchange visuals via the appropriate Internet gateway. Conceivably, images or text could be sent using wireless technology from a computer or a mobile Internet terminal to an article of clothing.

The main functions of the new prototypes are:

- To “be seen,” for security, publicity, recreational or aesthetic purposes
- To show one’s affiliation or support for a group
- To personalize one’s clothing according to the latest fashions
- To communicate or exchange information or to signpost advice.

Fabrics based on flexible display technology have the obvious potential to influence fashion designers, but they have a variety of other useful applications as well. OFFDs can be used as displays for mobile phones, PDAs (personal digital assistants), wearable computers and other portable electronic devices.

There is also enormous potential for firefighting and police applications. For example, information and warnings could be displayed on clothes—which could both increase public safety and help officers and firefighters to operate in remote and challenging conditions.

The interior of cars contains many flexible elements that could be used to display relevant information that might help drivers navigate or avoid accidents. Finally, houses and buildings could use OFFD technology to display or enhance drawings, pictures and lighting.

In this digital age, information is virtually everywhere and a multitude of screen and display technologies will be necessary to keep up with the demand. OFFDs have shown great promise as a new and interesting way to present images and information.

2.3 Passive textile displays based on electrochromical compounds

Materials that can undergo a reversible color change, upon the application of an external stimulus, are technically known as chromic materials. Research into the application of such species has been extensive due to the ability of color change to effectively convey important information, i.e. traffic lights, advertisement billboards etc. (Mortimer et al, 2006; Somani et al, 2003; Tehrani et al, 2006). Materials that display chromic properties are classified by the type of stimuli that induces their color change. For example, photochromics and thermochromics see a change in color when there is a change in light, or a change in heat, respectively. Both thermo- and photochromic materials have current applications within textile fields. Photochromics, when applied to textiles have been used in solar protection through the monitoring and notification of UV radiation levels (Shanmugasundaram, 2008). In addition, for added interest within fashion and interior furnishings, wallpapers treated with thermochromics, when heated by nearby

radiators, 'grow' flower buds across a vine (Sierra, 2008). Photochromic products include pillow covers which reveal a motif when exposed to sunlight (Zainzinger, 2009). When the heat or sunlight is removed, the flowers and motif disappears correspondingly.

On the other hand, an electrochromic compound is one in which a reversible change in color occurs when an electrical voltage is applied. Many materials express electrochromic properties, including metal oxides, the Prussian family, rare earth phthalocyanines and conducting polymer systems. Products that harness the fascinating spectroelectrochemical properties of electrochromic materials, currently available on the market, are predominantly rigid in their form and include the glass windows of buildings and cars which can darken reversibly (Sage Electrochromics, 2012; Gentex Corporation, 2012). Other proposed applications include re-usable price labels, camouflage materials and controllable light reflective or light-transmissive displays for optical information and storage (Mortimer et al, 2006; Rosseinsky et al, 2001; Silver et al, 1989).

The traditional structure of an electrochromic device (ECD) is that of a seven-layer electrochemical cell with a rigid sandwich structure (Figure 6).

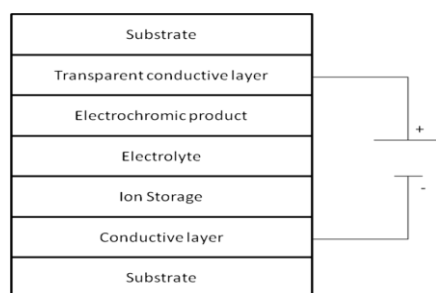


Figure 6: A traditional ECD with a seven-layer sandwich structure

An electrochromic material is coupled to both a suitable solid or liquid electrolyte (ionic conductor) and an ionic storage layer. These three layers are sandwiched between two conductors (electrodes), with at least one of these, also requiring transparency. These are then held between two protective substrates, typically transparent glass, completing the device. A number of academic and commercial research groups have been working on the development of ECDs that are flexible (Andersson et al, 2007; White et al, 2009; Coleman et al, 1999; Ma et al, 2008). For example, Mecerreyes and co-workers have published a flexible all-polymer ECD, using a plastic substrate (Mecerreyes et al, 2004). Poly(3,4-ethylenedioxythiophene), PEDOT, has been utilized, and acts simultaneously as both the electrode and the electrochromic material. The transparent conducting layer of the classical configuration is therefore eliminated, resulting in a device requiring only five-layers. However, flexible textiles treated with electrochromics are not readily available. Therefore, the combination of chromic materials with flexible textiles grants a new opportunity to create communicative flexible displays for clothing, interior furnishings or flags. The change in color could be used for protection and safety applications or for adding further interest or fashion to an item.

Five generations of EC displays have been realized since last ten years in GEMTEX laboratory. First, second and third generations use PET sheets with ITO transparent conductive layer (Figures 7-9), textile substrate containing an electrochromic compound is placed between them. Therefore, the hand is more plastic than textile. Fourth and fifth generations (Figures 10 and 11) are fully textile based without PET ITO coated sheets. The fourth generation is based on 3 layers' textile functionalized fabrics and the fifth generation is made of only one-layer textile substrate that is locally functionalized.

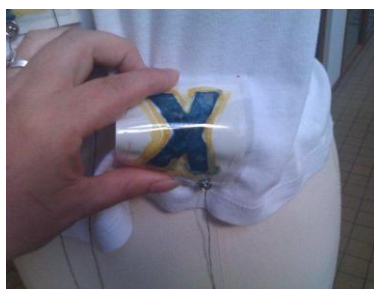


Figure 7: First generation (1G) of GEMTEX EC displays

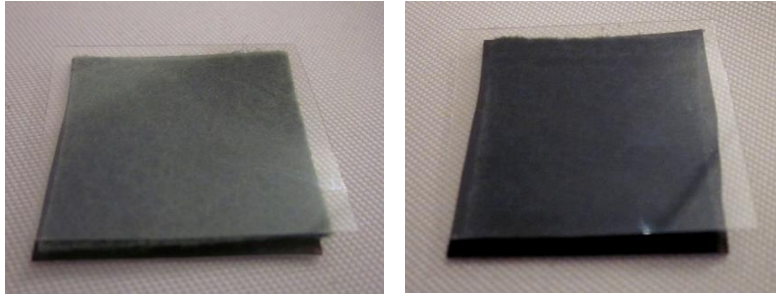


Figure 8: Second generation (2G) of GEMTEX EC displays

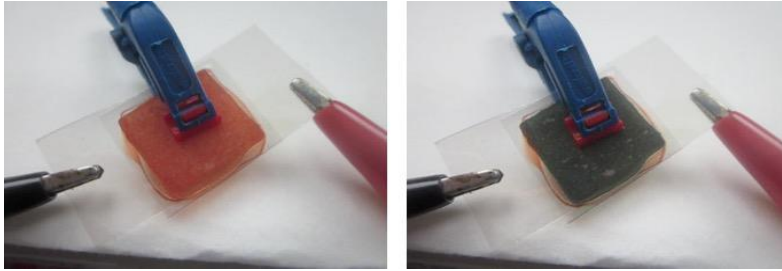


Figure 9: Third generation (3G) of GEMTEX EC displays

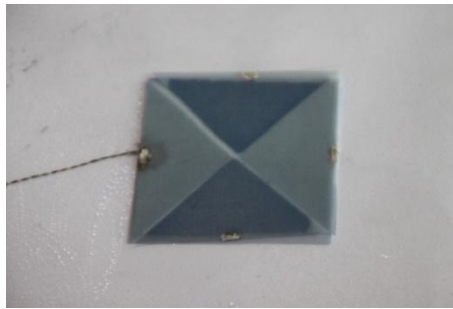


Figure 10: Fourth generation (4G) of GEMTEX EC displays

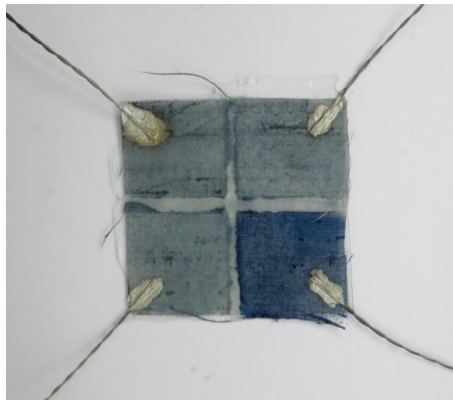


Figure 11: Fifth generation (5G) of GEMTEX EC displays (Moretti et al, n.d.)

3. CONCLUSION

New approaches towards the design and development of textile based flexible displays able to emit or reflect light should help designers to enhance their imagination and realize new exciting products (Koncar, 2005; Meunier et al, 2011; Kelly et al, 2013a; Kelly et al, 2013b; Moretti et al, 2014). Different areas are concerned such as fashion design, home textiles, technical textiles, car interior etc. The main issue that will

have to be addressed concerning optical fibers based displays is related to their cost and integration. Electrochromic displays on the other side should be improved in order to extend their life time and make them more reliable.

4. REFERENCES

- [1] Andersson, P., Forchheimer, R., Tehrani, P., Berggren, M.: "Printable All-Organic Electrochromic Active-Matrix Displays", *Advanced Functional Materials*, 17 (16), 3074-3082, 2007. doi: 10.1002/adfm.200601241
- [2] Coleman, J.P., Lynch, A.T., Madhukar, P., Wagenknecht, J. H.: "Printed, flexible electrochromic displays using interdigitated electrodes", *Solar Energy Materials and Solar Cells*, 56 (3-4), 395-418, 1999. doi: 10.1016/S0927-0248(98)00144-5
- [3] Gentex Corporation - A Smarter Vision: "Automotive Products" URL <http://www.gentex.com/automotive/product-categories> (last requested: 2012-08-15)
- [4] J. Silver. "Chemical chameleons for electronics," *New Scientist*, no. 1684, pp. 49-51, Sept. 1989.
- [5] Kelly, F.M., Meunier, L., Cochrane, C., Koncar, V.: "Polyaniline: Application as Solid State Electrochromic in a Flexible Textile Display", *Displays*, 34 (1), 1-7, 2013. doi: 10.1016/j.displa.2012.10.001
- [6] Kelly, F.M., Cochrane, C., Koncar, V.: "Evaluation of Solid or Liquid Phase Conducting Polymers within a Flexible Textile Electrochromic Device" *IEEE/OSA Journal of Display Technology*, 9 (8), 626 - 631, 2013. doi: 10.1109/JDT.2013.2255581
- [7] Koncar, V.: "Optical fiber fabric display – OFFD", *Optics & Photonics News*, 16 (4), 40-44, 2005. doi: 10.1364/OPN.16.4.000040
- [8] Ma, C., Taya, M., Xu, C.: "Flexible electrochromic device based on poly (3,4-(2,2-dimethylpropylenedioxy)thiophene)", *Electrochimica Acta*, 54 (2), 598-605, 2008. doi: 10.1016/j.electacta.2008.07.049
- [9] Mecerreyes, D., Marcilla, R., Ochoteco, E., Grande, H., Pomposo, J. A., Vergaz, R., Sánchez Pena, J. M.: "A simplified all-polymer flexible electrochromic device", *Electrochimica Acta*, 49 (21), 3555-3559, 2004. doi: 10.1016/j.electacta.2004.03.032
- [10] Meunier, L., Kelly, F.M., Cochrane, C., Koncar, V.: "Flexible displays for smart clothing: Part II — Electrochromic displays", *Indian Journal of Fibre & Textile Research*, 36 (4), 429-435, 2011.
- [11] Moretti, C., Tao, X., Koncar, V., Koehl, L.: "A Study on Electrical Performances and Lifetime of a Flexible Electrochromic Textile Device", *Autex Research Journal*, 14 (1), 2014. doi: 10.2478/aut-2014-0003
- [12] Moretti, C., Koncar, V.: Patent pending - FR 1770589, "Structure électro chromique comportant une couche support déformable", ENSAIT
- [13] Mortimer, R.J., Dyer, A. L. , Reynolds, J. R.: "Electrochromic organic and polymeric materials for display applications", *Displays*, vol. 27 (1), 2-18, 2006. doi: 10.1016/j.displa.2005.03.003
- [14] Rosseinsky, D.R, Mortimer, R. J.: "Electrochromic Systems and the Prospects for Devices," *Advanced Materials*, 13 (11), 783-793, 2001. doi: 10.1002/1521-4095(200106)13:11<783::AID-ADMA783>3.0.CO;2-D
- [15] Sage Electrochromics. Inc.: "Sage Glass Technology" URL <http://www.sage-ec.com/> (last requested: 2012-08-12)
- [16] Shanmugasundaram, O. L.: "Smart and Intelligent Textiles", URL <http://www.indiantextilejournal.com/articles/FAdetails.asp?id=852>. (last requested: 2018-10-17)
- [17] Sierra, M.B.: "Thermochromic", URL <http://www.techpin.com/thermochromic/> (last requested: 2008-05-26)
- [18] Somani, P.R., Radhakrishnan, S.: "Electrochromic materials and devices: present and future", *Materials Chemistry and Physics*, 77 (1), 117-133, 2003. doi: 10.1016/S0254-0584(01)00575-2
- [19] Tehrani, P., Isaksson, J., Mammo, W., Andersson, M. R., Robinson, N. D., Berggren, M.: "Evaluation of active materials designed for use in printable electrochromic polymer displays", *Thin Solid Films*, 515 (4), 2485-2492, 2006. doi: 10.1016/j.tsf.2006.07.149
- [20] White, C.M., Gillaspie, D. T., Whitney, E., Lee, S.H., Dillon, A. C.: "Flexible electrochromic devices based on crystalline WO₃ nanostructures produced with hot-wire chemical vapor deposition", *Thin Solid Films*, 517 (12), 3596-3599, 2009. doi: 10.1016/j.tsf.2009.01.033
- [21] Zainzinger, E. (2009, Nov.). Fashionable color changing flu-masks [Webpage]. Available: <http://www.talk2myshirt.com/blog/archives/3113> (last requested: 2009-11-03)



© 2018 Authors. Published by the University of Novi Sad, Faculty of Technical Sciences, Department of Graphic Engineering and Design. This article is an open access article distributed under the terms and conditions of the Creative Commons Attribution license 3.0 Serbia (<http://creativecommons.org/licenses/by/3.0/rs/>).

INNOVATIONS IN THE GRAPHIC ARTS, MEDIA AND PACKAGING FIELDS

Anastasios E. Politis

*HELGRAMED - the Hellenic Union of Graphic Arts and
Media Technology Engineers, Athens, Greece
University of West Attica, Egaleo, Greece
Hellenic Open University, Patras, Greece*

Abstract: *In recent years, some have predicted that printing and graphic arts will be eliminated by electronic and digital media. Within these predictions there was no future physical carriers of communication and paper would be replaced by monitors and screens, tablets and mobile devices.*

Back at DRUPA 1982, the introduction of the so-called "Desktop Publishing" has led to an exhibition under the title "Goodbye Gutenberg", predicting also that print was under threat by new electronic technologies. Hence, until today, graphic arts industry, printing and publishing and most of all packaging, present a continuous positive development, together with structural changes in the entire spectrum of research, industry and education.

Graphic Arts today is characterized by rapid technological developments, restructuring of design, management and production processes, and the application of various innovations. One of the most important indicators is the integration of basic and applied research in many fields, which leads to a new shape of the sector. In the present paper, issues concerning the following will be addressed (among others):

- Typography and its importance in the digital media domain*
- Evolution, Innovations and main trends in the graphic arts, printing and packaging industry*
- Digitalization and printing production (Industry 4.0, 3D printing)*
- The concept of Industrial Printing*

In this keynote paper, effort will be given to illustrate the trends and developments in graphic arts fields. Further, the parameters confirming that printing, paper, typography, bookbinding and packaging will stay alive in the digital era will be analyzed. In addition, the graphic arts sector and its positioning in the so-called "post-industrial" society, will be investigated and the new directions for the graphic arts research, industry and business as well as the requirements for education will be identified.

Key words: graphic arts innovations, typography, printing, packaging, industry 4.0, industrial printing

1. IS PRINT DEAD?

Many have predicted that printing and in general, the graphic arts sector will disappear... Those following the evolution and developments of the sector in the last decades might remember an exhibition during DRUPA 1982, with the title: "GOOD BYE GUTENBERG". In addition, some other predictions stated that print will be replaced by digital media. Well, it seems that up to today, such statements and predictions on the "death" of print do not seem to be a reality. Our field and the related sectors show a rather stable condition in terms of turnover and production, at least in Europe and North America, whereas in other continents, such as Asia, print is booming. The main driver for this is the packaging sector, which seems to be the most significant stakeholder of the printing industry worldwide. To give an example, even in Greece with the continuous crisis that takes place the last decade and where some 30% of printing companies disappeared, packaging printing shows a stable turnover increase of some 3,5 %.

Of course, nowadays, we are witnessing the expansion of digital communication and in particular the use of internet, social media, the enormous expanding of mobile devices, apps, and the web. However, the characteristics and in particular the nature of printed substrates combined with advanced technologies, such as finishing technologies reveal the strength of printing world and enhance the added value for a better communication. Haptic communication is the principal driver for this enhancement.

1.1 Print is NOT dead! - Some key paradigms

Tim Freeman, President at Printing Industries Alliance in a report entitled "PRINT - The reports of my death have been greatly exaggerated!", states that "Like Mark Twain in the late 1800's, much has been

written, fortunately prematurely, about the untimely demise of PRINT. As the world continues to examine the phenomenon of “fake news”, data hacks, and advertising ROI, the Print Drives America Foundation continues to promote the concept that PRINT is not only the largest communications media of all (larger than broadcast, internet, new media and all other media combined) but most importantly, the most effective” (Pialliance, 2018). In an article written by Morag published in “The Drum”, a global media platform and the biggest marketing website in Europe, “print, is re-affirming the reliability and authority of printed communication in so many ways” (Blazey, 2018). Following this, Morag states that “perhaps we should all stop proclaiming that certain media are ‘dead’ or ‘alive’. Undeniably both circulations of and ad spend in print media have fallen over recent years, but the fact is that print should still be considered a viable choice of medium depending on the end purpose of the communications.

Further, the article presents the Facebook's newspaper apology ad (Figure 1). The very gravity of Facebook's situation dictated a print apology. Print is where the Facebook story first broke, and so it is appropriate that the apology starts here. There is also the question of context: Print is a news environment, not a social environment – the connotations of apologising via social may have undermined the apology. It's no surprise that Facebook ran its apology in print – the combination of heritage, authority, gravity, context, performance and audience make it the most suitable medium for “comms” like this (Blazey, 2018).

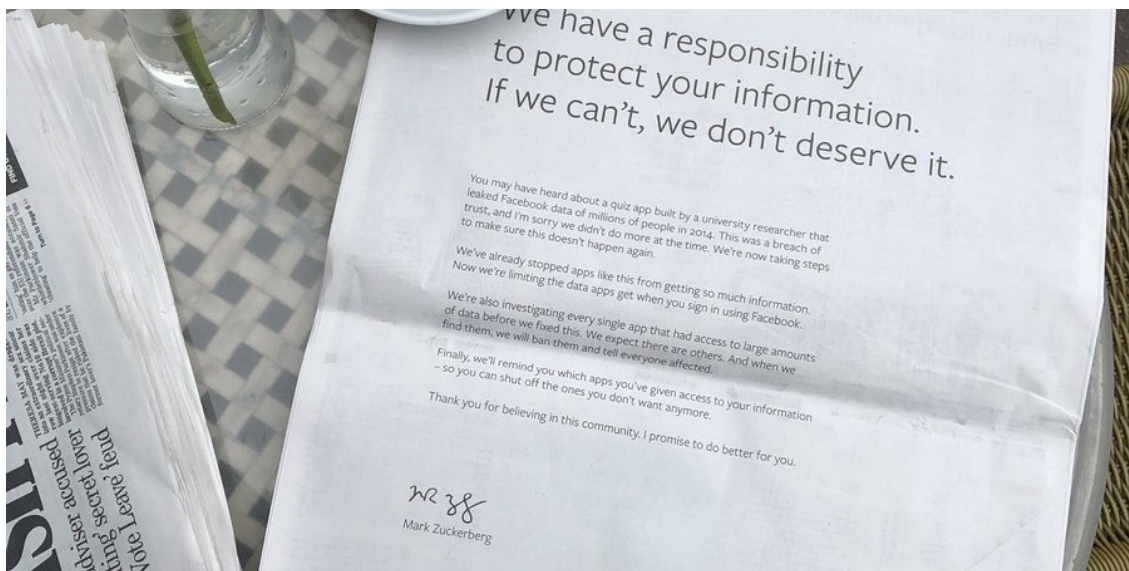


Figure 1: Facebook's newspaper apology ad

Source: <http://www.thedrum.com/opinion/2018/03/29/print-dead-then-why-do-even-the-tech-giants-use-it-their-apology-ads>

Another view on print media in relation with internet is stated at YouGov platform. “In a world of fake news, print is more trusted than Online media, particularly at the local level. 74% of respondents agree that they trusted the news and information in their local newspaper” over online sources. This trend is replicated by journalists – as published in WARC, Ogilvy Media Influence’s survey of 255 media professionals found that “52% of (journalists) now believe traditional media to be the most trusted source of news while social media is seen as the biggest contributor to the growth of fake news” (Blazey, 2018). As a conclusion, “Print possesses gravity and authority not held by newer channels. It has historically been the domain of births, deaths, marriages and major announcements As such, this sense of authority has always had applications for marketing – brand apologies and even product recalls traditionally run in print”.

2. TYPOGRAPHY AND ITS IMPORTANCE IN THE DIGITAL MEDIA DOMAIN

This leads us to consider the role of Typography in the digital age. Whereas typographic printing can be found only in collections and printing museums, the very role and significance of Typography is arising. This is taking place mainly because the principles of Typography are those that define quality and guidelines in every form of media, no matter the technology used (Politis, 2017).

Typography, together with paper and print, is directly related with quality reading. In addition, the haptic performance and sense of nature, is absolutely positively combined with humans, through handwriting. A study conducted by Vincent (Vincent, 2016), examined the topics of both reading and writing in the educational setting of universities.

The study revealed that using pen and paper for writing and reading as well as, and combined with, digital technologies remains part of the normative practices of University students. Motivations for using paper and pen are influenced by the haptic qualities of reading and writing – the feel and the smell of the paper and the grasp of the pen, the turn of the page, and extend also to the practical usefulness of note taking and writing in margins while reading.

There is no doubt that students have embraced the use of digital technologies in the educational setting of their university with enthusiasm but they have also found that the affordances of chirographic writing and the use of paper have special qualities that cannot be matched by digital media (Vincent, 2016). As such, the normative practices of students show that there is still a demand for pen and paper as well as keyboard and screen and that in some instances the use of paper is preferred.

3. DIGITAL TRANSFORMATION AND ITS IMPLICATIONS FOR GRAPHIC ARTS

Digital technologies play today a quite significant role in the media and graphic arts domain. However, digital transformation, digitalization or digitization has various interpretations and different meanings, which can be shortly defined as follows (Politis, 2018):

- Digital transformation - digitization in production processes in the printing industry (e.g. digital printing, digital prepress)
- Digital transformation - digitization in media with the evolution of digital and mobile media
- Digital transformation – digitization in production operation, business models and management (e.g. Industry 4.0, 3D printing, additive manufacturing)

This rather arbitrary classification, helps us to clarify both positive and possibly negative implications of digitization in the graphic arts fields. The conclusion from this interpretation of digitization is that no matter the digital evolution, print is evolving as well, mostly positively. Industry 4.0 is the most prominent step towards a new era for printing in the digital domain (Politis, 2018).

3.1 Industry 4.0 and graphic arts

Industry 4.0 is described as the 4th industrial revolution. Industrial revolution is an old term, used principally to classify the various steps of evolution in industrial operations and processes. However, the concept of Industry 4.0 appears as a global trend regarding the evolution in industrial manufacturing in the years to come. As such, it seems as a necessity for all industrial and manufacturing sectors to take under consideration the evolution that this concept brings. Hence, the term consists of several elements, which need to be carefully addressed and analysed. This analysis should lead to the determination of potential benefits for manufacturing operations and processes in various sectors (Drexler, 2018). In figure 2, the four industrial revolutions are illustrated.

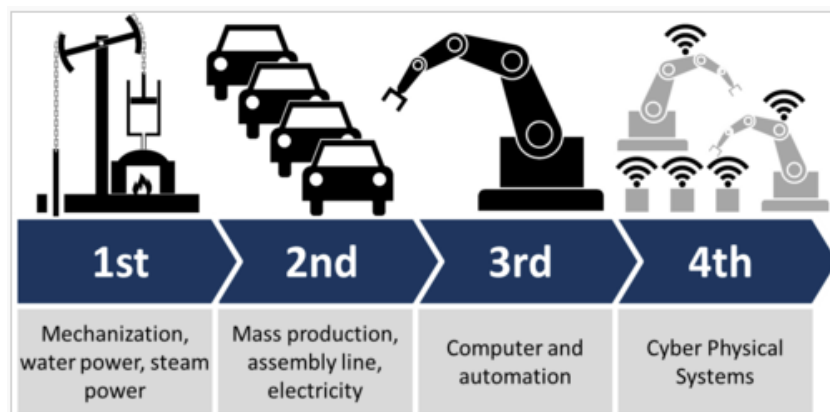


Figure 2: The four Industrial revolutions
Source: https://en.wikipedia.org/wiki/Industry_4.0

Industry 4.0 has been defined as a name for the current trend of automation and data exchange in manufacturing technologies. It includes cyber-physical systems, the Internet of things, cloud and cognitive computing and creates what has been called a “smart factory”. Industry 4.0 appears as an interesting global trend regarding the evolution in industrial manufacturing in the years to come. Since it has various definitions, interpretations, and elements, there is a necessity for specific definition of the general concept into certain sectors. Digitisation is considered as a principal element of Industry 4.0 (Politis, 2018).

As it concerns the graphic/media, printing and packaging industries, the generic Industry 4.0 trend is applied with the combination of certain elements that fit better to the nature of processes and operations in the industry. Vendors, organizations and scientists from the graphic arts and media – printing sectors could not stay out of the debate for manufacturing evolution caused by the Industry 4.0 trend. Numerous manufacturers are taking position within Industry 4.0. As such Industry 4.0 is classified / translated as Print 4.0, Finishing 4.0, Packaging 4.0 and Paper 4.0 (Politis, 2017).

A clear message from the investigation in the graphic/media sector is that not all Industry 4.0 elements are applicable at all sectors. The investigation for the graphic arts and related industries (printing, packaging, paper and finishing) show that generic elements of Industry 4.0 are adapted into specific applications in a more concrete manner at the level of manufacturers of graphic arts equipment and systems (Politis, 2017).

3.2 Digital business models

Extending digitization in the graphic arts and printing industry, Heidelberg claims that Digital business models are the future. (Heidelberg, 2018). According to Heidelberg, new digital business models such as software subscription contracts focus on the possibilities of cost-efficient print shop industrialization as digitization continues apace. Under the theme “Heidelberg goes digital, the new subscription business model offers a cost effective solution and simplified approach towards enabling end-to-end workflow automation and achieving optimal productivity, and a print shop’s business success is increasingly determined by how efficiently it handles data (Heidelberg, 2018).

Further, as it is stated by Bohan, printing companies today have to navigate the requirements of shorter run lengths, faster turnaround times and increasing costs, all while facing relatively stable print prices and higher consumables prices. With all of these challenges, it’s virtually impossible to maintain, yet alone increase, profitability without making changes to your current business model or operations (Bohan, 2018). Printing companies today have to navigate the requirements of shorter run lengths, faster turnaround times and increasing costs, all while facing relatively stable print prices and higher consumables prices. With all of these challenges, it’s virtually impossible to maintain, yet alone increase, profitability without making changes to your current business model or operations. According to Bohan, “the key to profitability and the solution to current challenges may be no further than workflow. An advanced workflow, should consider whether or not it drives positive impact on six key areas of printing business:

- Enhancing Customer Interaction
- Reducing Touchpoints
- Driving Productivity and Uptime
- Reducing Waste and Inventory
- Optimizing Consistency and Repeatability
- Providing Business Intelligence

4. CURRENT AND FUTURE TRENDS FOR GRAPHIC ARTS AND PRINTING INDUSTRY

As it is presented at DRUPA 2020 advertisement, six principal fields will dominate the exhibition in 2020, namely Print, Packaging production, Functional printing, 3D Printing, Future technologies and Industrial printing (Drupa, 2018). According to DRUPA website, Industrial Printing means Automation, robotics and new workflows in the production process as the next generation of Industry 4.0 (Drupa, 2018).

4.1 Industrial printing

Hence another interpretation for Industrial printing seems to be innovative concepts for a new era of printing, beyond traditional materials and substrates for totally new fields. According to this interpretation, Industrial printing is defined as the concept for applying print in medical and healthcare fields, in ceramics, and artificial “skin”, photovoltaics, and decoration items and artifacts. Based on a study published by the Greek portal “graphicarts.gr”, industrial printing expands the traditional printing processes in areas such as, Decoration, Multilayer materials, Ceramics, Fabrics and Glass (Graphicarts, 2018). According to the article, “Printing industry owners have to adapt to the evolving needs of consumers and buyers, which has allowed significant growth in four key market segments, namely decoration and multilayer materials, Printed electronics, Digital textile printing and 3D Printing. Smithers Pira's report – The Future of Operational and Industrial Printing by 2022 - estimates the value of the industrial and functional printing market at \$ 76.9 billion in 2017, predicting it will grow to \$ 114.8 billion by 2022 (Graphicarts, 2018).

5. PACKAGING- DEVELOPMENTS AND TRENDS

Packaging plays a crucial role in the world business and economy and it is extremely important for the global society and economy. Innovative developments at all levels are a mainstream procedure for packaging (supply chain, products and sales, transport, security, design, consumption) . Packaging is nowadays, a multi-disciplinary field, a rapidly evolving science and a dynamic industry with continuous positive indicators. In addition, packaging is the principal stakeholder for printing, with some 55% of printing worldwide to be directed on packaging Substrates (Politis, 2014).

A comprehensive research by Smithers Pira in its report on the Future of Global Packaging to 2022, shows that packaging demand will grow steadily at 2.9% to reach \$980 billion in 2022 (Smitherspira et al, 2018). In addition, according to Marketsandmarkets, the global packaging printing market was valued at USD 328.95 Billion in 2015 and is projected to reach USD 574.47 Billion by 2026, at a CAGR of 5.3% (Marketsandmarkets, 2018). All these illustrate the importance of packaging for the printing and graphic arts industry.

5.1. Packaging and the environment

The environment and its protection, the conservation of natural resources and energy saving, are nowadays key priorities for all modern societies. One of the most important features of packaging is its relationship to sustainability and environmental protection. The identification of practices, applications and procedures for controlling environmental and sustainability data relates to materials, production, handling and, more generally, to the lifecycle of the packaging.

Packaging, as an indispensable part of the product, but which is not consumed, is the most appropriate field where such policies (sustainability and environmental protection) are fully applicable (Pialliance, 2018). In this context, a variety of strategies and initiatives, as well as technologies, techniques and systems are being developed in the wider field of sustainability (Sarigiannidis et al, 2018). The environmental aspect of packaging is quite important since sustainability and the environment is considered as one of the principal issues for packaging production. Nowadays, packaging holistic design, materials and production implement sustainability concepts, in order to use less resources, recycle and protect the environment within the lifecycle of a product (Sarigiannidis, 2018).

6. (SOME) CONCLUSIONS

Printing and the graphic arts industry, show a rather positive development. Digitalization and digital transformation, together with innovations at all fields of the sector are the drivers towards this positive development. We, as researchers in the graphic arts fields should not only follow the trends, but lead the way on the transformation of our industry with intensive research for a bright future of our industry. This of course includes education as an integral part of the holistic evolution of graphic arts.

Such new - innovative tasks may include printing processes, substrates and materials, the formation of new structures in the Industry (e.g. Cultural and Creative Industries), and the role of Graphic Arts. Some indicative advanced research topics are presented here, as they are derived from the research department of HELGRAMED – The Hellenic Union of Graphic Arts and Media Technology Engineers. They are presented as indicators and good practices for further research:

- Colour Management, Measurement and Certification (Colour science – colour management systems)
- Holistic packaging design
- Innovative printing substrates and materials, inks and coatings
- Printing Science Hybrid printing, security and 3D printing
- Industrial printing
- Sustainability, environmental protection and energy efficiency
- Modern typographic design - Information and interface design
- Printed electronics and interactive information carriers – RFID-NFC
- Innovative business models, Life cycle Management, Lean Manufacturing, Production workflow management
- Industry 4.0 in the printing industry
- Standardization – A continuous development in ISO and other standards (e.g. ISO-12647)

7. REFERENCES

- [1] Blazey, M.: “Print is dead’ – then why do even the tech giants use it for their apology ads?”, Thedrum, URL: <http://www.thedrum.com/opinion/2018/03/29/print-dead-then-why-do-even-the-tech-giants-use-it-their-apology-ads> (last request: 2018-09-23).
- [2] Bohan, M.: “How Prinect Production Manager Will Reshape Your Business”, Heidelbergusa, URL: <https://news.heidelbergusa.com/2017/11/prinect-production-manager-reshape/> (last request: 2018-09-18).
- [3] Drexler, S.: “The 5 Factors of Industry 4.0, On digitizing Industry and Infrastructure, Industrial IoT/Industrie 4.0 Viewpoints”, Industrial-iot, URL: <https://industrial-iot.com/2016/08/5-factors-industry-4-0/>, (last request: 2018-10-11).
- [4] Drupa exhibition 2020, URL: https://www.drupa.com/?utm_source=drupa20%20besucher&utm_medium=email&utm_content=header&utm_campaign=news%20okt18%20en (2018-10-20).
- [5] Graphicarts , The top 4 sectors are growing faster in industrial printing, Graphicarts, URL: <http://www.graphicarts.gr/portal/showitem.php?artid=8188> (2018-09-11).
- [6] Heidelberger Druckmaschinen, “Digital business models are the future: Heidelberg achieves 100 worldwide installations of Prinect Production Manager”, Heidelbergusa, URL: <https://news.heidelbergusa.com/2018/10/digital-prinect-production-manager/> (last request: 2018-09-05).
- [7] Markets and markets, Packaging Printing Market by Printing Ink, Marketsandmarkets, URL: https://www.marketsandmarkets.com/Market-Reports/packaging-printing-market-153207109.html?gclid=CjwKCAjw8ajcBRBSEiwAsSky_ecQnTHgr4mN972nMDuCrB1C2b4npfF9cDbY3B1AvIbF4UwiwTxc_BoC_scQAvD_BwE (2018-10-13).
- [8] Pialliance, Print Drives America Foundation, Pialliance, URL: <http://pialliance.org/print-drives-america-foundation/>, (last request: 2018-10-07).
- [9] Politis, A.: “Industry 4.0: What does it mean for the Graphic Arts Industry?”, The 45th IARIGAI Conference, (Warsaw, Poland, 2018), 4-7.
- [10] Politis, A.: “The Graphic-Media Communication Science - Fields, Trends and the Contribution of Research Organizations”, The Scientific conference - Evolution Innovation in Graphic-media Science: Research, Industry Innovation and the Role of Education, (Hellenic Union of Graphic Arts and Media Technology Engineers - HELGRAMED, Athens, Greece, 2017).
- [11] Politis, A.: “Typography revisited: The importance of Typography in modern visual communication”. Aepm annual conference 2017, (The Museum of Typography, Chania Crete, Greece, 2017).
- [12] Politis, A.: “Transforming packaging buyer requirements to efficient solutions for packaging production”, ESKOWORLD Conference, 2014, (Athens, Greece, 2014).

- [13] Sarigiannidis Ch., Politis, A., Voutsinas, V.: “Packaging and Environment – a Comparative Analysis of MFCA, Full Costing and ABC Systems in Environmental Management Accounting (EMA)”, The 1st Hellenic Conference on Graphic Arts, (University of Ioannina, Ioannina, Greece, 2018).
- [14] Smithers Pira, The Future of Global Packaging to 2022, Smitherspira, URL: <https://www.smitherspira.com/industry-market-reports/packaging/the-future-of-global-packaging-to-2022> (2018-10-19).
- [15] Vincent, J.: “Students’ use of paper and pen versus digital media in university environments for writing and reading – a cross-cultural exploration”, Journal of Print Media and Media Technology Research, 5 (2), 97-106, 2016. doi: 10.14622/JPMTR-1602




© 2018 Authors. Published by the University of Novi Sad, Faculty of Technical Sciences, Department of Graphic Engineering and Design. This article is an open access article distributed under the terms and conditions of the Creative Commons Attribution license 3.0 Serbia (<http://creativecommons.org/licenses/by/3.0/rs/>).

PRINTING ADDED VALUE



THE IMPACT OF DIGITAL PRINTING MACHINES ON INDOOR AIR QUALITY

Savka Adamović¹ , Ivan Pinčjer¹ , Dragan Adamović² ,

Vladimir Zorić¹, Stefan Đurđević¹ 

¹University of Novi Sad, Faculty of Technical Sciences,

Department of Graphic Engineering and Design, Novi Sad, Serbia

²University of Novi Sad, Faculty of Technical Sciences, Department of Environmental Engineering and Occupational Safety and Health, Novi Sad, Serbia

Abstract: *The objective of the study is to evaluate the indoor air quality in digital printing facility during the three working weeks (120 hours). For that purpose, mass concentrations of suspended particulate matter of diameter less than 10 μm (PM_{10}) were monitored in addition to single-color and four-color digital machines. The cumulative mass concentrations values of PM_{10} for single-color digital machine were in the range from 1.36 to 9.90 $\mu\text{g}/\text{m}^3$, and they are almost 1.4 and 2.2 times higher compared to the same values for the four-color machine (0.97 - 4.44 $\mu\text{g}/\text{m}^3$). The obtained results could be useful for the risk assessment of indoor exposure to suspended PM_{10} particles, and for the creation of printing indoor air quality guidelines of the Republic of Serbia.*

Key words: digital printing, suspended particulate matter, indoor air quality

1. INTRODUCTION

Mass concentration has been one of the most commonly measured aerosol properties of indoor air quality, and the most important one for health and environmental effects. Many of epidemiological data suggesting that elevated levels of suspended particulate matters (PMs) are associated with an array of human health hazards (lowered immune systems, asthma or chronic coughs, even triggering heart attacks, etc.) (Wang et al, 2016). Therefore it is necessarily accurate monitoring data on mass concentration because it's right mass concentrations are the important basis for further calculations (chemical compositions or any specific property, such as isotopic content) (Wang et al, 2015).

PMs are complex mixtures of solid and liquid organic and inorganic substances (sulfate, nitrate, ammonia, sodium chloride, carbon, mineral dust and water). PMs were inhaled in a respiratory system with a potentially harmful effect on human health. Today, concentrations of suspended PMs in ambient air are quantitated based on the measurement of mass concentrations of particles with the diameter less than 10 μm (PM_{10}) and less than 2.5 μm ($\text{PM}_{2.5}$) (Vujić et al, 2010). During printing production processes, suspended PMs are produced and have an impact on the immediate environment, and therefore also to technical persons who directly serve these processes. Unfortunately, there is not enough information about indoor air quality during emission of suspended PMs by printing operations in the Republic of Serbia.

In printing techniques which ones using paper as a printing medium, sources of PMs are paper dusting and processes such as the collection, sorting, bonding and cutting of printed and unprinted paper. Dust consists of too short and insufficiently intertwined fibres of paper or filler particles that are not sufficiently bonded to the sheet of paper or are only bound by the action of static electricity. Dust also occurs in a paper who is inexpert circumcising a blunt printing knife in format or rolls (Prica et al, 2017). In digital printing technology, the sources of PMs are dust extraction, treatment processes of printing or unprinted paper and digital printing equipment.

The use of digital printing equipment (laser printers and photocopiers) has grown exponentially over the last decade. Digital printing equipment utilises a photosensitive drum to attract the toner powder and fuse it on the page with a set of rollers that apply high levels of pressure and heat. These toners are emitting particulate matters which are released via the board cooler, rear of the printer, paper tray and toner waste bin (Pirela et al, 2014). Since there is a plethora of epidemiological and toxicological evidence linking exposures to ambient particles with adverse health effects (Zhao et al, 2013) the high levels of PMs emissions have undoubtedly raised concerns about possible toxicity.

The objective of this study is to evaluate the impact of the type of digital machine on increasing of mass concentration of suspended PM_{10} particles in the ambient air of the digital printing office. The concentration levels of suspended PM_{10} particles in the ambient air of the digital printing office were monitored during three working weeks (120 hours or 40 hours per week). Also, the detected

concentrations of the suspended PM₁₀ particles emitted by the examined digital printing machines are compared with the emission limit values according to prescribed domestic and international legal acts.

2. METHODS

2.1 Digital printing office

During the three working weeks of monitoring suspended PM₁₀ particles, digital printing processes (electrophotographic procedure) were performed on single-color Xerox D95A and the four-color Xerox DocuColor 252 printing machines. The graphic material, offset paper ($G = 80 \text{ g/m}^2$) and cyan, magenta, yellow and black (CMYK) digital toners, manufactured by Xerox, were used. There are two employees in the digital printing office, but as the printing office is used for student education, and 2 to 5 students were present in practice during the monitoring.

2.2 Analysis of suspended PM₁₀ particles in the ambient air of the digital printing office

Mass concentrations of suspended PM₁₀ particles in the ambient air of the digital printing office were determined using the standard gravimetric measurement method (SRPS EN 12341: 2015). According to an SRPS EN 12341: 2015 method for the experiment, the following equipment and materials were used:

- a sampler for analysis of particulate matters (BAGHIRRA s.r.o., Czech Republic),
- an analytical balance (Kern analytical balance, model ABJ-120, Germany),
- filter paper with a diameter of 47 mm (Whatman, UK) and
- pincette.

The sampling of PM₁₀ suspended particles was carried out by a particulate matter sampler via a PM₁₀ filter paper which was placed on the duraluminum filter holder of the sampler. The masses of the filters paper before and after one hour of sampling were measured on the analytical balance, with an accuracy of $\pm 0.0001 \text{ g}$. Due to the accuracy of the results, do not touch the filter paper with fingers, but only with pincette.

The operational parameters of the sampler for analysis of suspended PM₁₀ particles for one-hour measurements during the three working weeks of monitoring are shown in Table 1.

Table 1: The operational parameters of the sampler for analysis of suspended PM₁₀ particles

Parameter	Interval
Ambient temperature (°C)	25 - 34
Ambient pressure (mbar)	1005 - 1014
Temperatures of sampler(°C)	24 - 32
Flow (l/min)	13.1 – 15.2
Flow for 1 h (l/min)	730 - 963

2.3 Calculation of the mass concentration of suspended PM₁₀ particles

The concentration levels of suspended PM₁₀ particles in the ambient air of the digital printing office were determined according to formula (1) (SRPS EN 12341: 2015):

$$Q_{PM_{10}} = \frac{m_2 - m_1}{V} \cdot 10^6 \quad (1)$$

Where are: $Q_{PM_{10}}$ - the quantity of suspended PM₁₀ particles ($\mu\text{g/m}^3$), m_1 and m_2 - the mass of the filter paper before and after sampling (g), respectively, and V - the volume of air passed through the device for 1 hour (m^3).

Daily eight-time values of PM₁₀ particles are calculated by a cumulative compilation of one-hour data updated every hour. Also, mass concentrations of suspended PM₁₀ particles were measured one-hour before the start of the operation of digital machines during sampling.

3. RESULTS AND DISCUSSION

Detected mass concentrations of suspended PM₁₀ particles before operation of digital machines (zero values) during monitoring were in the range from 0.77 to 0.88 µg/m³. Zero value show that some particle concentration was left in the air after the ventilation, but also that the particles migrate from the outside air into the ambient air of the printing office, which is not an isolated space. The detected mass concentrations of PM₁₀ particles during the eight-hour operation for the tested machines were reduced by the detected zero value to obtain real mass concentrations.

Variations of minimum and maximum mass concentrations, their cumulative and mean values for suspended PM₁₀ particles during the three working weeks monitoring for a single-color and four-color digital machine are shown in Table 2.

Table 2: Variations of mass concentrations of suspended PM₁₀ particles during three working weeks monitoring for tested digital machines

Data	Single-color Xerox D95A			Four-color DOCUCOLOR 252		
Working week	1 st	2 nd	3 rd	1 st	2 nd	3 rd
Total number of measurements	40	40	40	40	40	40
MIN $Q_{PM_{10}}$ (µg/m ³)	0.11	0.36	0.19	0.11	0.11	0.10
MAX $Q_{PM_{10}}$ (µg/m ³)	1.57	1.77	0.85	0.79	0.71	0.70
MIN cumulative value of $Q_{PM_{10}}$ (µg/m ³)	1.36	4.30	1.84	0.99	0.97	1.34
MAX cumulative value of $Q_{PM_{10}}$ (µg/m ³)	9.90	9.66	8.05	4.44	3.76	4.25
MIN mean value of $Q_{PM_{10}}$ (µg/m ³)	0.17	0.54	0.23	0.12	0.12	0.17
MAX mean value of $Q_{PM_{10}}$ (µg/m ³)	1.24	1.21	1.01	0.56	0.47	0.53

Analysing the influence of the type of digital machine on increasing the concentration of suspended PM₁₀ particles in the ambient air of the digital printing office, has been found that the significant contribution has single-color (Figure 1a) than the four-color digital machine (Figure 1b). The cumulative and mean values for the single-color digital machine were in the range: from 1.36 to 9.90 µg/m³ and from 0.17 to 1.24 µg/m³, respectively. The same values for a four-color digital machine are lower than 1.4 to 2.2 times and were in the range: from 0.97 to 4.44 µg/m³ (cumulative) and from 0.12 to 0.56 µg/m³ (mean value).

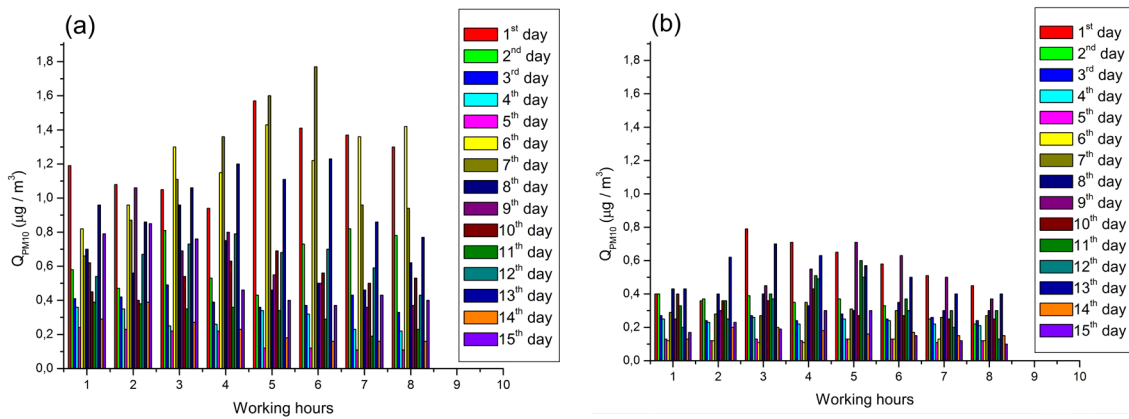


Figure 1: Mass concentrations of suspended PM₁₀ particles for eight-hour operation during ten days of monitoring in addition to (a) single-color Xerox D95A and (b) four-color Xerox DocuColor 252 printing machines

According to the manufacturer, during the operation of a digital machine, minimal amounts of paper dust and toner were emitted into the air. Most of the dust generated inside the machine goes through the exhaust gases and is retained on the filters. Dust consists primarily of particles and fibres of the paper and their levels depend on the composition and quality of the paper used. Less than 10 percent of the dust was produced by a toner cartridge (Xerox Corporation, 2017).

Air protection in Serbia is regulated by the Law on Air Protection ("Sl. glasnik RS", br. 136/09 i 10/2013) and the Regulation on the Conditions for Monitoring and Air Quality Requirements ("Sl. glasnik RS", br. 11/2010, 75/2010 i 63/2013) which are harmonized with the EU Directive (Council Directive 1999/30/EC). According to the above mentioned legal acts during the one-hour monitoring, the presence of suspended PM₁₀ particles in the ambient air is not allowed, while for 24 hours the emission limit values are 50 µg/m³. The investigated digital office was working only in one shift and for that reason was not conducted monitoring for 24 hours. Based on the highest cumulative values of mass concentrations of suspended PM₁₀ particles of 9.90 µg/m³ (single-color machine) and 4.44 µg/m³ (four-color machine) and assuming that the printing press operates the same capacity in three shifts, the values within 24 hours would be 29.70 and 13.32 µg/m³ respectively. Even three times higher concentrations do not exceed emission limit values (50 µg/m³) for 24 hours according to the above mentioned legal acts.

4. CONCLUSION

The monitoring conducted during the three working weeks showed that the digital printing process contributes to the quality of ambient air through the emission of suspended PM₁₀ particles. Comparing the influence of the type of digital machine on increasing the concentration of suspended PM₁₀ particles in the ambient air of the digital printing has been found that the more significant contribution has single-color regarding the four-color machine. The maximum cumulative values for the single-color digital machine are in the interval from 8.05 to 9.90 µg/m³ and almost 2.2 times higher than the same value for a four-color machine. Also, the maximum mean value during monitoring is 2.2 times higher for single-color compared to the four-color digital machine.

It is noticed that there is no form by which the concentration of suspended PM₁₀ particles for eight-hour hours is changed because the operation of digital machines is semi-automatic and depends on the organisation of the operator and the printing process circulation.

The Regulation of the Republic of Serbia and the EU Directive (2008/50/EC) do not define the emission limit values of suspended PM₁₀ particles during the eight-hour working hours. Therefore, the obtained results are the starting point in the future continuous monitoring of suspended PM₁₀ particles in digital but also in other printing techniques to get relevant data which would be supplemented by the laws of the Republic of Serbia.

5. REFERENCES

- [1] Institut za standardizaciju Srbije, SRPS EN 12341:2015 Vazduh ambijenta - Standardna gravimetrijska metoda merenja za određivanje PM₁₀ ili PM_{2,5} masene koncentracije suspendovanih čestica, Institut za standardizaciju Srbije, 2015.
- [2] Pirela, S.V., Pyrgiotakis, G., Bello, D., Thomas, T., Castranova, V., Demokritou, P.: "Development and characterization of an exposure platform suitable for physico-chemical, morphological and toxicological characterization of printer-emitted particles (PEPs)", *Inhalation Toxicology*, 26(7), 400-408, 2014. doi: 10.3109/08958378.2014.908987.
- [3] Prica, M., Adamović, S.: "Grafički materijali", (FTN Izdavaštvo, Novi Sad, 2017).
- [4] Službeni glasnik ("Sl. glasnik RS", br. 11/2010, 75/2010 i 63/2013): Uredba o uslovima za monitoring i zahtevima kvaliteta vazduha, Službeni glasnik, 2013.
- [5] Službeni glasnik ("Sl. glasnik RS", br. 136/09 i 10/2013): Zakon o zaštiti vazduha, Službeni glasnik, 2013.
- [6] The European Parliament and The Council Of The European Union, „Council Directive 1999/30/EC“, *Official Journal of the European Communities*, 42, 1, 1999.
- [7] The European Parliament and The Council Of The European Union, „Directive 2008/50/EC of the European Parliament and of the Council of 21 May 2008 on ambient air quality and cleaner air for Europe“, *Official Journal of the European Union*, 51, 1, 2008.
- [8] Vujić, B.B., Milovanović, D.B., Ubavin, D.M.: "Analiza koncentracionih nivoa čestičnih materija (PM₁₀, ukupnih suspendovanih čestica i čađi) u Zrenjaninu", *Hemijska industrija*, 64(5), 453-458, 2010. doi: 10.2298/HEMIND100323041V.
- [9] Wang, P., Cao, J.-J., Shen, Z.-X., Han, Y.-M., Lee, S.-C., Huang, Y., Zhu, C.-S., Wang, Q.-Y., Xu, H.-M., Huang, R.-J.: "Spatial and seasonal variations of PM_{2.5} mass and species during 2010 in Xi'an, China", *Science of the Total Environment*, 508, 477–487, 2015. doi: 10.1016/j.scitotenv.2014.11.007.

- [10] Wang, Y., Yang, W., Han, B., Zhang, W., Che, M., Bai Z.: "Gravimetric analysis for PM_{2.5} mass concentration based on year-round monitoring at an urban site in Beijing", *Journal of Environmental Sciences*, 40, 154-160, 2016. doi: 10.1016/j.jes.2015.09.015.
- [11] Xerox Corporation, The Safety of Xerox Products, Xerox, 2017, URL: https://www.xerox.com/downloads/usa/en/e/environment_safetyfacts.pdf (last request: 2018-06-21.).
- [12] Zhao, J., Gao, Z., Tian, Z., Xie, Y., Xin, F., Jiang, R., Kan, H., Song, W.: "The biological effects of individual-level PM_{2.5} exposure on systemic immunity and inflammatory response in traffic policemen", *Occupational and Environmental Medicine*, 70(6), 426-431, 2013. doi: 10.1136/oemed-2012-100864.



© 2018 Authors. Published by the University of Novi Sad, Faculty of Technical Sciences, Department of Graphic Engineering and Design. This article is an open access article distributed under the terms and conditions of the Creative Commons Attribution license 3.0 Serbia (<http://creativecommons.org/licenses/by/3.0/rs/>).

INFLUENCE OF THE INK AND SUBSTRATE PROPERTIES ON THE INK TRANSFER IN LITHOGRAPHY

Tomislav Cigula , Tamara Tomašegović , Tomislav Hudika , Davor Donevski 
University of Zagreb, Faculty of Graphic Arts, Zagreb, Croatia

Abstract: There are many parameters influencing transfer of the printing ink onto the printing substrates. Beside printing press characteristic one of most influential parameters is interface interactions in the offset blanket-printing ink-printing substrate system.

The aim of this paper is to determine printing ink and substrate properties as an influential parameter to the printing ink transfer, i.e. properties of the imprint. To achieve this goal, this research will be conducted in three steps. First, characterization of the printing substrates (coated and uncoated samples) and printing ink will be performed. The printing substrates will be characterized by determining smoothness of paper according to Bekk and surface free energy, while to printing ink's tack will be determined to detect property of the printing ink influencing the ink transfer. In the second stage a multipurpose printability testing machine will be used to produce laboratory prints. Finally, the prints will be characterized by conducting optical measurements (spectrophotometric and densitometric measurements) and determination of physical properties of the ink film (mass of the dried ink film).

The results of the research have proven that characteristics of the printing substrate and tack of the printing ink influence transfer of the printing ink onto the printing substrate, i. e. print quality.

Key words: lithography, printing ink, printing substrate, ink film

1. INTRODUCTION

Although other printing techniques are increasing their market share, offset is still the leader in the market share of the printing industry (Smith, 2017). The offset printing is a complex process where difference between printing and non-printing areas on the printing plate is achieved by their opposite physical-chemical properties (Kipphan, 2001) (Wilson, 2005). To disable adhesion of the printing ink on the non-printing areas, they must be covered by the water based solution – fountain solution. Furthermore, the ink transfer from the printing plate to the printing substrate is performed by the blanket cylinder (Figure 1).

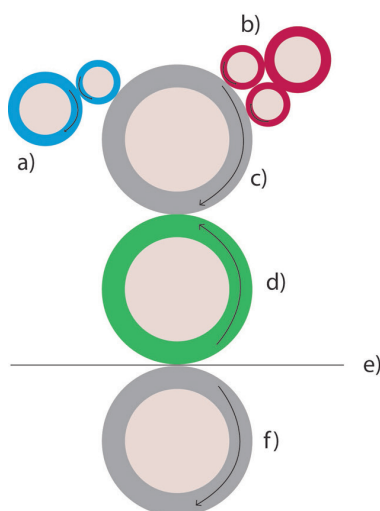


Figure 1: Basic offset printing unit: a) wetting unit, b) inking unit, c) plate cylinder, d) blanket cylinder, e) substrate and f) impression cylinder

The quality of the printing is influenced by many parameters including digital files, materials used in the process (printing substrate, printing ink, fountain solution, printing plate) and the process parameters of

printing press (e.g. printing speed, pressure, register, etc.) (Gallus, 2016). The scheme of the printing process parameters can be seen in Figure 2.

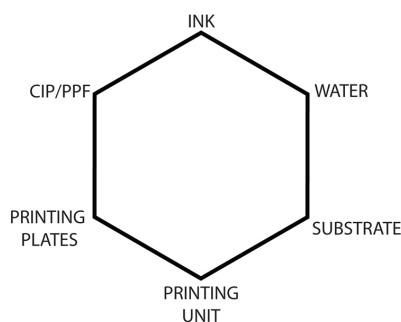


Figure 2: Offset printing process parameters

In order to achieve high printing quality, determination of the influence of each process parameters has to be performed and evaluated. In this paper investigation of the printing substrate and printing ink interaction has been performed.

2. MATERIALS AND METHODS

To achieve the aim of the research – determine printing ink and substrate properties as an influential parameter to the printing ink transfer, the research had three stages:

1. determination of the printing substrate and printing ink properties
2. making the imprints in laboratory surroundings
3. determination of the imprint characteristics

The printing substrates used in this research were two types of the fine art paper (gloss and matte coated) in the grammage of 300 gm⁻² and coated box board in the grammage of 305 gm⁻². On the other hand, printing inks were standard process offset inks (cyan, magenta, yellow and black).

Determination of the paper smoothness according to Bekk was performed using the ModularLine Smoothness Tester (Frank-Pti, n.d.).

To calculate the surface free energy of the printing substrates, contact angles of three reference liquids (water, glycerol, diiodomethane) were measured on each substrate by the use of Dataphysics OCA 30 goniometer. Sessile drop method was used to determine contact angle value. Measurements were conducted at room temperature. Drop of liquids was set to 1 µl, and the contact angle was measured 4 seconds after the first contact between solid and liquid. After that, surface free energy (SFE) and its polar (SFE^p) and dispersive (SFE^d) components were calculated in the Dataphysics' SCA 20 software by applying OWRK method (Owens et al, 1969).

The determination of the printing ink tack was performed using a IGT TackOscope III unit (IGT, n.d.). The measurements were conducted according to the ISO 12634:2017. This procedure included three steps at fixed temperature of 30°C. First 0.4 cm³ of ink was applied onto the distribution roller and the test was started by 30s of distribution time at the speed of 50 m/min. In second stage measurements of the tack was conducted at speed of 100 m/min for 60 seconds. In the third step tack was measured at the speed of 50 m/min for 90 seconds.

The sample imprints were produced in the laboratory by the use of the Pruefbau MZ II Multipurpose Printability Testing System (Pruefbau, n.d.). This laboratory unit enables printing in precisely defined conditions regarding amount of fountain solution and printing ink, printing speed and printing pressure. For the purpose of this experiment, the printing speed was 1 m/s⁻¹, printing pressure was 150 Ncm⁻², distribution time for the ink was set at 30 s, ink amount put into the inking unit was 0.2 cm³ and the application of the ink on the rubber form cylinder was set at 30 cycles.

Imprints were evaluated by weighing the dry ink film and the measuring colorimetric and densitometric values. The colorimetric and densitometric values were obtained using X-Rite eXact spectrophotometer (X-Rite, n.d.). Dry ink film was determined as difference between mass of the imprint and the mass of the printing substrate. Weighing was performed using Mettler Toledo XS205DU balance (Mettler Toledo, n.d.).

3. RESULTS AND DISCUSSION

In table 1 one can see characteristics of the printing substrates (fine art paper gloss designates as GLOSS, fine art paper matte designated as MATTE and coated box board designated as BOARD).

Table 1: Determined characteristics of printing substrates

	GLOSS	MATTE	BOARD
Smoothness of paper Bekk method [s]	535.98 ± 20.03	114.54 ± 3.2	102.26 ± 5.32
Surface free energy (SFE) [mN/m]	42.15	35.71	39.51
polar part of SFE (SFE ^p) [mN/m]	7.60	7.02	4.01
dispersive part of SFE (SFE ^d) [mN/m]	34.55	28.69	35.5

As one can see in table 1, GLOSS paper has by far the highest smoothness, and highest surface free energy and water absorption. On the other hand, BOARD has much lower polar part of the surface free energy in comparison to the GLOSS and MATTE.

Tack of printing ink is showed in table 2. Tack values presented in table 2 are the values at the end of the certain stage (measuring at the speed of 100 and speed of 50) as described in previous section.

Table 2: Ink tack value

	Cyan	Magenta	Yellow	Black
Tack at 100	164.56 ± 5.22	170.69 ± 1.36	223.35 ± 1.81	162.98 ± 2.27
Tack at 50	145.72 ± 2.72	154.12 ± 0.68	192.71 ± 0.68	144.59 ± 0.23

The tack values are higher at higher speed. The highest tack value has yellow ink while black ink has lowest tack. It can also be seen that differences between tack black, cyan and magenta is small, and yellow's tack is ca. one third higher than the tack of other inks.

Printing substrates was performed in laboratory using Printability Testing System with equal printing conditions (printing speed, printing pressure, amount of the printing ink) for all substrates and printing inks. In Figure 3 and 4 one can see the results of the imprint evaluation.

It is clearly visible that highest density is achieved when printing black printing ink on all substrates and lowest density values are measured on the substrates when printing yellow printing ink. Furthermore, higher values are achieved on fine arts paper in comparison to the coated board.

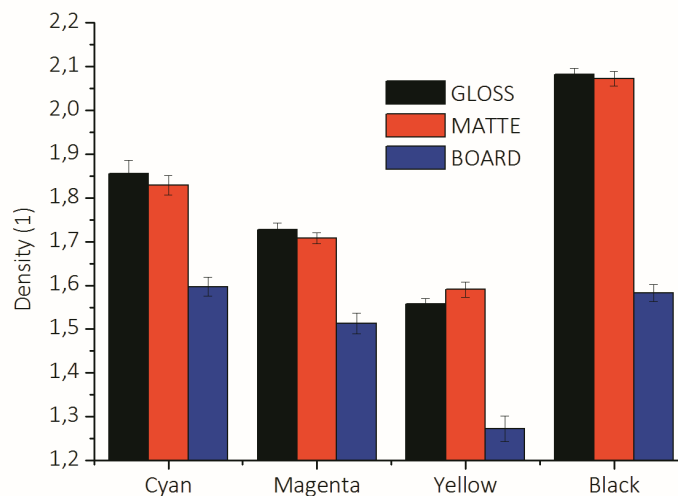


Figure 3: Density of process colours

The presented results of imprints density are opposite to the ink tack values. The ink tack values are given as a computation of a measured force when ink film is splitting between two rollers. Higher the ink splitting, higher the tack value, meaning that lower thickness of the ink film will be split and transferred onto the printing substrate as can also be seen in Figure 4.

On the other hand, it could be seen that higher smoothness and/or surface free energy (SFE) of the printing substrate leads to the higher density of the printed inks on it. Smoothness of the substrate means that the ink film formed on the substrate surface would be homogenous without higher amount of ink staying in the micro valleys on the substrate surface.

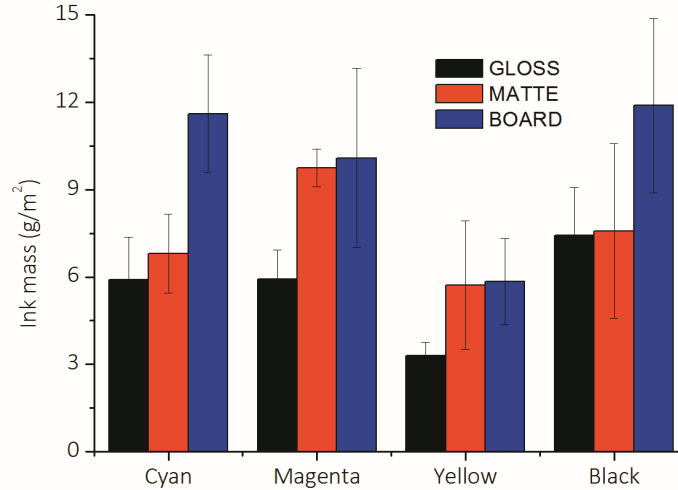


Figure 4: Mass of the dried ink layer

Opposite to the density values, the transferred ink film mass is highest on the BOARD printing substrate and lowest on the GLOSS substrate. Moreover, difference between ink film mass on the fine arts paper is small for cyan and black but high for magenta and yellow, where ink film mass on the MATTE is similar to the mass on the BOARD.

The results presented in Figure 3 and 4 show that ink on the BOARD substrate is better absorbed into the substrate causing higher reflection of light from the surface, i. e. lower density value. This is probably consequence of bulkier structure of the BOARD substrate. Nevertheless, the method used for the dried ink film mass computation is showing higher deviations, so it should be improved in the future evaluations. Calculation of the colour difference was made using ΔE_{ab} formula as defined in the ISO 12647-2: 2013. The results of the colour difference calculation are presented in Figure 5. The signs in the graph designate printing substrate combinations which were used in calculation.

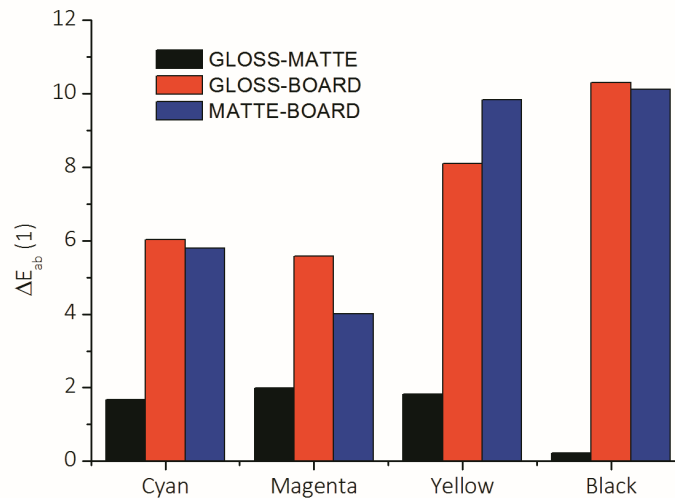


Figure 5: ΔE value between colours printed on investigated printing substrates

The highest difference between fine arts papers and paper board is present when printing black ink. Black ink is achromatic and higher density (Figure 3) leads to the lower L value, i.e. high colour difference. Similar behaviour is present in the reproduction of yellow ink. Higher ink film density on the substrate surface increases the chroma of the ink. The colour differences between fine art papers and paper board are not acceptable, except for MATTE-BOARD difference in magenta.

4. CONCLUSIONS

The hypothesis of this research was that printing substrate's and printing ink's properties influence the ink transfer during printing process. For the purpose of this research some material properties, including printing substrate's surface free energy and smoothness and printing ink's tack value, were determined. To evaluate printing ink transfer, density, dry ink film mass and colour difference were measured.

The results of the investigation showed that chosen printing substrates have similar surface free energy value but different smoothness. On the other hand, yellow ink had much higher tack than other process inks. The obtained density values were much higher on the fine art papers, but the mass of the dried ink film was higher on the paper board. The colour differences were negligible between fine art papers, but unacceptable between fine arts papers and the paper board.

From the results of this research one can conclude that investigated printing substrates and printing ink properties influence ink transfer in the printing process. The process should be adjusted according to the materials properties. Furthermore, one should take into account the printing ink usage when determining printing process costs as it can be seen that density of the colour is not linear dependant to the ink mass on the imprint.

In addition, in the future research it is planned include determination of more printing substrate properties to better determine more precise links between imprint and printing substrate properties.

5. ACKNOWLEDGMENTS

This research is a part of the project UIP-2017-05-4081, *Development of the model for production efficiency increase and functionality of packaging*, supported by Croatian Science Foundation.

6. REFERENCES





- [1] Frank-Pti, ModularLine Smoothness Tester, Frank-Pti, URL: https://www.frankpti.com/index.php?controller=dataset&function=show_detail&id=96 (last request: 2018-08-28).
- [2] Gallus, Series of articles on factors influencing quality in offset printing (part 4), Gallus, 2016, URL: <https://www.gallus-group.com/en/gallus/whitepaper/2016/03/04/series-of-articles-on-factors-influencing-quality-in-offset-printing> (last request: 2018-09-22).
- [3] IGT, TackOscope III, IGT Testing Systems Pte Ltd, URL: <http://www.igt.com.sg/products/details/tackoscope-iii> (last request: 2018-09-14).
- [4] International Organization for Standardization (ISO), ISO 12634:2017 Graphic technology -- Determination of tack of paste inks and vehicles by a rotary tackmeter, International Organization for Standardization, 2017.
- [5] International Organization for Standardization (ISO), ISO 12647-2:2013 Graphic technology -- Process control for the production of half-tone colour separations, proof and production prints -- Part 2: Offset lithographic processes, International Organization for Standardization, 2013.
- [6] Kipphan, H.: "Handbook of Print Media", (Springer, Berlin, 2001).
- [7] Mettler Toledo, Balance XS205DU, Mettler Toledo, URL: https://www.mt.com/hr/hr/home/products/Laboratory_Weighing_Solutions/Analytical/Excellence/XS_Analytical_Balance/XS205DU.html (last request: 2018-09-25).
- [8] Owens, D. K., Wendt, R. C.: "Estimation of the surface free energy of polymers", Journal of Applied Polymer Science 13(8), 1741-1747, 1969. doi: 10.1002/app.1969.070130815.
- [9] Pruefbau, prüfbau Multipurpose Printability Testing Instrument MZ II and MZ E, Pruefbau, URL: <http://pruefbau.com/en/offsetdruck/> (last request: 2018-09-21).

- [10] Smith, S.: "Digital printing to continue to take market share from offset presses", Smithers Pira, 2017, URL: <https://www.smitherspira.com/news/2017/april/digital-print-takes-market-share-from-offset> (last request: 2018-10-02).
- [11] Wilson D. G.: "Lithography primer", 3rd ed, (PIA/GATFPress, Pittsburg, USA, 2005).
- [12] X-Rite, eXact Spectrophotometer, X-Rite, URL: <https://www.xrite.com/categories/portable-spectrophotometers/exact> (last request: 2018-09-24).



© 2018 Authors. Published by the University of Novi Sad, Faculty of Technical Sciences, Department of Graphic Engineering and Design. This article is an open access article distributed under the terms and conditions of the Creative Commons Attribution license 3.0 Serbia (<http://creativecommons.org/licenses/by/3.0/rs/>).

DIFFERENCE BETWEEN USING COLOURIMETRIC VALUES ($L^*a^*b^*$) OR OPTICAL DENSITY FOR RANDOM PRINT NONUNIFORMITY QUANTIFICATION

Ivana Jurič , Dragoljub Novaković , Ivana Tomić , Ana Lilić , Željko Zeljković
University of Novi Sad, Faculty of Technical Sciences,
Department of Graphic Engineering and Design, Novi Sad, Serbia

Abstract: Surface nonuniformity can appear at a print in two forms: random or as a systematic variation. Both types appear in digital printing, but in this study, an only random variation on the digital prints was analyzed. We used two methods for quantification of the nonuniformity: M Score and ISO methods, which are based on physical measurement of the prints, using one of the measuring instruments that measure the colourimetric ($L^*a^*b^*$ values) and densitometric (optical density) values. Samples used in this paper were generated using the software MATLAB - Macro Uniformity Toolbox add-in that is printed on the same paper using ink jet printing machine Epson Stylus PRO 7800. We used spectrophotometer Eye One Pro2 and software Measure Tool to measure samples. Other calculations are done in a software application in Microsoft Excel. Based on the results obtained in the research, it is concluded that both methods can be used to measure the random variation of the print nonuniformity.

Key words: random print nonuniformity, M Score, optical density, digital printing

1. INTRODUCTION

In the reviewed literature (Petersson, 2005; Christoffersson, 2004; Fahlcrantz, 2005; Sadovnikov et al, 2007; Weingerl et al, 2014; Rasmussen et al, 2006), there are several different definitions of print (non)uniformity. The general physical definition would be that the print nonuniformity is an unwanted variation of optical density (reflected light) from the print. Different types of print nonuniformity are presented in Figure 1. Two main groups are random and systematic nonuniformity.

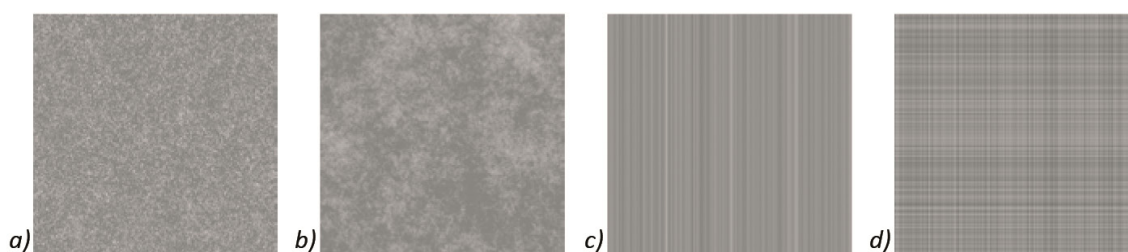


Figure 1: Different types of print nonuniformity: a) small-scale (graininess), b) large-scale (print mottle) random nonuniformity, c) stripes and d) wire mark texture – as systematic nonuniformity (Christoffersson, 2004)

In this paper, we only analyzed one type of print nonuniformity – **random print nonuniformity**. Print **nonuniformity** could be quantified using different methods: NU index (Rilovski, 2012), GLCM method (Hladnik et al, 2011; Jurič et al, 2015), standard ISO 13660, the method by (Christoffersson, 2004), etc. Common to all methods is that they are based on the Print Quality Analysis method. There is also a method based on the spectrophotometric measurements, and it is called M Score method.

The M Score method is based on spectrophotometric measurement and the analysis of the colourimetric values ($L^*a^*b^*$ values) and calculating ΔE colour differences, based on which one value is obtained in the range of 100 (uniform) to 0 (nonuniform) which determines the uniformity of the printing. Kraushaar described this method within the Fogra standard (Kraushaar, 2010). It is recommended that the test chart should be printed on the A3 format. After printing the test field should be divided into 46 columns and 59 rows, giving a tile of the size 6 x 6 mm. For each tile, $L^*a^*b^*$ values are measured. Then, for each row and each column, the mean $L^*a^*b^*$ value is calculated, and then the colour difference between the rows and between the columns is calculated, using ΔE_{00} or ΔE_{76} formula. According to these measured colour differences, M Score value is calculated. A detailed procedure for this method is shown in the paper (Jurič, 2018).

In this paper, we used two methods for print nonuniformity assessment: M Score and ISO 13660 method (the measured value of optical density was used for the ISO method, not as Print Quality Analysis).

2. MATERIALS AND METHODS

Samples used in this paper were generated using the software MATLAB - Macro Uniformity Toolbox (Rawashdeh, 2006), which is intended for simulation of surface nonuniformity in the printing process which was used in the paper (Rasmussen et al, 2006). In this add-in, it is possible to vary several parameters. For this research, only the amplitude (A) of the blotches was varied. On all samples, the background (base) colour is neutral gray (0.5) (Fahlcrantz, 2005; Lindberg et al, 2005), and the size of digital samples is $N = 2048$ px. For the simulation of random variation of nonuniformity, the function $RN.m$ (RN - Random noise) was used. The size of the blotches is defined by two values - p_{min} and p_{max} , which represent the maximum and minimum frequency. Both values were unchanged and amounted to $p_{min} = 20$, and $p_{max} = 100$. A different error level is achieved by varying the amplitude:

$$A = 0, 0.003, 0.006, 0.00975, 0.017, 0.026, 0.0496, 0.059, 0.074, 0.092, 0.13, 0.18$$

Simulated samples were printed at 160 x 160 mm. The selected printing technique for preparing samples was ink jet since based on previous research (Lindberg et al, 2005), it was concluded that prints obtained by ink jet printing were more uniform than those obtained by electrophotography.

The samples were printed on the Epson Stylus PRO 7800 digital ink jet machine. The machine settings were as follows: Paper - Single weighted Matte Paper, Print mode - Color I Profile - Epson Standard (sRGB). All samples were printed on uncoated paper IQ selection whiteboard (250 g/m²).

Test chart of 160 x 160 mm was divided into 20 rows and 20 columns, so in this case, the measuring tile was slightly larger (8 x 8 mm). Samples were measured using the spectrophotometer - *Eye One Pro2* and the *Measure Tool* software. The M Score value was calculated in a software application developed in Excel (Jurič, 2018). Both formulae (ΔE_{76} and ΔE_{00}) were used to calculate colour differences to check if there is a difference between them.

In addition to the M Score method, nonuniformity was measured using the optical density of the samples, more precisely based on the standard deviation of the measured optical density values for all tiles within a single sample. This method is similar to that described in ISO 13660 standard. Standard ISO 13660:2001 defines the methods and procedures for measuring different secondary quality attributes, as well as the print nonuniformity of monochromatic prints. The standard describes only one type of nonuniformity - random variations, which, depending on the frequency of the optical density variation, may be high - which is defined as graininess, or low - which is defined as mottling. Mottling represents macro-uniqueness and is defined as "aperiodic variation of optical density in all directions at frequencies smaller than 0.4 cycles/mm" (ISO, 2001). Mottling represents the standard deviation of optical density measurement.

3. RESULTS AND DISCUSSION

Results of print nonuniformity obtained with M Score method are presented in Figure 2. By changing the amplitude of the blotches, the M Score value is also changed. By increasing the amplitude (A), surface nonuniformity increases and the M Score values decreases. The sample S1 that is uniform has the highest M Score value (84.81 for ΔE_{76} and 85.67 for ΔE_{00}). The M Score gradually decreases, except that values for samples S3 and S4 are very similar, even for S4 slightly higher ($\Delta E_{76} = 71.04$ and 72.67, respectively). The same was observed for samples S7 and S8 ($\Delta E_{76} = 29.64$ and 29.44, respectively).

For each tile within a single sample, the optical density was measured based on which the average and standard deviation were calculated. The results are shown in Table 1 and Figure 3. Based on the results, it can be noticed that the average optical density is almost identical for all samples, while the standard deviation increases as the amplitude of blotches increases. So standard deviation of optical density could be used as a measure for the quantification of random nonuniformity.

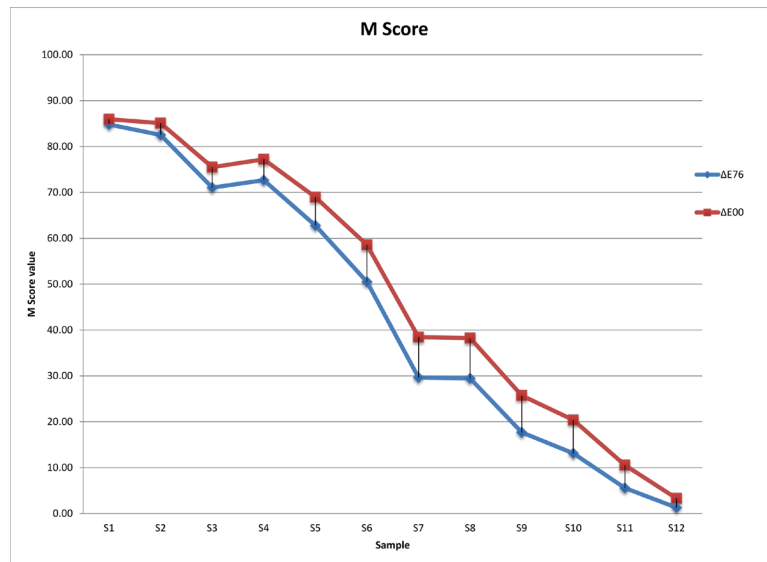


Figure 2: Obtained results of nonuniformity using M Score method

Table 1: Results of nonuniformity obtained using optical density (average D and standard deviation)

	S1	S2	S3	S4	S5	S6	S7	S8	S9	S10	S11	S12
Average D	0.387	0.385	0.384	0.387	0.384	0.386	0.385	0.386	0.386	0.383	0.382	0.389
Std	0.003	0.004	0.007	0.008	0.013	0.019	0.035	0.041	0.054	0.064	0.089	0.130

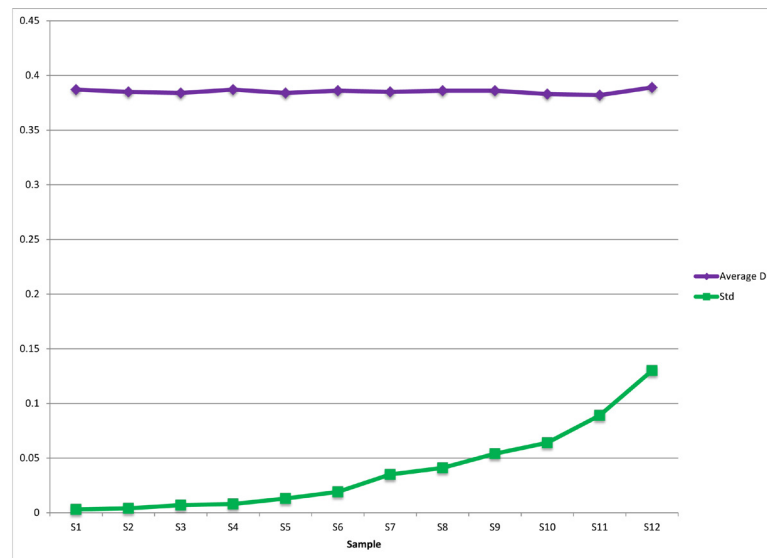


Figure 3: Obtained results of nonuniformity using optical density (average D and standard deviation)

4. CONCLUSIONS

As already mentioned, surface nonuniformity can be measured using different methods. Some methods are adapted for random measurement and some for measuring systematic variation. This paper examines the possibility of using two methods based on the measurement of the colourimetric coordinates ($L^*a^*b^*$ values) and the optical density of the field. Based on the obtained results, it can be concluded that both are suitable for measuring random variation. It is important to note that both methods are suitable when measuring a smaller test field because it is time-consuming if there is no automatic measuring instrument

for measuring the colourimetric coordinates ($L^*a^*b^*$ values) and the optical density. In the case of larger fields, methods based on Print Quality Analysis are more convenient for use.

5. ACKNOWLEDGMENTS

This work was supported by the Serbian Ministry of Science and Technological Development, Grant No.: 35027 "The development of software model for improvement of knowledge and production in graphic arts industry."

6. REFERENCES

- [1] Christoffersson, J.: "Evaluation of Systematic & Colour Print Mottle", MSc Thesis, Linköpings Universitet, 2004.
- [2] Fahlcrantz, C. M.: "On the evaluation of print mottle", PhD thesis, Stockholm University, 2005.
- [3] Hladnik, A., Mihael, L.: "Paper and board surface roughness characterisation using laser profilometry and gray level co-occurrence matrix", *Nordic Pulp and Paper Research Journal* 26(1), 99-105, 2011.
- [4] International Organization for Standardization (ISO), ISO/IEC 13660: 2001 Information Technology - Office Equipment - Measurement of image quality attributes - Binary Monochrome text and graphic images, International Organization for Standardisation and International Electrotechnical Commission, 2001.
- [5] Jurič, I., Karlović, I., Novaković, D., Tomić, I.: "Comparative study of different methods for the assessment of print mottle", *Color Research and Application* 41(5), 493-499, 2015. doi:10.1002/col.21984.
- [6] Jurič, I.: "Model za kontrolu površinske uniformnosti digitlanih otisaka", PhD thesis, University of Novi Sad, 2018.
- [7] Kraushaar, A.: "Evaluation of within sheet uniformity by means of M-Score", *Fogra*, 2010, URL: <http://www.fogra.org/index.php?menuid=263&downloadid=138&reporeid=206> (last request 2016-02-17).
- [8] Lindberg, S., Fahlcrantz, C. M.: "Perceptual assessment of simulated print noise with random and periodic structure", *Journal of Visual Communication and Image Representation*, 16(3), 271-287, 2005. doi: 10.1016/j.jvcir.2004.11.002.
- [9] Petersson, J.: "A Review of Perceptual Image Quality", Independent thesis Basic level, Linköping University, 2005.
- [10] Rasmussen, D.R., Donohue, K.D., Ng, Y.S., Kress, W.C., Gaykema, F., Zoltner, S.: "ISO 19751 macro-uniformity", *Proceedings of Electronic Imaging 2006*, (San Jose, California, USA, 2006), doi:10.1117/12.648086.
- [11] Rawashdeh, N.: "Macro Uniformity Toolbox (v2)", 2006, URL: <https://www.mathworks.com/matlabcentral/fileexchange/9882-macro-uniformity-toolbox--v2-?requestedDomain=true> (last request: 2016-01-04).
- [12] Rilovski, I.: "Influence of paper surface properties and toner type on digital print mottle", *Celuloza Si Hartie* 61, 4-9, 2012.
- [13] Sadovnikov, A., Lensu, L., Kälviäinen, H.: "Automated Mottling Assessment of Colored Printed Areas", *Proceedings of 15th Scandinavian Conference on Image Analysis*, (Springer, Berlin, Heidelberg, 2007), pages 621-630.
- [14] Weingerl, P., Hladnik, A.: "Objective methods for print inhomogeneity evaluation and their correlation with visual perception", *Journal of Imaging Science and Technology* 62(1), 2014. doi: 10.2352/J.ImagingSci.Technol.2018.62.1.010502.



INFLUENCE OF PLASMA TREATMENT ON PROPERTIES OF WAXED PAPERS

Igor Karlovits , Gregor Lavrič 

Pulp and Paper Institute, Ljubljana, Slovenia

Abstract: Barrier coatings of fibrous materials are of great interest for the packaging paper producers as increased resistance to oils, grease and other agents with the paper packaging increases the usability of the product. The barrier coatings have to withhold several parameters regarding resistance for the penetration of various agents, runnability on the machines regarding mechanical properties and also printability futures to enhance the packaging. Different sacks, bags and other products are mainly produced by coating the surface of the paper with the appropriate coatings which can be petroleum-based waxes, polymers solutions or pigments. By applying the barrier coatings the surface topography and porosity as well the surface chemistry is changed as the used polymers, waxes and other products which fill the fibrous network of the packaging change the macrostructure and induce different chemical compounds on the surface. These products are mainly printed with flexo technology. We have checked the grease resistance with the KIT test (Tappi T 559), dynamic contact angle change, the penetration of liquids and the surface coverage of plasma treated waxed and base papers. Our results indicate improved printability and liquid penetration but also the lowering of grease resistance after plasma treatment. The treatment is possible but further adjustments regarding plasma power and time of treatment are needed to find the optimal parameters for different kind of barrier coated papers.

Key words: waxed paper, plasma, dynamic contact angle, liquid penetration dynamics

1. INTRODUCTION

The waxed paper provides an economical choice for primary food packaging not only because of their versatility but also because of their safety as tasteless, odourless, non-toxic and relatively inert materials. Their widespread use in conventional packaging applications includes sandwich wraps and papers, bags, food trays, folding cartons, overwraps and many other types of packaging materials (Kit, 2010). The waxing material used is predominantly pure paraffin, often modified by the addition of microcrystalline wax and resins, particularly polyethylene. There are two general kinds of waxed paper: dry waxed, in which sheet is saturated with wax with none being left on the surface; and wet waxed, in which some wax is left as a film on the surface of the sheet (National Research Council, 1959). Recently different trends induced several changes on the market, one from the change of type of the barrier substance (removal of paraffin – change to biopolymer coatings), the need for packaging attractiveness improvement with multi-colour printing and food safety issues regarding contact with food and the migration of inks or other substances through the waxed paper. In her Bachelor theses, Sedlacekova (2017) made a comparison of different wrapping materials where the waxed paper has some beneficial properties as no composite layers are needed and the logistics point of view, the wax layer on the paper or paperboard improves the strength of the package making it unproblematic to stack. From the downside, waxed papers are harder to recycle because the wax layer should be separated (Coles et al., 2011). Also, trends of using recycled paper as a base paper instead of using virgin fibre cellulose materials (due to their availability and high prices) are having market potential regarding the decline of the reuse of the recycled materials for the newspaper or other graphic communication materials. Regarding food safety, the wrapping papers are mostly printed with water-based inks (with no VOCs or UV components) which induce that flexo printing is a dominant technology at the moment for decorating these kinds of papers. The waxed papers due to their surface treatment pose a challenge for water-based inks due to some natural incompatibilities, but the use of different surface modification methods like plasma or corona treatment there is a way to adhere the printing ink on the surface. Plasma is known as the fourth state of matter, it's a high-energy gas consisting of a mixture of ions, free radicals and photons. The energy by this particular gas allows changing the surfaces without affecting mass properties (bulk properties). Plasma flow is generated by submitting any gas, even simple air, to an electric field. This causes acceleration of free electrons that collide with gas atoms and molecules; depending on the type of collision and electron energy, ions or excited species are originated. Chemically reactive species are able to modify the surfaces with which they come into contact, by removing molecules (cleaning) or by adding functional groups (etching) (Brunelli, 2013). Researchers mainly tried using plasma for surface functionalization, but also some research work is found

regarding surface modification of cellulose-based or cellulose combined materials. It is well known that atmospheric pressure plasma activation in the air creates polar oxygen molecular groups on the surface, and thus increases the surface energy. Changes in the topography and electrostatic properties have also been reported. These changes were dependent on the type of the plasma gas as shown in work by Cornelius et al. (2017) where O₂, CF₄, or C₃F₆ gases were used on cellulose prior to papermaking and on the laboratory sheets. In a paper by a group of authors [Gonzaga et al., 2017] the analysis of elemental composition and identification of functional groups on the sample surface showed that chemical modifications occurred differently for each different plasma treatment. Contact angle measurements revealed that samples treated by O₂ plasma remained hydrophilic, whereas low receptivity to polar ($\theta > 120^\circ$) and non-polar ($\theta > 100^\circ$) liquids was observed for samples exposed to the SF₆ plasma. Regarding plasma treatment of papers for print quality improvement Pykönen (2010) in his PhD made an extensive research regarding the use of plasma on offset printability of papers. With plasma activation, it was possible to increase the surface energy and hydrophilicity of paper. Both polar and dispersion interactions were found to increase, although the change was greater in the polar interactions due to induced oxygen molecular groups. The results indicated that plasma activation takes place particularly in high molecular weight components such as the dispersion chemicals used to stabilize the pigment and latex particles. Surface composition, such as pigment and binder type, was found to influence the response to the plasma activation. The ink-setting rate decreased with linseed-oil-based inks, probably due to increased acid-base interactions between the polar groups in the oil and the plasma-treated paper surface. With mineral-oil-based inks, the ink setting accelerated due to plasma activation. Hydrophobic plasma coatings were able to reduce or even prevent the absorption of dampening water into pigment coated paper, even when the dampening water was applied under the influence of nip pressure. In another paper by Touminen et al. (2010) different surfaces modifications of surfaces were investigated and the results showed that the traditional surface treatment methods, i.e., flame and corona treatments, increased the surface energy by introducing oxygen-containing functional groups on the surfaces of LDPE and PP more than helium and argon plasma treatments. Only in the case of flame treatment, the higher surface energy and oxidation level led to better print quality, i.e., toner adhesion and visual quality, than the plasma treatments. The morphological changes observed on LDPE surface after flame treatment are partly responsible for the improved print quality. Atmospheric plasma treatments improved the print quality of LDPE and PP surfaces more than corona treatment. The electret phenomenon observed on LDPE and PP surfaces only after corona treatment is the most likely reason for the high print mottling and low visual quality of corona treated surface. As the research of the plasma treatment of waxed papers is scarce it motivated us to look further into the surface effects on these types of papers.

2. METHODS

We had three paper samples. One was the base paper which was waxed with two different type of wax compounds. The base paper had the grammage of 60 g/m² and specific volume of 1.50 cm³/g with a basic moisture content of 7%. The main material is recycled fibres recovered from the deinking process which were combined with fibrillated recycled fibres. To evaluate the effectiveness of the waxing for barrier properties we have made the test to evaluate the water and oil absorption properties of the papers. The test was carried out before and after plasma treatment. The plasma treatment was carried out in laboratory conditions for 60 s with an atmospheric plasma laboratory unit (O₂) with the power of 500W and 50 Pa pressure. The samples were tested before and after plasma treatment. For water resistance we have used several tests: the gravimetric Water vapour transmission rate (TAPPI T 464-om 18, with RH of 95%), the ultrasound method for the determination of the liquid penetration dynamics (Emtec PDA unit and proprietary method) and contact angle measurements were made using water on the Fibrodat 1100 device. The test the oil resistance we have used the so-called KIT test which is based on the Tappi T 559 measures the degree of repellence or anti-wicking of paper and boards which have been treated with fluorochemical sizing agents used to prevent wetting of the cellulose fibres of the material. Test solutions with varying strengths of castor oil, toluene, heptane and turpentine are used. The highest numbered solution (the most aggressive) that remains on the surface of the paper without causing failure is reported as the "kit rating" (maximum 12). To further evaluate the effect of the plasma treatment we have tried to print the samples with water-based inks using flexo technology, where optical density was used to evaluate the possibility of printing.

3. RESULTS

The results for the water transmission rate is presented in Figure 1.

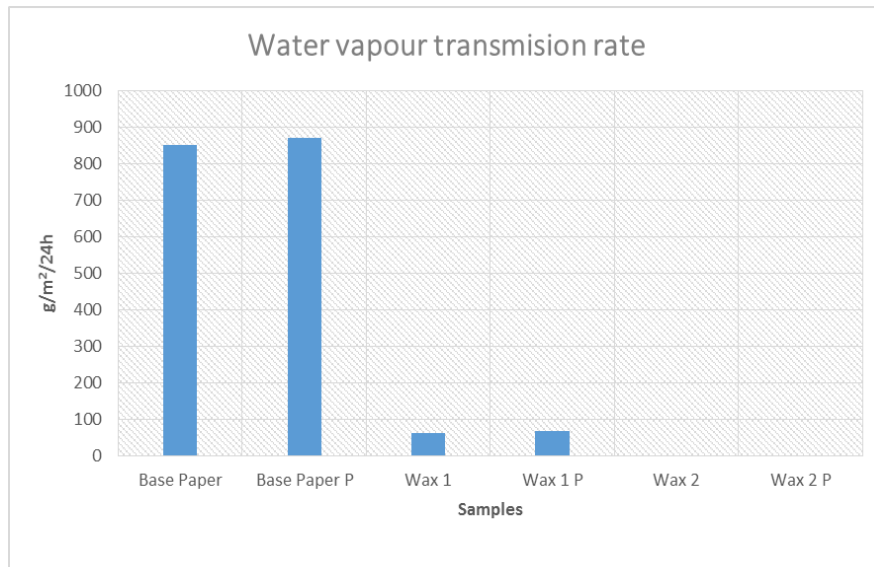


Figure 1: Water vapour transmission rate for the base and waxed papers

As we can observe as expected the non-waxed paper had a very high transmission rate $850 \text{ g/m}^2/24\text{h}$, while the waxed papers 1 had values $62 \text{ g/m}^2/24\text{h}$ and the waxed paper number 2 the lowest value of $8,7 \text{ g/m}^2/24\text{h}$. These were the results without the plasma treatment. After the plasma treatment there was a slight rise for the non-waxed base paper and the first waxed sample (from 850 to $870 \text{ g/m}^2/24\text{h}$ and 62 to $68 \text{ g/m}^2/24\text{h}$; while the third sample has dropped to $8 \text{ g/m}^2/24\text{h}$. These changes are very small due to the sensitivity of the test and we have tested the sample by the ultrasound measurement of penetration speed. The results are presented in Figure 2 and Table 1.

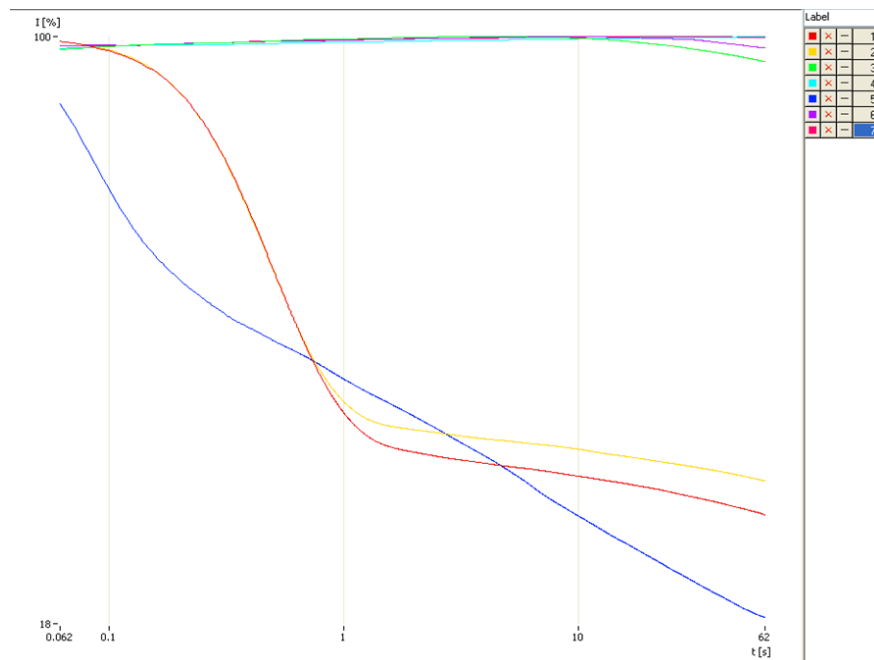


Figure 2: The penetration curves of water on different samples (curves 1 and 2 are base paper after plasma treatment, curve 3 wax 1 sample after plasma, curve 4 wax 2 after plasma and curve 5 base paper no plasma, curve 6 and 7 represent wax 1 and wax 2 sample with no plasma treatment)

Table 1: Penetration parameters of the PDA measurement

Sample	Base paper	Base paper P	Wax 1	Wax 1 P	Wax 2	Wax 2 P
Penetration parameters	Ci=70,45, Ct= 5,68	Ci=80,4 Ct= 54,166	Ci=0,0 Ct= 4,551	Ci=0,0 Ct= 9,516	Ci=0,0 Ct= 55,083	Ci=0,1 Ct= 59,933

Figure 2 and Table 1 indicate that only the sample without wax (base paper) was influenced and had quicker absorption while the samples which were waxed had almost no penetration of water prior and after plasma treatment. This indicates that the surface pore structure has not changed in the macro-pore region and this could be negative to the printing properties based on water, but good for barrier properties. The water absorption and sorption properties were also checked with the contact angle measurement using Fibrodat 1100. The results are presented in Table 2.

Table 2: Contact angles of the samples

Sample	Base paper	Base paper P	Wax 1	Wax 1 P	Wax 2	Wax 2 P
Contact angle (°) at 1s	54,51	37,18	96,06	103,9	94,94	99,16

The contact angle results also indicate that only the base paper had a decrease in contact angle (from 54,51° to 37,18° while the waxed papers had an increase in the contact angle measurements. This means that if we would like to print with water based inks the treatment does not bring any improvements.

As a final test before printing we have done the KIT test to test also the oil and grease repellency as this is an important property of the wrapping paper. The results are presented in Table 3.

Table 3: KIT values of the tested samples

Sample	Base paper	Base paper P	Wax 1	Wax 1 P	Wax 2	Wax 2 P
KIT number	1/1*	1	9/7*	6	7/8*	5

From Table 3 we can observe that here the plasma treatment caused some changes – lowered the oil and grease resistance of all samples. The base paper had the smallest KIT test value of 1 which means no barrier properties while the Wax 1 had the highest resistance value of 9 and 7 (for upper and downside) but decreased to 6 and sample Wax 2 decreased from 7/8 to 5. This means that the applied plasma treatment lowered the oil resistance of waxed papers by 1/3 of the value. This is most probably due to the small scale of surface watching which opened up the micropore structure which is suitable for the oil-based liquid absorption into the porous network.

After testing the properties we have tried to print the samples. For printing we have used the IGT F1 flexo laboratory printer with printing parameters of printing speed of 0.5 m/s, anilox force to printing form 60N, printing pressure was 90N and we have used HD flexo printing plates (1,4 mm thickness) and Doneck water-based inks with viscosity of 18s (measured with ISO Cup 4).

The printing on the base paper was no problem and the plasma treatment had a beneficial effect regarding optical density and ink coverage as we can see in Figure 3.



Figure 3: Print samples of the base paper (upper no plasma treatment lower after plasma treatment)

The increase in the optical density was around 30% for the plasma treated sample. No other print quality parameters were observed to change. The waxed paper on the other hand had a very poor printability as we can see in Figure 4.



Figure 4: Print samples of the waxed paper (upper sample wax 2 lower sampler wax 1 sample before plasma treatment)

As we can see in Figure 4 the waxed paper are unsuitable for good quality prints in water-based flexo technology due to poor ink adhesion and coverage. After plasma treatment a very interesting effect had occurred which we present in Figure 5.



Figure 5: Prints of plasma treated samples

From Figure 5 we can observe two distinct surfaces with a poor coverage and with an excellent coverage. Bot surfaces were under plasma treatment with the exception that the spherical part of the sample which has been in the plasma treatment had also been in contact with the base plate which heats up. It seems that the thermal effect induced by the plasma treatment had a better printability effect on the samples from the surface modification effort.

4. CONCLUSION

Using waxing as a barrier coating properties enhancement has a long tradition and is widely used. The changes in the surface modification technologies like plasma or corona gives possibilities of printing food contact safe inks which are water-based. In this preliminary study, we tested several methods to determine the effect of atmospheric plasma on water and oil barrier properties as well the possible changes in flexo printability. Our results indicate that the applied amount of surface modification induced by plasma did not lower the water resistance (the water vapour transmission rate, the penetration dynamics and the contact angle were slightly changed but with no major effect), but lowered the oil and grease resistance by 30%. The printability with water-based inks was not good, even after the plasma treatment which is in correspondence with the water/surface interaction test methods has shown. On the other hand as a very interesting phenomenon, the thermal effect within the plasma was observed

where excellent printability was achieved. These structural and morphological changes will be tested in the fore coming period, as well as the optimization of the plasma application process.

5. ACKNOWLEDGEMENTS

The work was carried out within the RDI project Cel. Cycle: "Potential of biomass for development of advanced materials and bio-based products"(contract number OP20.00365), co-financed by the Republic Slovenia, Ministry of Education, Science and Sport and the European Union under the European Regional Development Fund, 2016-2020. The authors also want to thank Ita Junkar from the Jožef Štefan Insitute for the help with the plasma treatment.

7. REFERENCES

- [1] Brunelli E.: "The potential of plasma technology", URL <http://www.paperindustryworld.com/not-only-sustainable-the-potential-of-plasma-technology/> (last request 2018-10-07)
- [2] Coles R. and Kirwan M. eds.: "Food and Beverage Packaging Technology", 2nd ed, (Blackwell Publishing Ltd, New Delhi, 2011), page 101.
- [3] Cornelius, C., Saquing, C., Venditti, R., McCord, M., Bourham, M.: "The Effect of Atmospheric Pressure Plasma on Paper and Pulps", *BioResources*, 12 (4), 8199-8216, 2017.
- [4] Gonzaga de Camargo, J.S., de Menezes, A. J., da Cruz, N.C., Rangel, E.C., de Oliveira Delgado-Silva, A.: "Morphological and Chemical Effects of Plasma Treatment with Oxygen (O₂) and Sulfur Hexafluoride (SF₆) on Cellulose Surface", *Materials Research*, 20 (2), 842-850, 2017. doi: 10.1590/1980-5373-mr-2016-1111
- [5] Kit L. Yam (Ed.): "The Wiley Encyclopedia of Packaging Technology", 3rd ed, (John Wiley & Sons, 2010) page 910. doi: 10.1002/9780470541395
- [6] National Research Council (U.S.). Food Protection Committee." Food-packaging Materials: Their Composition and Uses; a Report", National Academies, 1959
- [7] Pykönen M.: "Influence of Plasma Modification on Surface Properties and Offset Printability of Coated Paper", PhD Thesis, Åbo Akademi University, Finland, 2010
- [8] Sedlacekova Z.: "Food Packaging Materials Comparison of Materials Used for Packaging Purposes", Bachelor Degree International Business and Logistics Thesis, Helsinki Metropolia University of Applied Sciences, 2017.
- [9] Tuominen, M., Lahti, J., Lavonen, J., Penttinen, T., Räsänen, P. J., Kuusipalo, J.: "The Influence of Flame, Corona and Atmospheric Plasma Treatments on Surface Properties and Digital Print Quality of Extrusion Coated Paper", *Journal of Adhesion Science and Technology*, 24 (3), 471-492, 2010. doi: 10.1163/016942409X12561252292224



COMPARISON OF COLOUR REPRODUCTION BY PENTAX K10D DIGITAL CAMERA EMPLOYING POLYNOMIAL MODELS AND ICC BASED COLOUR MANAGEMENT TOOLS

Ondrej Panák , Natálie Kailová , Markéta Držková 

University of Pardubice, Faculty of Chemical-Technology

Department of Graphic Arts and Photophysics, Pardubice, Czech Republic

Abstract: This paper deals with the characterization of a Pentax K 10 digital camera in order to be used in colorimetric measurements in a custom built setup employing a LED light source. The experiment focuses on colour characterization using several polynomial transformation models in comparison to ICC based colour characterisation. Altogether 5 polynomial models are applied and evaluated by capturing set of uniform colour patches. Preliminary results indicate, that the complexity of the model does not markedly improve the prediction of CIELAB values.

Key words: digital camera, calibration, characterisation, polynomial models, colour prediction

1. INTRODUCTION

Digital *RGB* cameras can be utilised in applications mapping dynamic colour change of thermochromics surfaces (Abdullah et al, 2010; Smith et al, 2001; Farina et al, 1994; Vejrazka et al, 2007; Cukurel et al, 2012; Bourque et al, 2015; Panák et al, 2018). In such cases, the most important information is the information about the magnitude of colour change in dependence of temperature. The *RGB* signal recorded by the camera has to be transformed into colorimetric representation. There are several methods that could be employed: spectral characterisation of camera sensors (Cheung et al, 2005; Sole et al, 2016; Jiang et al, 2013), neural networks (Cheung et al, 2004) and polynomial modelling (Cheung et al, 2004; Westland et al, 2012; Bianco et al, 2009; Johnson, 1996; Hong et al, 2001; Finlayson et al, 2015).

Polynomial modelling requires uniform illumination and stable conditions in order to obtain reproducible results (Cheung et al, 2004; Westland et al, 2012; Bianco et al, 2009). A set of about 60 colour patches applied as training set seems to be enough to obtain good colorimetric prediction (Hong et al, 2001). The polynomial modelling transforms linearized *RGB* values into *CIE*XYZ colorimetric values. An example of polynomial model is shown in Equation 1.

$$\begin{aligned} X &= a_{1,1}R + a_{1,2}G + a_{1,3}B + a_{1,4}RG + a_{1,5}RB + a_{1,6}GB + a_{1,7}R^2 + a_{1,8}G^2 + a_{1,9}B^2 + a_{1,10} \\ Y &= a_{2,1}R + a_{2,2}G + a_{2,3}B + a_{2,4}RG + a_{2,5}RB + a_{2,6}GB + a_{2,7}R^2 + a_{2,8}G^2 + a_{2,9}B^2 + a_{2,10} \\ Z &= a_{3,1}R + a_{3,2}G + a_{3,3}B + a_{3,4}RG + a_{3,5}RB + a_{3,6}GB + a_{3,7}R^2 + a_{3,8}G^2 + a_{3,9}B^2 + a_{3,10} \end{aligned} \quad (1)$$

Polynomial model can be more or less complex. Polynomial models of second degree seem to be enough good to predict colorimetric data from *RGB* values (Hong et al, 2001). The polynomial transformation can be expressed in matrix form by Equation 2 (Cheung et al, 2004; Westland et al, 2012; Bianco et al, 2009).

$$\mathbf{T} = \mathbf{D} \mathbf{A} \quad (2)$$

Matrix \mathbf{T} represents $n \times 3$ values of *XYZ* and matrix \mathbf{D} is matrix of $n \times m$ extended values of *RGB*. The n represents the size of the set, e.g the number of colour patches or pixels. From Equation 1 the m is 10 ($R, G, B, RG, RB, GB, R^2, G^2, B^2, 1$). Matrix \mathbf{A} represents coefficients of selected polynomial model. In order to obtain coefficients of the model, colour patches of some training set have to be recorded. Then the matrix \mathbf{A} can be found by Equation 3.

$$\mathbf{A} = \mathbf{D}^+ \mathbf{T} \quad (3)$$

Matrix \mathbf{T} represent known set of *CIE*XYZ values of training colour patches. Matrix \mathbf{D}^+ is a pseudoinverse (Cheung et al, 2004; Westland et al, 2012; Bianco et al, 2009) matrix, determined from known set of *RGB* values of training colour patches. When coefficients of the polynomial model are known, any *RGB* combination can be transformed into *CIE*XYZ combination using Equation 1. Extension of the polynomial model can reduce the error for about 50 % (Bianco et al, 2009; Johnson, 1996; Hong et al, 2001; Finlayson et al, 2015), but only in case of stable capturing conditions (Finlayson et al, 2015).

The aim of the paper is to compare two approaches of transforming *RGB* data into *CIELAB* data in the setup we have applied in our previous study (Panák et al, 2018). The first approach is ICC based transformation in Adobe Photoshop. The second approach applies custom built algorithms of different polynomial models.

2. EXPERIMENTAL

2.1 Devices

Raw digital *RGB* image data were captured by Pentax K10D camera with SMC Pentax-DA 1:4(22) 16–45 mm ED–AL lens. A Falcon Eyes’ ring LED source DVR-630DVC with diffusor was utilized as a flat diffusive illumination with CRI value equal to 94, as specified by the producer (Falconeyes, 2018). Colorimetric parameters of colour patches were measured by Hunterlab UltraScan Vis spectrophotometer with SCI d/8 geometry.

2.2 Colour charts

Three colour charts were applied in this study. The first one was X-Rite ColorChecker Passport Photo with 24 patches, including 6 patches of neutral colours (See Figure 1). Colorimetric data provided by the producer (Xritephoto, 2018) were applied as a reference. The second custom made Profiling colour chart contained 80 colour patches including 8 neutral colours (see Figure 2). The third Testing colour chart contained another 80 colour patches that were selected randomly and were different from colour patches in Profiling colour chart (see Figure 3). Profiling and Testing colour patches were cut out of the NCS Index 1950 sample collection (NCS Colour AB, 2017) and their reference *CIEXYZ* colorimetric data were captured by Hunterlab UltraScan Vis spectrophotometer (D50, 2° observer). These charts were subdivided each in four parts, so the size matches approximately the size of ColorChecker Passport.

2.3 Methods

The digital camera was placed into the middle of a circular opening of the light source. The distance of the light source from the surface of measured sample was about 38 cm. The space between the light source and the sample was covered by a protective skin with an internal white diffusive surface, to prevent the negative effect of the outer environment. The sensitivity of the camera was set to ISO 200 and optimal shutter speed and aperture were found and kept constant over the experiment. The focal length of the lens was adjusted so the captured colour chart took about one fourth of total area captured by the sensor.

Stability of camera output was investigated by capturing 300 images of a white substrate with diffusive coating and white balance target of ColorChecker in 7 seconds intervals. Camera Raw 7.0 module of Adobe Photoshop CS4 software was used to obtain 16 bit *RGB* tiff images from raw *DNG* file. The stability was evaluated in terms of development of *RGB* values over time. Capturing of the sequence started after at least 30 minutes from switching on the light source. After this time the intensity of the source is stabilised. All colour charts described in previous chapter were captured in a sequence one after each other and they were processed later.

In order to perform fairly good linearization of *RGB* values, first the optimal transformation of *DNG* file into *TIFF* file had to be found. This was done by preparing set of 16 bit *TIFF* images out of one *DNG* file of CholorChecker in Camera Raw 7.0 module, where values of selected parameters were set to certain value or option. These parameters were: Exposure, Blacks, Brightness, Contrast, Curves, Details, and *DNG* profile. All other parameters were of 0 value. A custom made *DNG* profile of the camera was generated by ColorChecker Passport software. Only neutral colour patches of ColourChecker were considered in the procedure. The objective was to determine coefficients of Equation 4:

$$C_i = a_i R_i^{h_i} \quad (4)$$

where C_i is value of X , Y , or Z and R_i is value of R , G , and B respectively. The setup of Camera Raw 7.0 resulting in the best fit was considered in further processing of all other images. Coefficients of Equation 4 found for the best fit were used in linearization of *RGB* values of all colour patches.



Figure 1: ColorChecker Passport



Figure 2: Profiling colour chart



Figure 3: Testing colour chart

In the ICC based colour transformation the camera ICC profile had to be created. It was done in i1Profiler software from linearized 16 bit *RGB* TIFF file of ColorChecker. Created profile was assigned to all colour charts and the image was converted to *CIELAB* using absolute colorimetric rendering intent in Adobe Photoshop CS4. Obtained images were saved as 16 bit TIFF file. Mean *CIELAB* values of each colour patch were compared to reference *CIELAB* values in Matlab 2015 by means of ΔE_{00} applying predefined function (Westland et al, 2012).

Based on the information in (Cheung et al, 2005), all together 5 polynomial models (see Table 1) were tested using the general Equation 2. The coefficient matrix **A** was found by Equation 3 applying the *pinv* function in Matlab. In one case, the matrix **A** was found while linearized *RGB* values of CholorChecker were set to be the training set. In the second case, linearized *RGB* values of Profiling colour chart were set as training set. Each polynomial model with generated coefficients was then applied to linearized *RGB* values of all colour patches mentioned in 2.2. Linearization of *RGB* values of all colour patches was done according to neutral colour patches of corresponding training set. Obtained theoretical colorimetric representation was compared to reference colorimetric data by means of ΔE_{00} .

Table 1: List of polynomial models represented by formulation of matrix **D**

D1	[<i>R</i> <i>G</i> <i>B</i>]
D2	[<i>R</i> <i>G</i> <i>B</i> 1]
D3	[<i>R</i> <i>G</i> <i>B</i> <i>RGB</i> 1]
D4	[<i>R</i> <i>G</i> <i>B</i> <i>RG</i> <i>GB</i> <i>RB</i> <i>R</i> ² <i>G</i> ² <i>B</i> ² 1]
D5	[<i>R</i> <i>G</i> <i>B</i> <i>RG</i> <i>GB</i> <i>RB</i> <i>R</i> ² <i>G</i> ² <i>B</i> ² <i>RGB</i> <i>R</i> ² <i>G</i> <i>G</i> ² <i>B</i> <i>B</i> ² <i>R</i> <i>R</i> ² <i>B</i> <i>G</i> ² <i>R</i> <i>B</i> ² <i>G</i> <i>R</i> ³ <i>G</i> ³ <i>B</i> ³ 1]

3. RESULTS AND DISCUSSIONS

3.1 Stability of the camera output

Figure 4a shows the development of *RGB* values over time when capturing of the sequence started immediately after switching on the camera. It can be seen that the camera white balance is not kept constant. After approximately three minutes, some splitting of the magnitude id *R*, *G* and *B* values can be observed. Figure 4b shows the case, when capturing started 40 minutes after switching on the camera. The white balance was kept constant over time. Therefore the capturing of all colour patches started always at least 40 minutes after the camera was switched on. Some noise in the signal intensity can be observed, most probably due to a mechanical shutter of studied camera. The evaluation of variability in *CIELAB* colour space of ColorChecker can be found elsewhere (Panák et al, 2018).

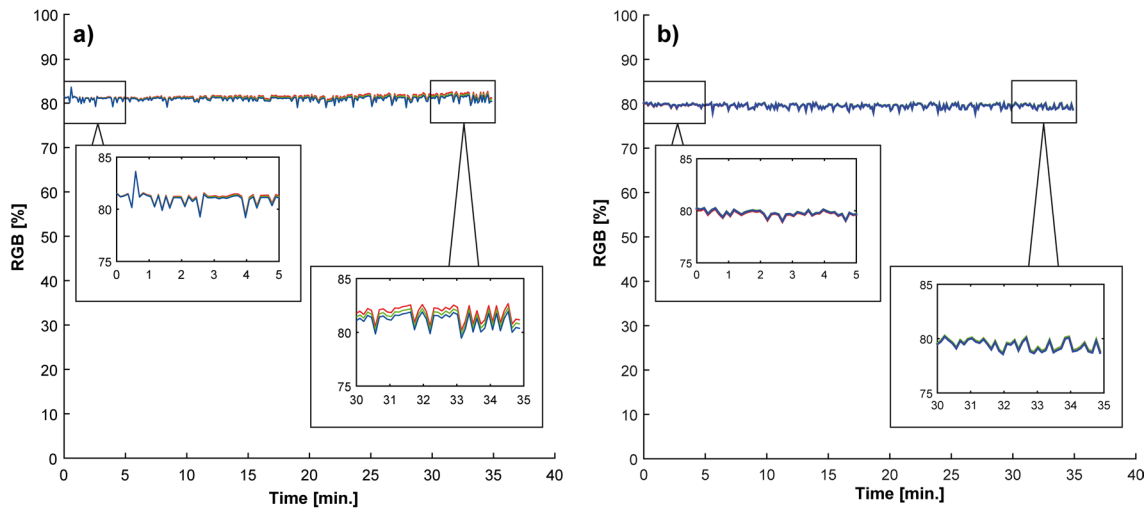


Figure 4: Camera output stability

3.2 DNG to TIFF transformation

The best setup of transforming DNG file into TIFF tile in Camera Raw 7.0 was setup described in the Table 2 as setup C4. Figure 5a illustrates the fit of $X(R)$, $Y(G)$ and $Z(B)$ dependencies according to general formula in Equation 4. Setup C13 is shown in Figure 5b for comparison, where obtained data do not fit the exponential function as good as in case of C4. Change in the exposition (C3-C8) did not affect the quality of regression. Setup C4 was applied in creation of RGB TIFF files of all colour patches.

Table 2: Determination coefficients R^2 of $X(R)$, $Y(G)$ and $Z(B)$ functions for different setups of Camera Raw 7.0.

	Exposure	Blacks	Brightness	Contrast	Curves	Details	DNG profile	R_c		
								R	G	B
C1	0,00	0	+50	+25	linear	implicit	custom	0.9921	0.9904	0.9912
C2	0,00	5	+50	+25	linear	0	custom	0.9911	0.9893	0.9902
C3	1,00	5	0	0	linear	implicit	custom	0.9997	0.9999	0.9998
C4	0,90	5	0	0	linear	implicit	custom	0.9999	0.9997	0.9998
C5	0,80	5	0	0	linear	implicit	custom	0.9997	0.9999	0.9998
C6	0,70	5	0	0	linear	implicit	custom	0.9997	0.9999	0.9998
C7	0,60	5	0	0	linear	implicit	custom	0.9997	0.9999	0.9998
C8	0,50	5	0	0	linear	implicit	custom	0.9997	0.9999	0.9998
C9	0,00	0	0	0	linear	implicit	custom	0.9993	0.9997	0.9995
C10	0,00	0	0	+25	linear	implicit	custom	0.9996	0.9999	0.9998
C11	0,00	5	0	+25	linear	implicit	custom	0.9965	0.9952	0.9957
C12	0,00	5	+50	0	linear	implicit	custom	0.9912	0.9891	0.9903
C13	0,00	5	+50	+25	linear	implicit	ACR 4.4	0.9912	0.9891	0.9900
C14	0,00	5	+50	+25	middle contr.	implicit	ACR 4.4	0.9908	0.9888	0.9900
C15	0,00	5	+50	+25	middle contr.	implicit	Adobe	0.9912	0.9892	0.9904
C16	0,00	5	+50	+25	middle contr.	implicit	custom	0.9912	0.9891	0.9903

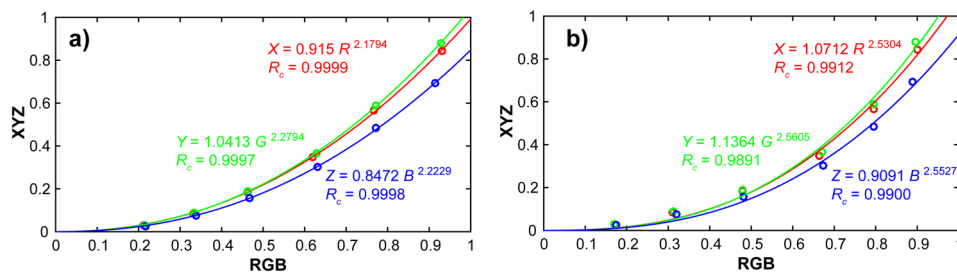


Figure 5: Regression of $X(R)$, $Y(G)$ and $Z(B)$ dependencies for setup C4 (a) and C13 (b)

3.3 ICC based colour transformation

The colour difference ΔE_{00} together with difference in attributes is presented in Table 3. As expected, the colour difference on ColorChecker is fairly low, not exceeding the value 2 (see Figure 6a). In case of the Profiling and Testing colour chart the worst prediction, ΔE_{00} exceeds the value 4, is for brown and dark green colours (see Figure 6b,c). The unsatisfactory colour prediction could be affected by indirect glare effects observed during the measurement. The surface of Profiling and Testing colour patches was semi-matte, glossier when compared to patches of ColourChecker. Some variability due to stability of camera output can also have a slight influence on the magnitude of ΔE_{00} .

Table 3: Colour differences in case of ICC based RGB to CIEAB transformation

		ΔE_{00}	ΔL	ΔC	ΔH
Median	ColorChecker	0.71	0.25	0.39	0.34
	Profiling	2.35	1.62	0.73	0.84
	Testing	2.25	1.09	0.75	0.80
Minimum	ColorChecker	0.12	0.01	0.03	0.05
	Profiling	0.47	0.01	0.05	0.00
	Testing	0.68	0.03	0.01	0.00
Maximum	ColorChecker	1.92	1.80	0.96	1.31
	Profiling	4.84	4.76	2.26	4.10
	Testing	5.82	5.05	2.55	4.12

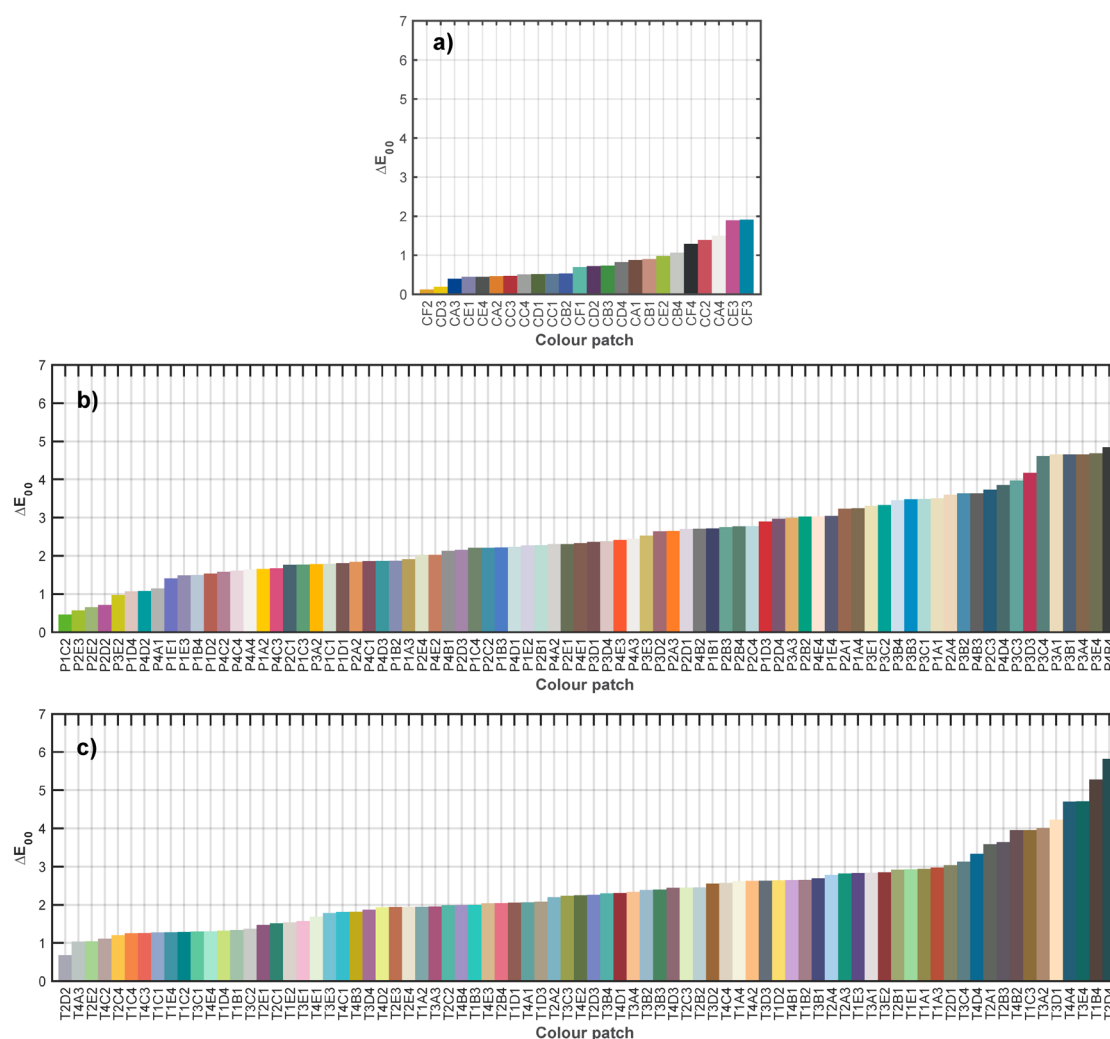


Figure 6: Colour difference between predicted and reference CIELAB values of ColourChecker (a), Profiling (b) and Testing(c) colour chart in case of ICC based RGB to CIELAB transformation.

3.4 Polynomial models

The colour difference between predicted and reference *CIELAB* values of the process, where ColorChecker was set to be the training set, is presented in Table 4 and Figure 7. The best results are obtained for polynomial model D3 (See table 1 in 2.3) but models D1, D2 and D4 predicted colour of all patches with similar results. The black colour patch of ColorChecker target exhibits the largest colour difference in all D1–D5 models. In case of Profiling and Testing colour

target worse prediction can be observed especially in darker green and violet colours. Model D5 predicted very poorly the colour representation of light colour patches and saturated orange patches in Profiling and Testing colour chart. The approach applying polynomial models seems to have worse results, than the ICC based transformation.

Table 4: Colour differences in case of polynomial transformations – ColorChecker as training set

		D1	D2	D3	D4	D5
Median	ColorChecker	1.42	1.26	1.29	0.89	0.21
	Profiling	2.34	2.17	2.11	2.37	3.61
	Testing	1.97	1.88	1.92	2.10	3.84
Minimum	ColorChecker	0.19	0.19	0.18	0.13	0.00
	Profiling	0.80	0.48	0.56	0.35	0.69
	Testing	0.66	0.57	0.71	0.36	0.64
Maximum	ColorChecker	2.65	5.62	4.22	4.81	3.15
	Profiling	6.66	6.74	6.74	6.78	37.87
	Testing	6.86	6.04	5.69	5.79	37.98

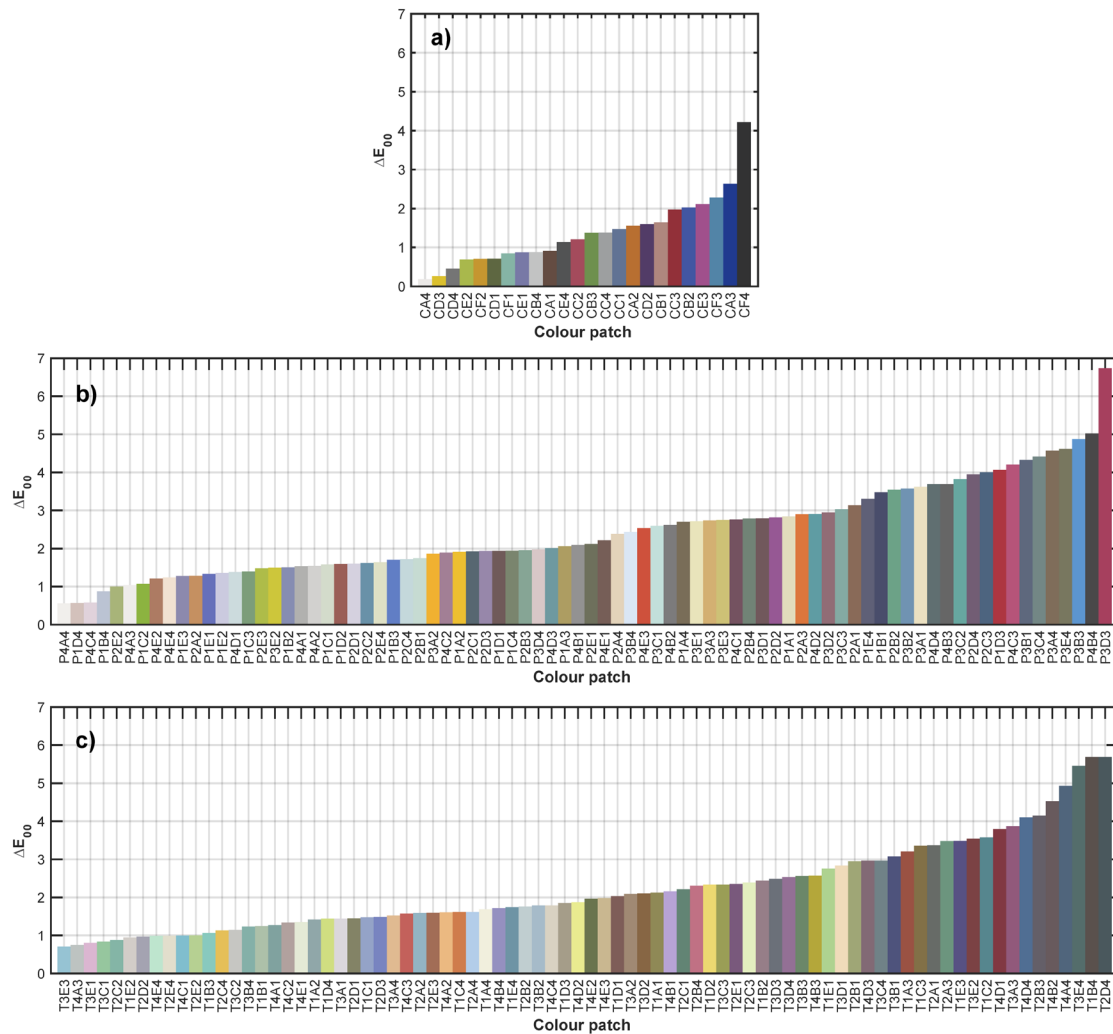


Figure 7: Colour difference between predicted and reference CIELAB values of ColourChecker (a), Profiling (b) and Testing(c) colour chart in case of application of D3 polynomial model utilising ColorChecker as training set.

When the Profiling colour chart was utilised as training, significant improvement can be seen on prediction of CIELAB values of Profiling and Testing charts' colour patches (see Table 5 and Figure 8).

The ΔE_{00} does not exceed value 2 for about 75 % of Profiling and Testing colour charts' patches. However, the prediction of ColorChecker patches gets worse especially when D4 model is applied. Again, more complicated models do not dramatically improve the colour prediction. The difference between goodness of prediction between ColorChecker and custom made colour charts is assigned to different diffusive properties of colour patches.

Table 5: Colour differences in case of polynomial transformations – Profiling colour chart as training set

		D1	D2	D3	D4	D5
Median	ColorChecker	2.66	2.70	2.65	2.85	2.41
	Profiling	1.25	1.18	1.26	0.90	0.87
	Testing	1.28	1.30	1.19	1.15	1.24
Minimum	ColorChecker	0.89	1.19	1.13	0.93	0.63
	Profiling	0.43	0.42	0.44	0.13	0.22
	Testing	0.25	0.20	0.19	0.21	0.42
Maximum	ColorChecker	4.21	7.04	7.39	11.81	6.81
	Profiling	4.69	4.70	4.47	3.30	3.32
	Testing	5.84	3.89	3.86	3.74	6.32

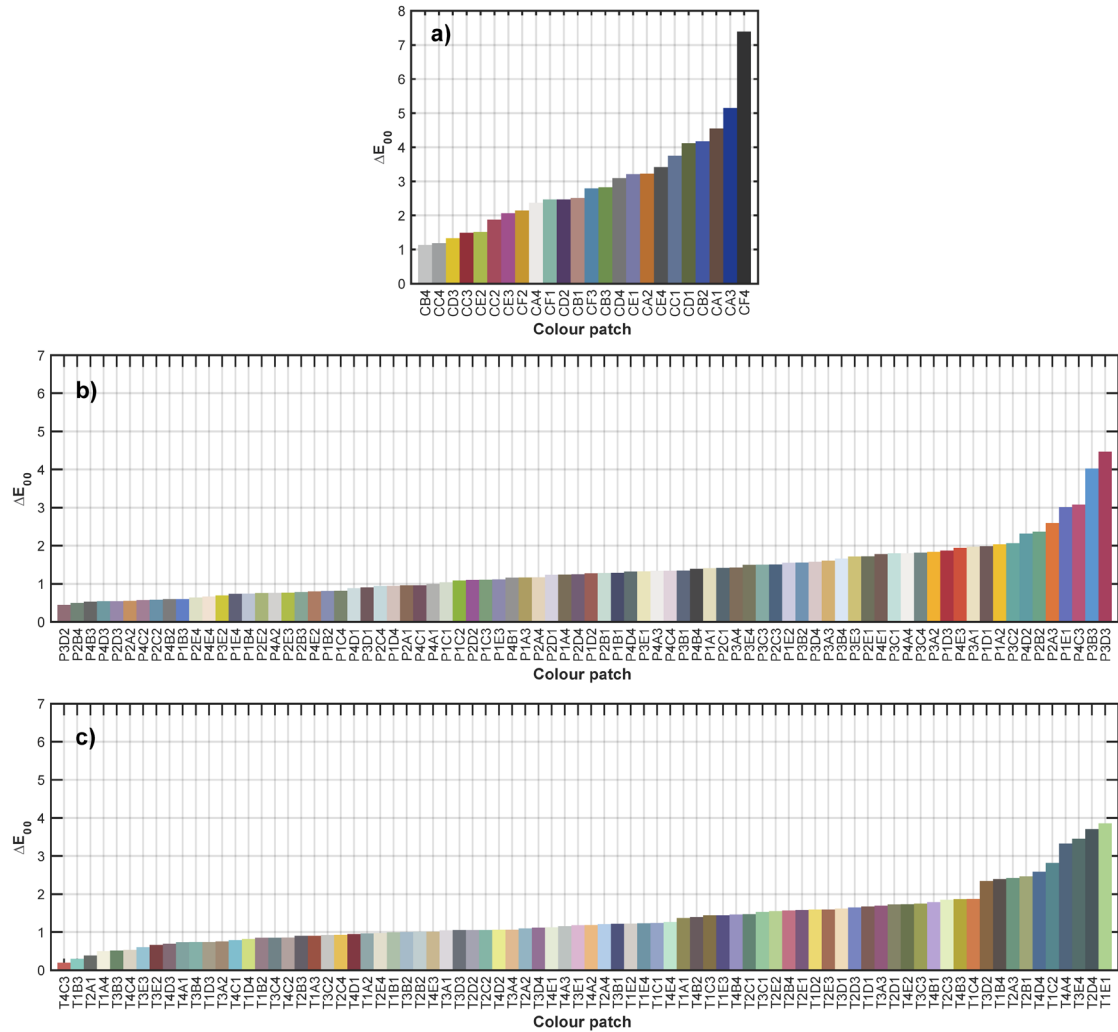


Figure 8: Colour difference between predicted and reference CIELAB values of ColourChecker (a), Profiling (b) and Testing(c) colour chart in case of application of D3 polynomial model utilising Profiling colour chart as training set.

4. CONCLUSIONS

Two approaches of transforming *RGB* values to *CIELAB* values were evaluated, one ICC based transformation and 5 transformations using polynomial models of different degrees. Custom made test charts and ColorChecker Passport were utilised in model preparation and evaluation of *CIELAB* prediction. When the ColorChecker is used as the training set in preparation of ICC profile and also determination of polynomial models, the ICC based transformation performs slightly better. When the custom made training set was applied, the prediction was better only in case of colour patches of the same surface properties. Obtained results show, that more complicated polynomial models do not have serious impact on the goodness of *CIELAB* prediction.

5. REFERENCES




- [1] Abdullah, N., Talib, A.R.A., Jaafar, A.A., Salleh, M.A.M., Chong, W.T.: "The basics and issues of thermochromic liquid crystal calibrations", *Experimental Thermal and Fluid Science*, 34(8), 1089–1121, 2010. doi: 10.1016/j.expthermflusci.2010.03.011
- [2] Bianco, S., Schnettini, R., Vanneschi, L.: "Empirical modeling for colorimetric characterization of digital cameras", *International Conference on Image Processing*, 16th, 2009, 3469-3472, 2009. doi: 10.1109/ICIP.2009.5413828
- [3] Bourque, A.N., White, M.A.: "Control of thermochromic behaviour in crystal violet lactone (CVL)/alkyl gallate/alcohol ternary mixtures", *Canadian Journal of Chemistry*, 93, 22–31, 2015. doi: 10.1139/cjc-2014-0251
- [4] Cheung, V., Hardeberg, C. Li, J., Connah, D., Westland, S.: "Characterization of trichromatic color cameras by using a new multispectral imaging technique", *Journal of the Optical Society of America A* 22(7), 1231–1240, 2005. doi: 10.1364/JOSAA.22.001231
- [5] Cheung, V., Westland, S., Connah D., Ripamonti, C: "A comparative study of the characterisation of colour cameras by means of neural networks and polynomial transforms", *Coloration Technology*, 120, 19-25, 2004. doi: 10.1111/j.1478-4408.2004.tb00201.x
- [6] Cukurel, B., Selcan, C., Arts, T.: "Color theory perception of steady wide band liquid crystal thermometry", *Experimental Thermal and Fluid Science*, 39, 112–122, 2012. doi: 10.1016/j.expthermflusci.2012.01.015
- [7] Falcon Eyes, "DVR-630D/630DVC", Falconeyes, URL: <http://www.falconeyes.com.hk/Product.aspx?id=1512> (last request: 2018-03-02).
- [8] Farina, D.J., Hacker, J.M., Moffat, R.J., Eaton, J.K.: "Illuminant invariant calibration of thermochromic liquid crystals", *Experimental Thermal and Fluid Science*, 9, 1–12, 1994. doi: 10.1016/0894-1777(94)90002-7
- [9] Finlayson, G. D., Mackiewicz, M., Hulbert, A.: "Color Correction Using Root-Polynomial Regression", *IEEE Transactions on Image Processing*, 24(5), 1460-1470, 2015. doi: 10.1109/TIP.2015.2405336
- [10] Hong, G., Rhodes, P. A., Luo, M. R.: "A study of digital camera colorimetric characterization based on polynomial modelling", *Color Research & Application*, 26, 76-84, 2001. doi: 10.1002/1520-6378(200102)26:1<76::AID-COL8>3.0.CO;2-3
- [11] Jiang, J., Liu, D., Gu, Jinwei., Susstrunk, S.: "What is the space of spectral sensitivity functions for digital color cameras?", *Applications of Computer Vision (WACV)*, (IEEE, 2013), 168-179. doi: 10.1109/WACV.2013.6475015
- [12] Johnson T.: "Methods for characterizing colour scanners and digital cameras", *Displays* 16(4), 183-191, 1996. doi: 10.1016/0141-9382(96)01012-8
- [13] Panák, O., Držková M., Kailová N., Syrový T.: "Colorimetric analysis of thermochromic samples in different forms employing a digital camera", *Measurement* 127, 554–64, 2018. doi: 10.1016/j.measurement.2018.06.025
- [14] Smith, C.R., Sabatino, D.R., Praisner, T.J.: "Temperature sensing with thermochromic liquid crystals", *Experiments in Fluids*, 30(2), 190–201, 2001. doi: 10.1007/s003480000154
- [15] Sole, A., Farup, I., Tominaga, S.: "Image based reflectance measurement based on camera spectral sensitivities", *El – Measuring, Modeling, and Reproducing Material Appearance*, 2470-1173, 2016. doi: 10.2352/ISSN.2470-1173.2016.9.MMRMA-360
- [16] Vejrazka, J., Marty, Ph.: "An alternative technique for the interpretation of temperature measurements using thermochromic liquid crystals", *Heat Transfer Engineering*, 28(2), 154–16, 2007. doi: 10.1080/01457630601023641

- [17] Westland, S., Ripamonti, C. Cheung, V.: “Computational colour science using MATLAB”, 2nd ed, (John Wiley & Sons Ltd., Chichester, 2012).
- [18] X-Rite, “ColorChecker Targets”, Xritephoto, URL:
http://xritephoto.com/ph_product_overview.aspx?ID=1192&action=Support&SupportID=5884&catid=28 (last request: 2018-09-20).



© 2018 Authors. Published by the University of Novi Sad, Faculty of Technical Sciences, Department of Graphic Engineering and Design. This article is an open access article distributed under the terms and conditions of the Creative Commons Attribution license 3.0 Serbia (<http://creativecommons.org/licenses/by/3.0/rs/>).

FUTURE DEVELOPMENT OF SECURITY PRINTING AND RFID MARKS

Iskren Spiridonov , Kosta Shterev , Tatyana Bozhkova 
University of Chemical Technology and Metallurgy,
Department of Printing Arts, Pulp and Paper, Sofia, Bulgaria

Abstract: *In the current research are described various ways to protect secure documents, labels and packages, and the different security printing techniques applied today and the way they will evolve in future. Security end products constitute a wide variety of different types of documents, packages, labels and cards. The degree to which these need protection from counterfeiters, forgers and terrorists depends upon how deleterious their illegal procurement and misuse is to human welfare and financial stability. In order to reduce forgery and counterfeiting, the printing industry uses a big range of variable security methods and via different combinations, a high security document is achieved. Security printing devices are often categorized as overt, covert and machine-readable. Another advantage that the security printer has today is the ability to produce security documents on nontraditional, nonporous substrates such as plastic and polymer - biaxially oriented polypropylene. Due to this complexity in its chemical structure documents and banknotes have a greater abrasion resistance and lower rate of tampering. Our research will aim not only to configure well known methods of security printing arts, but as well get a deeper view of what is coming up next and how for example could the RFID marks become an affordable and reliable security features of our future production.*

Key words: security printing, substrates, inks, printing technologies, RFID

1. INTRODUCTION

Security printing is the field of the printing industry that deals with the printing of items such as banknotes, cheques, passports, tamper-evident I labels, product authentication, stock certificates, postage stamps and identity cards. The main goal of security printing is to prevent forgery, tampering, or counterfeiting.

Different types of printing techniques are suited to different applications. Sometimes a heavier weight of ink is needed on the substrate in order for the security feature to work properly. In other instances is needed to use a technique that uses a more delicate approach, so that the detailing in the artwork adds to the security.

In recent days and in an overgrowing market, the industry of Security printing is struggling to bring up new ideas, with more security features and less costs. Vital parts in Printing Industry play the latest approaches in the field of chemistry. The ability to produce security documents on nontraditional, nonporous substrate such as plastic and polymer is not anymore a futuristic technology, but an adequate solution in several spheres (Warner et al, 2005).

2. METHODS IN SECURITY PRINTING

2.1 Substrates in Security Printing

Substrates for printing are mainly paper, polymer and cardboard. Security substrates can be designed and manufactured with special features and considerations to protect documents from counterfeiting or alteration of information (forgery). On Figure 1 there is a classification shown on both types of substrates used in security printing – mainly on banknotes. In some specific cases, substrates can be personalized and produced with certain features and unique securities in order to improve the level of protection and to prevent from counterfeiting and forgery. Most banknotes are made of heavy paper, almost always from cotton fibers for strength and durability, in some cases linen or specially coloured or forensic fibers are added to give the paper added individuality and protect against counterfeiting. Some countries, including Nigeria, Romania, Mexico, New Zealand, Israel, Singapore, Malaysia, United Kingdom and Australia, produce polymer (plastic) banknotes, to improve longevity and allow the inclusion of a small transparent window (a few millimeters in size) as a security feature that is difficult to reproduce using common counterfeiting techniques (Izdebska et al, 2015). Polymer banknotes are banknotes made from a polymer such as bi-axially oriented polypropylene (BOPP). Polymer banknotes last significantly longer than paper

notes, causing a decrease in environmental impact and a reduced cost of production and replacement. In November 2011 Canada joined the list of countries using polymer currency as it began the introduction of a new banknote series (Polygrafia Magazine).

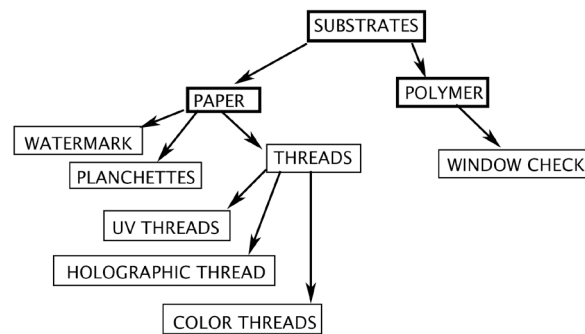


Figure 1: Security features in substrates

2.2. Security inks

A wide variety of security inks can be used in documents, packages, labels, and cards. In addition to security printing inks, the printer can also use overprint varnishes and laminates to help deter counterfeiting. It should be noted that many security printing inks depend upon the absorption of UV radiation and its re-emission as visible light. Therefore, to work properly, many security designs and devices must be printed on UV-dead or uncoated paper. On other media they will only work if there are no UV brighteners in the substrates (Vuaroz et al, 2003):

- Fluorescent dyes;
- Iridescent inks;
- Photochromic ink;
- Phosphorescent inks;
- Thermochromic ink;
- Optical variable ink;
- Infrared ink;
- Machine readable inks;

On Figure 2 can be observed most of the security inks, divided in three branches: overt, covert, semi-covert.

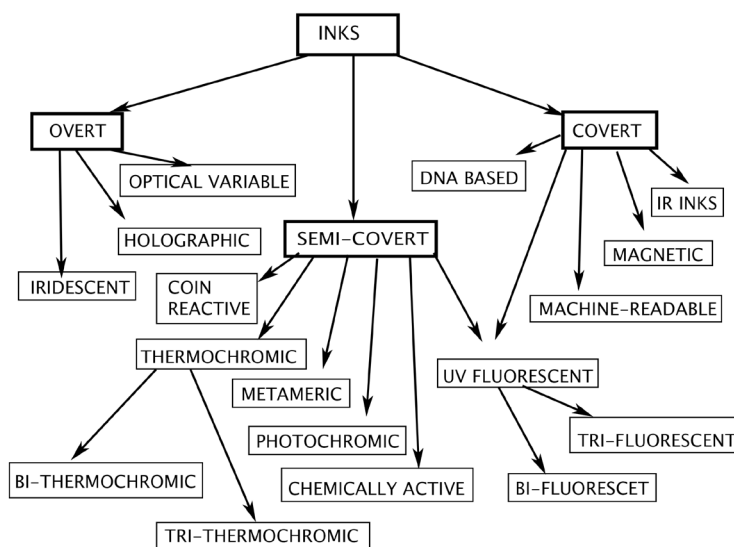


Figure 2: Security features within inks

2.3. RFID hidden security features

RFID, which is an acronym for Radio Frequency Identification, is not a new technology. It was first used in the late 1960's, but it has only become more widespread with advances in technology.

RFID Systems consist of a transponder, also known as a tag, which is basically a microchip connected to an antenna. The tag is mounted to an item, such as a pallet of goods in a warehouse, and a device called a reader communicates with the tag via radio waves. Depending on the type of tag that is used, the reader can receive detailed information or it can receive data as simple as an identification number.

RFID is similar to barcode systems in which data, such as a price, is accessed when the barcode is read. The main difference is that the barcode must come in direct contact to an optical scanner/reader and the RFID tag can transmit to the reader via radio waves and does not have to be in direct contact. An RFID reader can receive data from as many as 1,000 tags per second.

The radio signals can go through many non-metallic substances such as rain, fog, snows, dirt and grime, painted surfaces, etc. This gives RFID tags a distinct advantage over optically read items, such as barcodes, which would be useless under similar conditions (Vig, 2007; Khan, 2014; Printing Knowledge).

The many uses for RFID technology include:

- Smart labels and security labels
- Product and inventory management
- RFID chips in car keys for security
- Theft control
- Placement on pharmaceuticals to prevent counterfeited drugs from entering the legal supply chain
- Increased efficiency in admissions into entertainment or sporting events
- Increased efficiency in toll road payments
- Monitoring the whereabouts of luggage, library books, livestock, etc.

It is predicted that RFID use will continue to increase. It is unlikely to ever be as cost-effective as barcoding, but it will become dominant in areas where barcoding and other optically read technologies are not effective.

RFID Tag Categories

The basic types of RFID tags can be classified as read/write and read only. The data stored on read/write tags can be edited, added to, or completely rewritten, but only if the tag is within the range of the reader. The data stored on a read only tag can be read, but cannot be edited in any way. Read/write tags are much more expensive than read only tags, so they are not used for tracking most commodity items. RFID tags are further categorized as:

- Active tags, which contain a battery that powers the microchip and allows it to transmit a signal to the reader.
- Semi-active (or semi-passive) tags, which contain a battery to run the circuitry of the chip, but must draw power from the magnetic field created by the reader in order to communicate with the reader.
- Passive tags, which rely solely on the magnetic field created by the radio waves sent out by the reader to create a current that can be received by the antenna within the passive tag (Printing Knowledge)

RFID Tag Shapes and Sizes

RFID tags can be manufactured in several different shapes and sizes depending on the type of application in which they will be used.

- Some are the size of a pencil lead or are less than a half-inch in length and can be inserted under the skin of animals and livestock.
- Screw-shaped tags are used to identify specific trees.
- Rectangular RFID tags found in some products are used as an anti-theft device.
- Large, heavy duty tags that are several inches in length, width, and depth are used to track large containers or large vehicles such as trucks or rail cars.

Printing

With most types of printed applications, such as labels, the user is unaware of the existence of the chip and antenna because of the different methods of concealing them on the document. Some printers (such as label printers) purchase inlays (containing the RFID) that are already manufactured and then incorporate them into their printed products.

3. FUTURE TRENDS IN SECURITY PRINTING AND RFID TAGS

With the overgrowing markets and needs of greater security features, RFID tags can be evolved in taking care for the high security of shares. Since a single share presented on a special piece of paper can be the key to a big amount of money and thus to become an attractive product for counterfeiting. RFID tags in several ways can improve the ranking of security end product and at a descent price for production can save a lot of trouble and inconvenience.

There are several ways to achieve this security feature but at a reasonable price a more adequate roll will play to the top the passive tags – they which rely solely on the magnetic field created by the radio waves sent out by the reader to create a current that can be received by the antenna within the passive tag (Wikipedia, 2018; Printing Knowledge). Components of passive RFID system:

- An antenna is attached to a microchip.
- The antenna allows the chip to transmit information to a reader, which also has an antenna.
- The reader is the device that actually sends out the radio waves to create a magnetic field. A passive RFID tag draws its power from this magnetic field, which powers the circuits in the microchip allowing it to transmit data back to the reader.
- Reader transmits to a computer system.
- The computer passes data onto a network.
- Software determines how the data received should be used (Printing Knowledge)

These passive RFID tags (shown on *Figure 3*) are much cheaper and can be pre-ordered and attached as a hidden label on the share already printed sheet of paper, or in search for a greater security, they can be ordered built in the paper, ready to print over.



Figure 3: Passive RFID Tag

After having the shares printed and with an RFID tag already built in (Figure 4), the further need is only to prepare the RFID tag reader. This can automatically prevent the needs of eye checks for watermarks and other common security features for high end security products that can be manipulated easily.



Figure 4: Hidden RFID Tag in Shares

4. CONCLUSSIONS

In the high demand of security and an the more creative counterfeiting methods for gaining fortune in an illegal way, our society should move to a higher level of security to any of the common day branches and try its best to protect the welfare of our products in order to preserve stable growth in markets.

In our research we have followed the how process of security features in high end products and the trends to its future development. On a daily basis shares are not an everyday product, that will be used, but their value and the cost of its forgery and counterfeiting can become a great loss for its holder. Using machine-readable methods for shares in order to prevent counterfeiting will be a new method for this sphere in the printing industry. A slight rise of production price but a greater security level can be achieved by implementing a passive RFID tag within each share stock blanc itself thus a reader can at first check tell if the shareholder owns an original share.

Moving on to the next level of security in any kinds of security documents and products is mandatory in order to stay one step ahead of criminals. RFID tags can provide vast possibilities to achieve it.

5. REFERENCES

- [1] Izdebska, J., Sabu, T.: "Printing on Polymers Fundamentals and Applications", (Elsevier Inc., Amsterdam, 2016).
- [2] Khan, S., Lorenzelli, L., Dahiya, R.: "Technologies for printing sensors and electronics over large flexible substrates: a review", IEEE Sensors Journal, 15 (6), 3164-3185, 2014.
doi: 10.1109/JSEN.2014.2375203

- [3] Polygrafia Magazine, "Security Elements used in the printing of banknotes", URL: <http://polygrafiimagazine.bg/> (last request: 2018-10-21)
- [4] Printing Knowledge, Security Features | RFID, URL: <http://www.printingknowledge.com/security-features-rfid/>
- [5] Vig, R.: "General Overview of Overt & Covert Security Features for Brand Protection in Inks and Coatings", URL: <http://www.tappi.org/content/events/07place/papers/vig.pdf> (last request: 2018-10-21)
- [6] Vuarnoz, A., Amrein, O., Veya, P.: Patent - WO2003020834A1, "Ink composition comprising optically variable pigments, use of the composition, optically variable pigment and method of treating said pigment, 2003.
- [7] Warner, R. D., Adams, R. M.: "Introduction to Security Printing", (PA: PIA/GATF Press, Pittsburgh), Chapters 1-2;4-9
- [8] Wikipedia: "Security Printing", URL: https://en.wikipedia.org/wiki/Security_printing (last request: 2018-10-21).



© 2018 Authors. Published by the University of Novi Sad, Faculty of Technical Sciences, Department of Graphic Engineering and Design. This article is an open access article distributed under the terms and conditions of the Creative Commons Attribution license 3.0 Serbia (<http://creativecommons.org/licenses/by/3.0/rs/>).

APPLICABILITY OF STANDARD GREY SCALE FOR REPORTING PERCEIVED COLOR DIFFERENCE OF PRINTS ENHANCED WITH PEARLESCENT PIGMENTS

Ivana Tomić¹ , Rafael Huertas² , Luis Gómez-Robledo² ,

Sandra Dedijer¹ , Ivana Jurič¹ 

¹ University of Novi Sad, Faculty of Technical Sciences,

Department of Graphic Engineering and Design, Novi Sad, Serbia

² University of Granada, Faculty of Science, Department of Optics, Granada, Spain

Abstract: Printed materials that exhibit goniochromism pose a challenge not only for colour measurement but also for estimating colour differences. A common procedure for determining perceived colour difference implies assessing colour pairs by means of a standard grey scale. This method was proven to be adequate for estimating, among others, perceived differences of low chroma goniochromatic samples found in the automotive industry, as well as for assessing colour differences of conventional prints. In this work, we were interested in the applicability of the same approach for estimating colour differences of printed samples enhanced with pearlescent pigments. Such prints are regarded as goniochromatic and depending on the type of the pigment, can exhibit very high chroma in angles close to specular reflection. This may pose a problem in evaluating colour differences because grey scale only shows a change in lightness. In addition, in some illumination/viewing geometries the differences between the two samples can be higher than those presented in the grey scale. Nine colour pairs (low-chroma digitally printed samples enhanced with three types of pearlescent pigments) were assessed in six viewing/illumination angles by a panel of ten observers. Our results show that chroma of the samples did not influence significantly inter- and intra-observer agreement, implying that grey scale references can be used for determining the perceived differences between chromatic samples. SDC grey scale provided sufficient range of colour differences only for the limited set of printed samples, leading to the conclusion that for assessing the differences of printed samples enhanced with pearlescent pigments it is necessary to use reference scale with higher difference range.

Key words: grey scale, colour difference, goniochromism, pearlescent pigments

1. INTRODUCTION

Iridescence or goniochromism is the property of a material or a surface which appear to change the colour with the change of the viewing angle or the angle of illumination (Meadows et al, 2009). In printing, the goniochromatic effect is often achieved with pearlescent pigments (Maile et al, 2005; Weitzel, 2008), that are characterised by their interference colour – colour seen in the specular angle. Pearlescent pigments are mostly used in packaging, where their main purpose is to enhance the printed material. In such application, pigments are normally dispersed in the colour base or different types of coatings and applied as the last colour in the sequence (Weitzel, 2008). The resulting impression highly depends on the base colour, i.e. the colour printed beneath the pearlescent layer. Since the surface of the material on which pigments are applied absorb colour that is complementary to the interference colour, the most prominent visual effect is seen in the case when pigments are applied onto the dark surfaces. On the other hand, the effect is almost absent if pigments are deposited on the white substrate (Klein, 2009; Tomić et al, 2018).

The angle-dependent colour change of goniochromatic materials also leads to the higher or lower perceived difference when two goniochromatic samples are observed in different angles. As the description of goniochromatic materials colour requires multi-angular colour measurement (as explained in ASTM E2539 – 12), so does the estimation of their colour differences. Assuming the movement of the observer, the differences should be estimated for one angle of illumination (45° with respect to the perpendicular to the sample) and six viewing angles calculated from the specular reflection and marked as “aspecular” or “asp”: - 15°, 15°, 25°, 45°, 75° and 110°.

For visual estimation of colour differences, it is common to use a reference. It can be an anchor pair considered as reference difference or a gray scale. In a grey scales there are a number of colour pairs ordered in increasing or decreasing differences between them. It is commonly used for such purposes the

standard grey scale from the Society of Dyers and Colourists' (SDC, 2018) which contains nine pairs of grey chips. The pair marked as 1 indicates the highest colour difference and the pair 5 smallest difference between the two samples. This scale is normally used to evaluate fading (ISO, 2013), but was also successfully employed for estimating colour differences between printed samples of large colour difference (Huang et al., 2011), as well as the goniochromatic samples used in automotive industry (Martínez, 2013; Melgosa et al, 2014).

The biggest drawback of SDC scale is that it only shows the change in lightness. Also, it covers a certain range of colour differences, meaning that it might be inappropriate for estimating perceived disparity between two very distinct colour samples. In the case of printed samples enhanced with pearlescent pigments, the range of the differences is much wider in comparison to the goniochromatic samples found in the automotive industry. Also, the samples are often very chromatic, where the disparities in chroma significantly contribute to the perceived colour difference.

In this work, we were interested in whether the SDC grey scale would be appropriate for estimating colour differences of prints enhanced with pearlescent pigments, concerning the range of the presented differences. Also, since grey scale shows mostly change in lightness, we will check if it would be less useful for assessing the differences of very chromatic samples.

2. METHOD

2.1 Samples

As the visual effect produced by pearlescent pigments highly depends on the colour of the surface on which they are applied, we choose three base colours – black, grey and white (paper). Choosing the achromatic base colours ensured that the hue of the samples will be determined only by the pearlescent pigments in the coating layer, as well as that the chroma will decrease gradually with the increase of the viewing angle. The lightness of the base colour influenced the intensity of the perceived effect – on black samples the chroma was very dominant in the near-specular angles, while on white it was almost absent. The colour patches of size of 10x10 cm, of the mentioned colours were printed in Xerox DocuColor 252 digital printing machine on 300 g/m² matte art paper - type 2 in (ISO, 2013). The colour coordinates of dry prints are given in Table 1 (average of 3 measurements obtained with SpectroDens spectrophotometer).

Table 1: CIELAB colour coordinates of three base colours (geometry 45°/0°, illuminant D65 and Standard Observers CIE1964)

Colour	L^*	a^*	b^*
Black	15.75	-1.64	-1.73
Grey	50.56	-1.8	-1.29
White (paper)	93.46	0.21	-3.1

After drying, prints were enhanced with three types of Iriodin pearlescent pigments – 221 Rutile Fine Blue, 223 Rutile Fine Lilac and 231 Rutile Fine Green (Merck, 2018). Pigments were dispersed in the aqueous ink base (WBA base S) in the concentration of 15%. They were deposited on the prints via screen printing (mesh size of 68 lines/cm), where two layers of coating were deposited wet-on-wet. The drying was done during one minute at the temperature of 140° C.

All three pigments have the same composition (mica + titanium dioxide) and only differ in the thickness of the TiO₂ layer that leads to distinct interference colours – blue, lilac and green. With the decrease of the aspecular angle, the colour of the samples shifts to the lower wavelengths, i.e. appears more bluish. Figure 1 shows CIELAB colour coordinates of enhanced prints measured in the aspecular angle of 45°. The samples where the base colour was white exhibit very high lightness and low chroma (triangles in Figure 1). With the decrease of the lightness of the base colour (grey and black samples), chroma gradually increased.

2.2 Experimental setup

Visual assessment of printed samples was conducted in the completely dark room using Byko-Spectra effect cabinet (BYK, 2018). This cabinet is specially designed for evaluating effect coatings and materials

since its tilting table allows positioning samples in 6 angles specified in ASTM E2539-12 (ASTM, 2012): -15 asp, 15 asp, 25 asp, 45 asp, 75 asp and 110 asp.

Figure 2 depicts the interior of the Byko-Spectra cabinet during the experiment. Colour sample pair was placed in the middle of the tilting table, while the SDC grey scale was positioned above the pair. Since our colour samples were bigger than the grey chips, to facilitate the assessment, we used a black mask with an aperture equal to the greyscale pair's size (Figure 2).

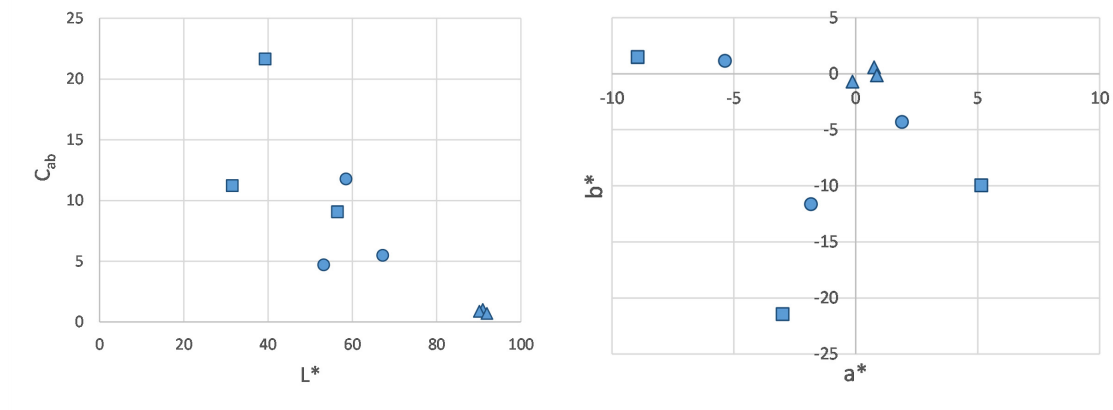


Figure 1: CIELAB colour coordinates of 9 colour samples used in the experiment. Triangles, circles and squares mark samples where the base colour was: white, grey and black, respectively. Measurements were performed in the aspecular angle of 45° asp using Photo Research 745 spectroradiometer (1° visual field) placed in the same position as the observers in the visual experiment.



Figure 2: Experimental setup – SDC grey scale and the test colour pair with black cover

The colour pair to be assessed consisted of the samples with the same base colour as shown in table 2. In the repetitions of experiment, the position of the samples (left or right) was randomly changed. The CIELAB colour coordinates of the samples were obtained from the measurements of Photo Research 745 spectroradiometer (1° visual field) placed just in the same position as the observers. Since the light source in the cabinet differs from CIE illuminants, transformations to CIELAB were made by taking into account the reflectance of the reference white (during the measurement placed at the position of the samples). The coordinates were obtained for each one of the viewing angles. In Table 2, colour, absolute lightness and chroma differences for all nine pairs are given for the angle of 45° asp, while Figure 3 shows the change of colour difference of each pair with the change of the viewing angle.

Table 2: The colour pairs used in the study (differences correspond to the viewing angle of 45° asp)

Colour pair	The base colour of the samples 1 and 2	Pearlescent pigment colour		ΔE_{ab}	$ \Delta L^* $	$ \Delta C^*_{ab} $
		Sample 1	Sample 2			
1	Black	Blue	Green	29.24	17.16	12.59
2	Black	Blue	Lilac	16.09	7.79	10.43
3	Black	Green	Lilac	30.31	24.27	2.07
4	Grey	Blue	Green	15.86	8.70	6.28
5	Grey	Blue	Lilac	9.77	5.28	7.06
6	Grey	Green	Lilac	20.06	17.04	2.15
7	White	Blue	Green	1.09	0.81	0.06
8	White	Blue	Lilac	1.83	0.99	0.23
9	White	Green	Lilac	2.79	2.55	0.18

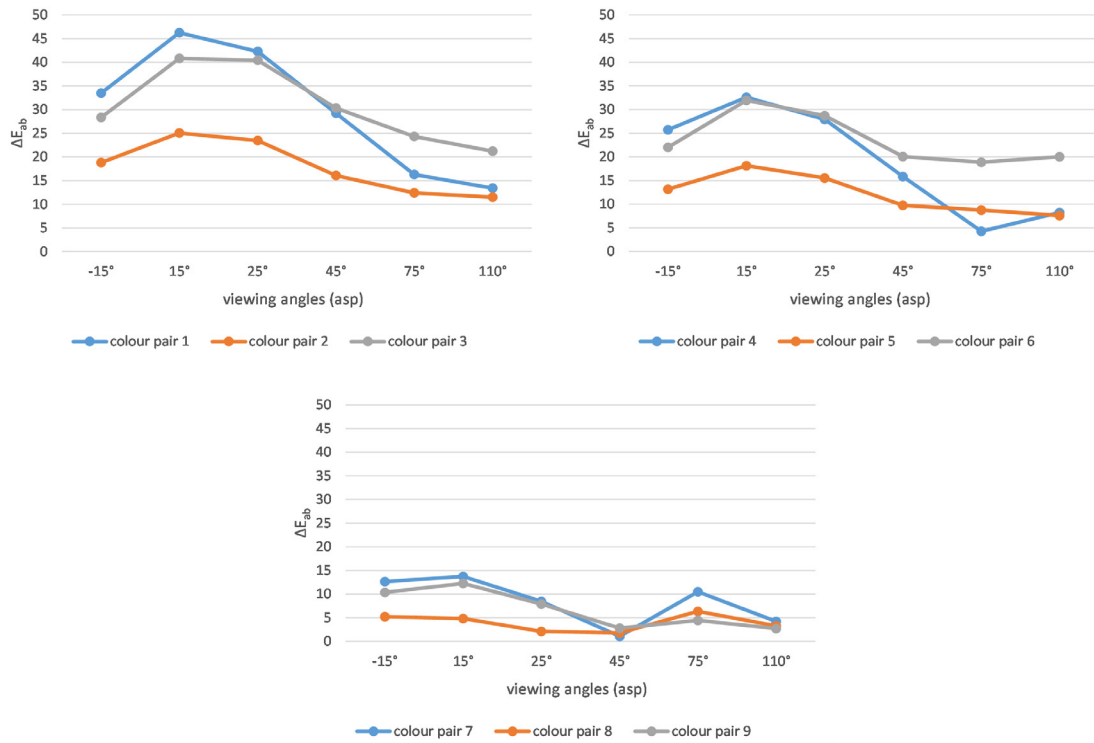


Figure 3: Colour differences of the colour pairs with (a) black, (b) grey and (c) white base colour

The colour pairs with black base colour (pairs 1-3, Figure 3a) exhibit the highest colour differences, where the disparities in both lightness and chroma were significant. On the contrary, the samples with white background (colour pairs 7-9, Figure 3c) were the least different. In the latter case, the change in lightness was the most prominent. It is noticeable that all the colour pair used in the experiment had colour difference above ΔE_{ab} of 1, while the majority belonged to the range of large colour differences ($\Delta E_{ab} > 5$).

Colour differences between the samples changed significantly with the change of a viewing angle as seen in Figure 3. In all the cases the differences were the highest in the angle of 15°. By increasing the viewing angle, the differences decreased, which can be attributed both to the decrease of lightness and chroma as seen in Figure 4 and 5. While in the low aspecular angles the hue of the samples is quite dominant, in the angles far from aspecular they appear as almost achromatic.

This trend was seen for the black and grey background pairs, while for the colour pairs with white base colour there is an additional increase of colour differences in the angle of 75° asp (Figure 3c and Figure 6). The increase of difference in the abovementioned angle was mainly due to the change in lightness as shown in Figure 6.

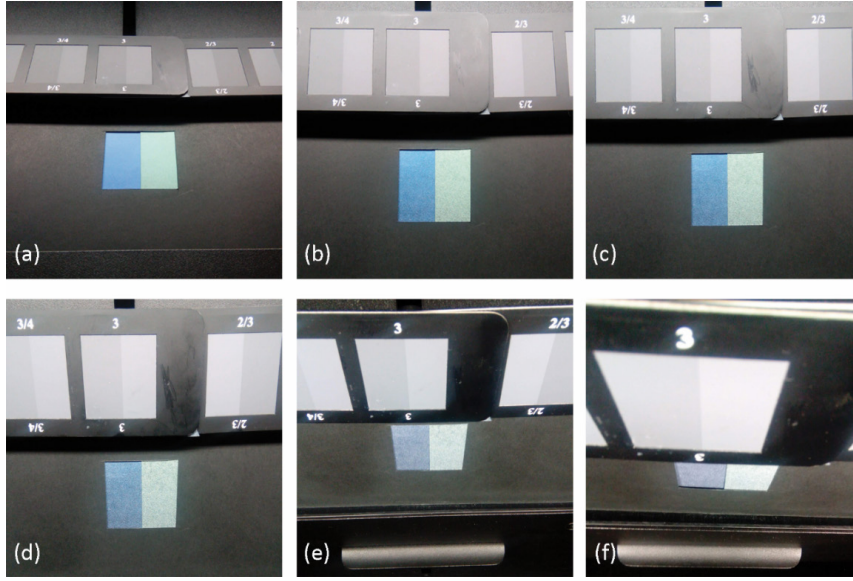


Figure 4: The appearance of the colour pair 1 observed in the aspecular angles of (a) -15° , (b) 15° , (c) 25° , (d) 45° , (e) 75° and (f) 110°

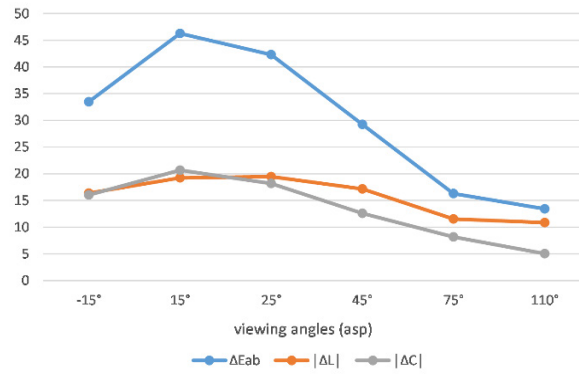


Figure 5: Colour, lightness and chroma differences of colour pair 1 in the six viewing angles

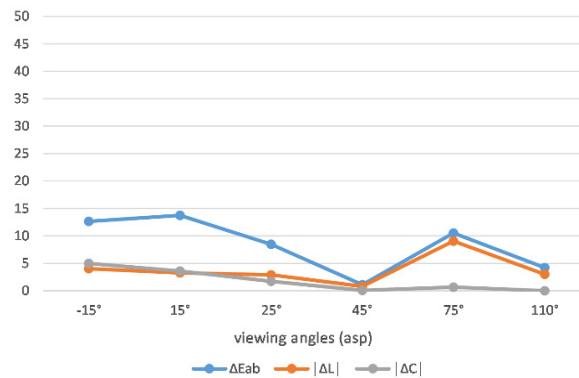


Figure 6: Colour, lightness and chroma differences of colour pair 7 in the six viewing angles

Due to its position in the viewing cabinet, the grey scale was not illuminated uniformly (Figure 2). As it was shown (Melgosa et al, 2016) this can result in a significant colour change of the specific grey scale pair with the change of the viewing angle. Hence, the grey scale colour pairs were measured in the same way as test pairs and the differences were obtained in the form of ΔE_{ab} . Minimum and maximum differences (corresponding to the pairs 5 and 1 in SDC grey scale) in all 6 viewing angles are presented in Table 3.

Table 3: Measured range of ΔE_{ab} colour differences of the grey scale in different viewing angles

Aspecular angle	Min ΔE_{ab}	Max ΔE_{ab}
-15	1.15	12.76
15	1.87	12.29
25	1.92	12.78
45	1.81	13.70
75	0.90	15.70
110	0.62	15.10

As it can be seen the highest measured difference in the grey scale is 15.70 ΔE_{ab} in the angle of 75°. In the rest of the angles, the differences were a bit lower. It implies that in the Byko-Spectra cabinet the SDC grey scale would be appropriate for assessing colour pairs with maximum ΔE_{ab} of 16 CIELAB units.

2.2 Experimental setup

Ten observers (3 females and 7 males) participated in the experiment. They all had normal to corrected-to-normal vision and normal colour vision. Four participants can be regarded as experts, while six were naïve. The observers passed 2 minutes of adaptation to the environment looking inside the cabinet and, prior to the assessment, were asked to evaluate 5 colour pairs to be able to familiarise with the experiment. They were instructed to evaluate the colour pair presented in the centre of their visual field concerning the greyscale. Intermediate values to those presented in the greyscale were allowed. Observers were also encouraged to report differences that are out of the grey scale. Such responses were noted as “no answer” and were processed as such.

In one session each observer assessed all 9 colour pairs in 6 viewing angles (54 assessments in total). The session lasted approximately 30 minutes and was repeated three times. The repetitions were conducted in different days in order not to exhaust the observers and to avoid memory effects.

The values in SDC greyscale indicate the degree of fading and are expressed on an ordinal scale. Also, in different viewing angles, the distinctness between grey pairs was perceived differently. In consequence, the responses given by the observers could not be used in their raw form since they did not provide any information about the perceived colour difference. To relate observers' responses to the visual colour difference (ΔV) we scaled them to ΔE_{ab} , commonly used for such a task (Martínez, 2013; Melgosa et al, 2014). The colour differences between greyscale pairs in each of the viewing angles were obtained and related to SDC values via fourth polynomial fitting (Martínez, 2013). The visual differences were then calculated from the observers' responses by using the corresponding polynomial.

For assessing the agreement between perceived and measured colour differences we used Standardized Residual Sum of Squares - STRESS index (Melgosa, 2011):

$$STRESS = \frac{\sum (\Delta E_i - F \Delta V_i)^2}{\sum F^2 \Delta V_i^2} \quad \text{for} \quad F = \frac{\sum \Delta E_i^2}{\sum \Delta E_i \Delta V_i} \quad (1)$$

where ΔE is colour difference obtained by measurement, and ΔV - the perceived difference for the set of colour pairs N ($i=1, \dots, N$). This metric is limited in the range of 0-100, where 0 denotes perfect agreement, i.e. no difference between measured and observed values.

The same metric was used to obtain intra- and inter-observer variability (Melgosa, 2011). To estimate the variations in the responses of a single observer with repeated assessment (intra-observer agreement) his/hers mean responses from three sessions were compared against responses from individual trials. The variation in responses between observers (inter-observer agreement) was obtained by replacing ΔE_i and ΔV_i with the mean responses of one observer and the mean responses of the whole group of observers. The final values for both inter- and intra-observer agreement were the mean values from all the observers participating in the experiment (Melgosa, 2011).

3. RESULTS AND DISCUSSION

By taking into account the measured colour differences of our colour pairs and the highest differences measured in the grey scale in each of the viewing angles (Table 3), for assessing the reliability of observers' responses we divided the sample pairs into two groups. In the first group were colour pairs with ΔE_{ab} that fall within the range of the differences presented in the grey scale (*within the range group*), while in the second pairs with ΔE_{ab} that exceeds the highest difference in grey scale for the respective angle (*out of the range group*).

The first group (*within the range group*) consisted of 25 pairs in total (counted in all angles), mostly samples with the white base colour as well as grey and black base colour samples in the angles far from specular. The highest chroma difference within the group was 7.89, while the highest lightness difference was 10.85.

Second (*out of the range*) group had 29 pairs in total. In this group, there were no samples with white base colour. The highest chroma difference in out of the range group was 20.69, while lightness differences ranged up to 28.8.

The intra- and inter-observer variability were calculated for both groups of samples. Table 4 summarises the results of intra-observer variations for each one of the observers. Results for colour pairs where observers missed to give an answer (the perceived difference was higher than shown in grey scale in at least one repetition) were excluded from the analysis.

Table 4: Intra-observer variability (*n* – naïve, *e* – expert)

Observer	1	2	3	4	5	6	7	8	9	10	Mean
Experience	e	e	n	n	n	n	e	e	n	n	
Within the range group	16.67	24.24	28.13	25.91	40.40	31.90	26.18	27.73	27.74	31.62	28.05
Out of the range group	18.67	19.05	23.70	20.53 ^a	19.07 ^b	28.00	34.45	20.61 ^c	17.86	30.24 ^d	23.31

^a calculated by excluding 5 pairs due to the missing answers

^b calculated by excluding 1 pair due to the missing answer

^c calculated by excluding 21 pairs due to the missing answers

^d calculated by excluding 8 pairs due to the missing answers

The within-subject agreement for the first group of sample pairs can be regarded as satisfactory, except in the case of observer 5. If the observer 5 were excluded from the further analysis, the mean STRESS value would be 26.68 which is a bit higher than reported in the assessment of automotive goniochromatic samples (Melgosa, 2014).

In most of the cases, an agreement was slightly better for pairs whose colour differences exceed the range presented in the grey scale. It seems that observers tend to assign the value 1 of the grey scale (higher difference) to all the test samples pairs exceeding the color difference in the grey scale, which resulted in better agreement between repetitions. This result, however, should be taken with caution due to a large number of pairs that were excluded from the analysis. Namely, four observers out of ten (3 naïve and 1 experienced) reported perceived differences out of the grey scale range. This was mostly the case for the pairs observed in near specular angles (-15° asp, 15° asp and 25° asp), where the chroma was more accentuated. None of the observers reported higher differences in the angles far from the specular, where all the samples appeared almost achromatic.

In average, for the sample pair with differences within the SDC grey scale range, expert observers showed better intra-agreement (STRESS of 23.7 in comparison to 30.96 for naïve). For the out of the range pairs, the results of experts and naïve observers were almost the same.

During the experiment, the majority of the observers reported difficulties to assess the differences when the presented colour pair appeared more chromatic (when pairs were observed in the near-specular angles, where both of the samples exhibit higher chroma). To evaluate if the mentioned issue was reflected in their answers, i.e. if the ratings were more certain in their assessment in cases when presented samples appeared more achromatic, their intra-observer agreements were calculated for the colour pairs with chroma differences lower than 1 (14 pairs in total), for colour pairs where ΔC^*_{ab} was in

the range of 1-5 (20 pairs) and for those where their chroma difference was larger than 5 (20 pairs). Results are presented in Figure 7.

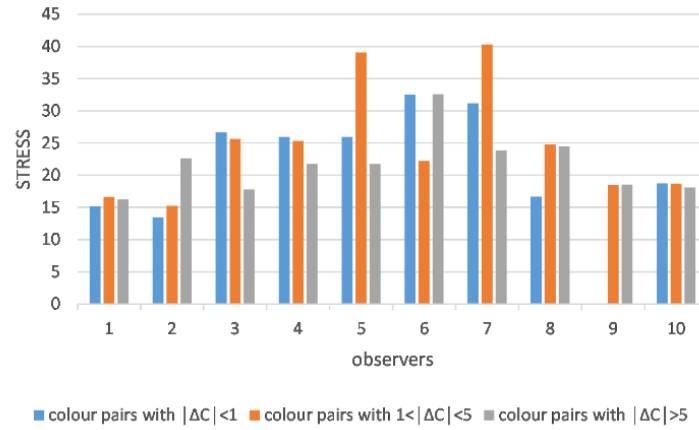


Figure 7: Inter-observer agreements for colour pairs with a distinct range of chroma difference

Obtained results (Figure 7) indicate that the chromaticity of the samples did not influence the within-subject agreements significantly. Even though the observers had difficulties to grade very chromatic colour pairs, their responses in three repetitions were quite coherent.

The inter-observer agreement for within the range group was 25.43, while for the samples that exceeded the grey scale range it was 19.36 (with 22 pairs excluded from the calculation due to at least one missing answer). If the agreement was calculated for the observers who reported the differences for all the colour pairs, the STRESS index was 24.23. Similar values can be found in (Melgosa, 2014; Huang, 2011). Observers agreed well in their answers even in the case where differences were clearly out of the reference range. This is an interesting finding, suggesting that the ratters assumed that the difference is within the range of presented reference and judged the pairs accordingly.

Inter-observer agreements for expert and naïve observers are shown in Table 5. The expert observers tend to agree more in their answers, both for the sample pairs within and out of the SDC grey scale difference range (Table 5).

Table 5: Inter-observer agreements

Observers	Expert	Naïve
Within the range group	21.89	26.25
Out of the range group	16.39 ^a	24.65 ^b

^a calculated by excluding 21 pairs due to the missing answers

^b calculated by excluding 10 pairs due to the missing answers

In order to assess the agreement of the observers' answers concerning chroma difference of the colour pair, STRESS index was also calculated for the responses given to the pairs with low, middle and large chroma differences. The results are presented in Table 6.

Table 6: Inter-observer agreements for colour pairs with a distinct range of chroma difference

	$ \Delta C^*_{ab} < 1$	$1 < \Delta C^*_{ab} < 5$	$ \Delta C^*_{ab} > 5$
STRESS	24.81	26.34	16.86

It is clear that the agreement between observers was much better when judging colour pairs with higher chroma difference (Table 6). Since chroma of the colour pair normally decreased in the angles further from the specular, this result can indicate that judging the sample pair was more difficult when it was positioned almost vertically (Figure 4, e and f).

The relationship between perceived and measured colour differences was evaluated only for the colour pairs whose differences were within the range of the SDC grey scale. The STRESS value (calculated for all observers and based on their mean answers) was 30.86. The obtained result is significantly lower than reported in (Melgosa, 2014) and indicate a satisfactory correlation between perceived and measured values.

4. CONCLUSIONS

In this work, we evaluated the possibility of using standard SDC grey scale for reporting the perceived differences of printed samples enhanced with pearlescent pigments. The goniochromism of such samples leads to the perception of very different colours with the change of the viewing angle, where the final impression highly depends on the base colour. Since the SDC grey scale shows only the change in lightness, we assumed that it would be less efficient for assessing differences of highly chromatic samples.

Our sample set consisted of achromatic prints (black, grey and white) enhanced with three types of pearlescent pigments (Iriodin 221 Rutile Fine Blue, 223 Rutile Fine Lilac and 231 Rutile Fine Green), enabling the perception of different hues in the angles close to specular. The chroma of the samples decreased with the increase of the viewing angle, producing the significant change of both perceived and measured colour difference between the samples with the change of the angle of view. The color pairs were built with samples with the same base colour and different pigment in the coating layer.

Measured colour differences (ΔE_{ab}) of our colour pairs revealed that mostly the pairs with white base colour (where pigments were deposited on unprinted paper), as well as few greys and black samples observed in the angles farther from specular, exhibit the differences that were within the range of those presented in SDC grey scale. In the real-world application (printing of packaging, for example) pearlescent pigments are rarely printed directly on the paper/cardboard. In fact, they are often used to accentuate the design, mostly overprinting dark and colours with dominant hue. This means that the range of the differences between samples in practice often exceeds the difference range presented in SDC scale.

Even though half of the sample pairs were out of the range of colour difference of the SDC scale the observers were asked to rate them. Interestingly enough, six out of ten observers did not report higher differences. We believe that the reason for this was the fact that the differences between our colour pairs consisted both of difference in lightness and chroma, which made the evaluation more difficult than in other works (Melgosa 2014).

Intra- and inter-observer variability obtained for the colour pairs with differences that were within- and out of the range of those presented in grey scale were satisfactory. Experienced observers showed better agreements in their responses, as expected. In addition, observers gave consistent answers in three repetitions and agreed quite well when estimating pairs with high chroma difference.

The relationship between perceived and measured (ΔE_{ab}) differences was estimated only for colour pairs where ΔE_{ab} was within the range of grey scale. The correlation between the observers' answers and measured values was satisfactory, meaning that the SDC grey scale can be used to estimate differences for pearlescent prints with differences up to 16 ΔE_{ab} .

By taking all the results into account, we can conclude that the grey scale can be used for estimating differences of samples with dominant chroma. For assessing the perceived disparities of printed samples enhanced with pearlescent pigments, it is necessary to use reference scale with a higher range of colour differences than those presented in the SDC scale. Since chroma did not significantly influence the observers' responses, the scale can be formed with grey pairs.

5. ACKNOWLEDGEMENTS

The research is supported by the Ministry of Education, Science and Technology Development of the Republic of Serbia, project number: 35027 *“Development of software model for scientific and production improvement in graphic industry”* and by the Spanish State Agency of Research (AEI) and the Ministry for Economy, Industry and Competitiveness (MIMECO) by means of the grant number FIS2017-89258-P with European Union FEDER (European Regional Development Funds) support.

The samples used in this study were partially printed in Squeegy Print printing house. The authors would like to express their sincere gratitude to Bojan Bačkalić for sharing his facilities and for his help and comments, as well as to volunteers from the Department of Optics (University of Granada, Spain) who participated in the visual experiment.

6. REFERENCES

- [1] ASTM International: ASTM E2539 – 12. “Standard Practice for Multiangle Color Measurement of Interference Pigments”, 2012. URL www.astm.org (last request: 2017-03-07).
- [2] BYK: Light Booths, URL <https://www.byk.com/en/instruments/products/?a=2&b=20&f=0&faction> (last request: 2018-08-20).
- [3] Huang, M., Liu, H., Cui, G., Luo, M.R.: “Research on large color difference evaluation using printed samples”, Proceedings of 4th International Congress on Image and Signal Processing, Vol 5. (IEEE: Shanghai, China, 2011), pages 1753-1756. doi: 10.1109/CISP.2011.6100543.
- [4] International Organization for Standardization: ISO 105-A02:1993. “Textiles -- Tests for colour fastness -- Part A02: Grey scale for assessing change in colour”, 1993. URL <https://www.iso.org/standard/3785.html> (last request: 2018-09-08).
- [5] International Organization for Standardization: ISO 12647-2:2013. “Graphic technology -- Process control for the production of half-tone colour separations, proof and production prints -- Part 2: Offset lithographic processes”, 2013. URL <https://www.iso.org/standard/57833.html> (last request: 2018-09-08).
- [6] Klein, G. A.: “Industrial Color Physics”, (London, GB: Springer, 2010.), pages 91-92.
- [7] Maile, F. J., Pfaff, G., Reynders, P.: “Effect pigments—past, present and future”, Progress in Organic Coatings 54(3), 150-163, 2005. doi: 10.1016/j.porgcoat.2005.07.003.
- [8] Martínez, J.: “Testing the AUDI2000 colour-difference formula”, Master thesis report - Color in Informatics and Media Technology, Universidad de Granada, 2013.
- [9] Meadows, M. G., Butler, M. W., Morehouse, N. I., Taylor, L. A., Toomey, M.B, McGraw, K.J., Rutowski, R. L.: “Iridescence: views from many angles”, Journal of the Royal Society Interface 6(2), S107–S113, 2009. doi: 10.1098/rsif.2009.0013.focus.
- [10] Melgosa, M., García, P. A., Gómez-Robledo, L., Shamey, R., Hinks, D., Cui, G., Luo, M. R.: “Notes on the application of the standardized residual sum of squares index for the assessment of intra- and inter-observer variability in color-difference experiments”, JOSA A 28(5), 949-953, 2011. doi: 10.1364/JOSAA.28.000949.
- [11] Melgosa, M., Gómez-Robledo, L., Cui, G., Li, C., Ferrero, A., Bernad, B., Campos, J., Richard, N., Fernández-Maloigne, C.: “Using a standard grey scale for colour change in a multi-angle colour-assessment cabinet”, Proceedings of 4th CIE Expert Symposium on Colour and Visual Appearance, (CIE: Prague, Czech Republic, 2016), pages 93-94.
- [12] Melgosa, M., Martínez-García, J., Gómez-Robledo, L., Perales, E., Martínez-Verdú, FM., Dauser, T.: “Measuring color differences in automotive samples with lightness flop: a test of the AUDI2000 color-difference formula”, Optics Express 22(3), 3458-67, 2014. doi: 10.1364/OE.22.003458.
- [13] Merck: Iriodin®, URL <https://www.merckgroup.com/en/brands/pm/iriodin.html> (last request: 2018-04-03).
- [14] SDC: SDCE Grey Scale, URL <https://www.sdcenterprises.co.uk/products/sdc-assessment-aids/grey-scale> (last request: 2018-08-20).
- [15] Tomić, I., Dedijer, S., Novaković, D., Jurič, I.: “Artificial neural networks for optimising camera-based colour measurements of prints enhanced with pearlescent pigments”, Coloration Technology 134(5), 364-372, 2018. doi: 10.1111/cote.12346.
- [16] Weitzel, J.: “Special effect pigments in printing inks”, In: Pfaff, G.: (Ed.) “Special Effect Pigments, 2nd Ed”, (Hannover, Vincentz Network, 2008.), pages 171-194.



SPECTROSCOPIC EVALUATION OF THERMOCHROMIC PRINTED CARDBOARD BIODEGRADATION

Marina Vukoje , Rahela Kulčar , Katarina Itrić , Mirela Rožić 

University of Zagreb, Faculty of Graphic Arts, Zagreb, Croatia

Abstract: Municipal solid waste, containing mostly organic fraction, paper and board, wood and textiles, continues to be a major environmental problem. In addition, paper and cardboard are the most important sources of packaging materials. Packaging waste comprising about one-third of all municipal solid waste, mainly plastic and paper based. Anaerobic degradation is one of the most environmentally friendly methods for solid organic waste treatment and widely applied for bio-energy production. In this study, the biodegradation potential of three different cardboard materials (Umca Color - UC, Propack - PP, Lux Pack - LP) and UV curable screen printing thermochromic ink applied on them (UV), were studied using the soil burial test under anaerobic conditions. Unprinted and printed cardboard samples were evaluated for changes over 4 months by FT-IR spectroscopy. FTIR spectra revealed the existence of CaCO_3 and kaolin in cardboard coating. No significant changes occurred in the FTIR spectra of unprinted cardboard samples during biodegradation. In addition, FTIR spectra showed the presence of polyurethane acrylate in the UV thermochromic printing ink since all typical vibrational bands of polyurethane acrylate (3385 cm^{-1} (NH stretching), $2955\text{--}2855\text{ cm}^{-1}$ (symmetric and asymmetric CH_2 stretching), 1726 cm^{-1} (C=O stretching), 1365 cm^{-1} (C–N stretching) and 1111 cm^{-1} (C–O–C stretching), 810 , 987 and 1408 cm^{-1} ($\text{CH}_2=\text{CH}$), 1636 cm^{-1} (C=C stretching), 1064 , 1195 and 1296 cm^{-1} (C–O stretching)) were obtained. After biodegradation of all three prints a decrease of band intensities located in the $2955\text{--}2855\text{ cm}^{-1}$ range (symmetric and asymmetric CH_2 stretching), carbonyl peak around 1726 cm^{-1} , ester linkages at $1260\text{--}1200\text{ cm}^{-1}$ and $1100\text{--}1000\text{ cm}^{-1}$ range (C–O stretching vibration) were observed. The changes in those bands may indicate the breaking down of the ester linkages, which lead to changes in polymeric structure of polymerized thermochromic ink. The highest changes in the whole spectral range were observed for the printed PP and LP cardboard, mainly in the $2955\text{--}2855\text{ cm}^{-1}$ spectral range and carbonyl peak around 1720 cm^{-1} . In addition, the changes to the dynamic colour properties of the samples were described. The highest changes in colour after biodegradation were observed for PP-UV sample, followed by UC-UV sample. This can be explained by the best absorption of ink into the cardboard structure. The studied spectroscopic methods individually are not effective methods for the evaluation of thermochromic prints changes during degradation studies, but in a combination, they can give a brief insight into the state of material.

Key words: biodegradation, cardboard, thermochromic ink, ATR – FTIR spectroscopy, colorimetric properties

1. INTRODUCTION

According to Holik 2013 the ratio of the worldwide consumption of the different paper and board grades has changed in the past and will continue to change in the future according to technical, economical, and social evolution and developments in the individual countries and in the world. The consumption of packaging grades have increased, graphic paper grades have stagnated, while the newsprint consumption has declined. The changes in costumers' behaviour have increased the demand for packaging materials, such as the growth in internet shopping and demand for small packaged foods (Holik, 2013). In order to fulfil consumers' expectations, packaging should be functional and attractive. Lately, intelligent packaging serves as a media for providing consumers with the necessary information about quality and safety of the packaging. Thermochromic printing inks, which can be applied on different printing substrates, can convey a message to the consumer based on the colour of the ink they are seeing.

Thermochromic printing inks are chromogenic or colour changing inks, which exhibit a colour change with exposure to different temperatures. They come in two forms: as liquid crystals or leuco dyes (Seeboth et al, 2013). Both types of thermochromic inks are usually encapsulated to enable easier handling. The sizes of microcapsules are in the range of 3 to $5\text{ }\mu\text{m}$, which makes them at least ten times larger than the average pigment particle. The most widely used system for microencapsulation of thermochromic inks involves urea or melamine and formaldehyde systems, gelatine–gum arabic and epoxy resins (Fujinami, 1996). Commercially available thermochromic printing inks based on leuco dyes are consisted of microencapsulated leuco dye–developer–solvent systems and a resin binder (Seeboth et al, 2013). In

thermochromic leuco dye–developer–solvent system thermochromic effects are based on changes of absorption caused by molecular interactions of the incorporated functional dye within its microenvironment (MacLaren et al, 2003; Seeboth et al, 2007; White et al, 1999). The thermochromic effect is caused by the formation of leuco dye–developer complexes in a reversible equilibrium redox reaction between leuco dye and developer. The reaction is triggered by interactions between the complex and the solvent during the melting or crystallization process (Seeboth et al, 2007).

Previous studies about thermochromic inks mainly investigated the chemical composition of the leuco dyes inside the microcapsules and their changes (Hajzeri et al, 2015; Panák et al, 2017; Raditoiu et al, 2016). For the commercially available thermochromic printing inks, different studies have been conducted for the purpose of their colorimetric properties and UV stability (Friškovec et al, 2013; Kulčar et al, 2011, 2010; Rožić et al, 2015). Studies dealing with biodegradability aspects showed that that polymerized ink vehicle (vegetable oil + resin) in thermochromic offset ink is more stable than the polymer resin present in UV curable screen printing thermochromic ink. SEM micrographs indicated a notably higher stability of offset ink binder and accordingly lower deformation of the microcapsules (Vukoje et al, 2018, 2017b).

The European laws require reducing the amount of all kinds of produced waste streams either by prevention, reusing or recycling (European Commission, 2008). Preventing the occurrence and reduction of waste generation is the most important step in sustainable waste management. But, if the waste is produced, than it should be recycled (by means of material or organic recycling) or used for energy production (Vukoje et al, 2018). 40% of collected paper for recycling is wet and is not suitable for production of recycled paper but is suitable for organic recycling (Murphy et al, 2006). In addition, paper based products contaminated with food are not desirable in paper recycling facilities due to cleaning difficulties, which leads to contamination issues (Twede et al, 2015). During production of recycled paper with the classic flotation deinking process a certain types of prints may cause certain problems, for example UV curable inks due to visible speck contamination and for water based inks due to low brightness or/and pronounced colour shade.

Biodegradation of paper products is dependent upon the crystalline/amorphous ratio in cellulose, presence of lignin and different additives in paper (Van Wyk et al, 2003). Variety types of paper and cardboard are being used nowadays for different graphic products and applications, differing in their composition or coatings applied. Pinzari *et al.* (2010) showed that clay and aluminium could inhibit fungal development during biodegradation of paper more than CaCO_3 . During anaerobic biodegradation, excessive amounts of calcium can lead to precipitation of carbonate and phosphate affecting the biomass activity and buffer capacity loss while heavy metals originating from printing inks or fillers in paper can accumulate to potential toxic concentrations (Chen et al, 2008). Sridach et al, (2007) studied biodegradation of four commercial barrier coated boards (*i.e.*, internally-sized uncoated board, one-side polyethylene coated board, double-side polyethylene coated board, and multilayer laminated board) using a soil burial test in a laboratory scale. Results showed that the base-board of four different barrier-coated paperboards was found to be biodegradable in a soil environment, but the coating layer remained intact during biodegradation. Sample size and microbial population affected the rate of the biodegradation process but the directionality of the samples did not. According to Nazhad et al, (2006), the polyester-coated boards were found to be biodegradable. The fibrous component of the boards was degraded in a very short time while degradation of the coated materials of the boards was influenced by the formulation of the coating.

2. METHODS

2.1. Materials

Three different cardboard materials were used in biodegradation test. The used cardboards are representing different classes of cardboards (Table 1) according to their properties and quality.

Table 1: Cardboard classification

Cardboard samples	Abbreviation	Grammage, g/m ²	Classification
Lux Pack	LP	350	GC1
Propack	PP	350	GT2
Umca Color	UC	350	GD2

All three cardboard samples were printed with thermochromic ink in order to examine how it affects the process of biodegradation. One leuco dye based, screen-printing UV curable thermochromic ink produced by CTI® was used for printing. The thermochromic ink was coloured in purple below its activation temperature ($T_A=31\text{ }^{\circ}\text{C}$) and changed to pink above the activation point. The biodegradation of unprinted (UC, LP, PP) and printed cardboard (UC-UV, LP-UV, PP-UV) samples was studied using the soil burial test under anaerobic conditions as it will be described in the text. Thickness of all unprinted cardboard samples was determined according to T411 standard using Enrico Toniolo DGTB001 Thickness Gauge. Print thickness values were obtained by subtracting the measured values of the thickness of unprinted paper from the measured values of thickness of paper with print. Average values of twenty measurements are presented as mean \pm SD.

2.2. Printing

The printing trials were carried out using the screen printing device (Siebdruckgeräte von Holzschuher K.G., Wuppertal), employing 60/64 mesh. The cardboards were printed in full tone, under the same conditions. The printed samples were dried under the UV irradiance (30 W/cm) using Technigraf Aktiprint L 10-1 device.

2.3. Soil burial experiments

Soil was sieved to less than 2 mm particle size. Large plant materials, stones, and other inert materials were removed. Laboratory soil burial experiments were conducted at room temperature $25\pm 3^{\circ}\text{C}$ by placing the neat and printed cardboard samples horizontally in laboratory glass containers filled with soil. Samples were cut in 4 x 5 cm. All the samples were buried for 14, 32, 50, 80 and 120 days in glass containers filled with the soil. The water content of the soil was adjusted to 60% of its maximum water retention capacity. The commercial available reagent was used in order to allow the development of anaerobic conditions. The existence of anaerobic conditions was proved with *Anaerotest* (Merck) strips.

2.4. Fourier transform infrared (FTIR) spectroscopy

The ATR spectra of the cardboard samples, unprinted as well as printed with the ink before and after the soil burial, were measured using Shimadzu FTIR IRAffinity-21 spectrometer with the Specac Silver Gate Evolution as a single reflection ATR sampling accessory with a ZnSe flat crystal plate (index of refraction 2.4). The IR spectra were recorded in the spectral range between 4000 and 400 cm^{-1} at 4 cm^{-1} resolution and averaged over 15 scans.

2.5. Colorimetric Measurements

Spectral reflectance was measured by using Ocean Optics USB2000+ spectrometer using 30mm wide integrating sphere under (8:di) measuring geometry (diffuse geometry, specular component included). The printed samples were heated/cooled on the full-cover water block (EK Water Blocks, EKWB d.o.o. Slovenia). Its temperature was varied by thermostatically controlled water block. Reflectance spectra were measured in one heating/cooling cycle by heating them from 15 to 50°C and then cooling them back to 15°C . The measurements were performed in the steps of 1nm for the spectral region from 400 to 750 nm. Ocean Optics SpectraSuite software was used for the calculation of the CIELAB values from measured reflectance. The D50 illuminant and 2° standard observer were applied in these calculations. Colour differences were calculated using the CIEDE2000 total colour difference formula (CIE Central Bureau, 2004).

3. RESULTS AND DISCUSSION

3.1. Thickness of the samples

Different thickness of the prints resulted from the different absorption capacity of the used cardboards and its specific surface free energy, as well as their compatibility with the used thermochromic UV ink which was studied in the previous research (Vukoje et al, 2017).

Table 2: Thickness of used cardboards

	Thickness, mm	Increase in thickness due to UV print/(lm), mm
LP	0.563±0.003	
LP-UV		0.010±0.003
PP	0.494±0.008	
PP-UV		0.003±0.007
UC	0.453±0.008	
UC-UV		0.005±0.008

3.2. FTIR spectra of used cardboards

Results in Figure 1 show that FTIR spectra of all unprinted cardboard materials are almost the same, indicating that the coating layer in all samples is made of the same substances.

In the fingerprint region, a broad band centred at about 1390 cm^{-1} is detected, followed by the peaks around 1091 , 1031 , 1001 , 912 , and 700 cm^{-1} indicating the presence of kaolin in the coating formulation (Grilj et al, 2012). The bands observed at 869 and 711 cm^{-1} (shoulder) can be attributed to the out-of-phase CO_3 bending vibration and the in-plane CO_2 bending vibration of calcium carbonate. Results show that for the formulation of coating, CaCO_3 and kaolin as pigment were used. Somewhat smaller intensities and broadening of the vibrational bands on the LP samples may indicate the smaller content of the coating layer, followed by the UC sample. The sharpest vibrational bands on the PP samples may indicate the highest content of the coating on the surface.

From the Figs. 2-4 it can be seen that no significant changes occurred during biodegradation. The intensity of the kaolin and CaCO_3 bands decreased mostly after 120 days of biodegradation. Only in the case of LP cardboard, the vibrational bands were weaker and poorly defined after 120 days indicating the highest rate of biodegradation and loss of coating fillers.

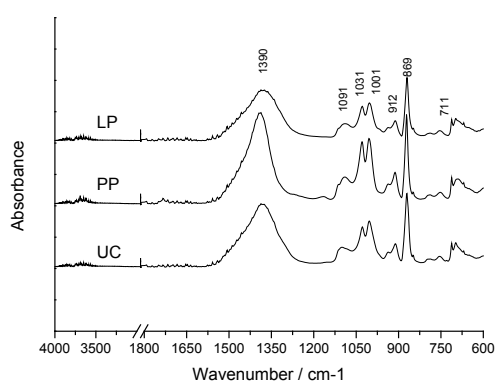


Figure 1: The ATR-FTIR spectra of unprinted cardboard samples before biodegradation test

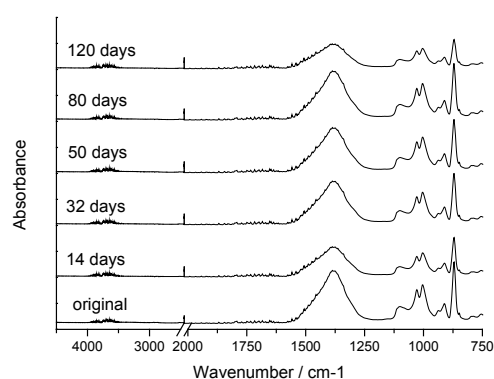


Figure 2: The ATR-FTIR spectra of unprinted UC cardboard samples before and after biodegradation test

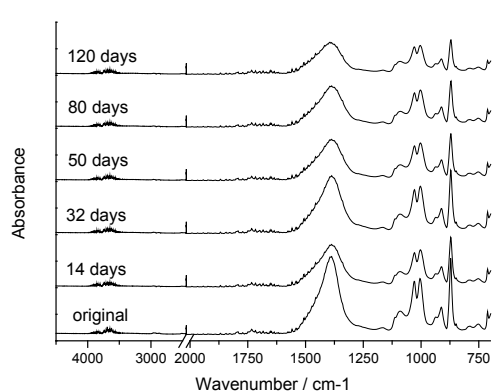


Figure 3: The ATR-FTIR spectra of unprinted PP cardboard samples before and after biodegradation test

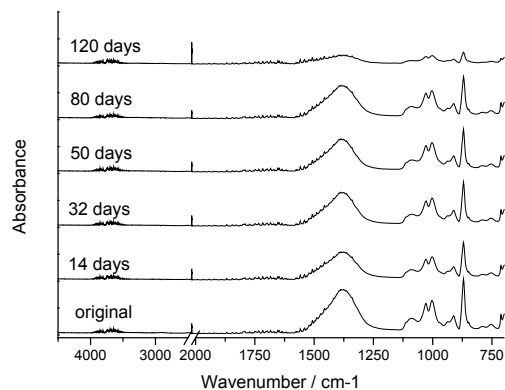


Figure 4: The ATR-FTIR spectra of unprinted LP cardboard samples before and after biodegradation test

3.3. FTIR spectra of thermochromic prints

Our previous research of FTIR studies of thermochromic offset and UV curable screen printing inks showed that the observed vibrational bands most likely originated from the thermochromic ink resin and were not the result of the vibrational modes of the thermochromic composites within the microcapsules present in a significantly smaller amount. In addition, the vibrational bands of microcapsules wall material (which are present in a significantly smaller amount) which are covered with a polymer resin (present in higher amount), are probably covered and overlapped with vibrational bands of polymer resin (Vukoje et al, 2018, 2017b).

The IR spectra of the thermochromic ink (Figure 5), show all typical vibrational bands of polyurethane, such as the bands at 3385 cm^{-1} (NH stretching), $2955\text{--}2855\text{ cm}^{-1}$ (symmetric and asymmetric CH_2 stretching), 1726 cm^{-1} (C=O stretching), 1462 cm^{-1} (ring stretching modes of phenyl moiety), 1363 cm^{-1} (C–N stretching) and 1111 cm^{-1} (C–O–C stretching) (Vukoje et al., 2018). In addition, the acrylate vibrational bands at 810 , 987 and 1408 cm^{-1} (in-plane and out-of-plane deformation of the vinyl group ($\text{CH}_2=\text{CH-}$)), as well as the bands at 1636 cm^{-1} (double bond (C=C) stretching), vibrational bands at 1064 , 1195 and 1296 cm^{-1} (vibrational modes of functionalities consisting of oxygen atom (C–O stretching)) were also present. The band at 1462 cm^{-1} could be also assigned to bending of the methylene groups present in acrylate as well, while the band at 1271 cm^{-1} could arise from the C–N stretching and C–O stretching in polyurethane and acrylate (Vukoje et al, 2018).

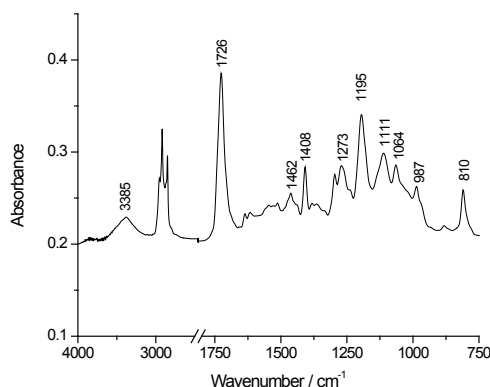


Figure 5: The ATR-FTIR spectra of UV curable thermochromic ink at 23°C

The IR spectra, measured in attenuated total reflectance (ATR) mode, of the UV curable thermochromic prints on all samples, UC, PP and LP, were very similar for the PP-UV and UC-UV sample. Some differences can be seen for the LP-UV sample, probably due to thicker layer of ink on the cardboard surface (Fig. 6). For example, thicker layer of thermochromic ink on LP-UV sample may also be confirmed by the absence of kaolin vibrational band at 1001 cm^{-1} that is present in UC-UV and PP-UV sample. The band at 1001 cm^{-1} is not present in the thermochromic ink (Figure 5) but it can be seen in FTIR spectra of all unprinted cardboards (Figure 1). In addition, some differences can be seen in the IR spectra of thermochromic ink and obtained prints. The bands at 1408 , 1294 , 1192 and 1062 cm^{-1} in the IR spectra of the prints were weaker and poorly defined due to polymerization of polyurethane acrylate during UV curing (Vukoje et al., 2018). In the case of prints, carbonyl peak at 1726 cm^{-1} (in thermochromic ink) was shifted towards lower values in the case of LP-UV sample (1720 cm^{-1}) and towards higher values in the case of UC-UV and PP-UV (1740 cm^{-1}) after polymerization.

The IR spectra of the thermochromic UV prints on the cardboard samples before and after 14, 32, 50, 80 and 120 days of biodegradation are shown in Figs. 7, 8 and 9. The spectra of the prints are vertically displaced for visual clarity. After biodegradation, especially for 120 days, the changes of vibrational band intensities in the whole spectral range can be seen. A decrease of vibrational band intensities located in the $1100\text{--}1000\text{ cm}^{-1}$ range (attributed to the ester C–O stretching vibration), $1260\text{--}1200\text{ cm}^{-1}$ range (attributed to carbonyl oxygen linkage) and carbonyl peak around 1726 cm^{-1} were observed after degradation for all prints (Figs. 7, 8 and 9). These changes indicate the breaking down of the ester linkages, leading to the changes in polymeric structure. In the ranges of $1100\text{--}1000\text{ cm}^{-1}$ and $1260\text{--}1200\text{ cm}^{-1}$, the highest changes were observed for the printed LP-UV sample, followed by print on PP-UV

sample. In addition, the changes in the spectral range 2955–2855 cm^{-1} corresponding to symmetric and asymmetric CH_2 stretching, were the highest in the case of LP-UV printed sample, indicating the highest change in polymeric structure, followed by PP-UV sample. A vibrational band around 1030 cm^{-1} was obtained in the IR spectra of the UV prints on all samples after biodegradation could be associated with silicates (Si-O stretching) adsorbed on the prints from the soil (Vukoje et al, 2018).

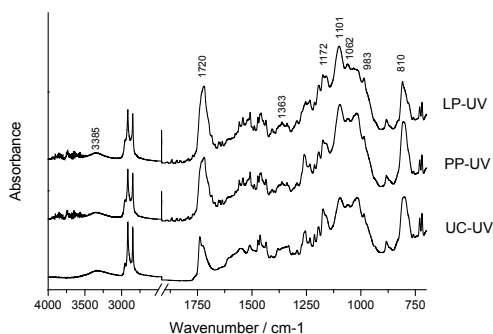


Figure 6: The ATR-FTIR spectra of printed cardboard samples before biodegradation test

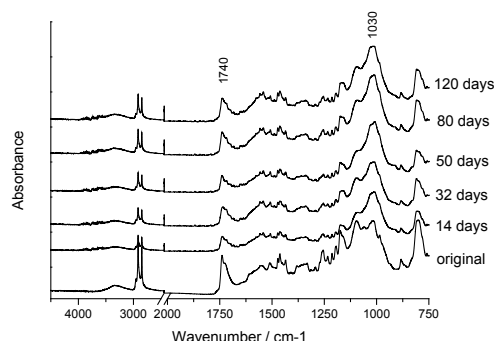


Figure 7: The ATR-FTIR spectra of printed UC-UV cardboard samples before and after biodegradation test

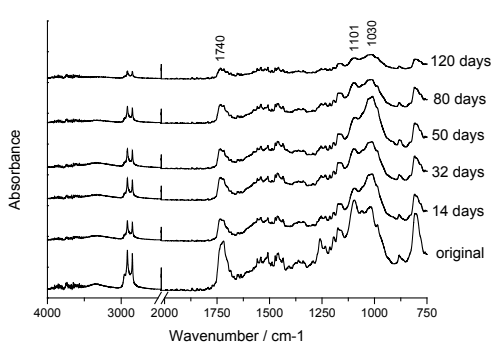


Figure 8: The ATR-FTIR spectra of printed PP-UV cardboard samples before and after biodegradation test

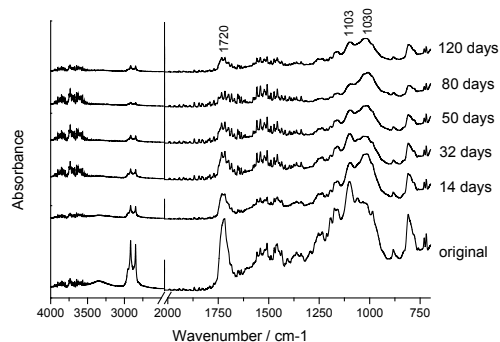


Figure 9: The ATR-FTIR spectra of printed LP-UV cardboard samples before and after biodegradation test

3.4. Colorimetric properties of thermochromic prints

Besides FT-IR spectroscopy, the second way of thermochromic UV curable prints biodegradability evaluation is measurement of their dynamic colorimetric properties. The reflectance spectra of thermochromic UV curable prints measured with spectrometer during heating are shown in Figure 10. Process is continuous and no abrupt change was observed. Reversible colour change is present in all samples, implying that the thermochromic effect has not been lost during biodegradation, but it was significantly reduced after 120 days of biodegradation.

Figure 11 shows colour hysteresis of prints on cardboards before and after 50 and 120 days of biodegradation. Colour hysteresis describes temperature dependence of colour for L^* component of colour. Samples appear differently during the two reversible thermochromic reactions (change of colour from purple to pink). This is probably because by heating, the microcapsules change their shape and position, they may become larger or more on surface, so for the opposite effect of the cooling process it is necessary to invest more energy for the same effect, i.e. lower temperature are needed to bring the colour of the sample into its initial state. In addition, Figure 11 shows the influence of biodegradation after 50 and 120 days on colour hysteresis. After 50 days of biodegradation, only a slight changes occurred. The loops become smaller for all the samples, the smallest were observed for LP-UV sample, while the highest changes were observed for the PP-UV sample. However, after 120 days of biodegradation remarkable changes were observed – the TC effect is almost destroyed in PP-UV sample, whereas the resulting loop remained very small on UC-UV and LP-UV samples.

In perfectly reversible process TC sample should return to the same colour after completing the whole heating/cooling cycle and colour hysteresis of such a samples has a closed loops. The degree of reversibility of TC change can be also evaluated by the opening of hysteresis loop at low temperatures,

i.e. by total colour difference of sample measured between heating and cooling at temperature well below the final chromic temperature (Kulčar et al, 2010).

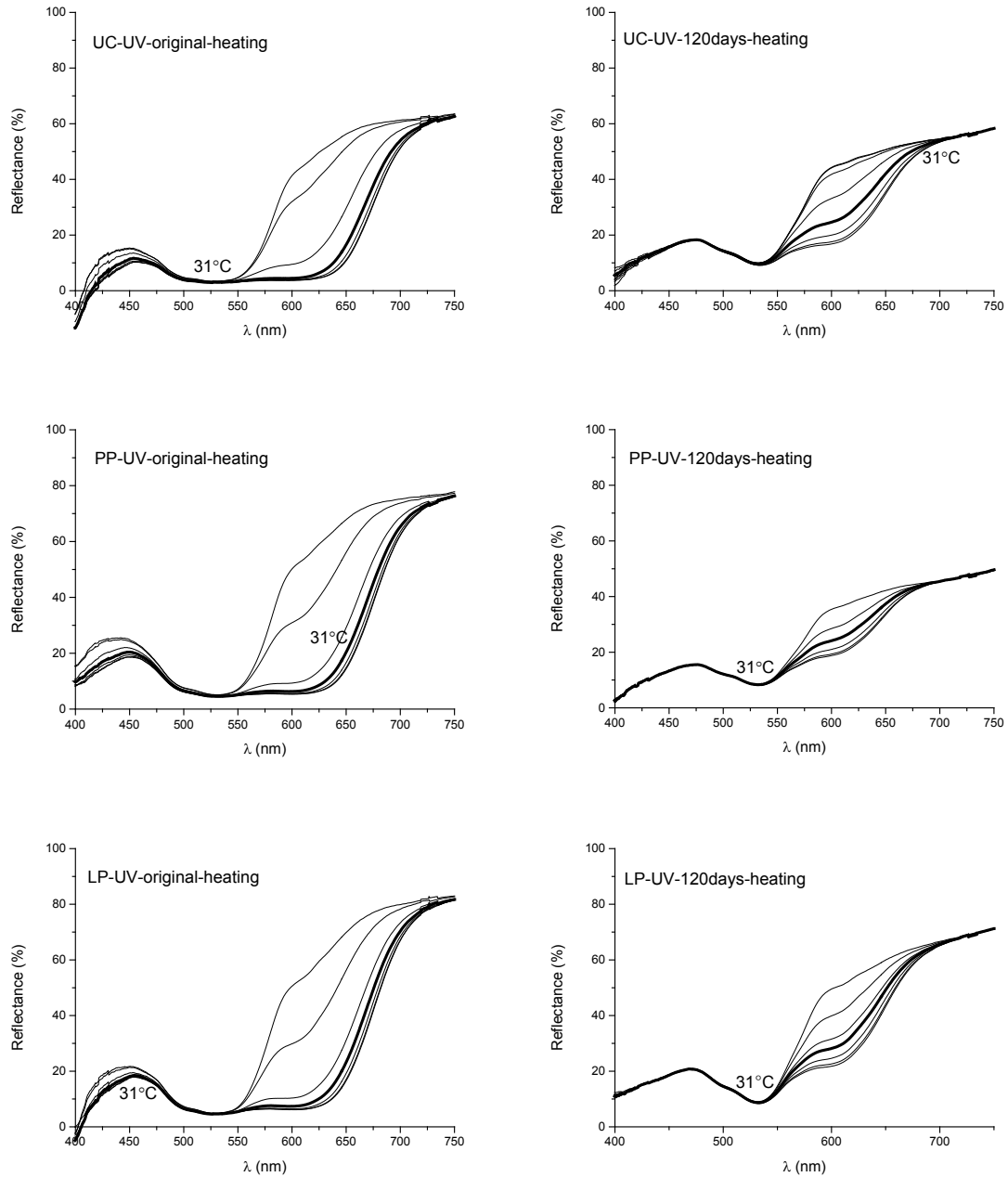


Figure 10: Reflectance spectra of printed UC-UV, PP-UV and LP-UV cardboard samples measured during heating and cooling

Results of total colour difference obtained for the original samples are given in Table 3. Results show that PP-UV sample has smallest total colour difference, followed by UC-UV sample. The highest total colour difference was obtained on LP-UV sample. This behaviour can be explained by the absorption of thermochromic ink in cardboards (Table 1). PP cardboard shows the highest absorption rate of ink into its structure (smallest increase in thickness after printing) while the LP cardboard shows almost no absorption of ink into its structure (highest increase in thickness after printing) (Table 1). In addition, in previous research the smallest surface tension between thermochromic ink and cardboard was obtained in the case of PP-UV sample (3.41 mJ m^{-2}) followed by UC-UV (6.40 mJ m^{-2}). The highest surface tension

was achieved in the case of LP-UV print (11.88 mJ m^{-2}) (Vukoje et al, 2017a). This means that the high surface tension between thermochromic ink and cardboard creates resistance and prevents the absorption of ink into the cardboard, resulting in higher total colour difference.

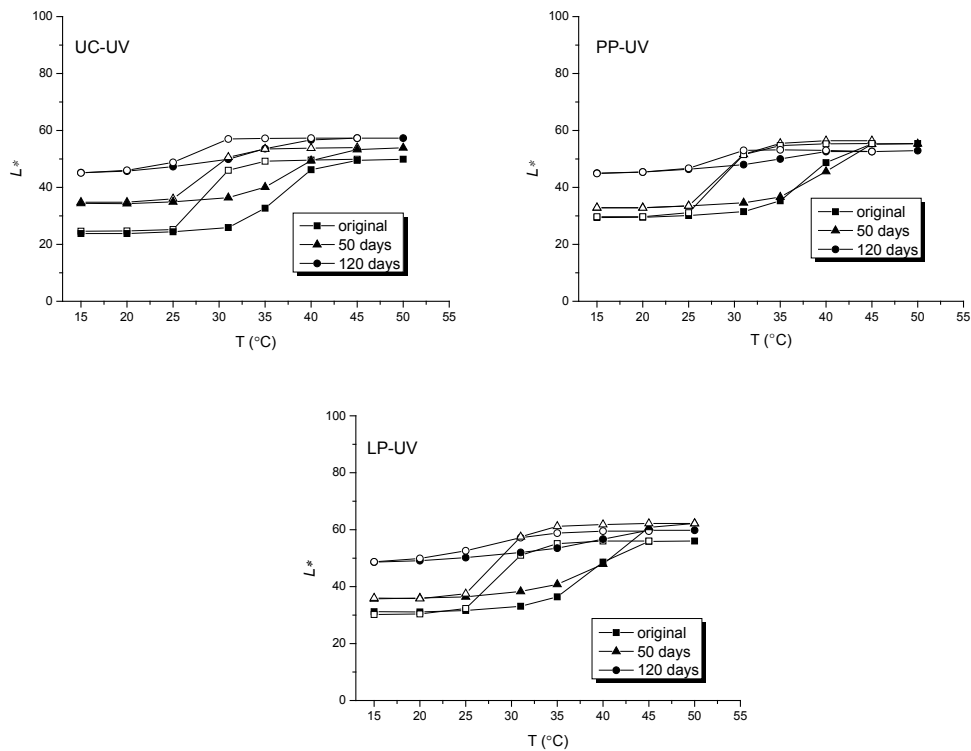


Figure 11: CIELAB lightness L^* of three thermochromic UV curable prints on cardboard samples in dependence on temperature at heating (solid signs) and cooling (open signs)

In addition, the PP-UV sample which shows the highest rate of ink absorption, results in the highest colour changes after 120 days of biodegradation. This can be explained by the thickness of the ink binder that covers the microcapsules. This is in the accordance with our previous research. Microcapsules that are probably made of biodegradable melamine resin, are promoting rate of biodegradation (Vukoje et al, 2018). The print obtained on cardboard that absorbs more thermochromic ink, shows higher rate of biodegradation, since microcapsules are exposed to bacteria. If the microcapsules are covered with a thinner layer of ink polymer resin, the higher rate of biodegradation will be achieved.

Table 3: Total colour difference (CIEDE2000) between heated and cooled of the sample at 15°C.

CIEDE2000	
Sample	original
PP-UV	0.27
UC-UV	1.49
LP-UV	2.70

4. CONCLUSION

The studied spectroscopic methods individually are not effective methods for the evaluation of thermochromic prints changes during degradation studies, but in a combination, they can give a brief insight into the state of material. Thermochromic printing inks are functional materials with a complex structure, which provide information about a product to which it is applied. In the case of thermochromic printing inks, the studies have shown that FTIR spectroscopy mostly shows the vibrational bands of binder present in a larger amount (compared to the ratio of the microcapsules) but it does not show the changes occurring inside the microcapsules. In addition, the effect of the temperature during measurements does

not significantly affect the spectrum change. The obtained spectrum shows the changes of the binder vibrational bands occurred during biodegradation. By colorimetric measurements, the samples are monitored in the visible part of the spectrum, in controlled temperature conditions during the heating and cooling process. Based on the resulting spectrum, it can be accurately determined when the thermochromic effect stops. In this case, FTIR spectroscopy showed the degradation of the thermochromic printing ink binder, but it doesn't show the change and degradation of the microcapsules, whereas colorimetric measurements showed the loss of thermochromic effect, pointing to the degradation of the microcapsule. However, in order to determine the overall degree of the samples biodegradation, other parameters such as weight loss during biodegradation should be considered as well. In this case, the measurements show that the greatest colour degradation is observed on the sample showing the highest absorption of thermochromic ink.

4. ACKNOWLEDGMENTS

The authors are grateful for the support of the University of Zagreb, Grant under the title "Modifications of conventional graphic materials with nanoparticles and chromogenic materials, and their health safety.

5. REFERENCES

- [1] Chen, Y., Cheng, J.J., Creamer, K.S.: "Inhibition of anaerobic digestion process: A review", *Bioresource Technology* 99(10), 4044–4064, 2008. doi: 10.1016/j.biortech.2007.01.057.
- [2] CIE Central Bureau: "Colorimetry", 3rd ed, (CIE Central Bureau Vienna, 2004).
- [3] The European Parliament and The Council Of The European Union, "Directive 2008/98/EC of the European Parliament and of the Council of 19 November 2008 on waste and repealing certain directives", *Official Journal of the European Union*, 51, 312/3-312/30, 2008.
- [4] Friškovec, M., Kulčar, R., Klanjšek Gunde, M.: "Light fastness and high-temperature stability of thermochromic printing inks", *Coloration Technology* 129(3), 214–222, 2013. doi: 10.1111/cote.12020
- [5] Fujinami, F.: Patent US5500040 - Ultraviolet-curable thermochromic ink composition, 1996.
- [6] Grilj, S., Klanjšek Gunde, M., Szentgyörgyvölgyi, R., Gregor-Svetec, D.: "FT-IR and UV / VIS analysis of classic and recycled papers", *Papíripar* 56(4), 7–13, 2012.
- [7] Hajzeri, M., Bašnec, K., Bele, M., Klanjšek Gunde, M.: "Influence of developer on structural, optical and thermal properties of a benzofluoran-based thermochromic composite", *Dyes and Pigments* 113, 754–762, 2015. doi: 10.1016/j.dyepig.2014.10.014.
- [8] Holik, H. (Ed.): "Handbook of Paper and Board", 2nd ed, (Wiley – VCH, 2013).
- [9] Kulčar, R., Friškovec, M., Hauptman, N., Vesel, A., Klanjšek Gunde, M.: "Colorimetric properties of reversible thermochromic printing inks", *Dyes and Pigments* 86(3), 271–277, 2010. doi: 10.1016/j.dyepig.2010.01.014.
- [10] Kulčar, R., Friškovec, M., Klanjšek Gunde, M., Knešaurek, N.: "Dynamic colorimetric properties of mixed thermochromic printing inks", *Coloration Technology* 127(6), 411–417, 2011. doi: 10.1111/j.1478-4408.2011.00338.x.
- [11] MacLaren, D.C., White, M.A.: "Dye–developer interactions in the crystal violet lactone–lauryl gallate binary system: implications for thermochromism", *Journal of Materials Chemistry* 13(7), 1695–1700, 2003. doi: 10.1039/b302249h.
- [12] Murphy, J.D., Power, N.M.: "A Technical, Economic and Environmental Comparison of Composting and Anaerobic Digestion of Biodegradable Municipal Waste", *Journal of Environmental Science and Health Part A* 41(5), 865–879, 2006. doi: 10.1080/10934520600614488.
- [13] Nazhad, M.M., Sridach, W., Retulainen, E., Kuusipalo, J., Parkpian, P.: "Biodegradation potential of some barrier-coated boards in different soil environments", *Journal of Applied Polymer Science* 100(4), 3193–3202, 2006. doi: 10.1002/app.23591.
- [14] Panák, O., Držková, M., Kaplanová, M., Novak, U., Klanjšek Gunde, M.: "The relation between colour and structural changes in thermochromic systems comprising crystal violet lactone, bisphenol A, and tetradecanol", *Dyes and Pigments* 136, 382–389, 2017. doi: 10.1016/j.dyepig.2016.08.050







- [15] Pinzari, F., Zotti, M., De Mico, A., Calvini, P.: "Biodegradation of inorganic components in paper documents: Formation of calcium oxalate crystals as a consequence of *Aspergillus terreus* Thom growth", *International Biodeterioration & Biodegradation* 64(6), 499–505, 2010. doi: 10.1016/j.ibiod.2010.06.001.
- [16] Raditoiu, A., Raditoiu, V., Nicolae, C.A., Raduly, M.F., Amariutei, V., Wagner, L.E.: "Optical and structural dynamical behavior of Crystal Violet Lactone - Phenolphthalein binary thermochromic systems", *Dyes and Pigments* 134, 69–76, 2016. doi: 10.1016/j.dyepig.2016.06.046.
- [17] Rožić, M., Kulčar, R., Jamnicki, S., Lozo, B., Gregor-Svetec, D.: "UV stability of thermochromic ink on paper containing clinoptilolite tuff as a filler", *Cellulose Chemistry and Technology* 49(7-8), 693–699, 2015.
- [18] Seeboth, A., Klukowska, A., Ruhmann, R., Löttsch, D.: "Thermochromic Polymer Materials", *Chinese Journal of Polymer Science (English Edition)* 25(2), 123–135, 2007. doi: 10.1142/S0256767907001923.
- [19] Seeboth, A., Lotzsch, D.: "Thermochromic and thermotropic materials", (CRC Press by Taylor & Francis Group, Boca Raton, Florida, USA, 2013).
- [20] Sridach, W., Hodgson, K.T., Nazhad, M.M.: "Biodegradation and recycling potential of barrier coated paperboards", *BioResources* 2(2), 179–192, 2007.
- [21] Twede, D., Selke, S.E., Kamdem, D.-P., Shires, D.: "Cartons, Crates and Corrugated Board, Handbook of Paper and Wood Packaging Technology", 2nd ed, (DesTech Publications, Inc., Lancaster, Pennsylvania, USA 2015).
- [22] Van Wyk, J.P.H., Mohulatsi, M.: "Biodegradation of Waste Cellulose", *Journal of Polymers and the Environment* 11(1), 23–28, 2003. doi: 10.1023/A:1023883428359.
- [23] Vukoje, M., Miljanić, S., Hrenović, J., Rožić, M.: "Thermochromic ink–paper interactions and their role in biodegradation of UV curable prints", *Cellulose* 25(10), 6121–6138, 2018. doi: 10.1007/s10570-018-1970-5.
- [24] Vukoje, M., Rožić, M.: "Various Valorisation Routes Of Paper Intended For Recycling – A Review", *Cellulose Chemistry and Technology* 52(7-8), 515–541, 2018.
- [25] Vukoje, M., Rožić, M., Cigula, T.: "The role of adhesion on thermochromic printed cardboard biodegradation", *ANNALS of Faculty Engineering Hunedoara – International Journal of Engineering* 15, 75–82, 2017a.
- [26] Vukoje, M., Rožić, M., Miljanić, S., Pasanec Preprotić, S.: "Biodegradation of thermochromic offset prints", *Nordic Pulp & Paper Research Journal* 32(2), 289–298, 2017b. doi: 10.3183/npprj-2017-32-02-p289-298.
- [27] White, M.A., LeBlanc, M.: "Thermochromism in Commercial Products", *Journal of chemical education* 76(9), 1201–1205, 1999. doi: 10.1021/ed076p1201.



PAPER AS A SUBSTRATE



PRINTABILITY CHARACTERISTICS OF PAPER MADE FROM A JAPANESE KNOTWEED

Gregor Lavrič¹ , Tanja Pleša¹ , Ana Mendizza² ,
Maruša Ropret² , Igor Karlovits¹ , Diana Gregor-Sveteč² 

¹ Pulp and Paper Institute, Ljubljana, Slovenia

² University of Ljubljana, Faculty of Natural Sciences and Engineering, Ljubljana, Slovenia

Abstract: Cereal straw and bagasse are presently the leading non-wood plants used in production of paper, though many fast-growing perennial plants have been studied for their suitability for paper manufacturing, too. In the present study the use of Japanese knotweed, as one of the most invasive alien plant species in Slovenia, as alternative raw material for papermaking is demonstrated. Paper was made of 55% Japanese knotweed and sulfate cellulose produced from 60% eucalyptus and 40% conifer fiber. The paper with the basic weight of 90 g/m² was manufactured on the pilot paper machine at the Pulp and Paper Institute. Among printability characteristics paper brightness, colour, yellowness, roughness, air permeability, specular gloss, print penetration, picking, and print unevenness were determined. The preliminary research has shown, that Japanese knotweed, as a cheap local raw material, could be used in paper making industry, though the fiber processing and paper making process must be improved in order to obtain good printability.

Key words: graphic paper, Japanese knotweed, printability characteristics

1. INTRODUCTION

A vast number of plants represent potential sources of paper fibers. Many of them were used experimentally, some of them commercially, mostly on a small scale, at various times and places (Britt, 1964). They still are used mainly in forest deficient countries, but also elsewhere as alternative fiber source for production of all kind of papers (Novak, 2004). In countries where wood is unavailable in sufficient quantities non-wood annual plants and agricultural residues are becoming important raw materials (Obi Reddy et al, 2014). Cereal straw and bagasse are presently the leading non-wood plants used in production of paper, followed by reeds and bamboo, though many fast-growing perennial plants, such as prairies and tropical grasses, leaf fibers from tropical plants have been studied for their suitability for paper manufacturing, too (Obi Reddy et al, 2014; Biermann, 1996). Compared to wood sources, nonwood plants and agricultural residues offer several advantages including short growth cycles, moderate irrigation, and fertilization requirements and low lignin content, resulting in reduced energy and use of milder chemicals during pulping (Saikia et al, 1997). Certain fast growing plants are seen as invasive alien plant species. They are a big challenge in the European ecosystem, because they displace local vegetation, destroy agricultural land and cause damage to European economy, as they are mostly daily removed and burned. One of the most invasive alien plant species in Slovenia is Japanese knotweed. Japanese knotweed is a fast-growing and strong clump-forming perennial, with tall, dense annual stems. It has hollow stems with distinct raised nodes that give it the appearance of bamboo, and they may reach a maximum height of 3–4 m each growing season (Royal Horticultural Society, 2018). In the European project the use of Japanese knotweed, as alternative raw material for papermaking is researched, with the goal to define a first small-scale industrial process of paper production from Japanese knotweed. Besides mechanical properties, printability is one of the most important paper characteristics. It tells us how paper behaves during a printing process. Printability depends on the interactions between the paper and printing ink at the given printing process variables. The print quality is strongly affected by the ink-paper interactions, an uneven absorption and distribution of ink components is one of the primary causes for defects, such as unevenness and mottle (Rousu et al, 2003). In the present research, a paper made from Japanese knotweed is described, with the emphasis on its printability characteristics.

2. METHODS

Paper was made of 55% Japanese knotweed using only plant stem as fibre source. The sulphate process was used in order to remove lignin. The sulphate cellulose produced from 60% eucalyptus and 40%

conifer fibers was added to Japanese knotweed. The paper with the basic weight of 90 g/m² was made on the pilot paper machine at the Pulp and Paper Institute. In the Figure 1 the Japanese knotweed plant and chopped stems are presented (Mežnarič Osole et al, 2015).



Figure 1: Japanese knotweed and chopped stems

Paper samples were conditioned in a standard atmosphere according to standard ISO 187, at the temperature of 23°C and relative humidity of 50%. The basic paper properties: basic weight (ISO 536), thickness and density (ISO 534), moisture content (ISO 287) were determined according to standardised methods. An optical microscope Leica S9i was used to take a picture of the paper surface. The surface roughness and porosity were determined using Bendtsen roughness and air permeability tester (ISO 8791-2, ISO 5636-2). Water absorptiveness was assessed as Cobb value (ISO 535). Among optical properties ISO brightness (ISO 2470), yellowness (DIN 6167), opacity and transparency (ISO 2471), absorption and scattering (ISO 9416), specular gloss (ISO 8254-1) were determined on felt (A) and wire (B) side. Among colorimetric properties, the CIELAB colour coordinates L^* , a^* , b^* , chroma C^* and hue h were measured. Print penetration was determined according to IGT W24 method and pick velocity according to ISO 3783. For picking or pick velocity we have used the middle viscous picking oil which has a value of 48 Pas. The print unevenness was determined with the image processing using GLCM (Gray Level Co-Occurrence Matrix) based texture features. The full tone prints were done on Pruefbau printability tester using offset test inks with process parameters of 200N, 0,3cm³ ink quantity and printing speed of 1m/s. The samples were dried for 24 hours to enable chemical drying and allow time for ink levelling out and the prints were scanned in 300 spi. For the image processing we have used the GLCM option of the radiomics package for R programming language. The samples were averaged from 4 angles (0°,45°,90°,135°) with an offset of 1 pixel.

3. RESULTS AND DISCUSSION

In Table 1 the basic properties of paper are presented. Low density of paper results from the absence of any filler added and from the brought distribution of fiber dimensions, resulting in poorer alignment of fibers and web connectivity. High standard deviation for thickness and density of paper suggest that paper is less homogeny, with higher variation in thickness and density as papers obtained from the wood fibres.

Table 1: Basic properties of paper given as mean value and standard deviation

Sample	Basic weight (g/m ²)	Thickness (μm)	Density (kg/m ³)	Moisture content (%)
Paper from JK	90.9 ± 2.37	157 ± 19.15	586.2 ± 76.91	4.73 ± 0.22

In Table 2 surface and optical properties of paper are presented. High value of surface roughness and air permeability show that paper is less dense, with high porosity and surface unevenness. Despite of high air permeability and low density, water absorptiveness is low, mainly because sizing agents were added in the paper production process. Low value of lightness and ISO brightness, beside positive values of colour coordinates a^* and b^* tell us, that paper has “natural” yellow look. That is confirmed with the quite high value of yellowing index. As bleaching of fibres was not applied obtained values were expected. Both values of scattering and absorption coefficient are in the range of unbleached chemical pulp. A high surface roughness coincides with a low value of specular gloss. The measurements on felt and wire side revealed the only noticeable difference in surface roughness.

Table 2: Surface and optical properties of felt and wire side of paper

Properties	Felt side	Wire side
Water absorptiveness C_{60} (g/m ²)	12.01	16.84
Surface roughness (ml/min)	2080	1820
Air permeability (ml/min)	540	540
ISO brightness (%)	39.88	39.40
Yellowness (%)	35.70	36.04
Florescence (%)	0.26	0.02
Opacity (%)	98.94	98.59
Transparency (%)	8.51	9.62
Absorption coefficient (m ² /kg)	7.06	6.97
Scattering coefficient (m ² /kg)	35.81	35.14
Specular gloss (%)	4.33	/
L* / a* / b*	78.01 / 2.41 / 16.22	77.86 / 2.47 / 16.35
C* / h	16.40 / 81.54	16.53 / 81.41

In Table 3 some of the printing properties that were determined are presented. The picking of paper is defined as the damage of the paper surface caused by tensile force during the printing operation. The pick velocity is defined as the velocity at which picking starts. Higher is the surface strength of the paper, the higher is velocity. The pick velocity around 2 m/s is for uncoated paper adequate. Viscosity velocity product (VVP) with the value around 100 confirms, a good pick resistance of paper. Good surface strength was influenced by the type of fibres, where the presence of long fibres improved the strength, by the treatment of fibres and proper surface sizing.

Low print gloss means that ink has poor reflective properties. It is related to excessive ink penetration into the paper and high surface roughness. Print penetration is related to absorption, roughness and porosity of paper surface. A rather high value of print penetration obtained is the result of high oil absorptiveness and porosity of paper surface.

Table 3: Printing properties of paper given as mean value and standard deviation

Sample	Pick velocity (m/s)	Print penetration (1000/mm)	Print gloss (%)
Paper from JK	2.03 ± 0.19	30.74 ± 0.95	2.93 ± 0.08

In Table 4 GLCM parameters, which describe the print unevenness are presented. The GLCM entropy is the measure of spatial disorder, and a high value obtained means that structure (texture) is less organized and the image is nonhomogeneous. GLCM values are dimensionless and in this case the entropy is rather high which indicates high mottling which can be also notices in Figure 1. GLCM Contrast is very dependent on the angle orientation of the inhomogeneous areas and this value indicates that is prominent in all directions.

Table 4: GLCM parameters of paper given as mean value and standard deviation

Sample	GLCM energy	GLCM correlation	GLCM entropy	GLCM contrast
Paper from JK	0.0001 ± 0.00002	0.805 ± 0.054	9.203 ± 0.141	453.64 ± 124.83

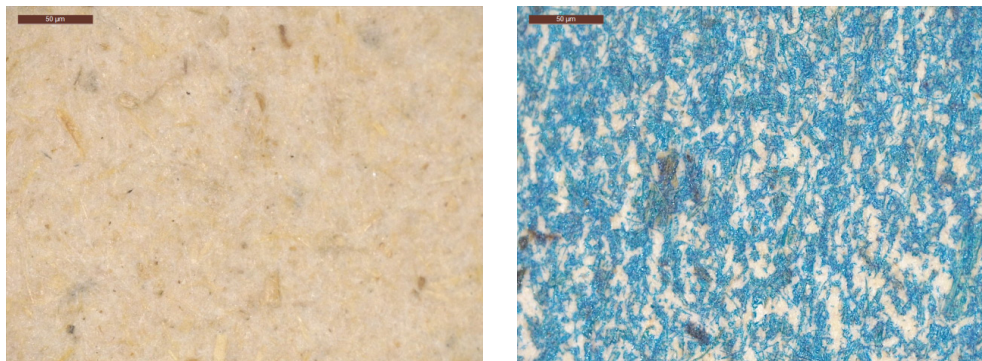


Figure 1: OM image of paper surface and print

4. CONCLUSIONS

Paper obtained from Japanese knotweed was produced on a pilot paper machine, in order to access the possibility of producing a paper with the adequate properties from the annual plant residue. The roughness of the paper and porosity are quite high, and the specular gloss low, which could be improved with better refining of fibers, cleaning to remove impurities, by adding the filler and by calendaring. Good surface strength and low water absorptiveness are connected to appropriate level of sizing of paper surface. The higher unevenness of surface, and larger number of impurities present, resulted in mottling. The brightness of paper is quite low, also because lignin and extractives were not completely removed in the fiber processing steps, and because no bleaching was applied.

The preliminary research has shown, that Japanese knotweed, as a cheap local raw material, could be used in paper making industry. However, to reach good printability characteristics of paper, mainly the fiber processing must be improved.

5. ACKNOWLEDGMENTS

Research is a part of the project "APPLAUSE - Alien Plant Species from harmful to useful with citizens' led activities", which is co-financed by EU Regional Development Fund.

6. REFERENCES

- [1] Biermann, C.J.: "Handbook of pulping and papermaking", 2nd ed, (Academic Press, Inc., San Diego, USA, 1996), page 633.
- [2] Britt, K.W.: "Handbook of pulp and paper technology", (Reinhold Publishing Corporation, New York, USA, 1964), page 44.
- [3] Mežnarič Osole, G., Jelenec, N., Dekleva, K.: "A friendly enemy Japanese knotweed in the paper laboratory", (Ljubljana, SI: Muzej za arhitekturo in oblikovanje, 2015)
- [4] Novak, G.: "Grafični materiali", (Naravoslovnotehniška fakulteta, OT, Ljubljana, SI: Univerza v Ljubljani, 2004), page 67.
- [5] Obi Reddy, K., Uma Maheswari, C., Shukla, M., Muzenda, E.: "Preparation, Chemical Composition, Characterization, and Properties of Napier Grass Paper Sheets", Separation Science and Technology 49(10), 1527-1534, 2014. doi: 10.1080/01496395.2014.893358.
- [6] Rousu, S., Gane, P., Eklund, D.: "Distribution of offset ink constituents in paper coating and implication for print quality", Proceedings of TAPPI Advanced Coating Fundamentals, (Chicago, USA, 2003).
- [7] Royal Horticultural Society, Japanese knotweed, Royal Horticultural Society, 2018, URL <https://www.rhs.org.uk/advice/profile?PID=218> (last request: 2018-09-27).
- [8] Saikia, S.N., Goswami, T., Ali, F.: "Evaluation of pulp and paper making characteristics of certain fast growing plants", Wood Science and Technology 31(6), 467-475, 1997. doi: 10.1007/BF00702569.



© 2018 Authors. Published by the University of Novi Sad, Faculty of Technical Sciences, Department of Graphic Engineering and Design. This article is an open access article distributed under the terms and conditions of the Creative Commons Attribution license 3.0 Serbia (<http://creativecommons.org/licenses/by/3.0/rs/>).

THE EFFECT OF BEATING ON THE DYEING OF CELLULOSE

Öznur Özden ¹ , Sinan Sönmez ² 

¹ *Istanbul University, Faculty of Forest, Department of Forest Product Chemistry and Technology, Istanbul, Turkey*

² *Marmara University, School of Applied Sciences, Department of Printing Technologies, Istanbul, Turkey*

Abstract: *Dyes and pigments are important colorants used in dyeing of paper, cardboard, fabric, food, plastic, wood materials. The dyes and pigments used for this are very diverse and have a wide range. With the increasing in demand for dyed paper day by day, the development of new technologies has become necessary. Since the natural colour of the paper is not much of a concern, the papers have been started to be dyed in different shapes to obtain products with shades ranging from bright pastel to dark and saturated tones. Tone and density can be adjusted according to need and requests. Colouring in paper is usually coloured by adding pigments or dyes to the pulp during pre-production preparation. Almost 95% of dyed papers are prepared in this way. For this purpose, direct acidic and basic dyes are used. The effectiveness used pigment or dye varies depending on the raw material and the environmental conditions. The purpose of this study, beating and pH is to improve the effect on cellulosic dyeing and paper properties. For this, two different types of pulp were selected as bleached softwood kraft pulp (BSWP) and bleached hardwood kraft pulp (BHWP). The dyeing process was carried out using four different colours in the beaten and the unbeaten pulp (60minute with Valley's beater). They produced sheets from the dyed pulp. It was made colour measurements on the produced sheets and compared obtained values. The results will help to give an idea of the effectiveness of coloured inks used during printing on coloured paper.*

Key words: dye, pigments, beating, kraft pulp

1. INTRODUCTION

Wood fibers are divided into two groups as softwood and hardwood. Hardwood is from deciduous trees such as birch, eucalyptus and poplar. Hardwood fibers, for example European birch, are usually 1-1.5 mm long and 16-22 µm in diameter. Softwood is from coniferous trees such as spruce and pine. Softwood fibers on the other hand, for example European spruce or pine, are 2.5-3.6 mm long and 24-59 µm in diameter (Daniel, 2009; Karlsson, 2006).

By Casey; "Any type of fiber used in paper making can be painted, but they take different colours. The difference in the characteristics of the fibers according to the tree type is effective in this. Hardwood pulp fibers are more round and bulky than softwood fiber. They have a larger surface area than a similar weight of softwood fiber. Since in dyeing paper the surface of the fiber is dyed, the same amount of dye used on a hardwood pulp will produce a lighter shade than on softwood furnish. In a mixed furnish containing a blend of both types of fiber, the shade will be lighter if the proportion of hardwood pulp is increased" (Casey, 1980).

Nowadays new technologies have been developed for painted paper. Because the natural colour of the paper is not very popular, the paper has started to be painted in different ways to produce products with shades ranging from glossy pastels to dark colours to saturated shades. Tone and density can be adjusted according to needs and requirements.

The papers are usually coloured by adding a colorant to the paper stock in the preparation stage. Nearly 95% of the dyed papers are prepared in this way. For this purpose, direct acidic and basic dyes are used. Since the paint penetrates all the fibers of the paper, the most efficient treatment is the dyeing of the substances (Drzewińska, 2008).

Beating or refining is one of the most important process in paper making.. It not only controls the properties of the finished sheet, as mentioned Often the effect of beating on strength (e.g. tensile, elastic modulus, Scott-Bond) is explained simply by increased inter fibre bonding. Most frequently it is assumed that bonding improves because beating increases fibre flexibility. Runnability increases cellulose of beating. It also affects the mechanical properties and structure of the paper (Hiltunen, 2003; Casey, 1980).

Beating process brings changes to the structure and properties of fibers, such as fiber swelling, fiber shortening, internal and external fibrillation, etc. Chemical pulp fibres swell as a result of beating. Fibre swelling is often called internal fibrillation (Lecourt, Sigoillot & Petit-Conil, 2010).

Writing and printing papers are usually produced from bleached chemical softwood or hardwood pulps. The quantity of these pulps and their brightness have an impact on the final optical properties of the paper produced.

2. MATERIAL AND METODS

Bleached softwood and hardwood kraft pulp were used for this study. Both pulp are supplied from a commercial paper mill. Bleached hardwood and softwood pulp in proportion 1:1, with beating degree 40°SR (Schopper Riegler). Pulp beating was carried out on laboratory scale in a Valley's beater according to Standard PN-ISO 5264-1:1999. Four-color dye was used to stain pulp. Paper was prepared from the dyed pulp in two different weights. The dyes were added to a 1,5 % pulp suspension at a temperature of 20 °C, with a pH of approx. 8. The contact time of dyeing substances with the pulp amounted to 30 minutes. Dyed sample papers were produced as handmade paper on a British paper machine (Figure 1, 2 and 3)

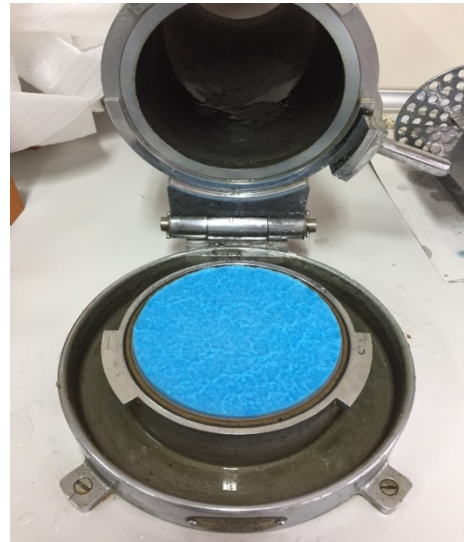


Figure 1: British type hand paper machine Figure 2: British type hand paper machine and painted paper sheet



Figure 3: Samples of paper painted in different colours

2.1 The Determination of Coloured Papers Properties

The thickness of the coated recycled paperboard samples were measured using a TMI Micrometer. Air permanence was measured used an L&W Air Permeance Tester (Tappi T 460 om – 88) and roughness was measured using a L&W Bendtsen Tester (Tappi T 479 om – 91). L*, a*, b* colour values of the coloured and white papers were measured using X-Rite eXact Densitometer. It was used A BYK Gloss Meter for determining gloss values of the printed samples and the coloured and white papers as ISO 2813 (Sonmez, 2017).

3. RESULTS AND DISCUSSION

Thickness, grammage, Porosity and Roughness are among the most important structural properties of paper that characterise for general description. The Physical properties of high grammage and Low grammage coloured papers are given in In Table 1 and Table 2. Roughness value of Low grammage coloured papers is lower than Low grammage coloured papers. Its means Low grammage coloured papers is smoother. But, they have more air permeability than them due to their low air permeability and thickness.

Table 1: The Properties of High Grammage Coloured Papers using Cyan, Magenta, Yellow and Black

Ink	High grammage			
	Grammage (g/m ²)	Thickness (μm)	Porosity (ml/min)	Roughness (ml/min)
Cyan	54	1	85	275
Magenta	74	1	79,1	379
Yellow	69	1	73,4	466
Black	46	1	89,5	232

Table 2: The Properties of Low Grammage Coloured Papers using Cyan, Magenta, Yellow and Black

Ink	Low grammage			
	Grammage (g/m ²)	Thickness (μm)	Porosity (ml/min)	Roughness (ml/min)
Cyan	36	0,5	178	186
Magenta	29	0,5	189	180
Yellow	32	0,5	279	196
Black	32	0,5	214	220

In Figure 4, the L* values of the coloured and white papers are given depending on the grammage change. Figure 4 showed that lightness values of the low grammage-coloured papers was higher than the high grammage-coloured papers.

While, compared the lightness value of the white paper, the use of Cyan, Magenta and Black inks in the coloured-paper production was decreased the Lightness values, the use of Yellow inks had not effected significantly. Lightness is a major indicator for a good print (Sonmez & Oguz, 2017). Therefore, the higher the lightness, the lower the colour saturation. So, Yellow-coloured paper has lower colour saturation than other coloured paper.

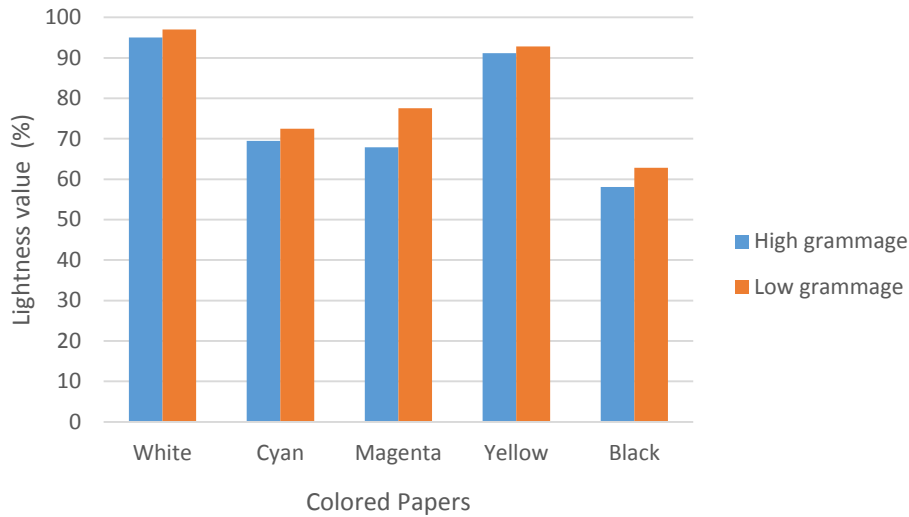


Figure 4: Lightness values of white paper and Coloured Papers using Cyan, Magenta, Yellow and Black

High chroma indicates high colour saturation, which is an important property for good quality paper, which including high colour gamut (Sonmez, 2011). Depending on the grammage change, the chroma values of the coloured and white papers are given in Figure 5. Having grammage of the coloured paper decreased, chrome values of all samples unlike Black were appear to be a noticeable reduced. These decrease were showed that colour gamut of the low grammage-coloured paper samples is the smaller than the low grammage-coloured paper samples. The higher chroma value was obtained in the high grammage-magenta-coloured paper.

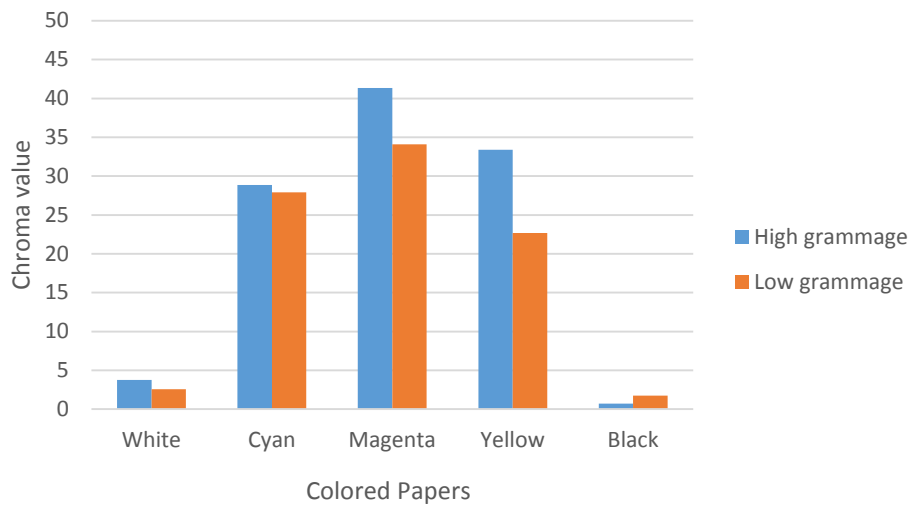


Figure 5: Chroma values of white paper and Coloured Papers using Cyan, Magenta, Yellow and Black

The gloss values of the all samples was measured at 60° and calculated Delta Gloss 60°. In, Figure 6, Calculated Delta Gloss 60° values were given depending on the grammage change. The grammage change decreased, the colored-papers produced using Magenta and Black inks were reduced the Delta Gloss 60° value. Conversely, the colored-papers produced using Cyan and Yellow inks were increased the Delta Gloss 60° value.

Generally, the coloration of the papers increased the gloss values. Increased the gloss was an important property the printability parameters, as the visual quality was advanced (Sonmez & Ozden, 2016).

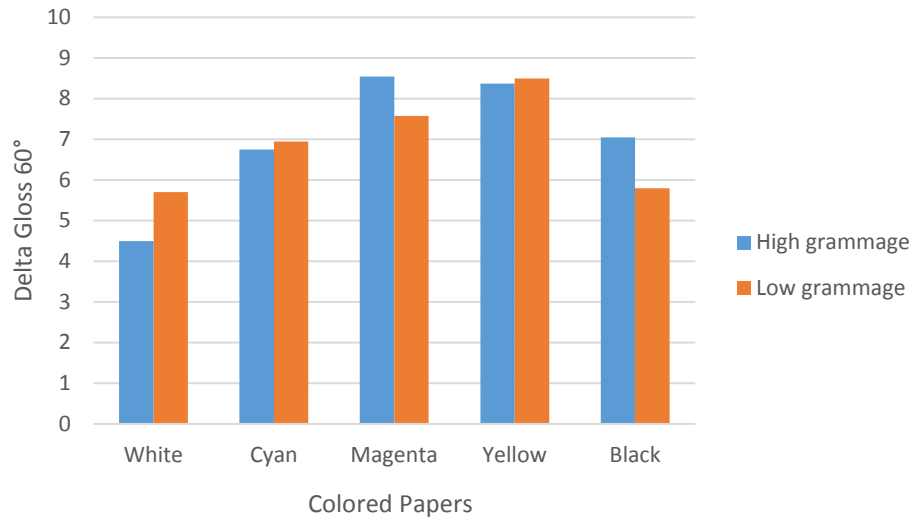


Figure 6: Delta Gloss 60° values of white paper and Coloured Papers using Cyan, Magenta, Yellow and Black

In Figure 7, the Delta E (ΔE) values of the coloured and white papers are given depending on the grammage change. Figure 7 showed that Delta E (ΔE) values of the low grammage-coloured papers was higher than the high grammage-coloured papers. This result shows that obtained different colour saturation in the Low and high grammage coloured papers.

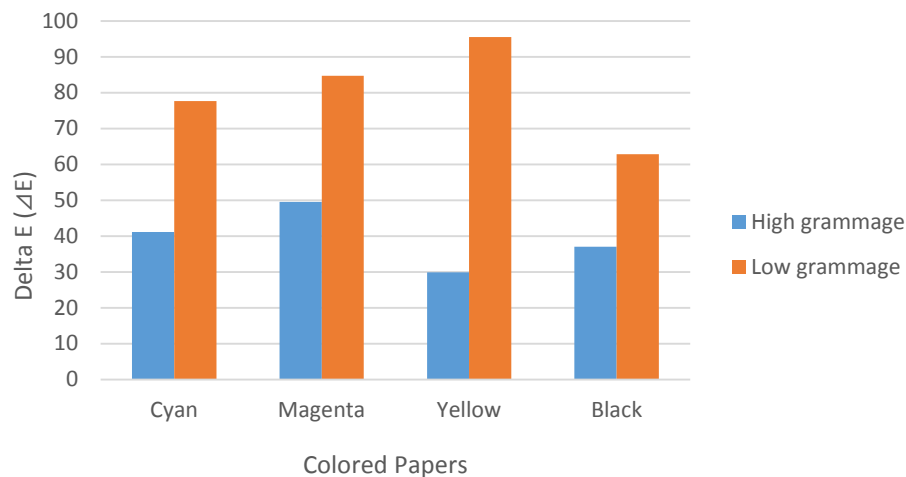


Figure 7: Delta E (ΔE) values of white paper and Coloured Papers using Cyan, Magenta, Yellow and Black

4. CONCLUSIONS

1. Lightness values of the low grammage-coloured papers was higher than the high grammage-coloured papers. Due to the fact that Yellow-coloured paper has high lightness, its colour saturation is lower than others coloured papers.
2. Grammage of the coloured paper decreased, chrome values of all samples unlike Black were appear to be a noticeable reduced. The higher chroma value was obtained in the high grammage-magenta-coloured paper. This show that the colour saturation value of the high grammage-magenta-coloured paper is high others coloured papers.
3. The coloured-papers produced using Cyan and Yellow inks were increased the Delta Gloss 60° value.
4. Delta E (ΔE) values of the low grammage-coloured papers and high grammage-coloured papers obtained different values. This result shows different colour saturation in the Low and high grammage coloured papers.




5. REFERENCES

- [1] Ander, P., Geoffrey, D.: "Differences between Scots pine and Norway spruce TMP pulps as revealed by the HCl method". Proceedings of IMPC: International Mechanical Pulping Conference (Södra Berget IMPC, Sundsvall, Sweden, 2009), pages 322-324.
- [2] Casey, J.P.: "Pulp and Paper Chemistry and Chemical Technology, 3rd ed. (Wiley, New York, 1980), pages 1627-1664.
- [3] Casey, J.P.: "Pulp and Paper Chemistry and Chemical Technology, 3rd ed. (Wiley, New York, 1980), pages 821-958.
- [4] Hiltunen, E.: "On The Beating Of Reinforcement Pulp", (Laboratory of Paper Technology Reports, Espoo, 2003).
- [5] Drzewińska, E.: "The Influence of Pulp on the Colour of Dyed Papers", *Fibres & Textiles in Eastern Europe* 16(1), 103-107, 2008.
- [6] Karlsson, H. *Fibre Guide: "Fibre analysis and process applications in the pulp and paper industry"*, (AB Lorentzen & Wettre, Kista, 2006).
- [7] Lecourt, M., Sigoillot, J. C., Petit-Conil, M.: "Cellulase-assisted refining of chemical pulps: Impact of enzymatic charge and refining intensity on energy consumption and pulp quality", *Process Biochemistry*, 45, 1274–1278, 2010. doi: 10.1016/j.procbio.2010.04.019.
- [8] Sonmez, S.: "Development of Printability of Bio-Composite Materials Using *Luffa cylindrica* Fiber", *Bioresources*, 12(1), 760-773, 2017.
- [9] Sonmez, S., Oguz, M.: "Investigation of Effect of Hot-Folio Printability of Mineral Pigments", *Oxidation Communications*, 40(2), 963-972, 2017.
- [10] Sonmez, S.: "Interactive Effects of Copolymers and Nano-sized Pigments on Coated Recycled Paperboards in Flexographic Print Applications", *Asian Journal of Chemistry*, 23(6), pages 2609-2613, 2011.
- [11] Sonmez, S. ve Ozden, O. (2016). : "The Use of Ultraviolet (UV) Ink in Prints of Paperboards Coated Carboxymethyl Cellulose (CMC)", *Proceedings of V. International Printing Technologies Symposium*, (V. International Printing Technologies Symposium, Istanbul, Turkey, 2016), page 215-133.



© 2018 Authors. Published by the University of Novi Sad, Faculty of Technical Sciences, Department of Graphic Engineering and Design. This article is an open access article distributed under the terms and conditions of the Creative Commons Attribution license 3.0 Serbia (<http://creativecommons.org/licenses/by/3.0/rs/>).

THE QUALITY ASSESSMENT OF BOOKBINDING STRENGTH FOR POLYVINYL ACETATE ADHESIVE (PVAc) AND NANO-MODIFIED PVAc ADHESIVES

Gorana Petković , Suzana Pasanec Preprotić , Marina Vukoje 
University of Zagreb, Faculty of Graphic Arts, Zagreb, Croatia

Abstract: One of the most common and cost-effective book binding method is adhesive binding method suitable for medium volume books (50-250 pages). Depending on run volume and printing technology, different adhesive binding techniques can be used. In this research, for short run book production, double-fan binding was used, because it can achieve up to 20% higher binding strength compared to perfect binding technique. In addition, for adhesive binding book production, polyvinyl acetate dispersions (PVAc), hot-melts (HM) and polyurethane adhesives (PUR) can be used. Today, water-based PVAc adhesives are more environmentally acceptable and numerous studies dealing with modification of PVAc adhesives have been carried out, in order to achieve the comparable or higher quality of adhesive joints for selected application. The aim of this research is to improve the binding performance of PVAc adhesive by adding 1% of nanoparticles, specifically hydrophobic fumed silica (SiO_2) or hydrophilic fumed titanium dioxide (TiO_2) powder. ISO specifies a test method (ISO 19594) for the quality assessment of adhesive binding by pulling out a single sheet from a book block, page-pull test. Pulled sheets have to be evaluated visually and in a consistent manner, since during the procedure the sheet can be pulled out completely without significant damage, ruptured roughly parallel to the binding edge, ruptured not parallel to the binding edge or show significant adhesive penetration. In this research, the binding strength of 8 specimens, at 4 different test positions (10%, 25%, 50% and 90% of the total number of pages), for 5 different groups of book blocks and 3 different types of PVAc adhesive (neat PVAc, PVAc + 1% SiO_2 , PVAc + 1% TiO_2) was evaluated. All the measurements were performed under the same conditions (volume, trimmed size, binding technique and conditions, drying and pressing time). For the evaluation of quality assessment of bookbinding strength, different paper types were used for each group - woodfree uncoated, woodfree coated, containing wood – bulky, woodfree office and office paper containing recycled fibres. According to ISO 19594 standard, quality levels for the binding strength of adhesive bound products are not enough. It is also necessary to calculate the coefficient of variation in order to evaluate the consistency of binding quality. According to obtained results, visual evaluation of test sheets and book blocks opening behaviour, the best quality was achieved for book blocks with PVAc + 1% SiO_2 adhesive. Compared to a neat PVAc, the binding strength for all groups of book blocks was 10 - 26% higher while coefficient of variation was 43 – 71% lower. Results for PVAc + 1% TiO_2 adhesive did not show any significant improvement or deterioration of the binding strength while coefficient of variation was notably lower, 4% - 58%, compared to neat PVAc.

Key words: binding strength, page-pull test, polyvinyl acetate adhesive, nano-modified adhesive

1. INTRODUCTION

According to European Federation for Print and Digital Communication volume of printed books will decline in favour of short runs, just-in-time, digitally printed books, together with an increased use of electronic publishing. Future business models have to meet new customer's requirements by switching to short run production, elimination of overstocking, allowing the customer to "sell first and print later", enabling versioning and personalization (Intergraf, 2015). All above described business models eliminate the need for storage and reduce publisher's profitable risk, but also may cause a reduction of delivery time and require constant and higher degree of the end product quality (Petković et al, 2017). Due to advancement in adhesive binding technology and shorter delivery time, adhesive binding is growing in popularity across all types of books and it is suitable for medium volume books (5-250 pages). The adhesive binding technique directly influence the quality of the end product. In perfect binding, the spine of the book block have to be mechanically pre-treated, in order to get higher roughness and enlargement of surface for adhesive application. In double-fan binding, book blocks are bending on both sides during adhesive application, allowing penetration of adhesive between leaves. The binding strength of double-fan binding is up to 20% higher with more uniform adhesive application (Petković et al, 2017). Currently used adhesives in bookbinding belong into three main categories: water-based emulsions (e.g. PVAc), hot melts (e.g. EVA) and reactive hot melts (e.g. PUR). Selection of adhesive type depends upon the nature of adherends, performance requirements, production volume and bonding processes. For the optimum performance,

adhesive should have excellent flexibility, toughness (without stiffness) and fatigue resistance. In addition, adhesive should have the ability of application in low-cost, high-speed processes and it should be able to survive storage conditions and repetitive stress (Petrie, 2008). Today, water-based adhesives are considerably more environmentally, they have the highest market share and they are mainly used in the paper industry (46.3%) (Jović et al, 2011). Water-based polyvinyl acetate adhesive (PVAc) has many desirable features and advantages, with only few limitations, as presented in Table 1.

Table 1: Main advantages and limitations of PVAc adhesive

	FEATURE	REFERENCE
ADVANTAGES	easy and wide for application (paper, plastic, metal foil, leather, cloth, wood, etc.)	(Paris, 2000; Šedivka et al, 2015)
	low cost and availability	(Ebnesajjad, 2008; Paris, 2000; Thomson, 2014)
	no toxicity problems	(Packham, 2005; Paris, 2000; Thomson, 2014)
	no aging problems	(Rebsamen, 1983)
	dried film holds high joint flexibility	(Thomson, 2014)
	does not damage the equipment	(Thomson, 2014)
	provides invisible, colourless and transparent glue lines	(Ebnesajjad, 2008; Salvini et al, 2009; Thomson, 2014)
LIMITATIONS	low resistance to weather and moisture	(Ebnesajjad, 2008; Salvini et al, 2009)
	poor resistance to most solvents	(Ebnesajjad, 2008; Salvini et al, 2009)
	slow setting speed	(Packham, 2005)
	curing for 1-7 days is recommended before handling	(Ebnesajjad, 2008)

Besides binding technique and adhesive selection, the proper paper selection is crucial to the end product quality as well. Compatible materials selection provides the best performance properties of book products, including page-pull, lay-flat and easy-open flexible spine characteristics (Petrie, 2008). The number of possible substrates, coatings and end uses are seemingly limitless, but 92% of all printed books in Europe are printed on woodfree paper (Intergraf, 2017).

Various studies have been focused on improving the properties of PVAc adhesives through their modification, especially by nanoparticles addition (nano clay, cellulose nanofibrils, silica or titanium dioxide) (Bardak et al, 2016; Wen et al, 2008; Aydemir et al, 2016; Laskowska et al, 2017). Properties of different conventional materials can be changed by nanoparticles addition while their small amount can cause significant changes in properties (Ramljak, 2017). In addition, these modifications can cause some side effects, such as a lower shelf-life, yellowing of adhesive or reduction of their performance (Tanket et al, 2016; Bonnefond et al, 2013). The adhesive industry continues to develop, and it is focus on improvements in drying mechanisms, bond strength, flexibility and application versatility.

2. MATERIALS AND METHODS

2.1 Materials

2.1.1 Paper

For a book production five types of paper were used as listed in Table 2. All of them belong to a different paper type group, based on fibre composition.

Table 2: List of used papers

TRADE NAME	TYPE	GRAMMAGE [g/m ²]	ABBREVIATION
Amber Graphics	woodfree uncoated	100	WFU
Garda Gloss	woodfree coated	115	WFC
Munken White	containing wood (bulky)	90	CW
Navigator Universal	woodfree, office	80	WF office
Recy Office	containing recycled (100%), office	80	CR office

2.1.2 Adhesive

Used polyvinyl acetate adhesive (Signokol L) is water dispersion of vinyl acetate homopolymers with polyvinyl alcohol and addition of plasticizers. According to material safety data sheet, it has 45 ± 2% of solid

content and the varying amount of water (0 – 5 %) can be added. Preliminary study showed that the best adhesion was achieved with 0 – 2.5% of water (Petković et al, 2016) and thus in this research, no water was added in order to eliminate water as an influential factor.

2.1.3 Nanoparticles

For PVAc adhesive modification, hydrophobic fumed silica (SiO₂, AEROSIL R 8200) and hydrophilic fumed titanium dioxide (TiO₂, AEROXIDE P25) were used. Both are odourless, solid, white powders with approximately same tamped density (140 g/L), but a different BET surface area (135 – 185 m²/g - SiO₂; 35 – 65 m²/g – TiO₂) and assay based on ignited material (SiO₂ ≥ 99.8%; TiO₂ ≥ 99.5%).

2.2 Methods

2.2.1 Adhesive preparation

Three types of adhesives were used – neat PVAc adhesive and PVAc adhesive modified with 1% of SiO₂ and 1% of TiO₂ nanoparticles. After adding 1% of nanoparticles to neat PVAc adhesive, IKA T 25 digital ULTRA-TURRAX disperser was used for mixing and adhesive homogenisation. Adhesive was stirred for 15 minutes, firstly 5 minutes at lower stirring speed (from 3500 to 7000 rpm) and then 10 minutes at 7000 rpm. The same mixing procedure was used for both nano-modified adhesives.

2.2.2 Specimens preparation

For the determination of binding strength, 120 book blocks were made (24 for each paper type). According to ISO 19594 standard guidelines, at least five specimens for each test should be used. In this research, 8 specimens for each test were measured. All book blocks were unprinted, without covers, with volume of 100 pages and 165 x 240 mm in trimmed size. Binding units were individual leaves, bonded with double-fan binding technique, pressed for 48 and dried for 72 hours. Spine width was 5-7 mm, depending on paper type and grammage. Binding was performed at room temperature of 20 ± 5 °C and relative humidity of 35 – 75 %.

2.2.3 Determination of the tensile index (T)

Tensile index (T) was determined according to standard method (ISO 1924-1). Measurements were performed on Enrico Toniolo Dynamometer Tensomini Super machine. Tensile index can be calculated from paper tensile strength according to Equation 1.

$$T = \frac{F}{g} \left[\frac{Nm}{g} \right] \quad (1)$$

Where: F – tensile strength, g – paper grammage.

2.2.4 Determination of the binding strength (BS)

According to ISO 19594, the binding strength is evaluated by pulling out a single sheet from the book block and measuring the maximum force resulting from the page-pull procedure. Page-pull test was performed according ISO 187, standardized conditioning and testing atmosphere, on IDM Page Pull Tester (model P0011). In addition to measurement of the maximum force, it is necessary to inspect all tested sheets, record their states and classify them in one of four categories listed in Table 3. Tested sheets marked with D should be excluded from any calculation. Tested sheets marked with B or C should be marked with “>” and excluded from the calculation of the coefficient of variation.

Table 3: Test sheet state classification

STATE OF TESTED	A	pulled out completely without significant damage
	B	ruptured roughly parallel to the binding edge
	C	with the rupture extending to the binding edge
	D	with significant glue penetration

The binding strength (BS) of the specimen is calculated according to ISO 19594:2017 and Equation 2. The quality levels for the evaluation of obtained binding strength results are listed in Table 4.

$$BS = \frac{F_{max}}{l} \left[\frac{N}{cm} \right] \quad (2)$$

Where: F – maximum force, l – spine length.

Table 4: The ISO 19594 quality levels for the evaluation of binding strength (QL_{BS})

QUALITY LEVEL (QL_{BS})	BINDING STRENGTH [N/cm]
very good durability	> 7.0
good durability	≤ 7.0 ; > 6.1
sufficient durability	≤ 6.1 ; > 5.1
poor durability	≤ 5.1

The quality levels for the consistency of binding quality, based on coefficient of variation (CV), are listed in Table 5.

Table 5: The ISO 19594 quality levels for the consistency of the binding quality (QL_{CV})

QUALITY LEVEL (QL_{CV})	COEFFICIENT OF VARIATION
very good consistency	≤ 0.10
good consistency	> 0.10; ≤ 0.15
sufficient consistency	> 0.15; ≤ 0.20
poor consistency	> 0.20

2.2.5 Determination of drape factor (DF)

Drape factor (DF) of paper is the main factor influencing the book block opening behaviour (drapeability). It represent single unglued sheet of paper and indicates how much leverage a paper is capable of exerting at the glue line (Jermann, 2008). After measurement of paper extend length, until it drops one inch at the leading edge, drape factor was evaluated according to Equation 3.

$$DF = \frac{l}{2.54} \times 10 \quad (3)$$

Where l represents extend length of paper.

3. RESULTS

3.1 Paper tensile index

Calculated tensile index values, for machine (MD) and cross (CD) directions are presented in Table 6.

Table 6: Paper tensile indexes

PAPER	TENSILE INDEX (MD) [Nm/g]	TENSILE INDEX (CD) [Nm/g]
WFU	47.09	23.29
WFC	31.66	18.41
CW	45.68	16.96
WF office	76.03	28.51
CR office	41.15	14.03

3.2 Binding strength quality and binding quality consistency

Every book block specimen, with spine thickness of at least 10 mm, should be tested at minimum three test positions (10 %, 50 % and 90 % of total number of pages). Book blocks with thickness less than 10 mm can be tested only at one test position. During page-pull procedure, 8 specimens for every adhesive and paper type were measured at four different test positions – 10 %, 25%, 50 % and 90 % (binding unit: 5, 13, 25 and 45). All binding strength results are listed in Tables 7 – 11, with the state of tested sheet classification

(A-D), total mean values, standard deviation and coefficient of variation. Considering the obtained results and quality levels listed in Tables 4 and 5, description of a binding strength and binding quality consistency is presented. Considering the mean values for binding strength and coefficient of variation of neat PVAc as reference value, percentage for durability and consistency improvement (e.g. binding strength enhancement and coefficient of variation reduction) is calculated and presented in the two last rows of each table.

Table 7: Binding strength (BS) and coefficient of variation values (CV), for WFU book blocks, with binding (QL_{BS}) and consistency (QL_{CV}) quality levels. Durability and consistency improvement of nano-modified adhesives compared with a neat PVAc [%].

WFU – 100 g/m ² [N/cm]																								
	PVAc (reference)								PVAc + 1% SiO ₂								PVAc + 1% TiO ₂							
	10%		25%		50%		90%		10%		25%		50%		90%		10%		25%		50%		90%	
1	9.89	A	5.64	B	9.44	A	18.3	D	9.14	A	9.46	A	16.3	D	10.0	A	8.42	A	8.73	A	12.4	D	8.33	A
2	7.85	A	9.44	B	9.39	A	9.8	C	10.0	A	14.4	D	9.71	A	9.35	A	8.67	A	8.61	A	12.5	D	9.27	A
3	8.46	A	13.9	D	8.39	A	18.2	D	10.4	A	9.14	B	9.02	C	9.69	A	9.10	A	15.1	D	9.21	A	8.08	A
4	9.96	C	9.71	A	9.79	B	9.64	A	9.89	A	10.2	B	10.3	C	9.37	A	10.1	D	9.10	A	15.8	D	7.25	A
5	9.60	A	8.83	B	9.50	A	16.8	D	10.1	A	14.4	D	14.7	D	9.52	A	8.87	A	9.14	A	8.83	B	7.66	A
6	9.96	A	9.94	B	4.79	B	9.27	A	8.81	A	9.52	C	9.14	A	9.42	A	9.35	A	9.46	A	6.81	A	9.50	A
7	9.71	A	18.3	D	8.54	A	16.3	D	9.39	A	9.48	A	9.62	A	9.08	A	9.00	B	6.75	A	15.3	D	7.42	A
8	8.29	A	6.04	A	5.04	B	8.42	C	16.3	D	9.25	A	14.2	D	9.39	A	8.87	A	14.4	D	6.66	A	8.75	A
\bar{x}	8.669								9.562								8.437							
σ	0.988								0.379								0.888							
BS	> 8.7								> 9.6								> 8.4							
QL (BS)	very good durability								very good durability								very good durability							
CV	0.109								0.039								0.105							
QL (CV)	good consistency								very good consistency								good consistency							
durability improvement (BS enhancement):									+ 10.30 %									- 2.68 %						
consistency improvement (CV reduction):									- 63.89 %									- 4.26 %						

Table 8: Binding strength (BS) and coefficient of variation values (CV), for WFC book blocks, with binding (QL_{BS}) and consistency (QL_{CV}) quality levels. Durability and consistency improvement of nano-modified adhesives compared with a neat PVAc [%].

WFC – 115 g/m² [N/cm]																										
	PVAc (reference)								PVAc + 1% SiO ₂								PVAc + 1% TiO ₂									
	10%		25%		50%		90%		10%		25%		50%		90%		10%		25%		50%		90%			
1	3.08	A	3.81	A	2.10	A	7.69	A	5.98	A	3.73	A	3.25	A	4.02	A	2.62	A	2.25	A	5.73	A	8.83	A		
2	5.42	A	2.44	A	2.54	A	3.29	A	6.69	A	6.04	A	4.56	A	8.54	A	5.75	A	3.79	A	2.96	A	2.83	A		
3	2.25	A	3.80	A	2.60	A	8.50	A	4.85	A	4.27	A	3.35	A	6.02	A	2.87	A	4.85	A	3.54	A	2.12	A		
4	2.17	A	2.77	A	2.91	A	6.44	A	5.39	A	5.98	A	3.46	A	4.69	A	4.58	A	2.29	A	2.60	A	3.33	A		
5	3.92	A	2.69	A	4.98	A	3.62	A	5.48	A	3.48	A	4.00	A	5.64	A	2.79	A	3.35	A	5.31	A	3.52	A		
6	5.75	A	5.19	A	3.31	A	5.79	A	4.60	A	3.23	A	3.92	A	4.67	A	2.29	A	4.75	A	2.64	A	2.46	A		
7	3.68	A	2.50	A	2.19	A	7.58	A	6.12	A	4.08	A	6.52	A	5.10	A	2.37	A	2.35	A	2.04	A	4.83	A		
8	3.21	A	7.21	A	2.67	A	3.39	A	6.69	A	6.79	A	6.87	A	5.95	A	3.62	A	2.96	A	5.44	A	5.46	A		
\bar{x}	4.047								5.125								3.662									
σ	1.810								1.300								1.494									
BS	4.0								5.1								3.7									
QL (BS)	poor durability								sufficient durability								poor durability									
CV	0.447								0.254								0.408									
QL (CV)	poor consistency								poor consistency								poor consistency									
durability improvement (BS enhancement):									+ 26.64 %									- 9.50 %								
consistency improvement (CV reduction):									- 43.28 %									- 8.83 %								

Table 9: Binding strength (BS) and coefficient of variation values (CV), for CW book blocks, with binding (QL_{BS}) and consistency (QL_{CV}) quality levels. Durability and consistency improvement of nano-modified adhesives compared with a neat PVAc [%].

CW – 90 g/m² [N/cm]																								
	PVAc (reference)								PVAc + 1% SiO₂								PVAc + 1% TiO₂							
	10%		25%		50%		90%		10%		25%		50%		90%		10%		25%		50%		90%	
1	11.5	D	8.31	A	13.7	D	9.69	C	10.2	A	17.7	D	10.9	A	10.6	A	9.96	B	8.29	A	15.8	D	8.94	A
2	4.23	A	9.67	A	8.94	A	9.81	A	9.81	A	10.1	A	9.31	A	13.3	D	15.4	D	16.7	D	10.6	D	8.94	A
3	9.75	B	9.06	A	5.60	B	9.81	A	9.56	C	9.23	A	9.79	A	17.6	D	15.4	D	13.5	D	9.89	A	7.58	B
4	9.25	A	9.81	A	7.71	C	9.85	A	10.1	A	16.6	D	9.89	A	9.39	A	9.35	A	9.31	A	14.7	D	7.04	A
5	20.0	D	9.92	A	14.7	D	9.58	A	9.75	A	9.58	A	10.7	A	18.2	D	9.44	A	13.4	D	9.71	A	7.25	A
6	8.60	C	9.58	A	8.10	A	15.1	D	9.33	B	17.5	D	9.67	A	10.2	B	7.67	A	14.3	D	7.83	B	9.38	A
7	14.9	D	14.9	D	9.50	B	13.2	D	10.1	A	10.2	B	10.1	A	9.23	B	9.44	A	7.31	A	8.10	A	7.77	B
8	7.92	B	9.83	A	8.37	C	9.17	B	9.33	A	9.08	A	9.56	A	9.31	A	9.04	A	16.3	D	9.39	A	8.85	A
\bar{x}	8.837								9.828								8.659							
σ	1.434								0.500								0.878							
BS	> 8.8								> 9.8								> 8.6							
QL (BS)	very good durability								very good durability								very good durability							
CV	0.159								0.051								0.100							
QL (CV)	sufficient consistency								very good consistency								good consistency							
durability improvement (BS enhancement):									+ 11.21 %									- 2.01%						
consistency improvement (CV reduction):									- 68.13 %									- 37.01 %						

Table 10: Binding strength (BS) and coefficient of variation values (CV), for WF office book blocks, with binding (QL_{BS}) and consistency (QL_{CV}) quality levels. Durability and consistency improvement of nano-modified adhesives compared with a neat PVAc [%].

WF office – 80 g/m ² [N/cm]																								
	PVAc (reference)								PVAc + 1% SiO ₂								PVAc + 1% TiO ₂							
	10%		25%		50%		90%		10%		25%		50%		90%		10%		25%		50%		90%	
1	3.96	A	9.04	A	4.08	A	15.6	D	9.87	A	8.96	C	15.7	D	8.73	A	8.81	A	8.62	A	9.21	A	8.12	A
2	9.29	A	9.56	A	8.89	A	7.94	B	8.77	A	10.3	A	8.75	C	15.2	D	9.25	B	8.81	A	8.21	A	8.12	A
3	5.64	A	9.44	A	15.2	D	9.04	C	8.85	B	10.3	A	9.48	A	8.67	B	8.60	A	9.17	A	9.14	A	9.08	A
4	9.64	A	6.42	A	8.92	B	10.1	D	10.0	C	8.89	C	9.54	A	8.71	A	7.44	A	8.35	A	5.48	A	7.85	A
5	7.10	C	8.95	C	7.62	A	14.8	D	10.5	A	9.85	B	9.60	C	10.4	C	8.60	A	7.56	A	5.83	A	9.04	A
6	9.33	A	9.31	B	8.87	A	18.2	D	8.89	A	9.12	A	10.0	C	14.1	D	9.33	A	9.00	A	7.17	A	8.73	A
7	8.71	A	9.17	A	9.56	A	9.06	C	8.98	A	10.1	A	9.94	A	9.19	A	9.35	A	8.92	A	15.6	D	9.35	A
8	7.94	A	9.21	A	5.19	A	5.79	C	8.71	A	8.75	B	9.27	C	16.4	D	7.46	A	8.44	A	16.2	D	6.94	A
\bar{x}	8.063								9.406								8.334							
σ	1.875								0.637								0.984							
BS	> 8.1								> 9.4								> 8.3							
QL _(BS)	very good durability								very good durability								very good durability							
CV	0.235								0.067								0.118							
QL _(CV)	poor consistency								very good consistency								good consistency							
durability improvement (BS enhancement):									+ 16.65 %								+ 3.36 %							
consistency improvement (CV reduction):									- 71.37 %								- 49.58 %							

Table 11: Binding strength (BS) and coefficient of variation values (CV), for CR office book blocks, with binding (QL_{BS}) and consistency (QL_{CV}) quality levels. Durability and consistency improvement of nano-modified adhesives compared with a neat PVAc [%].

CR office – 80 g/m ² [N/cm]																								
	PVAc (reference)							PVAc + 1% SiO ₂							PVAc + 1% TiO ₂									
	10%		25%		50%		90%		10%		25%		50%		90%		10%		25%		50%		90%	
1	8.56	C	9.46	A	9.79	A	9.89	B	9.08	A	9.23	A	9.54	A	7.92	B	9.54	B	12.5	D	9.19	A	6.98	A
2	9.35	A	5.89	A	7.89	A	9.14	C	9.29	B	9.64	A	8.42	A	8.02	A	8.10	A	7.96	A	7.62	A	8.12	A
3	7.54	A	8.62	A	5.69	A	12.3	D	8.64	A	9.27	A	7.54	C	8.92	A	9.52	B	8.27	A	8.25	A	7.06	A
4	4.23	B	6.94	C	8.00	A	9.83	C	9.48	A	9.31	A	9.21	A	7.60	A	9.50	A	8.67	A	8.25	A	6.67	B
5	5.04	A	4.54	A	7.64	C	9.37	B	8.19	C	9.29	B	8.67	A	8.98	A	8.21	A	9.29	A	9.21	B	6.44	A
6	4.58	C	7.94	C	8.67	A	12.0	D	9.33	A	9.25	A	9.14	A	7.98	B	10.4	D	8.02	A	9.04	A	7.37	B
7	6.52	C	9.71	C	6.98	B	8.29	C	8.54	A	9.42	A	7.17	A	8.77	A	8.52	A	8.12	A	7.06	A	6.50	B
8	6.67	B	8.00	C	7.80	B	9.00	B	9.87	C	9.35	B	8.10	A	8.54	B	7.73	A	9.29	A	7.87	A	8.75	A
\bar{x}	7.720							8.804							8.171									
σ	1.737							0.627							0.773									
BS	> 7.7							> 8.8							> 8.2									
QL (BS)	very good durability							very good durability							very good durability									
CV	0.230							0.071							0.094									
QL (CV)	poor consistency							very good consistency							very good consistency									
durability improvement (BS enhancement):								+ 14.03 %							+ 5.84 %									
consistency improvement (CV reduction):								- 69.27 %							- 58.97 %									

3.3 Book opening behaviour

Book blocks may show large differences in their opening behaviour, which mainly depends upon the nature of adhesive, binding technique and used paper. Figures 1 – 5 show differences in opening behaviour for book blocks made of the same paper type, but with different adhesive applied. Book block opening place was the same for all book blocks, at 75% of total number of pages - between page 74 and 75.



Figure 1: Opening behaviour of WFU book blocks (PVAc; PVAc + 1%SiO₂; PVAc + 1%TiO₂)



Figure 2: Opening behaviour of WFC book blocks (PVAc; PVAc + 1%SiO₂; PVAc + 1%TiO₂)

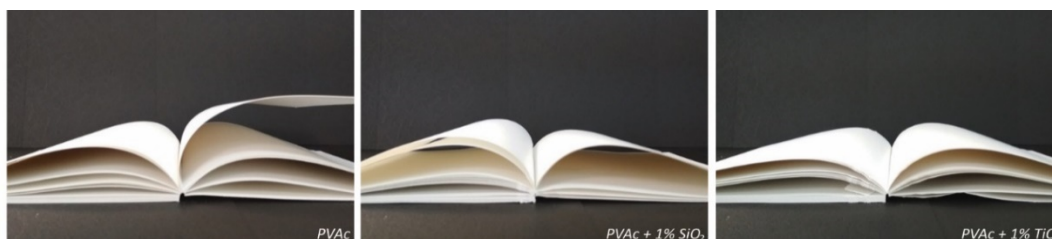


Figure 3: Opening behaviour of CW book blocks (PVAc; PVAc + 1%SiO₂; PVAc + 1%TiO₂)

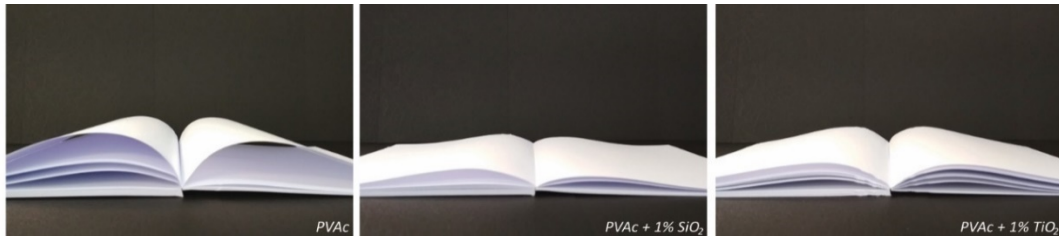


Figure 4: Opening behaviour of WF office book blocks (PVAc; PVAc + 1%SiO₂; PVAc + 1%TiO₂)



Figure 5: Opening behaviour of CR office book blocks (PVAc; PVAc + 1%SiO₂; PVAc + 1%TiO₂)

Paper drape factor values for machine direction (MD) of all used papers are listed in Table 12.

Table 12: Paper drape factor values

PAPER	WFU	WFC	CW	WF office	CR office
DRAPE FACTOR (MD)	33	30	29	27	25

4. DISCUSSION

According to the page-pull binding strength results (as quality measure of the binding quality) durability of 12 out of 15 groups of book blocks was classified as very good (> 9,8 N/cm to > 7.7 N/cm). Other 3 groups (WFC paper) have poor or sufficient durability (3.7 N/cm to 5.1 N/cm). Due to the fact that paper sets the criteria for a book's structure (Jermann, 2004), all together with adhesive and paper-adhesive compatibility the criteria for a binding quality, it is necessary to observe how paper type can affect the binding quality. Thus, three different characteristics must be observed: paper bindability (binding strength), paper strength (tensile index) and paper stiffness (drape factor).

Maximum binding strength was achieved for CW book blocks (> 9.8 to >8.6 N/cm), followed by WFU (> 9.6 to > 8.4 N/cm), WF office (> 9.4 to > 8.1 N/cm) and CR office (> 8.8 to > 7.7 N/cm) book blocks. The poorest binding strength was achieved for WFC book blocks (3.7 to 5.1 N/cm) (Figure 6). The binding strength order was the same for all used adhesives. Considering the paper type, obtained order of results was expected. CW paper is the most suitable for adhesive binding since it is uncoated and it has rough surface, high tearing resistance and limited stiffness (Pasanec Preprotić, 2012). WFU and WF office papers are also suitable for adhesive binding, but they have smoother surface with more fillers and binders, which can affect the binding strength (Džogaz, 2007). CR office paper is unpredictable due to the presence of different impurities and it can be unsuitable for adhesive binding or any binding at all (Lozo, 2004; Petković et al, 2017). WFC paper is not suitable for adhesive binding. It has high paper stiffness and smooth, coated surface, which covers cellulose fibres (Džogaz, 2007). This facts can also be confirmed with state of tested sheets (A-D), as presented in Tables 7-11. During page-pull test procedure, it was important to visually evaluate state of tested sheets, because there are different types of adhesive joint failures – adhesive and surface failure. In the case of adhesive or cohesive adhesive failure, state of tested sheet is marked with "A". In the case of surface or internal surface failure, state of tested sheet is marked with "B" or "C". In case of significant glue penetration, it is not possible to pull out tested sheet and this failure is marked with "D". Most "D" states were recorded for CW book blocks, due to high surface roughness. "A" states were the most recorded for all book blocks. Remarkable number of "B" and "C" states was recorded for CR book blocks that can be linked to paper type, unpredictable size and share of recycled cellulose fibres and impurities.

Machine direction tensile index was quite similar for WFU, CW and CR paper (41.15 to 47.09 Nm/g, respectively). WF office paper showed the highest tensile index – 76.03 Nm/g, while WFC showed the

lowest value – 31.66 Nm/g. Considering the obtained results for binding strength, paper strength can be directly linked to binding strength quality. However, adhesive-paper compatibility remained the main factor for binding strength (Figure 6).

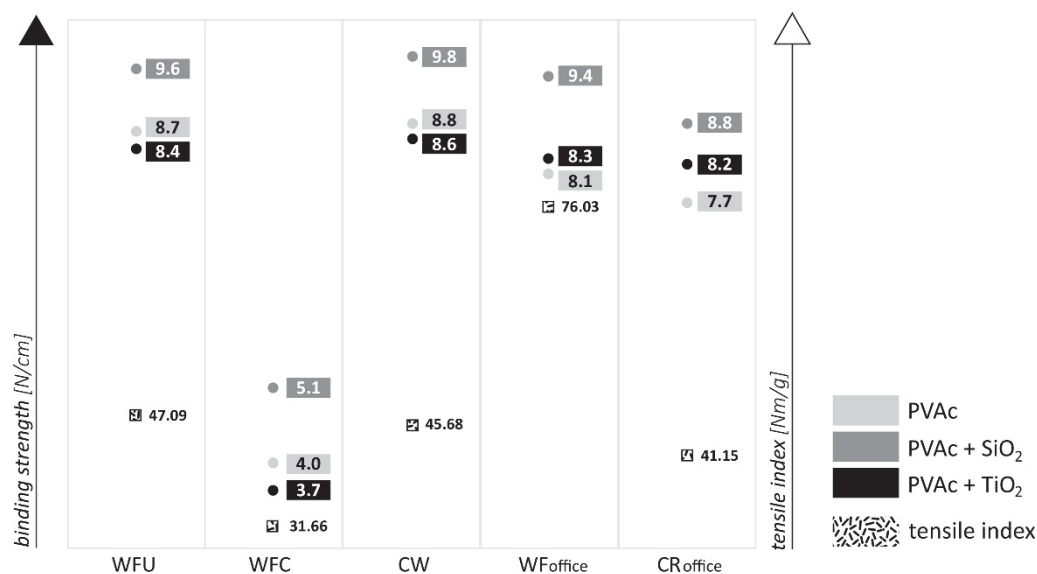


Figure 6: Comparison of binding strength (marked with circle) for different paper type book blocks and importance of tensile index (marked with square)

The aim of this study was the improvement of the PVAc adhesive binding performance by nanoparticles modification, namely by 1% of SiO₂ and TiO₂ nanoparticles. Enhancement of binding strength was achieved by 1% of SiO₂ nanoparticles, for all types of book blocks (26.64 – 10.30%). By adding TiO₂ nanoparticles, binding strength remained almost unchanged (-2.68 – 5.84%). In addition, another important feature was the reduction of coefficient of variation by adding SiO₂ nanoparticles (43.28 – 71.37%), as the main factor of the binding quality consistency.

It was also necessary to observe differences between binding strength results considering the test position – front, middle or rear. For WFU, CW and WF office papers, which are suitable for adhesive binding, binding strength values for neat PVAc were larger at front and rear part of the book block then in the middle. For PVAc adhesive with 1% of SiO₂ nanoparticles, results were uniform. The increase in uniformity for PVAc adhesive with 1% of TiO₂ nanoparticles was not important, since considerably higher binding strength for TiO₂ adhesive modification was not achieved.

The best binding performance of adhesive depends upon the binding strength, but also upon the visual and tactical experiences of end user. For good end user experience, book opening behaviour should have satisfactory characteristics, including lay-flat, easy-open flexible spine and adequate spine opening. Different adhesive – paper combinations show large differences in book opening behaviour. Papers with higher drape factor are stiffer and they tend to remain rigidly upright when book is open or they require a force in order to get fully opening of a book into a readable position. When book is fully open, the joint between leaves is subjected to peeling forces, which can be controlled by motion of the spine (Bracić, 2017; Jermann, 2004). In a fully flat opening, the most user-friendly type of opening, it is hard to achieve durable book blocks, especially with coated papers (Figure 2). In addition, a surface adhesion failure can occur between the paper and its coatings when applying elastic adhesives that allow movement, such as PVAc. This was confirmed with a poor to sufficient binding strength results and poor consistency for WFC book blocks. Completely opposite to a flat opening, is fixed spine which prevents any movement and users have to hold the book open (Figure 1 and 3; PVAc). This can be explained by higher drape factor of WFU and CW papers compared to other papers in this research. However, the possibility of durable book blocks with controlled spine opening (Figure 1 and 3; PVAc + 1% SiO₂; PVAc + 1% TiO₂) production was achieved by using nano-modified adhesive (especially PVAc + 1% SiO₂). Controlled spine opening was also achieved for book blocks made of WF and CR office papers with neat PVAc and PVAc modified with 1% TiO₂ (Figure 4 and 5; PVAc; PVAc + 1% TiO₂). WF office paper in combination with PVAc + 1% SiO₂ showed very good binding quality, according to its binding strength results. In addition, it can be classified as book block with the best binding performance in this research (Figure 4; PVAc + 1% SiO₂) due to a flat spine opening book

blocks. Opening behaviour of CR book blocks was controlled, but uneven and slack (Figure 5; PVAc + 1% SiO₂). As it was already mentioned, unpredictable properties of recycled paper made it impossible to give a correct conclusions and predictions for opening behaviour and binding strength, e.g. binding performance of CR office book blocks.

5. CONCLUSIONS

The right binding type selection usually depends on the book function, content, number of pages, printing budget and target group. However, reduction of printed book volumes and delivery time leads to the increase in popularity of adhesive bonded books. According to paper-adhesive compatibility, selection of paper and adhesive should be done before the production process begins. The aim of the research was to improve the binding performance of PVAc adhesive, by its modification with SiO₂ and TiO₂ nanoparticle, which reflected the binding strength and book opening behaviour. Considering the obtained results of binding strength and visually evaluation of book opening behaviour, WFC paper is not suitable for double-fan adhesive binding with PVAc adhesive at all. All other used papers are suitable and in addition, they showed very good durability. By adding SiO₂ nanoparticles, the binding strength increased by 10.30 - 16.65% respectively, for all groups of papers suitable for binding (WFU, CW, WF and CR office). Notable increase or decrease in binding strength with TiO₂ nanoparticles was not recorded. In addition, book blocks bound with PVAc modified with 1% SiO₂ adhesive showed more uniform adhesive application through all test positions – front, middle and rear part of the book block. Reduction of coefficient of variations was achieved for both adhesives modified with nanoparticles (43.28 – 71.37% SiO₂; 4.26 – 58.97% TiO₂), which can guarantee better consistency of binding quality. Despite the end product page-pull test results for the evaluation of binding performance, visual evaluation of book block opening behaviour should be done as well. The best easy-open, lay-flat opening behaviour was achieved for combination of WF office paper and PVAc + 1% SiO₂ adhesive. By adding SiO₂ nanoparticles in PVAc adhesive, book blocks made of stiff papers (WFU, CW) had more openable book behaviour. Although, the price of PVAc adhesive with 1% SiO₂ nanoparticles increased, obtained advantages are of particular importance for the end product quality. During nano-modified adhesive preparation, it is of great importance to achieve good distribution of nano particles, in order to avoid particle aggregation. In addition, it is important to find an optimum content of nano particles, because at higher contents the properties may deteriorate.

6. ACKNOWLEDGMENTS

The authors are grateful for the support of the University of Zagreb, Grant under the title: "Modifikacije konvencionalnih grafičkih materijala nanočesticama i kromogenim materijalima i njihova zdravstvena ispravnost" ("Modification of conventional graphic materials with nanoparticles and chromogenic materials and their health safety").

7. REFERENCES

- [1] Bardak, T., Tankut, A.N., Tankut, N., Sozen, E., Aydemir, D.: "The effect of nano-TiO₂ and SiO₂ on bonding strength and structural properties of poly (vinyl acetate) composites", *Measurement* 93, 80-85, 2016. doi: 10.1016/j.measurement.2016.07.004.
- [2] Bonnefond, A., Reyes, Y., Peruzzo, P., Ronne, E., Fare, J., Paulis, M., Leiza, J.R.: "Effect of the Incorporation of Modified Silicas on the Final Properties of Wood Adhesives", *Macromolecular Reaction Engineering* 7(10), 527-537, 2013. doi: 10.1002/mren.201300117.
- [3] Bracić, M.: "Utjecaj krutosti papira na kvalitetu bešavne forme s PUR ljepljivom", MSc thesis, University of Zagreb, 2017.
- [4] Džogaz, N.: "Ispitivanje kvaliteta knjiga povezanih na mašini za lepljeni povez Horizon BQ-270", BSc thesis, University of Novi Sad, 2007.
- [5] Ebnesajjad, S.: "Adhesives Technology Handbook", 2nd ed, (William Andrew, Norwich, USA, 2008), page 114.
- [6] Intergraf: "2015 Intergraf European Book Market Report", European Federation for Print and Digital Communication, 2015.
- [7] Intergraf: "2017 Intergraf European Economic Report – The evolution of the European graphic industry", European Federation for Print and Digital Communication, 2017.

- [8] Jermann, P.: "Reflections on Book Structures – part 2", Temper Productions, 2004, URL: <http://temperproductions.com/Bookbinding%20How-to/Reflections/reflect2.htm> (last request: 2018-05-06).
- [9] Jermann, P.: "Reflections on Book Structures – part 3", Temper Productions, 2008, URL: <http://temperproductions.com/Bookbinding%20How-to/Reflections/Reflections%203%20-%20Spine%20Control.pdf> (last request: 2018-06-04).
- [10] Jović, M., Buhin, Z., Krobot, I., Lučić Blagojević, S.: "Analysis of the Environmental Sustainability of the Adhesive Technology", *Kemija u industriji* 60(5), 269-276, 2011.
- [11] Laskowska, A., Kozakiewicz, P.: "Surface Wettability of Wood Species from Tropical and Temperate Zones by Polar and Dispersive Liquids", *Drvena industrija* 68(4), 299-306, 2017. doi: 10.5552/drind.2017.1704.
- [12] Lozo, B.: "Doprinosi optimiranju kvalitete novinskog papira", MSc thesis, University of Zagreb, 2004.
- [13] Packham, D.E.: "Handbook of Adhesion", 2nd ed, (John Wiley & Sons, Chichester, England, 2005), pages 136-138. doi: 10.1002/0470014229.
- [14] Paris, J.: "Adhesives for paper, board and foils", *International Journal of Adhesion & Adhesives* 20(2), 89-90, 2000.
- [15] Pasanec Preprotić, S.: "Čvrstoća knjižnog bloka u ovisnosti o starenju", PhD thesis, University of Zagreb, 2012.
- [16] Petković, G., Rožić, M., Vukoje, M., Pasanec Preprotić, S.: "Interactions in polyvinyl acetate – paper adhesive joint and influence on its adhesion parameters", *Proceedings of International Symposium on Graphic Engineering and Design 2016*, (University of Novi Sad, Novi Sad, Srbija, 2016), pages 91-101.
- [17] Petković, G., Pasanec Preprotić, S., Banić, D.: "Evaluation of finished product quality depending on paper properties and binding technique", *Polytechnic and Design* 5(3), 237-247, 2017. doi: 10.19279/TVZ.PD.2017-5-3-19.
- [18] Petrie, E.M., *Bookbinding Adhesives*, ASI Adhesives & Sealants Industry, 2008, URL: <https://www.adhesivesmag.com/articles/87133-bookbinding-adhesives> (last request: 2018-09-05).
- [19] Ramljak, A.: "Adhezijska svojstva polivinil acetatnog ljepila", BSc thesis, University of Zagreb, 2017.
- [20] Rebsamen, W., *Adhesive Binding Library Books, The New library scene*, 1983, URL: http://www.mekatronicsinc.com/machines/Werner_1983.pdf (last request: 2018-09-05)
- [21] Salvini, A., Saija, L.M., Finocchiaro, S., Gianni, G., Giannelli, C., Tondi, G.: "A New Methodology in the Study of PVAc-Based Adhesive Formulations", *Journal of Applied Polymer Science* 114(6), 3841-3854, 2009. doi: 10.1002/app.31032.
- [22] Šedivka, P., Bomba, J., Böhm, M., Boška, P.: "Influence of Temperature on the Strength of Bonded Joints", *BioResources* 10(3), 3999-4010, 2015.
- [23] Thomson, P.: "Bookbinding Tutorial: Glues – Tips, Techniques, Types & Recipes", *ibookbinding*, 2014, URL: <https://www.ibookbinding.com/blog/bookbinding-gluing-tips-techniques-types-info/> (last request: 2018-08-30).
- [24] Wen, N., Tang, Q., Chen, M., Wu, L.: "Synthesis of PVAc/SiO₂ latices stabilized by silica nanoparticles", *Journal of Colloid and Interface Science* 320(1), 152-158, 2008. doi: 10.1016/j.jcis.2007.11.059.



CHANGES IN THE OPTICAL PROPERTIES OF HEMP OFFICE PAPERS DUE TO ACCELERATED AGEING

Ivana Plazonić , Lahorka Malnar , Vesna Džimbeg-Malčić 
Željka Barbarić-Mikočević , Irena Bates 
University of Zagreb, Faculty of Graphic Arts, Zagreb, Croatia

Abstract: *This research observes alteration in optical properties of two commercially available hemp office papers exposed to various methods of accelerated ageing. Both handmade office papers, natural colored and non-chlorine bleached were formed from 100% hemp plant fiber. In order to establish their optical stability under controlled conditions two different accelerating ageing treatments were carried out for the period of 24 hours as a simulation of different degradation processes that naturally occurs in cellulosic materials: thermal oxidation (TO) and photo-oxidation (PO). Before and after ageing treatments the changes in the optical properties of papers were monitored by X-rite DTP 20 spectrophotometer and obtained differences in Reflectance index (R), Euclidean difference (ΔE_{00}^*) and Yellowness Index (YI E313) have been discussed. The results have shown how the paper optical stability is dependent upon manufacturing process. Namely, it was found that bleached hemp pulp provide better optical stability of papers than unbleached hemp pulp.*

Key words: accelerated ageing, hemp fiber, office papers, optical properties

1. INTRODUCTION

Behavior of paper as a multi-component material is strongly dependent upon the nature, origin and characteristics of its each component as well as upon their interactions (Area, 2011). The paper components can be classified according to their origin, chemical structure and function such as: fibers (composed mainly of cellulose, but also of lignin, hemicelluloses and other minor components), mineral particles (talc, kaolin, calcium carbonate, etc.), natural sizing agents (as starch or rosin) or synthetic ones (as alkyl ketene dimer (AKD) and alkenyl succinic anhydride (ASA)), colorants and other substances (Area, 2011). From the moment of its formation, paper suffers deterioration due to endogenous (pH, metal ions, lignin, degradation products) and exogenous (heat, humidity, light, oxygen, pollutant gases) contributors (Area, 2011; Strlič et al, 2004). However, heat and moisture are considered as two of the most important environmental influences on the stability of papers e.g. yellowing and loss of strength (Karlović et al, 2012). From the viewpoint of the paper industry ageing are irreversible changes that occur slowly over time and in paper substrate ageing process results with the deterioration of useful properties that can render it unsuitable for its primary usage. Therefore, an accelerated ageing test is a practical way to predict the physical and chemical changes occurring naturally in a paper in a relatively short period. In a practice, a numerous accelerated ageing tests with various aging conditions are used for evaluation and ranking paper substrates on their permanence. Some of the standard techniques of accelerated ageing are moist-heat (80 °C and 65% RH), dry-heat (105 °C) and treatment with a xenon arc lamp (Karlović et al, 2012). The concept of accelerated ageing test is simple. Namely, the rate of most chemical reactions in a paper sample increases when temperature is increased and those chemical changes affecting the physical properties of a paper. Paper optical stability is extremely important in graphic industry because it contribute, more than any other factor, to the overall paper appearance and appeal (Thompson, 2004). As a result of paper ageing, optical properties are significantly changed (Jääskeläinen et al, 2007). The optical properties of the paper are very sensitive to its structure. Cellulose is the major structural component of paper. Pure cellulose absorbs visible light only to a small extent (380–550 nm), while absorption in near UV spectral region (300–380 nm) is more pronounced. It is therefore in that spectral range most of the damage in cellulose is induced during exposure to electromagnetic radiation (Strlič et al, 2004). It is proven how the type and quality of the raw material is crucial for the longevity of the product. Namely, already degraded recycled fibers will lead to a less durable paper than high-quality virgin fibers, especially cotton ones (Strlič et al, 2004). Other components of paper also influence its stability, the major one being another natural polymer, lignin with high capacity to absorb ultraviolet light (absorption maximum at wavelength of 200–210 nm and at 270–280 nm) (Jingjing, 2011). Many other organic and inorganic components in the paper network structure (such as fillers, adhesives, pigments, binders, etc.) strongly influence on the paper optical stability as well. In general, the brightness (B), the lightness (L^*) of the CIEL*a*b* color system and the whiteness

(W) of paper decline, while the yellowness and the b^* (shift to yellow) and a^* (shift to red) coordinates of the CIEL*a*b* 20 color system increase after exposing to accelerated ageing.

2. MATERIALS AND METHODS

2.1 Materials

2.1.1 Hemp office paper

In this research two commercially available hemp office papers (grammage 90 gm⁻²) were used as samples:

Natural hemp paper – handmade sustainable paper made from 100% hemp plant fiber with wildgrass is unbleached, uncoated printer-compatible (Laser and Inkjet) paper in natural color with natural deckled edge. Paper manufacturer is Distant Village, US.

Bleached hemp paper – handmade sustainable paper made from 100% hemp plant fiber is non-chlorine bleached uncoated printer-compatible Laser and Inkjet) paper in cream color with natural deckled edge. Paper manufacturer is Distant Village, US.

2.2 Methods

2.2.1 Aging Treatments

In order to obtain optical stability of hemp containing papers under controlled degradation levels, two different accelerating ageing treatments were carried out as a simulation of different degradation processes that naturally occurs in cellulosic materials.

- Thermal oxidation: it was carried out on all laboratory formed papers at 60°C in oven for 24 hours in absence of light. It is well known that thermal oxidation induces the breakage of chemical bonds in cellulose and the formation of carbonyl, carboxyl, and hydroperoxide groups (Cocca et al., 2011).
- Photo-oxidation: papers were exposed in a Cofomegra Solarbox 1500e Xenon Test Chamber with a Xenon light source for 24 hours. Irradiation was kept at a constant power of 550W/m² and at a temperature of 60°C. Photooxidative reactions result in an increase of carbonyl content, carboxyl, and hydroperoxide groups (Cocca et al., 2011).

2.2.2 Optical Properties Analysis

Characterization of accelerate aged paper samples was discussed through optical properties analysis (Reflectance index, Euclidean difference and Yellowness Index) and compared to unaged (control) paper samples. Monitored optical measurements were repeated 20 times on each paper.

- Reflectance index (R)

Papers reflectance spectra measurements were processed using X-rite spectrophotometer with standard illuminant D65 and 2-degree observer, in the interval of the wavelengths from 400 nm to 700 nm for every 10 nm. Reflectance spectra values (R) were measured for all paper samples before ageing (R_{unaged}) and after accelerated ageing (R_{aged}) and gained results are presented as ΔR according to Equation (1):

$$\Delta R = R_{unaged} - R_{aged} \quad (1)$$

- The colour differences or Euclidean difference (ΔE_{00}^*)

Colorimetric CIE L*a*b* values of all laboratory papers before and after accelerated ageing were carried out by means of X-rite spectrophotometer. Color data were calculated under illuminant D65 (daylight 6500°K), 2 standard observers, sphere geometry, specular component included, and UV energy included. The instrument was calibrated against a white standard tile. In the CIE L*a*b* color space the value L* represents the lightness of the color and the value +a* represents redness or the value -a* represents greenness, and the +b* value represents yellowness or the value -b* represents blueness (Kipphan, 2001). The color differences or Euclidean difference (ΔE_{00}^*) of all analyzed paper substrates were calculated with the following equation (Luo, 2001), using the corresponding starting material (unaged paper substrate) as reference:

$$\Delta E_{00}^* = \left(\frac{\Delta L'}{k_L S_L} \right)^2 + \left(\frac{\Delta C'}{k_C S_C} \right)^2 + \left(\frac{\Delta H'}{k_H S_H} \right)^2 + R_T \frac{\Delta C'}{k_C S_C} \frac{\Delta H'}{k_H S_H} \quad (2)$$

- Yellowness index (YI E313)

The Yellowness Index (paper discoloration) is an indication of the degree to which a specimen surface is different to the ideal white in the yellow direction. In this research, it is used to indicate the influence of a two different accelerating ageing treatments on the change of straw-containing paper color during ageing. The measurements were performed in accordance with ASTM Method 313 (YI E313) by spectrophotometer X-Rite DTP 20 at D65/2°. On each paper sample, on different locations, 10 values were measured. Yellowness index according to the ASTM Method E313 is calculated as follows:

$$YIE313 = \frac{100 \times (C_x X - C_z Z)}{Y} \quad (3)$$

where X, Y, Z are the CIE tristimulus values, C_x and C_z are coefficients (D65/2°: $C_x = 1.2985$, $C_z = 1.1335$) (Hunter Associates Laboratory, 2008).

3. RESULTS

The changes in the optical stability of hemp office papers after exposing to accelerated ageing were analyzed and experimental results are presented at Figures 1-5.

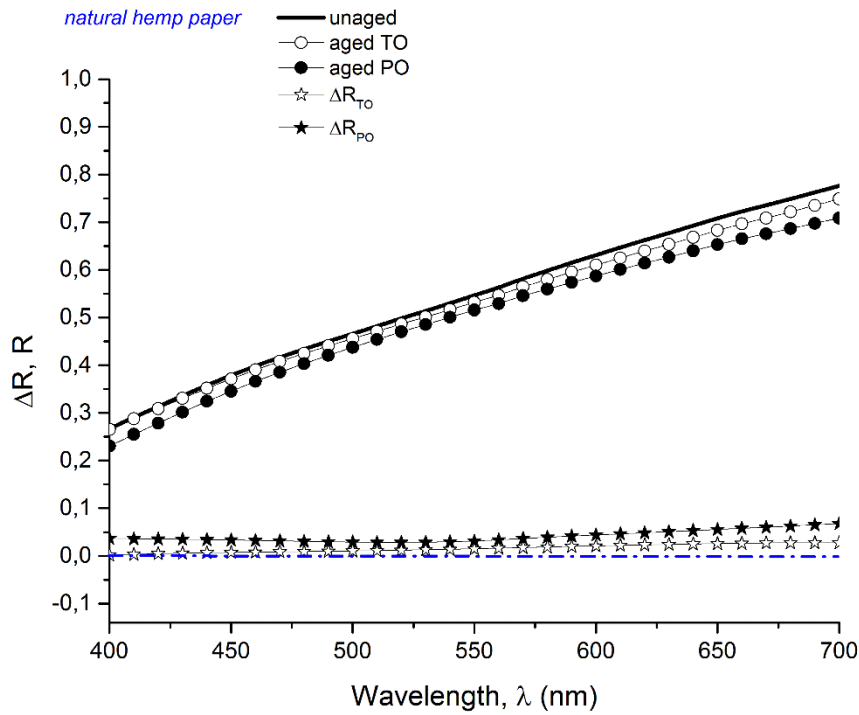


Figure 1: The impact of accelerated ageing on natural hemp paper reflectance

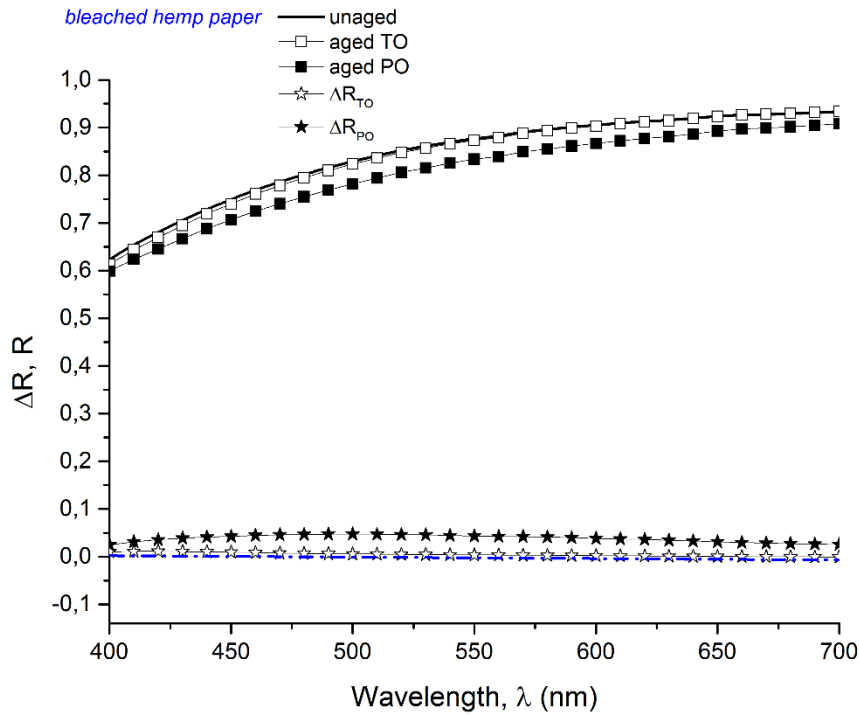


Figure 2: The impact of accelerated ageing on bleached hemp paper reflectance

From Figures 1 and 2 it is visible that both hemp office papers (natural and bleached) show more noticeable changes in reflectance values after exposure to UV/VIS radiation by xenon lamp (PO) compared to those aged only by thermal oxidation (TO). All examined hemp papers substrates after TO and PO ageing treatment have shown similar deviations in whole spectrum. For better observing and comparing changes on both analyzed papers, relative changes of reflectance ($\Delta R/R_{\text{unaged}}$) are summarized at Figure 3.

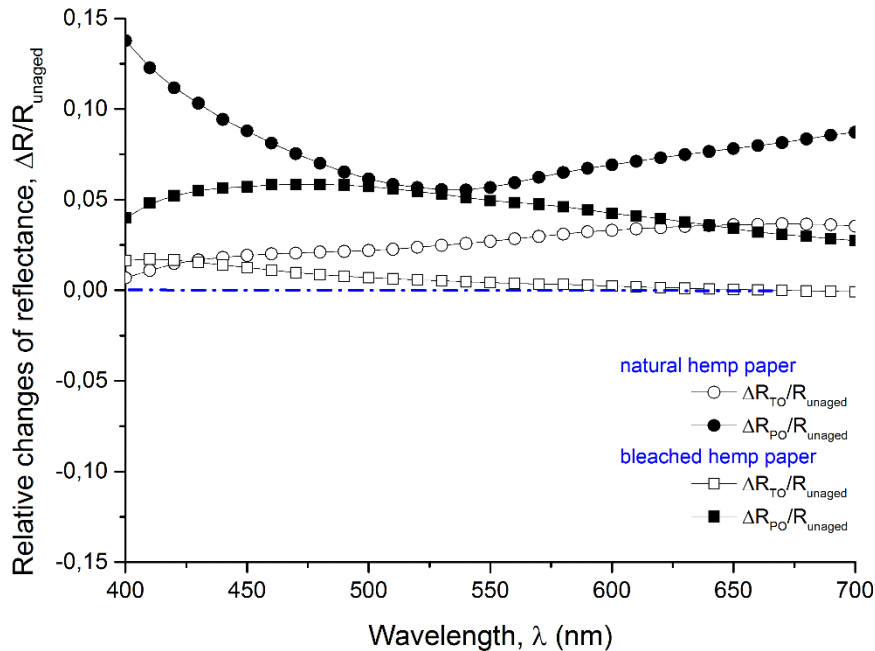


Figure 3: The relative changes of the reflectance of the hemp papers after ageing depending on ageing method

From relative changes of the reflectance values, we can see that maximum difference is achieved in blue (400-460 nm) and red part (620-700 nm) of spectrum for natural hemp papers, while for bleached hemp papers max $\Delta R/R_{\text{unaged}}$ is on 500 nm. The treatment with a xenon lamp (PO) had the strongest influence on natural hemp papers, where difference in the red part of the spectrum have reached 8.7% and in blue part 13.8%. Recorded maximum relative changes of reflectance for bleached hemp paper was 5.8% at wavelength 500 nm.

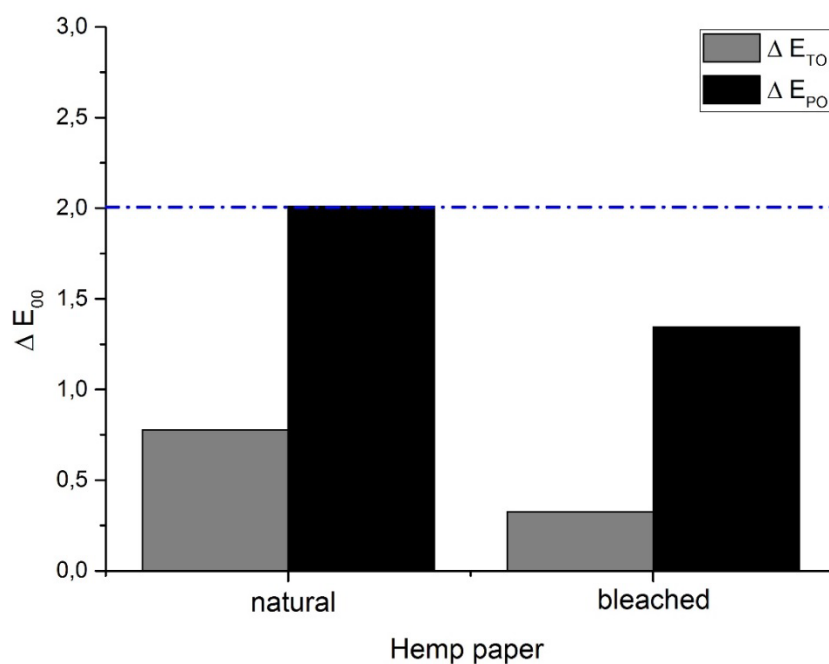


Figure 4: Euclidean difference

The calculated color differences or Euclidean difference (ΔE_{00}^*) values by equation 2 are presented at Figure 4. Color difference values caused by thermal-oxidation (TO) ageing are minor (from 0.32 to 0.78), while the color differences values are up to 2.01 for natural hemp paper aged by photo-oxidation (PO). Namely, according to tolerance definition $\Delta E_{00}^* \leq 2$ is classified as very small noticeable difference for standard observer while $\Delta E_{00}^* = 5$ is big noticeable difference in the color whose standard observer can recognized (Zjakić, 2007). From these results it is evident that office paper formed from bleached hemp pulp exhibits better optical stability to artificial ageing (by thermal-oxidation and by photo-oxidation) than papers formed from natural unbleached pulp.

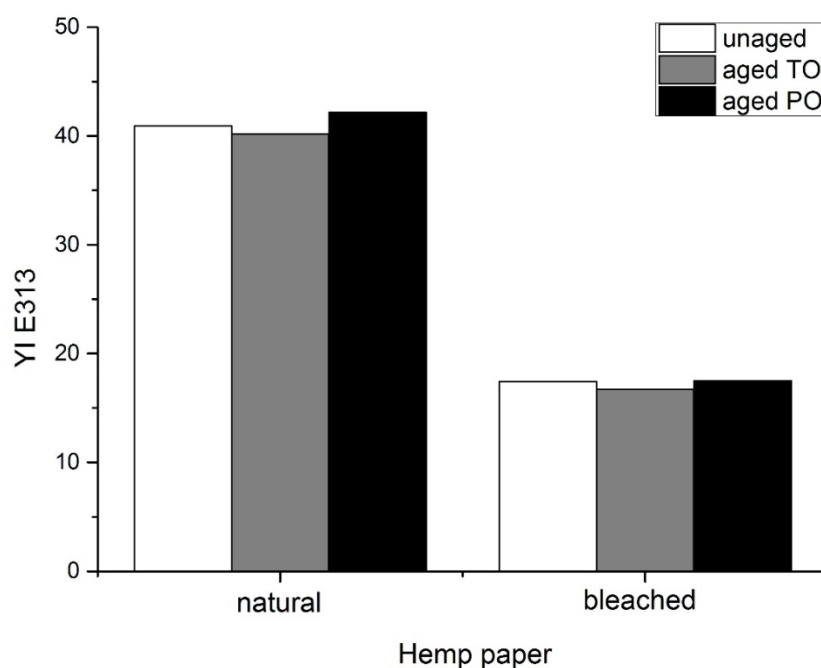


Figure 5: Yellowness Index

Figure 5 shows the influence of two accelerated ageing techniques (thermal and photo-oxidation treatment with a xenon lamp) on the Yellowness Index of the papers.

The tested papers differ significantly in yellowness (natural hemp paper: $YI_{E313} = 40.9$, bleached hemp paper: $YI_{E313} = 17.4$), the values confirm expected that natural hemp paper is more yellowish than bleached hemp paper. After 24 hours of treatment with heat and a xenon lamp, the results indicate that bleached hemp paper yellowed more slowly than natural hemp paper. Paper discoloration for both analyzed types of hemp paper (natural and bleached) due thermal-oxidation is not noticed.

4. DISCUSSION

Generally, paper as lignocellulose material undergo light-induced yellowing. Most responsible component for paper photo yellowing is lignin which contains numerous chromophores that efficiently absorb UV radiation. The mechanism of lignin photo-oxidation can be described as follows: primary chromophores from lignin absorb the light with 300 to 400 nm wavelengths → break of etheric bonds and creation of free radicals → reaction between free radicals and lignin → formation of ketyl radicals → phenoxy and ketone radicals → production of yellow quinone and chromophores with secondary chromophores → light-induced destruction of lignin and yellowing of paper (Nemati et al., 2011). Therefore, to remove the residual lignin and chromophores inside the pulp is a main purpose of bleaching the pulp. 50% of bleached mechanical pulps are currently produced using dithionite (hydrosulfite) bleaching which react with the chromophores present in the lignin of pulp to make less colored compounds, and consequently to give a brighter aspect to the pulp (El-Sakhawy, 2005). As both office papers analyzed in this study were handmade, from 100% hemp plant fiber it is to be expected that in some percentage they contain lignin. Lignin content in hemp fiber is usually 2-5% (Thomsen et al., 2005.). Bleaching process have made optical properties of hemp paper more stable due accelerated ageing comparing to those papers made from natural unbleached hemp fibers.

5. CONCLUSIONS

The effect of accelerated ageing on hemp office papers optical stability was studied. Taking into account all obtained results, the following could be concluded:

- Exposure to a xenon light source for 24 hours causes more rapidly yellowing of both papers than exposure to heat influence.
- The changes in optical properties due to accelerated ageing are more pronounced for the unbleached hemp office papers but still standard observer cannot recognize it.

6. REFERENCES

- [1] Area, M.-C., Cheradame, H.: "Paper aging and degradation: recent findings and research methods", *BioResources* 6(4), 5307-5337, 2011.
- [2] Cocca, M., D'Arienzo, L., D'Orazio, L.: "Effects of Different Artificial Agings on Structure and Properties of Whatman Paper Samples", *ISRN Materials Science*, 7, 2011. doi:10.5402/2011/863083.
- [3] El-Sakhawy, M.: "Effect of bleaching sequence on paper ageing", *Polymer Degradation and Stability* 87, 419-423, 2005. doi: 10.1016/j.polymdegradstab.2004.10.002.
- [4] Hunter Associates Laboratory, Inc.: "Yellowness Indices", *Insight on Color* 8(15), 2, 2008.
- [5] Jääskeläinen, A-S., Liitiä, T.: "UV/VIS reflectance spectroscopy reveals the changes in fibre chemistry during ageing", *SpectroscopyEurope* 19 (5), 11-13, 2007.
- [6] Jingjing, L.: "Isolation of lignin from wood", BSc thesis, Saimaa University of Applied Sciences, 2011.
- [7] Karlovits, M., Gregor-Svetec, D.: "Durability of Cellulose and Synthetic Papers Exposed to Various Methods of Accelerated Ageing", *Acta Polytechnica Hungarica* 9 (6), 81-100, 2012.
- [8] Kipphan, H.: "Handbook of Print Media", (Springer, Verlag, 2001.).
- [9] Luo, M. R., Cui, G., Rigg, B.: "The development of the CIE 2000 colour difference formula: CIEDE2000", *Color Research & Application* 26 (5), 340-350, 2001. doi:10.1002/col.1049.
- [10] Nemati, M., Hemmasi, A. H., Talaeipour, M., Samariha, A.: "Studying the effect of photo-yellowing on the brightness property of chemi-mechanical pulping paper", *Cellulose Chemistry and Technology* 47(12), 93-109, 2013.

- [11] Strlič, M., Kolar, J.: "Ageing and stabilisation of paper", (National and University Library, Ljubljana, 2004.), page 211.
- [12] Thompson, B.: "Printing Materials: Science and Technology", (Pira International, Leatherhead, 2004.), page 591.
- [13] Thomsen, A. B., Rasmussen, S. K., Bohn, V., Nielsen, K. V., Thygesen, A.: "Hemp raw materials: The effect of cultivar, growth conditions and pretreatment on the chemical composition of the fibres", Forskningscenter Risoe, 1507, 30, 2005.
- [14] Zjakić, I.: "Upravljanje kvalitetom ofsetnog tiska", (Hrvatska sveučilišna naklada, Zagreb, 2007.), page 245.



© 2018 Authors. Published by the University of Novi Sad, Faculty of Technical Sciences, Department of Graphic Engineering and Design. This article is an open access article distributed under the terms and conditions of the Creative Commons Attribution license 3.0 Serbia (<http://creativecommons.org/licenses/by/3.0/rs/>).

THE INVESTIGATION OF USING ZIRCONIUM OXIDE MICROSPHERES IN PAPER COATING

Yasemin Sesli , Zafer Ozomay , Emine Arman Kandirmaz , Arif Ozcan 

Marmara University, School of Applied Sciences, Printing Technologies, Istanbul, Turkey

Abstract: Paper and cardboard are the raw materials frequently used in the printing industry. Pulp structure in papermaking process, surface roughness, and strength of electricity, moisture, thickness, thermal conductivity and optical properties are important parameter that influences printing quality. The surface structure of paper and cardboard needs to be improved for the quality prints. Among the methods of reducing paper surface roughness, sizing, coating and calendering processes can be counted. In the surface coating process, fillers are added to the formulations differently from sizing. While these fillers increase absorption, they also affect colour, opacity, gloss, surface roughness, contact angle etc. Materials containing zirconium oxide; due to the increase of strength, unaffected by chemical agents, high opacity and whiteness, it finds different usage area. In this study sizing and surface coating processes have been carried out in order to improve the surface properties of the paper, to improve the gloss, yellowness, whiteness, absorbency and contact angle of the paper. For this purpose, cationic starch and zirconium oxide coating formulations were prepared and applied onto paper with a paper coating tester under laboratory conditions. In addition, surface sizing with cationic starch has been done as a reference. Coated, sized and standard office type base papers were printed with IGT C1 offset printing test with magenta ink. The colour and gloss values of all printed and unprinted samples were measured. Printed samples, coated papers, surface sized papers and base papers were subjected to lightfastness test according to BS4321 and colour and gloss changes were examined with blue wool scale. The contact angle, absorbency and surface energies of all the obtained surfaces were determined. As a result, it has been found that zirconium oxide-added paper coatings have less glossy but lower contact angle and higher absorbency than surface sizing. It has been determined that the coated paper have worst yellowness and gloss changes with light aging. As a result, the addition of zirconium oxide to the coating improves printability.

Key words: zirconium oxide, surface coating, surface energy, contact angle, sizing

1. INTRODUCTION

Paper is a composite structure with different porosity ratios of cellulose fibers (Thompson, 2004). But nowadays, paper is not used in industry as raw. Expectations also increased due to the development of visual media and the increase in consumer expectations. Printability parameters (smoothness, roughness, brightness, opacity and whiteness) of the paper must be good for the printing industry (Özcan et al, 2017). In print systems, print quality is strongly dependent on the adherence of paper and ink, and the fixation of the ink on the printing material. The surface characteristics of the paper are of great importance in the process of absorption and settling of the liquid ink to the paper surface. The surface properties of the paper directly affect the print quality. Surface smoothness or roughness is the most important feature of paper (Aydemir, 2014). The coating is one of the processes to give some properties on paper. The main purpose of this process is to fill the gaps on the paper by covering a thin film of pigment, binder and various additives on the base paper to coat a smooth surface. Pigment is one of the components of the coating process, and one or more pigments used in the coating in an amount ranging (Lehtinen, 2000).

Zirconium oxide is used in for aesthetic purposes in dentistry with its surface shape, transparency and colour feature; as a building material for nuclear reactors due to their high melting point, corrosion resistance and low neutron absorption; due to the flammable property in the military; making magnet due to its super conductive property at low temperatures (Çalışır, 2011; Tosun, 2007). In this study, surface sizing and surface coating processes were performed with the aim of developing the surface properties of paper with zirconium oxide (improvement of gloss, jaundice, absorbency and contact angle of paper).

The contact angle is measured by forming a liquid drop on a solid standing on a flat and horizontal plane. Surface tension exists on all interfaces; It is called inter-surface tension or “inter-surface free energy” (Erbil, 1997). The contact angle was first proposed and formulated by Young (Young, 1805) as the angle between the solid surface and the tangent drawn to the droplet surface passing through the triple point of the air-liquid-solid phases (Farris et al, 2011). In terms of printability, low contact angle on paper surface is

desirable. Offset printing is important for water-ink balance, which means that if the contact angle is low, it means wetting more areas with less humidity, which means more bright colours and fewer problems. In case of surface coating, low contact angle causes more area to get wet. Thanks to the -OH groups in the structure of binders such as starch, they form more hydrogen bonds with water and allow for printing with less ink to larger areas.

2. METHODS

In order to determine the effect of zirconium oxide microparticles on the printability, Zr powder was obtained from Alfa Aesar. Particle size distributions of all powder were determined on Malvern Mastersizer equipment. The powder characteristics of ZrO₂ used in this study are given in Table 1.

Table 1: Powder characteristics ZrO₂ powder.

Item	Zr
Vendor	Alfa Aesar
Shape	Irregular
Theoretical density, g/cm ³	6.51
Particle size	
D ₁₀	1.95
D ₅₀	6.97
D ₉₀	26.72
Purity, %	99.9

Uncoated papers with 80 g/m² grammage were used in surface sizing and coating operations. The parameters of base paper used in this study are given in Table 2. Cationic starch-based surface sizing was applied on the standard paper surfaces to the control group. Mixture of cationic starch with 7.5% concentration was heated to 90°C for this process. This hot sizing solution was cooled down to 60°C afterwards, and it was applied on the surface of paper with Meyer rod (Number 2) in the paper coating device. Then, the same process was repeated for the coating operations, too, and 2.7% ZrO₂ was added to the sizing solution in addition. The surface sizing was applied for drying, and coated paper samples were both left in air-drying for 24 hours at 23±1°C and 50±2% relative humidity.

Table 2: Parameters of the base paper used in the study

Properties	Standard	Paper
Grammage (g/m ²)	ISO 536	80
Thickness (μm)	TAPPI T411	190
Whiteness (D65/10) (%)	ASTM E313	99
Gloss (TAPPI 60°/75°)	T480 om-92	4.9
Yellowness	ASTM E313	0.06

The original, sized and coated papers were printed with Dyoboard DB-5600 Process Magenta commercial offset printing ink using an IGT C1 offset printability test device under 300 N/m² pressure printing conditions. CIE L*a*b* values of the print results were measured using X-Rite eXact hand-held spectrophotometer according to ISO 12647-2:2013, between a spectral range of 400 nm to 700 nm, under a D50 light source, 2° observer, polarized filter, and 0/45-degree geometry. The colour differences formula was given below. Calculations were made by taking the average of five measurements. ΔL*, Δa*, Δb*: Difference in L*, a*, and b* values between specimen colour and target colour.

Lightness is represented by the L^* axis which ranges from White to Black. The red area is connected to the green by the a^* axis, while the b^* axis runs from yellow to blue.

$$\Delta E = \sqrt{\Delta L^2 + \Delta a^2 + \Delta b^2} \quad (1)$$

Gloss measurements were made with BYK-Gardner GmbH glossmeter according to ISO 2813:2014 60° geometry. All printed and unprinted samples were subjected to light aging test in accordance with BS 4321:1969 standard. Following the light aging test, CIE $L^*a^*b^*$, gloss and yellowness measurements were performed one more time for all the samples. For light aging procedure, first of all the CIE $L^*a^*b^*$ colour values and gloss of the samples were measured. Then, printed and non-printed samples were exposed to light aging in a sealed cabinet on the Solarbox 1500 device under constant UV light for 192 hours according to BS 4321-1969 standard. The CIE $L^*a^*b^*$ colour and gloss values of the printed and unprinted samples exposed to fading were measured one more time, and the differences between the initial values and values measured after the light-fastness test were calculated. The contact angle and total surface energy measurements of the papers were performed by PocketGoniometer PGX+ in accordance with ASTM D5946 standard.

3. RESULTS AND DISCUSSION

SEM image and size distribution of zirconium oxide microparticles are given in Figure 1. Zirconium particle size is polydisperse and the largest particle has been determined to be 10 μ m. This creates the desired porous surface for the coating process.

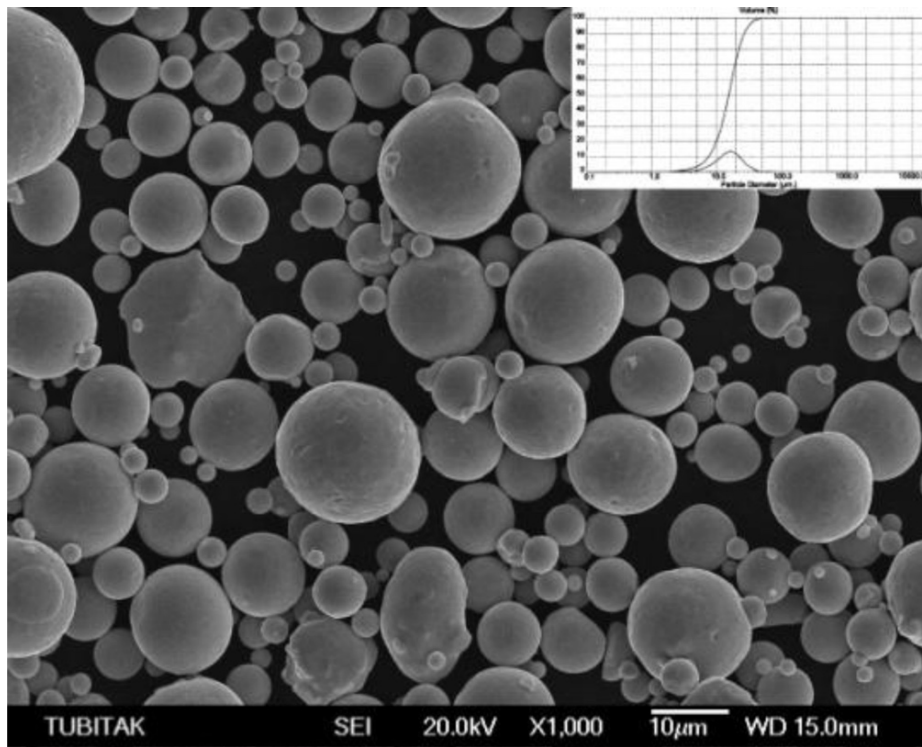


Figure 1: Scanning electron micrograph of ZrO_2 powder and particle size distribution curve

The colour properties were measured after complete drying on coated, sized and uncoated paper. Colour is calculated by delta E of transactions uncoated how it differs from paper. When Figure 2 is examined, it is concluded that the sizing process does not change the colour much and delta difference is not detected by the eye because it is below 3. However, it was determined that the colour changed very much in the coating process and shifted towards yellow. The reason for this shift is added into the origin zirconium coating. The colour of zirconium is yellowish white and the microparticulation increases the roughness and the light is more yellow.

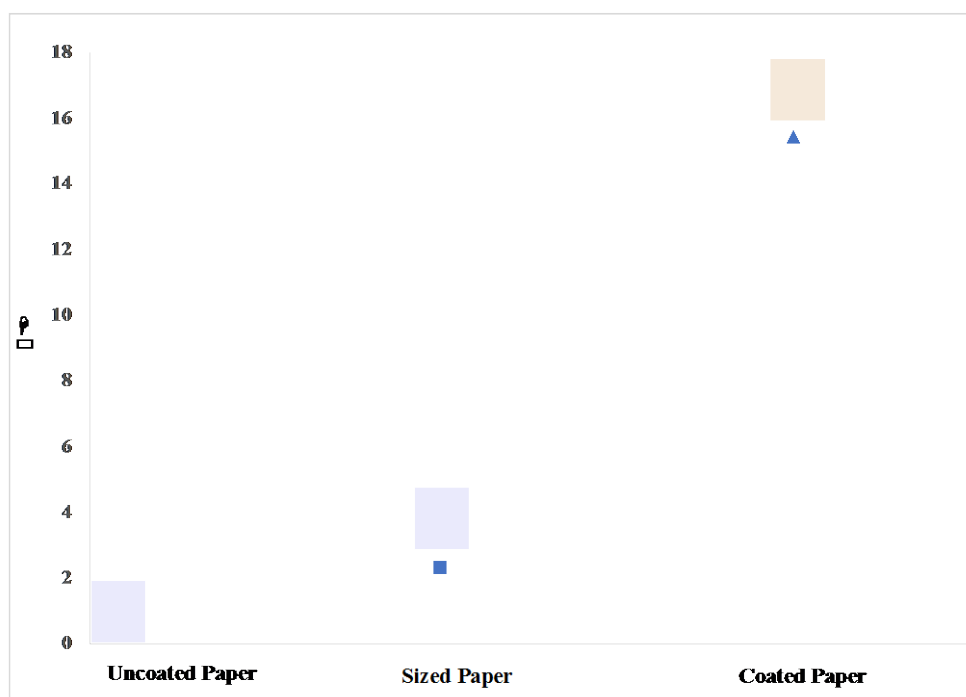


Figure 2: Colour differences of coated, sized and uncoated paper

The gloss of coated, sized and uncoated paper was measured. When the obtained data were examined (Figure 3), it was determined that the most glossy paper belonged to the sized paper containing the most binders. It has been seen that the processes are made more glossier than uncoated paper. Because more polymers were added to the environment, this caused an increase in the crystalline gloss of the polymer. Zirconium, which is added to the coating, creates folds on the surface and has a gloss smaller than the size paper because it causes the diffusion of light.

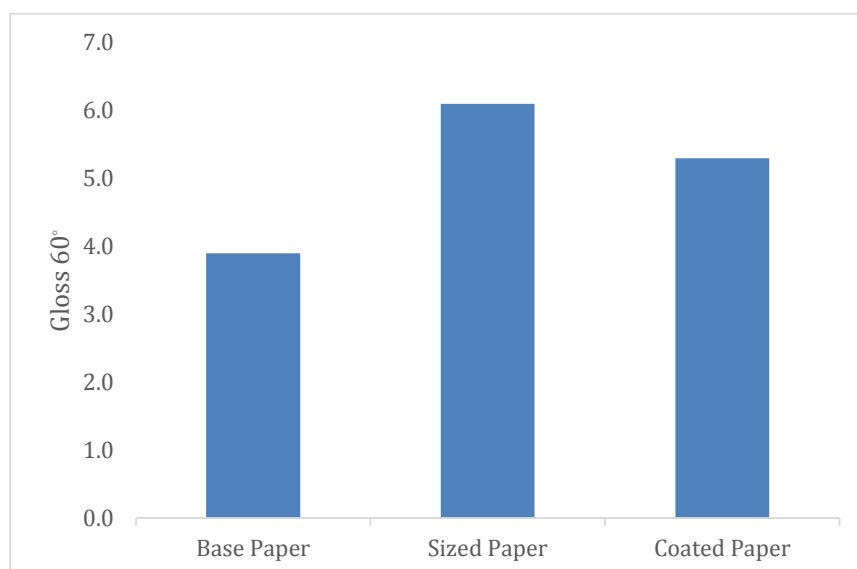


Figure 3: Gloss changes of coated, sized and uncoated paper

Total surface energy (Table 3) results showed that base paper has the lowest surface energy, zirconium coated paper has highest surface energy. The roughness of the zirconium microparticles on the surface reduces the contact angle, thus providing better wettability, i.e., less space to be printed. Surface energy and contact angle values were compatible with each other.

Table 3: Total surface energy and Contact Angle values according to ASTM D5946 method

Process	Total Surface Energy (mJ/m ²)	Contact Angle
Base paper	33,8	86,5
Coated paper	52,9	33,5
Sized paper	50,3	36,4

The prints were made on three different paper and colour properties were compared. When Figure 4 is examined, there is a noticeable differentiation in the colour of the printing on the treated paper. Because the paper and the pigments were not allowed to be dragged into the paper, thus the colour became more exacerbated and increased to some yellow. This means printing in more areas with less ink in print. So, the printing has been improved. Also, zirconium gave a little more absorbency and increased the colour difference.

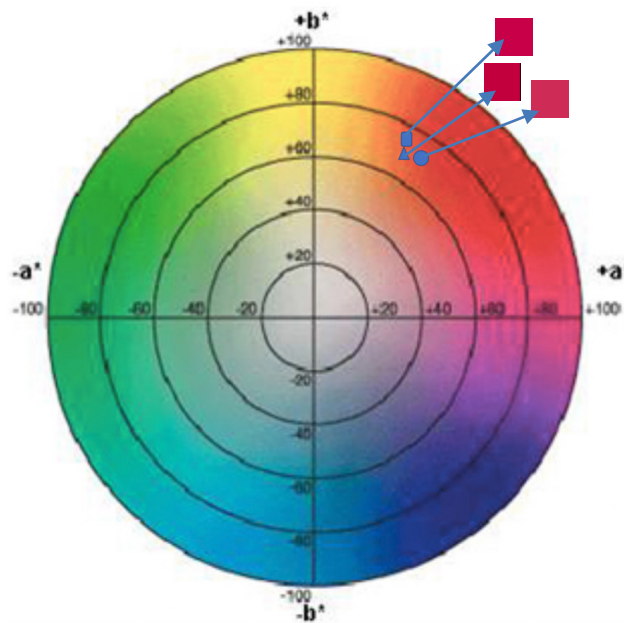


Figure 4: Colour changes of coated, sized and uncoated printed paper

The glosses of printed papers are similar to unprinted papers; however, it has been found that the gloss values are greatly increased due to the resin in the ink content (Figure 5).

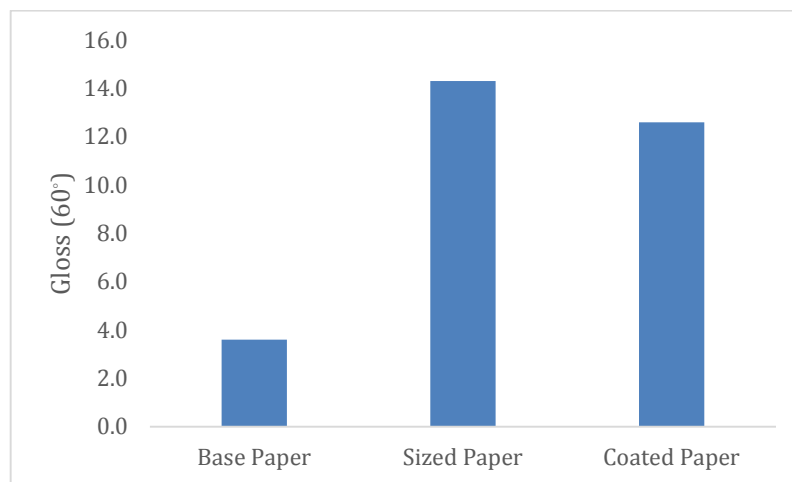


Figure 5: Gloss changes of coated, sized and uncoated printed paper

4. CONCLUSIONS

As a result, zirconium microparticles were produced and used in paper coating. Zirconium added coated papers printed with less ink. The gloss of both coatings and printed paper is enhanced by the processing. However, the shifting of the colour to yellow is a negative feature in the coating. Some negative influencing component (blue pigment) into ink can be eliminated from this problem. For this reason, it is determined that zirconium oxide can be used effectively in paper coatings.

5. ACKNOWLEDGMENTS

This work was supported by Marmara University, Scientific Research Projects Committee (M.U. BAPKO) under grant FEN-D- 060918-0513.

6. REFERENCES

- [1] Aydemir, C.: "Kağıdın Yüzey Pürüzlülüğünün, Baskı Renk Değişimi, Işık Haslığı ve Baskı Parlaklığına Etkisi", Marmara Fen Bilimleri Dergisi, 26 (3), 81-88, 2014.
- [2] Birdi, K.S.: "Handbook of Surface and Colloid Chemistry", (Boca Raton, CRC Press Inc., 1997), pages 259-306.
- [3] Çalışır, G.H.: "Farklı Zirkonyum Oksit Altyapılar Üzerine Farklı Teknikler ile Uygulanan Üstyapı Porseleninin Renk ve Şeffaflık Üzerine Etkilerinin İncelenmesi", PhD Thesis, İstanbul Üniversitesi Sağlık Bilimleri Enstitüsü, Protetik Diş Tedavisi ABD, 2011.
- [4] Farris, S., Introzzi, L., Biagioni, P., Holz, T., Schiraldi, A., Piergiovanni, L.: „Wetting of biopolymer coatings: Contact angle kinetics and image analysis investigation“, Langmuir, 27 (12), 7563-7574, 2011. doi: 10.1021/la2017006
- [5] Lehtinen, E.: "Pigment Coating and Surface Sizing of Paper", (Fapet Oy, Helsinki, 2000.), pages 61-66.
- [6] Ozcan, A., Zelzele, O.B.: "The effect of binder type on the physical properties of coated paper", MSU Journal of Science, 5 (1), 399-404, 2017. doi: 10.18586/msufbd.322353
- [7] Thompson, B.: "Printing Materials: Science and Technology", (Pira International Ltd., Leatherhead, 2004).
- [8] Tosun, T.: "Kuron ve köprü protezlerinde zirkonyum", Dentalife, 22, 18- 26, 2007.
- [9] Young, T.: "III. An essay on the cohesion of fluids", Philosophical transactions of the royal society of London, 95, 65-87, 1805. doi: 10.1098/rstl.1805.0005



© 2018 Authors. Published by the University of Novi Sad, Faculty of Technical Sciences, Department of Graphic Engineering and Design. This article is an open access article distributed under the terms and conditions of the Creative Commons Attribution license 3.0 Serbia (<http://creativecommons.org/licenses/by/3.0/rs/>).

QUALITY PERFORMANCE TESTING FOR BASE PAPER OF CORRUGATED PAPERBOARD BY DSC METHOD

Barnabás Tóth¹ , László Koltai² , Péter Böröcz³ 

¹ Óbuda University, Doctoral School on Materials Sciences and Technologies, Hungary

² Óbuda University, Rejtő Sándor Faculty of Light Industry and Environmental Protection Engineering, Budapest, Hungary

³ Széchenyi István University, Department of Logistics and Forwarding, Győr, Hungary

Abstract: Using a suitable paper quality of packaging structures is an element process in the packaging industry, mainly on producing corrugated paperboards. (Robertson, 2012) The base-papers are the most significant constituent of Corrugated Cardboards, contain mainly organic substances (e.g. cellulose, hemicellulose and lignin etc.) which are appropriate for thermo-analytical studies. The quality of the base-papers mainly defined by the primer cellulose, recycled paper and other incrust materials content. At the same time, it is difficult for users to precisely separate base papers that exhibit differences in mechanical and quality properties, as their ulterior identification is virtually impossible. (Holmberg et al, 1995) The testing methods such as CCT, RCT, FCT, COBB, bursting etc. are supported by statistical technique, but do not provide perfectly accurate results. (Caulfield et al, 1988) The reason is the deviation of testing results. In this paper, we publish the primary results of the thermoanalytical research for determination of different paper types. Applying a Differential Scanning Calorimetries (DSC) method, it is possible to study endotherm and exotherm spectrums of paper's raw materials. During a heating process each component react in different ways, both of their physical and chemical characteristic. Due to their various organic substances content, these values are different referring for similar results of the finished products, which determines their mechanical and quality properties during their use (Soares et al, 1995). The results show that this method on the one hand can be helpful to testing the paper during packaging producing process on the other hand after using as a packaging. Using a DSC apparatus helps showing the differences between the various organic substances, which allow to measure obvious and exact results for each base-paper. This test method can help classify base paper types in a simple and transparent manner and be of use in tracing quality problems of papers.

Key words: corrugated cardboard, base-paper, cellulose, thermo-analytical technique, heatflow, DSC

1. INTRODUCTION

The main chemical components of the base papers using for corrugated board are cellulose, hemicellulose and lignin. This finished material involves other incrust materials and extenders which constitute a complex chemical system (Soares et al, 1995). Knowing the exact components of corrugated cardboard papers are elementary for industrial processes and for consumers, because the mechanical and physical properties of these paper-based packaging, based on the chemical structure of it (Robertson, 2012). The thermo-analytical scanning calorimetry (DSC) analysers allows the identification of each substances according to it's natural origins which behaves on different ways during the test. Physical and chemical properties of each component can paraphrase accurately the investigated paper, independently from the condition of papers and effects of the environment on it. Contrary to currently used test methods (CCT, RCT, FCT, COBB etc.) can provide reproducible test results from the same samples (Caulfield et al, 1988).

2. THERMO-ANALYTICAL DSC METHOD

Using a DSC (Differential Scanning Calorimetry) apparatus is type of the Thermo-analytical test methods. The DSC measures the physical and chemical changes as a function of temperature. The thermal analysis provides information for the typify temperature peaks, which refer to characterization changes for each components. On the other hand derivative values proportional to the quantity of the transformed material, can be obtained (Haines, 2012). The method based on energy changes which can be monitored occurring in a given component during the heating and temperature keeping or cooling period. The test can measure the heat flow differences between the sample and the reference jars due to absorbed and released heat in function of temperature. In the most widespread DSC equipment a constant heating rate is used, and the

heat flow differential between the sample and the reference material is registered as a temperature differential ratio. The formula for the measure heat flow is shown below:

$$\frac{dH}{dt} = C_p \frac{dT}{dt} + f(T, t) \quad (1)$$

where dH/dt is DSC heat flow signal

C_p is a sample heat capacity (heat specific x weight)

dT/dt is heating rate

$f(T, t)$ is heat flow that function of time at an absolute temperature (kinetic)



Figure 1: DSC equipment apparatus, its test cell and nitrogen tank

During the test a differential thermal analysis curve of the sample is recorded, where the abscissa represents temperature or time, with the heat flow (set according to the exothermic or endothermic nature of the change) shown on the ordinate. For example, Figure 2 shows the characteristic curve of a high cellulose content paper's examination result.

The temperature at which a transformation takes place (initial temperature) is shown by the intersection of the extension of the base line and the tangent to the inflexion point. The conclusion of the temperature dependent transformation is shown by the peak of the curve.

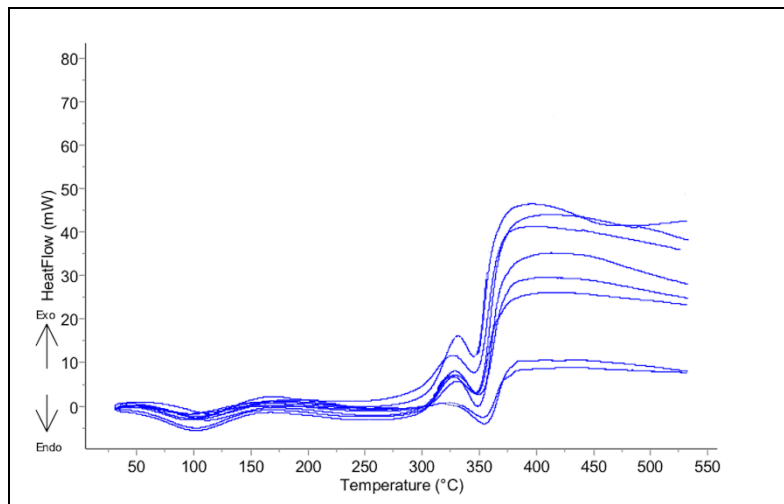


Figure 2: DSC curves of pure cellulose

The enthalpy of the transformation is proportional to the area between the curve and the baseline (the correct ratio can be defined through measuring a known material). Through the post-measurement analysis the temperature interval, peak temperature, heat flow, and heat in ratio of mass for the transformation can be expressed.

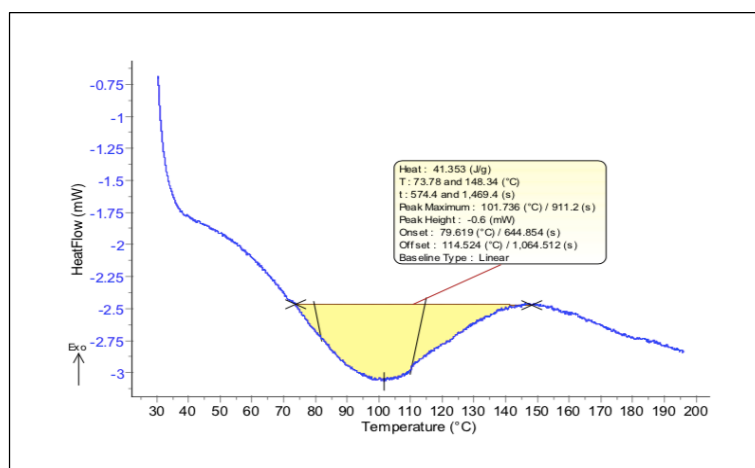


Figure 3: A sample DSC curve at the measurement of a paper sample

3. MEASUREMENT AND ANALYSIS

For the series of measurements 5 different materials are tested, pure cotton, soft wood sulphite pulp, “Kraft liner” base paper, filler material I., filler material II.

Table 1: Tested materials list with specific properties.

Tested material	Source	Content
Pure Cotton	Natural cotton treated with NaOH	Cellulose
Soft wood Sulphite pulp	Pine treated by sulphite method	Cellulose, hemicellulose, lignin
“Kraft liner” base paper	Pine treated by sulphate method	Cellulose, hemicellulose, lignin & inorganic components
Filler material I.	Mined minerals	Kaolin
Filler material II.	Mined Minerals	CaCO ₃

3.1 Test procedure

1. Preparation of test samples 8-20 mg sample take place in 30 µl jar, which exact weight measure with precision mg weight measurement apparatus.
2. A reference jar and a jar filled with the sample have to be placed into the Setaram DSC measuring device.
3. A predefined test program have to be performed.
4. Using nitrogen purge during examination.
 - a. Heating the test chamber of the measuring device to 30°C and keeping it at this temperature for 10 minutes.
 - b. Heating the test chamber up to 540°C at a rate of 10K/min.
 - c. Recording temperature differentials between the sample to be examined and the reference jar.
 - d. Analysing the data on the basis of peak temperatures and heat flow.
5. Performing the measurement on 5 samples per base paper and presenting the results obtained and their averages graphically.

4. RESULTS AND DISCUSSION

Table 2: DSC results of the tested materials

Tested materials	Avg.	T max [°C] endothermic	T max [°C] exothermic	Heatflow [mW]	Mass [mg]
Pure Cotton	Avg.	350	400	38	9,8
Soft wood Sulphite pulp	Avg.	275	400	65	12
“Kraft liner” base paper	Avg.	325	370	20	11
Filler material I.	Avg.	500	-	-	20,24
Filler material II.	Avg.	490	-	-	20,24

As the results show in Table 2. Most measured temperature peaks belong to endotherm and exothermal processes refer to the tested materials. In case of pure cotton shows accurate temperature peak at 350 °C as a specific endotherm peak and shows another peak at 400 °C as an exothermal. The Soft wood Sulphite pulp behave under the test nearly identically, produced same peaks endo- and exothermal at 275°C and 400°C. The examination adverts to “Kraft liner” base paper at 325°C as an exothermal and 370°C as a endotherm result. In the table are several dates are missing because it was not detected any exothermic maximum and heat flow value. The tested material with a higher cellulose content resolved on higher temperature on about 400°C and its thermal degradation starts at a higher temperature than the hemicellulose and lignin contain pulp. Results can be explained the structural different between the cellulose and hemicellulose. The cellulose it is a longer and more pure polysaccharide chain molecule than the hemicellulose which is a shorter polysaccharide and it is contained different hexoses and pentoses. And The studied extenders mined minerals (kaolin & CaCO₃) show no significant temperature peaks or thermal degradation in this examination range.

5. CONCLUSIONS

Table 3: Test zones with temperature range, peaks and reaction types

Zones	Temperature range [°C]	Temperature peaks [°C]	Reaction types
I.	0-100°C	100°C	Chemically bound water leaving
II.	100-250°C	250°C	Decomposition of extractable materials
III.	250-350°C	275°C	Decomposition
IV.	350-550°C	325°C & 350°C; 400°C	Decomposition
V.	Over 550°C		Decomposition

Results can be explained that at lower temperature, the samples behave on similar way, mainly the chemically bonded water leave from each materials (Saher et al, 2011; Yang, Yan, Chen Et al, 2006). At higher temperature between 200 to 400 °C decomposition of extractable materials shown due to weight loss processes with different temperature peaks (Saher et al, 2011). In case of “Kraft liner” base paper the decomposition starts at 250°C and has its temperature peak at 325°C. Pure cellulose starts to decompose at 275°C and lasts until 350°C. The soft wood sulphite pulp starts decomposition at 220°C and it has its own temperature peak at 400°C hemicellulose and lignin behave nearly similar way in the examined temperature range. Extenders show no significant endotherm or exothermal changes under the test (Haiping et al, 2006).

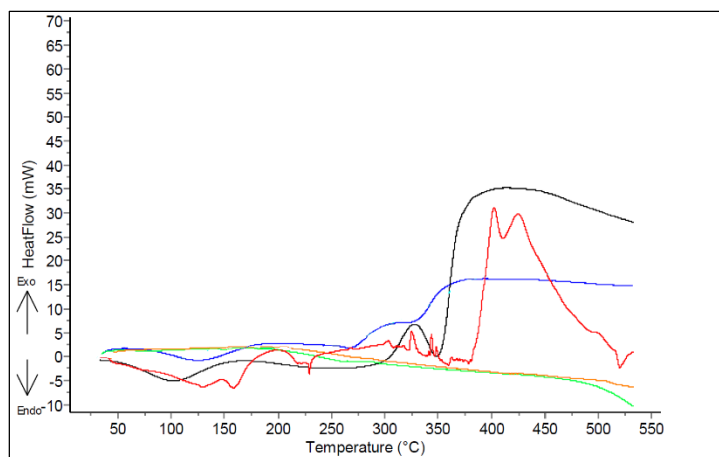


Figure 4: DSC curves of pure cotton-black, Soft wood sulphite pulp-red, Kraft liner base paper-blue, kaolin-green and CaCO_3 with brown colour

Table 4 shows the various DSC curves summarize on which the differences between the results of tested materials are shown. The reactions based on the content of cellulose. Materials which contain greater amount of cellulose, their cellulose molecules start its decomposition under a shorter range of the test-in opposite of lower cellulose content-and shown their typify temperature peaks by the results of the end of an exothermal reaction chain, which lead to its total charring. (Haiping et al, 2006; Yang et al, 2006). This conclusion can explain the results of the examined materials and shown its main differences and coherences in substances, which can be used for an accurate thermo-analytical identification independently from its multiple chemical components.

7. REFERENCES

- [1] Caulfield, D. F., Gunderson, D. E.: "Paper testing and strength characteristics", The 1988 paper preservation symposium, 1988 October 19-21 (Washington, DC. Atlanta, GA, 1988), pages 31-40.
- [2] Haines, P. J.: "Thermal methods of analysis, principles, applications and problems", Journal of Thermal Analysis, 45(1-2), 1995. doi: 10.1007/BF02548698
- [3] Haiping, Y., Hanping, C., Chuguang, Z.: "Characteristics of hemicellulose, cellulose and lignin pyrolysis", Fuel, 86(12-13), 1781-1788, 2007. doi: 10.1016/j.fuel.2006.12.013
- [4] Holmberg, M., Winqvist, F., Lundström, I., Gardner, J. W., & Hines, E. L.: "Identification of paper quality using a hybrid electronic nose", Sensors and Actuators B Chemical, 27(1-3), 246- 249, 1995. doi: 10.1016/0925-4005(94)01595-9
- [5] Robertson, G. L.: "Paper and paper-based packaging materials. Food packaging, principles and practice", 3rd ed, (CRC Press, Boca Raton, 2012).
- [6] Saher, F. I., El-Amoudy, E. S., Shady, K. E.: "Thermal Analysis and Characterization of some Cellulosic Fabrics Dyed by a New Natural Dye and Mordanted with Different Mordants", International Journal of Chemistry, 3(2), 40-54, 2011. doi: 10.5539/ijc.v3n2p40
- [7] Soares, S., Camino, G., Levchik, S.: "Comparative study of the thermal decomposition of pure cellulose and pulp paper", Polymer Degradation and Stability, 49(2), 275-283, 1995. doi: 10.1016/0141-3910(95)87009-1
- [8] Tsujiyama, S., Miyamori, A.: "Assignment of DSC thermograms of wood and its components", Thermochimica Acta, 351(1-2), 177-181, 2000. doi: 10.1016/S0040-6031(00)00429-9
- [9] Yang, H., Yan, R., Chen H., Zheng, C., Lee, D.H., Liang, D.T.: "In-depth investigation of biomass pyrolysis based on three major components: hemicellulose, cellulose and lignin", Energy & Fuels, 20(1), 2005. doi: 10.1021/ef0580117



© 2018 Authors. Published by the University of Novi Sad, Faculty of Technical Sciences, Department of Graphic Engineering and Design. This article is an open access article distributed under the terms and conditions of the Creative Commons Attribution license 3.0 Serbia (<http://creativecommons.org/licenses/by/3.0/rs/>).

GRAPHIC MATERIALS AND PROCESSES EFFICIENCY



UV ENERGY CURING OF DIELECTRIC LAYER FOR SCREEN PRINTED CAPACITIVE CHEMICAL SENSORS

Miha Golob 

The Secondary School of Multimedia and Graphic Technology Ljubljana, Ljubljana, Slovenia

Abstract: Functional printing is becoming a new standard in the printing industry and new materials are being developed for use with conventional printing methods. The purpose of our research was to successfully print and measure the change in capacitance of a multi-layered interdigitated capacitor, when exposed to water vapour in air. Commercially available printing inks were applied, including one silver-based conductive ink and one dielectric ink. Conductive structures with resolution of up to 300 microns were printed with a screen density of 120 lines/cm. Two-layered elements of dielectric printing ink and an additional layer of conductive ink were successfully applied onto a printing substrate coated with a conductive indium tin oxide layer. Capacitance of a parallel-plate and interdigitated capacitor was determined by implementing variation in the position of electrodes for measurements. The results confirm that the change of UV energy applied for curing of the dielectric ink has no significant influence on the capacitance of printed sensors, as opposed by the factor of capacitor function and surface area. Capacitance was greater when measured as a parallel-plate capacitor with dielectric layer between two electrodes and a larger surface area than interdigitated in-plane capacitor printed on the same sample. Dissipation factor diminishes with higher UV energy applied for curing of the dielectric ink. Sensor response to changes in relative humidity is even and can be reproduced. Change of capacitance of sensor is higher with increase in relative humidity, thus the prepared sensors are properly responsive.

Key words: screen printing, chemical sensor, functional printing, UV energy

1. INTRODUCTION

Printed electronics is a technology that merges electronics manufacturing and text/graphic printing. By this combination it is feasible to manufacture high-quality electronics products that are thin, flexible, wearable, lightweight, of varying sizes, ultra-cost-effective, and environmentally friendly. Fabrication of various types of sensing devices is seen as one of many possible applications in the field of printed electronics, for example, environmental sensors (temperature, humidity, gas concentration, ion concentration), biosensors (glucose, blood pressure, DNA), pressure sensors (floor mat sensor, touch sensor, explosion sensor), and light sensors (Suganuma, 2014).

Among different sensing principles, sensors based on resistance changes-chemoresistors, and capacitive changes-chemocapacitors, have attracted considerable research interest because they fulfil the low energy consumption criterion. Both sensor types can be fabricated with conventional microelectronic-micromachining processes as well as functional printing and they operate at room temperature offering low power consumption. Their response is usually fast and reversible and present good sensitivity to polar analytes (Botisalas et al, 2013).

The operating principle of planar interdigitated capacitance sensor (IDCS) basically follows the rule of two parallel plate capacitors, where electrodes open up to provide a one sided access to material under test (MUT) [Abdul Rahman et al, 2014]. In an IDCS the sensitivity to variations of the conductivity or permittivity depends on the penetration of the electric field inside a MUT contributing to the capacitance and impedance between electrodes (Mamishhev et al, 2004). Depending on the geometric configuration of the electrodes the electric field lines can penetrate deeper or less deep. The capacitance of an IDCS always depends on the dielectric properties of the MUT and the geometry of the electrodes (Guadarrama-Santana et al, 2014). When the sensitive layer (commonly a polymer) interacts with the chemicals present in the environment, the chemically sensitive layer changes its conductivity (σ), dielectric constant (ϵ) or its effective thickness (d). The interdigitated capacitance (IDC) chemical sensor can then detect a change in capacitance and/or impedance due to a change of the dielectric constant and thickness of the layer. IDC chemical sensors have been investigated by many researchers because they are inexpensive to manufacture and easily integrated with other sensing components and signal processing electronics (Mamishhev et al, 2004).

Since the electrodes of an IDCS are coplanar, the measured capacitance will give a high signal-to-noise ratio. Consequently, the electrode pattern of the IDCS can be repeated many times to get a strong signal.

The term “interdigitated” refers to a digit-like or finger-like periodic pattern of parallel in-plane electrodes, used to build up the capacitance associated with the electric fields that penetrate into a material sample (Abdul Rahman et al, 2014).

Chemical sensors constitute a large portion of all interdigital sensors described in the literature. They are used in detection of various gases, chemicals, moisture, organic impurities, etc. A typical chemical interdigital sensor design is to deposit interdigital electrodes on an insulating substrate (Mamishhev et al, 2004). Application of electrodes can be achieved by using common printing methods such as screen printing. Polymer inks containing electrically conductive particles are the most common choice for this purpose in the field of printed electronics, with silver particles offering the lowest resistivity (Žveglič, 2011). The electrodes are then coated with a thin layer of material that is sensitive to the concentration of chemicals present in the ambient atmosphere. When the sensor is exposed to ambient chemicals, changes in capacitance are the result of the change of dielectric constant and effective thickness of the sensitive layer (Mamishhev et al, 2004). Coating material often consists of derivatives of metacrylic acid, such as Poly(2-hydroxyethyl metacrylate) or pHEMA (Reddy, 2011), Poly(butyl methacrylate) or PBMA and Poly(ethyl methacrylate) or PEMA (Oikonomou et al, 2011), Polyvinylpyrrolidone or PVP, Poly(ethyleneimine) or PEI, polyhydroxystyrene or PHS (Botisalas et al, 2013).

2. METHODS

Electrodag PM-470 conductive screen-printable ink (Acheson Colloiden B.V., Netherlands) was used. It contains finely distributed silver particles in a thermoplastic resin. Its density is about 2140 kg/m³ and the solid content 58–62 %. CFSN6057 Suntronic Dielectric 681 dielectric screen-printable ink with density of approximately 1270 kg/m³, dielectric constant specified at $\epsilon = 4.76$ (@ 1 MHz) and breakdown voltage using direct current at 3100 V at layer thickness 25,4 μm . Recommended curing of the dielectric ink by the manufacturer is 650 mJ/cm².

RokuPrint SD 05 semi-automatic screen printing machine with adjustable table KO03 and pneumatic squeegee mechanism PR01 was used for printing. Printing forms with resolution of conductive structures of up to 300 microns were prepared on a high-modulus monofilament polyester plain weave mesh 120/34Y. A squeegee with a hardness of 75° Sh was used. For printing substrate, clear polyethylene film, coated on one side with indium tin oxide (ITO) was used.

Double layer prints (wet-on-dry) of dielectric ink (CFSN6057 Suntronic Dielectric 681) were made on conductive side of ITO coated film. Two samples of four different double layer prints were prepared and each layer of the sample cured with UV energy of 600, 1200, 1800, and 2400 mJ/cm², respectively. UV curing was carried out using Aktiprint L 10-1 UV dryer. Additional layer of conductive ink was printed (wet-on-dry) on top of the dielectric layer for each sample. The drying procedure involved placing the printed substrate level on a work bench for 5 min at room temperature and curing at 170 °C for 5 min in infrared tunnel Shrink Machine BS-B400.

The measurement of the change in capacitance of prepared sample sensors was carried out using Boonton 72B capacitance meter at the frequency of 1 MHz. Sample response to relative humidity was carried out in a measurement chamber with approximately 1 L volume after first neutralizing the measurement chamber with nitrogen gas with gas flow of 1,1 L/min. All measurements were conducted at temperature of 26 °C.

3. RESULTS

3.1 Capacitance measurements

Figure 1 depicts the placement of electrodes used in capacitance measurements of prepared sensor. The dielectric layer was placed between a conductive layer of indium tin oxide (ITO) on the surface of the substrate and a geometry of interdigitated sensor electrodes screen printed with conductive ink in the same plane (Lo, HiS, HiR, and Sb) on the surface of the dielectric layer.

Two different capacitor configurations were used, based on the position of the electrodes and dielectric layer. Measurements between electrodes Lo-ITO and Sb-ITO were carried out using parallel plate configuration. Measurements between electrodes Lo-HiS and Lo-HiR had the characteristics of an interdigitated capacitor (Figure 2).

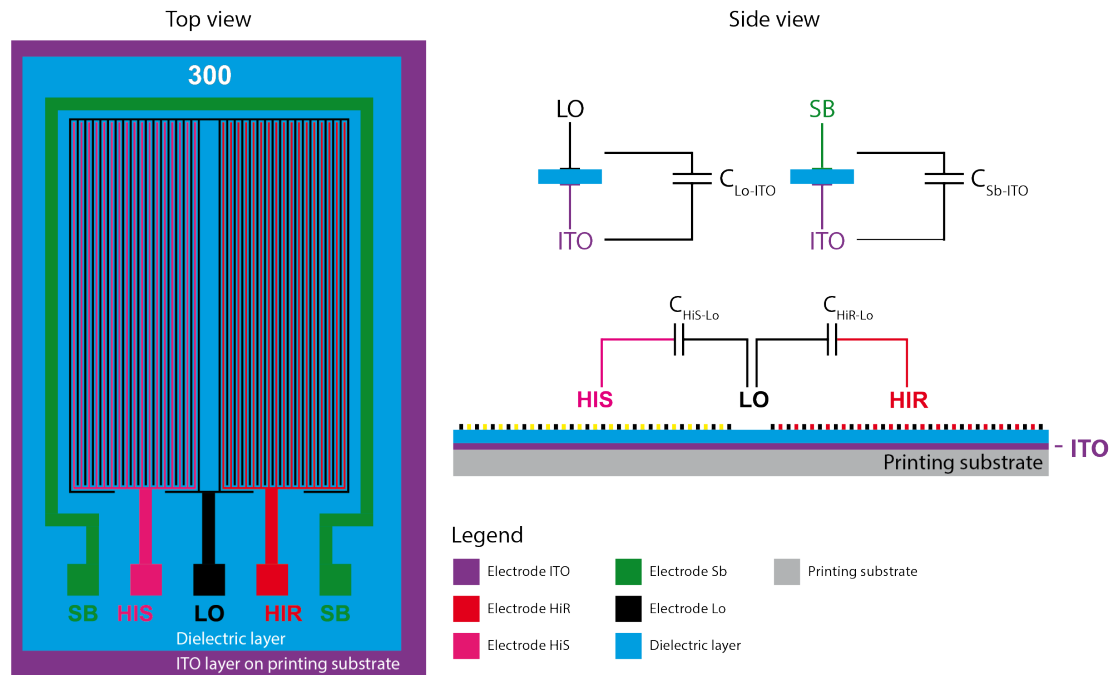


Figure 1: Schematic view of sensor electrode and dielectric layer placement.

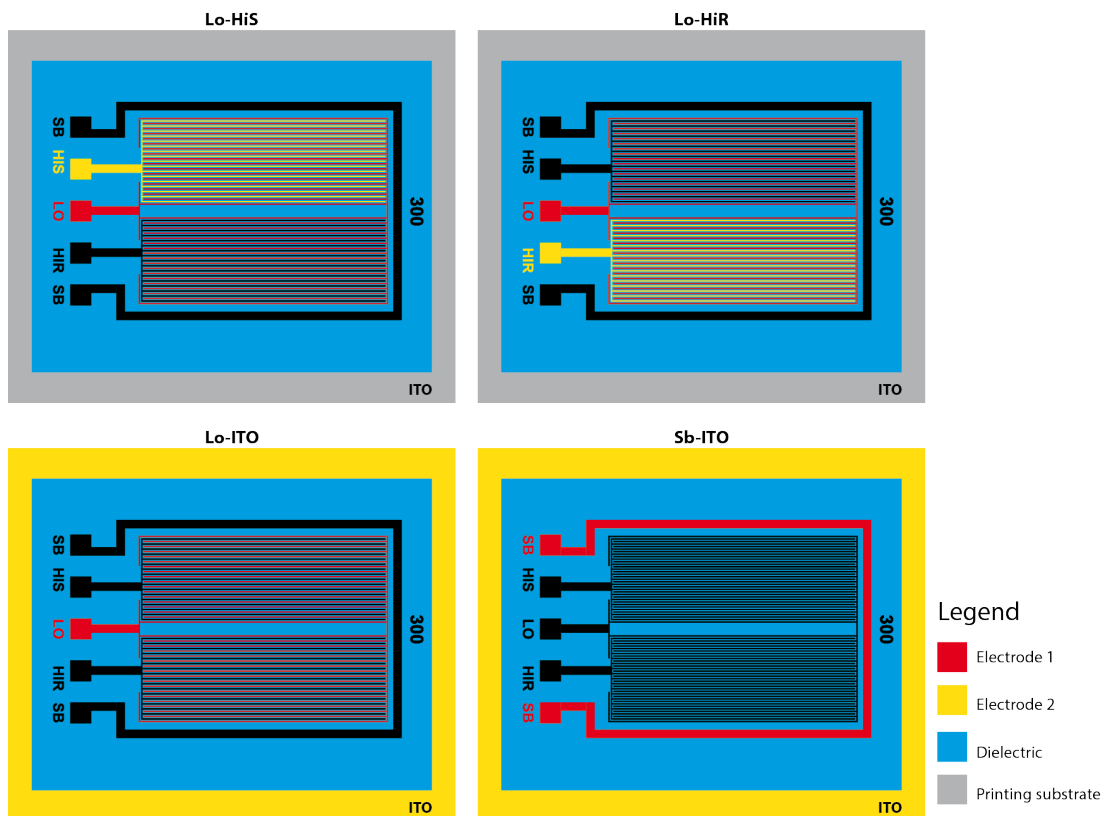


Figure 2: Electrode configuration for capacitance measurement.

Figure 3 shows the results of capacitance of prepared capacitors in relation to configuration of electrodes for measurement and UV energy used for curing of the dielectric layer. Out of eight prepared sensors, we experienced only one shortcircuit of a sample cured with UV energy of 600 mJ/cm². Measurements show that the influence of UV energy used for curing of the dielectric functional ink is small. On the other hand

we observed an increase in capacitance with the increase of surface of the electrodes. For parallel-plate capacitors with a dielectric layer between electrodes, capacitance C is defined as:

$$C = \varepsilon \varepsilon_0 \frac{A}{d}, [\text{pF}] \quad (1)$$

where A is the surface of the electrodes, d is the thickness of dielectric layer, ε is the dielectric constant, ε_0 is constant value defined as $\varepsilon_0 = 8,854 \cdot 10^{-12} \text{ F m}^{-1}$ (Breurer et al, 1993; Horvat, 2015). The capacitance of parallel-plate Lo-ITO capacitor is approximately 50 % greater than the capacitance of parallel-plate Sb-ITO configuration and approximately 70 % greater than the average of Lo-HiS/Lo-HiR interdigitated capacitor measurements. The latter is shown as an average since both capacitors use identical geometry and differences in measurements were negligible. Higher capacitance of Lo-ITO configuration may be caused by some advantages of interdigitated sensor design on one side and increased surface on the other, when compared to measurement results of capacitance between electrodes Sb-ITO and Lo-HiS/HiR.

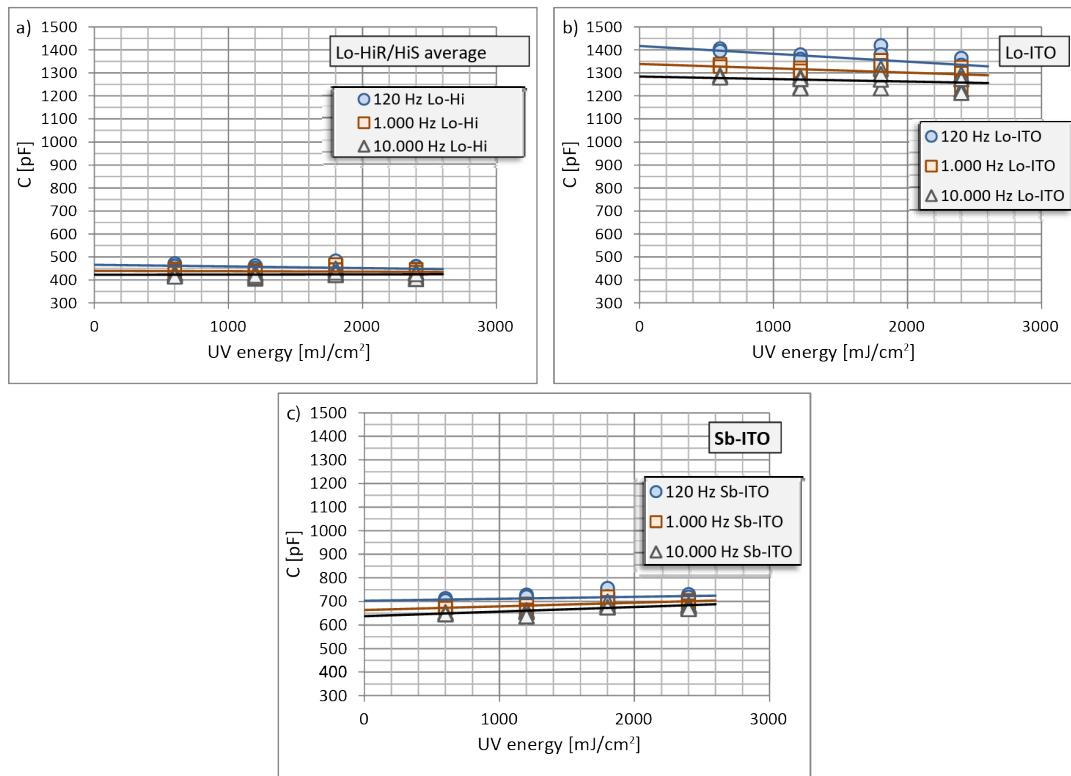


Figure 3: Capacitance measurement of screen-printed capacitors at different frequencies and different configuration of electrodes for measurement: (a) Lo-HiS/Lo-HiR average, (b) Lo-ITO, (c) Sb-ITO.

Surface area of different electrodes used in measurements is presented in figure 4.

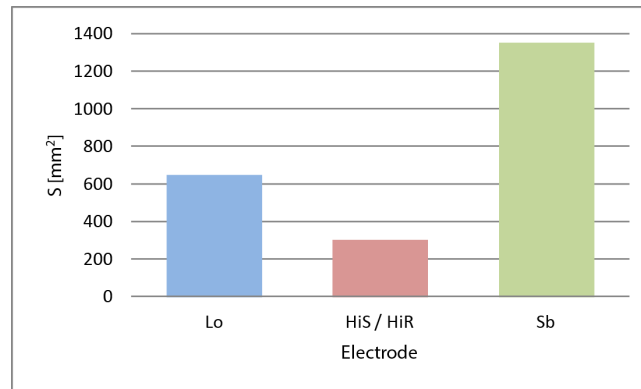


Figure 4: Surface of electrodes used in capacitance measurements (from left to right: Lo, HiS/HiR, Sb).

3.2 Dissipation factor

Dielectric loss quantifies a dielectric material's inherent dissipation of electromagnetic energy (e.g. heat). In a capacitor made of a dielectric placed between conductors it is quantified as the dissipation factor (DF), a measure of loss-rate of energy of a mode of oscillation in a dissipative system. It is the reciprocal of quality factor, which represents the "quality" or durability of oscillation. It can be parameterized in terms of either the *loss angle* δ or the corresponding loss tangent $\tan \delta$ (Horvat, 2015).

Based on the specification provided by dielectric ink manufacturer, the dissipation factor ($\tan \delta$) corresponds to DF = 0.013 (@1 MHz). Based on the measurements represented in figure 5 we can observe that the dissipation factor diminishes with increase in UV energy used for curing of dielectric layer and an increase in frequency of measurement. The biggest variations in measurements were observed when frequency of 120 Hz was used.

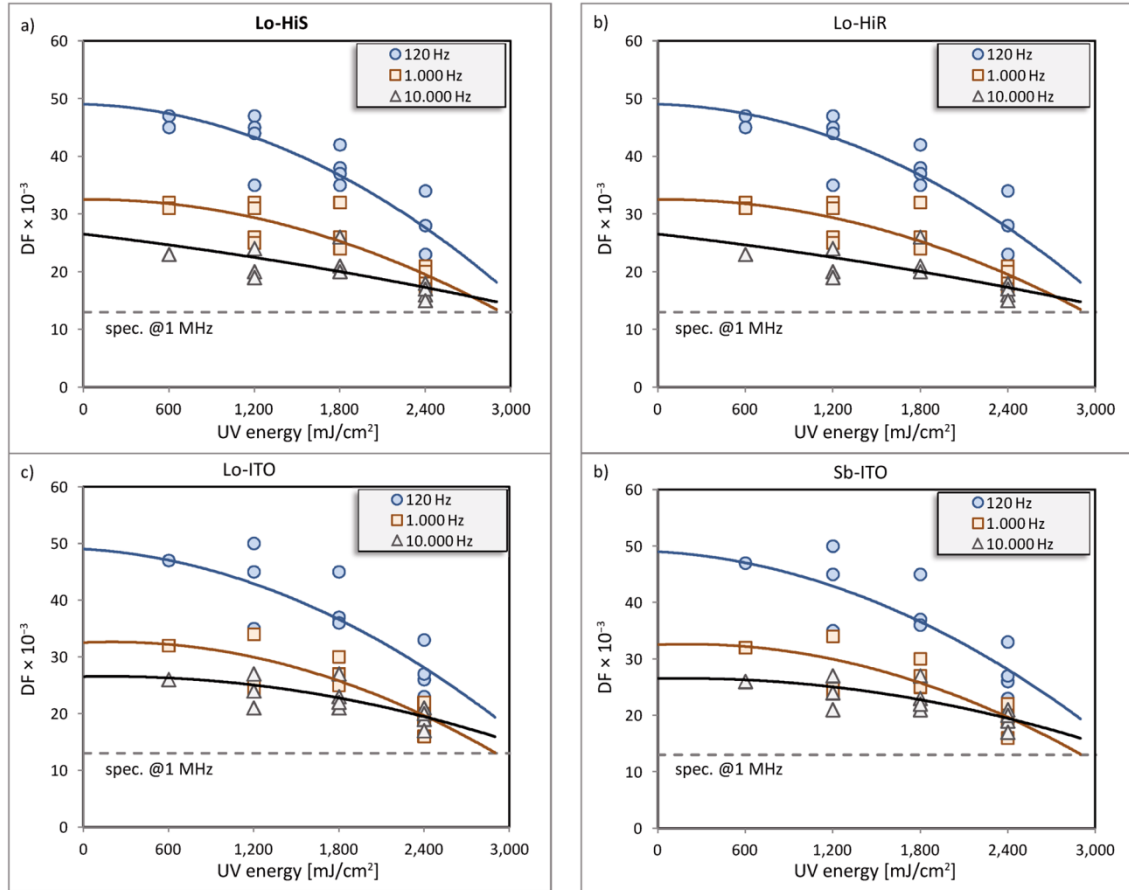


Figure 5: Dissipation factor measurements of screen-printed capacitors at different frequencies and different configuration of electrodes for measurement (a) Lo-HiS, (b) Lo-HiR, (c) Lo-ITO, (d) Sb-ITO.

3.2 Sensor response to change in relative humidity

Sensor with dielectric layer that was cured at UV energy of 2400 mJ/cm^2 was considered to be the most appropriate to study the response to changes in relative humidity, based on the measurements of capacitance and dissipation factor (Figure 6). In-plane interdigitated electrode geometry Lo-HiR, was used for measurements of sensor response.

First measurements of sensor response were made at relative humidity of 45 %. The base value of capacitance when the measurement chamber was filled with nitrogen gas was in the range of 250 pF. When water vapour was introduced to the measurement chamber the capacitance slowly increased to approximately 340 pF (figure 7). In comparison, the drop in capacitance was quicker, when the chamber was being purged with nitrogen gas. Sensor was characterized in transient state with six consecutive measurements made and all of them showed a similar response in change of capacitance.

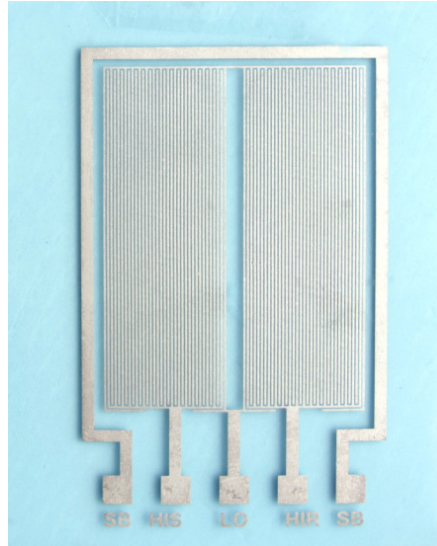


Figure 6: Sample sensor with conductive 300 micron interdigitated structure screen printed on two layer dielectric cured with UV energy 2400 mJ/cm².

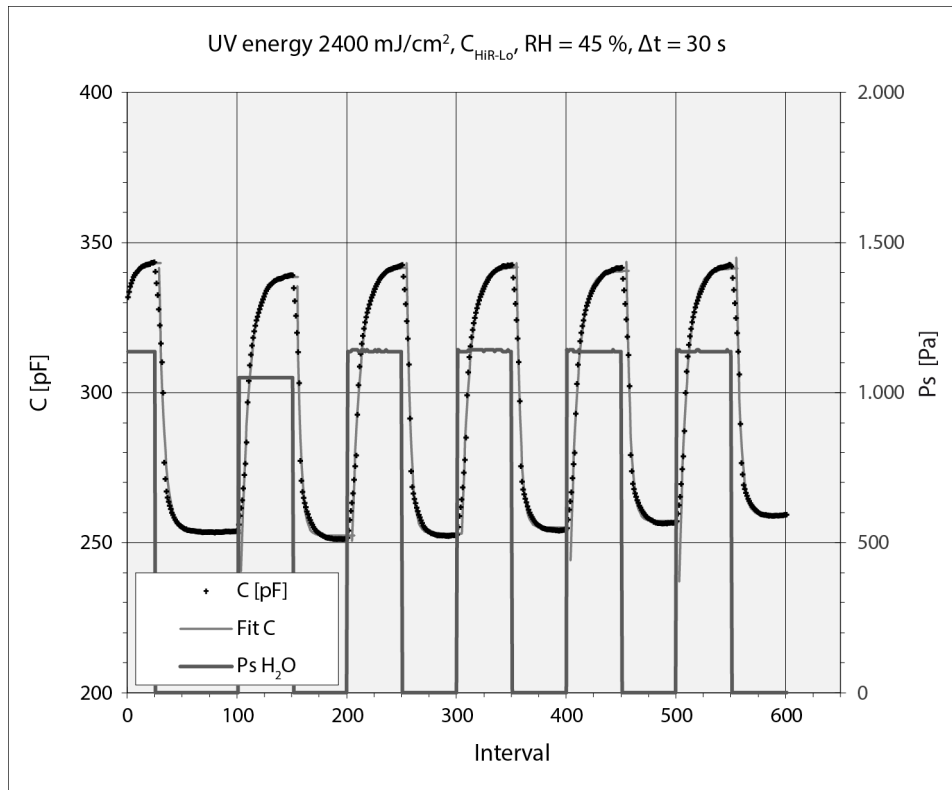


Figure 7: Sensor response to the change in relative humidity of 45 % in the measurement chamber.

Second measurements of sensor response were made at relative humidity of 53 %. The base value of capacitance when the measurement chamber was filled with nitrogen gas was in the range of 260 pF. When water vapour was introduced to the measurement chamber the capacitance slowly increased to approximately 370 pF (figure 8). This shows that sensor response was greater when higher values of relative humidity were introduced and that the sensor is properly responsive. Six consecutive measurements were made. First and second measurements of capacitance differ from the rest, due to an error on the nitrogen gas inlet at the measurement chamber.

The time interval used for individual measurements of sensor response was 30 s.

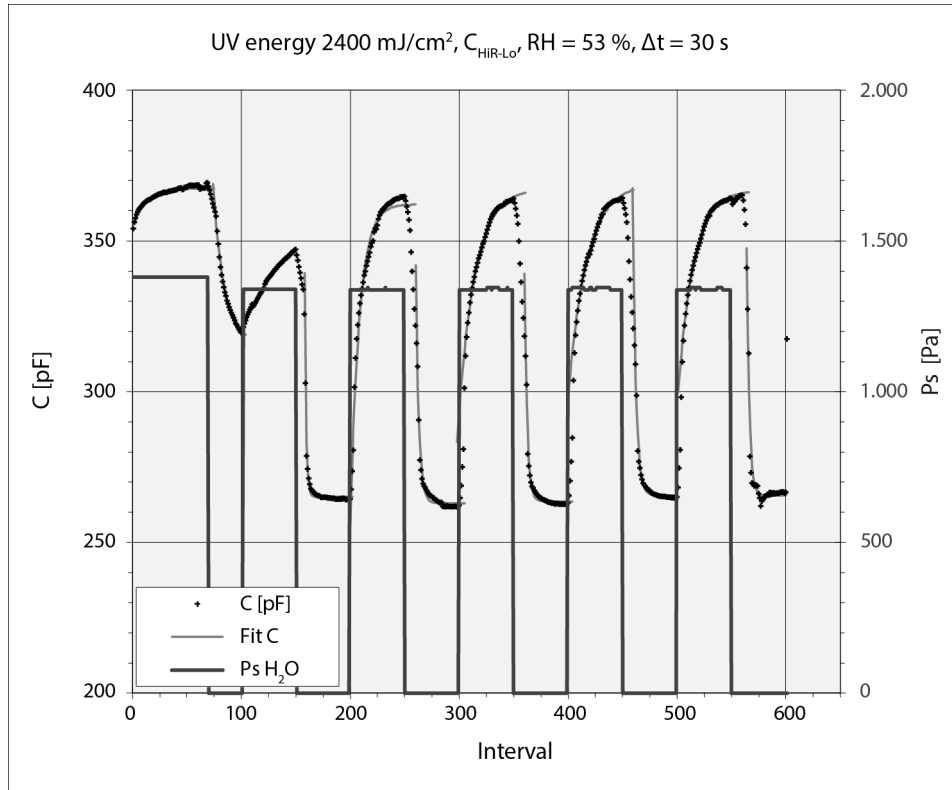


Figure 8: Sensor response to the change in relative humidity of 53 % in the measurement chamber.

4. DISCUSSION

Differences in capacitance of sensors were due to different placements of electrodes and therefore changes in geometry and surface of electrodes. Based on very low differences between capacitance measurements of samples with dielectric layer cured at different UV energy dose we can conclude that the layer was sufficiently polymerized at UV energy of 600 mJ/cm². This figure closely reflects the recommendations of printing ink manufacturer which state that UV energy of 650 mJ/cm² is needed for complete curing of the ink. On the other hand the dissipation factor measurements showed that there was still room for improvement in terms of quality of capacitor as the samples cured at higher UV energy were closer to the value of DF = 0.013 (@1 MHz) stated by the ink manufacturer.

Capacitance of sensor changes with the increase of dielectric constant of the dielectric used. The sensor response to change of relative humidity in the measurement chamber was expected as the dielectric constant of water is $\epsilon \sim 55$ (@100 °C) and the dielectric ink used was specified by the manufacturer at $\epsilon = 4.76$ (@ 1 MHz). When using relative humidity of 53 % to measure the sensor response, the base value of capacitance when the measuring chamber was purged with nitrogen gas was approximately 10 pF greater, in comparison to measurements made at 45 % relative humidity. We can conclude that the short time interval between measurements caused a temporary saturation of dielectric layer with water molecules, when the relative humidity in the measurement chamber was higher. Longer time interval between measurements could help prevent this. The results also show that sensor response was greater when higher values of relative humidity were introduced and indicate that similar results could be obtained if higher values of relative humidity were used. Sensor response to water vapour was slower when compared to response to the purge of measurement chamber with nitrogen gas. The designed sensor was reversible and did not get overly saturated when exposed to molecules of water vapour. The sensor response was more or less uniform throughout the measurements, although errors were recorded due to a malfunction of the nitrogen gas inlet

5. CONCLUSIONS

Screen printed multi-layered interdigitated capacitors have been fabricated on ITO coated PE substrate with printing resolution of 300 microns using commercially available printing inks. The influence of UV energy used for dielectric layer curing and sensor geometry was considered for practical use of prepared chemical sensors. The potential of the devices for sensing has been evaluated for relative humidity capacitive sensing, by preparing samples with dielectric layers cured at different UV energy, whose electrical permittivity and thickness is sensitive to changes in relative humidity. The characterization of the sensors in transient state offered reproducible measurements when exposed to 45 % and 53 % relative humidity. The signal obtained from measurements was both stable and reproducible. In future efforts the described technique could be used with different dielectric materials used to study sensor response to different gas analytes, and eventually implemented in applications such as an electronic nose.

6. ACKNOWLEDGMENTS

The author acknowledges the support of Marta Klanjšek Gunde, National Institute of Chemistry, Marijan Maček, University of Ljubljana, Faculty of Electrical Engineering, and Matej Pivar, University of Ljubljana, Faculty of Natural Sciences and Engineering.

7. REFERENCES

- [1] Abdul Rahman, M.S., Mukhopadhyay, S.C., Yu, P.-L.: "Novel sensors for food inspection: Modelling, Fabrication and Experimentation", (Springer, New Delhi, 2014), chapter 2.
- [2] Botisalas, A., Oikonomou, P., Goustouridis, D., Ganetsos, Th., Rapis, I., Sanopoluou, M.: "A miniaturized chemocapacitor system for the detection of volatile organic compounds", *Sensors and actuators B: Chemicals* 177, 776–784, 2013. doi: 10.1016/j.snb.2012.11.050.
- [3] Breurer, H., Breurer, R.: "Atlas klasične in modern fizike", (DZS, 1993, Ljubljana), pages 150–157.
- [4] Guadarrama-Santana, A., García-Valenzuela, A., Pérez-Jiménez, F., Polo-Parada, L.: "Interdigitated capacitance sensors in the mm scale with sub-femtoFarad resolution suitable for monitoring processes in liquid films", *Revista Mexicana de Física* 60, 451–459, 2014.
- [5] Horvat, M.: "Tisk in analiza pasivnih elektronskih elementov", PhD thesis, NTF - Naravoslovnotehniška fakulteta, Ljubljana, 2015.
- [6] Mamishev, A.V., Sundara-Rajan, K., Yang, F., Du, Y., Zahn, M.: "Interdigital sensors and transducers", *Proceedings of the IEEE International Conference on Communications 2004*, (IEEE, San Diego, 2004), pages 808–844. doi:10.1109/JPROC.2004.826603.
- [7] Oikonomou, P., Salapatras, A., Manoli, K., Misiakos, K., Goustouridis, D., Valamontes, E., Sanopoulou, M., Raptis, I., Patsis, G. P.: "Chemocapacitance response simulation through polymer swelling and capacitor modelling", *Procedia Engineering* 25, 423–426, 2011. doi:10.1016/j.proeng.2011.12.105.
- [8] Reddy, A.S.G., Narakathu, B.B., Atashabar, M.Z., Rebros, M., Rebrosova, E., Joyce, M.K.: "Fully printed flexible humidity sensor", *Procedia Engineering* 25, 120–123, 2011. doi: 10.1016/j.proeng.2011.12.030.
- [9] Suganuma, K.: "Introduction to printed electronics", (Springer Science+Business Media, New York, 2014), pages 1–31.
- [10] Žveglič, M., Hauptman, N., Maček, M., Klanjšek Gunde, M.: "Screen-printed electrically conductive functionalities in paper substrates", *Materials and technology* 45(6), 627–632, 2011.



© 2018 Authors. Published by the University of Novi Sad, Faculty of Technical Sciences, Department of Graphic Engineering and Design. This article is an open access article distributed under the terms and conditions of the Creative Commons Attribution license 3.0 Serbia (<http://creativecommons.org/licenses/by/3.0/rs/>).

ANALYSIS OF THE INTERACTIONS IN THE “VARNISH – PHOTOPOLYMER” SYSTEM

Tomislav Hudika , Tamara Tomašegović , Tomislav Cigula , Ante Poljičak 
University of Zagreb, Faculty of Graphic Arts, Zagreb, Croatia

Abstract: Varnishing of the printed product is often carried out by means of a photopolymer flexographic printing plate. Various types of varnishes interacting with a photopolymer material can cause chemical changes in its surface layer and affect the acceptance and transfer of varnish to the print. The aim of this paper is to describe the interactions of different types of varnishes and standard styrene-isoprene-styrene flexographic printing plate and to analyse the influence of varnishes on the surface layer of the photopolymer material. Types of varnishes used in this research are matt and gloss water-dispersive varnish, oil-based and UV varnish. Their interactions with the printing plate were analysed using different methods: contact angles of the varnishes on the printing plate were measured, and surface free energy of the printing plate was calculated before and after application of the varnishes. Experiments of the swelling of printing plate were carried out in order to assess the effect of the varnishes on the chemical changes in the photopolymer material. Microscopic images of the photopolymer exposed to varnishes and FTIR-ATR spectra were obtained in order to capture visible changes on the printing plate's surface. The results of the research will allow for an assessment of the suitability of a specific type of varnish for flexographic printing.

Key words: photopolymer, varnish, swelling, contact angle, surface free energy

1. BACKGROUND

Flexography is a relief printing technique that uses rotary actions to transfer ink from photopolymer printing plate onto substrate. Flexography developed from the use for low quality images, to a method of wide implementation in printing - from newspaper, packaging to books with capability of using the wide range of printing substrates.

The printing process is simpler than the offset printing and it's the only letterpress process that is in wide use. The main feature is the soft photopolymer flexible printing plate and low viscosity ink, so it makes it possible to print on substrates of different surface properties and roughness, both absorbent and non-absorbent (Brajnović, 2011).

Flexographic inks have very similar viscosity to gravure inks (0,05-0,5 Pas). Flexographic inks are transferred onto the printing plate by the inking unit with a usage of the anilox roller. The viscosity is very important because it influences the ink and varnish properties, with the requirements such as squeezing of the ink or varnish out of the anilox cells (Havlínová et al, 1999).

The solvents used in flexographic printing most often are ethyl acetate, isopropyl alcohol and water. They are used as a component of the inks or as the cleaning agent for the printing plate. Varnishing is often conducted by photopolymer flexographic printing plate. Different types of varnishes interact differently with the photopolymer material. As well as the inks, varnishes can cause physical and chemical changes in the surface of the photopolymer material, which can lead to mechanical issues and low print quality (Tomašegović, 2016). Most common types of varnishes were used in this research: matt and gloss water-dispersive varnish, oil-based and UV varnish.

In this research, experiments of the swelling of printing plate were carried out in order to assess the effect of the varnishes on the chemical changes in the photopolymer material. Contact angles of the varnishes on the printing plate and surface free energy of the photopolymer material were calculated. Microscopic images of the photopolymer exposed to varnishes were obtained in order to capture visible changes on the printing plate's surface that would affect the quality of image reproduction.

The aim of this experimental work was to analyse the influence of different varnishes on the surface of the photopolymer printing plate in order to assess its suitability for the use with the specific varnish. This research enabled an assessment of the impact and suitability of a specific type of varnish for flexographic printing.

2. EXPERIMENTAL SETTINGS AND METHODS

2.1. Swelling of the photopolymer material

Swelling is common phenomena in the printing process. The deformation of the photopolymer printing plate is caused when the ink and solvents enter the material, resulting with problems in the printing process. In Figure 1, an infographic of the result of swollen photopolymer printing plate can be seen.

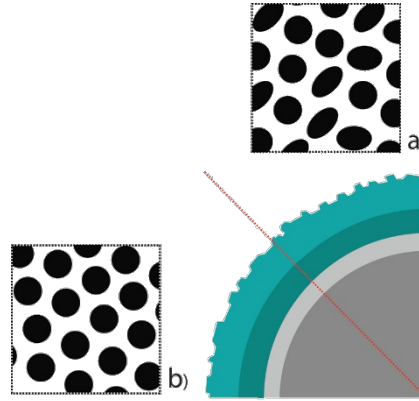


Figure 1: Infographics of swollen photopolymer; a) swollen photopolymer that leads to deformation of printing elements, b) normal, un-swollen photopolymer with stable printing elements

Problems that occurs due to the swelling are:

- a) Lack of register (misalignments of printing elements, poor pre-press calibration and colour imperfection)
- b) Problems with tolerances in the printing machine
- c) Poor print quality (distortion, errors, overlaps that can occur on the final product)
- d) Costs (decreased sleeve lifespan that causes more frequent sleeve replacing, additional cost of maintenance, poor print quality that leads to repetition of entire process, loss of customer)
- e) Dot gain due to swollen or deformed plates. It occurs most likely with use of aggressive inks, solvents, cleaners that cause the plates to swell (Jenkins, 1985; Liu et al, 2013).

In this experiment, swelling of the photopolymer sample was carried out in four varnishes mentioned in 2.1. Swelling experiments were performed until the equilibrium (normalized degree of swelling) was reached (Tomašegović et al, 2016). Measurements were performed by gravimetric method using analytical scale Mettler Toledo XS205 (MT laboratories, n.d.) in a controlled environment with a constant temperature of 23°C and relative humidity of 55±2 %.

Photopolymer samples were immersed in varnishes for periods up to 300 minutes, after which the weighing showed that the equilibrium of swelling was reached. Normalized swell ratio (M_t) for control periods of 5, 20, 40, 80, 120, 180, 240 and 300 minutes of immersion was calculated using Equation 1:

$$M_t = \frac{m_t - m_0}{m_0} \cdot 100\% \quad (1)$$

where m_t stands for the weight of the swollen polymer at a time t , and m_0 for the weight of the dry polymer sample before the immersion. Before each weighing, samples were quickly cleaned with acetone which causes minimal photopolymer swelling (Tomašegović, 2016). Swelling dynamics of the photopolymer material due to the effects of the varnishes was observed.

2.2. Contact angles of varnishes and surface free energy of photopolymer

Contact angle (Figure 2) is a quantitative measure of wetting of solid surface with a liquid. It can be described geometrically as the angle formed by the tangents on liquid drop and the solid surface at the three-phase boundary where a liquid, gas and solid come in contact. One can divide contact angles to static and dynamic one. The difference between contact angle hysteresis is referred as advancing or receding contact angle.

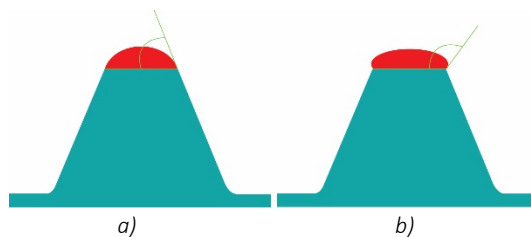


Figure 2: Difference between two contact angles of inks on flexographic printing element:
a) low contact angle, b) high contact angle

This feature is important and connected to surface wettability. High wettability results from the higher surface energy of solid that pulls the liquid down with strong attracting force. This feature makes the droplet to spread out on the solid surface. The surface tension of the liquid in this case is weaker than the surface free energy of the solid. Wetting is important for high-quality and stable printing process (Tryznowski et al, 2018).

For this research, static contact angles of four varnishes were measured on the surface of a classic, styrene-isoprene-styrene based LAMS printing plate. Used varnishes were matt and gloss water-based (water-dispersive) varnish, oil-based and UV varnish. Contact angles were measured using Dataphysics OCA30 goniometer and its program support. Static contact angle of varnishes on the printing plate were measured using the needle-in sessile drop method, with the volume of the drop of 10 μl . Measurements were taken at the point of the stabilization of the drop on the polymer surface.

Surface free energy of the printing plate was calculated using the contact angles of three probe liquids (water, diiodomethane and glycerol) and OWRK method (Owens et al, 1969). Volume of the probe liquid drops was 1 μl , and the sessile drop method was used. Measurements of the contact angle were taken 4 seconds after the initial contact of the liquid and solid.

2.3. FTIR-ATR spectroscopy and microscopy

In order to analyse the chemical changes in the surface layer of the printing plate samples after swelling, FTIR-ATR spectra of the photopolymer in transmittance mode was collected. Since the FTIR-ATR method provides the information about the vibrations of certain chemical bonds only in the depth of 1-2 μm of the analysed sample, changes in the spectra could be used to explain the changes occurring in the surface layer of the material after the exposure to different varnishes (Tomašegović, 2016).

In order to check for the possible visible damage and changes on the photopolymer surface caused by the immersion in varnishes, microscopy of the printing plate surface was performed before and after the immersion in varnishes. Olympus BX51 microscope was used for this purpose, and the magnification was set to 200x (Olympus, n.d.).

3. RESULTS AND DISCUSSION

3.1. Swelling of the photopolymer material

Swelling experiments were performed in order to assess the resistance of the photopolymer to the specific varnish, i.e. to determine if the varnish penetrates the photopolymer matrix and/or partially dissolves it. Figure 3 presents the dynamics of photopolymer swelling in different varnishes. Water-based varnishes have a negligible impact on the tested material – maximal normalized degree of swelling is cca. 0.5% of the solid sample weight (Figure 3a) – b). After 300 minutes of the immersion, swelling equilibrium is reached. In Figure 3c, one can see the dynamics of swelling of the sample immersed in the UV-curable varnish. It is visible that the swelling process starts to slow down after cca. 200 minutes, and that the normalized degree of swelling reaches 1.1% after 300 minutes. This is acceptable from the point of the graphic reproduction process, but it is evident that the swelling process continues even after 5 hours. Therefore, the interaction of the UV varnish and flexographic printing plate should be monitored for higher run lengths.

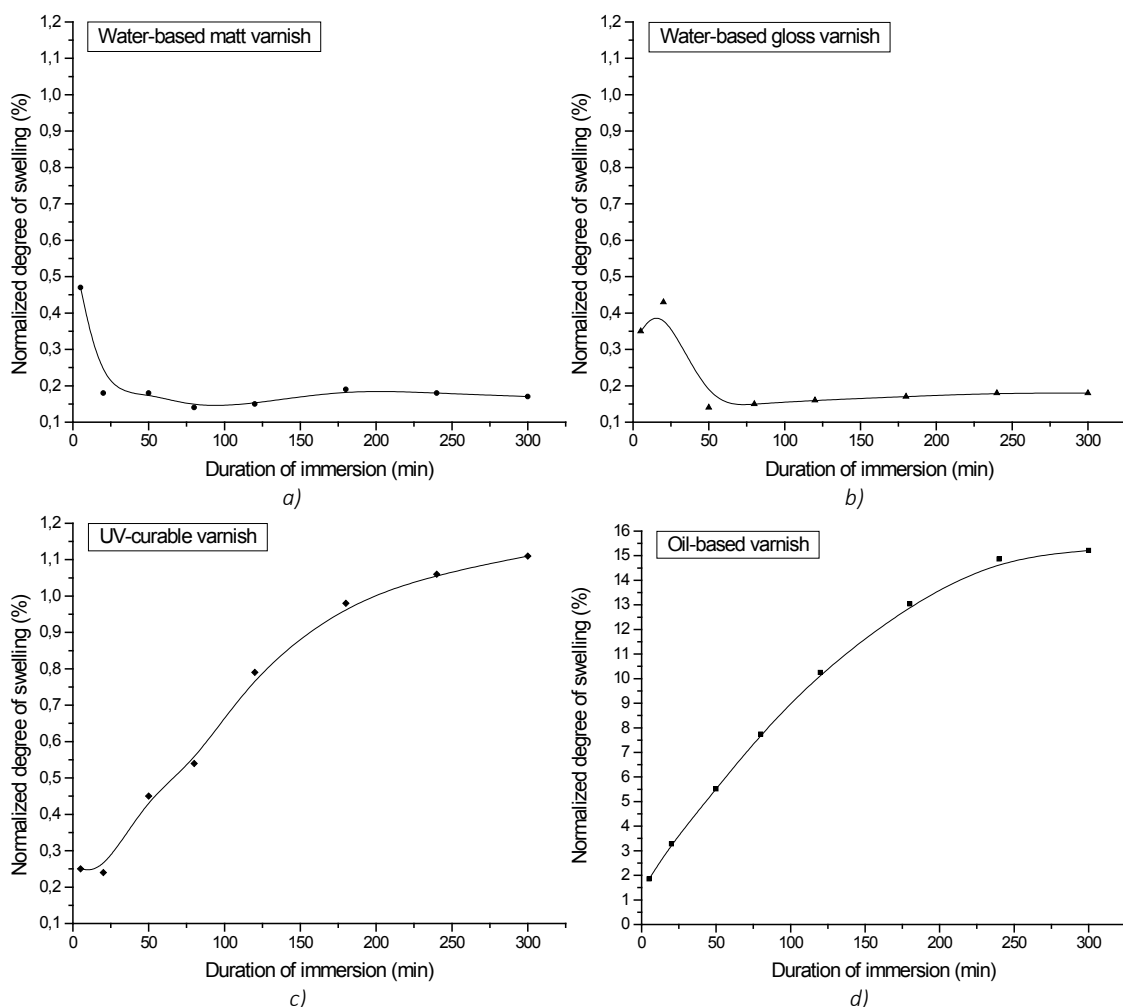


Figure 3: Swelling dynamics of the photopolymer immersed in different varnishes: a) water-based matt varnish, b) water-based gloss varnish, c) UV-curable varnish, d) oil-based varnish

Oil-based varnish causes significant swelling of the photopolymer material (Figure 3d). The swelling process starts to slow down after 250 minutes, but normalized degree of swelling reaches 15.2% after 300 minutes without achieving equilibrium. One can conclude that the solubility parameters of this oil-based varnish and the photopolymer used in this research are too similar (Hansen, 2007) for the varnish to be used in the reproduction system that includes tested printing plate.

3.2. Contact angles of varnishes and surface free energy of photopolymer

In order to address the effect of the prolonged exposure of the photopolymer to the varnishes, wettability of the varnishes on the photopolymer surface was assessed by the contact angle measurements. Furthermore, surface free energy (SFE) of the photopolymer not exposed to the varnishes was compared to the surface free energy of exposed ones.

Figure 4. presents the contact angles of the varnishes on the photopolymer surface. It is visible that the water-based gloss varnish displays the best wettability of the photopolymer among tested varnishes, and the oil-based varnish the poorest one. Poor wettability of the oil-based varnish on the photopolymer could be assigned to the air-polymerization of the oil-based coating, and to its thickness.

Since the water-based flexographic varnishes are basically dispersions of the acrylic resin in water and some alcohol, their primary drying mechanism is by coalescence (Resino, n.d.). Therefore, due to the separation of the water and resin part, wetting of these varnishes on the flexographic printing plate is not poorer than that of the UV-varnish.

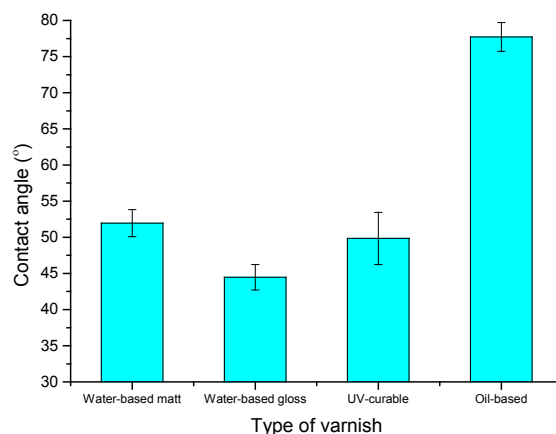


Figure 4: Contact angles of varnishes on the printing plate

In Figure 5, one can see the total SFE of the photopolymer samples exposed to the swelling in varnishes, compared to the non-swollen sample.

It is visible that the immersion of the photopolymer in the varnishes for 5 hours does not affect the total SFE drastically, except for the oil-based varnish. Since weighing showed the photopolymer remains swollen even 24 hours after the immersion in the oil-based varnish, the drastic increase of the surface free energy can be assigned to the presence of the varnish molecules inside the photopolymer matrix.

Since the photopolymer material used in this research is a low-polarity type of material, all the changes of the total SFE are closely followed by the changes of the dispersive SFE.

The decrease of the total (and dispersive) SFE after the immersion in water-based and UV varnishes points to two possibilities: the degradation of the photopolymer and/or migration of the low-molecular weight waxes from the volume of the material to its surface (Matsubara et al, 2011).

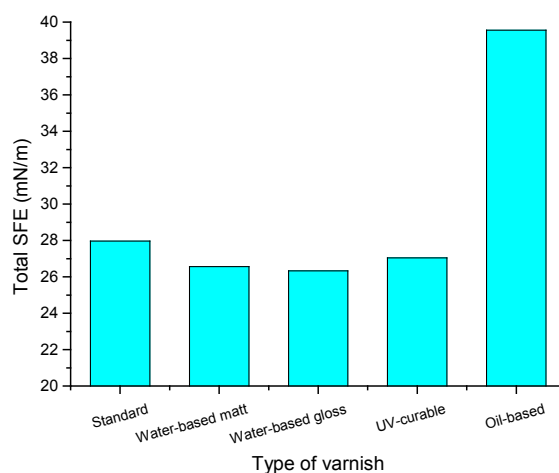


Figure 5: Total surface free energy of the printing plate after the immersion in varnishes

Polar SFE of the photopolymer before the swelling is close to 0 (0.01 mN/m). After the immersion in the varnishes and drying (Figure 5c), polar SFE slightly increased for all samples. However, this increase still results with very low values (< 0.8 mN/m). It can be concluded that, based on the types of changes of photopolymer's SFE, all tested varnishes except for the oil-based one should be suitable for application in the graphic reproduction with used printing plate.

3.3. FTIR-ATR spectroscopy and microscopy of the photopolymer surface

Figure 6. presents the FTIR-ATR spectra of the photopolymer samples taken after they were immersed in the varnishes for 5 hours and left to dry for 24 hours. The wavelength ranges presenting the changes in the vibrations of the types of chemical bonds are shown in Figures 6a) and 6b).

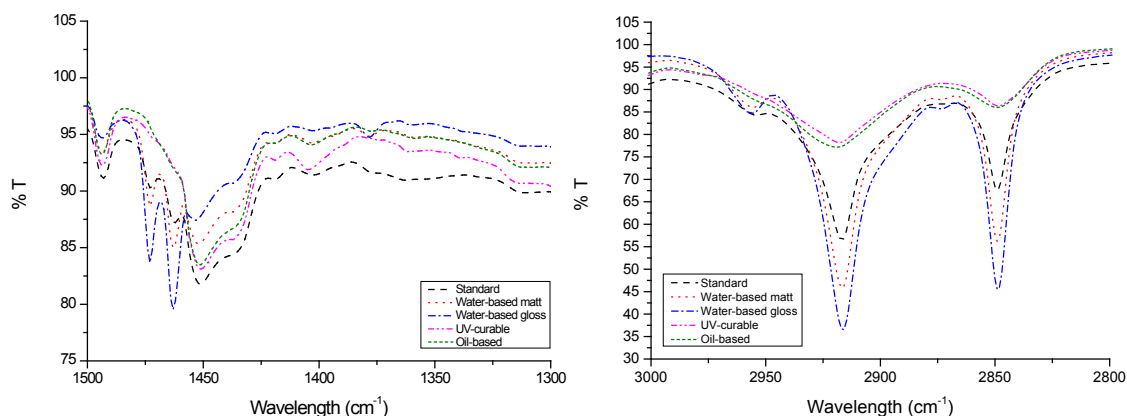


Figure 6: FTIR-ATR spectra of the photopolymer after swelling in varnishes: a) wavelength range of 1300 – 1500 cm^{-1} , b) wavelength range of 2800 – 3000 cm^{-1}

Figure 6a) presents the first wavelength range of interest: 1300 – 1500 cm^{-1} . It is visible that the samples which have been immersed in water-based varnishes present two peaks which are not prominent for the other samples: one at 1462 cm^{-1} and the other at 1472 cm^{-1} . They correspond to the aromatic C=C stretch. Other distinctive peak at 1378 cm^{-1} for the sample immersed in water-based gloss varnish corresponds to the CH_3 and CH_2 bending, or the C-H methyl rocking in the alkenes (Bardakçı, 2007). Since these peaks are not present for all photopolymer samples, it can be concluded that their presence presents the changes caused by residual of the varnishes in the photopolymer surface layer.

The peak at 1404 cm^{-1} is more pronounced for the sample immersed in UV varnish, and corresponds to the symmetrical C=O stretch (Kumar Trivedi et al, 2015). Since this peak is present in all analysed spectra, it can be concluded that it presents the changes occurring in the material structure as a direct consequence of the exposure to the varnishes. Likewise, all peaks in Figure 6b) are present for all samples, but display different transmittance. These peaks are characteristic for the tested photopolymer material. Peak at 3005 cm^{-1} corresponds to the =C-H stretch and points to the increased unsaturation in the sample after treating it with water-based gloss varnish. Peaks at 2849 cm^{-1} and 2916 cm^{-1} correspond to the C-H stretching in alkanes. Their decreased transmittance after treating the material with water-based varnishes could point to the migration of the waxes from the bulk of the photopolymer to the surface – and therefore the decreased SFE. This explanation could be applied for the peak at 2875 cm^{-1} , as well – it is present only for the samples treated with water-based varnishes and corresponds to the C-H stretching vibration.

The increased transmittance of these peaks after treating the photopolymer with UV and oil-based varnishes indicates that these varnishes do not cause the migration inside the material. However, they do affect the surface structure by decreasing the amount of the present characteristic C-H bonds, possibly by dissolving the compounds from the surface layer and/or incorporating in the material structure (Tomašegović, 2016).

Microscopic images of the photopolymer surfaces were taken after the swelling in the varnishes and drying. Images presented in Figure 7. were taken in the transmission light, with the magnification of 200x.

Figure 7a) presents the photopolymer surface that has not been immersed in the varnish. One can see the initial surface texture on the sample. Figure 7b) presents the photopolymer surface after it has been immersed in water-based matt varnish. The appearance of the surface is slightly changed which corresponds to the decrease of the dispersive (and total) SFE (Figure 5), but no signs of the significant material dissolving/damage are evident.

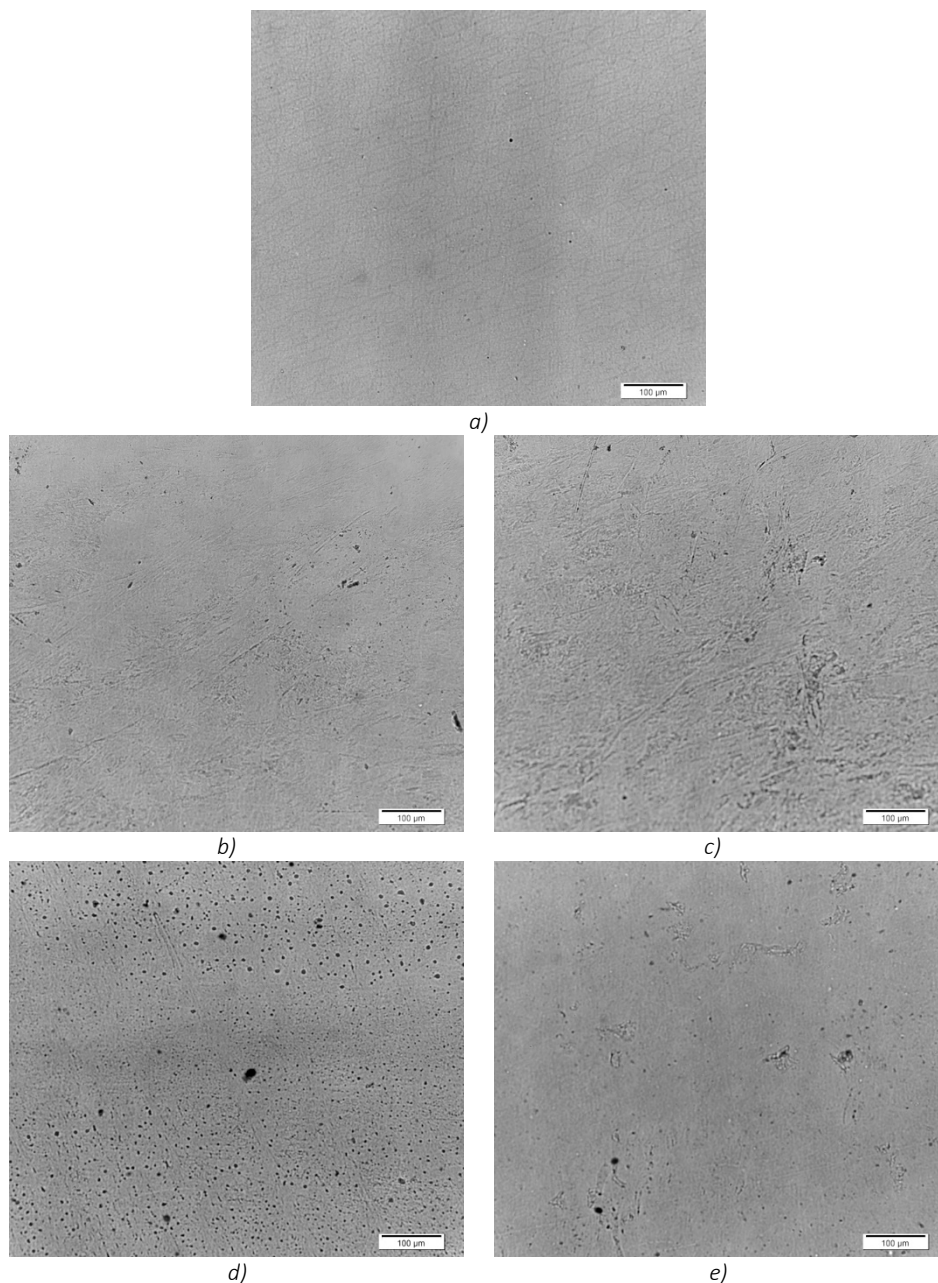


Figure 7: Surface of the photopolymer after swelling in varnishes at 200x magnification: a) non-immersed sample, b) immersed in water-based matt varnish, c) immersed in water-based gloss varnish, d) immersed in UV-curable varnish, e) immersed in oil-based varnish

In Figure 7c), which presents the photopolymer surface after the immersion in water-based gloss varnish, one can notice the subtle signs of the surface damage in form of the cracks on the material. Since the water-based gloss varnish causes the most prominent decrease of the total and dispersive SFE of the photopolymer among the used varnishes, it could be concluded that the visible material degradation takes place on the surface. These changes are corresponding to the changes in FTIR-ATR spectra presented in Figure 6.

UV varnish, on the other hand, causes the visible *pitting dissolution* on the photopolymer surface (Figure 7d). Based on the results of the swelling experiments, the changes of the surface free energy and FTIR-ATR spectra, it can be concluded that UV flexographic varnish penetrates the photopolymer material, and causes both swelling and partial dissolution.

Finally, the effect of the oil-based varnish on the photopolymer can be observed in Figure 7e). No prominent degradation is evident after the immersion. However, oil-based varnish caused the extensive swelling of the material and stayed incorporated in the photopolymer even after 24 hours.

4. CONCLUSION

The aim of this research was to characterize the influence of common varnishes used in graphic reproduction on the photopolymer material flexographic printing plate is made of. After immersion in the varnishes for defined period, changes in the plate's surface free energy components was observed, as well as the visible changes on the material surface.

It can be concluded that water-based and UV-curable varnishes can be used in the reproduction system with expected changes of the printing plate's SFE under 6%. Water-based varnishes cause noticeable decrease of the photopolymer's SFE. The decrease of the total (and dispersive) SFE after the immersion in water-based and UV varnishes points to two possibilities: the degradation of the photopolymer and/or migration of the low-molecular weight waxes from the volume of the material to its surface.

Swelling of the photopolymer in water-based varnishes was negligible, while the normalized degree of swelling reached 1.1% for UV-curable varnish.

Oil-based varnish affected the photopolymer material by causing prominent normalized degree of swelling that reached 15% after 5 hours. Furthermore, oil-based varnish remained in the photopolymer structure and caused the increase of total and dispersive SFE by cca. 30%. FTIR-ATR spectra showed that all varnishes affect the chemical bonds in the photopolymer surface, either by remaining integrated in the material, or by directly causing the changes in the material structure.

Based on the results obtained in this research, it can be concluded that the effects of the varnishes used to print with flexographic printing technique should definitely be monitored depending on the run length, in order to avoid the possible problems with coating quality as a result of the printing plate's surface changes and degradation.

5. ACKNOWLEDGEMENTS

This research is part of the project UIP-2017-05-4081, *Development of the model for production efficiency increase and functionality of packaging*, supported by Croatian Science Foundation.

6. REFERENCES

- [1] Bardakçı, B.: "FTIR-ATR spectroscopic characterization of monochlorophenols and effects of symmetry on vibrational frequencies", *Journal of Arts and Sciences* 7, 13-19, 2007.
- [2] Brajnović, O.: "Adjustment of the photopolymer printing forms to match new qualitative requirements", MSc thesis, University of Zagreb, 2011.
- [3] Hansen, C. M.: "Hansen Solubility Parameters: A User's Handbook", 2nd ed, (CRC Press, Boca Raton, 2007).
- [4] Havlíková, B., Cicák, V., Brezová, V., Horňáková, L.: "Water-reducible flexographic printing inks—rheological behaviour and interaction with paper substrates", *Journal of Materials Science* 34(9), 2081-2088, 1999. doi: 10.1023/A:1004511826583.
- [5] Jenkins, J.: "The effects of common solvents on different types of flexographic printing plates", PhD thesis, Rochester Institute of Technology, 1985.
- [6] Kumar Trivedi, M., Branton, A., Trivedi, D., Nayak, G., Bairwa, K., Jana, S.: "Fourier transform infrared and ultraviolet-visible spectroscopic characterization of ammonium acetate and ammonium chloride: an impact of biofield treatment", *Modern Chemistry & Applications* 3(3), 2329-6798, 2015.
- [7] Liu, J., Zheng, X. J., Tang, K. Y.: "Study on the gravimetric measurement of the swelling behaviors of polymer films", *Reviews on Advanced Material Science* 33(5), 452-458, 2013.
- [8] Matsubara, T., Oda, R.: Pat. 20,110,308,412, "Block copolymer composition for flexographic printing plates", 2011.
- [9] MT laboratories, Balance XS205DU, Mettler Toledo, URL: https://www.mt.com/us/en/home/products/Laboratory_Weighing_Solutions/Analytical/Excellence/XS_Analytical_Balance/XS205DU.html (last request: 2018-09-25).
- [10] Olympus, Microscopy Resource Center, URL: <http://www.olympusmicro.com/brochures/pdfs/bx51.pdf> (last request: 2018-09-25).
- [11] Owens, D. K., Wendt, R. C.: "Estimation of the surface free energy of polymers", *Journal of Applied Polymer Science* 13(8), 1741-1747, 1969. doi: 10.1002/app.1969.070130815.

- [12] Resino, spec. varnish, Resino Trykfarver A/S, URL:
http://www.resino.dk/index.php?option=com_content&view=article&id=28&group=10&Itemid=206&lang=en (last request: 2018-09-25)
- [13] Tomašegović, T.: "Fuctional model of photopolymer printing plate production process", PhD thesis, University of Zagreb, 2016.
- [14] Tomašegović, T, Beynon, D., Claypole, T., Mahović Poljaček, S.: "Tailoring the properties of deposited thin coating and print features in flexography by application of UV-ozone treatment", Journal of Coatings Technology and Research 13(5), 815-828, 2016. doi: 10.1007/s11998-016-9794-4.
- [15] Tryznowski, M., Żołek-Tryznowska, Z., Izdebska-Podsiadły, J.: "The wettability effect of branched polyglycerols used as performance additives for water-based printing inks", Journal of Coatings Technology and Research 15(3), 649–655, 2018. doi: 10.1007/s11998-018-0055-6.



© 2018 Authors. Published by the University of Novi Sad, Faculty of Technical Sciences, Department of Graphic Engineering and Design. This article is an open access article distributed under the terms and conditions of the Creative Commons Attribution license 3.0 Serbia (<http://creativecommons.org/licenses/by/3.0/rs/>).

DEFINITIVE SCREENING DESIGN FOR THE OPTIMIZATION OF FLEXOGRAPHIC WATER-BASED CYAN DYE REMOVAL FROM AQUEOUS SOLUTION BY nZVI-INDUCED FENTON PROCESS

Vesna Kecić¹ , Miljana Prica¹ , Đurđa Kerkez² , Ognjan Lužanin³ ,
Milena Bečelić-Tomin² , Dragana Tomašević Pilipović² , Anita Leovac Mačerak² 

¹University of Novi Sad, Faculty of Technical Sciences,

Department of Graphic Engineering and Design, Novi Sad, Serbia

²University of Novi Sad, Faculty of Sciences, Department of Chemistry,
Biochemistry and Environmental Protection, Novi Sad, Serbia

³University of Novi Sad, Faculty of Technical Sciences,
Department of Production Engineering, Novi Sad, Serbia

Abstract: *The paper investigates the potential use of nano-zero valent iron (nZVI) particles as a cheap, natural and effective catalyst in Fenton-like process for the removal of water-based Cyan dye from synthetic aqueous solution and printing effluent. The production of nZVI nanoparticles is based on the environmentally friendly method, so-called green synthesis, using the extract from natural product, oak leaves. Characterization of oak-nZVI by SEM, EDS and TEM revealed the surface and spatial structural characteristics, as well as the morphology of the synthesized nanomaterial. The experiments were carried out in a batch mode technique, investigating the influence of dye concentration (20-180 mgL⁻¹), nanoparticles dosage (0.75-60 mgL⁻¹), H₂O₂ concentration (1-11 mM) and pH value of the solution (2-10) on the decolorization efficiency. A new generation of experimental designs, the definitive screening design (DSD), was used to optimize the process conditions, considering the individual and interaction effects of the factors that influenced the percentage of dye degradation. The optimum degradation efficiency of Cyan dye in synthetic solution was 87.24%, within the operational parameters: initial dye concentration of 20 mgL⁻¹, nZVI dosage of 25.69 mgL⁻¹, H₂O₂ concentration of 6.88 mM and pH value of 2. Under the optimum conditions real printing effluent was treated, and decolorization efficiency of 70.85% was achieved. The obtained experimental results show that the Fenton process is effective for the degradation of printing dye, implying to the fact that future work should be explored with additional Fenton process catalyst and for other printing dyes.*

Key words: definitive screening design, nano zero valent iron, Fenton process, optimization, dye removal

1. INTRODUCTION

The printing industry is one of the most complex manufacturing industrial chains, covering the entire production cycle from raw materials (dyes, solvents, developers, photochemical baths) to final products (cardboard boxes, food packaging, newspapers, catalogues). The main environmental issue arising from printing process primarily regards water pollution, where the type and concentration of hazardous and harmful substances depends on the primary and secondary raw materials used in the production process, chemical reactions, process parameters, intermediates and final products (Kecić et al, 2017; Wang et al, 2018). However, the highest environmental load arises from dyes, known as difficult-to-eliminate organic compounds. Dyes released from printing industry are categorized as major ecological hazards, due to their non-biodegradability and chemically, photolytically and biologically highly stable nature (Kecić et al, 2018). Even in low concentrations, dyes are highly visible, they contribute to the esthetic pollution, reduce the photosynthetic activity within the water body and affect the symbiotic process. In addition, dyes affect the aquatic life and food chain, causing chemical pollution. The hazardous, toxic and carcinogenic nature of dyes is also well known, where a various physiological disorders in aquatic organisms happen by the consumption of dyes via food chain (Khemila et al, 2018). Solvent-based printing dyes primarily achieved a large market share, but the fact that they contain up to 60% of volatile organic compounds, which have a potentially negative impact on the working and living environment, have led to their substitution with water-based dyes. The colored dye effluent discharge from printing facilities is a growing concern worldwide and their treatment is always a challenging. The previous period in the field of environmental science and technology is characterized by the application of various techniques in the field of textile wastewater treatment (Mijin, 2017). However, printing

wastewater generated after printing process are usually discharged into water bodies without previous treatment, therefore polluting environment in a large scale. Thus, there is a great need for the disclosure of alternative, efficient and cost-effective treatment effective techniques that will remove dyes from large volumes of printing effluents.

Various biological and physio-chemical processes, effective but still quite expensive, are used in order to remove dyes from effluents: adsorption, membrane filtration, microbial degradation, coagulation and ion exchange (Punzi et al, 2015; Lin et al, 2016; Brito et al, 2018; Lin et al, 2017). Among the mentioned remediation process, advanced oxidation processes (AOPs) are proven as highly effective in the oxidation of organic pollutants, due to the generation of highly reactive species – hydroxyl radicals ($\text{HO}\cdot$) in the medium, which are capable to attack the majority of persistence organic compounds. In Fenton system $\text{HO}\cdot$ are generated through the catalytic reaction of $\text{Fe(II)}/\text{Fe(III)}$ in the presence of hydrogen peroxide. So far, various iron sources have been applied, categorizing the Fenton process as heterogeneous, homogeneous and Fenton-like process (Bilinska et al, 2016). Recently Fenton-like system have demonstrated high removal efficiency towards the application of nZVI particles as catalyst, mainly because of its nontoxic form, small particle size, large specific surface area, high density and high chemical reactivity in aqueous media. Based on these characteristics, the nZVI technology could become a promising approach for treating industrial dyes wastewater (Stefaniuk et al, 2016).

In this study application of nZVI-induces Fenton process was performed in order to achieve decolorization of water-based cyan dye synthetic aqueous solution and real printing effluent. The influence of fundamental operative parameters, such as dye concentration, catalyst dosage, hydrogen peroxide concentration and pH, as well as the process optimization were evaluated by using novel DSD method.

2. MATERIALS AND METHODS

2.1 Reagents

Hydrogen peroxide (30%) was obtained from NRK engineering, Serbia, NaOH (>98.8%) was purchased from POCH, while cH_2SO_4 (>96%) was produced by J.T. Baker. All chemicals used in this study were of analytical grade and employed without further purification.

Cyan flexographic dye (Figure 1) was supplied from Flint group. This dye was used during water-based flexographic process in one printing facility in Novi Sad. Samples of wastewater were obtained from same printing facility. Aqueous dye solution was prepared by dissolving appropriate amounts of Cyan dye with deionized water to the desired concentration. The final pH of the solution was adjusted by 0.10 molL^{-1} NaOH and H_2SO_4 . Deionized water was used throughout this experiment.

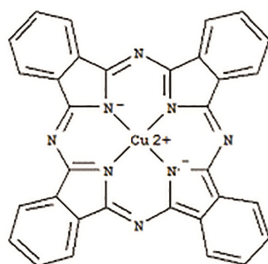


Figure 1: Chemical structure of Cyan pigment

2.2 Preparation and characterization of nZVI

nZVI particles were prepared through the "green" synthesis method, as previously reported by Machado et al (2013) where 37 g of dried oak leaves were mixed with 1000 ml of deionized water on a magnetic stirrer for 20 min at 80°C. The resulting mixture was filtered with Büchner Vacuum Filtration Funnel and 0.1 M Fe(III) solution was added in the mixture in a volume ratio of 1: 3. Ferric iron was reduced to Fe(0) and ZVI particles precipitated instantly according to the mixture color turned from yellow to dark brown. In that way, a Fe(0) concentration of 1.395 gL^{-1} in nanomaterial was obtained.

The structure, composition, particle shape and size distribution of the prepared nanomaterial were characterized by Scanning electron microscopy (SEM; Hithchi S-4700 Type II), energy dispersive spectrum (EDS) and transmission electron microscopy (TEM; Philips CM 10).

The synthesized nanoparticles are characterized by a spherical shape and a size of about 50 nm, without expressed particle aggregation and agglomeration (Figure 2), due to dispersive and stabilizing characteristics of oak leaves (Poguberović et al, 2016).

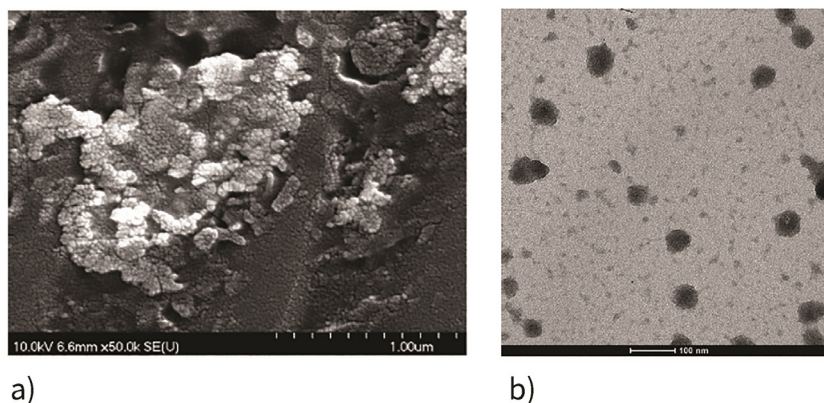


Figure 2: a) SEM i b) TEM microscopic display of nano zero valent iron (Poguberović et al, 2016)

2.3 Experimental procedure

A different dose of nZVI ($0.75 - 60 \text{ mgL}^{-1}$) was added in a samples of 250 mL aqueous dye solution within a dye concentration of $20 - 180 \text{ mgL}^{-1}$. After the pH adjustment with NaOH and cH_2SO_4 a certain amount of H_2O_2 (1-11 mM) was added in the mixture. Samples were shaken in a glass beaker on a JAR apparatus (FC6S Velp Scientific, Italy) at 120 rpm and constant temperature of 23°C .

After the reaction time has elapsed, residual Cyan concentration was determined in the filtrate by measuring the absorbance of the aqueous solutions at 636 nm with UV/VIS spectrophotometer (UV-1800 PG Instruments Ltd T80+ UV/VIS, Japan). The Cyan removal efficiency was calculated using the equation (1):

$$E(\%) = A_0 - A / A_0 * 100 \quad (1)$$

where the A_0 indicates the absorption of dye before Fenton-like treatment and A indicates the dye absorption after the treatment. All the experimental data were recorded in duplicate.

2.4 Statistical analysis

To quantify and elucidate the effects of four influencing factors (initial dye concentrations, catalyst dosage, pH and hydrogen peroxide concentrations) on Cyan removal efficiency, a new three-level design of experiments – DSD was selected to develop mathematical models. Besides the fact that allows a significant reduction in the number of experiments, DSD is very effective in estimating linear and nonlinear effects. In that way assessment of active effects, two-factor interactions effects, and purely quadratic effects in a single step with a minimal number of runs can be obtained. The specific levels for each factor are listed in Table 1. A total of 28 runs were designed: 13 experimental runs conducted in duplicate with two extra central points. By invoking the Effect Sparsity Principle, a model-selection strategy could determine which effects are actually active (Libbrecht et al, 2015).

Table 1: Factors and Levels for Cyan removal efficiency

Factors	Value	Coded value	Level		
			-1	0	+1
Initial dye concentration	mgL^{-1}	X1	20	100	180
Catalyst dosage	mgL^{-1}	X2	0.75	30	60
pH	-	X3	2	6	10
Hydrogen peroxide concentration	mM	X4	1	6	11

3. RESULTS AND DISCUSSIONS

3.1 Evaluation of DSD model

In order to characterize the system under the influence of different process conditions: dye concentration, catalyst dosage, pH and hydrogen peroxide concentration, DSD statistical analysis was applied. The results of the 28 experimental runs indicated decolorization efficiency range from 1.67 to 83.45% for Fenton-like process. In this way, the assumption that the Cyan removal process is largely dependable on the applied experimental conditions is confirmed, and it may be concluded that the individual parameters contribute to the efficiency of the Fenton process to a certain extent.

In order to derive the regression model that best fits the obtained results, JMP's regression analysis was applied. The regression model includes the first-order (main effects), second-order (quadratic), and two-way interaction terms and they were fit using a forward stepwise regression. Three popular modern measures of model performance: the corrected Akaike Information Criterion (AICc) and the Bayesian Information Criterion (BIC) and RMSE (Root Mean Square Error) were used to determine a model that best predicted process performance. Smaller values of AICc and BIC indicate better prediction capability or performance. In addition to the standard selection criteria, the models should contain all tested input parameters, which is from the engineering point of view extremely important in this problem.

Analysis of variance (ANOVA) was performed to provide more information concerning the model and the results are presented in Table 2. The quadratic regression model is statistically significant as p-value is less than 0.05, suggesting 95% confidence level. Moreover, due to the p-value higher than 0.05, lack of fit test is not significant, which is desirable, as it indicates that any predictor left out of model is considered insignificant and the established model predicts the experimental data very well.

Table 2: ANOVA results

Source	DF	SS	MS	F ratio
Model	11	19914.545	1810.41	41.414
Error	16	699.446	43.72	Prob>F
C. Total	27	20613.991	-	<0.0001
Lack of Fit	14	691.127	49.366	1.550
Pure error	2	8.319	4.159	Prob>F
Total error	16	699.446	-	0.0803

The R^2 value of 97% demonstrates that the quadratic regression model fits the data properly. The value of adjusted R^2 is 94.3%, which reveals good relationship between the expected values and the actual values. A very small difference between these two coefficients indicates the absence of too much overfitting.

Table 3: The chosen regression model

Descriptive factor	Value
R^2	0.966
R^2 Adjusted	0.943
RMSE	6.612
Mean of response	30.436
Number of experiments	28

The coefficients of significant main parameters, their square members and dual factor interactions for the obtained model obtained are shown in Table 4.

Table 4: Significant main parameters coefficients, their square members and dual factor interactions for the obtained model

Factor	Estimated parameters	Standard error	t value	Probability> t
Dye concentration	-2.918	1.478	-1.97	0.0659
Catalyst dosage	-1.067	1.478	-0.72	0.4811
H ₂ O ₂ concentration	-1.043	1.478	-0.71	0.4909
pH	-26.380	1.478	-17.84	<0.001
Fe*Fe	-3.881	3.281	-1.18	0.2542
Dye * H ₂ O ₂	-7.707	2.014	-3.83	0.0015
Fe * H ₂ O ₂	-1.075	1.867	-0.58	0.5729
H ₂ O ₂ * H ₂ O ₂	-19.293	3.086	-6.25	<0.001
pH * pH	36.006	3.518	10.23	<0.001

Bold values indicate statistically significant model factors, specifically the pH value, interaction between dye and hydrogen peroxide concentration, as well as the square member of pH. The order of significance is determined based on the estimated values of the parameters: pH < H₂O₂*H₂O₂ < dye*H₂O₂ < pH*pH.

3.2 Optimization of nZVI-induced Fenton process

Despite the limited number of papers that implement DSD analysis as the main factor of the experiment, it has been established that the capability and flexibility of the JMP 13 software can provide significant advancement in the optimization process, which, for the ultimate goal, maximizes the dye removal efficiency compared to the technological conditions described in Table 1. The optimization of the process conditions is carried out within the limits of the tested variables (Table 1). The prediction profile with optimal values is shown in Figure 3.

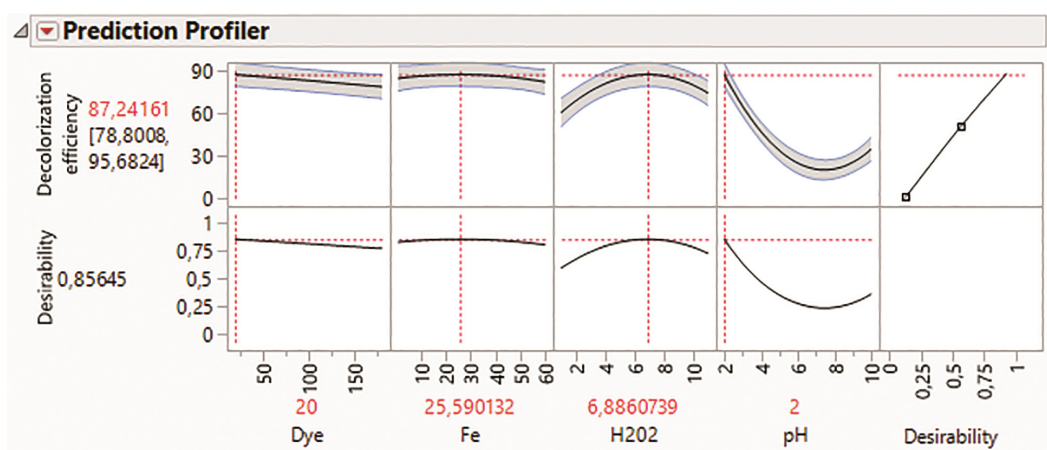


Figure 3: Optimal process conditions for nZVI-induced Fenton process

Based on the obtained results, the following optimal conditions were determined: dye concentration of 20 mgL⁻¹, catalys dosage of 25.59 mgL⁻¹, pH value of 2 and hydrogen peroxide concentration of 6.89 mM, where the statistical model proposes the process efficiency of 87.24%. The obtained results are consistent with the significant factors shown in Table 4, indicating that the decolorization efficiency increases significantly with the decrease of pH and dye concentration. The experimental verification of the process optimization was performed with eight additional experiments, yielding the following decolorization efficiencies: 89.63; 84.78; 85.20; 83.50; 84.35; 83.58; 84.27; 90.73. On the basis of experimentally obtained values, a 95% confidence interval was calculated [83.41 - 88.09%]. The value of decolorization efficiency predicted by the adopted regression model (Figure 3) is 87.24% and fits in the experimentally obtained confidence interval, which shows that the adopted regression model good describes the process of dye removal.

3.3 Real effluent treatment

In order to determine the possibility of using the synthesized nanomaterial, a real effluent generated after the printing process and colored with a cyan dye was subjected to nZVI-induced Fenton treatment within the optimal doses of the tested parameters. The dye removal efficiency was monitored for a period of 120 minutes and the results indicated that degradation efficiency after 60 minutes was 70.85% where the maximum efficacy was achieved with a longer reaction time, but with a slight increase (up to 76.69%). Compared to the treated synthetic cyan dye solution, the efficiency of the Fenton process in the case of a real effluent was lower. This behavior is due to the presence of a various organic and inorganic compound in the complex effluent matrix. Different species can achieve an inhibitory effect on the dye degradation process, behaving as hydroxyl radical catchers and thereby achieving competition for active sites on the surface of the catalyst.

4. CONCLUSIONS

The results obtained in this work indicated that the DSD approach can be effectively used to investigate factors that affect decolorization efficiency during the nZVI-induced Fenton process. Four investigated process parameters (initial dye concentration, catalyst dosage, pH and hydrogen peroxide concentration) were studied via modeling using the DSD approach. Application of this experiment design method enabled a reduction of the large number of traditional experiments to only 28, where all experimental runs were performed in duplicate, followed with two additional central points. The accuracy and reliability of the mathematical models were confirmed by validation experiments.

Based on the experimental results, it can be concluded that the decolorization efficiency increases with the decrease of pH value and dye concentration, which are the most significant parameters. High decolorization efficiency, up to 87% is obtained in the case of synthetic dye solution, while a lower expected efficiency of 76% is achieved within the wastewater treatment under determined optimal conditions.

This study enriches understanding of Fenton-like process for the cyan dye removal from synthetic dyes solution and real printing effluent and demonstrates that DSD is a feasible method to investigate the mechanism of Fenton-like process.

5. ACKNOWLEDGMENTS

The authors acknowledge the financial support of the Ministry of Education, Science and Technological Development of the Republic of Serbia within the Projects No. TR 34014 and III43005.








6. REFERENCES

- [1] Bilińska, L., Gmurek, M., Ledakowicz, S.: "Comparison between industrial and simulated textile wastewater treatment by AOPs – Biodegradability, toxicity and cost assessment", Chemical Engineering Journal 306, 550-559, 2016. doi:<https://doi.org/10.1016/j.cej.2016.07.100>.
- [2] Brito, M., Veloso, C., Santos, L., Bonomo, R., Fontan, R.: "Adsorption of the textile dye Dianix® royal blue CC onto carbons obtained from yellow mombin fruit stones and activated with KOH and H₃PO₄: kinetics, adsorption equilibrium and thermodynamic studies", Powder Technology 339, 334-343, 2018. doi: 10.1016/j.powtec.2018.08.017.
- [3] Kecić, V., Kerkez, Đ., Prica, M., Lužanin, O., Bečelić-Tomin, M., Tomašević Pilipović, D., Dalmacija, B.: "Optimization of azo printing dye removal with oak leaves-nZVI/H₂O₂ system using statistically designed experiment", Journal of Cleaner Production, 202, 65-80, 2018. doi:[doi:10.1016/j.jclepro.2018.08.117](https://doi.org/10.1016/j.jclepro.2018.08.117).
- [4] Kecić, V., Kerkez, Đ., Prica, M., Rapajić, S., Leovac Maćerak, A., Bečelić-Tomin, M., Tomašević Pilipović, D.: "Optimization of Cyan flexo dye removal by nano zero-valent iron using response surface methodology", Journal of Graphic Engineering and Design 8, 35 – 45, 2017. doi: 10.24867/JGED-2017-2-035.
- [5] Khemila, B., Merzok, B., Chouder, A., Zidelkhir, R., Leclerc, J., Lapicque F.: "Removal of a textile dye using photovoltaic electrocoagulation", Sustainable Chemistry and Pharmacy 7, 27-35, 2018. doi: 10.1016/j.scp.2017.11.004.

- [6] Libbrecht, W., Deruyck, F., Poelman, H., Verberckmoes, A., Thybaut, J., De Clercq J., Van Der Voort, P.: "Optimization of soft templated mesoporous carbon synthesis using Definitive Screening Design", *Chemical Engineering Journal*, 259, 126–134, 2015. doi: 10.1016/j.cej.2014.07.113.
- [7] Lin, C., Chiang, C., Nguyen, M., Lay, C.: "Enhancement of fermentative biohydrogen production from textile desizing wastewater via coagulation-pretreatment", *International Journal of Hydrogen Energy* 42 (17), 12153-2158, 2017. doi: 10.1016/j.ijhydene.2017.03.184.
- [8] Lin, J., Ye, W., Baltaru, M., Tang, Y., Bruggen, B.: "Tight ultrafiltration membranes for enhanced separation of dyes and Na₂SO₄ during textile wastewater treatment", *Journal of Membrane Science* 154, 21-228, 2016. doi: 10.1016/j.memsci.2016.04.057.
- [9] Machado, S., Pinto, S., Grosso, J., Nouws, H., Albergaria, J., Delerue-Matos, C.: "Green production of zero-valent iron nanoparticles using tree leaf extracts", *Science of the Total Environment*, 445–446, 1–8, 2013. doi: 10.1016/j.scitotenv.2012.12.033.
- [10] Mijin, D.: "Printing dyes and adhesives", (Faculty of Technology and Metallurgy, Beograd, 2015). (in Serbian)
- [11] Poguberović, S., Krčmar, D., Maletić, S., Konya, Z., Tomašević Pilipović, D., Kerkez, Đ., Rončević, S.: "Removal of As(III) and Cr(VI) from aqueous solutions using "green" zero-valent iron nanoparticles produced by oak, mulberry and cherry leaf extracts", *Ecological Engineering*, 90, 42–49, 2016. doi: 10.1016/j.ecoleng.2016.01.083.
- [12] Punzi, M., Anbalagan, A., Börner, R., Svensson, B.M., Jonstrup, M., Mattiasson, B.: "Degradation of a textile azo dye using biological treatment followed by photo-Fenton oxidation: Evaluation of toxicity and microbial community structure", *Chemical Engineering Journal*, 270, 290-299, 2015. doi:10.1016/j.cej.2015.02.042.
- [13] Stefaniuk, M., Oleszczuk, P., Ok, Y.: "Review on nano zerovalent iron (nZVI): From synthesis to environmental applications", *Chemical Engineering Journal* 27, 618–632, 2016. doi: 10.1016/j.cej.2015.11.046.
- [14] Wang, R., Xin, J., Wang, Z., Gu, W., Wei, Z., Huang, Y., Qiu, Z., Jin, P.: "A multilevel reuse system with source separation process for printing and dyeing wastewater treatment: A case study", *Bioresource Technology* 247, 1233-1241, 2018. doi: 10.1016/j.biortech.2017.09.150.



TREATMENT OF WASTEWATER CONTAINING DYE MIXTURE USING PYRITE CINDER IN HETEROGENEOUS FENTON PROCESS

Đurđa Kerkez ¹ , Milena Bečelić-Tomin ¹ , Aleksandra Kulić ¹ ,
Dragana Tomašević Pilipović ¹ , Anita Leovac Mačerak ¹ ,
Božo Dalmacija ¹ , Miljana Prica ² 

¹University of Novi Sad, Faculty of Sciences, Department of Chemistry,
Biochemistry and Environmental Protection, Novi Sad, Serbia

²University of Novi Sad, Faculty of Technical Sciences,
Department of Graphic Engineering and Design, Novi Sad, Serbia

Abstract: *Dyes and pigments are important industrial chemicals. The structures of dyes can be very diverse and complex, so the treatment of wastewater containing these chemicals can be very challenging. Fenton process is particularly attractive and effective to degrade a wide range of dyes. In order to reduce the expenses related to applying these processes, the use of waste materials in the heterogeneous Fenton process, as alternative sources of catalytic iron, is recently investigated in scientific literature. In this study effluent was obtained from dye house unit of carpet factory (Serbia) and it contained the mixture of six commercial dyes. Pyrite cinder, a residue from sulfuric acid production, was also used in this process as a source of catalytic iron. Effluent decolourization rate reached 75% under optimal condition. Additionally, the research included further characterization of obtained effluent in terms of mineralization and metal leaching. A significant degree of mineralization was achieved under the applied conditions. Although, dye degradation was satisfactory, the metal content of the solutions after the process suggests that an additional treatment step, by using lime, is necessary. Results indicated that the applied waste material is effective as iron source in modified Fenton processes for treatment of effluent containing mixture of dyes.*

Key words: dyes, pyrite cinder, Fenton process, decolourization, mineralization

1. INTRODUCTION

Textile manufacturing is one of the largest industrial producers of wastewaters, which are characterized by strong colour, highly fluctuating pH, high chemical oxygen demand (COD), and biotoxicity. Under typical reactive dyeing conditions, not all dyes bind to the fabric; depending on the class of dye, up to 50% of the initial dye remains in the spent dye bath in its hydrolysed form, which has no affinity for the fabric and results in a coloured effluent. Dyes are known to be non-degradable under the typical aerobic conditions found in conventional biological treatment systems and adsorb very poorly biological solids, resulting in residual colour in discharged effluents (Becelić-Tomin et al, 2014), (Gozmen et al, 2009). Advanced oxidation processes (AOPs) are the most attractive technologies for dye wastewater treatment, able to oxidize quickly and non-selectively a broad range of pollutants (Chang & Chern, 2010; Ilinoiu et al, 2013; Saravanan et al, 2014). Fenton process is particularly attractive and effective to degrade a wide range of dyes. It is also relatively cheap and easy to perform compared to other AOPs processes. On the other hand, classical Fenton process implies continuous loss of iron ions due to formation of solid sludge and also a heavy load of counter ions. This can be avoided by employing heterogeneous Fenton processes. A great deal of interest has developed in the degradation of different dyes by modifying the Fenton system and/or introducing novel alternative iron sources. Numerous researchers (Dukkancı et al, 2010), (Kasiri et al, 2008), (Kusic et al, 2007), (Wu et al, 2013) have shown that H₂O₂ can oxidize organic pollutants in the presence of solid catalysts which contain iron. One of the potential waste materials that can be used as catalytic iron source is Fenton process is pyrite cinder. Pyrite cinder (PC) is generated in sulfuric acid production, and a high content of iron oxide of this type of waste, in the form of hematite and magnetite, is the basis for the research regarding the possibility of its use as a source of catalytic iron in the modified heterogeneous Fenton processes in wastewater treatment. In this paper optimum operating conditions were established in order to achieve the highest decolourization efficiency of textile industry effluent when using PC. Also the characterization of the obtained effluent in terms of leached metals and arsenic as well as the determination of mineralization efficiency was performed.

2. METHODS

Textile industry effluent was obtained from dye house unit of carpet factory (Serbia) and it contained the mixture of six commercial dyes: Tectilon Yellow 3R (317 mg/l); Tectilon Red 2B (182 mg/l); Tectilon Blue 4R (179 mg/l); Maxilon Yellow GL (5.2 mg/l); Maxilon Red 3GLN (9.3 mg/l) i Maxilon Blue TL (9.3 mg/l), as well as different thickeners and additives in total concentration of 12.5 g/l. It was characterized by using standard laboratory procedures. The PC used in this work was a remnant after the combustion of pyrite in the production of sulphuric acid in the chemical industry in Serbia. All solutions were prepared with deionised water. All experiments were conducted at room temperature ($25 \pm 0.5^\circ\text{C}$). The relative standard deviations (% RSD) obtained ($n = 3$) were below 10%. The experiments were conducted on a jar test apparatus (FC6S Velp Scientifica, Italy), where reactive mixtures with 0.25 l volumes were continually mixed in 1 l laboratory cups, at 150 rpm. The experiments were performed in the following manner: firstly, the appropriate PC dosage was added to the model dye solution, which was followed by pH adjustment to the desired value and the addition of the required amount of H_2O_2 . Decolourization of the textile industry effluent was monitored by absorbance (A) at $\lambda_{\text{max}} = 411 \text{ nm}$ for (UV/VIS spectrophotometer, Shimadzu, Japan). The efficiency of dye decolourization was obtained by the application of the following formula (1):

$$\text{Decolourization efficiency [\%]} = ((A_0 - A_t)/A_0) * 100\% \quad (1)$$

Where: A_0 – represents the initial absorbance of dye solution and A_t – represents absorbance of dye solution after a certain time t .

Decolourization kinetic analysis was determined by using mathematical model of the author (Behnajady, Modirshahla, Ghanbary et al, 2007). Characterization of the treated effluent in terms of leached metals and arsenic was performed before and after adjusting the pH to 7.5-8 by atomic absorption spectrometry AAS (Perkin Elmer AAnalyst™ 700). Determination of mineralization obtained effluents was performed by determination of total organic carbon (TOC) using Elementar Liqui Germany Toc analyzer and chemical oxygen demand (COD) using the standard method.

3. RESULTS AND DISCUSSION

The effect of PC concentration on the decolourization efficiency of textile industry effluent is shown in Figure 1a. Increasing concentrations of PC lead to an increase in the concentration of iron ions in the Fenton process, and on the other hand to the available surface on which the reaction takes place, which causes a greater production of $\text{HO}\cdot$ radicals to a certain amount (Daud & Hameed, 2010). The decolourization efficiency of textile industry effluent at higher concentrations of PC (40 and 80 g/l) was satisfactory ranging between 74.5 and 78.3%.

As further amount increase of PC did not significantly affect the decolourization efficiency, the following experiments used the PC concentration 40 g/l.

Figure 1b shows the decolourization efficiency in the dependence of the applied initial hydrogen-peroxide concentration. The highest decolourization efficiency was obtained at an initial concentration of 50 mM. The effect of the decolourization efficiency reduction at higher H_2O_2 concentrations can be explained by the phenomenon in which molecules of H_2O_2 exhibit the "scavenging" effect towards $\text{HO}\cdot$ and lead to the formation of less reactive species such as HO_2 (Hassan & Hameed, 2011).

Changing the pH values can have an influence on the heterogeneous Fenton reactions which take place on the catalyst surface (Zhao & Hu, 2008). The results indicate that the Fenton process with the use of PC as a source of iron, similar to the conventional Fenton process, shows the highest efficiency for pH=3, and the downward trend in the decolourization efficiency with increasing the pH values (Figure 1c) (Arslan-Alaton & Teksoy, 2007). The acidity of the PC itself contributed to the reduction of the dye solution pH.

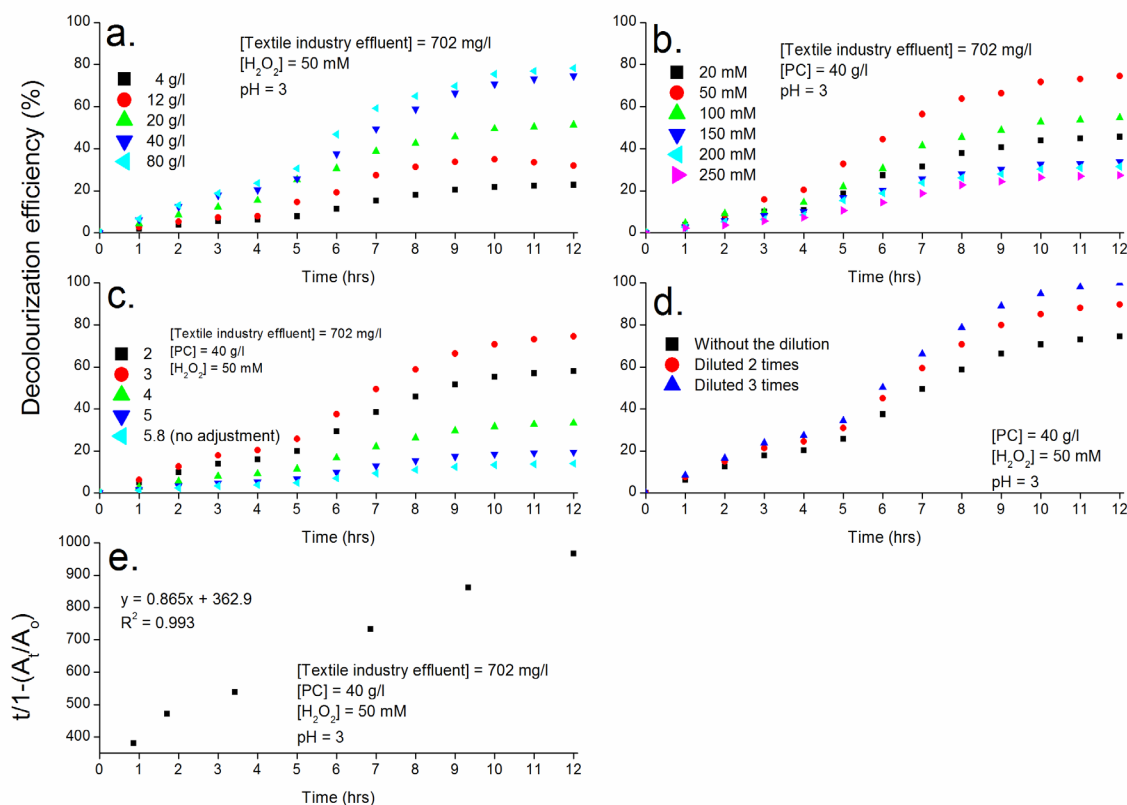


Figure 1: Optimization of textile industry effluent solution decolourization, a. Effect of PC dosage; b. Effect of H_2O_2 concentration; c. Effect of initial solution pH; d. Effect of initial dye concentration; e. Kinetics

The effect of the initial concentration of dye on the decolourization efficiency is given in Figure 1d. It can be seen that with the increase of the dye concentration there is a reduction in the decolourization efficiency. The increase in concentration implies an increase in the number of dye molecule but with the same amount of $OH\cdot$ radicals present, which causes this effect. Also, in the heterogeneous Fenton processes, reactions are partially carried out on the surface of the catalyst, so that when the dye concentration is high, the number of active sites is reduced due to the competitive adsorption of dye molecule (Chen et al, 2008).

Regarding the kinetic analysis, the resulting value of the derived coefficients indicate that using PC as a source of iron in a heterogeneous Fenton process takes longer period of time to achieve effective decolourization in comparison to a homogeneous Fenton processes (Figure 1e.). Similar studies have also shown that Fenton treatment of wastewater, including those from the textile industry, requires longer reaction time to achieve high efficiency primarily due to the very complex composition and high concentration of different colours and additives (Galeano et al, 2011).

In this research the untreated PC, with a high content of other metals, was used. Therefore metal leaching in dye solution after the applied Fenton process was investigated, when the pH value of the examined effluents after the treatment was 3. pH value and the metal content indicated the necessity of an additional step for the treatment of effluents in order to remove residual leached metals. Namely, lead, copper, chromium and cadmium were leached above the emission limit values according to "Official Gazette", 67, 2011, [14]. Among the leading technologies, that are recommended and used for the removal of potentially toxic substances from the effluent, precipitation is the most widely used for the removal of metals from industrial effluents. In this experiment, we used the lime, which was added to treated effluents, while maintaining the pH value in the range 7.5-8, in order to meet the requirements [14]. At the same time, this value is close to the pH range which helps to minimize the solubility of the hydroxides of most metals.

It can be concluded that the addition of lime in the reaction mixtures after the Fenton process contributed to a significant reduction in the metal content in the investigated solutions. After adjusting the pH by using lime, the emission limit values for metals are met.

The mineralization level of the studied heterogeneous Fenton effluent after the treatment is usually determined by measuring the degree of removal of total organic carbon (TOC), and the degree of reduction of chemical oxygen demand (COD). Removal of COD depends entirely on the complete mineralization of the dye molecule, while the reduction in TOC values is primarily attributed to the fragmentation of highly-complex structures of dye molecules on relatively simpler organic fragments, such as carboxylic acids, aldehydes, ketones, alcohols etc. These parameters were measured in the initial solution and in effluent after the Fenton treatment when applying optimal conditions (Table 1).

Table 1: COD and TOC values before and after application of the heterogeneous Fenton process

		COD mg O ₂ /l	TOC mg C/l
Textile industry effluent	Before treatment	7893	2500
	After treatment	4110	1760
	% Removal	47.9	29.6

5. CONCLUSIONS

PC has been proved to be a superior catalyst for decolourization of textile industry effluent in a modified Fenton process 75% of decolourization was achieved. Also a significant degree of mineralization was achieved under the applied conditions. Although, dye degradation was satisfactory, the metal content of the solutions after the process suggests that an additional treatment step, by using lime, is necessary to remove the remaining metals from the water. Overall using this waste material as an alternative source of catalytic material for dye degradation is a cost-effective method for making textile wastewater viable for further treatment and minimizing possible negative environmental effects.

6. ACKNOWLEDGMENTS

The research was funded by the Ministry of Education, Science and Technological Development (Project III43005).

7. REFERENCES

- [1] Arslan-Alaton, I., Teksoy, S.: "Acid dyebath effluent pretreatment using Fenton's reagent: Process optimization, reaction kinetics and effects on acute toxicity", *Dyes and Pigments*, 73, 31-39, 2007. doi: 10.1016/j.dyepig.2005.09.027
- [2] Becelic-Tomin, M., Dalmacija, B., Rajic, Lj., Tomasevic, D., Kerkez, Dj., Watson, M., Prica, M.: "Degradation of Anthraquinone Dye Reactive Blue 4 in Pyrite Ash Catalyzed Fenton Reaction", *The Scientific World Journal*, 2014. doi: 10.1155/2014/234654
- [3] Behnajady, MA., Modirshahla, N., Ghanbary, F.: "A kinetic model for the decolorization of C.I. Acid Yellow 23 by Fenton process", *Journal of Hazardous Materials*, 148(1-2), 98-102, 2007. doi: 10.1016/j.jhazmat.2007.02.003
- [4] Chang, MW., Chern, JM.: "Decolorization of peach red azo dye, HF6 by Fenton reaction: initial rate analysis", *Journal of the Taiwan Institute of Chemical Engineers*, 41(2), 221-228, 2010. doi: 10.1016/j.jtice.2009.08.009
- [5] Chen, A., Ma, X., Sun, H.: "Decolorization of KN-R catalyzed by Fe-containing Y and ZSM-5 zeolites", *Journal of Hazardous Materials*, 156(1-3), 568-75, 2008. doi: 10.1016/j.jhazmat.2007.12.059
- [6] Daud, NK., Hameed, BH.: "Decolorization of Acid Red 1 by Fenton-like process using rice husk ash-based catalyst", *Journal of hazardous materials*, 176(1-3), 938-44, 2010. doi: 10.1016/j.jhazmat.2009.11.130
- [7] Dukkanci, M., Gunduz, G., Yilmaz, S., Yaman, YC., Prikhodko, RV., Stolyarova, IV.: "Characterization and catalytic activity of CuFeZSM-5 catalysts for oxidative degradation of Rhodamine 6G in aqueous solutions", *Applied Catalysis B Environmental*, 95(3-4), 270-278, 2010. doi: 10.1016/j.apcatb.2010.01.004

- [8] Galeano, AL., Vicente, MA., Gil, A.: "Treatment of municipal leachate of landfill by Fenton-like heterogeneous catalytic wet peroxide oxidation using an Al/Fe-pillared montmorillonite as active catalyst", *The Chemical Engineering Journal*, 178, 146-153, 2011. doi: 10.1016/j.cej.2011.10.031
- [9] Gozmen, B., Kayan, B., Gizir, A.M., Hesenov, A.: "Oxidative degradations of reactive blue 4 dye by different advanced oxidation methods", *Journal of Hazardous Materials*, 168, 129–136, 2009. doi: 10.1016/j.jhazmat.2009.02.011
- [10] Hassan, H., Hameed, BH.: "Fe–clay as effective heterogeneous Fenton catalyst for the decolorization of Reactive Blue 4", *The Chemical Engineering Journal*, 171(3), 912-918, 2011.
- [11] Ilinoiu, EC., Pode, R., Manea, F., Colar, LA., Jakab, A., Orha, C., Ratiu, C., Lazau, C., Sfarloaga, P.: "Photocatalytic activity of a nitrogen-doped TiO₂ modified zeolite in the degradation of Reactive Yellow 125 azo dye", *Journal of the Taiwan Institute of Chemical Engineers*, 44(2), 270–278, 2013. doi: 10.1016/j.jtice.2012.09.006
- [12] Kasiri, MB., Aleboyeh, H., Aleboyeh, A.: "Degradation of Acid Blue 74 using Fe-ZSM5 zeolite as a heterogeneous photo-Fenton catalyst", *Applied Catalysis B Environmental*, 84(1), 9-15, 2008.
- [13] Kusic, H., Loncaric Bozic, A., Koprivanac, N., Papic, S.: "Fenton type processes for minimization of organic content in coloured wastewaters. Part II: Combination with zeolites", *Dyes and Pigments*, 74(2), 388-395, 2007. doi: 10.1016/j.dyepig.2006.01.050
- [14] Ministry of Energy, Development and Environmental Protection of Republic of Serbia, "Regulation on limit values of pollutants in water and deadlines for their achievement", *Official Gazette*, 67 (2011), 13–41
- [15] Saravanan, R., Gupta, VK., Narayanan, V., Stephen, A.: "Visible light degradation of textile effluent using novel catalyst ZnO/g-Mn₂O₃", *Journal of the Taiwan Institute of Chemical Engineers*, 45(4), 1910-1917, 2014. doi: 10.1016/j.jtice.2013.12.021
- [16] Wu, J., Lin, G., Li, P., Yin, W., Wang, X., Yang, B.: "Heterogeneous Fenton-like degradation of an azo dye reactive brilliant orange by the combination of activated carbon-FeOOH catalyst and H₂O₂", *Water Science & Technology*, 67(3), 572–578, 2012. doi: 10.2166/wst.2012.596
- [17] Zhao, Y., Hu, J.: "Photo-Fenton degradation of 17 β -estradiol in presence of a-FeOOH and H₂O₂", *Applied Catalysis B Environmental*, 78(3-4), 250-258, 2008. doi: 10.1016/j.apcatb.2007.09.026



EXAMINATION OF THE APPLICATION POSSIBILITIES OF WASTE RED MUD IN TREATMENT OF COLORED EFFLUENT

Aleksandra Kulić¹ , Milena Bečelić-Tomin¹ , Đurđa Kerkez¹ ,
Gordana Pucar Milidrag¹ , Vesna Kecić² , Miljana Prica² 

¹University of Novi Sad, Faculty of Sciences, Department of Chemistry,

Biochemistry and Environmental Protection, Novi Sad, Serbia

²University of Novi Sad, Faculty of Technical Sciences,

Department of Graphic Engineering and Design, Novi Sad, Serbia

Abstract: *The most important component of coloured wastewaters is the synthetic dyes, which cause negative effects on aquatic ecosystems due to great solubility and persistence. Previous research points out that the heterogeneous Fenton process can be applied as an effective treatment of this type of wastewater. In this paper, the possibility of using waste red mud (RM), as a catalyst for the Fenton reaction, has been investigated. Sample of wastewater was obtained from the local textile industry, as follows: effluent before and after biological treatment. The optimization process was carried out using the response surface methodology, where the pH value, the concentration of H₂O₂ and the catalyst dose was varied. The following optimal reaction conditions were obtained for raw effluent: pH=3.26; [H₂O₂]=10 mM; [RM]=0.09 g, while for effluent after biological treatment: pH=3; [H₂O₂]=4.28 mM; [RM]=0.1 g. Under the given conditions, the efficiency of the Fenton process was 61.83 and 79.65%, respectively.*

Key words: Fenton, red mud, RSM, CCD, effluent

1. INTRODUCTION

Large quantities of discharged coloured wastewaters from textile mills are characterized by high chemical oxygen demand, suspended solids, heavy metals, salts, etc. The use of multiple technological processes (dyeing, finishing, sizing, washing, rinsing) contributes to the highly variable nature of textile effluents (Babuponnusami & Muthukumar, 2014; Soltani & Safari, 2016).

Biological treatment processes are widely used because they are economical, but after all not able to efficiently degrade present synthetic dye molecules in the wastewaters. So, advanced oxidation processes (AOPs) can be used in order to mineralise dyes in textile effluents (Benatti & Tavares, 2008). Among them, Fenton process is known as a reaction between hydrogen-peroxide (oxidant) and iron species (catalyst) to generate highly reactive hydroxyl radicals (HO•) that can efficiently degrade dye molecules (Bezerra et al, 2008; Davarnejad & Azizi, 2016; Gebrati et al, 2018). The wide range of materials can be used as catalysts in heterogeneous Fenton processes, where even industrial solid wastes can find its purpose (Gebrati et al, 2018). One of them is red mud (RM) from alumina factory that could be used, because it is consisted of iron minerals among others constituents. Nowadays researches are oriented towards combining these processes for achieving a satisfactory level of coloured effluent purification (Benatti & Tavares, 2008). Also, evaluation of optimal experimental conditions must be conducted, where response surface methodology (RSM) can be used as a tool. The main types of RSM designs are full factorial design, central composite design (CCD), Box-Behnken design and D-optimal design (Lodha & Chaudhari, 2007).

In this study, CCD was used to optimize heterogeneous Fenton process parameters (pH value, initial H₂O₂ concentration and catalyst dose) for obtaining satisfactory decolourization of raw textile effluent and effluent after biological treatment. Moreover, as a catalyst in Fenton reaction was used RM after thermal modification at 550°C.

2. METHODS

2.1 Materials

Commercially purchased chemicals, 30% H₂O₂, H₂SO₄ and bovine liver catalase, were used in this work without any further purification (Sigma-Aldrich Company). Waste RM collected from the alumina factory (Bosnia and Herzegovina) was used as catalyst in the heterogeneous Fenton process after thermal modification (RM-550). The main steps of catalyst preparation are shown in the figure 1. Coloured

effluents from local textile mill (Serbia) were collected before and after biological treatment, named as *rawEF* and *afterBT*, respectively. Table 1 shows characterization of these wastewaters.

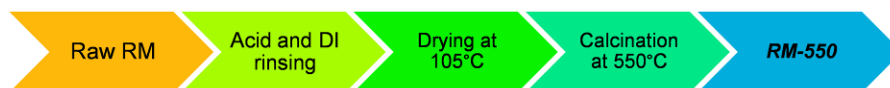


Figure 1: Steps of thermal modification of RM

Table 1: Main characteristics of coloured effluents

Parameter Effluent	COD (mgO ₂ /l)	BOD (mgO ₂ /l)	Total N (mgN/l)	Total P (mgP/l)	pH value	Color
rawEF	627	360	16	0.1	6.9	Dark purple
afterBT	497	127	12	2.6	7.7	Black

2.2 Heterogeneous Fenton process

Decolourization of textile effluents were conducted as follows: convenient amount of RM-550 was added to 100 ml of real sample, after what pH value was set with diluted H₂SO₄. Next, initial concentration of H₂O₂ was added and mixing of this mixture was set at 120 rpm at JAR test apparatus during a predetermined time. For termination of Fenton reaction 1 ml of catalase solution (0.1 g/l) was added to the mixture. The catalyst was separated by centrifugation (Sigma 3-30K) for 5 minutes at 10000 rpm. Evaluation of treatment efficacy was executed by measuring absorbance at UV/VIS spectrophotometer (UV 1800, Shimadzu, Japan), $\lambda_{\max}(\text{rawEF})=579.5$ nm and $\lambda_{\max}(\text{afterBT})=592$ nm. Percent of dye degradation was calculated according to the formula (1).

$$\frac{A_0 - A}{A_0} \cdot 100 = \text{Decolourization}(\%) \quad (1)$$

Where A_0 was initial absorbance value for effluent, and A value was sample absorbance after specified reaction condition and time.

2.3 Experiment design

Effect of three independent variables (A-pH value, B-initial concentration of H₂O₂ and C-dosage of RM-550) on response-decolourization efficacy, were investigated employing CCD experimental design and RSM by the software Design-Expert 7.0.0. (Stat-Ease Inc., Minneapolis, USA). The actual values of coded maximum, central and minimum levels (-2, -1, 0, +1, +2) for each variable are given in table 2.

Table 2: Coded and actual values for experimental parameters

Symbol	Parameter	Unit of measure	Range of independent variables				
			-2	-1	0	+1	+2
A	pH value	-	1.98	3.00	4.50	6.00	7.02
B	Initial concentration of H ₂ O ₂	mM	0.61	3.00	6.50	10.0	12.4
C	Initial dosage of RM-550	g	0.03	0.05	0.08	0.10	0.12

3. RESULTS

According to the CCD 20 experimental probes were designed, where probes 1-8 presents full factorial design, 9-14 star design and 15-20 central point repetitions. The order of runs, the real values of factors, the actual experimental and predicted values for the decolourization efficiency of both effluents, rawEF and afterBT, are given in Table 3. The actual values of the response vary between 1.02 to 69.1% and 2.79 to 92.5%, respectively. For both effluents the relation between the independent variables and observed response was described by a second order polynomial model and the experimental data were fitted by square function. Also, ANOVA test was implemented and significant interactions between variables such as pH and initial H₂O₂ concentration (AB), pH and RM-550 dose (AC), initial H₂O₂

concentration and RM-550 dose (BC), as well as (A²), (B²), (C²) are presented in table 4. Further, these interactions are also presented as 3D graphs in the figure 2 and 3.

Table 3: The matrix of the experimental design, with actual and predicted values for dependent variables

Std Order	Run Order	Parameter			Decolourization efficiency (%)			
		pH	c(H ₂ O ₂)	m(RM-550)	rawEF		afterBT	
					Actual	Predicted	Actual	Predicted
1	18	3.00	3.00	0.05	39.9	45.1	58.8	57.0
2	1	6.00	3.00	0.05	1.02	16.5	6.44	12.3
3	15	3.00	10.0	0.05	38.5	46.0	64.6	71.4
4	16	6.00	10.0	0.05	7.34	13.1	15.5	16.1
5	10	3.00	3.00	0.10	54.6	61.8	77.0	86.2
6	9	6.00	3.00	0.10	23.6	29.1	41.9	44.8
7	8	3.00	10.0	0.10	69.1	66.6	75.5	79.4
8	14	6.00	10.0	0.10	21.8	29.6	15.9	27.5
9	7	1.98	6.50	0.08	57.6	53.5	82.2	76.2
10	19	7.02	6.50	0.08	12.6	-1.62	2.79	-5.05
11	20	4.50	0.61	0.08	67.5	53.8	56.2	51.3
12	4	4.50	12.4	0.08	59.8	55.0	57.7	48.8
13	17	4.50	6.50	0.03	38.2	24.3	48.9	46.8
14	3	4.50	6.50	0.12	56.7	52.2	92.5	80.8
15	5	4.50	6.50	0.08	50.7	57.2	39.7	57.6
16	11	4.50	6.50	0.08	58.9	57.2	69.5	57.6
17	2	4.50	6.50	0.08	56.5	57.2	53.4	57.6
18	12	4.50	6.50	0.08	57.2	57.2	57.7	57.6
19	6	4.50	6.50	0.08	60.4	57.2	71.8	57.6
20	13	4.50	6.50	0.08	56.5	57.2	51.1	57.6

Table 4: ANOVA test results for quadratic model

Source	Model	A	B	C	AB	AC	BC	A ²	B ²	C ²
<i>rawEF</i>										
Sum of squares	6865.6	3670.2	1.67	943.9	9.34	8.55	7.80	1761.4	14.0	647.3
df	9	1	1	1	1	1	1	1	1	1
Mean square	762.9	3670.2	1.67	943.9	9.34	8.55	7.80	1761.4	14.0	647.3
F value	6.33	30.5	0.01	7.83	0.08	0.07	0.06	14.62	0.12	5.37
P value	0.0040	0.0003	0.9086	0.0188	0.7864	0.7953	0.8043	0.0034	0.7406	0.0429
<i>afterBT</i>										
Sum of squares	10730.6	7968.5	7.52	1400.2	56.4	5.53	223.4	872.7	102.0	69.4
df	9	1	1	1	1	1	1	1	1	1
Mean square	1192.3	7968.5	7.52	1400.2	56.4	5.53	223.4	872.7	102.0	69.4
F value	8.59	57.4	0.05	10.1	0.41	0.04	1.61	6.29	0.73	0.50
P value	0.0012	<0.0001	0.8206	0.0099	0.5381	0.8458	0.2334	0.0311	0.4114	0.4956

4. DISCUSSION

Determination of statistically significant independent variables was conducted through Fisher's test (table 3) (Lodha & Chaudhari, 2007; Soltani & Safari, 2016). 6.33 and 8.59 were F-values for quadratic model, for both effluents respectively, which implies the statistical importance of the model. Further, p-values <0.05 point out which model terms are significant and p-values >0.1 indicate which model terms are not significant. Based on this explanation terms of importance are A, C, A² and C² for decolourization efficacy of coloured textile effluents. The coefficients of determination (R²) for process efficiency were 0.8507 and 0.8854, for rawEF and afterBT effluent, respectively. Thus indicating that the applied model was statistically significant and modelled responses fit well with experimental data.

Three-dimensional surface plots were applied to represent the interaction between the examined parameters. According to the table 3 and ANOVA test, the pH value is one of the significant parameters which affect heterogeneous Fenton process efficiency, thus controlling the catalytic activity of RM-550 and H_2O_2 stability. Interaction between pH and initial H_2O_2 concentration was examined at constant RM-550 dose (0.08 g) (fig. 2a, 3a). Even when changing the entire H_2O_2 concentration range, a low pH is responsible for a high decolourization percentage, which is in accordance with the literature data where is stated that Fenton process is most effective in the narrower pH range (2-4). Lower efficacy can be explained due to H_2O_2 instability at higher pH values, where it starts to break down on molecular oxygen without forming a sufficient amount of HO^\bullet (Torrades & Garcia-Montano, 2014; Nidheesh, 2015)). Interaction between pH and RM-550 dosage was examined at constant H_2O_2 concentration (6.50 mM) (fig. 2b, 3b). A noticeable trend of growth of heterogeneous Fenton process efficiency can be seen with lowering pH values and increasing RM-550 dose. According to the literature data (Bezerra et al., 2008; Soltani & Safari, 2016)) catalyst dosage is in direct proportion to a Fenton process efficacy, because with its increase there is a larger amount of available active sites, which produce HO^\bullet and therefore the organic pollutant degradation increases. Highest process efficiency was achieved at pH 3.00 and 0.10 g for rawEF (69.1%) and at pH 4.50 and 0.12 g for effluent afterBT (92.5%), thus confirming the previous statement. There is also a possibility of dye molecule adsorption to occur on the surface of RM-550, and therefore increasing discoloration of coloured effluents. Interaction between RM-550 dosage and initial H_2O_2 concentration was examined at constant pH (4.50) (fig. 2c, 3c). It is evident that H_2O_2 concentration has only slight effect on decolourization of rawEF, in contrast to the catalyst dose. On the other hand, highest dye removal is achieved with lower H_2O_2 concentration and highest RM-550 dosage, where with increasing of oxidant concentration Fenton process efficiency is decreasing. This trend could be associated with sufficient production of HO^\bullet from H_2O_2 on the surface of the catalyst, and therefore providing rise of both effluents colour removal (Nidheesh, 2015; Davarnejad & Azizi, 2016; Soltani & Safari, 2016).

The desired goal of the model is to maximize decolourization efficiency to achieve highest treatment performance. The optimum values of the independent variables are shown in table 5 for both observed effluents. After verification through a further experimental test the result indicates that the efficiency was in good correlation with the predicted values. Achieved decolourization was 61.8% and 79.7% for rawEF and afterBT, respectively, which can be due to the low content of present heavily biodegradable organic matter and dyes.

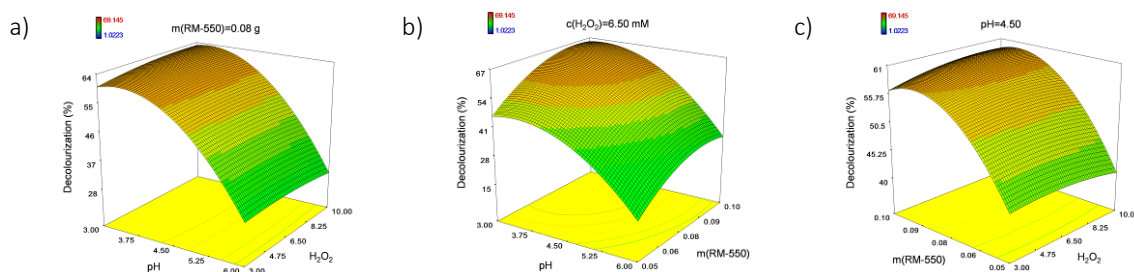


Figure 2: The effect of pH value, initial H_2O_2 concentration and RM-550 dosage on the decolourization efficiency of effluent rawEF

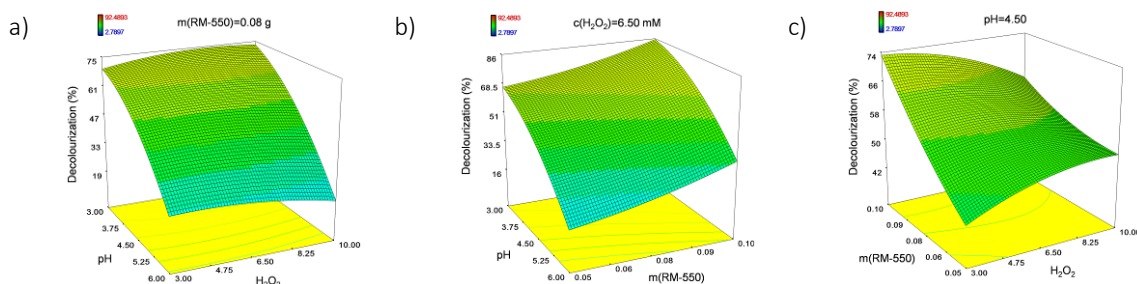


Figure 3: The effect of pH value, initial H_2O_2 concentration and RM-550 dosage on the decolourization efficiency of effluent afterBT

Table 5: Optimal values for the independent variables and heterogeneous Fenton process efficiency

Coloured effluent	pH	c(H ₂ O ₂)	m(RM-550)	Decolourization efficiency (%)	
				Actual	Predicted
rawEF	3.26	10	0.09	61.8	67.3
afetrBT	3.00	4.3	0.10	79.7	86.5

5. CONCLUSIONS

The aim of this paper was investigating the possibility of thermally treated waste red mud as a catalyst in the heterogeneous Fenton process of decolourization of textile wastewaters. Two effluents were treated, and those were raw wastewater and after biological treatment. The optimization of this process was carried out by applying the central composite design, with variation of main Fenton reaction parameters (pH, initial H₂O₂ concentration and RM-550 dose). Based on the experimental results, an empirical relationship between the response and independent variables was obtained, expressed by a second-order polynomial equation, as well as by 3D surface plots. The following optimal reaction conditions were obtained for raw effluent: pH=3.26; [H₂O₂]=10 mM; [RM]=0.09 g, while for effluent after biological treatment: pH=3; [H₂O₂]=4.28 mM; [RM]=0.1 g. Under the given conditions, the efficiency of the Fenton process was 61.8 and 79.6%, respectively, due to different effluent characteristics. Namely, it is assumed that the higher decolourization efficiency after biological treatment was achieved due to partial degradation of dye molecules. Because of this, lower rates of hydroxyl radical production was required and therefore lower hydrogen peroxide consumption.

6. ACKNOWLEDGEMENTS

This research was financed by the Ministry of Education, Science and Technological Development of Republic of Serbia (Project III43005).

7. REFERENCES

- [1] Babuponnusami, A. & Muthukumar, K.: "A review on Fenton and improvements to the Fenton process for wastewater treatment", *Journal of Environmental Chemical Engineering*, 2(1), 557-572, 2014. doi: 10.1016/j.jece.2013.10.011
- [2] Benatti, C.T. & Tavares, C.R.G.: "Fenton's Process for the Treatment of Mixed Waste Chemicals", In book: *Organic Pollutants Ten Years After the Stockholm Convention - Environmental and Analytical Update*, 247-266, 2012. doi: 10.5772/31225
- [3] Bezerra, M.A., Santelli, R.E., Oliveira, E.P., Villar, L.S., Escalera, L.A.: "Response surface methodology (RSM) as a tool for optimization in analytical chemistry", *Talanta* 76, 965-977, 2008. doi: 10.1016/j.talanta.2008.05.019
- [4] Davarnejad, R. & Azizi, J.: "Alcoholic wastewater treatment using electro-Fenton technique modified by Fe₂O₃ nanoparticles", *Journal of Environmental Chemical Engineering*, 4(2), 2016. doi: 10.1016/j.jece.2016.04.009
- [5] Gebrati, L., Achaby, M.E., Chatoui, H., Laqbaqbi, M., Kharraz, J.E., Aziz, F.: "Inhibiting effect of textile wastewater on the activity of sludge from the biological treatment process of the activated sludge plant", *Saudi Journal of Biological Sciences*, 2018. doi: 10.1016/j.sjbs.2018.06.003
- [6] Lodha, B. & Chaudhari, S.: "Optimization of Fenton-biological treatment scheme for the treatment of aqueous dye solutions", *Journal of Hazardous Materials*, 148(1-2), 459-466, 2007. doi: 10.1016/j.jhazmat.2007.02.061
- [7] Nidheesh, P.V.: "Heterogeneous Fenton catalysts for the abatement of organic pollutants from aqueous solution: a review", *RSC Advances*, 5(51), 2015. doi: 10.1039/C5RA02023A
- [8] Soltani, R.D.C. & Safari, M.: "Periodate-assisted pulsed sonocatalysis of real textile wastewater in the presence of MgO nanoparticles: Response surface methodological optimization", *Ultrasonic Sonochemistry*, 32, 181-190, 2016. doi: 10.1016/j.ultsonch.2016.03.011
- [9] Torrades, F. & García-Montaña, J.: "Using central composite experimental design to optimize the degradation of real dye wastewater by Fenton and photo-Fenton reactions", *Dyes and Pigments*, 100(1), 184-189, 2014. doi: 10.1016/j.dyepig.2013.09.004



© 2018 Authors. Published by the University of Novi Sad, Faculty of Technical Sciences, Department of Graphic Engineering and Design. This article is an open access article distributed under the terms and conditions of the Creative Commons Attribution license 3.0 Serbia (<http://creativecommons.org/licenses/by/3.0/rs/>).

CHARACTERIZATION OF COATED PRINTS WITH FRAGRANCED MICROCAPSULES

Rastko Milošević¹ , Nemanja Kašiković¹ , Živko Pavlović¹ ,
Mladen Stančić² , Raša Urbas³ 

¹University of Novi Sad, Faculty of Technical Sciences,
Department of Graphic Engineering and Design, Novi Sad, Serbia

²University of Banja Luka, Faculty of Technology,
Graphic Engineering Department, Banja Luka, Bosnia and Herzegovina

³University of Ljubljana, Faculty of Natural Sciences and Engineering,
Department of Textiles, Graphic Arts and Design, Ljubljana, Slovenia

Abstract: *Microcapsules are used in various fields of application, such as in pharmacy, medicine, agriculture, chemical industry, construction industry, food industry, biotechnology, electronics. Fragranced and PCM (phase change materials) microcapsules also found their use in the printing and the textile industries, where they are applied in the combination with the appropriate ink or varnish on the desired substrate material. Microcapsules are applied either by coating or by different printing techniques, which main advantage is the ability to transfer the microcapsules onto desired areas of the substrate material without or with as little damage as possible, thus allowing the deposited microcapsules to fulfil their basic functionality. The aim of this research was to investigate the morphologic characteristics of the fragranced microcapsules and the coated prints using selected varnish and different fragranced microcapsules concentrations, as well as to determine how variable concentrations of the applied microcapsules in the varnish affect the optical characteristics of the coated prints. Performed SEM (scanning electron microscopy) and spectrodensitometric analyses of the coated prints revealed that both the coating process without microcapsules, as well as the different fragranced microcapsules' concentration in the coated water-based varnish, significantly affected both the morphologic and the optical characteristics of the coated prints.*

Key words: fragranced microcapsules, coating, offset printing, morphology, optical characteristics

1. INTRODUCTION

Different coatings are used today in the printing industry in order to add a new value to the printed products or to enrich them by enhancing their visual, protective or functional properties (application of different microcapsules' types) (Kipphan, 2001; Gosh, 2006). Microcapsules are used in different fields of application, such as in medicine, pharmacy, agriculture, biotechnology, electronics, chemistry, construction, food, printing and textile industry. They can be applied on various substrates, using numerous transfer techniques (coating or different printing techniques: screen and flexo printing, sheet-fed and web offset printing, gravure, pad printing, inkjet and xerography), which enable precise microcapsules' deposition on the specific areas of the printing substrate, though before application they need to be pre-mixed with the printing ink or the printing varnish (Gosh, 2006; Urbas et al, 2017; Starešinič et al, 2011; Rodrigues et al, 2009; Goetzendorf-Grabowska et al, 2004; Goetzendorf-Grabowska et al, 2008; Chovancova et al, 2008; Milošević et al, 2016). In addition to the visual and the tactile aspects of the printed matter, the progress of the printing technology also enabled the integration of scents, by applying microcapsules containing fragrances (Rose, 2007).

Microcapsules are tiny spheres, usually consisting of two parts (core and shell), which enables the encapsulated active agent (core material) to reach the "target" areas without being affected by the environment through which it passes, while its microscopic size allows the consumption of very small active agent quantity (Gosh, 2006; McShane et al, 2009; Dubey et al, 2009; Microtek Laboratories). Microcapsules used in printing applications can be activated by using different activation mechanisms, such as by external pressure, abrasion and heat or light application (Gosh, 2006; Boh et al, 2008; Nelson, 2001; Sensor Products).

Applied microcapsules enable different functionalities to the final, printed product, but they will to a certain extent change basic features of the prints such as physical (thickness, grammage, surface roughness), mechanical and optical characteristics (colour, opacity and print gloss) (Blanco-Pascual, 2014;

Pavić, 2015; Tarnopol, 2009; Urbas et al, 2015; Manojlović, 2013). A surface characteristic of the printed surface has a huge impact on the type and the amount of the reflected light from the printed surface, which affects the print quality and the overall appearance of the prints. Morphologic characteristics of the prints are dependent on the printing substrate properties, its surface structure (smoothness, roughness), texture, degree of transparency, type of the coating and complex rheological and surface tension properties of the coatings used (Karlović, 2010; Karlović et al, 2011; Satas et al, 2000). Basic properties of the microcapsules, such as morphology, microcapsule formation, size and volume distributions, can be determined using optical, scanning electron microscopy (SEM) or transmission electron microscopy (TEM) in combination with the appropriate image analysis software (Rodrigues et al, 2009; Urbas et al, 2015; Peña et al, 2009).

The aim of this research is to determine basic morphologic and optical characteristics of the functional coatings with scents, produced by an automatic coating technique using water-based varnish in which fragranced microcapsules in water suspension were added, as well as to investigate how different concentrations of the microcapsules in the coating layers affect morphologic and optical characteristics of the coated prints. Conducted SEM and optical characteristics analysis of the produced functional coatings revealed that the application of the microcapsules, in the varnish, significantly affected morphologic and optical characteristics of the coatings.

2. METHODS

In this research, for the coating process were used fragranced mono-core microcapsules in water suspension, which were made by modified in situ polymerization method (Šumiga, 2013). The microcapsule core material was made of different essential oils combination, with the fragrances of sage, rosemary and lavender, while the microcapsule shell was made of partially methylated trimethylol melamine (Melamin, Slovenia). As a printing substrate was used a commercially available matte coated paper (GardaMatt Art, Lecta, Spain) which basic characteristics provided by the producer (thickness, basis weight, specific volume and CIE whiteness) were presented in Table 1.

Table 1: Basic characteristics of used paper

Paper	Surface finish	Basis weight (ISO 536)	Specific volume	Thickness (ISO 534)	CIE-whiteness (ISO 11475)
GardaMatt Art	matte coated	130 g/m ²	0.85 cm ³ /g	111 µm	121.3 CIE

The C-375 water-based printing varnish was based on the stabilised water dispersion of acrylic resins (styrene acrylic emulsion), with the addition of the polyethylene wax. Selected varnish is suitable for the protection of the printed packaging in the food industry (without direct contact with the food) and is characterised by its high gloss and abrasion resistance (Cinkarna Celje, Slovenija).

Chosen substrate material was firstly printed using a four-color sheet-fed offset printing machine (KBA Performa 74, Koenig & Bauer, Germany) using only cyan ink (Diatone® PREMIUM+, Sakata inx, Japan). Printing was done according to standard printing production conditions, using Libra VP digital printing plate (Kodak, USA). Before coating process, microcapsules were premixed with the varnish (for 10 min., at 800 rpm) using the HS-30D WiseStir mixer (Witeg Labortechnik GmbH, Germany). The application of the varnish with the fragranced microcapsules, onto the printing substrate, was done using an automatic coating technique (K303 Multi Coater, RK PrintCoat Instruments Ltd, UK), with a rod that allows maximum varnish deposition thickness of 12 µm (coating speed was 8 m/min). Previously printed samples were coated with the mixture of varnish and four different fragranced microcapsules mass concentrations in the varnish: 0%, 1%, 7% and 15%. After coating procedure, all the samples were dried at room temperature (25°C, 55% relative humidity) for 24 hours.

Selected fragranced microcapsules and the coated samples were prepared and photographed using scanning electron microscopy (SEM; JSM 6060 LV, Jeol, Japan) to obtain microcapsules' and coated samples' morphology. Generated images were also analysed using an image analysis software (ImageJ, USA) (ImageJ, n.d.) in order to determine microcapsules' size/volume distributions. Determination of the fragranced microcapsules diameters was based on the 500 measurements on different SEM images. After SEM analyses, several optical characteristics of the prints were determined in order to investigate the effects of varnish and different microcapsules concentrations application. Following print quality

parameters were determined: solid-tone print density, tone value increase (TVI) and relative spectral reflectance, using spectrodensitometer SpectroDens (Techkon, Germany).

3. RESULTS

3.1 SEM analysis of the fragranced microcapsules and the coated samples

Scanning electron microscopy (SEM) and subsequent image analyses of the obtained SEM images were employed in order to investigate the fragranced microcapsules' properties (Figure 1a) in the coated varnish layers, to determine their size/volume distributions (Figure 1b), as well as to investigate the properties of the coated samples' surfaces made by using different fragranced microcapsules mass concentrations in the varnish: 0% (C_0% sample), 1% (C_1% sample), 7% (C_7% sample) and 15% (C_15% sample), Figure 2. In the Figure 1 are presented morphology (1a) and size/volume distribution (1b) of the fragranced microcapsules in water suspension, that were used for automatic coating process in combination with the water-based varnish. As it can be observed from the Figure (1a), the fragranced microcapsules have regular, spherical shape, possessing a smooth surface and relatively uniform sizes. Obtained size distribution curve is positively skewed with relatively narrow distribution (blue curve in Figure 1b), where 92.08% of the sampled fragranced microcapsules had the diameter between 1 μm and 3 μm . The mean diameter of the sampled fragranced microcapsules was 2.08 μm (st. dev. 0.63), while the minimum and the maximum recorded diameters were 1.06 μm and 4.60 μm . In contrast to the fragranced microcapsule size distribution, the volume distribution curve (red curve in Figure 1b) is almost symmetrical, showing normal volume distribution, where 17.62% of all sampled fragranced microcapsules (sizes between 2.5 μm and 3 μm) participated with 30.36% in the total fragranced microcapsules volume amount.

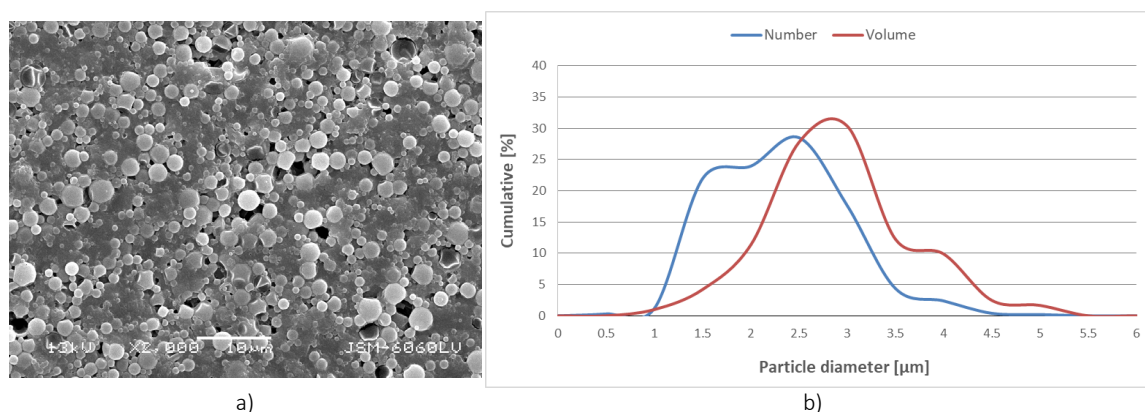


Figure 1: *Fragranced microcapsules in water suspension (a) (SEM; 1.000× magnification), with their size and volume distributions (b)*

From Figure 2, it can be noticed that used matte coated paper for printing and coating, possesses relatively rough surface structure (Figure 2a), which is also observed in the case of printed sample (Figure 2b) where due to paper's uneven surface structure nonuniform ink deposition of the solid tone patch was obtained (darker, left half of the SEM image). The prints made by solely varnish (Figure 2c), sample C_0%, has very smooth and uniform surface structure, while the sample coated using varnish and microcapsules in the mass concentration of 1% (C_1% sample), Figure 2d, has slightly rougher surface structure with several fragranced microcapsules on top of it. The prints made with the fragranced microcapsules in the mass concentration of 7% (C_7%), Figure 2e, possess even rougher surface structure, while the samples coated with the varnish and microcapsules in the mass concentration of 15% (C_15% sample), Figure 2f, possess the roughest and the least uniform surface structure, with visible fragranced microcapsules spread all over the surface of the sample. By increasing the concentration of the fragranced microcapsules in the varnish, the surface of the coated samples became more and more non-uniform and rough. Transferred microcapsules on the coated samples were undamaged, which prove that automatic coating technique is adequate and can be successfully used for coating process of the fragranced microcapsules.

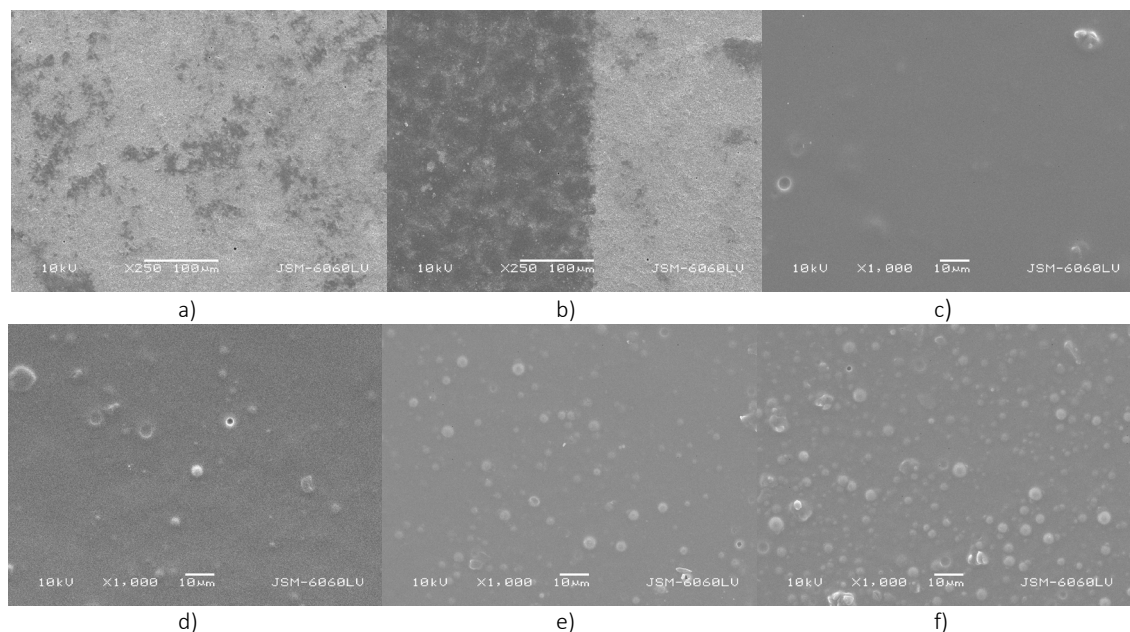


Figure 2: Surfaces of the blank paper (a), printed paper C (b), and printed and coated samples C_0% (c), C_1% (d), C_7% (e), C_15% (f), (SEM; 250× and 1000× magnifications)

3.2 Analysis of the print quality parameters

From the presented solid-tone print density results in Figure 3, it can be observed that all recorded print density values were below reference values (red line) given by ISO standard (ISO 12647-2:2004, 2004). Coating process with the varnish only (without microcapsules) led to solid-tone print density increase (C_0% sample) which is a result of varnish colour and transparency characteristics. Addition of fragranced microcapsules in the mass concentration of 1% in the varnish, slightly raised the resulted solid-tone print density value (C_1% sample), while the coating process with increased microcapsules' concentrations in the varnish (7% and 15%) led to gradual print density decline. Varnishing process without fragranced microcapsules produced darker prints compared to uncoated prints, while the higher concentrations of the microcapsules in the varnish (7% and 15%) led to gradual print density values drop, which is a result of microcapsules shell material white colour.

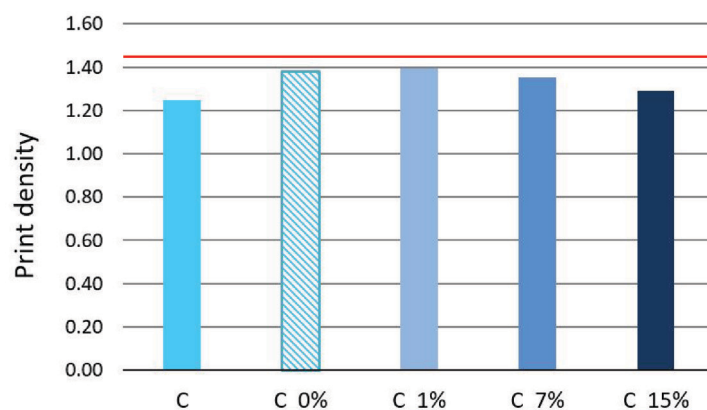


Figure 3: Measured solid-tone print density of printed and coated samples

In Figure 4 are presented obtained TVI values, as well as aimed ISO TVI values (dashed purple line) which correspond to defined printing conditions (printing process, screen ruling, paper and printing plate types) according to ISO standard (ISO 12647-2:2004, 2004). TVI reproduction curve of printed, uncoated sample (C, cyan curve) almost match the reference ISO TVI values (dashed purple line), indicating good print quality, regarding this print quality parameter. Obtained TVI data have a very similar trend as previously

analysed solid-tone print density data. Namely, coating process using only varnish (C_0%, dashed cyan curve) produced much higher TVI values over the whole tonal range, comparing to solely printed samples (C sample). The highest TVI values were recorded on the samples coated with varnish and fragranced microcapsules in the mass concentration of 1% in it (C_1%, light blue curve). The next increase of the fragranced microcapsules concentration in the varnish (C_7% sample), led to a decline of TVI values. This trend continued in the case of the samples coated using the highest microcapsules concentration in the varnish as well (C_15% sample), where the lowest TVI values were obtained, comparing to all coated samples.

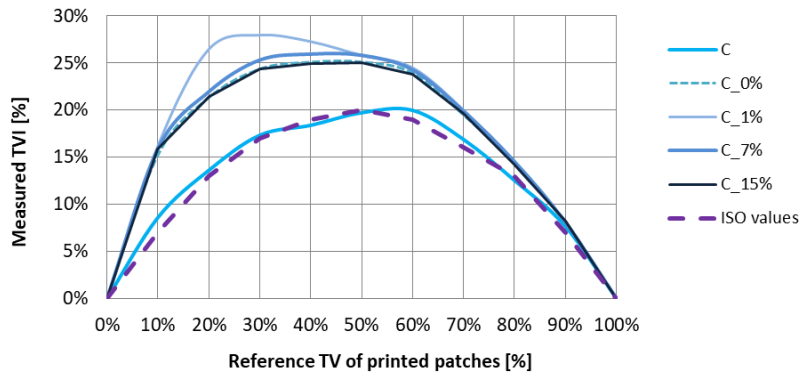


Figure 4: Measured TVI of the samples

In Figure 5 are presented measured relative spectral reflectance values of only printed (C) and printed and coated samples (C_0%, C_1%, C_7% and C_15%). This parameter was measured on the solid-tone patches printed using an offset printing press and a cyan ink. It can be noticed that all obtained relative spectral reflectance curves have almost identical shape, which describes the measured colour of the printed cyan ink patches (Figure 5).

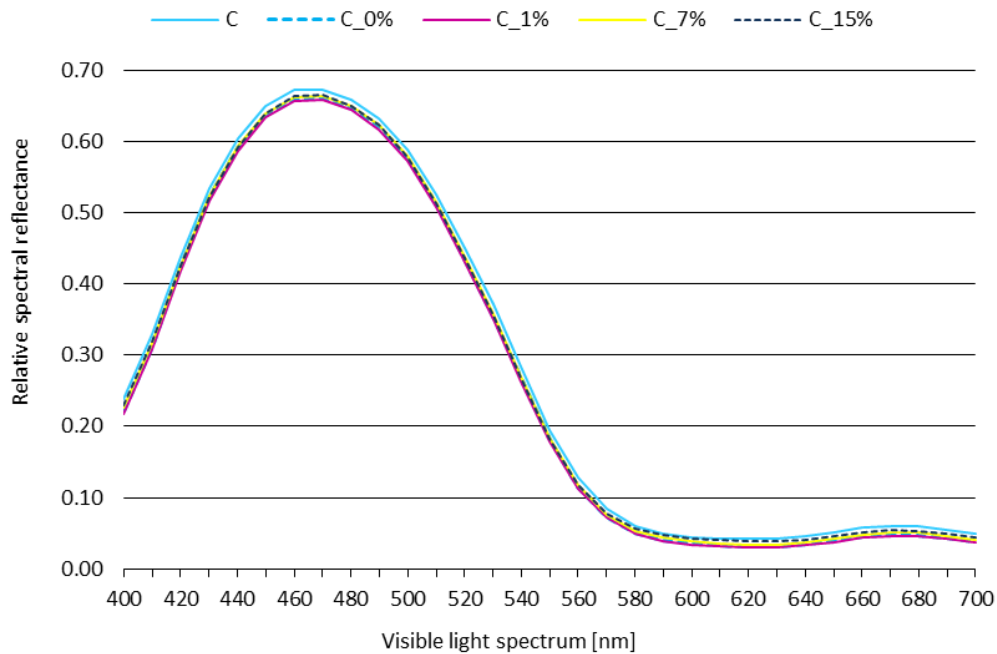


Figure 5: Measured relative spectral reflection of the samples

It can be noticed that on the solely printed sample (C sample, solid cyan curve) were recorded the highest relative spectral reflectance values, meaning that the colour of this sample was the lightest one. The sample where slightly lower relative spectral reflectance was obtained is the one printed and coated with fragranced microcapsules in the mass concentration of 15% (C_15% sample, dashed navy blue curve)

which is due to high concentration of microcapsules in the varnish that have white coloured shell, so the corresponding intensity of spectral reflectance will be higher compared to the samples coated using varnish with lower microcapsules' quantity. The darkest sample, i.e. the sample where the lowest spectral reflectance values were recorded was the sample printed and coated using fragranced microcapsules in the mass concentration of 1% (C_1% sample, solid magenta curve), which almost match the reflectance curve of the slightly lighter sample coated without microcapsules (C_0% sample, dashed cyan curve).

4. CONCLUSIONS

Presented results showed that the automatic coating technique is a nondestructive process for microcapsules transfer and that it can be successfully used for the coating process with varnish and different concentrations of fragranced microcapsules. This was proved by the SEM images where a lot of undamaged microcapsules were transferred on the paper substrate. Used fragranced microcapsules in the water suspension had very regular, spherical shape, smooth surface. Even though a visual inspection of the SEM images showed that microcapsules' sizes are relatively uniform, their size distribution curve is positively skewed with relatively narrow distribution while the volume distribution curve is almost symmetrical (normal volume distribution). The higher the fragranced microcapsules concentration in the coated varnish layer, the higher the surface nonuniformity and roughness of the applied coatings, as well as more microcapsules were observed on the surface of the coated samples.

Coating process with fragranced microcapsules changed to certain extent basic optical characteristics of the printed samples. On the coated samples without fragranced microcapsules were recorded higher solid-tone density values (darker prints) compared to only printed samples, while the higher concentrations of the fragranced microcapsules in the varnish (7% and 15%) led to a gradual print density decline, which is a result of white colour of the microcapsules shell material.

Similarly, as in the case of solid-tone print density data, coating process of printed samples led to a dramatic increase of TV, which was even higher after addition of microcapsules in 1% mass concentration in the varnish. Following two increases of microcapsules' percentage in the varnish (7% and 15%), resulted in a slight TVI decrease.

Obtained relative spectral reflectance curves of all samples have almost identical shape, but they have slightly different amplitude. Namely, coating process, without and with small microcapsules concentration of 1%, produces darkest colour samples (the lowest spectral reflectance values), comparing to only printed sample. Higher fragranced microcapsules concentrations in the varnish produced coated samples with a lighter colour (high spectral reflectance values) which is the consequence of the white colour of the microcapsules' shell.

5. ACKNOWLEDGMENTS

This research was supported by the Serbian Ministry of Science and Technological Development, Grant No: 35027 "The development of software model for improvement of knowledge and production in the graphic arts industry".

6. REFERENCES

- [1] Blanco-Pascual, N., Koldeweij, R.B.J., Stevens, R.S.A., Montero, M.P., Gómez-Guillén, M.C., Ten Cate, A.T.: "Peptide Microencapsulation by Core-Shell Printing Technology for Edible Film Application", *Food Bioprocess Technology* 7(9), 2472-2483, 2014. 10.1007/s11947-014-1256-3.
- [2] Boh, B., Šumiga, B.: "Microencapsulation technology and its applications in building construction materials", *Materials and Geoenvironment* 55(3), 329-344, 2008.
- [3] Chovancova, V., Pekarovicova, A., Fleming, I.P.: "Production of 3D Structures in Printing", *Proceedings of the 57th TAGA Annual Technical Conference 2005*, (Toronto, Ontario, 2008), pages 93-94.
- [4] Dubey, R., Shami, T.C., Bhasker Rao, K.U.: "Microencapsulation technology and applications", *Defence Science Journal* 59(1), 82-95, 2009.
- [5] Goetzendorf-Grabowska, B., Krolikowska, H., Gadzinowski, M.: "Polymer Microspheres as Carriers of Antibacterial Properties of Textiles: A preliminary Study", *Fibres & Textiles in Eastern Europe* 12(4), 62-64, 2004.

- [6] Goetzendorf-Grabowska, B., Królikowska, H., Bąk P., Gadzinowski, M., Brycki, B., Szwajca, A.: "Triclosan Encapsulated in Poli (L,L-lactide) as a Carrier of Antibacterial Properties of Textiles", *Fibres & Textiles in Eastern Europe* 16(3), 102-107, 2008.
- [7] Gosh., K.: "Functional coatings by Polymer Microencapsulation", (Wiley-VCH, Weinheim, Germany, 2006.), pages 3; 153; 177; 235.
- [8] ImageJ: "Download", URL <https://imagej.nih.gov/ij/download.html> (last request 2016-06-26).
- [9] International Organization for Standardization: ISO 12647-2. "Graphic technology – Process control for the production of half-tone colour separations, proof and production prints - Part 2: Offset lithographic processes", International Organization for Standardization, 2004.
- [10] Kipphan, H.: "Handbook of Print Media", (Springer-Verlag Berlin Heidelberg, Germany, 2001.), page 142.
- [11] Karlović, I.: "Karakterizacija kolorimetrijskih i geometrijskih osobina oplemenjenih površina u štampi", PhD thesis, Department of Graphic Engineering and Design, University of Novi Sad, Novi Sad, Serbia, 2010.
- [12] Karlović, I., Novaković, D.: "Effect of Different Coating Amounts on the Surface Roughness and Print Gloss of Screen Coated Offset Prints", *Journal of Imaging Science and Technology* 55(2), 020501-1 – 020501-10, 2011.
- [13] Manojlović, S.: "Bonding Microcapsules to Different Types of Substrates", BSc Thesis, University of Ljubljana, Slovenia, 2013.
- [14] Microtek Laboratories Inc.: "Technical overview: Microencapsulation", URL <http://www.microteklabs.com/technical-overview.html> (last request 2015-09-24).
- [15] Milošević, R., Kašiković, N., Pavlović, Ž., Stanković Elesini, U., Urbas, R.: "The Possibility of Microcapsules Application Using Pad Printing Technology", *Proceedings of the 8th GRID Symposium 2016*, (Faculty of technical sciences, Novi Sad, Serbia, 2016), pages 47–55.
- [16] McShane, M., Ritter, D.: "Microcapsules as optical biosensors", *Journal of Materials Chemistry*, 20(38), 8189-8193, 2010. 10.1039/C0JM01251C.
- [17] Nelson, G.: "Microencapsulation in textile finishing", *Review of Progress in Coloration and Related Topics*, 31, 57–64, 2001. doi.org/10.1111/j.1478-4408.2001.tb00138.x.
- [18] Pavić, N.: "Possibility of Microcapsule Application in Screen and Offset Printing Techniques", MSc thesis, University of Novi Sad, Serbia, 2015.
- [19] Peña, B., Casals, M., Torras, C., Gumí, T., Garcia-Valls, R.: "Vanillin release from polysulfone macrocapsules", *Industrial and Engineering Chemistry Research* 48(3), 1562–1565, 2009. 10.1021/ie801133f.
- [20] Rodrigues, S.N., Martins, I.M., Fernandes, I.P., Gomes, P.B., Mata, V.G., Barreiro, M.F., Rodrigues, A.E.: "Scentfashion®: Microencapsulated perfumes for textile application", *Chemical Engineering Journal* 149(1-3), 463–472, 2009. doi.org/10.1016/j.cej.2009.02.021.
- [21] Rose, H.: "Scent Encapsulated in Printed Products", URL https://projekt.beuth-hochschule.de/fileadmin/projekt/sprachen/sprachenpreis/erfolgreiche_beitraege_2007/1._Preis_07_-_Scent_Encapsulated_in_Printed_Products_-_Heike_Rose.pdf, (last request: 2017-04-03).
- [22] Satas, D., Tracton, A.A.: "Coatings Technology Handbook", (Boca Raton, FL, USA, 2000.), page 187.
- [23] Sensor Products Inc.: "Tactile Pressure Indicating Sensor Film", URL <https://www.sensorprod.com/prescale/product-pages/prescale/prescale.pdf> (last request 2017-04-04).
- [24] Starešinič, M., Šumiga, B., Boh, B.: "Microencapsulation for Textile Applications and Use of SEM Image Analysis for Visualisation of Microcapsules", *Tekstilec* 54(4-5), 80–103, 2011.
- [25] Šumiga, B.: "Informational approaches in the design of chemical microencapsulation processes", PhD thesis, University of Ljubljana, Slovenia, 2013.
- [26] Tarnopol, P.B.: "Scenting process", URL <http://www.google.com.gt/patents/WO2011002997A1?cl=en> (last request 2018-06-10).
- [27] Urbas, R., Milošević, R., Kašiković, N., Pavlović, Ž., Stanković Elesini, U.: "Microcapsules application in graphic arts industry: a review on the state-of-the-art", *Iranian Polymer Journal* 26 (7), 541–561, 2017. 10.1007/s13726-017-0541-1.
- [28] Urbas, R., Stanković Elesini, U.: "Color differences and perceptive properties of prints made with microcapsules", *Journal of Graphic Engineering and Design* 6 (1), 15-21, 2015.



© 2018 Authors. Published by the University of Novi Sad, Faculty of Technical Sciences, Department of Graphic Engineering and Design. This article is an open access article distributed under the terms and conditions of the Creative Commons Attribution license 3.0 Serbia (<http://creativecommons.org/licenses/by/3.0/rs/>).

POLY[(VINYL ALCOHOL) - (STEARIC ACID)] SYNTHESIS AND USE IN LAVENDER OIL CAPSULATION

Arif Ozcan , Emine Arman Kandirmaz 

Marmara University, School of Applied Sciences, Printing Technologies, Istanbul, Turkey

Abstract: Block polymers are used frequently in medicine, nanotechnology, paint, cosmetic and many other fields. Generally, one of the blocks produced is hydrophilic and the other hydrophobic. With amphiphilic polymers, molecules in the lipophilic structure can be encapsulated. Encapsulation is being used industrially for the reason that it is easier to transport a substance chemically without deterioration and is less affected by environmental effects. Amphiphilic block copolymers composed of hydrophilic and hydrophobic monomer units are used in micellization. Copolymers can form different morphological structures, which can be repeated under controlled conditions, depending on the composition of the block copolymer in the aqueous medium, the concentration of the copolymer in the medium, the interactions between the hydrophilic chains forming the shell, the addition of the acid, base or salt, the organic solvent used, the polarity of the solvent used and the relative solubilities of the blocks in the solvent. In these systems, while the core acts as a repository that allows the active substances to be dissolved, the shell part provides the hydrophilic property to the whole system. With amphiphilic polymers, molecules in the lipophilic structure can be encapsulated. In the first part of this work, stearic acid substituted polyvinyl alcohol-hydrophilic lipophilic polymer was synthesized with acidic esterification reaction and the chemical structure of the polymer enlightened with ATR-FTIR. ¹H-NMR method was used to determine the composition ratio of the polymer. In the second part of the study, lavender oil was added to the obtained polymer system and encapsulation was carried out after the interaction of the lavender oil and lipophilic end of polymer. The obtained capsule size analysis was performed by SEM. At the end of the work, paper coating formulations were prepared with microcapsules containing lavender oil and coated on standard office paper. The color and gloss properties of the coatings are measured. The results showed that the stearic acid substitute PVA polymer could be used in lavender oil encapsulation and made a suitable encapsulation for paper coatings.

Key words: block polymer, encapsulation, lavender oil, stearic acid, PVA

1. INTRODUCTION

Microcapsulation is the process in which the solid, liquid or gaseous compounds are taken up with a film material around them (Mars et al, 1990; Dubey et al, 2009) where the inner material is called the core, the corona, the active substance, and the outer material is called the shell, shield or wall. The capsule used is inert to the internal structure. so that the core structure is protected without degradation (Thies, 1996). The entire microencapsulation process essentially involves three separate processes that are separate from each other. The first process is to create a wall layer around the interior material. Second, the inner material is prevented from escaping from the formed outer wall layer. Besides, the outer wall layer should also prevent the ingress of unwanted materials which may damage the material inside. It takes place during the third process when the inside material is taken out at the beginning and at the right time This technique has been employed in a diverse range of fields from chemicals and pharmaceuticals to cosmetics and printing (Xiang et al, 1998; Cummings et al, 1996; Preston et al, 2001).

Microcapsules having a size of 1-100 µm are formed by coating an active inner material with a membrane which does not react with this substance (Moutinho et al, 2009). Microencapsulation of odor, drugs, vitamins, oils etc. protects the active material from oxygen, light, moisture, heat factors. It facilitates the transport of the active substance and also prevents it from evaporating during the stock and market. At the same time, it provides the spreading of the active substance in desired amount by the help of controlled release mechanisms. Many methods can be used to release active substance. Some of those; pH, electric current, ultrasound, heat etc.

The commonly used microcapsulation techniques are coacervation, (Cost E32, 2002; Pruszyński, 2003; Moutinho, 2009) interfacial polymerization (Moutinho et al, 2011; Zhu et al, 2012; Suave et al, 2006) and “in situ” polymerization (Singh et al, 2010; Mervosh et al, 2009). Release mechanism, formation conditions, particle size, stability, usage area etc. effects microcapsule production technique. Microencapsulation technology has a lot of applications such as including pharmaceutical, chemical, food, cosmetics, perfumery, textiles, agriculture, etc. (Jegat et al, 2000; Soper et al, 2000).

Lavender oil is an odour that it is used in cosmetic, pharmacy, antimicrobial usage, and aromatherapy (Ascheri et al, 2003) lavender oil have been used perfumery industry as a pleasant fragrance or as an antimicrobial agent. But lavender oil is high volatile and gives reaction with light, oxygen and heat. The microcapsulation is use to prevent this effects (Mizuno et al, 2005; Ouall et al, 2006).

The paper industry has to increase paper quality due to the increased customer demands and competition (Kandirmaz et al, 2018). The final quality requirements of the paper in the hands of the end user depend on the surface properties, and in recent years the paper industry has focused on improving the paper surface properties and answer the customer demands (Ozcan, 2016; Aydemir et al, 2013). In addition to improving the printability of paper, the paper is attracting and attracting features. Some of the charm attributes are colour changing paper, odorous paper, effect paper. The easiest way to impart a paper smell is to add a scented compound to the paper production process. However, most perfumes undergo oxidation, losing smell easily in an open environment and having a yellowish colour. In addition, oil compounds, which can be used for permanent odour, are not readily dispersed in an environment containing inorganic materials such as paper and adversely affect the production process. For this reason, the odour can be microcapsulated to facilitate the use of scents in paper production so that the surrounding perfume can not evaporate, the paper can not change the colour and the negative properties are reduced (Hirech et al, 2003; Jang et al, 2005; Brown et al, 2003; Chograni et al, 2010; Madene et al, 2006; Xiang et al, 1998; Pruszynski, 2003). The use of microcapsules in paper production can be accomplished by two methods, such as the addition of during the production and the coating on the paper surface. It is easier to apply with the coating on the paper surface because the homogenization process takes off and the production process is simplified.

For this purpose, stearic acid substituted PVA polymer was synthesized in this study and lavender microencapsulation with this polymer was performed. The coating formulations prepared with this microcapsule and cationic starch, papers coated with this formulation. The surface and printability properties of the resulting coatings were investigated.

2. METHODS

PVA, Stearic Acid, Citric acid, Ethanol, Sulphuric acid were obtained to Sigma Aldrich. Firstly, the wall material was synthesized. PVA (40 mmol), 200 mL of distillate water and stearic acid (10 mmol) were loaded to a three-necked glass flask equipped with a nitrogen inlet, a magnetic stirrer, a reflux condenser, and a thermometer. With the help of a dropping funnel, 1 ml H₂SO₄ was added drop by drop with 250 rpm stirring at 80 °C in an oil bath. The mixture was refluxed at 80°C for 24 hours. The solution was participated with ethanol. Substituted polymer was filtered and dried overnight at room temperature in a vacuum incubator. In the capsulation study; 1 g stearic acid substituted PVA polymer was dissolved in 50 ml distillate water, 2 hour stirred and the 1 ml lavender oil was added onto the solution. After 1 hour 4mL 1M citric acid was added the mixture and stirred 2 hours 500 rpm. Obtained capsules are filtered and dried. The obtained capsules chemical structure was enlightened with ATR-FTIR the morphological structures determined with SEM.

Cationic starch based surface coatings were applied to paper. The parameters of base paper used in this study are given in Table 1.

Table 1: Parameters of the base paper used in the study

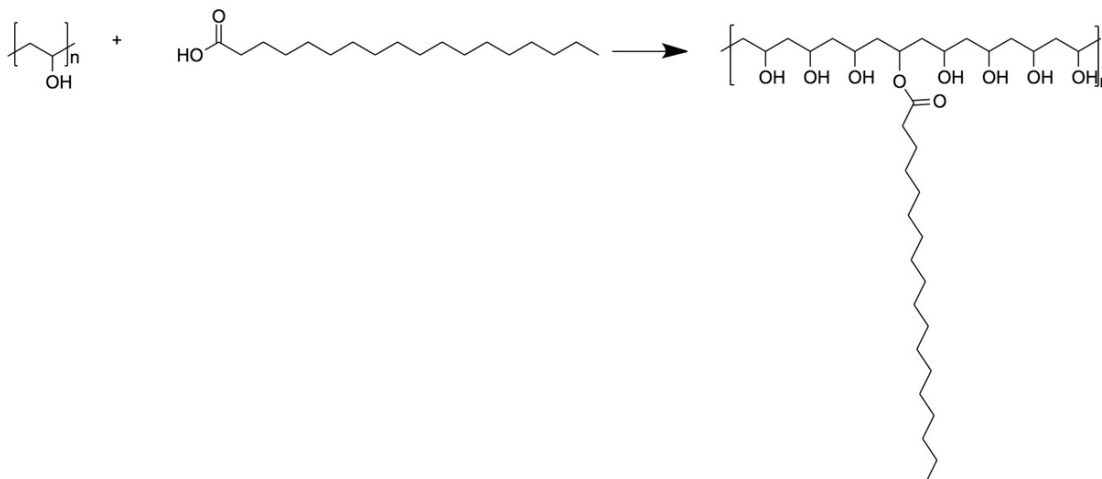
Properties	Standard	Paper
Grammage (g/m²)	ISO 536	80
Thickness (µm)	TAPPI T411	190
Whiteness (D65/10) (%)	ASTM E313	99
Gloss (TAPPI 60°/75°)	T480 om-92	4.9
Yellowness	ASTM E313	0.06

The sizing formulation applied consisted of 7.5% concentration of cationic starch, which was heated up to 90 °C, and the resulting hot-surface coating solution was cooled to 60 °C and then applied on to the paper surface using the MEYER rod with rod number 2 in a laboratory-type paper coating machine. The same

CIE L*a*b* values of The original, sized and microcapsule sized papers were measured using X-Rite eXact hand-held spectrophotometer according to ISO 12647-2:2013, between a spectral range of 400 nm to 700 nm, under a D50 light source, 2° observer, polarized filter, and 0/45-degree geometry. The colour differences formula was given below. Calculations were made by taking the average of five measurements. ΔL^* , Δa^* , Δb^* : Difference in L*, a*, and b* values between specimen colour and target colour. Lightness is represented by the L* axis which ranges from White to Black. The red area is connected to the green by the a* axis, while the b* axis runs from yellow to blue.

Gloss measurements were made with BYK-Gardner GmbH glossmeter according to ISO 2813:2014 60° geometry.

Stearic acid substitute polyvinyl alcohol was prepared via acidic esterification (fisher esterification) technique according to Figure 1.



ATR-FTIR and ^1H -NMR spectra was confirmed the expected structures. In Figure 2, the characteristic ^1H -NMR signals of stearic acid substitute polyvinyl alcohol can be seen. The proton on the stearic acid bounded carbon proton signal for Stearic acid substitute polyvinyl alcohol structure was appeared at 4,69 ppm in Figure 2. Additionally, the spectrum also showed characteristic peaks for proton of the hydroxyl-bonded carbon at 3.59 ppm, Symmetric protons on to PVA at 1.72 ppm, Symmetric protons on stearic acid at 1,23 ppm, Symmetric protons on stearic acid first carbon at 2,25 ppm and at 1.67-0,84 ppm, the protons at the end respectively. It is clear that, the synthesis was successfully realized. When the area ratios of the peaks at 4.69 ppm and 3.59 ppm are examined, it is calculated to have 1: 8 ratios. Accordingly, the amount of substitution was determined to be 11%.

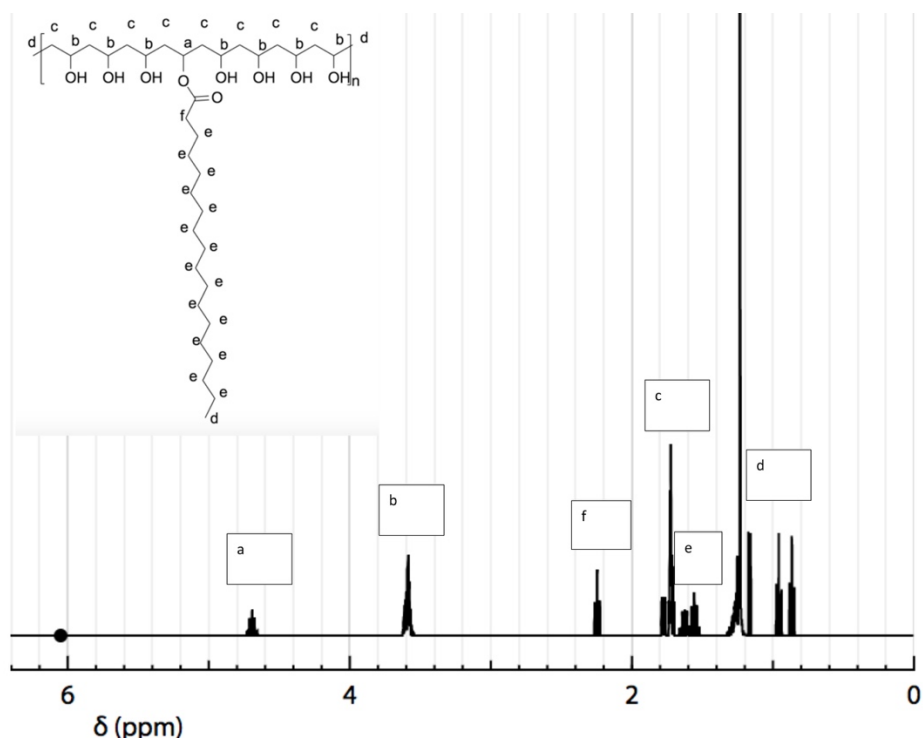


Figure 2: ^1H -NMR spectra of stearic acid substitute polyvinyl alcohol

Moreover, ATR-FTIR analysis supports the ^1H -NMR results. Figure 3a showed that; the characteristic C-H₂ asymmetric alkyl stretching bond vibration band for PVA appeared at 2915 cm^{-1} . Moreover, at 3307 cm^{-1} OH and Crystallization-sensitive band of PVA: 1090 cm^{-1} . Figure 3b showed that carbonyl group of stearic acid 1711 cm^{-1} and hydroxyl bands for free alcohol 3299 cm^{-1} . Stearic acid substitute PVA was seen Figure 3c. C-O-C=O esteric bond vibration was appeared onto 1644 cm^{-1} .

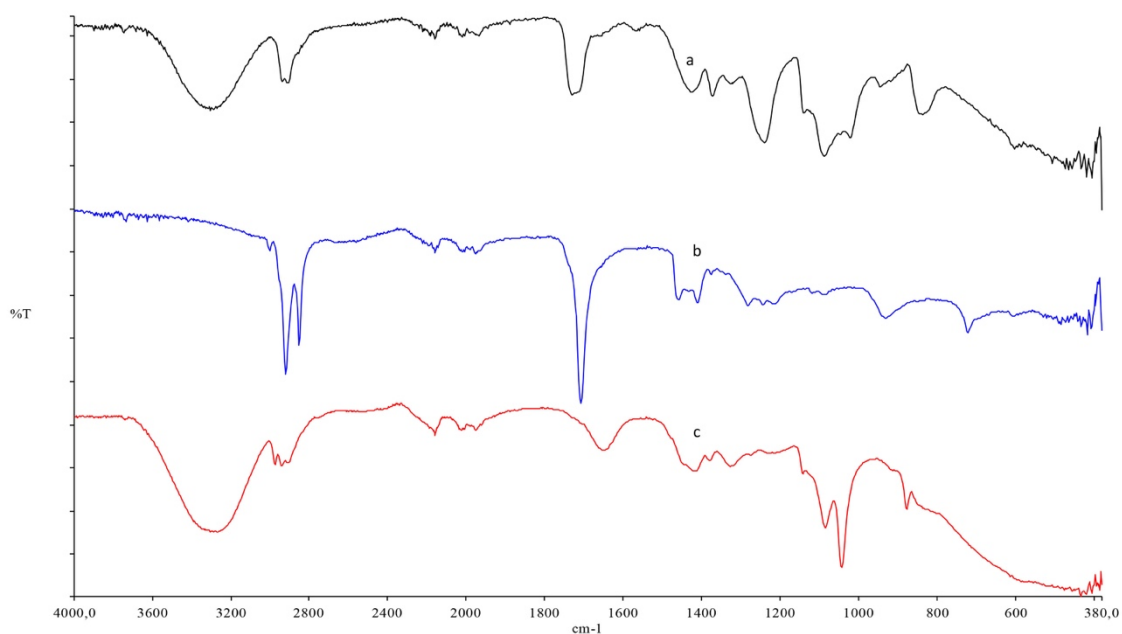


Figure 3: ATR-FTIR spectra of stearic acid substitute polyvinyl alcohol

Lavender oil capsulation with stearic acid substituted PVA polymer was carried out under acidic conditions. The chemical structure of the resulting microcapsules was illuminated by ATR-FTIR. When the ATR-FTIR

spectra were examined, it was found that only the polymer in which the peaks of the oil were not seen, that is, the whole oil was encapsulated.

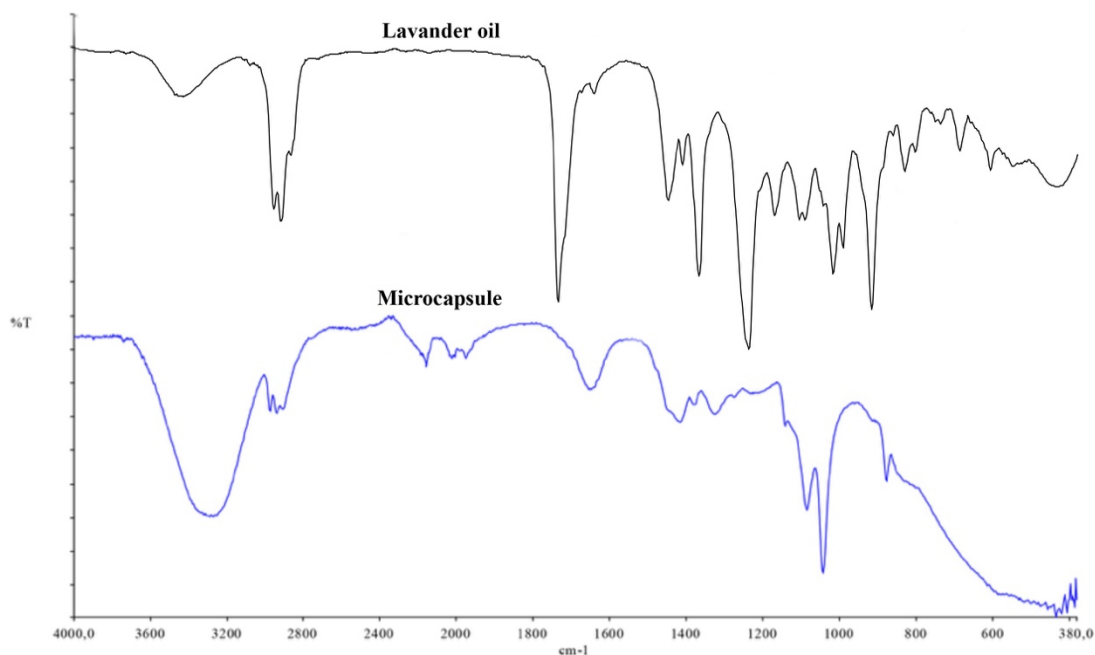


Figure 4: ATR-FTIR spectra of lavender oil microcapsule

When the microcapsule synthesis is examined, it is concluded that the encapsulation does not occur in basic pH only at extreme acidic pH. In addition, when the SEM images were examined, it was determined that the microcapsule size was homogeneous and about 13 nm.

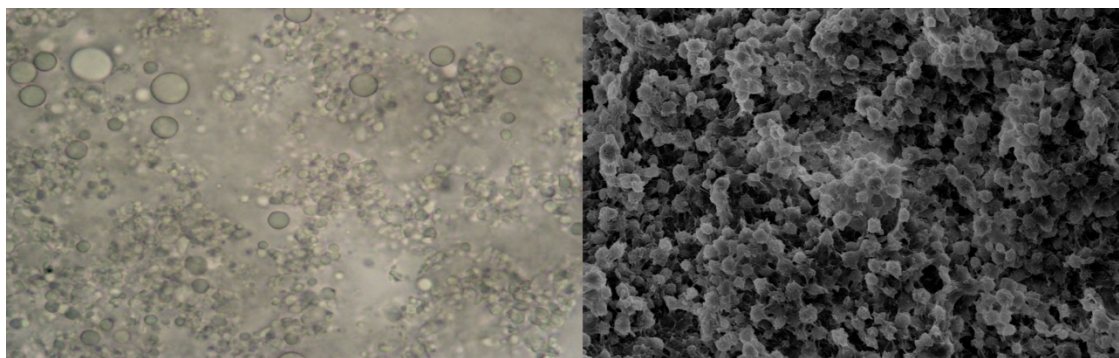


Figure 5: Optical and SEM images of lavender oil microcapsule

The formulations containing lavender oil capsules and cationic starch were coated on 80 g/m² paper. color and gloss values of coated and uncoated paper are given in the Table 2.

Table 2: Color and gloss values of paper and sized paper

Properties	Uncoated paper	Sized paper	Microcapsule added sized paper
L	90,87	89,80	90,23
a	2,29	2,48	2,37
b	-8,02	-8,3	-8,14
Gloss (TAPPI 60°)	4,5	9,3	7,9

When the table is examined, it is observed that the biggest change in the colour of the uncoated paper with the sizing process is colour goes to yellow. When the microcapsule was added to the starch, it was observed that the differentiation in the colour increased and the colour shifted to yellow more. When the colour differences between the obtained colours are calculated, it is concluded that the delta E value is in the values of 1,12 and 0,65 it is acceptable according to ISO 12647-2. When the gloss values were examined, it was found that the paper sized with starch had the highest gloss and microcapsule containing the second. All paper treated is higher than reference uncoated paper. This is due to the cationic starch applied to the environment. The reason for the decrease in the microcapsule is that the surface is slightly roughened by the capsules.

SEM images of uncoated paper, starch coated paper and microcapsule added starch coated paper are shown in Figure 6. When the Figure was examined, it was obtained that the microcapsule, where the surface was smoothed by applying starch, was spread uniformly on the surface and the coating was stable.

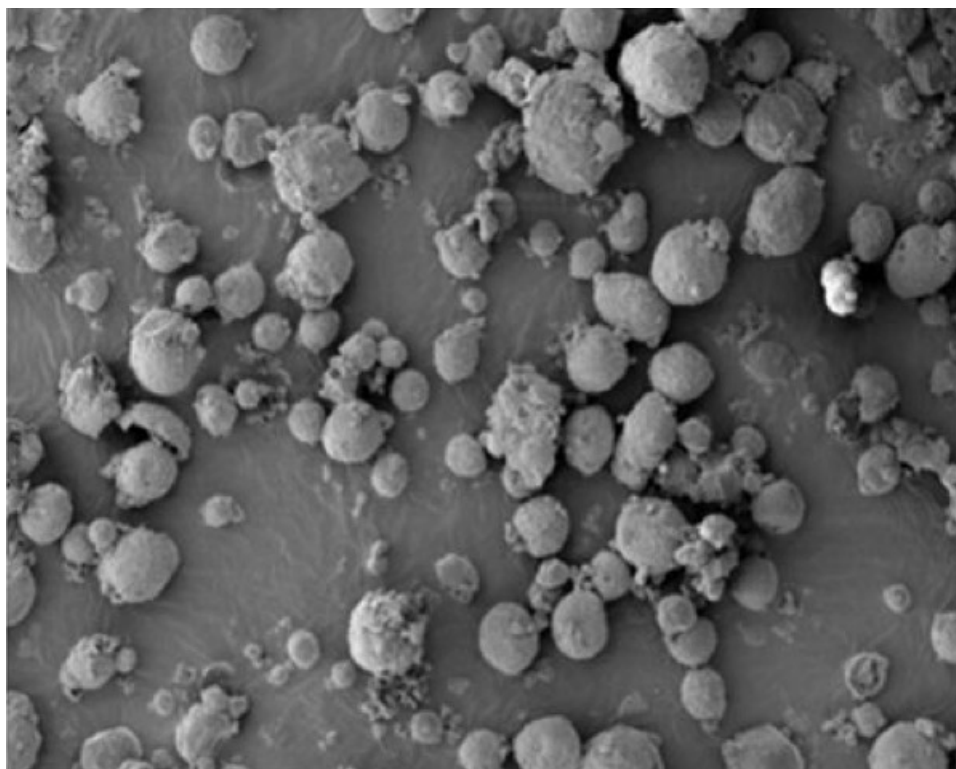


Figure 6: SEM images of microcapsule sized paper

4. CONCLUSIONS

Stearic acid substitute polyvinyl alcohol was synthesized by acidic esterification and it was used to prepare a new lavender microcapsule. $^1\text{H-NMR}$ and ATR-FTIR was confirmed the expected structures. SEM images showed that the microcapsule sizes are mono dispersed. The sizing formulations are prepared with these microcapsules and apply onto paper successfully. Colour and optical properties of microcapsule sized papers are not better than uncoated paper but the difference is between the acceptable limits according to ISO 12647-2. Gloss is higher than uncoated paper because of extra cationic starch. And the surface of the microcapsule sized papers more uniform and not bursted.

5. ACKNOWLEDGMENTS

This work was supported by Research Fund of the Marmara University. Project Number: FEN-C-DRP-110718-0411.






6. REFERENCES

- [1] Ascheri, D. P., Marquez, M. O., Martucci, E. T.: "Microencapsulação de óleo essencial de laranja: seleção de material de parede", *Ciência e Tecnologia de Alimentos* 23, 1-6, 2003. doi:10.1590/S0101-20612003000400002.
- [2] Aydemir, C., Özomay, Z., Karademir, A., Kandirmaz, E. A.: "Effects of matte coating on the paper surface and print density", *Science and Engineering of Composite Materials* 20(2), 141-145, 2013. doi: 10.1515/secm-2012-0070.
- [3] Brown, E. N., Kessler, M. R., Sottos, N. R., White, S. R.: "In situ poly (urea-formaldehyde) microencapsulation of dicyclopentadiene", *Journal of microencapsulation* 20(6), 719-730, 2003. doi: 10.1080/0265204031000154160.
- [4] Chograni, H., Zaouali, Y., Rajeb, C., Boussaid, M.: "Essential oil variation among natural populations of *Lavandula multifida* L. (Lamiaceae)", *Chemistry & biodiversity* 7(4), 933-942, 2010. doi: 10.1002/cbdv.200900201.
- [5] COST E32: "Memorandum of understanding: characterization of paper surfaces for improved printing paper grades", (European Concerted Research Action COST Action E32, Brussels, 2002).
- [6] Cummings, D. O., Lyons, A. V.: "Influence of Engineered Kaolin on Web Offset", *Proceedings of TAPPI Coating Conference* 1996, (TAPPI Press, Nashville, Atlanta, 1996), page 16.
- [7] Dubey, R., Shami, T.C., Bhasker Rao, K.U.: "Microencapsulation Technology and Applications", *Defence Science Journal* 59 (1), 82-95, 2009. doi: 10.14429/dsj.59.1489.
- [8] Hirech, K., Payan, S., Carnelle, G., Brujes, L., Legrand, J.: "Microencapsulation of an insecticide by interfacial polymerisation", *Powder Technology* 130(1-3), 324-330, 2003. doi:10.1016/S0032-5910(02)00211-5.
- [9] Jang, I. B., Sung, J. H., Choi, H. J.: "Synthesis of microcapsule containing oil phase via in-situ polymerization", *Journal of materials science* 40(4), 1031-1033, 2005. doi: 10.1007/s10853-005-6527-y.
- [10] Jegat, C., Taverdet, J. L.: "Stirring speed influence study on the microencapsulation process and on the drug release from microcapsules", *Polymer bulletin* 44(3), 345-351, 2000. doi: 10.1007/s002890050612.
- [11] Madene, A., Jacquot, M., Scher, J., Desobry, S.: "Flavour encapsulation and controlled release—a review", *International journal of food science & technology*, 41(1), 1-21, 2006. doi: 10.1111/j.1365-2621.2005.00980.x.
- [12] Mars, G. J., Scher, H. B.: "Controlled delivery of crop protecting agents", (Taylor and Francis, London, 1990.), page 65-90.
- [13] Mervosh, T. L., Stoller, E. W., Simmons, F. W., Ellsworth, T. R., Sims, G. K.: "Effects of starch encapsulation on clomazone and atrazine movement in soil and clomazone volatilization", *Weed Science* 43(3), 445-453, 2009.
- [14] Mizuno, K., Taguchi, Y., Tanaka, M.: "The effect of the surfactant adsorption layer on the growth rate of the polyurethane capsule shell", *Journal of chemical engineering of Japan* 38(1), 45-48, 2005. doi: 10.1252/jcej.38.45.
- [15] Moutinho, I. M. T., Kleen, A. M., Figueiredo, M. M. L., Ferreira, P.J.T.: "Effect of surface sizing on the surface chemistry of paper containing eucalyptus pulp", *Holzforschung* 63(1), 282-289, 2009. doi: 10.1515/HF.2009.046.
- [16] Moutinho, I.M.T.: "Physical & Chemical Interactions on Paper Surface - Impact on the Printability of Papers Produced with E. globulus Kraft Pulps", *Coimbra University for the degree of Doctor of Philosophy in Chemical Engineering*, 2009.
- [17] Moutinho, I.M.T., Ferreira, P.J.T., Figueiredo, M. L.F.: "Paper surface chemistry as a tool to improve inkjet printing quality", *Bioresources* 6(4), 4259-4270, 2011.
- [18] Ouall, L., Lahoussine, D.: WO, 2006027664A2, "Process for production nano-capsules containing a fragrance", 2006.
- [19] Ozcan, A.: "Para-Amino Benzoik asit Eklenmiş Kaplamalarının Kağıdın Fiziksel ve Optik özelliklerine Etkisinin İncelenmesi", *Proceedings of International printing technologies symposium 2016*, (Printistanbul, Istanbul, Turkey, 2016), pages 331-340.
- [20] Preston, J. S., Elton, N. J., Legrix, A., Nutbeem, C.: "The role of pore density in the setting of offset printed ink on coated paper," *Proceedings of TAPPI. Advanced Coating Fundamentals Symposium* 2001, (ACS, San Diego, USA, 2001), page 102.

- [21] Pruszyński, P.: "Recent developments in papermaking chemicals. In Chemical Technology of Wood", Proceedings of the International Conference Chemical Technology of Wood 2003, Pulp and Paper, (WPP, Bratislava, 2003), page 82-90.
- [22] Pruszyński P.: "Recent developments in papermaking chemicals", WPP Keynote Lectures 82-90, 2003.
- [23] Singh, M. N., Hemant, K. S. Y., Ram, M., Shivakumar, H. G.: "Microencapsulation: A promising technique for controlled drug delivery", Research in pharmaceutical sciences 5(2), 65-77, 2010.
- [24] Soper, J. C., Yang, X., Josephson, D. B.: "U.S. Patent No. 6,106,875", Patent and Trademark Office, 2000.
- [25] Suave, J., Dall'Agnol, E. C., Pezzin, A. P. T., Silva, D. A. K., Meier, M. M., Soldi, V.: "Microencapsulação: Inovação em diferentes áreas", Revista Saúde e Ambiente/Health and Environment Journal 7(2), 12-20, 2006.
- [26] Thies, C. A.: "Survey of microencapsulation processes. In Microencapsulation: Methods and industrial applications", (Marcel Dekker, New York, 1996), page 73-77.
- [27] Ural, E., Kandirmaz, E. A.: "Potential of fish scales as a filling material in surface coating of cellulosic paper", Journal of applied biomaterials & functional materials 16(1), 23-27, 2018. doi:10.5301/jabfm.5000378.
- [28] Xiang, Y., Desjumaux, D., Bousfield, D., Forbes, M. F.: "Preprints of the microcapsule", The Preprints of the Pan Pacific and International Printing and Graphic Arts Conference 1998, (Quebec, Canada, 1998), page 85.
- [29] Xiang, Y., Desjumaux, D., Bousfield, D., Forbes, M.F.: "The relationship between coating layer composition, ink setting rate and offset print gloss", Preprints of the Pan Pacific and International Printing and Graphic Arts Conference 1998, (Quebec, Canada, 1998), page 85.
- [30] Zhu, G. Y., Xiao, Z. B., Zhou, R. J., Yi, F. P.: "Fragrance and flavor microencapsulation technology", In Advanced Materials Research 535, 440-445, 2012.



STATISTICAL ANALYSIS OF ADHESIVE LAYER THICKNESS` DISTRIBUTION ON PERFECT BOUNDED BROCHURES

Magdolna Pál , Sandra Dedijer , Živko Pavlović , Bojan Banjanin , Jelena Vasić 
University of Novi Sad, Faculty of Technical Sciences,
Department of Graphic Engineering and Design, Novi Sad, Serbia

Abstract: *Perfect binding has become one of the most popular binding methods for low- and mid-range graphic products, but with the appearance of new adhesives and application techniques, it is more and more important for the production of high quality, short-run products too. The influencing factors of perfect binding quality are numerous, involving different parameters and aspects of graphic production. Along the paper's properties, book block parameters and spine preparation technique, the used adhesive and its application could have a direct influence on the paper/adhesive interaction and therefore on the adhesive bond quality, i.e. binding strength, too. In this study, a statistical analysis of overall adhesive layer thickness and its distribution along the book block spine has been performed. This analysis was aiming to investigate the influence of the book block volume and two gluing system set-up parameters, the nominal adhesive thickness and gluing length modification, on the adhesive application consistency. The statistical analysis showed that the book block volume had a significant influence on the obtained results of overall adhesive layer thickness (based on the p -value of 0.05) and the adhesive layer became more evenly applied to the block spine by increasing the book block volume. The influence of the nominal adhesive thickness and the glue length modification were also statistically significant (at level $p < 0.05$) on the obtained overall adhesive thickness, however, the corresponding post hoc tests showed that not all the observed groups differed significantly from each other. In addition, the obtained results for adhesive distribution along the book block spine showed more uniform application for the higher values of nominal adhesive thickness and glue length modification.*

Key-words: perfect binding, adhesive layer, book block spine

1. INTRODUCTION

Perfect binding is the most frequently used binding techniques for low and mid-range quality brochures with high-volume, primarily because of its suitability for mass production. Also, due to the development and availability of new adhesives, perfect binding has become an important finishing operation for the high-quality and short-run products, too (Kipphan, 2001; Liebau et al, 2001; Pasanec Preprotić et al., 2012). By its growing range of application, the quality control of perfect bounded products gained on importance. The page-pull test (also known as pull test) is the only standardized method available today for the quality assessment of perfect bindings, and it has an essential role in both quality verifications, the process and final control. Along with other test parameters (such as test position, specimen alignment and fixing, etc.) the specimen opening behaviour was identified to have a direct influence on results of page-pull tests (ISO 19594:2017, 2017). Uniform adhesive application can be recognized as a precondition for the adequate opening behaviour of the produced brochures, therefore the adhesive layer thickness and application consistency have particular importance. The desirable amount of adhesive layer thickness mostly depends on the size of the book block. Book blocks with higher volume (i.e. thicker) require a higher amount of adhesive and vice versa, for thinner book blocks thinner adhesive layer is sufficient to obtain the expected binding strength, spine shape stability and opening behaviour. Applying more adhesive than recommended will reduce the book block spine flexibility, making it more difficult to open and lay down flat without destroying the spine shape. Also, the adhesive consumption and overall production costs will increase, but also frequent work stoppage/downtime will slow down the production process due to the excess adhesive accumulation on the binding machines. Thinner adhesive layer than recommended will result in insufficient adhesion and binding strength, decreased book block integrity and reduced adhesive open-time (Lauren, 2017). The uniform adhesive application over the book spine is also fundamental in achieving high adhesive bond strength, the stability of the book block spine shape and adequate brochure opening behaviour. The uneven distribution of adhesive layer could directly affect the overall adhesive bond strength, but also the aesthetic feature of the finished brochure (wavy shape of the book block due to the unwanted local glue accumulation).

The scope of this investigation is limited to the statistical analysis of overall adhesive layer thickness and its distribution along the book block spine to investigate the influence of book block volume (thickness) and two gluing system set-up parameters, the nominal adhesive thickness and gluing length modification, on the adhesive application consistency.

2. MATERIALS AND METHODS

For this investigation the brochures' book blocks were prepared from commercially available uncoated, wood-free, offset paper with the basis weight of 80 g/m² (IQ Print, Mondi). The selected paper has good surface properties and smoothness and it is usually used for graphic products such as annual reports, magazines, books and brochures, printed with sheet-fed or web offset printing technique (Mondigroup, 2016). The brochures' covers were prepared from glossy coated cardboard with a basis weight of 300 g/m² (Nevia, n.d.). The binding operation was done on Horizon BQ-270 automated perfect binding machine with hot-melt adhesive Mitol-Termokol Ultra 2410/05 (Grafino, 2017), at working temperature of 170°C. The binding machine is equipped with a single-clamp, a double rollers gluing unit and a milling section for book block spine processing (Xerox Corporation, 2018).

The dimensions of the prepared brochures were 176 mm x 250 mm (width x height), while the book block thickness (the number of sheets, i. e. the volume) has been increased from 50 sheets up to 250 sheets, with the increment of 50 sheets. The specifications of prepared brochure samples (book block volume) and the binding process set-up parameters (nominal adhesive layer thickness and gluing length shortening) are presented in Table 1.

Table 1: Specifications of prepared brochure samples

Group number	Book block volume [no. of sheets]	Book block thickness [mm]	Nominal adhesive layer thickness [mm]	Glue line length shortening [mm]
1.	50 sheets	5	1.8 mm	-1.5 mm
2.	100 sheets	10		
3.	150 sheets	15		
4.	200 sheets	20		
5.	250 sheets	25		
6.	150 sheets	15	1.4 mm	0 mm
7.	150 sheets		2.2 mm	
8.	150 sheets		1.8 mm	
9.	150 sheets			

To investigate the influence of the observed parameters on the adhesive layer thickness distribution, after 3-side trimming each brochure sample was cut into 24 uniform segments along the book block spine, using a high-speed cutting machine (Perfecta 72 HTVC). The thickness measurement was carried out using a measuring magnifier with metric scale (field of view: 0 to 10 mm, minimum scale division: 0.1mm). Five brochure samples were prepared for each parameter settings and the thickness measurement was repeated three times on one segment, hence 15 measurements were carried out for each segment, or altogether 360 measurements for each parameter.

3. RESULTS AND DISCUSSION

The mean values of adhesive layer thickness, their standard deviations and corresponding coefficient of variations were calculated for the entire book block spine (overall values) and for each measuring position (adhesive layer profiles). The obtained results are presented in that manner. In Figure 1a-c the overall mean values and standard deviations are given for each parameter group, while Figures 2-4 are showing the adhesive layer thickness profiles along the book block spine likewise for each parameter group.

As it can be seen in Figure 1a, the overall mean values of adhesive layer thickness have the increasing tendency by increasing the brochures thickness, i.e. volume. For the thinnest brochures the overall mean value of adhesive layer thickness was 0.500 mm, while values of 0.591 mm, 0.741 mm, 0.863 mm and 0.894 mm were delivered for brochures with 10, 15, 20 and 25 mm thick book blocks, respectively.

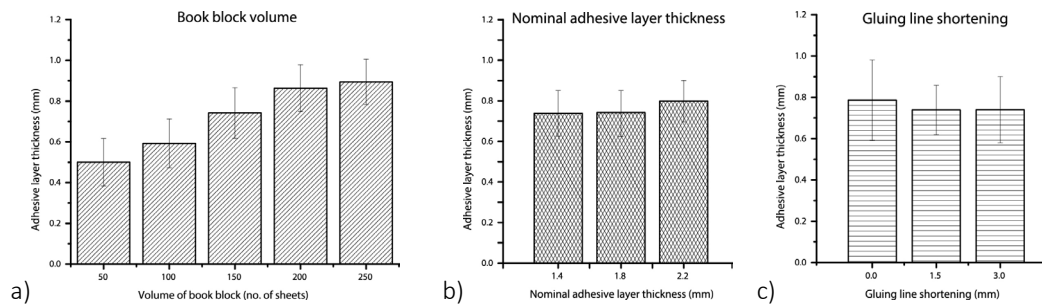


Figure 1: Overall mean values of adhesive layer thicknesses regarding to the book block thickness (a), nominal adhesive layer thickness (b) and gluing line shortening set-up values (c)

Comparing the results by nominal adhesive layer thicknesses (Figure 1b) it can be noticed that the obtained values were very similar, however a slightly increasing tendency is apparent. The mean values were 0.738 and 0.741 for nominal layer thicknesses of 1.4 mm and 1.8 mm, while for the brochures with the nominal layer thickness of 2.2 mm it was 0.798 mm. In addition, although the nominal adhesive layer thicknesses have been set much higher, none of the prepared samples had exceeded the adhesive layer thickness of 0.9 mm over the book block spine. The reason for that is the nominal adhesive thickness on the book block spine corresponds to the maximum adhesive thickness on the gluing rollers, which cannot be entirely transferred to the book block spine. By analysing the results regarding different gluing length values (Figure 1c), the overall mean values of adhesive layer thickness were also very similar, but a slight decreasing tendency can be noticed. With the shortening of 1.5 and 3 mm, the mean thicknesses were 0.741 and 0.740, while for the samples without gluing length modifications (i.e. with 0 mm shortening) the mean value of adhesive layer thickness was 0.787mm.

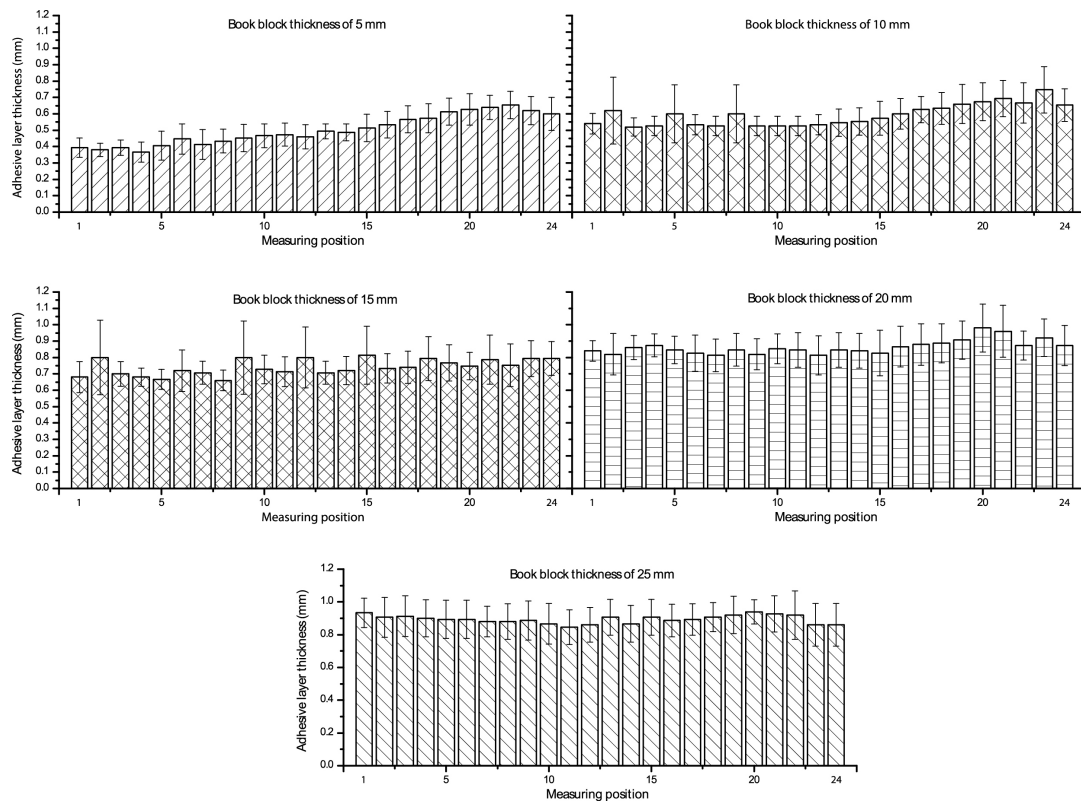


Figure 2: Adhesive layer thickness profiles for brochures with different book block thicknesses

From the adhesive layer profiles for brochures with different book block thicknesses (Figure 2) it can be noticed that in the case of thinner brochures (especially for 5 and 10 mm thick book blocks) the adhesive layer thickness had visible increasing tendency along the measuring positions, with ranges from 0.367 mm to 0.653 mm for book blocks of 5 mm and 0.520 mm ÷ 0.747 mm for book blocks of 10 mm.

Since position 1 corresponds to brochure's upper part, where the gluing process begins and position 24 corresponds to the brochure's bottom part, where the gluing was stopped, these increasing tendencies along the measuring points could indicate the undesirable glue accumulation at the end of the book block spine during the glue application process. For higher book block thicknesses this uneven adhesive application is not that distinct, however slight increasing tendency can also be noticed with ranges from 0.660 mm to 0.813 mm for 15 mm thick book blocks, from 0.813 mm to 0.980 mm for 20 mm thick book blocks and from 0.847 mm to 0.940 mm for 25 mm thick ones. The moderately low values of standard deviation indicate high consistency of the measured values (the ranges of the corresponding coefficient of variations were: $9.27\% \div 22.15\%$, $10.79\% \div 29.55\%$, $8.24\% \div 26.75\%$, $7.52\% \div 16.79\%$ and $7.84\% \div 16.02\%$, for samples with 5, 10, 15, 20 and 25mm thick book block, respectively).

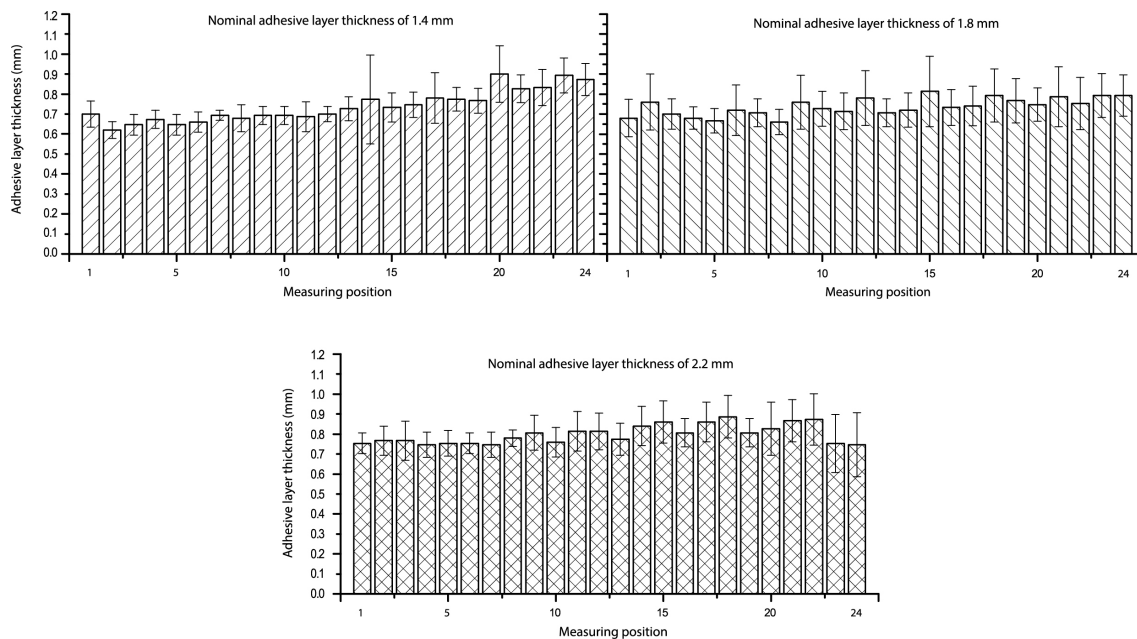


Figure 3: Adhesive layer thickness profiles for brochures with different nominal adhesive layer thicknesses

Comparing the obtained adhesive layer profiles for different nominal adhesive layer thicknesses (Figure 3), a mild increasing tendency can be observed along the measuring positions (from position 1 to position 24), although the overall mean values were very similar. These tendencies are more visible for the lowest nominal adhesive layer thickness value (1.4 mm), than for the other two nominal thicknesses. The ranges of obtained results were 0.620 mm \div 0.900 mm, 0.660 mm \div 0.813 mm and 0.747 mm \div 0.887 mm for nominal adhesive thicknesses of 1.4 mm, 1.8 mm and 2.2 mm, respectively.

By analysing the adhesive layer profiles regarding different gluing length values (Figure 4) a certain waviness of the adhesive layer can be noticed on the samples with no glue line shortening (set-up value of 0 mm). This waviness was most likely caused by the excessive adhesive application on the book block spine, especially at the beginning of the gluing process. The brochures with 1.5 mm shortening on both ends of the book block had more evenly spread adhesive layer, but the most uniform adhesive layer was achieved with the shortest gluing application (-3 mm) since there were no redundant adhesives at the ends of the brochures. The measured thickness values for both sample groups with shortened gluing line were in very similar range (0.66 mm \div 0.813 mm for -1.5 mm, and 0.673 mm \div 0.800 mm for 3 mm), while samples without gluing length modifications had higher maximum values (range 0.673 mm \div 0.960 mm) and more visible increasing tendency along the measuring positions.

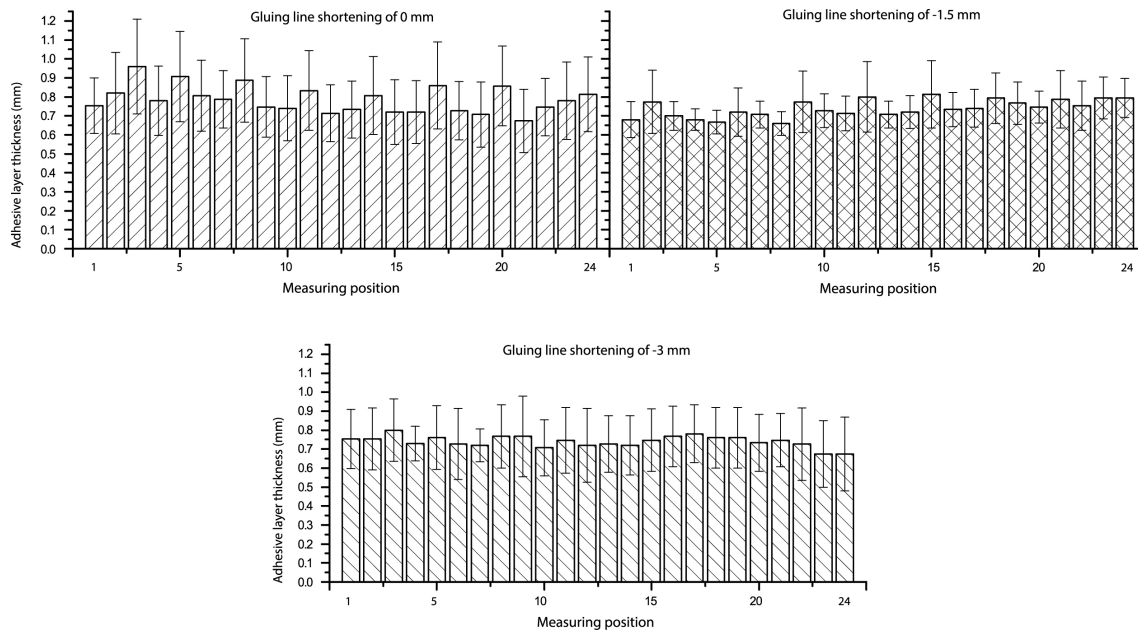


Figure 4: Adhesive layer thickness profiles for brochures with different gluing length

Although the presented graphs and profiles delivered useful information about the changes in applied adhesive layer thicknesses, they do not set out whether these changes are statistically significant. In order to determine the statistical significance of the differences in the obtained mean values of adhesive layer thicknesses regarding the observed parameter groups, detailed statistical analyses were done by one-way ANOVA and corresponding post hoc tests (Dunnett's T3). Besides the statistical significance delivered by ANOVA, the effect size (the practical significance) is also calculated for each sample group using partial eta squared. According to Cohen, the value of 0.01 is classified as a small effect, 0.06 as a medium effect, and 0.14 as a large effect (Pallant, 2005). Along ANOVA, where it was applicable, the correlation analysis was used to describe the strength and direction of the linear relationship between the measured adhesive layer thickness and measuring points. Preliminary analyses were performed to ensure no violation of the assumptions of normality, linearity, homogeneity (for ANOVA) and homoscedasticity (for correlation analysis). All the statistical analyses were done using IBM SPSS statistics software (version 20), with a significance level of $p < 0.05$ for ANOVA and $p < 0.01$ for correlation analysis.

Based on the results of ANOVA, in the case of book block volume, there is a statistically significant difference in mean values of the adhesive layer thicknesses with large effect size [$F(4, 1795) = 759.643$, $p = 0.000$, partial eta squared = 0.628]. Post hoc comparisons using the Dunnett's T3 test showed that all the mean values of adhesive layer thicknesses regarding to the different book block volume differ significantly ($M = 0.500$, $SD = 0.116$; $M = 0.591$, $SD = 0.119$; $M = 0.741$, $SD = 0.124$; $M = 0.863$, $SD = 0.115$ and $M = 0.894$, $SD = 0.111$). Results of one-way ANOVA for the nominal adhesive layer thickness showed that there was a statistically significant difference in mean values of the adhesive layer thicknesses, [$F(2, 1077) = 32.369$, $p = 0.000$], but with small effect size according to Cohen (partial eta squared = 0.057). The post hoc comparisons (Dunnett's T3) indicated that only the highest nominal adhesive layer thickness (2.2 mm) resulted in significantly different mean value ($M = 0.798$, $SD = 0.102$) comparing the other two, lower set-up values ($M = 0.738$, $SD = 0.112$ for samples with nominal adhesive layer thickness of 1.4 mm and $M = 0.741$, $SD = 0.124$ for samples with 1.8 mm thick nominal adhesive layer set-up). The mean values for the two lower thickness set up did not differ significantly. Regarding the gluing line shortening set-up, the results of one-way ANOVA have shown a statistically significant difference between the observed groups [$F(2, 1077) = 9.892$, $p = 0.000$], but with small effect size (partial eta squared = 0.018) like in the case of nominal adhesive layer thickness set-up. Based on the corresponding post hoc test (Dunnett's T3) it has been found that only the samples with no gluing line shortening gave statistically significant different mean value ($M = 0.787$, $SD = 0.195$) comparing the samples with glue line shortening of 1.5 mm and 3 mm ($M = 0.741$, $SD = 0.124$ and $M = 0.740$, $SD = 0.161$, respectively). The mean values of the two modified gluing length's groups did not differ significantly.

The results of conducted correlation analysis have shown a positive correlation between the measuring positions and the adhesive layer thickness in most of the observed parameters, however strong

correlations were registered only in two cases: for the book block thickness of 5 mm ($r=0.742$, $n=360$, $p<0.05$) and nominal adhesive layer thickness of 1.4mm ($r=0.637$, $n=360$, $p<0.05$). These results confirm the previously observed tendencies presented in Figure 2 and 3, that during the glue application process undesirable glue accumulation is happening at the end of the book block spine. For higher values of these parameters, the correlation coefficient (Pearson's r) values were much lower, indicating medium ($r=0.416$ for brochures with 10 mm thick book block) and small correlations ($r=0.216$ and $r=0.234$ for the book blocks of 15 and 20mm, respectively; $r=0.216$ and $r=0.242$ for the brochures with 1.8 and 2.2 mm thick nominal adhesive layer set-up) or no correlations at all ($r=-0.009$ for 25 mm thick book blocks). In the case of glue length modification, the results of correlation analysis were not as consistent as for the other two parameters, showing in one case medium positive correlation between the measuring positions and the adhesive layer thickness ($r=0.216$ for glue line shortening of 1.5 mm), in other small negative ($r=-0.129$ for samples with no gluing length modification) and in the third no correlations at all ($r=-0.074$ for glue line shortening of 3 mm).

4. CONCLUSIONS

In this paper, the influence of the book block volume and two gluing system set up parameters (nominal adhesive layer thickness and gluing length) on the overall adhesive layer thickness and its distribution along the book block spine has been analysed and presented. Based on the obtained results for overall mean values of adhesive layer thickness it can be conducted that it has a notable increasing tendency by increasing the brochures volume (i.e. thickness). For the nominal adhesive layer thickness, the same increasing tendency was fairly visible, as the decreasing tendency for the gluing length modification. These remarks are confirmed by the performed statistical analysis, one-way ANOVA and the corresponding post hoc tests. The obtained results of these tests imply that changes in brochure book block volume influence significant changes in adhesive layer thicknesses for all observed book block volumes (50-250 sheets). In case of two gluing system set-up parameters, the nominal adhesive layer thickness and the gluing length modification, significant differences were observed in the adhesive layer thickness values, but only for the higher amount of glue application (for the nominal thickness of 2.2 mm and with no gluing length modification). Regarding the adhesive layer distribution along the book block spine, the results of correlation analysis showed that the adhesive layer became more uniformly applied by increasing the book block volume, but also for higher values of nominal adhesive thickness and the shortest length of glue application.

5. ACKNOWLEDGMENTS

This work was supported by the Serbian Ministry of Science and Technological Development, Grant No.: 35027 "The development of the software model for improvement of knowledge and production in the graphic arts industry".

6. REFERENCES

- [1] Grafino: "Technical data for Termokol Ultra 2410/05 hot-melt adhesive", URL: <http://www.grafino.rs/proizvodi/graficki-lepkovi/%201.2./>, (last request: 2017-08-25).
- [2] International Organization for Standardization, ISO 19594:2017: "Graphic technology -Test method for the determination of the binding strength for perfect-bound products - Page-pull test working upwards", International Organization for Standardization, 2017.
- [3] Kipphan, H.: "Handbook of Print Media: Technologies and Production Methods", (Springer-Verlag, Heidelberg, 2001.). doi: 10.1007/978-3-540-29900-4
- [4] Lauren, O.: "How Spine Glue Thickness Can Affect Bookbinding Integrity", URL: <http://rsindustrial.com/blog/glue-thickness-bookbinding-integrity/>, (last request: 2018-03-10).
- [5] Liebau, D.; Heinze, I.: "Industrielle Buchbinderei" (Verlag Beruf+Schule, Paderborn, 2001.)
- [6] Mondigroup: "IQ Print: your reliable and flexible uncoated wood-free paper for offset printing", URL: <https://www.mondigroup.com/en/products-and-solutions/categories/office-and-professional-printing-papers/iq-print/>, (last request: 2017-08-28).

- [7] Nevia: "Technical data Nevia C2S". URL: https://static1.squarespace.com/static/56ab875f0ab3777445d9785e/t/57334e5759827ee074bc3657/1462980183566/CathayNevia_C2SNew.pdf, (last request: 2017-08-25).
- [8] Pallant, J.: "A step by step guide to data analysis using SPSS for Windows (Version 12)", (Allen & Unwin, Ligare, Sydney, 2005.).
- [9] Pasanec Preprotić, S., Babić, D., Tuzović, A.: "Research on adhesive joint strength dependency on loose leaf position in a text block", Tehnicki vjesnik- Technical Gazette, 19(1), 43-49, 2012.
- [10] Xerox Corporation: "Technical data for Horizon BQ 270", URL: <https://www.xerox.com/digital-printing/feeders-print-finishing/offline-finishers/horizon-bq270-perfect-binder/enus.html/>, (last request: 2018-01-28).



© 2018 Authors. Published by the University of Novi Sad, Faculty of Technical Sciences, Department of Graphic Engineering and Design. This article is an open access article distributed under the terms and conditions of the Creative Commons Attribution license 3.0 Serbia (<http://creativecommons.org/licenses/by/3.0/rs/>).

DEPENDENCE OF THERMAL CONDUCTIVITY AND HEAT RETENTION ABILITY OF FABRICS FROM DIGITAL PRINT PARAMETERS

Mladen Stančić¹ , Branka Ružičić¹ , Đorđe Vujčić¹ , Dragana Grujić² 

¹ University of Banja Luka, Faculty of Technology,
Graphic engineering, Banja Luka, Bosnia and Herzegovina

² University of Banja Luka, Faculty of Technology,
Textile engineering, Banja Luka, Bosnia and Herzegovina

Abstract: *The human body transforms the chemical energy of the food into the work and the heat through the process of metabolism. The produced heat through the skin is transferred to the environment. In this case, in the state of thermal equilibrium, the amount of heat produced is equal to the amount of heat lost by conduction, convection, radiation, evaporation and breathing. The process of conduction of heat is transferred from the body to the environment, through layers of clothing and air, with the person standing still. Conductivity of heat in clothes depends on the thermal conductivity of the fibers from which the clothes are made, the conductivity of the air trapped in the pores of the clothes and the air on the surface of the clothing, the surface of the clothing layer through which the heat and the thickness of the clothes pass. The amount of heat transferred by conduction is usually negligible because the clothing, by its characteristics, slows down heat transfer in this way. Additionally, ink layers made in printing process significantly affect the properties of textile materials and clothes made from these materials. And today textile materials are increasingly being subjected to the process of printing due to aesthetic requirements of the people. This paper investigates the influence of digital printing parameters on the thermo-physiological features of textile materials. The essential print parameter was a different number of passes. In this research were used textile fabric materials of 100% cotton fibers. With printing process parameters, such as number of passes in the print, it is possible to influence the amount of ink that is applied on and in printed material, and thus the achievement of desired values of thermal parameters of printed materials. The influence of print parameters to thermo-physiological properties of the material is evaluated through a thermal conductivity and heat retention ability. Results of the research demonstrated that, in addition to material composition, the printing process with its parameters have a significant influence on the thermo-physiological characteristics of textile materials. The values of the thermal conductivity of the printed samples show that the increase in the number of application of ink in the printing results in a rise in the value of thermal conductivity coefficient, and decrease in heat retention ability value.*

Key words: digital printing, textile materials, fabrics, thermal conductivity, heat retention ability

1. INTRODUCTION

Nowadays, from selected clothes is expected to satisfy aesthetic and fashionable requirements (Mecheels, 1992). Printing clothes makes aesthetic value of product more individual and fashionable. From technical aspect, process of printing clothes can be defined as process of transferring ink on textile substrate (Kašiković et al, 2014).

Currently the world's annual print of textile material is between 11 and 13%, that is more than 27 billion m² of textile substrates, with annual growth rate of 2% (Momin, 2008; Provost, 2009; Onar et al, 2012). The value of textile material printing industry in 2010 was 165 billion US\$. Textile material printing industry is under great pressure of constant changes. This market is seasonal and highly dependent on fashion trends (Gupta, 2001). Demands of customers are changing very fast, therefore the collections are changing frequently in two months (Özgüney et al, 2007). Trends on market, like: decrease in circulation, demands for higher print quality, rapid job change and short deadlines, unique and personalized print, have led to increased interest for digital printing in textile material printing (Kanik et al, 2004; Mikuž et al, 2005; Stančić et al, 2013). Digital printing efficiency, as flexible way of ink transfer on substrate in the form of a desirable design, is primarily reflected in respect of costs and time needed for production of smaller circulations (Novaković et al, 2010). Besides that, digital printing technique enables faster response to market demands and mass individualization.

More important, for clothes, is to meet the ergonomic and physiological requirements (Mecheels, 1992). Does clothing meet aesthetic and ergonomic demands customer easily evaluates before or during first

wearing. With physiological function it is different, and clothing with good physiological characteristics should make man does not feel heat or cold in different climatic conditions (Mecheels et al, 1976). Comfort is basic and universal need of human being and presents one of the most important aspects of clothing. During clothes wearing, heat and humidity produced by body has been stopped as layers of air before passing in the environment, resulting in characteristic microclimate between skin and clothing, defined as the feeling of comfort (Yoo et al, 2000; Grujić et al, 2010). Thermal effects largely contribute to the comfort of the individual, whereby a complex physiological and psychological factors together with clothes play an important role in defining the complex phenomenon of comfort (Andreen et al, 1953).

Human body with the process of metabolism constantly transforms food chemical energy into work and heat. Produced heat is transferred through skin and further through clothing system to the environment. Heat exchange processes in dressed and undressed human are qualitatively equal, while quantitatively depend on the thermodynamic properties of clothing, which presents separating surface between body and environment (Mecheels, 1991; Grujić, 2010). The process of heat exchange between body and environment itself is done by processes of: conduction, convection, radiation, evaporation and respiration (Stoecker et al, 1982). Greatest part of heat exchange is done by the process of convection. With this process heat is transferred by the movement of gas or liquid. Quantity of heat lost by the convection is determined with difference between temperature of clothing surface and air, and also with convective heat transfer coefficient, which is, in turn, determined with speed of air movement through clothing system (Persons, 2003). The physiological properties of clothing, and thus wearing comfort, could be expressed, apropos quantified, through heat and sorption properties of material (Huang, 2006; Das et al, 2007).

Previous research showed that thermal conductivity and heat retention ability of textile material is conditioned by structural properties of material. However, during printing process layer of ink is transferred on clothing. Part of printed ink covers clothing surface, while other part of ink fills pores between fibers in yarn. Thereby, printed ink presents new layer of material, actually additional barrier for the movement of air through the clothing. In order to get new scientific knowledge, this study examined influence of printing process, as one of the methods for increasing visual attractiveness of clothes, on physiological comfort of printed textile materials. Thereby was examined influence of digital ink-jet printing parameters and number of ink layers, on thermal conductivity and heat retention ability of cotton fabrics.

2. METHODS AND MATERIALS

Research of printing process influence on thermal conductivity and heat retention ability of fabric was performed on purpose-made fabric. Basic characteristics of examined fabric are shown in Table 1.

Table 1: Characteristics of material used in research

Sample	Material type	Type of weaves	Material composition (%)	Fabric weight (g/m ²)	Thread count (cm ⁻¹)
T-A	Fabrics	Single	Cotton 100 %	177,68	Vertical: Dv = 20 Horizontal: Dh = 20
Method			ISO 1833-1	ISO 3801	ISO 7211-2

For research purposes special test image has been developed. Test image was created using Adobe Illustrator CS5 software application, and was consisted of twelve patches dimension 20 x 20 cm, and coverage of 10%, 50% and 100% tonal values (TV) of yellow process color.

Printing of samples was done using ink-jet printing system Polyprint TexJet. Samples were printed with one, three and five ink applications, without intermediate drying in case of printing with more ink applications. Printing of samples has been done with resolution of 720 x 720 dpi, using water-based pigment colors DuPont Artistri Pigment- 5000 Series (yellow). After printing process, prints were exposed to drying process and fixation of printed inks. Samples were dried with heat effect at a temperature of 130 °C for 120 seconds, using device for drying imprints tp 4040s from manufacturer „Opremakv“.

Before laboratory measurements samples were air-conditioned for 24 hours at standard atmosphere (temperature of 20 °C and relative air humidity 60%). In order to achieve higher accuracy of the measurement results, more samples were measured with repetition on the individual samples. As measurement results were taken arithmetic means of ten times measured numerical values.

Heat conductivity is one of the criteria for the insulation properties of textile fabrics. Since all textile fibers, except glass-fibers, conduct heat better than air, the thermal insulation does not only depend on the specific conductivity of the material used but also of the air volume, which is contained in the textile material, i.e. of the structure and thickness of the textile material. (Grujić, 2010).

Heat conductivity measurement is based on the heat transfer from the warmer to the colder, i.e. on the principles of heat conduction. To measure the heat conductivity coefficient, a BT measurement medium with a heat source heated to 35 °C and a metered body with water VT is used. When measuring the sample, it is placed on the measuring body with water VT. When the temperature of the BT metering unit reaches a default value of 35 °C, the BT measurement body is placed face-up on the sample. The value of the heat flow ϕ is evident on the digital display of the device.

These values of the heat flow are used to calculate the thermal conductivity coefficient or thermal conductivity coefficient according to the expression (1) (Kato Tech Co. Ltd., 1998):

$$\lambda = \frac{\phi \cdot h}{A \cdot (T_{BT} - T_a)} \quad (1)$$

where:

- λ – coefficient of thermal conductivity [W/mK],
- A – surface of BT unit [0,0025 m²],
- h – thickness of material [m],
- T_{BT} – temperature of BT unit [K],
- T_a – temperature of room [K],
- ϕ – heat flow [W].

Heat retention or thermal insulation is greatest when the man is stationary, because then the air under the clothes is still. Determination of heat retention of the test materials, i.e. heat flow measurement, was performed with larger BT measuring unit, which is located in an anvil and heated to a temperature of 35 °C. At that time, the wind was constantly moving at a velocity of 1 ms⁻¹ at a temperature of 20 °C ± 2 °C. Constant movement of the air is achieved using the fan. The loss of heat or heat flow can be determined by the following methods: dry contact method, dry contactless method, wet contact method, wet contactless method. In determining the heat resistance of textile materials, a dry contactless method was used. From the heat flow values obtained, the heat retention of the textile materials is determined according to the expression (2) (Kato Tech Co. Ltd., 1998):

$$Rc = \frac{(T_s - T_a) \cdot A}{H_{ct}} \quad (2)$$

where:

- Rc – heat retention of textile [m²K/W],
- H_{ct} – dry heat flow, that goes through material [W],
- A – surface of BT unit [m²],
- T_s – temperature of BT unit (skin temperature) [°C],
- T_a – temperature of air in anvil (air temperature) [°C].

3. RESULTS AND DISCUSSION

Results of thermal conductivity of printed cotton fabrics research are shown in Figure 1. The results indicate that the increase of the number of ink layers applied results in an increase in the coefficient of thermal conductivity of printed cotton fabrics. By observing the value, it can be noticed that applying of the ink nearly doubles values of thermal conductivity coefficients of unprinted cotton fabrics. Figure 1 also shows that by increasing the tone value, the value of the coefficient of thermal conductivity increases, irrespective of whether the samples are printed with one, three or five ink layers. It can be noted that the increase of the coefficient of thermal conductivity is higher with the increase of the tone value and that the coefficient of thermal conductivity of three ink layers on 10% and 50% is similar to coefficient of thermal conductivity of 50% and 100% on samples with one ink layer respectively.

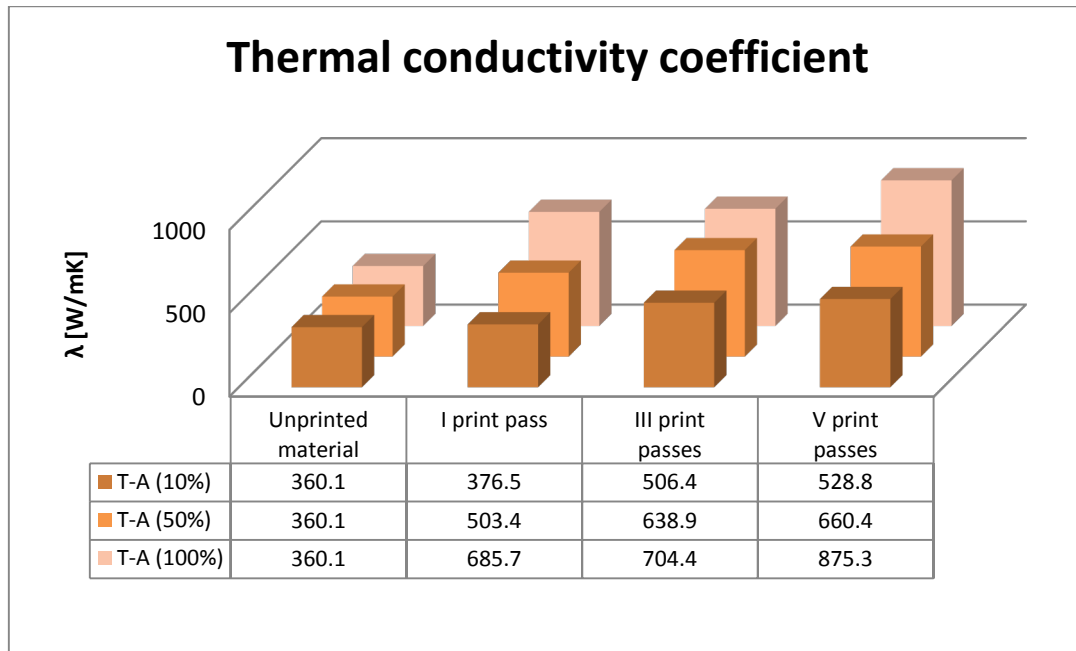


Figure 1: Thermal conductivity value of printed cotton fabrics

With research results analysis were obtained statistically reliable dependences of thermal conductivity on number of ink layers, which are presented in Table 2.

Table 2: Statistical analysis of thermal conductivity values of printed cotton fabrics

$\lambda = 315,678 + 3,159 \cdot TV + 41,575 \cdot IL$										
Multiple reg. coef.	Std. Error of the Estimate	$b_0 = 315,678$			$b_1 = 3,159$			$b_2 = 41,575$		
R^2	s	Std. Error	t	p	Std. Error	t	p	Std. Error	t	p
0,951	3,740,589	31,724	9,951	0,000069	0,339	9,327	0,000086	7,635	5,445	0,002
λ - Thermal conductivity coefficient TV – tone value IL – ink layers										

Results of heat retention of printed cotton fabrics research are shown in Figure 2. The results indicate that the increase of the number of ink layers applied results in a decrease of the heat retention of printed cotton fabrics. By observing the value, it can be noticed that by increasing the tone value, the value of the heat retention decreases, irrespective of whether the samples are printed with one, three or five ink layers. It can be noted that the decrease of the heat retention is lower with the increase of the tone value.

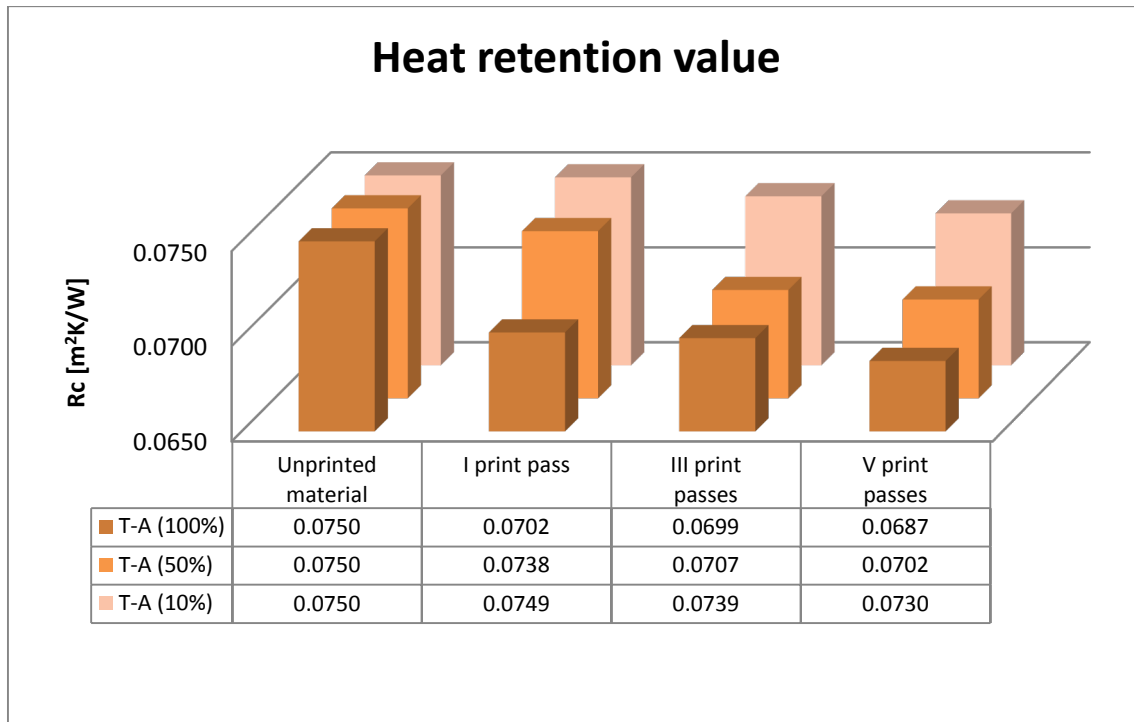


Figure 2: Heat retention value of printed cotton fabrics

With research results analysis were obtained statistically reliable dependences of heat retention on number of ink layers, which are presented in Table 3.

Table 3: Statistical analysis of heat retention values of printed cotton fabrics

Rc = 0,076 - 0,000048 · TV - 0,001 · IL										
Multiple reg. coef.	Std. Error of the Estimate	b ₀ = 3598,109			b ₁ = -7,110			b ₂ = -140,333		
R ²	s	Std. Error	t	p	Std. Error	t	p	Std. Error	t	p
0,886	152,640	129,453	27,795	1,4345 · 10 ⁻⁷	1,382	-5,145	0,002	31,158	-4,504	0,004
Rc – Heat retention value TV – tone value IL – ink layers										

4. CONCLUSIONS

In the presented research, influence of digital ink-jet printing process parameters on sorption properties of printed clothes, apropos on parameters of physiological comfort of printed clothes was tested. In that purpose, dependence of thermal conductivity and heat retention of printed cotton fabrics on variable factors of printing process was tested, i.e. from different tonal coverage and different number of ink layers. Measured values of thermal conductivity for tested fabrics behave in a manner that with increasing the number of ink layers in printing, and also increasing the tonal coverage, leads to thermal conductivity value increase. Measured values of heat retention for tested fabrics behave in a manner that with increasing the number of ink layers in printing, and also increasing the tonal coverage, leads to heat retention value decrease. Also, based on experimentally obtained results mathematical dependence models of thermal conductivity on printing parameters were created. These models could be used in real production conditions, during printing clothes made from these materials, and in order to adjust printing process parameters to get clothes for different purpose, with optimal both aesthetic and sorption properties, and all of that in order to get clothes with optimal comfort properties.

With printing process part of printing ink is transferred on material surface, and other part penetrates the interior of material and fills pores between yarn as well as pores between fibers. In this way in textile material is created additional barrier, which disturbs the free passage of air through textile material. Increasing the value of thermal conductivity and decreasing the value of heat retention by increasing tonal coverage and number of ink layers in printing is explained by the fact that increasing of these parameters leads to application of larger amount of ink on and in printed material. This leads to covering the larger quantity of fibers, and thus to reducing possibilities for free passage of air through textile material.

Measured values of thermal conductivity also show that closely equal values of thermal conductivity can be obtained with combination of number of ink layers and tone value. This fact is, in turn, important from an economic point of view, because it shows that similar values of sorption parameters can be obtained with smaller number of ink layers in printing by increasing tone value. In this way it is possible to achieve an increase in productivity, because time needed for printing process is being reduced, without affecting the values of sorption properties of printed cotton fabrics, and also the comfort of the clothes made from these materials.

Summarizing the results of the research it can be concluded that printing parameters have great influence on thermal conductivity and heat retention. In order to obtain further knowledge, in future research it is planned to test the impact of materials of different composition. Also, done research should be carried out, besides fabrics, on knitwear.

5. REFERENCES

- [1] Andreen, J.-H., Gibson J.-W., Wetmore O.-C.: "Fabric Evaluations Based on Physiological Measurements of Comfort", *Textile Research Journal* 23(1), 11-22, 1953.
doi:10.1177/004051755302300102.
- [2] Das, B., Das A., Kothari V., Fanguiero R., Araújo M.: "Moisture Transmission Through Textiles- Part I: Processes involved in moisture transmission and the factors at play", *AUTEX Research Journal* 7(2), 100-110, 2007.
- [3] Grujić, D.: "Influence of Fabric properties of Thermal Physiological Comfort of Clothing", PhD thesis, Slovenia Faculty of Mechanical Engineering, 2010.
- [4] Grujić, D., Geršak J., Ristić M.: "Uticaj fizikalnih i sorpcijskih svojstava tkanina na količinu upijenog znoja u odjeći", *Tekstil* 59(3), 68-79, 2010.
- [5] Gupta, S.: „Ink-jet Printing- A Revolutionary Ecofriendly Technique for Textile Printing“, *Indian Journal of Fibre and Textile Research* 26 (1-2), 156-161, 2001.
- [6] Huang, J.: "Thermal Parameters for Assessing Thermal Properties of Clothing", *Journal of Thermal Biology* 31 (6), 461-466, 2006. doi:10.1016/j.jtherbio.2006.03.001.
- [7] Kanik, M., Hauser P.-J., Parrillo-Chapman L., Donaldson A.: "Effect of Cationization on Inkjet Printing Properties of Cotton Fabrics", *AATCC Review* 4(6), 22-25, 2004.
- [8] Kašiković, N., Vladić G., Novaković D., Stančić M., Milošević R.: "Spektrofotometrijska analiza uticaja toplotnih dejstava na kvalitet otisaka", *Savremene tehnologije* 3 (1), 66-71, 2014.
doi:10.5937/savteh1401066K.
- [9] Kato Tech Co., Operating Instruction KES-F7: Manual for KES-F7 Thermo Labo II (Precise and Prompt Thermal Prosperity Measurement Instrument), Keskato, URL: <http://www.english.keskato.co.jp/products/pdf/F7.pdf> (last request: 2016-06-7).
- [10] Mecheels, J.: "Körper-Klima-Kleidung: Grundzüge der Bekleidungsphysiologie", (Schiele & Schon, Berlin, 1991.), page 65.
- [11] Mecheels, J.: "Anforderungsprofile für Funktionsgerechte Bekleidung", (DWI-Schriftenreihe des Deutschen Wollforschungsinstitutes an der TH Aachen, Aachen, 1992.), pages 263-268.
- [12] Mecheels, J., Umbach K.H.: "Hermophysologische Eigenschaften von Kleidungs-systemen", (Bekleidungsphysiologisches Institut Hohenstein e.V., Hohenstein, 1976.), page 25.
- [13] Mikuž, M., Šostar-Turk S., Pogačar V.: "Transfer of Ink-jet Printed Textiles for Home Furnishing into Production with Rotary Screen Printing Method", *Fibres and Textiles in Eastern Europe* 13(6), 79-84, 2005.
- [14] Momin, N.-H.: "Chitosan and Improved Pigment Ink Jet Printing on Textiles", PhD thesis, School of Fashion and Textiles, RMIT University, Melbourne, 2008.

- [15] Novaković, D., Kašiković N., Zeljković Ž., Agić D., Gojo M.: "Thermographic Analysis of Thermal Effects on the Change of Colour Differences on the Digitally Printed Textile Materials", Tekstil 59(7), 297-306, 2010.
- [16] Onar Çatal, D., Özgüney A. T., Akçakoca Kumbasar E.-P.: "The Influence of Rheological Properties of the Pretreatment Thickeners on Ink-jet Printing Quality", Tekstil ve Konfeksiyon 22(4), 309-316, 2012.
- [17] Özgüney, A.-T., Özerdem A., Özkaya K.: "Influences of Pretreatment on the Yellowing Occured During Screen Printing Process", Tekstil ve Konfeksiyon 17 (1), 45-51, 2007.
- [18] Persons, K.: "Human Thermal Environments: The Effects of Hot, Moderate and Cold Environments on Human Health, Comfort and Performance", 2nd ed., (Taylor and Francis, London, 2003.), page 240.
- [19] Provost, J., Ink Jet Printing on Textiles, Provostinkjet, URL: <http://provostinkjet.com/resources/SDC%2B%2BInk%2BJetPretreatment%2B4th%2BDec%2B03.pdf> (last request: 2016-06-7).
- [20] Stančić, M., Kašiković N., Novaković D., Grujić D., Milošević R.: "Thermal Load Effect on Print Quality of Ink Jet Printed Textile Materials", Journal of Graphic Engineering and Design 4(2), 27-33, 2013.
- [21] Stoecker, W.-F., Jones J.-W.: "Refrigeration and Air Conditioning", 2nd Ed., (McGraw- Hill, Singapore, 1982.), page 66.
- [22] Yoo, H.S., Hu Y.S., Kim E.A.: "Effect of Heat and Moisture Transport in Fabrics and Garments Determined with a Vertical Plate Sweating Skin Model", Textile Research Journal 70(6), 542-549, 2000. doi:10.1177/004051750007000612.



INHIBITION OF PREMATURE POLYMERIZATION OF CATIONICALLY CURABLE SYSTEMS BY TRIETHANOLAMINE

Jan Vališ , Bohumil Jašůrek , Zuzana Brůnová

University of Pardubice, Faculty of Chemical Technology,

Department of Graphic Arts and Photophysics, Pardubice, Czech Republic

Abstract: *This work concerns the inhibition of early polymerization of cationically polymerizable systems. Tested formulations contain 3,4-epoxycyclohexylmethyl-3,4-epoxycyclohexane carboxylate as a reactive monomer, triethanolamine as a stabilizer, and a photoinitiator. Three types of initiators were used: sulphonium salt (tris[4-[(4-acetylphenyl)sulfanyl]phenyl]sulfonium hexafluorophosphate), iodonium salt (iodonium (4-methyl-phenyl) [4-(2-ethylpropyl) phenyl] hexafluoro-phosphate)) and iron-arene salt (η^5 -2,4-cyclopentadien-1-yl) [(1,2,3,4,5,6- η)-(1-methylethyl)benzene]-iron hexafluorophosphate). Prepared formulations were periodically exposed at an increased temperature (60 °C). The long-term stability was tested by viscosity measurement. Viscosity change reflects changes in the distribution of molecular weights in the system or structural changes caused by premature polymerization. The flow behaviour was measured using rheometer Haake RotoVisco 1. The reactivity of the mixtures was tested by FTIR spectroscopy using Nicolet Avatar 320.*

Key words: cationic polymerization; inhibition; premature polymerization

1. INTRODUCTION

UV curable inks are mixtures of reactive components, photoinitiators and other additives. Apart from the rapid photo induced polymerization, these systems undergo the very slow, thermally induced polymerization, which leads to complete gelation. The rate of premature polymerization is influenced by storage temperature, reactivity of the components and thermal stability of the photoinitiators. The premature polymerization is undesirable, because viscosity affects strongly the print quality and a significant increase in viscosity may lead to an irreversible failure of the printing (mainly inkjet) system. Due to the key requirement for ink viscosity stability during storage in the dark and during the printing process, additives inhibiting premature polymerization are put into the ink formulation.

For cationically polymerized inks the amines are added as inhibitors (Takabayashi et al, 2006; Kondo, 2007). These substances react preferentially with the active species initiating the polymerization. They are added in small amounts (e.g. 0.01–0.1 wt. %) of the ink formulation. After UV exposition, all polymerization inhibitors are depleted by excessive generation of the reactive components (cations) and, sequentially, polymerization initiation and propagation take place.

In the case of cationic polymerization the reactive cations have a much longer lifetime (compared to radicals). Therefore even a small amount of cations prematurely generated in the dark promotes long-lasting polymerization, resulting in slow gelation of the formulation. One of the ways, how to suppress premature polymerization, is cation scavenging by the addition of some nucleophilic substance, e.g. amines (Crivello et al, 1998).

Some cationic photoinitiators (for example the diaryliodonium salts) can be decomposed not only by direct photo-decomposition after UV exposition, but also by redox reactions with suitable free radicals in the dark (Crivello et al, 1998; Yagci et al, 1998). If the premature decomposition of the cationic photoinitiator is supported by premature generation of such free radicals, radical scavengers as quinones or phenolic antioxidants should be effective as the inhibitors of premature polymerization. The use of antioxidants for the inhibition of premature polymerization of cationically polymerizable systems can be found in literature, e.g. (Toagosei America Inc., 2011; Rinker, 2010).

2. METHODS

Testing deals with the inhibition effect of triethanolamine (Figure 1a) on premature polymerization of systems consisting of epoxide monomer (Figure 1b) and various types of cationic initiators: iodonium (Figure 1c), sulfonium (Figure 1d), and iron-arene salts (Figure 1e).

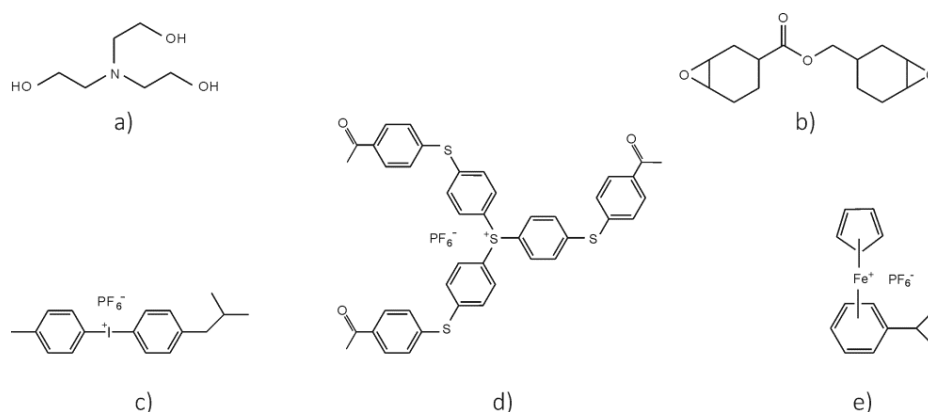


Figure 1: Used materials – (a) triethanolamine, b) 3,4-epoxycyclohexylmethyl-3,4-epoxycyclohexane carboxylate, c) iodonium (4-methyl-phenyl) [4-(2-ethylpropyl) phenyl] hexafluoro-phosphate, d) tris[4-[(4-acetylphenyl)sulfanyl]phenyl]sulfonium hexafluorophosphate, e) η^5 -2,4-cyclopentadien-1-yl [(1,2,3,4,5,6- η)-(1-methylethyl)benzene]-iron hexafluorophosphate

The efficiency of triethanolamine as a protecting agent of cationically curable systems against premature polymerization was tested by measuring of viscosity changes at room and elevated temperatures. Increase of viscosity reflects changes in the distribution of molecular weights in the system or structural changes caused by premature polymerization. The stability of prepared samples was measured during twenty three weeks. Part of samples was exposed to elevated temperature (60°C) few times (1; 1.5; 5; 5 and 11 hours). Flow curves of the samples were measured at 22°C in the range to 1000 s⁻¹ shear rate using a Haake Rotovisco 1 rotary viscometer equipped with a cone sensor C20/1. The viscosity was determined from the flow curve as a mean value of steady values of the apparent viscosities (Figure 2).

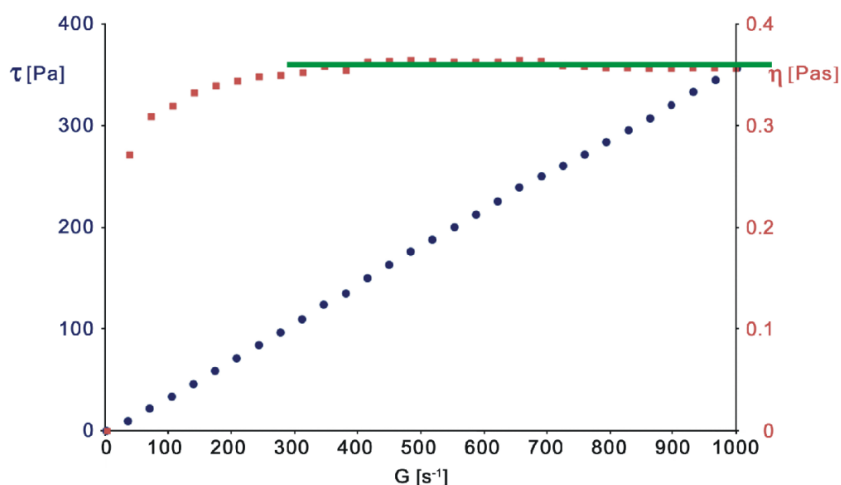


Figure 2: Example of the flow curve evaluation

The influence of additive on photoinitiated polymerization was tested by evaluation of conversion degree of the monomer after UV exposition. The infrared spectra were recorded by means of FTIR spectrometer Avatar 320 (Nicolet Instrument Corp., USA). The samples were irradiated by a medium pressure mercury lamp (UV tunnel Miniterm 220, Aeroterm, Czech Republic). The average UV dose per sample was 750 mJ/cm². The degree of conversion at time it was evaluated according to the formula:

$$\alpha_t = \frac{\frac{A_0}{R_0} - \frac{A_t}{R_t}}{\frac{A_0}{R_0}} \cdot 100 \quad (1)$$

where A_0 and R_0 are areas of the epoxide tripleband (approximately 800 cm^{-1}) and the reference carbonyl (1730 cm^{-1}) absorption bands before UV exposition, resp., A_t , R_t are areas of these absorption bands after UV exposition and the defined time lag (see Figure 3).

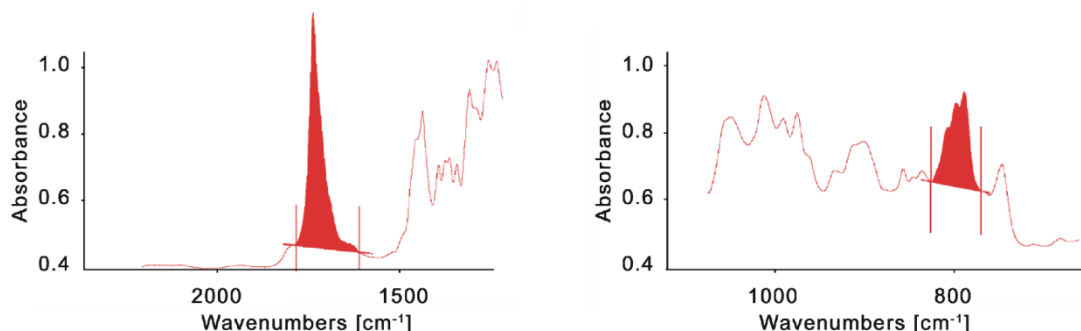


Figure 3: Example of the areas of absorption bands evaluation

3. RESULTS

The test results are summarized in Table 1. Samples 250 contained 3 weight % of the iodonium salt as a photoinitiator, samples 270 contained 3 weight % of the sulfonium salt as a photoinitiator and samples 251 contained 3 weight % of the organometallic salt as a photoinitiator. Samples A contained 1 weight % of the triethanolamine as an inhibitor of premature polymerization, samples C were stored in the refrigerator throughout the test period (4°C) and samples H were heated to 60°C .

Table 1: Results

Heating [hours]	0	1	2.5	7.5	12.5	23.5	(only H samples were heated*)	
Storage [weeks]	1	4	11	15	20	23	Premature polymerization	Conversion [%]
Sample	Upper limit viscosity [mPas]							
250	0.63	0.65	0.66	0.67	0.78	0.88	yes	98.7
250-H	0.63	0.61	0.67	0.79	1.06	1.46	yes	95.8
250-C	0.63					0.60	no	95.9
250A	0.44	0.44	0.44	0.41	0.44	0.42	no	56.7
250A-H	0.44	0.42	0.42	0.42	0.45	0.44	no	67.5
250A-C	0.44					0.44	no	66.1
270	0.57	0.57	0.54	0.57	0.57	0.53	no	88.1
270-H	0.57	0.58	0.54	0.58	0.58	0.58	no	87.8
270-C	0.57					0.57	no	92.0
270A	0.54	0.55	0.53	0.53	0.55	0.51	no	87.3
270A-H	0.54	0.52	0.52	0.52	0.56	0.55	no	87.9
270A-C	0.54					0.54	no	85.7
261	0.51	0.52	0.52	0.52	0.51	0.51	no	91.7
261-H	0.51	0.51	0.49	0.52	0.52	0.53	no	92.5
261-C	0.51					0.52	no	97.3
261A	0.46	0.47	0.46	0.45	0.48	0.48	no	89.5
261A-H	0.46	0.49	0.49	0.52	0.54	0.55	no	88.6
261A-C	0.46					0.51	no	90.8

*H samples were heated (60°C); C samples were stored in the refrigerator (4°C); A sample contained the amine

4. CONCLUSIONS

Premature polymerization occurs in mixtures containing the iodonium salt as photoinitiator mainly at elevated temperature, but also at room temperature (slightly). Addition of the triethanolamine effectively suppressed the premature polymerization of samples containing iodonium salt, but the presence of triethanolamine significantly reduces final degree of conversion (with iodonium salt as photoinitiator). Samples containing the iron-arene and the sulphonium photoinitiators did not show premature polymerization. The presence of triethanolamine in this case only slightly reduces the final degree of conversion. No sample stored in refrigerator showed premature polymerization.

5. REFERENCES

- [1] Crivello, J. V., Dietliker, K., edited by: Bradley, G.: "Photoinitiators for Free Radical, Cationic & Anionic Photopolymerization", 2nd ed, (John Wiley & Sons, Chichester, 1998).
- [2] Kondo, A.: EP 1 852 477 A1, "Ink set for inkjet, and method for forming image and inkjet recording device using the same", Konica Minolta Medical & Graphic Inc., 2007.
- [3] Rinker, K.: US 2010/0304284 A1, "Thermally stable cationic photocurable compositions", BASF Corporation, 2010.
- [4] Takabayashi, T., Sekiguchi, R.: US 2006/0050121 A1, "Activated light curable inkjet ink and image formation method", Konica Minolta Medical & Graphic Inc., 2006.
- [5] Toagosei America Inc., Aron Oxetane Technical Information, Aronalpha, URL: [http://instantadhesives.aronalpha.net/Asset/OXETANE TDS.pdf](http://instantadhesives.aronalpha.net/Asset/OXETANE%20TDS.pdf) (last request: 2018-07-21).
- [6] Yagci, Y., Reetz, I.: "Externally stimulated initiator systems for cationic polymerization", Progress in Polymer Science, 23 (8), 1485-1538, 1998. doi: 10.1016/S0079-6700(98)00010-0



© 2018 Authors. Published by the University of Novi Sad, Faculty of Technical Sciences, Department of Graphic Engineering and Design. This article is an open access article distributed under the terms and conditions of the Creative Commons Attribution license 3.0 Serbia (<http://creativecommons.org/licenses/by/3.0/rs/>).

GLYCEROL DERIVATIVES AS A MODERN PLASTICIZERS FOR STARCH FILMS

Zuzanna Żółek-Tryznowska, Łukasz Cichy

Warsaw University of Technology, Faculty of Production Engineering,
Mechanics and Printing Institute, Warsaw, Poland

Abstract: Due ecological reasons there is a considerable interest in biodegradable films made from renewable and natural polymers, such as starch. Starch films are not meant to totally replace conventional packaging polymer films, but they might be a competition in several application, where traditional packaging cannot function. Moreover, starch as a raw material exhibit many benefits, such as relatively low price, abundant, biodegradable, and edible. Films prepared from starches are isotropic, odourless, tasteless, colourless, non-toxic and biodegradable. Finally, they are nutritious and safe, so they are used in the marketing of food. Unfortunately, the starch films present poor tensile properties and sensitivity to moisture content.

In order to modify starch films properties the addition of various plasticizers is used. Commonly as a plasticizer water and glycerine is used. In this work, we use glycerol derivatives as a modern plasticizers for starch films obtained from potato starch by the tape casting technique, which allows to obtained films with constant thickness and 20 cm length. The influence of the ratio of various plasticizers: glycerol, pentaerythriolethoxylate, glycerol ethoxylate and Poligliceryn-3 on the mechanical properties and surface free energy was investigated. The plasticizers selected by us are characterized by a large number of functional hydroxyl groups. The starch films with the mixture of plasticisers reveal better usable properties and higher mechanical properties than with only one plasticizer. However, glycerol derivatives they cannot be used without the addition of glycerol. Furthermore, surface free energy was determinate by Owens-Wendt and van Oss-Chaudhury-Good method. The values of SFE are in the range 50–60 mJ/m² and higher than values of typical plastic films, which are used in packaging industry. Obtained starch films are characterized by quite high polar component of SFE, with may be related with the influence of hydroxyl groups.

Our results support the use of glycerol derivatives as modern plasticizers for biodegradable films and may open up new possibilities for applications of these compounds.

Key words: biodegradable films, starch, surface free energy, glycerol

1. INTRODUCTION

Plastic are commonly used in various industries, however one of the main recipient of them is packaging industry. In Poland the usage of plastics as a flexible films is estimated at around 13 kg per person per year. Furthermore, in the packaging industry only six plastics (HDPE, LDPE, PVC, PP, PS and PET) are used. Due their great packaging properties, such as good mechanical properties, gas and water barrier, plastic films have found application as excellent materials for packaging of food products. Plastic films are used in the packaging industry usually as single-use packaging, which means that after consuming, they must be recycled.

The main disadvantage of conventional plastic materials is the method of recycling. Utilization of plastic films is a problem due their non-degradability in natural environment, hence the European Union introduce the regulation of single-use plastics. In order to decrease the usage of conventional plastics, bio-based and biodegradable plastics are introduced. Some of the environmentally friendly polymers are already industrially produced (PLA, PHA, PCL, PEA), however the researchers search for new, cheap, with good properties plastics based on renewable and natural raw materials, for example polysaccharides (Lawton, 1996). Furthermore, the price of biodegradable PLA is still higher than conventional non-degradable PP or PET.

Starch is one of the most abundant naturally occurring substances (Pareta et al, 2006). Furthermore, it exists in various forms depending on the origin of the raw material (Sartori et al, 2016). Depending on origin of starch, give rise to a variety of films. The films based on maize (Pareta et al, 2006), banana (Sartori et al, 2016), cassava (Bourtoom et al, 2008, Souza et al, 2013), potato starch (Talja et al, 2007), have been already presented in the literature. The most widely used technique for the laboratorial production of starch-based films is casting method (Vicentini et al, 2002; Mali et al, 2005a; Müller et al, 2008). The suspension of starch in water is poured on Petri dish, while the thickness of the resulting films from the mass of suspension

poured on the plate. The film is drying at room temperature or in ovens with forced air. This method exhibits some disadvantages: (i) uncontrolled thickness of the starch film, (ii) long time of drying (24 h or more), (iii) limited and small size of obtained starch film, which enables to scale up the production to industrial scale. Addition of plasticizers to the starch films affects the properties such as water sorption, mechanical properties and glass transition temperature. Generally, as a plasticizers glycerine is used. However, also some of polyols, (sorbitol, xylitol) may be used as plasticizers (Talja et al., 2007). Furthermore, water sorbed in film acts also as plasticizer.

2. METHODS

Table 1: Properties of glycerine and its derivatives

Amount of glycerol or glycerol derivative was added into a solution of 4 g of starch in 100 g of water. Next, the film forming suspension was heated with continuous mixing over 95°C and kept for 5 min before letting it cool down to 50°C to obtain the film forming solution. Film forming solution was casted on a Teflon-coated plate placed on a K Paint applicator equipped in a spreader with gap 3 mm. The films were dried in a room temperature and humidity 30% RH.

Sample	Starch [g]	Glycerol [g]	Poliglycerol-3 [g]	Pentaerythiolethoxylate [g]	Glycerolethoxylate [g]
1	4	1.6	0.8	-	-
2	4	2.8	0.4	-	-
3	4	1.6	-	0.8	-
4	4	1.6	-	-	0.8
5	4	2.8	-	-	0.4
6	4	2.8	-	0.4	-

Contact angle of the obtained films was measured using a DSA 30E drop shape analysis system (Krüss, Germany). In order to measure contact angle, smooth and horizontal sessile drops of the liquids were deposited on a solid surface using needles of 0.5 mm diameter. The contact angle was measured on static drops. The drop shape analysis was done 15 s after the drop deposition with Tangent method 2. Environmental conditions were stable with temperature $23 \pm 0.5^\circ\text{C}$. The reported contact angle values are the mean of 6 probes on two films. The SFE was calculated using Owens-Wendt and van-Ossy-Good method.

Testing of mechanical properties of obtained starch films was performed using wick BT1-FB010TN.D30 tensometer (Zwick-Roell, Germany). Samples for the tests were prepared conforming to ISO 527-1. The width of the strip was 10 mm and the length was 100 mm for all tested films, and initial distance of the clamps was set to 50 mm. The speed of stretching was 100 mm min^{-1} . Tensile strength and elongation properties were determined from the stress-strain curves. For each film, at least 3 samples from two various films were tested and the mean values were taken as the final result.

3. RESULTS

We have prepared about 23 various starch films based on different properties of plasticizers. However, the quality of some of them did not allow for surface free energy and mechanical properties measurements. The properties of obtained films are presented in Table 3.

Table 3: Organoleptic properties of formed starch films

Sample	Colour	Smell	Flexibility	Extensibility
1	Transparent	Odourless	Flexible	Slightly stretchable
2	Transparent	Odourless	Very flexible	Very stretchable
3	Transparent	Odourless	Slightly flexible	Non stretchable
4	Transparent	Odourless	Slightly flexible	Non stretchable
5	Transparent	Odourless	Flexible	Stretchable
6	Transparent	Odourless	Flexible	Stretchable

The values of contact angle and surface free energy are listed in Table 4. The values of surface free energy (SFE) calculated by Owens-Wendt method and van Ossy-Good-Chaudhury method are listed in Table 5 and Table 6, respectively.

Table 4: Contact angles and SFE calculated using Owens-Wendt method of obtained films

Sample	Water [°]	Diiodomethane [°]	Formamide [°]
1	46.50	32.26	32.88
2	35.10	34.54	27.10
3	45.37	20.43	36.67
4	15.85	22.64	26.95
5	29.32	32.83	37.96
6	24.94	32.10	31.66

Table 5: Values of SFE together with polar and dispersive components calculated using Owens-Wendt method

Sample	Dispersive component [$\text{mJ}\cdot\text{m}^{-2}$]	Polar component [$\text{mJ}\cdot\text{m}^{-2}$]	SFE [$\text{mJ}\cdot\text{m}^{-2}$]
1	43.3	18.5	61.8
2	42.2	25.2	67.4
3	47.7	17.3	65.0
4	47.0	30.5	77.4
5	43.0	27.6	70.6
6	43.3	29.3	72.7

Table 6: Values of SFE together with its acid–base components and Lifshitz–Van der Waals calculated using van Ossy–Good–Chaudhury method

Sample	γ^W [mJ•m ⁻²]	γ^+ [mJ•m ⁻²]	γ^- [mJ•m ⁻²]	γ^{AB} [mJ•m ⁻²]	SFE [mJ•m ⁻²]
1	43.3	0.4	29.6	7.0	50.3
2	42.2	0.5	40.5	9.3	51.6
3	47.7	0.0	34.1	0.6	48.3
4	47.0	0.0	60.1	0.9	47.8
5	43.0	0.0	56.2	1.0	44.0
6	43.3	0.0	55.4	3.2	46.5

The mechanical properties of obtained films are listed in Table 7.

Table 7: Tensile strength and ultimate elongation of the investigated films

Sample number	Tensile strength [MPa]	Ultimate elongation [%]
2	2.06	89
5	1.76	25
6	3.92	80

4. DISCUSSION

We have received about 23 various starch films based on various content of plasticizers. However, some of obtained starch films exhibited fragility and non-flexibility. This films where so fragile that where broken in hands and it was unable to measure contact angle or tensile properties. Only six films where suitable for measurements of contact angle or tensile properties.

The measurements of static contact angles (CA) represent useful information regarding interactions between the coating and the liquid. In general, lower values of CA of water testify to greater wettability of surface and greater hydrophilicity. However, the values of CA of water provide rather greater affinity to water of obtained films.

To the best our knowledge, for the first time surface free energy of starch films were investigated. In this work, in order to calculate SFE two various methods were used: Owens–Wendt (OW) and Van Oss–Good–Chaudhury (VOCG). The surface free energy of coatings were evaluated by Owens–Wendt equation:

$$(1 + \cos \theta_i) \gamma_{li} = 2 \left(\sqrt{\gamma_{li}^d \gamma_s^d} + \sqrt{\gamma_{li}^p \gamma_s^p} \right) \quad (1)$$

where θ is the contact angle (CA) of testing liquid (deg), γ_{li} is the surface free energy (SFE) of the testing liquid, γ_{li}^d , γ_{li}^p is the dispersion and polar component of tested liquid and finally γ_s^d , γ_s^p are SFE of coating. The acid base theory by van Oss, Good and Chaudhury was used for determination of dispersive, i.e. non-polar Lifshitz–Van der Waals γ^{LW} , acid γ^+ , and base γ^- components of the PHU surface energy expressed by terms as acid component γ^+ (acceptor effect) and γ^- basic component (donor effect) (Good et al, 1991):

$$(1 + \cos \theta_i) \gamma_{li} = 2 \left(\sqrt{\gamma_i^{LW} \gamma_s^{LW}} + \sqrt{\gamma_i^{LW} \gamma_s^{LW}} + \sqrt{\gamma_i^{LW} \gamma_s^{LW}} \right) \quad (2)$$

where i refers to testing liquid and s refers to solid material. The values of SFE calculated with Owens–Wendt method and van Ossy–Good–Chaudhury method are listed in table 4 and 5, respectively. The values of total SFE calculated by both models, OW and VOGC, differ insignificantly. However, the values of SFE reveals that starch films may be printed without activation process. The highest difference can be observed for sample 3 and is equal nearly 30 mJ•m⁻². The values of Lifshitz–Van der Waals (non-polar) component are much higher than the values of acidic and basic components of SFE. Further, the values of basic component are much higher than values of acidic components. This is related with the presence of electron pairs of oxygen in ether or hydroxyl groups which are effective Lewis base sites. However, compering the acidic

component, it can be seen that sample 1 and 2 exhibited the highest “acidic” surface character, which may be related with addition of Polyglycerin-3.

Summarizing, all investigated starch films exhibited various values of γ^{AB} and γ^{LW} due various amount of plasticizers and free end-groups (hydroxyl) in the starch and plasticizers, despite their structure is quite similar. The tensile properties of obtained starch films are listed in Table 7. Obtained starch films, in comparison to conventional plastic films, reveal poor tensile properties. However, film with addition of glycerine and Poligliceryn-3 exhibited highest tensile strength.

5. CONCLUSIONS

In this work we have demonstrate novel application of glycerol derivatives. The most effective plasticizer for starch films is glycerine and water, however the addition of other glycerine derivatives may improve selected properties of starch films. Unfortunately, the use of other plasticizers or mixture of plasticizers with glycerine requires more research and work. Films that consist more than one plasticizer obtained the best results of surface free energy. The values of surface free energy are higher than the values of surface free energy of conventional plastic films used in packaging. The measurements of SFE shows, that starch films do not requires activation process prior printing. Furthermore, starch films may replace conventional plastics in single-use products, which production may be limited by the regulation of the European Union.

6. ACKNOWLEDGMENTS

Funding for this research was provided by the Faculty of Production Engineering, Warsaw University of Technology.

7. REFERENCES

- [1] Bourtoom, B., Chinnan, M.S.: “Preparation and properties of rice starch-chitosan blend biodegradable film” *LWT - Food Science and Technology* 41 (9), 1633-1641, 2008.
- [2] Good R.J., Chaudhury, M.K., van Oss, C.J.: “Theory of Adhesive Forces Across Interfaces” in “Fundamentals of Adhesion” (Springer-Verlag, Boston, USA, 1991) pages 153-172.
- [3] Lawton, J.W.: “Effect of starch type on the properties of starch containing films” *Carbohydrate Polymers* 29 (3), 203-208, 1996.
- [4] Mali, S., Grossmann, M., Garcia, M., Martino, M., Zaritzky, N.: “Mechanical and thermal properties of yam starch films” *Food Hydrocolloids* 19 (1), 157-164, 2005.
- [5] Müller, C., Yamashita, F., Laurindo, J.: “Evaluation of the effects of glycerol and sorbitol concentration and water activity on the water barrier properties of cassava starch films through a solubility approach” *Carbohydrate Polymers* 72 (1), 82-87, 2008.
- [6] Pareta, R., Edirisinghe, M.J.: “A novel method for the preparation of starch films and coatings” *Carbohydrate Polymers* 63 (3), 425-431, 2006.
- [7] Pareta, R., Edirisinghe, M.J.: “A novel method for the preparation of starch films and coatings” *Carbohydrate Polymers* 63 (3), 425-431, 2006.
- [8] Sartori, T., Menegalli, F.C.: “Development and characterization of unripe banana starch films incorporated with solid lipid microparticles containing ascorbic acid” *Food Hydrocolloids* 55, 210-219, 2016.
- [9] Souza, Ac., Goto, G.E.O., Mainardi, J.A., Coelho, A.C.V., Tadini, C.C.: “Cassava starch composite films incorporated with cinnamon essential oil: Antimicrobial activity, microstructure, mechanical and barrier properties” *LWT - Food Science and Technology* 54 (2), 346-352, 2013.
- [10] Talja, R.A., Helén H., Roos, Y.H., Jouppila, K.: “Effect of various polyols and polyol contents on physical and mechanical properties of potato starch-based films” *Carbohydrate Polymers* 67 (3), 288-295, 2007.
- [11] Vicentini, N., Sobral, P., Cereda, M.: “The influence of the thickness on the functional properties of cassava starch edible films” in *Plant Biopolymer Science: Food and Non-Food Applications* (RSC: Cambridge, UK, 2002) pages 291-300.








© 2018 Authors. Published by the University of Novi Sad, Faculty of Technical Sciences, Department of Graphic Engineering and Design. This article is an open access article distributed under the terms and conditions of the Creative Commons Attribution license 3.0 Serbia (<http://creativecommons.org/licenses/by/3.0/rs/>).

PACKAGING ADDED VALUE



PRODUCTION FACTORS INFLUENCING MECHANICAL AND PHYSICAL PROPERTIES OF FDM PRINTED EMBOSSED DIES

Bojan Banjanin , Gojko Vladić , Magdolna Pál ,
Vladimir Dimovski, Savka Adamović , Gordana Delić 
University of Novi Sad, Faculty of Technical Sciences,
Department of Graphic Engineering and Design, Novi Sad, Serbia

Abstract: Embossing technique is an essential operation in the print finishing process. It entails permanently changing the shape of the paper surface by applying pressure with the embossing die, so as to create a recessed or raised image. Embossing dies are made using conventional techniques such as chemical etching or milling. These techniques in the production of conventional embossing die imply the use of different machines and devices, plenty workspace, and often insufficient flexibility in quick job changes. By replacing conventional with additive manufacturing techniques, these problems imposed by the market can be overcome to a great extent.

Using additive manufacturing techniques in embossing dies production process requires prior understanding of factors influencing mechanical and physical properties of produced samples. Fused Deposition Modelling (FDM) technique is commonly used in additive manufacturing due to its simplicity and availability. The surface roughness of FDM produced embossing dies is an important factor which can alter the quality of the embossed paper material. Excellent mechanical properties of the die are also required due to pressure forces applied in the embossing process.

This paper aims to investigate the influencing process factors in FDM additive manufacturing found in current scientific researches and implement these findings for embossing dies production. Influence of these factors on surface roughness, tensile and compression strength, the quantity of used material and production time were investigated.

Findings imply that vast variety of process factors influence chosen dependent variables of samples printed with FDM technique. Many researchers have investigated these factors, but mainly in the field of industrial engineering, electronics and bioengineering. Hence, the importance of this paper is in finding a way to implement these findings in the field of graphic engineering and design.

Key words: Fused Deposition Modelling, embossing dies, FDM process factors, mechanical and physical properties

1. INTRODUCTION

In the graphic production process, there is a noticeable trend of reducing print runs, and increasing demand of personalized products with the capability of quick makeready times, which requires from manufacturers to finish a whole production process in one place. In personalized production, embossing dies (Figure 1) withstand a lower number of imprints; hence different approach of their production should be considered. Production of these dies needs to be simplified, to cost less and to satisfy all the necessary criteria such as high production precision and good mechanical and physical characteristics.

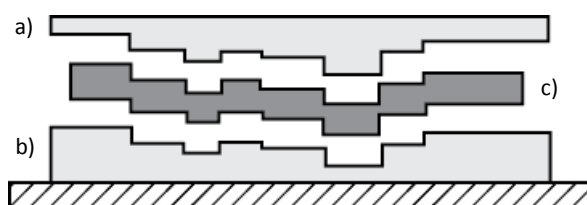


Figure 1: Embossing tool with a) male die and b) female die used for embossing c) paper

Recently, there appear to be more manufacturers of graphic equipment and materials who introduces additive manufacturing in their production process. Additive manufacturing (AM) techniques refer to the

production of 3D objects by adding material in successive layers. Mainly these techniques were used for the production of prototypes (rapid prototyping - RP), but recently they have been used for commercial, industrial purposes (Masood et al, 2004). Constant improvements in the area of additive manufacturing and wide availability of its techniques enabled their vast utilization in education and domestic production. One of the most represented 3D technique is based on material extrusion (also known as FDM – Fused Deposition Modelling). Synonyms for this technique are also: “plastic jet printing”, “thermoplastic extrusion” or “fused filament method” (Bogue, 2013). FDM technique is invented in the year 1988. By Scott Crump, but its commercialisation was done by Stratasys company in the year 1990. (Stratasys, 2016). A solid filament of material is fed into printing head where it is heated and pushed through nozzles onto a building platform where it is deposited in successive layers. Each layer of extruded material is cooled down and solidified once being deposited on the platform (Figure 2).

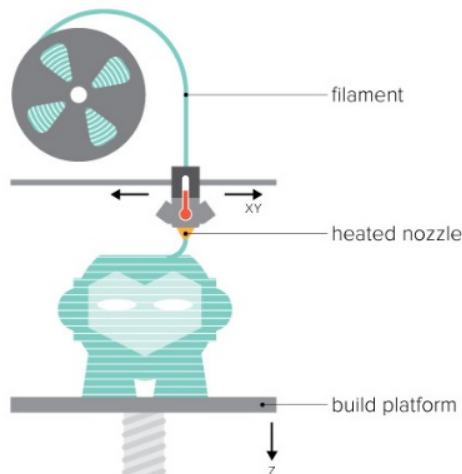


Figure 2: Principle of FDM printing process (3dlink, 2016)

Successive layers form a 3D printed object which has an anisotropic property (Ahn et al, 2002). Common materials used in FDM printing process are acrylonitrile butadiene styrene (ABS), polylactic acid (PLA), nylon, polycarbonate (PC), polyether ether ketone (PEEK), etc. Composite materials gain interest in academic circles due to the variety of improved properties which cannot be achieved only with a plain thermoplastic material. Clay, glass, wood and metal particles are often added to the thermoplastic matrix to improve one of the material properties. Objects produced with FDM technique have good mechanical properties but less surface quality which can be improved using one of the print finishing techniques (Yan et al, 1996; Wendel et al, 2008; Upcraft et al, 2003; Wong et al, 2012). FDM technique is characterized by its simplicity, availability of different printing materials and low price. Use of biodegradable materials such as polylactic acid (PLA) allows printed objects to be biodegradable which leads to a decrease in the negative effect on living and working environment.

Conventional techniques of embossing dies production are chemical etching and machining. Machining is carried out by removing excess material with machining tools in order to get the desired shape of the embossing die. Chemical etching techniques usually use nitric acid to remove certain parts of the embossing die. Both of these techniques produce by-products which can be hazardous to humans and their environment.

1.1 Parameters influencing embossing process

There are a lot of influencing parameters that affect the quality of embossed images on graphic products. They can be divided into three categories (Konstantinović, 1997):

- parameters of embossing die
- parameters of embossing substrate
- parameters of working parameters

Before production of embossing dies it is necessary to know optimal size and shape of embossing elements, the number of details, gap between elements on male and female die part and depth of embossing elements. Element precision, their size and number of impressions dictates the choice of die material. Brass and copper dies are used for high circulations and fine precision of embossing elements. Magnesium dies are softer and are used for lower circulation, pressure and lower quality of fine embossing elements (u-emboss, n.d; Rikard, 2016; Iggesund, 2018). The gap between elements on the male and female die is defined in the process of preparing files for filming. A small gap is used for embossing thinner papers, and larger ones are used for thicker papers often with rough surface structure. A depth of embossing elements is controlled in the process of chemical etching or machining.

Parameters of embossing substrate (usually paper) also affect the quality of the embossing process. Different papers require different die parameters and work parameters. If the elements on the embossing die are small and depth of embossing is large, it is necessary to acquire proper hardness, stiffness, toughness and elasticity of paper to achieve optimum embossing results. Essential paper characteristics are tensile and compressive strength and strain, hardness, stiffness, density and percentage of moisture in paper structure (Kirwan, 2013). If relative humidity in paper rises, plastic deformation will be higher (Konstantinović, 1997).

According to Konstantinović (1997), working parameters are applied pressure, the embossing die temperature and contact time between paper and die during the embossing process. In order to achieve plastic deformation of the embossing material, it is required to overcome its resistance. Plastic deformation is the objective criteria for determining embossing quality. According to Blechschmidt (2013), optimum embossing depth is between 0.3 mm and 0.6 mm. In embossing process, ultimate deformation is calculated as a sum of elastic, elasto-plastic and plastic deformation of material Eq. (1):

$$\varepsilon_{uk} = \varepsilon_e + \varepsilon_{ep} + \varepsilon_p \quad (1)$$

Where ε_{uk} is ultimate deformation, ε_e is elastic deformation, ε_{ep} is elasto-plastic deformation, and ε_p is plastic deformation. Wilken (ed. Holik, 2013) defines the embossing process as forming material by using pressure. Required pressure depends on the embossing area and specific material resistance Eq. (2):

$$F = c \cdot \sigma_0 \cdot A \quad (2)$$

where c stand for the correction factor. Elastic deformation of material ends after applying pressure, and the final result of embossing is defined by ultimate plastic deformation implied upon the material. By adjusting the gap between raised and recessed die, it is also possible to control embossing pressure. Blechschmidt (2013) points out that optimum pressure should be between 25 MPa and 35 MPa.

The temperature of the embossing die can also be regulated. The optimum combination of pressure and temperature will yield high-quality embossing result. The same results can be achieved by lowering the pressure and rising temperature or by applying greater pressure and lower temperature (Konstantinović, 1997). Contact time is defined as a time of applying pressure of embossing die on a substrate. By increasing contact time, plastic deformation of material increases. Contact time depends on the level of automation and construction of the embossing machine, the surface structure of embossing material, material properties as well as the type of embossing process (Konstantinović, 1997). Optimum contact time should be between 0.3 and 3 seconds (Blechschmidt, 2013).

1.2 Requirements for embossing dies produced using additive manufacturing

Embossing dies produced by one of the additive manufacturing techniques need to have good mechanical properties, smooth surface and good reproduction of fine embossing elements. In order to replace conventionally produced embossing dies with ones produced by AM technique, it is necessary to have a good quality of reproduced elements and to ensure the desired number of impressions without die failure. Satisfying embossing requirements using FDM produced dies will probably ensure desired quality by using other AM techniques such as vat photo polymerization, binder jetting, laser sintering etc.

To achieve these requirements, FDM printed dies have to overcome problems of surface quality (usually caused by “staircase effect”), mechanical strength and precise reproduction of fine elements. These output

variables are commonly researched in scientific circles and will be discussed in this paper. It is also of great importance to produce embossing dies for the least possible time and to ensure that usage of printing material is reduced as much as it is possible while retaining a good quality of dies.

2. FACTORS INFLUENCING QUALITY OF FDM PRINTED PRODUCTS

There are a great number of factors influencing the quality of objects produced using FDM 3D printing technique such as printing material properties, the height of deposited layers, type and percentage of infill, number of shells, extruding temperature, printing speed, print orientation, raster angle etc. Embossing dies produced with FDM technique require appropriate mechanical properties, surface roughness, and reproduction of small embossing elements, low price and production time in order to justify their use in the embossing process. Influence of the above-mentioned factors on the properties of FDM printed parts is discussed in the next chapter. First basic terminology must be defined.

Layer height (slice height, layer thickness) - This factor is the most researched in academic circles so far, and it refers to the thickness of the layer deposited by nozzle tip in “z” direction of the printing surface. This factor determines “resolution” of side surfaces of the FDM printed object. The lower the value of layer height is, the finer side surface quality will be achieved. By increasing layer height, the so-called “staircase effect” will be more visible leading to rougher side surfaces (Ahn et al, 2002; Mohamed et al, 2015).

Air gap - This parameter refers to the distance between two deposited filaments (rasters) on the same layer determining the percentage of object infill. Because of its anisotropic structure, FDM printed objects are formed with interlaced rasters trapping a certain amount of air between them. Smaller air gaps lead to the more compact structure of the 3D printed object with stronger inter-filament bonds and better mechanical properties (Ahn et al, 2002; Mohamed et al, 2015).

Raster width (bead width) – This parameter refers to the width of the deposited filament in “xy” direction, and it is commonly controlled by adjusting extruder temperature. Ahn et al. (2002). Wider raster width leads to part with the stronger interior but increased production time (Ahn et al, 2002; Mohamed et al, 2015).

Raster angle (raster orientation) – beside layer height, this is one of the most influencing parameters found in the literature. It refers to the angle between rasters and “x” axis of the print surface. Most commonly used values of this parameter are 0°, 45° and 90° but angles of 20°, 30°, 60° etc. are also investigated in the listed literature (Ahn et al, 2002; Mohamed et al, 2015).

Contour width – this parameter refers to the width of the layer’s outer contour also know as a shell which surrounds the part (Mohamed et al, 2015).

Contour to contour air gap - refers to the gap between outer contours if the part is printed with multiple contours (Mohamed et al, 2015).

Perimeter to raster air gap – this parameter refers to the gap between the innermost contour and the edge of the rasters in infill (Mohamed et al, 2015).

Build orientation – this parameter defines an angle between the printed object and build platform along “x”, “y” and “z” axis (Mohamed et al, 2015).

Type of infill - refers to the inner geometry of the printed object. There are many different shapes of inner infill like linear, hexagonal, diamond and some which have more of an aesthetic function (marroccanstar, catfill, sharkfill, etc.) (3dhubs, 2017).

Infill (percentage of infill) – determines gaps in the inner structure of 3D printed object. Variation in values in this parameter printed object will be more or less filled with deposited filament (3dhubs, 2017).

Number of contours (shells) – this parameter refers to the number of deposited filaments that form outer walls of the printed object. By varying values of this parameter, object will be printed with thinner or thicker walls (Mohamed et al, 2015).

Floor/roof thickness – these parameters are not thoroughly investigated in the academic community. They refer to number (commonly described through thickness) of first few layers (floor) or last few layers (roof)

printed with 100% linear infill. Adjusting these parameter allows the printed object to have a dense cover (3dhubs, 2017).

Nozzle temperature (model build temperature) – refers to the temperature of the heating element (nozzle) which controls the viscosity of the semi-molten material (Ahn et al, 2002).

Colour of the material – this parameter refers to the addition of different colorants to the base matrix of thermoplastic material used in FDM (Ahn et al, (2002).

Nozzle diameter – refers to the diameter of the printhead nozzle tip. Adjusting this parameter allows different raster widths to be extruded on the build platform (Ahn et al, 2002).

Envelope temperature (environment or build platform temperature) – This parameter refers to the temperature of the surrounding atmosphere during the printing process (Ahn et al, 2002).

In the work of Mohamed et al (2015) a review of the influencing process parameters on the quality of FDM printed objects are listed. It is important to choose which of these parameters are going to be analysed and which should be constrained in order to have a desirable quality of printouts. Classification of influencing factors derived from the works of Mohamed et al (2015) and Ahn et al. (2002) is presented in Table 1.

Table 1: Factors influencing the quality of FDM produced parts (Mohamed, Masood and Bhowmik, 2015; Ahn et al, 2002)

INFLUENCING FACTORS OF FDM PRINTING TECHNIQUE					
QUALITY OF 3D MODEL	ORIENTATION ON BUILD PLATFORM	SETTINGS OF FDM PRINTER	WORKING PARAMETERS	UNPROCESSED MATERIAL	ENVIRONMENTAL FACTORS
STL FILE	ALONG X AXIS	NOZZLE TEMPERATURE	AIR GAP	DENSITY	TEMPERATURE
	ALONG Y AXIS	NOZZLE DIAMETER	RASTER ANGLE	COLOUR	HUMIDITY
	ALONG Z AXIS	BUILD PLATFORM TEMPERATURE	TYPE OF INFILL		
		PRINTER CALIBRATION	RASTER WIDTH		
			LAYER HEIGHT		
			PERCENTAGE OF INFILL		
			OBJECT SHRINKAGE ALONG X, Y AND Z AXIS		
			FLOOR/ROOF THICKNESS		
			CONTOUR WIDTH		

3. SELECTION OF THE MOST INFLUENCING FACTORS AND OPTIMIZATION TECHNIQUES

In FDM process it is essential to choose the proper process parameters in order to improve surface roughness, dimensional accuracy, mechanical properties, build time and at the same time to reduce material consumption during the manufacturing of embossing dies.

For determining which processing factors are most influencing regarding specific output variables, Design of experiment (DOE) and Taguchi method are commonly utilized. DOE was introduced as a concept by Ronald Fisher (Fisher, 1925), but most investigations on this topic were done in academic community (Ranjit, 2001). In his work, Fisher demonstrated the usability of his concept in agriculture. He analysed the optimum amount of water, rain, sunlight, fertilizers and soil condition required to gain better harvest (Fisher, 1926).

Genichi Taguchi broadened the application of this method by introducing a new approach (Taguchi, 1986). This approach implies dividing a problem into two categories by using the logarithmic function of desired output as a target optimization function (called signal to noise – S/N ratio). Problems of optimization are divided into two categories:

- Static problems – more than one input variables directly determine the desired value of the output variable. Three approaches can be used: smaller-the-better (when the smallest value of output variable is desired), larger-the-better (when the highest value of output variable is desired) and nominal-is-better (when the desired value is predetermined, and no other values smaller or bigger than that value is desired)
- Dynamic problems – one input variable directly determine the value of the output value

Taguchi optimization technique is able to provide:

- Maximum return funds
- Most efficient settings of machines
- Efficient use of raw materials and energy
- Optimum distribution of work in order to reduce the required labour and production time

The goal of every production process is to achieve the best product quality, least failure and high productivity which can be achieved utilizing full factorial design. In that case, it is necessary to test the interaction between every input factor and their influence on output value which prolong production process and increase cost. In contrast to the full factorial design, the Taguchi method decreases the number of required experiments by using orthogonal arrays. Choosing the adequate orthogonal array is the most laborious task in the Taguchi method (Bolboaca et al, 2007).

Besides full factorial design and Taguchi method, there are some other techniques used in the optimization process. Thrimurthulu et al (2010) used a real coded genetic algorithm (GA) to develop an analytical model to predict the optimum part orientation for surface roughness. Horvath et al (2007) used DOE to study the three different input factors to improve the surface roughness of FDM printed ABS samples. Chung Wang et al (2007) integrated the Taguchi method with the grey relational analysis to improve the surface roughness of FDM printed parts by 62.27%. In the work of Sood et al (2010) central composite design (CCD) and analysis of variance (ANOVA) were used for optimization of mechanical properties of FDM parts by investigating the influence of five different input variables. Percoco et al (2012) also used CCD technique to analyse the influence of two process parameters, and chemical treatment of FDM printed parts on their compressive strength and mechanical behaviour. Rayegani and Onwubolu (2014) utilize group method for data handling (GMDH) and differential evolution (DE) for process parameter prediction and optimization of the FDM process. They investigated four input variables on tensile strength.

Usually, research papers are focused on one objective (output) parameter which needs to be optimized by investigating the influence of one input parameter (main effect) or their interactions. Hamel et al (2018) proposed the use of an approximation-assisted multi-objective optimization technique to quantify the performance of an AM system for specific use. The focus of their research is in design for manufacturing (DfAM) techniques and tools needed in the design process regardless of the AM system being used. Mohamed et al (2016) investigated the influence of six input variables on build time, feedstock material consumption and dynamic flexural modulus using Q-optimal response surface methodology. Analysis of variance (ANOVA) technique was used to test the adequacy and significance of mathematical models. As a result, the optimal setting of process parameters was determined. Authors proved that Q-optimal design type of response surface methodology was simple, efficient, powerful, flexible, cost-effective and reliable design for process optimization involving multiple input and output variables. In Table 2 Input factors and their influence on output variables investigated in the literature are listed.

Table 2: Input factors and their influence on output variables investigated in the literature

Input \ Output	Surface roughness (surface finish)	Dimensional accuracy and sample deformation	Static mechanical properties (tensile strength, compression strength)	Dynamic mechanical properties	Build time	Feedstock material
Layer height	Huang et al. (2018); Chung Wang, Lin and Hu (2007); Thrimurthulu, Pandey and Venkata Reddy (2004); Horvath, Noorani and Mendelson (2007); Nancharaiah, Raju and Raju (2010); Anitha, Arunachalam and Radhakrishnan, (2001)	Chung Wang, Lin and Hu (2007), Sahu, Mahapatra and Sood (2013); Zhang and Peng (2012); Nancharaiah, Raju and Raju (2010); Sood, Ohdar and Mahapatra (2009); Zhang and Chou (2008); Xinhua et al. (2015)	Huang et al. (2018); Sood, Ohdar and Mahapatra (2010); Chung Wang, Lin and Hu (2007); Chin Ang et al. (2006); Hamel, Salsbury and Bouck (2018)	Mohamed, Masood and Bhowmik (2016);	Mohamed et al. (2016); Hamel, Salsbury and Bouck (2018); Kumar and Regalla (2012); Nancharaiah (2011); Thrimurthulu, Pandey and Venkata Reddy (2004)	Mohamed, Masood and Bhowmik (2016);
Raster width	Nancharaiah, Raju and Raju (2010); Anitha, Arunachalam and Radhakrishnan, (2001)	Sahu, Mahapatra and Sood (2013); Zhang and Peng (2012); Nancharaiah, Raju and Raju (2010); Sood, Ohdar and Mahapatra (2009); Zhang and Chou (2008); Xinhua et al. (2015)	Masood, Mau and Song (2010); Rayegani and Onwubolu (2014); Percoco, Lavecchia and Galantucci (2012); Sood, Ohdar and Mahapatra (2010); Chin Ang et al. (2006); Ahn et al. (2002); Montero et al. (2001);	Mohamed, Masood and Bhowmik (2016); Arivazhagan, Masood and Sbarski (2011)	Mohamed et al. (2016); Kumar and Regalla (2012)	Mohamed, Masood and Bhowmik (2016)
Build orientation	Huang et al. (2018); Chung Wang, Lin and Hu (2007); Thrimurthulu, Pandey and Venkata Reddy (2004)	Chung Wang, Lin and Hu (2007); Sahu, Mahapatra and Sood (2013); Sood, Ohdar and Mahapatra (2009)	Huang et al. (2018); Rayegani and Onwubolu (2014); Sood, Ohdar and Mahapatra (2010); Chung Wang, Lin and Hu (2007); Chin Ang et al. (2006); Ahn et al. (2002); Jami, Masood and Song (2013)	Mohamed, Masood and Bhowmik (2016); Jami, Masood and Song (2013)	Mohamed et al. (2016); Kumar and Regalla (2012); Thrimurthulu, Pandey and Venkata Reddy (2004)	Mohamed, Masood and Bhowmik (2016)
Raster angle	Huang et al. (2018); Nancharaiah, Raju and Raju (2010)	Sahu, Mahapatra and Sood (2013); Nancharaiah, Raju and Raju (2010); Sood, Ohdar and Mahapatra (2009)	Huang et al. (2018); Masood, Mau and Song (2010); Rayegani and Onwubolu (2014); Percoco, Lavecchia and Galantucci (2012); Sood, Ohdar and Mahapatra (2010); Montero et al. (2001)	Mohamed, Masood and Bhowmik (2016); Arivazhagan, Masood and Sbarski (2011)	Mohamed et al. (2016); Kumar and Regalla (2012); Nancharaiah (2011)	Mohamed, Masood and Bhowmik (2016)
Air gap	Nancharaiah, Raju and Raju (2010)	Sahu, Mahapatra and Sood (2013); Nancharaiah, Raju and Raju (2010); Sood, Ohdar and Mahapatra (2009)	Rayegani and Onwubolu (2014); Sood, Ohdar and Mahapatra (2010); Chin Ang et al. (2006); Ahn et al. (2002); Montero et al. (2001)	Mohamed, Masood and Bhowmik (2016);	Mohamed et al. (2016); Nancharaiah (2011)	Mohamed, Masood and Bhowmik (2016)
Type of infill	Chung Wang, Lin and Hu (2007); Horvath, Noorani and Mendelson (2007)	Chung Wang, Lin and Hu (2007); Xinhua et al. (2015)	Masood, Mau and Song (2010); Chung Wang, Lin and Hu (2007); Chin Ang et al. (2006); Hamel, Salsbury and Bouck (2018)	Arivazhagan and Masood (2012); Arivazhagan, Masood and Sbarski (2011)	Hamel, Salsbury and Bouck (2018)	
Printing speed	Huang et al. (2018); Anitha, Arunachalam and Radhakrishnan, (2001)	Zhang and Peng (2012); Zhang and Chou (2008); Xinhua et al. (2015)	Huang et al. (2018)			
Nozzle temperature	Horvath, Noorani and Mendelson (2007)	Xinhua et al. (2015)	Ahn et al. (2002); Montero et al. (2001)	Arivazhagan and Masood (2012)		
Number of contours			Hamel, Salsbury and Bouck (2018)	Mohamed, Masood and Bhowmik (2016);	Mohamed, Masood and Bhowmik (2016); Hamel, Salsbury and Bouck (2018)	Mohamed, Masood and Bhowmik (2016)
Support style	Chung Wang, Lin and Hu (2007)	Chung Wang, Lin and Hu (2007)	Chung Wang, Lin and Hu (2007)			
Colour			Ahn et al. (2002); Montero et al. (2001)			
Contour width					Kumar and Regalla (2012)	

In Figure 3 presence of most investigated input factors in literature listed in Table 2 are presented.

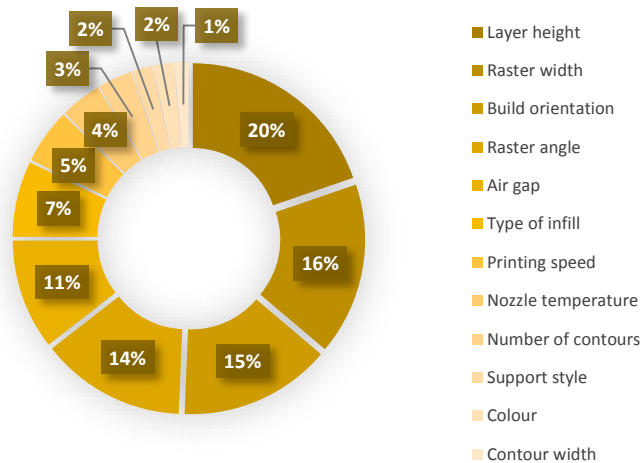


Figure 3: Most investigated input factors found in literature listed in Table 2

From Table 2 and Figure 3 it can be seen that layer height is one of the most investigated input factors in the presented literature followed by raster width, build orientation and raster angle. Their influence on mechanical properties of FDM printed samples and the accuracy of their dimensions are thoroughly investigated.

Factors that influence output variables such as surface roughness, dimensional accuracy, tensile and compression strength, build time and feedstock consumption found in literature and that are chosen as important for the production of FDM printed embossing dies are presented in Table 3.

Table 3: Output variables important for quality of FDM produced embossing dies and their most influencing input variables found in the literature

Output variable	Input variable
Surface roughness (surface finish)	<ul style="list-style-type: none"> - Layer height (Anitha, Arunachalam and Radhakrishnan, 2001) - Layer height (Horvath, Noorani and Mendelson, 2007) - Layer height (Nancharaiah, Raju and Raju, 2010) - Layer height (Huang et al. 2018)
Dimensional accuracy	<ul style="list-style-type: none"> - Layer height (Xinhua et al. 2015) - Build orientation (Chung Wang, Lin and Hu, 2007) - Raster width (Nancharaiah, Raju and Raju, 2010) - Build orientation (Sood, Ohdar and Mahapatra, 2009) - Raster width (Zhang and Peng, 2012) - Build orientation (Sahu, Mahapatra and Sood, 2013) - Print speed (Zhang and Chou, 2008) - Build orientation (Chung Wang, Lin and Hu, 2007)
Tensile strength	<ul style="list-style-type: none"> - Air gap (Ahn et al. 2002) - Raster angle (Montero et al. 2001) - Build orientation (Chung Wang, Lin and Hu, 2007) - Air gap (Masood, Mau and Song, 2010) - Build orientation (Huang et al. 2018)
Compression strength	<ul style="list-style-type: none"> - Air gap (Chin Ang et al. 2006) - Raster width (Percoco, Lavecchia and Galantucci, 2012)
Build time	<ul style="list-style-type: none"> - Build orientation (Thrimurthulu, Pandey and Venkata Reddy, 2004) - Layer height (Nancharaiah, 2011) - Layer height (Kumar and Regalla, 2012) - Layer height (Mohamed, Masood and Bhowmik, 2016) - Layer height (Hamel, Salisbury and Bouck, 2018)
Feedstock consumption	<ul style="list-style-type: none"> - Air gap (Mohamed, Masood and Bhowmik, 2016)

Table 3 shows a selection of factors which are identified as important for the production of FDM embossing dies. It can be seen that layer height is most influencing factor regarding surface finish and build time. Build orientation and raster width are detected as most influencing on dimensional accuracy. Air gap and build orientation are found to be important factors regarding tensile strength. Compression strength is mostly affected by an air gap and raster width according to the listed literature.

4. CONCLUSIONS

Proper selection of influencing process parameters on the production of embossing dies printed using FDM technique is essential task due to the abundance of various parameters and their setting. Each of these parameters affects the quality of produced die in a certain degree. Knowing which parameters influence desired output variables and adjusting their values to get the optimum quality of embossing die is crucial in implementing additive manufacturing in graphic industry. A lot of work is done on investigating influencing factors of FDM 3D printing technique on quality of produced parts, so there are many resources which can aid in decision making in the production process of embossing dies. Most researches are done regarding the influence of process parameters on mechanical properties, dimensional accuracy and surface finish of FDM printed samples. Input parameters such as layer height, raster width and build orientation are also widely investigated in inspected literature, and general guidelines for adjusting these parameters are provided in respect to the desired outcome. Factors such as a number of contours, nozzle temperature, printing speed and type of infill are less represented and investigated in the research community, so there is still space for further research. Output variables such as feedstock consumption and build time are essential in the process of replacing the conventional production of embossing dies with additive manufacturing techniques and deserves more investigation.

It is evident that layer height is one of the most influencing factors regarding the quality of surface finish. Build orientation is identified as the most important factor for getting the precise dimension of FDM printed samples. For acquiring best tensile strength, build orientation and air gap plays an important role. Build orientation defines the orientation of rasters, and the way object is printed on build platform which affects anisotropy of FDM printed objects altering its mechanical properties. Air gap contributes to the porosity of printed object. Larger air gaps between deposited layers and rasters will lead to the looser inner structure of printed sample decreasing its mechanical properties. Build time appears to be most affected by layer height. Thicker the height of layer is, faster the sample will be printed. The increase of layer height, on the other hand, leads to the rougher surface of the printed sample. Specific recommended values of these parameters are purposely left out because they vary between different printers, feedstock material, dimensions and purpose of desired object etc.

By being aware of the complexity of the FDM process, one can take into consideration all constituting factors for specific use and find their optimum values for getting desired output variables. Applying information presented in this paper can lead to better understanding and solving issues which can appear during the production of FDM printed embossing dies.

5. ACKNOWLEDGMENTS

The research is supported by the Ministry of Education, Science and Technology Development of the Republic of Serbia, project number: 35027 "Development of software model for scientific and production improvement in graphic industry"

6. REFERENCES

- [1] 3D Hubs: "What is 3D Printing? The definitive guide to additive manufacturing", 2018, URL: <https://www.3dhubs.com/what-is-3d-printing#owledge-base> (last request 2018-07-17).
- [2] 3dlink: "Fdm-technologie 3d printer", 2016, URL: <https://www.3dlink.nl/2016/08/23/ddd-drop-printer-in-zeeland/fdm-technologie/> (last request 2018-07-20).

- [3] Ahn, S., Montero, M., Odell, D., Roundy, S., Wright, P.: "Anisotropic material properties of fused deposition modeling ABS", *Rapid Prototyping Journal*, 8 (4), 248-257, 2002. doi: 10.1108/13552540210441166
- [4] Anitha, R., Arunachalam, S., Radhakrishnan, P.: "Critical parameters influencing the quality of prototypes in fused deposition modelling", *Journal of Materials Processing Technology*, 118 (1-3), 385-388, 2001. doi: 10.1016/S0924-0136(01)00980-3
- [5] Arivazhagan, A., Masood, S., Sbarski, I.: "Dynamic mechanical analysis of FDM rapid prototyping processed polycarbonate material", *Proceedings of the 69th annual technical conference of the society of plastics engineers 2011*, (SPE, Boston - Massachusetts, 2011), pages 950-955.
- [6] Arivazhagan, A., Masood, S. H.: "Dynamic mechanical properties of ABS material processed by fused deposition modelling", *International Journal of Engineering Research and Applications*, 2 (3), 2009-2014, 2012.
- [7] Blechschmidt, J.: "Papierverarbeitungstechnik", (Hanser Verlag, München, 2013)
- [8] Bogue, R.: "3D printing: the dawn of a new era in manufacturing?", *Assembly Automation*, 33 (4), 307-311, 2013. doi: 10.1108/AA-06-2013-055
- [9] Bolboacă, S., Jäntschi, L.: "Design of Experiments: Useful Orthogonal Arrays for Number of Experiments from 4 to 16", *Entropy*, 9 (4), 198-232, 2007. doi: 10.3390/e9040198
- [10] Chin Ang, K., Fai Leong, K., Kai Chua, C., Chandrasekaran, M.: "Investigation of the mechanical properties and porosity relationships in fused deposition modelling-fabricated porous structures", *Rapid Prototyping Journal*, 12 (2), 100-105, 2006. doi: 10.1108/13552540610652447
- [11] Chung Wang, C., Lin, T. W., Hu, S. S.: "Optimizing the rapid prototyping process by integrating the Taguchi method with the Gray relational analysis", *Rapid prototyping journal*, 13 (5), 304-315, 2007. doi: 10.1108/13552540710824814
- [12] Fisher, R.A.: "Statistical Methods for researcher Workers", (Oliver and Boyd, London, 1925.)
- [13] Fisher, R.A.: "The arrangement of field experiments", *Journal of the Ministry Agriculture of Great Britain*, 33, 503-513, 1926.
- [14] Hamel, J. M., Salsbury, C., Bouck, A.: "Characterizing the effects of additive manufacturing process settings on part performance using approximation-assisted multi-objective optimization", *Progress in Additive Manufacturing*, 3 (3), 123-143, 2018. doi: 10.1007/s40964-018-0043-5
- [15] Holik, H.: "Handbook of paper and board", Revised and Enlarged Edition, (Wiley-VCH Verlag, Weinheim, 2013.)
- [16] Horvath, D., Noorani, R., Mendelson, M.: "Improvement of Surface Roughness on ABS 400 Polymer Using Design of Experiments (DOE)", *Materials Science Forum*, 561-565, 2389-2392, 2007. doi: 10.4028/www.scientific.net/MSF.561-565.2389
- [17] Huang, B., Meng, S., He, H., Jia, Y., Xu, Y., Huang, H.: "Study of processing parameters in fused deposition modeling based on mechanical properties of acrylonitrile-butadiene-styrene filament", *Polymer Engineering & Science*, 1-9, 2018. doi: 10.1002/pen.24875
- [18] Iggesund: "Embossing and debossing", URL: <https://www.iggesund.com/en/knowledge/knowledge-publications/graphics-handbook/finishing/hot-foil-stamping12/> (last request 2018-02-02).
- [19] Jami, H., Masood, S. H., Song, W. Q.: "Dynamic response of FDM made ABS parts in different part orientations", *Advanced Materials Research*, 748, 291-294, 2013. doi: 10.4028/www.scientific.net/AMR.748.291
- [20] Konstantinović, V.: "Tehnologija grafičke dorade I i II", (Zavod za udžbenike i nastavna sredstva, Beograd, 1997.)
- [21] Kumar, G. P., Regalla, S. P.: "Optimization of support material and build time in fused deposition modeling (FDM)", *Applied Mechanics and Materials*, 110-116, 2245-2251. 2011. doi: 10.4028/www.scientific.net/AMM.110-116.2245
- [22] Masood, S.H., Song, W.Q.: "Development of new metal/polymer materials for rapid tooling using fused deposition modelling", *Materials & Design*, 25 (7), 587-594, 2004. doi: 10.1016/j.matdes.2004.02.009
- [23] Masood, S. H., Mau, K., Song, W. Q.: "Tensile properties of processed FDM polycarbonate material", *Materials Science Forum*, 654-656, 2556-2559, 2010. doi: 10.4028/www.scientific.net/MSF.654-656.2556

- [24] Mohamed, O., Masood, S., Bhowmik, J.: "Optimization of fused deposition modeling process parameters: a review of current research and future prospects", *Advances in Manufacturing*, 3 (1), 42-53, 2015.
- [25] Mohamed, O. A., Masood, S. H., Bhowmik, J. L.: "Mathematical modeling and FDM process parameters optimization using response surface methodology based on Q-optimal design", *Applied Mathematical Modelling*, 40 (23-24), 10052-10073, 2016. doi: 10.1016/j.apm.2016.06.055
- [26] Montero, M., Roundy, S., Odell, D., Ahn, S.H., Wright, P.K.: "Material characterization of fused deposition modeling (FDM) ABS by designed experiments", *Society of Manufacturing Engineers*, 10, 1-21, 2001.
- [27] Nancharaiah, T., Raju, D. R., Raju, V. R.: "An experimental investigation on surface quality and dimensional accuracy of FDM components", *International Journal on Emerging Technologies*, 1 (2), 106-111, 2010.
- [28] Nancharaiah, T.: "Optimization of process parameters in FDM process using design of experiments", *International Journal of Emerging Technology*, 2 (1), 100-102, 2011.
- [29] Percoco, G., Lavecchia, F., Galantucci, L. M.: "Compressive properties of FDM rapid prototypes treated with a low cost chemical finishing", *Research Journal of Applied Sciences, Engineering and Technology*, 4 (19), 3838-3842, 2012.
- [30] Ranjit, K.R.: "Design of Experiments Using the Taguchi Approach: 16 Steps to Product and Process Improvement", (John Wiley, New York, 2001.)
- [31] Rayegani, F., Onwubolu, G.: "Fused deposition modelling (FDM) process parameter prediction and optimization using group method for data handling (GMDH) and differential evolution (DE)", *The International Journal of Advanced Manufacturing Technology*, 73 (1-4), 509-519, 2014. doi: 10.1007/s00170-014-5835-2
- [32] Rikard: "The Graphic Designer's Guide to Embossing – ZevenDesign", 2016, URL: <https://zevendesign.com/graphic-designers-guide-embossing/> (last request 2018-03-15).
- [33] Sahu, R., Mahapatra, S. and Sood, A.: "A Study on Dimensional Accuracy of Fused Deposition Modeling (FDM) Processed Parts using Fuzzy Logic", *Journal for Manufacturing Science & Production*, 13 (3), 183-197, 2013. doi: 10.1515/jmsp-2013-0010
- [34] Sood, A., Ohdar, R., Mahapatra, S.: "Improving dimensional accuracy of Fused Deposition Modelling processed part using grey Taguchi method", *Materials & Design*, 30 (10), 4243-4252, 2009. doi: 10.1016/j.matdes.2009.04.030
- [35] Sood, A., Ohdar, R., Mahapatra, S.: "Parametric appraisal of mechanical property of fused deposition modelling processed parts", *Materials & Design*, 31 (1), 287-295, 2010. doi: 10.1016/j.matdes.2009.06.016
- [36] Stratasys Ltd: "3D Printing & Additive Manufacturing | Stratasys", 2016, URL: <http://www.stratasys.com> (last request 2017-12-07).
- [37] Taguchi, G.: "Introduction to Quality Engineering: Designing Quality into Products and Processes", (Asian Productivity Organization, New York, 1986.)
- [38] Thrumurthulu, K., Pandey, P. Venkata Reddy, N.: "Optimum part deposition orientation in fused deposition modelling", *International Journal of Machine Tools and Manufacture*, 44 (6), 585-594, 2004. doi: 10.1016/j.ijmachtools.2003.12.004
- [39] U-emboss: "Detailed Information on Materials | U-Emboss.com", n.d. URL: <http://u-emboss.com/information/materials-for-die-making/detailed-information-on-materials/> (last request 2017-12-24).
- [40] Upcraft, S., Fletcher, R.: "The rapid prototyping technologies" *Assembly Automation*. 23 (4), 318-330, 2003. doi: 10.1108/01445150310698634
- [41] Wendel, B., Rietzel, D., Kühnlein, F., Feulner, R., Hülde, G., Schmachtenberg, E.: "Additive processing of polymers", *Macromolecular materials and engineering*, 293 (10), 799-809, 2008. doi: 10.1002/mame.200800121
- [42] Wong, K. V., Hernandez, A.: "A review of additive manufacturing" *ISRN Mechanical Engineering*, 1-10, 2012. doi: 10.5402/2012/208760
- [43] Xinhua, L., Shengpeng, L., Zhou, L., Xianhua, Z., Xiaohu, C., Zhongbin, W.: "An investigation on distortion of PLA thin-plate part in the FDM process", *The International Journal of Advanced Manufacturing Technology*, 79 (5-8), 1117-1126, 2015. doi: 10.1007/s00170-015-6893-9
- [44] Yan, X., Gu, P.: "A review of rapid prototyping technologies and systems", *Computer-Aided Design*, 28 (4), 307-318, 1996. doi: 10.1016/0010-4485(95)00035-6

- [45] Zhang, Y., Chou, K.: "A parametric study of part distortions in fused deposition modelling using three-dimensional finite element analysis", Proceedings of the Institution of Mechanical Engineers, Part B: Journal of Engineering Manufacture, 222 (8), 959-968, 2008. doi: 10.1243/09544054JEM990
- [46] Zhang, J., Peng, A.: "Process-Parameter Optimization for Fused Deposition Modeling Based on Taguchi Method", Advanced Materials Research, 538-541, 444-447, 2012. doi: 10.4028/www.scientific.net/AMR.538-541.444



© 2018 Authors. Published by the University of Novi Sad, Faculty of Technical Sciences, Department of Graphic Engineering and Design. This article is an open access article distributed under the terms and conditions of the Creative Commons Attribution license 3.0 Serbia (<http://creativecommons.org/licenses/by/3.0/rs/>).

COMPRESSION RESISTANCE OF SMALL PAPERBOARD PACKAGING SHAPES

Josip Bota , Sonja Jamnicki Hanzer , Dubravko Banić , Maja Brozović 
University of Zagreb, Faculty of Graphic Arts, Zagreb, Croatia

Abstract: Rectangles are the most common packaging shapes. Their stability under compression can vary according to different types of paperboard as well as panels ratios. Rectangular shapes have advantages in transportation and production but are not the only shapes that paperboard packaging has to offer. This paper investigates seven packaging shapes with different cross-sections while keeping the same height and amount of material used. The tested shapes were made with two types of paperboard (with recycled fibre and virgin pulp) and different grammage. The testing was conducted using a modified Crush Test (Lorentzen & Wettre Crush Tester). The results showed that cylinder shape has the most compression resistance while triangular prism and rectangular prism (1:4 panel ratio) the least. Testing rectangles with different panel ratios together with the results of other shapes led to the conclusion that compression resistance mainly depends on the size of the panel. If a shape has larger (less number of) panels it has less resistance to vertical pressure (stackability).

Key words: paperboard packaging, packaging shapes, compression resistance, stackability

1. INTRODUCTION

Primary and secondary packaging play two important roles: product safety and communication with the consumer. Packaging can have additional benefits and setbacks but this paper is focused on the technological aspect of shape. Shape of the packaging is usually determined according to multiple factors: budget - cost of material, production and transportation, brand - recognizable and unique shape, product requirements - products conditions needed to avoid spoilage or damage.

The other aspect of shape is the communicational role. Packaging can have multiple effects on customers. The experiment from Becker et al., (2011) showed that angular packaging shape may inspire intense taste sensations and that designers should create the package according to taste of the food product. According to Pantin-Sohier, (2009) shapes have an effect on the brand image, but this is mostly focused on plastic packaging and packaging materials that are more versatile and moldable. Shapes and size can attract or alienate a consumer (Al-Turaif, 2009) and can also have a big impact when consumers are subjected to time pressure decision making (Silayoi et al, 2004), even different panel ratios of rectangular packaging can influence the purchasing decision (Raghubir et al, 2006).

On the other hand, unique packaging shapes can raise the production and transport cost. Transport packages made from corrugated cardboard are mostly rectangular shape. Accordingly most of the primary and secondary packaging are rectangular as well in order to easily and tightly fit the transport boxes to ensure safety of the product and the packaging. Unique shapes usually need additional inserts or cushioning materials to avoid damage of the packaging during transport. Also, paper and paperboards are recyclable materials (Kirwan, 2011) and there are defined in paperboard grades (DIN Standard 19303 "Paperboard - Terms and grades") according to different levels of recycled/secondary fibre, type of pulp, coatings and color. This has an impact on mechanical properties of paperboard. Recycling can decrease density, tensile and bursting strength, but can increase tear strength (Wistara et al, 1999). Mechanical properties of paperboard like other materials have a cumulative effect when applied to shapes (Vable, 2012). So the same sheets of material will have various results according to shape.

Instruments exist for testing compression and stacking resistance of transport packages and which are in adherence to ISO 12048 Packaging - "Compression and stacking tests" but they are not adequate for testing low forces and small packaging shapes. There are no instruments or standards for testing compression resistance of small paperboard packaging. Crush test instruments (Ring and Edge Crush test, ISO 12192:2011 and ISO 3037:2013 respectively) are used to characterize the compression resistance of elements for corrugated paperboard. They have a smaller testing format and can record weaker forces thus appropriate to obtain the needed results.

The goal of this paper is to investigate what prism shape has the best/worst compression resistance and compare it within different paperboard grades and grammages.

2. METHODS

2.1 Materials

The paperboards chosen are commonly used for packaging of food, drugs and other products. Paperboard specifications, grades (according to DIN Standard 19303 "Paperboard - Terms and grades") and nomenclature are seen in Table 1. The paperboard was conditioned according to the ISO 187:1990 standard at temperature of 23°C ± 1°C and humidity RV 50% ± 2% before and during the testing.


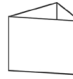
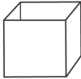
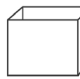
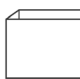
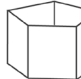
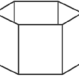
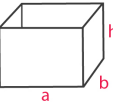
Table 1: Paperboard samples nomenclature and specifications

sample name	grammage	grade	thickness	manufacturer
GD230	230 g/m ²	GD2(recycled/secondary fibre)	0,29 mm	Umka color®
GD280	280 g/m ²	GD2(recycled/secondary fibre)	0,36 mm	Umka color®
GD350	350 g/m ²	GD2 (recycled/secondary fibre)	0,45 mm	Umka color®
GC250	250 g/m ²	GC1 (virgin mechanical pulp)	0,41 mm	Ningbo®
GC270	270 g/m ²	GC2(virgin mechanical pulp)	0,46 mm	AllyKing®

2.2 Samples

To test the compression resistance of shapes, just the bases were used, in order to isolate the influence of the closing, locking and other flaps commonly found in packaging layouts. Test samples were prepared by using the same amount of material. Each sample had the same surface area (250 mm x 50 mm) but differed in the positions of creasing lines to achieve seven types of shapes. The fibre orientation is vertical in order to ensure the highest degree of compression resistance, and how it is commonly oriented in packaging production. The shapes and their specifications are seen in Table 2. The glue area is the same on each shape and is glued by using a water based dispersion of polyvinyl acetate with additives (Signokol®) which is commonly used in the packaging line.

Table 2: Paperboard samples nomenclature and specifications

	Cylinder	Triangular prism	Rectangular prism (1:1)	Rectangular prism (2:3)	Rectangular prism (1:4)	Pentagonal prism	Hexagonal prism	
shape								
dimensions (mm)	Ø 79,6 h = 50	a = 83,3 h = 50	a = 62,5 h = 50	a = 75 b = 50 h = 50	a = 100 b = 25 h = 50	a = 50 h = 50	a = 41,6 h = 50	a= width b= length h= height (in millimeters)

2.3 Measurement procedure

After the glue was completely dry (24h after gluing) the samples were tested with vertical pressure using a modified Crush test instrument (Lorentzen & Wettre Crush Tester). The samples were pressed between two plates so the force was applied on the upper and lower edges of the shapes. The test speed (movement of the upper plate) was 48,0 mm/min. The instrument records the maximum force that the samples withstand till barreling occurs (shape deformation). Each shape and material was tested with ten identical samples.

2.4 Calculations

In order to compare different shapes and types of paperboard and to omit the influence of grammage a compression index was calculated. The formula was devised resembling the bursting index from the ISO 2759-2001 standard.

$$I = \frac{F}{g} (N \cdot g/m^2) \quad (1)$$

I - Compression index (N·m²/g); F - Force of vertical pressure (N); g - Grammage of paperboard (g/m²)

3. RESULTS AND DISSCUSION

The results in Figure 1 show compression resistance force for seven investigated shapes each made from five different paperboards. According to the results cylinder shape showed the highest compression resistance by far. This confirmed previous research that cylinders and cones have better dynamic strength than rectangular ones (Hoffmann, 2000). Collectively it is visible that the GC270 sample showed the best results in all shapes except with the cylinder shape, the best result there was GD350. In the cylinder shape of the GD350 sample we can assume that maybe the larger grammage gives additional support in relation to other shapes. This is an interesting finding and should be additionally explored. GD270 is made from virgin mechanical pulp and was expected to overperform paperboards with recycled fibre but it wasn't clear at what grammage would GD paperboards show same characteristics as GC. The least compression resistance for GD230 and GD280 was with triangular prism shape but for the GD350, GC250 and GC270 it was with the rectangular prism (1:4) shape. The smaller panels of the rectangular prism (1:4) in the weaker material could act as a type of support for the object. From the results it is also visible that the GD350 paperboard with recycled/secondary fibre could replace GD250 for all types of shapes.

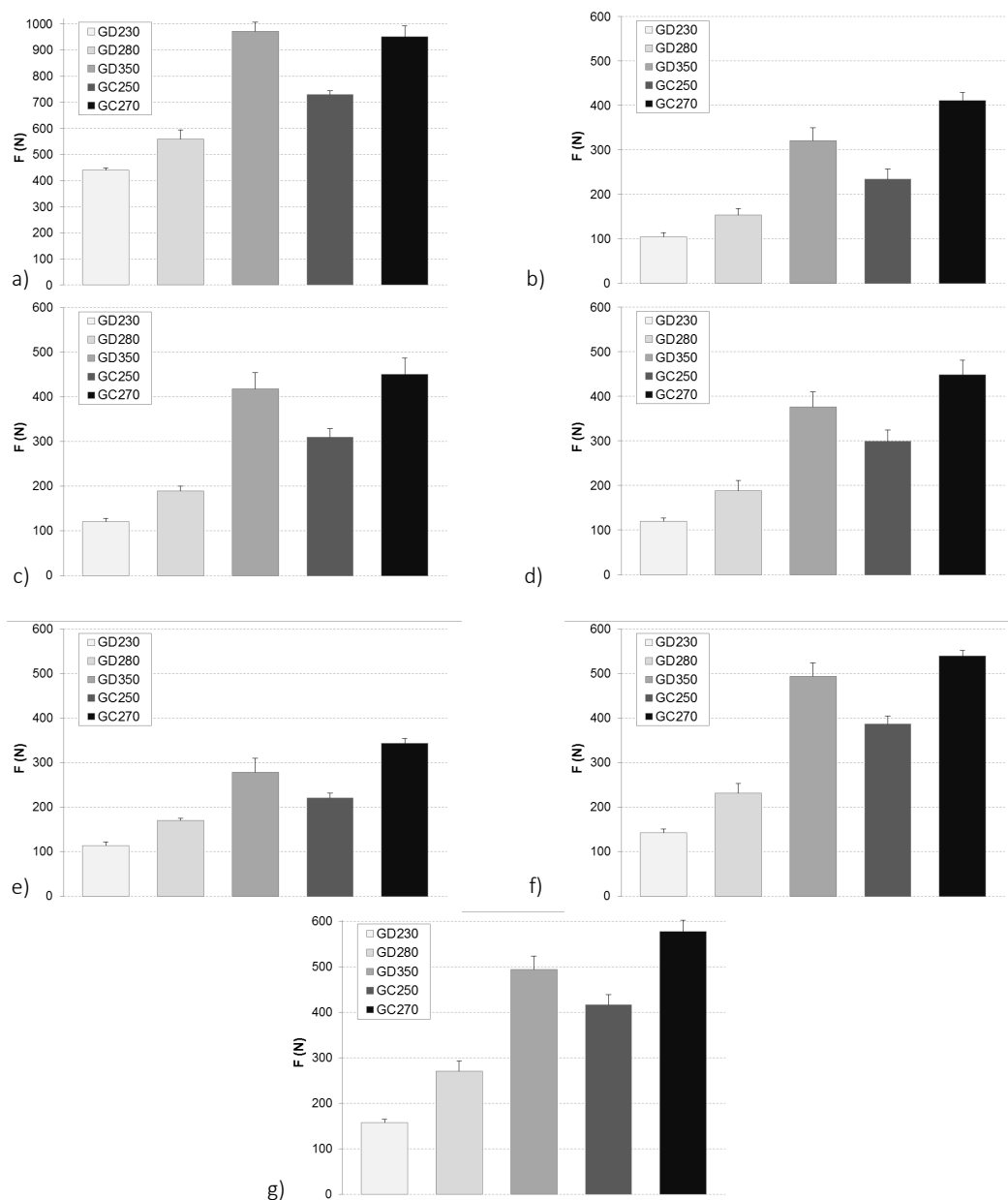


Figure 1: a) Cylinder; b) Triangular prism; c) Rectangular prism (1:1); d) Rectangular prism (2:3); e) Rectangular prism (1:4); f) Pentagonal prism; g) Hexagonal prism

In order to compare the performance of paperboards according to shape, the cylinder shape values (as the highest in all samples) were set as a benchmark. This calculation is presented in Table 3. The shapes are listed from the highest values to the lowest except in the case of triangular prism for the GD230 and GD280. Cylinder shape can't be easily compared to other shapes because it doesn't have any creasing or folding (no sharp edges), so no visible panels. It can be viewed as a shape with endless amount of panels. All samples were made from the same amount of material so if the shape has more panels the panels are smaller in size. It can be seen that the smaller the panel the higher the compression resistance. Large panels, as a weak point can be best observed in the case of rectangular shapes with different panel rations.

Also, the results show that when the grammage of GD2 paperboard is larger, the lesser the difference between the cylinder and other shapes. The same case can be observed with the GC grade paperboards. This can be credited to the material thickness and other mechanical properties of the paperboards that change with the increase of thickness and weight.

Table 3: Compression values in relation to the cylinder shape

	GD230	GD280	GD350	GC250	GC270
Cylinder	100,0%				
Hexagonal prism	35,7%	48,4%	50,9%	57,1%	60,8%
Pentagonal prism	32,5%	41,4%	50,8%	53,1%	56,9%
Rectangular prism (1:1)	27,4%	33,9%	43,0%	42,6%	47,5%
Rectangular prism (2:3)	27,2%	33,7%	38,7%	41,0%	47,2%
Triangular prism	23,8%	27,4%	28,6%	32,1%	43,3%
Rectangular prism (1:4)	25,9%	30,4%	33,0%	30,3%	36,1%

But to fully compare the values with excluding the grammage of paperboard a Compression index was calculated according to formula in Section 2.4. The results of compression indexes are displayed in Table 4. The compression index shows the neutral specification of material and how does each material perform according to shape. GC270 paperboard shows, by far, the highest values across all shapes and paperboards. According to these results it can be said that the GD350 is equivalent to the GD250 sample. From these results it can also be seen the larger the grammage the better the index. The biggest difference is seen between GD280 and GD350.

Table 4: Compression index of paperboard samples in comparison with shape

	Compression index (N·m ² /g)				
	GD230	GD280	GD350	GC250	GC270
Cylinder	1,914	1,999	2,778	2,918	3,519
Hexagonal prism	0,683	0,968	1,414	1,667	2,140
Pentagonal prism	0,623	0,827	1,411	1,549	2,001
Rectangular prism (1:1)	0,525	0,677	1,196	1,242	1,673
Rectangular prism (2:3)	0,520	0,674	1,074	1,198	1,660
Triangular prism	0,456	0,549	0,917	0,938	1,524
Rectangular prism (1:4)	0,495	0,608	0,795	0,884	1,272

It is important to note the there is a difference in volume of the shapes. Cylindrical prism has the biggest volume followed by hexagonal prism and the volume further drops when the shape has fewer numbers of panels. When grouping the tested shapes it is important to note that some shapes like pentagonal and cylinder prism cause a waste of space when packed for shipping, and that type of packaging would require additional fillers. According to previous research and mathematical papers it is theorized and proven that hexagonal shapes are an optimal structure and the best material-volume ratio(Hales, 1999; R  z, 2016). This theory is applied in furniture construction and proven to be best in impact behavior, energy absorption and compression (Guo et al., 2010; Wang et al., 2009; Wang, 2009) which is also used in filling constructions for 3D printing (Lu et al., 2018).

4. CONCLUSIONS

This research was aimed to investigate the difference between small packaging shapes together with the use of different types of paperboards. For this research a new type of testing was developed using Crush test instrument. The results led to these conclusions:

- Cylinder shape proved to be the best option for vertical compression resistance when using the same amount of material, followed by hexagonal prism, pentagonal prism, rectangular prism (1:1), rectangular prism (2:3), triangular prism and rectangular prism (1:4)
- The weak points of angular prisms are large panels. They decrease the compression resistance if compared with smaller panels.
- The gap of compression resistance values between different shapes is smaller when using larger grammage.
- Paperboards with recycled/secondary fibres display weaker mechanical properties for compression resistance when compared with paperboards made from virgin mechanical pulp.
- 350 g/m² GD2 can substitute 250 g/m² GC1 paperboard in the case of compression resistance
- Hexagonal prism is show as an optimal solution due to better compression resistance and larger volume for the same amount of material, with minimal losses of space in collective transportation.

This research is limited to the samples tested in the paper and should be expanded in further research. Multiple variables should be additionally tested separately (size of paperboard sheets, size and heights of shapes, other types of paperboard grades and grammages). Those results should also be compared with results of packaging shapes with different types of closing components (flaps, crash lock, glued locks... etc.)

5. REFERENCES

- [1] Al-Turaif, H.: "Surface coating properties of different shape and size pigment blends" *Progress in Organic Coatings*, 65 (3), 322–327, 2009. doi: 10.1016/j.porgcoat.2009.01.001.
- [2] Becker, L., van Rompay, T.J.L., Schifferstein, H.N.J., Galetzka, M.: "Tough package, strong taste: The influence of packaging design on taste impressions and product evaluations", *Food Quality and Preferences*, 22 (1), 17–23, 2011. doi: 10.1016/j.foodqual.2010.06.007
- [3] Guo, Y., Hou, J., Xu, W., Cao, G.: "Comparison Studies on Strength Properties of Corrugated and Honeycomb Composite Paperboards". *Proceedings of 17Th IAPRI World Conference on Packaging* (International Association of Packaging Research Institutes: Tianjin, China, 2010)
- [4] Hales, T.C.: "The honeycomb conjecture", *Discrete & Computational Geometry*, 25 (1), 1–22, 1999.
- [5] Hoffmann, J.: "Compression and cushioning characteristics of moulded pulp packaging", *Packaging Technology and Science*, 13 (5), 211–220, 2000. doi: 10.1002/1099-1522(200009)13:5<211::AID-PTS515>3.0.CO;2-0
- [6] Coles, R., Kirwan, M. eds.: "Paper and Paperboard Packaging, in: *Food and Beverage Packaging Technology*", (Oxford, Wiley-Blackwell, 2011), page 213. doi: 10.1002/9781444392180.ch8
- [7] Lu, C., Qi, M., Islam, S., Chen, P., Gao, S., Xu, Y., Yang, X.: "Mechanical performance of 3D-printing plastic honeycomb sandwich structure", *International Journal of Precision Engineering and Manufacturing-Green Technology*, 5 (1), 47–54, 2018. doi: 10.1007/s40684-018-0005-x
- [8] Pantin-Sohier, G.: "The Influence of the Product Package on Functional and Symbolic Associations of Brand Image", *Recherche et Applications en Marketing (English Edition)*, 24 (2), 53-71, 2009. doi: 10.1177/205157070902400203
- [9] Raghubir, P., Greenleaf, E.A.: "Ratios in Proportion: What Should the Shape of the Package Be?" *Journal of Marketing*, 70 (2), 95–107, 2006. doi: 10.1509/jmkg.70.2.95
- [10] Rätz, T.: "The silent hexagon: explaining comb structures", *Synthese*, 194 (5), 1703-1724, 2016. doi: 10.1007/s11229-016-1014-3
- [11] Silayoi, P., Speece, M.: "Packaging and purchase decisions: An exploratory study on the impact of involvement level and time pressure", *British Food Journal*, 106 (8), 607-628, 2004. doi: 10.1108/00070700410553602
- [12] Vable, M.: "Mechanical Properties of Materials", 2nd ed, URL <http://madhuvable.org/wp-content/uploads/2016/04/Entire%20Book%202018.pdf> (last request: 2018-10-17)

- [13] Wang, D.M., Wang, Z.W., Liao, Q.H.: "Energy absorption diagrams of paper honeycomb sandwich structures", *Packaging Technology and Science*, 22 (2), 63–67, 2009. doi: 10.1002/pts.818
- [14] Wang, D.: "Impact behavior and energy absorption of paper honeycomb sandwich panels", *International Journal of Impact Engineering*, 36 (1), 110-114, 2009. doi: 10.1016/j.ijimpeng.2008.03.002
- [15] Wistara, N., Young, R.A.: "Properties and treatments of pulps from recycled paper. Part I. Physical and chemical properties of pulps", *Cellulose*, 6 (4), 291–324, 1999.



© 2018 Authors. Published by the University of Novi Sad, Faculty of Technical Sciences, Department of Graphic Engineering and Design. This article is an open access article distributed under the terms and conditions of the Creative Commons Attribution license 3.0 Serbia (<http://creativecommons.org/licenses/by/3.0/rs/>).

THE INFLUENCE OF THE TYPE OF A BEVERAGE ON ITS PACKAGING SHAPE

Gordana Delić , Gojko Vladić , Bojan Banjanin , Jelena Vasić 

University of Novi Sad, Faculty of Technical Sciences,
Department of Graphic Engineering and Design, Novi Sad, Serbia

Abstract: A lot of research today implies that packaging attributes have an essential role in attracting consumer attention, creating expectations and influencing product choice. Many studies have documented that people match a variety of tastes, aromas, and flavours to other sensory features, such as shapes and colours. This study investigates the influence of the type of a beverage on its packaging shape. The study is designed to discover what packaging materials, the shape of packaging body and the type of packaging opening consumers prefer for each beverage: milk (chocolate milk, milkshake), soda, juice, yoghurt, fruit yoghurt, water and ice coffee. The investigation was conducted through a survey where participants were asked to choose a packaging shape from a variety of presented shapes. The stimuli that were used were grayscale photographs of packaging without any graphic design applied. These packaging differed not only in shape but also in materials from which they were made and the type of opening system. The result implies that participants that consumed a certain type of drink on regular basis were more open for new different atypical packaging shapes. On the other hand, for products that they consumed less, they preferred a packaging that was most commonly presented and placed on the market where they live. Also, these results support the view of many researchers that delicate and subtle flavours were best presented in packaging with rounded and curvy shapes, while sour and intense flavours are best presented with angular shapes. Characteristic that turned out to be very important was the shape of the packaging body but in terms of ergonomics and ease of use. It was found that there is a positive correlation between aesthetic features and ergonomic features of the packaging. These findings are relevant to those researchers interested in taste-vision correspondences, it should contribute to product communication, and it can be used as a base for future research focused on packaging shape and ergonomics.

Key words: beverage, drink, packaging, shape, ergonomics

1. INTRODUCTION

A growing body of empirical research suggests that packaging has replaced the role of salespersons in the communication with consumers at the point of purchase. Today, most consumers postpone their purchase decisions to the moment when they find themselves in the store, so the first impression between the consumer and a product, or to be more precise, the packaging of the product has become relevant. However, communication through packaging has become more challenging, since the number of products that are offered is rapidly increasing. In such an environment cluttered with products, purchase decisions are often not based on a systematic and critical evaluation of product features, but rather on heuristic and fast processing of packaging cues. Marketers respond to this development by using various visual techniques to increase the consumer's attention, such as the use of original materials, shapes, and colours in their packaging (Ooijen et al, 2016).

The traditional functions of packaging for beverage and food are to protect the products from degradation processes (primarily produced by environmental factors, such as oxygen, light and moisture), to contain the product, and to provide consumers with ingredient and nutritional information. The packaging here acts as a barrier between the food product and the outside environment while avoiding the migration of harmful substances from the packaging to the food. Materials that have traditionally been used in beverage/food packaging include glass, metals (aluminium, foils and laminates, tinplate, and tin-free steel), paper and paperboards, and plastics. The right selection of the packaging material plays a vital role in maintaining product quality and freshness during distribution and storage. Packaging for beverage often combines several materials to exploit each material's functional or aesthetic properties. New advances in this field include the development of multilayer systems, new approaches based on active or intelligent packaging, or materials with lower environmental impacts as bio-based polymers. The use of plastics in beverage packaging has continued to increase due to the low cost of materials and functional advantages (such as thermosealability, microwavability, optical properties, and unlimited sizes and shapes) over traditional materials such as glass and tinplate (Ramos et al, 2015). Packaging openability and usability is an area that has been explored by ergonomics in its various aspects: biomechanical, anthropometric, and

also the cognitive, which involves perception and comprehension of the information provided. The packaging openability and usability is important especially for products such as beverages that are meant to be used in “to go” situations. In this situations, opening that requires the use of scissors wouldn’t be the best way to go, but the opening system that includes a simple twist motion such as screw thread caps, or packaging that includes a straw hole (and a straw) would be easier to use (Bonfim et al, 2015). Over the past three decades, a lot of research has highlighted how beverage and food packaging can inform, tempt, and bias the consumer, both at the point of sale, as well as during consumption. Ongoing investigations suggest that even relatively minor adjustments to the visual design of the packaging, such as to the shapes, colours, orientations, and positions of design elements, can significantly impact consumer’s product evaluations and purchase intent either positively or negatively (Simmonds et al, 2018; Steenis, 2017; Vladić et al, 2015). With improvements in packaging technology come new opportunities for packaging design. One such trend is the ability to introduce transparency into a wide range of product packaging. Results suggested that transparent packaging increased willingness to purchase, expected freshness, and expected quality, as compared to packaging that used food imagery instead. Also, participants assumed the products to be tastier, to be more innovative etc. (Westerman et al, 2013).

Ooijen et al. (2016) investigated the influence of atypicality of packaging on product quality perception. The researchers found support for the hypothesis that atypical packaging design enhances the processing of product information, and improves the recall of product claims presented on the product. They found that the persuasiveness of weak and strong product claims on the packaging was affected by whether the packaging design was typical or atypical. When packaging was atypical, strong claims resulted in a higher quality judgment, but weak claims resulted in a lower willingness to pay - compared to when packaging was typical. Therefore, atypical packaging may not always be beneficial for product evaluation (Ooijen et al, 2016).

Most drink and food products come in packaging of a particular shape or form, whose attributes prime various concepts in the mind of the consumer. A growing body of empirical research now demonstrates that people associate different basic tastes and taste words with specific packaging shapes. While it may be evident that semantic knowledge concerning products, based on the packaging and design elements (e.g., typeface, logo, images), can guide the taste expectations that consumers generate about a given product, many research work has been done to demonstrate that this happens even with unfamiliar stimuli. Specifically, shape features (e.g., straight vs curvy, or symmetrical vs asymmetrical) have been shown to influence the taste that people naturally associate with a given shape. It was found that people match tastes and shape features in a manner that is significantly non-random and both packages and their respective shape-related features can convey information about the likely taste of a product (Velasco, 2016; Becker et al, 2011; Valesco et al, 2014; Machiels et al, 2016; Husić-Mehmedović et al, 2017). In a similar field, research was done to investigate whether shape-taste correspondences would influence consumers’ expectations concerning coffee. Amongst other findings, the results revealed that the coffee was expected to be more aromatic from narrower diameter mugs, the coffee associated with shorter mugs was expected to be both bitterer and more intense, and the coffee was expected to be sweeter from wider diameter mugs (Doorn et al, 2017).

There are also researches focused on the influence of the packaging colour on packaging perception. In food packaging, light and pale colours are often used to highlight product healthiness. What has been found is that positive health cues may also convey another crucial information about the taste of the product which with pale colours often gets a negative connotation.

As it has been presented in previous text, a lot of research today implies that packaging attributes have an important role in attracting consumer attention, creating expectations and influencing product choice. Many studies have documented that people match a variety of tastes, aromas, and flavours to other sensory features, such as shapes and colours. This study investigates the influence of the type of a beverage on its packaging shape, materials of the packaging, and the type of packaging opening system. The investigation was done through a survey where the participants were asked to define the packaging with the best aesthetic and ergonomics features for a certain type of a beverage. Investigated beverages were: milk (chocolate milk, milkshake), soda, juice, yoghurt, fruit yoghurt, water and ice coffee.

2. METHODS

The research was conducted through a survey completed by 30 participants. The age range of participants was 21-22. Demographic data of participants such as gender was also collected. In the first part of the survey, participants were asked to define which beverage they usually consume at lunch break at college

or work and to define the most important characteristics they look for while buying that product. The next series of questions of the survey was divided into seven parts that included the same questions, but in each part the questions were focused on a different kind of beverage. These were: milk (chocolate milk, milkshake), soda drink, juice, yoghurt, fruit yoghurt, water, and ice coffee. For each type of beverage, participants were asked to choose the most suitable packaging from 6 different types of presented packaging. By selecting a type of packaging, they were asked to define the reasons for choosing that packaging and then they were broth to a series of questions related to the selected type of packaging. Here, the chosen type of packaging was divided into several version of that packaging. The versions varied mostly in shape of the body or in type of an opening system. The participants had the task to choose the version with the best aesthetics, the packaging with the most comfortable shape, the packaging with the best opening and the packaging with the best closing system. As mention, these series of question repeated for every type of beverage. Since all the packaging were evaluated as products that are used outside of the home, at college or work, all the questions and stimuli were formed with a focus on that. The participants could take as much time as they needed to complete the survey.

2.1 Stimuli used in the research

The stimuli that were used in the survey were grayscale photographs of packaging without any graphic design applied. These packaging differed not only in shape but also in materials from which they were made and the type of opening system. Stimuli that were used can be divided into 6 types of packaging that differ in a base material or basic shape from which they were made. Each type is marked with a letter: group A: plastic cup-shaped packaging; group B: plastic bottle; group C: glass bottle; group D: bag-shaped packaging; group E: metal can packaging; group F: packaging made of plastic-coated carton known as tetra pak (in upcoming text referred to as tetra pak). Also, within one group there were more variations of that type of a packaging in order to divide them by a body shape, opening or closing system. Variations within one group are marked with a number. All packaging had about the same volume, so the size of the packaging was not an influencing factor. Based on this division there were 36 different packaging. All the packaging used as stimuli in this research are shown in Figure 1. The layout of one question from the survey is shown in Figure 2.

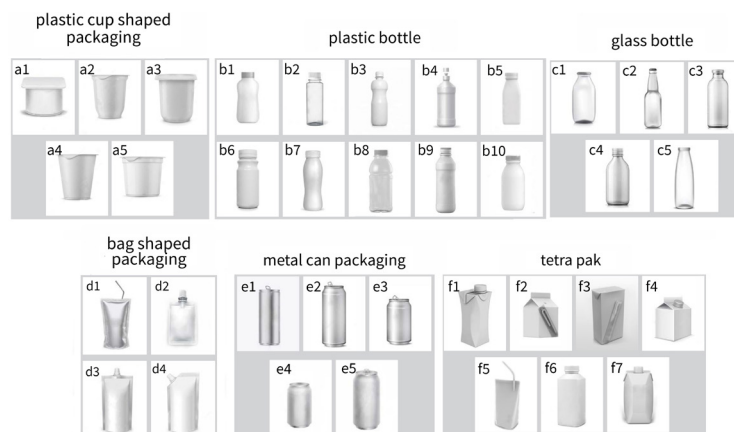


Figure 1. Packaging that were used as stimuli in this research

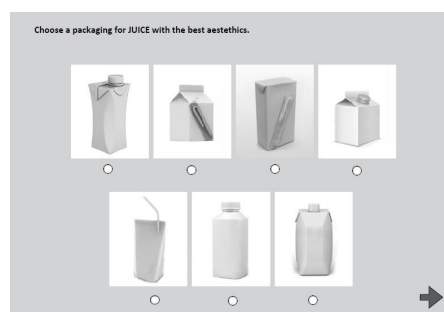


Figure 2: Example of one question from the survey

3. RESULTS AND DISCUSSION

The responses from 30 participants were collected and presented graphically. At the question: “What do you usually drink during lunch break at college/work..?” the most frequent answer was water (70%), as shown in Figure 3. At the question: “What is most important to you when choosing a beverage?” most frequent answer was the quality of the product inside it and portability and convenience to carry it in a purse/bag. Other answers can be seen in Figure 4.

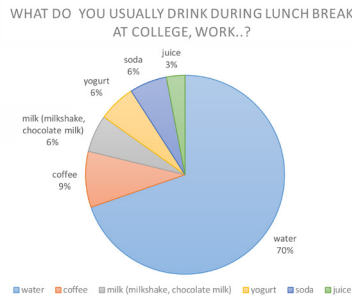


Figure 3: The most consumed beverages by participants



Figure 4: The most important features of the product considered while purchasing rated by participants

3.1 Aesthetic and ergonomic features of the packaging

Since the purpose of this research was to investigate the type of a beverage as an influencing factor on choosing the packaging shape, the collected responses given by participants of the packaging with the best aesthetic features and most comfortable shape were analysed within one type of a beverage.

Milk (milkshake, chocolate milk) - Collected responses of packaging for milk (milkshake, chocolate milk) with the best aesthetic features and the most comfortable shape are presented in Figure 5. As it can be seen in Figure 5, for milk (milkshake, chocolate milk) participants prefer plastic bottles, glass bottles and tetra pak packaging. From those, based on the number of responses, packaging with the best aesthetic features were b2, b7, f1 and f6 (Figure 5a), and the most comfortable shape of the packaging had the packaging b7 and f1 (Figure 5b). Participants preferred tetra pak mainly because it is practical for use and portable, it has a good opening system and the packaging material is light. As the best feature of plastic packaging, they emphasised a good closing system.

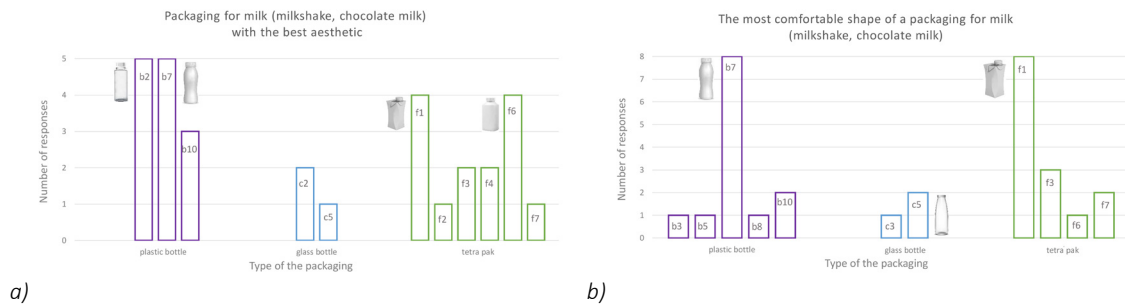


Figure 5: Packaging for milk (milkshake, chocolate milk) with the best aesthetic (a) and the most comfortable shape (b) based on participants' ratings

Soda drink - Collected responses of packaging for soda drink with the best aesthetic features and the most comfortable shape are presented in Figure 6. As it can be seen, for soda drink participants prefer plastic bottles, glass bottles and metal can packaging. From those, based on the number of responses, packaging with the best aesthetic features were b2, b9, e1 and e2 (Figure 6a), and the most comfortable shape of the packaging had the packaging b3, e2 and e3 (Figure 6b). Participants preferred plastic bottles mainly because they thought it is standard packaging for that product (soda), it is practical for use and portable, it has a good closing system and the packaging material is light. The most common reason for choosing a metal can packaging was the standard shape of the packaging on which they are used to, and they liked the aesthetic of that type of the packaging.

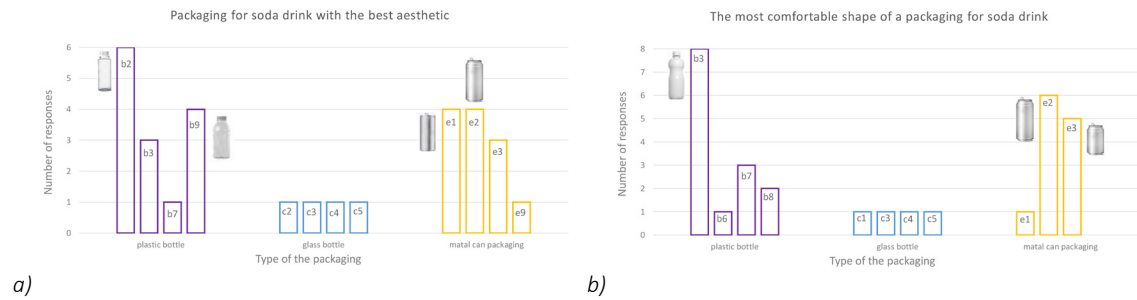


Figure 6: Packaging soda drink with the best aesthetic (a) and the most comfortable shape (b) based on participants' ratings

Juice - Collected responses of packaging for juice with the best aesthetic features and the most comfortable shape are presented in Figure 7. As it can be seen for juice, participants prefer plastic bottles, glass bottles, bag-shaped packaging, metal can packaging and tetra pak packaging. From those, based on the number of responses, packaging with the best aesthetic features were b2, c5 and d4 (Figure 7a), and the most comfortable shape of the packaging had the packaging b3, b7 and d4 (Figure 7b). Participant preferred plastic packaging because it has a good closing system, it is practical for use and portable, it is comfortable for hand gripping, it has a stable stand (it stays steady on the table) and because the packaging material is light. The second most common choice was bag-shaped packaging, mostly because they thought it is standard packaging for that type of a beverage and the material of the packaging is light.

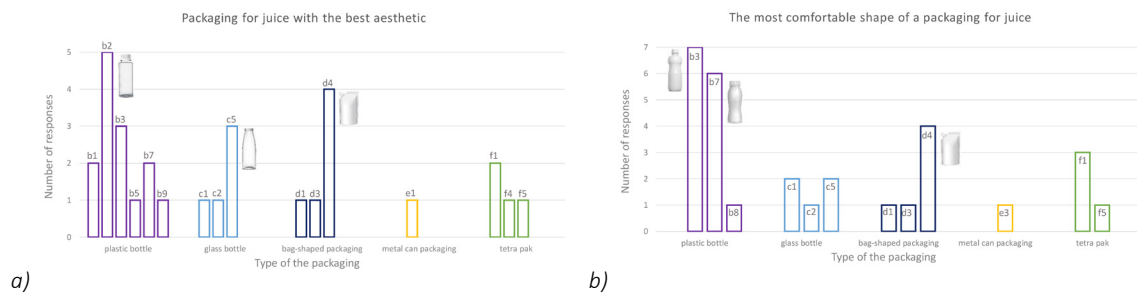


Figure 7: Packaging for juice with the best aesthetic (a) and the most comfortable shape (b) based on participants' ratings

Yoghurt - Collected responses of packaging for yoghurt with the best aesthetic features and the most comfortable shape are presented in Figure 8. As it can be seen for yoghurt, participants prefer plastic bottles, tetra pak packaging, plastic cup-shaped packaging and glass bottles. From those, based on the number of responses, packaging with the best aesthetic features were b7 and b5 (Figure 8a), and the most comfortable shape of the packaging had the packaging b7 (Figure 8b). Participants preferred plastic packaging because it has a good opening and closing system, it is practical for use and portable and it is comfortable for hand gripping.

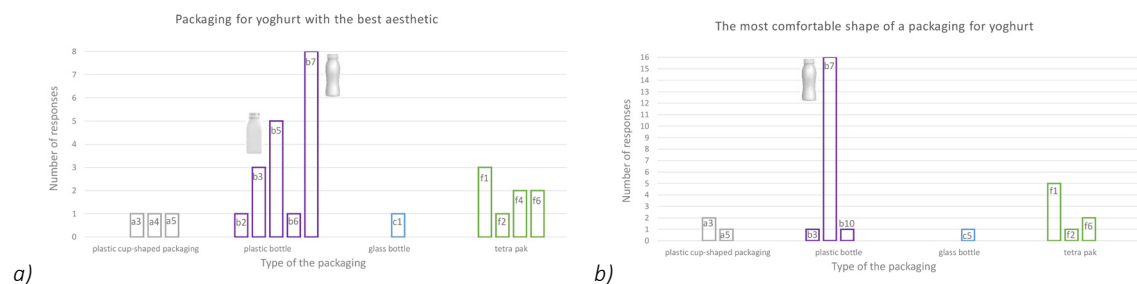


Figure 8: Packaging for yoghurt with the best aesthetic (a) and the most comfortable shape (b) based on participants' ratings

Fruit yoghurt - Collected responses of packaging for fruit yoghurt with the best aesthetic features and the most comfortable shape are presented in Figure 9. As it can be seen for fruit yoghurt, participants prefer plastic bottles, plastic cup-shaped packaging and tetra pak packaging. From those, based on the number of responses, packaging with the best aesthetic features was b7 (Figure 9a), and the most comfortable shape of the packaging had the packaging b7 (Figure 9b). Participant preferred plastic packaging because they think it is a standard packaging for that type of a beverage, it has a good opening and closing system, it is practical for use and portable, it is comfortable for hand gripping and it has a stable stand (it stays steady on the table).

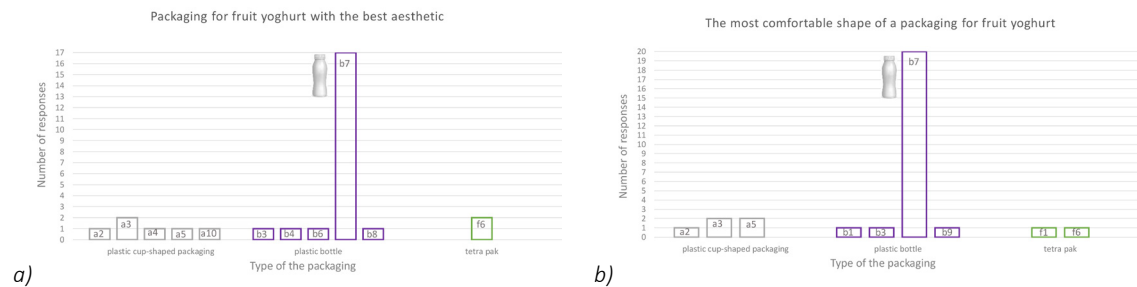


Figure 9: Packaging for fruit yoghurt with the best aesthetic (a) and the most comfortable shape (b) based on participants' ratings

Water - Collected responses of packaging for water with the best aesthetic features and the most comfortable shape are presented in Figure 10.

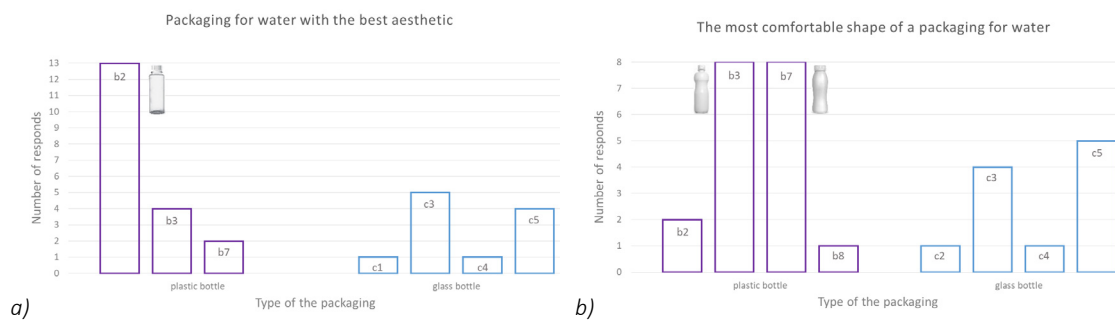


Figure 10: Packaging for water with the best aesthetic (a) and the most comfortable shape (b) based on participants' ratings

As it can be seen in Figure 10, participants prefer plastic bottles and glass bottles for water packaging. From those, based on the number of responses, packaging with the best aesthetic features was b2 (Figure 10a), and the most comfortable shape of the packaging had the packaging b3 and b7 (Figure 10b). Participant preferred plastic packaging because they thought it is a standard packaging for that type of a drink, it has a good opening and closing system, it is practical for use and portable and it is comfortable for hand gripping. The second most common choice was glass bottles, mostly because they are good for the environment, and their aesthetic features.

Ice coffee - Collected responses of packaging for ice coffee with the best aesthetic features and the most comfortable shape are presented in Figure 11. As it can be seen for ice coffee, participants prefer plastic cup-shaped packaging, plastic bottles, glass bottles, metal can packaging and tetra pak packaging. From those, based on the number of responses, packaging with the best aesthetic features was a4, b7 and e1 (Figure 11a), and the most comfortable shape of the packaging had the packaging a2 and b7 (Figure 11b). Participant preferred plastic cup-shaped packaging because it was made from a light material and it had a stable stand (it stays steady on the table). The second most common choice was plastic bottles because they have a good opening and closing system, it is practical for use and its portable, it is comfortable for hand gripping and it has a stable stand. The third most common choice was a metal can packaging mostly because participants preferred their aesthetic features.

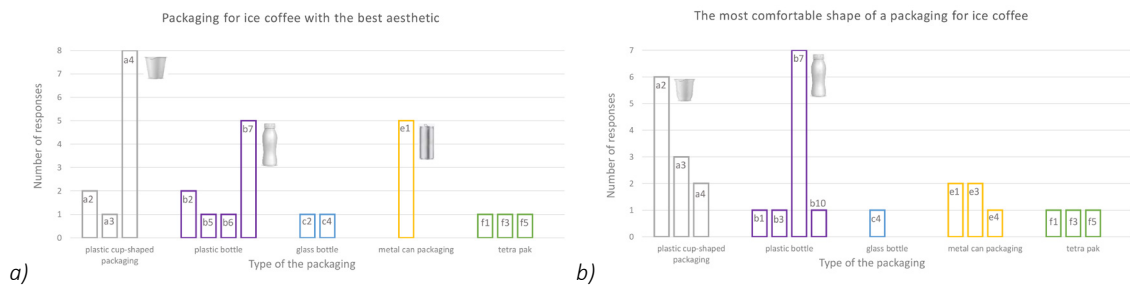


Figure 10: Packaging for ice coffee with the best aesthetic (a) and the most comfortable shape (b) based on participants' ratings

3.2 Opening and closing system of the packaging

Since the results of the best opening and closing system of the packaging were almost unanimous, they are presented together for every type of beverage in Figure 11. As it can be seen, for milk (milkshake, chocolate milk) the best opening and closing system had the packaging f6. For yoghurt and fruit yoghurt the packaging that was rated the most was b7, and for water it was b3. For soda drink, participants rated packaging b3 and e2 as the ones with the best opening and closing system, and for juice, it was b3 and d4. When it comes to ice coffee, based on participants' rating packaging b7 and a2 were mostly chosen as the best in this category.



Figure 11: Packaging with the best opening and closing system based on participants' rating

Between types of beverages, a diversity in answers was found. For milk (milkshake, chocolate milk) participants preferred plastic bottles and tetra pak packaging. For soda drink participants preferred plastic bottles and metal can packaging. As packaging for juice, participants preferred plastic bottles and bag-shaped packaging. For yoghurt and fruit yoghurt participants preferred plastic bottles. For water, participants preferred plastic bottles and glass bottles, and finally, for ice coffee they preferred plastic bottles and plastic cup-shaped packaging. However, it can be easily noticed that plastic bottles take a large share as a preferred packaging, regardless of the type of the beverage. Even though the plastic bottle is appropriate to every type of a beverage, its shape varies from one beverage to another. For milk, yoghurt, ice coffee and other delicate and subtle flavours, packaging with rounded and curvy shapes were a more common choice, while for soda drink and other sour and sharp flavours complex packaging with angular shapes were a more common choice. The complex packaging was also a common choice for water. When choosing a packaging with the most comfortable shape, participants were focused mostly on the body of the packaging. Often the packaging that was rated as one with the best aesthetic features was also a packaging rated as the one with the most comfortable shape. This means that packaging with good aesthetic values was perceived as a comfortable one, or vice versa, packaging with comfortable shape was perceived as eye pleasing. Since the investigated packaging were evaluated as products that are used outside of the home, results showed that portability, convenience in carrying, opening and closing system were crucial factors in selecting a packaging. For packaging with the best opening and closing system, those with screw thread caps were a clear choice for most types of beverages. When observing the responses of participants separately it is noticed that participants that consumed a certain type of beverage on regular basis were more open for new different atypical packaging shapes. On the other hand, for products that they consumed less, they preferred a packaging that was most commonly presented and placed on the market where they live.

4. CONCLUSIONS

Based on the results of the survey, it can be concluded that the type of a beverage is an influencing factor to its packaging shape. Results collected by a survey indicate that there was a difference in choice of the most suitable packaging between each beverage type. The most common packaging choice, regardless of beverage type, was a plastic bottle. Even though the plastic bottle was defined as appropriate to every type of a beverage, its chosen shape varied from one beverage to another. Packaging with rounded and curvy shapes was a more common choice for beverages with delicate and subtle flavours, while complex packaging with angular shapes was a more common choice for sour and intense flavours and water. Often the packaging that was rated as one with the best aesthetic features was also a packaging rated as the one with the most comfortable shape. This means that packaging with good aesthetic values was perceived as a comfortable one, or vice versa, packaging with comfortable shape was perceived as eye pleasing. Since the investigated packaging were evaluated as products that are used outside of the home, at college or work, as expected, results showed that portability, convenience in carrying, opening and closing system were crucial factors in selecting a packaging. When observing the responses of participants separately, it was noticed that participants that consumed a certain type of beverage on a regular basis were more open for new, different atypical packaging shapes. On the other hand, for products that they consumed less, they preferred a packaging that was most commonly presented and placed on the market where they live. These findings are relevant to those researchers interested in taste-vision correspondences, it should contribute to product communication, and it can be used as a base for future research focused on packaging shape and ergonomics.

5. ACKNOWLEDGENTS

The research is supported by the Ministry of Education, Science and Technology Development of the Republic of Serbia, project number: 35027 "Development of software model for scientific and production improvement in graphic industry".

6. REFERENCES

- [1] Bonfim, F. H.C., Paschoarelli, L.C.: "Visualization and Comprehension of Opening Instructions in Child Resistant Packaging", *Procedia Manufacturing* 3, 6153-6160, 2015. doi:10.1016/j.promfg.2015.07.906.
- [2] Becker, L., Rompay, T.J.L., Schifferstein, H. N. J., Galetzka, M.: "Tough package, strong taste: The influence of packaging design on taste impressions and product evaluations", *Food Quality and Preference* 22, 17-23, 2011. doi:10.1016/j.foodqual.2010.06.007.
- [3] Doorn, G., Woods, A., Levitan, C.A. Wan, X., Valesco, C., Bernal- Torres, C., Spence, C.: "Does the shape of a cup influence coffee taste expectations? A crosscultural, online study", *Food Quality and Preference* 96, 201-211, 2017. doi:10.1016/j.foodqual.2016.10.013.
- [4] Husić- Mehmedović, M., Omeragić, I., Batagelj, Z., Kolar, T.: "Seeing is not necessarily liking: Advancing research on package design with eye-tracking", *Journal of Business Research*, 80, 145-154, 2017. doi:10.1016/j.jbusres.2017.04.019.
- [5] Machiels, C.J.A., Karnal, N.: "See how tasty it is? Effects of symbolic cues on product evaluation and taste", *Food Quality and Preference*, 52, 196-202, 2016. doi:10.1016/j.foodqual.2016.04.014.
- [6] Mai, R., Symmank, C., Seeberg-Elverfeldt, B.: "Light and Pale Colors in Food Packaging: When Does This Package Cue Signal Superior Healthiness or Inferior Tastiness?", *Journal of Retailing*, 94 (4), 426-444, 2016. doi:10.1016/j.jretai.2016.08.002.
- [7] Mead, J. A., Richerson, R. "Package color saturation and food healthfulness perceptions", *Journal of Business Research*, 82, 10-18, 2018. doi:10.1016/j.jbusres.2017.08.015.
- [8] Ooijen, I., Fransen, M. L., Verlegh, P. W.J., Smit, E. G.: "Atypical food packaging affects the persuasive impact of product claims", *Food Quality and Preference*, 48, 33-40, 2016. doi:10.1016/j.foodqual.2015.08.002.
- [9] Ramos, M., Valdés, A., Mellinas, A. C., Garrigós, M. C.: "New Trends in Beverage Packaging Systems: A Review", *Beverages*, 1(4), 248-272, 2015. doi:10.3390/beverages1040248.

- [10] Simmonds, G., Woods, A. T., Spence, C.: “‘Show me the goods’: Assessing the effectiveness of transparent packaging vs. product imagery on product evaluation”, *Food Quality and Preference*, 63, 18-27, 2018. doi: 10.1016/j.foodqual.2017.07.015.
- [11] Steenis, N. D., Herpen, E., Lans, I. A., Ligthart, T. N., Trijp, H. C. M.: “Consumer response to packaging design: The role of packaging materials and graphics in sustainability perceptions and product evaluations”, *Journal of Cleaner Production*, 162, 286-298, 2017. doi: 10.1016/j.jclepro.2017.06.036.
- [12] Valesco, C., Salgado-Montejo, A., Marmolejo-Ramos, F. Spence, C.: “Predictive packaging design: Tasting shapes, typefaces, names, and sounds”, *Food Quality and Preference*, 34, 88-95, 2014. doi: 10.1016/j.foodqual.2013.12.005.
- [13] Velasco, C., Woods, A. T., Petit, O., Cheok, A. D., Spence, C.: “Crossmodal correspondences between taste and shape, and their implications for product packaging: A review”, *Food Quality and Preference*, 52, 17-26, 2016. doi: 10.1016/j.foodqual.2016.03.005.
- [14] Vladić, G., Kecman, M., Kašiković, N., Pal, M., Stančić, M.: “Influence of the shape on the consumers perception of the packaging attributes”, *Journal of Graphic Engineering and Design*, 6 (2), 27-32, 2015. UDC: 655.3.066.25:159.937.522.
- [15] Westerman, S.J., Sutherland, E.J., Gardner, P.H., Baig, N., Critchley, C., Hickey, C., Mehigan, S., Solway, A.: “The design of consumer packaging: Effects of manipulations of shape, orientation, and alignment of graphical forms on consumers’ assessments”, *Food Quality and Preference*, 27, 8-17, 2013. doi: 10.1016/j.foodqual.2012.05.007.



THE INFLUENCE OF PRINTING PROPERTIES OF SCREEN PRINTED ELECTRODES ON SENSITIVITY MEASURED WITH CYCLIC VOLTAMMETRY

Urška Kavčič¹ , Tanja Pleša 

¹Pulp and Paper Institute, Ljubljana, Slovenia

Abstract: Disposable screen printed electrodes are widely used for environmental monitoring such as water quality test, heavy metals detection and gas pollutants. (Hayat et al, 2014; Li et al, 2012) Screen printed electrodes used for electrochemical detection consist of three electrodes: auxiliary, working and reference electrode. The working electrode is the principal electrode on which electrochemical reactions are performed, while the reference and auxiliary electrodes are used to complete the electronic circuit. (Hayat et al, 2014) To produce efficient screen printed electrodes the modification of the electrode surface or altering of the geometry of electrode can be done. Researchers mostly modify the surface of the electrode, but on the other hand, there are many properties that can be changed and optimized at the beginning, in the process of screen printing.

In the presented research the influence of the modification of the working electrode area and conductive ink thickness on the final electrochemical activity was evaluated. Besides that, a modification of conductive printing ink was done using carbon nanotubes. Finally, electrochemical activity of all samples was analyzed with potassium ferricyanide $K_3[Fe(CN)_6]$. It was found that the highest impact on electrochemical activity has conductive ink thickness. Working electrode area also affects the electrochemical activity, but less, while modification of conductive ink with the addition of carbon nanotubes does not have significant influence. The main reason for that was immersing of nanotubes into the ink and consequently, the specific surface of the modified working electrode remains comparable to non-modified one.

Key words: screen printed electrodes, printing properties, cyclic voltammetry

1. INTRODUCTION

Disposable screen printed electrodes (SPE) are widely used for environmental monitoring such as water quality test, heavy metals detection and gas pollutants. (Hayat et al, 2014; Li et al, 2012) Screen printed electrodes used for electrochemical detection consist of three electrodes: auxiliary (AE), working (WE) and reference (RE) electrode (Figure 1). A RE is mostly printed with silver printing ink, while AE and WE can be printed also with different conductive printing inks (carbon, gold etc.). The WE is the principal electrode on which electrochemical reactions are performed, while the RE and AE are used to complete the electronic circuit (Hayat et al, 2014).

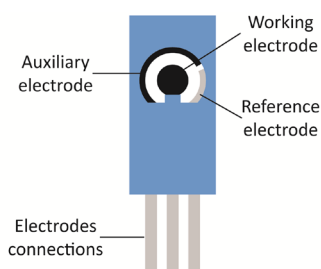


Figure 1: Screen printed electrode

There are two main strategies to produce efficient SPEs (Mohamed, 2016): (1) modification of electrode by depositing several substances or (2) altering the geometry of electrode or used printing inks. For the detection of a target analyte, researchers mostly use modified commercially available SPEs (DropSens, Metrohm Autolab, Gamry etc.). (Menart et al, 2017; Gusmão, 2017; López-López, 2017) That way, the most important property of the SPE is its modification. But on the other hand, there are many properties that can be changed and optimized at the beginning, in the process of screen printing. The sizes of all three electrodes, the conductive ink, the thickness of the conductive ink and consequently the conductivity of the electrodes can all be variables.

Researchers focus on both, modification of commercially available electrodes and also on altering the geometry. Jadav (Jadav et al, 2018) presents a development of silver/carbon screen printed electrode for determination of vitamin C in fruit juices. In his article he presents the whole process from formulation of conductive ink and screen printing process to analysis of electrochemical performance of screen printed electrode. Jewell and co-authors (Jewell et al, 2016) present the interactions between printing ink solvent, printed ink conductivity and process consistency. Oppositely to the printing process and used materials Garcia (Garcia et al, 2010) and Prasek (Prasek et al, 2012) focus on the geometry of the screen printed electrodes. Garcia with co-authors was focused on changing design parameters (the area of WE and AE, the distance between them and the overlap length between them). They found out that the only key parameter that influences the performance of the sensor is the area of the WE. Prasek was changing the geometrical size of RE and AE and found out that areas and materials of those two electrodes can markedly influence detection limit of the sensor.

In the first part of the presented research, the influence of WE area, the carbon ink thickness (and consequently the conductivity) on the final electrochemical behaviour by using cyclic voltammetry was analysed. In the second part of the research, the influence of addition of carbon nanotubes (CNT) into carbon ink was researched. The electrochemical performance of all SPEs was analysed with cyclic voltammetry. Cyclic voltammetry technique enables the study of the modified SPEs performance, by using a ferricyanide solution, being the redox couple peaks intensities (e.g. $K_3Fe(CN)_6/K_4Fe(CN)_6$) frequently used as sensitivity indicators (Sharma et al, 2010; Couto et al, 2016). For the cyclic voltammetry, 2.5 mM potassium ferricyanide $K_3[Fe(CN)_6]$ in 0.1 M KCl solution was used and cyclic voltammogram for each SPE was scanned. By altering the WE area, conductive carbon ink thickness and with modification of conductive carbon ink with CNT the enhancements in the sensor sensitivity could be achieved.

2. METHODS

SPEs were firstly designed in accordance with Dropsens potentiostat dimensional requirements. Three SPEs with different WE area (diameter of 2, 3 and 4 mm) were designed (Figure 2). After that, multi-layer screen printing followed. Firstly, contacts (electrodes connections) and RE were printed with silver printing ink (SC), then AE and WE electrode with carbon printing ink (PE) and at the end dielectric printing ink. For SPEs printing, the printing inks, printing and curing conditions as presented in Table 1 were applied. As a printing material, synthetic paper Monotex L 175 BG 254 g/m² (Feron, Germany) was used.

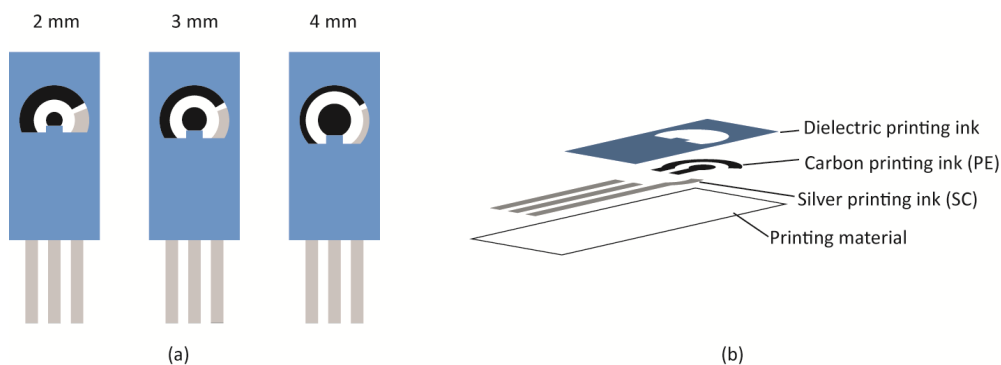


Figure 2: Samples of SPE with 2, 3 and 4 mm WE diameter (a) and multi-layer SPE (b)

Table 1: Used printing and curing conditions

Abbreviation	Printing ink	Producer	Ink type	Mesh count [lines/cm]	Curing conditions
PE	PE-C200 Carbon resistive ink	Applied Ink Solution, US	Carbon printing ink	77-55	5 min @ 120 °C
SC	CRSN 2442, SunTronic Silver 280	Sun Chemical	Silver printing ink	120-31	10 min @ 120 °C
Dielectric	CFSN6057 SunTronic Dielectric 681	Sun Chemical	Dielectric printing ink	90-45	600 mJ/m ²

2.1 The influence of WE area, ink thickness and sheet resistance on cyclic voltammetry

In the first part of the research, the variation of WE area and WE printing ink thickness was analysed. All samples had contacts and RE printed using silver conductive ink SC, while WE and AE were printed with PE ink in two thicknesses (PE ink was printed in one or in two layers) (Figure 2 (b)). After curing, the thickness of the dry ink was measured using micrometre (Lorentzen & Wettre, Sweden). The resistance of conductive ink lines was measured using LCR-300 Voltcraft multimeter and sheet resistance was calculated for both thicknesses.

2.2 The influence of carbon nanotubes on cyclic voltammetry

In the second part of the research, the influence of CNT addition into PE ink on electrochemical activity was analysed. 0.4 % of multi-walled carbon nanotubes (Sigma-Aldrich, USA) were added to the PE carbon ink. The printing and curing were applied under the same conditions as PE ink (see Table 1).

2.3 Cyclic voltammetry

After printing, an electrochemical activity using cyclic voltammetry was analysed. The electrochemical performance of all SPEs was analysed using 100 μ l of 0.1 M KCl solution containing 2.5 mM potassium ferricyanide $K_3[Fe(CN)_6]$ and cyclic voltammogram for each screen printed electrode (with different WE area, WE conductive ink thickness and CNT addition) was scanned. Cyclic voltammograms were scanned using Dropsens μ Stat 300 Bipotentiostat with the parameters presented in Table 2.

Table 2: Cyclic voltammetry parameters

Parameter	Value
Current range	auto
E_{begin}	0.22 V
E_{vtx1}	-0.15 V
E_{vtx2}	0.5 V
Estep	0.002 V
Scan rate	0.05 V/s
n scan	1

The important parameters for a cyclic voltammogram are the peak potentials and peak currents. (BASi, 2018) So, at the end, the final comparison of the cyclic voltammograms peak currents of the samples printed with different WE area and different ink thicknesses as well the influence of the CNT addition in PE ink was checked.

3. RESULTS AND DISCUSSION

3.1 The influence of WE area, ink thickness and sheet resistance on cyclic voltammetry

The final area of a WE and its conductivity (which is a consequence of ink thickness) influence the final signal of cyclic voltammetry. The actual areas of WEs of different diameters are presented in Table 3. In Table 4 the final ink thicknesses of the WEs printed once (1 \times PE) and twice (2 \times PE) and corresponding sheet resistances of the samples are presented.

Table 3: Diameters and actual areas of samples WE electrodes

WE diameter [mm]	WE actual area [mm ²]
2	3.061
3	7.169
4	12.863

Table 4: Printing ink thicknesses of WE and AE and corresponding sheet resistances

Sample	Thickness [μm]	Sheet resistance [Ω/sq]
1 \times PE	21	137
2 \times PE	28	46

In Figures 3, 4 and 5 cyclic voltammograms of 2.5 mM potassium ferricyanide $\text{K}_3[\text{Fe}(\text{CN})_6]$ in 0.1 M KCl for different WE diameters (2, 3 and 4 mm) and for different WE ink thicknesses (1 \times PE and 2 \times PE) are presented. When changing the potential from 0.22 V to -0.15 V and through 0.5 V back to the starting potential the current that is produced presents electrochemical properties of the analyte. The maximum current achieved during the cyclic voltammetry scanning (one or more peaks) has to be as high as possible, which can be regulated also with WE area and its conductivity. In Figures 3, 4 and 5 it can be seen that the peaks are getting higher with larger WE diameter. The difference between the minimum and maximum current peaks at 1 \times PE samples is 7.93 μA when using SPE with 2 mm diameter of WE, when the diameter is 3 mm the difference is 20.27 μA , and when using the largest, 4 mm diameter WE the difference increases to 29.88 μA . When analysing samples with higher thicknesses and conductivities (2 \times PE) the peaks are getting even higher. After comparison of the influence of WE diameter and ink thickness on cyclic voltammetry, it is clearly seen that the final conductivity of the WE influences the cyclic voltammetry more than the WE diameter itself.

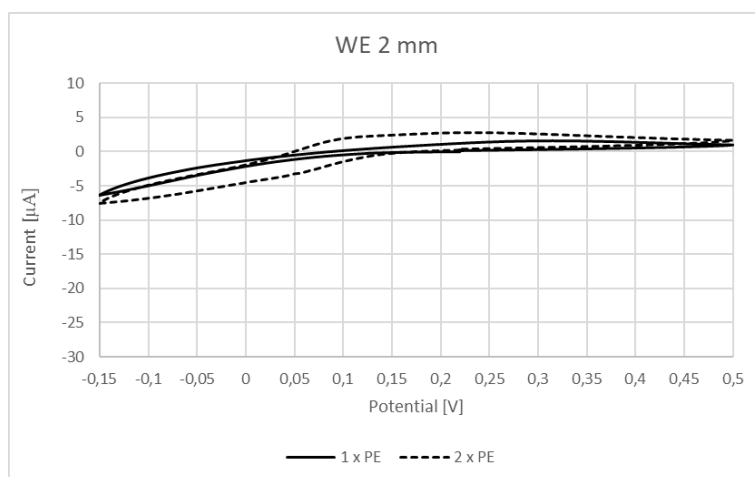


Figure 3: Cyclic voltammograms of SPE with 2 mm WE diameter in two thicknesses

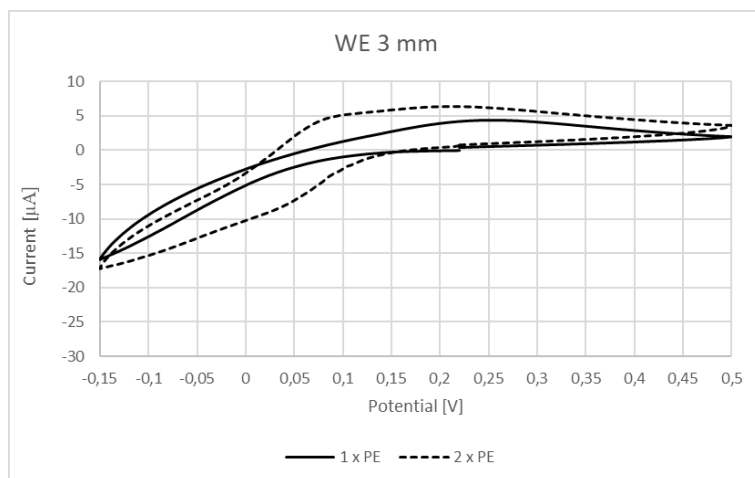


Figure 4: Cyclic voltammograms of SPE with 3 mm WE diameter in two thicknesses

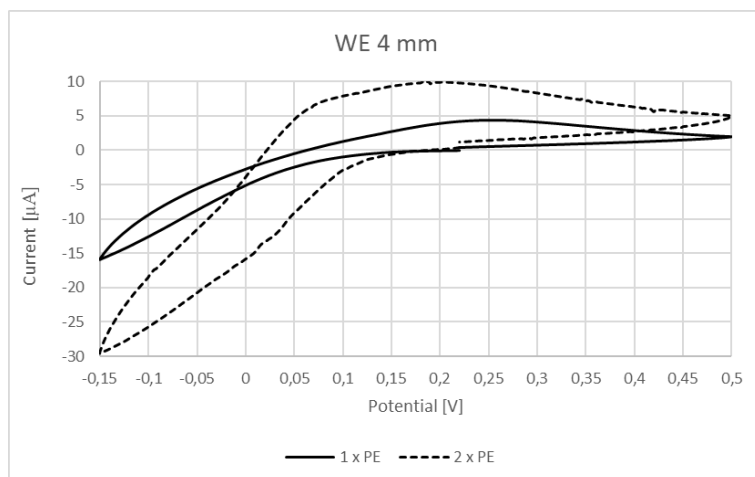


Figure 5: Cyclic voltammograms of SPE with 4 mm WE diameter in two thicknesses

3.2 The influence of carbon nanotubes on cyclic voltammetry

The functionalization of the SPE WEs is often used to enhance the final response of cyclic voltammetry. While comparing the different graphical properties on the final cyclic voltammetry response, the functionalization of WE was one of the variables changed during the experiment. Regarding literature, the functionalization is often done with nanotubes addition, so it was expected to get a better response in comparison to SPEs printed without CNT. But when cyclic voltammograms were scanned for samples with CNT ($1 \times \text{PE} + \text{CNT}$) the current peaks were comparable to those without CNT ($1 \times \text{PE}$) as presented in Figure 6.

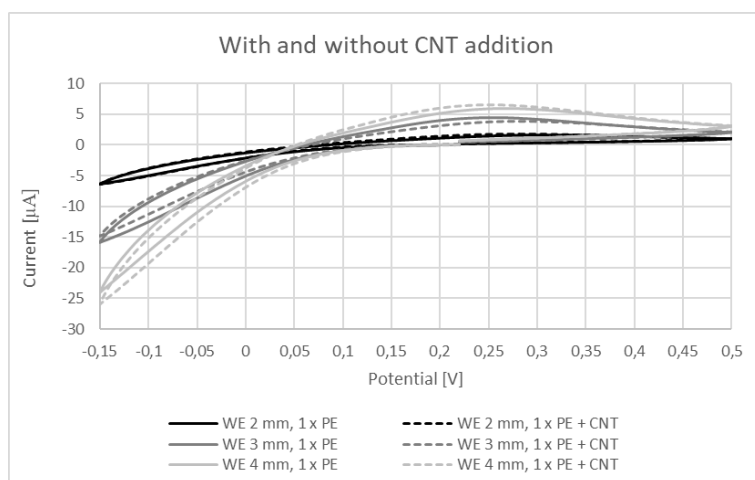


Figure 6: Cyclic voltammograms of SPE with different diameters of non-functionalized ($1 \times \text{PE}$ – solid line) and with CNT functionalized ($1 \times \text{PE} + \text{CNT}$ – dashed line) ink WE

While the results of cyclic voltammetry of non-functionalized and with CNT functionalized SPE were so comparable the surface of the both WE were scanned at scanning electron microscopy – SEM. In Figure 7 we have presented the surfaces of both and it is seen that the surface roughness is very similar, which can be attributed to the very small size of CNT (in comparison to conductive ink thickness) which were immersed into the ink and not remained at the surface of the WE. Consequently, the surface area changed just a little in comparison to non-functionalized SPE and the final response did not increase significantly.

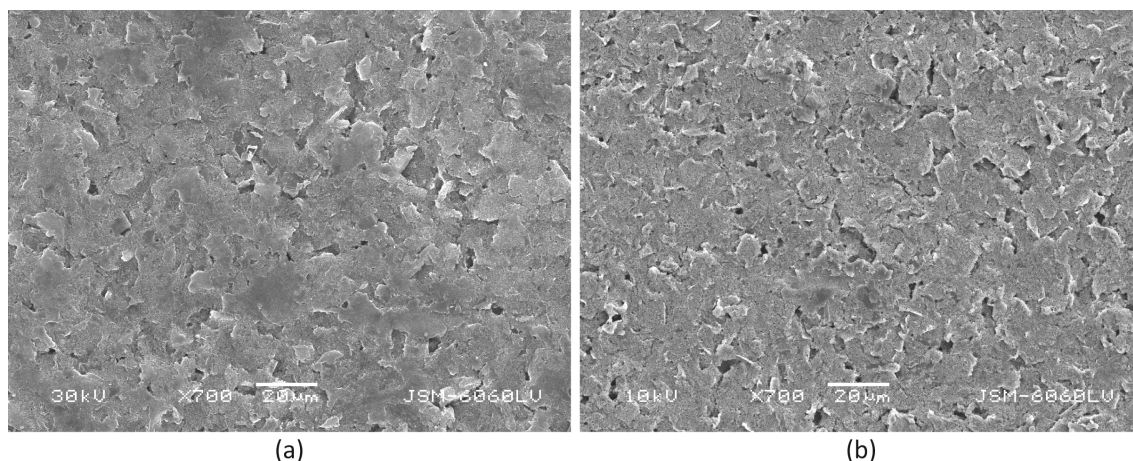


Figure 7: 700 × magnification of non-functionalized ($1 \times \text{PE}$) – (a) and functionalized ($1 \times \text{PE} + \text{CNT}$) – (b) surface of WE

4. CONCLUSIONS

Screen printing process offers many possibilities for printing SPE. The variations in thickness, conductivity and WE area can be easily achieved. Besides that, the functionalization of the ink can be freely done (for example with incorporation of chemical functionalized materials into the ink). In the presented research there are presented all the aforementioned properties and the final evaluation with cyclic voltammetry analysis was conducted. It was shown, that the conductivity of the WE (i.e. printing ink thickness) influences the cyclic voltammetry response much more than the WE diameter (even though also the diameter of the WE contributes the current change). Regarding WE functionalization, it was shown that CNT that are mixed into the printing ink sink into the ink and do not remain at the surface of WE. Consequently, the final response of WE printed with added CNT is just comparative to those without CNT. In the future analysis, the functionalization of the very top of the surface should be done and it is expected that with CNT on the top of WE surface would enlarge the specific area of the WE and consequently increase the response of the cyclic voltammetry.

5. ACKNOWLEDGEMENTS

Slovenian Research Agency is gratefully acknowledged for funding via J2-8182 "Catalytically-assisted high efficiency and low-cost nanostructured sensors based on modified screen printed electrodes for analytical chemistry" project.

6. REFERENCES

- [1] BASi.: "Cyclic Voltammetry - Data Analysis", URL https://www.basinc.com/manuals/EC_epsilon/Techniques/CycVolt/cv_analysis (last request: 2018-10-18)
- [2] Couto, R.A.S., Lima, J.L.F.C., Quinaz, M.B.: "Recent developments, characteristics and potential applications of screen-printed electrodes in pharmaceutical and biological analysis." *Talanta* 146, 801-814, 2016. doi: 10.1016/j.talanta.2015.06.011.
- [3] Garcia, D. E., Chen, T.H., Wei, F., Ho, C.M.: "A Parametric Design Study of an Electrochemical Sensor." *JALA: Journal of the Association for Laboratory Automation*, 15 (3), 179-188, 2010. doi: 10.1016/j.jala.2010.01.007.
- [4] Gusmão, R., López-Puente, V., Yate, L., Pastoriza-Santos, I., Pérez-Juste, J., González-Romero, E.: "Screen-printed carbon electrodes doped with TiO₂-Au nanocomposites with improved electrocatalytic performance", *Materials Today Communications*, 11, 11-17, 2017. doi: 10.1016/j.mtcomm.2017.02.003.
- [5] Hayat, A, Marty, J. L.: "Disposable Screen Printed Electrochemical Sensors: Tools for Environmental Monitoring" *Sensors*, 14 (6), 10432-10453, 2014. doi: 10.3390/s140610432

- [6] Jadav, J.K., Umrana, V.V., Rathod, K.J., Golakiya, B.A.: "Development of silver/carbon screen-printed electrode for rapid determination of vitamin C from fruit juices", *LWT - Food Science and Technology*, 88, 152-158, 2018. doi: 10.1016/j.lwt.2017.10.005
- [7] Jewell, E., Philip, B., Greenwood, P.: "Improved Manufacturing Performance of Screen Printed Carbon Electrodes through Material Formulation", *Biosensors*, 6 (3), 30, 2016. doi: 10.3390/bios6030030.
- [8] Li, M., Li, Y.T., Li, D.W., Long, Y.T.: "Recent developments and applications of screen-printed electrodes in environmental assays—A review", *Analytica Chimica Acta*, 734, 31-44, 2012. doi: 10.1016/j.aca.2012.05.018.
- [9] López-López, L., Miranda-Castro, R., de-los-Santos-Álvarez, N., Miranda-Ordieres, A.J., Lobo-Castañón, M.J.: "Disposable electrochemical aptasensor for gluten determination in food." *Sensors and Actuators B: Chemical*, 241, 522-527, 2017. doi: 10.1016/j.snb.2016.10.112.
- [10] Menart, E., Jovanovski, V., Hočevár, S.B.: "Novel hydrazinium polyacrylate-based electrochemical gas sensor for formaldehyde", *Sensors and Actuators B: Chemical*, 238, 71-75, 2017. doi: 10.1016/j.snb.2016.07.042.
- [11] Mohamed, H.M.: "Screen-printed disposable electrodes: Pharmaceutical applications and recent developments", *TrAC Trends in Analytical Chemistry*, 82, 1-11, 2016. doi: 10.1016/j.trac.2016.02.010.
- [12] Prasek, J., Trnkova, L., Gablech, I., Businova, P., Drbohlavova, J., Chomoucka, J., Adam, V., Kiyek, R., Hubalek, J.: "Optimization of planar three-electrode systems for redox system detection", *International Journal of Electrochemical Science*, 7 (3), 1785-1801, 2012.
- [13] Sharma, M.K., Agarwal, G.S., Rao, V.K., Upadhyay, S., Merwyn, S., Gopalan, N., Rai, G.P., Vijayaraghavan, R., Prakash, S.: "Amperometric immunosensor based on gold nanoparticles/alumina sol-gel modified screen-printed electrodes for antibodies to *Plasmodium falciparum* histidine rich protein-2", *Analyst*, 135 (3), 608-614, 2010. doi: 10.1039/B918880K.



NOTICEABILITY AND RECALL OF VISUAL ELEMENTS ON PACKAGING

Dorotea Kovačević , Maja Brozović 

University of Zagreb, Faculty of Graphic Arts, Zagreb, Croatia

Abstract: *Product packaging protects the content from the environment, but also serves to display information relevant to consumers. Some product information, like warning messages, should be both noticeable and memorable. The purpose of the study was to explore how people pay attention to visual elements on packaging and how well they recall them. The investigation was especially directed towards a particular visual element – a safety pictogram. The study consisted of two parts: an eye tracking experiment which measured the participants' visual attention while viewing the packaging, and a follow-up memory test which assessed the ability of the participants to recall elements from the packaging. The packaging was designed especially for the purpose of the experiment. It was presented on-screen and viewed by 130 participants. The visual elements displayed on the packaging were: an illustration, a product name, a logo, a pictogram and the quantity information. Eye-tracking measures used were time to first fixation on each of the visual elements on the packaging and total fixation duration on an element. A list test was used for assessing the recall of visual information in the absence of the packaging. The illustration was the visual element recalled by most of the participants (reported by 80% of the participants), followed by the product name (reported by 59% of the participants). Only 18% of the participants mentioned that they saw the pictogram. The analysis of the eye movements and the visual attention showed that the most easily noticed visual element was the product name, while the illustration had the longest viewing period. Furthermore, the participants who detected the pictogram faster and viewed it longer also recalled it better. However, the association between visual attention and memory was not revealed for all visual elements on the packaging. The findings could be relevant for designers and those interested in the communication aspect of packaging.*

Key words: packaging, eye-tracking, recall, pictogram

1. INTRODUCTION

The basic role of packaging is to protect its content from the environment. Concurrently, it serves to display information relevant to consumers. Some product information, like warning messages, should be both noticeable and memorable. Noticeability is necessary because if a warning message is not detected, it can have no effect on safe behavior (Young et al, 1999). The memorability of a warning is important because warning information might not be accessible during the use of a product and exposure to associated hazards (Wogalter et al, 2002). A high level of warning recall was found to be related to compliance behavior (Wogalter et al, 1991) and the perception of the safety of the product (Stark et al, 2008).

Previous studies have shown that memorability and visual attention are linked. This was demonstrated in the case of pictures (Mancas et al, 2013), advertisements (Crespo et al, 2007), and also in the case of warning labels (Strasser et al, 2012). Many studies that investigated the association between attention and memory employed eye tracking technology (Krugman et al, 1994; Strasser et al, 2012). For example, Krugman et al (1994) used an eye tracking measure (i.e. time spent attending to a warning) to demonstrate that longer viewing time can be associated with the viewer's performance at a recall test. The results of the study done by Strasser et al (2012) also indicated that directing attention to a warning can improve recall of the warning information. They measured the time to first fixation on the warning and the dwell time duration to investigate the connection between visual exploration and correct recall.

The effectiveness of eye tracking evaluations in user-centered design research is well known. It was used as a tool for accessing how people view a stimuli and what attracts their attention in a great deal of studies in this field. To name a few, Velásquez (2013) used an eye tracker to investigate how users perceive different elements on a web page instead of using a survey. Renshaw et al (2003) also recorded eye movements of participants to explore how specific designs affect visual processing. Strasser et al (2012) demonstrated that eye movement measures can reflect viewing patterns of participants who observed textual and graphic warning labels.

In this study, our aim was to use eye tracking measures in the context of packaging design and users' information processing. The intention was to explore how people pay attention to different visual

elements on packaging and how well they recall them. More particularly, we measured the amount of time the participants spent attending to each of the elements and tested its association with the participants' performance in a free memory recall test. The investigation was especially directed towards a particular visual element – a safety pictogram.

2. METHODOLOGY

The experiment consisted of two parts. The first part was an eye tracking measurement of the participants' visual attention while viewing the packaging. The second part was a follow-up memory test which assessed the ability of the participants to recall the visual elements on the packaging.

130 people (87 women and 43 men) were recruited, and all voluntarily participated in the study. Their age ranged from 19 to 40 ($M = 22.31$, $SD = 3.14$). All had normal or corrected-to-normal vision.

The experiments were conducted in a laboratory testing room at the University of Zagreb, Faculty of Graphic Arts. The stimulus was a picture of packaging presented on-screen, on a Lenovo computer display (model LEN L1900pA) with a resolution set to 1280 x 1024 pixels and a refresh rate of 60 Hz. The participants' visual attention was recorded with a Tobii Eye Tracker X60 (sampling rate of 60 Hz, accuracy of 0.5 degree). Eye tracking measures used as dependent variables were: time to first fixation (in seconds) and total fixation duration (in seconds) on each element on the presented packaging. Figure 1 shows the packaging used as stimuli. The packaging was designed for a fictitious brand of air freshener. The main visual elements displayed on the packaging were: an illustration, a product name, a logo, a pictogram and the quantity information.

Before the experiment started, the participants were instructed that they will participate in eye tracking testing, and that their task will be to view the example of the packaging in the same way as they would in their everyday life. They were informed that the viewing time would be limited and that they would be given a question at the end of the testing. In order to avoid goal directed visual search, the participants were not informed about the type of the question. After calibration, the participants fixated a symbol "x" in the middle of the screen and then the image of the packaging was presented in the duration of 5 seconds. Immediately after the packaging presentation, a list test was used for assessing the recall of visual information. The measurement of recall was done by asking the participants to list any elements of the packaging they could remember. After the completion of the task, the participants were debriefed and thanked.

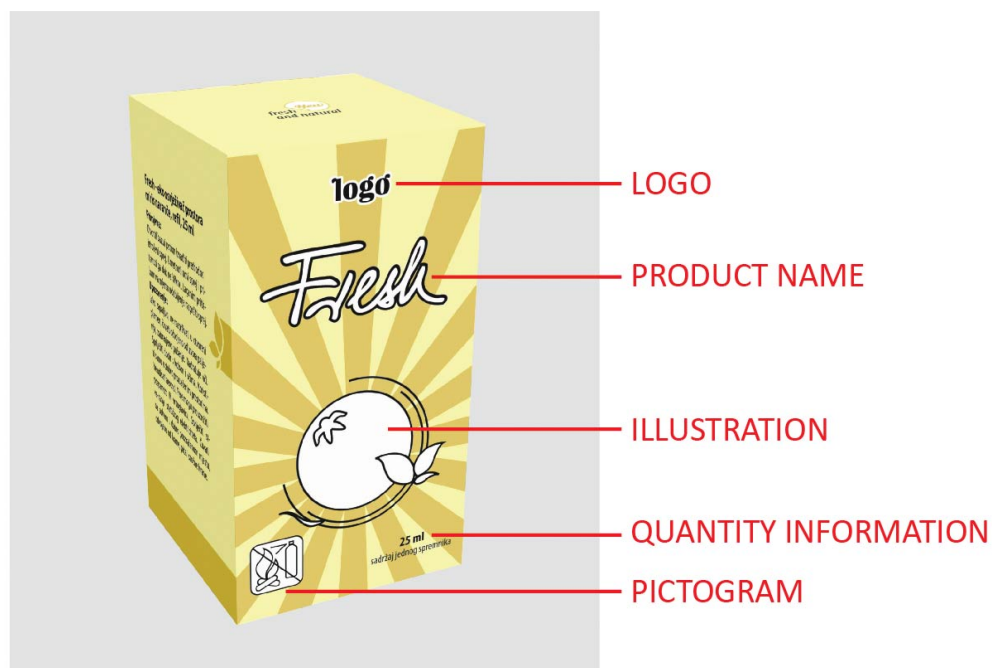


Figure 1: Picture of the packaging used as stimuli in the experiment

3. RESULTS

3.1 Visual attention

Table 1 shows the descriptive statistics for the two measures of the participants' visual attention (i.e. time to first fixation and total fixation duration) grouped by visual elements. The time to first fixation and fixation duration data were analysed with a separate repeated-measures analyses of variance (ANOVA). The results indicated significant differences in the time to first fixation on different visual elements, $F(4, 456) = 245.42, p < 0.01$. Since the pictogram was the focus of our investigation, pairwise t-tests were performed between the pictogram and each of the tested visual elements. The pictogram was fixated faster ($M = 2.50, SD = 0.56$) than the quantity information ($M = 2.78, SD = 0.61$), $t(114) = -4.92, p < 0.01$. However, it was fixated slower than the product name ($M = 0.81, SD = 0.43$), $t(114) = -23.60, p < 0.01$, and the illustration ($M = 1.02, SD = 0.52$), $t(114) = -21.09, p < 0.01$. There was no significant difference in the time to first fixation between the pictogram and the logo ($p = 0.21$).

A significant difference was found in the duration of fixations on different visual elements, $F(4, 516) = 87.023, p < 0.01$. The pairwise t-tests revealed that the pictogram was fixated longer ($M = 2.83, SD = 1.30$) than the logo ($M = 1.85, SD = 1.63$) and the quantity information ($M = 2.42, SD = 1.36$). However, it was fixated less than the illustration ($M = 4.22, SD = 1.38$) and the product name ($M = 4.20, SD = 1.14$).

3.2 Memory

Figure 2 shows the results of the memory test. The bars represent the total number of participants who mentioned each of the visual elements in the test. Cochran's Q test showed that the differences between memorizing the visual elements were significant, $\chi^2(4) = 201.26, p < 0.001$. The post hoc comparisons performed between the pictogram and each of the visual elements showed that the participants mentioned the pictogram less than the illustration $\chi^2 = 66.39, p < 0.01$, and the product name, $\chi^2 = 37.04, p < 0.01$. However, there was no significant difference in memorability between the pictogram and the logo ($p > 0.05$), and between the pictogram and the quantity information ($p > 0.05$).

Table 1: Descriptive statistics for eye tracking measurements

		Visual element				
		Illustration	Product name	Logo	Pictogram	Quantity information
Time to first fixation	Mean	1.02	0.81	2.34	2.50	2.77
	Standard Deviation	0.52	0.43	0.88	0.56	0.61
Total fixation duration	Mean	4.21	4.20	1.85	2.83	2.42
	Standard Deviation	1.38	1.14	1.63	1.29	1.36

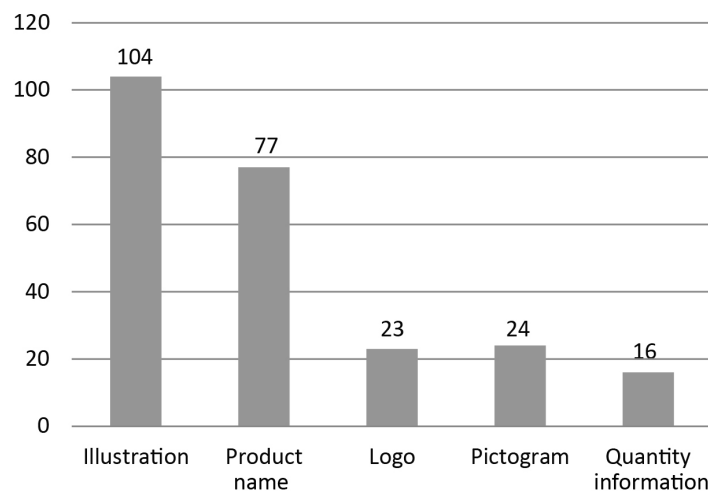


Figure 2: Number of participants who mentioned each of the visual elements in the memory test

3.3 Visual attention and memory

The degree of association between the measures of visual attention and memory was calculated using Spearman's correlation analyses. Only the significant correlations are reported. There was a positive relationship between the time to first fixation on the logo and its memorability $r_s = .198, p < 0.05$. There was a negative relationship between the time to first fixation on the pictogram and its memorability $r_s = -.211, p < 0.05$, indicating that the participants who noticed the pictogram faster also recalled it better. The analysis of the total fixation durations revealed a significant association between the duration of fixation on the pictogram and its memorability $r_s = .210, p < 0.05$.

4. DISCUSSION

One of the intentions of the present study was to measure the visual attention that the participants direct towards elements on the packaging, with a special interest in the perception of the safety pictogram. Two measures were used; the time to first fixation on the visual element as a measure of noticeability (the ability of an element to attract attention) and the duration of fixations landing on the visual element as a measure of the ability of an element to hold one's attention. The results showed that the most noticeable object on the packaging was the product name, while the least noticeable object was the quantity information. The high level of noticeability could be the result of positioning the product name in the upper part of the packaging. The low noticeability of the quantity information can be explained not only by the lower positioning, but also by the low visual saliency derived from the small size of the element and the dominance of the background pattern.

Although the safety pictogram required less time to be noticed than the quantity information, it appears that it was not easily detected. This could be due to the design features of the pictogram. Previous research has shown that the pictogram's design characteristics such as size and thickness can affect its noticeability (Kovačević et al, 2018). In relation to the size of the packaging and the size of other elements, the dimensions of the pictogram were small, which probably had a negative influence on the pictogram's visual prominence and its ability to attract attention. On the other hand, the ability of the pictogram to hold one's attention was somewhat better. The results indicated that the participants viewed it longer than the quantity information, and also longer than the logo. This was expected, since previous research suggested that more complex visual forms need more fixations to be processed (Zusne, 1964). The structure of the pictogram used in our experiment was noticeably more complex than the logo.

The participants dedicated most of their attention to the illustration. This was the element on the packaging that had the longest total fixation duration. This result is in line with previous studies which found that graphics attracted more attention than other elements. For example, Piqueras-Fiszman et al (2013) investigated the consumers' attention to the design of jam jars and found that graphics presented on the packaging attracted more attention to itself than the text, resulting with increased fixation duration. In general, fixation duration tends to be longer on informative visual elements than on less informative elements (Unema et al, 2005). In our experiment, the illustration was the most informative object because it provided information about the most distinctive characteristic of the product – its fragrance. The longer fixation duration also indicates that the illustration was more engaging in some way (Just et al, 1976), or relevant for viewers (Jacob et al, 2003).

The results of the memory test supported the dominant role of the illustration, indicating that the illustration was the visual element recalled by most of the participants (reported by 80% of the participants), followed by the product name (reported by 77% of the participants). Only 18% of the participants mentioned that they saw the pictogram. The power of the illustration to be recalled better than the pictogram element can be explained by the visual saliency of the illustration. Some previously done memory-based studies have shown that the saliency of an object can be a good predictor of its memorability (Dubey et al, 2015; Borkin et al, 2016). The most prominent elements within an image are likely to be remembered (Dubey et al, 2015), and the illustration was undoubtedly the visual cue that stood out the most. It was designed as the largest and the brightest element on the packaging, with a central position highlighted by the background texture. Perhaps some other design features of the pictogram that make it more salient would generate better recall. Many warning researchers have reported about the connection between salient warnings and memorability. Fienmann (1988) found that the warning symbol which was recalled more often than the other symbols in the study had better

graphic qualities which made it more conspicuous. Torres et al (2007) revealed that overtly positioned warnings in print ads provide a higher warning recall.

A higher recall of a warning message is often associated with deeper cognitive processing of the message, measured through a greater number of fixations and viewing duration (Crespo et al, 2007). Some of our results support this connection between recall and visual attention. The correlation analyses revealed that the participants who detected the pictogram faster and viewed it longer also recalled it better. Similar findings are reported by Strasser et al (2012) who found that warnings that attracted attention more quickly and had longer dwell time duration were associated with better recall. However, the association between visual attention and memory was not revealed for all visual elements in our study. The lack of consistency in results for all the elements is probably caused by the variety of their attributes that produced different visual effects. For example, the color and recognisability of an object enhance memorability (Borkin et al, 2013), but do not necessarily affect the measures of the visual attention. Also, participants tend to remember the warning messages which they perceive as being important (Lehto et al, 1993), so the perception of the relevancy of each of the elements on the packaging might also affected the recall test performance. Finally, increasing the amount of information on packaging may affect the recall of an individual element (Scammon, 1977), so, when analysing the obtained results, the effect of visual clutter on the packaging should definitely be taken into consideration.

5. CONCLUSIONS

Since packaging often provides product-related safety information, which is especially important to be recalled, a particular research focus in the present study was on the safety pictogram. By connecting the results of the free memory recall test with the eye tracking results, the study demonstrated the connection between attention and recall to some extent, but also touched upon some issues associated with safe product use.

The main finding of the study is that the memorability of the pictorial warning could benefit from emphasizing its noticeability. However, eye tracking results suggested that the link between the visual attention and the recall was not revealed for all elements on the packaging. Thus, any further conclusions about memorability and attention in reference to the design of the product packaging should not be generalized. Another finding is related to the communication role of the packaging. While the illustration and the product name had high levels of recall, the safety pictogram was recalled by only a small number of participants. This brings to light the questionable effectiveness of safety communication derived from the packaging design used in our study, and suggests that more effort should be put into testing the determinants of effective design of the safety pictorial in future research. Also, future studies should investigate the influence of color, which was, due to the preliminary nature of our study, omitted as an independent factor in the present work. In addition, various packaging designs and compositions of the elements could be differently perceived, so these variables should also be worthy of more research attention in the future.

6. REFERENCES

- [1] Borkin, M. A., Bylinskii, Z., Kim, N. K., Bainbridge, C. M., Yeh, C. S., Borkin, D., Pfister, H., Oliva, A.: "Beyond memorability: Visualization recognition and recall", *IEEE Transactions on Visualization and Computer Graphics* 22(1), 519–528, 2016. doi: 10.1109/TVCG.2015.2467732.
- [2] Borkin, M. A., Vo, A. A., Bylinskii, Z., Isola, P., Sunkavalli, S., Oliva, A., Pfister, H.: "What makes a visualization memorable?", *IEEE Transactions on Visualization and Computer Graphics* 19(12), 2306–2315, 2013. doi: 10.1109/TVCG.2013.234.
- [3] Crespo, A., Cabestrero, R., Grzib, G., Quirós, P.: "Visual attention to health warnings in tobacco advertisements: An eye-tracking research between smokers and non-smokers", *Studia Psychologica* 49(1), 39–51, 2007.
- [4] Dubey, R., Peterson, J., Khosla, A., Yang, M-H., Ghanem, B.: "What makes an object memorable?", *Proceedings of The IEEE International Conference on Computer Vision 2015, (ICCV, Santiago, Chile 2015)*, pages 1089-1097. doi: 10.1109/ICCV.2015.130.
- [5] Friemann, K., 1988.: "The effect of adding symbols to written warning labels on user behavior and recall", *Human Factors: The Journal of the Human Factors and Ergonomics Society* 30(4), 507–515, 1998. doi: 10.1177/001872088803000411.

- [6] Jacob, R.J.K., Karn, K.S.: "Commentary on Section 4 - Eye tracking in human-computer interaction and usability research: Ready to deliver promises", *The Mind's Eye* 573–605, 2003. doi: 10.1016/B978-044451020-4/50031-1.
- [7] Just, M.A., Carpenter, P.A.: "Eye fixations and cognitive processes", *Cognitive Psychology* 8(4), pp.441–480, 1976. doi: 10.1016/0010-0285(76)90015-3.
- [8] Kovačević, D., Brozović, M., Možina, K.: "Do prominent warnings make packaging less attractive?" *Safety Science* 110, 336–343, 2018. doi: 10.1016/j.ssci.2018.08.031.
- [9] Krugman, D.M., Fox, R. J., Fletcher, J. E., Flscher, P. M., Rojas, T. H. : "Do adolescents attend to warnings in cigarette advertising? An eye-tracking approach", *Journal of Advertising Research* 34(6), 39–52, 1994.
- [10] Lehto, M.R., Papastavrou, J.D.: "Models of the warning process: important implications towards effectiveness", *Safety Science* 16(5-6), 569–595, 1993. doi: 10.1016/0925-7535(93)90024-8.
- [11] Mancas, M., Le Meur, O.: "Memorability of natural scenes: The role of attention", *Proceedings of 2013 IEEE International Conference on Image Processing 2013, (ICIP, Melbourne, Australia, 2013)*, pages 196–200. doi: 10.1109/ICIP.2013.6738041.
- [12] Piqueras-Fiszman, B. Velasco, B., Salgado-Montejo, A., Spence, C.: "Using combined eye tracking and word association in order to assess novel packaging solutions: A case study involving jam jars", *Food Quality and Preference* 28(1), 328–338, 2013. doi: 10.1016/j.foodqual.2012.10.006.
- [13] Renshaw, J.A., Finalay, J.E., Tyfa, D., Ward, R.D.: "Designing for visual influence: An eye tracking study of the usability of graphical management information", *Proceedings of Human-Computer Interaction - INTERACT 2003, (IFIP TC13, Zurich, 2003)*, pages 144–151, 2003.
- [14] Scammon, D.L.: ""Information Load" and consumers", *Journal of Consumer Research* 4(3), 148, 1997. doi:10.1086/208690.
- [15] Stark, E., Kim, A., Miller, C., Borgida, E.: "Effects of including a graphic warning label in advertisements for reduced-exposure products: Implications for persuasion and policy", *Journal of Applied Social Psychology* 38(2), 281–293, 2008. doi: 10.1111/j.1559-1816.2007.00305.x.
- [16] Strasser, A.A., Tang, K.Z., Romer, D., Jepson C., Cappella J.N.: "Graphic warning labels in cigarette advertisements: Recall and viewing patterns", *American Journal of Preventive Medicine* 43(1), 41–47, 2012. doi:10.1016/j.amepre.2012.02.026.
- [17] Torres, I.M., Sierra, J.J., Heiser, R.S. "The effects of warning-label placement in print ads: A social contract perspective", *Journal of Advertising* 36(2), 49–62, 2007. doi:10.2753/JOA0091-3367360203.
- [18] Unema, P.J.A., Pannasch, S., Joos, M., Velichkovsky, B. M.: "Time course of information processing during scene perception: The relationship between saccade amplitude and fixation duration", *Visual Cognition* 12(3), 473–494, 2005. doi: 10.1080/1350628044000409.
- [19] Velásquez, J.D.: "Combining eye-tracking technologies with web usage mining for identifying Website Keyobjects", *Engineering Applications of Artificial Intelligence* 26(5-6), 1469–1478, 2003. doi: 10.1016/j.engappai.2013.01.003.
- [20] Wogalter, M.S., Rashid, R., Clarke, S.W., Kalsher, M.J. : "Evaluating the behavioral effectiveness of a multi-modal voice warning sign in a visually cluttered environment", *Proceedings of the Human Factors Society Annual Meeting* 35(10), 718–722, 1991. doi:10.1177/154193129103501033.
- [21] Wogalter, M.S., Conzola, V.C., Smith-Jackson, T.L.: "Research-based guidelines for warning design and evaluation", *Applied Ergonomics* 33(3), 219–230, 2002. doi: 10.1016/S0003-6870(02)00009-1.
- [22] Young, S.L., Lovvoll, D.R. "Intermediate processing stages: Methodological considerations for research on warnings", (Taylor & Francis, London, 1999), pages 27–52.
- [23] Zusne, L., Michels, K.M.: "Nonrepresentational shapes and eye movements", *Perceptual and Motor Skills* 18(1), 11–20, 1964. doi:10.2466/pms.1964.18.1.11.



USER-CENTERED APPROACH TO PRODUCT DESIGN FOR PEOPLE WITH VISUAL IMPAIRMENTS

Monika Rastovac¹ , Jurica Dolić² , Jesenka Pibernik² , Lidija Mandić² 

¹Q-Bit d.o.o., Zagreb, Croatia

²University of Zagreb, Faculty of Graphic Arts, Zagreb, Croatia

Abstract: *The aim of this research was to investigate the application of the user-centred design process to the design and development of a product and its packaging suitable for people with visual impairments. The product and packaging had to be accessible to stakeholders on both sides - not only to visually impaired end users but also to the workers with visual impairments in the production process. The accessibility features had to function in conjunction with other presentation and functional requirements of the product and packaging. In order to adapt the design for people with visual impairments, research of optimal design process was conducted using combination of contextual design with other user-centred methods. Rapid prototyping was used to create full-scale physical packaging models and product moulding tools for evaluation. Additional subjective evaluation using semantic differential was carried on users without visual impairments to establish the perception of pragmatic and hedonic quality of the packaging.*

Key words: packaging, product design, visual impairment, Braille, user-centred Design, contextual design

1. INTRODUCTION

User-Centred Design (UCD), which is a subset of Human-Centred Design (HCD), is an approach to design of interactive products in which the deep understanding of users' needs and potentials presents a key factor for design decisions throughout the design process. With the ever-rising demands and expectations from the consumers in the competitive markets, employing UCD approach to product development has become a necessity rather than a choice. It is particularly important to include users when designing accessible products (Alzuhair et al, 2014). In many cases, visually impaired users have significantly different mental models than users without impairments, so it is challenging for designers to take into account the visually impaired user's needs (Sanchez, 2008). However, integrating UCD approach into a design process for an accessible product can be challenging. Designers are often faced with limited access to the visually impaired population, so UCD methods which could provide most insights from a limited number of participants should be beneficial. Participation in UCD activities could become demanding for the disabled users, so the number and scope of activities should be reasonable and planned to have the user involved just where his or her input is needed. Often, visually impaired users represent just one of the target groups, so the design should also accommodate requirements of the general population, or should be designed according to inclusive design principles.

Visually impaired population considers research of accessibility methods in packaging as one of the top priorities (Van der Geest et al, 2015). However, there is little existing research into applying UCD principles and methods for package design accessible to visually impaired users. In one such study (Barbosa et al, 2018), authors applied Guidance for Project Development procedure, developed by Merino (Merino, 2016) for the development of accessible packaging proposal. They examined several aspect of accessibility of product packaging including methods of opening the package and access to the product.

This paper explores UCD process adjustments in order to establish a user-centred design process which would help designers address most of the challenges they are facing when designing accessible products for people with visual impairments. The process and its' implementation is presented through a case study of designing accessible mould and packaging of bar soap.

2. CASE STUDY: SOUVENIR SOAP AND PACKAGING DESIGN

The proposed process was implemented into design of a souvenir soap mould and packaging for the "Soap with dots" (SWD) project for a non-commercial association for people with visual impairments "Martin's cape". The soaps are manufactured by blind and low vision workers. The design requirements

included that the packaging should be accessible to blind and low vision workers in the process of packaging the soaps and to blind and low vision end users in the process of handling the packaging and accessing the product. Since it has a function of a souvenir, the product should also appeal to users without visual impairments. The design requirements for the soap mould was that it supports more accessible and safer manufacture process for workers with visual impairments. The design should support manufacture of soaps with various surface (relief) designs.

3. UCD PROCESS FOR PEOPLE WITH VISUAL IMPAIRMENTS

Since techniques and methods that support user-centred design (Abrams, 2004; Maguire, 2001) and contextual design (Beyer et al, 1997; Holtzblatt et al, 2014) are well documented, this paper won't go into their explanation, but rather how they were implemented into the proposed design process.

Inclusion of the user into the design process start with contextual inquiry sessions in the form of semi-structured interviews with the users at their workplace, place or residence or the place where the problem occurs (eg. grocery store). Interviewer is followed by an assistant who records what users want, care about and interact with, as well as observations of non-verbal communication (eg. body language). In the interpretation and data consolidation process, affinity diagramming was used to reveal key issues and gain a better understanding of the users and their world. Through persona creation, gained issues were made more actionable and easier for designers to implement through the ideation and validation processes. In the next stage, insights gained from the contextual inquiry are translated into design concepts. In this stage, emphasis is placed on exploring various possibilities and producing a high number of novel design concepts that could address the accessibility issues while at the same time accommodating other design requirements. Rapid prototyping is used to produce low-fidelity functional prototypes of the design concepts. If needed, the low-fidelity prototypes can be supported with 3D visualizations to gain better understanding of the design features.

Since testing a high number of variations could be demanding for the users with visual impairments, but also resource consuming for the development team, informal expert reviews are used to reduce the number of design concepts that will undergo usability testing and user experience evaluation and to determine any major accessibility omissions in the design concepts.

The usability testing is based on completing a set of tasks. Completion time, number of errors, and task completion are measured and observations about participants manipulation with the products are recorded. Moderators should generally avoid assisting the participants while performing tasks. Participants are interviewed after each tested sample for providing deeper insights into their experience. The results from usability testing are used for design selection and refinements, and the process is repeated until the design criteria is met.

After the usability tests, the chosen design concepts are evaluated by users without visual impairments. Measuring user experience is a rather active and expanding field of research, with many evaluation techniques and methods present, but also many problems and challenges still to solve (Hornbæk, 2006). One of the widely used user experience evaluation method, and applicable to the design and production context (Roto et al, 2009), is AttrakDiff (Hassenzahl et al, 2003) - a questionnaire based on the semantic differential method and designed to measure pragmatic and hedonic qualities of interactive products, as well as the product's attractiveness. The most recent version of AttrakDiff evaluation method, AttrakDiff 2 (Hassenzahl, 2004), consists of 28 word pairs which are used to evaluate following dimensions of design: Pragmatic Quality (PQ), Hedonic Quality – stimulation (HQ-S), Hedonic Quality – Identity (HQ-I) and Attractiveness (ATT). Decisions on the final design are based on the results of both usability testing and subjective evaluation.

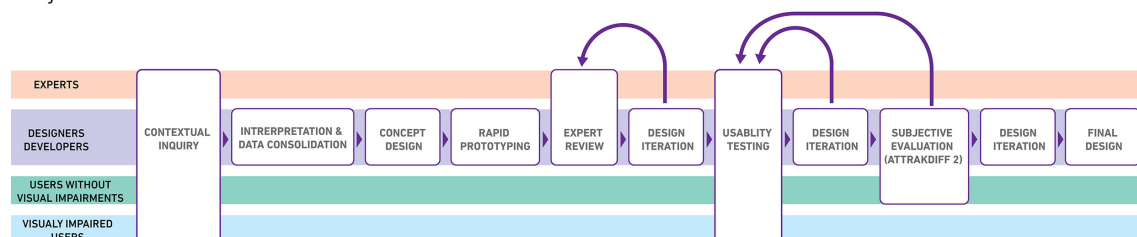


Figure 1: Proposed User-Centred Design process for people with visual impairments

Since the mould for soap manufacture is a speciality product developed primarily for blind and low-vision users and the visual aspect of the product isn't relevant, process for designing the mould was modified and didn't include subjective evaluation of visual features.

4. SOAP MANUFACTURING MOLD DESIGN PROCESS

The design process began with conducting contextual inquiry with the blind and low-vision manufacture workers. A total of 3 participants were interviewed. The interviews were focused on the current process of the bar soap manufacturing and key issues for the blind and low vision workers. It was identified that the existing generic moulds for manufacturing of the soap that are widely available aren't suitable for use. They are made from rigid polymers and usually feature multiple slots that cannot be separated. Since the soap mass is heated to 70°C during the casting, difficulties with manipulating the moulds could lead to injury of the worker. Separating the soap from the mould after casting was stressed as one of the most important challenges to workers in the production process. Participants also indicated problems with manufacture of multi-layered soaps with existing moulds.

Based on the insights gained from the contextual inquiry, a concept of a modular mould was developed to aid the users in easier separation of the soap and the mould (Figure 2). The design featured a movable bottom plate which enables easier soap extraction from the mould. The plate is interchangeable and can feature different embossed designs for producing soaps with relief features on the top surface. Rapid prototyping method was used to build a functional prototype of the design. The prototype was created by fused deposition modelling (FDM) 3D printing technique (Figure 3).

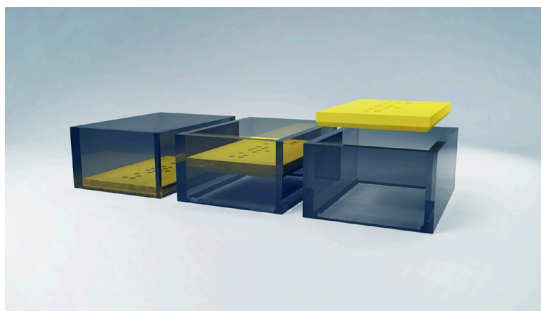


Figure 2: Visualization of the modular mould design



Figure 3: 3D printed prototype of the mould design

In the next phase, usability tests were conducted with the developed prototype. The mould was tested with 3 participants without vision deficiencies in the soap production facility. Usability test results indicated problems with the plate separation from the rest of the mould. Problems were addressed in the next iteration of the design and a new 3D printed physical prototype was created for usability test on the target audience.

Usability test with the participants from the contextual inquiry showed no significant problems with using the proposed modular design of the mould. After establishing the final design, a version of the mould for production of multi-layered soaps was developed (Figure 4). Two usability tests, first with the workers without visual impairments and after with low vision workers, were conducted to validate the developed design.

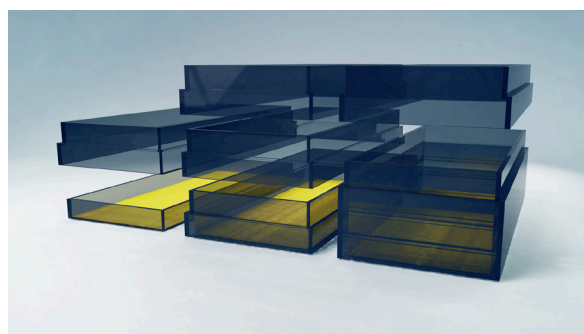


Figure 4: Variant of the mould design for manufacture of multi-layered soaps

5. SOAP PACKAGING DESIGN PROCESS

Contextual inquiry was used to gain insights into everyday interaction of blind and low vision users with packaged goods, with an emphasis on handling of the bar soap packaging from the perspective of the end user and from the perspective of the soap manufacture worker. Participants were asked to provide elaborate comments for the bad and good examples of existing packaging design practices in regard to accessibility for blind and low-vision users, as well as to provide their ideas for enhancement of the existing packaging designs. The interviews were conducted in two sessions, one week apart, with 1 blind and 6 low-vision participants.

All insights were categorized and analysed prior to concept design phase. Participants singled out wrapped packaging as the most difficult to open, as well as most difficult to package the product into. Shrink wrapped cardboard packaging was also found to be impractical to open due to lack of tactile features. Braille lettering was stated as helpful for identifying the content of the packaging and other relevant information, but it was stated as unnecessary for indication of the opening area on the packaging. According to participant insights, a simple tactile feature, such as a dot, notch or a tab on the cardboard box lid would be a sufficient pointer to a blind or a low-vision user.



Figure 5: Initial design concepts

Insights were used to develop 12 different bar soap packaging concepts by using rapid prototyping method in combination with 3D visualizations (Figure 5). Functional cardboard prototypes were created on Zünd M-800 digital flatbed cutter. Expert review was conducted to narrow the number of samples that are going to be tested to 5 samples (Figure 6). The chosen designs were modified according to the reviewers feedback. Functional prototypes of the modified designs were created for the purpose of testing with users. Sample 1 and 2 presented a more traditional approach of the cardboard box design for bar soaps, while Samples 3, 4, and 5 presented a more novel approach. All designs had accessibility features for easier opening and access to the product.

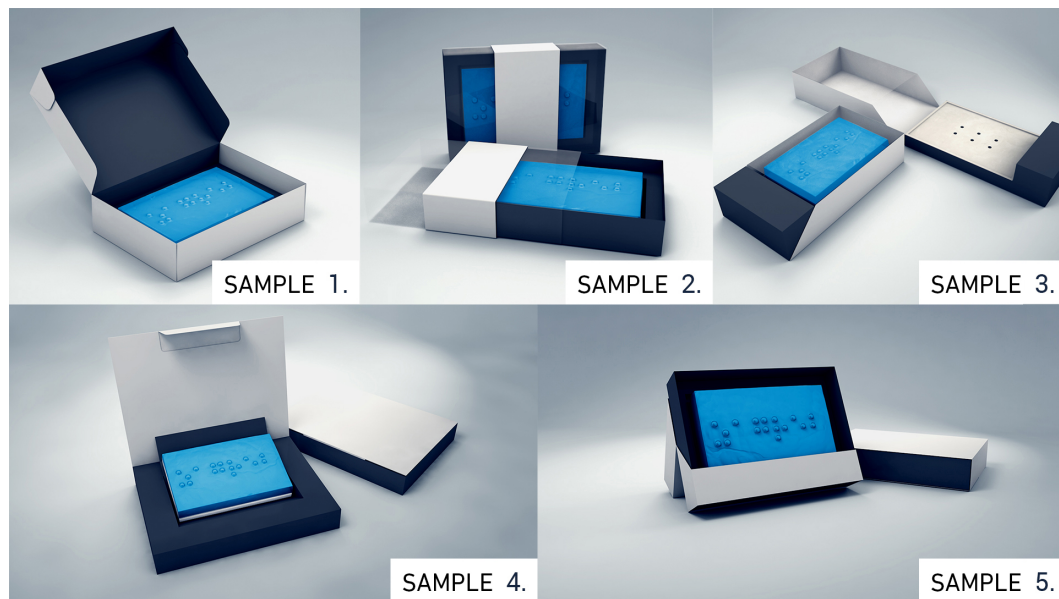


Figure 6: Selected design samples after the expert review process

Usability testing was conducted on 7 users that participated in contextual inquiry. Both the tasks of opening the packaging and packaging the soap into the cardboard box were tested. Observations about the speed of conducting the tasks, errors while conducting the tasks and the way users manipulated with the packaging and the product during the tasks were recorded. After each task, participants were asked to evaluate the packaging in regard of ease of use and accessibility features, as well to identify any pain points in their experience while performing given tasks.

Samples 1 and 3 had weak usability results, with Sample 1's design being especially problematic during the action of closing the box, due to presence of flaps that needed to be tucked into the designated spaces. Samples 2, 4, 5 were found to offer similar level of usability, with the participant's slight preference toward Sample 4.

After usability testing with blind and low-vision users, a subjective evaluation was conducted with users without visual impairments. The evaluation is conducted on cardboard prototypes of 5 Samples. All Samples featured identical colour and surface properties of the material used to eliminate their influence on the results. 20 participants evaluated each of the Samples by semantic-differential questionnaire which featured 28 word-pairs from AttrakDiff method and a 7 point Likert scale for each word pair. The research was conducted in a controlled environment and each sample was presented on a neutral background and in the same lighting conditions.

Results show that Sample 1 was rated lowest compared to the rest of the samples in regard to all dimensions of quality and attractiveness (Figure 7). Sample 2, while having the similar results for pragmatic quality compared to Sample 4 and 5, has scored low for the hedonic quality dimensions and attractiveness. Sample 5 had the best results for both hedonic quality dimension and attractiveness, with Sample 4 receiving the second highest scores. However, although being perceived as best design overall, Sample 5 was rated as the most unpredictable and cumbersome design (Figure 8).

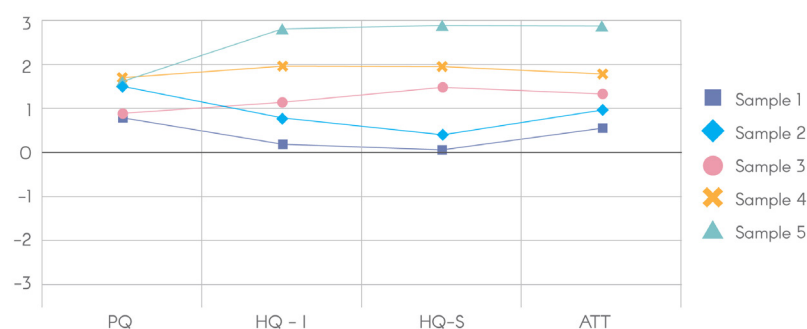


Figure 7: Graph of the mean values for the AttrakDiff subjective evaluation results for each of the quality dimensions

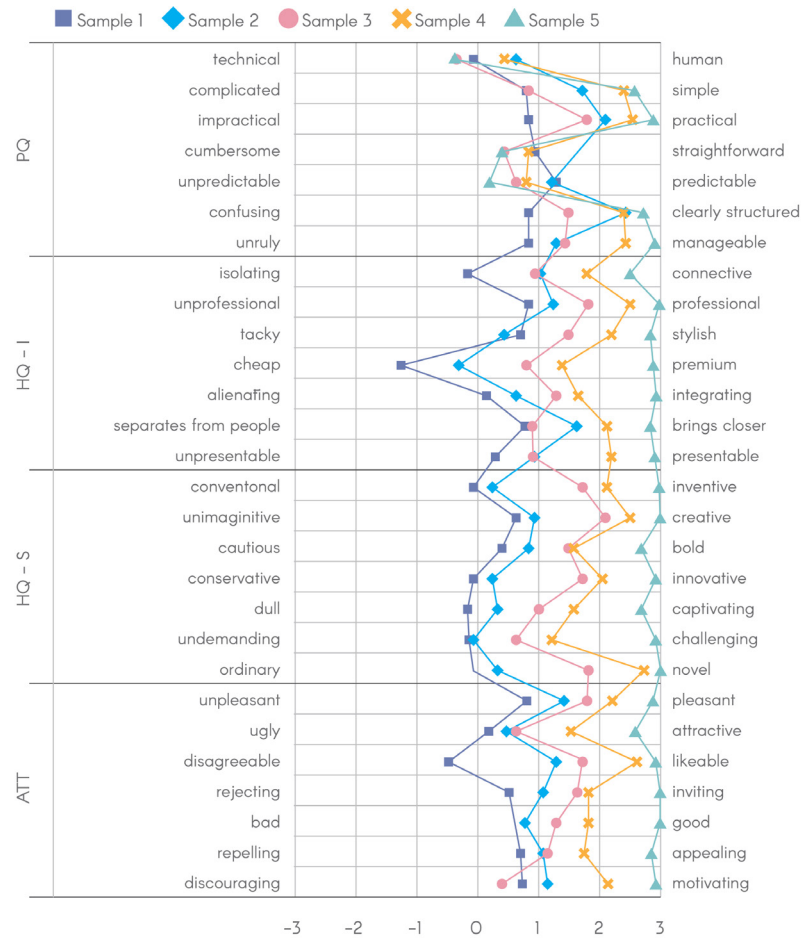


Figure 8: Graph of the mean values for the AttrakDiff subjective evaluation results for each word pair

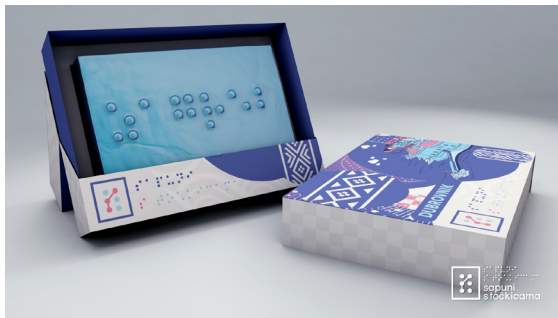


Figure 9: Visualization of soap design and visual appearance of the packaging based on Sample 5



Figure 10: Visualization of soap design and visual appearance of the packaging based on Sample 4

Based on the results of usability testing and AttrakDiff 2 evaluation, the manufacturer opted to use two packaging designs, Sample 4 and Sample 5, for its' soap product range. The visual identity for the product and packaging was created and applied to packaging designs, as well as the range of soap designs manufactured with the developed moulds (Figure 9, 10).

6. CONCLUSION

Designing physical products accessible to people with visual impairments still presents a significant challenge to many designers. The inclusion of users in the design process is a necessity, but can introduce several challenges, so the selection of the techniques and methods should be optimised. The proposed User-Centred design process for people with visual impairments was successfully applied to the case of designing packaging of accessible packaging for souvenir bar soap manufactured by blind and low-vision

users. Further research is needed to develop subjective evaluation methods for user experience measurement more suited to the users with visual impairments, so they can be included in the relevant phases of the proposed design process.

7. REFERENCES

- [1] Abras, C., Maloney-Krichmar, D., Preece, J.: "User-centered design", Encyclopedia of Human-Computer Interaction, Sage Publications, Thousand Oaks, 2004.
- [2] AlZuhair, M. S., Najjar, A. B., Kanjo, E.: "NFC based applications for visually impaired people - A review", Proceedings of IEEE International Conference on Multimedia and Expo Workshops (ICMEW, Chengdu, 2014), pages 1-6. doi: 10.1109/ICMEW.2014.6890657.
- [3] Barbosa, M. L. de A., Ribeiro, G. Y. A., Soares, I. G., Okimoto, M. L.: "Accessible Packaging: A Study for Inclusive Models for Visual Impairment People", Proceedings of the AHFE International Conference on Ergonomics in Design 2018, (AHFE, Orlando, Florida, 2018), pages 282–292.
- [4] Beyer, H., Holtzblatt, K.: "Contextual design: defining customer-centered systems", (Elsevier, San Diego, 1997).
- [5] Van der Geest, T. M., Buimer, H. P.: "User-centered priority setting for accessible devices and applications", Proceedings of Mensch und Computer 2015 – Workshopband, (Mensch und Computer, Oldenbourg: De Gruyter, Stuttgart, 2015), pages 383–389.
- [6] Hassenzahl, M.: "The Interplay of Beauty, Goodness, and Usability in Interactive Products", Human-Computer Interact 19(4), 319-349, 2004. doi: 10.1207/s15327051hci1904_2.
- [7] Hassenzahl, M., Burmester, M., Koller, F.: "AttrakDiff: Ein Fragebogen zur Messung wahrgenommener hedonischer und pragmatischer Qualität", Proceedings of Mensch und Computer 2003, (Mensch und Computer, Verlag, 2003), pages 187–196.
- [8] Holtzblatt, K., Beyer, H.: "Contextual Design: evolved", Synth. Lect. Human-Centered Informatics 7(4), 1-91, 2014. doi: 10.2200/S00597ED1V01Y201409HCI024.
- [9] Hornbæk, K.: "Current practice in measuring usability: Challenges to usability studies and research", International Journal of Human-Computer Studies 64(2), 79-102, 2006. doi:10.1016/j.ijhcs.2005.06.002.
- [10] Maguire, M.: "Methods to support human-centred design", International Journal of Human-Computer Studies 55(4), 587–634, 2001. doi: 10.1006/ijhc.2001.0503.
- [11] Merino, G. S. A. D.: "Guia de Orientação para Desenvolvimento de Projetos: Uma metodologia de Design Centrado no Usuário", (NGD/UFSC, Florianópolis, 2016).
- [12] Roto, V., Obrist, M., Väänänen-Vainio-Mattila, K.: "User experience evaluation methods in academic and industrial contexts", Proceedings of ACM CHI 2009 (CHI, Boston, 2009).
- [13] Sanchez, J.: "User-Centered Technologies for Blind Children", Human Technology- An Interdisciplinary Journal on Humans in ICT Environments 4(2), 96-122, 2008. doi:10.17011/ht/urn.200810245832.



CHITOSAN AND RICE STARCH FILMS AS PACKAGING MATERIALS

Urška Vrabič Brodnjak ¹, Dimitrina Todorova ²

¹University of Ljubljana, Faculty of Natural Sciences and Engineering,
Department of Textiles, Graphic Arts and Design, Ljubljana, Slovenia

²University of Chemical Technology and Metallurgy,
Department of Pulp, Paper and Graphic Art, Sofia, Bulgaria

Abstract: Producers of bio-based materials are keen on replacing oil-based packaging materials with green, sustainable materials which also have improved mechanical, antimicrobial, barrier properties. One of the most nontoxic and widely used polymers are polysaccharides, chitosan being one of them.

This research shows the preparation, characterisation of the chitosan and rice starch films. The aim of the research was to improve the mechanical, moisture and optical properties of chitosan, rice starch and composite chitosan-rice starch film using ultrasonic treatment. Our research was focused on the effect of ultrasonic treatment on the solutions for the preparation of the mentioned films.

The results showed that an ultrasonic treatment improved elasticity, moisture resistance and that films were more transparent. Elongation at break and tensile strength increased, especially at blend films. Moreover, moisture content showed a decrease proportional to an increase in thickness with decreasing film solubility at all treated samples. The surface at untreated blend film was more uneven compared to chitosan and rice starch films, which improved after the treatment. However, preparing film solutions with ultrasound is an improved procedure to increase many properties of biodegradable films and in this form could be used as packaging materials.

Key words: materials, food, blend films, biodegradability, sustainability

1. INTRODUCTION

Producers of bio-based materials are keen on replacing oil-based packaging materials with green, sustainable materials which also have improved mechanical, antimicrobial, barrier properties (Bourtoom & Chinnan, 2008), (Caner et al, 1998). One of the most nontoxic and widely used polymers are polysaccharides, chitosan being one of them. It is a natural polysaccharide, derived with the deacetylation of chitin (Krochta & De Mulder-Johnston, 1997). Chitosan has also attracted interest in packaging, especially in the food packaging area as edible films and coatings (Vrabič Brodnjak, 2017). It is known that chitosan films have great mechanical properties, e.g. they are flexible, long lasting, have good strength and increase storage life of fresh food (Xu et al, 2005). They also have good barrier properties against grease due to the positive charge on the amino group under acidic conditions, where chitosan binds negatively charged molecules. Moreover, chitosan films exhibit excellent oxygen-barrier properties, due to their high crystallinity and hydrogen bonds between molecular chains (Cheng, Chen, Liu et al, 2010). On the other hand, there are many other natural polymers, which could be used as materials for packaging. One of them is also rice starch. Due to the high amount of amylase, rice starch is attractive for food packaging as a film barrier (Xu et al, 2005). It has also been used to replace plastic film barriers as it has good mechanical properties (Bourtoom & Chinnan, 2008), (Krochta & De Mulder-Johnston, 1997), (Xu et al, 2005). Rice is the most widely used basic food in the world. Due to different climates, soil characteristics and cultures, more than 240 000 registered varieties of rice exist in the world and consequently as many different types of rice starch, (Xu et al, 2005).

This research shows the preparation, characterisation of the chitosan and rice starch films. The aim of the research was to improve the mechanical, moisture and optical properties of chitosan, rice starch and composite chitosan-rice starch film using ultrasonic treatment. Previously, no research was conducted on the blend of rice starch and chitosan film, and a subsequent improvement of the properties with ultrasound. Our research was focused on the effect of ultrasonic treatment on the solutions for the preparation of the mentioned films. Using ultrasound is an environmentally friendly process and it can be used for all solutions in order to improve biodegradable films. Such a treatment and materials could be used as a substitute for packaging films that are currently on the market.

The results showed that an ultrasonic treatment improved elasticity, moisture resistance and that films were more transparent. Elongation at break and tensile strength increased, especially at blend films. Moreover, moisture content showed a decrease proportional to an increase in thickness with decreasing

film solubility at all treated samples. The surface at untreated blend film was more uneven compared to chitosan and rice starch films, which improved after the treatment. However, preparing film solutions with ultrasound is an improved procedure to increase many properties of biodegradable films and in this form could be used as packaging materials.

2. METHODS

2.1 Materials

Chitosan, with molecular weight 20kDa and deacetylation degree higher than 85%, was purchased from Sigma Aldrich (Austria). Rice starch was obtained from Farmalabor Srl (Italy), with moisture content of 14%, 1% of proteins and 0.6% of ashes. Malic acid (98%) was purchased from Sigma Aldrich (Austria). Glycerol, obtained from Sigma Aldrich (Austria), was also used as a plasticiser.

2.2 Preparation of film-forming rice starch and chitosan dispersions

The rice starch dispersion was prepared by dissolving 2 g of rice starch in 100 ml of distilled water and glycerol (40% w/w) was added as a plasticiser. The solution was mixed until it gelatinised (85 °C for 20 min) and then cooled to room temperature.

The chitosan solution was prepared by dissolving 2 g of chitosan in 100 ml (2% w/w) malic acid and glycerol (40% w/w) was added as a plasticiser. The solution was mixed at 90 °C for 5 minutes until chitosan was not dispersed and after that cooled to room temperature. Before cooling down, the film solution was filtered through a polyester screen (mesh no. 140 with mesh opening 160 µm) with aspiration to remove small lumps in the solution.

2.3 Preparation of solution for chitosan-rice starch blend film

The rice starch-chitosan film was prepared by mixing 100 ml of 2% rice starch solution with 100 ml of 2% chitosan solution. After that, 40% of glycerol as a plasticiser (w/w; of total solid weight in solution) was added into the mixed solution. The total solution for blend film was mixed at 800 rpm for 5 minutes at room temperature and then filtered through a polyester screen with the same mesh opening as at the chitosan solution. The aspiration was performed in order to remove small lumps in the solution.

After the aspiration, the solutions (for chitosan, rice starch film and blend film) were put into an ultrasonic bath (Asonic, Ultrasonic bath), using constant 35 kHz frequency for 15 minutes (Cheng, Chen, Liu *et al*, 2010).

2.4 Preparation of casting films

After the aspiration and the treatment, the mixtures (untreated and treated) were cast onto petri dishes (50 ml), spread thinly, uniformly and dried at 55 °C for 10 hours. After the films were peeled off from the dishes, they were cooled at room temperature (23 °C; 55% RH). The films were stored in desiccators at 60% RH for further investigations.

2.5 Characterization of films

2.5.1 Film thickness

The thickness of films was measured with a precision digital micrometre Mitutoyo Corporation, Japan, to the nearest 0.0001 µm at 5 random locations on each film.

2.5.2 Moisture content

Moisture content was determined by measuring weight loss upon drying in a laboratory oven at 105 ± 1 °C until constant weight. Five samples per each films were tested and the results were expressed in percentage.

2.5.3 Water vapour permeability (WVP)

To determine the WVP of films, the ASTM E96 standard desiccant method was used [19]. The test cups were filled with silica gel (RH = 16% in the cup), where a sample was placed between the cup and the ring

cover of each cup [20]. There was an air gap of 11 mm between the silica gel and the underside of the placed film. To ensure the best results of WVP, a silicone sealant was applied around the cup edge. The films with the exposed area of 50 cm² were tested at 90 ± 2% RH and 38 ± 2 °C for 24 hours. Three replicas per each film were tested.

2.5.4 Tensile properties

Tensile strength (TS) and elongation at break (E) of the films were determined on a tensile testing machine Instron 6022. The samples were analysed in standard atmosphere 23 °C ± 1 °C of temperature and 55% ± 2% of relative humidity. The cross speed head was 0.15 mm/s. The films of 6 cm in length and 0.7 cm in width were used, and a minimum of five probes for each sample was tested. During the sample stretching, several load and elongation data per second were recorded until a break of the sample occurred.

2.5.5 Surface properties – Scanning electron microscope (SEM)

The SEM micrographs of film surfaces were taken with a scanning electron microscope (JSM -6060 LV). The instrument was operated at 10 kV, at the magnification 400×.

3. RESULTS AND DISCUSSION

3.1 Thickness, moisture content and water vapor permeability

The thickness of films influences water vapour properties. The nature of films from biopolymers is mostly hydrophilic; therefore, the thickness influences water barrier and mechanical properties. In our research, the thickness (mean values) of films was used in the calculations for water vapour properties (TS). Table 1 presents a comparison of untreated and treated films, and it can be seen that chitosan-rice starch blend film treated with ultrasound exhibits better WVP than the untreated samples. In our research, glycerol as a plasticiser was added, whereas the ultrasonic treatment had the biggest impact on WVP (Brodnjak, 2017), (Rhim et al, 2006). Previous research has explained that chitosan films have great oxygen but poor water vapour barriers, which is due to their hydrophilic character, which was also proved in our research (Dias et al, 2010), (Butler et al, 1996).

From the obtained results, it can be seen that the best water vapour properties characterise the chitosan-rice starch film treated with ultrasound (3.37 ± 0.29 g mm/m²/day kPa, i.e. is by two times lower than at the untreated sample). The same trend is detected at chitosan and rice-starch film. The WVP of untreated chitosan film decreased with the treatment from 9.11 to 8.47 g mm/m²/day kPa.

Table 1: Results of thickness, moisture content and water vapor permeability

	Sample	Thickness (μm)	Moisture content (%)	WVP (g mm/m ² /day kPa)
Untreated	Chitosan film	210 ± 2.5	11.3 ± 0.55	9.11 ± 0.36
	Rice starch film	205 ± 5.0	10.8 ± 0.69	6.45 ± 0.75
	Blend film	215 ± 3.3	9.5 ± 0.23	7.92 ± 0.17
Treated with ultrasound	Chitosan film	207 ± 6.7	10.8 ± 0.47	8.47 ± 0.24
	Rice starch film	203 ± 4.2	9.6 ± 0.18	5.45 ± 0.36
	Blend film	216 ± 1.2	9.0 ± 0.78	3.37 ± 0.29

The presence of rice starch in blend films can form highly cross-linked systems, preventing water molecules from penetrating into composite films (Thakur et al, 2016). The values of moisture content of the untreated films were higher than of treated ones. The highest moisture content characterised the untreated chitosan film (11.03%) and the lowest the treated blend film (9.0%). The acoustic activation in ultrasonic bath caused differences in the tested films. In the case of addition of glycerol, at all tested films, the observed behaviour can be a consequence of an increase in free volume, and a consequent decrease in WVP and moisture content. The reason is in the high content of glycerol, which was present at all samples. The ultrasonic treatment affected all films regarding moisture absorption, with a decrease

between 0.5 and 1%. The decrease was not major, yet the impact on the solution and afterwards on other film properties was detected.

3.2 Tensile properties

The results of tensile strength and elongation at break of untreated and ultrasound treated films are presented in Figure 1. They demonstrated that tensile strength increased with the ultrasonic treatment at all treated films. Better results of tensile strength are at treated samples and the maximum occurred at the blend of chitosan-rice starch film. The values of untreated films are slightly higher, but still comparable to those reported in the literature (Rivero et al, 2009). The highest increase was detected at the blend of chitosan-rice starch film, i.e. by 30%, and at chitosan film by 18%. The treated rice starch film had a lower increase, i.e. by 4%. Elongation at break (E) is an indicator for film extensibility and is determined as the point when a film breaks at tensile testing. The values of elongation at break were affected by the ultrasonic treatment. The highest elongation at break characterised blend films, which with an ultrasonic treatment increased by 8%. At the rice starch and chitosan film, elongation increased by 2.5% at both samples. The values of elongation are higher at all samples due to the added plasticiser, i.e. glycerol. Nevertheless, the elongations at break was better at all treated samples also because of the increase in solubility and homogeneity of all film solutions, due to the acoustic activation in the ultrasonic bath.

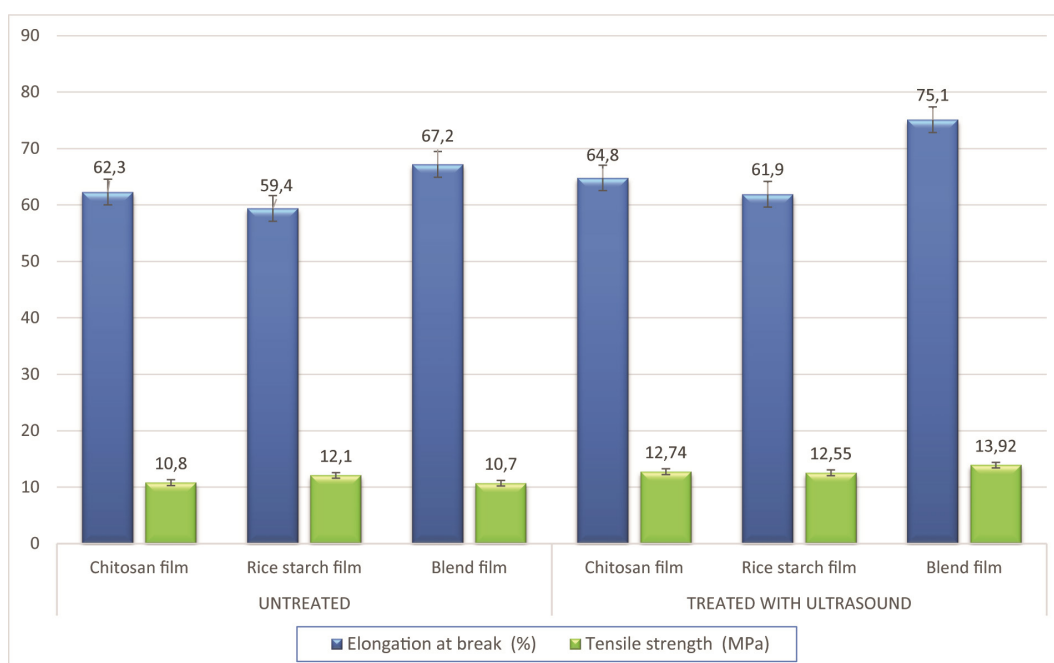


Figure 1: Tensile properties of untreated and ultrasound treated chitosan, rice starch and blend films

3.3 Surface properties

Surface properties were determined with scanning electron microscope (SEM) in order to analyse the effect of ultrasound treatment of film solutions on final product-packaging films. SEM micrographs of untreated and treated films are presented in Figure 2 (a–f). All figures show the surface of films at 400x magnification and voltage 10 kV. The 10kV voltage was used since at higher voltage, film samples would get damaged very quickly and the determination of the surface would not be correct. The same was at 400x magnification, as higher magnifications degrade the surface of analysed films.

The surface micrographs revealed a smoother, even surface at all treated films. As seen in Figure 2a, the untreated chitosan film is less smooth and not as even as the film treated with ultrasound (Figure 2b). The same trend is seen in Figures 2c and 2d, where the SEM micrographs of rice starch are shown. From Figure 2c, it can be seen that the untreated rice starch film has a more irregular surface than the chitosan film.

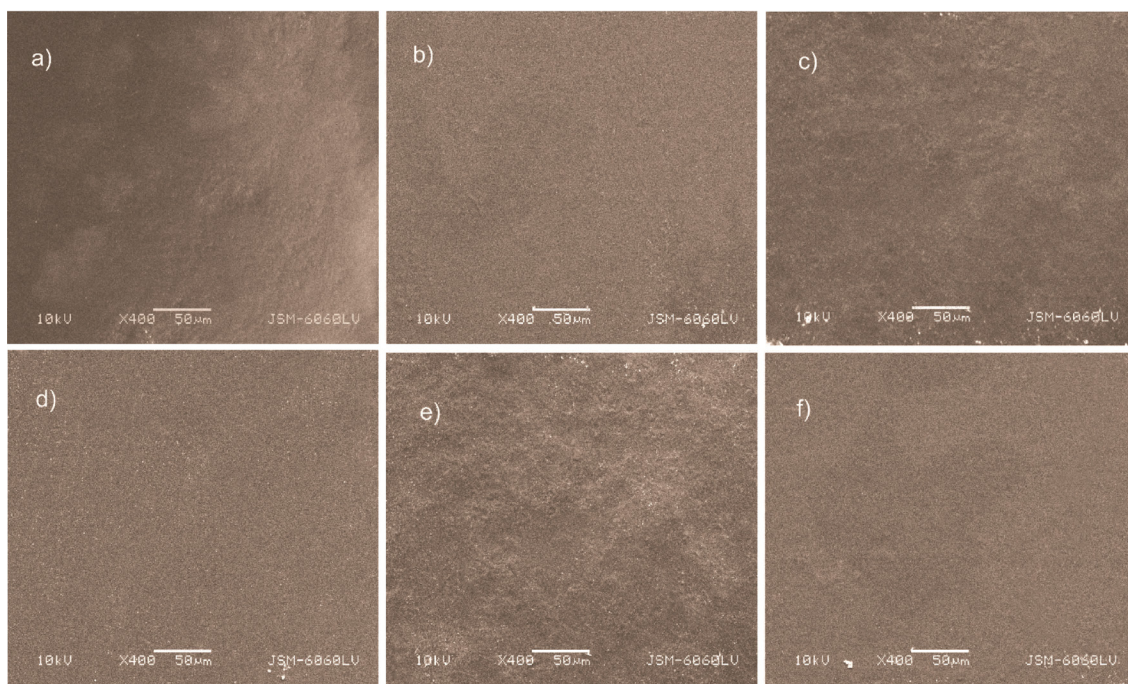


Figure 2: Surface properties of untreated and ultrasound treated films a) untreated chitosan film, b) treated chitosan film, (c) untreated rice starch film, d) treated rice starch film, e) untreated blend chitosan-rice starch film, f) treated blend chitosan-rice starch film

4. CONCLUSIONS

From our research and analysis we came to the conclusion that the ultrasonic treatment caused homogeneity of the surface and it is a good indicator for better structural and mechanical properties, compared to the untreated films. The surface of films improved at all treated films. The mechanical resistance of treated films was improved, especially at blend film. By mixing these two polymers, characteristics of the film improved and with an ultrasonic treatment, the properties got even better.

Nevertheless, the elongations at break were better at all treated samples also because of the increase in solubility and homogeneity of all film solutions, due to the acoustic activation in the ultrasonic bath. The results demonstrated that tensile strength increased with the ultrasonic treatment at all treated films. Better results of TS are at treated samples and the maximum occurred at the blend of chitosan-rice starch film. The presence of rice starch in blend films can form highly cross-linked systems, preventing water molecules from penetrating into composite films. Such behaviour was confirmed at our research due to the inclusion of glycerol and rice starch as well, since they interfere with cross-links, resulting in decreased water solubility.

In general, the ultrasonic treatment helps to obtain a smoother and homogeneous surface. New studies are necessary to find the best ultrasonic procedures (regarding treatment times and frequency) to prepare the films.

5. ACKNOWLEDGMENTS

This research was supported by the COST action CA15118 (FoodMC). The authors would like to thank University of Ljubljana, Faculty of Natural Sciences and Engineering, Department of Textiles Graphic Arts and Design, Ljubljana, Slovenia for financial support and University of Chemical Technology and Metallurgy, Department of Pulp, Paper and Printing Art in Sofia.

6. REFERENCES

- [1] Bourtoom, T., Chinnan, M. S.: "Preparation and properties of rice starch-chitosan blend biodegradable film", *Food Science and Technology*, 41(9), 1633-1641, 2008. doi: 10.1016/j.lwt.2007.10.014
- [2] Brodnjak, U. V.: "Experimental investigation of novel curdlan/chitosan coatings on packaging paper", *Progress in Organic Coatings*, 112, 86-92, 2017. doi: 10.1016/j.porgcoat.2017.06.030
- [3] Butler, B. L., Vergano, P. L., Testin, R. F., Bunn, J. M., Wiles, J. L.: "Mechanical and barrier properties of edible chitosan film as affected by composition and storage", *Journal of food Science*, 61(5), 953-956, 1996. doi: 10.1111/j.1365-2621.1996.tb10909.x
- [4] Caner, C., Vergano, P.J., Wiles, J.L.: "Chitosan film mechanical and permeation properties as affected by acid, plasticizer, and storage", *Journal of Food Science*, 63(6), 1049-1053, 1998. doi: 10.1111/j.1365-2621.1998.tb15852.x
- [5] Cheng, W. J., Chen, J. C., Liu, D. H., Ye, X. Q., Ke, F. S.: "Impact of ultrasonic treatment on properties of starch film-forming dispersion and the resulting films", *Carbohydrate Polymers*, 81(3), 707-711, 2010. doi: 10.1016/j.carbpol.2010.03.043
- [6] Dias, A. B., Müller, C. M. O., Larotonda, F. D. S., Laurindo, J.: "Biodegradable films based on rice starch and rice flour", *Journal of Cereal Science*, 51(2), 213-219, 2010. doi: 10.1016/j.jcs.2009.11.014
- [7] Rivero, S., García, M. A., Pinotti, A.: "Composite and bi-layer films based on gelatin and chitosan", *Journal of Food Engineering*, 90(4), 531-539, 2009. doi: 10.1016/j.jfoodeng.2008.07.021
- [8] Rhim, J. W. , Hong, S. I. , Park, H. M. , Perry, K. W. N.: "Preparation and characterization of Chitosan-Based Nanocomposite Films with Antimicrobial Activity", *Journal of Agricultural and Food Chemistry*, 54(16), 5814-5822, 2006. doi: 10.1021/jf060658h
- [9] Krochta, J.M., De Mulder-Johnston, C.: "Edible and biodegradable polymer films: challenge and opportunities", *Food Technology*, 51, 61-74, 1997.
- [10] Thakur, R., Saberi, B., Pristijono, P., Golding, J., Stathopoulos, C., Scarlett, C., Vuong, Q.: "Characterization of rice starch-l-carrageenan biodegradable edible film. Effect of stearic acid on the film properties", *International journal of biological macromolecules*, 93(Pt A), 2016. doi: 10.1016/j.ijbiomac.2016.09.053
- [11] Vrabč Brodnjak, U.: "Influence of ultrasonic treatment on properties of bio-based coated paper", *Progress in organic coatings*, 103, 93-100, 2017. doi: 10.1016/j.porgcoat.2016.10.023
- [12] Xu, X.Y., Kim, K.M., Hanna, M. A., Nag, D.: "Chitosan-starch composite film: preparation and characterization", *Industrial Crops and Products*, 21(2), 185-192, 2005. doi: 10.1016/j.indcrop.2004.03.002



THE USE OF THE GREEN CHEMISTRY CONCEPT IN THE SYNTHESIS OF PACKAGING MATERIAL BASED ON POLYLACTIDE

Nevena Vukić ¹ , Tamara Erceg ¹ , Vesna Teofilović ¹ , Ljubiša Nikolić ²,
Suzana Cakić ², Borislav Simendić ³, Ivan Ristić ¹ 

¹University of Novi Sad, Faculty of Technology, Novi Sad, Serbia

²University of Niš, Faculty of Technology, Leskovac, Serbia

³Higher Technical School of Professional Education, Novi Sad, Serbia

Abstract: A world without plastics, or synthetic polymer materials, seems unimaginable today. During the last decade, the share of synthetic polymer consumption used in packaging industry increased to 42%, in relation to the total consumption of polymers. Wide use of polymer materials leads to generation of large amount of waste. Environmental pollution, as well as alarming reduction of fossil fuels have led to the implementation of the strategies for pollution control, pollution prevent, energy and resources saving. Growing awareness of global pollution consequences has rised these concerns on the level of the Green Chemistry concept. Green Chemistry is a multidisciplinary field where chemistry science and industry meets each other in order to design products and strategies for elimination of harmful substances. It is well known that the most important primary sources of feedstock for polymer materials production are fossil fuels. Increasing demand for polymers, has imposed the need for fossil fuels replacement by renewable resources for its synthesis. In this paper we have shown the implementation of the Green Chemistry principles in the synthesis of packaging material based on polylactide (PLA). Polylactide is one of the most promising polymers because of its biocompatibility, biodegradability and the fact that it can be produced from the biobased feedstocks. In accordance with modern ecological requirements, packaging material should be degradable or biodegradable and also economic. The use of PLA has a growing trend, therefore, today it takes an important place in packaging industry, especially because the properties of PLA films are comparable to standard petroleum based flexible packaging materials. The main purpose of this study was to syntheses packaging material based on polylactide by microwave synthesis as a method which implement some of the Green Chemistry principles. Microwave synthesis of PLA meets requirements of biobased polymers from the aspect of energy and time saving production of this biodegradable material. The microwave-assisted synthesis of PLA provides homogenous heating of reaction mixture, significant reduction in polymerization time, decreased consumption of organic solvent and, in the same time, high molecular weight polymers.

Key words: polylactide, packaging, green chemistry, microwave synthesis

1. INTRODUCTION

The reducing of waste production is one of the major challenges of the present era. Polymers represent the largest segment of global waste, this leads to the problems such as recycling and decomposition of polymer materials. Also, fossil resources have been reduced and the increasing concentration of carbon dioxide in the atmosphere has focused attention on the development of biopolymer materials, such as polylactide (PLA). The production of polylactide presents numerous advantages: it can be obtained from a renewable agricultural source (like corn starch or sugar cane), it is compostable and recyclable, its production consumes quantities of carbon dioxide, it provides significant energy savings, and the physical and mechanical properties can be manipulated through the polymer architecture (Auras et al, 2004).

Among the use of polylactide in the field of electronic, textile, pharmacy and medicine, industrial production is directed to the field of packaging industry. The use of PLA in packaging, especially in food, is increasing due to biodegradability of this material because polymer packaging materials can be contaminated by biological substance and foodstuff, which makes the recycling of these materials impracticable and most of the time not economically convenient. PLA is extremely versatile and can be injection molded into plastic parts, extruded into sheet or film, foamed, thermoformed or spun into fibers and filaments. This material also provides an excellent surface for printing and graphics. The high natural surface energy combined with good ink receptivity allows PLA to be used on conventional equipment using standard printing inks. Due to its higher cost, the initial focus of polylactide as a packaging material has been in high value films, food and beverage containers, coated papers and rigid thermoforms. PLA

may have packaging applications for a broader array of products as new and emerging production technologies lower its production costs. The use of PLA as a packaging material has increased mainly in the area of fresh products where polylactide is being used as a food packaging material for short shelf life products. PLA is also recognized as safe material for use in food packaging, but the use of this polymer as food packaging material can be limited because of the ductility, thermal and barrier properties (Arrieta et al, 2013; Martino et al, 2011). As the price for polylactide production drops and new facilities produce higher volumes of this polymer, new applications will be pursued.

It is possible to manipulate with PLA physical, mechanical and barrier properties by changing its chemical composition, and varying its molecular characteristics. It is also possible to blend polylactide with other polymers and to use nanomaterials and nanotechnologies in structuring of this material, making it a good biodegradable alternative for use in polymer packaging. If we compare PLA with other polymer packaging materials, we can note that polylactide has lower melting (T_m) and glass transition temperature (T_g) than poly(ethylene terephthalate) (PET) and polystyrene (PS), which make this polymer better for heat sealing and thermal processing. Polylactide is a clear, colorless thermoplastic when quenched from the melt and it is similar in many aspects to polystyrene (PS) (Auras et al, 2003; Madhavan Nampoothiri et al, 2010). But it is important to emphasize that thermal and mechanical properties of PLA are higher than the other biodegradable polyesters (polybutylene succinate - PBS, polyhydroxybutyrate - PHB and polycaprolactone - PCL).

The monomer lactic acid has two optical isomers, L and D, resulting in polymers that can present three forms: PLLA, PDLLA and PDLA. The stereochemistry, the ratio of L and D isomers, influences on polylactide properties and degradability (Abdel-Rahman et al, 2011). Direct polycondensation of lactic acid gives only the low molecular weight polymer, poly(lactic acid). It is equilibrium reaction, with water as by-product, which should be removed during the synthesis, in order to get higher conversions. Removing of water during the synthesis, as well as using a coupling agent to obtain higher molecular weights makes this process longer, more complicated and more expensive. For the preparation of high molecular weight polymer, cyclic lactide is used as monomer for the ring opening polymerization (ROP) (Figure 1) (Nice et al, 2003). ROP process demands high purity of the monomer, specific catalyst and solvent. Depending on methods, it requires high temperature, high pressure or vacuum. Traditional methods of PLA synthesis require large consumption of energy, time and reagents. Polymerization in organic solvent takes place from 4 to 50 hours depending on applied mechanism, temperature, catalyst and solvent. The applied temperature ranges from 40 to even 280 °C. Long polymerization time and high temperature require significant quantities of energy.

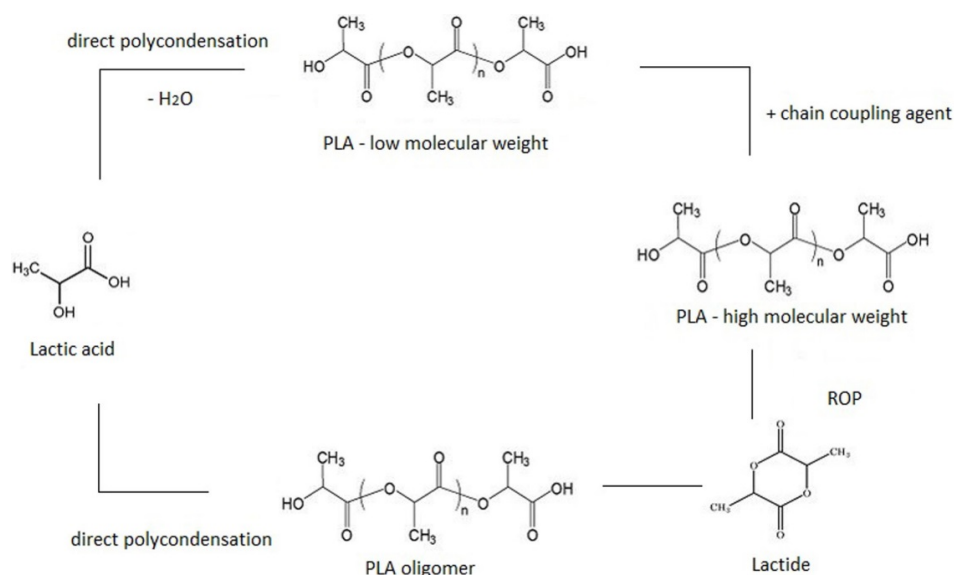


Figure 1: Synthesis of polylactide via direct polycondensation and via ROP method.

Difficulties that occur during the traditional methods of PLA synthesis can be overcome using a microwave heating as a solution which lies in the concept of Green Chemistry. The Green Chemistry concept seeks to redesign the materials that make up the basis of our society and our economy, in ways which are harmless for humans and the environment and possess intrinsic sustainability. In this concept,

by minimizing the hazard portion of the equation, using innocuous chemicals and processes, prevention is the approach to risk reduction. Green Chemistry has been enormously successful in devising ways to reduce pollution through efficiency of materials synthesis, catalysis, and improvements in solvent technology. Alternative synthesis methods have been applied to reduce energy consumption in the industry, and biobased feedstocks are decreasing our reliance on deficit fossil resources. In Table 1 are shown Twelve Principles of Green Chemistry which are a comprehensive set of design guidelines that have guided Green Chemistry development for many years (Anastas et al, 1998).

Table 1: The Twelve principles of Green Chemistry

1. Prevention It is better to prevent waste than to treat or clean up waste after it has been created.	2. Atom Economy Synthetic methods should be designed to maximize the incorporation of all materials used in the process into the final product.	3. Less Hazardous Chemical Syntheses Wherever practicable, synthetic methods should be designed to use and generate substances that possess little or no toxicity to human health and the environment.
4. Designing Safer Chemicals Chemical products should be designed to effect their desired function while minimizing their toxicity.	5. Safer Solvents and Auxiliaries The use of auxiliary substances (e.g., solvents, separation agents, etc.) should be made unnecessary wherever possible and innocuous when used.	6. Design for Energy Efficiency Energy requirements of chemical processes should be recognized for their environmental and economic impacts and should be minimized. If possible, synthetic methods should be conducted at ambient temperature and pressure.
7. Use of Renewable Feedstocks A raw material or feedstock should be renewable rather than depleting whenever technically and economically practicable.	8. Reduce Derivatives Unnecessary derivatization (use of blocking groups, protection/deprotection, temporary modification of physical/chemical processes) should be minimized or avoided if possible, because such steps require additional reagents and can generate waste.	9. Catalysis Catalytic reagents (as selective as possible) are superior to stoichiometric reagents.
10. Design for Degradation Chemical products should be designed so that at the end of their function they break down into innocuous degradation products and do not persist in the environment.	11. Real-time analysis for Pollution Prevention Analytical methodologies need to be further developed to allow for real-time, in-process monitoring and control prior to the formation of hazardous substances.	12. Inherently Safer Chemistry for Accident Prevention Substances and the form of a substance used in a chemical process should be chosen to minimize the potential for chemical accidents, including releases, explosions, and fires.

Microwave heating simplifies and accelerates the reaction of polymerization of lactide that lasts only 5-30 minutes. Sensitivity of the reaction to impurities and moisture from the air is significantly reduced due to the fact that the reaction takes place very quickly, so there is no need for recrystallization of monomers or carrying out of reaction under the vacuum (Ristić et al, 2012; Nikolić et al, 2010). Homogenous heating of the whole reaction mixture and high transfer energy per unit of time result in faster polymerization rate (Nikolić et al, 2010; Singla et al, 2012). Microwave synthesis allows obtaining a high molecular weight polymer in a short time in improved yield (Nikolić et al, 2010).

In this paper is shown how we can obtain applicable packaging material whose complete life cycle is put in ecological framework by implementing some of the Green Chemistry principles in the synthesis of PLA, emphasising the aspects of saving energy and resources accomplished using microwave reactor. The synthesis of polylactide as a biobased material that degrades in natural environment, also fits into the Green Chemistry concept.

2. METHODS

L-lactide (3,6-Dimethyl-1,4-dioxane-2,5-dione) and tin (II)- ethylhexanoate were supplied from Sigma-Aldrich. Toluene was procured from LACH-NERs.r.o. L-lactide was purified by recrystallization with methanol and placed in evaporating dish. Catalyst, tin (II)-ethylhexanoate, was added together with toluene. After homogenization of reaction mixture, the toluene was evaporated in vacuum, at 60 °C. Then the reaction mixture was closed in ampules which were put in a “Discover” focus microwave reactor, CEM Corporation, Matthews, NC, USA. Polymerization was performed at frequency of 2.45 GHz and power of 150 W, for 5, 10 and 20 minutes.

The molecular structure of obtained samples was analysed by Fourier Transform-Infrared Spectroscopy (FTIR), using a Shimadzu M850 Model FT-IR Spectrophotometer. The scans were recorded in the range of 4000-400 cm^{-1} .

Thermal properties of synthesized materials were investigated in nitrogen atmosphere using a TA Q20 Differential Scanning Calorimeter. Hermetically sealed aluminium pans containing around 5 mg of samples were prepared. The scans were recorded by heating of samples from -50 to 200 °C, at a rate of 10 °C /min. Data for melting temperature (T_m), crystallization temperature (T_{cc}) and glass transition (T_g) were recorded and are reported.

For the determination of the surface energy of the synthesized polylactide samples, the contact angle measurement was performed on the Drop Shape Analyzer DSA25 KRUS. The contact angle is measured using the image of a sessile drop at the points of intersection between the drop contour and the surface.

3. RESULTS AND DISCUSSION

Temperature and power change with reaction time were demonstrated at Figure 2. Lactide absorbs microwaves, and as a result of microwave heating and heating realised during the exothermic reaction, the temperature of reaction mixture linearly increases with the time in first 250 s. The loop on the curve originates from the presence of both - monomer and polymer in reaction mixture, which have different ability to absorb microwaves. Monomer is more polar than polymer and, therefore, possesses greater ability to absorb microwaves. Microwave irradiation was automatically switched off after 500 s, after reaching a temperature of 100 °C. The applied power of 150 W at the beginning of reaction dropped to zero after reaching an appointed temperature of 100 °C. After 500 s, the power of 40 W was sufficient for performing the polymerization.

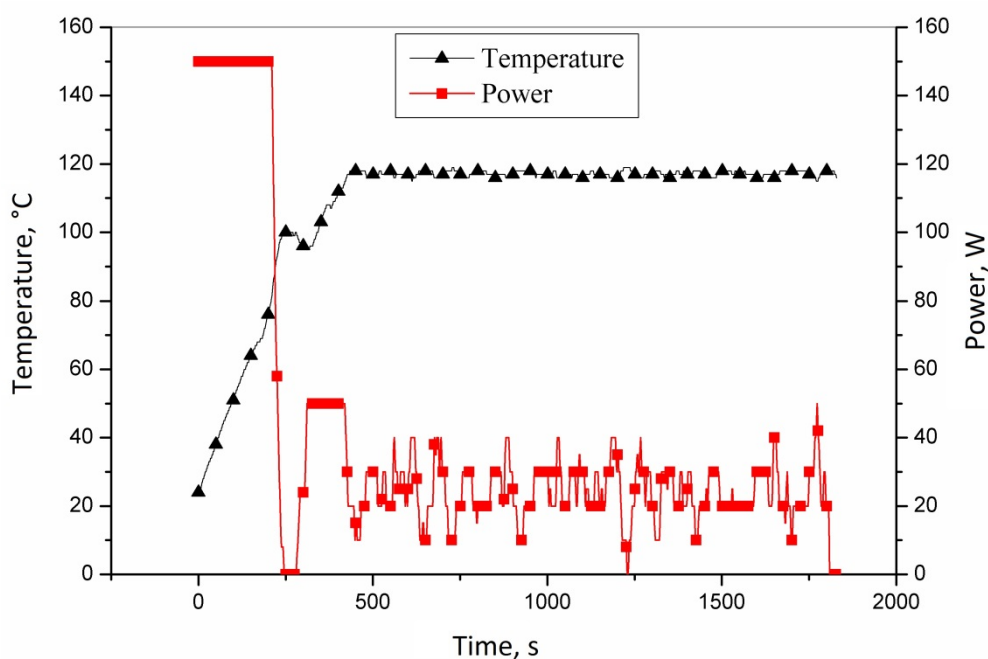


Figure 2: Temperature and microwave radiation power dependence on reaction time

The molecular structures of synthesized polymers were confirmed by FTIR (Figure 3). The broad peak at 3485 cm^{-1} is attributed to the O-H stretching. The two peaks at 2985 and 2891 cm^{-1} correspond to symmetric and asymmetric -CH_2 stretching. Sharp peak at 1750 cm^{-1} is attributed to C=O stretching vibrations. Peak at 1454 cm^{-1} corresponds to -CH_2 bending. C-O-C stretching vibrations are detected at 1257 and 1099 cm^{-1} .

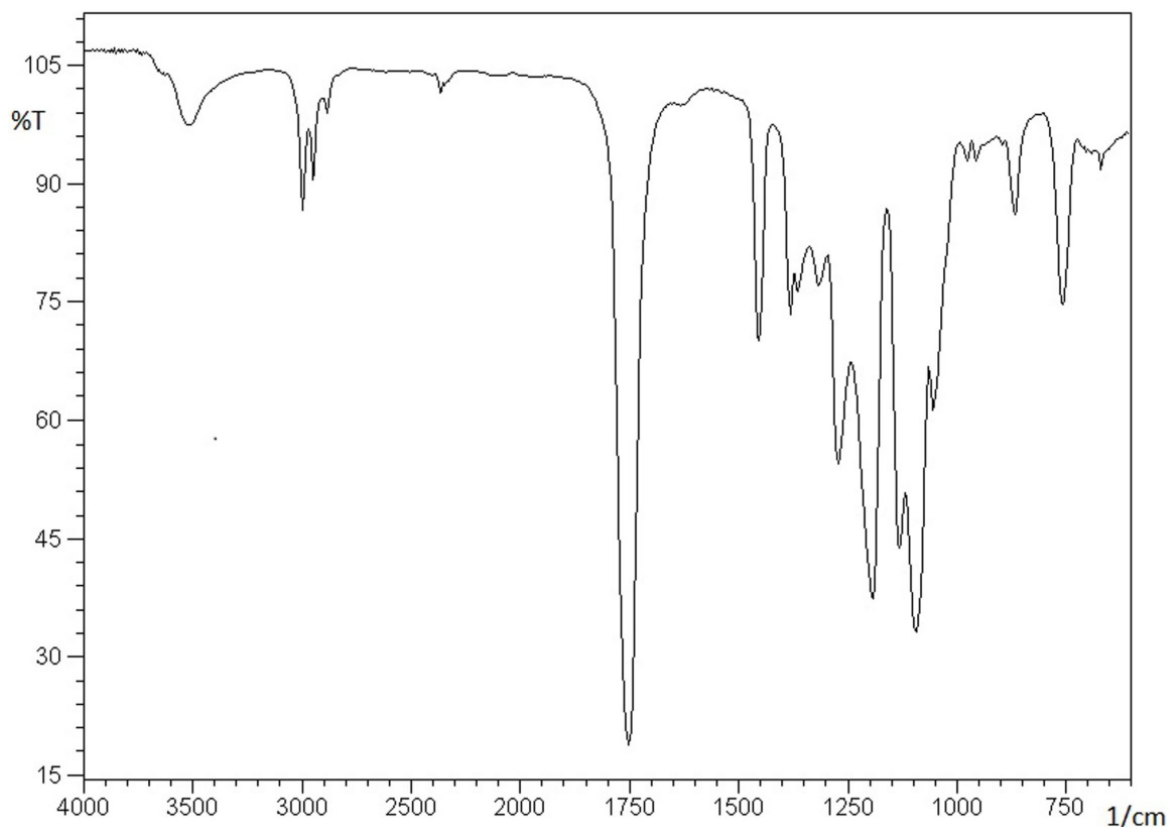


Figure 3: FTIR spectrum of polylactide.

Thermal properties of synthesized samples were analyzed by differential scanning calorimetry (DSC). Obtained results have showed that glass transition temperature (T_g) and melting temperature (T_m) values of analyzed samples increase with increasing in duration of polymerization reaction (Table 2). However, as the reaction time increases, the temperature of “cold” crystallization (T_{cc}) increases, as result of higher molar mass of polymer achieved after longer reaction time.

Table 2: Thermal properties of PLA samples obtained from DSC curves.

	Reaction time [min]	T_g [°C]	T_{cc} [°C]	T_m [°C]
PLA 1	5	42	86	154
PLA 2	10	44	92	155
PLA 3	20	47	98	159

Higher surface energy of packaging materials will provide more satisfactory printing properties without surface treatment. If higher surface energy is needed for processing, the surface can be treated by corona discharge. Figure 4 shows water drops recorded on the instrument for the contact angle measurement, based on which the surface energy values of the polylactide materials are calculated. The obtained surface energy values of the synthesized PLA materials are shown in the Table 3. All samples have the similar surface energy, which is satisfactory high for further processing of this material.

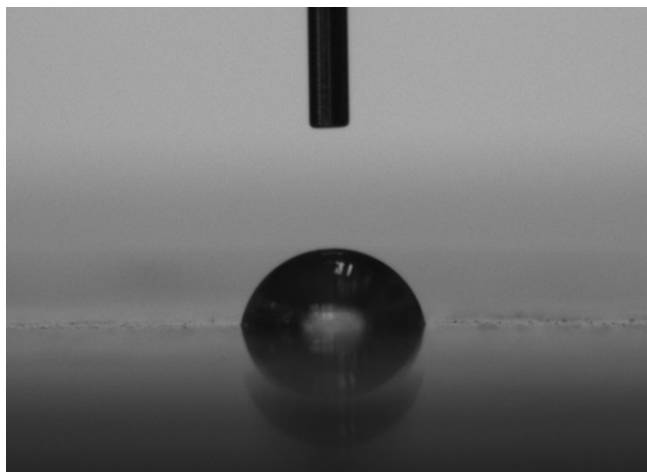


Figure 4: Water drops on synthesized polylactide material

Table 3: Surface energy of synthesized polylactide material

Sample name	Reaction time [min]	Surface energy [mN/m]
PLA 1	5	36.8
PLA 2	10	37.4
PLA 3	20	37.1

4. CONCLUSIONS

Poly lactide meets many requirements as a packaging thermoplastic and is suggested as a commodity resin for general packaging applications. Over the past decade, new polymerization methods are discovered and they allow the economical production of high molecular weight PLA, and this have resulted in an expanded use of PLA for consumer goods and packaging. Because polylactide is compostable and derived from renewable sources, it has been considered as one of the solutions to alleviate solid waste disposal problems and to lessen the dependence on petroleum-based polymers for packaging materials. These facts have faced scientific community with necessity for development energy efficient process for polylactide obtaining. In accordance with the Green Chemistry concept, microwave synthesis of PLA can be applied. Microwave synthesis gives high molar weight PLA with quite regular structure in improved yield. Shorter polymerization time and reduced consumption of energy and resources accompanied with desired properties of polymer, make microwave synthesis applicable to contemporary requirements. The use of microwaves enables homogenous heating of reaction mixture, lower consumption of organic solvent and drastic reduction in polymerization time, obtaining high molecular weight polymers. In this research polylactide based materials were synthesised using microwave method and molecular structures, and thermal properties of obtained samples were investigated. Particular consideration was given to the surface energy of obtained polymer materials. The presented results confirm that microwave synthesis can be an adequate method for preparing of PLA materials which can be used for packaging applications. The answer on question how do the microwave synthesis of polylactide affects the other properties which are important for packaging materials (such as mechanical or barrier), requires further investigation.

5. ACKNOWLEDGEMENTS

This paper were supported by Ministry of Science and Technological Development, Republic Serbia, contract grant number III 45022.

6. REFERENCES

- [1] Abdel-Rahman, M. A., Tashiro, Y., Sonomoto, K.: "Lactic acid production from lignocellulose-derived sugars using lactic acid bacteria: Overview and limits", *Journal of Biotechnology* 156(4), 286-301, 2011. doi: 10.1016/j.jbiotec.2011.06.017.
- [2] Anastas, P. T., Warner, J. C.: "Green Chemistry: Theory and Practice", (Oxford University Press: New York, 1998.), page 30.
- [3] Auras, R., Harte B., Selke S.: "An Overview of Polylactides as Packaging Materials", *Macromol. Biosci.* 4, 835-864, 2004. doi: 10.1002/mabi.200400043.
- [4] Auras, R. A., Harte B., Susan S., Hernandez R.: "Mechanical, Physical, and Barrier Properties of Poly(Lactide) Films", *Journal of Plastic Film and Sheeting* 19(2), 123-135, 2003. doi: 10.1177/8756087903039702.
- [5] Arrieta, M. P., López, J., Ferrándiz, S., Peltzer M. A.: "Characterization of PLA - limonene blends for food packaging applications", *Polymer Testing* 32(4), 760-768, 2013. doi: 10.1016/j.polymertesting.2013.03.016.
- [6] Madhavan Nampoothiri, K., Nair, N. R., John, R. P.: "An overview of the recent developments in polylactide (PLA) research", *Bioresource Technology* 101(22), 8493-8501, 2010. doi: 10.1016/j.biortech.2010.05.092.
- [7] Martino, V. P., Jimenez A., Ruseckaite, R. A., Avérous, L.: "Structure and properties of clay nano-biocomposites based on poly(lactic acid) plasticized with polyadipates", *Polymers for Advanced Technologies* 22(12), 2206-2213, 2011. doi: 10.1002/pat.1747.
- [8] Nice, G.W., Gluaser, T., Connor, E.F., Mork, A., Waymounth, R.M., Hedrick, J.L.: "In Situ Generation of Carbenes: A General and Versatile Platform for Organocatalytic Living Polymerization" *Journal of the American Chemical Society*, 125(10), 3046-3056, 2003. doi: 10.1021/ja021084+.
- [9] Nikolić Lj., Ristić I., Adnadjević B., Nikolić V., Jovanović J., Stanković M.: "Novel Microwave-Assisted Synthesis of Poly(D,L-lactide): The Influence of Monomer/Initiator Molar Ratio on the Product Properties", *Sensors* 10(5), 5063-5073, 2010. doi: 10.3390/s100505063.
- [10] Ristić I.S., Nikolić Lj.B., Cakić S.M., Radičević R.Ž., Pilić B.M., Budinski-Simendić J.K.: "Poli(laktid)-dostignuća i perspektive", *Savremene tehnologije* 1(1), 67-77, 2012.
- [11] Singla P., Kaur P., Mehta R., Berek D., Upadhyay S.N.: "Ring-Opening Polymerization of Lactide Using Microwave and Conventional Heating", *Procedia Chemistry* 4, 179-185, 2012. doi: 10.1016/j.proche.2012.06.025.



PRINTING QUALITY



INVESTIGATION OF COLOR REPRODUCTION ACCURACY OF DIFFERENT INK JET AND ELECTROPHOTOGRAPHICAL PRINTING SYSTEMS

Rumyana Boeva , Iskren Spiridonov , Simeon Yordanov ,
Tatyana Bozhkova , Zhivko Ivanov 
University of Chemical Technology and Metallurgy,
Department of Pulp, Paper and Printing Arts, Sofia, Bulgaria

Abstract: *The main goal of this paper is to define and compare the reproduction accuracy and color quality of different digital printing systems. The chosen digital printing systems are from both commonly used types – ink jet and electrophotography. The printers used for experiment in this study are: HP Indigo 5500, Canon IPF 9400, HP Latex 370, Agfa Anapurna M2540 FB. The media used are: glossy and matt coated papers, uncoated papers, photo paper, Jet coat paper, Polypropylene, PVC, vinyl. On above mentioned digital printing systems and media have been printed several test forms with big number of test charts and different control elements. The test forms are containing the following control elements: 240 Pantone colors for assessment of color difference from the original Pantone colors, color charts for generating of ICC profiles, 3D volume and 2D color gamut for different media and printing systems, charts for measuring of color characteristics of main and secondary colors, charts for evaluation of tone value increase, etc. A big number of experimental results are obtained for the most important printing quality parameters – color difference from original Pantone colors, color gamut volume, accuracy of reproduction expressed by tone values, etc.*

Key words: printing quality, color reproduction accuracy, digital printing

1. INTRODUCTION

During the past few years the main driving force of technical development is established by digital technology, which advances ever so greatly in all scientific domains, in economy and in industry. The new generation machines, equipment, systems and materials contribute to improved performance, better quality, greater ecology and cost efficiency. New printing technologies offer reductions in the use of materials and energy, as well as shorter machine setup time and decrease of maculatures. In this context, the development of graphic technologies is a strive to ameliorate the efficiency of at least one of the three main principles of every business, namely – rapidity, quality and production costs.

Digital print is a new generation technology in comparison to all known methods of printing information on paperback or any other type of carrier. With the development of information technologies, the application of this printing method increases as well. It picks up steam in the Graphic industry, as the tendency is for it to go into full industrial use for the production of packages and labels in small and medium circulations (Kachin et al, 2004, Kachin et al, 2000). This paper is the first part of a series of researches, which are focused on different classes of digital printing machines as the latter are used in a variety of applications, such as commercial Printing, outdoors advertisement, Packaging and Labels, etc.

2. EXPERIMENTAL

Reaching the set goals was aided by the use of different measurement tools – densitometer, spectrophotometer, which served to examine the accuracy and quality of tonal and colour reproduction in digital printing machines. In order to maintain result reproducibility, a specialised test form was developed and used. The test form consists of:

- ECI 2002 test chart with 1485 patches for colorimetric assessment and generating of ICC profiles;
- Test charts with 0, 5, 10, 20 to 100% for all process colors and their double overlays;
- Positive and negative lines of different width and number of colors for assessment in order to detect the thinnest lines, which could be reproduced from the given material by the examined printing systems;
- Test images for visual analyses;
- Small positive and negative text of different size;
- Vignettes.

A multitude of colorimetry and densitometry methods were used. The goal of this paper is to render examination results on the accuracy and quality of tonal and colour reproduction in ink-jet and electrophotographical digital print as a multitude of assessment methods related to tonal and colour reproduction accuracy were selected regarding the Pantone colouring system, colour characteristics of solid primary colors, tone value increase, assessment of 3d and 2d color gamut shape and values, visual analyses of images, reproduction of thin positive and negative line art and lines, as well as fonts with small size in one, two and more colours (Kachin, 2004; Kipphan, 2001). The following digital machines have been used to carry out the experiment:

- Agfa Anapurna M 2540FB – ink-jet printer with UV inks;
- Canon IPF 9400 – ink-jet printer with water-based inks;
- HP Latex 370 – ink-jet printer with water-based inks;
- HP Indigo 5500 – electrophotographical printer with toner inks.

Used media to perform the experimental analyses are:

- Offset uncoated paper – 120 g/m²;
- Matte Coated paper – 150 g/m²;
- Glossy Coated paper – 150 g/m²;
- Paper “Jetcoat” – 200 g/m²;
- Glossy Photo paper – 190 g/m²;
- Polypropylene – 160 g/m²;
- Self-adhesive PVC – glossy – 135 g/m²;
- Vinyl – 440 g/m².

3. RESULTS AND DISCUSSION

Due to the large dataset obtained from the thorough research on the precision and quality of tonal and colour reproduction for ink-jet and electrophotographical digital print, this paper will only include the results, obtained during the experiments with HP Indigo 5500, loaded with offset uncoated paper and glossy coated. The examination included assessment of colour characteristics of test prints, simulating specially selected Pantone colours. Also there is a measurement of the colour coordinates as per the CIE Lab system with included calculation and comparison of ΔE_{76} and ΔE_{00} according to (ISO 12647-2:2013). A dedicated software product was used to render the 2D and 3D visualisation and a comparison between the colour gamuts of the examined media was made with a standard ICC profile FOGRA47 and FOGRA51.

In order to compare the quality of tonal and colour reproduction of catalogue and selected Pantone system colours, one must calculate the colour difference ΔE for a set number of colours. In order to calculate ΔE , one must first obtain the colour coordinates of all colours according to the CIE Lab system. The reference values are the colour coordinates as per (ISO 12647-2:2013).

Process control for the production of half-tone colour Colour differences are derived using the following formulas:

- colour difference ΔE_{76} :

$$\Delta E_{76}^* = \sqrt{(L_1^* - L_2^*)^2 + (a_1^* - a_2^*)^2 + (b_1^* - b_2^*)^2} \quad (1)$$

- colour difference ΔE_{00} :

$$\Delta E_{00}^* = \sqrt{\left(\frac{\Delta L'}{K_L S_L}\right)^2 + \left(\frac{\Delta C'}{K_C S_C}\right)^2 + \left(\frac{\Delta H'}{K_H S_H}\right)^2 + R_T \frac{\Delta C'}{K_C S_C} \frac{\Delta H'}{K_H S_H}} \quad (2)$$

Where: L – lightness/brightness
C – saturation
H – hue

The measurements of colour coordinates are made using a spectrophotometer under the following conditions:

- Standard light illuminant - D50;
- 2° standard observer;
- No polarisation filter;
- Aperture – 4mm;
- A white backing has been used.

3.1 Investigation of color reproduction accuracy of digital printing systems and calculation of ΔE for Pantone colours

In order to examine the reproduction precision of the fundamental Pantone colours, the colour coordinates (Lab) for the media listed above have been measured. Figure 1 represents the basic Pantone colours.



Figure 1: Basic Pantone colours used in experiment

In order to examine the reproduction precision of the basic Pantone colours, the colour coordinates (Lab) for the media listed above have been measured. Figure 43 represents the basic Pantone colours. Figure 2 represents a selection of Pantone colours.

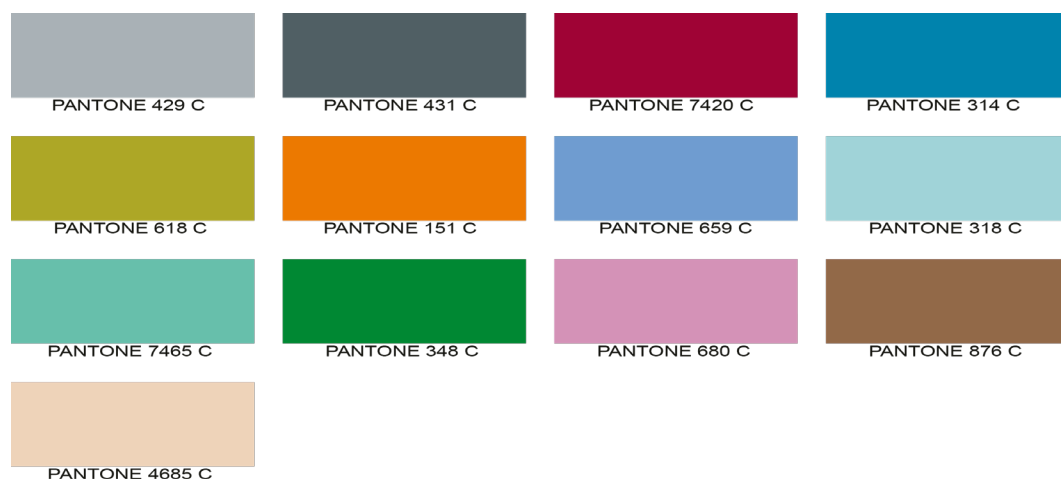


Figure 2: Selection of Pantone colours used in experiment

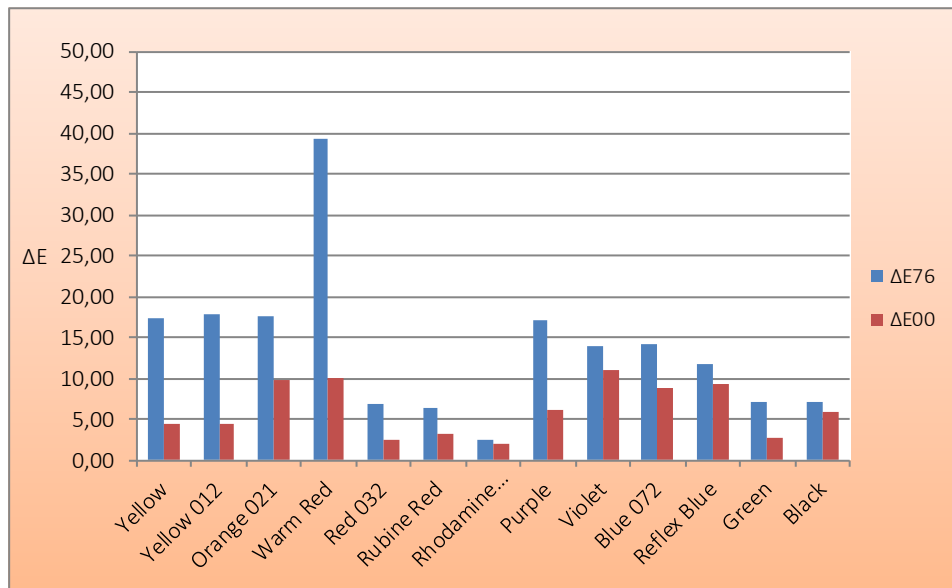


Figure 3: Comparison of the colour differences, according to CIE Lab, between the basic Pantone colours with ΔE_{76} and ΔE_{00} for Offset uncoated paper printed through HP Indigo 5500

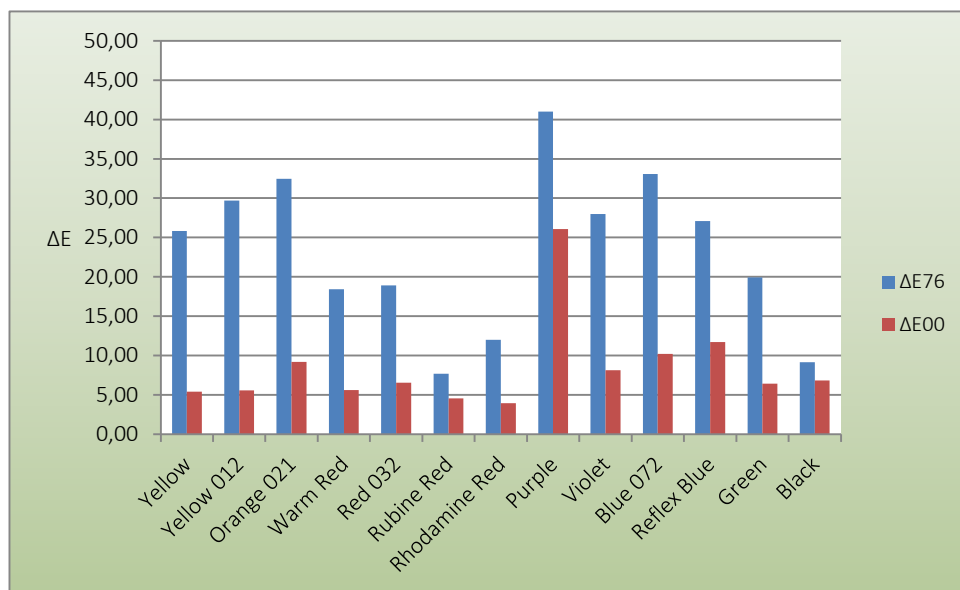


Figure 4: Comparison of the colour differences, according to CIE Lab, between the basic Pantone colours with ΔE_{76} and ΔE_{00} for Glossy Coated paper printed through HP Indigo 5500

Figure 3 and Figure4 shows the comparative graphs for comparison of the colour differences, according to CIE Lab, between the basic Pantone colours with ΔE_{76} and ΔE_{00} for offset uncoated paper printed through HP Indigo 5500 and comparison of the colour differences, according to CIE Lab, between the basic Pantone colours with ΔE_{76} and ΔE_{00} for Glossy Coated paper printed through HP Indigo 5500. Due to the extensiveness of the measurements and the multitude of obtained results, this paper presents only an excerpt there to concerning the stated printing machine and the printing media, used in conjunction with it. Tables 1 and 2 show all results derived from ΔE calculations.

Table 1: Experimental results for color reproduction accuracy obtained for basic Pantone colours

Fundamental Pantone colours			ΔE_{76}			Count of colours corresponding to the average limitations (total of 13)			ΔE_{00}			Count of colours corresponding to the average limitations (total of 13)		
Nº	Digital machine	Media	$\Delta E_{avg.}$	ΔE_{min}	ΔE_{max}	$\Delta E < 3$	$\Delta E < 5$	$\Delta E > 5$	$\Delta E_{avg.}$	ΔE_{min}	ΔE_{max}	$\Delta E < 3$	$\Delta E < 5$	$\Delta E > 5$
1	HP Indigo 5500	Offset uncoated paper	13,77	2,40	39,23	1	0	12	6,17	2,00	11,06	3	3	7
2	HP Indigo 5500	Matte coated paper	22,59	5,69	44,13	0	0	13	7,04	2,56	11,70	1	1	11
3	HP Indigo 5500	Glossy coated paper	23,33	7,95	33,84	0	0	13	7,06	4,10	11,33	0	3	10
4	HP Latex 370	Self-adhesive PVC	25,16	5,23	45,05	0	0	13	7,20	3,00	12,23	1	1	11
5	Canon IPF9400	Photo paper	25,37	5,57	46,77	0	0	13	7,40	2,93	12,62	1	1	11
6	HP Latex 370	Jetcoat paper	25,50	5,95	43,98	0	0	13	7,45	3,91	12,20	0	2	11
7	Agfa Anapurna M2540	Vinil	25,87	7,66	45,88	0	0	13	8,26	3,65	12,09	0	2	11
8	HP Latex 370	polypropylene	25,98	7,70	41,01	0	0	13	8,48	3,95	26,06	0	2	11

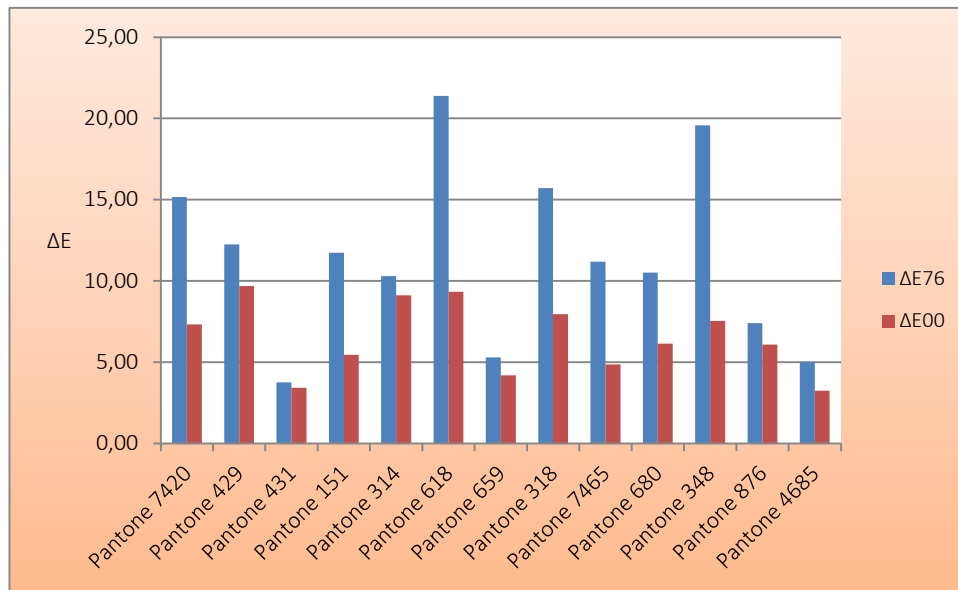


Figure 5: Comparison of the colour differences, according to CIE Lab, between the selected Pantone colours with ΔE_{76} and ΔE_{00} for Offset uncoated paper printed through HP Indigo 5500

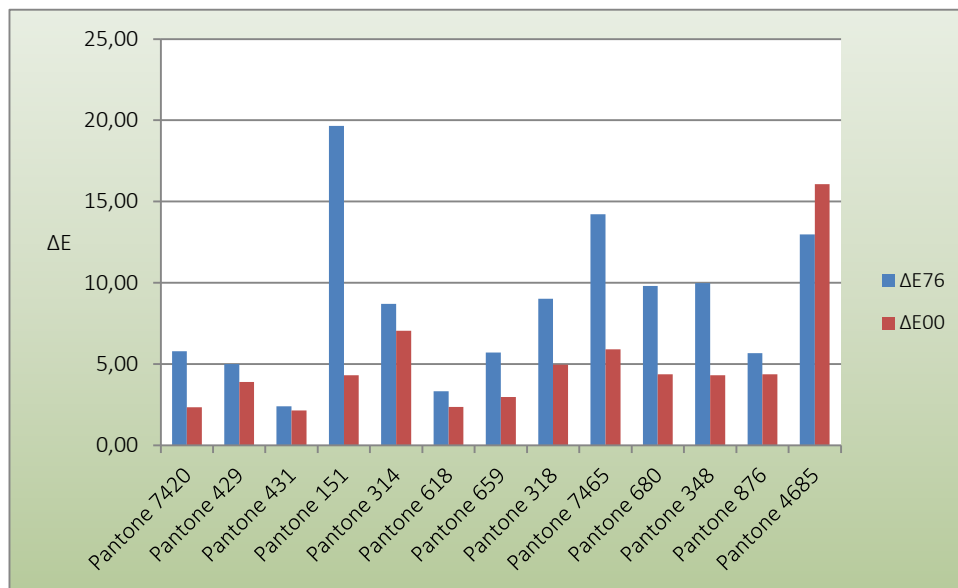


Figure 6: Comparison of the colour differences, according to CIE Lab, between the selected Pantone colours with ΔE_{76} and ΔE_{00} for Glossy Coated paper through HP Indigo 5500

Figure 5 and Figure 6 shows the comparative graphs for comparison of the colour differences, according to CIE Lab, between the selected Pantone colours with ΔE_{76} and ΔE_{00} for Offset uncoated paper printed through HP Indigo 5500 and comparison of the colour differences, according to CIE Lab, between the selected Pantone colours with ΔE_{76} and ΔE_{00} for Glossy Coated paper through HP Indigo 5500

Table 2: Experimental results for color reproduction accuracy obtained for selected Pantone colours

Selected Pantone colours			ΔE_{76}			Count of colours corresponding to the average limitations (total of 13)			ΔE_{00}			Count of colours corresponding to the average limitations (total of 13)		
No	Digital machine	Media	ΔE_{avg}	ΔE_{min}	ΔE_{max}	$\Delta E < 3$	$\Delta E < 5$	$\Delta E > 5$	ΔE_{avg}	ΔE_{min}	ΔE_{max}	$\Delta E < 3$	$\Delta E < 5$	$\Delta E > 5$
1	HP Latex 370	polypropylene	7,16	1,42	23,94	2	4	7	3,30	0,48	6,21	7	3	3
2	HP Latex 370	Self-adhesive PVC	7,21	2,31	24,17	2	3	8	3,36	1,25	6,40	8	2	2
3	Agfa Anapurna M2540	Vinil	7,34	2,31	22,03	3	3	7	3,44	1,43	8,47	8	2	3
4	HP Latex 370	Jetcoat paper	7,44	2,03	24,30	2	3	8	3,48	1,18	7,44	7	3	3
5	HP Indigo 5500	Matte coated paper	7,59	1,69	18,68	2	2	9	3,83	1,49	5,95	4	7	2
6	Canon IPF9400	Photo paper	8,28	3,72	21,07	0	3	10	4,18	1,99	7,15	5	3	5
7	HP Indigo 5500	Glossy coated paper	8,63	2,41	19,65	1	1	11	5,00	2,15	16,07	4	7	2
8	HP Indigo 5500	Offset uncoated paper	11,49	3,76	21,39	0	1	12	6,49	3,25	9,68	0	4	9

3.2 Investigation of Tone value increase for digital printing systems on different papers

The tone value increase is an indicator, which defines tone and colour reproduction and under certain conditions it influences the image depth field. This is one of the most important measured values, serving to control the printing process and is directly linked to the quality of the printed image [Kachin, 2004]. In order to define the tone value increase for the separate prints, one performs densitometric measurements of tonal fields in the interval between 5% and 100%.

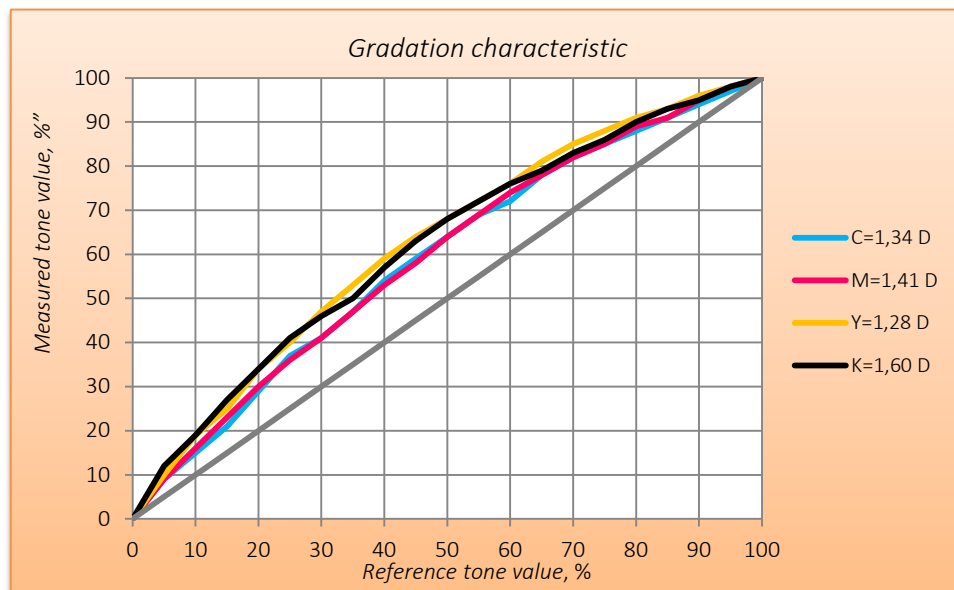


Figure 7: Dependency between the reference and measured tone value (gradation characteristic) for Offset uncoated paper printed through digital printer HP Indigo 5500

Figure 7 represents the dependency between the set and measured tone value, for offset paper, as this correlation is a gradation characteristic of reproduction for the four primary colours (CMYK). From this figure it is apparent that with the four primary colours (cyan, magenta, yellow and black) we can observe significant uniform increase in the range up to 20%, after which one can observe that with black and yellow there is a slightly higher measured tone value, which varies for both colours in the range between 30% and 70%. The increase of tone value with black and yellow varies between 4 and 7 units, compared to cyan and magenta. The figure above also demonstrates the extensive similarity of tone values for cyan and magenta across the range.

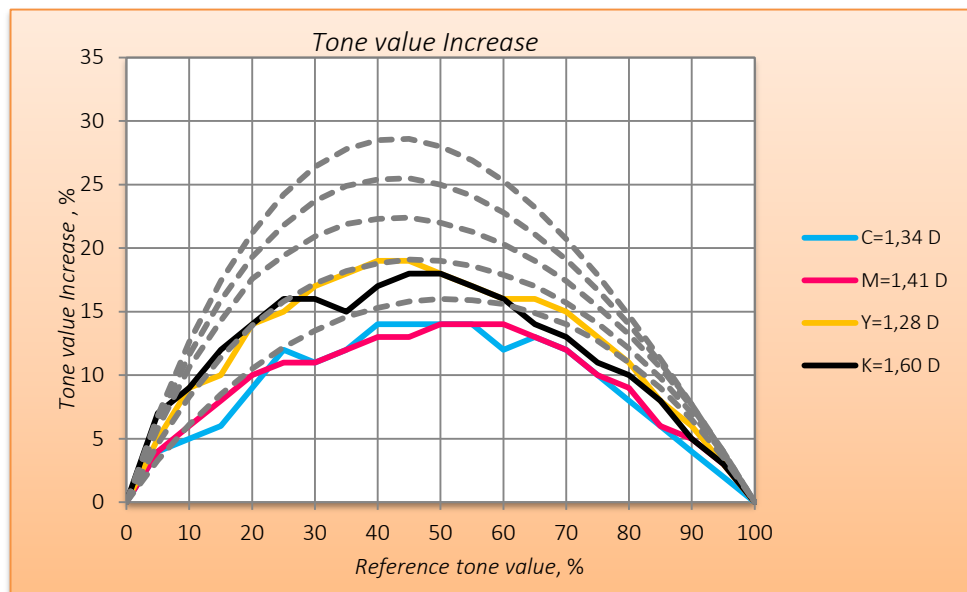


Figure 8: Tone value Increase for the four primary colours and standard curves as per ISO 12647-2:2013 for Offset uncoated paper printed through digital printer HP Indigo 5500

Figure 8 contains the correlation between the reference tone value and the increase of tone value for cyan, magenta, yellow and black, all printed on offset paper, compared to the standard curves as per ISO (ISO 12647-2:2013). The figure shows that cyan shows lower measured values in the range between 5% and 100% compared to the reference curves (A-E) as stated in ISO (ISO 12647-2:2013). Magenta shows that in terms of light tones (0% to 20%) there is full coincidence with curve A and after the 20% mark the results are lower than the standard. Yellow displays relatively identical measured values, compared to the reference curve B up to the mid tones, after which it drops down to curve A between 50% and 70%. The black colour results in solid measurements of tone value increase between 0% and 30%, after that the values start varying between 30% and 50%, and in the dark tones, the measurements are lower in pitch than the reference ones. None of the experimental curves shows significant increase of tone value. TVI of cyan and magenta is relatively the same.

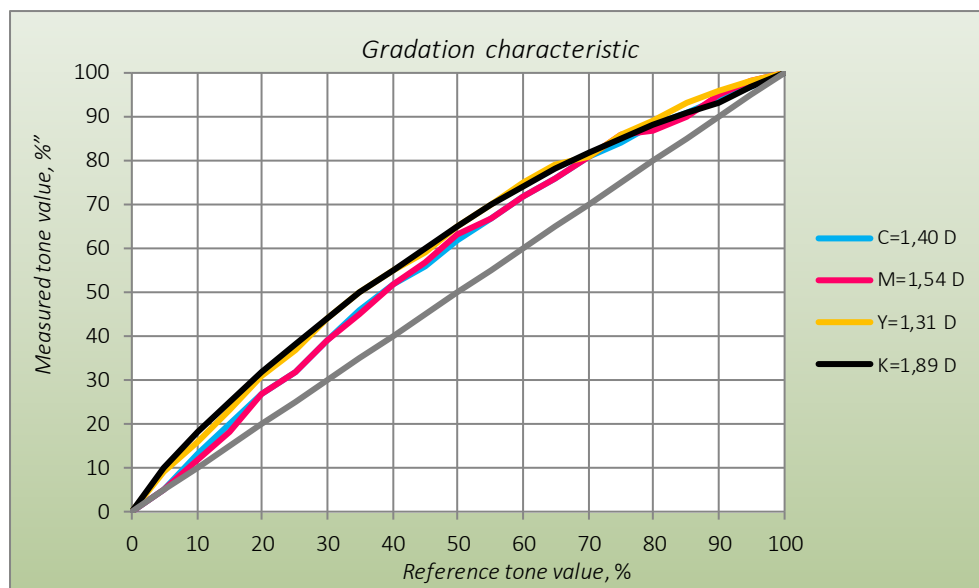


Figure 9: Dependency between the reference and measured raster tone (gradation characteristic) for gloss paper printed through digital printer HP Indigo 5500

Figure 9 shows the dependency between the reference and measured tone values, for gloss paper, which represents the gradation characteristic of reproduction for the four primary colours (CMYK). The figure shows that for these four colours (cyan, magenta, yellow and black) one can observe the rather even increase as cyan and magenta almost coincide in the range between 20% and 70%. Yellow and black have slightly higher values compared to the other two colours.

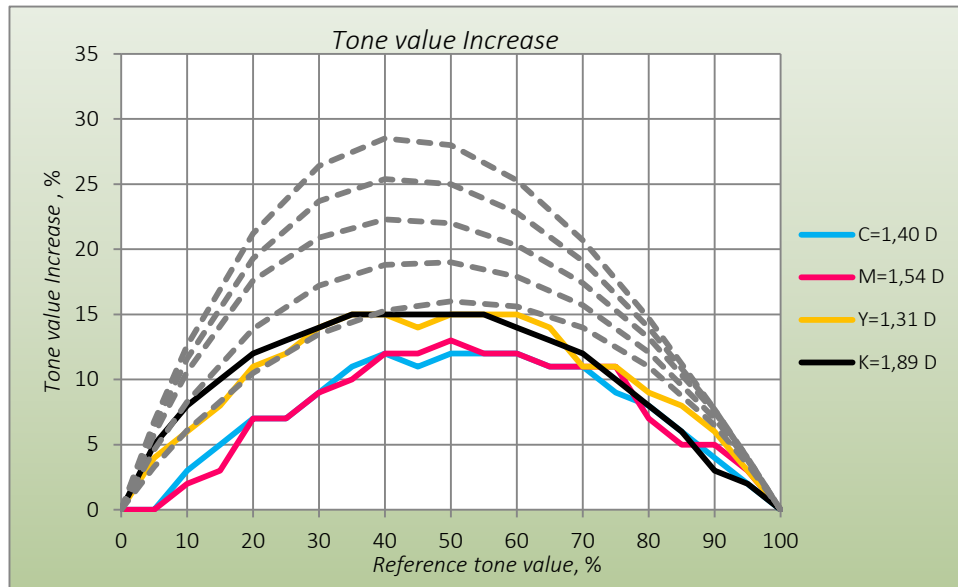


Figure 10: Tone value Increase for the four primary colours and standard curves as per ISO 12647-2:2013 for gloss paper printed through digital printer HP Indigo 5500

Figure 10 shows the correlation between the reference tone value and the increase of tone value for cyan, magenta, yellow and black, all printed on gloss paper, compared to the standard curves as per ISO (ISO 12647-2:2013). The figure shows that the experimental curves of cyan and magenta, for the increase of tone value, are significantly lower in terms of values compared to the reference curves (A-E) as stated in (ISO 12647-2:2013). Both colours (cyan and magenta) are with approximately identical values throughout the test. In the case of the yellow and black colours one observes smoother increase as both colours, in the range 0% to 40% follow the reference curves closely and after the mid tones yellow shows slight decrease between 40% and 50%. This figure does not show a peak increase shift for both light and dark tones due to the fact that the four colours have lower measured values, compared to the references. However, this may also lead to inaccuracy of tonal and colour reproduction. From the cyan and magenta curves, it is clear that there is 0% increase in the first 5% of the reference tone value.

3.3 Investigation of color gamut volumes and comparison of 2D and 3D color gammuts of different digital printing systems

One important function, which is used to visualise the colours, as reproduced by any given machine, is the 2D and 3D representation of the respective colour gammuts. This paper also uses 2D and 3D representations. The 2D representation of colour gammuts with different cross-sections along the L-axis of the CIE Lab colour space allows for good visual comparison of colours in light, mid and dark tones, as well as comparison of a large number of colour gammuts at once. The 3D representation of colour gammuts allows a complex visual assessment for the 3D body of the colour gammut. It is appropriate for the visualisation and comparison of ore or two colour gammuts.

In order to perform the comparison for the colour gammut of the examined prints from the corresponding digital printing presses – HP Indigo 5500, Agfa Anapurna M2540, Canon IPF9400 and HP Latex 370 it is necessary to provide a 3D visualisation with a standard ICC profile FOGRA 47 for uncoated papers and FOGRA 51 for coated papers with the ultimate goal to achieve visual representation for the colour gammuts. The 3D visualisation of the ICC colour profiles was performed using the software PROFILE MAKER 5.10. To compare the colour gammut on offset uncoated paper, a standard ICC profile was used FOGRA 47.

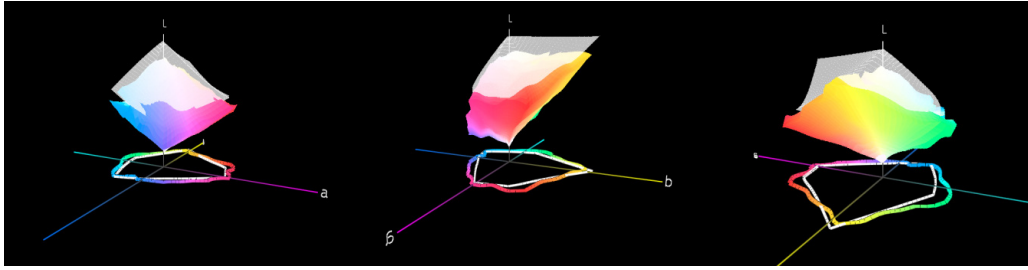


Figure 11: 3D visualisation (Lab system) of an ICC profile of offset paper printed through HP Indigo 5500 and FOGRA 47

From figure 11 one can observe, that the colour gammut of FOGRA47 is significantly larger than the one of the offset paper, which was printed through the HP Indigo 5500. It is also noticeable, that in certain areas the colour gammut of the tested digital machine – material is able to reproduce colours, which FOGRA47 could not [fogra.org, eci.org]. It is also clear that with offset paper one obtains better colour reproduction of the light hues of the yellow-red and the blue-green areas. In FOGRA 47, however, one notices better reproduction of darker hues.

As a comparison platform for the colour gammuts of matte paper, gloss paper, vinyl, photo paper, Jetcoat paper, polypropylene and self-adhesive film, the ICC FOGRA 51 profile has been used:

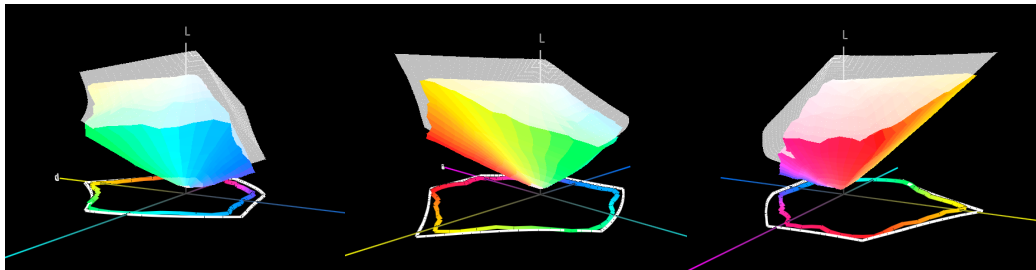


Figure 12: 3D visualisation (Lab system) of an ICC profile of gloss paper printed through HP Indigo 5500 and FOGRA 51

Figure 12 shows that the colour gammut of FOGRA51 is significantly larger compared to the gloss paper printed through the HP Indigo 5500. It is also observed that in certain areas, the colour gammut of the tested digital machine – material is able to reproduce colours, which FOGRA51 cannot. It is also clear that with gloss paper one obtains, once more, better colour reproduction of the light hues of the yellow-red and the blue-green areas. In FOGRA 51, however, one notices better reproduction of darker hues.

Figure 13 depicts a 2D visualisation of the colour gammuts of the tested media. The data shows that the most accurate tone and colour reproduction occurs on matte and gloss papers printed through HP Indigo 5500, as they coincide in all areas. The smallest colour gammut occurs with offset paper printed through the same machine. This phenomenon is due to the fact, that offset paper is considered an uncoated print media and has more porous structure, thus causing more ink intake in comparison to coated media.

Table 3: Volume of the colour gammut

No	Machines	Used media	Volume of the colour gammut ΔE^3
1	HP Indigo 5500	Offset uncoated paper	202 479
2	HP Indigo 5500	Matte Coated paper	293 021
3	HP Indigo 5500	Glossy Coated paper	314 299
4	Agfa Anapurna M2540	Vinyl	244 498
5	Canon IPF 9400	Glossy Photo paper	246 780
6	HP Latex 370	Paper “Jetcoat”	236 614
7	HP Latex 370	Polypropylene	254 321
8	HP Latex 370	Self-adhesive PVC	244 983

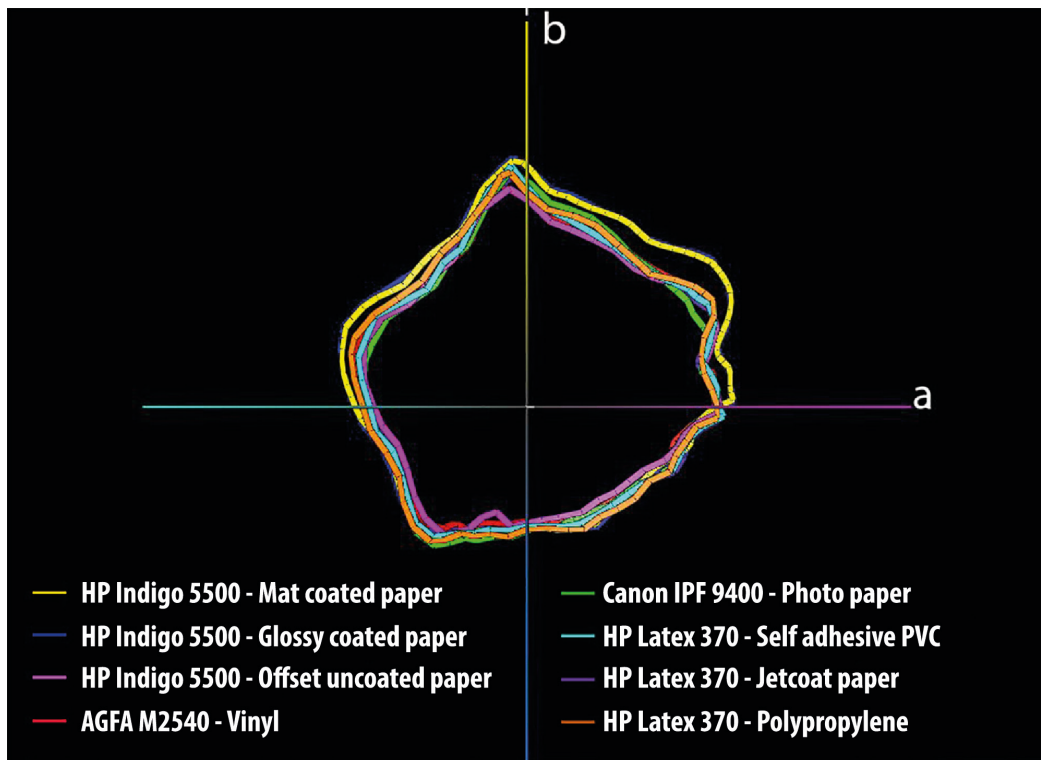


Figure 13: 2D visualisation of the colour range of all types of media, used within the scope of the experiment

4. CONCLUSIONS

Based on the results obtained within the scope of this paper, the following conclusions could be presented:

1. Colour reproduction accuracy is an ever more important factor provided by the increasing usage of digital printing systems, especially in the production of packages, labels and other. In spite of the extended colour gamut in most any digital printing system some of the fundamental problems originate from the insufficient colour reproduction accuracy – especially with Pantone. After printing 240 Pantone colours, a colorimetric measurement and appropriate analyses it was established that:

- The average colour difference in ascending order between the set Pantone colours and the measured prints is:
 - 1) ΔE_{00} avg. HP Indigo 5500 varies between 3,83 and 7,06 (ΔE_{76} avg. from 7,59 to 23,33)
 - 2) ΔE_{00} avg. HP Latex 370 varies between 3,30 and 8,48 (ΔE_{76} avg. from 7,16 to 25,98)
 - 3) ΔE_{00} avg. Canon IPF9400 varies between 4,18 and 7,40 (ΔE_{76} avg. from 8,28 to 25,37)
 - 4) ΔE_{00} avg. Agfa Anapurna M2540 varies between 3,44 and 8,26 (ΔE_{76} avg. from 7,34 to 25,87)
- The minimal colour difference in ascending order is $\Delta E_{00} = 0,48$ (HP Latex 370) up to 4,10 (HP Indigo 5500)
- The maximal colour difference in ascending order is $\Delta E_{00} = 5,95$ (HP Indigo 5500) up to 26,06 (HP Latex 370)

From the received results one may conclude that the highest colour reproduction accuracy of the Pantone colours is achieved while using the machine HP Indigo 5500 followed by all the other examined printing systems. Therefore, the present paper focuses mainly on its results as closest to ISO12647-2:2013. However, the average colour difference ΔE is relatively high and could be the source of some inaccuracy perception, especially with pretentious customers who often insist on a maximal tolerance of $\pm 1 \div 2 \Delta E$. For some of the Pantone colours, one receives very good and low values of ΔE such as $\Delta E_{00} = 0,48$ (HP Latex 370).

2. Colour gamuts and their volume are of special significance when the print quality is defined. The largest colour gamut was obtained with HP Indigo 5500 ($\Delta E^3 = 314\,299$), followed from HP Latex 370

($\Delta E^3 = 254.321$), Canon IPF9400 ($\Delta E^3 = 246.780$) and Agfa Anapurna M2540 ($\Delta E^3 = 244.498$). The standard colour gamuts of FOGRA52 were best met by the HP Indigo 5500, followed by HP Latex 370 and Agfa Anapurna M2540.

3. The tone value increase and colour characteristics of primary colours are important for the research of comparable visual results of digital print compared to the conventional printing processes. The experiment established that the TVI curves of digital printing systems differ significantly from their standardised counterparts. For the most cases, the curves follow the standards for light and dark hues and differ in the mids.

From the presented graphic material, depicting the dependency between the reference and measured colour tone, representing the gradation characteristics, one may observe a uniform increment of the colour tone for the four primary colours with all tested media.

For the most part of the tested media, one observes that within the first 5% of the reference there is 0% increase of the colour tone for some of the colours. Another interesting fact, which becomes apparent from these graphics, is that with most any media, the obtained values during the primary colours measurements are slightly lower in the light and mid hues – up to the 60% mark. On the one hand this does not lead to any significant increase of the colour tone, but the very fact that there are lower values obtained for the CMYK across most of the media could also lead to some inconsistencies in tonal and colour reproduction. From the results obtained herein, one could begin to understand how important it is to adhere as much as possible to the recommendations of the ISO standards in order to be able to optimise and to maintain the print quality so that the customer's highest requirements, with respect to the end product, are fully met. This is especially important with the print of packages, labels and other.




5. REFERENCES

- [1] Kachin, N., Spiridonov, I.: "Optical Density and Colour Difference in Printing on Different Types of Paper", Cellulose Chemistry And Technology, 39 (3-4), 255-264, 2004.
- [2] Kachin, N., Spiridonov I.: "Printing Processes - Part 1, Theoretical bases", (Pleyada, Sofia, 2000.)
- [3] Kipphan, H.: "Handbook of Print Media", (Springer-Verlag Berlin Heidelberg, Heidelberg, 2001). doi: 10.1007/978-3-540-29900-4
- [4] International Organization for Standardization, ISO 12647-2:2013 Graphic technology - Process control for the production of half-tone colour separations, proof and production prints - Part 2: Offset lithographic processes, International Organization for Standardization, 2013.



© 2018 Authors. Published by the University of Novi Sad, Faculty of Technical Sciences, Department of Graphic Engineering and Design. This article is an open access article distributed under the terms and conditions of the Creative Commons Attribution license 3.0 Serbia (<http://creativecommons.org/licenses/by/3.0/rs/>).

INVESTIGATION OF UV ARTIFICIAL AGEING OF OPTICAL CHARACTERISTICS OF PRINTED IMAGES

Rumyana Boeva , Iskren Spiridonov , Yordanka Ivanova 
University of Chemical Technology and Metallurgy, Faculty of Chemical Technology,
Department of Pulp, Paper and Printing Arts, Sofia, Bulgaria

Abstract: Over time, the printed images are ageing, and this may be due to different factors like natural ageing of paper and ink, temperature, humidity, sun light and human intervention. The main goal of this research is determination of the influence of artificial UV ageing on the colour characteristics of the printed images for mostly used papers, inks and offset printing technology. Two types of papers have been selected for the experiment in terms of their wide use and distribution on the all printing markets – uncoated offset paper and mat coated paper. Printing test evaluation form designed for this research test has been used. In real printing conditions in printing houses on two selected papers have been printed the test form with big number of control strips and elements for colour measurements. The optical properties of papers, colour characteristics of test charts for used papers, inks and printing presses were measured before and after artificial UV ageing time periods. The colour differences, changes of colour gamut volumes, 3D and 2D gamut are calculated too. Great changes in the colour characteristics of the printed images have been identified. The results show huge changes in many of critical colours from human perception point of view.

Key words: colour characteristics, offset printing, colour difference, ageing of materials, UV ageing, optical characteristics of papers

1. INTRODUCTION

The main problems encountered in the long storage of some types of print production are associated with deterioration of colour characteristics and loss of information from them. Changing the colour range and the colour difference that arise are due to the aging of the inks (Saldivar-Guerrero et al, 2016; Rosen et al, 2001).

Natural aging is a rather slow process. Therefore, in the present experiment, a study of the changes that occur with the printed output over time in artificial UV radiation with a simulation of the actual conditions under which the different printing outputs can be subjected (Kachin et al, 2004; Dolezalek, 2004).

2. METHODS

2.1 Materials and conditions of the experiment

Two wide used and popular types of papers have been chosen for the experiment:

- Uncoated offset paper – with weight 80 g/m²;
- Mat coated paper – 130 g/m².

On the paper samples the following analyses were made:

- Estimation of weight, [g/m²] (EN ISO 536:1998);
- Fibre composition, (by microscopic method) (ISO 9184-3:1990);
- The pH of the water extraction according to (ISO 8947-83). Based on estimation of the pH of the water extract the alkalinity or acidity is determined of the paper.

The results of the analysis of the two types of printed papers are given in Table 1.

Table 1: Characterization of used papers in experiment

Type paper	Weight, [g/m ²]	Fibre composition	pH of the water extract before UV ageing	pH of the water extract after UV ageing
Offset uncoated paper	80	Sulfate Pulp of Softwood 75% Sulfate Pulp of Hardwood 25%	7.9	7.2
Mat coated paper	130	Sulfate Pulp of Hardwood 80% Sulfate Pulp of Softwood 20%	7.7	7.0

The results shows, that in the offset uncoated paper content of coniferous wood is predominantly in the composition of the Sulfate Pulp of Softwood, while the matte coated paper predominates the Sulfate Pulp of Hardwood. At the same time, the pH of the water extraction for both types of paper changes slightly, indicating no significant changes in the chemical composition of the fibrous material components.

2.2 Selection of prints that meet all the offset printing technology requirements

The printing of the test sheets in this experiment was carried out on a Heidelberg Speedmaster four-color offset printing machine, size 35x50 cm, model SX 52-5-L with ANICOLOR inking unit. Implemented print plates were positive acting and were exposed by Computer to Plate System – Kodak. A special test form, which contains a multiple test charts and patches, have been designed for this experiment (Timar et al, 2016; Sonderegger et al, 2015; ISO 13656:2000; ISO 2846-1:2006).

- Inks - Huber Group - Maxima Series: Cyan - 43 F 50 MX, Magenta - 42 F 50 MX, Yellow - 41 F 50 MX, Black - 49 F 50 MX;
- Dampening solution – 6% isopropanol content, pH = 5.3, to 10 ± 1 ° C.

The printing of the test forms is carried out under the following conditions:

- Sequence of the inks – Black, Cyan, Magenta, Yellow.

Optimal inking quantity is predetermined by the ISO (ISO 12647-2:2013) recommendation and maximum print contrast method for each combination of paper-ink-printing machine. Table 2 gives the test values for optimal inking.

Table 2: Optimal Inking Values for Used Papers

Type paper	Cyan	Magenta	Yellow	Black
Offset uncoated paper	1.10	1.10	0.95	1.20
Mat coated paper	1.55	1.60	1.45	1.75

2.3 Experiment conditions

Artificial UV ageing was conducted in a Q-SUN Xenon Tests camera, which uses a full-spectrum xenon lamp to reproduce the material damaging wavelength. The camera for UV aging irradiation in the UVA and UVB spectrum in the range of 320 - 800nm. In experiment are used fluorescent UV lamps (UVA - 351 and UVB - 313EL). They provide the ability to simulate sunlight with a peak at 340 nm.

The measurements were done on intervals: 0 hours, 6 hours, 12 hours, 24 hours, 36 hours, 48 hours, 72 hours, 144 hours and 200 hours. Colour measurements were performed with spectrophotometer GretagMacbeth Spectrolino and X-Rite i1i0: GM Profile Maker, GM Measure Tool и GM Profile Editor and i1Profiler. Measurement conditions – standard light source D50, measuring geometry 45°/0° or 0°/45°, 2° standard observer (ISO 13655:2017; Rosenberg, 2004; European Color Initiative; ICC.1:2004-10; ISO 2470:2002).

3. RESULTS AND DISCUSSION

3.1 Influence of UV ageing on global colour change expression expressed by $\Delta E_{\text{average}}$ and ΔE_{max}

The parameters investigated in this section shows us the global influence of UV radiation on the colour characteristics of printed images. Data from spectrophotometric measurements were used to calculate ΔE_{ab} from CIE $L^*a^*b^*$ values (ISO 2846-1:2006; ISO 13656:2000; ISO 13655:2017). As reference CIE $L^*a^*b^*$ values, those measured prior to exposure to artificial UV ageing paper - 0 hours were used.

For investigation of the global change in the colour differences of 999 colour patches in the test form, the values of $\Delta E_{ab}^{\text{Average}}$, $\Delta E_{ab}^{\text{Max}}$ and $\Delta E_{2000}^{\text{Average}}$, $\Delta E_{2000}^{\text{Max}}$ in the various stages of UV ageing for both types of paper examined were calculated. Following figures (Figures 1 to 4) present the graphical dependence of the colour difference expressed by, $\Delta E_{ab}^{\text{Average}}$, $\Delta E_{ab}^{\text{Max}}$ and $\Delta E_{2000}^{\text{Average}}$, $\Delta E_{2000}^{\text{Max}}$ on both types of paper in the duration of artificial UV ageing.

3.1.1 Study of the average colour difference - $\Delta E_{ab}^{\text{Average}}$ for both types of papers

The colour difference $\Delta E_{ab}^{\text{Average}}$ - the mean arithmetic colour difference of the measured 999 fields of the TC 6.02 scale before and after being subjected to artificial UV ageing, have been calculated by formula:

$$\Delta E_{\text{AVERAGE}} = \frac{\Delta E_{\text{Sample / Original}}^{\text{Field 1}} + \Delta E_{\text{Sample / Original}}^{\text{Field 2}} + \dots + \Delta E_{\text{Sample / Original}}^{\text{Field 999}}}{999}, \quad (1)$$

where, $\Delta E_{\text{Sample / Original}}^{\text{Field}}$ – colour difference between a specific sample colour field and the same field of the original untreated sample.

Table 3 presents the values of $\Delta E_{ab}^{\text{Average}}$ in the process of artificial UV ageing for mat coated and offset uncoated paper.

Table 3: Change in $\Delta E_{ab}^{\text{Average}}$ for both types of paper in the process of artificial UV ageing

UV ageing hours	0	6	12	24	36	48	72	144	200
$\Delta E_{ab}^{\text{Average}}$ – mat	0	0.89	1.2	2.16	2.96	3.79	5.62	9.54	14.34
$\Delta E_{ab}^{\text{Average}}$ – offset	0	0.48	0.61	1.11	1.49	2.04	2.85	4.91	6.67

The data in Table 3 shows an increase in colour difference $\Delta E_{ab}^{\text{Average}}$ with an increase in UV exposure time. The colour change in the mat coated paper up to the 6th hour of UV ageing $\Delta E_{ab}^{\text{Average}} < 1$, therefore has an almost invisible colour difference. By the 36th hour the difference is $\Delta E_{ab}^{\text{Average}} < 3$, therefore there is a visually relatively small, slightly distinct difference. After 72 hours, a significant peak is observed, with the colour difference drastically increasing $\Delta E_{ab}^{\text{Average}} > 6$ and reaching $\Delta E_{ab}^{\text{Average}} = 14.34$ at the 200th hour, therefore there is a relatively large visual difference, very noticeable.

The experimental results for offset uncoated paper shows, that up to 6 hours of UV ageing, $\Delta E_{ab}^{\text{Average}} < 1$, therefore there is an almost invisible colour difference. By the 72th hour the difference is $\Delta E_{ab}^{\text{Average}} < 3$, therefore there is a visually relatively small, slightly distinct difference. At the 200th hour of $\Delta E_{ab}^{\text{Average}} > 6$, there is therefore a visual difference, very noticeable.

From the data obtained in Table 3, it can be seen that the increasing of $\Delta E_{ab}^{\text{Average}}$ for mat coated paper and uncoated offset paper is almost uniform over time, reaching values for 200h irradiation for mat paper to $\Delta E_{ab}^{\text{Average}} = 14.34$, and for offset paper up to $\Delta E_{ab}^{\text{Average}} = 6.67$.

On average, for 1 hour UV ageing, the change in $\Delta E_{\text{average}}$ is:

- Mat coated paper - $\Delta E_{ab}^{\text{Average}} = 0.07$;
- Offset uncoated paper - $\Delta E_{ab}^{\text{Average}} = 0.03$.

$\Delta E_{ab}^{Average}$ for mat paper after 200h UV ageing reaches 2 times higher than offset uncoated paper. The reason is the greater thickness of the ink layer of the mat coated paper relative to the other paper. The thicker layer means more saturated colours and a bigger change in ageing.

3.1.2 Investigation of the maximum colour difference obtained (ΔE_{max}) for both types of paper

The maximum colour difference - ΔE_{max} is obtained from 999 measured fields of the TC 6.02 scale before and after being subjected to artificial UV ageing. Table 4 presents the values of ΔE_{max} in the artificial UV ageing process for mat coated paper and offset uncoated paper.

Table 4: Changes in the maximum color difference ΔE_{max} obtained for both types of paper in the process of artificial UV ageing

UV ageing hours	0	6	12	24	36	48	72	144	200
$\Delta E_{max} - \text{mat}$	0	5.48	6.45	9.15	9.67	10.74	17.78	29.86	57.59
$\Delta E_{max} - \text{offset}$	0	2.04	2.96	4.17	4.92	5.88	7.88	19.84	31.41

Table 4 shows that for the colour change in the mat coated paper, the values of the maximum colour difference are considerably high, yet at the 6th hour $\Delta E_{max} = 5.48$ units, and from the 72th hour to the 200th it has a significantly high peak reaching $\Delta E_{max} = 57.59$ at the 200th hour. Therefore there is a relatively large visual difference, very noticeable.

For uncoated offset paper the colour difference up to 12 hours is $\Delta E_{max} < 3$, therefore there is a visually relatively small, slightly distinct difference. After 24 hours, up to 200 hours, the colour difference dramatically increased, with a relatively high peak between 72 hours and 200 hours, reaching $\Delta E_{max} = 31.41$ at 200 hours, therefore there is a noticeable colour difference.

On average for 1 hour UV ageing, the change in ΔE_{max} is:

- for coated mat paper - $\Delta E_{max} = 0.29$;
- for uncoated offset paper - $\Delta E_{max} = 0.16$.

The maximum colour difference for mat coated paper after 200 hours of UV ageing reaches 2 times higher values than uncoated offset paper. The reason is the greater thickness of the ink layer of the coated mat paper relative to the uncoated offset paper. The thicker layer means more saturated colours and consequently a larger change in ageing.

3.1.3 Investigation of the average colour difference for – $\Delta E_{2000}^{Average}$ for both types of papers

Table 5 presents the data for $\Delta E_{2000}^{Average}$ and for mat coated and offset uncoated paper in the process of UV ageing.

Table 5: Changes in $\Delta E_{2000}^{Average}$ for coated mat paper and uncoated offset paper in the UV ageing process

UV ageing hours	0	6	12	24	36	48	72	144	200
$\Delta E_{2000}^{Average} - \text{mat}$	0	0.55	0.72	1.21	1.53	1.93	2.83	4.88	7.68
$\Delta E_{2000}^{Average} - \text{offset}$	0	0.31	0.38	0.69	0.9	1.24	1.68	2.91	4.06

The data in Table 5 shows an increase in the colour difference $\Delta E_{2000}^{Average}$ with gaining of the UV radiation time. The colour change in the coated mat paper up to 12 hours of UV radiation $\Delta E_{2000}^{Average} < 1$, therefore has an almost invisible colour difference. Until 72 hours, the difference is $\Delta E_{2000}^{Average} < 3$, therefore there is a visually relatively small, slightly distinct difference. After 144 hours to 200 hours, the colour difference dramatically increased by $\Delta E_{2000}^{Average} > 6$ to reach $\Delta E_{2000}^{Average} = 7.68$ at 200h, therefore there is a relatively large visual difference - very noticeable.

There is an almost invisible colour difference for uncoated offset paper up to 36 hours of UV radiation - $\Delta E_{2000}^{Average} < 1$. Up to 144 hours there is a difference of $\Delta E_{2000}^{Average} < 3$, small, slightly distinct difference, and at the 200th hour it reaches $\Delta E_{2000}^{Average} = 4.06$.

From the data in table 5 it is seen that the increasing of $\Delta E_{2000}^{Average}$ for coated mat paper and uncoated offset paper is almost uniform over time, reaching values for 200h radiation at matte paper to $\Delta E_{2000}^{Average} = 7.68$ and for offset paper to $\Delta E_{2000}^{Average} = 4.06$.

On average for 1 hour UV ageing, the change in $\Delta E_{2000}^{Average}$ is:

- for coated mat paper - $\Delta E_{2000}^{Average} = 0.04$,
- for uncoated offset paper - $\Delta E_{2000}^{Average} = 0.02$.

The average colour difference (2000 formula) for mat coated paper after 200 hours of UV ageing reaches 2 times higher than offset uncoated paper.

3.1.4 Investigation in the maximum colour difference - (ΔE_{2000}^{Max}) for both types of papers

Table 6 shows the data for ΔE_{2000}^{Max} for coated mat paper and uncoated offset paper in the UV ageing process.

Table 6: Changing the maximum colour difference ΔE_{2000}^{Max} obtained for both types of papers in the process of artificial UV ageing

UV ageing hours	0	6	12	24	36	48	72	144	200
$\Delta E_{2000}^{Max} - \text{mat}$	0	4.59	5.96	8.56	9.09	9.68	9.25	12.81	19.53
$\Delta E_{2000}^{Max} - \text{offset}$	0	1.76	2.5	3.62	4.34	4.55	5.9	7.9	10.92

From the received data table 6 it can be seen that on the coated mat paper the values of the maximum colour difference are significantly large and at the 6th hour $\Delta E_{2000}^{Max} = 4.59$ units and at the 200th hour it reaches $\Delta E_{2000}^{Max} = 19.53$, therefore it has a relatively large visual difference, very noticeable.

The data obtained for uncoated offset paper shows up to 12 hours the difference is $\Delta E_{2000}^{Max} < 3$, therefore there is a visually relatively small, slightly distinct difference. After 72 hours to 200 hours, the colour difference dramatically increased $\Delta E_{2000}^{Max} > 6$ to reach $\Delta E_{2000}^{Max} = 10.92$ at the 200th hour, therefore there is a marked difference.

Table 6 shows that the increasing of ΔE_{2000}^{Max} for coated mat paper and uncoated offset paper is almost uniform over time, reaching values for 200 hours of exposure to matte paper to $\Delta E_{2000}^{Max} = 19.53$, and for offset uncoated paper to $\Delta E_{2000}^{Max} = 10.92$.

On average for 1 hour UV ageing, the change in ΔE_{2000}^{Max} is:

- for uncoated mat paper - $\Delta E_{2000}^{Max} = 0.1$,
- for uncoated offset paper - $\Delta E_{2000}^{Max} = 0.05$.

The maximum colour difference for mat coated paper after 200 hours of UV ageing reaches 2 times higher than offset uncoated paper.

3.2 Investigation of the influence of artificial UV ageing on Brightness, Yellowness and paper colour for both types of papers

The brightness, yellowness and colour are the most important optical characteristics of papers. That is why in the present paper there are performed an experiment over their influence of UV radiation.

3.2.1 Graphic representation of the effect of artificial UV ageing on the Brightness depending on the time of the two types of papers

The paper Brightness was measured with a Gretag Macbeth SpecroEye Spectrophotometer at a standard light illuminant - CIE D65, Brightness R457 (according to ISO470: 2002).

Figure 1 shows the graphical dependence of the influence of artificial UV ageing on the Brightness of coated mat and uncoated offset papers.

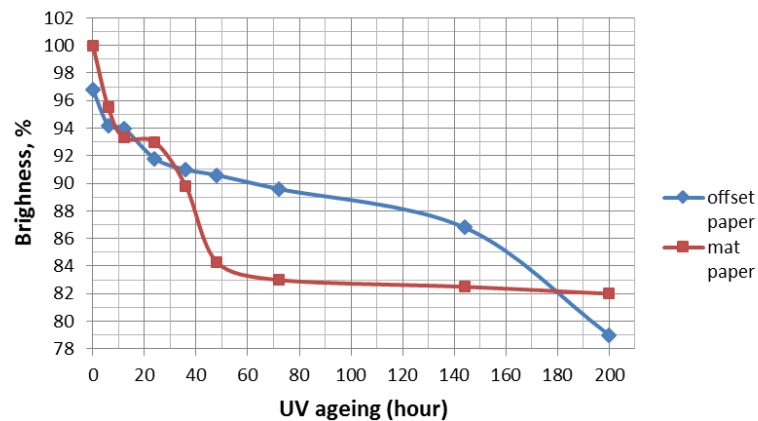


Figure 1: Influence of artificial UV ageing on Brightness of coated mat and offset uncoated papers

From Figure 1 it can be seen that with increasing hours of artificial UV ageing the Brightness decreases. On the coated mat paper from 0 hour to 48 hour, a drastic reduction in Brightness of ≈ 16 units is observed and reaches 18 units at 200 hours. While uncoated offset paper, a drastic reduction in Brightness occurs almost throughout the UV exposure range, reaching 17.8 units for 200 hours of exposure.

3.2.2 Graphic representation of the effect of artificial UV ageing on the Yellowness depending on the time of the two types of papers

The Yellowing of the paper is a very important indicator, especially for printing papers. The reason for its increase is the influence of UV rays, the increase of the temperature and humidity of the environment, the harmful gases in the atmosphere (especially SO_2), the type of used fibrous materials and the ways of their production. Figure 2 shows the graphical dependence of the influence of artificial UV ageing on the Yellowness coated mat and offset uncoated paper.

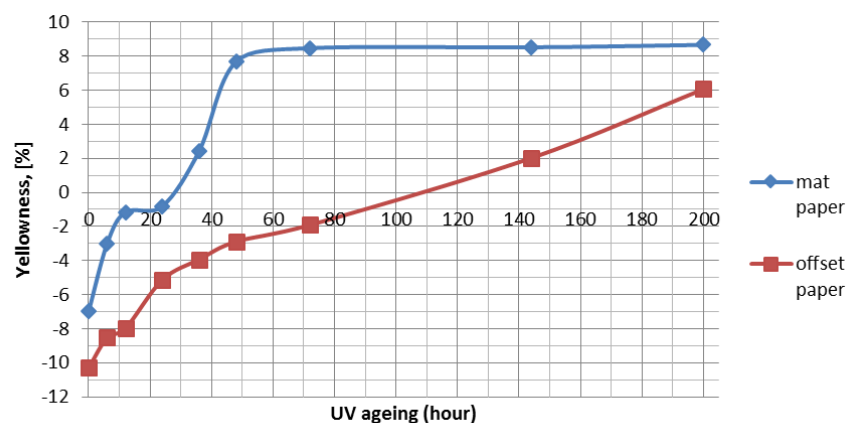


Figure 2: Influence of Artificial UV Ageing on the Yellowness coated Mat and Offset uncoated Paper

From Figure 2 it can be seen, that for both papers - the Yellowness is increasing for longer exposure. For coated mat coated papers, the UV radiation observed a drastic increase in yellowness to 48 hours was 14.68 units. After 48 hours the yellowness changed relatively little, reaching 15.66 units. For offset uncoated paper, the increase in yellowness is almost constant throughout the UV ageing interval, reaching 16.9 units.

3.3 Investigation of the change in 2D and 3D colour gamut, depending on the time of artificial UV ageing, and examination of the variation of the volumes of the colour gamut depending on the time of artificial UV ageing.

By estimating of changing of the colour gamut it can be judged the presence and direction of change of colour characteristics. They are presented in two ways in a 3D and 2D form. In a 3D form, the colour range gives a lot of general information about the colour changes of the three axes L, a and b.

The 2D representation is a cross-section of the 3D gamut graph on the CIE L axis, thus a colour gamut gives very accurate colour information characteristics at each specific L (light) value.

Test charts TC 6.02 were measured with a X-Rite SpectroScan Spectrophotometer before and after being subjected to artificial UV ageing at 0, 6, 12, 24, 36, 48, 72, 144 and 200h.

The data obtained from the spectrophotometer were used to create ICC colour profiles. ICC colour profiles are created with ProfileMaker 5.10 and i1Profiler. The Colour Setting settings of the created profiles (for 6, 12, 24, 36, 48, 72, 144 and 200 hours of artificial UV ageing) differ only in the total amount of dark tones (TAC), as it is different for different types of paper.

The following figures (Figures 3 to 6) show 3D visualizations and 2D incisions before and after UV ageing for both types of papers.

3.3.1 Determination of influence of UV ageing on the 3D colour gamut of mat coated paper and offset uncoated paper

With specialized software and hardware, colour patches are measured, ICC colour profiles are generated and a 3D colour model of the gamut is selected. The resulting 3D gamut's have a characteristic pear-shaped shape and show the colour change during artificial UV ageing.

The chart of Figure 3 compares the colour gamut (viewed at different angles) of engraved mat coated paper before (the outer triangular contour) and after (inner triangular contour) subjecting it to UV ageing. During UV ageing for the mat coated paper there is a decrease in the volume of the 3D body shape in light, medium and dark tones. The greatest change in volume is in the light, then in the middle and the smallest in the dark tones.

The chart of Figure 4 compares the colour gamut (viewed at different angles) to offset uncoated paper before (outer triangular contour) and after (inner triangular contour) subjecting to UV ageing. During UV ageing on uncoated offset paper there is decreasing tendency in the volume of the 3D body in light, medium and dark tones. The greatest change in volume is in the light, then in the middle and the smallest in the dark tones.

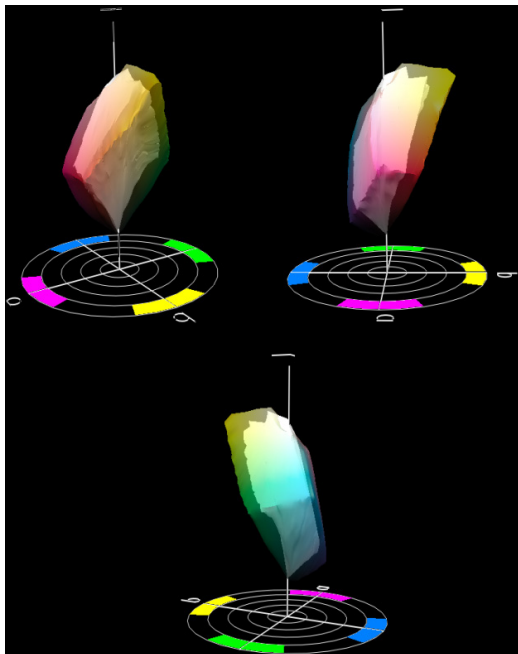


Figure 3: Influence of UV ageing on 3D color gamut on mat coated paper (before ageing – outside contour, after ageing – smaller (inside) contour)

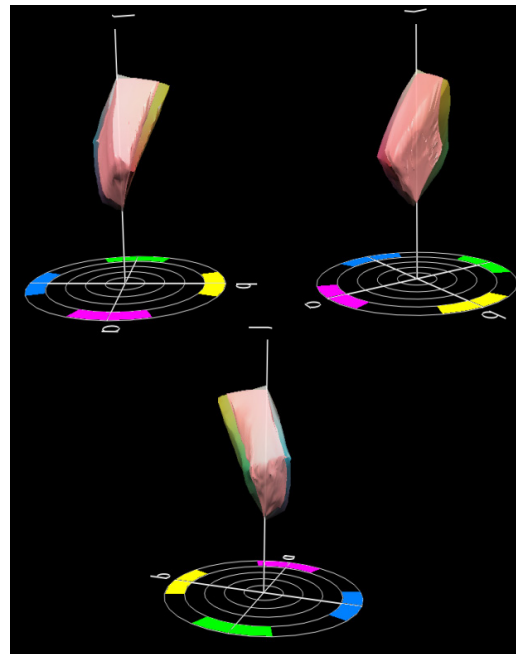


Figure 4: Influence of UV ageing on 3D color gamut on offset uncoated paper (before ageing – outside contour, after ageing – smaller (inside) contour)

3.3.2 Determination of influence of UV ageing on 2D colour gamut of both types of papers

The graphical representation of the colour gamut in the 3D colour space gives a comprehensive assessment of the variety of colours that are reproduced at the given paper-machine-ink combination. In order to make a more complete characterization of the colour change of the print image as a result of UB ageing for coated mat paper, a cut of the 3D body of the colour gamut at $L = 25$ (dark tones), $L = 50$ (medium tones) and $L = 75$ (light tones), where L is the coordinate of the light colour.

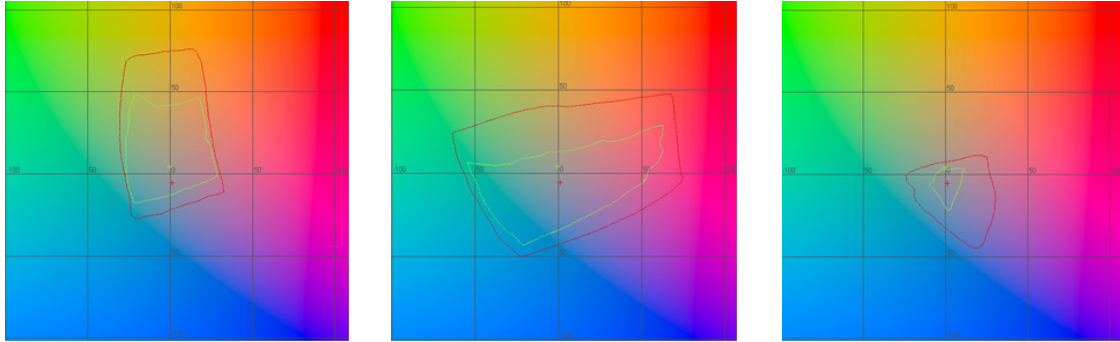


Figure 5: CIE Lab colour space gamut for $L = 75$, $L = 50$ and $L = 25$ for coated mat paper (outside red contour – before UV ageing; inside green contour – after UV ageing)

From Figure 5 it can be seen that in mat coated paper in light, medium and dark tones the colour gamut before UV ageing is significantly greater, than that after UV ageing.

In cross section of CIE $L = 75$ the colour shift in the yellow-red and blue areas is noticeable after ageing. The shift is to the yellow area, which can be explained by the yellowing of the paper itself. In section $L = 50$ there is an even greater displacement in all areas, with a relatively large difference in the red-green area. At $L = 25$ there is a significant change in the blue area. This means that these colours either "disappear" or are replaced with the same, but with less intensity and with another colour tone.

In Figure 6 is a sectional view of the 3D body of the colour gamut at $L = 38$ (dark tones), $L = 50$ (average tones) and $L = 75$ (light tones).

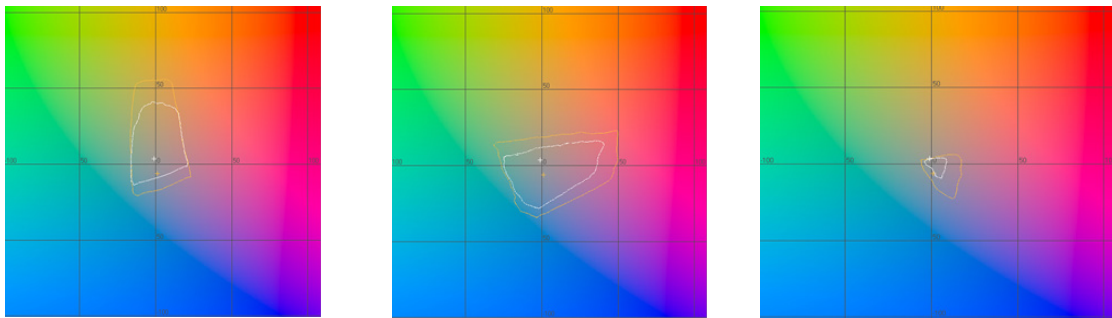


Figure 6: CIE Lab colour space gamut for $L = 75$, $L = 50$, and $L = 38$ for uncoated offset paper (outside red contour – before UV ageing; inside white contour – after UV ageing)

From Figure 6 it can be seen that for offset uncoated paper in light, medium and dark tones the colour gamut before UV ageing is significantly higher than that after UV ageing. In cross section of CIE $L = 75$, the colour shift in the yellow and blue areas during ageing is noticeable, while in the cabbage and the red area there is almost no change. The shift is to the yellow area, which can be explained by the yellowing of the paper itself. In section $L = 50$, offset is visible in all areas except in light blue areas. In $L = 25$ there is a significant change in the blue and red areas. This means that these colours either "disappear" or are replaced with the same, but with less intensity and with another colour tone.

4. CONCLUSIONS

During the experiment, the obtained results shows significant changes in colour characteristics observed in the UV ageing process, and a correlation between UV irradiation and colour difference ΔE . The colour difference reached, after 200h of ageing, $\Delta E_{ab}^{Average}$ is 14.34 units for coated mat paper and twice as low as 6.67 units for uncoated offset paper. With the 2000 colour difference formula $\Delta E_{2000}^{Average}$, for offset uncoated paper the difference is - 4.06, and for mat coated papers $\Delta E_{2000}^{Average}$ - 7.68. The maximum difference obtained ΔE_{ab}^{Max} for coated mat paper is 57.59 units and there are twice lower values of 31.41 unsuitable offset uncoated paper. For mat coated paper, ΔE_{ab}^{Max} = 19.53 units and 10.92 units for offset uncoated paper. This indicates that some of the colours undergo a huge change - they "disappear" or go into another colour gamut.

After exposure to the UV ageing of papers, it was found that paper Brightness was reduced. In the coated mat paper the reduction reaches 18 units, the most drastic being this reduction to about 48 hours. On uncoated offset paper there is a more uniform Brightness reduction throughout the irradiation process of 17.8 units. Accordingly, the Yellowness is increased, with the coated mat paper being 16.9 units, and the uncoated offset paper is 15.66 units.

After the 3D visualization analysis and the 2D sections of the colour gamut in the UV ageing process, a significant decreasing of 38 ÷ 40% was recorded in the volumes of the 3D body. The reduction of area of the 2D cross sections after irradiation for both types of papers is - for the mat paper 38 % and for offset is 21%. A large colour shift from the blue and red areas of the colour gamut of the printed images is found after the UV ageing of papers. In the field of light tones there is a significant displacement from green and red to yellow areas and less displacement in blue areas. In the middle tones there is a contraction in all areas, and in the dark tones there is a significant shift in the blue regions. In all key tones the colours are transforming with less saturation and different colour hue.

5. REFERENCE

- [1] Dolezalek, F.: "Characterization data for offset, newspaper and screen printing", URL: <http://www.fogra.org/products-de/icc/Readme04e.pdf> (last request: 2018-10-21)
- [2] European Color Initiative, ECI offset profiles, URL: www.eci.org (last request: 2018-10-21)
- [3] International Color Consortium, Specification ICC. 1: 2004-10 Image technology colour management–Architecture, profile format, and data structure, International Color Consortium, 2004.
- [4] International Organization for Standardization, ISO 13656:2000 Graphic technology - Application of reflection densitometry and colorimetry to process control or evaluation of prints and proofs, International Organization for Standardization, 2000.
- [5] International Organization for Standardization, ISO 2470:2002 Paper, board and pulps – Measurement of diffuse blue reflectance factor (ISO Brightness), International Organization for Standardization, 2002.
- [6] International Organization for Standardization, ISO 2846-1:2006 Graphic technology - Application of reflection densitometry to process control or evaluation of prints and proofs, International Organization for Standardization, 2006.
- [7] International Organization for Standardization, ISO 12647-2:2013 Graphic technology -Process control for the production of half-tone colour separations, proof and production prints - Part 2: Offset lithographic processes, International Organization for Standardization, 2013.
- [8] International Organization for Standardization, ISO 13655:2017 Graphic technology - Spectral measurement and colorimetric computation for graphic arts images, International Organization for Standardization, 2017.
- [9] Kachin, N., Spiridonov, I.: "Optical Density and Color Difference in Printing on Different Types of Paper", Cellulose Chemistry and Technology, 39 (3-4), 255-264, 2004.
- [10] Rosen, M., Imai, F., Jiang, X., Ohta N.: "Spectral Reproduction from Scene to Hardcopy: Image Processing", Proceedings of SPIE 2001, (Photonics West 2001 - Electronic Imaging, San Jose, California, 2001), pages 31-41. doi: 10.1117/12.410822
- [11] Rosenberg A.: From Europe to ISO: „What is the intention of the new Colour Scale for Offset“, FOGRA Extra, 9, 2004.




- [12] Saldivar-Guerrero, R., Cabrera, Álvarez E. N., Leon-Silva, U., Lopez-Gonzalez, F. A., Delgado Arroyo, F., Lara-Covarrubias, H. and Montes-Fernandez, R.: "Quantitative Analysis of Ageing Condition of Insulating Paper Using Infrared Spectroscopy", *Advances in Materials Science and Engineering*, 2016. doi: 10.1155/2016/6371540
- [13] Sonderegger, W., Kránitz, K., Bues, C. T., Niemz, P.: "Aging effects on physical and mechanical properties of spruce, fir and oak wood," *Journal of Cultural Heritage* 16 (6), 883-889, 2015. doi: 10.1016/j.culher.2015.02.002.
- [14] Timar, M. C., Varodi, A. M., Gurău, L.: "Comparative study of photodegradation of six wood species after short time UV exposure," *Wood Science and Technology*, 50 (1), 135-163, 2016. doi 10.1007/s00226-015-0771-3.



© 2018 Authors. Published by the University of Novi Sad, Faculty of Technical Sciences, Department of Graphic Engineering and Design. This article is an open access article distributed under the terms and conditions of the Creative Commons Attribution license 3.0 Serbia (<http://creativecommons.org/licenses/by/3.0/rs/>).

REPEATABILITY AND REPRODUCTION ACCURACY IN ELECTROPHOTOGRAPHY FOR COLOR DIFFERENCE EVALUATIONS

Sandra Dedijer , Ivana Tomić , Magdolna Pál ,

Ivana Jurić , Živko Pavlović , Neda Milić 

University of Novi Sad, Faculty of Technical Sciences,
Department of Graphic Engineering and Design, Novi Sad, Serbia

Abstract: *In this paper, we have investigated the applicability of electrophotography, in terms of repeatability and reproduction accuracy, for color difference evaluations. When performing color difference evaluations with printed samples, the printing technique used may more or less influence the color reproduction. In order to evaluate the influence of reproduction accuracy and short term repeatability in electrophotography on color difference evaluation, we chose to examine the color reproduction of five initial color centers which were varied in their lightness. For color difference calculation we used CIE2000 color difference formula. It was shown that the expected color differences were not obtained in all cases and for all colors used whereas the variability is not only influenced by the color center but also by the level and direction of lightness variation.*

Key words: electrophotography, color difference, CIE00

1. INTRODUCTION

Evaluation of color can be performed through instrumental, objective assessment of color stimuli, or visual, subjective one based on human color perception (Brainard, 2003; Gulrajani, 2010; Fairchild, 2013).

The objective color analysis usually encompasses the examination of the color differences between various colored stimuli using appropriate color difference equations such as CIELAB (CIE76), CIELUV, CMC, BFD, CIE94, CIE00 (Xin et al, 2001; Xu, Yaguchi et al, 2002; Hong et al, 2006; Ho et al, 2004; Laborie et al, 2010). In the graphic industry, color difference is usually calculated using CIE76, CIE00 or CMC formula. Each of them performs best under a specific, more or less unique set of reference conditions whereas different results might, in some color regions, be quite significant (Xin et al, 2001). CIE94 (ΔE_{94}) and CIE00 (ΔE_{00}) are two, so called advanced formulae, are tended to adjust the numerical expression of difference to the way human observers perceive differences depending on the location of the color in color space and its intensity introducing the weighting factors into basic equation (ΔE_{ab}). These equations are highly recommended for use with color-differences in the range of 0.0 to 5.0 ΔE units for prints and textile (Ho et al, 2004; SpectraCal, 2018). The previous research has proven that CIE00 have a strong agreement with human perception in regards to lightness, chroma and hue of the tested colors (Mangine et al, 2005; Pant et al, 2010; Ortiz-Jaramillo et al, 2016; Pant et al, 2012; SpectraCal, 2018).

Color difference calculations are usually performed between target color stimuli and corresponding reproduced match. The pass/fail decision is generally made on the basis of the established color difference threshold which will differ in ΔE value depending upon the area of application and color difference formulae used: a difference of 5 ΔE may be acceptable in some applications, whereas for other, differences over 1 ΔE may be unacceptable (Dedijer et al, 2017).

In the graphic arts and printing industry, for most demanding works, the maximum acceptable ΔE color difference is 1.5 ΔE . According to ISO standard for offset printing, tolerances are even more stretched (ISO 12647-2:2013): up to 5 ΔE_{ab} for Cyan, Magenta, Yellow and Black or 3.5 ΔE_{00} (perceptual assessments) for Cyan, Magenta, Yellow and 5.0 for Black.

In digital printing, according to IDEAlliance Digital Press Certification Program, it is suggested that in color difference evaluation CIE00 equation should be used whereas color difference of 5 ΔE_{00} should not be exceeded through all the patches of the Digital Press Control Strip 2011. Tolerances for the short term and long term repeatability for the primary and secondary colors should not exceed color difference value of 3 (Idealliance, 2018).

In color differences evaluation, where a series of color tests are to be compared with a color reference, influence of printing technology should be omitted or at least minimal and known and taken into consideration.

In this research, we have investigated the possibilities of using electrophotography, digital printing technique, for the purpose color difference evaluation. We have aimed to preliminary establish to which extend the used printing technique alter the targeted color difference. We have been driven with general recommendations of the IDEAlliance certification program for electrophotography printing technique.

2. MATERIALS AND METHODS

In order to evaluate the level of reproduction inconsistency which will be directly influenced by the printing technique used, we chose five initial color centre (Xu et al, 2002)(Table 1). Their lightness of samples was varied in the steps of ΔE 0.5, where the changes were made in both directions: by lowering and increasing the value. The smallest color difference from the initial color was 0.5, while the largest was set to be 5. We created one color test chart (Figure 1) with all five colors and all color patches with targeted color difference values. The targeted digital L,a,b data of each color patch were calculated on the basis of expected color difference value ΔE_{ab} , L, a, and b values of five initial color centres and following formulae (Gulrajani, 2010; Fairchild, 2013, Stone et al, n.d.):

$$\Delta E_{ab} \text{ color difference: } \Delta E_{ab} = \sqrt{[\Delta L^2 + \Delta a^2 + \Delta b^2]} \quad (1)$$

where:

ΔL - the lightness difference: $\Delta L = L_1 - L_2$,

Δa and Δb - chromaticity differences: $\Delta a = a_1 - a_2$, $\Delta b = b_1 - b_2$,

L_1, a_1, b_1 - lightness and chromaticity coordinates of sample 1 (CIE color centre); L_2, a_2, b_2 - lightness and chromaticity coordinates of sample 2 (targeted color patch).

The L,a,b data were then recalculated to RGB values (CIE D50 standard illuminant and standard 2° observer; 0-1 scale) and used for of the generation of color patches size of 2x2 cm (sRGB, .tiff format). For this purpose, we employed MATLAB® R2013a. The patches were used for color test chart creation in Adobe® Illustrator® CS6 software. The PDF file for printing was generated according to PDF/X-4 guidelines.

The created color test charts were printed on matte coated 300 g/m² paper using calibrated digital printing machine for XEROX Versant 80 Press (printing technique: electrophotography). According to recommendations for the short term repeatability (Idealliance, 2018) three sheets were printed for each sampling time: 0 hour (sheets 1), 1 hour after (sheets 2) and 24 hour after (sheets 3). The measurements were done on each sheet for each patch trice. The average values of 9 color measurements were used for color difference calculation. The colorimetric measurements were performed using Techkon SpectroDens Advanced spectrophotometer (measurement geometry: 0°/45° with respect to CIE D50 standard illuminant and standard 2° observer). Measurement is performed on black, matte backing.

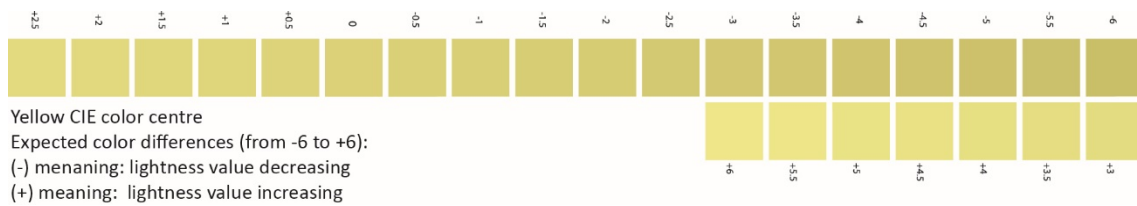


Figure 1: One part of the generated color test chart (one color - yellow)

For calculation of reproduced color difference, we used ΔE_{00} (Stone et al, 2018):

$$\Delta E_{00} = \sqrt{[(\Delta L'/K_L S_L)^2 + (\Delta C'/K_C S_C)^2 + (\Delta H'/K_H S_H)^2 + R_T(\Delta C'/K_C S_C)(\Delta H'/K_H S_H)]} \quad (2)$$

where

$$\Delta L' = L'_1 - L'_2$$

$$\Delta C' = C' - C'_2$$

$$\Delta H' = 2(C'_1 C'_2)^{\frac{1}{2}} \sin(\Delta h'/2)$$

$$\Delta h' = h'_1 - h'_2$$

$$S_L = 1 + \frac{0.015(L'-50)^2}{\sqrt{20+(L'-50)^2}}$$

$$\begin{aligned}
S_c &= 1 + 0.045\overline{C'} \\
S_H &= 1 + 0.015\overline{C'}T \\
T &= 1 - 0.17 \cos(\overline{h'} - 30^\circ) + \\
&+ 0.24 \cos(2\overline{h'}) + 0.32 \cos(3\overline{h'} + 6^\circ) + 0.20 \cos(4\overline{h'} + 63^\circ) \\
R_T &= -\sin(2\Delta\theta) R_C \\
\Delta\theta &= 30 \exp\left\{-[(\overline{h'} - 275^\circ)/25]^2\right\} \\
R_C &= 2 \sqrt{\frac{\overline{C'}^7}{\overline{C'}^7 + 25^7}} \\
L' &= L^* \\
a' &= (1 + G)a^* \\
b' &= b^* \\
C' &= (a'^2 + b'^2)^{1/2} \\
h' &= \tan^{-1}(b'/a') \\
G &= 0.5 \left(1 - \sqrt{\frac{\overline{C_{ab}^*}^7}{\overline{C_{ab}^*}^7 + 25^7}}\right) \\
K_L &= 1; K_c = 1; K_h = 1; \text{ default values.}
\end{aligned}$$

Table 1: CIELAB chromaticity parameters of the test color centers (CIE1931 Standard Colorimetric Observer) (Xu et al, 2002)

CIE color centre	L ₁	a ₁	b ₁	C ₁	h ₁ °
Red	44.38	36.91	23.33	43.67	32
Green	56.09	-32.13	0.44	32.13	179
Blue	35.60	4.83	-30.18	30.56	279
Yellow	86.65	-6.92	47.15	47.66	98
Gray	61.65	0.11	0.04	0.12	20

Short term repeatability was evaluated according to ΔE_{00} values computed between all combinations of press sheets: sheets 1 (0 hour) and 2 (1 hour), sheets 1 (0 hour) and 3 (24 hours), and sheets 2 (1 hour) and 3 (24 hours) (Ideaaliance, 2018).

3. RESULTS AND DISCUSSION

On Figure 2a are presented calculated color differences (ΔE_{00}) for red color. The straight line represents the ideal color reproduction, theoretically achievable targeted/ reproduced color difference ratio. According to the results, the color differences reproduced on the first and second set of prints exhibited moderate to large discrepancies from targeted values whereas reproduced color differences were of lower value for the whole range. The least deviations were observed on sheets 3 (printed after 24 h). Color difference values calculated for the sheets 1 and sheets 2 are somewhat similar, where the deviations were higher if the targeted color difference value was higher too. On Figure 2b-d are presented absolute differences in lightness and chromaticity coordinates. It can be noticed that the difference in chromaticity values take a share in overall color difference, although initially only lightness value of color patches was changed.

On Figure 3a are presented calculated color differences (ΔE_{00}) for green color where the straight line represents the ideal reproduction. It can be seen that the color differences reproduced on all three sets of prints are reflecting smaller discrepancies from targeted values except for the prints 2 and values defined through lightness decrease. On Figure 3b-d are presented absolute differences in lightness and chromaticity coordinates. The difference in chromaticity values take a share in overall color difference, but in much lower range in comparison to the red color.

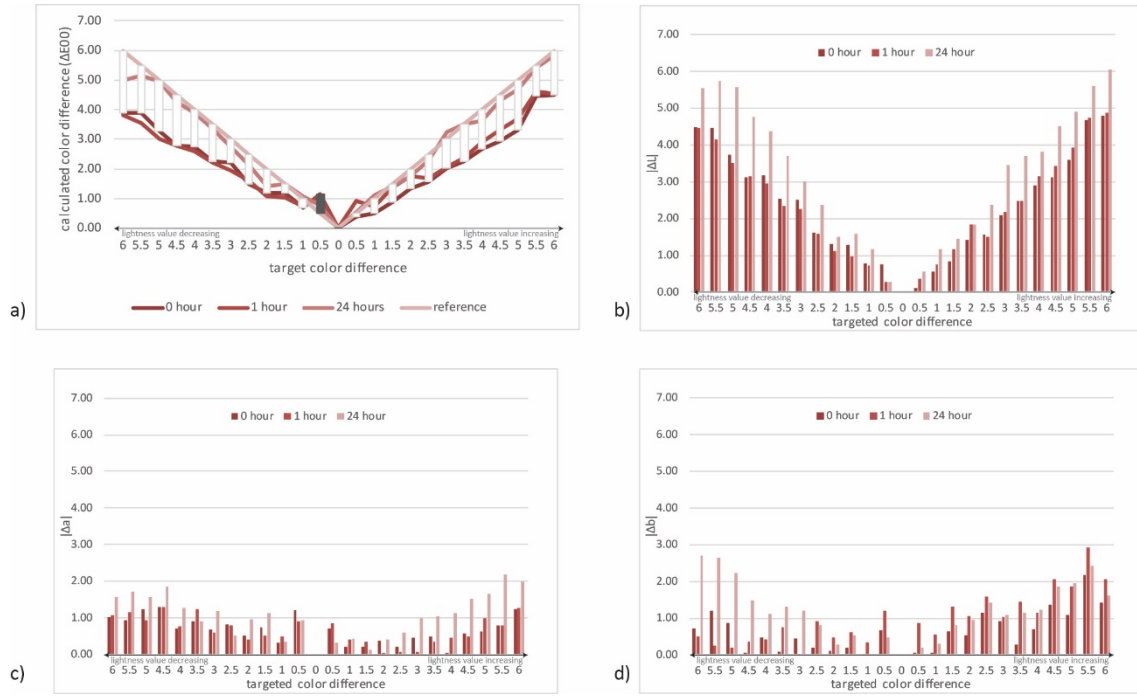


Figure 2: Red CIE color centre: a) color difference (ΔE_{00}), b) lightness difference (absolute values), c) difference in chromaticity coordinate a (absolute values), d) difference in chromaticity coordinate b (absolute values)

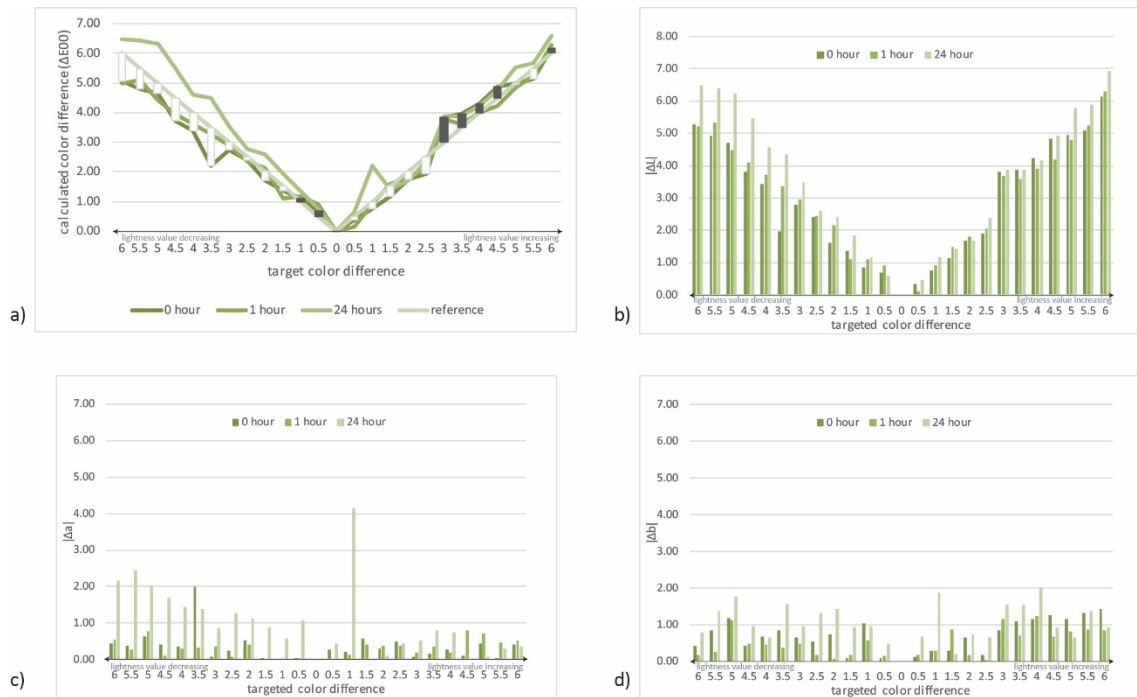


Figure 3: Green CIE color centre: a) color difference (ΔE_{00}), b) lightness difference (absolute values), c) difference in chromaticity coordinate a (absolute values), d) difference in chromaticity coordinate b (absolute values)

On Figure 4a are presented calculated color differences (ΔE_{00}) for blue color which exhibits the same pattern in color differences reproduction as the red color. On Figure 4b-d the one can see the results of the absolute differences in lightness and chromaticity coordinates. It can be noticed that the difference in chromaticity values take a share in overall color difference, but in much lower range in comparison to the red color.

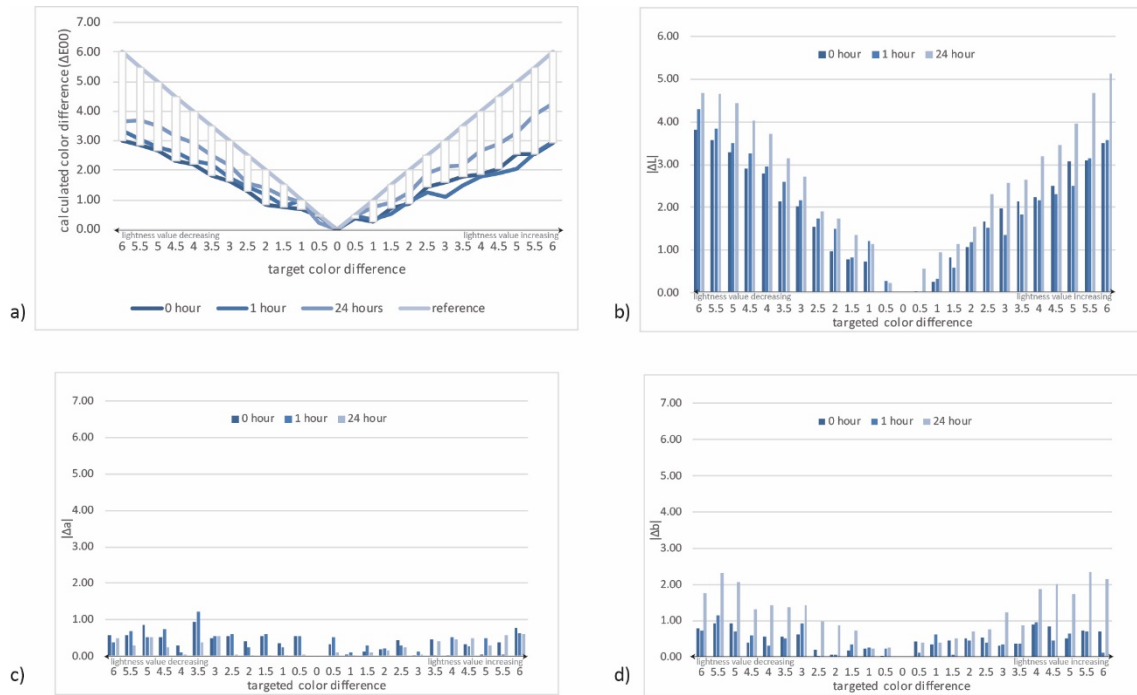


Figure 4: Blue CIE color centre: a) color difference (ΔE_{00}), b) lightness difference (absolute values), c) difference in chromaticity coordinate a (absolute values), d) difference in chromaticity coordinate b (absolute values)

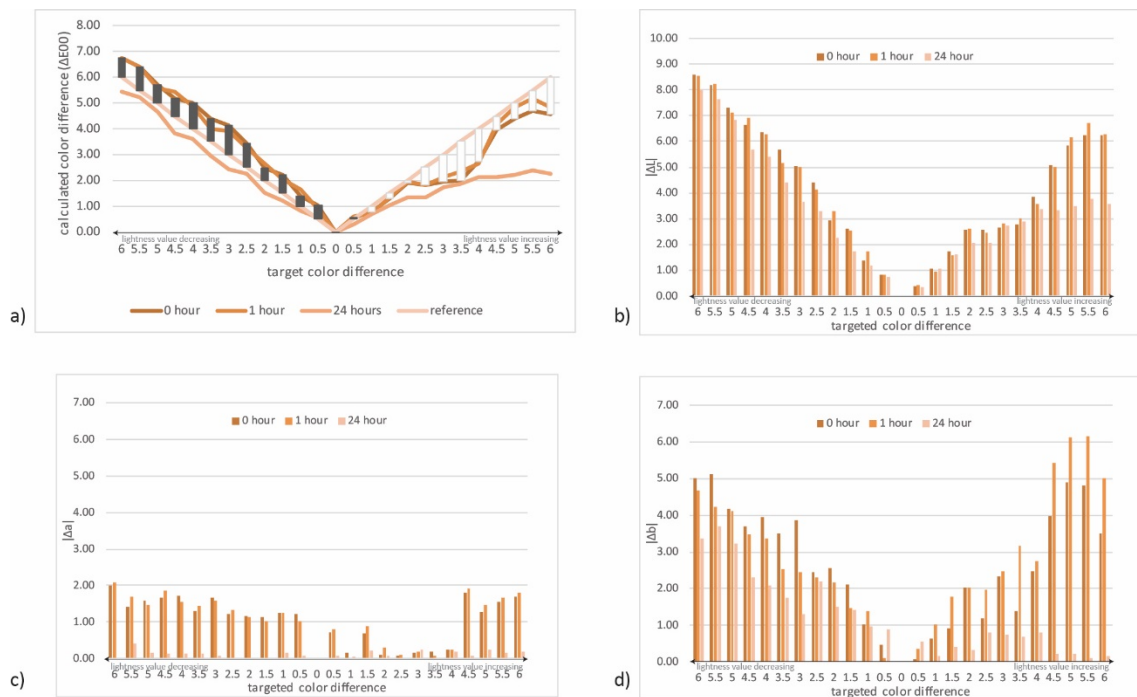


Figure 5: Yellow CIE color centre: a) color difference (ΔE_{00}), b) lightness difference (absolute values), c) difference in chromaticity coordinate a (absolute values), d) difference in chromaticity coordinate b (absolute values)

On Figure 5a are presented calculated color differences (ΔE_{00}) for yellow color. It can be noticed color differences reproduction differs in dependence of sheet set as well as the fact if the lightness value was decreased or increased. The more accurate reproduction is achieved when the lightness value was decreased, especially in the case of sheets 3 (printed after 24 hours). On Figure 5b-d are presented absolute differences in lightness and chromaticity coordinates. It can be noticed that the difference in chromaticity values take a considerable share in overall color difference, especially in the case of chromaticity coordinate b.

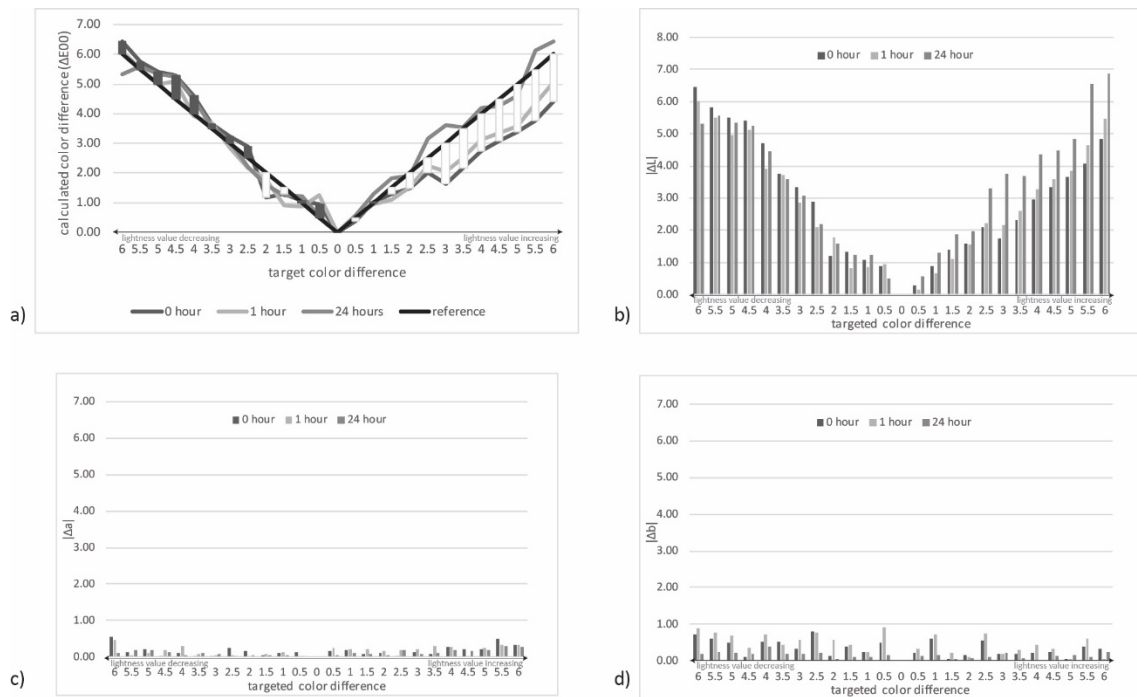


Figure 6: Gray CIE color centre: a) color difference (ΔE_{00}), b) lightness difference (absolute values), c) difference in chromaticity coordinate a (absolute values), d) difference in chromaticity coordinate b (absolute values)

On Figure 6a are presented calculated color differences (ΔE_{00}) for gray color which exhibit rather similar reproduction accuracy to yellow CIE color centre. The most accurate reproduction is achieved when the lightness value was decreased. On Figure 6b-d are presented absolute differences in lightness and chromaticity coordinates. It can be seen that the difference in chromaticity values take a rather small part in overall color difference.

Table 2: Coefficient of variation (average value)

CIE color centre	Coefficient of variation (average value) (%)								
	0 hour			1 hour			24 hours		
	L	a	b	L	a	b	L	a	b
Red	0.70	1.11	2.31	0.71	1.10	2.35	0.72	1.06	1.22
Green	0.95	1.51	6.22	0.66	0.92	8.80	0.49	2.25	8.80
Blue	1.06	7.35	0.84	0.94	6.95	0.97	0.90	9.91	0.78
Yellow	0.42	2.71	0.16	0.43	2.58	1.51	0.22	0.81	0.95
Gray	0.97	11.48	10.66	0.97	11.03	9.88	0.80	4.89	3.94

In Table 2 are presented results of the calculated coefficient of variation for L, a and b color coordinates, for all CIE color centres and all groups of sheets. According to the low coefficient of variation (varying from 0.22% up to 11.48%, in dependence of color and sheet set), it can be stated that the measurement was stable and repeatable throughout all sheets in all three sets. The variation in L value was under 1%, while higher variations were between values of the chromaticity coordinates.

In Table 3 are given results of color difference calculations between sheets 1 (0 hour), 2 (1 hour) and 3 (24 hours). As it was in introduction section highlighted, upper tolerance for the short term repeatability assessment is restricted to color difference value of 3. This request was not fulfilled in case of red, green and yellow CIE color centre and sheet set 1 and 2 in contrast to sheet set 3. The highest deviation was calculated for the yellow color.

Table 3: Color difference values between sheets 1 (0 hour), 2 (1 hour) and 3 (24 hours) (ΔE_{00})

Measuring field	CIE color centre														
	Red			Green			Blue			Yellow			Gray		
	Color difference ΔE_{00}														
	0/1	0/24	1/24	0/1	0/24	1/24	0/1	0/24	1/24	0/1	0/24	1/24	0/1	0/24	1/24
6	1.06	5.61	6.18	0.27	4.75	4.88	0.83	1.53	0.72	0.41	8.76	9.12	0.98	2.01	1.17
5.5	0.73	6.02	5.98	0.70	4.59	4.66	0.62	1.83	1.26	0.49	8.65	8.94	1.12	2.76	1.70
5	0.82	5.92	6.16	0.23	4.59	4.80	0.72	1.84	1.13	0.34	8.41	8.72	0.89	2.84	1.98
4.5	1.07	5.82	6.27	0.62	4.54	4.94	0.67	1.80	1.24	0.68	8.66	9.25	1.18	2.85	1.74
4	0.82	6.39	6.44	0.57	5.06	5.33	0.73	1.64	0.93	0.37	8.77	9.00	0.71	2.78	2.16
3.5	0.86	5.75	5.90	1.77	4.59	4.73	0.70	1.83	1.37	0.13	8.79	8.73	1.40	2.86	1.48
3	0.83	6.36	6.80	0.52	5.05	5.39	0.58	1.36	0.83	0.47	9.03	9.08	0.93	2.74	1.85
2.5	1.00	5.92	6.23	0.35	5.03	5.16	0.55	1.48	1.07	0.28	8.30	8.57	0.67	2.40	1.78
2	0.88	6.70	7.11	0.85	4.85	5.08	0.89	1.67	0.86	0.64	8.19	8.70	1.97	3.34	1.50
1.5	0.83	6.34	6.86	0.26	4.86	5.11	0.49	1.56	1.13	0.33	8.18	8.38	0.89	2.89	2.00
1	1.03	6.66	7.16	0.59	5.49	5.70	0.82	1.38	0.72	0.73	7.63	8.32	1.17	3.12	1.96
0.5	0.67	6.59	7.07	0.56	5.29	5.75	0.71	1.38	0.87	0.41	7.44	7.76	1.48	2.60	1.36
0	1.18	6.70	7.53	0.38	5.59	5.93	0.47	0.91	0.54	0.43	7.38	7.79	1.35	2.90	1.56
0.5	0.80	6.62	6.90	0.58	5.34	5.72	0.48	1.02	0.91	0.38	7.27	7.59	1.26	2.17	1.09
1	0.92	6.92	7.50	0.27	4.97	5.22	0.46	0.72	0.49	0.48	7.16	7.55	1.56	2.51	1.03
1.5	0.77	6.80	7.16	0.23	5.43	5.29	0.66	0.93	0.77	0.49	6.97	7.27	1.60	2.41	1.03
2	0.76	6.79	7.32	0.23	5.56	5.56	0.45	0.67	0.47	0.41	6.67	7.06	1.33	2.49	1.24
2.5	1.15	6.87	7.53	0.22	5.54	5.74	0.65	0.82	0.70	0.44	6.63	6.91	1.23	1.90	1.21
3	1.14	6.79	7.75	0.61	5.24	5.82	0.91	0.68	0.99	0.37	6.94	7.24	0.96	1.18	0.77
3.5	1.08	7.36	7.60	0.62	5.35	5.60	0.65	0.64	0.84	0.43	7.13	7.05	1.08	1.63	1.01
4	0.94	6.92	7.60	0.66	5.11	5.67	0.80	0.92	0.85	0.55	6.61	7.08	1.01	1.49	0.62
4.5	0.80	7.04	7.49	0.97	5.80	6.10	0.59	0.77	1.22	0.52	5.74	5.91	1.20	1.70	0.90
5	0.78	7.21	7.67	0.47	6.19	6.44	1.05	0.82	1.17	0.31	5.30	5.32	1.13	1.69	0.57
5.5	1.05	6.61	7.12	0.26	5.93	5.92	0.35	1.07	1.38	0.26	5.28	5.20	0.80	0.68	0.72
6	1.06	6.90	7.51	0.24	6.21	6.12	0.54	1.01	1.44	0.46	5.52	5.57	0.71	0.88	0.31
average	0.92	6.54*	6.99*	0.52	5.24*	5.47*	0.65	1.21	0.96	0.43	7.42*	7.68*	1.14	2.27	1.31

4. CONCLUSIONS

The presented research was conducted in order to investigate the possibilities of using electrophotography, digital printing technique, for the purpose of color difference evaluation. The conclusions derived were as follows:

- Presented results have shown that the expected accuracy in color differences reproduction was not obtained in all cases and for all colors used.
- The reproduction accuracy is dependent on whether the color difference was affected by initial variations in color lightness, in positive or negative direction, color itself as well as the time frame in which was printing exhibited (sets 1, 2 and 3).
- The variability in terms of color difference accuracy reproduction was also influenced by changes in chromaticity coordinates which were initially left unchanged. Their variations are assumably influenced by electrophotographic printing process. This is especially noticeable in the case of yellow color.
- In the case of three CIE color centres (yellow, red and green), the color difference value requested for successful short term repeatability was not achieved, although color difference between sheets 1 and sheets 2 were exceptional (less than 1). For yellow color, the highest deviation from the upper bound of tolerance was exhibited.
- Generally, the size of the initially defined color difference and the accuracy of reproduction is in inverse correlation.
- According to the coefficient of variation values, it can be stated that the measurement was stable and repeatable throughout the experiment thus did not influence the parameters used to evaluate reproduction accuracy or short term repeatability.

5. ACKNOWLEDGMENTS

This work was supported by the Serbian Ministry of Science and Technological Development, Grant No.: 35027 "The development of the software model for improvement of knowledge and production in the graphic arts industry".



6. REFERENCES

- [1] Brainard, D. H.: "Color Appearance and Color Difference Specification", (Elsevier, Amsterdam, 2003.), pages 191-216.
- [2] Dedijer S., Tomić I., Spiridonov I., Boeva R., Jurič (Rilovski) I., Milić N., Đurđević S.: "Ink - jet imprints in just noticeable color difference evaluation", *Bulgarian Chemical Communications*, 49 (L), 140- 147, 2017.
- [3] Fairchild, M.D.: "Color Appearance Models", (John Wiley & Sons , Chichester, 2013)
- [4] Gulrajani, M. L.: "Colour measurement principles, advances and industrial applications", (Great Abington Cambridge, UK, Woodhead Publishing Limited in association with The Textile Institute Abington Hall, Granta Park, 2010)
- [5] Ho, K. M. R., Cui, G., Luo, M. R., Rigg, B.: "Assessing colour differences with different magnitudes", *Proceedings of the Interim Meeting of the International Color Association, Brazil 2004*, (Brazilian Color Association, Lisbon, 2004), pages 117-120.
- [6] Hong, G., Luo, M. R.: "New algorithm for calculating perceived colour difference of images", *The Imaging Science Journal*, 54 (2), 86-91, 2006. doi.org/10.1179/174313106X98737.
- [7] Ideaalliance: "Digital Press Certification Program", URL <http://connect.idealiance.org/HigherLogic/System/DownloadDocumentFile.ashx?DocumentFileKey=ef430ae7-2fcc-cd3a-2ff3-eab28265eaa1>, (last request: 2018-08-01)
- [8] Laborie, B., Vienot, F., Langlois, S.: "Methodology for constructing a colour-difference acceptability scale", *Journal of Ophthalmic and Physiological Optics* 30 (5), 568-577, 2010. doi.org/10.1111/j.1475-1313.2010.00765.x.
- [9] Mangine, H., Jakes, K., Noel, C.: "A Preliminary Comparison of CIE Color Differences to Textile Color Acceptability Using Average Observers", *Color Research and Application* 30 (4), 288-294, 2005. doi.org/10.1002/col.20124
- [10] Ortiz-Jaramillo, B., Kumcu, A., Philips, W.: "Evaluating color difference measures in images", *Proceedings of the 8th International Conference on Quality of Multimedia Experience, Lisbon 2016*, (Instituto de Telecomunicações, Lisbon, 2016), pages 1-6.
- [11] Pant, D.R., Farup, I.: "Riemannian Formulation of the CIEDE2000 Color Difference Formula", *Proceedings of the 18th CIC: Color Science and Engineering Systems, Technologies, and Applications, San Antonio 2010*, (Society for Imaging Science and Technology, San Antonio, 2016), pages 103-108.
- [12] Pant, D.R., Farup, I.: "Riemannian formulation and comparison of color difference formulas", *Color Research and Application* 37(6), 429-440, 2012. doi.org/10.1002/col.20710.
- [13] SpectraCal: "Visual Color Comparison: A Report on Display Accuracy Evaluation", URL <http://www.spectracal.com/Documents/White%20Papers/Visual%20Color%20Comparison.pdf>, (last request: 2018-02-07).
- [14] Stone, M., Szafir, D.A., Setlur, V.: "An Engineering Model for Color Difference as a Function of Size", URL https://research.tableau.com/sites/default/files/2014CIC_48_Stone_v3.pdf, (last request: 2018-02-07).
- [15] Xin, J. H., Lam, C. C., Luo, M. R.: "Investigation of parametric effects using medium colour difference pairs", *Color Research and Application* 26 (5), 376-383, 2001. doi.org/10.1002/col.1053.
- [16] Xu, H., Yaguchi, H., Shioiri, S.: "Correlation between visual and colorimetric scales ranging from threshold to large color difference", *Color Research and Application* 27(5), 349-359, 2002. doi.org/10.1002/col.10081.



© 2018 Authors. Published by the University of Novi Sad, Faculty of Technical Sciences, Department of Graphic Engineering and Design. This article is an open access article distributed under the terms and conditions of the Creative Commons Attribution license 3.0 Serbia (<http://creativecommons.org/licenses/by/3.0/rs/>).

STUDY OF COLOUR CHANGE IN THE COURSE OF DRYING ON PRINTS CREATED USING OFFSET PRINTING TECHNOLOGY

Csaba Horvath , Pál Görgényi-Tóth 
Óbuda University, Institute of Media Technology and
Light Industry Engineering, Budapest, Hungary

Abstract: *The research presented in the article describes the colour changes resulting from the drying of printing ink. In technical terminology, this colour change is called dryback (Schulz et al, 2005). Different print technologies use different inks (solvent-based, inks dried by oxidation, inks dried by UV radiation), but all of them are affected by dryback. This means that the ink still wet after printing has colour properties different from ink after it is dried. During the printing process it is usually possible to measure the colour properties (lightness, blue-yellow, red-green content, density) of the still wet print by the machine. A polarizing filter is installed in spectrophotometers in order to perform this measurement, which tries to measure the colour characteristics of the print, eliminating surface reflection. The research is designed to determine the point when the paint can be considered dried on the carrier (paper), to describe – using mathematical equations – the changes in the colour characteristics during the drying process, and then to design a device which is able to determine – using the mathematical model – what colour characteristics the still wet print will have after complete drying. In our article we intend to describe the first tests and the resulting conclusions.*

Key words: printing inks, carrier drying, autotype prints, density, colour stimulus difference, colour change

1. OBJECTIVES OF THE RESEARCH

Industrial printing inks solidify on the paper through various drying mechanisms. There are differences between the drying processes of the 'classic' ink dried by oxidation, a solvent based ink, and an ink dried by UV radiation. In the case of offset technology, ink drying is a complex process. Polymerization caused by oxidation (that is why prints are powdered in case of sheetfed offset ink; due to their size, the particles create an air vent between two sheets, allowing free airflow between the sheets), evaporation (for example gravure or flexo ink), and penetration (ink of cold-set printing dries this way) also play their part in the process of drying (INKFORMATION, 2011). As experience shows during the drying process, different values in terms of color characteristics (density, color stimulus difference) are shown once ink has fully dried on the paper, as compared to color characteristics measured right after printing. This phenomenon is called back-drying (Şahinbaskan et al, 2010). Factors influencing the ink drying process:

- additives in the ink containing dryers,
- ink viscosity,
- quantity and quality of the lubricant used during printing,
- ambient air temperature,
- ambient air humidity,
- paper surface,
- paper volume and aA value,
- air flow (oxygen concentration changes in case of air flow).

In our research the role of these factors within the drying process was examined. That is, only those ones of these parameters that can be changed. We intend to measure colour changes during drying after as many ways of modifications as possible.

Our goal is to define the change based on the exact measurements of a mathematical model, to develop a software for the existing measuring devices (densitometer, spectrophotometer) using an algorithm based on the mathematical model, or to make a new measuring device. This software could be used to determine the post-drying color characteristics of a specific color in the printing stage, in order to achieve the original colors of the sample after the dryback of the wet print.

For the research, we have defined three phases of the experiments. The first series of experiments are carried out in a laboratory, while the pilot measurements in the second phase of the experiment are

intended to confirm the results of the laboratory tests. The third step is the production trial, where our results are confirmed or adjusted in operational conditions.

We have selected offset printing for the measurements made in pilot and operational conditions. This is the technology, where the ink used dries in the most complex way, and colour change is also the most striking here. Offset printing is the most complex printing technology: liquid lubricant is necessary for the selectivity of the image areas and the non-image areas, and rheometer data (viscosity, tack value) must be changed in order to make the ink suitable for printing.

To conduct the experiments, from among the papers most frequently used in the printing industry, we selected 3 different print media types of the same square meter weight (100 g/m²), however of different structure and characteristics:

- offset (uncoated)
- glossy paper (coated)
- and optical bleach-free paper.

The measurements were started with the 4 colours [Cian, Magenta, Yellow and Black (Key)] of autotype printing, since these are the colours typically used for colour printing. These four colours are used for determining the mathematical correlations, and later the basic colours of the direct colours are used for the checking and correction of the mathematical formula.

The first phase of the experiments was conducted at the Hungarian company of Sun Chemical Corporation, where the color changes of the printed inks were modeled and measured with ink testing instruments under laboratory circumstances. At first, the temporal changes of colors were recorded under the specific circumstances of temperature and humidity. Density and hues of each sample are (L*, a*, b*) measured, then they are calculated according to the colour stimulus difference contained in the excel table included in the publication (Sharma et al, 2005).

2. RESEARCH METHODS

IGT C1 Offset and Letterpress Proofer Series test printing machine was used for the basic experiments conducted in the ink laboratory (Figure 1).



Figure 1: IGT C1

The test strip printed with the test printing machine represented the measurement fields with 100% fill ratio. The inks of Sunchemical SunLit Intense Process were used for the tests with all the three selected carriers. Rheometer data of the inks are shown in Table 1.

Table 1: Data of the examined inks

	INT09	INT41	INT39	INT38	INT24	INT75
Viscosity Rheometer 50s-1, 23°C (Pa.s)	45-60	45-60	70-90	75-95	42-55	42-55
Yield value Rheometer 2s-1, 23°C (Pa.s)	65-120	65-120	90-170	90-170	60-100	55-100
Tack Thwing Albert 800 rpm (g.m)	7,5-10,5	7,5-10,5	8,5-11,5	9-12	8,5-11,5	8,5-11,5

Ink density was set to similar values in the case of all carriers (in the case of coated paper: DC=1.5, DM=1.6, DY=1.4, DK=1.5, uncoated paper: DC=1.45, DM=1.45, DY=1.25, DK=1.45, and bleach-free paper: DC=1.5, DM=1.6, DY=1.4, DK=1.6).

The colours were measured with X-Rite eXact type spectrophotometer (device settings: D50 and 45/0 diffuse illumination, 2° viewing angle, without M1 filter). The measurements were based on measuring the colours L^* , a^* , b^* , L^* , C, H, X, Y, Z and the density values. Device repeatability was 0.01 – 0.02.

Based on the continuous measurement of the air temperature and relative humidity in the measurement room, it can be concluded that both the temperature and the humidity were constant during the measurement (the temperature was 25°C, while relative humidity was 48% – 52%).

3. SUMMARY OF THE RESULTS

During the measurements, the changes in the colour components were measured through one hour, then the measurements were repeated after a few days (when the ink was expected to be completely dry) in order to compare the previous values to the values of the completely dry ink colours. We also intend to perform the examination of the ink drying process in order to determine when an ink layer can be considered completely dry, and no further colour change can be expected. (note to X-Rite company: it would be nice to design an application allowing measurement intervals for automatic measurement, so that measurements could be made for 24 or even 48 hours in every fifteen minutes.)

The changes are illustrated in diagrams as well, and the diagrams include the formula of the function best fitting the curve, as well as its regression. The regression values are almost always 98–99, which means that the calculated curve fits the measured data. When illustrating the brightness values versus time, the following changes were noticed (Figures 2–4):

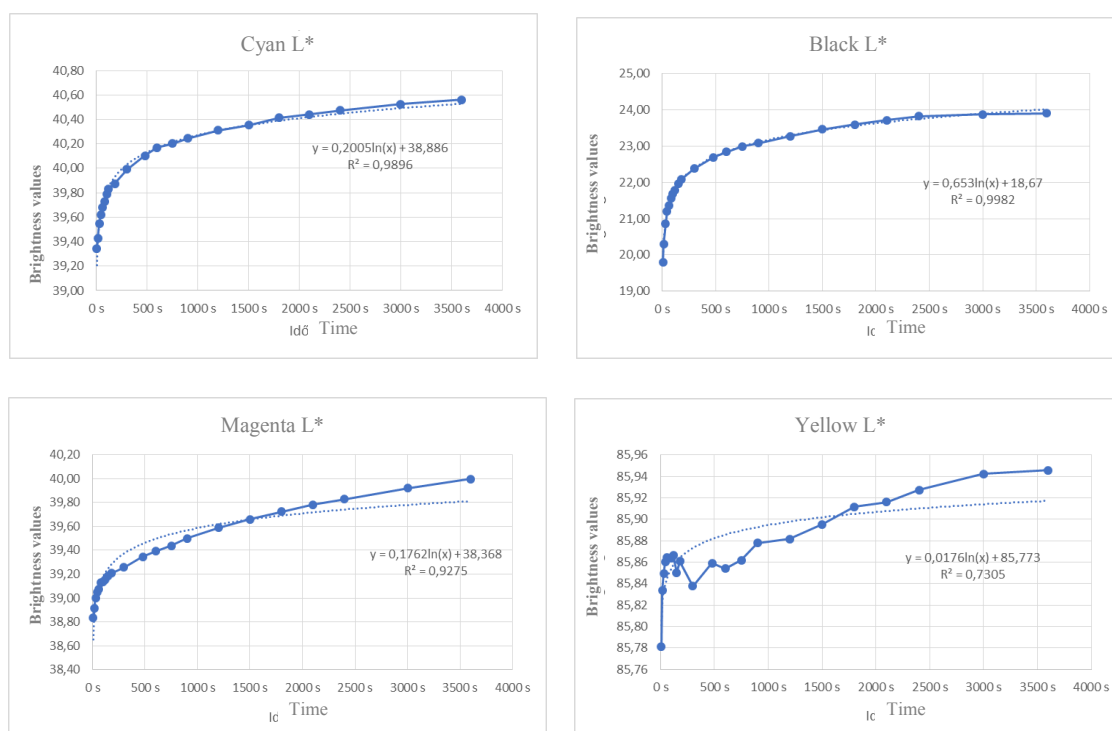


Figure 2: Brightness values in case of bleach-free paper

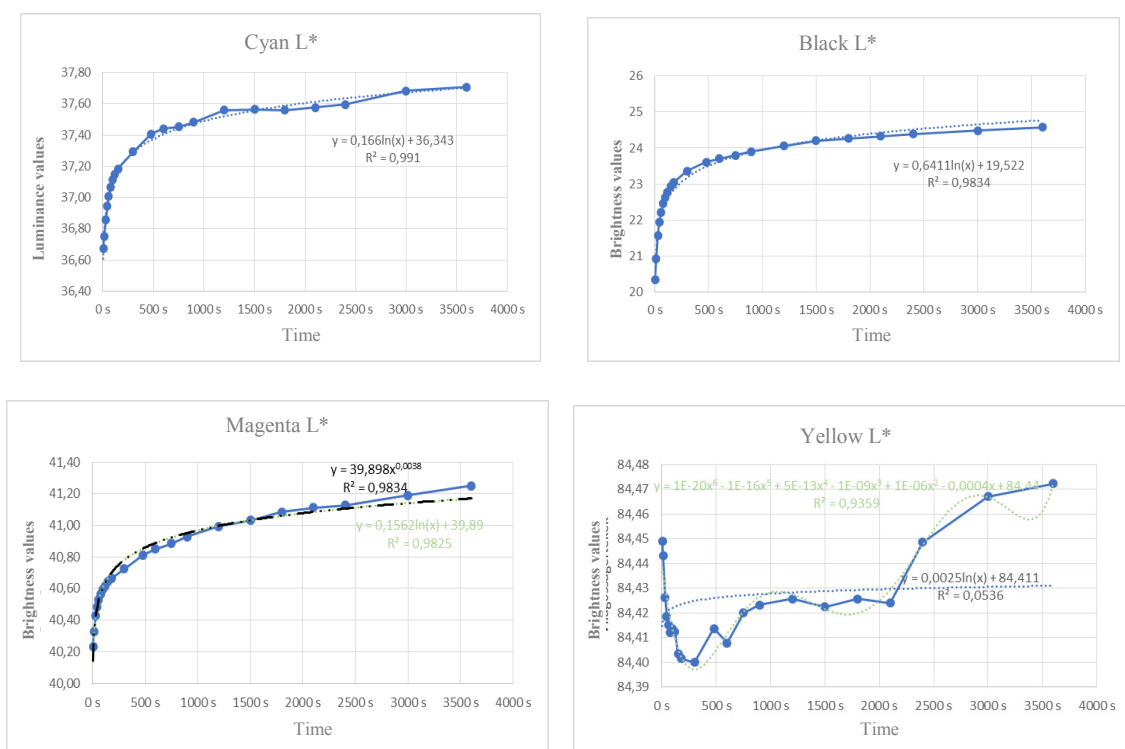


Figure 3: Brightness values in case of uncoated paper

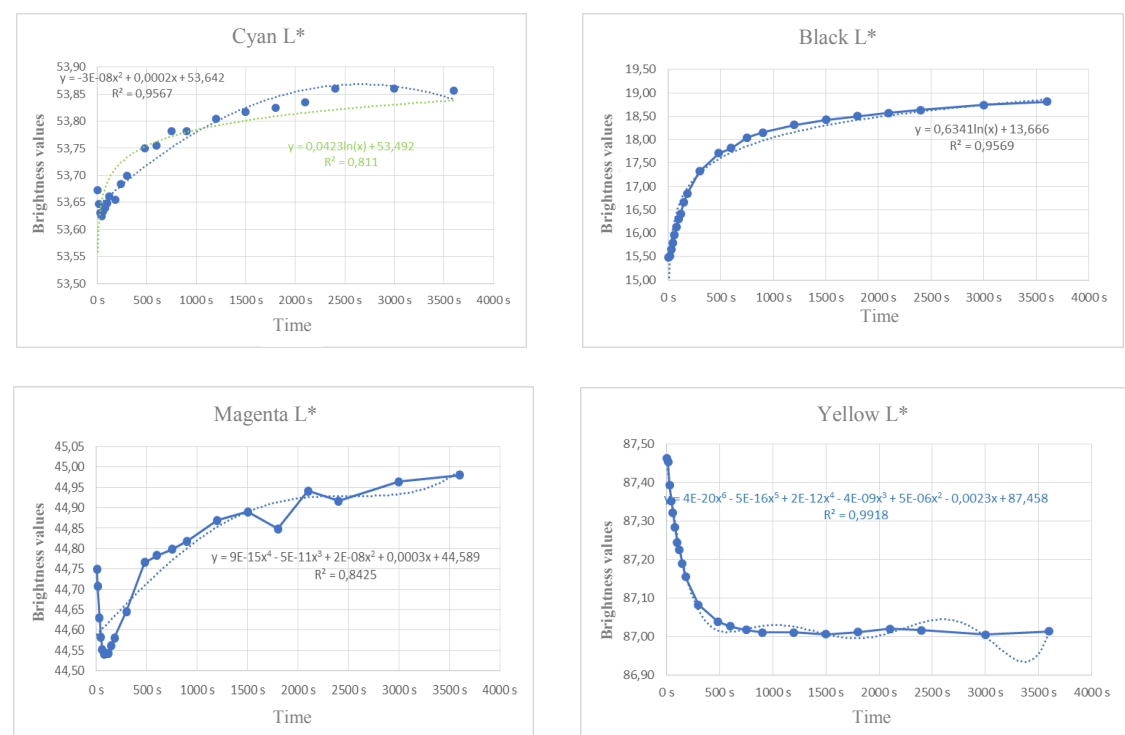


Figure 4: Brightness values in case of coated paper

In the large part of the measurements the brightness values changed versus time, according to a natural logarithm function. The exceptions were: yellow colour in case of coated and uncoated papers, and magenta as well in case of coated papers.

The colour changes measured on a* b* plane are shown in Figures 5–7. (The time of the measurement is indicated on the measurement points to identify the curve changes).

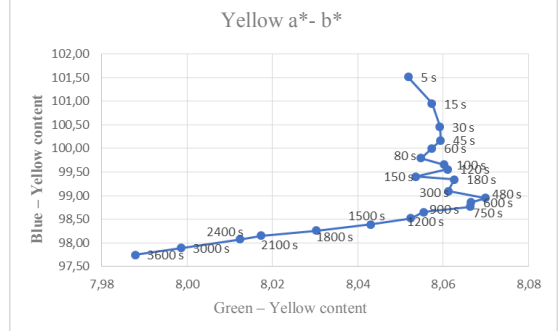
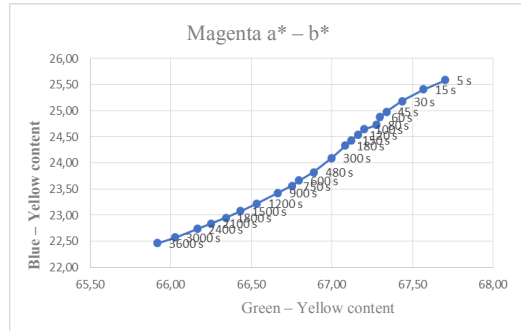
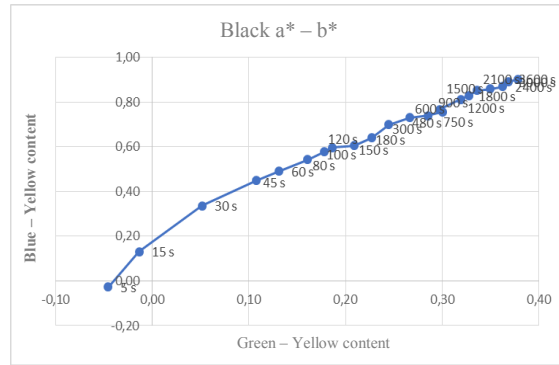
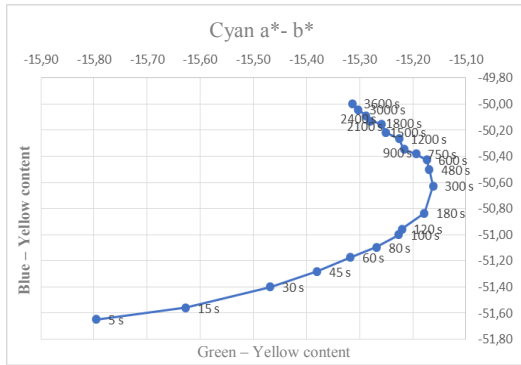


Figure 5: Changes shown in $a^* - b^*$ plane in case of bleach-free papers

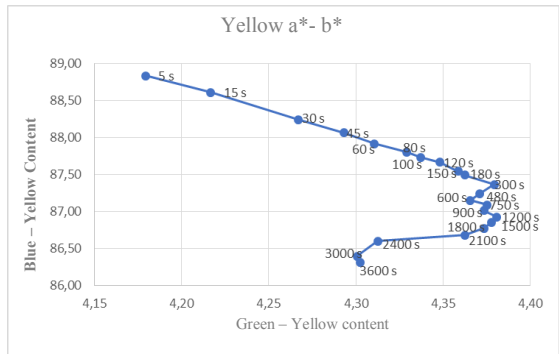
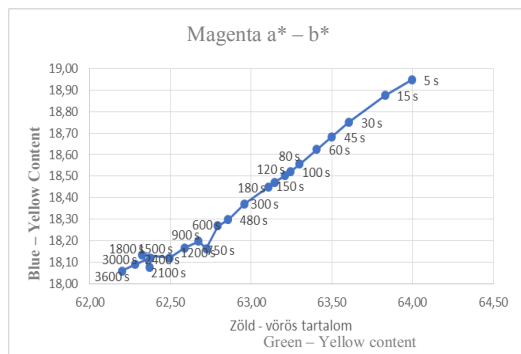
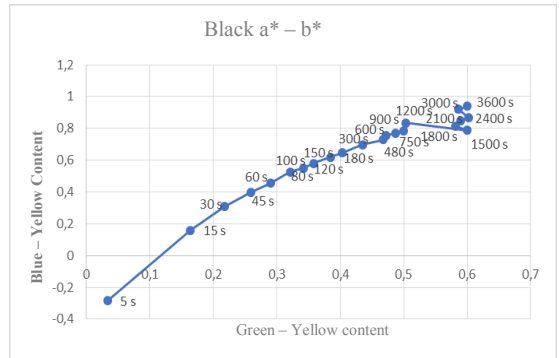
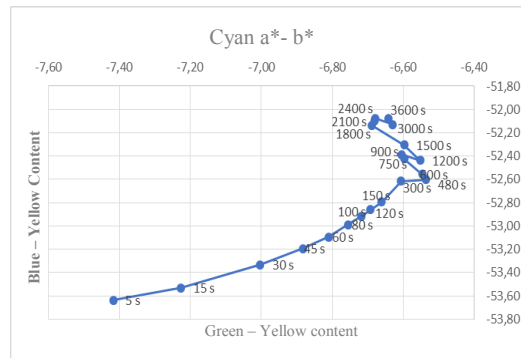


Figure 6: Changes shown in $a^* - b^*$ plane in case of uncoated papers

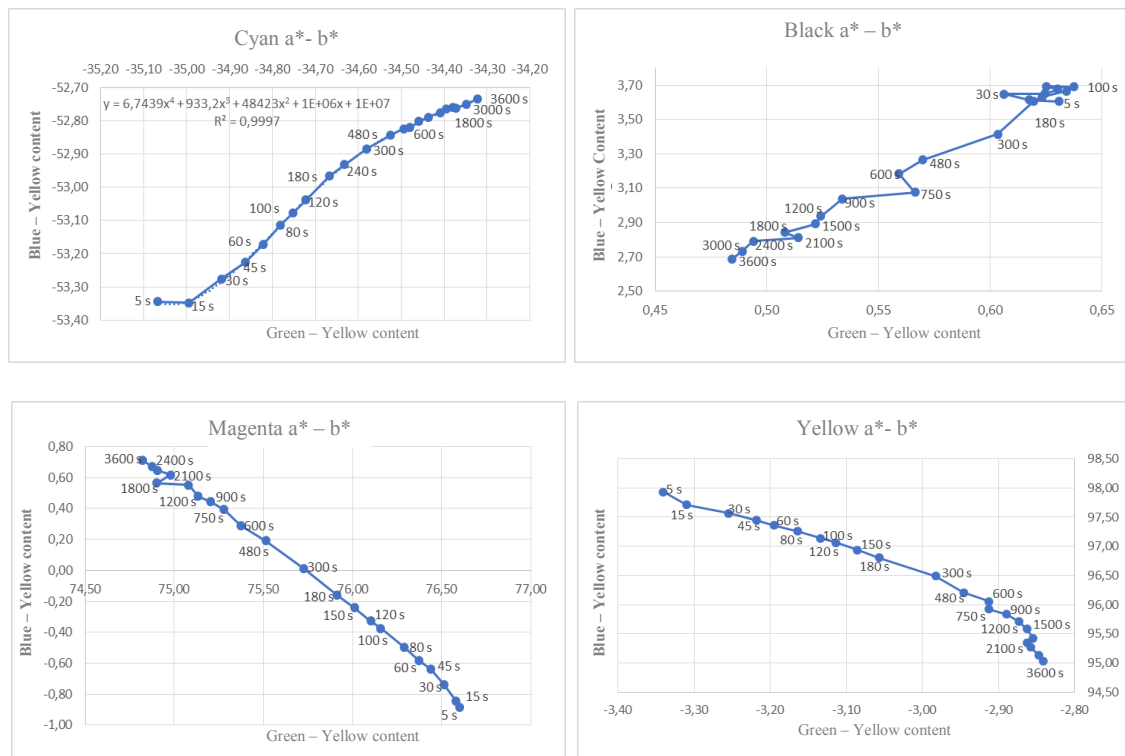


Figure 7: Changes shown in $a^* - b^*$ plane in case of coated papers

In case of all paper types the blue – yellow content of cyan colour shifted towards the blue, while in case of green – red content it shifted towards the red. The colour of cyan ink shifted towards the reddish blue in case of all paper types. Magenta shifted towards the yellow and the red, and when it was used on coated paper, it shifted towards the blue. In case of all the three paper types the black colour showed monotone increase towards yellow – red, so the colour got darker.

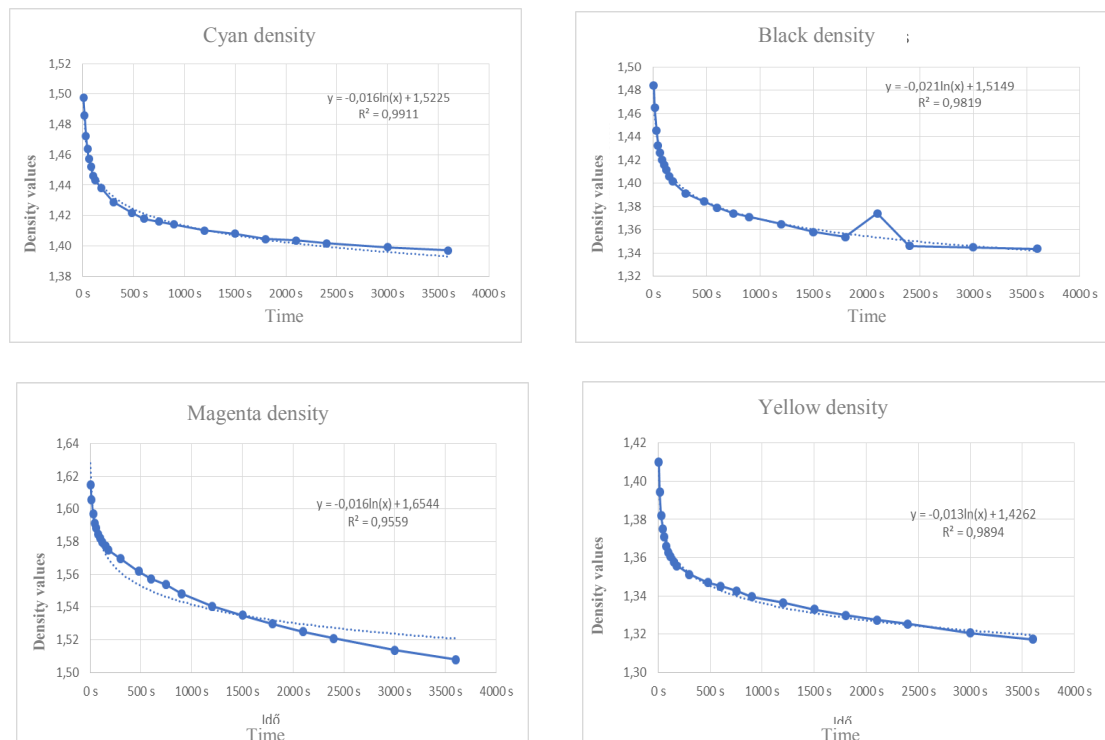


Figure 8: Density changes in case of bleach-free papers

In case of all the three paper types yellow changed differently during the drying process; yellow shifted towards green, red shifted towards blue, while blue shifted towards green.

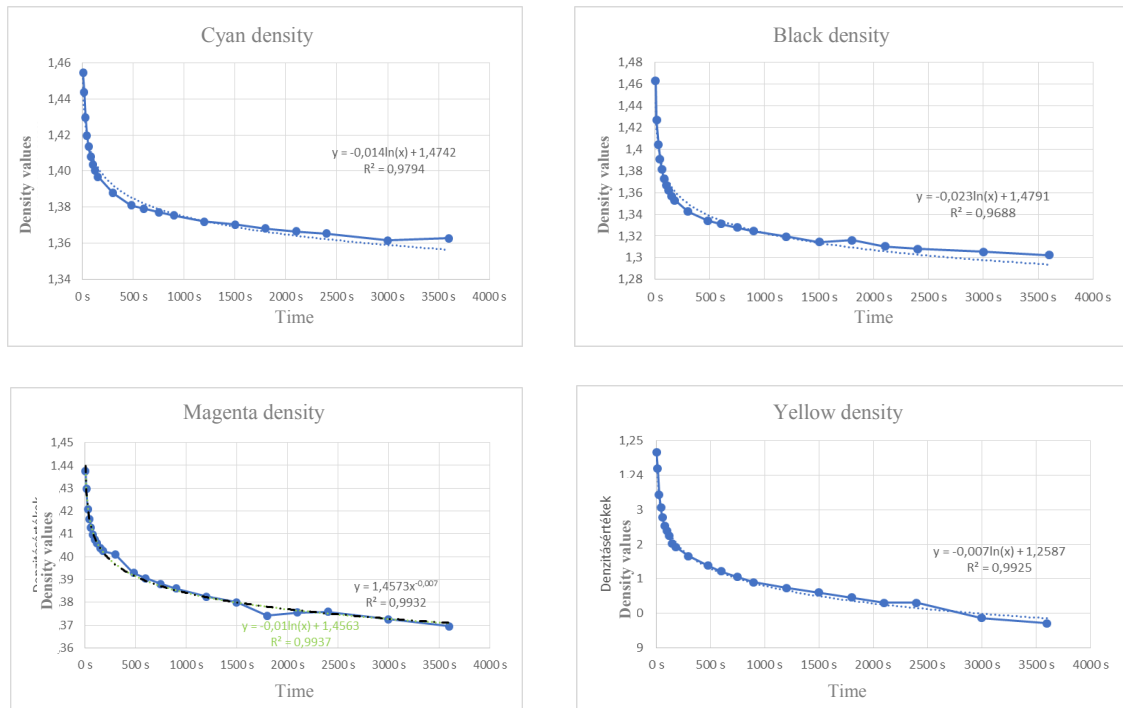


Figure 9: Density changes with uncoated papers

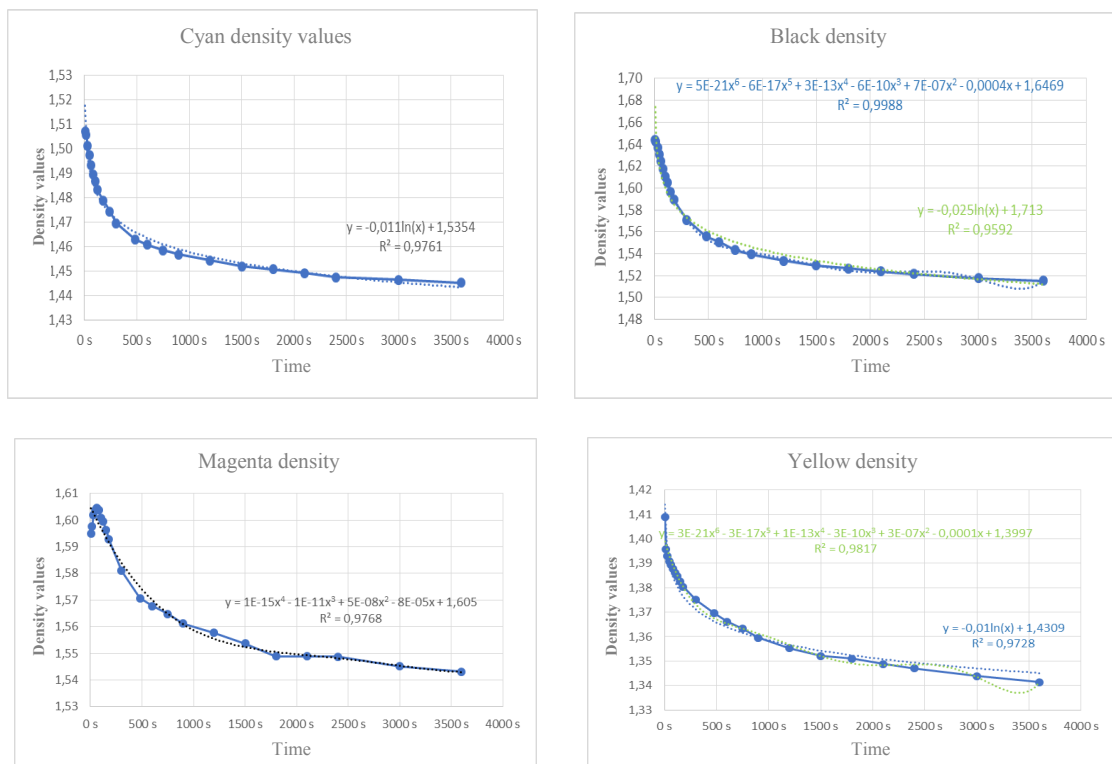


Figure 10: Density changes in case of coated papers

The curves of the density values are monotonous decreasing, following natural logarithm (at some points n-degree polynomial) function, growing fast up to 500s, then slowing down. This is due to the in reflection of the red paint, which can be eliminated by polarization filter.

After a certain period of time (3–4 days later) the ink was totally dry. At this point we repeated the measurements on the colour components, and with the use of the method mentioned above we calculated the colour stimulus difference between the colour of the dry ink and the ink in the drying process. The results are shown in Figures 11–13:

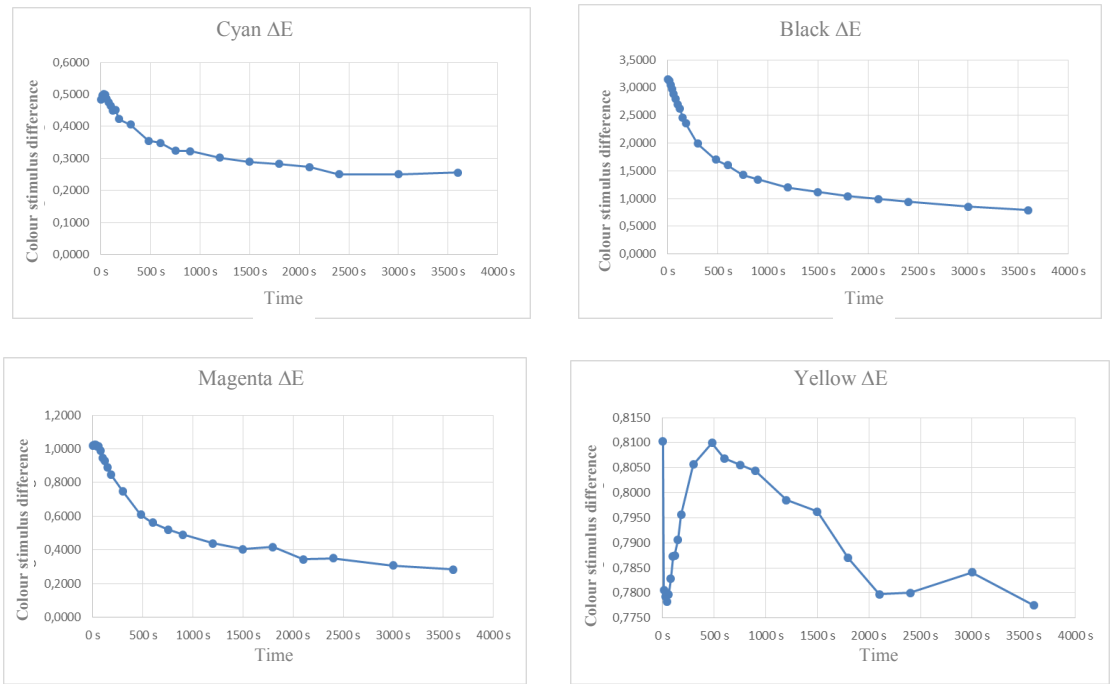


Figure 11: Changes in colour stimulus difference in case of coated paper

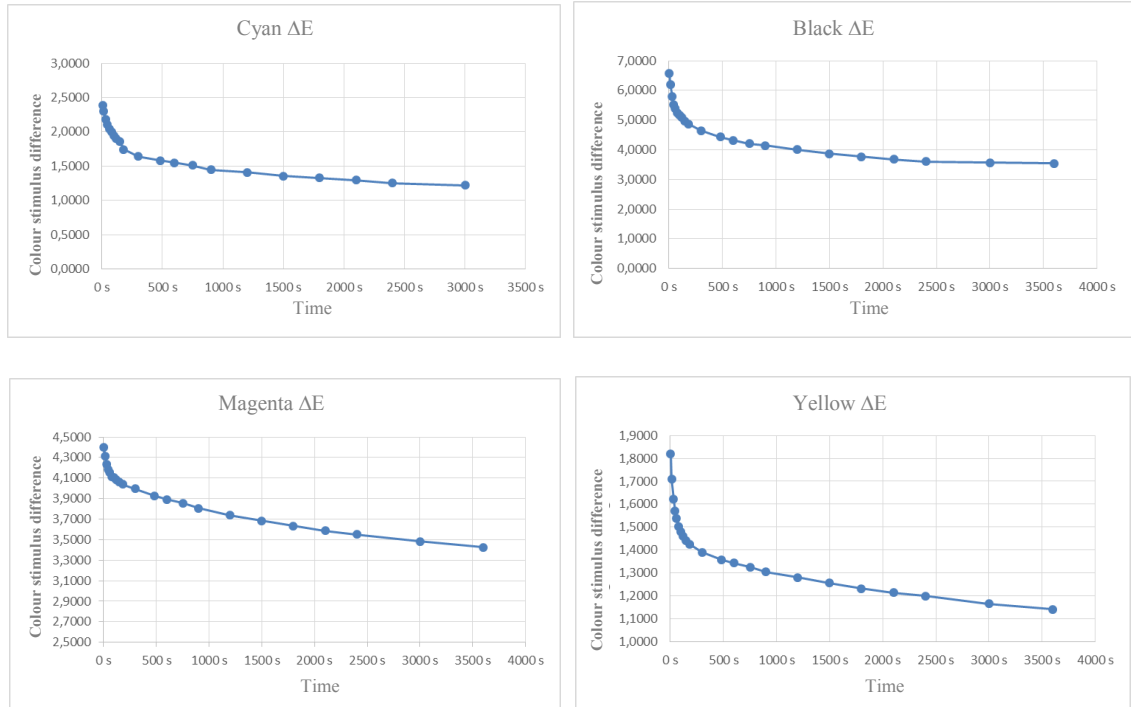


Figure 12: Changes in colour stimulus difference in case of bleach-free paper

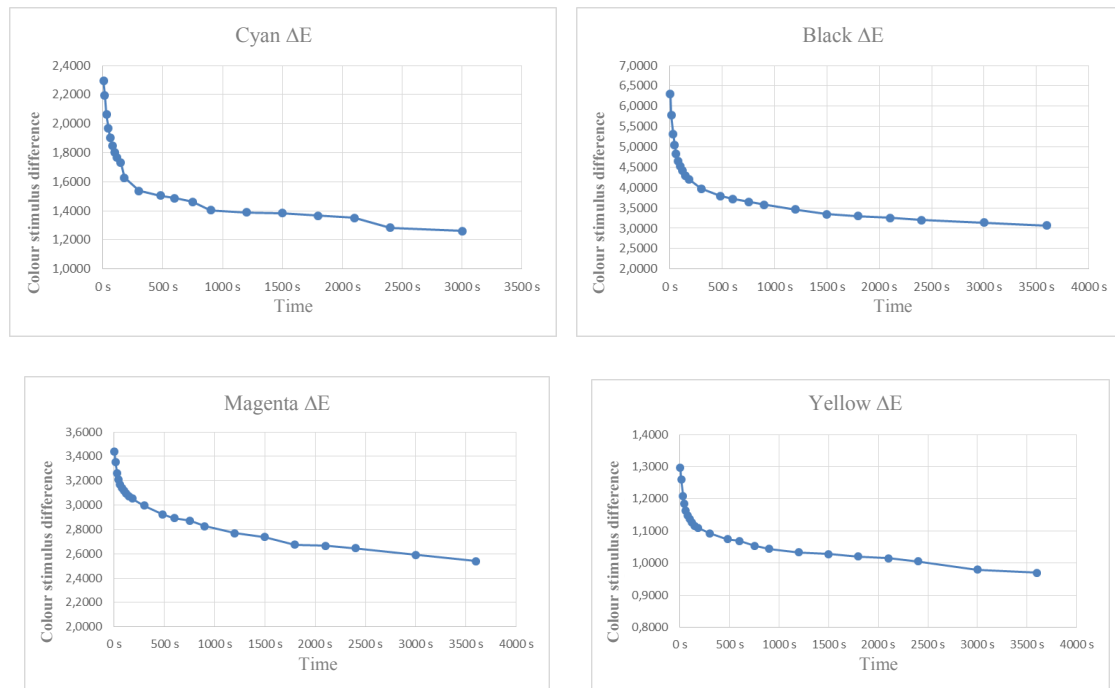


Figure 13: Changes in colour stimulus difference in case of coated paper

The colour stimulus difference calculations clearly show the trend of drying, that is – although none of the inks reached the final colour on paper – the colour stimulus difference between the colours is smaller and smaller. It is also true to these diagrams that the changes are faster during the first 500 seconds, and as the ink starts to dry, the ΔE change gets slower as well.

4. CONCLUSION

During our research we have found that ink colour change appearing on the paper follows the same curves (except for a few cases), and the colour is changed similarly over time on the same type of paper. The colour stimulus difference of completely dry ink changes following the same trend (monotonous decrease), only the magnitude of the difference varies.

In pilot plant trials we continue examining the functions describing differences and changes. In addition to examining colour and density values, we intend to examine changes in the colour angles, in brightness, therefore each variable parameter mentioned at the beginning of this article will be changed. By way of rubbing we will experiment the exact time when an ink can be considered dry, and we will draw further conclusions later.



5. REFERENCES

- [1] INKFORMATION, Test methods for offset inks and substrates, Huber Group, 2011.
URL: http://www.hubergroup.net/pdf-files/inkformarion/INKFORMATION_4_en_02.pdf
(last request: 2018-10-24)
- [2] Şahinbaşkan, T., Köse, E.: "Modelling of time related drying changes on matte coated paper with artificial neural networks", Expert Systems with Applications, 37 (4), 3140-3144, 2010.
doi: 10.1016/j.eswa.2009.09.068
- [3] Schulz, P., Endrédy, I.: "Angol-magyar nyomdaipari értelmező szótár", Mérnök és Nyomdász Kft., Budapest, 2005
- [4] Sharma, G., Wu, W., Edul, N. D.: "The CIEDE2000 color-difference formula: Implementation notes, supplementary test data, and mathematical observations", Color Research & Application, 30 (1), 21-30, 2005. doi: 10.1002/col.20070



© 2018 Authors. Published by the University of Novi Sad, Faculty of Technical Sciences, Department of Graphic Engineering and Design. This article is an open access article distributed under the terms and conditions of the Creative Commons Attribution license 3.0 Serbia (<http://creativecommons.org/licenses/by/3.0/rs/>).

INFLUENCE OF PRINTING SPEED AND RADIATION DOSE ON THE CURING OF UV INKS AND VARNISHES

Bohumil Jašůrek , Jan Vališ , Michaela Hozmanová
University of Pardubice, Faculty of Chemical Technology,
Department of Graphic Arts and Photophysics, Pardubice, Czech Republic

Abstract: *This work is focused on curing of UV curable printing inks and varnishes and evaluation of the conversion degree after printing with various printing speeds (between 4 and 10 thousands of sheets per hour) and settings of curing units. Five sets of process offset printing inks (SunCure® FLM – Sun Chemical, Suncure® Starlux – Sun Chemical, UltraCURA® Sens – Flint Group, NewV Pack MGA® Premium – Huber Group, Sicura Litho Nutriplast – Siegwirk) and one UV curable varnish (ExCure All Round EXC90006 – Toyo Ink) were tested. Printing inks and varnish were printed on KBA Rapida 142 6+L and curing of inks/varnish was examined by Fourier transform infrared spectroscopy. The results show the importance of optimization of both the printing speed and the settings of curing units to achieve appropriate curing connected with good adhesion, no surface tackiness and maximum elimination of migrating components from cured inks that is important mainly in food packaging.*

Key words: UV ink, UV varnish, curing, polymerization, infrared spectroscopy

1. INTRODUCTION

Photoinitiated polymerization of multifunctional monomers and oligomers is one of the most efficient methods to produce highly cross-linked polymer networks. It has found a large number of commercial applications (printing inks and varnishes, coatings, adhesives, etc.), because of its unique advantages (rapid curing time, enhanced material properties, elimination of volatile organic compounds, etc.).

To ensure quality printing and trouble-free subsequent processing of the order is necessary to ensure sufficient ink/varnish drying. Insufficient drying of UV curable inks/varnishes may result in blocking, ink set-off, lower ink/varnish adhesion to printed substrate and increased migration of the printing ink/varnish components. Migration of ink components is very important mainly in food packaging and products intended for children. With this are connected regulations that need to be followed. Between most important belongs Regulation (EC) No 1935/2004 on materials and articles intended to come into contact with food, Regulation (EC) No 2023/2006 about Good Manufacturing Practice for the production of food contact articles, Directive 2007/42/EC relating to materials and articles made of regenerated cellulose, Regulation (EU) No 10/2011 on plastic materials and articles intended to come into contact with food and Swiss ordinance on materials and articles in contact with food (SR 817.023.21) (EUPIA, 2018; Grabitz, 2017). In addition to this, some big companies have their own regulations, for example Nestlé (Nestlé Guidance Note on Packaging Inks) (Nestlé, 2016).

Drying of UV curable printing inks and varnishes is influenced by many factors. Between most important belongs composition of inks/varnishes (type and amount of photoinitiators, monomers, oligomers, pigments, additives), type of UV source (mostly medium pressure mercury lamp or UV LED), UV dose connected with printing speed and intensity of irradiation, presence of inhibitors (oxygen for free radical polymerization and basic substances or humidity for cationic polymerization), thickness of printed ink/varnish, printed substrate etc.

To evaluate the drying of UV curable inks, printers often use simple methods that may not provide the correct information about ink drying. Methods such as Tape test, friction of printing with solvent-impregnated cloth, observing of surface tackiness by touch are used. One of the sophisticated methods for evaluation of drying of UV curable inks is infrared spectroscopy. This method gives information on chemical groups containing polar bonds, or bonds whose dipole moment changes during vibration and from changes of infrared spectra (before and after curing) can be evaluated degree of conversion of cured inks (Škola et al, 2016).

This work is focused on curing of five sets of process offset printing inks (UV curable) and one UV varnish and evaluation of the conversion degree after printing with various printing speeds and settings of curing units. For evaluation of conversion degree, the Fourier transform infrared (FTIR) spectroscopy was used.

2. MATERIALS AND METHODS

This work investigates curing of five sets of process UV offset printing inks from various producers and one UV varnish from TOYO Ink. Tested inks and varnish are summarized in Table 1. One-side coated cardboard Serviliner GD2 (250 g/m²) was used as printed substrate. All inks and varnish were printed on printing machine KBA Rapida 142 6+L equipped with 6 printing units and one varnish unit. Maximum speed of this machine is 15 000 sheets/hour with maximum format 1 020×1 420 mm. The printing speed was changed from 4 000 to 10 000 sheets/hour (in first step for all inks and varnish from 4 000 to 7 000 sheet/hour and in second step for well-cured inks at 7 000 sheets/hour also at higher printing speeds to 10 000 sheets/hour. The power of curing units (equipped with medium pressure mercury lamps) was changed from 70 to 100 % (step 10 %). On Figure 1 is shown printed sheet (Suncure® Starluxe).

Table 1: Tested inks and varnish

Producer / ink	Type of ink
Fling Group / UltraCURA® Sens	Process Cyan VW17-508S
	Process Magenta VW17-308S
	Process Yellow VW17-108S
	Process Black VW37-908S
Huber Group / NewV pack MGA® premium	Process Cyan 43UG 5000M
	Process magenta 42UG 5000M
	Process Yellow 41UG 5000M
	Process Black 49UG 5000M
Siegwerk / Sicura Litho Nutriplast	Process Cyan 70-111140-3
	Process Magenta 70-801280-2
	Process Yellow 70-300629-6,
	Process Black 70-900479-0
Sun Chemical / SunCure® FLM	Process Cyan FLM25
	Process Magenta FLM27
	Process Yellow FLM26
	Process Black FLM46
Sun Chemical / Suncure® Starluxe	Process Cyan USL25
	Process MagentaUSL 27
	Process Yellow USL26
	Process Black USL46
Toyo Ink / ExCure all round EXC90006	Varnish



Figure 1: Printed sheet (Sun Chemical/Suncure® Starluxe, 7 000 sheets/hour, 80 %)

Printed inks (dot area 100 %) were measured by FTIR spectrometer (Avatar 320, Thermo Scientific, USA) with ATR (Attenuated Total Reflectance) attachment using diamond crystal in range from 4 000 to 400 cm^{-1} at room temperature. Infrared spectrum of every ink at every printing speed was measured four times. Furthermore, the infrared spectrum of uncured inks and varnish was measured. All tested inks and varnish polymerize by free radical polymerization. This type of inks/varnishes is based on acrylate chemistry. The degree of conversion (DC, Equation 1) was evaluated from the decrease of the absorption band (maximum at 809 cm^{-1}) area belonging to the acrylate double bond. Carbonyl group (1 730 cm^{-1}) as internal standard was chosen (Colthup et al, 1990).

$$\text{DC} = 1 - (A_t/A_0) \times 100 \quad (1)$$

where A_0 is the ratio of areas of acrylate double bond and internal standard uncured ink/varnish and A_t is the ratio of areas of acrylate double bond and internal standard after printing. Figure 2 shows decrease of absorption band of acrylate double bond after curing with two printing speed and different setting of curing unit compared to uncured ink for cyan and magenta (Huber Group, NewV pack MGA® premium). All cyan, yellow and black inks have very similar shape and neighbourhood of absorption band with maximum 809 cm^{-1} . Acrylate double bond of magenta inks (from all producers) and UV varnish partially overlapped with another band. From this reason, area of absorption band (809 cm^{-1}) of magenta inks and UV varnish was evaluated by deconvolution of overlapped bands too.

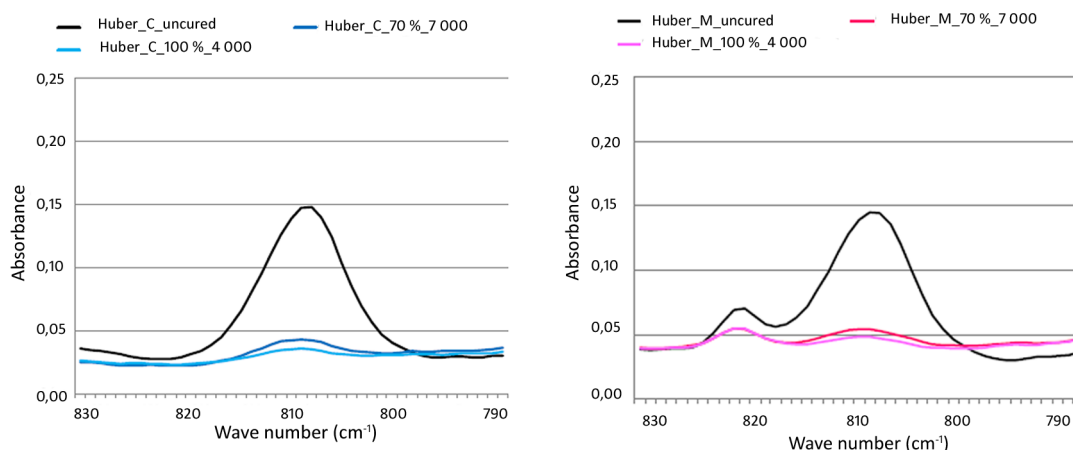


Figure 2: Decrease of acrylate double bond band (max. 809 cm^{-1}) during curing (Huber Group, NewV pack MGA® premium). Printing speed 4 000 and 7 000 sheets/hour, setting of curing unit 70 and 100 %. Cyan – left figure, Magenta – right figure.

3. RESULTS AND DISCUSSION

Evaluated DC of UV varnish is shown in Figure 3. It is apparent that differences between two ways of evaluation (with and without deconvolution) are minimal (mostly in range of standard deviation).

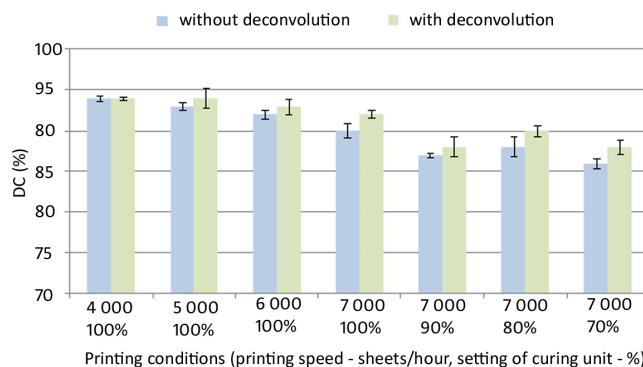


Figure 3: DC of UV varnish (ExCure all round EXC90006 from TOYO Ink) with different printing conditions

For printing speeds between 4 000 and 6 000 sheets/hour (curing unit set on 100%) were reached similar DC and UV varnish was well cured. DC reached with printing speed 7 000 and different setting of curing unit were lower and varnish is not fully cured as with lower printing speeds.

Figures 4–8 shown DC of all tested inks. Inks from Flint Group (UltraCURA® Sens) are on Figure 4. It is apparent that all process inks (UltraCURA® Sens) are well cured at speeds 4 000 and 5 000 sheets/hour. Cyan, yellow and black inks are also well cured at 6 000 and 7 000 sheets/hour but not magenta inks, where DC decrease and magenta ink is not sufficiently cured at this speeds.

For inks from Huber Group (NewV pack MGA® premium) is result similar (Figure 5). All process inks are well cured at printing speeds up to 5 000 sheets/hour. Yellow ink is well cured to 6 000 sheets/hour and magenta with black inks to 7 000 sheets/hour (setting of curing unit 100 %).

Inks from Siegwark (Sicura Litho Nutriplast) were all well cured to 7 000 sheets/hour (with setting of curing units 100 %). When the setting of curing units was lower (at printing speed 7 000 sheets/hour), the DC decrease and inks cannot be well cured (Figure 6).

Figure 7 shown DC of inks SunCure® FLM from Sun Chemical. All process inks are well cured to 8 000 sheets/hour. Cyan and magenta till 10 000 and black till 9 000 sheets/hour. Second type of inks from Sun Chemical (Suncure® Starlux) are well cured till 7 000 sheets/hour (Figure 8). Problematic is yellow ink (for both sets of Sun Chemical inks), where the decrease in DC is most significant).

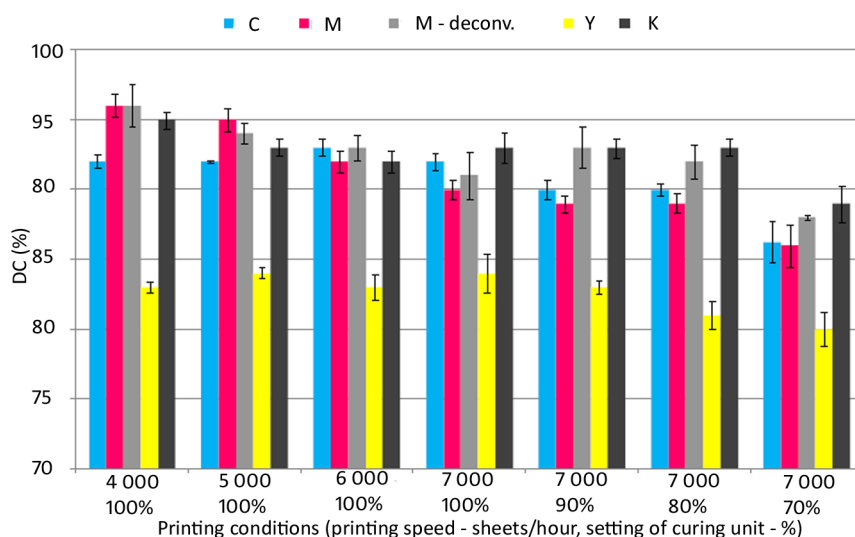


Figure 4: DC of inks UltraCURA® Sens (Flint Group) with different printing conditions

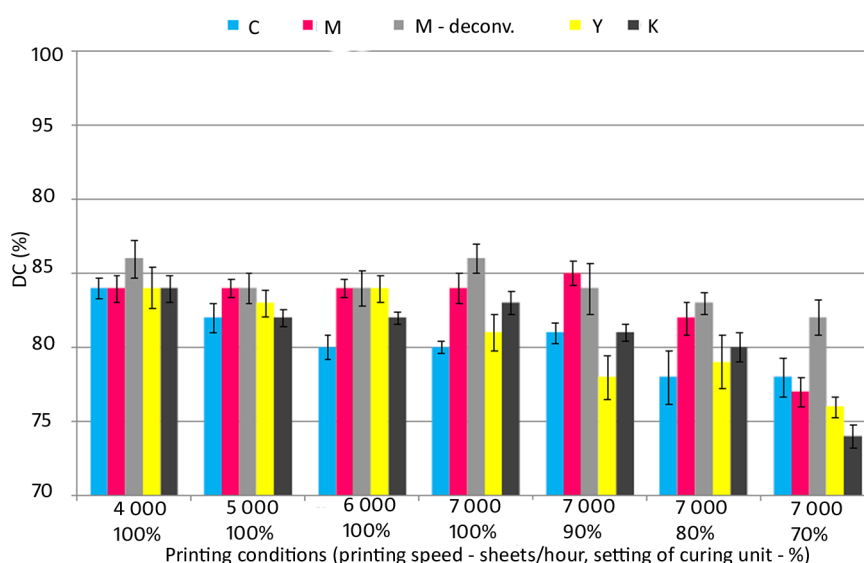


Figure 5: DC of inks NewV pack MGA® premium (Huber Group) with different printing conditions

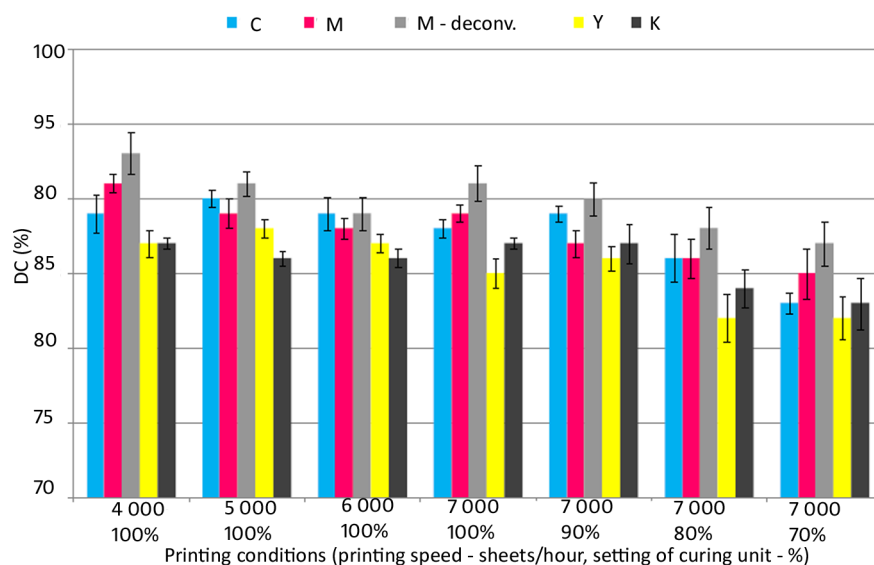


Figure 6: DC of inks Sicura Litho Nutriplast (Siegwerk) with different printing conditions

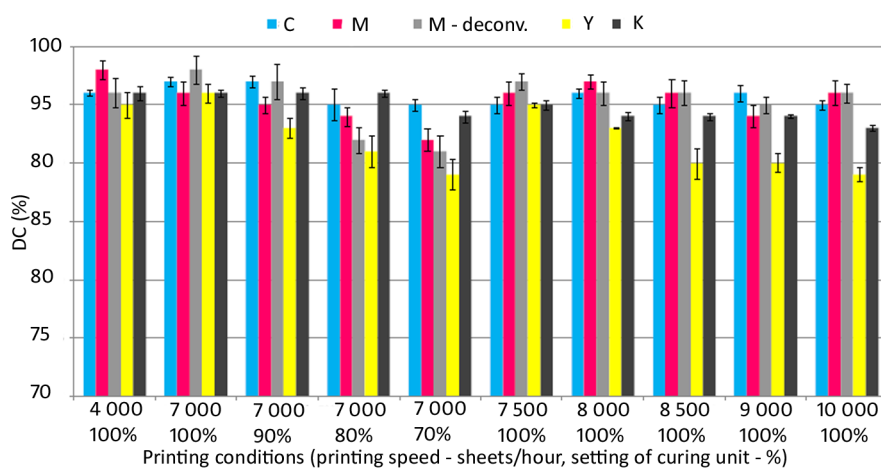


Figure 7: DC of inks SunCure® FLM (Sun Chemical) with different printing conditions

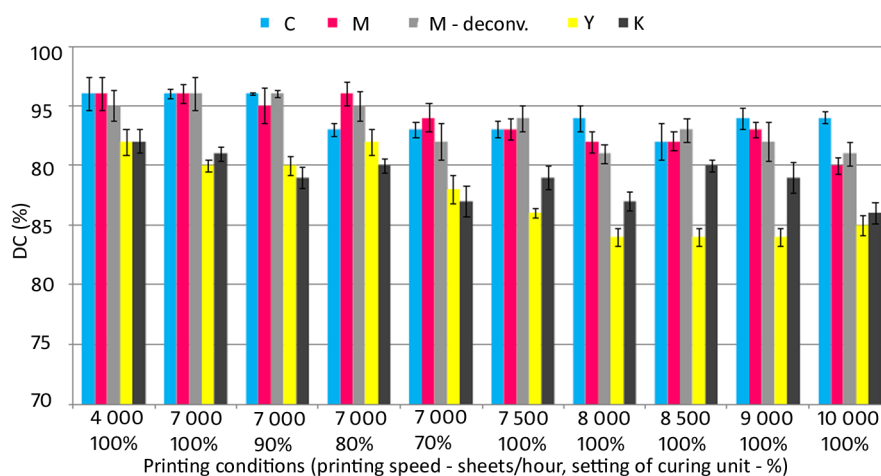


Figure 8: DC of inks Suncure® Starlux (Sun Chemical) with different printing conditions

CON-TROL-CURE® UV Fastcheck™ Strips Key Chart (Figure 9) was used for evaluation of UV dose at different printing speeds. Control strips were stick on printing substrate and with same conditions exposed to UV radiation in printing machine. From colour changes was evaluated UV dose (Table 2).

Table 2: UV doses for different printing speeds evaluated with CON-TROL-CURE® UV Fastcheck™ Strips Key Chart

Printing speed (sheets/hour)	UV dose (mJ/cm ²)
4 000–5 000	150
6 000–7 000	100
8 000–10 000	75

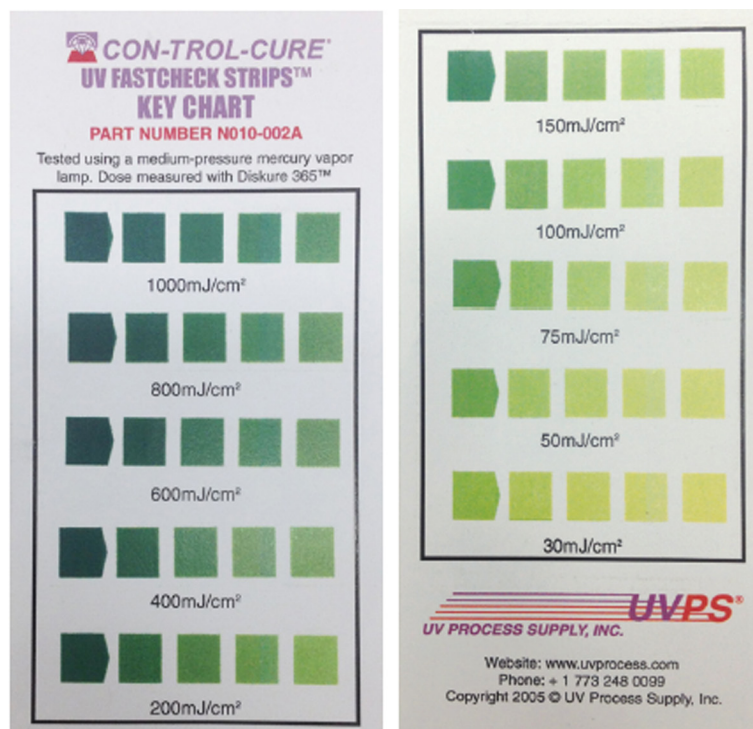


Figure 9: CON-TROL-CURE® UV Fastcheck™ Strips Key Chart (UV Process Supply, Inc.) for evaluation of UV dose

5. CONCLUSION

Important parameter that has to be controlled during print with UV curable inks is their adequate curing. When the curing of UV inks is insufficient, it can result for example in lower ink adhesion, blocking and increased migration of ink components from the cured film. Simple methods used in printing companies to evaluate ink curing (for example Tape test) cannot provide true information. In this work was curing of UV inks and varnish evaluated by FTIR spectroscopy. Results show differences in curing of inks from various producers (Flint Group, Huber group, Siegwerk and Sun Chemical), where all process inks (CMYK) were well cured in range of printing speeds from 5 000 to 8 000 sheets/hour. The best result was reached with inks from Sun Chemical (SunCure® FLM).

6. REFERENCES




- [1] Colthup, N. B., Daly, L. H., Wiberley, S. E.: "Introduction to Infrared and Raman Spectroscopy", 3rd ed, (Academic Press, Massachusetts, 1990.).
- [2] EuPIA: "Guideline on Printing Inks applied to the non-food contact surface of food packaging materials and articles", Eupia, URL: http://www.eupia.org/uploads/tx_edm/111114_EuPIA_Guideline_for_Food_Packaging_Inks_-_November_2011_corr_July_2012_under_review.pdf (last request: 2018-09-18).
- [3] Grabitz, A.: "Printing ink legal assessment after the decline of German printing ink ordinance", RadTech Europe Conference 2017, (Rad Tech, Prague, Czech Republic, 2017), 17-19.

- [4] Nestlé, Nestlé Guidance Note on Packaging Inks, Argus-analysen, URL: <http://www.argus-analysen.de/assets/plugindata/poola/nestle-guidance-note-on-packaging-inks-2016-08.pdf> (last request: 2018-09-18).
- [5] Škola, O., Jašůrek, B., Veselý, D., Němec, P.: “Mechanical properties of polymer layers fabricated via hybrid free radical-cationic polymerization of acrylate, epoxide, and oxetane binders”, *Progress in Organic Coatings*, 101, 279–287, 2016. doi: 10.1016/J.PORGCOAT.2016.08.020



© 2018 Authors. Published by the University of Novi Sad, Faculty of Technical Sciences, Department of Graphic Engineering and Design. This article is an open access article distributed under the terms and conditions of the Creative Commons Attribution license 3.0 Serbia (<http://creativecommons.org/licenses/by/3.0/rs/>).

RUBBING FASTNESS OF GREEN INK PRINTED ON TEXTILE USING SCREEN PRINTING TRANSFER TECHNIQUE

Ana Lilić , Nemanja Kašiković , Nada Miketić 
University of Novi Sad, Faculty of Technical Sciences,
Department of Graphic Engineering and Design, Novi Sad, Serbia

Abstract: *Printing on textile surfaces is possible using either direct or transfer method. The transfer method is a complex technique in which, the first, design is transferred to a flexible substrate via digital or screen printing, after which the transfer to textiles is carried out. To apply the colour to the material, heat pressure is used. Different environmental influences can affect such printed material. Some of them are rubbing, heat, UV radiation, moisture, washing, etc. In this study, an analysis of the impact that rubbing has on the print will be done. Rubbing treatment of the prints was done according to ISO 105-X12 standard. Colour changes of the printed textile materials to dry rubbing treatment were characterized by the spectrophotometric measurements. In the given analysis, two different types of cotton material were used as a printing medium. Both materials are 100% cotton, however, they differ in the weight of the fabric. The first material has a weight of 150 g/m² and the other has 190 g/m².*

Key words: rubbing, transfer printing, textile, colour difference

1. INTRODUCTION

Textile printing can be best described as the art and science of decorating a fabric with a colourful pattern or design (Tippet, 2005). The saga of digitally printing and dyeing of fabrics, yarns and garments involves a past of a few decades, a dynamic present and likely a bright future. This introduction accounts for the origins and evolution of textile printing to digital solutions. It identifies some of the many creators and pioneers of these technologies and assesses their impact on the textile printing industry (Cahil, 2006). Printing on textile surfaces is possible using either direct or transfer method. Transfer printing is the term used to describe textile and related printing processes in which the design is first printed on to a flexible non-textile substrate and later transferred by a separate process to a textile. Transfer printing process could be divided into: sublimation transfer, melt transfer, film release and wet transfer. The reasons why this technique is still popular are numerous. The production of short runs and repeated orders is much easier to produce, sometimes it is easier to produce complex design on the paper than on the textile, designs could be printed on cheap substrate before the transfer to the more expensive textile materials, and sometimes this is the only way to make certain special effects on garments or garment panels. The designs that are printed on paper, decrease both storage space and costs, as relatively cheap equipment is needed (printing machines, irons, etc.). Later, the design may be applied to the textiles with relatively low skill input and low reject rates (Rattee, 2003). The clothes are usually exposed to external influences such as washing, heat, abrasion, UV light, etc. (Kašiković et al, 2017). The resistance of the material to rubbing will be analysed in this article. Samples will be exposed to the rubbing procedure and afterwards will be measured the quality of the print and compared with the original. As a result, the effect of rubbing will be shown and whether it affects the visual quality of the print.

2. MATERIALS AND METHODS

In the given analysis, two different types of cotton material were used as a printing medium. Properties of these materials are shown in Table 1.

An appropriate test map consisting of three fields of size 12x5 cm was prepared for study. Heat transfer papers (150 g/m²) were printed using screen printing technique (M & R Sportsman E Series, printing speed was 15 cm/sec, the hardness of the squeegee 80° Shore Type A, the printing pressure 275.8×10^3 Pa and the snap-off distance 4 mm, 55 and 90 threads/cm). The ink used for printing the transfer paper is Sericol Texopaque Classic OP Plastisol. Afterwards, from the transfer paper, the test card was transferred to the textile material by heat pressure for 10 seconds. Three different temperatures were used for this process (160, 170 and 180 °C).

Electronic crockmeter Testex textile instrument LTD. TF411 (rubbing head diameter 16 mm, vertical pressure 9 N, rubbing stroke 104 mm, according to the ISO 105x12/D02 standard) was used as an instrument for analysis.

Spectrophotometric measurements and visual control of printed samples were performed after the printing process and after exposure to the rubbing effect, the samples being subjected to rubbing at 500, 1000 and 1500 times. Colorimetric measurements were made using the HP 200 measuring device (D65 lighting, 2° standard observer, d/8 measuring geometry).

Colour differences between treated and untreated samples were calculated using ΔE_{94} formula. Colour difference value can be translated to human perception reference as $0 < \Delta E < 1$ - the difference cannot be noticed; $1 < \Delta E < 2$ - small colour difference, visible to "trained" eye; $2 < \Delta E < 3,5$ - Medium colour difference, visible to "untrained" eye; $3,5 < \Delta E < 5$ - Obvious colour difference; $\Delta E > 5$ - Massive colour difference (Novaković, 2008).

Untreated and treated samples were scanned using a Canon CanoScan 5600F scanner that was set to 600 spi resolution without auto correction function.

Table 1: Properties of the used textile materials

Tests	Type of weaves	Material composition (%)	Fabric weight	Thread count (cm ⁻¹)	
				Vertical	Horizontal
Material 1	Single	Cotton 100%	150	14	19
Material 2	Single	Cotton 100%	190	15	16
Method			ISO 1833	ISO 3801	ISO 7211-2

3. RESULTS AND DISCUSSION

In Figures 1 and 2 are presented values of the colour difference between the samples immediately after printing and after rubbing procedure which occurred 500, 1000 and 1500 times.

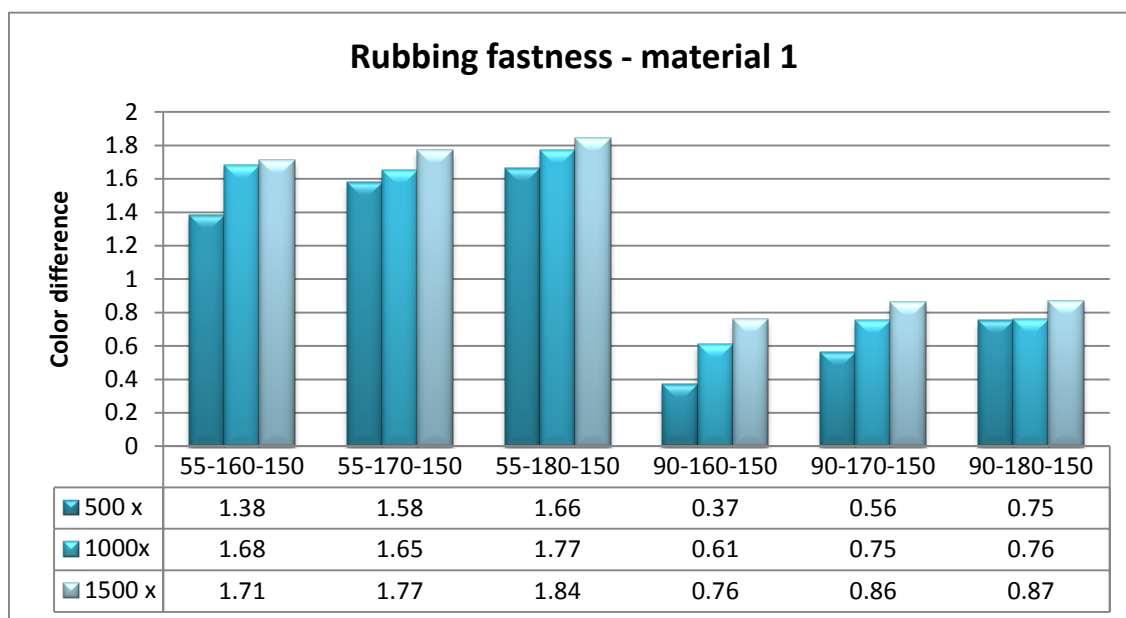


Figure 1: Colour difference between the samples immediately after printing and after rubbing procedure – material 1 (Remark: numbers 55 and 90 represent threads/centimetre, number 160, 170 and 180 represent temperature in °C; number 150 represent fabric weight for material 1)

From the given analysis, it can be seen that a change in colour has occurred with the increase in the rubbing repetition. Likewise, the rise in temperature is increasing in colour difference value. Results do not exceed the value of 2, which means that difference can be noticed only by “trained” eye. This means that although the device detects changes, the average human see samples as identical. The biggest change in ΔE value can be observed in the case where the temperature is highest and number of threads per centimetre is 55. The colour difference value in this example is 1,84.

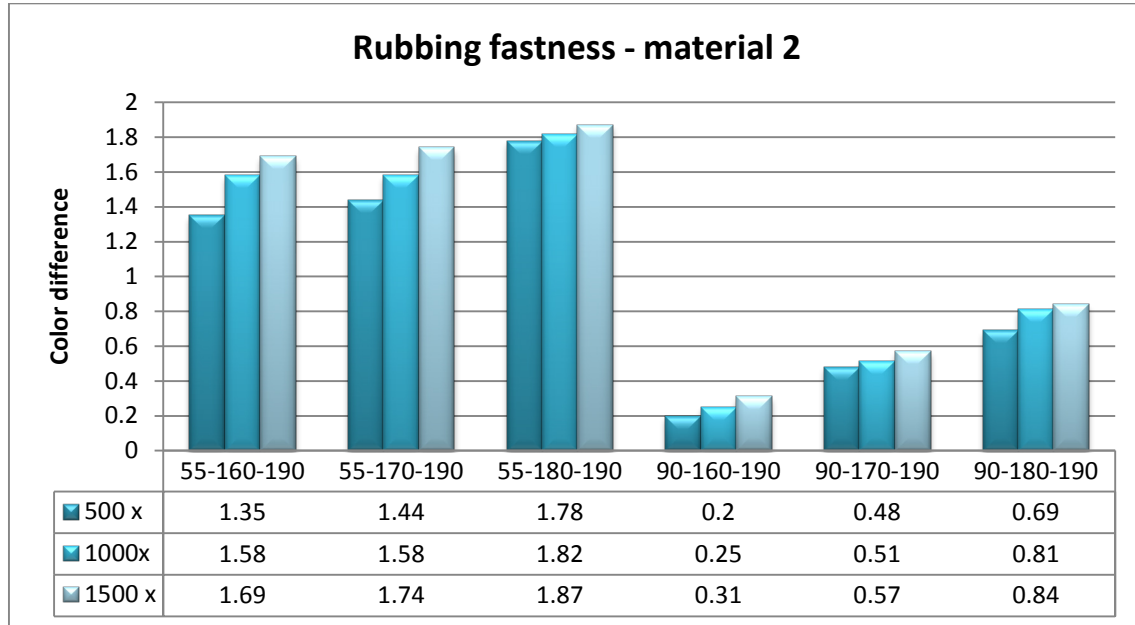


Figure 2: Colour difference between the samples immediately after printing and after rubbing procedure – material 2
(Remark: numbers 55 and 90 represent threads/centimetre, number 160, 170 and 180 represent temperature in °C; number 190 represent fabric weight for material 2)

By comparing these materials, it has been established that the material 2 provides more permanent proof. This result is consequence of the higher fabric weight. Higher fabric weight can cause the colour to seep deeper into the structure, leaving a smaller layer of paint on the surface that can be damaged. Another characteristic that affects the quality of the print is thread count of screen printing mesh. Prints created with greater thread count screen shows better rubbing fastness as a result of lower amount of ink deposited. The thinner the colour layer is, the less pigments can be removed, resulting in a lower value of colour difference between samples before and after rubbing mechanism. Likewise, lower temperature when transferring paper to material results in better durability of colour.

Figures 3, 4, 5 and 6 show scanned samples using a Canon CanoScan 5600F scanner after rubbing procedure. First samples shown in each group are original samples scanner right after printing process.

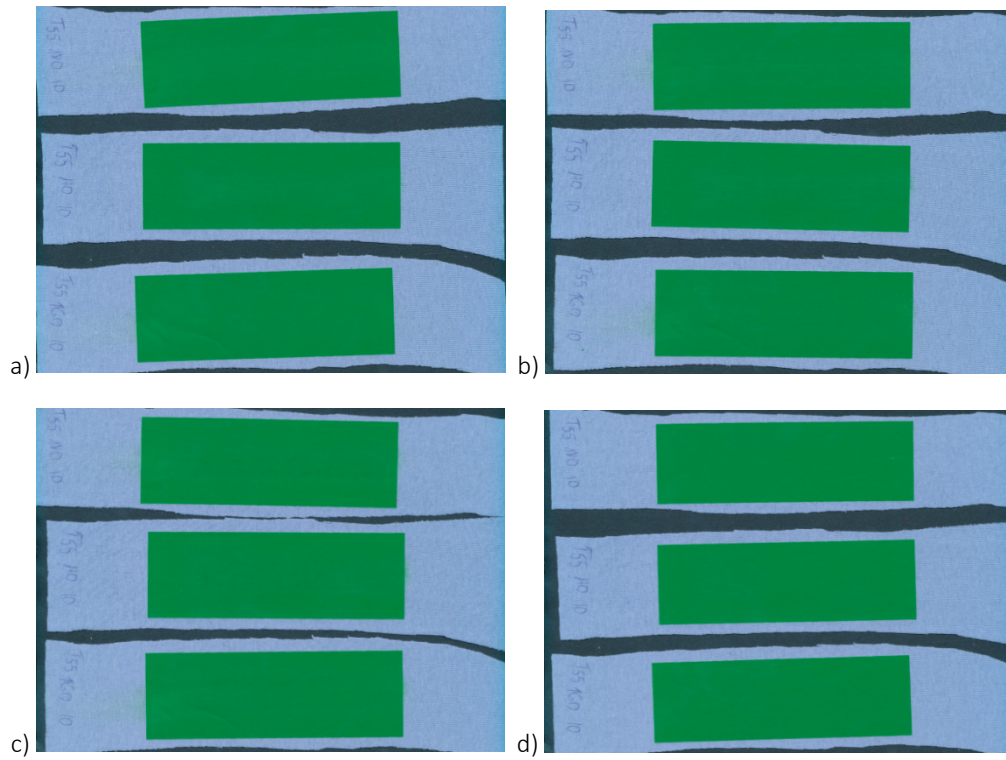


Figure 3 (part 2): Scanned samples (55 thread/cm, 160, 170 and 180°C) after printing process and rubbing treatment – material 1: a) after printing process, b) after 500 x rubbing repetitions, c) after 1000 x rubbing repetitions, d) after 1500 x rubbing repetitions

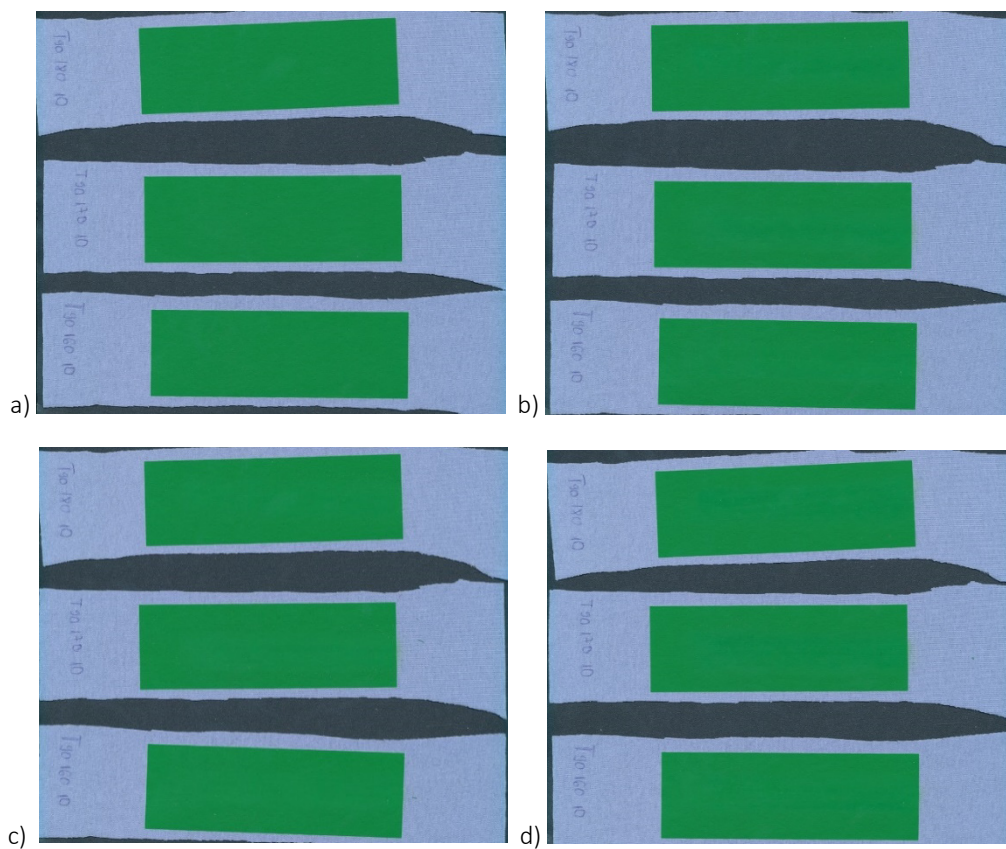


Figure 4: Scanned samples(90 thread/cm, 160, 170 and 180°C) after printing process and rubbing treatment – material 1: a) after printing process, b) after 500 x rubbing repetitions, c) after 1000 x rubbing repetitions, d) after 1500 x rubbing repetitions

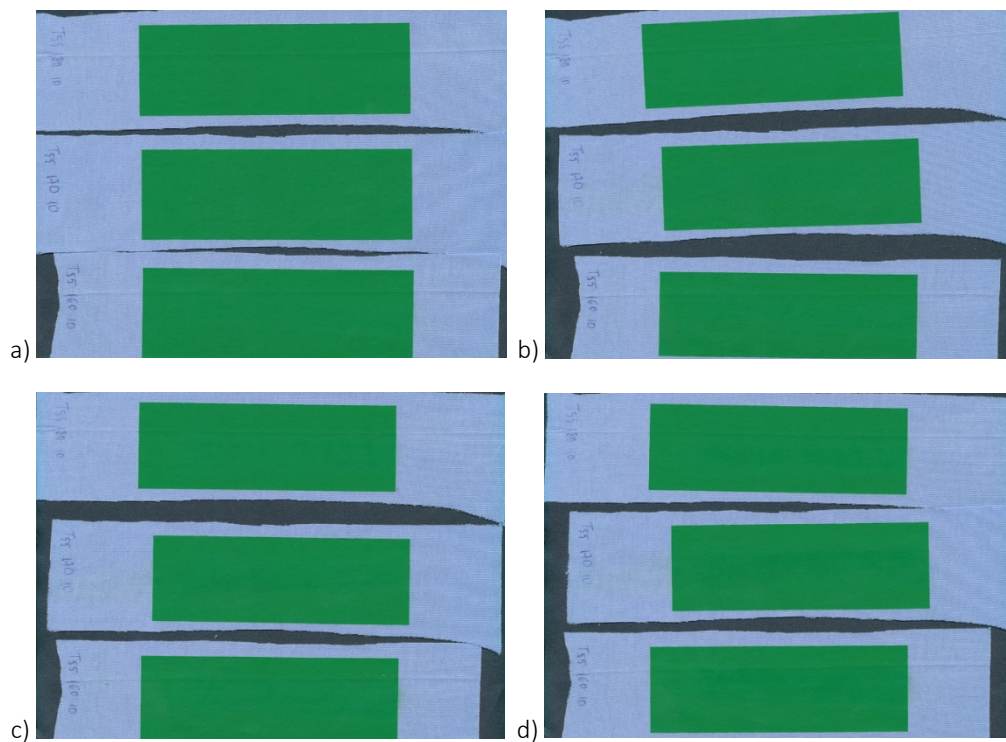


Figure 5: Scanned samples (55 thread/cm, 160, 170 and 180°C) after printing process and rubbing treatment – material 2: a) after printing process, b) after 500 x rubbing repetitions, c) after 1000 x rubbing repetitions, d) after 1500 x rubbing repetitions

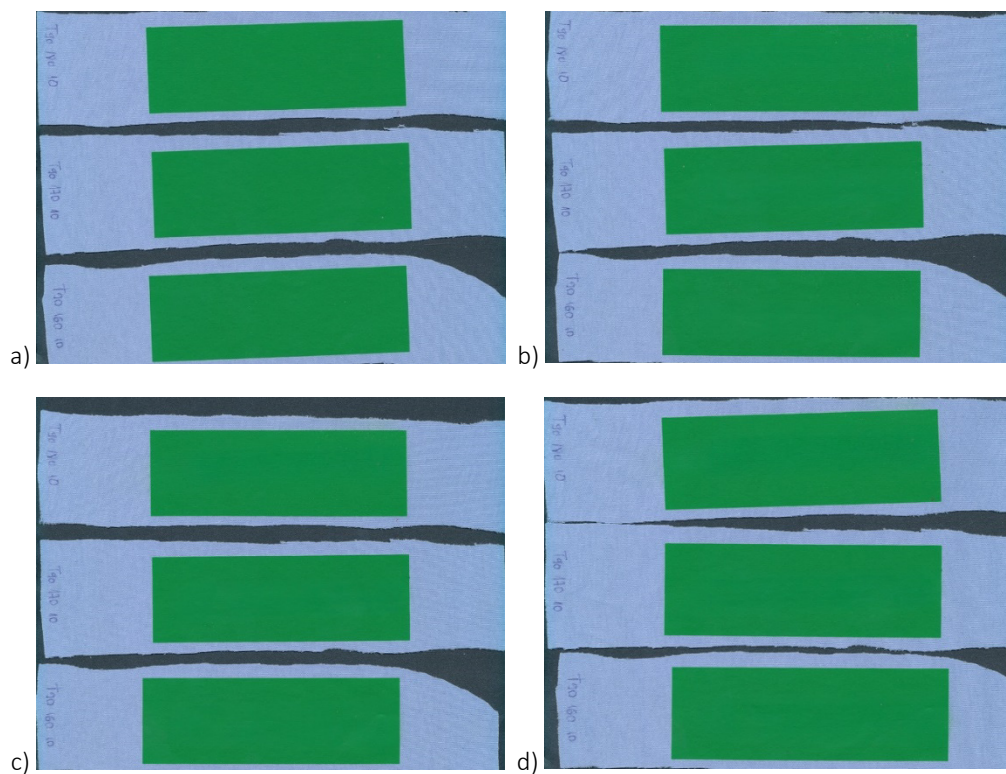


Figure 6: Scanned samples (90 thread/cm, 160, 170 and 180°C) after printing process and rubbing treatment – material 2: a) after printing process, b) after 500 x rubbing repetitions, c) after 1000 x rubbing repetitions, d) after 1500 x rubbing repetitions

Although measurements were made on two different materials, as well as different screen thread, it can be concluded that there are no visible changes in samples. If the rubbing continues, the colour difference will reach the level at which the eye will notice the difference. However, this study shows that the balance of various factors such as material properties, screen thread count and temperature in transfer process can sustain the quality of print.

4. CONCLUSIONS

Transfer printing is highly accepted technique on the market. Some of the advantages are economical aspect such as low cost transfer paper, inexpensive equipment and also fast response to sales demand. This analysis was performed to examine the stability of the prints produced by transfer screen printing in case of rubbing. Although the results showed that there was a difference between the samples immediately after printing and after rubbing procedure, the quality of the prints remained constant. Colour difference values will be higher but those values will not be high enough to cause significant visible damage.

5. ACKNOWLEDGMENTS

This work was supported by the Serbian Ministry of Science and Technological Development, Grant No.:35027 "The development of software model for improvement of knowledge and production in graphic arts industry".

6. REFERENCES

- [1] Cahill, V.: "Digital printing of textiles", 1st ed, (Woodhead Publishing Limited, Abington England, 2006).
- [2] Kašiković N., Stančić M., Spiridonov I., Novaković D., Milošević R., Grujić D., Ružičić B.: "The effect of washing temperature and number of washing cycles on the quality of screen printed textiles materials", Bulgarian Chemical Communications 49, 130-139, 2017.
- [3] Novaković D., Karlović I., Pavlović Ž., Pešterac Č.: "Reprodukciona tehnika- priručnik za vežbe", (Fakultet tehničkih nauka, Novi Sad, 2008).
- [4] Rattee I. D.: "Transfer printing in textile printing", In: Miles, L.W.C. (ed.) Textile Printing, 2003.
- [5] Tippet, B. G.: "The evolution and progression of digital textile printing", URL <http://brookstippett.com/docs/Print2002-BGT.pdf> (last request: 2018-5-22).



© 2018 Authors. Published by the University of Novi Sad, Faculty of Technical Sciences, Department of Graphic Engineering and Design. This article is an open access article distributed under the terms and conditions of the Creative Commons Attribution license 3.0 Serbia (<http://creativecommons.org/licenses/by/3.0/rs/>).

DETERMINING AND SELECTING SCREEN PRINTING FORM PARAMETERS FOR PRINTING ON PAPER AND TEXTILE

Rozália Szentgyörgyvölgyi¹ , Erszébet Novotny² , Milán Weimert³ 

¹ Óbuda University, Sándor Rejtő Faculty of Light Industry and
Environmental Protection Engineering, Budapest, Hungary

² ANY Security Printing Company, Budapest, Hungary

³ Stencil Consult Bt, Budapest, Hungary

Abstract: The technology of screen printing is a chain of work processes which include many variants. Of all the parameters influencing the technology most occur due to the presence of screen mesh in the process. Reproduction ability doesn't simply require adherence to the technological steps but also needs a continuous creative and flexible approach and comprehensive knowledge of the entire procedure. Before preparing the printing stencil, serious planning is required; it needs to be determined during this process what stencil is needed to realize the expected quality of the print.

The goal of the examinations is to determine and choose the parameters of screen printing forms for creating the best possible quality screen printing stencils to be used with paper and textile printing, and the improvement of the quality of the screen preparation process for direct screen printing on paper and textile substrates. From the point of view of the quality of the print, the critical issues of the technology of stencil preparation is the planned thickness of the stencil, reaching the necessary Rz values, and the lighting conditions of accurate printing element reproduction. We have made prints with printing forms chosen by the parameters examined and analysed the quality of prints.

Key words: screen printing form, Rz, EOM, screen printing on paper and textile

1. INTRODUCTION

The technology of screen printing presents many challenges for the user. The most conflicting factor in the challenges of technology is probably the presence of screen mesh itself in the technology. While fulfilling its task, it often results in ragged edges of prints, blocks the flow of ink, distorts light like an optic strand, makes precise screen lighting difficult, and also might create problems with keeping the accuracy of the colour line up, since the forces affecting it during screen printing might change due to pressure and possible chemical effects of the chemical substances used. All of these can be kept under control with precise and astute planning and preparation, with the knowledge of the proper techniques, and by using the right tools and materials. The wide selection of media available also presents a challenge. An even tension of the screen mesh is an important parameter, and it must be set to be the same quality at a later time as it was before. In case of quality deviations, many problems might occur indirectly from screen tension, such as colour line up, colour correctness and size keeping. The final quality of the stencil is also affected by the continuously changing, wearing coating trough edges, and is also might affect the final result. When lighting the stencil, a weakening light source can affect the useful life of the stencil during printing, under or over tanning can harm the resolution of the print, or might push the distribution indicators of a properly set ink system to an unwanted direction. The thickness of the under tanned stencil might change due to the not polymerized and washed out developing parts, so we are once again facing a different print thickness and possibly shade of colour. In case of industrial screen printing, not only the colour correctness of the print, but also the expected resistance, the tensile strength and thermal expansion are also determined beforehand, so when preparing the stencil, we must be able to determine exactly what materials need to be used to prepare the printing stencil. The choice of textile provides the approximate thickness of the stencil, and the available resolution. The tension of the textile can be adjusted to the printing press or manual printing. The useful life of the printed image and the stencil depend on the correct selection of emulsion. It depends on the coating how thick the print is going to be, and how even the prints produced are going to be. The printing elements are created at exposure, and these must be in the correct ratio with the film positive, thus ensuring the right reproduction of the print. The developing is responsible for the clean print image (Leicester Print Workshop, 2018; Hurtz GmbH, 2018).

The goal of the examinations is to determine and choose the parameters of screen printing forms for creating the best possible quality screen printing media to be used with paper and textile printing.

2. METHODS

The elements of the screen printing form (stencil) generally examined are the thickness of the stencil, the EOM (Emulsion Over Mesh), the Rz value of the stencil (evenness of the surface of pressing side), the quality of printing edges and the quality of printing duct. Knowing these parameters helps deduce the quality of the prints, its possible faults and expected reproduction capability. The expected ink coat thickness of the print is a necessary parameter amongst the pre-determined characteristics of the print. In case of screen technology, it can be varied according to the requirements of the customer, and by choosing the thickness of the stencil within the framework of possibilities provided by the technology. In case of optimal stencil thickness it is approximately the same on the entire surface of the print, but in case of printing with a stencil which is too thick, the middle of the print is going to be thinner. Emulsion Over Mesh (EOM) shows the thickness of the stencil in μm , not counting the thickness of the textile. The value represents how thick of an emulsion coat was created during coating exceeding the thickness of the textile. The effects of a too thick or a too thin EOM value can be detected on the prints as typical faults. The Rz value of the stencil represents surface roughness. This value is provided in μm , according to the following principles: between 3 and 12 μm the Rz value is considered good. Below 3 μm and above 12 μm the value is not suitable. The higher the value, the more rough is the surface of the stencil, and it has a direct effect on the quality of the print. In case of a low Rz value, ink is pressed between the print and the printing stencil at the indentations on the edges of the squeegees, and the image will have blurry contours, and will not represent clearly the image to be reproduced (Figure 1). It greatly harms the quality of the print in case of both raster prints and half-tone prints (Peyskens, 2003; Sefar Inc., 1999).

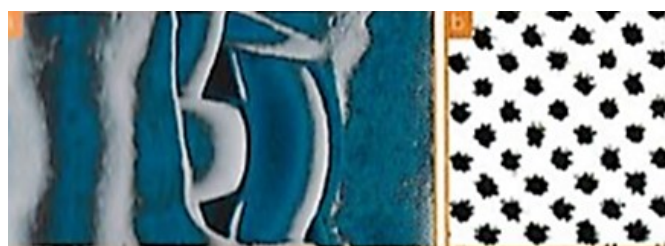


Figure 1: The effect of high Rz value on the quality of prints (Peyskens, 2003)

The determination of the quality of printing edges is done by optical examination, analysing the edges of the stencil. In case of adequate quality, the structure of the textile due to its weaving does not affect the printing edges of the stencil, and the emulsion follows the lines of the printing elements independent of the textile. The evenness of the emulsion at the edges of printing elements is called “mesh bridging”. In case of optimal lighting, the points, lines and print parts of the print match the parts on the film positive exactly. In case of overexposed stencils, the size of the printing elements might differ greatly from the ones on the film positive (Figure 2), and it leads to colour deviation, incorrect spectral, point distortion, and print part loss of the print (Sefar Inc., 1999).

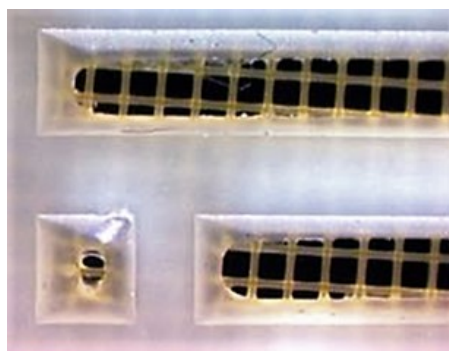


Figure 2: Closure of line in case of overexposure (Ulano, 2018)

Significant influencing factors of print quality are also the openness of the printing duct, and therefore the quality of the squeegees created by the emulsion. In ideal case the printing duct is completely free of obstacles, therefore it does not block the flowing of ink. The squeegees are almost 90° (Figure 3), so the capillary effect can help the ink to move through the stencil optimally (Sefar Inc, 1999).

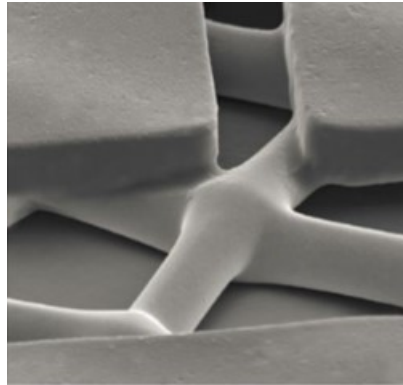


Figure 3: Squeegees of adequate quality (MacDermid Autotype Ltd., 2018)

Of all screen meshes of which screens are made of, we used SEFAR meshes made in Switzerland. These textiles have a quality of PET 1500, reduced elasticity and plasma surface treatment. The textiles are made of high viscosity polyester, have even weaving, are wearing resistant, keep their tension set at screen tensioning, are suitably elastic, and resistant to the inks and chemical substances used during printing, preparation and after treatments. Two different, simply weaved textiles were chosen, based on the planned prints and examinations; both has different weaving density (textile strand / cm). Material SEFAR PET 77.48 Y was used for textile printing, and SEFAR PET 120.34 Y material was used for paper printing (Table 1), taking the ink thickness to be reached and maximum print resolution to be reached into consideration.

Table 1: General identifying parameters of screen meshes

Screen mesh parameter	Screen mesh type	
	77.48 Y	120.34 Y
Colour	Yellow	Yellow
Weaving	1-1	1-1
Tolerance (peace thread)	2	3
Mesh density (thread/cm)	77	120
Mesh-thread diameter (µm)	48	34
Mesh thickness (µm)	80	55
Tolerance (µm)	4	3
Mesh elongation (µm)	77	45
Maximum tension (N/cm ²)	35	28

Layering takes place with a two component Diazo UV Polymer emulsion. Its medium 7000 mPa viscosity and relatively high, 40% dry matter content provides the necessary resistance in case of both water and solvent soluble inks; at the same time adequately thick emulsion coat can be created on both types of textiles.

During the examinations the following materials were used: SEFAR 4 pneumatic Tension Device, SEFAR Tensiocheck, GRÜNIG G COAT 415 Coating Machine, GRÜNIG Coating Tub, BOCHONOW 1100 Horizontal Drying Cabinet, BOCHONOV Developing Box, KIWO ProfiWash Spray Gun, BOCHONOW 2-3-5 kW Exposure Device, BOCHONOW 2000 Manual Screen Printing Table, DEFELSKO DFT Ferro Coating Thickness Gauge, MAHR PocketSurf II Surface Roughness Device, PEAK Microscope.

The screens were layered by manual and an automatic GRÜNIG G Coat 415 machine, with a GRÜNIG coating trough with a 1.0 radius edge. The manual coating is used for preliminary testing, and machine coating is used for preparing the printing stencils, in order to have greater accuracy. The coating speed, the angular offset of the troughs, the pressure exerted by the troughs to the textile, and the emulsion distribution time before starting the pulling, in case of an automatic GrÜNIG coating machine, can be set,

so the desired coating result can be set by parameters. When choosing the edge of the trough, a medium sharp, 1.25 R radius trough was selected. Following the layering of emulsion, the stencils were dried in horizontal position in a BOCHONOW 1100 drying cabinet. Lighting was also taken care of by a BOCHONOW product, traditional, metal halogen bulb. After the exposure, the development of the stencil took place in a BOCHONOW washing and developing tub, completed with a KIWO Profiwash spray gun. Printing was done on a manual screen printing table, BOCHONOW 2000 Model 70/10 “A” vacuum table, with counterweight frame motion.

3. RESULTS AND DISCUSSION

Prior to preparing the printing stencils, examinations were carried out to determine the best technique to have the expected quality of the printing form. The following examinations were carried out:

- Examination regarding the tension keeping of the screen mesh
- Layering examinations
 - Examining the effect of coating trough edge
 - Examining the effect of coating speed
 - Examining the effect of the amount of emulsion
 - Comparing coating techniques
 - Examining the effect of emulsion viscosity
- The effect of screen lighting ratio on the quality of the stencil
- Examination of prints on textile and paper media

3.1 Examination regarding the tension keeping property of the screen mesh

The process was started by tensioning the screen mesh on the screen frame. In order to have adequate tension and tension evenness, three tensioning techniques had been compared previously by preliminary testing; the tensioning values of a screen printing stencil tensioned with 15 minutes and 35 minutes of textile relaxation time, and one with quick, no textile relaxation time. The goal was to reach 21 N/cm² screen tension in case of the 120.34 screen mesh, and 18 N/cm² tension in case of the 77.48 screen mesh used for printing textile. The results of the tension measurements of test screens are in Table 2. The most suitable was the result of screens made with 35 minutes of relaxation time.

Table 2: Tension keeping properties of textiles in case of various tensioning technologies

Tensioning technologies	Tension, N/cm ²					
	77.48 Y screen mesh			120.34 Y		
	Tension at the end	1 hour later	4 hours later	Tension at the end	1 hour later	4 hours later
Quick, no textile relaxation time	20	18	16	22	22	22
15 minutes of textile relaxation time	20	18	17	20	21	21
35 minutes of textile relaxation time	20	19	18	19	20	21

3.2 Layering examinations

In the course of testing, we compared the R_z values and the emulsion thickness (Emulsion Over Mesh) values. Comparison and measurement of the effects of coating troughs with various radius were carried out using SEFAR PET 1500 120.34 Y screen mesh, with 2/2 manual coating and Azocol Z 140 emulsion (Table 3). The examination showed that the greater the radius of the coating trough when coating the greater the EOM value.

Table 3: The effect of various coating troughs on stencil thickness

Radius of the coating trough	Stencil thickness, μm
0,50	8
1,00	10
1,25	12

The effect of various coating speeds on the stencil thickness and their comparison regarding various SEFAR screen meshes with 2/4 layering were simulated with a Grünig G coat 415 automatic screen coating machine. The screen meshes were coated with Azocol Polyplus S emulsion. The results of the examination are shown in Table 4. The examination showed that in case of the same type of textile, the slower is the coating, the thicker is the resulting emulsion coat. Another conclusion of the test is that the less dense is the screen mesh, the greater effect the speed of coating has on the attainable stencil thickness.

Table 4: The effect of various coating speeds on stencil thickness

Screen mesh type	Stencil thickness, μm					
	Coating speed, cm/min					
	600	500	400	300	200	100
77.48	28	30	32	34	35	37
100.40	26	26	26	27	28	31
120.34	24	25	27	26	25	26
140.34	16	16	17	17	18	19

The effect of various emulsion amounts on the stencil thickness with 2/2 layering were simulated with a Grünig G coat 415 automatic screen coating machine. The layering was done with Azocol Polyplus S emulsion (Table 5). The examination showed that the more emulsion is present in the coating trough, the thicker the coat will be when the coating parameters are the same. On the other hand, the larger the exposed area on the textile, the greater is the difference due to the different amount of emulsion.

Table 5: The effect of emulsion amounts on stencil thickness when the coating and emulsion is the same

Screen mesh type	EOM values, μm	
	saturated in 15 mm high	saturated in 5 mm high
120.40	11	10
120.37	21	17
120.32	34	26

The comparison of various coating techniques regarding stencil thickness were simulated with a Grünig G Coat 415 automatic screen coating machine, with Azocol Polyplus S emulsion (Table 6). The result of the examination is that if the emulsion is coated in a greater number of times, the final result will be much thicker.

Table 6: Measured on "wet on wet" coating stencil/the same emulsion, coated in a different way

Screen mesh type	EOM values, μm		
	2/2 coating	2/3 coating	2/4 coating
100.40	7	14	22
120.34	5	10	14
140.34	5	7	10

In order to have the best Rz values, the effect of additional print side coating after the intermediate drying of the stencil was examined on a GRÜNIG G Coat 415 automatic screen coating machine, with Azocol Z 140 emulsion (Table 7). The results of the examination showed that the additional coating resulted in a minimal change of 1 μm in stencil thickness.

Table 7: Effect of additional coating stage on the thickness of stencil/ the same emulsion, coated in a different way

Screen mesh type	EOM values, μm		
	2/2+1 coating	2/3+1 coating	2/4+1 coating
100.40	8	16	23
120.34	6	11	15
140.34	6	8	11

The effect of differences in emulsion viscosity on stencil thickness were examined on a Grünig G Coat 415 automatic screen coating machine, with Azocol Z 140 emulsion. The results in Table 8 showed that due to the density differences in colder emulsion, stencil thickness had a higher value than the values of a similar coating done using emulsion of a higher temperature.

Table 8: The effect of emulsion temperature differences on stencil thickness, coated with the same type of emulsion of different temperature

Screen mesh type	EOM values, μm	
	15°C	21°C
100.40	9	7
120.34	6	5
140.34	5,5	5

Based on the evaluation of the results of manual coating tests, the following parameters were chosen for preparation of screens to be used for the prints:

- 77.48 screen mesh for printing cotton textile
 - 2/2 emulsion coating (2x on printing side, 2x on squeegee side coating)
 - emulsion coating with a coating trough with 1.25 R radius edge
 - fully filled coating trough (to 15 mm height)
 - emulsion temperature 21 C° (temperature of printing room)
 - on a Grünig G Coat 415 automatic coating machine the emulsion layering with coating speed 600 cm/min.
- 120.34 screen mesh for printing paper
 - 2/1 + 1 emulsion coating (2x on printing side, 1x on squeegee side coating, an after intermediate drying 1x coating from printing side)
 - emulsion coating with a coating trough with 1.25 R radius edge
 - fully filled coating trough (to 15 mm height)
 - emulsion temperature 21 C° (temperature of printing room)
 - on a Grünig G Coat 415 automatic coating machine the emulsion layering with coating speed 400 cm/min.

In the course of the examinations, our goal was to reach the desired stencil parameters, and based on our previous experience, it was easily reached with the help of a GRÜNIG G Coat 415 automatic coating machine. The parameters of the coated screens are in Table 9.

Table 9: The parameters of stencils used for final lighting and printing tests

Stencil	Screen mesh parameters					
	Screen mesh	Screen tension, N/cm ²	Coating technology	Stencil thickness, μm	EOM, μm	R _z , μm
Textile printing stencil	SEFAR PET 1500 77.48.Y	21	2/2+1	91	21	7,7
Paper printing stencil	SEFAR PET 1500 120.34.Y	21	2/1+1	57	14	8,6

The screens positioned as layers were dried in a BoOCHONOW 1100 horizontal dryer, on 38 °C temperature and 120 minutes of drying time. The temperature was checked in every 30 minutes using a mobile thermometer. The temperature fluctuation was not greater than 3 °C, and it did not exceed the upper limit of 41 °C. After drying, the even distribution of the emulsion coats of the screens were checked at a number of points, using a layer thickness measuring device. The results were values within the tolerance of the measuring tool (1 µm), therefore we concluded that the dried emulsion coats are even, and there are no differences in thickness at the various points of the screen printing stencils.

3.3 The effect of screen lighting ratio on the quality of the stencil

To identify the proper lighting values, KIWO EXPOCHECK calculating film was used. By using the test film, simulating 10 different exposure times on a stencil, we were able to define the underexposure limit of the coated screen within one exposure cycle, with the help of colour change during emulsion polymerization. Overexposure limit was defined by the comparison of the size of positive and negative lines, which are the same size on the film, measured on the stencil. Developing was done with cold water and a KIWO PROFIWASH developing spray gun. The optical identification of exposure quality was carried out by the following parameters of the stencils. The colour of underpolymerized stencil is weaker, and it will be visible due to the thinning of the stencil because during developing the not fully solidified underexposed emulsion on the squeegee side will be washed out. In case of overexposure, due to point and line increase (under lighting), the positive and negative lines which are the same size on the film will close up and increase on the stencil, producing a different size. Following the identification of the correct minimal exposure value, the exposure time was defined with the help of a microscope, where the best possible resolution was found and stencil was fully tanned, taking into consideration the following: quality of printing edges, the angle of printing duct, the quality of mesh bridging, and the printing element sizes determined at the location where positive and negative lines meet (Figure 4).

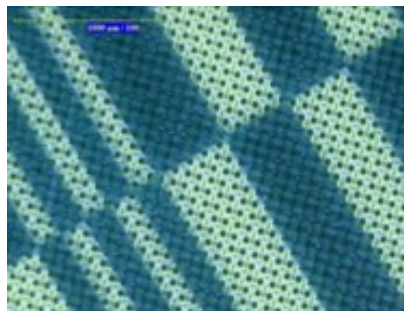


Figure 4: Size concordance of positive and negative lines

The following exposure values were detected during the examinations, which were carried out using KIWO Expocheck film, containing printing elements (Tables 10 and 11).

Table 10: The basis of exposure tests are the lighting parameters of 120.34 Y stencils

Stencil	Exposure time, s			
	Entire exposure	Minimum exposure	Optimal exposure	Over exposure
Textile printing stencil	240	120	168	190

Table 11: The basis of exposure tests are the lighting parameters of 77.48 Y stencils

Stencil	Exposure time, s			
	Entire exposure	Minimum exposure	Optimal exposure	Overexposure
Paper printing stencil	240	110	132	214

3.4 Examination of prints on textile and paper media

The prepare stencil was printed on white, 100 % cotton substrate, using black BOMO-Print LAC FLEX water soluble ink. The printing of the stencil for the printing of the paper was carried out using Maraster RS solvent soluble screen ink from the manufacturer MARABU. A commercial, white organic cotton T-shirt material was chosen as textile media. Art paper IGEPA CircleOffset 100 g/m² was chosen for paper media. The inspection of the quality of the print prepared with solvent based ink on paper media was done by digital microscope. The quality of the print edges, evenness and at selected locations, the correctness of the size were examined and compared to the image on the film positive to be reproduced, as shown on Figures 5 and 6.

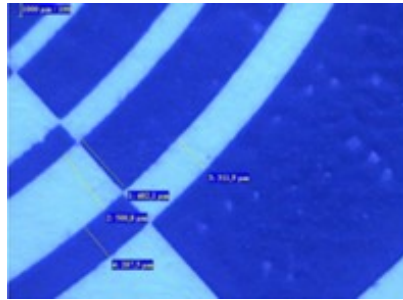


Figure 5: Size concordance of positive and negative curving lines on the print

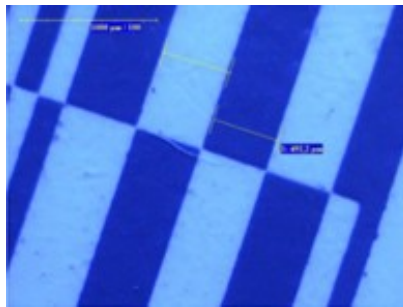


Figure 6: Size concordance of positive and negative straight lines on the print

The positive and negative lines which were to be the same size on the print showed a deviation value of less than 10%. The print edges are clean, with contours, the interfering effect of the textile is minimal, barely noticeable, and there is no raggedness detected. The corners of the prints are precise, well defined, the 90° angle tips are sharp, and no print loss can be seen. When comparing the raster points of the film positive and the print, the size differences on the print and film were only 1 to 3 µm, and it means less than 1% of deviation. The raster print shows optically acceptable image, although the edges have less contour than the line elements. The excellence of the results of the spectrophotometer measurements well represents that there is a 5% deviation in general between various shades. At the same time, the greatest difference between the values measured on the print and on the film was only 10%. The results of the measurements conducted show that the printing stencil has a very good quality, and the image on the film is reproduced on the media very well. The ink distribution is minimal, the print has sharp and contour image, and sizes have only minimal deviations. Both curved and straight lines are free of raggedness and waves. Thanks to the additional printing side coating, the stencil squeegees are sharp and due to their even stencil thickness, there are no protuberances at the edge of the print. There is no ink smearing at the circular measurement elements. Due to the proper stencil thickness and thanks to the additional coating, the layer of ink created is adequate. The stencil can be printed fully, there are no areas which are not printed due to ink blockage; except for the limit due to physical limits originating from the screen mesh and the emulsion resolution capability, which defines an approximately 120 µm size as the lower printable limit.

The inspection of the quality of print on cotton textile is done by checking the contours of the image, the line size retention at printing, the possible print distortions between the edges of the print, the sharpness

of lines, the coating property of the print, and the bleeding of the print edges. Measurement points were chosen on the film used for printing on cotton media: a circular, a line, and a fine resolution text area. The coating property of the black print is very strong despite the absorbing white textile substrate; when stretching the media, it does not crack or break, and keeps its colour. The print edges have contour, the distribution of ink is average, and there is no strong bleeding along the textile strands. It can be observed very well at the nonprinting element print which is about 100 μm thick and located at the edge of the circular printing element; it did not slur on the print (Figure 7).



Figure 7: Checking the position of ink blurring on the print

We have measured the 1 mm line thickness ensured by the film at the line print with the help of a measuring field magnifier (Figure 8). Taking into consideration the stretching capability of the textile, the size of the print did not deviate significantly from the size expected. The lines show sharp contours, and thanks to the sharp print edges, the ink has almost three dimensional effect despite the minimal coat thickness.

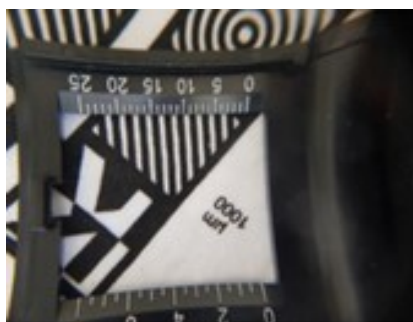


Figure 8: Checking the size of lines on the print

All characters were fully printed in the fine, small text area; the printing elements have contour and are well defined. The resulting stencil is of good quality, its coat thickness is optimal, and its Rz value is excellent despite the fact that the substrate of the stencil is a 77.48, medium “homespun” weaved screen mesh. The edges of the stencil are straight, the textile does not decrease the resolution capability of the emulsion. Due to adequate exposure, the squeegees are almost at a right angle, the stencil is developed to the necessary rate and without remnants, thus ensuring an adequate printing duct for the screen ink flow.

4. CONCLUSIONS

The goal of this work is to perfect the preparation of a screen printing stencil, and the improvement of the quality of the screen preparation process for direct screen printing on paper and textile substrates. The right stencil was chosen by examinations. From the point of view of the quality of the print, the critical issues of the technology of stencil preparation is the planned thickness of the stencil (EOM), reaching the necessary Rz values, and the lighting conditions of accurate printing element reproduction. We have made prints with printing forms based on the parameters examined, and analysed the quality of prints. The measurements conducted show that the printing stencils were of very good quality.

Measurements conducted with the help of a microscope showed that on average, the print image on the film was reproduced on art paper with less than 5% deviation. The examination of the textile print was carried out with less precise measurements, but with inspections fitting to the base characteristics of the media. Excellent stencil and print have resulted from the effect of even and straight edges of the print contours, the size keeping of the lines, the non-distorted and not blurred full image, and the ink with excellent covering capabilities.





5. REFERENCES

- [1] Hurtz GmbH: "Screen printing frames" URL: <https://www.hurtz.de/en/products/frames/screen-printing-frames> (last request: 2018-09-12).
- [2] Leicester Print Workshop: "A brief history of screenprinting", URL: http://www.leicesterprintworkshop.com/printmaking/screenprinting/a_brief_history_of_screenprinting/ (last request: 2018-09-12).
- [3] MacDermid Autotype Ltd.: "Anleitung - Belichtungsgeräte", URL: <http://autotype.macdermid.com/how-to-guides/details/206/anleitung-belichtungsgerate> (last request: 2018-09-20).
- [4] Peyskens, A.M.: "Sztatészítés Műszaki Alapelvek", (SaatiPrint S.p.A., Budapest, 2003).
- [5] Sefar Inc.: "Handbook for screen printers", (Sefar Printing Division, Thal, 1999.)
- [6] ULANO: "Frequently Asked Questions" URL: <http://www.ulano.com/FAQ/FAQexposure.htm> (last request: 2018-09-21).



© 2018 Authors. Published by the University of Novi Sad, Faculty of Technical Sciences, Department of Graphic Engineering and Design. This article is an open access article distributed under the terms and conditions of the Creative Commons Attribution license 3.0 Serbia (<http://creativecommons.org/licenses/by/3.0/rs/>).

LS FITTING OF THE MATERIAL PROPERTIES INFLUENCING THE PRINT QUALITY IN FLEXOGRAPHIC REPRODUCTION SYSTEM

Tamara Tomašegović , Tomislav Cigula , Juraj Huzjak , Marija Prša 
University of Zagreb, Faculty of Graphic Arts, Zagreb, Croatia

Abstract: *Printing quality is influenced by numerous parameters and by the material interactions in the ink-plate-substrate system. The aim of this paper is to characterize and quantify influential parameters in the flexographic reproduction system by using the method of the least squares (LS fitting). Specifically, this paper deals with influential properties of the printing plates and porous printing substrates (paper, board). Printing plate with its properties and interaction with the printing ink and substrate during the printing process affects the parameters of the print. Different properties of analysed porous substrates define properties of the print such as tonal values/dot gain and optical density. Measured properties of different printing substrates (papers and boards with different types of coatings) are used to build a quantification system of influencing parameters for the quality of the print using two different types of printing plates (patterned and non-patterned). Substrate parameters included in this research are roughness, surface free energy and gloss, while the surface free energy analysis was used to define printing plate properties. Results have shown that the least squares method can be applied to define the suitability of a particular type of printing plate for printing on different materials and enable optimization when selecting the material parameters in the flexographic reproduction system.*

Key words: flexography, printing plate, printing substrate, paper, board, LS fitting

1. INTRODUCTION

Flexography is a printing technique used primarily in the packaging and label production, as well as in novel applications such as functional printing. It utilizes an elastic photopolymer printing plate, which enables the usage of different types of substrates (Kipphan, 2001; Page Crouch, 1998).

Many parameters influence the quality of the print in flexography: photopolymer plate used for the printing plate production (Matsubara et al, 2011), bump and compensation curves applied to the plate, properties of anilox roller, type of tape placed under the printing plate to adjust its deformation, properties of the printing ink and printing substrate (Bollström et al, 2013) and control of the printing process (Mahović Poljaček et al, 2013).

Improvements of the flexographic printing plate's mechanical and surface properties in the past decade have been implemented in order to widen the possibilities of the application of flexography in graphic reproduction. For example, patterned textures have been applied to the surface of the printing elements on the printing plate in the plate making process (Kodak, n.d.); (Flint, n.d.). The increased surface roughness of the printing plate consequently enables better adsorption of the printing ink to the printing plate, and improved transfer of the ink to the printing substrate, reducing the fingering and enhancing the visual impression of the print. Surface patterns can be applied to the plate only in high coverage area (> 80%) or in the whole range of tonal values, depending on the type of the ink, substrate and printing plate itself.

Different types of printing substrates can be used in flexography. Among them, foil and paper/board are the most common. Adjustment of the printing plate's coverage values is necessary for each printing substrate because of the influence of the substrate's properties on the transfer and behaviour of the ink on its surface in the printing process.

Main properties of the printing substrate that influence the properties of the print to extent are roughness, surface free energy, smoothness and gloss. Each of these properties in relation to the properties of the printing plate itself will result with different quality of the print properties (optical density and tonal value, i.e. tone value increase (Johnson, 2008; Tomašegović, 2016.).

The aim of this paper was to quantify the influence of the parameters of the printing substrate on the properties of the print, when using patterned and non-patterned printing plate. In order to achieve this, least square (LS) fitting in matrix form was applied. LS fitting method enabled assigning the "weight coefficients" to each of the substrate parameters that affect the properties of the print (optical density and tonal values). In this way, the strength of the each property of printing substrate related to optical density and specific tonal value (5%, 40%, 80%) on the print could be assessed.

The quantification of the substrate parameters influencing the print quality in flexography can be used to predict and assess the suitability of a particular printing substrate for the usage with the chosen flexographic printing plate and ink.

2. MATERIALS AND METHODS

For this research, four types of paper/board printing substrates were used: matt 100 g/m², offset gloss 115 g/m², coated 245 g/m² and silk 350 g/m². Properties of substrates, including roughness, gloss and surface free energy were determined prior to printing.

Measurements of the substrate roughness were performed with a TR200 roughness tester (PortableTesters.com, n.d.). Roughness parameters were determined by measuring ten measurements on the printing side of the substrate. Five measurements were performed in the direction of paper grain and five measurements perpendicular to the paper grain direction.

For the purposes of this experiment, the value taken into account was Ra parameter (the arithmetic mean of the profile in the individual measurement).

Paper gloss was measured using a gloss meter Elcometer 407, which measures reflective glare. Light intensity is registered over a small range of reflected angles. The intensity of the light depends on the material and the angle of illumination. For the purpose of obtaining correct results of the measurements, ranging from high gloss to matt surfaces, three different geometries and three different ranges (BYK, n.d.) have been defined. All surfaces were measured at an angle of 20°, 60° and 85°.

In order to calculate the surface free energy of the printing substrates, contact angles of three probe liquids (water, glycerol, diiodomethane) were measured on each substrate by means of goniometer Dataphysics OCA 30. Temperature set for the measurements was 23±1 °C. Eight drops of 1 µl were applied on the solid surface (printing substrate), and the contact angle was measured 4 seconds after the drop has touched the solid surface. Sessile drop method was used for the measurements. After that, surface free energy (SFE) and its polar (SFE^p) and dispersive (SFE^d) components were calculated using OWRK method (Owens et al, 1969.).

Materials used for the experiment were commercial styrene-isoprene-styrene based LAMS photopolymer flexographic printing plates and black UV flexographic ink. Two variations of printing plates made from the same material were used: patterned and non-patterned type. The purpose of the surface pattern on the flexographic printing plates is to increase the surface roughness and consequently the amount of the ink transferred to the printing substrate. Pattern was applied to the surface of the printing plate in the whole coverage area: from 1% to 100%. Surface free energy of printing plates was ~ 30 mN/m, of which up to 0.5 mN/m consisted of polar component, and the rest of the dispersive.

Printing process was carried out by means of IGT F1 unit (IGT, n.d.). Prior to printing on the substrates used in this experiment, both types of plates were printed with using 10 probe samples in order to stabilize the printing process. Since different types of printing substrates were used, no compensation curves were applied during the production of the plates. Printing parameters, which were kept fixed during the printing process, were adjusted by aiming the optical density of 1.5 on 100 matt paper. Anilox force was set to 300 N; printing force to 50 N, and printing speed was 0.3 m/s.

After the printing process, optical density (D) and tonal values (TV) on the prints were measured by means of X-rite eXact device. Tonal value was measured on 5%, 40% and 80% of nominal coverage value in order to examine highlights and mid-tones, as well as shadows.

Collected results were used to build a matrix for least square (LS) fitting (Björck, 1996.). Input parameters were Ra, gloss, SFE^p and SFE^d of the substrates. The reason for not using the total SFE of substrates alongside its components was the singularity of the constructed matrix, which would compromise the accuracy of the results. Output matrixes consisted of vectors representing D and TV at 5%, 40% and 80% for patterned and for the non-patterned printing plates. All input parameters were normalized (0-1). In this way, eight LS fitting sets were constructed. The weight coefficients for each of the substrate parameters (Ra, gloss, SFE^p and SFE^d) influencing the print properties (D, TV) were estimated in this way. The results were compared for the prints obtained with patterned and non-patterned printing plate in order to assess the qualitative variations of the print when using different substrate-plate combinations (Johnson, 2008.).

3. RESULTS AND DISCUSSION

3.1. Properties of printing substrates

In order to quantify the influence of the chosen parameters of the printing substrate that influence the properties of the print, the variation of their features needed to be present. Figure 1 displays the measured properties of chosen printing substrates.

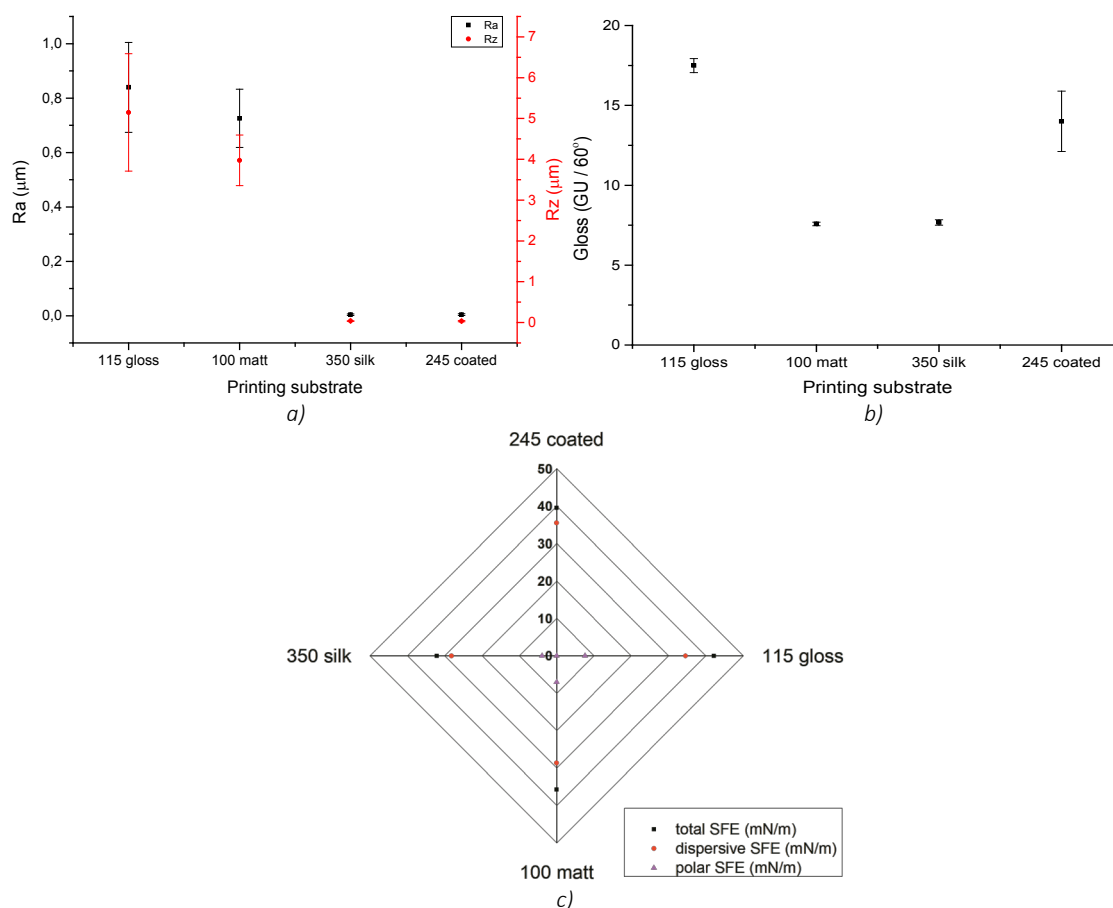


Figure 1. Measured properties of printing substrates: a) roughness parameter R_a , b) gloss, c) surface free energy

For the inclusion in matrix prepared for LS fitting, only R_a parameter (Figure 1a) was chosen to represent roughness in the model, since R_a and R_z are not independent. Furthermore, R_a parameter showed less deviation. The range of measured R_a was from $0.004 \mu\text{m}$ to $0.84 \mu\text{m}$, depending on the printing substrate.

Values of gloss measurements chosen for the LS fitting were fixed at 60° in order for them to be comparable and assure the validity of the model. In Figure 1b, one can see that the values of the gloss for measured surfaces range from $7.5 - 18 \text{ GU}$. Highest deviations of the measurements are present for the 245 coated substrate.

Figure 1c presents the surface free energy (SFE) components of the printing substrates used in this research. Substrate 115 gloss has the highest value of the total SFE at 42.15 mN/m . 350 silk presents the lowest value of total SFE: 32.1 mN/m . All substrates have a dominant dispersive SFE component, with polar component lower than 10 mN/m . Specifically, lowest polar component is present for 245 coated substrate, and it amounts only 0.01 mN/m .

3.2. Properties of prints

Figure 2 (a-c) presents the results of measurements performed on the prints obtained by patterned and non-patterned printing plate. Results of the total value measurements are presented in Figure 2a-b, and optical densities on the prints are visible in Figure 2c.

Measured tonal values show the similar trend for the prints obtained by patterned and non-patterned printing plate. Substrates *350 silk* and *245 coated* present lower tonal values than substrates *100 matt* and *115 gloss*. This can be explained by the higher roughness of substrates *100 matt* and *115 gloss* (Figure 1a).

When comparing the tonal values obtained by patterned and non-patterned printing plate on the same substrate, it is visible that the patterned printing plate produces higher tonal value increase – because of the higher amount of the ink present on the plate itself and therefore transferred to the print.

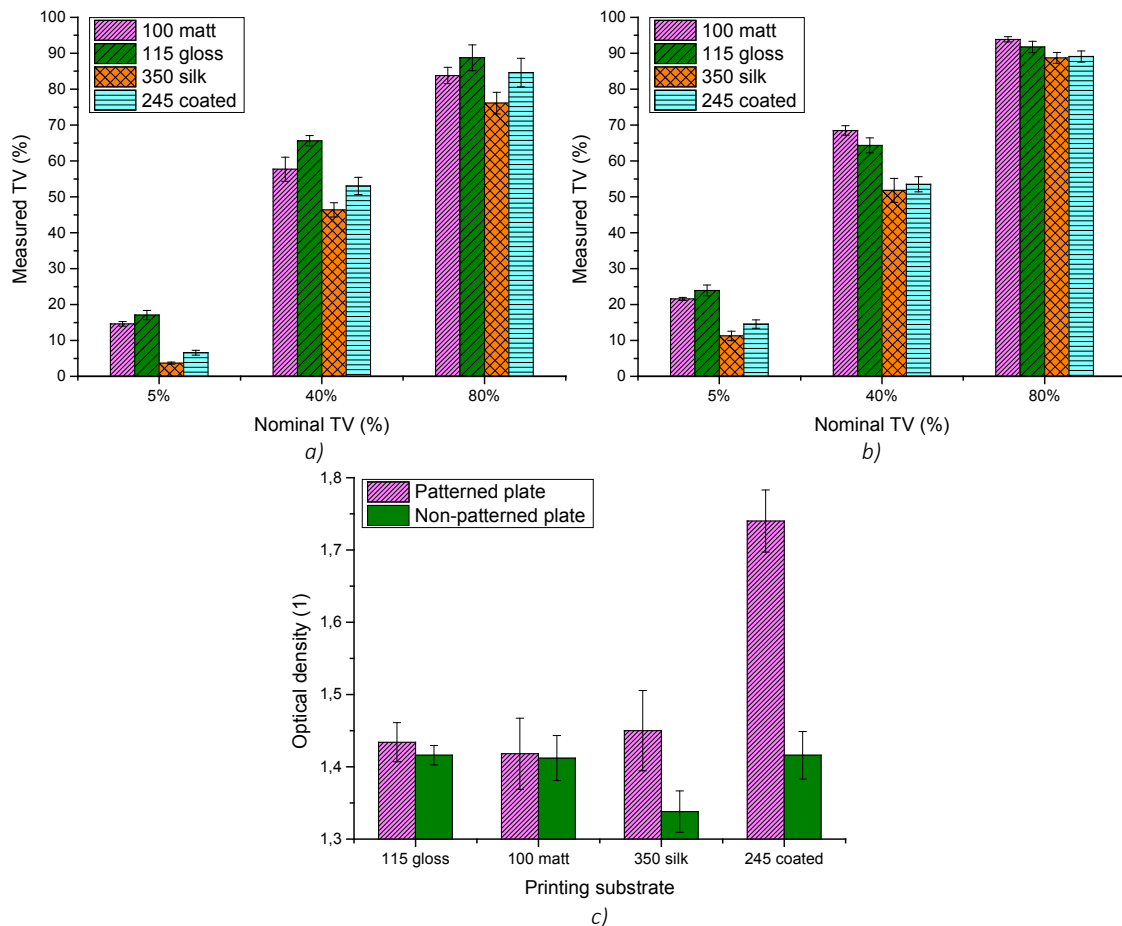


Figure 2. Measured properties of prints: a) tonal values obtained by non-patterned printing plate, b) tonal values obtained by patterned printing plate, c) optical density

Optical density measured on the prints is highest when using the patterned printing plate and *245 coated* substrate; and lowest when using non-patterned plate and *350 silk* substrate (Figure 2c). As expected, optical density on the substrate is higher when printing with the patterned printing plate, specifically on the substrate that possess low roughness (*350 silk* and *245 coated*).

Furthermore, the print on substrate *245 coated* with the patterned printing plate has significantly higher optical density than the rest of the printed samples. This could be explained by the almost non-existent polar component of this substrate – specifically, of the substrate's coating. When transferring a higher amount of the ink with the patterned printing plate to this substrate, due to the properties of the coating, penetration of the ink into the substrate before the drying could be decreased. This will result with higher measured optical density.

It can be concluded that all presented printing substrate parameters have an impact on the tonal values and optical density on the prints obtained by patterned and non-patterned printing plates. However, the effects of those parameters are individual and different for each substrate property.

It is therefore necessary to quantify those influences in order to assess their degree of impact on the properties of the flexographic print.

3.3. LS fitting

After analysis of the results, the application of the least squares method in the matrix form (LS fitting) was applied in order to interpret the obtained measured values in the context of the quality of the prints. The aim was to predict the trends of optical density and tonal values on prints produced using different printing substrates and patterned/non-patterned printing plates. Figure 3 presents the weight coefficients for chosen parameters of the substrates that influence the properties of the print when using patterned and non-patterned plate. The impact can have a positive or negative sign, presenting the proportional or inversely proportional connection, respectively.

It is visible that some parameters have generally negligible effect on the properties of the print, specifically polar component of the surface free energy of the substrate (with the exception of the influence on optical density when using rough printing plate, Figure 3a-c), due to its low values on substrates and printing plates compared to the dispersive component. The obtained results point to the dominant impact of the roughness of the substrate, gloss and dispersive component of the surface free energy on the analysed properties of the print.

The influence of the substrate roughness with positive sign is present for both printing plates for the tonal values on the prints (Figure 3a-b). This influence was similar for all tonal areas: highlights, mid-tones and shadows. Higher roughness of the substrate will generally, regardless of the type of printing plate, result with a higher tone value increase on the print due to the deformation of the screen element on the print.

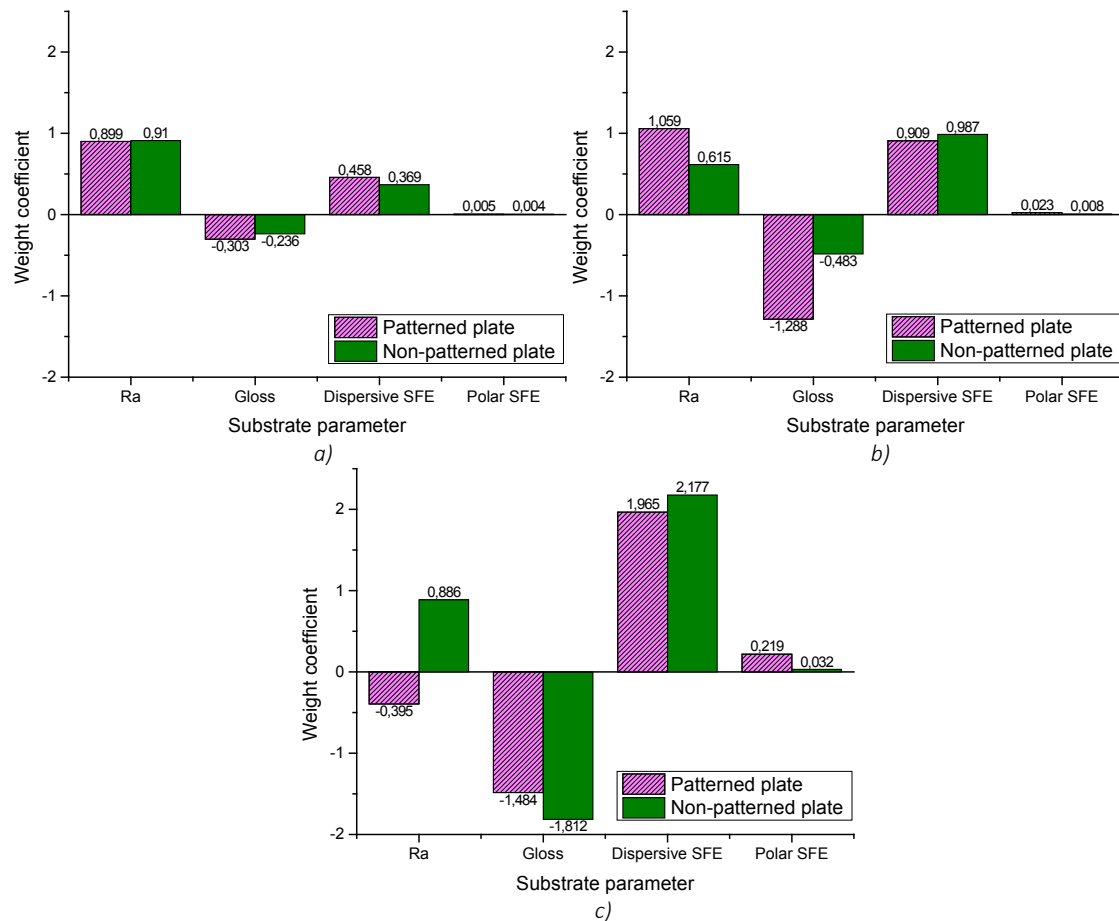


Figure 3. Weight coefficients of influential parameters of substrates for: a) tonal value of 5% on prints, b) tonal value of 80% on prints, c) optical density on prints

The roughness of the substrate affects positively the optical density on the prints obtained by non-patterned printing plate, while the influence on the prints obtained by patterned printing plate is negative (Figure 3c). It is visible that the transfer of the printing ink (and thus the optical density on the print) is improved when a rough and smooth surface (rough printing plate and smooth printing substrate

or vice versa) are used in the printing process. In the smooth-to-smooth or rough-to-rough system, amount of the transferred ink will be decreased.

Other substrate parameters (gloss, dispersive and polar surface free energy) influence the tonal values with the same sign throughout the measured range, regardless of the type of used printing plate.

Gloss, which can be associated with the type of the substrate coating, has an impact with a negative sign on the optical densities and increase of the tonal values. It can be concluded that the increased gloss of the substrate due to the use of specific coatings reduces the ability of the ink adsorption on the printing substrate and its penetration into the substrate. Therefore, optical density and the increase of tonal values on the print (dot gain) are reduced compared to the prints on substrates with coatings which do not possess, among other properties, high gloss.

The dispersive component of surface free energy has an influence with positive sign. The UV flexographic ink used in this experiment is mainly composed of non-polar components (polymers, oligomers, waxes, etc.). Therefore, when the contact with the printing substrate with pronounced dispersive component of surface free energy is achieved, the ink transfer is improved. This will be manifested by the increased tonal values on the print, as well as with increased optical density.

The LS fitting made it possible to connect the properties of the printing substrate and the print when varying the media between them in the printing process - printing plate. The results obtained by the LS method provided a mathematical weight to the interpretations of the influence of printing substrates and plates on flexographic print, specifically in the case of evaluation and linking of multiple parameters.

4. CONCLUSIONS

The aim of this research was to quantify the influential parameters in the flexographic reproduction system using the least squares method, and to define the interaction of a particular type of printing substrate and printing plate. This enables the optimization of the flexographic printing system.

Roughness, gloss and surface free energy were measured on the chosen printing substrates, and the printing process was carried out using patterned and non-patterned printing plate. Obtained prints were used to measure optical density (D) and tonal values (TV) on prints at certain percentages (5%, 40% and 80%). Based on the collected data, a model presenting the weight coefficients of the influential parameters in flexographic system was developed using the least squares method. Fitting was applied for both patterned and non-patterned printing plate.

Based on the obtained results, one can conclude that optical density is enhanced when a combination of smooth printing substrate and rough printing plate (or vice versa) is used in the reproduction process. Furthermore, increased roughness of the printing substrate will result with increased tonal values on the print. Increased gloss has an impact with negative sign on optical density and dot gain on prints produced by both types of printing plates due to the surface properties of the coatings and decreased penetration of the ink in the coated paper/board.

Increased dispersive component of the surface free energy has a positive effect on the increase of tonal values and optical density on the print when using chosen standard UV flexographic ink.

Polar component of surface free energy, due to its low values on both printing plate and substrate, has a weak impact on the properties of the print.

This research has shown that the qualitative properties of the prints (represented by D and TV) obtained by the materials used in this experiment are dominantly affected by roughness, gloss and dispersive component of the surface free energy of the substrate. Furthermore, it is possible to quantify the influence of these parameters using LS fitting.

In accordance with the qualitative requirements, it is therefore possible to choose a combination of patterned/non-patterned printing plate and substrate in order to optimize the flexographic printing system.

5. ACKNOWLEDGMENTS

This research is part of the project UIP-2017-05-4081, *Development of the model for production efficiency increase and functionality of packaging*, supported by Croatian Science Foundation.

6. REFERENCES

- [1] Björck, A.: "Numerical methods for least squares problems", PhD thesis, Linköping University, Linköping, 1996.
- [2] Bollström, R., Tobjörk, D., Dolietis, P., Salminen, P., Preston, J., Österbacka, R., Toivakka, M.: "Printability of functional inks on multilayer curtain coated paper", Chemical Engineering and Processing: Process Intensification 68, 13-20, 2013. doi: 10.1016/j.cep.2012.07.007.
- [3] BYK, Gloss measurement, BYK-Gardner GmbH, URL:
- [4] https://www.byk.com/fileadmin/byk/support/instruments/theory/appearance/en/Intro_Gloss.pdf (last request: 2018-09-16).
- [5] Flint, Flint NeXT technology, Flint Group, URL:
<https://www.flintgrp.com/en/products/flexographic/nyloflex-next/> (last request: 2018-09-16).
- [5] IGT, IGT: F1 printability tester, IGT Testing Systems, 2016, URL:
[http://www.igt.nl/image/data/IGT/Downloads/IGT%20F1%20brochure%20\(ENG\).pdf](http://www.igt.nl/image/data/IGT/Downloads/IGT%20F1%20brochure%20(ENG).pdf)
 (last request: 2018-09-16).
- [6] Johnson, J.: "Aspects of flexographic print quality and relationship to some printing parameters", PhD thesis, Karlstad University, 2008.
- [7] Kipphan, H.: "Handbook of Print Media", (Springer, Berlin, 2001).
- [8] Kodak, Kodak NX technology, Kodak, URL:
http://graphics.kodak.com/KodakGCG/uploadedFiles/Products/Computer-to-plate/Flexo_CTP/TRENDSETTER_NX_Imager/Tab_Contents/TSNX_sellsheet.pdf
 (last request: 2018-09-16).
- [9] Mahović Poljaček, S., Cigula, T., Tomašegović, T.: "Meeting the quality requirements in flexographic plate making process", Proceedings of IC 2012, (Budapest, Hungary, 2012), pages 62-69.
- [10] Matsubara, T., Oda, R.: Pat. 20,110,308,412, "Block copolymer composition for flexographic printing plates", 2011.
- [11] Owens, D. K., Wendt, R. C.: "Estimation of the surface free energy of polymers", Journal of Applied Polymer Science 13(8), 1741-1747, 1969. doi: 10.1002/app.1969.070130815.
- [12] Page Crouch, J.: "Flexography Primer", 2nd ed, (PIA/GATF Press, Pittsburgh, 1998).
- [13] PortableTesters.com, TR200 Surface Roughness Tester, PortableTesters.com, URL:
<https://portabletesters.com/product/tr-200-surface-roughness-tester/> (last request: 2018-09-19).
- [14] Tomašegović, T.: "Functional model of photopolymer printing plate production process", PhD thesis, University of Zagreb, 2016.



© 2018 Authors. Published by the University of Novi Sad, Faculty of Technical Sciences, Department of Graphic Engineering and Design. This article is an open access article distributed under the terms and conditions of the Creative Commons Attribution license 3.0 Serbia (<http://creativecommons.org/licenses/by/3.0/rs/>).

IMPACT OF TYPE OF INK AND SUBSTRATE ON COLORIMETRIC VALUES OF INKJET PRINTS

Jelena Vasić¹ , Nemanja Kašiković¹ , Milana Đurđević

¹ University of Novi Sad, Faculty of Technical Sciences,
Department of Graphic Engineering and Design, Novi Sad, Serbia

Abstract: *This research aims to characterize the quality of prints printed with inkjet printing technique, depending on the type of UV ink and printing substrate. Printing substrates were chosen as trending substrates for digital printing used for both indoor and outdoor applications and thus may be affected with a variety of different agents during production and in general use. The results led to the conclusion that on various substrates, HP HDR250 Scitex inks shown better results, as well as that fastness properties very much depend on the type of pigment in ink.*

Key words: digital printing, inkjet, ink, substrate, colour difference

1. INTRODUCTION

In addition to electrophotography, inkjet printing technology is currently one of the simplest and most popular digital printing technique that takes precedence in the field of short runs (Kašiković et al, 2016). The printing process is contactless, which means that there is no need for an intermediate carrier for transfer of the ink on the substrate (Kipphan, 2001). Since this is the main advantage of this printing technique, it allows printing on a large number of different substrates (paper, cardboard, textile, foils, glass, metals etc.) that other printing techniques cannot use. Besides that, inkjet printing enables usage of a large number of different colours, as well as large format prints (Kašiković et al, 2016). Due to all its advantages, this printing technique has broad application – home use (HP, Epson, Canon), printing on textiles (Canon, Seiren, Minolta, Durst), production of printing plates (Polychrome, Iris), 3D printing (3D System, Z Corporation) and printing for medical needs (Iris, Sterling Diagnostics) (Majnarić, 2015).

The main inkjet technologies are continuous and drop on demand inkjet. Continuous inkjet is based on dyeing the substrate with fine droplets that a very brittle oscillating body continually ejects from the nozzle. During this process, it is possible to produce and then transfer thousands of droplets to the substrate depending on the charge – electric field deflects charged droplets, while the uncharged ones dye the substrate. On the other hand, in drop on demand inkjet technology, a droplet is produced when needed. The main drop on demand technologies are thermal, piezo, electrostatic and stream inkjet (Kipphan, 2001; Majnarić, 2015).

1.1 Inkjet inks

The most demanding component in inkjet printing is ink. The chemical composition and ink formulation in inkjet dictate not only the quality of the print but also determine the characteristics of the droplets as well as the reliability of the printing system. All inks for inkjet contain two components – colorants and base. Since low viscosity is the main characteristic of the inkjet inks, the base is the most abundant component. Its task is to ensure the formation of small droplets of colour and their proper distribution from the printheads, as well as the good bonding to the substrate. Use of a large number of different substrates requires the application of different liquids as a base for inkjet – water, microemulsions, oils. As such fluids behave differently in contact with the rigid surfaces, several drying mechanisms are available – penetration, evaporation, phase change from a liquid state to a solid state or gel, and a chemical reaction. Depending on the drying process, it is possible to use different inks (hot-melt, UV, solvent, latex etc.) (Majnarić, 2015).

1.1.1 UV inkjet inks

Unlike other inkjet inks, UV inks dry at the moment under the influence of UV light. Implementing the UV inkjet technology requires adjusting of the composition of UV inks and their compatibility with UV light sources. Since polymerization is the base of the UV drying process, UV inkjet inks must contain the following components: pigments (15-20%), prepolymers (20-35%), monomers and oligomers (10-20%), photoinitiators (5-10%) and accessories (1-5%). The essential component of the ink are photoinitiators which absorb UV light and start the polymerization process. Considering UV light sources, the most

effective ones are quicksilver lamps, that have the highest emission in the electromagnetic UV spectrum (200-380 nm), which is why they are often applied. However, as their radiation is detrimental to human health, the use of LED light sources is increasing though they are less efficient. UV inks allow printing of a wide range of materials, including coated and uncoated substrates, flexible materials and rigid individual sheets several centimetres thick (Majnarić, 2015).

2.1 Colour fastness to rubbing

The fastness of the colour is crucial in attaining commercially acceptable prints which may be affected with a variety of different agents during production and in general use. Exposure of the colour to these agents can induce both change in and loss of colour from the substrate, producing variation in saturation and hue. Measuring colour fastness is essential to assess the durability of a colorant (Valdeperas-Morell et al, 2012). Colour fastness refers to the resistance of colour to fade or bleed of a printed substrate to various types of influences e.g. water, light, rubbing, washing, perspiration etc. Colour fastness to rubbing (also known as the "Crock test") is commonly tested to determine the quality of a collared substrate regarding the fixation of the colour to the substrate. The fastness properties depend on the properties of the substrate, as well as on the composition of ink (mainly the type of pigment). For example, black colour is carbon-based; therefore the pigment particles are large which is the main reason for its poor rubbing properties (Kiron, n.d.).

This research aims to characterize the quality of prints printed with inkjet printing technique, depending on the type of UV inks and printing substrate.

2. MATERIALS AND METHODS

Rubbing fastness was studied on two sets of six different substrates – paper, cardboard, akyplac, printolyte, forex and plexiglass. All substrates were printed with HP Scitex 11000 Industrial Press with two different types of ink. One set was printed using HP HDR230 Scitex inks (hereinafter referred to as P samples) optimized for paperboard applications and other using HP HDR250 Scitex inks (hereinafter referred to as U samples) optimized for flexible and rigid media, including paperboard and plastics. Properties of used substrates are presented in the continuation.

- Paper – coated, grammage (weight) 250 g/m² (hereinafter referred to as sample 1),
- cardboard – three-layers, thickness: 1.6 mm, grammage 600g/m² (hereinafter referred to as sample 2),
- akyplac – thickness: 3 mm (hereinafter referred to as sample 3),
- printolyte – thickness: 2.6 mm (hereinafter referred to as sample 4),
- forex – thickness: 3 mm (hereinafter referred to as sample 5) and
- plexiglass – white, thickness: 3 mm (hereinafter referred to as sample 6).

These substrates were chosen as trending substrates for digital printing used for both indoor and outdoor applications. Printed test form (Figure 1) included four measuring fields sized 12 x 4 cm with 100% tone value of all process colours (cyan, magenta, yellow, black).

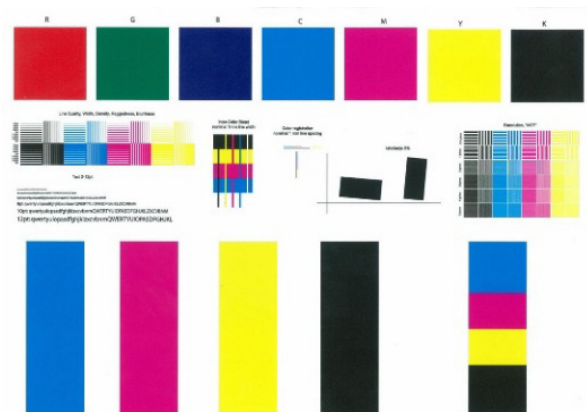


Figure 1: The appearance of the used test form

The samples were tested using Testex TF411 electronic crock meter in three cycles with different number of strokes depending on the substrate (Table 1). The number of strokes was determined with first noticeable changes within the first cycle.

The test method used in this paper is the standard colour fastness to rubbing dry method according to the ISO 105-X12:2016 (ISO, 2016). Crockmeter, consisting of a flat surface to hold the specimen and circular rubbing surface (rubbing finger), covered with a white cotton fabric, exerts a downward force on a specimen when moving back and forth along the straight line of 100 mm (Yogesh, 2017).

Table 1: The number of strokes within one cycle depending on the substrate

Substrate	Number of strokes within one cycle
Paper	1500
Cardboard	500
Akyplac	100
Printolyte	500
Forex	50
Plexiglass	300

The instrumental measurement (CIE $L^*a^*b^*$) was conducted with SpectroDens directional $0^\circ/45^\circ$ measurement geometry, D50 standard illuminant and 2° standard observer. The following formula was used to calculate the colour difference based on the measured CIE Lab components:

$$\Delta E = \sqrt{\Delta L^* + \Delta a^* + \Delta b^*} \quad (1)$$

where L^* represents the achromatic coordinate of the light, and a^* and b^* chromatic coordinates of the CIE Lab colour space (Smyth, 2009). The values measured after each rubbing cycle are compared with the values measured before rubbing, as well between the 1st and the 2nd, and the 2nd and 3rd rubbing cycle. The colour differences can be classified into certain categories depending on their values:

- $0 < \Delta E < 1$ - the imperceptible difference,
- $1 < \Delta E < 2$ - very small difference,
- $2 < \Delta E < 3,5$ - medium difference,
- $3,5 < \Delta E < 5$ - big difference and
- $\Delta E > 5$ massive difference (Smyth, 2009).

3. RESULTS AND DISCUSSION

3.1 P samples

Figure 2 gives a graphic representation of the colour difference values for the Black process colour of the P samples. When compared to the initial values, the values measured on all samples after each rubbing cycle are greater than 5, which belongs to the domain of massive visual differences. The measured values compared to the previous rubbing cycle are in the field of medium and big differences for samples P1 and P5, while the difference for other samples remains massive.

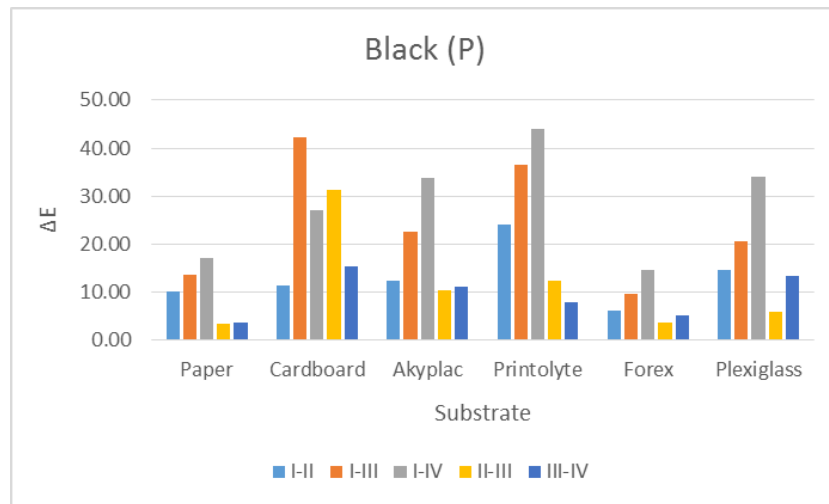


Figure 2: Graphic representation of the colour difference values for the Black process colour of the P samples

Figure 3 gives a graphic representation of the colour difference values for the Cyan process colour of the P samples. When compared to the initial values, the values measured on all samples after each rubbing cycle vary from medium to massive difference. The measured values compared to the previous rubbing cycle vary from the imperceptible to massive differences. The graphic shows that the lowest colour difference values are measured for samples P1 and P2.

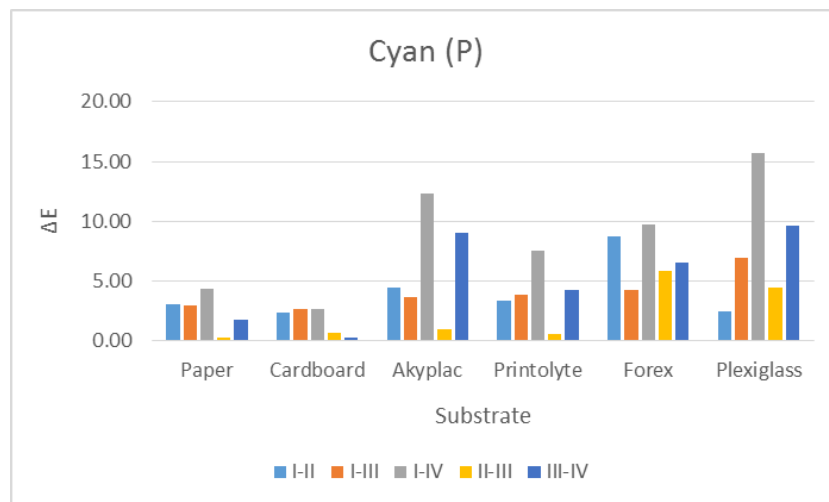


Figure 3: Graphic representation of the colour difference values for the Cyan process colour of the P samples

Figure 4 gives a graphic representation of the colour difference values for the Magenta process colour of the P samples. When compared to the initial values, the values measured on all samples after each rubbing cycle vary from big to massive difference. The measured values compared to the previous rubbing cycle vary from the medium to massive differences.

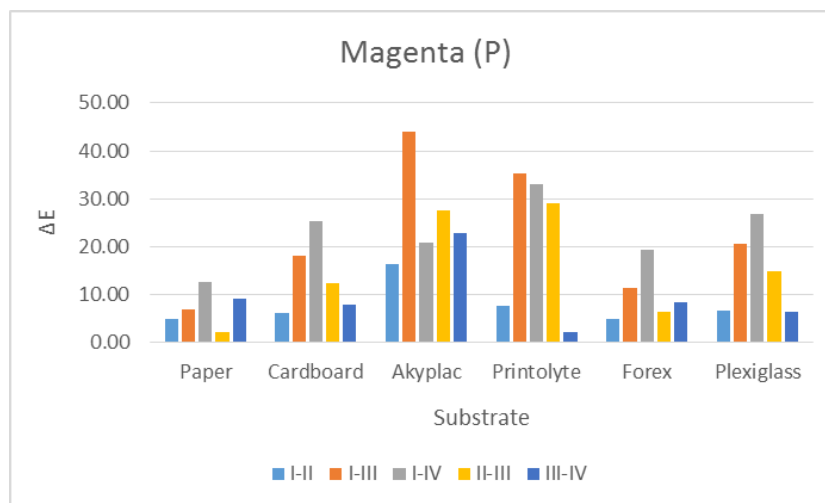


Figure 4: Graphic representation of the colour difference values for the Magenta process colour of the P samples

Figure 5 gives a graphic representation of the colour difference values for the Yellow process colour of the P samples. When compared to the initial values, the values measured after each rubbing cycle vary from medium (for P1 and P5 samples) to massive difference. The measured values compared to the previous rubbing cycle vary from the imperceptible to massive differences. The graphic shows that the lowest colour difference values are measured on the P5 sample, with no measurement showing a massive difference.

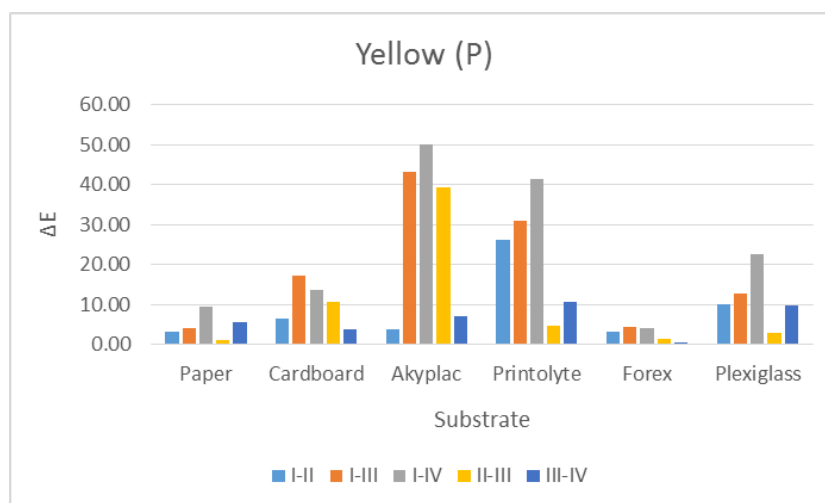


Figure 5: Graphic representation of the colour difference values for the Yellow process colour of the P samples

3.1 U samples

Figure 6 gives a graphic representation of the colour difference values for the Black process colour of the U samples. When compared to the initial values, the values measured after each rubbing cycle are greater than 5, which means that there is a massive visual difference between the cycles. The measured values compared to the previous rubbing cycle vary from medium to massive differences.

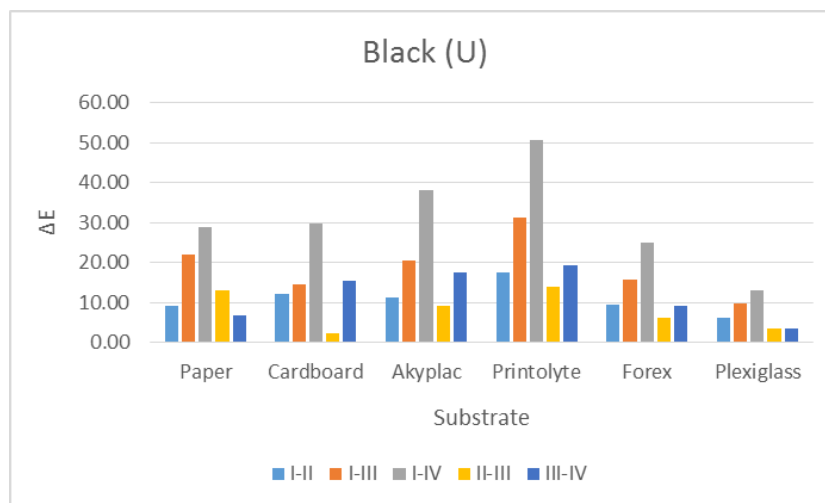


Figure 6: Graphic representation of the colour difference values for the Black process colour of the U samples

Figure 7 gives a graphic representation of the colour difference values for the Cyan process colour of the U samples. When compared to the initial values, the values measured on all samples after each rubbing cycle vary from medium to massive difference. The measured values compared to the previous rubbing cycle vary from the imperceptible to massive differences. The graphic shows that the lowest colour difference values are measured on the U5 sample.

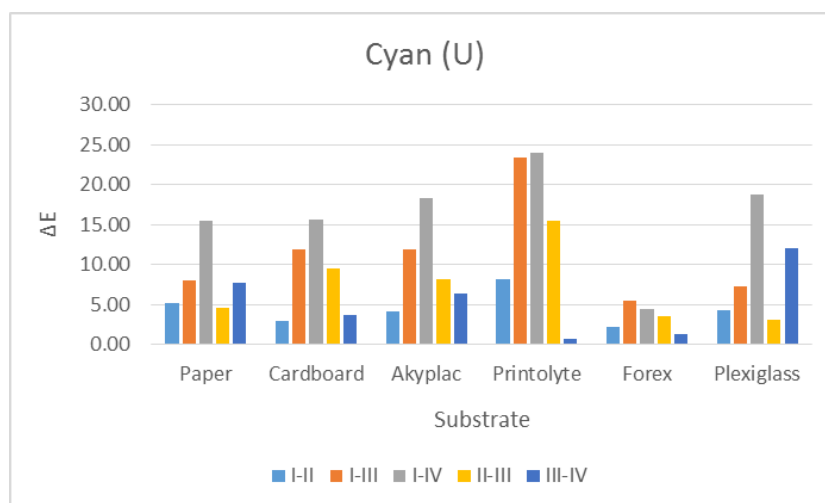


Figure 7: Graphic representation of the colour difference values for the Cyan process colour of the U samples

Figure 8 gives a graphic representation of the colour difference values for the Magenta process colour of the U samples. When compared to the initial values, the values measured on all samples after each rubbing cycle vary from medium to massive difference. The measured values compared to the previous rubbing cycle vary from the imperceptible to massive differences. The graphic shows that the biggest colour difference values are measured on the U2 sample.

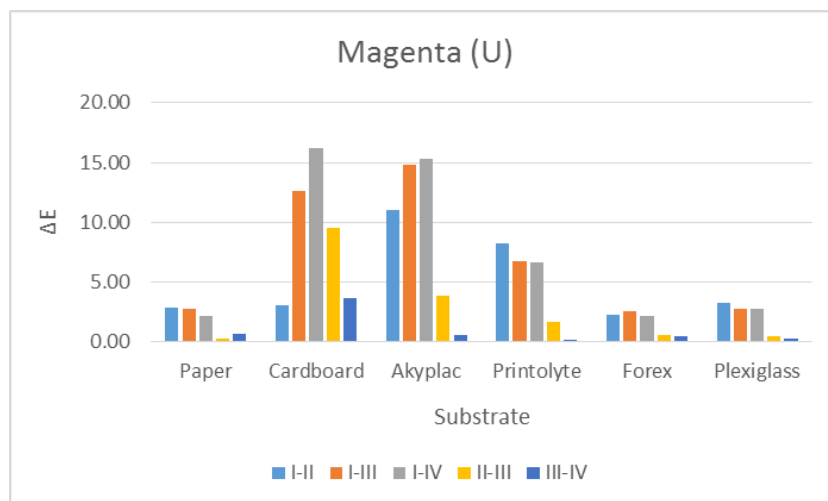


Figure 8: Graphic representation of the colour difference values for the Magenta process colour of the U samples

Figure 9 gives a graphic representation of the colour difference values for the Yellow process colour of the U samples. When compared to the initial values, the values measured after each rubbing cycle are greater than 5, which means that there is a massive visual difference between the cycles. The measured values compared to the previous rubbing cycle vary from the imperceptible to massive differences. The graphic shows that the lowest colour difference values are measured on the U5 sample.

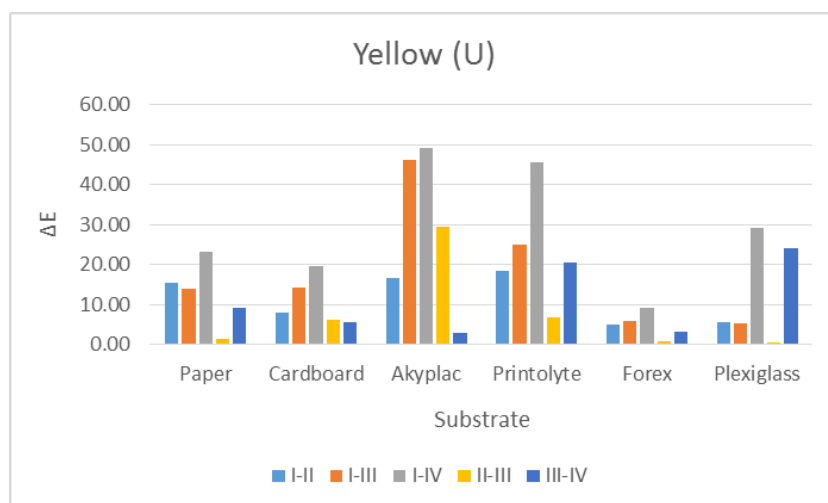


Figure 9: Graphic representation of the colour difference values for the Yellow process colour of the U samples

Obtained results lead to the conclusion that, when printed using HP HDR230 Scitex inks (P samples), the lowest colour difference values are measured for the cyan process colour, where specimens P1 and P2 showed particularly good results. The most significant colour difference values were measured for the black process colour, particularly for specimens P2 and P4. On the other hand, when printed using HP HDR250 Scitex inks (U samples), the lowest colour difference values are measured for the magenta process colour, where specimens U1, U5 and U6 showed particularly good results. The most significant colour difference values were measured for the black process colour on all specimens.

4. CONCLUSIONS

Trending substrates for digital printing used for both indoor and outdoor applications are often exposed to various types of influences. All tested materials had different characteristics as well as the applied colours. According to expectations, the results led to the conclusion that on different substrates, HP HDR250 Scitex inks (U samples) shown better results. However, paper and cardboard substrates shown better results when printed with the HP HDR230 Scitex inks. The analysis also confirmed that fastness properties very much depend on the type of pigment in ink, since black colour which is believed to have large pigment particles showed the poorest rubbing properties.

Future research could include a more detailed analysis of the chemical composition of the ink to investigate whether any component other than pigments affects the rubbing fastness and to what extent. Besides, a uniformed number of strokes within one rubbing cycle for all substrates could be considered.

5. ACKNOWLEDGMENTS

This work was supported by the Serbian Ministry of Science and Technological Development, Grant No.: 35027 "The development of software model for improvement of knowledge and production in graphic arts industry."

Also, this work was supported by the companies NSPlakat and Print Grupa Zagreb who provided and printed the samples.

6. REFERENCES

- [1] International Organization for Standardization (ISO), ISO 105-X12:2016: Tests for Colour Fastness, Part X12: Colour Fastness to Rubbing, International Organization for Standardization, 2016.
- [2] Kašiković, N., Novaković, D., Jurič, I.: "Digitalna štampa – praktikum za vežbe", (FTN Izdavaštvo, Novi Sad, 2016), pages 9, 13
- [3] Kiron, M. I., Rubbing Fastness Test | Color Fastness to Rubbing, Textile Learner, URL: http://textilelearner.blogspot.com/2011/08/color-fastness-to-rubbing-rubbing_1201.html (last request: 2018-08-19)
- [4] Kipphan, H.: "Handbook of Print Media: Technologies and Production Methods", (Springer-Verlag, Berlin, 2001), pages 63-64
- [5] Majnarić, I.: "Osnove digitalnog tiska", (Sveučilište u Zagrebu Grafički Fakultet, Zagreb, 2015), pages 150 -207
- [6] Smyth, S.: "The Print and Production Manual", 11th ed, (Pira International Ltd., Leatherhead, 2009).
- [7] Valldeperas-Morell, J., Carrillo-Navarrete, F.: "Understanding and Improving the Durability of Textiles", (Elsevier Science, 2012), pages 82-103
- [8] Yogesh, T., Measurement of Rubbing Fastness, Textile Mates, 2017, URL: <https://www.textilemates.com/measurement-rubbing-fastness/> (last request: 2018-08-19)



© 2018 Authors. Published by the University of Novi Sad, Faculty of Technical Sciences, Department of Graphic Engineering and Design. This article is an open access article distributed under the terms and conditions of the Creative Commons Attribution license 3.0 Serbia (<http://creativecommons.org/licenses/by/3.0/rs/>).

EDUCATION



A NOVEL APPROACH TO GRAPHIC COMMUNICATION EDUCATION

Jure Ahtik , Tanja Nuša Kočevar 

University of Ljubljana, Faculty of Natural Sciences and Engineering, Ljubljana, Slovenia

Abstract: *Working as educators for future graphic communications experts we have to have two things in mind: how to prepare students for the real market opportunities and how to make their portfolios better. Scientific pedagogical approach was taken to do so and it is based on simulating a real-world environment: working with real world companies on real life examples, organizing students into advertising agencies where everybody has its predefined role, working in steps and competing with others. First step in our process is to divide all participants into teams of five. Each member of a team can choose his or her role: leader, designer, copywriter, speaker or technician. These roles were determined by studying different types of modern creative environments. Next step is team-building. Team has to begin working together and the final results of this cooperation is team's identity (name, logo). First real life assignment is done with a help of real advertising agency. We invite an art director to present a brief of a real order which every group will be working on for six weeks. Each week teams get live feedback from the agency. The assignment that follows in the next six weeks is done directly for the customer. This is possible because of the experience students get when working for/with advertising agency. The final step is organizing an event, a public exhibition of work that was done in the semester. The developed process prepares our students for the job hunting. In the paper, we explain which are the most important steps and approaches a modern educator should take to prepare their students for the real life. Results are presented as an analysis of final works, employees, co-operators and other experts in the process.*

Key words: education, graphic communication, advertising, market, team work

1. INTRODUCTION

Generations are changing, jobs are different as they were just a few years ago. Young generations of future employees have to be prepared in a different way, as the market has different expectations.

In the field of graphic communications, design, advertising ... changes are rapid and jobs have changed a lot. In the process of education, teaching stuff has a difficult task to adopt their approach of preparing young professionals to the new world. Learning basics is as important as it ever was. Having a solid base to build on is therefore necessary. But how to build on this base? What approaches should educators take, to prepare their students to the job market? How to accomplish, that students will have some real-world experience even before they finish their education? This is the main challenge in nowadays education. Teachers therefore should be encouraged to turn focus on different types of learning processes.

In today's environment of complexity and rapid change, work is characterized by collaboration among people from variety of disciplines. Tasks for solving complex problems are too big and diverse and thus require teamwork and many kinds of expertise (Davis, 2015).

Teamwork is a context of education, where communication for learning is stimulated and consequently student-centered experience could be purposefully achieved (Dunne et al, 2010). Benefits of teamwork in educational process are numerous. However, teamwork is not a preferable method for achieving design results for students. Therefore the instructor should emphasize the importance of teamwork skills to the students before the class and identify and underline those skills during team projects (Page et al, 2003).

2. METHODS

Simulating a real-world condition starts with creating a simulated advertising agency and follows with a team-building. Majority of work is done on two projects, first one with a help of a real advertising agency and the second directly to a real customer.

2.1 Creating a simulated advertising agency

A team is created by joining five students. Each one gets his one role in which he or she functions until the end of the semester. These roles are:

- art director (leader of the group),
- graphic designer,
- copywriter (and lecturer),
- pitcher (speaker, presenter) and
- technician (problem solver).

Roles were defined by analysing jobs in advertising agencies and represent main fields of work in any graphic or communication task. Art director, graphic designer, copywriter and pitcher come directly from real life and on the market already defined jobs. Technician on the other hand, has been added as an important part when analysing work that students do. We believe, that one person, that takes the burden of solving problems as soon as they appear, makes all the other jobs much more manageable.

Students can distribute roles by themselves and they cannot be changed or rotated. The main reason is that they have to learn how to react in situations that are outside of their comfort zones, the same as in a real world. This is also manageable because a semester lasts for only 15 weeks and sticking to the same role, even if you don't like it, can be accomplished. At the end, we usually get 10 groups that are competing to the end of the semester.

2.2 Team-building

Second step in our novel approach is team-building – each new established team has to begin working together and each member has to begin getting used to their new role (job). We have designed this team-building as a 4-hour workshop which results in a team identity. Time limited steps in this workshop are:

1. Each member in a team writes down 10 words that describe him.
2. Papers with words are passed to other members in a group and each one deletes two words in each paper he/she gets that he/she at least agrees with.
3. At the end, group has five papers where only two word are left on each. Altogether that's 10 words on which all members in a group can agree.
4. 10 words are then connected into the short story of any kind.
5. Pitcher has to stand up and read the story out loud.
6. The following step takes the most time: based on their story, each team has to build a sculpture. Before the team-build they are all told to bring all kind of materials they would like to use, such as old packaging, colour pencils, Legos, cardboard, glue etc. Using these materials they represent their stories in a sculpture that can be very abstract. Sculptures need to stand by themselves and can be any size the team wants (Figure 1).
7. Sculptures are presented.
8. Teams simplify their sculptures and design logos/signs out of it.
9. Teams define names of their simulated agencies, based on stories and sculptures.
10. At the logo and team name is joined and team's identity is established (Figure 1).



Figure 1: An example of a sculpture (left) and a final logo (right), made by team INIXI in 2018

Two main goals are accomplished: students start to work together as a team and each team has its new graphic identity through which they communicate in the future projects.

2.3 Working on a first project

The first project isn't done directly to the customer, but through and with the help of an advertising agency. It all starts with an agency introduction and follows with a brief or a real customer order the agency has. The presentation is usually done by an art director who is also present on seven following lectures. Students get a weekly feedback from the lecturer and from the art director as well. The goal of a first project is to learn how a real agency works and how students should respond to their tasks, according to their given roles in their teams. At the end, students give a final presentation of their solutions and usually one of them gets picked by the agency and developed to the end with the help of authors.

Example: in 2018 we worked together with PR agency Sidera on a project for Huawei Slovenija. The goal was to make Slovenian inspired EMUI themes for Huawei mobile phones. Eight of this themes are now available on EMUI theme store (Figure 2).



Figure 2: Few of the EMUI themes designed by the students as their first project

2.4 Working on a second project

The first project gives students some knowledge about the design process which is the base for the second project. The second project again starts with a design brief, presented directly by the customer, not the agency. Teams have seven weeks to complete the brief's goals. Weekly feedbacks and lectures support students' work, but mostly they work independently. Therefore students and lecturers have to take more responsibility for project development, from conception to completion, because there is no help from the advertising agency. Goals have to be completed, no matter what. Second project ends with a public exhibition.

Important note to that is, that students have to learn how to trust their own creativity and to become strong and self-conscious individuals who will be able to go out there and find a job that they prefer.

Example: in 2018 we worked directly with the Basketball association of Slovenian on promoting the world cup qualifying games for the Slovenian national basketball team (current European champions). Billboards and online advertising based on the winning visual identity are still being used at this moment (Figure 3).

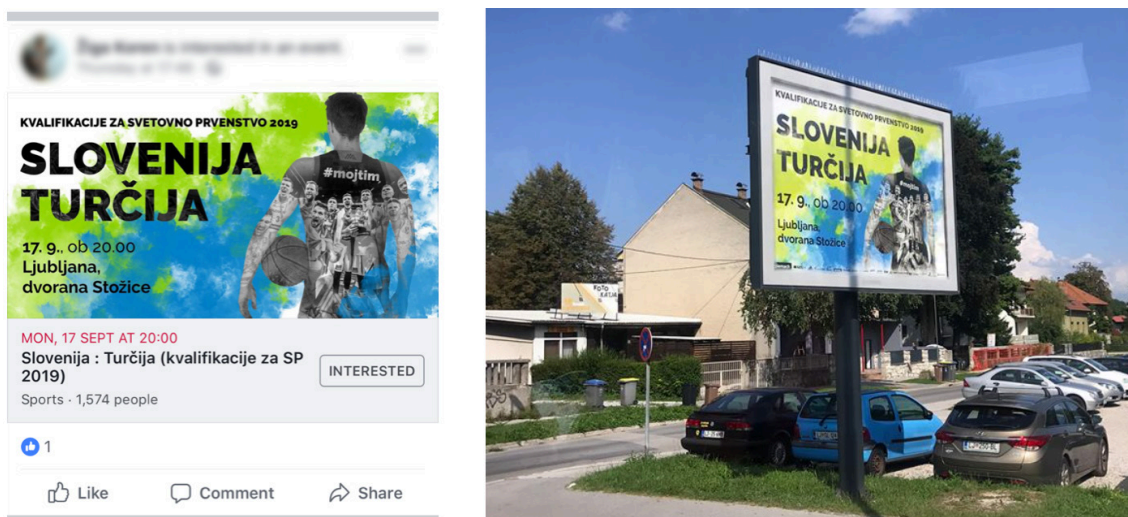


Figure 3: Facebook advertisement (left) and billboard with a winning visual identity

2.5 Creative process

When we work on both real-world projects, the creative process is divided into several stages:

1. **Research:** students have to understand a market that a customer is working on, to know competition and to be aware of target groups.
2. **Analysis or redefinition:** students have to understand customers' communication solutions and how they are using them.
3. **Outline and construction:** first step in constructing the solution is to apply rules, primary graphic elements and basic designs.
4. **Application and design:** students define final communication elements, such as logo, typography, colours, secondary elements, etc.
5. **Production:** based on application and design, all communication media is prepared.
6. **Usage:** the final stage is not done by students but by a customer. An important thing of this final stage is that an author is able to step out of the usage and that a customer is able to communicate by himself.

2.6 Using ICT

In the process of managing the described approach to graphic communication education, there is a lot of communication and task management that has to be done. Using information and communications technology (ICT) is a proposed and well established way of engaging students and lecturers to communicate. In the creative process there is usually a big amount of data that needs to be transferred between different parties and using cloud based solution has proven to be the most useful way to do it. It is also important to archive all history of changes that has been done to developing products. In our novel approach to education we use ICT for (Bouarab-Dahmani et al, 2015; Hamiti et al, 2014; Digitalna Slovenija 2020, 2016):

- communication (e-mail and other messaging tools, such as Google Talk or Discord),
- data sharing and commenting (cloud based storage, such as Google Drive or Dropbox),
- archiving (cloud based storage, such as Google Drive or Dropbox).

3. RESULTS

Students, who attended the course the last three years, were asked to deliver critical evaluation of the course by answering the online research questionnaire. Some of the students still study and some of them already have a job. The encompassed questions were qualitative as well as quantitative. Majority of questions asked students to specify their level of agreement or disagreement on a Likert scale (1–5), where 5 means that they totally agree and 1 means that they totally disagree. In some cases students could pick one from the given answers and there were also some questions where students could

response in a descriptive manner. 53 students filled out the questionnaire. The questions covered the following topics:

- general questions,
- course enrolment examination,
- team work,
- project work,
- general contentment with the course.

In the general part of the questionnaire students were asked to explain why they chose the course. The majority of them mentioned the positive recommendation of students from previous years as a motive. Many students selected the course because they like to design in general or they wanted to work with real clients and agencies. Those students want to build their career as graphic designers. Some of them were motivated by the interesting presentation of the course and some students wanted to challenge themselves in a team work. One of the students wrote that the reason for choosing the course was the fact that there is no written exam.

Too many students want to join the *Media visualization* course each academic year. With the aim to perform a quality course work, we decided to limit the enrolment with the enrolment examination. 50 students (95,3%) confirmed the examination as an appropriate method for enrolment limitation, and 23 students (52,3%) approved the content of the examination assignment.

Students predominantly have good opinion on team work. 25 students (47,2 %) valued team work as very good and only one student (1,9 %) as very bad. 34 (64,2 %) students established that their role in the team was appropriate, what shows that preliminary decisions about their work and estimation about their competences were correct.

Answers about the team composition revealed that group members did not perceive two roles as very important, these are the role of a pitcher (speaker, presenter) and the role of a technician (problem solver). Most of the students evaluated the two mentioned roles as important (level 4), for the pitcher 20 students (37,7 %) and for the technician 19 students (35,8 %). These two roles were also the only ones that were evaluated as not important at all by a few students, the pitcher by 3 (5,7 %) and the technician by 4 (7,5 %).

The questionnaire also enclosed questions about the guided team building that was performed at the beginning of the course. 28 students (52,8 %) answered that it was very important for creation of a team's identity and nobody valued that it wasn't important at all. 24 students (45,3 %) estimated that the team building was very important for further work of the team, but 5 students answered that it was not important (2 students chose option 1 and 3 students chose option 2 on the 1–5 scale).

Students also wrote some suggestions; draw of the team members, the possibility to change the role in the team and to have more designers in the group.

Project work was the next part of questionnaire. 30 students (56,6 %) evaluated presentations and the overall role of the agency's representative on the course very important. 5 of them (9,4 %) had neutral and 2 of them (3,8 %) had negative opinion.

Having weekly presentations, student could accompany other students work. 26 students (49,1 %) strongly agreed with that, 9 students (17 %) were neutral and 3 students (5,7 %) disagreed. Very similar is students' opinion on weekly reviews of their work. 54,7 % of them thought that they are important and 69,8 % of them believed that there was enough time for them each week. 28,3 % of students would like to have more time for reviews.

Students were asked for their opinion about lectures. Some of them would like to learn even more from agency representatives while they appreciated their opinion and their reviews.

In the conclusion, 28 (52,8 %) students strongly agreed that they improved their teamwork competence. 34 (64,2 %) students think that the course extensively influenced the project realization capabilities in the field of media communications, and 27 (50,9%) thought that the course definitely influenced their critical relations to their own works.

A little smaller percent of students (43,4 %) strongly agreed that they improved their presentation skills, 28% agree and 22,6 % are neutral. Only 2 students (3,8 %) strongly disagreed and 1 student (1,9 %) disagreed with the statement mentioned above.

One of the last question was "Do you think that the course improved your employment possibilities?" 15 students (28,3 %) thought that their employment possibilities strongly improved, 22 students answered that the possibilities improved, 13 students were neutral, 2 students disagreed and only 1 student strongly disagreed with that.

4. DISCUSSION

According to the results where the students' opinion on the course are presented, we can establish that the course meets the students' initial expectations. However, the survey reveals some interesting suggestions and opinions we are going to consider in the future, such as:

- adjusting roles in each team to distribute the amount of work more equally,
- changing the content of the enrollment exam and
- inviting more real-world lecturers/experts into the course.

Through the whole process mentors evaluated actual results as well as student's individual progress respectively subject-specific competencies.

5. CONCLUSIONS

Simulating a real-world environment has proven to be a useful way of educating a future graphic communications professional. We strongly believe, that students, educated by our approach, have more work experiences and better portfolios to show to their future employees. An important goal that we have accomplished with our approach is that we are able to show students, how does advertising industry look and feel like and to help them decide if this really is something they would like to do. In the future, we are planning to use and develop this novel approach on post graduate study program (beginning in 2018/19 academic year). We have also began testing the approach on smaller groups of students and more targeted projects what also shows very good results.

Working with real agencies we would like to teach students other skills too, such as negotiating and selling ideas, maintain schedules, appreciate deadlines, and with introducing the teamwork, we would like to demonstrate the experience of working in an industry with people of diverse ideas, abilities, opinions and noteworthy, various routines.

6. ACKNOWLEDGMENTS

We would like to thank the following advertising and PR agencies that trusted and helped us develop our education approach: Yin+Young, Agencija 101, Sidera and Rubikon GRAL.


7. REFERENCES

- [1] Bouarab-Dahmani, F., Tahi, R.: "New Horizons on Education Inspired by Information and Communication Technologies", *Procedia - Social and Behavioral Sciences* 174, 602-608, 2015. doi: 10.1016/j.sbspro.2015.01.589.
- [2] Davis, M.: "Interdisciplinarity and the Education of the Design Generalist", *The Education of a Graphic Designer* (Allworth Press, New York, 2015).
- [3] Digitalna Slovenija, Digitalna Slovenija 2020, Strategija razvoja informacijske družbe do leta 2020, Digitalna Slovenija, 2016, URL: http://www.mju.gov.si/fileadmin/mju.gov.si/pageuploads/DID/Informacijska_druzba/DSI_2020.pdf (last request: 2018-06-21).
- [4] Dunne, E., Rawlins, M.: "Bridging the Gap Between Industry and Higher Education: Training Academics to Promote Student Teamwork", *Innovations in Education and Training International* 37(4), 361-371, 2010. doi: 10.1080/135580000750052973.
- [5] Hamiti, M., Reka, B., Baloghová, A.: "Ethical Use of Information Technology in High Education", *Procedia - Social and Behavioral Sciences* 116, 4411-4415, 2014. doi:10.1016/j.sbspro.2014.01.957.
- [6] Page, D., Donelan, J. G.: "Team-Building Tools for Students", *Journal of Education for Business* 78(3), 125-128, 2013. doi: 10.1080/08832320309599708.



© 2018 Authors. Published by the University of Novi Sad, Faculty of Technical Sciences, Department of Graphic Engineering and Design. This article is an open access article distributed under the terms and conditions of the Creative Commons Attribution license 3.0 Serbia (<http://creativecommons.org/licenses/by/3.0/rs/>).

IMPLEMENTATION OF CAPACITIVE TOUCH SENSORS ON ARTWORKS FOR AUGUMENTATION OF USER EXPERIENCE OF BLIND AND VISUALLY IMPAIRED USERS

Marija Jevtić, Deja Muck, Helena Gabrijelčič Tomc 
University of Ljubljana, Faculty of Natural Sciences and Engineering,
Department of Textiles, Graphic Arts and Design, Ljubljana, Slovenia

Abstract: *This research presents the results of the study in which the artworks are exhibited to blind and visually impaired persons and an automatic verbal tour guide with capacitive sensors is implemented. The aim of the research is the development of a prototype for audio interpretation of 3D printed artworks for enhancement of the experience of blind and visually impaired persons. The proposed solution enable the blind and visually impaired persons to touch and hear information when accessing the 3D printed object, i.e. after the approaching of the 3D object and the user's touch there is a programmed synchronised turn on of the voice explaining the set of information about the object. For each touched form (shape) of the artwork the blind and visually impaired person has a complete insight in relation with other shapes in the vicinity, and consequently the user is able to experience the whole artwork, to comprehend what it is all about, which artistic movements or age it belongs to, the handwriting of artist, and in the context of experiencing the exhibition place, the concept of the exhibition, etc. In front of each artwork there is a plate in Braille alphabet with the name of the artist, year of its creation, used technique, and the name of the gallery. Further, in the results the technology of the sensors is presented, their composition and the implementation in 3D printed objects is explained and based on a usability testing advantages and disadvantages of the presented application of capacitive sensors are critically discussed.*

Key words: capacitive touch sensors, 3D printed artwork, blind and visually impaired, accessibility, augumentation

1. INTRODUCTION

Most museums and galleries present and exhibit reproductions of sculptures, paintings and other artefacts interpreted with the languages (usually 3D tactile) that enable the accessibility of the art for blind and visually impaired persons. These models are usually hand-made by artists and thus provide artistic 3D interpretation of the original artwork. However, many 2D art works and new media products are still not available for the target groups with visual limitations. Here, some rear exceptions (museums) have to be mentioned, i.e. State Tactile Museum Omero (Ancona, Italy) or The Art Institute of Chicago (Illinois, United States of America) that implemented tactile displays dedicated to blind people. In order to increase and accelerate the "translation" process of interpretation from visual into tactile several computer aided approaches have been developed over the past few years. Recent studies suggest that only tactile interpretation with 3D models (even in the case when they optimally reproduce the original image) is not enough for a complete understanding and enjoyment of an artwork (Feucht et al, 2018). In Figure 1 computer approach is presented that aimed to facilitate experiencing an artwork. The Kinect sensor is placed at the distance of 1 m from tested model. The test starts with calibration of manual tracking (requested by applied method) and the registration of a manual model on users' hands (Wang et al, 2012).

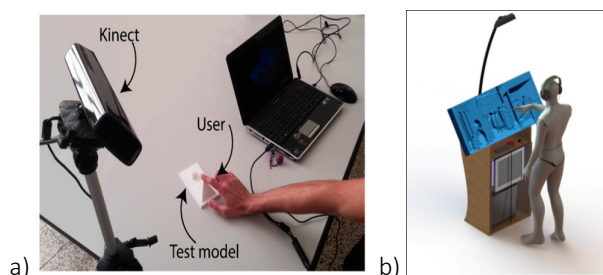


Figure 1: a) Touch identification hardware b) user in front of a model

Blind people who understand the original artistic work are, in fact, subject to many factors (e.g. the person's sensitivity and capability, previous experience, the size and quality of the tactile model); for this reason, when the interpretation is verbal, the quality of verbal guidance is essential in order to appreciate the best possible reproduction of artistic relief of a particular image. Such verbal description is usually provided by an informed person (employees of the museum, accompanying person, etc.) that help the blind person to build a complete mental image of the tactile model. However, the presence of another person can be viewed as a limiting factor in the enjoyment of works of art, since a blind person is forced to discover through the perspective of someone else; art is a language that requires autonomy and freedom to be fully captured (Foreword et al, 2009).

In the presented research the technical part is primarily considered and, consequently, the functioning mode of a tactile transfer of voice, where capacitive sensors play an important role. The task of sensors is to collect different information regarding certain processes. These units can be used before or after the processes. Sensors detect properties that can be measured and converted into some useful form, usually into electric signals. Sensors are also named convertors. Converter is device transforming signal of one physical size into signal of another physical size. Capacitive sensors for detection of moving are contact or non-contact devices having ability to measure precisely / detect position and / or position change of moving object. The following example in Figure 2 illustrates the installation of the capacitive sensor in the model, which there can be tested voice reproduction on.

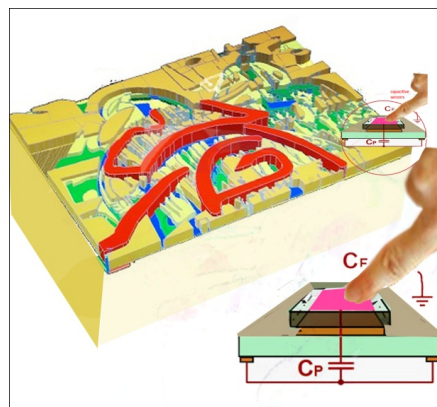


Figure 2: Instalation of the capacitive sensor in an artwork

The accessibility of the artworks should be enabled with the adequate technical equipment of the galleries. In Figure 3a the example of a blind person trying to experience the artwork is shown, on the left there is a 2D painting and on the right a 3D object (Okamoto et al, 2013).

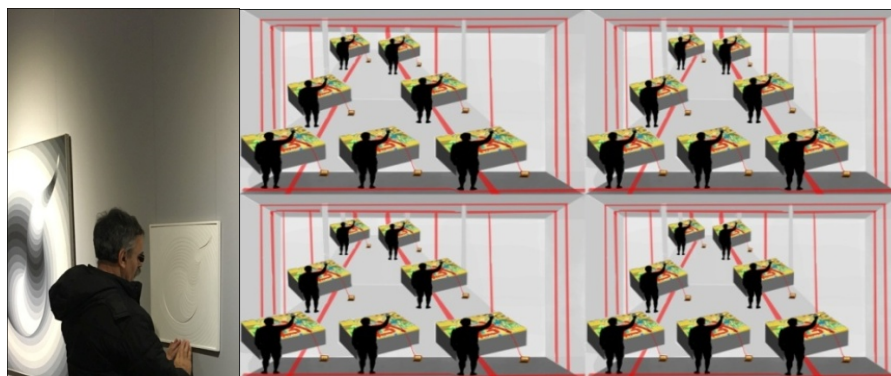


Figure 3: 3D object, 2D picture and blind person (left), people in the gallery receive information about work with the help of an automatic verbal guide (right)

The aim of the research is the development of the methodology and a prototype of a technical solution for audio interpretation of 3D printed artworks for enhancement of the experience of blind and visually impaired users. With this purpose the capacitive sensors were used and implemented in the installation of 3D printed objects that improved the user experience when interacting with the art work.

2. METODS

In Figure 4 experimental concept is described including on one side users/participants (blind and visually impaired persons) and capacitive touch sensors. When new trends in the art for the blind are introduced new frontiers are opened giving the space for the implementation of sensors, speech synthesizer, 3D printed objects etc.

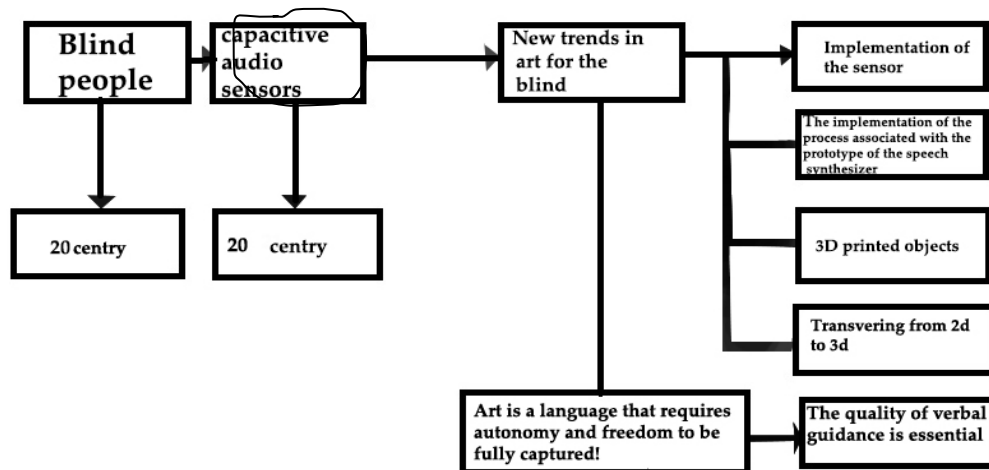


Figure 4: The schematic presentation of experimental

In the study twenty blind or visually impaired persons participated. The performance of the analysis took place in the art gallery where the artworks were exhibited. Five of the respondents said that there was no need to introduce audio guidance, due to an explanation in the form of Braille beside the model. These persons were blind from the birth and have excellent knowledge of Braille alphabet. Fifteen respondents confirmed the need for the audio guidance, due to the fact that they have lost the vision later in the lives and were not blind from the birth. Consequently, they did not learn Braille alphabet and for them the verbal guidance was indispensable. After the implementation of the process associated with the prototype of the speech synthesizer and verbal guidance, the testing was performed on a target group, that discovered the disadvantages and advantages of the performance and whether the synthesizer with the capacitive sensor was sufficiently persuasive to allow the blind and the visually impaired to fully grasp the artwork. The results of the testing is presented in Table 1 and 2, where Table 2 represents the results of the exploration of capacitive sensors according to their speed, sensitivity, pass time, financial profitability, and wider use (Bert, 2018). The examples in Figure 5 show a 3D printed model and a 3D model shaped in Auto Cad with the marked locations where the capacitive sensors can be touched.

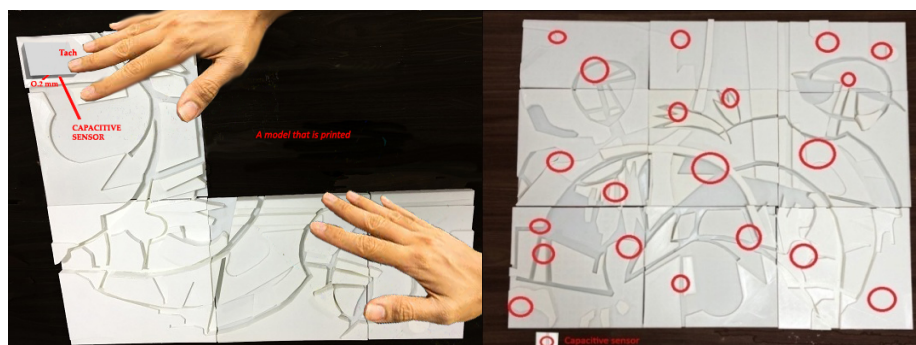


Figure 5: The appearance of a capacitive sensor (left) and 3D printed model with the locations of the capacitive sensors (right)

In Figure 6 the functions of capacitive touch sensors and Installations of the automatic verbal guides in the gallery are presented, which enable the visitors to receive information about artworks.

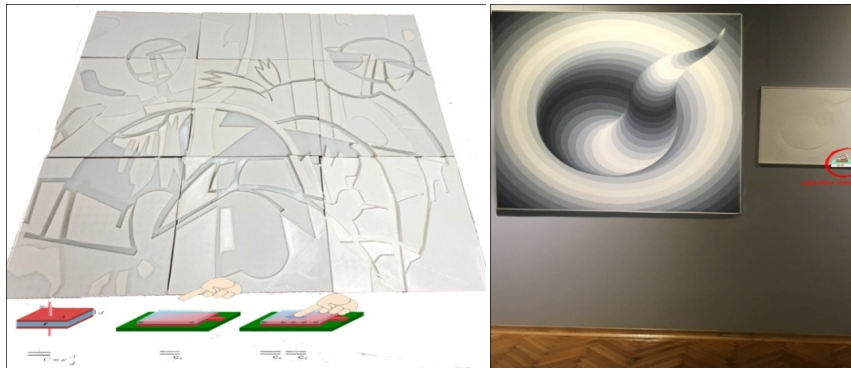


Figure 6: Functions of capacitive touch sensors (left), Installations of the automatic verbal guides in the gallery (right)

3. RESULTS

The results of the research were 3D printed objects (carefully planned and prototyped with 3D modelling). 3D printed objects were developed from the artworks and each 3D model had implemented a speech sensor, which activation was enabled with the touch of the 3D object's surface. After being entitled to approach the 3D object and to touch its surface, a voice sensor transmitted audio information about the artwork, its properties, its surface and its size, what color it is, what is the texture, in which direction it extends, where the dents and bumps are, how are the edges formed and if they are smooth or sharp. In Figure 7 the activities of the participants are schematically presented.

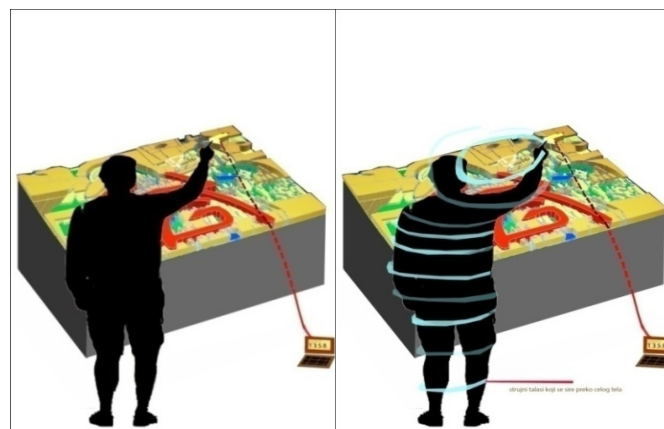


Figure 7: Participants in the research (visitors in the gallery) that through voice command and touch activities receive information about the artwork using an automatic verbal guide including capacitive sensors.

This research was conducted in order to discover if there is necessary to install capacitive sensors into printed models. Touch capacitive sensor were installed in each exhibited 3D objects allowing the visitors to activate it by moving hand over it. During the examinations each participant gave data about the age and how old he/her was when he/her lost the sight. In Table 1 the participants are presented with gender, age, time of vision los and if according to their experience they consider capacitive sensors as usefull solution or not. Based on this table, it can be concluded that majority (12) participants of both genders were able to use successfully the capacitive sensors and express the opinion that their implementation is useful. When analysing the gender of the participants, the results show that 6 women and 6 men evaluated the capacitive sensors as useful and the same gender ration was also present for the participants that were not favourable for the proposed solution.

Table 1: Results of the participants' evaluation of the implementation of capacitive sensors in 3D printed artworks

No.	Gender	Time of vision los	Age	For (yes) / against (no) capacitive sensors
1	Lady	58	83	yes
2	Lady	50	72	yes
3	Lady	55	65	yes
4	Lady	12	56	no
5	Lady	32	50	yes
6	Lady	41	55	yes
7	Lady	11	39	no
8	Lady	19	47	no
9	Lady	22	68	yes
10	Lady	42	59	yes
11	Man	0	44	no
12	Man	44	75	yes
13	Man	26	45	yes
14	Man	24	65	no
15	Man	43	50	yes
16	Man	7	41	no
17	Man	36	67	yes
18	Man	15	38	no
19	Man	33	57	yes
20	Man	50	84	yes

Further, usability testing was performed with a questionnaire about the capacitive sensors' sensitivity, speed and time of turning on the audio guide, about financial effects and wider use (table 2). Here, 18 participants were questioned and their evaluation about the sensors properties were recorded. In Table 2, we can conclude that capacitive sensor developed for the analysed 3D models were not evaluated as useful for wider use. In our opinion this was due to the plastic materials, which the sensors were built from. The participants responded to financial profit with great portion of dislikes, while they have better evaluated pass time, speed; and the best evaluated was sensitivity.

Table 2: Evaluation of the properties of capacitive sesors

Participants	Sensitivity	Spid	Release time	Financial profitability	Wider use
1	Good	Good	Good	Good	Medium
2	Good	Good	Medium	Medium	Medium
3	Good	Medium	Good	Medium	Good
4	Good	Medium	Good	Good	Bad
5	Good	Good	Medium	Medium	Medium
6	Good	Medium	Good	Good	Good
7	Good	Good	Medium	Medium	Medium
8	Medium	Good	Good	Medium	Bad
9	Good	Good	Medium	Medium	Medium
10	Good	Medium	Good	Medium	Medium
11	Good	Good	Medium	Good	Bad
12	Good	Good	Medium	Medium	Bad
13	Medium	Good	Good	Good	Bad
14	Good	Medium	Good	Good	Medium
15	Good	Good	Good	Medium	Bad
16	Good	Good	Mediium	Good	Bad
17	Good	Medium	Good	Good	Medium
18	Good	Good	Medium	Medium	Bad

4. CONCLUSIONS

In the paper the successful collaboration of the art and the technology is presented. Capacitive touch sensors were implemented in 3D models done from the artists in order to enable the blind and visually impaired persons more comprehensive experience of the art. In further researches, the technology of capacitive audio sensors is going to be improved and new printed artworks are going to be tested. Besides, for the valuable testing of usability and user experience the performance and issue based matrices are going to be performed with additional tools and analysis.

5. REFERENCES

- [1] Bert T.: "Sensitivity to Social Contingency in Adults with High-Functioning Autism during Computer-Mediated Embodied Interaction ", Plan de Estudios Combinados en Medicina, PhD thesis, Facultad de Medicina, Universidad Nacional Autónoma de México, Mexico City, Mexico, 2018.
- [2] Feucht, F.C.; Holmgren, C.R.: "Developing Tactile Maps for Students with Visual Impairments: A Case Study for Customizing Accommodations", *Journal of Visual Impairment & Blindness* 112(2), 143–155, 2018.
- [3] Foreword., Catherine K.: "Groundwork for a History of Blindness", (French University, 2009).
- [4] Okamoto, T., Mitsui, C., Yamagishi, M., Nakahara, K., Soeda, J., Hirose, Y., Miwa, K., Yamano, A., Matsusha, T., Uemura, T., Takeya, J.: "V-shaped organic semiconductor with solution processability, high mobility, and high thermal durability", *Advanced Materials* 25(44), 2013, 6392 – 6397. doi: 10.1002/adma.201302086.
- [5] Wang, M., Chang, J., Jens, K., Zhang, J.J.: "A Framework for Digital Sunken Relief Generation Based on 3D Geometric Models" The Media School, Bournemouth University, Poole, Germany. *The Visual Computer*, 28(11), 1127–1137, 2012. doi: 10.1007/s00371-011-0663-y.



© 2018 Authors. Published by the University of Novi Sad, Faculty of Technical Sciences, Department of Graphic Engineering and Design. This article is an open access article distributed under the terms and conditions of the Creative Commons Attribution license 3.0 Serbia (<http://creativecommons.org/licenses/by/3.0/rs/>).

DETERMINING THE FRAMEWORK FOR ŽIŽKA MONUMENT 3D REPRODUCTION

Tanja Nuša Kočevar ¹ , Anja Škerjanc ¹, Ana Porok ²,
Tomaž Jurca ², Matej Pivar ¹, Helena Gabrijelčič Tomc ¹ 

¹University of Ljubljana, Faculty of Natural Sciences and Engineering, Department of Textiles,
Graphic Arts and Design, Chair of Information and Graphic Arts Technology, Ljubljana, Slovenia

²Plečnik House, Ljubljana, Slovenia

Abstract: *In this research the development of the framework for 3D interpretation of Plečnik's Žižka Monument is presented. Jože Plečnik was a very known Slovenian architect, that design many personal, public and sacral buildings, mainly in Ljubljana, Wien and Prague. The design of Jan Žižka (Czech commander-in-chief) monument was never realised and was therefore a subject of the research of Plečnik's specialists. The features of the monument can be, according to their shape, topology and level of details, basically divided in two parts, i.e. 1. architectural part that is chalice-like stage and 2. eight human and one animal (horse) models that are more organic and highly detailed. The experimental part presents a framework for the inventory of available documentation that were collected and categorised, processed and selected with the purpose of further procedures. After the examination and the analysis of the documentation, the next step of determination and extraction of graphic, artistic and stylistic information from the documents were performed and implemented in 3D models of architectural and sculptural part. The research included also preparation of the models, 3D printing, assembly and finishing. The last phases of the framework were defined as exhibition, promotion and evaluation. In the results the overall framework for the creation and construction of 3D interpretation is presented and estimated.*

Key words: Žižka monument, architect Jože Plečnik, cultural heritage, 3D reproduction, framework determination

1. INTRODUCTION

Implementation of workflows including digital data and media in documentation, preservation and presentation of cultural heritage is a multi-layered process. After the acquisition of the target data, the processes of data storage, archivation and managing are interlaced with the aim of keeping the data accuracy and adding them values with the processing and analysis. In the steps that follow, i.e. presentation, interpretation and reproduction, 3D technologies (3D scanning, 3D printing, 3D computer aided modelling and design) are widely used and applicable due to their accuracy, repeatability and mostly non-invasive nature. The implementation of these technologies in the framework, however, should not be overlooked especially to the more subtle aspects of the cultural object(s) included in the study, i.e. preserving the details of the work and author's style.

3D printing is strongly established in cultural heritage for preservation, restoration and reproduction of cultural assets (Balletti et al, 2017). 3D printed objects can be in cultural heritage used for study and research, as an accessible media for blind and visually impaired persons in museums and galleries, for restoration and reproductions, for 3D interpretations as didactic tools etc. Authors Saorin et al (2017) presented 3D interpretation of sculptural heritage as an educative tool. In the research, 2D digital and tangible 3D printed replicas were produced and tested as spatial interpretation features on the users (students). The results shown that 3D approach (3D models, 3D prints, 3D interactive presentations) was more successful in teaching and learning process in comparison with classical 2D approach (Saorin et al, 2017).

Many researchers discovered that 3D prints are risk-free accurate reproductions of a cultural and natural heritage artefacts which physical properties are important. Authors Wilson et al (2018) demonstrated that when considering semantic differentials, exploratory factor analysis and statistic physical properties of 3D printed replicas can be evaluated by the visitors of the museums. In the research, six different 3D prints were analysed produced with different 3D printing technologies. Methodology inductive creation of the categories was used to define categories of the replicas surface texture, weight and aesthetic value. The results found out that the most important was verisimilitude, robustness, quality (Wilson et al, 2018).

Rossetti et al. used rapid prototyping and 3D printing to construct accessible interactive 3D architectural objects of cultural sites. 3D models, 3D printed tactile reproduction and interactive solutions that enabled to the blind persons the audible explanation of the semantic information were tested. The results presented that the approach was a suitable accessible extension of the exhibited objects that offer to the blind person's autonomy and satisfying exploration of the cultural heritage (Rossetti et al, 2018).

The aim of the research is the establishment of a framework and the presentation of the initial phases of 3D reproduction of Žižka monument, i.e. a non-realised work of a known Slovenian architect Jože Plečnik. The main challenge of the research was the documentation, which was inconsistent in terms of included elements (architectural part, number of figures) and figures details (role of the figures, requisites), and consequently the definition of the robust framework that would result in successful 3D interpretation.

2. EXPERIMENTAL

The proposal for the 3D reproduction of Žižka monument was launched by the Plečnik House in Ljubljana. Jan Žižka was a famous Czech army leader and the monument was meant to be settled in Prague. The monument was never realised, presumably due to some nationalistic standpoints of the Czech committee in Žižka monument competition (year 1913) (Berglund, 2017).

At the beginning of experimental only the starting and final framework phases were known, i.e. documentation and final exhibition of the 3D reproduction in Plečnik house (title of the Exhibition: Plečnik and the Sacred). During the development-creative process, the following phases were defined: 1. analysis of documentation, 2. interpretation with 3D modelling, 3. 3D printing, 4. assembling and finishing, 5. exhibition and promotion and 6. evaluation, as is presented in Figure1.

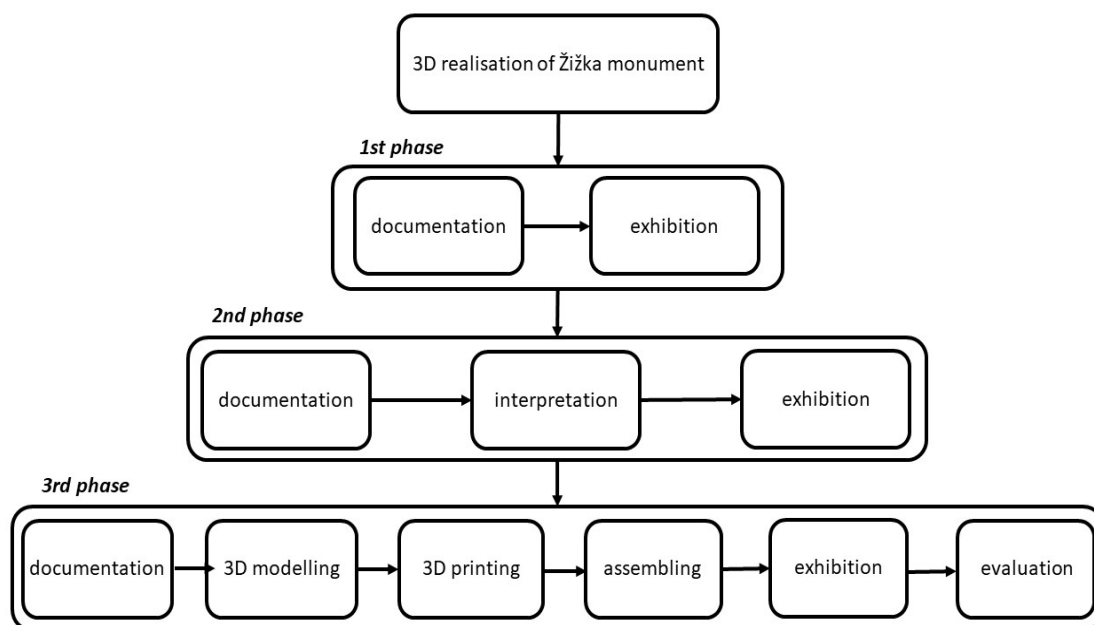


Figure 1: Framework of 3D interpretation of Plečnik's Žižka monument

3. RESULTS AND DISCUSSION

In the results the framework is presented with the determined sequence of the research phases and the steps for the creation of the 3D reproduction. Besides, initial 3D prototypes and 3D models of the geometrical stage of the monument and complex humans' and animal models are shown.

3.1 Documentation and analysis

Documentation

Plečnik drew many sketches and architectural plans for the monument and presumably the last versions were also the inspiration for the construction of a wooden scale model, which documentation is actually limited to only one photo with a side image acquisition and non-detailed features image presentations. Besides a photo of a wooden scale model, the accessible documents (provided by Plečnik house and The Museum and Galleries of Ljubljana) of monument were: two hand drawn sketches of the author, one architecture plan and one two pages long written source (Berglund, 2017). The provided documents were not consistent, revealing different possibilities of performance and especially including almost no information about the details of monument elements (figures and requisites). Consequently, the research work included gathering and analysis of additional historical (written and image) references about Husite movement, Husite soldiers, Czech national hero Jan Žižka and battle and prayer equipment (caliche, sword, shield) and Plečnik expression style (when presenting national leaders, horses and and battle and prayer requisites).

Processing and analysis of the documents

According to the professional opinion of the specialists in Plečnik creations the photo of wooden scale model of the monument could have been taken as the most relevant reference for further work, however in the photo there were only silhouettes of the elements reproduced. With the image processing the parts of the photo were processed with the aim to reveal additional details of the elements as is presented in Figure 2.

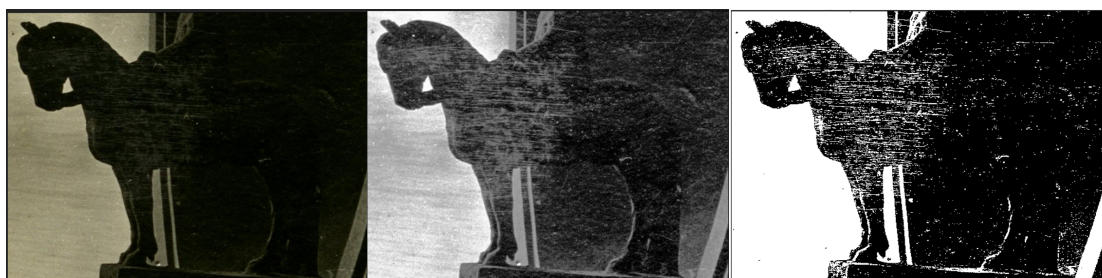


Figure 2: Part of the photo "Plečnik house" (Berglund, 2017) of a wooden model and two processed images

The results of image processing discovered that the methodology was not successful enough, so that the further analysis was based mainly on observational studies of the photo of wooden scale model and with the cues of spatial perception deduction of the possible topology of the parts of the monuments. Framework of documentation phase is presented in Figure 3.

3.2 3D modelling

Before 3D modelling started the parts of the monument were divided in two main parts considering the geometry, shapes and forms in the illustrated and photo references, i.e. architectural part and sculptural part. Architectural part consisted of monument foundation: a.) three level structure - base with stairs and plato level carrying the pillars and the altar carrying main caliche and cavalry Jan Žižka), b.) caliche in a form of one quarter of hemisphere and c.) five pillars. The sculptural part included: a.) one monk and one husite soldier standing on the plato level; b.) military commander Jan Žižka on the horse standing on the altar and five Husite soldiers each standing on pillars. The sculptural part was further analysed and in 3D modelling phase considered as figures (monks, commander and Husite soldiers), clothes, shoes and accessories (coats, trousers, caps, etc.) and requisites (caliche, swords, shields, helmets).

The 3D modelling phase consisted of two experimental parts. The first part was the analysis of possible automatized approaches for extracting 3D models from hand drawn illustrations and one photo of wooden scale model (Berglund, 2017; Chen et al, 2013; Jackson et al, 2017). The second part was the manual detailed modelling which special attention was on figure/cloths/requisite details and geometry of the architectural part. In Figure 4 framework of the 3D modelling phase is shown.

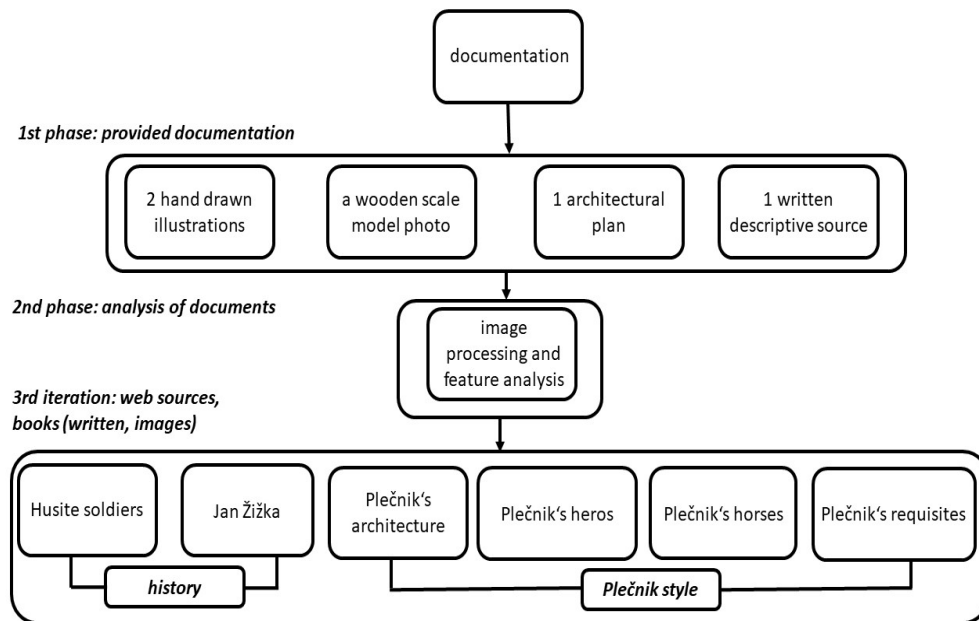


Figure 3: Framework of documentation phase and analysis

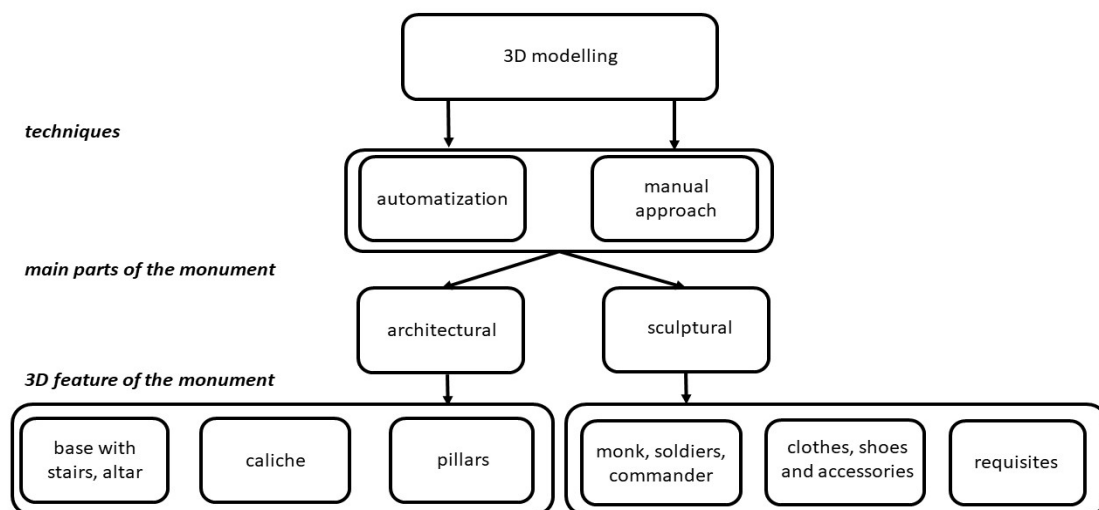


Figure 4: Framework of the 3D modelling

The first part of figures creation was performed using a programme Make Human, an open source tool for character modelling. The characters were then transferred to 3D program Blender where dresses were added and other characters' accessories, such as swords, shields, a chalice and helmets. When modelling the figures, sculpt tools were used to add details and their correct features. For creation of clothes, the process of cloth simulation was used and sculpt tools for correction of details. On figure 5, a 3D model of a soldier is shown.

The architectural part of the monument was also modelled using Blender. The most challenging part to create was a cut-off sphere/chalice and changing thickness of its wall. The sphere is the largest part of the monument and bearing in mind the FDM printing technology it was necessary to create a model with a suitable well modelled topology.

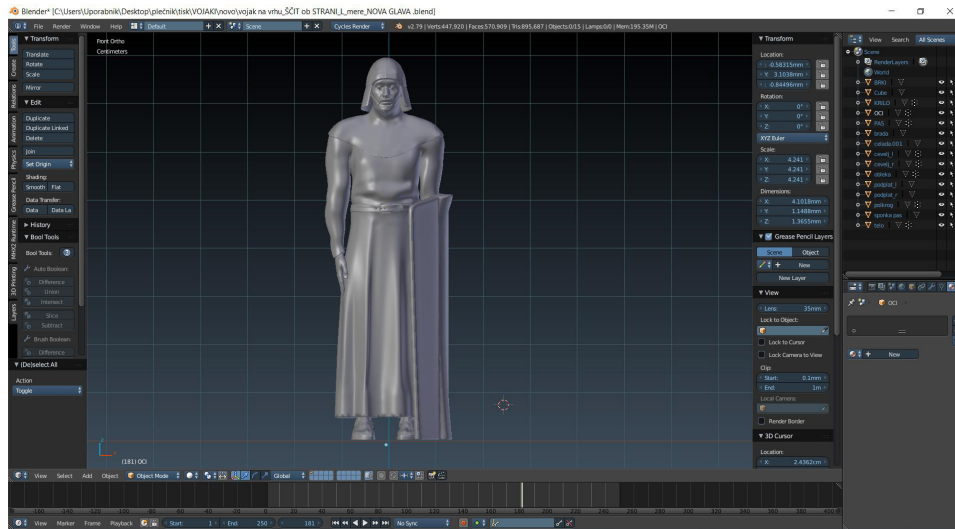


Figure 5: 3D model of a soldier in Blender computer programme

3.3 3D printing

Before the 3D printing, the models were prepared according to the topology properties (level of details) of the parts of the monument's 3D model. The framework of 3D printing and preparation of the models is presented in figure 6.

3D model of the architectural part was divided (cut) into smaller elements according to the demands of the used 3D printer. When cutting the model, it was necessary to create smaller object with planes that can be easily put and glued together. It is also important to print the model that doesn't require much support structure for printing. Our monument was divided into 58 smaller parts. 3D printing process was performed with two technologies, i.e. stereolithography (figures with clothes, accessories and requisites) and FDM (architectural parts).

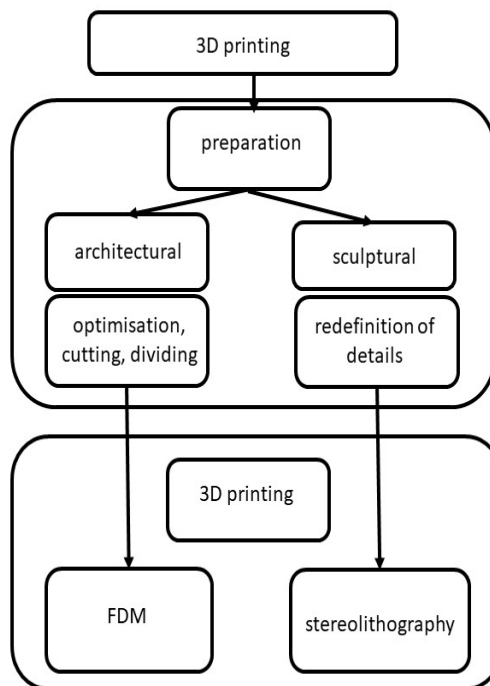


Figure 6: Framework of 3D printing and preparation of the models

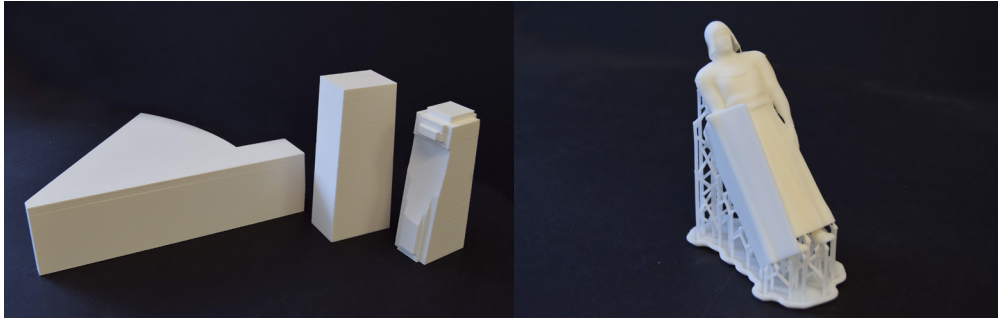


Figure 7: Parts of the monument printed with FDM 3D printing technology on the left and a model of a soldier printed with stereolithography on the right

3.4. Assembling and finishing

Assembling and finishing of the 3D printed reproduction included gluing of the architectural parts, sanding with sanding paper, UV fixation of 3D objects printed with stereolithography, removing of the support structure, filling seams of the model with putty and colouring with matte white colour spray. Figure of framework of assembling and finishing of 3D printed objects is presented in Figure 8.

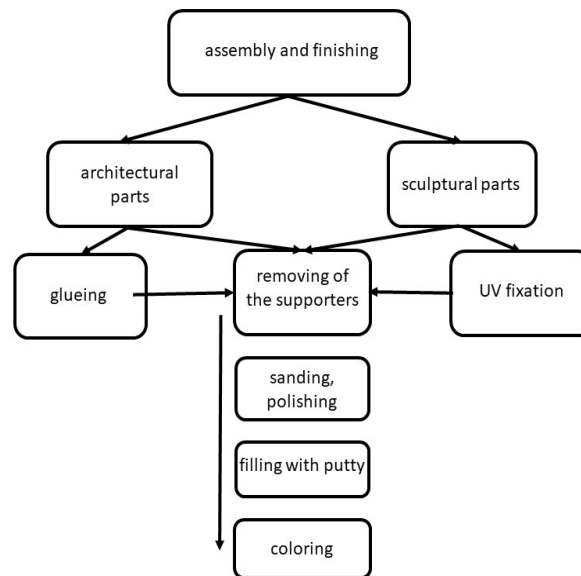


Figure 8: Framework of assembling and finishing of 3D printed objects

On figure 9, process of removing supporters from a model printed with stereolithography is presented and the phase of gluing architectural parts of the model printed with FDM technology.

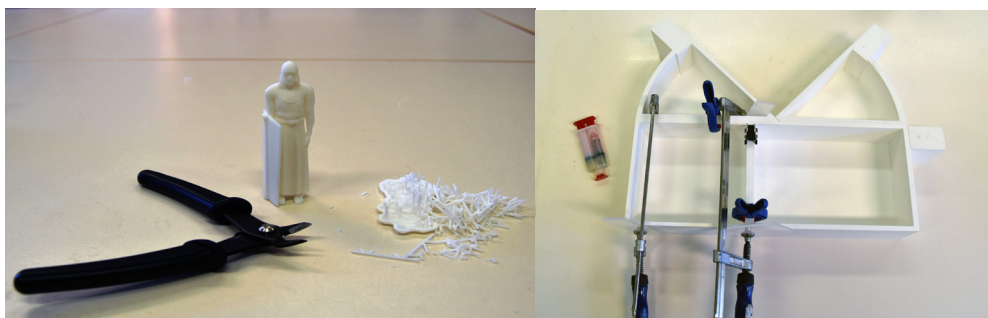


Figure 9: Two phases of 3D printed model assembling, removing of supporters and glueing

3.5 Exhibition and promotion

The model of the Žižka monument is going to be presented in The Plečnik house in Ljubljana. Due to its fragility, especially models of human figures and a horse have some small, fragile parts, is going to be protected with the transparent cover. Visitors of the museum will be able to explore and evaluate the scale model of Plečnik's unrealised project.

3.6 Evaluation

In further researches, the evaluation of the results is going to be performed in more phases. Printed 3D interpretation is going to be analysed considering geometrical accuracy and reproduction of the style and details in architectural and sculptural parts. Moreover, the focus of the analysis is going to be also the observers' estimation, when comparing references, visualisation and 3D printed reproduction.

4. CONCLUSIONS

In the contribution the development of framework for Žižka monument 3D reproduction is presented. Due to non detailed illustration and image references 3D reproduction was not possible to be performed with a noticeable level of interpretation that was implemented especially in 3D modelling phase. With the use of 3D technologies it was possible to "make alive" Žižka monument that otherwise would remain documented only in the few references. The 3D printed monument is going to be a permanent item exhibited in Plečnik house in Slovenian capital town Ljubljana.

5. REFERENCES

- [1] Balletti, C., Ballarin, M., Guerra, F.: "3D printing: State of the art and future perspectives", *Journal of Cultural Heritage*, 26, 172-182, 2017. doi: 10.1016/j.culher.2017.02.010
- [2] Berglund, B.: "Castle and Cathedral in Modern Prague: Longing for the Sacred in a Skeptical Age", (Central European University Press, London, 2017), page 280.
- [3] Chen, T., Zhu, Z., Shamir, A., Hu, S.M., Cohen-Or, D.: "3-Sweep: Extracting Editable Objects from a Single Photo", *ACM Transactions on Graphics*, 32 (6), 195, 2013.
- [4] Jackson, S.A., Bulat, A., Argyriou, V., Tzimiropoulos, G.: "Large Pose 3D Face Reconstruction from a Single Image via Direct Volumetric CNN Regression", *IEEE International Conference on Computer Vision (ICCV, Venice, Italy, 2017)*, pages 1031-1039.
- [5] Rossetti, V., Furfari, F., Leporini, B., Pelagatti, S., Quartaa, A.: "Enabling Access to Cultural Heritage for the visually impaired: an Interactive 3D model of a Cultural Site", *Procedia Computer Science*, 130, 383-391, 2018. doi: 10.1016/j.procs.2018.04.057
- [6] Saorín, J.L., Carbonell-Carrera, C., Cantero de la Torre, J., Meier, C., Aleman, D.D.: "Three-Dimensional Interpretation of Sculptural Heritage with Digital and Tangible 3D Printed Replicas", *Turkish Online Journal of Educational Technology* 16 (4), 161-169, 2017.
- [7] Wilson, P.F., Stott, J., Warnett, J. M., Attridge, A., Smith, M. P., Williams, M. A.: "Museum visitor preference for the physical properties of 3D printed replicas", *Journal of Cultural Heritage*, 32, 176-185, 2018. doi: 10.1016/j.culher.2018.02.002



NEW INITIATIVE TO EDUCATE THE “POSTPRESS: BINDING, FINISHING AND MAILING” AS OBLIGATORY COURSE-UNIT AT ÓBUDA UNIVERSITY

Piroska Prokai , Csaba Horvath 

Óbuda University, Institute of Media Technology and
Light Industry Engineering, Budapest, Hungary

Abstract: *This online course-unit (lecturing at the Obuda University) assembled by the authors, is a primer that serves a dual role for today's students of graphic communication. The course is an introduction to the process of post-press technologies and the different kind of bookbinding technologies, what is solid base for any printer professional that wants or needs to learn how does it works the end of in the printing house. The knowledge based on our revised manuscripts of well-known Hungarian printing industry professionals as Lajos Papp (Horvath et al, n.d.) and Gyorgy Toth (Prokai et al, n.d.). The curriculum contains presentations, videos, tests and tasks for home work. The course is presented during one semester. The credit point value of the course is 2. The students are following the lectures online week by week. They need to pass six tests and complete six home works assignments to monitor their progress. This course is designed for the students of Obuda University.*

Key words: postpress, book-binding education, finishing technologies, e-learning

1. INTRODUCTION

This English language online course-unit (lecturing at the Obuda University) assembled by the author, is a primer that serves a dual role for today's students of graphic communication. The main task of the students in this course is to design and virtually create their own future efficient and sustainable enterprise in graphic communication using the binding, finishing and mailing tool box while also considering the associated social responsibility (CSR) aspects.

This course is designed for the students of Obuda University, who are studying the undergraduate academic course of “Light industry engineering” and their specification is the graphic communication. The fulfilment of this course in English language is criteria to get their degrees.

2. UNIVERSITY, FACULTY – THE PLACE OF EDUCATION

Obuda University is a dynamic and thriving institution located in Budapest, heart of Hungary, heart of Europe. For 132 years of existence, the educational excellence has remained paramount. The history of our institution is spanning over three centuries. Obuda University was established as of 1 January 2010, as a legal successor of Budapest Tech – and its legal predecessors, namely Donat Banki Technical College, Kalman Kando Technical College, and the Technical College of Light Industry. The fundamental mission of the University is to serve science and the future by transferring and developing knowledge at high standards and by research and innovation. The high level education is going on in various faculties and centres. These faculties are found in the parts of Budapest and Szekesfehervar. Obuda University has six faculties:

- Banki Donat Faculty of Mechanical and Safety Engineering,
- Kando Kalman Faculty of Electrical Engineering,
- Keleti Karoly Faculty of Economics,
- John von Neumann Faculty of Information Technology,
- Rejto Sandor Faculty of Light Industry and Environmental Engineering,
- Alba Regia Faculty of Engineering (Szekesfehervar).

Obuda University constantly builds and develops a competitive institution of higher education meeting the criteria and regulations of the European Higher Education Area (Figure 1).

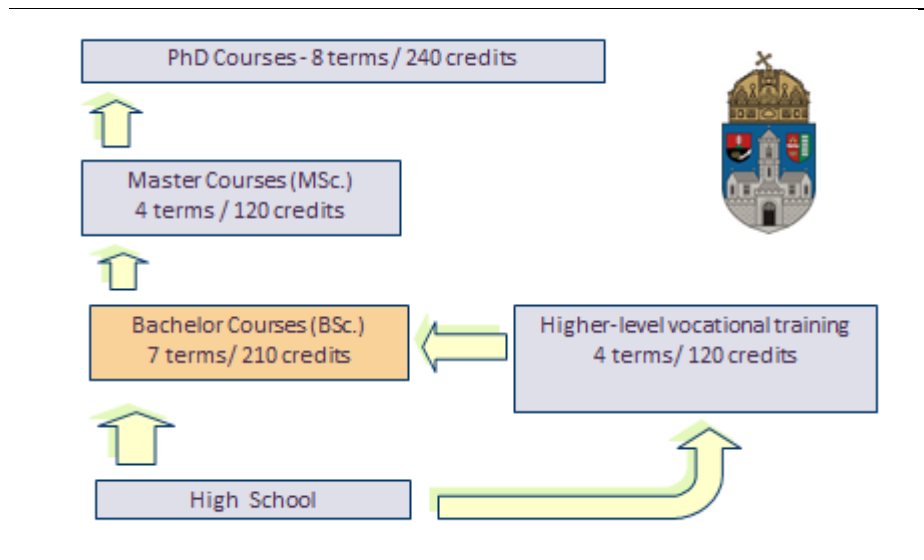


Figure 1: Education system of Obuda University

Rejtő Sándor Faculty of Light Industry and Environmental Engineering offers three BSc programs: Light Industry Engineering, Industrial Design Engineering, Environmental Engineering, and a MSc program in Light Industry Engineering.

- The bachelor's program in Light Industry Engineering prepares students for the control and supervision of manufacturing processes related to their specialisation. After completing the fundamental courses in engineering, with basic technical and engineering skills they can choose from the following specialisations: Print media, packaging design and technologies; Industry system development and quality management.
- Engineers, with a BSc degree in Industrial Design Engineering will be able to initiate, compile and implement projects, to carry out analyses using relevant design methods and to professionally justify the implemented work procedures. They will have competence in comprehensive product design, taking into consideration aesthetic, usability, market, safety, and implementation aspects, as well as historic, cultural, social, economic, industrial and natural environmental factors related to industrial design and product development. Specialisations: Product Design and Product Management.
- BSc Environmental Engineers will possess the necessary up-to-date vocational and technological skills needed to reduce and prevent environmental damage and pollution. They are trained to be capable of making environmental studies. We offer the Light Industry specialisation.
- Those who earned the BSc degree can continue their studies on the Light Industry Engineering MSc program. The training is organised in cooperation with the Faculty of Wood Sciences of University of West Hungary. Graduates of the BSc program may also continue their studies in the Engineering Teacher Master program in cooperation with Trefort Ágoston Centre for Engineering Education.

3. CRITERIA SUBJECT

By the regulation of Obuda University the undergraduate students have to cover four credits from the criteria subjects to get their degrees. An example can be seen on the Table 1. The criteria lectures units are optional presented in English or German languages.

This subject is prepared and proposed to the student who had chosen the "Print media, Packaging design and technologies" specialization instead of the Hungarian language blended version. The Obuda University's future aim is to educate bilingual engineers, who can speak fluently in English beside their mother language. It is the reason we created this subject in English. Our faculty's dean motivates the teacher staff to create more e-learning subjects as an obligatory. Our project is the pilot one.

Table 1: Curriculum of Light Industry Engineering course (BSc.) for full time students

No.	Main fields of study	Credit [Pts]
1	Natural Science Fundamentals	41
2	Economics and Human Studies	20
3	Technical Fundamentals	75
4	Specializations <div style="margin-left: 20px;"> <input type="checkbox"/> Print media, Packaging design and technologies <input type="checkbox"/> Fashion product technologies <input type="checkbox"/> Industrial system development and quality management </div>	69
5	Optional course-units	6
6	Criteria Subjects (English or German) - optional	4
7	Thesis	15
Sum:		210

4. E-LEARNING COURSE UNIT OF “POSTPRESS: BINDING, FINISHING AND MAILING”

The knowledge base of the course is founded on the new American and German. It is an English language online course unit, managed by the E-learning system of Obuda University. This optional criteria subject is educated by credit-based (2 credit points). The length of the programme is one semester (14 weeks), opened for all undergraduate students (not only for OE students).

4.1 Why the bookbinding?

The graphic arts industry has experienced tremendous change in the last quarter century. While the prepress and press areas have received the majority of the attention from the trade media, the bindery and finishing areas have gone largely unnoticed ... until now. The product variety of the finishing industry is illustrated in the overview shown in Figure No.2. In this subject we focus the bookbinding operation.

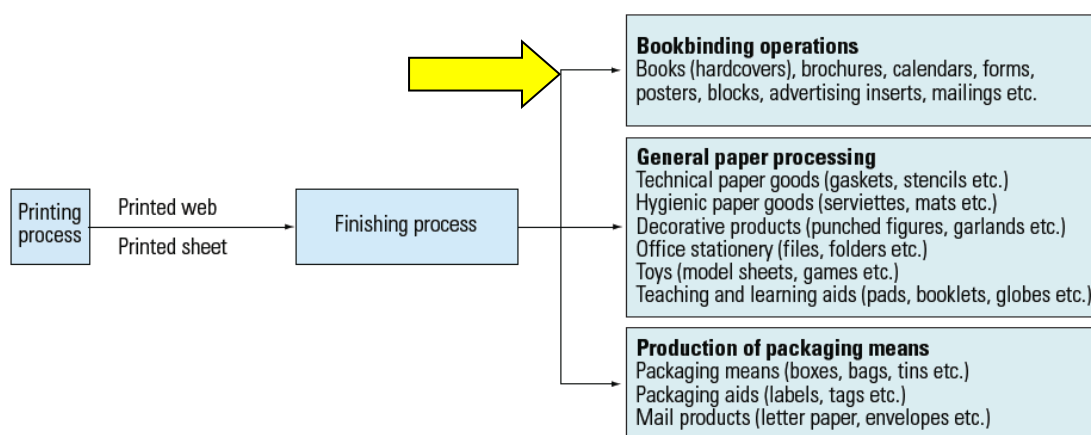


Figure 2: Print finishing products (Kipphan, 2001)

The course is a primer that serves a dual role for today's students of graphic communication. It's an introduction to the world of binding, finishing and mail preparation. It's also a first pass – a necessary first coat – that will provide a solid base for any printer who wants or needs to know more about the postpress technologies, about the final word of printing. The presentation has been recorded with voice-over with help of Camtasia software.

The curriculum contains presentations, videos, tests and tasks for home work. The course is presented during one semester. The credit point value of the course is 2. The students are following the lectures online week by week. They need to pass six tests and complete six homework assignments to monitor their progress. They finish the course unit with a closing test. The description, brief curriculum and the requirements are on the Table 2.

Table 2: Printing technologies No.3 (Binding, finishing and mailing) – brief curriculum and requirements

ÓBUDA UNIVERSITY						
Rejtő Sándor Faculty of Light Industry and Environmental Engineering			Faculty	Media Technology and Light Industry		Institute
Hungarian title of the course:		Nyomdaipari technológiák 3. (kötészet és továbbfeldolgozás)			Neptun code:	RMTNT3NTNE
English title of the course:		Printing technologies No. 3 (bookbinding and finishing)			Credit:	3
Type (compulsory/obligatory):		optional, criteria	Education Type	online	Semester :	7
Study field: Light Industry engineering						
Lecturer:		Dr. Csaba Horváth, Piroska Prokai				
Required preliminary knowledge:		Nyomdaipari technológiák 2. (Printing technologies No. 2)				
Weekly teaching hours:	Lecture:	1	Practical work:	0	Laboratory work:	1
Exam type:		e	Language of course:	English	In timetable:	Thursday 09:50 -- 11:30
CURRICULUM						
Abstract:						
The course is a primer that serves a dual role for today's students of graphic communication. It's an introduction to the world of binding, finishing and mail preparation. It's also a first pass – a necessary first coat – that will provide a solid base for any printer who wants or needs to know more about the postpress technologies, about the final word of printing.						
Requirements						
Attendance at lectures:						
It is online subject. The rules of education and exam directory (TVSZ) are the guidelines.						
Exams and tests (types, data)						
Test	6 pcs		6 x 5 points			
Home work	6 pcs		6 x 8 points			
Closing test	on 14th week		32 points			
Improver closing test	1 st week of examination period					
Requirements for qualification:						
The students have to write min. 6 tests, and outline min. 6 home works. Closing test is obligatory.						
0 - 49	(1)	fail				
50 - 59	(2)	pass				
60 - 69	(3)	satisfactory				
70 - 84	(4)	good				
85 - 100	(5)	excellent				
In the latter case: re-take examination paper in week 14 or/and once more within the first 10 days of the examination period.						

The detailed curriculum can be followed on the Table 3 and Table 4. All the files (marked ■) are loaded to the platform of E-learning system. The students load up their home works and closing test to this platform. The six tests are passed by the students on the platform of E-learning system (<https://elearning.uni-obuda.hu/>).

Table 3: Printing technologies No.3 (Bookbinding and finishing) – the detailed curriculum of Lectures No. 1-7

Lecture	Subject	Test/Homework
No. 1	<p>Introduction (Presentation No. 1)</p> <p>The course "Bookbinding and finishing" is an online course. The education is organized by the E-learning system of Óbuda University.</p> <p>The tests, the home works, the practices and the valuating are managed through the E-learning system.</p> <p>Lecturer: Dr. Csaba Horvath, Piroska Prokai</p> <ul style="list-style-type: none"> Teachers' introducing (video) Sample of Europass CV (pdf) Sources to learn, required Binding, Finishing and mailing: The Final Word (Tedesco et al, 2005), Handbook of Print Media (Kipphan, 2001) Source to learn, proposed Sappi 06 The Standard (Sappi North America, 2012) Bookbinding (Morlok et al, 2018) 	<ul style="list-style-type: none"> <u>Students cv's</u> <p>Students are needed to create and submit their CV's in English. Format: Europass</p>
No. 2	<p>Cutting and Die-cutting</p> <ul style="list-style-type: none"> Presentation No.2 Cutting: step by step (educational video) PERFECTA 132 TS High-speed Cutter (video) MM Granit three-knife trimmer (video) Bobst SPrintera 106 PER Die cutter (video) 	<ul style="list-style-type: none"> <u>Test No.1</u>
No. 3	<p>Folding</p> <ul style="list-style-type: none"> Presentation No.3 Buckle fold principles (animation video) Knife fold principle (animation video) Operating of MBO M80-K folder (video) Herzog+Heynemann Pharma Line folder (video) 	<ul style="list-style-type: none"> <u>Test No.2</u>
No. 4	<p>Assembling Blocks, Saddle Stitching, Sewing</p> <ul style="list-style-type: none"> Presentation No.4 Kolbus book block production (video) Saddle stitcher Primera (video) MM Ventura sewing machine (demo video) Meccanotecnica sewing (video) 	<ul style="list-style-type: none"> <u>Test No.3</u>
No. 5	<p>Perfect Binding</p> <ul style="list-style-type: none"> Presentation No.5 MM Alegro perfect binder (video) Kolbus perfect binder (video) Adhesive binding: tips and tricks (pdf) 	<ul style="list-style-type: none"> <u>Test No.4</u>
No. 6	<p>Case Making and Book Cover Producing</p> <ul style="list-style-type: none"> Presentation No.6 MM Colibri backgluing (video) MM Diamant Bookline (video) MM Ribbon inserting (video) Hardcover vs. Paperback: Which option is better? (pdf) Hard cover case maker (video) 	<ul style="list-style-type: none"> <u>Test No.5</u>
No. 7	<p>Finishing Short Print Runs (Digital Finishing)</p> <ul style="list-style-type: none"> Presentation No.6 Photobook technology (video) Paperfox equipment (videos) Digital finishing (pdf) 	<ul style="list-style-type: none"> <u>Test No.6</u>

Table 4: Printing technologies No.3 (Bookbinding and finishing) – the detailed curriculum of Lab practice No. 8 - 14

Practices	Subject	Test / Homework
No. 8 - 9	<i>Design and making of name card and wall calendar</i> <ul style="list-style-type: none"> ▪ Presentation No.8-9 ▪ Working regulations in the printing lab (pdf) ▪ A practical guide making name card (video) ▪ A practical guide to make personalized wall calendar (video) ▪ Blazon of Óbuda University (jpeg) ▪ Sample for name card design (pdf) ▪ Graphic Design (pdf) (Prokai et al, n.d.) ▪ Design of calendars (URL) 	<ul style="list-style-type: none"> ▪ <u>Homework No.1-2.</u> First the student design their name card and personalised wall calendar for next year. Than they make and finished them alone following the video intentions in the printing lab. (Lab supervisor supports them.)
No. 10	<i>Art of Marbling</i> <ul style="list-style-type: none"> ▪ Presentation No.10 ▪ How to paint on Water for Paper Marbling? (video) 	<ul style="list-style-type: none"> ▪ <u>Homework N.3</u> The students produce different patterned paper sheets with marbling art. They can use them for endpaper or cover of their handmade book. (Lab supervisor supports them.)
No. 11-12	<i>Assembling a hard-covered book by handmade technology</i> <ul style="list-style-type: none"> ▪ Presentation No.11-12 ▪ Handmade bookbinding tutorial (video) 	<ul style="list-style-type: none"> ▪ <u>Homework No.5</u> Students assemble by hand a hardcover, sawn book step by step from recycled paper using their marbled paper. (Lab supervisor supports them.)
No. 13	<i>Visit in a bookbinder company</i> <ul style="list-style-type: none"> ▪ Presentation No.13 (Intention for the visit.) ▪ Introducing the company (video) 	<ul style="list-style-type: none"> ▪ <u>Homework No.6</u> Students create a report about the company visit focusing the things what they liked. The company visit guided by teachers.
No. 14	<i>Closing test (45 minutes)</i>	

5. CONCLUSION

The “Printing technologies No.3 (Binding, finishing and mailing)” course unit was launched in fall semester of 2018, two month ago. That’s way we haven’t got enough experiences about it. We only hope this course-unit will be a successful and popular program very soon, supported the marketing of the paper-based communication.

The Obuda University is so open to collaborate with other universities:

- to split the education of ‘Lean and green printing’,
- to develop this course-unit together,
- students from other universities are welcome.

In this case you should contact to the author to get login, etc.

6. ACKNOWLEDGEMENTS

We say a special thanks to Mr. Tibor Sándor – who is the managing director of Müller-martini Magyarország Kft. for his help. He supported us with videos and a lot of technical material to make the presentations.

7. REFERENCES

- [1] Horvath, C., Papp, I.: "Nagyüzemi könyvgyártás", (book under preparation)
- [2] Kipphan, H.: "Handbook of Print Media", (Springer Verlag, Heideleberg, 2001.), page 1208.
- [3] Morlok, F., Waszelewski, M., Wright, C.: "Bookbinding: A Comprehensive Guide to Folding, Sewing, & Binding", (Princeton Architectural Press, Princeton, 2018.), page 420.
- [4] Prokai, P., Tóth, G.: "Kötészeti technológiák", (book under preparation)
- [5] Sappi North America: "The Standard 06 - Bindery Techniques", (Sappi North America, Boston, 2012.), page 88.
- [6] Tedesco, T. J., Clossey D., Hershey, J.: "Binding, Finishing and Mailing: The Final World", (PIA/GATFPRESS, Pittsburgh, 2005.), page 388.



© 2018 Authors. Published by the University of Novi Sad, Faculty of Technical Sciences, Department of Graphic Engineering and Design. This article is an open access article distributed under the terms and conditions of the Creative Commons Attribution license 3.0 Serbia (<http://creativecommons.org/licenses/by/3.0/rs/>).

HOW TO MASTER MODULAR REALITIES IN ART, SCIENCE AND TECHNOLOGY — WITH NEW ELECTRONIC MEDIA, AND FOR A BETTER FUTURE OF WORK

Peter Purg 

University of Nova Gorica, School of Arts, Nova Gorica, Slovenia

Abstract: *The MAST project is developing an applied study module at the intersections of Art, Science and Technology, combining methodologies and practices that intertwine the academic sphere closely with the Culture and Creative Sectors. Nurturing a critical perspective on the historical, economical, social and above all cultural relevance of this interdisciplinary blend within the new digital shift, MAST develops innovative, ICT-enhanced teaching and learning methods. Students from different countries and disciplines will, under mentorship of engineers, scientists and artists, in partnership with relevant NGOs and industry partners, jointly tackle challenges emerging from the paradox between the obviously disparate agendas of Europe's ambition towards innovation on the one side, and the need for social equity on the other. In the present contribution, besides discussing MAST's Visual Identity Design in Pedagogical Context as well as contextualizing Web-design and Production as a uniquely Transversal Academic Collaboration process, Social Media shall be presented in their potential of becoming a Collective Reflection Tool, whereas the electronic publishing potential of Open Courses on Interoperable Platforms will be delineated. These four key aspects will indicate a vision of sustaining the impact of new curricula for a fair digital future that may keep a dynamic balance between the (European, competitive) need for simultaneously sustaining innovation and social agendas. The first piloting year of MAST poses the overarching challenge about the future of work in the context of electronic media, and seeks to develop (in both students, professionals and academia) positive digital-domain worker profiles. Integrating new media and electronic publishing approaches, these workers are able to think about future independently and freely, in a bold trans-disciplinary manner, and act ethically across Creative & Cultural Sectors and high technologies.*

Key words: electronic dissemination, social media, web-design, visual identity, open courseware, social agenda, innovation

1. INTRODUCTION TO THE MAST PROJECT

Currently in its first year, the project "Master Module in Art, Science and Technology" (MAST) is developing an applied study module at the intersections of art, science and technology, combining methodologies and practices that will intertwine the academic sphere closely with the industry realms of the Culture and Creative Sectors (CCS). Nurturing a competent perspective on the historical, economical, social and above all cultural relevance of this interdisciplinary blend within the new digital shift, the project will apply innovative, ICT-enhanced teaching and learning methods. Gradual work-placement combined with support for spin-out or start-up and career self-management will instigate such innovation capacities in both students and the academy that are linked to the real and foreseeable CCS industry needs, but still critically reflect (its) realities and paradoxes. MAST is already in 2018/19 offering a range of five international workshops (Portugal, Austria, Hungary, Croatia, Slovenia), where students from three universities will face an interdisciplinary challenge, seeking innovative solutions with support of excellent mentors, artists, scientists, engineers, curators and producers.

However, to enable a most positive collision of the three realms, the project will need to let creatively collide (and combine, if not blend) the tech-innovation paradigm and the social equity agenda models. Technologies are always political and have a social impact, in that they codify certain values into material culture thus enabling (or limiting) individual and societal possibilities. Therefore, hard-won values — like social justice, strong labor, gender equality, and quality culture — will be linked with new digital innovations. In its tectonic ethical orientation, the module shall explore how progressive Social Europe (SE) agenda values can be coded into innovations, as well as how social groups and movements may use media and (high) technology to forward the values of SE. Experts from different fields will learn how to understand artists (i.e. their poetical, metaphysical, philosophical and ethical premises) and translate these divergent ideas into possible solutions that may reach all the way from industry-oriented innovative technologies to social innovation.

This GRID 2018 contribution may be considered especially relevant and interesting in the "Electronic publishing and new media" context due to the MAST consortium agreeing on a method that integrates the pedagogic process with the visual identity and website development of the project (BA students taking over the responsibility, under deep involvement of internal and external mentors). Besides discussing Visual Identity Design in Pedagogical Context and contextualizing Web-design and Production as a uniquely Academic Collaboration process, the Social Media use shall be sketched in its potential of becoming a Collective Reflection Tool, along with a presentation of the electronic publishing potential of Open Courses on Interoperable Platforms. These four key aspects will delineate a vision of sustaining the impact of new curricula for a fair digital future that may keep a dynamic balance between the (European, competitive) need for innovation on the one hand and social agendas on the other.

2. THE CHALLENGE BETWEEN INNOVATION AND SOCIAL AGENDAS (BACKGROUND)

For Europe to successfully remodel its economy in a global competition, it must re-imagine innovation on —European terms. MAST therefore attempts to create sea t of teaching and learning (as well as collaboration) methods by which the art, science, and technology crossover can be embedded with SE values, regardless of the particular application domain. Technologies are always political and have a social impact, in that they codify certain values into material culture, thus enabling (or limiting) individual and societal possibilities (c.f. the current perspective on creative value chains in "Mapping the Creative Value Chains executive summary by the European Commission (2017)). In this sense, technologies are a form of legislation outside the traditional space of politics: they are rarely democratic, transparent, or even acknowledged. Science is currently being productively challenged by participatory practices of citizen science and coproduction, and thus MAST represents a hybrid approach combining principles from art, design, sociology, politics, and other key Social Sciences and Humanities disciplines, as well as engineering and technology.

Surpassing the 'Silicon-Valley' modeled technical culture that in its deep structures principally opposes the social cohesion in both the national and local, as well as a global sense, MAST promotes a clear European vision as well as academic practice that aims to succeed in integrating the values of Social Europe into the entire chain of technology creation as well as use (including education). Studies agree (European Comission, 2017) that Europe is hamstrung by the tension between regressive technological ideology and what this project considers to be essential European social values of its ICT practitioners and their communities. The MAST graduates as European ICT, creative media and applied arts or design creators will need to be able to consider the social costs within a design as readily as they can do that with power, efficiency or the ergonomic aspects of a design or prototype. Over 90% of Europe's search market belongs to Google, with the leftovers divided up between mostly non-European enterprises ("Here's How Dominant Google Is In Europe" (Rosoff, 2014)) and this lack is increasingly echoed for mobile platforms, browsers, etc. but even worse for whole genres of product ideas! Nevertheless, MAST embraces the fact that particularly in the Art+Sci+Tech crossover, there are key Soft skills that can only be developed on higher education level through well-designed training, in order to achieve positive social progression & sustainability (STEPS, 2014).

Many of the most important production tools for digital media artists today are not the results of for-profit companies, but collaboratively designed using the ascending methods of free/open non-proprietary software and other technologies, as well as horizontal coordination of work and management models. Art and design training contributes to business, while art and commerce have always had a productive tension. The MAST consortium does ignore this tension, but rather to address it fully. This includes not only teaching business culture, but more broadly organizational techniques, which may be expressed in many forms. In particular, the project will seek to explore the ways that art, science, and technology crossover may be socially impactful in a variety of enterprise organizational forms, including business, non-profit, free/open software, platform collaborative, and others. MAST thus develops the intellectual framework and concrete repertoire by which responsible research and innovation can engender ICTs that strengthen the best qualities of the European social model. It does this by developing an educational module on HE level that corresponds to all relevant educational quality criteria (Quality and relevance in higher education (European Comission, 2018a). With it the graduate students of the MAST module will be in capacity to build an overall better electronic (publishing, communication, business etc.) world; their co-workers can have better jobs, and their users or customers can have products and services that do not undermine their culture, their way of (quality) life.

3. NEW APPROACHES TO ELECTRONIC PUBLISHING (METHODOLOGICAL DISCUSSION)

The dissemination activities lie at the core of the MAST project and are focused on outreach actions that will spread the knowledge and collaboration outside of the consortium and partners directly involved in the project. Such actions will deepen collaboration and attract members of the industries towards potential collaboration on future educational activities and career development. The key objectives are to make the target groups aware of the MAST project, and keep following its messages as well as key (interim) results; to provide all needed mechanisms and an electronic platform (website, newsletter and social media) that informs the target groups about the project; and not least to build MAST as a brand that the target groups can associate with and use in their own communication as well as multiply accordingly for exploitation reasons, to eventually broaden the project's impact not only horizontally (taking over of models and practices) but also vertically (policy and business impact).

3.1 Visual Identity Design in Pedagogical Context

To reflect the academic as well as social and not least economic values and production principles argued for above, the visual identity of the MAST project was conceived in collaboration with students, who took over the leading role in graphically designing the logotype and the outlines of the project's visual communication. A student who responded to an open invitation at the School of Arts, University of Nova Gorica, and was chosen for the task, accepted the first brief and discussed the visual identity at the project's kickoff meeting with the representatives of the project consortium (in which two partner institutions are explicitly concerned with dissemination activities).

The logotype of the project has been gradually developed subsequently by including both lexemic (letter M for MAST) as well as semantic elements (drop as a graphical element of most diverse possible meanings, denoting both natural sciences as well as the fluid character) of the project. Eventually a project-internal Visual Identity Handbook has been developed, with a special consideration of its use in digital realms (black-and-white, optimized low-resolution usage). The student involved in the development of the logotype is foreseen to take part in the piloting of the MAST module as such, in order to better reflect its identity and iterate own development of graphic design skills. The social (collective) reflection of the developed logotype was a key factor in its development, for which collaborative (Google) online documents were used in order to assure everyone's access not only to the development files in real-time, but also to give possibility of relevant, structured feedback, the tracking of versions etc.

3.2 Web design and Production as a Transversal Academic Collaboration

The web-design process was integrated into the pedagogical process even much deeper than the graphic design of the visual identity. Together with the undersigned project coordinator, the lecturer of web-design in the first year of the undergraduate programme (Digital Arts and Practices) developed a stratified task, in which the students gradually developed possible wireframes for the project website, therein considering the possible semantic and symbolic interactions of the art-science-technology fields. Simultaneously they were discussing (and applying) the abovementioned Visual Identity, with which they developed a mutual interdependence (both were developed at the same time). Their guest mentor, also a renowned media artist, became the main programmer and webmaster to the MAST site.

After several sessions the most convincing website designs were chosen (by a mixed group of mentors and peers), upon which a most compatible Wordpress web-design theme was chosen and purchased, also reflecting the functional needs of the educational context that the project is primarily embedded in. The most interested and at the same time skilful student was chosen to collaborate on preparatory activities for the development of the theme into the actual website, upon which the below signed project coordinator and the PR (communications) officer of the project gradually filled in the contents of the website. At the time of writing the present contribution, the website launch at www.mastmodule.eu (MAST Consortium, 2018) is shortly due, and the social media presence is to be gradually developed on public level. A revision and consolidation of the electronic public relations (publications) strategy in the light of the recent project developments is planned within the following weeks.

3.3 Social Media as a Collective Reflection Tool

The public events of the project that will have an impact not only on the academic communities involved, but also on the broader environment, consist of intensive learning events and so called pop-up events, as well as an annual "Interfacing Academy" event for showcasing and evaluation of the developed innovations, as well as the academic module as a whole. These events shall be promoted and disseminated publically via the project website and the related social media (Twitter, Facebook and Instagram profiles of MAST) that will all involve relevant stakeholders from in and around the MAST community, as well as externals. They shall involve a broad variety of stakeholders, including students, artists, engineers, scientists, guest lecturers, policy makers and industry representatives. The dissemination of central messages of the project will be delivered through a regular newsletter, sent out to a gradually assembled list of relevant e-mail addresses as well as featured on the website and promoted through relevant social media.

The social media activity will be designed and coordinated (moderated) in a way to stimulate feedback that will be sought both about the structure and contents of the module's curriculum, as well as the quality and relevance of the (prototyped, or speculatively designed) innovations that the student groups will develop during the academic cycle. The data will be eventually used for evaluation the project and fine-tuning the structures of the curriculum (courses, assessment forms, methodologies, inter-course connections etc.).

3.4 Open Courses on Interoperable Platforms

The success of initiatives such as MAST depends on an effective knowledge sharing strategy. This strategy will consider five areas of emphasis: organizational context, interpersonal and team characteristics, cultural characteristics, individual characteristics, and motivational factors. Each of these dimensions needs to be approached with a different method, but in an integrated fashion considering its interdependencies. Each consortium partner will contribute with different perspectives (such as industry, research, arts and science) on the different components of MAST (curriculum, mobility, partnering strategies, teaching methodologies and disciplines) to create a best practices book that will outline a collaboration framework for Art, Science and Technology and best practices featured therein. It is to be available publically in the form of an e-book via a web service, at no cost.

The consortium shall develop a so called 'cross-sector innovation transfer' business plan, based on online media. This integrated format shall both deepen and widen the impacts of MAST, including long-term sustainability, the main focus being on how to assure a lasting continuation and/or legacy of the project activities. This activity shall also develop a knowledge transfer model through a free of charge (open) online course, with a wide variety in both artistic and technical content, involving experts from various fields. The course shall equip participants with digital, entrepreneurial and design/art knowledge and thus foster students from art and cultural institutions to acquire interdisciplinary skills and experiences with emerging technologies. Even if designed as a widely offered online course, it shall be used also in the entry stages of the MAST module piloting, in the second academic cycle. The online seminar shall be accompanied by a digital forum, possibly embedded into social media such as Facebook or Twitter, where students of any related field could share their questions, experiences and discuss the lessons learned with both peers and professionals, curators, entrepreneurs and artists from the field(s).

4. SUSTAINING THE IMPACT OF NEW CURRICULA FOR A FAIR DIGITAL FUTURE (CONCLUSIONS AND OUTLOOK)

The above methods and approaches indicate at how the MAST project attempts to use new media and digital publishing tools to disseminate and evaluate the project's activities and products. It still remains to be validated whether these approaches shall actually serve the purpose planned, however it may be argued already that these tools and methods do reflect the contemporary realities of communication and collaboration found in the interdisciplinary field of art, science and technology. Moreover, they also bring about important topical implications, such as the current academic year's challenge to the students: *'How can work, collectives, or enterprises be designed to ensure a more inclusive, supportive, verdant, and open society?'* Along the way of developing efficient solutions to meaningful challenges in the realm of technological innovation, the MAST community should explore how key choices in art, design, and technology can help or harm a virtuous circle of progressive European social values. Among many other policies, documents, proclamations and practices on both European and national as well as local and non-

governmental levels, these values are well reflected in the current European Pillar of Social Rights (European Commission, 2018b) that is about delivering new and more effective work-related rights for citizens, built upon 20 key principles along the chapter of Equal opportunities and access to the labor market; Fair working conditions; as well as Social protection and inclusion. The underlying assumption so far is that the future of (electronically supported, digitally dominated) work should belong to (or at least be championed by) profiles who are able to think about future independently and freely, in trans-disciplinary manner, inserting and transforming existing solutions and products into new scenarios that would be solved or transferred to industry realms, ranging from CCS to high technologies and social services. The ideal MAST graduate should act as a coordinator and an integrator in these realms, remaining in positive (if not utterly creative) control over her or his (and our common) digital tools and electronic platforms.

5. ACKNOWLEDGMENTS

This contribution rests on the project conception and legacy of the MAST project, conceived by the MAST consortium and supported by the European Commission (Communications Networks, Content & Technology; CONNECT I.3 Unit – Audiovisual Industry & MEDIA programme), where it is necessary to note that *the content of this contribution reflects the views only of the author(s), including the MAST consortium), and the European Commission cannot be held responsible for any use which may be made of the information contained therein.* The MAST consortium combines a host of hi-profile institutions with excellent references across the science-art-technology triangle. Partner roles in the MAST consortium typically combine academic, managerial and professional (business) profiles with two institutions of big outreach capacity, as well as several topically relevant associate partners: University of Nova Gorica, School of Arts (Slovenia) in the managerial (consortium coordination) role is joined by Madeira Interactive Technologies Institute (Portugal) and Technical University Graz, Institute of Spatial Design (Austria) in academic as well as research & development roles. Kersnikova Institute (Slovenia) and Kitchen Budapest (Hungary) represent the entrepreneurial production partners, while networking and outreach are covered by Culture Action Europe (Belgium/EU) and the Croatian Cultural Alliance / Unicult programme (Croatia). Associated partners are: EQ-Arts (Netherlands); University of Madeira – UMa (Portugal); Stromatolite (Sweden/UK); The University of Arts Belgrade (Serbia); Institute for Development and International Relations – IRMO (Croatia); Hakan Lidbo Audio Industries (Sweden); European Creative Business Network – ECBN (EU wide); European Digital Art and Science Network (EU wide).

6. REFERENCES

- [1] European Commission: "Mapping the Creative Value Chains. A study on the economy of culture in the digital age. Executive Summary", 2017, URL <https://publications.europa.eu/en/publication-detail/-/publication/4737f41d-45ac-11e7-aea8-01aa75ed71a1/language-en> (last request: 2018-09-28).
- [2] STEPS: "Soft Skills; Training; Enabling; Progression & Sustainability", 2014, URL s3.amazonaws.com/2seas-us/page_ext_attachments/1685/STEPS_MAG_Nov2014_EN.pdf (last request: 2018-09-28).
- [3] European Commission: "Quality and relevance in higher education", 2018a, URL http://ec.europa.eu/education/policy/higher-education/quality-relevance_en (last request: 2018-09-28).
- [4] Rosoff, M.: "Here's How Dominant Google Is In Europe". Business Insider, 2014, URL <http://www.businessinsider.com/heres-how-dominant-google-is-in-europe-2014-11> (last request: 2018-09-28).
- [5] MAST Consortium: "Mast Module", URL www.mastmodule.eu (last request: 2018-10-07).
- [6] European Commission: "European Pillar of Social Rights", 2018b, URL https://ec.europa.eu/commission/priorities/deeper-and-fairer-economic-and-monetary-union/european-pillar-social-rights/european-pillar-social-rights-20-principles_en (last request: 2018-10-07).



© 2018 Authors. Published by the University of Novi Sad, Faculty of Technical Sciences, Department of Graphic Engineering and Design. This article is an open access article distributed under the terms and conditions of the Creative Commons Attribution license 3.0 Serbia (<http://creativecommons.org/licenses/by/3.0/rs/>).

DEFINITION IN SCIENTIFIC AND TECHNICAL DISCOURSE

Jelisaveta Šafranji , Marina Katić

University of Novi Sad, Faculty of Technical Sciences,
Department of Fundamental Sciences in Engineering, Novi Sad, Serbia

Abstract: *The paper deals with the notion of definition as one of the rhetorical functions used by writers of scientific and technical English to provide information about a given concept or object. Specifically, definition is an explanation of a concept or objects that distinguishes this concept or object from all others. It is one of the most important and frequently employed rhetorical functions in English for Science and Technology discourse. At the instructional level it is found frequently in association with physical concepts, e.g. physical objects. When dealing with objects, definition is the process of stating what a given object is, either by describing its physical structure, its use or purpose, the way in which it functions, or a combination of two or all of them. It is an essential part of organized thinking and, thus, it is basic to scientific and technical discourse. A definition locates its subject in a class and then proceeds to point out the characteristics that make it differ from other items in that class and that, therefore, allow it to be assigned to a subclass. This process is a special variant of the process of classification. A definition simply sets its subject in a limited scheme of classification. The process of definition is a natural way the mind works. The language of definition should be as logically precise as possible. The purpose of a definition is to limit the meaning of a word which stands for an object in an acceptable way. For this purpose metaphorical language is not used in scientific and technical discourse, because the essence of metaphor is not to limit meaning but to extend meaning by developing new and complex ranges implicit in the literal base. Definitions are expressed either explicitly or implicitly in scientific and technical discourse. Explicit definition is that type of definition which makes clear through phrasing that a particular concept is being defined. Implicit definition presents information also, but it does not present it in defining terms. The paper investigates how definitions are made in lectures with a view to the development of a more appropriate pedagogy for teaching the comprehension of this important language function.*

Key words: definition, scientific and technical discourse, rhetorical function

1. INTRODUCTION

Definition is one of the most important and frequently employed rhetorical functions in EST (English for Science and Technology) discourse. At the instructional level it is found frequently in association with physical concepts, e.g. physical objects. When dealing with objects, definition is the process of stating what a given object is, either by describing its physical structure, its use or purpose, the way in which it functions, or a combination of two or all of them. It is an essential part of organized thinking and, thus, it is basic to scientific and technical discourse (Swales, 2004).

Definition locates its subject in a class and then proceeds to point out the characteristics that make it differ from other items in that class, and therefore, allow it to be assigned to a subclass. This process is a special variant of the process of classification. A definition simply sets its subject in a limited scheme of classification.

The process of definition is a natural way the mind works. The language of definition should be as logically precise as possible. The purpose of a definition is to limit the meaning of a word which stands for an object in an acceptable way. For this purpose metaphorical language is not used in scientific and technical discourse, because the main function of metaphor is to extend meaning by developing new and complex ranges implicit in the literal base. Definitions are expressed either implicitly or explicitly in scientific and technical discourse.

2. IMPLICIT DEFINITION

An implicit definition is usually found in a paragraph of information which contains particular kinds of information often mixed with other kinds of information, that are given by a definition, usually formal or sometimes semi-formal. In a paragraph of implicit definition the defining information is scattered through or mixed with other kinds of information and should be abstracted from the paragraph and put together as a definition by the reader. It is only possible for the reader to do this when he knows what kinds of

information make up a definition, i.e., the term being defined, the class to which the term belongs, and the differences which distinguish the term from all other terms of the same class.

Example 1. Print Media

Topical surveys on the significance and use of print media prove that the need for print media is growing worldwide. This is indicated by the fact that at the end of the millennium Time Magazine acknowledged the socio-cultural significance of the invention and utilization of book printing and elected Johannes Gutenberg's work as the most crucial event of the millennium. It is true that the age of electronic media has started; however printed information is and remains omnipresent. Depending on level of education, income, and household type, between US\$ 20 and US\$ 55 per month and household were spent in Germany in 1997 on books, brochures, magazines, and newspapers. The market for print products offers more variety than ever before. Usually, printed products are categorized into commercial printing and periodicals. This classification differentiates printed matter with regard to its frequency of publication. Since the production process also depends largely on these basic conditions, print shops usually specialize in one or the other market segment. Commercial printing refers to print products that are produced occasionally (e.g., catalogues, brochures, leaflets, business cards, etc.). Periodicals are printed matter that appears periodically (e.g., newspapers, journals, magazines). Publishing houses and companies are the typical clients for periodicals printing. Another way of categorizing printed products is by splitting them into special product groups (Kipphan, 2001).

Implicit defining information is *buried* in a paragraph whose primary purpose is not to define but something else. The specific rhetorical function of this paragraph is that of *description*, in this case a *function description* of a print media. Buried in the information supporting this rhetorical function of description is information which can be presented in the form of an explicit formal definition, if extracted and reordered to produce an explicit formal definition.

Implicit definitions are found frequently in English for Science and Technology. They are more frequently found in technical books or articles written for more advanced students, engineers or experts in particular fields. They are not explicitly stated but given by implication, thus, they make use of context and, at times, the reader's previous knowledge, to make clear what the given concept is.

Since definitions are often given by implication in English for Science and Technology, the reader should learn to recognize these definitions and to be able to frame the information in defining terms, which means to have a more formal, clear, and precise grasp of the information presented.

3. EXPLICIT DEFINITION

Explicit definition can be classified into three broad types on the basis of how much and what kinds of information each type gives the reader and how precise that information is. These three types are: formal definition, semi-formal definition and non-formal definition. Besides, definition by stipulation and expanded definition are also explicit definitions.

3.1. Formal definition

It provides maximum information at the highest possible level of precision. This is the traditional type of definition and it consists of three parts:

- the term or concept being defined (the species);
- the family or class to which the term belongs (the genus),
- the differences between the term being defined and all other members of the class (differentia). It is usually found in a single sentence.

For example, in the sentence

Engineering is the process of harnessing or directing the forces and materials of nature for the use and convenience of man.

The elements of a formal definition can be seen as an equation:

<i>The term being defined</i>	=	<i>Class</i>	+	<i>Differences defined</i>
Engineering		is the process		of harnessing or directing the forces and materials of nature for the use and convenience of man.

There are several methods of defining. Most commonly they are:

- definition by purpose,
- definition by operation,
- definition by example,
- definition by use or function,
- definition by physical description, or
- definition by a combination of two or more methods

The kind of information given in the differences depends on what method of defining the writer chooses. These different methods of defining can be seen in the following examples.

Example 2. Formal definition in EST by purpose

Guillotine is a machine used for trimming stacks of paper.

The term being defined is *guillotine*. It is a member of a class (group) of things called *electronic devices*, and it differs from other electronic devices in its purpose which is to trim stacks of paper.

The kind of difference here is *purpose*; thus, the method of defining is definition by purpose.

Example 3. Formal definition in EST by physical description

Paper guillotine consists of a base at least 1 foot (30 cm) long on each side for small work with a long, curved steel blade, often referred to as a knife, which is attached to the base at the top right-hand corner.

In this case the definition is by physical description because the writer names the parts which compose a guillotine.

Example 4. Formal definition in EST by operation

When the knife of a guillotine or paper cutter is pulled down to cut paper, the action resembles that of a pair of scissors, only instead of two knives moving against each other, one is stationary.

In this case the definition is by operation description because the writer explains the operational procedure.

3.2. Semi-formal Definition

A semi-formal definition is the most frequently used type of explicit definition. It contains almost as much information as a formal definition except that the class is left out (Swales, 2011). The reasons why the class is left out are usually:

- because the writer feels that the class will be obvious to the reader, or
- because the class is so large that it is meaningless, so that he can present the definition in formal form. Examples of classes of this type are *science*, *device*, *process*, *word*, etc.

Example 5. A ceramic is a combination of one or more metals with a non-metallic element, usually oxygen. (A semi-formal definition in EST by physical description)

In the above example the class: *chemical compound* is not stated because obviously the writer assumes that this is information the reader possesses. Instead he gives the reader information about the physical characteristics of the term being defined, i.e., what a *ceramic* is made of. Method of defining here is definition by physical description.

Semi-formal definitions of the formal definition given in Examples 2, 3, and 4 would read:

Example 6. Guillotine is used for trimming stacks of paper.

Example 7. Paper guillotine consists of a base, and curved steel blade.

Example 8. When the knife of a guillotine or paper cutter is pulled down to cut paper, the action resembles that of a pair of scissors, but one of them is stationary.

3.3. Non-formal Definition

The most common types of non-formal definition are those definitions given by synonym and antonym.

3.3.1. Definition by Synonym

It simply presents a word or short phrase which is an approximate equivalent to the term being defined. Synonyms are often presented as appositives, or in parentheses (Miller, 1984).

Example 9. The printing areas of the printing plate are oleophilic or ink-accepting and water-repellent or hydrophobic.

3.3.2. Definition by Antonym

Definition by antonym is the second most common type of non-formal definition. In this type of definition the writer gives a word that means the opposite of the word being defined. In such cases the author is usually assuming that the antonym is a word the reader will understand, and therefore, he can use it to learn the meaning of the word being defined (Hayot, 2014).

Example 10. Hydrophilic is the opposite of oleophilic.

Closer explanation of last definition:

Hydrophilic: A quality of certain papers, components of paper or non-image areas of lithographic plates that cause them to absorb and/or be receptive to water. In offset lithography, a hydrophilic substance is likely to be receptive to water and fountain solutions and repellent to oils and oil-based inks.

Oleophilic: A quality of certain papers, components of paper, or the image areas of lithographic printing plates that causes them to have an affinity for oils and oil-based inks. Oleophilic substances are likely to repel water. Oleophilic substances are also called lipophilic and are considered hydrophobic.

3.4. Definition by Stipulation

It is a special type of explicit definition in which a particular term has a particular meaning in a given situation, but does not necessarily have that meaning in other situations. There are two types of stipulation: mathematical stipulation and specifying stipulation.

3.4.1. Mathematical Stipulation

Mathematics uses a great deal of stipulation when specifying the meaning of the symbols in an equation or formula. Mathematical definitions are a special type as the *language* of mathematics is universal, i.e. we are dealing with a set of symbols universal in form (Harmon & Reidy, 2002).

Example 11. Let A and B be any two sets. A mapping of A into B is an operation \emptyset which assigns to each element a of A a well determined element of B which we denote $\emptyset(a)$ and call the image of a under \emptyset .

In the above stipulate definition the term *mapping* is being defined. It belongs to the class "*an operation \emptyset* " and sum of differences are "*which assigns to each element a of A ...*"

Example 12. Printing is a reproduction process in which printing ink is applied to a printing substrate by pressure, in order to transmit information (images, graphics, text) in a repeatable form using an image-carrying medium (e.g., a printing plate). (Definition by mathematical stipulation in graphic engineering)

Thus, the pressure (P) used in printing presses is defined by the Equation 1:

$$P = dF/dA \quad (1)$$

where **dF** denotes the force (in Newtons), and **dA** the surface (in sq meters).

In the above example the definition of *pressure* is given by equation and then the meaning of the symbols in this equation is specified.

3.4.2. Specifying Stipulation

This kind of stipulate definition is used very frequently by scientists when they coin names for new discoveries or assign new terms or apply old terms in new ways to activities, processes, or objects resulting from their research. Thus, reports and papers contain the following expression:

When the term X is used in this paper, it means so and so.

Example 13. Definition by specifying stipulation

- a) In information theory "*entropy*" means "*information*" or "*freedom of choice of an information source*".
- b) "Failures due to excessive deformation are those which produce excessive deflection, and depend primarily upon relative module of elasticity of the material. *Here in*, resistance to over deformation is termed *stiffness of the member*."
- c) "In this text, a measure of the ability of a member to resist overstressing is referred to as *strength of the member* and stress always means *force per unit area*."

In the above quotations the writer is stipulating the meaning of "*entropy*", "*resistance to over deformation*" and "*a measure of the ability of a member to resist overstressing*" and "*stress*". All these terms and phrases have particular meaning in this given situations, but they have different meanings in other situations, e.g., in other fields of science.

All the above mentioned explicit definitions (formal, semi-formal, non-formal, and definition by stipulation) are given in one single sentence. But very often one single sentence is not enough to explain a new concept or object and the reader needs more information.

3.5. Expanded Definition

One sentence long formal definition cannot give enough information to satisfy the reader's understanding. If an idea or a complex object is being explained, it is necessary to develop the definition further by making use of examples, comparisons, contrasts, cause and effect, time order, space order and other explanatory devices. An expanded definition has its core in the form of a definition. How it is developed depends on the nature of the concept or term being defined and the writer's own approach to it. Most expanded definitions are fairly short, usually not longer than a paragraph, but some may require an essay of several thousand words or even a volume.

The most common ways in which definitions are expanded are classification, description (all types), exemplification, illustration, explication, and operation.

3.5.1. Definition Expanded by Classification

Throughout recorded history creative men as well as scientists, have first given names to something new and then made definitions of the things they have named, so others could understand. Likewise, the concept of classification has been developed because the things surrounding us are so numerous, that humans needed to see them in a perspective small enough for the human minds to grasp. Thus, they have learned to relate things with some elements in common, and think about them in terms of their classes, their common factors, which let them think more clearly. In other words, through classification, man has organized the world around him. That is why definitions are most commonly developed or expanded by classification.

Example 14. The printing press is the equipment with which the printing process is performed. Processing press includes the following areas of function: materials processing (e. g., inking, printing, substrate transportation), drive (motors and transmission elements), control system (e. g., sensors, actuators, and control processors), support and covering area (frame, bearings, guides, guards).

The core generalization is the formal definition stated at the beginning of the paragraph. This formal definition is then expanded by classification in which the other members of the class are given. Then each member of the class is physically described.

3.5.2. Definition Expanded by Description

In order to classify things, man first had to observe how things were similar or different in their physical natures and in the way they worked. Thus, he learned to describe. It should be noted that definition, classification and description (which together add up to explanation) are all essential to scientific thinking and thus, they are found most commonly in scientific writing (Gross, 2006).

Example 15. We might define production as the way material is transformed by factory methods into things wanted by society. For example, the sales orders are taken and the raw material is ordered. The raw material is received and manufacturing orders are fed to the plant at a rate and sequence at which the plant can handle them. Now the raw material is converted at various stages to assembled units

In the above paragraph, semi-formal definition given in the first sentence is the core generalization. *Production* is the term being defined, and *as the way material is transformed by factory methods... by society* is the sum of differences, which distinguishes this term from all other members of the class which is not mentioned. Then this semi-formal definition is expanded by example, which is indicated by the phrase *for example*; then by process description in which there is a time ordered series of related activities.

3.5.3. Definition Expanded by Exemplification

One sentence definition is very often expanded by examples to give the reader a specific case or a general one of the generalization represented by the core idea, i.e., by a formal definition (Fahnestock, 2009).

Example 16. Acceleration is a change in the speed or velocity of an object per unit of time.

$$A = v/t$$

$$v = s/t$$

There are two time units in the expression for acceleration for example, miles per hour per hour (mi/hr/hr) or meters per second per second (m/sec/sec).

For example, an automobile at rest has an initial velocity of 0 miles per hour. As the car begins to move, it is accelerated from zero velocity to some new velocity in the first second it moves. The velocity of the automobile changes as long as the acceleration continues. The change in the velocity also can be a negative one. The driver can apply the brakes of the automobile and slow the car down. The change in velocity in this instance is known as deceleration or negative acceleration.

The formal definition given in the first sentence is expanded, first, by a general example since the reader is told that there are two general time units in the expression for acceleration. Then the writer tells the reader a specific case of acceleration of an automobile.

3.5.4. Definition Expanded by Illustration

It is very often found in technical writing. The writer uses it when he wants to make his definition clear by referring the reader to a picture, a graph, or any other visual aid. This kind of illustration is called visual illustration. When the writer wants to give the reader a very specific, detailed example, this type of illustration is a special kind of example and it is called illustration in words.

Example 17. Hardness

Hardness is a measure of the resistance of a material to permanent deformation. It is commonly measured by placing an indenter in contact with the material being tested. A known load is placed upon the indenter, as shown schematically in Fig.1-11(a). The indenter material is much harder than the specimen, with hardened steel, tungsten carbide, or diamond being commonly used. After the indentation has been made, the indenter is removed (Fig.1-11b). The hardness number depends on the geometry of the indentation and the type of test used. The type of test often leads to some confusion. The four different types of hardness tests are summarized in Table 1-1, and it is seen that different types of indenters are used for different tests. The hardness number depends on the applied load and the shape of the indentation, for the first three tests shown (Brinell, Vickers, and Knoop). For the Rockwell hardness test, both the shape of the indenter and the load are specified. The hardness number depends only on the depth to which the indenter penetrates the specimen. The hardness tests given in Table 1-1 have been found to be convenient and have evolved as standard tests.

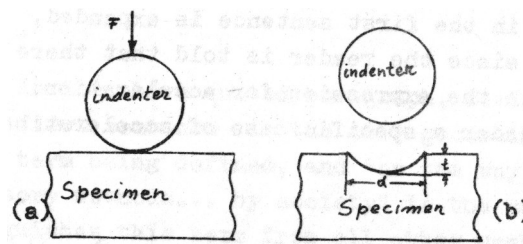


Fig.1 The hardness test (a) A loaded indenter is placed in contact with the specimen. The indenter is shown as a sphere; however, other shapes are also used. (b) The hardness number depends on the indentation that remains when the indenter is removed. The dimension d is used in the Brinell test, whereas t is used in the Rockwell test. From M.M. Eisenstadt, *Introduction to Mechanical Properties of Materials*, 2012:137

The above definition of *hardness* is expanded by illustration in words and in visual aids. The writer describes how the hardness is measured (tested) by referring the reader to a picture which is supposed to help him visualize the things he is describing.

3.5.5. Definition Expanded by Explication

This is a special type of expanded definition. In this type of definition the writer takes those words in the original definition which are presumed not known to the reader and defines each of them, so that the reader can, when he has read the entire discussion, put together all of the definitions and understand the original definition more clearly (Bazerman, 1998).

Example 18. Fluid Velocity

We define fluid velocity at a point, or the flow velocity (at a point) as the velocity (a vector) of a fluid element relative to a certain reference frame. If the reference frame is not specifically defined, then it corresponds to the reference frame in which the flow is studied. By the flow speed, or the speed of the fluid at a point, we mean the magnitude of the flow velocity (or, in other words, the magnitude of the fluid

velocity at a point). If the flow is uniform everywhere in the region of space considered, we speak of the stream velocity, or of the stream speed.

Note that when defining the fluid velocity at the point we used the concept of a reference frame. Since it is impossible to detect the absolute motion of a system by studying its response to the action of forces, only relative and not absolute motion through space can be detected. This statement describes what is known as the Newtonian relativity. As a result, when we say that a fluid flows we are considering its motion relative to a certain frame of reference.

From: J.P.Freidberg, *A self-consistent two-fluid model*, 2008:78

In the first sentence of this paragraph the writer gives a formal definition of the *fluid velocity at a point* which is also the core generalization. Then he explains what he means by *flow speed*, *stream velocity* and *reference frame*. Because both physical paragraphs develop the same core generalization they add up to one conceptual paragraph. After the reader has read the entire conceptual paragraph and put together all of the definitions he will be able to understand the original definition, stated in the first sentence of the first physical paragraph, more clearly.

3.5.6. Definition Expanded by Operation

It is a special type of expanded definition in which the writer tells the reader what to do (usually some physical activity) in order to experience the thing being defined. This type of definition is often given as a set of instructions, either direct or indirect, which enable the reader to feel or see or somehow experience the terms being defined.

Example 19. Letterpress Printing and Letterpress Printing Presses

Letterpress printing (sometimes also called book printing) is now considered to be a largely “extinct” process, except for its descendent, flexographic printing, which is winning more and more of the packaging printing market, just as indirect letterpress printing also prevails in certain parts of this sector. In spite of this, it deserves equal treatment with the other two printing processes in this historical section, because it was from letterpress printing that everything else developed. It has still not yet been proven conclusively whether Johannes Gutenberg accomplished his pioneering discovery between 1440 and 1450 in Mainz or in Strassburg, so both towns honour Gutenberg equally. His invention is based on three things: cast print types, a hand-casting instrument to make these types, and a printing press designed for this purpose, which was adapted from the wine presses of the time.

Friedrich Koenig set about mechanizing the hand press completely, which led to the pioneering invention in 1811/12 of the first automatic cylinder press. In the course of the following years both the drive mechanism (e.g., “rack drive”, “railway motion”, and circular motion – i.e., planetary drive) and the operating principle of cylinder printing presses underwent constant development. In the latter respect, we should distinguish the most important forms: stop cylinder, single-revolution, and two-revolution presses. Common to them all was the back-and-forth motion of the printing form bed, the “carriage.” The flat letterpress printing form was attached to it in a lockup form. The carriage ran on rollers and, apart from the two-revolution presses, was moved back and forth by a thrust crank. An impression cylinder positioned above it, which in the case of the single and two-revolution presses rotated continuously, produced the contact pressure (for single-revolution presses it had a double-sized impression cylinder and one revolution per printed sheet, and for two-revolution presses it had a correspondingly smaller impression cylinder and two revolutions per printed sheet); the sheet of paper was brought into contact with it by using a so-called “swing gripper”. These sheet feeders in particular underwent numerous further developments up to full automation (Kipphan, 2001).

4. CONCLUSION

Definition is one of the rhetorical functions used by writers of scientific and technical English to provide information about a given concept or object. The process of definition is a natural way the mind works. The purpose of definition is to limit the meaning of a word which stands for an object in an acceptable way. Specifically, definition is an explanation which distinguishes this concept or object from all others. They are expressed implicitly and explicitly in scientific and technical discourse. In a paragraph of implicit definition the defining information is scattered through or mixed with other kinds of information and

should be abstracted from the paragraph and put together as a definition by the reader. They are not explicitly stated but given by implication, thus, they make use of context and, at times, the reader's previous knowledge, to make clear what the given concept is. Explicit definition is the type of definition which makes clear through phrasing that a particular concept is being defined. It is stated obviously and in detail, leaving no room for confusion or doubt.






5. REFERENCES

- [1] Bazerman, C.: "Shaping written knowledge: The genre and activity of the experimental article in science" (University of Wisconsin Press, Madison, 1998).
- [2] Eisenstadt, M. M.: "Introduction to Mechanical Properties of Materials, Indiana State University", Physics Today 25(5), 54-54 2008. doi:10.1063/1.3070856.
- [3] Freidberg, J.P.: "Plasma Physics and Fusion Energy", 1st ed., (Cambridge University Press, Cambridge, 2008), Chapter 10.
- [4] Fahnestock, J.: "Rhetorical figures in science", (Oxford University Press, New York, 2009).
- [5] Gross, A. G.: "Starring the text: The place of rhetoric in science studies". (Southern Illinois University Press, Carbondale, 2006).
- [6] Harmon, J. E., Reidy M.: "Communicating science: The scientific article from the 17th century to the present", (Oxford University Press, New York, 2002).
- [7] Hayot, E.: "The Elements of Academic Style Writing for the Humanities", (Columbia University Press, New York, 2014).
- [8] Kipphan, H.: "Handbook of Print Media", (Springer, Berlin, 2001).
- [9] Miller, C. R.: "Genre as social action", Quarterly Journal of Speech 70(2), 151–176, 1984. doi: 10.1080/00335638409383686.
- [10] Swales, J. M.: "Genre analysis: English in academic and research settings", (Cambridge University Press, Cambridge, 2011).
- [11] Swales, J. M.: "Research genres: Explorations and applications", (Cambridge University Press, Cambridge, 2004).
- [12] Trench, B.: "Internet: Turning science communication inside-out", (Routledge, New York, 2008), 185-198.



© 2018 Authors. Published by the University of Novi Sad, Faculty of Technical Sciences, Department of Graphic Engineering and Design. This article is an open access article distributed under the terms and conditions of the Creative Commons Attribution license 3.0 Serbia (<http://creativecommons.org/licenses/by/3.0/rs/>).

USING MODERN INFORMATION TECHNOLOGY TO ENRICH THE PRESENTATION OF RESULTS IN SCIENTIFIC PUBLICATIONS

Gojko Vladić , Dragoljub Novaković , Gordana Delić ,
Rastko Milošević , Stefan Đurđević 
University of Novi Sad, Faculty of Technical Sciences,
Department of Graphic Engineering and Design, Novi Sad, Serbia

Abstract: *It has been almost two decade since electronic formats entered mainstream in scientific paper publishing. PDF (portable document format) has become without any doubt most used electronic publishing format. Wide adoption of this format offered easy exchange of the information presented conventionally through text and images, which was widely adopted. On the other hand it has been little over a decade since 3D artwork, java script and SWF applications are supported by PDF, but adoption of all of these advanced features is quite low. With technological advancements augmented and virtual reality are becoming useful tools also. Same as in the case of PDF there is the problem, all across the board of scientific fields, of slow adoption of new Information communication technology ICT. This paper aims to explore and present some of the new ICT features that could help improve presentation of scientific results and also to illuminate the reasons they are rarely used in publications.*

Key words: PDF, augmented reality, multimedia, scientific publishing

1. INTRODUCTION

Using text and images in scientific publishing, and publishing in general, has its long history. This way of presenting the content was transferred to internet and electronic publishing. With technological advancements of electronic publishing formats new communication opportunities arouse. While migration to the internet was done quite fast and it was met with enthusiasm, this was not the case with usage of full capabilities of the electronic publishing formats such as Portable Document Format. Furthermore new technologies such as augmented reality are becoming more available and used each day, but their adoption and integration in scientific publications remains insignificant. This paper aims to explore and present features that could help improve presentation of scientific results and also to illuminate the reasons they are rarely used by authors.

1.1 Portable document format

Portable Document Format (PDF) can be used to present and exchange electronic content reliably, independent of hardware or software system. Adobe PDF was invented in beginning of '90 and by now it became an open standard maintained by the International Organization for Standardization (ISO). It meets ISO 32000 standards for electronic document exchange, including special-purpose standards such as PDF/A for archiving, PDF/E for engineering, and PDF/X for printing and variety of accessibility standards for people with disabilities. PDFs is based on the PostScript language and can contain fonts, vector graphics, raster images, links, buttons, form fields, audio, video, business logic, they can be signed electronically and can be easily viewed using various free software. Java support is present since 2000. and since 2004. PDF files may contain three dimensional objects using U3D or PRC, and various other data formats (Acrobat.adobe, 2018). Despite continuous improvements in the PDF capabilities there is little to no adoption of these capabilities in scientific publishing. Other than information presented conventionally through text and images, advanced features are not used even when there is clear need for them. Good examples are the medical illustrations, which have always been handicapped by being restricted to two dimensions even though three dimensional imaging and scanning is available and used for some time now (Ziegler, 2011; Maunsell, 2010).

1.2 Augmented and virtual reality

This interaction technology overlays computer-generated virtual elements onto real-world environment images. Augmented reality became well known technology only with recent advancements in the hardware of the mobile devices. These advancements made it possible to capture the real world images, process them, while simultaneously process the virtual content and to combine them in to augmented

reality which is shown on the device's display. Concept is based on the information displayed and image overlay which are context-sensitive, depending on the observed objects and by enhancing perception of reality by combining physical and digital content and giving additional value, in information terms. This technology is widely available through different applications, mostly intended for the mobile devices. (Zhu et al, 2004; Azuma, 1997; Azuma et al, 2001). Although there are technological variations, basically augmentation is produced after a series of digital data transformations. First, the real video image is captured and transformed. Then, this image is processed in order to determine position of the markers (containing an image pattern that is compared to patterns stored in a database). Next, the algorithm determines pattern orientation as the base for the coordinates frame and calculates the real position of the digital camera in relation to the physical marker. After that, the virtual objects are placed over the markers, and the final image is rendered and sent to the display (Soares, et al, 2012). Production of the AR content has become fairly easy and there are researchers suggesting that it should become standard practice to be incorporated into figures representing structural data (Wolle et al, 2018).

In contrast to augmented reality, virtual reality completely replaces outside world with computer generated one. Special head set is needed in order to emerge in to virtual world. VR technology is in its first stage of adoption and as such is still rather exotic in hardware and software sense. In the literature overview there are no references of using this technology in order to present scientific data, but there are numerous references for usage in the education.

2. CONSIDERATION OF THE BENEFITS

Today scientific research results are or could be captured as three-dimensional (3D) data, for example modern Scanning Electron Microscope SEM equipped with 3DSM solution can produce 3D image in real time and it is possible to obtain a precise quantitative 3D model suitable for visualization and analysis of the 3D surface with generation of complete metrology reports. These 3D scans can be easily presented in the research papers but often they are not.

Good illustration can be found in graphic engendering, as there is often a need for graphical presentation of a colour coordinates or a colour gamut. Both colour and gamut are often presented with still image of Lab colour space, but information value of that image is close to none, as observer can perceive only two dimension and needing all three dimensions in order to comprehend the full information. Using to full extent PDF 3D capabilities can be improve understanding of colour data, as shown in Figure 1. In order to comprehend 3D space at least three orthographic images are needed, but problems with size and legibility are apparent. Interactive 3d representation showing colour space with colour position can be rotated and zoomed in order to get a real sense of colour positions in Lab colour space.

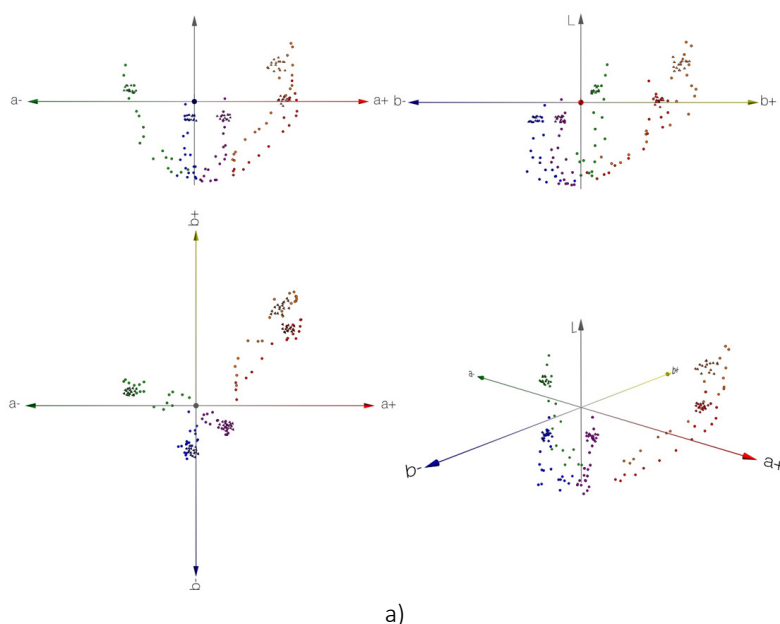
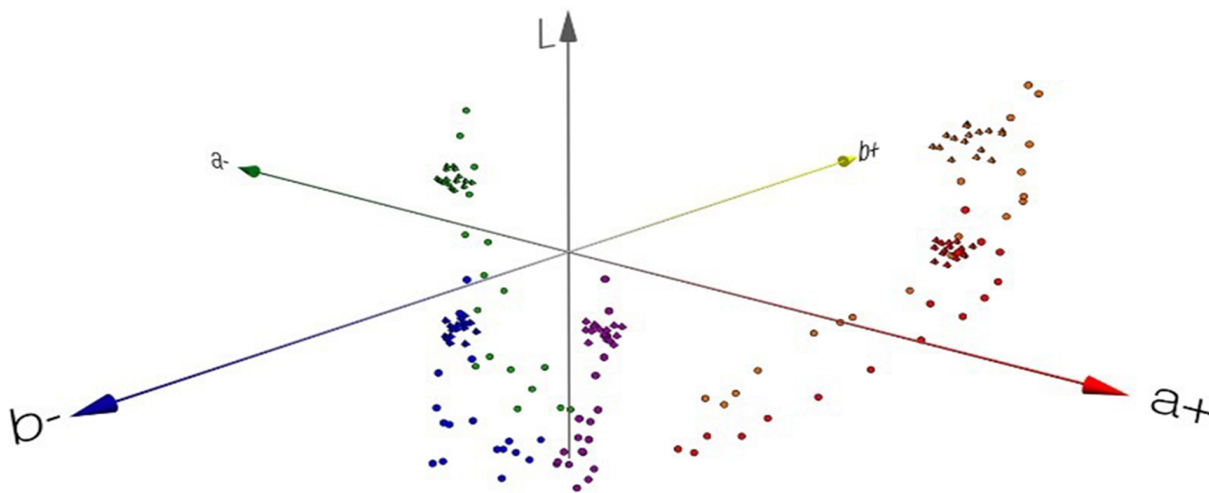


Figure 1 (part 1): a) Static orthographic images of Lab colour space



b)

Figure 1 (part 2): b) Interactive 3D representation
Click the image for 3D in the electronic edition of proceedings

This is achieved by constructing 3D model of Lab space, using specialized colour analysis application capable of 3D visualization or any 3D modelling application by imputing colour coordinates.

In case of PDF, universal three-dimensional (U3D) or PRC file format must be used for interpretation by PDF. Universal 3D is a binary file format that contains all necessary information to describe a 3D scene graph. This includes the geometry data, palette definitions, lighting, cameras ("views"), texturing and pre-defined animations ("motions") (Newe, et al, 2013). U3D is a compressed file format standard for 3D computer graphics data, standardized by Ecma International in 2005 as ECMA-363 in order to facilitate data exchange. It can be inserted into PDF documents and interactively visualized by Acrobat Reader, since version 7. PRC is older file format which has been pushed aside by more popular U3D.

PDF format has integrated support for video (including H.264), audio, and other multimedia. Adding the video and other multimedia to the scientific publication can vastly improve presentation of experimental methodology, results, etc. Figure 3 shows the static frame (image of the break in the tensile test of ABS and PLA 3D printed sample, but in electronic version of the proceedings break can be observed in real time and important differences between two materials can be seen, which are omitted in static image.

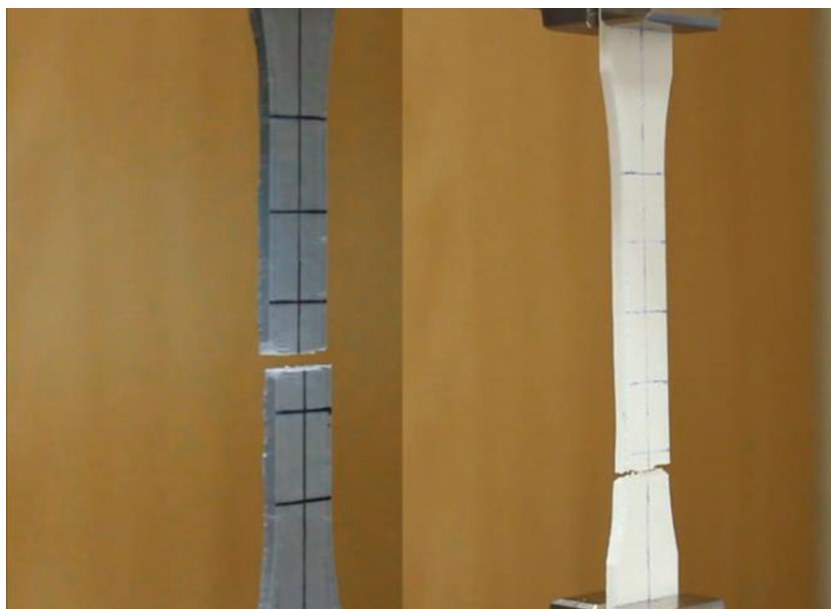


Figure 3: Static images of a tensile test, *Click the image for video in the electronic edition of proceedings*

PDF also supports attachment of Adobe Flash applications shockwave file (SWF). This format offers integration of the interactive application suitable for presentation of interactive graphs and great verity of other use. Over the time SWF became obsolete due to security issues and is really supported without separate installation for operating system or internet browsers.

Similar results can be achieved by using augmented reality technology with the difference that content is not embedded in to the PDF file for witch viewer needs to be installed on to the device, but in the separate application. This application is produced for each platform iOS, Android or Windows in which 3D, video, or other content is triggered by the image. This offers possibility for seamless combination of printed media and multimedia content. Such content can be manipulated and navigated using touch screen of the mobile device or other AR device, as shown on augmented 3D graph example of Graphmented app, figure 2.

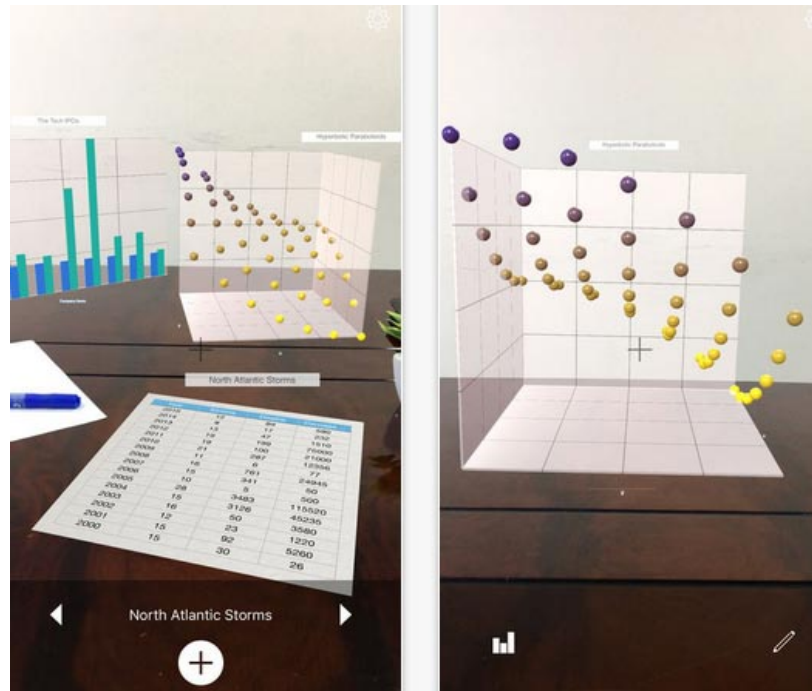


Figure 2: Graphmented app example of augmented reality data presentation

Alongside simple mobile applications such as Graphmented, augmentation can be achieved by using much more versatile software such as Unity and Vuforia combination which enables video and other multimedia formats to be included in augmented reality application, with addition of potential for full customization of the application.

Usual process for generating augmented reality application consists of material preparation. Makers, or triggers must be well defined imaged with contrast areas in order to be recognized by the machine. Alternative is to use dedicated QR codes which in case off Apple phones offer automatic play of augmented content even without specialized application.

Procedure for generating augmented reality applications starts with preparation of 3D models following standard procedure of geometry generation and optimization for reproduction on a mobile device, although most modern mobile devices have powerful graphic hardware that can render very complex 3D scenes. Depending on the platform certain format of 3D files must be saved. Preparation of video or other media content is done with usual editing software and saved in appropriate format. Content can be stored in the application which enables offline use, or it can be uploaded on the internet and downloaded by the application at time of use. When markers and content is ready they are connected using software such as Unity for creation of the application interface interactivity and 3D environment, and Vuforia engine for easy insertion of augmentation.

3. CHALLENGES IN ADOPTION AND IMPLEMENTATION

Spatial presentation, multimedia and possibility to interact with data representation offers better insight and encourages curiosity. Technical possibility for all of this is present in the most popular electronic publishing format, used by more than 500 million users worldwide, for more than a decade. Big publishers promoted and encouraged authors to embed 3D data directly into their publications, Elsevier “Authors of selected Elsevier journals are invited to enrich their online articles by providing supplementary 3D models” yet there is very little content supported with this technology. Augmented reality in comparison to PDF is still novelty and used seldom. Having all this in mind, it must be asked “Why don’t authors use the advantages?”.

In informal interviews different reasons were stated for not using all the capabilities of available technology. Reasons differed depending on the field of study, majority of authors do not know about the possibilities at all, and when introduced to the possibilities did not recognize potential in their field. Skills required for preparation of content are also deterring factor, as academics in most scientific field are not familiar with 3D modelling, multimedia production or trained for it.

Relative obscurity of U3D file format and lack of support by the mayor 3D modelling applications is also one of the reasons among authors who are familiar with the PDF format possibilities. Specialized conversion applications are often needed as there is no possibility to directly save U3D format. Although, this is somewhat emended by variety of online converters.

Closed file formats of laboratory equipment and software manufacturers could also be significant factor. For example MRI, CT or ultrasound in medical science often produce DICOM format which is hard to translate in to other formats and sometimes it is hard to even view them using independent software.

Last factor are the editors and reviewers of scientific publications who do not promote and insist on presentation of results in the best way possible, by using up to date technologies.

All the previously mentioned obstacles are in relation to PDF format, while augmented reality technology is considered as a game like feature, and majority of scientific authors are unfamiliar with the process of creating augmented reality application and content.

4. CONCLUSIONS

Despite obvious advantages of using modern information communication technology to enrich the presentation of results in scientific publications examples are seldom encountered. 3D data is produced as a result of research, but not presented in that form, instead it is reduced to 2D imagery. This results in loss of valuable information. Technology to support better presentation of scientific research is present and it should be used to its full potential. Obstacles discussed in this paper could be overcome by proper education, promotion and stimulation of scientific authors and journal editors. Having in mind tough road of full PDF features adoption, it can be foreseen that augmented reality will not be significantly present in scientific publications for a long time.

6. ACKNOWLEDGMENTS

The research is supported by the Ministry of Education, Science and Technology Development of the Republic of Serbia, project number: 35027 “Development of software model for scientific and production improvement in graphic industry”.

7. REFERENCES

- [1] Acrobat, URL: <https://acrobat.adobe.com/us/en/> (last request: 2018-10-12).
- [2] Azuma R, Bailiot Y, Behringer R, Feiner S, Julier S, MacIntyre, B.: “Recent Advances in Augmented Reality”, IEEE Computer Graphics and Applications 21(6), 34–47, 2001. doi: 10.1109/38.963459
- [3] Azuma, R.: “A Survey of Augmented Reality”, Teleoperators and Virtual Environments, 6(4), 355–385, 1997, doi: 10.1162/pres.1997.6.4.355
- [4] Maunsell J.: “Announcement regarding supplemental material”, The Journal of Neuroscience, 30(32), 10599–10600, 2010, URL: <http://www.jneurosci.org/content/30/32/10599.short> (last request: 2018-08-15)

- [5] Newe, A., Ganslandt, T.: "Simplified Generation of Biomedical 3D Surface Model Data for Embedding into 3D Portable Document Format (PDF) Files for Publication and Education", PLoS ONE 8(11), e79004, 2013. doi: 10.1371/journal.pone.0079004
- [6] Soares, A, Andrade, A., Lamounier, E., Cardoso, A.: "Virtual and Augmented Reality: A New Approach to Aid Users of Myoelectric Prostheses", 2012. doi: 10.5772/50600
- [7] Wolle, p., Müller, M. P., Rauh, D.: "Augmented Reality in Scientific Publications—Taking the Visualization of 3D Structures to the Next Level", ACS Chemical Biology, 13(3), 496–499, 2018. doi: 10.1021/acscchembio.8b00153
- [8] Zhu, W., Owen C. B., Li H., Lee J.: "Personalized In-store E-Commerce with the PromoPad: an Augmented Reality Shopping Assistant", Electronic Journal for E-commerce Tools and Applications, 1(3), 1-19, 2004. doi=10.1.1.83.8198
- [9] Ziegler, A., Mietchen, D., Faber, C., Hausen, W., Schöbel C., Sellerer, M., Ziegler, A.: "Effectively incorporating selected multimedia content into medical publications", BMC Medicine, 9, 17, 2011. doi: 10.1186/1741-7015-9-17



© 2018 Authors. Published by the University of Novi Sad, Faculty of Technical Sciences, Department of Graphic Engineering and Design. This article is an open access article distributed under the terms and conditions of the Creative Commons Attribution license 3.0 Serbia (<http://creativecommons.org/licenses/by/3.0/rs/>).

NOVEL TECHNOLOGIES



THE MODELING OF FACIAL RECOGNITION PROCESS IN PROSPECTIVE OF SIMULATION TECHNIQUES

(A methodical elaboration through the built-in modules of Matlab)

Jozef Bushati ¹ , Virtyt Lesha ² , Dea Strica ³ 

¹University of Shkodra, Shkodra, Albania

²Polytechnic University of Tirana, Tirana, Albania

³University of Tirana, Tirana, Albania

Abstract: *Biometrics is a field of study and dissemination that brings a host of contributing domains in an integrated way to generate products that find multiple applications particularly in creating an individual's identity. Modeling biometric processes reveals a series of discussions in various fields, mainly in medicine and in the digital image processing field. These discussions range from the simulation levels of these models to those of application and concrete products that use biometric systems for identifying and recognizing individuals. Indeed, over many biological parameters of an individual to be identifiable, there is the face that generates a lot of information about the physical data of the individual. According to specific studies, facial components combined according to different methods can be used to design simulation models that come in aid of generating closed-source and dedicated programs of biometric recognition (Das, 2018).*

This paper deals with a simulation model, through the Matlab test-bench, of the facial recognition process. The model is created at the proposal level for the subject field and gives the limits and recommendations for improvements and further developments of this simulation method.

The modeling methodology includes two parts; the first part is the Matlab program that has been coded in such a way that it takes some images that represent the faces of different people published in the open-source database on the Internet; the second part is the creation of a database that retains these images to enable face identification when entering a new image program. The facial search and retrieval process are built through some built-in functions that the latest versions of Matlab offer.

Finally, the simulation model provides a new facial identification model that leaves room for further discussion and limits to the relatively small number of face images that can support the database in Matlab.

Key words: biometrics, test-bench, database, identification

1. INTRODUCTION

Face recognition is a process under which persons are subject to biometric verification and authentication for purposes such as camera surveillance, biometric passports, biometric facial identification for research and development purposes, and so on (Buhrow, 2016). As one of the biometric identification methods, facial identification is more popular and has a lot of advantages over others where the main one consists in relatively large distance identification compared to other methods such as eye iris, sound, trace of fingers, etc (Bourlai, 2016).

Among the 6 biometric identifying methods considered, facial identification has shown greater suitability in a Machine-Readable Travel Documents (MTRD) system based on several evaluation factors such as: perception and suitability to the population, adaptability to electronic data processing equipment, etc. (Chityala et al, 2014). The following figure shows the suitability of facial identification in comparison to other biometric methods (Datta et al, 2015). As a biometric system, a system of face recognition operates in two methods: face verification and face identification. Face verification includes matching a one-to-one approach that compares an image to another image whose identity is known. An application of this method is the use of a biometric passport. Face identification includes one-to-many matching where a face image is compared to some face images that are stored on a database. Also, this method finds use when it is necessary to identify a face image that is closer to the face image being tested (Newman, 2009).

Further face recognition development has brought a lot of development of image processing software in the sense of the parameters of these information processing machines, such as development of memory suitable for storing images with higher levels than just textual information. In addition, requests and advances in this regard are also represented in database developments, their management as well as storage of visual and multimedia data; it is natural that in this case the budgets and the financial capacities for these purposes are imposed.

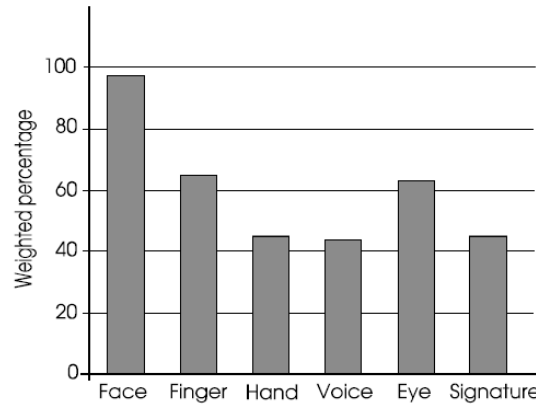


Figure 1: Level of suitability to an MTRD system of 6 biometric Identification attributes

The use of face recognition includes a series of defined algorithms which, through the development and simulation by respective programs, move on these identification processes

The algorithms developed in face recognition processes: are Eigenface, Gabor jets, Fisherface, etc. In this paper we discuss and elaborate the Eigenface method in terms of its improvement in the simulation software environment and the provision of further proposals for the performance of this method.

Finally, automatic face identification faces multiple challenges with various technical aspects such as when we have an environmental impact on an image such as damage to the figures that will be identified, photographing under undesirable effects of light, making pixel elements prevent to perform with images, etc.

2. METHODOLOGY

The face images, presented as multidimensional matrices, are subject to image processing through algorithms that have shown high interest in the computer vision in general. Surveys on this subject include algebraic and statistical methods for extracting and further elaboration these images.

In concrete applications, rather than simulation environments, the facial identification consists on some processes that are taken into consideration. In principle, as input of the system, the facial image is subjected to observation by a sensor that records the values of facial image pixels; image pixels can be monochromatic or colored and for each image type, specific attributes are required for image identification and recording as inputs in the system.

Facial image is considered as a two-dimensional matrix that, after switching to the scanning of the sensor, requires normalization in fixed dimensions of the $m \times n$ size of matrix and this is predetermined for each facial image that may have different dimensions, depending on the distance when the face image was taken from the sensor.

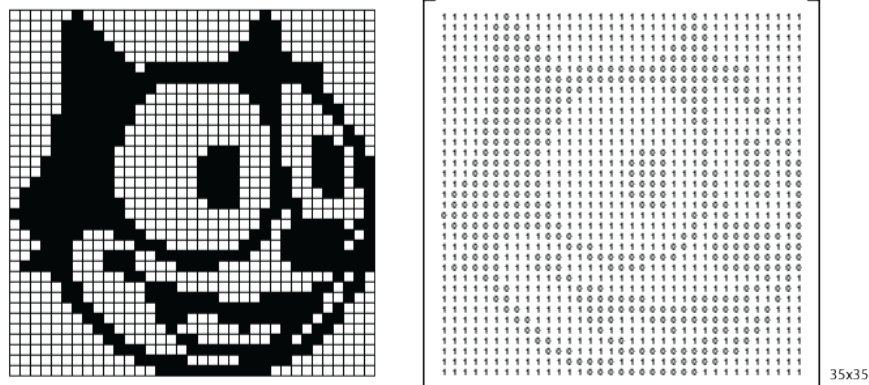


Figure 2: Monochromatic image expressed in bites

Face image and image processing in general, specifies and analyzes each pixel of the image in question and the dimensions of the images that are subject to normalization and greatly affect the processing capabilities of the computing machines; the purpose of the computing machine is to normalize the image in fixed dimensions $m \times n$. As a result, processing methods face this challenge because in high values of dimensions, several disadvantages arise where the most commonly required costly calculation capabilities in case of these high-dimensional images.

The most common face image processing model is the Principal Component Analysis (PCA) dimensioning technique; the first component of this approach is the linear combination of the original image dimensional dimensions.

The most common case in simulation and application development facilities is multiple analysis assuming that the extraction processing and the principal manifold are linear. Once facial image is normalized and extracted from the facial image database, it behaves as a linear subspace from the image subspace.

In the case of our simulation model, we have considered one of the most common methods of linear analysis that is the Eigenface technique which is subject to probabilistic models.

The Eigenface method was proposed for the first time by Turk/Pentland. In the case of our study, an improved version was taken into account by highlighting the advantages it includes and the limits it pursues under this modified model.

The simulation environment is Matlab R2017, which has already built-in functions that support image processing applications and, consequently, the biometric case.

The simulation takes into consideration a database of 400 face images that are included in the program; this database is valid for performing the identification of face images that will be inserted for matching.

The developed code adapts the Eigenface method with a treatment other than classic approach in the sense of the size of the database in terms of the number of facial images supported. Also, the other modification that is applied to the classical Eigenface method considers of the time of execution of face recognition.

The simulation model consists of two parts: the creation of the database execution code and the main code used to read this database required for the recognition process (Jain et al, 2011).

The face recognition simulation considers 400 different persons in the modeling process. The modification consists on intervening the two cycles needed to complete the creation of the database and introducing a subset for each cycle leading to the minimization of the time of reading the database in the main code of the face recognition and further increasing the number of supported of face images in the database.

Also, for each execution of 400 face images, the time of execution was measured as in the case of the Eigenface class method and the improved version of this method. Finally, the graphical presentation of each case is enabled thus showing the comparison between the two Eigenface methods regarding the time execution.

3. RESULTS

In the simulation discussed in this paper, the methodology is reflected in detail in the results section where the findings and determining elements discussed in the above sections are provided.

Specifically, in our simulation we have used 400 face images which are placed as input on the improved model of Matlab simulation; against the standard simulation model in question, the performance of each simulation model is determined in terms of the time needed for executing the face image recognition process for the database at all.

In function of this approach, we have found the execution time for each image's recognition of 400 images per standard and improved algorithm. Moreover, through Matlab simulations we have defined the trend-line for each simulation model; this trend-line is of the "General Model Gauss8" type of the eighth order.

The approximation equation by the "General Model Gauss8" method is theoretically the following:

$$f(x) = a_1 \times \exp\left(-\left(\frac{x-b_1}{c_1}\right)^2\right) + a_2 \times \exp\left(-\left(\frac{x-b_2}{c_2}\right)^2\right) + a_3 \times \exp\left(-\left(\frac{x-b_3}{c_3}\right)^2\right) + a_4 \times \exp\left(-\left(\frac{x-b_4}{c_4}\right)^2\right) + a_5 \times \exp\left(-\left(\frac{x-b_5}{c_5}\right)^2\right) + a_6 \times \exp\left(-\left(\frac{x-b_6}{c_6}\right)^2\right) + a_7 \times \exp\left(-\left(\frac{x-b_7}{c_7}\right)^2\right) + a_8 \times \exp\left(-\left(\frac{x-b_8}{c_8}\right)^2\right) \quad (1)$$

where, the coefficients a_1 , b_1 , etc. consist of the approximation line determinants according to the "General Model Gauss8" method. The values of the above constants are presented below for both the simulation model and the improved simulation.

Table 1: Trendline coefficients according to the General Gauss8 algorithm for the classic simulation model

Coefficients (with 95% confidence bounds)	The values Standard Algorithm	The values Improved Algorithm
a1	2.229 (-114.7, 119.1)	1.491 (-24.18, 27.16)
b1	320.4 (200.2, 440.5)	339.3 (281, 397.5)
c1	320.4 (200.2, 440.5)	38.3 (-127.3, 203.9)
a2	320.4 (200.2, 440.5)	0.7382 (-15.77, 17.25)
b2	107.4 (-1490, 1705)	166.5 (122.5, 210.6)
c2	128.4 (-3073, 3330)	25.69 (-80.65, 132)
a3	2.336 (-40.91, 45.59)	0.2948 (-3.196, 3.786)
b3	218.1 (134.5, 301.8)	79.68 (40.61, 118.8)
c3	27.72 (-110.5, 165.9)	21.83 (-44.45, 88.11)
a4	2.136 (-38.29, 42.56)	1.278 (-27.25, 29.81)
b4	-5.647 (-146, 134.7)	200 (126.7, 273.3)
c4	51.78 (-287.9, 391.4) 1.086 (-1.765, 3.937)	37.51 (-237.7, 312.8)
a5	1.086 (-1.765, 3.937)	2.746 (2.54, 2.952)
b5	172 (165, 178.9)	22.5 (-16.04, 61.03)
c5	13.04 (-5.923, 32)	105.3 (-34.39, 245)
a6	1.192 (-42.31, 44.69)	1.591 (-6.449, 9.632)
b6	367.4 (316.5, 418.2)	129.1 (-35.42, 293.6)
c6	21.2 (-159, 201.4)	42.5 (-242.1, 327.1)
a7	1.498e+12 (-4.008e+17, 4.008e+17)	2.426 (0.3012, 4.551)
b7	4823 (-4.472e+07, 4.473e+07)	396.1 (345.9, 446.2)
c7	858.8 (-4.351e+06, 4.353e+06)	42.06 (-48.42, 132.5)
a8	2.552 (-103.3, 108.4)	2.687 (-2.356, 7.729)
b8	273.9 (206.3, 341.4)	267.4 (168.7, 366.1)
c8	30.49 (-197.2, 258.2)	69.94 (-738.5, 878.4)

Below we have presented the relevant trend charts for each model, the standard and the improved one.

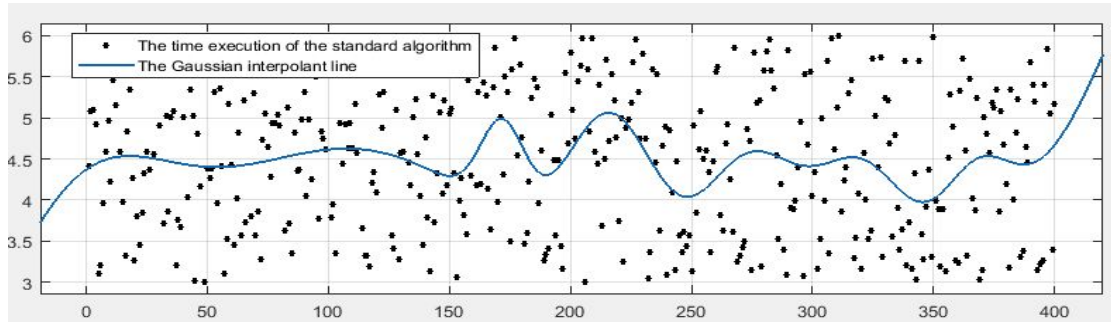


Figure 3: A graph showing the dependency of the execution time for the recognition of each face image for the standard model

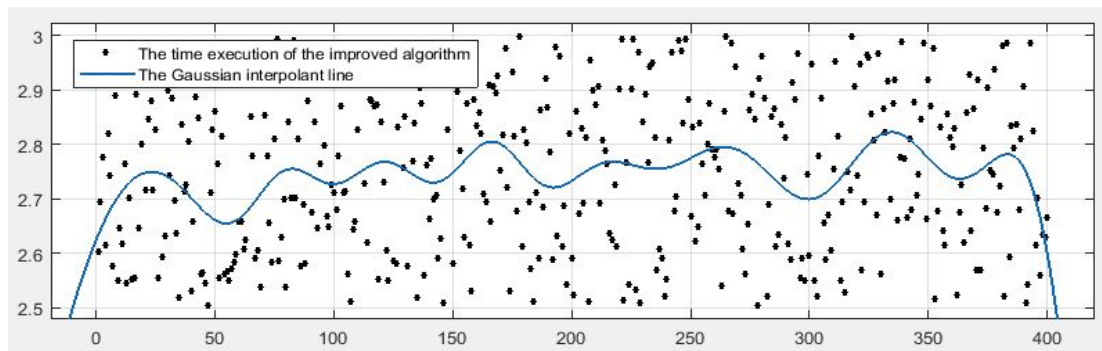


Figure 4: A graph showing the dependency of the execution time for the recognition of each face image for the improved pattern

We can confirm, from the graphs presented above, the time execution needed to perform the recognition process for the improved model of the simulation, is lower in comparison to the classical model. In the corresponding graph of the improved simulation model the biggest value of the time execution needed to perform the recognition does not exceed 2.9 sec whereas in the standard model graph the lowest execution time is above 3.5 sec. Also, presented below are the supporting data of the trend-line performance and the execution time of which 400 imaging images of the simulation model.

Table 2: A table showing the performance data of two models

	SSE_Standard Algorithm	R-squared_Standard Algorithm	Adjusted R-square_Standard Algorithm	RMSE_Standard Algorithm
Standard Algorithm	268.8	0.06352	0.006235	0.8456
Improved Algorithm	7.484	0.06752	0.01048	0.1411

Both simulation models support the "NonLinearLeastSquares" method and are not robust. The algorithm used to program the approximation method "Gauss8" is "Trust-Region". Further details are as follows:

1. *DiffMinChange* – 1.0e-8
2. *DiffMaxChange* – 0.1
3. *MaxFunEvals* – 600
4. *MaxIter* – 400
5. *TolFun* – 1.0e-6
6. *TolX* – 1.0e-6

4. CONCLUSIONS AND DISCUSSIONS

In this paper we discussed about the field of biometric face recognition regarding performance of the Eigenface algorithm (Gonzalez et al, 2018).

The importance of the Eigenface model, as an algorithm for biometric facial identification processes, plays an important role and provides space for continuous reconfigurations and modifications that improve the performance of the models in question in different terms where one of them is the time of facial identification execution versus a certain database.

In our model we have implemented a simulation model through Matlab software (R2017a), which realizes the face recognition process including an open source database of 400 facial images (Solomon et al, 2011). The purpose of this paper was to present a simulation model that deals inside it with a modified version of the Eigenface algorithm; the modeling was intended to give the results of this improvement of the Eigenfaces algorithm in terms of the execution time of identifying a facial image.

The modification, carried out in the Eigenface algorithm, was the intervening in the respective cycles by introducing a subset into the algorithm. Also, the modification of this modeling was the intervention standard code that makes it possible to read the database that is further applied in the basic model algorithm (Nixon et al, 2013).

Also, to reflect the results in time, we simulated through Matlab a "Gauss8 approximation" algorithm model that generates a threefold reflection performance of the standard Eigenface algorithm versus the improved algorithm (Bolle et al, 2004). Along with the graphical data of Gauss8 approximation, specific and supporting parameters are also given, where they are considered as computable coefficients (Petrou et al, 2015).

Because of the Gauss8 method simulations, it is concluded that the execution time of the facial image identification process for the standard Eigenface algorithm has extremes that show greater time values compared to the improved pattern (Vacca, 2007).

Disputes and discussions that arise from this study leave spaces for improvements in the terms of time needed to perform facial identification process performances as well as the size of the database needed to keep the face images; in relation to the database arises the challenge of designing models that go hand in hand with the improvement of the model's quality in relation to the execution.




5. REFERENCES

- [1] Bolle, R. M., Connell, J. H., Pankanti, S., Ratha, N. K., Senior, A. W.: "Guide to biometrics", (Springer-Verlag, New York, 2004), doi: 10.1007/978-1-4757-4036-3.
- [2] Boutilier, T.: "Face Recognition Across the Imaging Spectrum", (Springer International Publishing, Switzerland, 2016), doi: 10.1007/978-3-319-28501-6.
- [3] Buhrow, W. C.: "Biometrics in support of military operations: Lessons from the battlefield", (CRC Press, Florida, USA, 2016).
- [4] Chityala, R., Pudipeddi, S.: "Image processing and acquisition using Python", (CRC Press, Florida, USA, 2014).
- [5] Das, R.: "The science of biometrics: Security technology for identity verification", (Routledge, New York, 2018), doi: 10.4324/9780429487583.
- [6] Datta, A. K., Datta, M., Banerjee, P. K.: "Face detection and recognition: Theory and practice", (Taylor & Francis, Florida, USA, 2015), doi: 10.1201/b19349.
- [7] Gonzalez, R. C., Woods, R. E.: "Digital image processing", 4th ed, (Pearson, New York, 2018).
- [8] Jain, A. K., Li, S. Z.: "Handbook of face recognition", (Springer-Verlag, London, 2011), doi: 10.1007/978-0-85729-932-1
- [9] Newman, R.: "Security and access control using biometric technologies", (Cengage Learning, US, 2009).
- [10] Nixon, M. S., Aguado, A. S.: "Feature extraction and image processing for computer vision", 3rd ed, (Academic Press, Oxford, UK, 2013), doi: 10.1016/C2011-0-06935-1.
- [11] Petrou, M., Petrou, C.: "Image processing: The fundamentals", 2nd ed, (John Wiley & Sons, Chichester, 2015), doi: 10.1002/9781119994398.
- [12] Solomon, C., Breckon, T.: "Fundamentals of digital image processing: A practical approach with examples in Matlab", (John Wiley & Sons, Chichester, 2011), doi: 10.1002/9780470689776.
- [13] Vacca, J. R.: "Biometric technologies and verification systems", (Elsevier - Butterworth Heinemann, Amsterdam, 2007).



© 2018 Authors. Published by the University of Novi Sad, Faculty of Technical Sciences, Department of Graphic Engineering and Design. This article is an open access article distributed under the terms and conditions of the Creative Commons Attribution license 3.0 Serbia (<http://creativecommons.org/licenses/by/3.0/rs/>).

DEVELOPING AUGMENTED REALITY APP FOR SMART PACKAGING

Stefan Đurđević¹ , Dragoljub Novaković¹ , Savka Adamović¹ ,
Frank Boadu², Adriana Rodríguez Lezaca³, Željko Zeljković¹

¹University of Novi Sad, Faculty of Technical Sciences,
Department of Graphic Engineering and Design, Novi Sad, Serbia

²University Printing Press, Kwame Nkrumah University
of Science and Technology (KNUST), Kumasi, Ghana

³SENA, National Training Service, Bogota, Colombia

Abstract: *Augmented Reality technology is increasingly present smart packaging feature. This paper presents the development of the smart packaging application that will provide information on the state of the product in packaging using the Augmented reality technology as a result. In order to control the product state, freshness control labels were printed with stimuli-responsive dyes in the form of specific code. These dyes are conceivable for all environmentally sensitive goods during storage and transport such as food, seeds, pharmaceuticals, cosmetics, electronics etc. These dyes are very useful for controlling the product freshness because they do not require an additional power supply and they can be monitored optically via the smart device camera. Stimuli-responsive dyes can report different environmental influences such as water/moisture, temperature, light, pressure, pH, etc. in a one-bit binary state or in gradually changing optical properties. The aim of the paper is the development of the application that will provide product freshness information based on packaging design (product type) and different environmental influences.*

Key words: augmented reality, product quality, smart packaging, smart labels, stimuli-responsive dyes

1. INTRODUCTION

There is a long list of various “smart materials” that enhance smart packages. These include shape memory alloys to control the opening and closing of packages depending on environmental conditions, piezoelectric materials to provide power for lighting and audio features on packaging, smart adhesives that can be used in conjunction with smart labels, thermochromic inks to show when optimal or dangerous temperatures have been reached, etc. (Furht, 2011). There are features and benefits of combining these smart materials with Augmented Reality technology. In this paper, we will describe how to develop the smart labels and augmented reality app for identifying product state. A smart label will be printed with screen printing inks tone sensitive to the change of essential parameters for the preservation of product state (time, temperature, UV rays, humidity, etc.), and the Augmented Reality app will be developed in Swift program language for new iOS 11 devices.

1.1 Stimuli-responsive dyes

Stimuli-responsive or sensitive dyes change their absorption spectrum through induced transformations of light, temperature, pH, water, etc. The most-known organic compound in this category is spiropyran; its reversible closure properties are extensively examined. Induced by heating and light irradiation, it becomes coloured (Hunger, 2003).

In recent years stimuli-responsive dyes are used for the printing, packaging, security (brand protection, traceability, tamper-evidence), medical sterilisation, heat and radiation curing, food retorting, coding and marking, etc. (Siltechlimited, 2018).

Smart inks can respond to the following sources of stimulation (Sfxc, 2018):

- Gamma Radiation
- UV Radiation
- Temperature (Heat or cold)
- Steam
- Ethylene Oxide
- Infrared Radiation etc.

Thermochromic inks or dyes are temperature sensitive (Stančić et al, 2013) compounds that change colour gradually in response to fluctuations in temperatures. There are both irreversible and reversible types (Sfxc, 2018).

1.2 Smart Labels

There are different types of smart labels developed for smart packaging. In this paper, we are based on creating Augmented Reality application for the specific thermochromic label. These labels were developed by Đurđević et al. (Đurđević et al, 2017). The labels were printed in the first pass, with thermochromic ink and after drying process in the second pass, labels were printed with conventional ink (Figure 1).

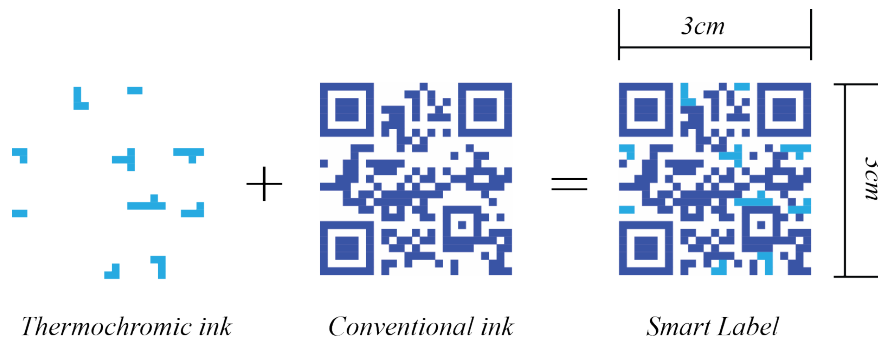


Figure 1: Thermochromic Smart label printing process

1.3 Smart packaging

Smart packaging provides enhanced functionality that can be divided into two submarkets: active packaging and intelligent packaging (Packagingdigest, 2018). Active packaging is packaging, which has an extra function in addition to that of providing a protective barrier against external influence. It can control, and even react to, phenomena taking place inside the package. Intelligent packaging monitors to give information on the quality and state of the packed product. Smart, intelligent or clever packaging is defined as a packaging technique containing an external or internal indicator for the active product history and quality (Febech et al, 2000).

1.4 Augmented Reality Technology

AR-technology has huge possibilities, and only technology and imagination set the limit on what can be achieved with it. AR-technology can be used in many fields such as commercial, games, navigation, tourism, medicine, military, maintenance, etc. (Azuma, 1997; Sielhorst et al, 2004; Jung et al, 2008; Reitmayr et al, 2004; Platonov et al, 2006). In recent years, a wide variety of AR technologies and applications have been developed (Van Krevelen et al, 2013; Caudell et al, 1992).

The term “Augmented Reality” was coined by Caudell and Mizell (Caudell et al, 1992) in 1992, as superimposing environment whose elements are merged with augmented computer-generated images creating a mixed reality (Furht, 2011). Unlike virtual reality, which creates an artificial environment, Augmented Reality uses the existing environment and overlays new information on top of it. That means Augmented Reality requires less computation resource than Virtual Reality (VR) because it only needs to render the overlaid objects instead of every pixel on the screen.

Augmented Reality combines real and virtual, it is interactive in real time and registered in 3D (Azuma, 1997). Combines real and virtual means that information or animations are displayed on the same screen as the user sees the actual world on or through, to enhance what the user can see and read out from real-world objects. Interactive in real time means that the user can interact with whatever information is displayed in the AR system. For instance, a user might look at a food packaging and is provided information about the food manufacturer and by clicking on this information the user can get the other food product list or the manufacturer’s website (Figure 2). Registered in 3D means that virtual information is displayed and aligned with the real-world object (Tholsgard, 2014).

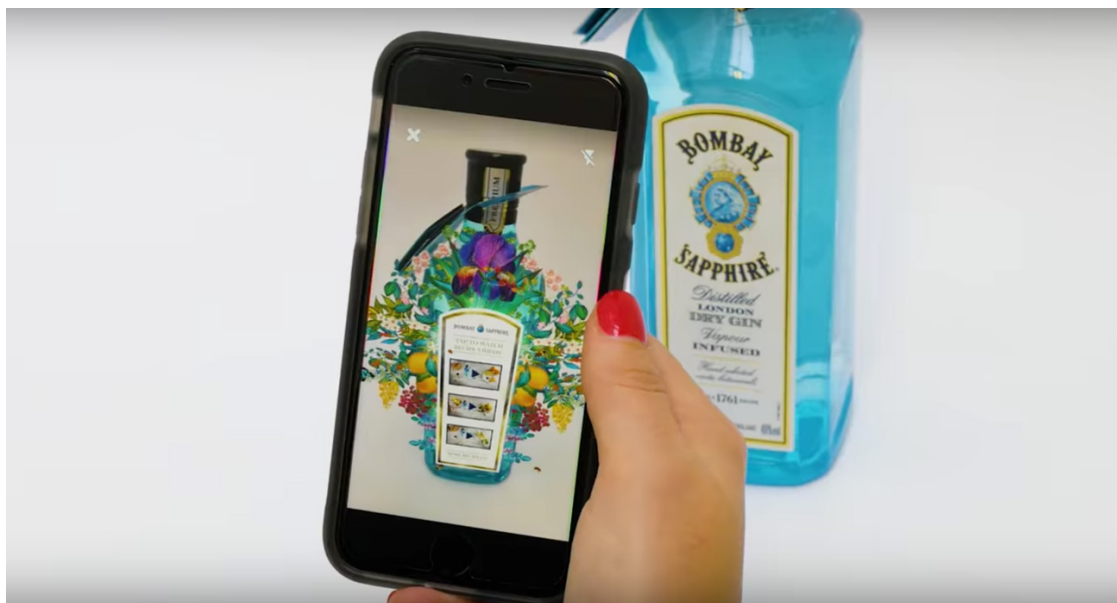


Figure 2: Augmented Reality App activated after product label scan

1.5 Problem Description

This work aims to develop the Augmented Reality app that is possible to check the product state via comparing packaging design (product type) and smart thermochromic label. The Smart thermochromic label was the previous research, and its development can be found in Đurđević et al. (Đurđević et al, 2017) article.

2. METHODS AND TOOLS

The following applications were used for the Augmented Reality smart packaging application development: 3D Studio Max for 3D modelling of freshness indicator, Xcode 9.4.1 and Swift 4 for programming application for iOS devices, as well as the Adobe Illustrator CC, Adobe Photoshop CC and Sketch for creating design interface of the application.

3. RESULTS

The basis of this application is the Smart Label image consisting fields printed with conventional inks and fields printed with irreversible thermochromatic inks that disappear if they reach the higher temperature in the ambient than the activation temperature (for the used type of ink 30oC). Developing code for this type of smart packaging labels is shown in previous research (Đurđević et al, 2017).

Smart labels are applied to existing packaging, where the first target is the segment of packaging design side to applied label, second is the non-activated label code design, and the third is the label code in the activated form. In this way, the device recognises the product and the status of the label code, and by linking this two information gives freshness state of the product. For example, if the frost product is concerned, activating the thermochromatic ink will signal that the product was thawed during storage, and because of that, it is not fresh anymore. Parts of the user interface design were created in vector graphics software from the Adobe CC package, Adobe Illustrator, and integrated into UI design software Sketch (Figure 3). Finally, user interface design from Sketch is used in Xcode.

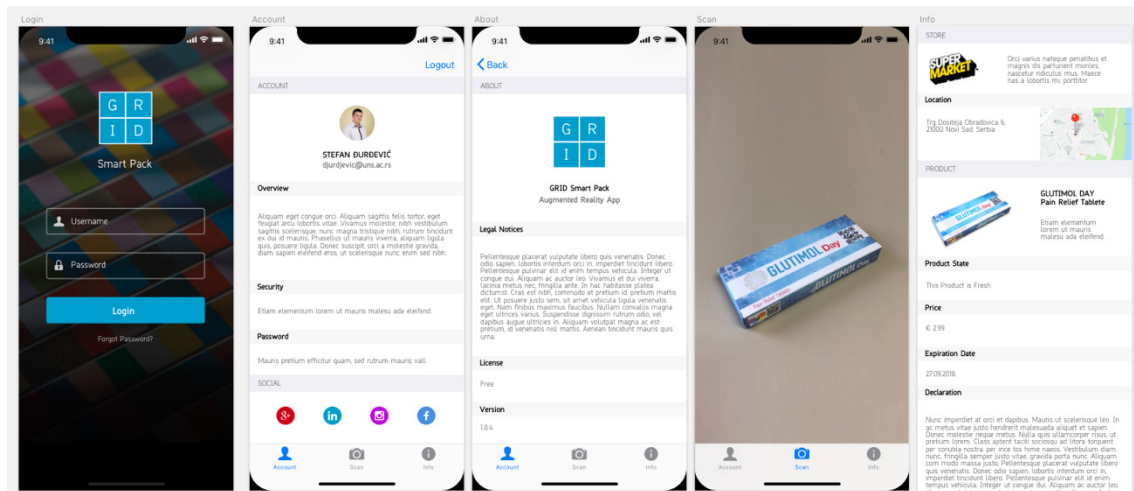


Figure 3: Smart Packaging Application UI development in Sketch

It can be seen that based on the GPS location, additional information about the identified product is also loaded on the interface, such as the price, the declaration, the store, the expiration date. Figure 4 shows View Controllers in Xcode. Application interface screens can be found in figure 3.

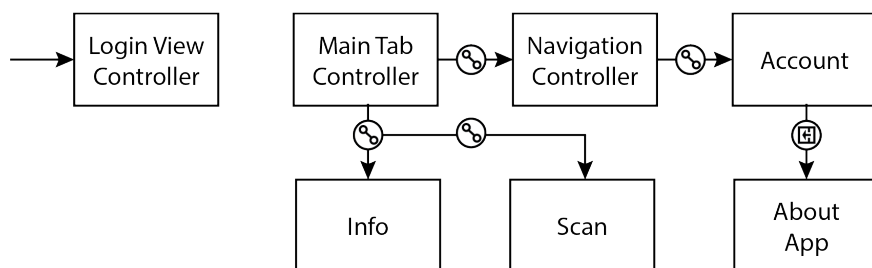


Figure 4: Augmented Reality app View Controllers connections in xCode

The "Scan" tab allows you to launch an AR camera that recognises the product and its freshness and prints data within the "Info" tab. Below is the code that is associated with the View Controller "Scan" tab and "Scan" tab in use while the application is running on a smartphone (Figure 6).

First, it is necessary to import code packages for Augmented Reality and User Interface development.

```

import Foundation
import UIKit
import ARKit

```

Then in this part of code buttons are linked with View Controllers.

```

class SecondViewController: UIViewController {
    @IBOutlet weak var sceneView: ARSCNView!
    @IBOutlet weak var label: UILabel!

```

This part of the code is responsible for 3D object Fresh animation setup (fade duration, rotation, spin action, etc.).

```

let fadeDuration: TimeInterval = 0.3
let rotateDuration: TimeInterval = 10
let waitDuration: TimeInterval = 0.5

```

```

lazy var fadeAndSpinAction: SCNAction = {
    return .sequence([
        .fadeIn(duration: fadeDuration),
        .rotateBy(x: 0, y: CGFloat.pi * 360 / 60, z: 0, duration: rotateDuration),
        .wait(duration: waitDuration),
        .fadeOut(duration: fadeDuration)
    ])
}()

lazy var fadeAction: SCNAction = {
    return .sequence([
        .fadeOpacity(by: 0.8, duration: fadeDuration),
        .wait(duration: waitDuration),
        .fadeOut(duration: fadeDuration)
    ])
}()

```

In this part of the code, we can see product state 3d models. We can see three product states depending on product type and label state combination (fresh, check again, do not use).

```

lazy var freshNode: SCNNode = {
    guard let scene = SCNScene(named: "Fresh.scn"),
        let node = scene.rootNode.childNode(withName: "fresh", recursively: false) else { return SCNNode() }

    let scaleFactor = 0.010
    node.scale = SCNVector3(scaleFactor, scaleFactor, scaleFactor)
    node.eulerAngles.x = 0
    node.runAction(SCNAction.rotateBy(x: 0, y: 0, z: 0, duration: 0.0))

    return node
}()

lazy var checkNode: SCNNode = {
    guard let scene = SCNScene(named: "Check.scn"),
        let node = scene.rootNode.childNode(withName: "check", recursively: false) else { return SCNNode() }

    let scaleFactor = 0.1
    node.scale = SCNVector3(scaleFactor, scaleFactor, scaleFactor)
    return node
}()

lazy var doNotNode: SCNNode = {
    guard let scene = SCNScene(named: "Do not use.scn"),
        let node = scene.rootNode.childNode(withName: "doNot", recursively: false) else { return SCNNode() }

    let scaleFactor = 0.25
    node.scale = SCNVector3(scaleFactor, scaleFactor, scaleFactor)
    node.eulerAngles.x += -.pi / 2
    return node
}()

override func viewDidLoad() {
    super.viewDidLoad()
    sceneView.delegate = self
    configureLighting()
}

```

```

func configureLighting() {
    sceneView.autoenablesDefaultLighting = true
    sceneView.automaticallyUpdatesLighting = true
}

override func viewWillAppear(_ animated: Bool) {
    super.viewWillAppear(animated)

    resetTrackingConfiguration()
}

override func viewWillDisappear(_ animated: Bool) {
    super.viewWillDisappear(animated)
    sceneView.session.pause()
}

@IBAction func resetButtonDidTouch(_ sender: UIBarButtonItem) {
    resetTrackingConfiguration()
}

```

Here is the part of the code to give the information to a user to move the camera to detect smart packaging.

```

func resetTrackingConfiguration() {
    guard let referenceImages = ARReferenceImage.referenceImages(inGroupNamed: "AR Resources",
bundle: nil) else { return }
    let configuration = ARWorldTrackingConfiguration()
    configuration.detectionImages = referenceImages
    let options: ARSession.RunOptions = [.resetTracking, .removeExistingAnchors]
    sceneView.session.run(configuration, options: options)
    label.text = "Move camera around to detect smart packaging"
}
}

```

```

extension SecondViewController: ARSCNViewDelegate {

```

This part of the code will render information about packaging name and state after detection.

```

func renderer(_ renderer: SCNSceneRenderer, didAdd node: SCNNode, for anchor: ARAnchor) {
    DispatchQueue.main.async {
        guard let imageAnchor = anchor as? ARImageAnchor,
            let imageName = imageAnchor.referenceImage.name else { return }
        let overlayNode = self.getNode(withImageName: imageName)
        overlayNode.opacity = 0
        overlayNode.position.y = 0.2
        overlayNode.runAction(self.fadeAndSpinAction)
        node.addChildNode(overlayNode)

        self.label.text = "Smart packaging detected: \"\(imageName)\""
    }
}

func getPlaneNode(withReferenceImage image: ARReferenceImage) -> SCNNode {
    let plane = SCNPlane(width: image.physicalSize.width,
        height: image.physicalSize.height)
    let node = SCNNode(geometry: plane)
    return node
}

```



```

func getNode(withImageName name: String) -> SCNNode {
    var node = SCNNode()
    switch name {
    case "Glutamol day fresh state":
        node = freshNode
    case " Glutamol day check product state":
        node = checkNode
    case " Glutamol day do not use":
        node = donotNode
    default:
        break
    }
    return node
}
}

```

To build the application on a mobile device, Xcode 9.4 and programming language, Swift was used. Figure 5 shows the xCode screen while App is running in test mode on a mobile device.

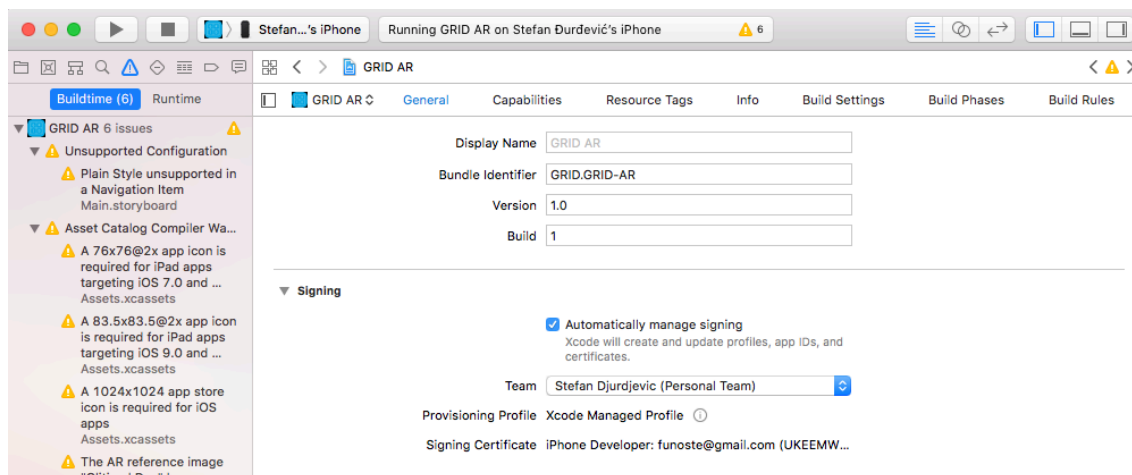


Figure 5: Building Smart Packaging Application on iPhone in Xcode

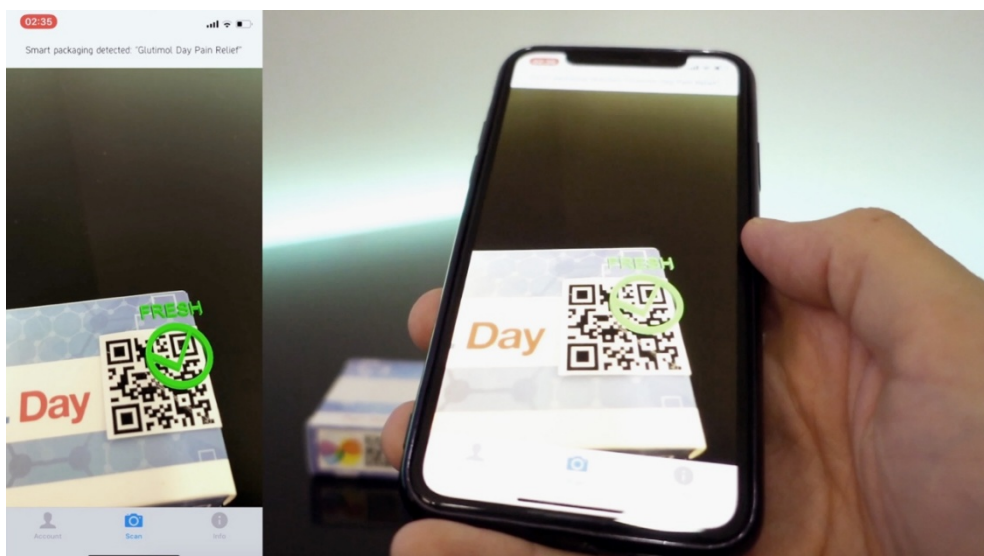


Figure 6: AR Smart Packaging App Demo

4. DISCUSSION

The final application is a working AR application; it fully meets all the requirements for an AR application. As a result, the service was able to show the product state (freshness) depending on smart label state and packaging image target and to provide a variety of information in a very accurate and fast way. The application also has GPS working features to personalise information depending on the phones GPS location. GPS integration can help the application to recognise the Store and find the product price depending on location.

5. CONCLUSION

The AR concept of the smart packaging shows that it is possible to create an application for reading content and checking the product freshness in smart packaging using smart labels. Current technological advances ensure the implementation of such a control system. In the future, we expect the fall in prices of smart inks for printing smart labels and greater development of AR. Advances in powerful CPU, camera, accelerometer, GPS, and solid state compass are present in all mobile phones today, making them the best handheld platform for this AR system. However, their small display size is less than ideal for 3D user interfaces, but it is expected that in the future this system will be able to adapt and head mounted displays (HMD) and spatial displays.

6. ACKNOWLEDGEMENTS

This work was supported by the Serbian Ministry of Science and Technological Development, Grant No.:35027 "The development of software model for improvement of knowledge and production in graphic arts industry".

7. REFERENCES


- [1] Azuma, R. T.: "A Survey Of Augmented Reality", *Presence Teleoperators and Virtual Environments* 6(4), 1997, 355-385. doi: 10.1162/pres.1997.6.4.355
- [2] Camigniani, J., Furht, B., Anisetti, M., Ceravolo, P., Damiani E., Ivkovic. M.: "Augmented Reality Technologies, Systems and Applications." *Multimedia Tools and Application*, 51(1), 341 – 377, 2010. doi: 10.1007/s11042-010-0660-6
- [3] Caudell, T., Mizell, D.: "Augmented Reality: An Application of Heads-Up Display Technology to Manual Manufacturing Process", *Proceedings of Twenty-Fifth Hawaii International Conference on System Sciences*, volume 2, (Kauai, HI, USA, 1992) 659 – 669. doi: 10.1109/HICSS.1992.183317
- [4] Đurđević, S., Novaković, D., Zeljković, Ž., Kašiković, N.: "Thermochromic inks and augmented reality as part of novel smart packaging solutions", *Proceedings of 2nd International Printing Technologies Symposium Printistanbul, 2. (Printistanbul, Istanbul: Marmara Üniversitesi, 2017)*, 153-159.
- [5] Febech, B., Hellstrom, B., Henrysdotter, G., Hjulmand, M., Nilsson, J., Rudinger, L., Sipilainen, T., Solli, E., Svensson, K., Thorkelsson, A., Tuomaala, V.: "Active and intelligent food packaging: A Nordic report on the legislative aspects", (Nordic Council of Ministers, Copenhagen, 2000).
- [6] Furht, B.: "Handbook of Augmented Reality", (Springer Publishing Company, New York, 2011).
- [7] Hunger, K.: "Industrial Dyes: Chemistry, Properties, Applications", (WILEY-VCH Verlag GmbH & Co. KGaA, Weinheim, 2003).
- [8] Jung, K., Lee, S., Jeong, S., Choi, B.: "Virtual Tactical Map with Tangible Augmented Reality Interface", *Proceedings of International Conference on Computer Science and Software Engineering*, volume 2 (Wuhan, China, 2008), 1170-1173. doi: 10.1109/CSSE.2008.1305
- [9] Packagingdigest, "Smart Packaging", *Packagingdigest*, URL: <http://www.packagingdigest.com/smart-packaging> (last request: 2018-10-24).
- [10] Platonov, J., Heibel, H., Meier, P., Grollmann, B.: "A mobile markerless AR system for maintenance and repair", *Proceedings of IEEE/ACM International Symposium on Mixed and Augmented Reality*, (ISMAR, Santa Barbard, CA, USA, 2006), 105-108.
- [11] Reitmayr, G., Schmalstieg, D.: "Collaborative Augmented Reality for Outdoor Navigation and Information Browsing", *Proceedings of the Second Symposium on Location Based Services and TeleCartography*, (Vienna University of Technology, Austria, 2004), 53-62.

- [12] Sfxc, "SFXC | Special Effects and Coatings", Sfxc, URL: <https://www.sfxc.co.uk/products/chameleon-thermochromic-ink-trail-pack-for-paper-board-and-textiles> (last request: 2018-03-24).
- [13] Sielhorst, T., Obst, T., Burgkart, R., Riener, R., Navab, N.: "An Augmented Reality Delivery Simulator for Medical Training", International Workshop on Augmented Environments for Medical Imaging - MICCAI Satellite Workshop, 2004.
- [14] Siltechlimited, "Siltech limited smart inks", Siltechlimited, URL: <http://siltechlimited.com/> (last request: 2018-03-23).
- [15] Stančić, M., Kašiković, N., Novaković, D., Milošević, R., Grujić, D.: "Thermal Load Effect on Print Quality of Ink Jet Printed Textile Materials", Journal of Graphic Engineering and Design, 4 (2), 27-33, 2013.
- [16] Tholsgard, G.: "3D rendering and interaction in an augmented reality mobile system", (UPPSALA University, Department of Information Technology, 2014), page 7.
- [17] Van Krevelen, R., Poelman, R.: "A Survey of Augmented Reality Technologies, Applications and Limitations", The International Journal of Virtual Reality, 9(2), 1-20, 2010.



© 2018 Authors. Published by the University of Novi Sad, Faculty of Technical Sciences, Department of Graphic Engineering and Design. This article is an open access article distributed under the terms and conditions of the Creative Commons Attribution license 3.0 Serbia (<http://creativecommons.org/licenses/by/3.0/rs/>).

PDF METADATA AND ITS CONVERSION TO XJDF

Thomas Hoffman-Walbeck 

Stuttgart Media University, Faculty Print and Media, Stuttgart, Germany

Abstract: *In this paper, we show an example of how a product description such as the specifications of the print substrate can be embedded as metadata in a PDF file using a well-documented technology for variable data printing. We demonstrate the corresponding data structures in PDF. Moreover, we are explaining how these structures can be integrated in a PDF file and retrieved afterwards with a JAVA program. In addition, this metadata is converted into XJDF, which can be passed on to a commercially available workflow management system. The basic structure of XJDF is explained as well as its generation with JAVA.*

Key words: Metadata, PDF, PDF/VT, XJDF, PrintTalk, JDF, CSV, Web-to-Print, Workflow Management System

1. INTRODUCTION

Typically, a production department of a print service provider (PSP) imports content data - mostly PDF - and metadata - in formats like JDF or private XML - into a Workflow Management System (WMS). PDF contains the layout definition of the pages that are supposed to be printed, while the metadata incorporates the overall product specification as well as production issues. Metadata inside PDF are rarely used for specifying the product or even controlling the production. Extended Metadata Platform (XMP) (ISO 16684-1:2012, 2012), for example, is mainly used for storing information about page components (like images) or about the PDF document itself (like contact details of the author). The XMP metadata structure is not suitable for defining a product and its product parts.

The PSP usually receives PDF documents from the print buyer (PB) or some agency via an email attachment, FTP-server, portal or some cloud storage. Metadata concerning the product definition, however, is generated by the MIS of the PSB or by some PB's Enterprise Resource Planning System (ERP). The MIS-employee has to learn the PB's product intentions and fill them in the system. Only in the case of Web-to-Print (W2P) the PDF and the metadata stem from the same source, i.e. the W2P-Server. In all other cases, the content data and the product specification are using different communication channels, which can be time-consuming to synchronize. Anyhow, even with W2P two different files need to be handled simultaneously. Thus, it would be easier if the product definition could be stored inside the PB's PDF, in particular since it describes the view of the PB's intention concerning the product in the first place. This metadata could be generated by a W2P or even by the customer himself, using a plug-in for a layout software for example.

The necessary technology became available with PDF/VT (ISO 16612-2:2010, 2010), an extension of PDF 1.6 for transactional and variable data printing. Now, however, this is part of PDF 2.0 (ISO 32000-2:2017, 2017). The technology allows to define different product parts and to assign individual pages of a PDF document to just these product parts. In addition, the final product as well as each product part may refer to their own metadata structure, in which one can specify detailed technical information. As an example, the desired printing substrates of the product parts or the overall binding intent may be given. While PDF 2.0 provides the general file structure, the CIP4 organization specified the necessary semantics in the papers "ICS-Common Metadata for Document Production Workflows" (Prosi, 2015) and "ICS-IntentMetadata.PDF.1.5 ISO Draft" (Meissner, 2015). In this context, please refer also to the draft ISO standard ISO/CD 21812-1 about print product metadata in PDF files (ISO/DIS 21812-1).

At first, we will outline in this paper the technical structure of the PDF metadata with the help of an example (a booklet with a cover and content). Moreover, we will explain how to implant such structure into a PDF file by a JAVA program. The second part of this paper shows how to extract this information from the PDF file and how to convert the data into a suitable input format for a WMS like JDF (Meissner, 2018), XJDF (Meissner, 2018) and CSV (Wikipedia, 2018). However, in this paper we will only describe in detail the conversion to XJDF through a JAVA program. Since the XJDF can be employed to generate a new job within the WMS it will be embedding into a PrintTalk (Confluence.cip, 2018;

Confluence.cip, 2015) business object of type “purchase order”. Finally, we will show what kind of results can be gained when importing the generated PrintTalk/XJDF file into a commercially available WMS. Figure 1 shows the modules of the implementation. Software ① and ② are stand-alone prototype applications. The user enters details in a dialogue mask of program ① in order to provide the necessary metadata. Note that ① will be executed by a PB, while ② will precede the PSPs WMS.

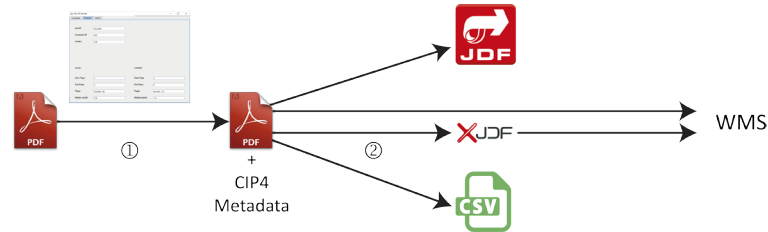


Figure 1: Structure of the software applications: ① writes CIP4 metadata into a PDF, ② reads the metadata and converts it to JDF, XJDF and CSV.

2. METHODS

For both ① and ② we are using the SDK IntelliJIDEA 2018.1 (Jetbrains, 2018) and the JAVA version 9.0.1. For reading and writing the PDF/VT-structures, we employ the libraries PDFlib und PDI 9.1.2 (Pdfliib, 2018) of the company PDFlib GmbH. Furthermore we include different external libraries for the XJDF conversion in ②: istack-commons-runtime-2.16.jar, jaxb-core-2.2.7.jar, jaxb-impl-2.2.7.jar, FastInfoset-1.2.12.jar, commons-configuration-1.9.jar, commons-io-2.4.jar, commons-lang-2.6.jar, commons-logging-1.1.1.jar, activation-1.1.1.jar, jaxb-api-2.2.7.jar, jsr173_api-1.0.jar, junit-4.10.jar, commons-lang3-3.4.jar, xJdfLib-0.13.jar, xPrintTalkLib-0.13.jar, hamcrest-core-1.1.jar, annotations-13.0.jar, jaxb2-basics-runtime-0.9.1.jar. The generated PDF should not be compressed, in order to analyse the file with a standard text editor. Moreover the tool “Enfocus Browser Vers. 3.0” is very helpful to study the dictionary hierarchy in PDF.

3. RESULTS

In subsection 3.1, we will explain the document part (DPart) hierarchy inside PDF, which might reference to one or more pages (page objects). Each DPart can also reference to an object called Document Part Metadata (DPM), which in turn can contain technical details about the document part. We will present a particular example. Then we will show in subsection 3.2 how to generate DPart und DPM object using the PDFlib library for JAVA. The following two section cover details concerning ②. In section 3.3, we will present the basic structure of XJDF. Section 3.4 primarily covers the conversion of the metadata information into XJDF using the library xJDF of CIP4. Finally, in subsection 3.5 we will demonstrate the XJDF import into a WMS.

3.1 Metadata structure

Figure 2 shows an example of a simplified PDF/VT structure. In the right-hand side, there are the normal page objects, in the left-hand side the DPart objects.

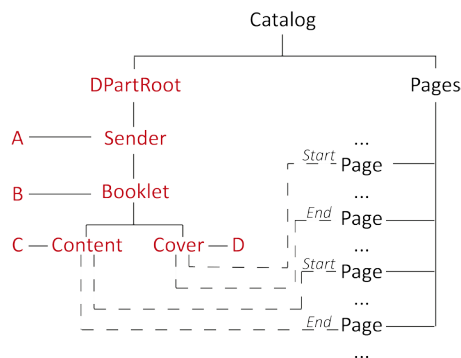


Figure 2: DPart hierarchy with DPMs A, B, C and D

The leaves of the Dpart-tree are the product parts. They contain the information about the first and the last page of the product part. The page number in the PDF document does not give the references, but rather as the page object number, which identifies the PDF page object.

The actual definitions of the four DPart objects inside PDF are to be seen in figure 3. Please note that all of them are contained on one stream object. Each DPart is a dictionary that begins with “<<” and ends with “>>”. PDF dictionaries have two parts per entry. The first one is called *key* (e.g. /Type), the second one is called *value* (e.g. /Dpart).

```
stream
11 0
34 63
9 126
6 181
<</Type/DPart/Parent 9 0 R/DPM 12 0 R/Start 22 0 R/End 29 0 R>>
<</Type/DPart/Parent 9 0 R/DPM 35 0 R/Start 39 0 R/End 74 0 R>>
<</Type/DPart/Parent 6 0 R/DPM 10 0 R/DParts[ 78 0 R]>>
<</Type/DPart/Parent 80 0 R/DPM 7 0 R/DParts[ 81 0 R]>>
endstream
```

← Cover

← Content

← Sender

← DpartRoot

Figure 3: DPart objects in side PDF

Each DPart in figure 2 and 3 refers to a specific DMP, which hold information like the intended print substrate or about the contact details of the PB. In application ① the user provides this data via a GUI, which is partially shown in figure 4. The entries in the text fields of the GUI are stored in a XML preferences file in order to make them available for the next launch of the program. The entries can, of course, alternatively edited directly in the XML file.

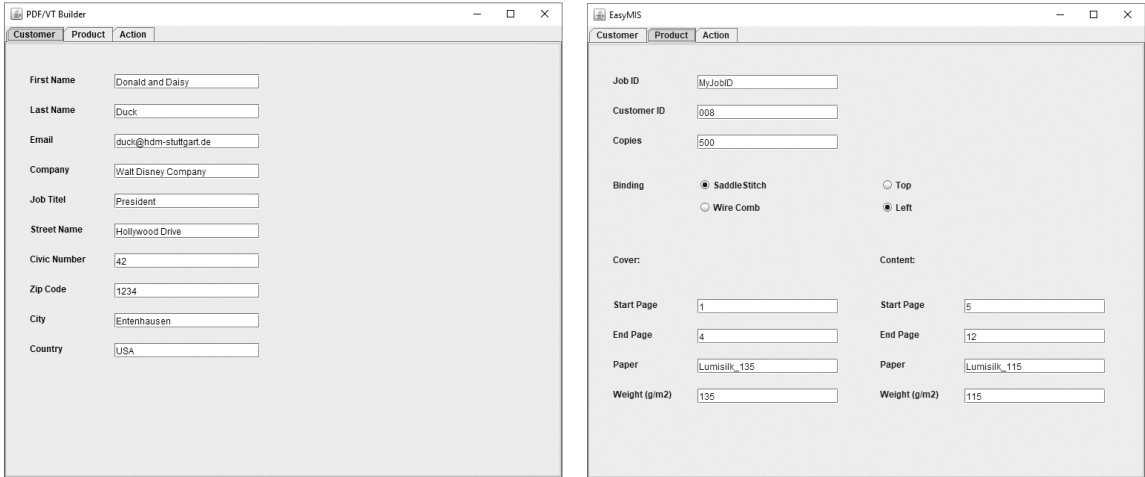


Figure 4: GUI of application ①

The structures of three (slightly text formatted) DPMs can be seen Figure 5. The first one contains information about the sender, the second one some characteristics about the final product, including the binding intent. The product properties concerning the cover of the brochure are given in the third DPM. In this example, only the dictionaries CIP4_BindingIntent and CIP4_MediaIntent have been embedded. In similar manner, one can add other resources like CIP4_ColorIntent, CIP4_ or CIP4_FoldingIntent. The metadata for the content has been omitted in figure 5.

```

<</DPM<</CIP4_Root<</CIP4_Metadata<<
    /CIP4_Conformance(base)
    /CIP4_Creator(Disney)
    /CIP4_JobID(MyJobID)
    /CIP4_Sender<<
        /CIP4_Contact<<
            /CIP4_Person<<
                /CIP4_FirstName(Daisy and Donald)
                /CIP4_Lastname(Duck)
                /CIP4_JobTitel(Presedent)>>
            /CIP4_Address<<
                /CIP4_City(Entenhausen)
                /CIP4_Country(USA)
                /CIP4_PostalCode(1234)
                /CIP4_StreetName(Hollywood Drive)
                /CIP4_CivicNumber(42)>>
            /CIP4_ComChannel<<
                /CIP4_Email(duck@hdm-stuttgart.de)
                /CIP4_ChannelType(Email)>>
            /CIP4_Company<<
                /CIP4_OrganizationName(Walt Disney Company)>>
>>
>>
>>
>>
>>
>>

<</DPM<</CIP4_Root<<
    /CIP4_Production<<
        /CIP4_DescriptiveName(Cover)>>
    /CIP4_Intent<<
        /CIP4_ProductType(WrapAroundCover)
        /CIP4_MediaIntent<<
            /CIP4_MediaQuality(lumisilk_135)
            /CIP4_MediaWeight(135)>>
>>
>>
>>
>>

```

Figure 5: DPM structures in PDF example

3.2 Writing metadata into PDF

Figure 6 shows a snippet of the code for writing the metadata into the PDF file. In the first two lines, the PDFLib is open and the PDF file is read. In the next two lines DPM dictionaries are generated, that are called CIP4_Intent and CIP4_Media_Intent. Here POCA stands for “PDF Object Creation API” and is a PDFlib set of methods for creating objects like DPMs.

In the following line the dictionary CIP4_Media_Intent is filled in with the key-value pair CIP4_Media_Intent/coverPaperWeight, whereas CIP4_MediaWeight is a metadata term defined in [1] and coverPaperWeight an internal variable that holds the corresponding string that the user has filled in via the GUI. The method “P.poca_insert” requires a String in the second parameter. The last line inserts the dictionary CIP4_MediaIntent as a key/value pair into the CIP4_Intent dictionary. Using this technology one can construct the tree of dictionaries in figure 5.


```

...
p=new pdfLib();
...
docIn = p.open_pdi_document(inFile, "");
...
p.begin_dpart("dpm=" + dpm);
...
CIP4_Intent = p.poca_new("containertype = dict usage=dpm");
...
CIP4_MediaIntent = p.poca_new("containertype = dict usage=dpm");
...
p.poca_insert(CIP4_MediaIntent, "type=string key=CIP4_MediaWeight value="+{"+coverPaperWeight+"}");
...
p.poca_insert(CIP4_Intent, "type=dict key=CIP4_MediaIntent value=" + CIP4_MediaIntent);
...

```

Figure 6: Writing a DPart and DPMs into PDF

3.3 XJDF

An introduction into XJDF technology can be found in (Meißner, 2017) and in (Meissner, 2018). Here we only want to describe the XJDF outcome of software ②. The XJDF element in figure 7 is embraced by a PrintTalk element.

```

<ptk:PrintTalk version="2.0" payloadID="5bf27d60-cc4f-4ed3-86a4-3a2a88b6900c" Timestamp="2018-
06-07T12:52:16Z" xmlns:ptk="http://www.printtalk.org/schema_2_0" xmlns:xjdf="http://www.CIP4.org/
JDFSchema_2_0">
  <ptk:Request>
    <ptk:PurchaseOrder Currency="Euro" BusinessID="4711">
      <xjdf:XJDF Category="Product" DescriptiveName="Final Broschur" JobID="MyJobID"
        Types="Product">
        <xjdf:ProductList>
          <xjdf:Product Amount="500" DescriptiveName="Broschur (root)" ID="ID_broschur"
            IsRoot="true"
            ProductType="booklet">
            <xjdf:Intent Name="BindingIntent">
              <xjdf:BindingIntent BindingOrder="Collecting" BindingSide="Left"
                BindingType="SaddleStitch"/>
            </xjdf:Intent>
            <xjdf:Intent Name="LayoutIntent">
              <xjdf:LayoutIntent Pages="12"/>
            </xjdf:Intent>
          </xjdf:Product>
          <xjdf:Product Amount="500" DescriptiveName="Cover" ID="ID_Cover" IsRoot="false"
            ProductType="WrapAroundCover">
            <xjdf:Intent Name="MediaIntent">
              <xjdf:MediaIntent MediaQuality="Lumisilk_135" MediaType="Paper"
                NamedWeight="135"/>
            </xjdf:Intent>
            <xjdf:Intent Name="LayoutIntent">
              <xjdf:LayoutIntent Pages="4"/>
            </xjdf:Intent>
          </xjdf:Product>
        </xjdf:ProductList>
        ...Analogue structure for the product part „Content“...
      </xjdf:ProductList>
      <xjdf:ResourceSet Name="Contact" ProcessUsage="Input">
        <xjdf:Resource ID="Contact_8fb6beef-0c72-43b5-a42a-cb3d53b4b262">
          <xjdf:Contact ContactTypeDetails="Customer">
            <xjdf:Address City="Entenhausen" CivicNumber="42" Country="USA"
              PostalCode="1234" Street="Hollywood
              Drive"/>
            <xjdf:ComChannel ChannelType="Email" Locator="duck@hdm-stuttgart.de"/>
            <xjdf:Company OrganizationName="Walt Disney Company"/>
            <xjdf:Person FamilyName="Duck" FirstName="Donald and Daisy"
              JobTitle="President"/>
          </xjdf:Contact>
        </xjdf:Resource>
      </xjdf:ResourceSet>
      <xjdf:ResourceSet Name="RunList" ProcessUsage="Input">
        <xjdf:Resource ID="RunList_7a226b95-f194-4ae1-839f-b5888b8cc032">
          <xjdf:Part ProductPart="ID_RunList_Cover"/>
          <xjdf:RunList NPage="4" Pages="1 4">
            <xjdf:FileSpec URL="https://www.hdm-stuttgart.de/print40/Flyer.pdf"/>
          </xjdf:RunList>
        </xjdf:Resource>
        <xjdf:Resource ID="RunList_6b34765a-fd03-49e4-b5db-798801b3b97a">
          <xjdf:Part ProductPart="ID_RunList_Content"/>
          <xjdf:RunList NPage="8" Pages="5 12">
            <xjdf:FileSpec URL="https://www.hdm-stuttgart.de/print40/Flyer.pdf"/>
          </xjdf:RunList>
        </xjdf:Resource>
      </xjdf:ResourceSet>
    </xjdf:XJDF>
  </ptk:PurchaseOrder>
</ptk:Request>
</ptk:PrintTalk>

```

Figure 7: PrintTalk element with XJDF sub-element

Sub-element of the `PrintTalk` is the business object `Request`, which in turn contains the `PurchaseOrder` element (see (Confluence.cip4, 2018)). `XJDF` is a child element of `PurchaseOrder`. Next, we find the `ProductList` in the hierarchy. In our example, there are three products in this list. First, there is the final product with the value of the attribute `IsRoot` equals `true`. Next, the product parts “cover” and “content” are also defined as product elements with attributes `IsRoot` equal `false`. Each those products contain one (or more) `Intent` element(s), which describe the product or the product parts from the PB’s point of view. Each `Intent` resource is specialized further by a `Name` attribute and the according sub-element. Here, the final product contains a `BindingIntent`, the product parts `MediaIntents`, which define the printing substrates. In each of them specific `LayoutIntents` have been incorporated. Note that the attributes of these elements are not derived from a corresponding DPM dictionary in the PDF file but rather from the `DPart` structures (see figure 3).

`ResourceSets` succeed the `ProductList`. Each `ResourceSet` contain one or more `Resources`, which in turn can describe physical (like paper used by PSB, not defined in our example) or logical entities like `RunLists`. The two `RunLists` in Figure 7 define the PDF pages of the product parts cover and content. The attributes `NPage` denotes the “Number of Pages” and `Pages` the range of pages in the document. Note that here the sequential page numbers in the document are referred to, while in figure 3, the PDF internal page object numbers are stored.

3.4 Reading metadata from PDF and converting it into XJDF

Figure 8 and 9 show some code snippets for the extracting metadata out of a PDF/VT file. Reading the metadata is actually mostly straightforward: In the first line, the `PDFlib` is opened, in the next the PDF document is parsed in. After that, a path of a dictionary is specified from which entries would be determined. This is done in the last two lines. The individual entries in the dictionary are accessed in the notation of an array.

```
...
p = new pdflib();
...
docIn = p.open_pdi_document(inFileFullName, "");
...
path = "/Root/DPartRoot/DPartRootNode/DPM/DPM/CIP4_Root/CIP4_Metadata/
        CIP4_Sender/CIP4_Person";
firstName = p.pcos_get_string(docIn, path + "[" + 0 + "].val");
lastName = p.pcos_get_string(docIn, path + "[" + 1 + "].val");
...
```

Figure 8: Reading values from a PDF/VT dictionary

Figure 9 shows a snippet of the method concerning the computing of page numbers using PDF page object numbers. Here it is assumed that the page objects in the PDF file have the same order as the pages in the PDFD file. The page object numbers can be arbitrarily. This assumption, however, is not true in general (see F.4.2 in (ISO 32000-2:2017, 2017), p. 885)

```
double getPageNumber(String PDFPageObject) {
...
pageObjectNumber = p.pcos_get_number(docIn, "pcosid:" + PDFPageObject);
...
int dict_length = p.pcos_get_number(docIn, "length:" + "pages");
...
for (i = 0; i < (int) dict_length; i++) {
    if (pageObjectNumber == p.pcos_get_number(docIn, "pcosid:" + "pages" + "[" + i + "]"))
        pageNumber = i;
...
    return (pageNumber + 1);
}
```

Figure 9: Calculating a page number from PDF page objects

Figure 10 shows a snippet of the translation of the metadata to XJDF as shown in figure 7. Here the CIP4 library `xjdfLib` is used. In the first part, the resource `MediaIntent` is defined. The values `CIP4_PaperCover` and `CIP4_PaperCoverWeight` are derived from the PDF metadata and were originally put into the GUI of software ① by user. In the second section, the product part `Cover` is set and

resource `MediaIntentCover` is added. The third paragraph determines the XJDF-structure with the `ProductList` (`broschur`, `cover` and `content`). The generation of the `ResourceSets` are skipped in figure 10. In the last part, finally, the `PrintTalk` envelope is built around the XJDF structure.

```
...
//Create MediaIntent for Cover
MediaIntent mediaIntentCover = new MediaIntent();
mediaIntentCover.setMediaType(MediaType.PAPER);
mediaIntentCover.setMediaQuality(CIP4_PaperCover);
mediaIntentCover.setNamedWeight(CIP4_PaperCoverWeight);
...
//create Cover and add mediaIntent for Cover
ProductBuilder productBuilderCover = new ProductBuilder(CIP4_Copy_Count);
Product cover = productBuilderCover.build();
cover.setDescriptiveName("Cover");
cover.setIsRoot(false);
cover.setProductType("Product");
cover.setID("ID_Cover");
cover.setProductType(CIP4_ProductTypeCover);
productBuilderCover.addIntent(mediaIntentCover);
...
// create xjdf and add product (parts)
XJdfBuilder xJdfBuilder = new XJdfBuilder(CIP4_JobID, "Product", "Final Broschur");
xJdf = xJdfBuilder.build();
xJdfBuilder.addProduct(broschur);
xJdfBuilder.addProduct(cover);
xJdfBuilder.addProduct(content);
...
// create PrintTalk and embrace xJDF
PrintTalkNodeFactory ptkNf = new PrintTalkNodeFactory();
PrintTalkBuilder ptkBuilder = new PrintTalkBuilder();
PurchaseOrder purchaseOrder = ptkNf.createPurchaseOrder("4711", "Euro", xJdf);
ptkBuilder.addRequest(purchaseOrder);
PrintTalk printTalk = ptkBuilder.build();
...
```

Figure 10: Generating XJDF

3.5 Importing XJDF into a WMS

The XJDF file from figure 7 was put in a suitable hot-folder of the Heidelberger Prinect WMS (Heidelberg). Doing that a job with the two parts “content” and “cover” is automatically created. Figure 11 also shows that the customer details, the binding intent and the number of copies are already set.

The screenshot displays the Prinect WMS interface with a sidebar on the left showing a tree structure with 'End product', 'Content', and 'Cover'. The main area contains several form sections:

- Address:** Name: Walt Disney Company, Street: Hollywood Drive, PO Box: , Postal Code: 1234, City: Entenhausen, Region: , Country Code: , Country: USA, Extended Address: .
- Communication Channels:** Email: duck@hdm-stuttgart.de.
- Person:** Title: , First Name: Donald and Daisy, Family Name: Duck, Name Suffix: , Additional Name: , Job Title: President.
- Details:** (Empty text area)
- Binding:** Binding type: Saddle Stitch, Comment: .
- Delivery:** Overproduction: 0.0 %, Delivery quantity: 500.

Figure 11: Prinect reads XJDF Resource “Contact”

One can observe in figure 12 that the printing substrate and the number of pages of the product part content has been recognized. The same applies for the cover.

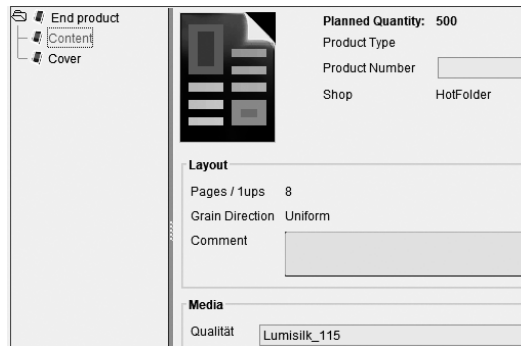


Figure 12: Prinect reads XJDF Product Part “Content”

4. DISCUSSION

The specifications concerning the metadata used here are draft versions only (Meissner, 2018; ISO/DIS 21812-1) and thus subject to change. It is not advisable to start a product development based on this still unstable ground.

The outcome of the conversion has also been imported into a WMS. The metadata has been partly recognized.

The software ① and ② are not meant to become industry solutions. For that, the programming got to be much more error tolerant and more general. Reading the metadata from PDF/VT, for example, need to be implemented more universal and cannot assume a certain structure as it has been the case in our project. Thus, software ① and ② are working fine in conjunction, but ② will most likely fail if it reads PDF/VT with CIP4 metadata that has been generated by some other program and some other library. Moreover, we concentrated on a single product type, i.e. a booklet with cover and content. Even for this example, we did not address every aspect – for example, neither the colour properties of the product nor the actual formats are considered.

5. CONCLUSIONS

The feasibility of the interfaces is proven. The problem in practice will be the generation of the metadata. There are several obvious scenarios that are right for this new approach like Web-to-print or forwarding jobs to a subsidiary or partner of the PSP. It might become a bit more questionable, if the PB needs to fill out a form, as it is the case with this prototype software. In this scenario, a steady and firm collaboration between PB and PSP might be a necessary assumption for the start.

6. ACKNOWLEDGMENTS

I would like to thank PDFlib for providing me with a temporary license for their library.

7. REFERENCES


- [1] Heidelberg, Prinect, Heidelberg,
URL: https://www.heidelberg.com/global/en/lifecycle/workflow/prinect_overview.jsp
(last request: 2018-07-18)
- [2] International Organization for Standardization: ISO 16612-2:2010. “Graphic technology - Variable data exchange - Part 2: Using PDF/X-4 and PDF/X-5 (PDF/VT-1 and PDF/VT-2)”, International Organization for Standardization, 2010.
- [3] International Organization for Standardization: ISO 16684-1:2012. “Graphic Technology – Extensible Metadata Platform (XMP) specification”, International Organization for Standardization, 2012.

- [4] International Organization for Standardization: ISO 32000-2:2017. "Document Management - Portable Document Format - Part 2: PDF 2.0", International Organization for Standardization, 2017.
- [5] International Organization for Standardization: ISO/DIS 21812-1. "Graphic technology — Digital data exchange — Print product metadata for PDF files — Part 1: Architecture and core requirements for metadata", International Organization for Standardization, Draft 2018.
- [6] JetBrains, IntelliJ IDEA, JetBrains, URL: <https://www.jetbrains.com/idea/> (last request: 2018-07-19)
- [7] Meissner, S.: "ICS-IntentMetadata.PDF.1,5", confluence.cip4, URL: <https://confluence.cip4.org/display/PUB/XJDF>, (last request: 2018-05-13)
- [8] Meissner, S.: "XJDF Specification 2.0 – final", confluence.cip4, URL: <https://confluence.cip4.org/display/PUB/XJDF> (last request: 2018-07-09)
- [9] Meissner, S.: "Print Talk", confluence.cip4, URL: <https://confluence.cip4.org/display/PUB/PrintTalk> (last request: 2018-05-13)
- [10] Meissner, S.: "JDF Specification 1.6-final", confluence.cip4, URL: <https://confluence.cip4.org/display/PUB/XJDF> (last request: 2018-05-16)
- [11] Prosi, R.: "ICS — Common Metadata for Document Production Workflows", confluence.cip4, URL: <https://confluence.cip4.org/display/PUB/ICS+Documents> (last request: 2018-05-13)
- [12] Wikipedia, CSV (Dateifformat), Wikipedia, URL: [https://de.wikipedia.org/wiki/CSV_\(Dateifformat\)](https://de.wikipedia.org/wiki/CSV_(Dateifformat)) (last request: 2018-05-25)



© 2018 Authors. Published by the University of Novi Sad, Faculty of Technical Sciences, Department of Graphic Engineering and Design. This article is an open access article distributed under the terms and conditions of the Creative Commons Attribution license 3.0 Serbia (<http://creativecommons.org/licenses/by/3.0/rs/>).

EVOLUTION OF GRAPHIC DESIGN AS AN WORLDSKILLS INTERNATIONAL COMPETENCE IN RUSSIA

Taisiya Konygina , Olga Minaeva, Andrey Ermakov
WorldSkills Russia, Moscow, Russia

Abstract: *In this article we tell about development graphic design as a competence WorldSkills Russia. Article analyzes new format of knowledge testing (Demonstration exam by WorldSkills Russia) and progress of Russian graphic designers - participants of WorldSkills International Competition.*

Key words: skills, young professionals, graphic design, education, digital

1. INTRODUCTION

WORLDSKILLS is a center for improving and developing skills. We emphasize the importance of training and education for young people, industry and society, helping young professionals to become the best in their chosen profession. Founded in 1950, WorldSkills is an international organization that promotes vocational, technical, and service-oriented education and training. We are raising vocational training standards in 78 WorldSkills member countries, working with young people, educators, governments and industries, creating workforce and working talent today to help with future employment. WorldSkills brings together youth, industry, and educators to teach young people about professional skills and show them how to become the best in their chosen specialty. From traditional crafts to multidisciplinary occupations in the field of industry and services, with the support of partners, industries, government, volunteers and educational institutions, WorldSkills has a direct impact on the growth of professional skills throughout the world. Today it is the world's largest and largest competition, in which young skilled workers, university and college students take part as participants, and well-known professionals, specialists, industrial trainers and mentors as experts who evaluate the assignment (Minaeva, 2013).

CHAMPIONSHIP is a multifaceted event, where the leaders of state bodies and educational institutions, representatives of industry and public organizations meet, the place where the most important and topical issues related to professional skills are discussed. WorldSkills Championships are held every two years in various countries and are the most important event in the field of training and skill improvement, comprehensively reflecting all areas from industry to services. The contestants are winners of the national championships of professional skills of the WorldSkills member countries. They demonstrate both the level of their technical training, as well as their individual and collective qualities, solving the tasks set for them, which they study and / or perform in their workplace. Their success or failure speaks not only about their personal professional qualities, but also about the level of professional training in the country they represent, and the general level of quality of services in the home countries of the participants (Milchin, 2011).

In WorldSkills championships, competences are combined into 6 thematic blocks: construction, IT, industrial production, civil transport services, services, creativity and design.

2. METHODS

Since 2017, college graduates in Russia are passing the Demonstration exam.

The WorldSkills Demonstration exam is a form of state final certification of graduates in secondary vocational education programs of educational institutions of higher and secondary vocational education, which provides for:

- modeling of real working conditions for graduates to demonstrate professional skills;
- an independent expert assessment of the tasks of the demonstration exam, including experts from enterprises;
- determination of the level of knowledge and skills of graduates in accordance with international requirements.

The Demonstration exam is conducted to determine students and graduates of the level of knowledge and skills that enable them to conduct professional activities in a particular field and (or) to work in a specific profession or specialty in accordance with WorldSkills Russia standards.

The inclusion of the Demonstration exam format in the state final certification procedure for students of professional educational organizations is a model for independent assessment of the quality of training, facilitating the solution of several tasks of the vocational education system and the labor market without additional procedures (Minaeva, 2016).

Graduates who have passed certification tests in the format of the Demonstration exam are given the opportunity to:

- simultaneously with the confirmation of the level of development of the educational program in accordance with the federal state educational standards, to confirm their qualifications in accordance with the requirements of the WorldSkills international standards without undergoing additional certification tests,
- confirm their qualifications in individual professional modules demanded by enterprises-employers and receive a job offer at the stage of graduation from an educational organization,
- simultaneously with obtaining a diploma of secondary vocational education, obtain a document confirming the qualification recognized by enterprises operating in accordance with WorldSkills Russia standards.

This Methodology was developed in order to provide methodological assistance to the executive authorities of the constituent entities of the Russian Federation exercising public administration in the field of vocational education, educational organizations implementing secondary vocational education programs, other organizations and enterprises participating in the pilot testing of the demonstration exam in WorldSkills Russia standards and determines format, order of its organization and implementation, including the requirements for the procedure and participants (Minaeva, 2015).

For educational organizations conducting certification tests in the format of the demonstration exam is an opportunity to objectively assess the content and quality of educational programs, material and technical base, qualification level of teaching staff, as well as areas of activity, in accordance with which to determine the points of growth and further development (Kusheleva, 2012).

After passing the demo exam, the graduate receives a Skills-passport, which indicates the number of points scored for each module. The employer is very convenient to look at what the employee is strong.

Demonstration exam in Russia is passed on a variety of competencies. I would like to tell more details about the "Graphic Design" competency. Graphic design refers to a multitude of competencies and aspects. The variety of competences in this industry is very large, so usually the people employed in it are specialists of a narrow profile. As a result, a team can be engaged in graphic design, in which each participant has their own strengths, specialization and role in the development process.

Graphic design specialists can work with external and internal customers, creating unique solutions that meet their needs. They can also print or post products online. This area is characterized by direct interaction with the client, which requires developed communication skills to successfully achieve the goals set by the customer. In the field of graphic design interaction skills, research, design, technical skills are appreciated. This, in turn, requires an understanding of the target audience, markets, trends, cultural differences and customer desires. Such specialists should be able to work in formal and informal teams or independently (Kusheleva, 2015).

Upon completion of the research and planning phase, the task is interpreted for its execution using the appropriate specialized software. Work must comply with the technical requirements for the withdrawal or placement online. For such specialists, it is important to understand all stages of work, including limitations related to the printing process. These skills are also applied when changing or improving projects.

Within the scope of this sphere, various employment options are possible. These include external work, entrepreneurship, work in an advertising company, design bureau, typography or a company that has a design department. Both wide and narrow specialization is possible. The latter is typical for graphic designers, graphic artists, prepress specialists, type design, typesetters, font artists, image processing specialists, illustrators, art directors, production managers, digital printing specialists, information designers, packaging specialists, publishers (Vilberg et al, 2003).

3. RESULTS

Russian participants in international competitions show all the best and best results in the competence of "Graphic Design". At the international championship, which took place last year in Abu-Dhabi, our participant took fifth place in the world and received a medallion for professional skills. This year at the European competition EuroSkills-2018, which took place in the Hungarian capital Budapest, the representative of Russia won the first place and received a gold medal.

Russia is preparing to host the world championship, which will be held in Kazan in 2019, in full swing. Within the framework of training, participants in the competence of graphic design take part in national championships of other countries, where they compete out of competition, but by number of points they have repeatedly taken first places.

Graphic design in Russia keeps pace with the times. Gradually, multimedia publications are crowding out print. WorldSkills Russia has launched a line of DigitalSkills championships related to information technology and graphic design is also represented there. Participants at the championships are engaged in the development of interactive publications, create website design.

4. REFERENCES

- [1] Kusheleva T.: "Business organization", (FGOU SPO :MIPK MIP I. Fedorova, Russia, 2012.)
- [2] Kusheleva T.: "Economics of organization", (FGOU SPO :MIPK MIP I. Fedorova, Russia, 2015.)
- [3] Milchin A.: "Preparation and editing of the book's apparatus: How to make a book convenient for the reader", (University book, School of publishing and media business, Russia, 2011.)
- [4] Minaeva, O.: "Cheat for Adobe InDesign CS5.5", (FGOU SPO :MIPK MIP I. Fedorova, Russia, 2013.)
- [5] Minaeva O.: "Layout. Book Design Requirements", (FGOU SPO :MIPK MIP I. Fedorova, Russia, 2016.)
- [6] Minaeva O.: "InDesign course + interactive features", (FGOU SPO :MIPK MIP I. Fedorova, Russia, 2015.)
- [7] Vilberg G., Forsman, F.: "ABC book design", (SPBGPU, Russia, 2003.)



© 2018 Authors. Published by the University of Novi Sad, Faculty of Technical Sciences, Department of Graphic Engineering and Design. This article is an open access article distributed under the terms and conditions of the Creative Commons Attribution license 3.0 Serbia (<http://creativecommons.org/licenses/by/3.0/rs/>).

CONTENT-AWARE IMAGE COMPRESSION WITH CONVOLUTIONAL NEURAL NETWORKS

Alena Selimović , Aleš Hladnik 

University of Ljubljana, Faculty of Natural Sciences and Engineering,
Department of Textiles, Graphic Arts and Design, Ljubljana, Slovenia

Abstract: *Traditional image compression algorithms treat all image regions equally, regardless of their content, often resulting in reconstructed images that do not correlate well with human perception. Content-aware compression, on the other hand, prioritizes image regions that are more relevant to the interpretation of an image and encodes them at a higher bitrate, i.e. without loss or with less loss, than the rest of the image. Our paper explores the multi-structure region of interest (MS-ROI) model, a convolutional neural network, which enables the localization of multiple regions of interest (ROIs) in an image. The localization is expressed as a corresponding saliency map, which identifies the relevance of individual image regions and provides a saliency value for each pixel of the given image. This information is then used to guide the compression. The saliency values are discretized into multiple levels and more important levels are encoded with a higher quality factor Q than the less important ones, allowing for most of the reduction in image resolution to occur in non-salient image regions. Because the generated saliency maps produce soft boundaries between salient and non-salient image regions, smooth transitions between these regions are achieved. The obtained image is then encoded further using the standard JPEG algorithm with a uniform Q factor, resulting in the final image of the standard JPEG format. Our model was trained on the Caltech-101 image dataset and its performance was tested on two other image datasets. Presented are the obtained saliency maps for several images, as well as the results of content-aware compression, which are compared to the standard JPEG compression at different Q factors. For an objective comparison and evaluation of the quality of the obtained images, various standard quality metrics were used, i.e. mean squared error (MSE), peak signal-to-noise ratio (PSNR), structural similarity index (SSIM) and multi-scale structural similarity index (MS-SSIM).*

Key words: convolutional neural networks, image compression, JPEG, saliency maps, MS-ROI

1. INTRODUCTION

The primary objective of image compression is to reduce the amount of bits that is required for the image data to be stored or transmitted. Traditional lossy image compression algorithms, such as the widely adopted JPEG standard, take advantage of repetitive, redundant or imperceptible image data, and of the limitations of the human visual system, to encode the data more efficiently and reduce the file size. While the goal is to preserve the perceptual quality of an image, the approximation of the represented content results in the development of some unavoidable visual artifacts, which worsen the interpretability of the reconstructed images. Blocking effects, ringing artifacts and blurring, which are most characteristic for JPEG compression, appear as a consequence of the discontinuities between adjacent 8x8 pixel blocks and the elimination of high frequencies. Because the algorithm treats all image regions equally, regardless of their content, the compression artifacts are equally visible in the image background as well as in foreground objects. In order to minimize the visibility of these unwanted artifacts in the decoded images, numerous approaches that focus on obtaining a more accurate reconstruction of the original signal have been proposed (Dong et al, 2015; Dong et al, 2016a; Tao et al, 2017).

Content-aware compression methods, on the other hand, encode the content in a way that corresponds more to the manner in which the human eye interprets the image. Because the degree of human interest in different image regions varies according to what we perceive as more relevant for understanding the image, content-aware compression prioritizes the more important image regions, i.e. the regions of interest (ROIs), and enables them to be preserved with less loss than the rest of the image.

Before the encoding process can be accomplished, a saliency map, corresponding to the image content, needs to be obtained. A saliency map partitions the image into several categories, depending on the image regions they contain, and therefore serves as the means for quantifying the relevance of individual regions. The provided contextual information about the image is then integrated into a compression scheme. Because the selected, more important image regions, are encoded at a higher bitrate than the

image background, the compression artifacts in the ROIs of the reconstructed images are less noticeable than those in the background.

1.1 Saliency maps

Saliency maps can be obtained using different techniques. In recent years convolutional neural networks (CNNs) have been used successfully in a variety of image processing and computer vision tasks and have enabled a more accurate localization, detection and segmentation of objects and ROIs in images. For the purpose of obtaining saliency maps in order to guide the image compression, these approaches are inappropriate due to the following drawbacks:

- i) The use of typical methods aimed at object localization results in an object's position being represented within a rectangular window, which does not capture the object's silhouette.
- ii) The image segmentation techniques subdivide an image into its constituent regions by classifying each pixel as either a part of a foreground object or a part of the background. The resulting saliency maps produce sharp boundaries between different regions, which is not needed for the purpose of image compression.

Saliency maps can also be based on visual saliency models. While these models accurately capture the fixations of the human eye, the fixations themselves do not encompass the object's edges, which prevents the models from capturing the complete extent of the object. As shown in (Yu et al, 2009), the use of saliency maps based on human fixations for the task of image compression results in blurred edges and a soft focus of the objects in the obtained image.

1.2 The MS-ROI model

The multi-structure region of interest (MS-ROI) model, proposed in (Prakash et al, 2017), is a CNN model that enables the localization of multiple ROIs. The architecture of the model consists of convolutional layers, which are followed by a nonlinear activation function and a max-pooling operation. Fully connected layers, typically added on top of the traditional CNN with the aim of producing the predicted categorical output, are removed and replaced with a GAP layer that applies a global average pooling. The GAP operation calculates the spatial average of each feature map (a three-dimensional tensor) from the convolutional layer preceding the GAP layer, reducing each feature map to a single value. The resulting vector is fed directly into the final, Softmax layer, which outputs the model's prediction. The weights connecting the GAP layer to the output layer encode the contribution of each feature map to the predicted class – the bigger the contribution of a specific detected visual pattern, the more weight it is given. A saliency map is obtained by mapping the weights of the final layer back to the last convolutional layer and calculating a weighted sum of the feature maps. Rather than picking only the most probable class (the highest activation), the activations are sorted from the index of the element with the lowest value to the index of the element with the highest value and a weighted sum of the five highest-scoring classes is taken, while the less probable classes are discarded. By applying a colourmap consisting of a range of cold and warm colours over the obtained greyscale saliency map, the final localization is expressed as a heatmap, which highlights the discriminative ROIs specific to the predicted classes. The most important image regions are represented with the red colour, whereas the least important image regions are represented with the dark blue colour.

The two significant modifications made to the architecture of a traditional deep convolutional neural network - the removal of the fully connected layers and the inclusion of the GAP layer – in addition to choosing the five most probable classes instead of only one, enable the three important advantages of the MS-ROI model in comparison with the approaches of obtaining saliency maps, which are based on localization, segmentation or human fixation.

Firstly, the removal of fully connected layers allows for the model to retain the ability of convolutional layers to behave not only as feature extractors but also as object detectors, despite being trained only on image-level labels with no additional annotation provided (e.g. bounding box supervision or pixel annotation).

Secondly, an addition of the GAP layer provides the means for the network to determine the full extent of the object. If instead of the GAP operation the global max-pooling (GMP) was applied, it would force the model to discard all of the values except the highest one, enabling the model to identify only one discriminative part of the object in an image, but preventing it from highlighting the whole object. The employment of the GMP would therefore present a drawback similar to the usage of a visual saliency model.

Lastly, by using a weighted sum of the top five predictions instead of only the highest scoring class, the obtained heatmap enables the detection of multiple regions of interest, which can include objects belonging to different classes. The localization of multiple ROIs and the production of soft boundaries between different image regions create coherent heatmaps and enable smooth transitions from salient to non-salient regions in the reconstructed images.

1.3 The compression process

The JPEG compression algorithm treats all areas of the image with equal importance, using the same quality factor Q to encode them evenly. The heatmaps obtained by the MS-ROI model, on the other hand, enable a content-aware encoding with a variable factor Q . The generated heatmap provides a saliency value, located in the interval between 0 and 1, for each pixel of the given image. These values are then discretized into a range of levels, varying in their relevance. Pixels with a saliency value of 1 are categorized as the most important, while pixels with a saliency value of 0 are categorized as the least important. Finally, a range of JPEG quality levels from Q_l to Q_h , corresponding to the levels of importance, is chosen.

The compression process involves two encoding passes. In the first encoding pass, the less important levels, indicated by the cold colours on the heatmap, are encoded with lower Q factors (meaning a higher compression), whereas the more important levels, indicated by the warm colours on the heatmap, are encoded with higher Q factors (meaning a lower compression). The areas encoded at higher Q factors are therefore capable of preserving more information about the original image.

The second encoding pass employs a uniform Q factor, Q_{final} , to encode all regions equally. Because the final image is encoded using the standard JPEG encoder, decoding the image can be done by the standard JPEG decoder.

2. METHODS

The code for the MS-ROI model and the image compression was written in Python 3. The processing of the images was performed using the CUDA software on the Nvidia GPU with 8 GB of memory.

The model was trained on the Caltech-101 image dataset (Fei-Fei et al, 2006), which consists of 9144 monochromatic, greyscale and RGB images (representing the independent variables) belonging to 102 classes (representing the dependent variables). The last 15 images of each class were used for the validation set, whereas the remaining images were used for the training set. The training set and the validation set initially contained 7614 images (83.3%) and 1530 (16.7%) respectively, but during the training phase the size of the trainset was increased using real-time image augmentation. The original images were rotated up to 30 degrees, centrally scaled up to 30% and flipped horizontally and vertically. Every iteration produced a number of transformed images from each class that was approximately equal to the number of images that the class originally contained. Since the transformations were performed randomly, each iteration included different variations of the input images.

The implementation of the model was based on the pretrained VGG16 model (Simonyan et al, 2014), the architecture of which was modified by removing the fully connected layers at the top of the model and replacing them with three additional convolutional layers and a GAP layer. The 1000 nodes comprising the Softmax layer of the standard VGG16 model were replaced with 102 nodes, corresponding to 102 classes included in the Caltech-101 image dataset. The input images were resized to a fixed input size of 224x224 pixels. 3x3 pixel convolution filters with a stride of 1 and 2x2 pixel pooling windows with a stride of 2 were used for convolution and max-pooling. In total, the neural network consisted of 23 layers – 16 convolutional layers, each followed by a ReLU activation function, 5 max-pooling layers, following each of the 5 blocks of convolutional layers, a GAP layer and a final, Softmax layer. The combination of removing the fully connected layers, thereby decreasing the number of parameters, and adding a GAP layer, which in itself serves as a regularizer, reduced the risk of overfitting the model to the training data largely enough that the dropout was not needed.

Three different methods were used for weight initialization. In the unmodified layers of the VGG16 model the pretrained weights were initialized to the constant numbers. In the convolutional layers, added on top of the VGG16 model, the weights were initialized from the truncated Gaussian distribution using the standard deviation of 0.1, whereas the weights in the GAP layer were initialized using the Gaussian distribution. The reason for using the truncated normal distribution in each of the three additional convolutional layers was to reduce the risk of neuron saturation.

The cost was calculated using the cross entropy function and minimized using the Adam optimization algorithm with a learning rate of 0.0001 and the default values of the parameters beta 1, beta 2 and epsilon. The learning process included 100 iterations using a batch of 32 images.

In order for the model to be able to identify multiple ROIs, the matrix of sorted activations for each input image needed to be obtained. Instead of the more commonly applied argmax method, which finds the index of the element with the maximum activation, the argsort method was used to obtain and sort all the activations. The five highest scoring activations were picked for every input image and their weighted sum was taken. Matplotlib's Jet colourmap was used to generate the colour scheme.

The performance of the content-aware compression method based on the MS-ROI model was assessed on JPEG images from the Salicon dataset (Yu et al, 2015) and on uncompressed BMP images from the General-100 dataset (Dong et al, 2016b). The results of the MS-ROI based compression were compared to the standard JPEG compression at Q factors of 50, 30 and 70. For an objective comparison and evaluation of the quality of the obtained images, the mean squared error (MSE), peak signal-to-noise ratio (PSNR), structural similarity index (SSIM) and multi-scale structural similarity index (MS-SSIM) were used. Higher PSNR (measured in dB), SSIM and MS-SSIM values refer to a higher image quality, whereas a higher MSE indicates a bigger error in the reconstructed image. For all of the experiments, the chosen Q values for the first encoding pass of the MS-ROI compression method ranged from $Q_l = 30$ to $Q_h = 70$. The Q_{final} factor of the second encoding pass depended on the selected Q factor of the JPEG compression and the file size of the original image. When comparing the MS-ROI compression to the standard JPEG compression at $Q = 50$, the average Q_{final} was 57, at $Q = 30$ the average Q_{final} was 31, and at $Q = 70$ the average Q_{final} was 73. The maximum difference between the file sizes of the standard JPEG images and the images obtained using the MS-ROI model was 1%.

3. RESULTS

3.1 The accuracy and reproducibility of saliency maps

Because the quality of the final image is heavily dependent on the accuracy and reproducibility of the obtained heatmaps, the model was evaluated on input images representing different content and containing different semantic objects. Since the model's prediction (the matrix of activations) for the same input image is slightly different every time the image is passed through the network, different variations of the heatmaps are generated. To show that the model's prediction for the same input image varies only to some degree and to estimate the robustness of the model, as well as the reproducibility of the obtained heatmaps, some of the test images were passed through the network five times in order to obtain five different variations of the heatmap (shown in Figures 1 – 4).

As seen in Figures 1 and 2, the model is able to accurately identify one or a few clearly distinguishable salient image regions. Consequently, the similarity between the produced heatmaps is relatively high. In cases where the identification of the ROIs and the isolation of foreground objects from the background are more difficult (Figure 3) or where the input images do not contain any salient regions at all (Figure 4), the precision and the reproducibility of the generated heatmaps are lower.



Figure 1: Example of an input image with one salient region



Figure 2: Example of an input image with two salient regions

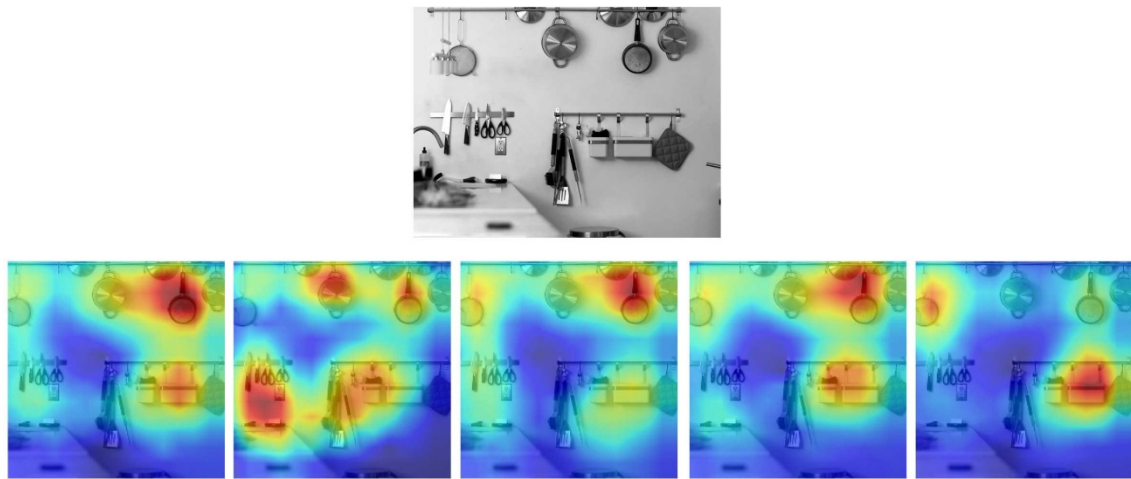


Figure 3: Example of an input image with several salient regions

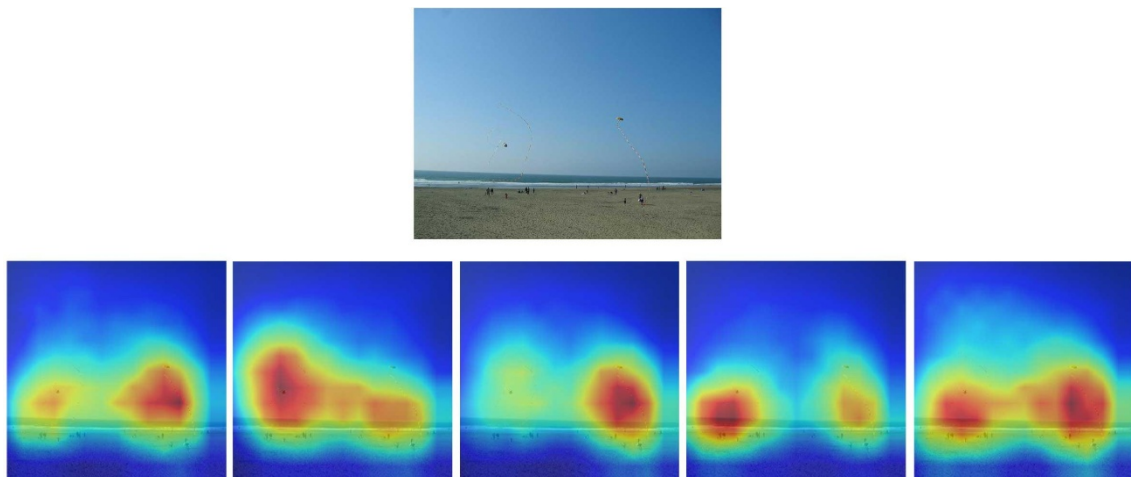


Figure 4: Example of an input image without salient regions

3.2 Objective evaluation of the quality of the reconstructed images

Table 1 presents the results of calculated quality metrics for the set of five images that contain distinct salient areas (Figure 5). The compression method based on the MS-ROI model outperforms the standard JPEG compression at $Q = 50$ for all five images, even though the file sizes of images that were compressed

using the MS-ROI method are all slightly smaller than those compressed using the JPEG algorithm. The most significant gain in PSNR, 1.61 dB, is achieved in the case of image 2 (snowboarder), the biggest improvement in SSIM, 0.0107, in the case of image 1 (bird), and the biggest gain in MS-SSIM, 0.0044 in the case of image 5 (elephant).

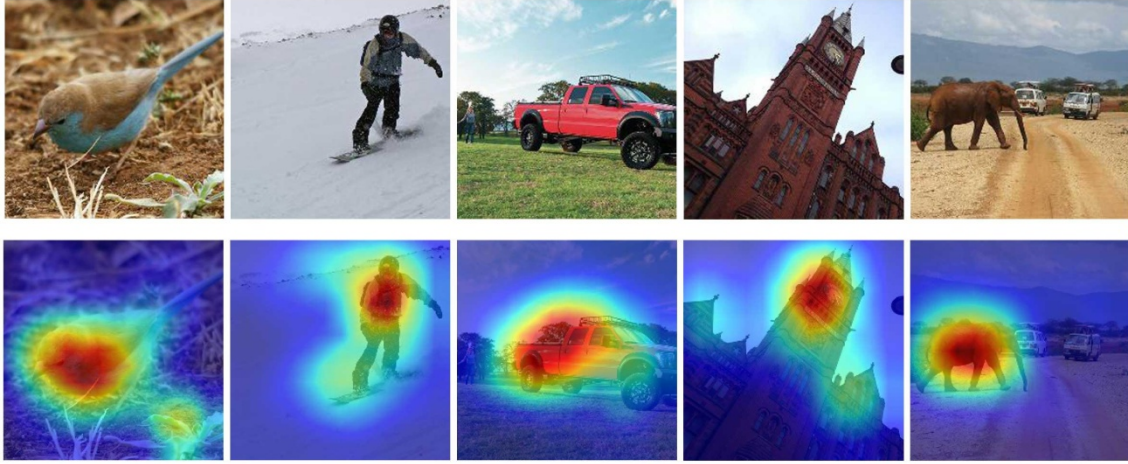


Figure 5: Five examples of images from the Salicon dataset and of their corresponding heatmaps

Table 1: Results of calculated quality metrics when comparing the MS-ROI compression to JPEG at $Q = 50$ – for the images with salient regions

	MSE	PSNR (dB)	SSIM	MS-SSIM	File size (B)
Image 1 (bird)					
JPEG	35.134	32.674	0.9616	0.9925	47436
MS-ROI	26.932	33.828	0.9723	0.9947	47014
Image 2 (snowboarder)					
JPEG	21.099	34.888	0.9590	0.9878	22171
MS-ROI	14.571	36.496	0.9669	0.9886	21951
Image 3 (truck)					
JPEG	114.50	27.543	0.9201	0.9846	56867
MS-ROI	80.481	29.074	0.9290	0.9878	56362
Image 4 (cathedral)					
JPEG	46.729	31.435	0.9233	0.9848	41895
MS-ROI	32.479	33.015	0.9261	0.9864	41669
Image 5 (elephant)					
JPEG	52.656	30.916	0.9230	0.9824	42718
MS-ROI	37.492	32.391	0.9336	0.9868	42301

The results of calculated quality metrics for the set of five images, which do not contain any salient areas or where their identification is more ambiguous (Figure 6), are displayed in Table 2. Because content-aware compression is intended for encoding images that depict some salient objects, the model's predictions were expected to be much less accurate in cases where the input images contained patterns, shapes or textures. Nonetheless, the PSNR values of the MS-ROI compression method turned out to be

higher than those of the JPEG compression for all images, with the exception of the last one (corals). Unlike the PSNR value, the SSIM and MS-SSIM indexes were improved only for image 1 (stone wall) and image 3 (leaves).

It is worth mentioning that, even in the cases where any of the PSNR, SSIM or MS-SSIM values of the MS-ROI compression were higher than for the JPEG compression, the improvement of the MS-ROI method over the JPEG method is much less significant than in the case of the images that contain clearly identifiable salient objects.

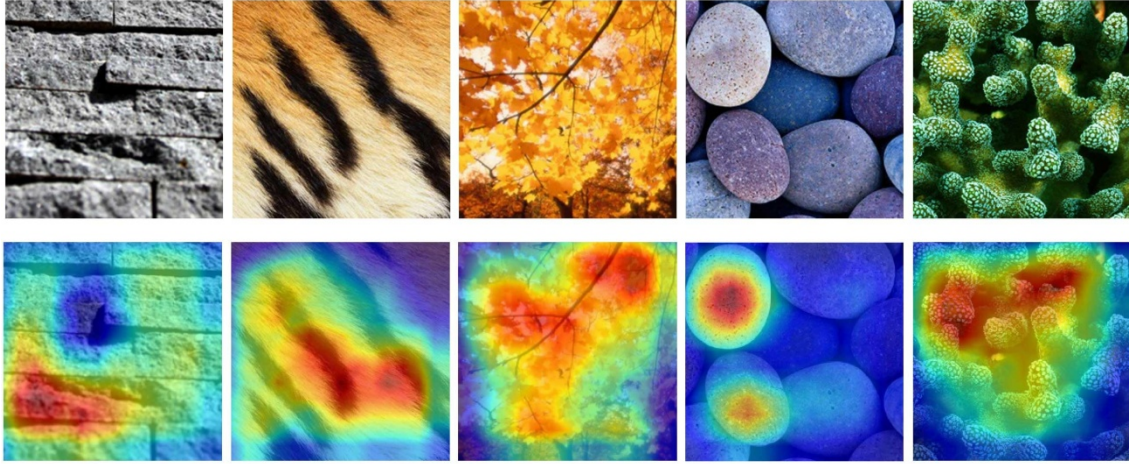


Figure 6: Five examples of images from the General-100 dataset and of their corresponding heatmaps

Table 2: Results of calculated quality metrics when comparing the MS-ROI compression to JPEG at $Q = 50$ – for the images without salient regions

	MSE	PSNR (dB)	SSIM	MS-SSIM	File size (B)
Image 1 (stone wall)					
JPEG	94.637	28.370	0.9639	0.9962	14331
MS-ROI	94.425	28.380	0.9644	0.9963	14457
Image 2 (tiger stripes)					
JPEG	96.061	28.305	0.8649	0.9812	24809
MS-ROI	94.273	28.387	0.8623	0.9808	24805
Image 3 (leaves)					
JPEG	25.258	34.107	0.9516	0.9897	23126
MS-ROI	25.201	34.117	0.9518	0.9899	23261
Image 4 (pebbles)					
JPEG	86.153	28.778	0.8672	0.9828	30722
MS-ROI	84.485	28.863	0.8657	0.9827	31003
Image 5 (corals)					
JPEG	48.866	31.241	0.9584	0.9915	68008
MS-ROI	55.054	30.723	0.9571	0.9908	68278

The model was also evaluated on 200 randomly chosen images from the Salicon dataset, which contains a total of 20000 images, and on 50 randomly chosen images from the General-100 dataset, which contains

a total of 100 images. The average PSNR and SSIM values for the selected images from the Salicon and General-100 dataset are shown in Table 3 and Table 4, respectively.

Table 3: PSNR and SSIM of 200 images from the Salicon dataset

	PSNR	SSIM
JPEG (50)	32.670	0.9658
MS-ROI	33.763	0.9735
JPEG (30)	29.521	0.8991
MS-ROI	30.134	0.9021
JPEG (70)	43.445	0.9910
MS-ROI	44.416	0.9958

Table 4: PSNR and SSIM of 50 images from the General-100 dataset

	PSNR	SSIM
JPEG (50)	32.827	0.9501
MS-ROI	33.184	0.9537
JPEG (30)	30.637	0.9375
MS-ROI	30.641	0.9379
JPEG (70)	34.902	0.9741
MS-ROI	34.968	0.9759

Results show that the MS-ROI compression method performs better than the standard JPEG compression, since the former is characterized by a higher PSNR and a better visual quality of the obtained images. As seen in Table 3, compression based on the MS-ROI model achieves an average gain of 1.09 dB in PSNR and a 0.0077 gain in SSIM against the standard JPEG compression at $Q = 50$, and an average gain of 0.97 dB in PSNR and 0.0048 in SSIM at $Q = 70$. Meanwhile, the improvement of the MS-ROI compression, when compared to the JPEG compression at $Q = 30$, is not as substantial, though the MS-ROI method still performs better and on average improves the PSNR by 0.61 dB and the SSIM by 0.0030.

Similarly, the MS-ROI based compression generates better results in comparison with the standard JPEG compression at $Q = 50$ for the images from the General-100 dataset. On average, the MS-ROI compression gains 0.36 dB in PSNR and 0.0036 in SSIM. However, when compared to the JPEG compression at $Q = 30$ and $Q = 70$, the results of the MS-ROI compression are much less prominent. When compared to the JPEG compression at $Q = 70$, on average, the MS-ROI compression improves the PSNR by 0.07 dB and the SSIM by 0.0018, while, when compared to the JPEG compression at $Q = 30$, the average gain in PSNR is only 0.0040 dB and only 0.0004 in SSIM.

Overall, the MS-ROI model performs better on images from the Salicon dataset. This can be explained by the fact that the General-100 dataset contains more images depicting textures and patterns compared to the Salicon dataset, which consists mostly of images of natural indoor and outdoor scenery with various salient regions. Furthermore, the General-100 dataset contains images of smaller dimensions than the Salicon dataset, which is therefore better suited for a content-aware compression task.

The obtained results were interpreted using a one-way analysis of variance (Anova). The purpose of the test was to determine whether the MS-ROI compression and the JPEG compression are actually different in the measured characteristics. Since the improvement of the MS-ROI compression over the JPEG compression was more significant for the images from the Salicon dataset than for the images from the General-100 dataset, Anova was performed for the former dataset. An improvement of the MS-ROI model over the standard JPEG compression is statistically significant if the p-value is less than the

significance level of 0.05. The test yielded p-values that were lower than the significance level, for both the PSNR and SSIM values, when comparing the MS-ROI model to the JPEG compression at Q factors of 30, 50 and 70, thereby rejecting the null hypothesis in favour of the MS-ROI model.

4. CONCLUSIONS

This paper explores the content-aware compression based on saliency maps obtained using a convolutional neural network - the MS-ROI model. We showed that by varying the quantization of compression, the MS-ROI based encoding is capable of achieving a better visual quality of the reconstructed images compared to the standard JPEG compression. Since the accuracy of the obtained heatmaps is highly dependent on the content of the input image, the performance of the MS-ROI compression is especially superior when images with clear semantic regions are used. Because the model allows for the detection of multiple salient image regions and produces soft boundaries between them, the transitions from regions encoded at higher and lower bitrates are smooth. Further experimentation with the MS-ROI model based on different CNN architectures is required to better understand the effect of the model implementation on the generated saliency maps and the resulting quality of the content-aware compression.

5. REFERENCES


- [1] Dong, C., Deng, Y., Loy, C. C., Tang, X.: "Compression artifacts reduction by a deep convolutional network", *Proceedings of IEEE International Conference on Computer Vision (ICCV) 2015* (Santiago, Chile, 2015), pages 576–584. doi:10.1109/ICCV.2015.73.
- [2] Dong, C., Loy, C. C., He, K., Tang, X.: "Image super-resolution using deep convolutional networks", *IEEE Transactions on Pattern Analysis and Machine Intelligence* 38(2), 295-307, 2016, doi:10.1109/TPAMI.2015.2439281.
- [3] Dong, C., Loy, C. C., Tang, X.: "Accelerating the super-resolution convolutional neural network", *Computer Vision – ECCV 2016* (Springer International Publishing, 2016), 391-407. doi: 10.1007/978-3-319-46475-6_25.
- [4] Fei-Fei, L., Fergus, R., Perona, P.: "One-Shot learning of object categories", *IEEE Transactions on Pattern Analysis and Machine Intelligence* 28(4), 594-611, 2006. doi: 10.1109/TPAMI.2006.79.
- [5] Prakash, A., Moran, N., Garber, S., Dilillo, A., Storer, J.: "Semantic perceptual image compression using deep convolution networks", *Proceedings of Data Compression Conference (DCC) 2017* (Snowbird, UT, USA, 2017), pages 250-259. doi: 10.1109/DCC.2017.56.
- [6] Simonyan, K., Zisserman, A.: "Very deep convolutional networks for large-scale image recognition", *Proceedings of International Conference on Learning Representations 2015 (ICLR, San Diego, CA, 2015)*, pages 1-14.
- [7] Tao, W., Jiang, F., Zhang, S., Ren, J., Shi, W., Zuo, W., Guo, X., Zhao, D.: "An end-to-end compression framework based on convolutional neural networks", *Proceedings of Data Compression Conference (DCC) 2017* (Snowbird, UT, USA, 2017), page 463. doi: 10.1109/DCC.2017.54.
- [8] Yu, F., Seff, A., Zhang, Y., Song, S., Funkhouser, T., Xiao, J.: "LSUN: Construction of a Large-scale Image Dataset using Deep Learning with Humans in the Loop", 2015, URL <https://arxiv.org/abs/1506.03365> (last request: 2018-09-20).
- [9] Yu, S. X., Lisin, D. A.: "Image compression based on visual saliency at individual scales", *Proceedings of ISVC: International Symposium on Visual Computing, Advances in Visual Computing 2009* (5th International Symposium ISVC Las Vegas, NV, USA, 2009), pages 157-166. doi: 10.1007/978-3-642-10331-5_15.



© 2018 Authors. Published by the University of Novi Sad, Faculty of Technical Sciences, Department of Graphic Engineering and Design. This article is an open access article distributed under the terms and conditions of the Creative Commons Attribution license 3.0 Serbia (<http://creativecommons.org/licenses/by/3.0/rs/>).

DESIGNING THE EDUCATIVE APP FOR THE DETERMINATION OF TYPICAL SLOVENIA ROCKS

Anja Škerjanc¹, Tadej Abram¹, Aja Knific Košir¹, Rok Brajković²,

Žiga Fon³, Petra Žvab Rožič⁴, Helena Gabrijelčič Tomc¹ 

¹ University of Ljubljana, Faculty of Natural Sciences and Engineering,
Department of Textiles, Graphic Arts and Design, Ljubljana, Slovenia

² Geological Institution of Slovenia, Dimičeva Street 14, 1000 Ljubljana, Slovenia

³ Digied, e-learning development and production company, d.o.o., Žirovnica, Slovenia

⁴ University of Ljubljana, Faculty of Natural Sciences and Engineering,
Department of Geology, Ljubljana, Slovenia

Abstract: Applications presenting the content of a specific professional field are more frequently used for educational purposes. Not only that the interactive solutions including multimedia can more effectively transfer knowledge due to their property to offer a content on a demand, but they are also very attractive, they augment user experience, are able to present more spatial and time dependent data and they usually involve multisensory approaches including senses of vision, hearing and touching.

In the research the work frame and a design process of the educative app solution for geological purposes is presented. The aim of the app is to interactively determine stones by means to implement geological stone key. The experimental part presents the strategy phase, in which the target groups were defined, their needs were analysed and touching points for the successful networking, sharing and promotion were introduced. Next, app's functionalities and content types were created, based on the specification of professional field of geology. The content was categorised and labelled so that in the context of the whole app's structure required hierarchy and organisation of the content categories were introduced. User interface design began with simple layout sketches and with iterative approach that followed, more interactive prototypes were designed, developed and tested using the wireframes. In the results the final prototype and its design are presented with the evaluation of user-centred design approach that was implemented in the work frame.

Key words: stone key, user interface, design process, educative app, geology

1. INTRODUCTION

Interactivity is a potencial of action-reaction between different communication units (human – computer interaction). It is also a communication process and a dialog that considerably improve the effectiveness of education when it is applied in educative content (Jakupović, 2018). On technological level, multimedia interactive content are persistently gaining the popularity and the applicative value in new media. As was demonstrated, effectiveness of educational content and the quality of working memory is improved when the content is perceived (seen, heard and touched) and sensed (experienced) interactively and as such prompt the user to act, collaborate and continously self-evaluate the understanding and knowledge (Rias & Zaman, 2010). Nowadays trends of the known and respected universities is to offer without any costs and with open-access web workshops, seminars and other forms of educational activities, mentor support and effective evaluation of the knowledge (Mlakar & Štepic, 2018; Youngs, 2018).

When interactivity and multimedia in the learning process is discussed, the science of education should be considered and the Mayer's cognitive theory briefly introduced. Mayer's researches include theories of learning process, cognitive psychology and media technology. In the book about the multimedia in the education he presents the discoverings that the study content including only images or only text is less efficient as content including the combination of both content type. This principle of production of educative content, named also a principle of multimedia, is connected to the Mayer's theory of learning with multimedia and is a fundamental guide in multimedia design. The theory behind the principle of multimedia states that human being has two channels for information processing, that the working memory is limited and that a efficient learning is possible only when the student is cognitively active (Mayer, 2014).

Planning, production and development of interactive media are usually performed with two simultaneous processes that include the creator – the designer and the consumer – the user of the application. The designer is involved in the creative process of planning, designing and producing the media and implements

the methodologies of user-centred design that offer the augmentation of users' experience when consuming the media. The designer's work is a multi-layered process that usually include five elements of designing user experience – UX (Garret, 2011): 1. the strategy plane; 2. the scope plane; 3. the skeleton plane; 4. navigation and interface design and 5. surface level and sensory design. In the strategy plane the needs of the app's users and app's objectives are analysed, introduced and transpose in the concept of interactive media. In the second, scope phase the app's functionalities (interactive map, searching, etc.) and types of content (images, text, video) are be defined and categorised, the relevant touch points (social media) are defined and the strategy of communication through touch points is elaborated. In the third and fourth phase organisation, hierarchy, labelling and internal structure and skeleton of the app (information architecture) is established and navigation design is performed. With the start already in the fourth phase, interface design continues in the fifth, last phase of UX design, i.e. the app's surface level and sensory design.

When developing and designing of educative mobile application some important features should be included in the process and solution. The app's databases should be powerful and stable enough to support different functionalities (uploading new content, sharing etc.) and various type of multimedia content should be planned and created with the focus of successfully persuade all the target groups. As the interactive communication is more effective, when there is a direct and "personal" contact between the communicative units, the app should include virtual tutors or at least video or animated interactive tutorials. It is recommended that in the app there is a functionality of a self-evaluation process that should be effectively included on different learning levels. The basic functionalities (login, statistics etc.) should be designed according to the principles of user-centred design that had to be implemented also in the user interface design process. Further, features of personalisation are indispensable and can be developed directly from the profiled analysis of target groups and personas. These features should be planned and included as smart interactive elements and not as abusive additives (Still & Crane, 2016).

User-centred design is crucial in the educative apps' development, when in the framework of working phases special attention is given to the users, their cognitive processes, the environment of the use of the product (media), usability goals and especially the context of the media consumption. Here, user-centred design is a problem-solving multi-stage process which aim is the testing and the analysis of users' behaviour, experience and immersion when human-media interaction occurs. Besides, the evaluation of the usability and user experience is performed iteratively and in many consecutive phases of the product development, design, production and its actual use (William Albert & Tullis, 2013).

In this research we present the work frame and a design process of the educative app solution for geological purposes. The aim of the app is to interactively determine stones by means to implement geological key. The educative part of the solution includes step by step process of recognition and labelling of stones that can be found in Slovenian region. Consequently, the focus during the app's user interface and content development was the implementation of user-centred design that considered users' cognitive processes of understanding, learning and memory to achieve knowledge about the different stones' name, properties and origin, and consequently their geologic category.

2. EXPERIMENTAL

In the research work, professionals from three main research fields were included, i.e. geologists, graphic designers and programmers, which members were students and mentors. The work was directed by the creative director of the company Digied that covers the development and implementations of advanced user-oriented solutions for ICT supported education. In this contribution and its experimental part, we focus on designing the educative app that included the following phases:

- strategy phase;
- prototyping and wire frame design;
- graphic identity design;
- creation of functionalities and content;
- navigation and interface design;
- testing and design redefining;
- promotion of the project and educative application.

In **the strategy phase**, the timeline of the research work was carefully defined with the consideration of the goals and complexity of the tasks included in the work. While the geologists were developing the geological

key (defining three main groups of Slovenia stones: magmatic, metamorphic and sediment stones), i.e. the systematisation of labelling and categorisation of Slovenian stones, the target groups and their needs were defined and analysed by the graphic designers. Touch points for the successful networking, sharing and promotion were introduced and were active (for promotion, tracking of project working phases) already during the project work. The development of the information architecture started already in this first, strategy phase of the project (Figure 1).

Prototyping and wire frame design began with simple sketches and with iterative approach 4 stages of prototype were designed and tested (Figure 1). Each iteration was an upgrade of the previous version and all findings from the intermediate quick testing from the on defined prototype were implemented in the next version.

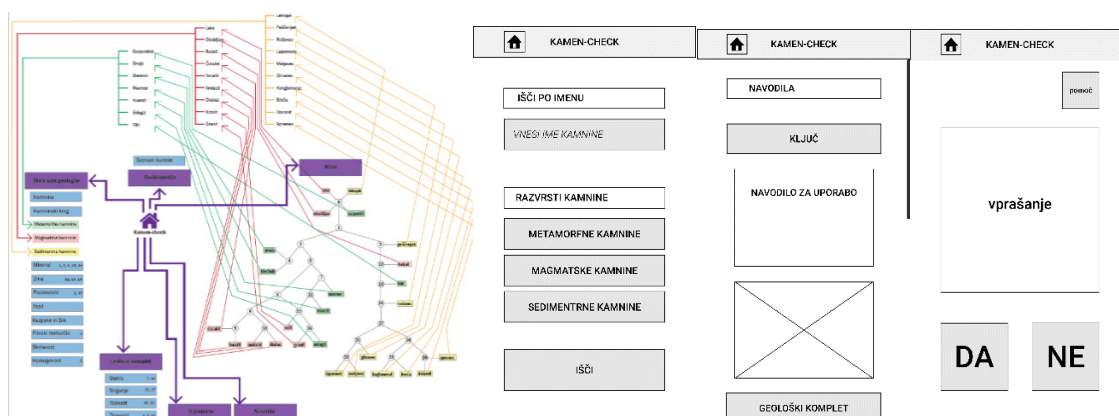


Figure 1: Information architecture, i.e. the structure, hierarchy and labelling of educative app and static prototype and wireframes

Graphic identity design originated from the main content elements of the interactive solution, i.e. stone. Graphic identity was determined with the logotype, selection of the colour pallet and font types. The symbol of the logotype, i.e. symbol of stone, was designed as a multi-sided geometrical object and the text part included a creative name of the application KamenCheck that means StoneCheck. A logotype version and selected fonts are presented in Figure 2.

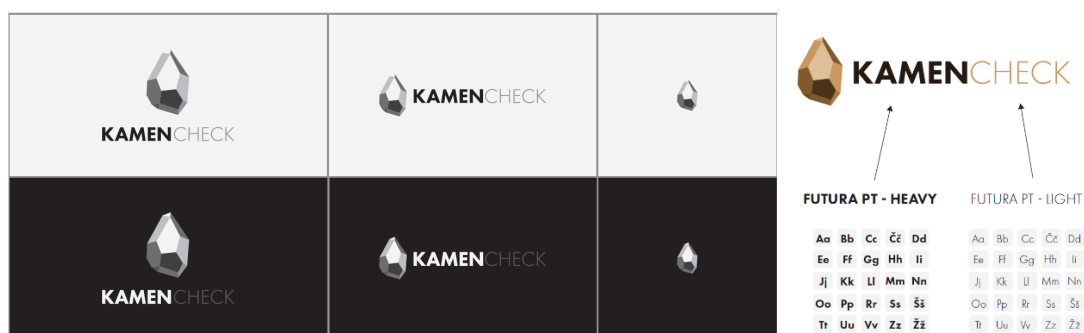


Figure 2: Elements of graphic identity and logotype

Next, **app's functionalities and content types were created** (photos, videos, 3D models, illustrations, text), based on the specification of professional field of geology. The photos of the selected stones were acquired in photo studio and beside regular photography also 360 records were performed. The letter was planned to be implemented in 360 video presentations of the stones and to be used as a photogrammetric records for additional AR interactive presentations of stones. The content was categorised and labelled so that in the context of the whole app's structure a successful hierarchy, organisation and categorisation were introduced. In Figure 3 shots from instructional video, explanatory photos and educative illustrations are presented.

Video content	Photos	Illustrations
		
		
		

Figure 3: Presentation of the video shots about the checking and defining the stone group (category), photos of the stones with the unit measurement and educative illustrations of geological process

Navigation and interface design was carefully planned and implemented considering the structure and the hierarchy of the content categories. Icons, buttons and other static and interactive elements were designed according to the principles and concepts of Material design, which guidelines were used also for the design of the layout, i.e. composition and arrangements of the graphic elements of the user interface. Moreover, the user interface design implemented also some of the state of the art principles of human perception and the findings of our intermediate usability testing.

Testing of the wireframes and prototypes was performed on a smaller number of users (No. = 5) with the focus of discovering issues, errors, inconsistencies and non-uniformity.

Usability testing implemented performance metrics, i.e. the representative users were asked to freely use an educative application, while the developers observed users' performance and recorded the usability issues. After each testing, the design was iteratively redefined.

Promotion of the project and started already in the initial phase of the project with the development of effective communicative channels (social media and project's web site) so that in the project team the connective and collaborative atmosphere was created. After the communication was established internally, the promotion continued and is still in progress externally through target promotional activities on social media, contributions on symposiums and meetings, etc.

3. RESULTS AND DISCUSSION

The workflow of the project was strongly imprinted by the creative design thinking methodologies and the results is a quality, functional educative application with the geological content. Phases of emphasizing, defining, ideating, prototyping and testing were iteratively and interchangeably included through a multi-layer process of the elaboration of a stone key and were implemented in a user-oriented interactive application with an attractive user interface and stylish colours, iconography, graphic elements and typography.

In the strategy phase three main target groups were defined, primary – middle school's teachers and pupils and elementary pupils between 10 and 13 years; secondary group: geoparks, elementary pupils, geological museums and persons interested in the field. The tertiary target group included the clients from the Institute for education and the financiers of the project. The content (photos, videos, illustrations and graphics) was produced with the high communicative value considering the geological specifications and the context of the user-oriented interface as is presented in Figure 4.

The approach of user-centred design was successful, resulting in educative didactic tool. In further researches, the usability testing is going to be performed at the elementary and middle schools and some improvements of the app's functionalities are going to be implemented (presentations of augmented reality of stones).

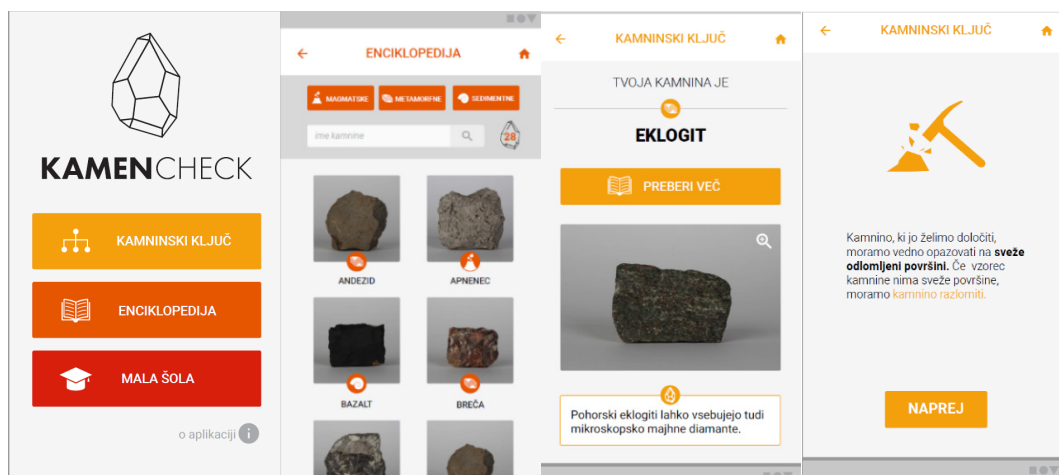


Figure 4: Final design of the educative app Kamencheck

In Figure 5 activities on social networks are presented that were the integral part of app's promotion strategy. Each step of the project work and the results were published and presented with the optimised web content and attractive visual communications, which aim was to introduce an educative application KamenCheck to the target groups and generate its exposure on the web. Beside the digital promotion also posters, leaflet and T-shirts were designed as is presented in Figure 5.

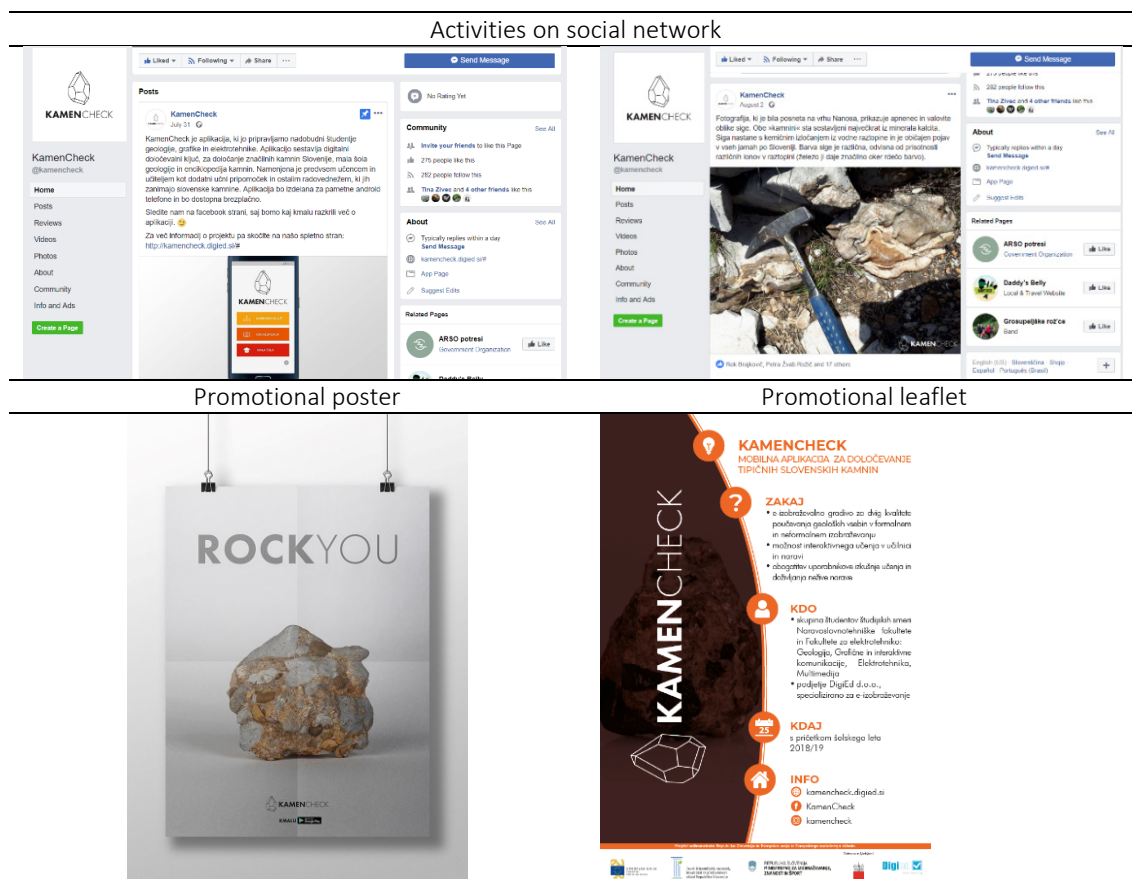


Figure 5: Activities on social network, promotional posters and leaflet

4. CONCLUSIONS

User centred design is an effective methodology that in our project resulted in successful design of educative app with the geological content. The evaluation of the app's interface, content design and usability discovered that the interactive solution is highly functional with a very good user experience and perfective design. The goals of the project were achieved, however, the results of user experience evaluation discovered that some functionalities could be improved, and that the usability of the app could be upgrade with AR presentation of stones that certainly could reinforce the educative effects and attractiveness of the solutions. 3D technologies (photogrammetry, scanning and 3D modelling) were indeed applied in the workflow, however the 3D model and texture optimisation and the reduction of topology details in the 3D stones' representations for the real-time presentations are complex procedures and consequently are still in the researching phase.

5. ACKNOWLEDGEMENTS

The project was financed by the Public Scholarship, Development, Disability and Maintenance Fund of the Republic of Slovenia, Ministry of Education, Science and Sport (Republic of Slovenia) and European Social Fund and was a part of Public tender project work with the economy and the non-economy in the local and regional environment - creative way to the knowledge 2017-2020. The authors of the contribution would like to thank the supporters of this project and all the dedicated participants involved.

6. REFERENCES

- [1] Garret, J. J.: "The Elements of User Experience: User-Centered Design for the Web and Beyond", 2nd ed, (New Riders, Berkeley, 2010).
- [2] Jakupović, E.: "V izobraževanju so čedalje bolj priljubljene multimedijske interaktivne vsebine", Ikt.finance, URL: <https://ikt.finance.si/8848337?cctest&> (last request: 2018-08-27).
- [3] Mayer, R. E.: "The Cambridge Handbook of Multimedia Learning", 2nd ed, (Cambridge University Press, New York, 2014). doi: 10.1017/CBO9781139547369
- [4] Mlakar, A., Štepic, M.: "Programi za animacijo". URL: <http://upomancaandrej.weebly.com/programi-za-animacijo.html> (last request: 2018-08-27).
- [5] Rias, R. M., Zaman, H. B.: "Learning with Multimedia: Effects of Different Modes of Instruction and Animation on Student Understanding", Jurnal Teknologi Maklumat & Multimedia 9, 57-70, 2010.
- [6] Still, B., Crane, K.: "Fundamentals of User-Centered Design: A Practical Approach", (CRC Press, Boca Raton, 2016).
- [7] Tullis, T., Albert, W.: "Measuring the User Experience, Second Edition: Collecting, Analyzing, and Presenting Usability Metrics", 2nd ed, (Morgan Kaufmann, Burlington, 2013).
- [8] Youngs, K.: "How to use 3D content in simulations for teaching and learning", Jisc.ac, URL: <https://www.jisc.ac.uk/blog/3d-in-teaching-and-learning-23-sep-2014> (last request: 2018-09-10).



© 2018 Authors. Published by the University of Novi Sad, Faculty of Technical Sciences, Department of Graphic Engineering and Design. This article is an open access article distributed under the terms and conditions of the Creative Commons Attribution license 3.0 Serbia (<http://creativecommons.org/licenses/by/3.0/rs/>).

DEVELOPMENTS IN DIGITAL PRINT STANDARDIZATION

Christos Trochoutsos^{2,3} , Anastasios Politis^{1,2,3}

¹ University of West Attica, Department of Graphic Arts Technology, Egaleo, Greece

² Hellenic Open University, School of Applied Arts, Patras, Greece

³ HELGRAMED - The Hellenic Union of Graphic Arts &
Media Technology Engineers, Athens, Greece

Abstract: Digital Printing has been established as one of the most rapidly evolving printing processes since its first introduction in 1982. In the years that followed, digital printing became the one significant new technology for print media production. Digital printing is continuously changing the print media landscape. Although, DP creates structural changes in production workflow and processes, it lacks in terms of print standardization, compared to offset printing for example, where consistent aim values and guidelines apply by means of ISO 12647-2. This drawback basically depends on two factors, which are interrelated. Firstly, there are many different technologies that are used in digital printing, and, each of them shows substantial difference in printing technology, substrates, data preparation, process control and image quality requirements. Secondly, compared to conventional printing, some digital printing technologies are still developing. After all, digital printing is versatile and variable in every way and cannot be standardized under a single standard.

A research on the digital printing technologies, processes and workflows is needed, to determine if a print specifications and quality controls (among them color management), can be applied in Digital Printing, and if possible, to which segment. Since color is very important to printing, especially in packaging and marketing applications, the print evolution demands for matching colors across technologies, substrates, materials and colorants. This paper intends to reveal the present status regarding Digital Printing Standardization. The question posed is whether standards can be applied and in which segments of digital printing either as technology or print sector (commercial decoration, packaging).

Within the paper, an analysis of the current industrial typical guidelines ranging from data creation all the way to printing will be made. Guidelines that are determined either by the manufactures of the digital printing machines, or by Institutes, such as FOGRA are reviewed for output process control and colour fidelity. As such, this paper can be regarded as a first attempt to preview the basis where standardization for digital printing processes can be developed.

Key words: digital printing, standardization, developments, technologies

1. INTRODUCTION

1.1 Introduction

Digital Printing (DP) has been established as a principal printing process since its first commercial introduction in the 90s. In the years that followed, digital printing became a significant new technology for print media production. Since then, Digital Printing has been developed rapidly and has brought about significant changes not only in printing itself but also in production workflow and in the total landscape of media market.

The establishment and the introduction of DP as well as its commercial application have led to predictions that this technology will eliminate traditional printing processes. Some older remember the title of an exhibition at a DRUPA (probably DRUPA 1982): “Good Bye Gutenberg”. This “apostrophe” has been related with the digitalization of the production processes in the prepress field, the Internet and digital publishing, as well as with the introduction of digital printing.

1.2 History of Digital Printing

The history of digital printing is relatively short compared to printing as a whole, which dates back to 1439, when German businessman Johannes Gutenberg created a press that started the mass production of books. The first digital printing presses came onto the market in the early 1990s.

In 1993 the world's first digital colour printing press was launched called Indigo. The name of the printing press series came from a company formed by Benny Landa in 1977 to develop the world's fastest

photocopier. Landa later discovered that the ink developed for the photocopier, called ElectroInk, could also be used in printers.

The first introduction of the Indigo printing machine, triggered a transformation in the printing world – all of a sudden, customers and print buyers were able to choose short-run, personalized, “high quality” print straight from prepress and the “desktop publishing” systems.

Print media industry expert Chris Baker, who worked as vice-president at HP and Indigo for five years, predicts that this growth will continue into the future: *"Digital print will be everywhere in the future. Digital printing will not just be used for commercial printing; it will be used for publishing and packaging. I believe that digital presses will be developed to go after the packaging market - the personalization of packaging will be huge in the future. Digital presses will also become faster and be designed to handle more types of printing,"* (printed.com, n.d.).

1.3 Facts & benefits of Digital Printing

The growth of digital printing can be attributed by the many benefits claimed that offers to customers:

- **Green:** This method of printing can boost the green credentials of any company. Unlike conventional printing, there are no pre-press stages between the digital document file and the final print, so there is no need for film plates or photo chemicals. The process can be very environmentally friendly when water based inks are used and no powders or coatings are applied. It is sometimes cost prohibitive to go completely green but there are ways to keep costs down without harming the environment more than absolutely necessary.
- **Speed:** Digital printing offers a quicker response time due to its minimal press setup. It simplifies the printing process, traditional plates and film are redundant, there is no press make-ready needed, no plate mounting, no registration adjustments and no ink keys. There are less steps and people involved in the printing process, and as result the final product can be delivered quicker.
- **Cost effective:** Enabling companies to make financial savings is another benefit offered by digital printing. Traditional printing services have always had quotas or minimum orders required when you used their services. However, because of the flexibility of the printing press, digital printing companies do not have these sorts of boundaries, proving the freedom for the businesses and individuals to save and get the exact amount that they need.
- **Short runs:** Digital printing is the ideal method of producing short- to medium-runs in more effective ways than traditional print. Digital data is easily stored and updated; therefore changes are easily made either prior to printing or in the following batch. Digital printing allows more effective print management: there's no need for bulk stock and no need to dump out of date stock. Some machines that use digital technology can not only print out the materials but also finish the final product at the same time. (inline post-press)
- **Print Enables Smarter Marketing:** Variable data printing gives direct marketing a highly effective way to talk to customers, allowing companies to tailor their message to their audience. Delivering the right message to the right people at the right time. QR codes have also linked printed materials to the digital realm. Digital printing facts include information about variable data and variable imaging. Because computers control the printing process it is much easier to change the content of the item while it is being printed. This adds a new level of customization and personalization that can greatly improve your finished product appeal (Pearl Print and Design, n.d.).

2. GUIDELINES AND SPECIFICATIONS FOR COLOR PRINTING

2.1 Color image quality in printing

The publishing industry is constantly changing. New disruptive digital printing techniques enter the market, standards continue to evolve or to be revised; electronic media allows print service providers to become communication providers. That implies more complex processes and related interactions.

Color image quality is a very important deciding factor for buyers of color imaging devices. It is therefore of utmost importance for manufacturers of imaging equipment such as digital presses, to pay special attention to this factor. After several years of market hesitation, digital presses have now become common (most of them). In today's printing market, where flexibility, variable content, shorter lead

times, and on demand publishing, are being demanded, digital presses represent an attractive supplement to conventional offset presses. It is important for customers of digital press equipment to be able to take into account the quality of the equipment, typically to be able to make a trade-off between price and quality. The total quality of a device is, however, a very complex entity, involving technical aspects such as expected lifespan, printing speed, accepted media, as well as customer relation aspects such as service agreements (Fogra, 2018).

There are indeed many factors that contribute to the quality of an image, such as spatial resolution, color depth, sharpness, naturalness, colorfulness, and visual artifacts (banding, streaking, grain, blocking, moire, etc.). There exists an ongoing effort to standardize the definitions of these and other image quality factors, as well as their assessment methodology.

Potential uses of quantifiable data on color image quality for manufacturers include the following:

- Tradeoff analysis of speed and implementation cost versus color image quality in image processing algorithm development
- Benchmarking of imaging systems and algorithms to other vendor's products
- Documentation of color image quality improvements resulting from efforts spent on optimization of technology parameters

For customers, it would obviously be advantageous to have access to reliable and objective information about the image quality that devices can provide when considering several alternatives for purchasing.

Every print shop is committed to a high level of quality. A basic prerequisite for this is to use meaningful rules, hence a standard. In standardization a distinction is often made between the specification of the final aim and the needed (process) steps to achieve that aim. A good example for the latter one is the PSO - Process Standard Offset, which has been successfully in place for years (Hardeberg et al, n.d.).

2.2 Color management

Two main components are needed to successful color management, no matter in offset printing or in digital printing. These are the **technology part** (meaning to have the appropriate hardware and software) and the proper **education** (understanding color management theory and the workflow knowledge).

Hardware is complicated, as it insists of different digital printing presses (and there are literally hundreds of models), different ink sets, different ink types, different substrates and so on.

Color measuring devices are used to measure the resulting colors of ink mixtures on the substrate. Standard devices are designed to measure on flat and even surfaces. Substrate properties can interfere with the measurement. Measuring colors correctly on those surfaces requires measurement equipment designed for that purpose. More information about measuring in different conditions can be found in section 2.4 (Gerrit, 2017).

Some of the major construction companies for digital presses have developed integrated tools to simplify and automate the colour management process. These tools ensure that the colour accuracy remains consistent and uniform across presses and sites and over time, without laborious manual calibration.

These tools usually consist of an Inline Spectrophotometer scans a colour chart to describe the individual colour space of a specific substrate (the "Media Fingerprint"). The DFE (Digital Front End) then automatically generates a dedicated ICC profile, ensuring accurate colour matching of that specific substrate against a given FOGRA, GRACOL etc. tool based on standard such as ISO 12647-2.

Accurate matching to these industry standards also enables seamless emulation of output from other print technologies (such as offset). A three-dimensional LUT is then used to regularly calibrate the press, automatically compensating for any variations in press conditions to return it to the baseline established by the Media Fingerprint, ensuring that colour output always remains consistent. On web-fed presses this process happens at a pre-determined interval, whereas on sheet-fed presses the operator is free to determine the frequency of calibrations. Media Fingerprints can be saved and shared between presses and sites, and over time, to ensure a consistent output regardless of where or when the file is printed.

2.3 Why digital printing is hard to standardize

Since there are many different printing technologies, processes and workflows it is under research to determine if a color management process can be applied in digital printing, and if possible, to which applications of digital print. The physics of the lithographic process doesn't vary from one model or machine to another. But, all digital press manufacturers have unique, patented processes.

The very term "digital" is misleading, because it refers to many disparate processes. Digital is commonly taken to mean toner/laser technology, but in the printing world, it may just as readily mean inkjet. Laser and inkjet are about as different as anything can be.

In the digital process, a crucial consideration for color quality is gamut-the range of color that a press can reproduce. The wider the gamut, the more colors can be printed. But gamuts of equal size are not always equal. One device may be weak in reds, another in blues. Sometimes, same size gamut can produce very different results.

Usually, **digital presses have a wider color gamut than the offset process**. Because the offset gamut is still the standard in many people's minds, this is often not understandable and is a more confusing fact. Unlike offset, **each digital press model has a difference color gamut**. All are different from offset. And it's even more complicated when considering also the spot colors reproduction and not just the conventional CMYK colors. There is also a belief that because of the massive range of applications, which is one of the key benefits of digital printing, this also makes it hard to standardize.

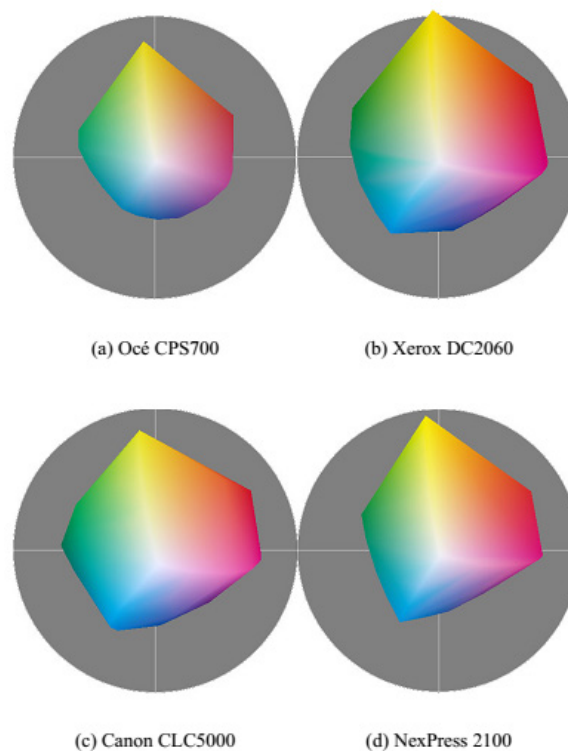


Figure 1: Different digital presses, different color gamuts

2.4 ISO 12647-2: Process Standard Offset

The Process Standard Offset (PSO) was developed by Fogra in co-operation with the German Printing And Media Industries Federation. It is the description of an industrially orientated and standardized procedure for the creation of print products. The PSO is in conformance with the international standardization series ISO 12647 and therefore internationally recognized.

By using PSO the quality of the production of a complete print product can be guaranteed, from data creation to the finished printing product. The PSO describes adequate testing devices and control methods by which the production process can be supervised, guided and proved. This includes measuring devices with spectral and densitometric settings, as well as suitable testing elements (for example test stripes). Furthermore, the PSO sets nominal values and tolerances for the print production that, relating to modern production materials, represents what is sensible and feasible (printed.com, n.d.).

The goal is to ensure that the production process is as efficient as possible and at the same time to ensure that interim and final results show a predictable quality of colour. In the printing industry very rarely data is printed where it was created. Customers often hand jobs to different print and media specialists. Printing plants collaborate in order to concentrate themselves on their core competences. This trend will continue and will extend across borders as well. The PSO and ISO 12647 are

in constant development in order to benefit the user. This way, quality becomes measurable, verifiable and reproducible. ISO 12647-2 is part of the ISO 12647, which contains the following:

- ISO 12647-1 - Part 1 Parameters and measurement methods
- ISO 12647-2 - Part 2 Standardized offset printing
- ISO 12647-3 - Part 3 Standardized press printing
- ISO 12647-4 - Part 4 Standardized gravure printing
- ISO 12647-5 - Part 5 Standardized screen printing
- ISO 12647-6 - Part 6 Standardized flexo-printing
- ISO 12647-7 - Part 7 Standardized digital printing

Unfortunately, part 7 is not about digital printing products, but for proof prints, that are printed with digital printers (GmG color, n.d.).

Process standard offset is a living process, so as the paper technology and other factors that affect printing changes, the standards may also change. For example, latest ISO 12647/2-2013 printing conditions and Fogra 51 and 52 it's the revised ISO standard printing conditions for sheet and web fed heatset-offset litho. This revision was published at the end of 2013 and it replaces the 2004 version. The main changes to the revised standard and the new data sets and profiles being developed by Fogra for coated and uncoated papers. Changes are also made due to the implications of the new spectrophotometer specifications, M1, in relation to the new 2013 version and the Fogra data sets.

- First, papers have been revised to better reflect the papers in current use with their high OBA (Optical Brightening Agents), so there are now 4 coated and 4 uncoated paper types in this new version, three more than the old 2004 version. These are now called 'Print Substrates' (PS), replacing the 'Paper Types' (PT) of the 2004 version.
- Colour differences are still measured and evaluated using De76, however De2000 tolerance values are also given.
- The new specifications for CIE Lab figures and TVI curves will result in new colour data sets and ICC profiles being needed. At present Fogra are working on a coated profile for PS1, based on a new dataset, Fogra 51 and an uncoated profile for PS5, also based on a new dataset, Fogra 52.
- This new version of 12647/2 is much more than just changing to new ICC profiles and new measurement figures. This change also may need new lighting, new spectrophotometers and changing digital proofing papers to have OBA/UV content.

One of main factors as referred to above for this new version of 12647/2 is to reflect the use of OBAs in papers. The viewing and lighting conditions standard, ISO 3664 was revised in 2009 in order to support the extra UV emissions caused by the OBA content. So, this is now within the standard and the latest D50 tubes will meet this requirement.

However, to measure accurately printed sheets a new spectrophotometer measurement standard is needed, M1. The 2004 standard uses M0 measurements, which do not correctly record the UV content of the paper, so can affect the accuracy of the ink colour readings.

The M1 spectrophotometer measures and allows for the UV content caused by the OBAs. For example, an M0 reading giving b at -4, on reading using M1 would result in a more accurate b -6.

Older spectrophotometers will not be able to read in the M1 mode; so, some updating of instruments is inevitable, both to off-line handhelds and on-press online devices.

Current 'approved' inkjet proofing papers are often OBA free. Proofing papers for the new profiles and M1 spectrophotometer readings will need to match the OBAs in the chosen paper type as closely as possible (Sherfield, 2014).

2.5 PSO and Digital Printing

After the success of the Standardization for Offset, the production also needs Digital Print Standardization for matching colors across technologies, substrates, materials. Process control needs to cover all print specific settings and the corresponding visual and instrumental measures, in order to establish a repeatable and stable printing condition. The process control measure therefore strongly depends on the printing technology and media used. Although process control is considered to be the responsibility of the print service provider some basic principles are important.

In the majority of such applications the **requirement could be termed as "matching offset"**. In light of this it stands to reason that where possible it would be good to make use of the established means to control

offset printing processes. This would include the usage of the same control wedges, measurement devices [in particular densitometers to measure the tone response] and, last but not least, the evaluation and the comparison of digital prints by means of press acceptance tests established for offset printing.

Press acceptance tests usually cover the solid coloration, the tone value increase [formerly known as dot gain] as well as grey reproduction. Those figures are compared against aim values derived from state of the art characterization data sets such as FOGRA39. Whilst ISO 12647-2 and hence PSO make provisions for a binary [conforming or not-conforming print] evaluation, manufactures of such solutions also offer a single value index also known as scoring value. Such scores typically range from 0% to 100% or from 1 star to 5 stars. The problem with these scores is that there is no agreed basis for their calculation so any score is somewhat proprietary and can't be compared among different vendors.

But **Process Standard Offset can't be applied in Digital Printing** in the same way. Contrary to digital printing the binary [Yes/No] evaluation of offset prints represents the results of many years' research and practical implementations. Still, some problematic aspects describe why the "offset concept" can't be transferred without some modification to the digital domain. That's the reason, why Fogra's working group created a new digital printing standard ISO 15311. Three of these main aspects are described below:

1. **Inadequate definition of the pertinent scope.** The usage of PSO for digital printing needs to be critically reviewed as there is no description as to what technologies and substrates it should be applied to. The term "digital printing" as a description for a given printing technology or imaging process is quite unsuitable. While the use of PSO for digital printing might be considered intuitive for toner based systems it is more than questionable for large format banner printing using UV-curing inkjet or textile printing using thermal processes.
2. **Lack of scientific knowledge and practical experience.** The various digital printing technologies are compared to conventional printing processes at a relatively early stage of their development and so that standardization activities and the necessary research is still scarce. This means that the implementation of procedures and methods which are successfully used in offset printing are not necessarily transferable to every kind of digital printing. Rather, such a "transfer" must be tailored and optimized for each use case, considering strengths and weaknesses of the pertinent imaging processes. Examples include the typical inkjet banding or a characteristic graininess as is found in some inkjet printing systems induced by coalescence. These digital-printing-specific problems might severely affect the final image quality but are not included in the "offset evaluation method toolbox". An audit or a compliance check in accordance with PSO ignores this property completely.
3. **Missing Link to underlying process parameters.** The primary aim of densitometry is to monitor the amount of colorant per area on a print. In order to measure the tone reproduction [the tonal response [CIEY] of the primary colours from 0 % to 100 %] the graphic arts industry uses the tone value, better known to some as apparent dot area. The solid densities and the tone value increase helped conventional process control reliably by indicating [with high sensitivity] press problems and monitoring the relative changes in tone reproduction of an image as it moved through the various stages of data preparation to a printing plate and eventually to the printed image. The underlying concept in ISO 12647-2 is that once the correct process colour solids and two-colour solid overprints are achieved, a satisfactory overall result can be reached by simply adjusting the tone value curve to match the specified tone value curve defined for the pertinent printing condition. **In general, this assumption can't be made for digital printing** although it is possible to measure solid density and tone value increase. This doesn't allow for any direct link to the underlying process parameters since they can't be easily identified. They are dependent on the imaging process and the interaction of the colorants with substrates used. For example, there is no doubling in inkjet printing. A possible evaluation of established doubling-slur patches thus leads to results that are hard to interpret by the user or are simply meaningless. Further it should be noted that densitometers mostly use a cross polarizer to reduce the effect of first surface reflections which reduce the measured differences between wet and dry prints. This may not be suitable for many digital printing technologies since it differs from colorimetric readings which are made without polarization filters. Note that the machine's internal use of density measurements for dedicated control processes, for example the control of the toner transfer to the photoconductor, is not considered as being inappropriate [it actually might be a very good solution]

2.6 Digital Print Standardization - ISO 15311

The basic prerequisite for printing predictable print quality is to use meaningful rules, hence a standard. In standardization a distinction is often made between the specification of the final aim and the needed (process) steps to achieve that aim. For digital printing the PSD – Process Standard Digital provides industrial typical guidelines ranging from data creation all the way to printing and is provided by Fogra. The ISO title is: *Graphic Technology - Requirements for printed matter for commercial and industrial production*. However, there is some discussion within ISO TC130 WG3 if the standard should be restricted to digital printing or not (since it can be applied also to conventionally printed products).

Contrary to ISO 12647-x, ISO 15311 is a multipart standard based on representative use cases (rather than printing technologies). Substantial contribution has been made in the Fogra digital printing working group (DPWG). The current structure looks as follows:

- ISO 15311-1 - Part 1 Parameters and measurement methods
- ISO 15311-2 - Part 2 Commercial production printing (almost published)
- ISO 15311-3 - Part 3 Large format printing (draft will be published as Fogra specification)
- ISO 15311-4 - Part 4 Additional parts based on use case (in discussion)

As far as the problematic aspects appear in digital printing in comparison to offset printing, Fogra proposes the following solutions:

1. The recently started multi-part standard ISO 15311 [Graphic Technology - Requirements for printed matter utilizing digital printing technologies for the commercial and industrial production] will provide a process-independent classification of the relevant use cases and applications and these will be accurately defined. Thus, for example, part 2 of ISO 15311 addresses commercial production printing while part 3 stipulates aim values and tolerances for large-format signage printing.
2. Fogra has applied for a research project that has started recently. It focuses on the development [and improvement] of objective methods for evaluating inhomogeneity and sharpness. First ideas were discussed during the last meeting of the DPWG (Fogra Digital Printing Working Group) and in the October 2010 ISO/TC130 WG3 meeting. In the short- and mid-term results from this research project can be expected that contribute to the vendorneutral, objective evaluation of the pertinent print image quality attributes.
3. Many manufacturers of digital printing systems are moving towards a colorimetric evaluation or inspection of their prints. This begins with the adjustment and calibration, via ICC profiling and ends with the colorimetric print quality evaluation. This development is already covered in the process independent definitions of contract proofs [ISO 12647-7] and the so-called “Validation Prints” [ISO/DIS 12647-8]. Both are fully defined without using any densitometric methods. The DPWG [Digital Printing Working Group] is working on a fullyfledged all colorimetry-based metrology including the respective statistical analysis [and uncertainty analysis] for process control and quality assurance (Kraushaar, 2010).

The Process Standard Digital has three main objectives:

- **Output process control** - Achieving a repeatable print output. Different output processes need to be checked against their known and constant behaviour.
- **Colour fidelity**. The second goal addresses a consistent colour communication by means of faithful image reproduction. Guide by the motto: “Printing the Expected” quality-oriented print service providers do first understand the needs and expectations of their clients and are second able to accurately reproduce that expectation. In that light the Process Standard extends the established way of colour reproduction namely the absolute reproduction (“Side-by-Side”) by means of an all new media relative colour reproduction.
- **PDF/-X compliant workflow**. As in this paper, an analysis of the current industrial typical guidelines from data creation all the way to printing will be made, it’s important that the entire workflow is subject to critical scrutiny as to its capacity for sustained achievement of consistent print quality and colour fidelity. So, Process Standard needs to provide guidelines for creating, preflighting and processing PDF based documents.

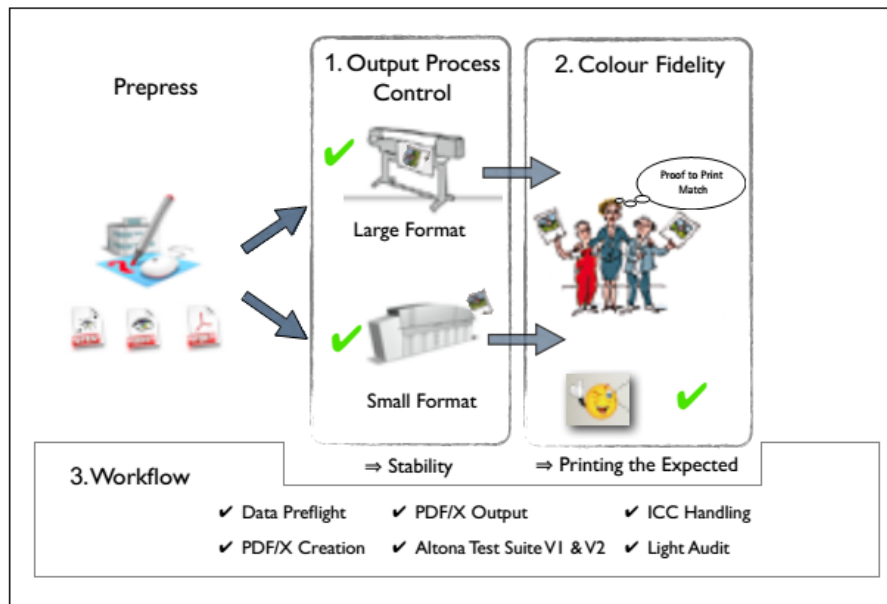


Figure 2: Fogra PSD-concept. Aiming for a consistent and predictable print quality

Standardization does not mean that materials such as substrates, inks, toner or machinery must be limited. On the contrary, standardization aims toward a manageable facilitation of a material and process diversity in terms of rigors and consistent print quality. Only then is it possible to identify suitable “combinations”, i.e. collection of a driving (RIP & colour management), a substrate, ink or toner and a printing press. Although many factors are the same in almost every digital printing press (for example the E.F.I. Fiery is used in most cases for RIP), as mentioned before, the publishing industry is constantly changing. New disruptive digital printing techniques enter the market. From xerography, to electrophotography and the latest one: nanotechnology, which is still being developed. That implies more complex processes and related interactions. To meet these changes the standardization process is designed as a “living document”.

2.7 Factors that affect quality of Digital Printing

The color gamut of a digital press (or any other imaging device) is the sum of all colors it can reproduce. Colors that are outside of this gamut cannot be reproduced. The color gamut, and in particular its size, is thus a quality factor. A press with a larger gamut than another is typically able to reproduce more saturated colors, which can be appreciated for many applications. The color gamut of a digital press depends on many factors such as substrate, toner/colorant, and halftoning algorithm. And unfortunately, every digital press has its own color gamut, as mentioned in section 2.3.

2.7.1 Substrate

Two main types are available: swellable and porous. In general, acid-free, buffered, and lignin-free paper bases are recommended for long-term storage.

Using swellable paper, its surface of this type of inkjet paper swells in the presence of the moisture in the water-based ink, allowing the colorants to penetrate the top layers. Swellable papers typically have three active layers: a protective top layer, a layer that fixes the ink droplets in place, and, below that, a layer that absorbs additional ink components. The paper base is sandwiched between two polyethylene layers and backed by an anti-curl coating and an antistatic layer. Premium swellable papers contain all of these layers, but less expensive ones may not. The polymer coating on swellable papers acts to maximize image brightness by keeping the colorants from spreading, and, to some extent, it protects the image from atmospheric pollutants. Images printed on coated paper may require a significant amount of drying time. On the other hand, the surface of porous paper is coated with very small, inert particles, which create numerous minute cavities in which the ink is deposited. These particles prevent the ink from spreading. Porous paper has a higher resistance to moisture and humidity. This paper requires minimal drying time, so the print can be handled immediately without fear of smudging. This type of print has no protective polymer layer; therefore, the colorants are susceptible to attack by atmospheric pollutants, such as ozone

and oxides of sulfur and nitrogen, which can be present in the environment in fairly high concentrations. Porous paper is preferred when pigment inks are used.

That's why in ISO 12647-2 there are different standards regarding the different type of paper, and the same difference have to be considered on digital printing.

2.7.2 Toner/Colorant

Dye Diffusion thermal transfer Prints In this process, which is also referred to as dye sublimation, heat transfers colorant from a donor ribbon to the final print. Dye diffusion thermal transfer printers frequently apply a clear protective layer to the print during the transfer process to prevent the image from smearing when rubbed. This process is frequently used for snapshot-size photo printers or in photo kiosks, where customers can print images in a few minutes. The permanence of these images has not been widely studied, and there is very little information available.

The majority of photo-quality printers use **inkjet technology**, in which very small droplets of ink are deposited onto paper. Inkjet prints vary widely not only in the composition of the colorants and paper, but also in stability. Inkjet images may be composed of dyes like those used in traditional photographic prints, or of pigments, which are the colorants used in paints. In general, pigments tend to be more stable than dyes.

Inkjet prints can be made on either uncoated or coated paper, but only coated paper will provide photo-quality prints. Plain, uncoated paper tends to absorb the ink, resulting in a blurred image and loss of color intensity. In high-quality paper, a coating prevents the ink from bleeding into the paper; this results in brighter, more saturated color and greater image detail. Coated papers may closely resemble traditional color print supports (IPI, 2004).

In **electrophotographic prints**, the same process used to produce office photocopies is used to make the prints. In electrophotography, toner is transferred to the paper base and then fused in place. The paper is usually uncoated, and the images are reasonably stable, because they are composed of pigment particles that are fused to the paper with a durable polymer binder material. This technology is used less widely than inkjet for photo-quality printing (Fogra, 2018) Electrophotography is the most widespread nonimpact-printing technology that exists. Many companies, like Xerox and Canon use variants of the electrophotographic principle with electrostatic powder toner, based on an invention of Chester Carlson from 1939 (HP, n.d.).

3. TYPICAL GUIDELINES RANGING FROM DATA CREATION ALL THE WAY TO PRINTING

Printing the expected is not easy. To standardize printing we need to have the same printing results and not just print the expected, but have the same output across different printing technologies, different substrates, and production batches.

Problems might occur not only on the output procedure, but in many occasions in input file formats as well. PFD files are container files and elements can include bitmap graphics in different color modes (RGB, CMYK, LAB, ...), vector elements, spot colors, overprints, transparencies, etc.

Depending on the creation application the result can be overly complex which leads to longer processing time and mistakes during PDF processing. Missing color management information (embedded profiles and output intent) leaves room to interpretation and errors.

PDF/X is the ideal data exchange format for the printing industry. The purpose of it is to facilitate graphic content exchange with specific requirements linked to production workflow needs. In the following table some typical tasks of the prepress side are provided to avoid faults.

Table 1: Typical tasks together with the corresponding party being responsible for that specific job

Nr.	Task	Responsible	Note
1	Data creation – open (application) files	Print service provider should inform the data deliverer about the status of the data integrity.	Providing a reliable visualization e.g. by means of a hard- or softproof based on the corrected (optimised) data is needed for colour critical jobs.
2	Providing Print-ready data – marked as PDF/X.	Data deliverer	
3	Preflight of data	Print service provider	
4	Agreement and negotiation about the output condition (printing condition)	Print service provider together with the client (print buyer)	These include the definition of the quality type for CMYK (and spot if present), the intended viewing distance, the reference characterization data set as well as the colour reproduction („Side-by-Side“ or media relative)
5	Printability of the substrate	Print service provider	Unless the manufacturer of the printing system has "certified" the pertinent substrate.
6	Process Conversion when data is not prepared for the intended printing condition	Print service provider	The print service provider is required to inform the print buyer about potential limitations preferably with a contract proof based on the re-separated data.

During the printing process, even more tasks are needed to ensure the right output. A printing system is only as good as its maintenance status. A printer has to:

- Follow manufacturer periodically recommended operations
- Ensure that both printing system and substrates used are in appropriate environment conditions
- Identify and check material combination
- Choose the desired print mode(s)
- Understand specific parameters for printer (hardware) and workflow (software)
- For drying/curing printing systems, the temperatures applied during printing and post-printing stages are very important for both printability and runnability
- Select colour reference(s). The achievable colour gamut results from the substrate and ink interaction and performance

Most important one the measurement procedure. To control colour adjustments and calibrations are needed and in many occasions the printer must create a specific characterization and profiling (e.g. ICC) for the specific job. This is not needed in offset printing, since the ICC profiles that are being used are provided by ISO 12647. In digital printing the characterization data set for the selected printing combination must be created and then the printing condition becomes a fully characterized printing condition. In this stage a typical ICC Output Profile will be generated, but in some occasions a device link profile may be also used.

Lastly, to validate the printing output the stability of the printing system for a given printing condition needs to be checked, as well as the deviation from aim values of the printing condition to be simulated. This is done by using the control strip or chart, using the properly measuring device in proper conditions and check the pass/fail tolerances adapted from already established validation print tolerances. Periodically calibration or re-calibration is recommended in case of a faulty evaluation. Monitoring and recording the pass/fail evaluation for tracking purposes is also recommended as it will show up trends useful to fix issues before they become problems.

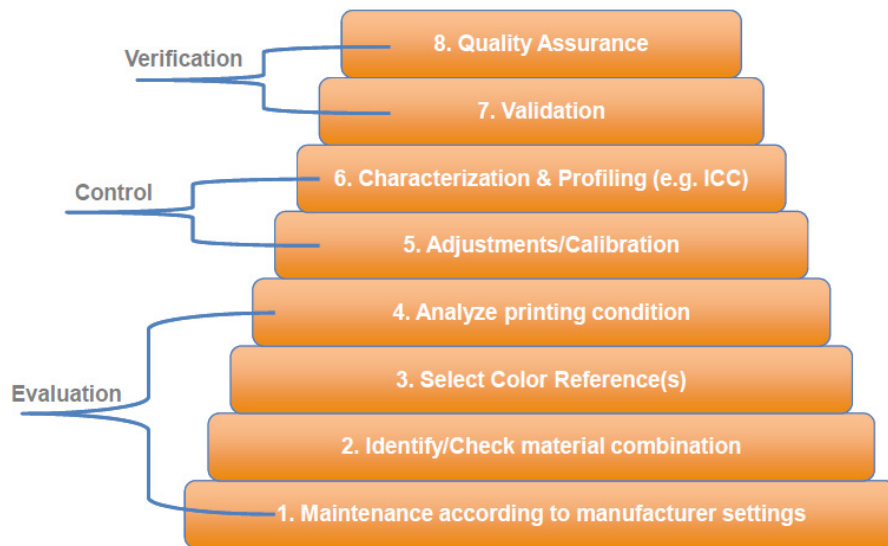


Figure 3: Process Control pyramid - 8 steps to success

4. FURTHER RESEARCH

Color image quality is of very high importance in a digital imaging device such as a digital press. For manufacturers and customers of such devices it is important to be able to quantify color image quality. Unfortunately, as of today there are no analytical techniques that can quantify color image quality in this context. Contrary to ISO 12647-x, ISO 15311 is a multipart standard based on representative use cases (rather than printing technologies). Despite this fact, some researches rely on experiments using ISO 126147-x. Some others rely on experiments involving real observers. We claim that the notion of color image quality is ultimately tied to the preferences of customers and end users. Because of this, a very useful tool to quantify color image quality is psychophysical experiments involving a panel of human observers. However, such experiments are relatively time consuming. Definitively, Yendrikhovskij (1999) hits the nail on the head when he states that “most studies on image quality employ subjective assessment with only one goal - to avoid it in the future.” Therefore, results from ongoing research toward analytical models for color image quality is eagerly anticipated. An example of such research is the development of metrics for color differences between complex images. However, much more use cases must be analyzed in different digital presses, different substrates, different settings etc. to assure a standardize process in digital printing. And this is even more complicated, since digital printing consists of commercial printing, large format printing, printing in special materials and so on. And nobody knows the evolution of digital printing by using nano technology. Landa’s presses are believed to print the same output no matter what (any size, any substrate and matching ISO 12647-2). Will this set a new standard for digital printing?

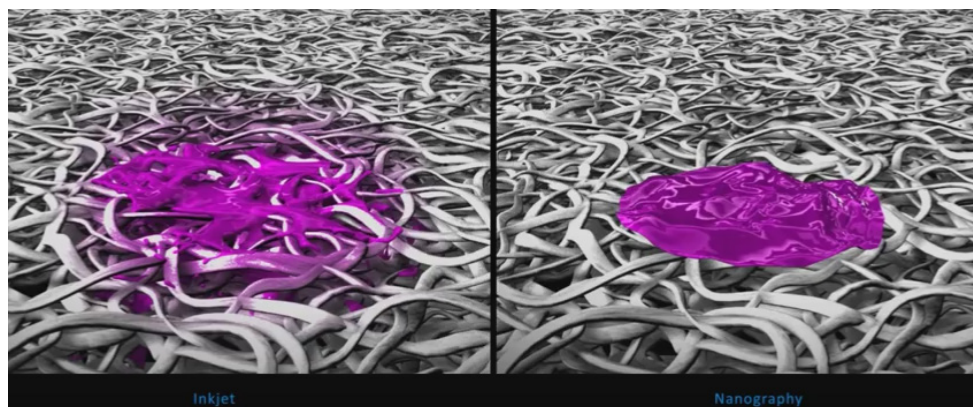


Figure 4: Landa’s nano-pigment toner penetration to substrate in comparison with inkjet

5. CONCLUSIONS

In summary, it can be stated that the underlying concept of ISO 12647-1/2/3 [including the recently started revision] is completely adequate for offset printing. In contrast, digital printing tailored to specific technologies is hard to imagine. Instead, a process-independent concept that addresses the individual applications with dedicated print quality measures seems more appropriate. The demand for a digital printing standard alongside methods for process control and quality assurance is evident. The use of established methods in offset printing, in particular by offset printers that also use digital printing systems might be quite useful - but it comes quickly to many limits that are outlined in this paper. Although it might be tempting to simply use the existing PSO system for digital printers, too, this has a poor technical basis and is, thus, likely to reduce the industry's confidence in certification altogether. Fogra is making research on Process Standardize Digital and there's still a lot of space for further research, as mentioned above. The various digital printing technologies are compared to conventional printing processes at a relatively early stage of their development and so that standardization activities and the necessary research is still scarce. This means that the implementation of procedures and methods which are successfully used in offset printing are not necessarily transferable to every kind of digital printing.

6. REFERENCES

- [1] Fogra: "Process Standard Digital Handbook, Step by step toward printing the expected", (Fogra Research Institute for Media Technologies, 2018).
- [2] Fogra, PSO - The Process Standard Offset, Fogra, 2017, URL: <https://www.fogra.org/en/fogra-standardization/standardization-psy/psy-e28093-the-process-standard-offset.html> (last request: 2018-5-08)
- [3] Gerrit, A.: "Innovative Solution Committed to Color, Color Management for Industrial Printing Applications", Slides from the conference In Print Show 2017. URL: <http://www.inprintshow.com/usa/conference/pdf/Gerrit-Andre.pdf> (last request: 2018-5-08)
- [4] Gmg color, New ISO standards for proof prints, Gmg color, URL: <https://www.gmgcolor.com/specials/new-iso-standard/> (last request: 2018-05-07)
- [5] Hardeberg, J. Y., Skarsbø, S. E.: "Comparing color image quality of four digital presses", URL: http://www.ansatt.hig.no/jonh/archive/ipgac02_iq.pdf (last request: 2018-05-02)
- [6] HP, HP Indigo Digital Offset Colour Technology, HP Development Company, URL: ftp://ftp.hp.com/pub/gsb/Indigo/Knowledge/Sales_New/Commercial/07-Technology_Supplies_Environment_Media/Technology/HP___Indigo___Digital___Offset___Color___Technology___WP.pdf (last request: 2018-06-05)
- [7] Image Permanence Institute (IPI), A consumer Guide to traditional and digital print stability, Image Permanence Institute, 2004. URL: http://www.imagepermanenceminstitute.org/consumerguide_traditional.pdf (last request: 2018-06-05)
- [8] Kraushaar, A.: "Process Standard Offset print [PSO] for Digital Printing? Between appropriate use and opportunism", Fogra Forschungsgesellschaft Druck, 2010, URL: <https://www.fogra.org/index.php?menuid=48&downloadid=222&reporeid=197> (last request: 2018-05-08)
- [9] Pearl Print and Design, The digital future of print, Pearl Print and Design, URL: <http://www.pearlprintdesign.com/the-digital-future-of-print/> (last request: 2018-5-08)
- [10] printed.com, History of Digital Print, URL: <https://www.printed.com/history-of-digital-print> (last request: 2018-05-02)
- [11] Sherfield, P.: "The new ISO 12647/2-2013 standard printing conditions and Fogra 51 and 52", The Missing Horse Consultancy Ltd, 2014, URL: <http://www.missinghorsecons.co.uk/wordpress/2014/06/the-new-iso-126472-2013-standard-printing-conditions-and-fogra-51-and-52/> (last request: 2018-5-08)
- [12] Yendrikhovskij, S. N., Blommaert, F. J. J., de Ridder, H.: "Color reproduction and the naturalness constraint", Color Research and Application 24(1), 52-67, 1999. doi: 10.1002/(SICI)1520-6378(199902)24:1%3C52::AID-COL10%3E3.0.CO;2-4



© 2018 Authors. Published by the University of Novi Sad, Faculty of Technical Sciences, Department of Graphic Engineering and Design. This article is an open access article distributed under the terms and conditions of the Creative Commons Attribution license 3.0 Serbia (<http://creativecommons.org/licenses/by/3.0/rs/>).

ACCESSIBILITY OF SLOVENIA'S MUSEUMS FOR BLIND AND VISUALLY IMPAIRED

Raša Urbas¹ , Ana Kuščer¹, Mexhid Ferati² , Urška Stankovič Elesini¹ 

¹University of Ljubljana, Faculty of Natural Sciences and Engineering, Department of Textiles, Graphic Arts and Design, Chair of Information and Graphic Arts Technology, Ljubljana, Slovenia

²Linnaeus university, Faculty of Technology, Department of Informatics, Kalmar, Sweden

Abstract: Accessibility of museums and other cultural institutions is not equal for all visitors. Since the perception of the human surroundings bases mainly on the visual experience, people with vision disabilities, either blind or visually impaired, are deprived of this kind of experience. Desiring to provide an equivalent user experience more and more institutions show the tendency of offering different variations of adjustments.

Adjustments for blind and visually impaired are usually limited to the use of existing exhibition materials for all visitors either in the form of audio guides, guides or brochures in Braille, tags in Braille, less often tactile objects, tactile maps, floor markings, larger signs or indicators, magnifying glass, and sound elements. Though it seems that numerous adjustments are being used, the reality shows that they are still rare. Besides that, these materials and adaptations usually do not fulfil the requirements of adequate museum experience therefore, the need of improving the current state is necessary.

In this paper an overview of needs and demands, which need to be fulfilled within the graphic arts and communication technologies possibilities, either for Braille, tactile or audio demands for presenting the lack of visual experience with blind and visually impaired, is presented.

Key words: adaptations, audio guide, blind and visually impaired, museums, tactile recognition, user experience

1. INTRODUCTION

People are multisensory living beings who are estimated to gain from 80–85% of their surrounding perception through vision (Politzer, 2008). Though it can be stated that we live in highly visual world where information is mainly visually experienced, people who cannot use all their senses are able to form a credible representation of surroundings (Kermauner, 2014). Therefore, it cannot be stated that the world structured with all senses is much more real than the one structures with one or more senses missing.

The blind and visually impaired are able to partially replace the missing sight with other senses, mainly by touch, as a contact sense, and hearing, as a distant sense (Hersh, 2008). They use the sense of touch to read Braille and other tactile recognizable elements, or to recognize certain objects. Hence, they can develop a much better hearing and recognize certain objects with the help of it. In spite of mentioned there are still numerous limitations in different user experiences. One of them is the accessibility of museums and other cultural institutions. Since they are mainly adjusted for visual, and sometimes audibly, presentations of a wide variety of exhibits, pieces, displays etc. people with vision disabilities, either blind or visually impaired, are deprived of this kind of experience. Desiring to provide an equivalent user experience more and more institutions show the tendency of offering different variations of adjustments (Levent et al, 2013a; Levent et al, 2013b).

Adjustments for blind and visually impaired are usually limited to the use of existing exhibition materials for all visitors either in the form of audio guides, guides or brochures in Braille, tags in Braille, less often tactile objects, tactile maps, floor markings, larger signs or indicators, magnifying glass, and sound elements. Though it seems that numerous adjustments are being used, the reality shows that they are still rare. Besides that, these materials and adaptations usually do not fulfil the requirements of adequate museum experience therefore, the need of improving the current state is necessary.

The use of graphic arts technologies and communication techniques enable numerous possibilities for adapting not only the exhibitions artefacts and objects, but also the written content and audio descriptions as well as some other variations (Bowe, 1993; Cullen, 2001).

Many museums have already successfully implemented the use of digital screens, multimedia visualizations on different devices, and most commonly the use of different audio guides (Othman et al, 2013). The latter, in particular, present a common way of providing additional information. Lately, audio guides are upgraded

with different applications that can be used on smart phones, tablets or similar devices. Users can access the audio guide with their device, either by downloading the application, or by using web based one.

Museum programs for the blind and the visually impaired roughly fall into the categories of verbal description tours and touch tours. Though this can significantly improve the museum user experience of blind and visually impaired, the content is in many cases defectively and inadequately presented. Namely, due to the fact that many exhibits, pieces, displays etc. are exclusively available for viewing only the lack of basic information (precise description of the size, the shape, the source material, the color etc.) deprives the blind and the visually impaired visitor of adequate presentation (Rice et al, 2006; Hall, 2009).

Some museums offer tactile elements, either as the original historical or art works, or as replicas, some offer different models or objects that are in a way related to the visual material. All these objects are, compared to the numerous exhibits and museum pieces, still very rare. Their rarity is not solely attributed to the production costs, but the depicting and their production must also be considered. Namely, objects, presented for normally sighted, carry in their visual representation numerous information – shape, size, color, surface and in some cases inner structure, composition, etc., which are, when adapted into the tactile presentation, usually strongly limited. It is very hard, if not sometimes impossible, to present for instance the shape, color and the length of persons hair, their facial properties (e.g. color of cheeks and lips, eyes, wrinkles ...), shape and pattern of their clothes, etc. Tactile impressions are limited, therefore depriving the information of presented object. The same could be said also for the written information in Braille. Additional information in text guides and brochures.

For ensuring an adequate museum accessibility and experience proper adaptations need to be made. The aim of this research was to establish the current state of adaptations for blind and visually impaired in Slovenia and on the bases of findings to prepare an overview of possibilities and solutions, which would offer the blind and the visually impaired comparable user experience as with the normally sighted. This paper offers an overview of needs and demands which need to be fulfilled within the graphic arts and communication technologies possibilities either for Braille, tactile or audio demands for presenting the lack of visual experience with blind and visually impaired.

2. RESEARCH METHODS

The research was divided into three parts – *preliminary*, *qualitative* and *quantitative research*.

The *preliminary research* consisted the study of the current situation in Slovenian museums and their accessibility for the blind and visually impaired. The objective was to establish whether and in what manner are Slovenian museums adapted for this group of visitors. Furthermore, our second goal was to establish if there are any audio applications being used, and if, what are their types. In the study 73 Slovenian museums and their collections were included. We examined the museums' websites to gather the information regarding their accessibility for the blind and visually impaired. The collected information was later upgraded with telephone interviews.

The *quantitative research* consisted of questionnaire in which we asked the respondents for the purpose of using smart phones and their experience with different applications, usage of computer and in general about the use of information-communication technology (ICT) in their everyday life. The questionnaires of quantitative research were sent by e-mail to the group of participants and their written results (answers) were later analysed. Thirteen interviewees participated in the research (4 female and 9 males), among which three had low vision, while others were blind.

At the end, the *qualitative research* was conducted. Seven blind people participated (2 female and 5 males, age from 20 to 51) in personal interviews where we have used the method of contextual inquiry. A smaller number of participants is attributed to the fact that the number of blind people in Slovenia is relatively small, among which not all are using ICT devices and tools. Interviews were performed in accordance to the previously prepared questions. Afterwards, we asked the interviewees to show us some of the tasks they usually perform on their smartphones, and, also, to show us some of the applications they use. The interviewees who use applications for navigation were asked to show us how they use them in context, of course, if possible. Results of all three research parts are presented in the continuation.

3. RESULTS AND DISCUSSION

3.1 Preliminary research results

The research has shown that there are 14 Slovenian museums that have some sort of adaptations with differing scope for the blind and the visually impaired (Figure 1).

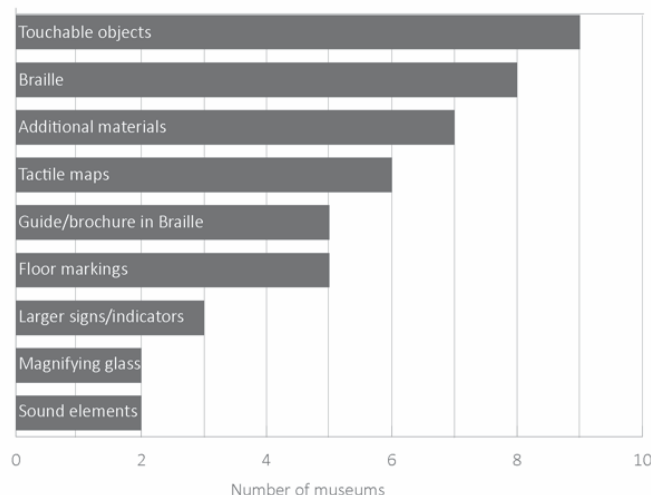


Figure 1: Accessibility of Slovenian museums for the blind and the visually impaired

Nine of those museums present diverse tactile objects (mostly as some sort of replicas). Often, there are only certain exhibition objects available as tactile objects, or only particular parts of the exhibitions. Eight museums display information in Braille (usually only labels for the presented objects and pieces), while five offer guide or brochure in Braille. Information written in Braille is very often less extensive than written in Latin. Guides and brochures for normally sighted are visually attractive and mainly image presented, while the written content is most often short and only basically informative. Due to the fact that images are not suitable for preparing this kind of material for the blind and the visually impaired, all the content needs to be in Braille. But when preparing in braille it must be considered that Braille has other demands than Latin – Braille needs to be of certain size, which is much larger than Latin and being written on Braille typewriters it is normally only one-sided. Therefore, prepared initial texts in Latin are, when rewritten in Braille, often shortened, offering this group of museum visitors less information. Research has also shown that seven Slovenian museums offer some sort of additional material (their type was not specified on the web pages), while six of them offer tactile maps, five have floor markings for easier navigation of the blind and the visually impaired, and three museums have larger signs for the visually impaired, or some type of indicators. The fact is, that majority of museums are either partially adapted for the blind and the visually impaired or present only temporary adapted exhibitions. The only fully adopted museum for the blind and the visually impaired is the Museum of post and telecommunications in Polhov Gradec, which offers tactile objects, Braille presented contents, sound elements, tactile maps and floor markings, thus enabling their blind and visually impaired visitors the possibility of independent museum visit (Figure 2).

Though there are several museums in Slovenia that offer audio guides for their visitors, only one museum in Slovenia offers an adapted audio guide for the blind and visually impaired, which offers visual descriptions of the exhibited objects. There are 16 museums in Slovenia that use the Nexto audio guide mobile application (Proxima, Slovenia) and none of the museums offer a mobile guide application that would be especially adapted for the blind and the visually impaired. Nexto application possesses no special adaptations for the blind and the visually impaired, but is somewhat accessible with VoiceOver (iOS) and Talkback (Android), and, therefore, can be used by the blind and the visually impaired visitors, as well as sighted ones.



Figure 2: Adaptations for the blind in the visually impaired in the Museum of post and telecommunications, Polhov Gradec

3.2 Quantitative research results

ICT technology today presents a part of everyday life. Its use is widespread among world population and it is not gender or age limited. Therefore, it is not surprising that even blind and visually impaired use smart devices and applications.

In the quantitative research, we wanted to establish in what way the blind and the visually impaired interact with mobile/smart devices, and for what purposes they use them. Research has shown that the blind and the visually impaired interviewees use their smart phones mainly for phoning (92,3%), using different applications, and texting (84,6%). Two thirds of respondents (69,2%) use their phone for web browsing and navigation (Figure 3). Furthermore, the research has shown that the use of smart phone helps blind and visually impaired with their everyday activities, enabling them greater independence.

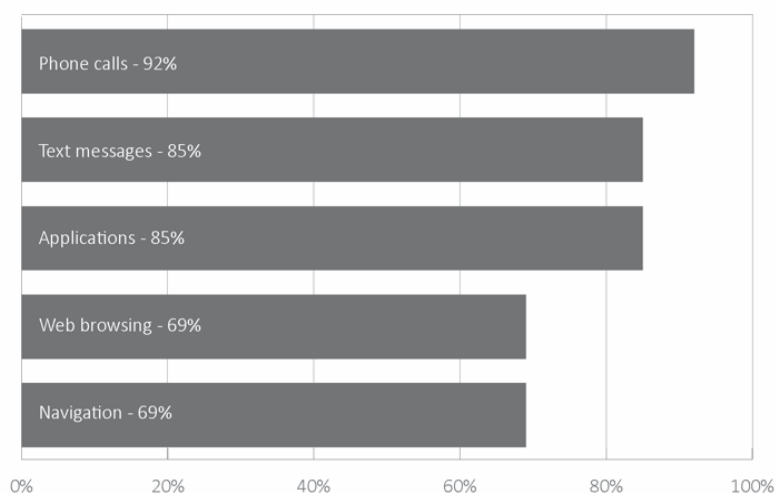


Figure 3: Usage of smart phones

We were also interested in what kind of applications and how often do they use them. Surprisingly quarter of respondents (23%) use 9 or more applications, while other (77%) use 6 or less. Among most frequently used applications are popular social media apps e.g. Facebook and Messenger, and at the same time navigation for blind and visually impaired applications (Moovit, Lazarillo, Navigation) and usual transportation applications (Slovenian versions – LPP Bus, Prevozi) (all 38%). The respondents also frequently use e-mail and music apps (31%), less often calendar, call and chat apps (Viber, Skype), health

and sports apps, online television, Siri, weather applications and YouTube (all 15%). They also use other applications (e.g. calculator, camera, Google, reminders etc.) though their use depends on the user. The blind and the visually impaired often rely also on applications developed intentionally for their use like Be my eyes and Tap TapSee.

It could be concluded from the research that the blind and the visually impaired use their smart devices in the same manner as normally sighted. Therefore, the use of ICT technology presents a useful tool for presenting the surrounding world not only in everyday life but also in the museums and other cultural activities. Smart devices present not only video content but can also be used as audio descriptors.

3.3 Qualitative research results

For determination of requirements and needs of technical and user experience properties of applications we interviewed blind persons (7) who had different experiences about museum visits. Majority of them have already visited different museums in Slovenia and abroad, where they have used an audio guide device or an audio application as a guide while the visit. Their experience differed. Some have used audio guide devices where the users input by themselves the number assigned to a certain object while other used audio guide devices that detects near-by objects. The interviewees agree that for a positive blind and visually impaired user experience audio guide device shouldn't have too many buttons and should be easy to use. Selecting a proper number assigned to object is easy if audio guides device is user friendly, on the other hand if it is complicated blind or visually impaired visitor can have problems with its use. With automated audio guide device (usually connected to NFC tags) some function problems can occur if presented objects are positioned too close together, when movement can trigger a beginning of another description audio tape. One of the interviewees also mentioned an experience from a museum where an application detected through a camera if a certain object was near, and, therefore, provided information about the object.

Regardless to the type of audio guides, recorded descriptions should include precise visual descriptions of objects, containing information about dimensions, colours, locations etc. Sometimes, a blind person has difficulties imagining how big a certain object is if it is only described in relative terms. However, if it is presented with specific information, like measurements, or compared to another object, it is easier for them to get an idea how the object looks like (Neves, 2008; Salzhauer et al, 2003). Also, it is useful to know the precise location of a certain object in comparison to the location of the other objects. Each element needs to have a correct description in the source code with simple input fields.

Research has shown that interactions with smart devices (phones, tablets, etc.) play an important role. Simplicity of use enables good user experience regardless of their purpose. Devices for audio guides can be more user friendly to the blind and visually impaired if they enable scrolling the screen in both directions, thus enabling the selection of certain recording or element, which can be selected by double clicking. Every time the users reach a new element, a beep goes on, and, at the same time, the phone vibrates so that the users know they are located on a new element. Sliding offers users more freedom while navigating then scrolling. Good examples of this practice are Talkback and Voice over. Application needs to follow the Web Content Accessibility Guidelines (WCAG 2.0) which explain how to make web content more accessible to people with disabilities (W3C, 2018).

In applications for the blind and the visually impaired the usage of graphic elements should be limited, however, if used, they should have an appropriate name in the code. If the application offers more buttons to choose from, or other options on the screen, it doesn't present an obstacle for the user, as long as they are presented in the correct manner. The research has also shown, that setting up a web-based application presents an advantage, thus it can be used on all operating systems.

With audio guides it is important to think about the usage of head phones, which offers visitors privacy during a visit. Headphones are usually paired, but because blind get a lot of information about the world around them through hearing, they prefer to use headphones only in one ear.

4. CONCLUSIONS

Research has shown that Slovenian museums offer different kind of adaptations for blind and visually impaired, though the majority bases on presenting some of the information in Braille or on exhibiting certain tactile objects. Because visual experience isn't enabled for the blind and visually impaired, for achieving adequate presentation exhibited items need to be either fully verbally or written presented.

For firstly mentioned, museums and other institutions usually use audio guides, which are also being used for normally sighted though voice recorded apertures. However, these guides are often not properly adapted for the use of blind and visually impaired. They lack of precise object descriptions and their user commands are not suitable for this group of people. In the contextual research, we have discovered that the blind and the visually impaired use their smart phones in a similar manner as the sighted, with the only difference that the navigation works differently. Therefore, the blind and the visually impaired are able to use all applications and web pages, as long as their code is written properly, so that it can be read with a screen reader. Furthermore, a code of the application needs to be written in a form of a screen reader compliant. In such a way, it will be accessible to the blind users with either TalkBack or VoiceOver. Application needs to follow the guides of the WCAG 2.0 standard.

Secondly mentioned written materials in Braille have usually content shortened because texts in Braille take up more space than ordinary texts due to the demands and standards of Braille. Thus, information is usually more scattered and does not satisfy the curious ones.

When the museum is made accessible, it is necessary to think about the achievement of the intended goals. A new relationship with the blind and the visually impaired who decided to stop going to museums needs to be formed, and, moreover, to attract those who have felt unwelcomed before, or have never visited a museum at all (Levent et al, 2013a).

5. REFERENCES

- [1] Bowe, F. G.: "Access to the Information Age: Fundamental Decisions in Telecommunications Policy", *Policy Studies Journal* 21(4), 756–74, 1993. doi: 10.1111/j.1541-0072.1993.tb02173.x.
- [2] Cullen, R.: "Addressing the digital divide", *Online Information Review* 25(5), 311–320, 2001. doi: 10.1108/14684520110410517.
- [3] Hall, C. A.: "Web Presentation Layer Bootstrapping for Accessibility and Performance", *Proceedings of the 2009 International Cross-Disciplinary Conference on Web Accessibility (W4A)*, (Madrid, Spain, 2009), pages 67–74. doi: <https://doi.org/10.1145/1535654.1535671>.
- [4] Hersh, M. A., Johnson, M. A.: "Assistive Technology for Visually Impaired and Blind People", (Department of Electronics and Electrical Engineering, University of Glasgow, Glasgow, 2008), page 52. doi: 10.1007/978-1-84628-867-8.
- [5] Kermauner, K.: "Avdio-haptično-virtualna Mona Lisa", *Časopis za kritiko znanosti, domišljijo in novo antropologijo* 42(255), 173–181, 2014.
- [6] Levent, N., Kleege, G., Pursley, J. M.: "Museum Experience and Blindness", *Disability Studies Quarterly* 33(3), 2013a.
- [7] Levent, N., Reich, C.: "Museum Accessibility: Combining Audience Research and Staff Training", *Journal of Museum Education* 38(2), 218–226, 2013b. doi: 10.1080/10598650.2013.11510772.
- [8] Lievrouw L. A., Livingstone S. eds.: "Perspectives on Internet Use: Access, Involvement and Interaction", in *The Handbook of New Media*, (editors: Lievrouw L. A., Livingstone S., SAGE Publications Ltd., London, 2006), pages 92–113.
- [9] Neves, J.: "Descriptive guides: Access to museums, cultural venues and heritage sites", in *Pictures painted in words: ADLAB Audio Description guidelines*, URL: <http://www.adlabproject.eu/Docs/adlab%20book/> (last request: 2018-02-24).
- [10] Othman, M. K., Petrie, H., Power, C.: "Measuring the usability of a smartphone delivered museum guide", *Procedia – Social and Behavioral Sciences* 97, 629–637, 2013. doi: 10.1016/j.sbspro.2013.10.282.
- [11] Politzer, T.: "Vision is our Dominant Sense", *Brainline*, URL: <https://www.brainline.org/article/vision-our-dominant-sense> (last request: 2018-04-15).
- [12] Salzhauer Axel, E., Hooper, V., Kardoulis, T., Stephenson Keyes, S., Rosenberg, F.: "ABS's Guidelines for Verbal Description", in *Art Beyond Sight: A Resource Guide to Art, Creativity, and Visual Impairment* (editors: Salzhauer Axel, E., Sobol Levent, N., New York: AEB and AFB Press, 2003), pages 229–237.
- [13] W3C, Web Accessibility Initiative (WAI): "Web Content Accessibility Guidelines (WCAG) Overview", W3C, 2018, URL: <https://www.w3.org/WAI/standards-guidelines/wcag/> (last request: 2018-09-04).



© 2018 Authors. Published by the University of Novi Sad, Faculty of Technical Sciences, Department of Graphic Engineering and Design. This article is an open access article distributed under the terms and conditions of the Creative Commons Attribution license 3.0 Serbia (<http://creativecommons.org/licenses/by/3.0/rs/>).

DESIGN



EFFECTS OF DIGITAL PRINTING APPLICATIONS ON CONTEMPORARY ART

Yeter Beris 

Altinbas University Vocational School, Graphic Design Department, Istanbul, Turkey

Abstract: Today's technology and innovations, which have a power in representing society's cultural values and emotions, offer new possibilities to the most important expression tools of social life. In fact, it is stated that with this power of representation, it shapes the cultures and societies as well. In this representation, art is stated to play an important role in shaping the expression of social emotions and life by being embedded in them and taking the support of technology (Schiuma, 2011). As a necessity for the age, humans now communicate through art, strengthening the individual expression in social life with advantages offered by technological production and incorporate new expression tools into their lives.

Continuing to explore the conveniences offered by technological life, humans continue their development in their social life through communication and interaction in the virtual world. Thanks to this interaction, digital communication channels have spread rapidly and the desire to access information easily has also created the technological infrastructure requirements that are able to provide, economical, high quality and personalized designs for demands changing consumer habits as requirement of this era, decreasing printing circulation due to this, and personalized designs taking center stage have accelerated the spread of digital inkjet printers with toner cartridges. Digital printing systems that have emerged since the year 2000 offer a new laboratory environment that today's artists can experience as a means of expression, beside their technological developments. Fine-Art print, with a view that acknowledges the importance of digital art in the technological life of our era, is a new expression tool worth mentioning its role and importance in contemporary art. Fine art print, as a term, defines the prints made by high-quality inkjet systems of images transmitted from digital files to the special production underprint materials under the supervision of the artist himself/herself.

In this research, fine art print technique which presents the artistic expression to the viewer with today's technology will be discussed. It is aimed to examine the values it adds to contemporary art and technological advantages as a production material that supports artistic expression and its effects on artists' material preferences.

Key words: fine art print, digital print, contemporary art

1. INTRODUCTION

After the industrial revolution, technological and scientific developments have facilitated human life, and the speed of life and technology have improved the way people communicate and learn. Due to this, the world wars which caused social and cultural destruction as well as the participation of technology in the life since the early 1900s, have also contributed to the transformation of the means of expression and the production techniques. After II. World War, the invention of the computer brought this change to an irreversible point. This great invention, which was the beginning of the modern era, has been the harbinger of the periods when technology has guided communication, the developments could not be kept up with and the art would meet technology.

The technological facilities offered by the computer in every field of life have been rapidly adopted by the people and have created more demands and the communication methods developed with urbanization have gained a strong momentum with the possibilities of the computer. Thanks to the digital communication, people can communicate in seconds by pressing a button and transfer information to many points of the world. Now in the age of such a speed, the development of faster communication methods in the business world has been inevitable. "The rapid dissemination of digital communication channels and the desire to easily access the information has also created the technological infrastructure where the demands are made to provide economic, and personalized designs of high quality" (Beris, 2015). It is also possible to see these developments in the printing sector, which has been commercially available since the 16th century. The printed media, which has been produced after days of preparation with traditional methods, are replaced by the personal design and communication channels that can be printed on all kinds of surfaces in digital tracks just in a few minutes. This change has been reflected in the computer and programming languages that have been developing since 1950 and has been seen in the artistic expressions of contemporary artists such as Andy Warhol. The reflections of this

interaction continued to develop at the same rate in 40 years. Today's art experiences individual expression and communication with the advantages offered by technological production and incorporates new means of expression. In other words, it has become one of the most important means of expression of cultural and social life with the power of representation in the expression of the cultural values and emotions of society. It is stated that this representation power shapes cultures and societies. In this representation, art plays an important role in the expression of social emotions and shaping life (Schiuma, 2011). Human beings are now communicating through art, empowering individual expression in social life with the advantages offered by technological production and include new means of expression. Referring to this change in the 1930s, W. Benjamin mentions "The artwork is not independent of the conditions in which it was born" and tells something about today. Fine art print refers to digital prints that are produced by controlling the high-resolution images that are transferred from digital files or digital media by the artist himself/herself and which belong to the artist. In other words, it defines the artistic special print made on the sub-printing materials also called specially produced media with the high-quality inkjet system of high quality.

In this age, which is thought together with the technological life, fine art print, which accepts the importance of digital art, appears as a new phenomenon worth mentioning its role and importance in contemporary art. Before discussing fine art print, which will be the material that will produce the original expression in contemporary art with a new language, it would be useful to take a brief look at the historical development of the art of print.

2. METHODS

In this paper, qualitative researches based on records and documents have been used in the field research. It has been referred to the scanning methods of resources recorded on the internet or resources such as professional books and periodicals and this study has been formed within the context of collection of the data of the impression and research based on the work experience from the past years.

3. HISTORY OF THE PRINTMAKING ART

Throughout the history, the artist presented his/her thoughts to the viewer starting from the walls of the cave and working on different materials such as paper-canvas, ink, oil paint, watercolor, acrylic, brush, pencil or other tools. The usage preferences of these materials have also varied according to the image imagined by the artist, the final satisfactory result and the visual presentation. It is not known that the artists at that time searched for the new materials since the artistic materials had negative effects on the permanence of the works for many years; however, the developing chemical techniques have found somehow a place in the art movements. This interest also created an environment that made you experience artistic production via original printed picture for the artists of the period who are looking for new expression and expression. The first engravings of the world-renowned German painter Albert Dürer, which are known to have been produced at the end of the 15th century, can be given as an example (Figure 1).



Figure 1: Adam and Eve, Albrecht Dürer, 1504, Engraving, Rijks Museum, Netherland
Source: <https://www.rijksmuseum.nl/en/rijksstudio/artists/albrecht-durer/objects#/RP-P-OB-1155,0>

The social-cultural developments of the urbanized communities, the technological and political structures caused the industrial revolution, which is defined as "the breaking point" in the social transformation and the reflection of these developments and searches has been included in the art movements. The inclusion of mass production lines, which are the extension of industrial production, has brought a cultural movement. The urban man who worked in the factory environment had created a separate world for him both to enjoy and rest at night parties. The artists of that period also found a new way of expression in this movement and printmaking art, which can be defined as a mass production band method in the art, created a perception of art in a new language. Posters of entertainment announcements such as cabarets and theaters in the entertainment world, which influenced the city culture of that period, attracted great attention. Printmaking art has become popular with intense interest thanks to these posters produced by mass production techniques such as lithography, wood printing, and engraving. These posters were highly appreciated by the low-income people who could not reach the works of art, and each of the painters who designed the posters created a new school of design that influenced the history of graphic art in Europe (Figure 2).



Figure 2: "Reine de Joie" Poster, Lithography, Henri de Toulouse-Lautrec, (French, 1864–1901)

Source: <http://www.artnet.com/artists/henri-de-toulouse-lautrec/art-nouveau-ms5QsHaTLycCljGbdjv-aw2>

The fact that production is affordable in every layer in the society and that artworks take place on the streets thanks to cheap production as posters have changed the value perception of the artwork. In this way, the original print art has survived to the present day and has been accepted in the art market. Printmaking Art, created by traditional methods in Europe, has become valuable in the art market as a result of the centuries of radical changes and cultural life. This cultural life has led to the establishment of modern art museums and engravings museums around the world, which recognize the value of the art of printmaking. At the same time, international print biennials and printmaking Competitions also offer activities supporting this interest (Tekcan, 2017).

In the last four decades, the intersection of digital technology with the art world has been thanks to the practices experienced by photographers and artists. Firstly, the photographer or artist applied digital imaging methods to develop his/her own art. These methods have produced demands, thanks to intensive research by scientists, the image quality of inkjet digital prints and ink and sub-printing materials have been developed. In other words, fine art print, among contemporary artists, has been used in the production of a limited number of reproductions or original works of art, since inks are more resistant to light fading with a wider range of colors. For this reason, it is now possible to see fine art print artworks exhibited in contemporary art museums.

The fine art print is based on digital inkjet technology. It is obtained by printing the digital artwork prepared in the digital environment by the artist himself/herself and by printing with a high-quality inkjet digital printing, by numbering in a limited number and by the artist's signature process. Thanks to the latest technological inventions and non-fading inks that incorporate intelligent systems, serial production can now be performed in order to meet the demands of digital production. In addition, high-resolution

fine art print practices can be done in a short time on a wide range of sub-printing materials using many materials such as canvas, handmade special papers, and watercolors. Although not yet produced at affordable prices, high-quality digital prints can be made with high costs and these satisfy artists. The fact that all kinds of machinery and material supplies of digital printing technology are imported from major countries is also a negative factor that makes it difficult for artists to prefer in terms of cost.

It would not be wrong to say that the foundation of fine-art print is based on the computer and programming language has developed since 1950. Frieder Nake, who started working on computer graphics and art in 1963, is an engineer who is known as one of the pioneers of computer art. When he studied mathematics in Stuttgart, Germany, he and Frieder Nake, A. Michael Noll and Georg Nees performed artistic experiments for the first time in the digital environment. These works were later published in 1965 at the Stuttgart University of Technology with the plotter called "Graphomat Z64", the legendary drawing machine of Konrad Zuse (Nake, 2012). These digital art examples drawn by algorithms that are stated to be entered by interpreting mathematically on ER 56, a room-sized computer, were exhibited in Stuttgart, Galerie Wendelin Niedlich in 1965 and this information can be found in Wikipedia (Figure 3).

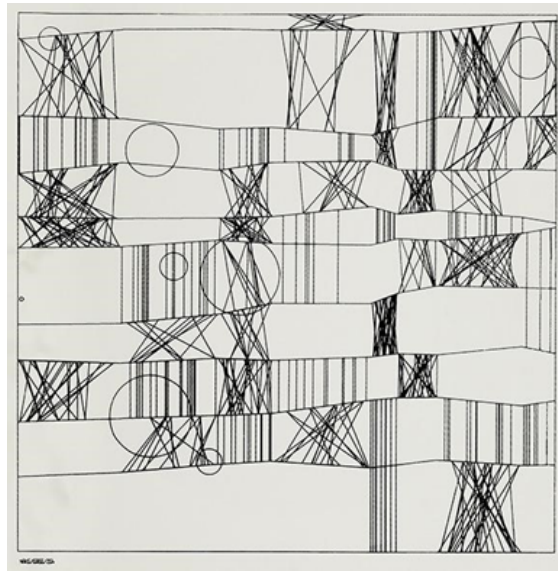


Figure 3: 1965, Frieder Nake tarafından Paul Klee'ye övgü (Frieder Nake Hommage à Paul Klee),
Source: <https://iq.intel.com/a-brief-history-of-digital-art>

From the 1960s on, new examples of digital art practices were introduced, a photo was scanned by engineers from Leon Harmon and Ken Knowlton, and the grayscale values were converted to various ASCII codes on the IBM 7040 computer and the image was re-created. The work "Nude" was found on the cover of the New York Times magazine, which was presented at a meeting although it was not seen as very successful for that period (Figure 4).

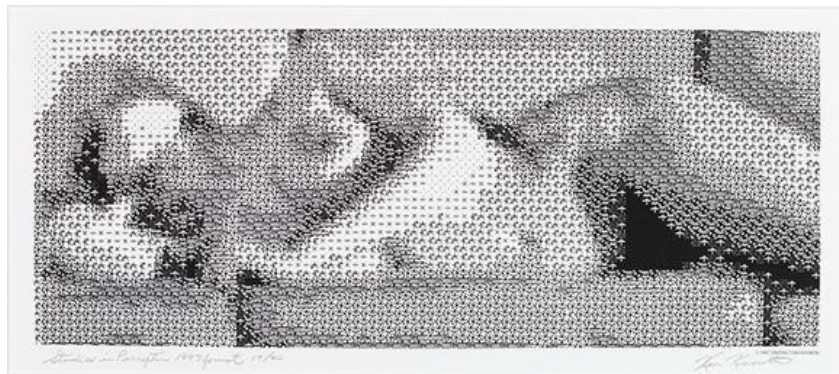


Figure 4: Nude, Bell Labs, 1967
Source: <https://iq.intel.com/a-brief-history-of-digital-art>

In the early 1980s, globally-powered computer companies, such as the IBM PC and Apple Macintosh, underpinned the artistic applications of digital media thanks to their breakthrough technological innovations in personal use. These discoveries have heralded the fact that there will be no life like before and incorporated technological systems that facilitate everyday life into our lives. In this period when the computer evolved from binary code to the graphics interface, the efforts of making the individual use of the computer at every moment of the social life provided the rise of computer games. Using the Commodore Amiga computer, one of the popular plays of that period, the American painter Andy Warhol, the most important representatives of the Pop Art movement, got a chance to experience digital art for the first time (Figure 5). The story of the first examples Andy Warhol experienced the digital art in the Commodore Amiga computers in 1985 that they were saved from the old archives almost 30 years after was announced by Andy Warhol Museum (Ford, 2014).



Figure 5: "Andy 2 "Image recovered from Andy Warhol's computer, 2014
Source: <http://edition.cnn.com/2014/04/24/us/andy-warhol-lost-art/index.html>

The opportunities promised by modern technology to today's art are the reflections of inventions of more than 100 years in which new tools have been presented to artists since 1800s. In the last 30 years, high-resolution digital printing systems, which have evolved from the days of the use of plotter and laser printers, have contributed to the increase in the interest and popularity of fine art Print with its technological ink structure which incorporates intelligent systems. The technological structure, which is now able to present the work prepared in the digital environment, with the desired dimensions and almost the desired sub-printing material, with a fine ink flow of millions of drops per second, has turned into an important opportunity. Accordingly, the development of specially produced sub-printing materials continues to inspire contemporary artists.

In the last 20 years, unlike the limited production of ink-jet color printers, which are used in business and offices, today's new system inkjet printers have improved the image quality of digital art print in incredible ways. Production in this machine track with production capacity in the desired scale can now be seen everywhere. In the light of 100 years of progress, artists have also embraced a new vision and understanding by exploring the use of photography. The new vision of chemists and some artists who use new dyes and pigments to improve science use technology to capture fresh and even ground-breaking interpretations of the rapidly changing world in which they live (Berger, 2005). Digital art prints, which have a large size placement in museums, exhibitions, and architectural buildings, are appreciated as a work of contemporary art by collectors in today's art market. As such, however, the extent to which digital technology will provide radical changes in artistic vision is not yet clear.

3.1 The Current Fine Art Print Practices

First of all, inkjet digital artworks have been defined as "Giclee" print by the printing engineer Jack Duganne. It was stated that these first artistic prints were produced in Iris printers in the early 1990s and that the original works began to fade or deteriorate after a certain period of time. Afterward, it has been stated that the life of the ink and sub-printing materials have been significantly increased by developing technologies and these problems have been eliminated (Nickelson, 2017).

In today's studio environments, using Adobe programs, artworks prepared electronically, with the advantages and facilities offers new opportunities for artists. As such, it stands out as an advantage for the artists who want to produce their work collectively. When an artwork is archived in a digital environment, it is possible to print the desired number of prints with minimum effort and cost. With the professional color separation process, which is controlled by the artist personally, the edition print of the work can be realized in a short time in determined numbers on order or demand without the need for a cost in mass production. The characteristic of edition printing defines the number of prints that can be done at the specified size. The work, which has been approved by the artist with the final print, means that there will be only 50 editions if 50 artistic prints are planned. These editions are called original prints and are printed and signed by the artist in person. In addition, in determining the number of editions, except for the total number of editions under the name of artist copies approved by the artist, there are artistic copies which the artist have and are decided according to the mixed edition and a total number of editions. Thus, by limiting the sale of the work to a certain number, whether it is a photo print or a picture, it turns into a situation where the material value of the work is shared among 50 buyers, which preserves the originality and increases its market value. It means that the artwork can reach low-income art-lovers at an affordable price. Thus, the artist can also share his/her work with more than one buyer through the editions. This sharing process makes contemporary artist prefer this way and this view becomes common.

The fine art print studios of the contemporary museums serving for the artists such as IMOGA in İstanbul and the high-quality print with the inkjet printing tracks in the range of millions of colours increase the interest. As such, the inkjet printing system has now a sensitive fine spraying technology like laser printing system. In addition to this advantage, it offers a possibility to print on many sub-printing materials, not only paper, and in almost every size. This creates an opportunity for the artist to adapt the visual she/he wants or needs as a new way of expression.

It is obvious that understanding the stages of this digital printing, the new way of expression takes time for artists and the language of digital software has a complex organization. For the artist, original pre-printing preparation for the designed work is a complex process which the artist can work with the help of another expert. This information environment which covers the digital printing technology that is produced by controlling outside, changing fast and sometimes seems complex is a challenging area which the artist does not dominate yet. This challenging informative and searching process covers the quality of artistic printing in the last three decades and accordingly deterioration, the variety of material, the technologic innovation increasing the option and digital printing processes developing over time. Assessing the longevity of artistic pressure characterized by a variety of ink and media combinations, resistant to fading of artistic prints, is an important consideration as well as being compelling by the artist. These factors include the stability of the printing to environmental conditions (lighting, moisture, and atmospheric pollutants) as well as post-printing options (such as polished printing and canvas prints and montage). Sometimes, as a result of the environmental conditions and after long years, it is possible to see fading of the artworks exhibited in the walls. This is a condition which is not appreciated by the artist. While the artist is able to use the artistic materials she/he uses with the traditional methods with a certain experience, she/he has little experience and knowledge about the stages of this new digital production. At this stage, the artist will either work with a specialist in a reliable studio environment or conduct extensive research and will continue to improve his/her experience by getting a professional training in this production technology. It is certain that it is not that affordable. The fact that the machinery and consumption costs of technology are at a high price is an obstacle for many artists to reach. Currently, there are the artists who prefer this technology, familiarity with the art market and the digital production belonging to the prominent artists. In Turkey, it is possible to see fine art prints of well-known painters of our country known in our country in the contemporary museums like IMOGA in contemporary museums and temporary exhibitions and in online sales (Figures 6, 7 and 8).



Figure 6: Burhan Dogancay, Fine Art Print, IMOGA Istanbul Museum of Graphic Art 2017, Istanbul, Turkey
Source: <https://imoga.org/collections/burhan-dogancay/products/copy-of-burhan-dogancay-02>



Figure 7: Adnan Coker, Fine Art Print, IMOGA Istanbul Museum of Graphic Art 2017, Istanbul, Turkey
Source: From Archives Of IMOGA Istanbul Museum of Graphic Art, 2017 Istanbul



Figure 8: Ergin Inan, Fine Art Print, IMOGA Istanbul Museum of Graphic Art 2017, Istanbul, Turkey
Source: From Archives Of IMOGA Istanbul Museum of Graphic Art, 2017 Istanbul

4. CONCLUSIONS

Today, what is called the Millennium Age, defines a time when the art and science, and design and engineering come together and the technology itself is experienced. This unity serves humanity in many vital areas such as the business world, communication, and transportation. In this period when universities have focused on R&D studies with multidisciplinary studies, we observe either the engineering courses in the design departments or the design courses in the engineering departments and the modern training modules following the change. In short, it is mentioned that technological developments are listed one after the other and the speed of science is difficult to follow.

In a rapidly changing social life, the contemporary artist will try to interpret this new world that she/he has lived and perceived by taking advantage of the opportunities of technology. The beginning of a new era where there is a threshold again after 100 years can be mentioned. In this technological life, it is an undeniable fact to use a technological production field that will serve to increase the accessibility of art to all segments of the society by reinterpreting. We are in the times when we witnessed the fact that contemporary artists who accept this fact are now working in a team. Edward Burtynsky, known as one of Canada's most respected photographers, is an inspiring example combining art with his internationally acclaimed scientific studies and the digital imaging and new media education center he established as a researcher as well as an artist. It is possible to illustrate many famous people who combine science with art. It is also a fact that, when there is so much flow of information, it is now a necessity to turn to the teamwork instead of being alone, to be able to discover new ways of expression as an artist. In this experimental environment, it would not be wrong to say that the works of art produced with the technology presented to the audience have enriched the artistic expression style and have been even inspiring. At this time, it is possible to see the signs that modern artists, who are open to science and innovation, will shape the art world in the future in the societies that have adapted technological life so much and, in an era, when fine art prints find a place in daily life.

From the 1990s onwards, thanks to these high-quality print courses, which have been covered by technological innovations and inkjet printers, the image quality in artistic prints has now been satisfactory for the artist. Since it is a newly discovered technological track, the problem of reaching for each artist and the high cost are concerns in terms of expenditures in Turkey. These technological tracks, which are imported and introduced to the market for the first time, are unfortunately very expensive, and therefore there are high-cost solutions for now. But in time these costs will be reduced, and in less costly times, it will be easier to supply. It is hoped that engineers and designers are trained to produce technological tracks and material that will eliminate the dependency on the import in Turkey. It is a necessity that a production technology with international standards is manufactured within country possibilities so that it is necessary to reach a stage where all kinds of machinery and consumption materials with affordable prices can be provided.

In a rapidly changing world in life, with a unique expression that captures the day, today's artists can present the works of art to the audience in dazzling exhibitions by using this technological track with the production capacity they want. Digital art prints, which cover a large space in museums, exhibitions, and architectural structures, are being discussed as a contemporary work of art as a growing value in the contemporary art market and among collectors. Today, it is not yet clear how much digital technology will provide radical changes in artistic vision. As mentioned above, it should be reiterated that these digital art prints are considered as original prints and with the signature of the artist and found in the archives of collectors in the art market. As a harbinger of a new era, fine art print expects to be discovered as an endless means of expression for contemporary artists who are beginning to find a place in the international art market.

6. REFERENCES



- [1] Berger, M.: "The Digital Fine Art Print—Opportunities and Challenges", Proceedings of International Conference on Digital Printing Technologies adlı NIP & Digital Fabrication Conference book, (Society for Imaging Science and Technology publishing, 2005).
- [2] Beris, Y.: "Analising of the graphic design and digital printing production communication", Proceedings of Print İstanbul 2015, (Marmara University, İstanbul, 2015), pages 295-308.
- [3] Ford, D.: "Andy Warhol's lost computer art found 30 years later", CNN web news, 2014, URL: <http://edition.cnn.com/2014/04/24/us/andy-warhol-lost-art/index.html> (last request: 2017-11-10).

- [4] Nake, F.: "Information aesthetics: an heroic experiment", *Journal of Mathematics and the Arts* 6(2-3), 65-75, 2012. doi: 10.1080/17513472.2012.679458.
- [5] Nickelson, J.: "Fine Art Inkjet Printing – The craft and art of the fine digital print", (Rocky Nook, San Rafael, 2017).
- [6] Schiuma, G.: "The Value of Arts-Based Initiatives", (Cambridge University Press, UK, 2011).
- [7] Tekcan, S.: IMOGA museum visits and the notes received in the interview with the artist, November 2017.



© 2018 Authors. Published by the University of Novi Sad, Faculty of Technical Sciences, Department of Graphic Engineering and Design. This article is an open access article distributed under the terms and conditions of the Creative Commons Attribution license 3.0 Serbia (<http://creativecommons.org/licenses/by/3.0/rs/>).

INFLUENCE OF BEER LABEL DESIGN ON MAKING DECISION ABOUT CHOOSING AND BUYING PRODUCT

Marina Heđa, Dean Valdec , Krunoslav Hajdek, Petar Miljković 
University North, Department of media design, Koprivnica, Croatia

Abstract: *In the brewing industry there is a great competition among beer producers and the constant struggle for dominance on the market. The beer label for glass packaging is an important means of communicating with the customer and it represents a key part of the whole packaging which sells the product. This paper researches the impact of primary packaging and beer label on customer perception and purchase of products. The aim of this study was to examine customers' perception of different elements of beer label design. Survey was conducted on a hundred adult males and females aged 18 to 65 years. The sample for conducting the survey consisted of six 0.5 bottles of different types of beer placed on the shelf. Based on the results of the research, conclusions were drawn about the influence and preference of the brand, about the elements that are crucial for the decision to purchase and the efficiency of individual graphic elements of the label.*

Key words: beer label, design, brand, packaging

1. INTRODUCTION

Beer is a product which is often consumed and belongs to a food group of products. Glass packaging is very suitable for packing beer due to its chemical and barrier properties. Dyed glass used for beer packaging is also a good light insulator that prevents the formation of harmful chemical reactions in beer caused by UV rays. Furthermore, the bottle shape itself contributes to mechanical resistance. The most efficient bottle shape is a relatively narrow bottle with a narrow long neck. According to its basic purpose, glass packaging belongs to a sales or primary packaging (Narodne-novine, 2005) which has the role of protecting and presenting the packaged product, containing information on the goods and allowing an easy use and wear of the product. Therefore, glass bottles have assumed absolute primacy in beer production. However, practice has shown that PET packaging is very practical and well accepted by consumers (Rujnić-Sokele, 2018).

Due to difficulties of printing on a glass bottle, the label is an integral part of beer packaging. Customers and label consumers have never been more demanding, more price-sensitive and more environmentally and health-conscious (Print magazine, 2018). Label represents a medium of visual communication which allows customers to get all the necessary information on the product, i.e. the information that encourages them to purchase. Since it is a product placed on the shelves in the store, the beer manufacturer can communicate with the customer exclusively through the visual display – the label. The label is a part of the packaging where the manufacturer should, by means of graphic elements, unite legally prescribed information with design elements that in a psychological way reach the customer's consciousness and encourage admiration (Solomon et al, 2006).

Consumer behaviour is influenced by a large number of factors (social, personal and psychological) which are interrelated and represent a starting point for understanding consumer behaviour (Kesić, 2006). From a marketing point of view, packaging should enable the product identification among competing products at the point of sale, contribute to the communication with the buyer, create an additional psychological value of the product, and facilitate the customer's purchase decision (Grbac & Meler, 2007). Product identification is the main task of beer labelling which should enable the customer to clearly identify the product within the variety of other products, which usually refers to the product name that is dominant on the label (Jurečić, 2004). The label must also describe the product, i.e. it must contain the information on the type of beer, content, composition, date and place of production, method of handling, etc. Glass bottles are recycled and reused in a way that they are cleaned and prepared for reuse using specifically defined processes which are carried out in breweries and are therefore classified as returnable packaging (Stipanelov Vrandečić, 2010).

2. BEER LABEL DESIGN

Label design together with the descriptive information makes the entity vital to the sale of the product, which is the ultimate goal of each beer maker. Product descriptions include all the information a customer needs in order to safely use the product. The label with its typography, colours, shape and other graphic elements has to retain its visual identity so that the customer could at first sight identify the manufacturer - the brewery (Mencer, 2011). An attractive and innovative graphic design of the label should promote the product. Due to the fact that beer is a part of a group of food products, it is allowed to be advertised. Beer producers often advertise their products regardless of its sales results. The design of the label needs to be changed after some time in accordance with its visual identity and identification of the manufacturer in order to keep the customer's attention and promote the product on the competitive market. Very often, specific beer labels are produced for events such as festivities or jubilees to promote the beer tradition.

The front label on the beer bottle is the first and most important part of the packaging that will be noticed at first by the potential buyer. The shape of the front label should be aligned with the cylindrical shape of the bottle, so in practice, the rounded forms of the front labels are often applied. It is a well-known rule that the composition of elements has a remarkable impact on the perception of the human eye and the perception of the general impression of aesthetics. The front label is placed on the body of the bottle in the optical centre, which is the imaginary line and is slightly above the geometric environment and corresponds to the ratio of the golden section. The composition of individual graphic elements on the label should show harmony in the human eye. The optical medium of the label is firstly noticed by the observer. Therefore, the name of the beer identifying the product is put in this position. Other elements are subordinated to the optical medium, and their size and position are determined by the importance of the information. When using the front label, it is important to pay attention to the amount of information since too much information in a small format may result in the lack of legibility and difficulties to find the desired data. The information on the front label should be divided into three to four groups and then adjusted to the size and placement of the text. The text on the front label of beer is most commonly written in uppercase, with the exception of the logo. Like colours, the selected fonts contribute to the brand personality (Ellis, 2018).

Illustration is often a constituent part of the label, and its role is to describe the text or to be a decorative part of the label. Illustrations on beer labels most often complement the typographic logo and describe the tradition of a particular brewery or a particular type of beer. Choosing illustrations in the form of drawings or photographs on packaging is a very complex task because the illustration speaks a lot about the product. Like the size of text, the number of colours should also be limited to several rankings in order to avoid unreadability. The beer label on the front contains textual information about the type of beer that is crucial for informing the potential buyer and its main purpose is to identify the product and aesthetically appeal to the buyer, while all other information is on the back label (Jurečić, 2004).

3. METHODOLOGY

The research was conducted through surveys on the persons who were not exclusively beer consumers. A sample of 100 respondents was selected without prior knowledge of their age and education, but with the same ratio of male and female respondents. The survey comprised the comparison of six different brands of beers: Pan Lager, Pan Zlatni, Carlsberg, Osječko, Karlovačko and Stella Artois. As a sample for conducting the survey, a printed real-size model was used, which represented a simulation of the shelf at a store where six types of beer were placed in glass packaging, a volume of 0.5 l. The front and back labels were visible on the glass bottles of the above beer type. Respondents were asked to reply to 10 questions after which it was possible to make a conclusion about the impact of the entire packaging on the customer, including the label and individual elements on the label. The questions were on multiple choice basis, so that the respondent could choose one of the answers which best describes his/her opinion. In addition, respondents were asked to give data on their gender, age and education. Thus, subgroups were defined within the examined sample of people providing the additional data on the subgroup preferences within the overall research.

Each of the above stated beer producers have profoundly shaped their visual identity. The colours and graphic elements on the labels have carefully been adjusted to the appearance of the bottle in order to arouse an adequate visual effect among potential customers. The goal of each label is to present the quality and the brand of the particular beer and eventually sell the product. Due to the fact that specific

beer consumers already have certain predispositions to the above stated products as a result of their previous experience with consumption of a particular beer type, the research comprised the investigation of the visual elements which arouse a certain cognition of the product. The first step of the analysis of consumer's behaviour was to find the reason why individuals prefer one beer or the service of another beer producer (Pindyck & Rubinfeld, 2005). The goal of the research was to establish which label design and which print design cause the most positive reactions among potential customers. Besides, it was important to determine which elements on the label attract the most attention and their impact on the decision to select and buy the particular product.

4. RESULTS AND DISCUSSION

The data on the age of the respondents were not previously known, nor was the targeting of a particular age group taken into account. The survey was conducted on adult persons, i.e. persons older than 18 years of age. When selecting the respondents, it was considered that the total sample covers all age groups alike, and the respondents were selected according to an intuitive visual assessment. Figure 1 shows the proportion of individual age groups of respondents according to predefined classes.

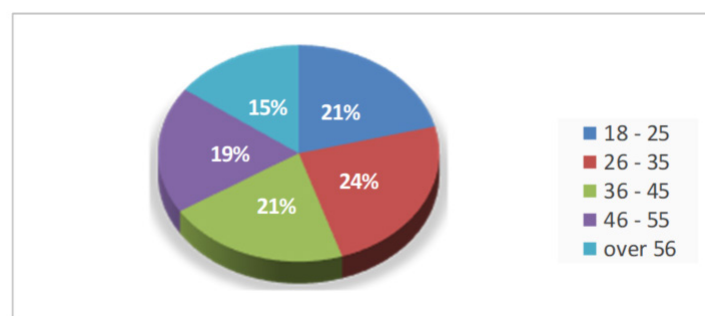


Figure 1: Ratio of respondents in the survey according to age groups

The data on the education of respondents are important for the presentation of the characteristics of the sample of the individuals surveyed. Figure 2 shows the educational profile of sample of respondents. As can be seen from the diagram below, the highest percentage comprises high-school graduates (60%). The percentage of undergraduates is twice lower (29%) and there are also primary school graduates (2%).

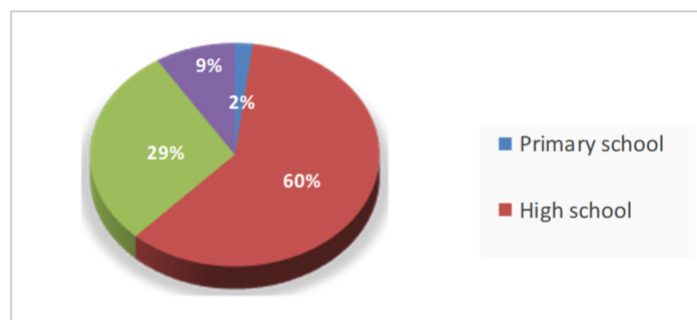


Figure 2: Ratio of respondents according to their degree of education

The question "Do you drink beer?" was replied as 'Yes' by 74% respondents. According to the gender, it was found that men consume more beer than women. A total of 82% of men claimed to consume beer while this percentage among women was 66% (Figure 3). This issue involves drinking beer, which does not have to be frequent, but is a general guideline for buying beer, as well as being in contact with a beer label. So this survey confirms that beer is a widely consumed product. The appearance of a packaging for consumer goods needs to be taken into consideration upon designing and manufacturing, because the decision to purchase such products depends on the first few seconds of seeing the product.

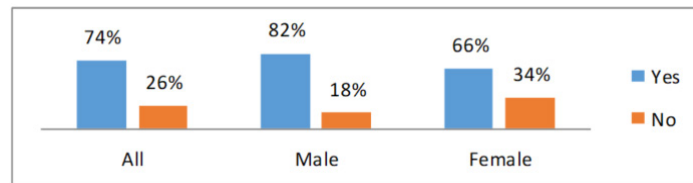


Figure 3: Ratio of respondents who consume beer

The preference to a particular brand among consumers was determined in the survey by the question "Do you always buy beer produced by the same manufacturer?". Every manufacturer's goal is to keep the customers of their products, investing considerable effort during the whole beer production process. The product itself is the most important for retaining customers, but it must be recognizable. It is the beer label that identifies a particular product and makes it recognizable. Due to the preference of the product on the store shelf, a particular consumer group seeks the label of its favourite beer, not paying particular attention to the label of other beer producers. However, a group of people experimenting with the consumption of different beers from different manufacturers is the main target group which may be affected by the appearance of the product and its advertising. People who do not always buy the same beer are prone to buying beer with a new label or even a new type of beer. The complexity of this area of research is the fact that it comprises two opposite concepts of the brand. There are people who are inclined to buy only their favourite brand, and people to whom it is not important who the manufacturer is. The research results have shown that most people (58%) buy beer by the same manufacturer. The tendency to buy the same beer is specifically present among men (74%), while women often buy various kinds of beer (42%).

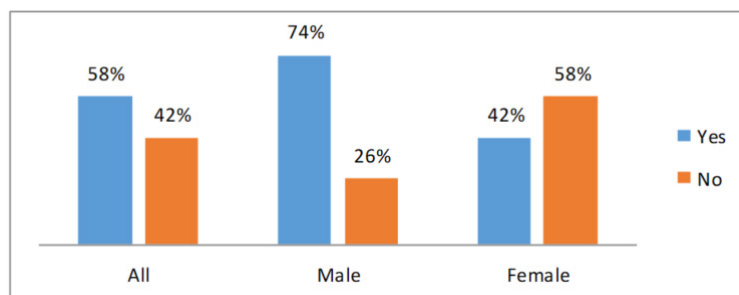


Figure 4: Respondents' ratio in tendency to buy a certain beer brand

When choosing which beer to buy, buyers have different criteria crucial upon selecting a particular beer. The taste of beer plays the most important role to a particular group of consumers when buying beer, while the appearance and the function of packaging are regarded as the less important beer selection criterion. Price represents the relationship between supply and demand of goods conditioned by the product brand. Price is a factor that significantly affects the selection and purchase of beer. Buyers are often willing to buy a cheaper product, ignoring the taste and quality of beer. The appearance and functionality of packaging also significantly influence the decision to buy beer. The design of packaging is especially important to buyers who do not consume beer, but only buy it for other person's consumption. Innovations regarding beer as a product and its packaging influence the buying decision because buyers like to experiment with products they often use, so they are often ready to buy a beer with a new taste or in a new and different packaging. The results of the research (Figure 5) show that beer taste is the most important criterion for beer selection and buying (31%), but price (28%) and packaging (27%) also play an important role, while product innovation is the least important criterion. The taste of beer is especially important for men while women pay more attention to the price of the product.

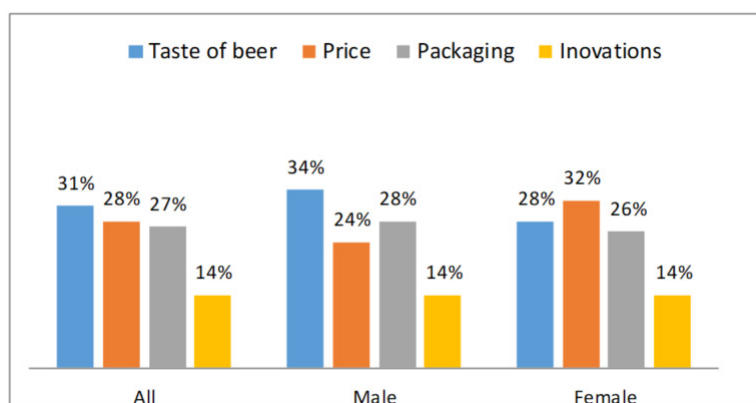


Figure 5: Impact of taste, price, packaging and innovativeness on beer selection

The reason why a customer buys a particular product, not the one produced by competition, represents a very important information for every manufacturer. It is in the interest of any manufacturer to know what is important in view of their beer packaging and label and what exactly attracts the buyer and makes him/her buy the beer if the content of the packaging is left out. Brand is a quality that buyers notice and is based on the experience they associate with the product. The goal of each manufacturer is to create a brand because the recognition of the product is sometimes a sufficient reason to purchase. Brand is a marketing phenomenon that sometimes creates the whole corporate culture based on a product or name. Therefore, a buyer who buys a particular brand feels as a part of the community which consumes that same beer. There is a very strong link between the manufacturer and the customer and it requires a lot of time and experience to create it. The design of the packaging and the label also make a very important effect on the purchase decision. The customer wants to experience pleasure, as it is the case with all other stuff he/she owns. An attractive appearance plays an important role upon purchase decision due to the fact that individuals make visual perceptions of the product. The functionality of the packaging itself can also have a major impact on the purchase, whereas to some people neither the brand nor the appearance is important, but the way in which the product is opened and consumed. The research results (Figure 6) have shown that the brand (43%) is more important than functionality (24%) and packaging design (33%), especially to men (46%), whereas women consider packaging design equally important (brand – 40%; packaging design – 40%).

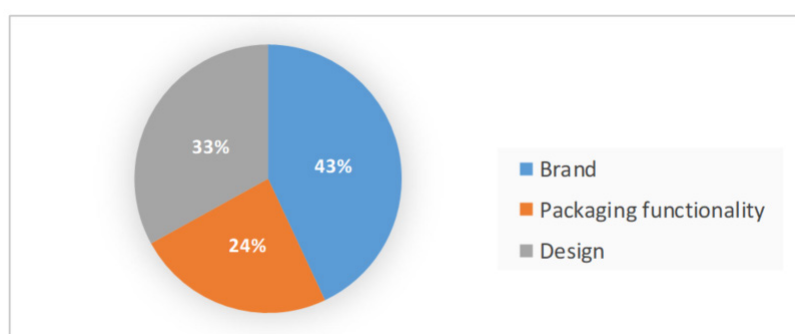


Figure 6: Impact of brand, functionality and design of packaging on beer selection

The question in the survey 'To what extent can the label design affect your purchase decision?' should investigate the customer's sensitivity to visual information on the label. The informations are created and designed to represent the product. Their composition, colours and position on the packaging should cause a positive visual reaction of the buyer. The impact of the layout of the label is not questionable. However, it is important to determine to what extent it affects a purchase decision. The awareness on the impact is an important factor upon creation of new elements on the label. The manufacturer is thus able to know the ratio of the people who will be interested in the new label or who will recognize the importance of a good design of the existing label and the existence of the label in general.

The research results (Figure 7) have confirmed the effect of the label design on the purchase decision. Most respondents are aware of the effect of the label design (it affects sometimes – 39%; it affects always – 45%). However, the label design makes an impact on the choice of beer only to 9% of respondents. The effect of the label design is higher among female respondents (54%) than among male respondents (46%).

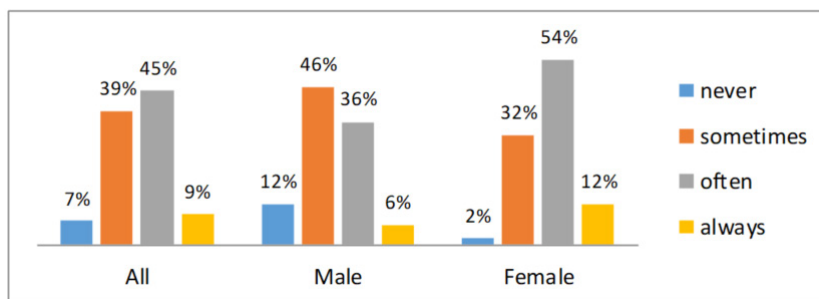


Figure 7: Effect of label design on beer purchase decision

The questions presented below refer to the concrete beer samples: Pan Lager, Pan Zlatni, Carlsberg, Osječko, Karlovačko and Stella Artois. The photographs of beer samples on the shelf were presented to respondents during the survey (Figure 8).



Figure 8: Beer samples compared in the survey

The question "Which of the labels most attracts your attention?" should determine the performance of a particular label to attract customer attention at a certain time. In direct sales of the product where the customer comes into direct contact with the product, it is extremely important for the customer to notice the product as soon as possible. In order to gain attention, the first few seconds are crucial when several different products of the same type are placed in front of the customer. The goal of every manufacturer is that their product is the first to be seen. The appearance of beer labelling plays a leading role in attracting attention, because the packaging of all beers packed in glass bottles is very similar. The bottle is designed so that the buyer notices its content, i.e. beer but not the kind of beer and the manufacturer. The label identifies the brand, and its appearance is a key indicator of beer type.

The results of the research (Figure 9) show that beer labels Stella Artois, Osječko, Pan Zlatni and Karlovačko are almost equally observed, while beer labels Carlsberg and Pan Lager draw less attention compared to the above stated labels. The labels that are most noticeable in the survey attract attention by the combination of easily visible colours such as red and shiny surfaces in gold, as well as the contrast between them and are placed in the centre of the packaging. The results show that the Carlsberg beer is the lowest positioned, so it can be concluded that the reason for this is the expectation of the observer that the label is placed in the middle of the bottle at the most visible location, which is not the case with this packaging sample.

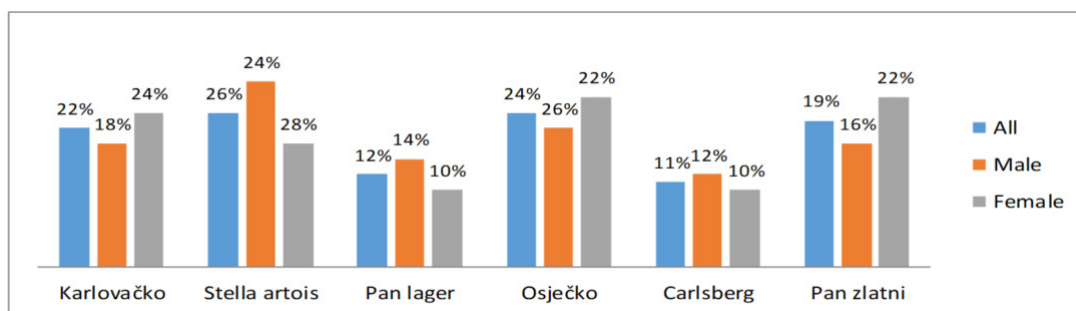


Figure 9: Ability of specific labels to attract customer's attention

The combination of colours on the beer label enables the perception of design elements. The selection of colours on the label describes the character of the product, i.e. the type of beer. Colour psychology has a great influence on marketing and customers are often unaware of these facts. It has been shown that colours arouse different moods and associations in humans, and that the human brain subconsciously associates certain experiences with colours. It has been determined that beer labels are dominated by white, green, red, gold, silver and black. Based on the knowledge of colour psychology, it could be concluded that these colours are intended to achieve the recognition of natural and high quality products. However, label designers use different shades to show the colour that is most similar to the colour of beer, as there are less and more bitter beers of various volumes of alcohol and different basic ingredients. The question "Which colour label best suits your expectations of beer?" should determine the success of the manufacturers in this field. Only respondents who claimed to consume beer were participated in this part of the survey in order to get better results, since people who do not consume beer have no expectations of the taste of the product. The results of the research (Figure 10) show that the combination of colours on the beer labels of Karlovačko, Osječko and Pan Zlatni best present the beer taste.

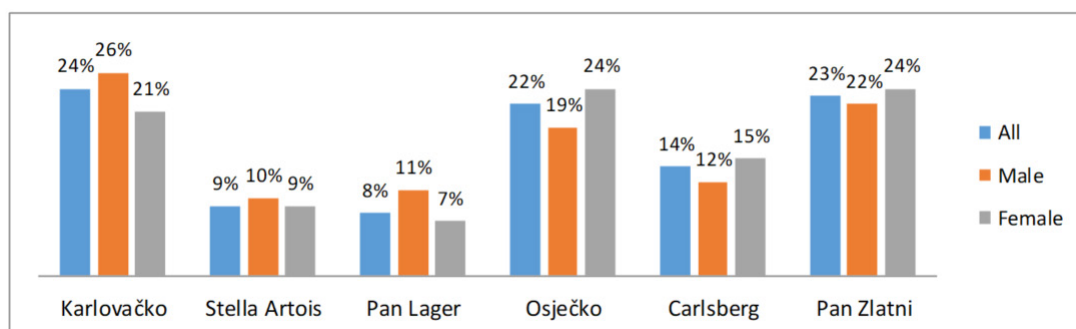


Figure 10: Perception of beer taste in view of colour combinations on the label

The elements on almost every beer label are the name of beer, information on the type of beer, an illustration that more closely describes the character of the beer or the producer and the background that contains the elements mentioned. All of the above elements are very important for the success of product presentation and successful sales. The name of the beer identifies the brand, the information on its content is necessary for the purchase decision because it tells what kind of product is contained in the packaging, while the illustration keeps the attention. The background or background texture used to form the background serves to attract the attention of the customer. The question "Which of the graphic elements have you first noticed?" should determine how much the particular elements of the label format and their size are associated with making beer selection decisions.

The results of the research (Figure 11) show that the name of the beer is first perceived. The name of the beer is located at the most visible place of the label in all beer samples and is considerably higher with respect to other typographic contents. It is highlighted by contrasting paint with the backing. The second place takes up the background colour or texture that dominates the label (31%).

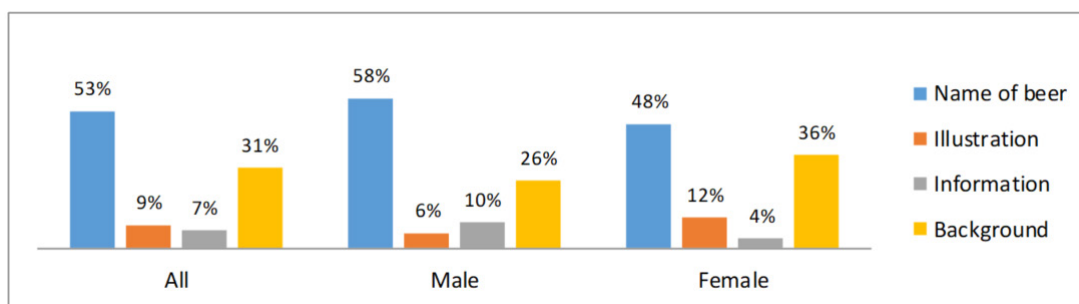


Figure 11: Effect of specific graphic elements on the label on beer selection

Production of a label consists of a series of related production processes. In order to create a graphic product of high quality which should present and promote the sales of the specific beer the co-operation of various market research experts, graphic designers and print technology professionals is required. When making a label, the goal is to get the best quality label at a lower price. However, although a label is relatively inexpensive, the editions are so large that any shift in the quality of the material used results in increased costs of a client. Despite the fact that beer is almost consumed by all the people and that sales are not questionable, significant resources are invested in the quality of the print and appearance of the label itself. The reason is a psychological experience with customers when they see something of a good quality.

Metalized paper used in the production of labels is applied because it has been proved that customers prefer shiny prints since the labels on plain paper do not point to high quality. Therefore, almost all manufacturers have introduced metallized papers into the process of producing their labels. Due to the effort invested in the quality of the label, the goal is that potential customers who do not necessarily have knowledge on printing and its capabilities recognize this quality. The survey investigated the success of comparable beer brands in recognizing and understanding the quality of label prints by consumers.

The quality of labels as graphic products in terms of print quality (Figure 12) was perceived by the respondents in all the samples with slight deviations. This information confirms that the beer label is a quality graphic product. High quality beer label printing is required for reasons of competitiveness with other manufacturers, as a proof of the quality of the brand and the durability of the label regarding mechanical influences when storing and handling.

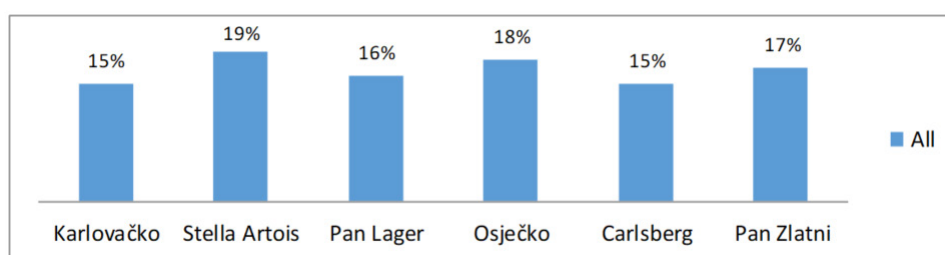


Figure 12: Perception of label quality in view of print quality

5. CONCLUSIONS

Based on the results of the research and the analysis of the results, conclusions are drawn on the influence and preference of the brand, the influence of the elements that are crucial to the decision to purchase and the productivity of some graphic elements on the label format. If the purchasing power with regard to the degree of education is not considered, it should be based on the fact that beer is a "popular" drink which everyone buys without being conditioned by a great purchasing power. Therefore, the appearance of the label must attract as many different target groups as possible.

Of all the participants who participated in the survey, 58% claimed they always bought beer from the same producer. These data indicate a rather great tendency to the purchase a particular brand. Men are more inclined to buy their favourite beer since research results show that as many as 74% of men always buy beer from the same producer. In female population this figure is considerably lower - 42%. The reason may lie in the fact that women consume less beer and show a tendency to seek new flavours.

In view of beer packaging, the brand is together with its appearance the most important factor affecting the buying decision. Men (46%), in higher proportion to women (40%), stress the brand as the most important factor. The name of the beer on the label is besides its colour the main representative of the brand and the beer producer. As many as 53% of respondents said the name of beer was the part of the label they first noticed. This information points to the significance of the brand as the most important factor in the entire brewing industry. The above stated data point to the conclusion that beer is a product which is primarily sold on the basis of a preference for a particular brand. Manufacturers recognize the importance of highlighting their brands, so beer labels are made in line with total visual identity for faster recognition.

The label has a significant impact on the sale of products, which is confirmed by the large share of respondents (45%) who responded in the survey that they are aware that the appearance of the label often affects beer selection. Apart from the content information on the product, the label significantly influences the sale by its design and aesthetic attractiveness. Women are especially prone to a visual impression. An attractive packaging is the most important reason for buying beer among as much as 42% of women who put it in the first place ahead of the brand's importance (40%) or packaging functionality (18%). Print quality can also affect sales of products because people want quality products. People think that quality prints are associated with a quality product and are therefore willing to buy a product that is in a more attractive and high quality packaging.

A good layout of the elements on the surface of the label, their size and contrast result in fast perception of the entire label. The research has shown that larger labels with stronger colour contrast and larger typographic elements are instantly noticed. The contrast between typography and background is conditioned by good readability, which results in the perception speed. Manufacturers recognize the importance of highlighting their name, and therefore this element is placed in the most visible place of the label. The name of the beer is so important that it stands out in several places on the entire packaging, for example, some labels on the bottleneck contain only a logo, and it is also highlighted on the back labels if the packaging contains them.

In comparison to the information recorded by typography, more important are regarded the information on the type of beer, origin and volume of alcohol, which can in some cases be found on the front label.

The illustrations are placed close to the logo and are primarily used to keep the viewer's attention on the label. They are usually painted in red, which is known as the colour that attracts one's attention. The illustrations show the character of beer or some drawings related to the brewery tradition. The background lines, textures, and coloured surfaces round off the look of the label and emphasize the information that the label contains. They are designed in accordance with the shape of the label, and their colour is aligned with other elements that are the carriers of information. Beer labels do not usually contain much colour, but are simple and easy to read.

Beer labels are high quality graphic products for the purpose of presenting and selling beers, as well as most of the printed packaging products. The quality of these products is conditioned by customer requirements whose goals are to get the most quality product at a lower price. Since customer satisfaction is the ultimate goal and the main bearer of the long-standing success of every brewery, advertising materials such as the label requires a lot of time and large investments into material resources to help customers recognize their quality and dedication.

6. REFERENCES

- [1] Ellis, M.: "How to design a beer label: the ultimate guide for craft brewers", 99designs, URL: <https://99designs.com/blog/packaging-label/beer-label-design/> (last request: 2018-07-23)
- [2] Grbac, B., Meler, M.: "Realizacija poslovne ideje – Od ideje do proizvoda/usluga", (ZT Zagraf, Zagreb, 2007).
- [3] Jurečić, D.: "Evaluacija elemenata vizualne informacije na grafičkoj opremi ambalaže", Magistarski rad, Sveučilište u Zagrebu, 2004.
- [4] Kesić, T.: "Ponašanje potrošača, II. izmijenjeno I dopunjeno izdanje", (Opinio d.o.o., Zagreb, 2006).
- [5] Mencer, I.: "Politika marketing miksa", (Rijeka, 2011).
- [6] Narodne-novine, Ministarstvo zaštite okoliša, prostornog uređenja i graditeljstva: "Pravilnik o ambalaži i ambalažnom otpadu", Narodne novine broj 97/05 i 115/05, URL https://narodne-novine.nn.hr/clanci/sluzbeni/2005_08_97_1894.html (last request: 2018-08-18)
- [7] Pindyck, S.R., Rubinfeld, L.D.: "Mikroekonomija", 5, (Mate, Zagreb, 2005).

- [8] Print magazin, Etikete i etiketiranje, Print-magazin,
URL: <https://www.print-magazin.eu/etikete-i-etiketiranje/> (last request: 2018-09-19)
- [9] Rujnić-Sokele, M.: "Plastična ambalaža – najbolji izbor za okoliš", Polimeri, 32(2), 92-94, 2018.
- [10] Solomon, M. R., Bamossy, G., Askegaard, S.: "Consumer Behaviour: A European Perspective", 3rd ed, (Prentice Hall, London, 2006).
- [11] Stipanelov - Vrandečić, N.: "Ambalaža", (Kemijsko-tehnološki fakultet, Split, 2010).



© 2018 Authors. Published by the University of Novi Sad, Faculty of Technical Sciences, Department of Graphic Engineering and Design. This article is an open access article distributed under the terms and conditions of the Creative Commons Attribution license 3.0 Serbia (<http://creativecommons.org/licenses/by/3.0/rs/>).

GEOMETRIC STYLE IN DESIGN OF URBAN LANDSCAPES

Milena Lakićević , Danka Kordić 

University of Novi Sad, Faculty of Agriculture, Department of Fruit Science, Viticulture,
Horticulture and Landscape Architecture, Novi Sad, Serbia

Abstract: *Designing landscapes in geometric style has a long history. Even open spaces in ancient Egypt, dating around 3000 BC, were shaped in a clear geometric form. Later throughout the history, geometric patterns evolved and the most impressive achievements in landscape architecture were reached in France during the period of baroque. Geometric patterns are also steady in Moorish and Islamic gardens and landscapes. Contemporary landscape designs rely on the heritage of previous epochs, but it is suited and adapted to the local environment and conditions. Geometric style is considered as formal or classical one and can be found in urban landscapes and parks worldwide. In this paper, we focused on an example from Serbia; we analyzed the design features of the main city park in town of Ruma, Serbia and proposed a new design concept in a geometric style. The presentation is supported by 2D and 3D graphical representations produced in SketchUp 2017 and Adobe Photoshop CS4. The special attention in the designing process was dedicated to plant material and selection of plants was determined by their visual and aromatic qualities. The new design included the constriction of water mirrors, using the reflection in water to enchase the aesthetic features of landscape elements.*

Key words: geometric style, urban landscapes, landscape architecture, Ruma (Serbia)

1. INTRODUCTION

Urban landscapes can be designed in different manners, and two main styles are: geometric (classical, formal) and natural (informal) one (Vujković et al, 2014). Geometric style has its origins in designing exteriors in ancient Egypt, and has evolved and improved ever since. Natural or informal style is referred to the design that does not recognize a regular or strict geometric pattern and its origins had been developed in Chinese and Japanese gardens. Nowadays, both styles are used equally and, in addition, they can also be combined. Combining geometric and informal style can be done in two ways: one single design can have traits of both styles forming a mixed style or one project can be consisted of two parts designed in geometric style (usually smaller, representative part) and natural style (usually larger backyards), and these zones are being separated by the architectural object.

After having its first outset in ancient Egypt, geometric style continued developing in the medieval period. From that timeframe Moorish and Islamic gardens were especially notable; some elements of their design are being incorporated in what we now consider a classic style. The most important elements conveyed from Moorish gardens are using plant material with intense color and scent properties (Kluckert, 2007). During the period of renaissance and mannerism, landscape architecture was blooming in Italy, and their landscape design was recognizable by intense use of topiary forms of trees and shrubs; it should be noted that this horticultural practice was established and known even in ancient Rome, but reached its peak during the period of renaissance. However, geometric style in landscape architecture is usually associated with the French baroque, and the most famous examples of that epoch are Versailles Park and Park of Vaux-le-Vicomte, both designed by André le Nôtre in the 17th century. Parks designed in later periods are simpler and used just some of the baselines established during baroque, such as symmetry and perspective principles (Motloch, 2001).

Landscape architecture nowadays relies on heritage from previous epochs, but at the same time aims to meet local conditions and fulfill contemporary demands. In this paper, we have demonstrated how geometric style can be applied in designing of urban zones on the example of the park in Ruma, Serbia.

2. METHODS

The aim of the paper was to analyze current and propose a new, geometric design for the park in Ruma. For that purpose we used several programs; for the representation of broader spatial context of the park we used R version 3.5.1 and QGIS version 2.18 (Figure 1), while the designing process was supported by SketchUp 2017 and Adobe Photoshop CS4 (Figures 2-4).

2.1 Description of the case study area

Town of Ruma is located in the north-west part of Serbia (Figure 1a) and the park situated in the central part of the town (Figure 1b).

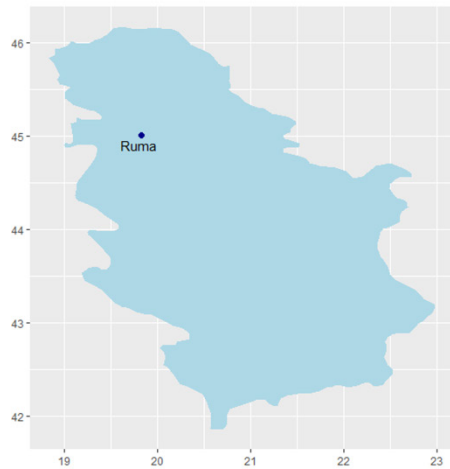


Figure 1a: Location of Ruma, Serbia

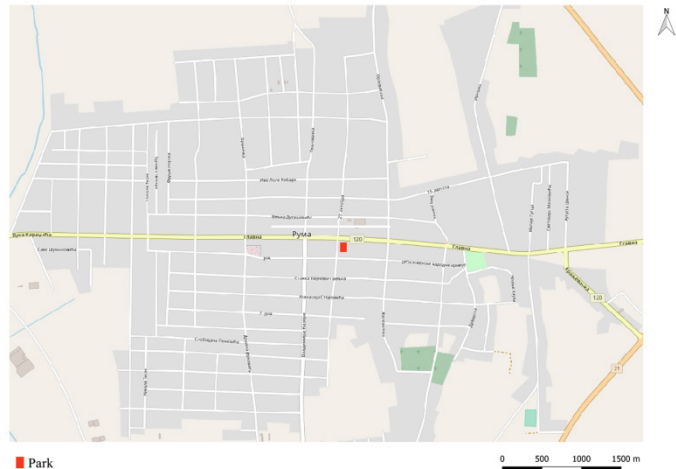


Figure 1b: Location of park in Ruma, Serbia

The park occupies 16.96 a, and due to its dimensions is often referred to as "small park" by the local inhabitants. The zone is primarily suited for children's play and the current design of the park has some of the geometric style features (Figure 2).



Figure 2: Current design of park in Ruma, Serbia

Next chapter explains one of the ways for introducing geometric style and proposes a new design for the park. One of the guidelines in the design process was to create a zone that would be appealing to larger number of visitors, and therefore promote tourist offer of the town (Tatović et al, 2014; Lakićević et al, 2011).

3. RESULTS

The park has a parallelogram shape, and in order to introduce symmetry principle the area was transacted by vertical and horizontal axis in the first phase of the designing process. This way it was ensured that all park elements will be paired and ordered in accordance to the distance from these two axes. At the intersection of the axes, there is a tree of silver lime (*Tilia tomentosa* Moench.), that is the dominant element in the park. Placing a larger tree or a water element in the central part of park is one of the characteristics of geometric landscape style. This type of disposal of the landscape elements was set in both Moorish and French baroque gardens.

Selection of the plant material was an important part of the designing process and even though we were dealing with the smaller space the idea was to introduce diverse plant material. For the designing process 15 different plant species were selected based on their visual and aromatic qualities (Figure 3). Among them, there is a tree of Serbian spruce (*Picea omorika* (Pančić) Purk) which was selected as an endemic species in Serbia that can be grown in urban areas. Introducing endemic and endangered species when re-designing or reconstructing green areas is important for promoting biodiversity and protecting local floristic elements. In addition, introducing local flora gives an area an authentic feature, namely the area can be easily distinguished and unique by the plants that have been chosen.

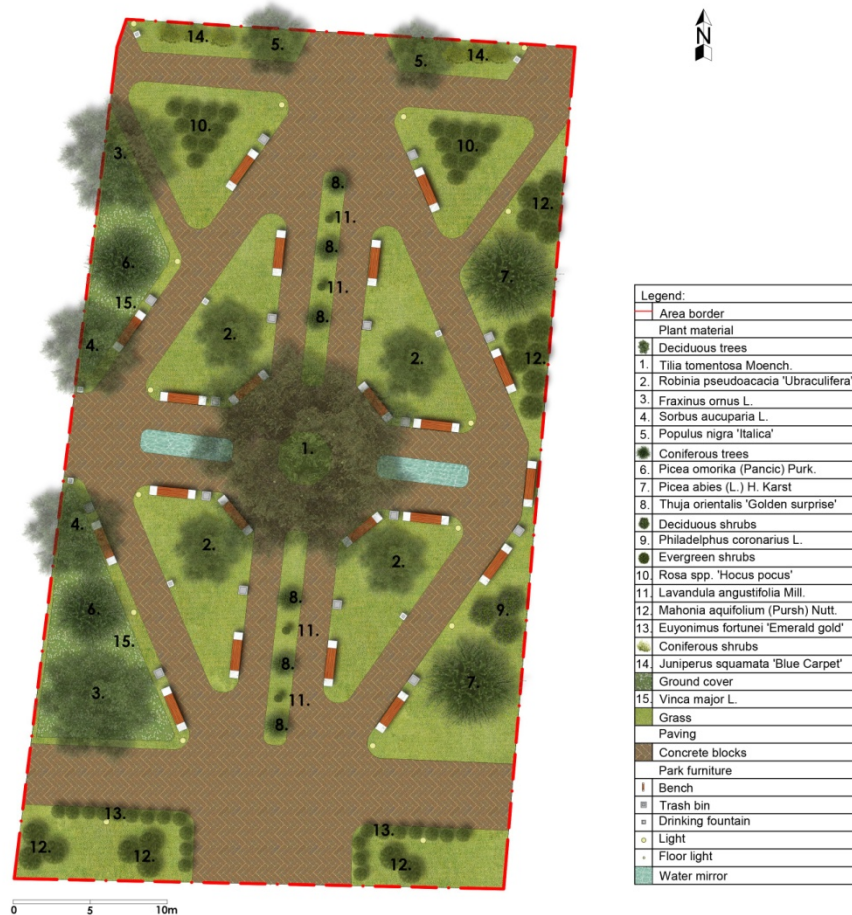


Figure 3: Proposed design of park in Ruma, Serbia

Some of the selected tree species proposed by new design such as, *Thuja orientalis*, *Tilia tomentosa*, *Juniperus squamata*, *Mahonia aquifolium*, etc. can be used for making topiary forms or hedges. Using these plants in the design was descended from Italian renaissance and French baroque gardens and it additionally emphasizes geometry pattern of the place. Besides that, some cultivars were selected based on the shape of tree crown and that is, for example, a form of black locust *Robinia pseudoacacia* 'Umbraculifera' which can be seen in many contemporary landscape architecture objects. Four trees of black locust were placed in the central part of the park on four large grass parterres. For emphasising

shape of trees water mirrors were put on the horizontal axis of the park, in between central lime tree and four triangular grass parterres.

Selection of plants was also determined by their aromatic qualities, and based on this prerequisite some of the plants used in the proposed design are: *Lavandula angustifolia*, *Philadelphus coronarius* and *Rosa* spp. Using aromatic plants is a tradition of Moorish gardens from medieval period, and they have been intensively used in landscaping ever since.

The park is designed for a short stay of visitors and therefore there are benches placed all across the park as well as candelabras and ground lightening.

Parts of the park, not covered by plant material, are paved by concrete boards and serve as pathways throughout the area. The new design is also presented in 3D view in order to get a complete image of the area (Figure 4).



Figure 4: 3D view of proposed design of park in Ruma, Serbia

The above figure depicts height, shape and colour of new design elements and their disposition in the park.

4. DISCUSSION

In the new design proposal, symmetry principle was clearly respected and plant material was carefully selected in order to emphasize a strict geometric pattern of the park structure. Aside from choosing plant material, design process included planning of pathways and they were formed with the idea to make quick and easy communication throughout the area.

Even though some design elements were taken from the previous epochs, the main goal was to create a zone adjusted to contemporary demands and needs. New design is primarily suited for a short rest of local inhabitants.

Software used in this paper proved to be convenient for this type of research; QGIS and R can be applied for a spatial analysis on a broader scale, while SketchUp and Adobe Photoshop can be used for the detailed design process. It should be noted that R can also be used different analysis of plant material that are not used in this research, but are important from environmental point of view (for example analysis of biodiversity indices, etc.) (Lakićević, 2018).

5. CONCLUSIONS

Two main styles in designing urban landscapes are geometric (formal) and natural (informal) one. While formal style follows strict geometric principles, informal one doesn't recognize any geometric patterns. These styles can be also combined in designing parks and other urban green structures.

In this paper, we focused on the geometric style and have shown how its principles can be applied in designing of urban areas, on the case study of the park in Ruma, Serbia. Geometric style follows up some

of norms established in previous epochs in development of landscape architecture. For designing the park in Ruma, we used some of the principles known and used from medieval time until nowadays. From medieval time, the most of the ideas where descended from Moorish landscape architecture and that included the following: using aromatic plant species and placing water mirrors in central part of the place. From French baroque, main elements that were relied on are: symmetry principle and selection of plants that can be used for making topiary forms. Making topiary forms was initially developed in Italy, and can be also seen in Italian renaissance gardens. Disposal of the landscape elements in the park reminds of both medieval Moorish and French baroque gardens. However, it should be noted that all elements were suited for contemporary demands and needs. New designed space should be appropriate for short stays of visitors and should improve tourist offer of the town of Ruma.

6. REFERENCES

- [1] Kluckert, E.: "European garden design: from classical antiquity to the present day", (Tandem Verlag GmbH, Oxford, 2007.), pages 32-39.
- [2] Lakićević, M., Srđević, B.: "Tourism evaluation of Topčiderski park in Belgrade", Zbornik naučnih radova Poljoprivrednog fakulteta 35(1), 127-135, 2011.
- [3] Lakićević, M.: "Environment and sustainable development", (University of Novi Sad - Faculty of Agriculture, Novi Sad, 2018.), pages 13-21 (In Serbian).
- [4] Motloch, J.L.: "Introduction to landscape design", (Willey, Austin TX, 2001.), pages 134-146.
- [5] Tatović, N., Lakićević, M., Matić, V., Rabotic, B.: "Potential of Kalemegdan complex as a tourist attraction of Belgrade", Turističko poslovanje 14, 81-90, 2014. doi: 10.5937/TurPos1414081T.
- [6] Vujković, Lj., Došenović, Lj.: "Garden design", (University of Banja Luka - Faculty of Forestry, Banja Luka, 2014.), page 23 (In Serbian).



© 2018 Authors. Published by the University of Novi Sad, Faculty of Technical Sciences, Department of Graphic Engineering and Design. This article is an open access article distributed under the terms and conditions of the Creative Commons Attribution license 3.0 Serbia (<http://creativecommons.org/licenses/by/3.0/rs/>).

EVOLUTION OF GESTALT PRINCIPLES IN CONTEMPORARY GRAPHIC DESIGN

Jonas Malinauskas

Vilnius College of Technologies and Design, Design faculty, Vilnius, Lithuania

Member of LGDA – Lithuanian Graphic Design Association

Abstract: *From the very beginning of XX century the principles of Gestalt helped humans to simplify and structure their visual surrounding. Despite aesthetic evolutions, it always helped to keep the clarity and readability of visual messages. Alas, development of global digital communications simulated the appearance of many stereotypes, clichés and templates, which has led to a loss of quality and originality, total convergence of visual language.*

Today, when marketing – orientated designers replaces visual artists creating posters and prints, attention and reconsideration of visual information, encoded in their graphics, gets a growing importance. Knowingly made visual errors, inaccuracies can not only attract the attention, but also encourage the viewers to re-think them. On the other side, ingeniously disintegrated parts of the composition or some “visual riddles” provokes the viewer to turn his intelligence on; as a result, the whole of the visual message acquires a much greater value than it’s separate parts.

The mentioned development of digital technologies also offers unlimited image transformation capabilities, and also encourages wider use of dynamic compositions, based on video formats. Quick visible changes or movements (from chaos to structure etc.) helps to attract and keep viewer’s attention.

The study of changes in Gestalt principles most of all concerns prints and poster as a universal genre of graphic design that combines individual artistic expression with adaptive graphic communication. The research of exchanges is based on analysis of examples of printed and digital Gestalt applications.

Key words: Gestalt, rules of gestaltung

„Design is the conscious effort to impose a meaningful order“

Victor Papanek

1. DEFINITION AND SHORT HISTORY OF THE OBJECT

Gestalt (*unified whole* - germ.) — unity of form, image, structure of some physical object or virtual model. Only few terms in the field of print and design have German origin, noting the contributions of scientists of this country in research of this area. Above all, it concerns the studies, made just before the First World War in Frankfurt Psychological Institute by young scientists Wolfgang Köhler, Max Wertheimer, and Kurt Koffka (Figure 1). Their researches were based on the ideas of Max Planck and Carl Stumpf about the link between physics and psychology. The young scientists collaborated on the founding of a new holistic attitude toward psychology called Gestalt theory, aspects of which were grounded on the earlier work of C. Stumpf.



Figure 1: The researches of Gestalt theory

Developing the studies of apparent movement, they came to conclusion of inherent nature of human vision. The essential sentence, describing the Gestalt phenomena, was "The whole is different from the sum of its parts" (Lupton et al, 2015) which due to possible translation mistake, sounds as "the whole is greater than the sum of its parts". Most of specialists, including psychologists and communication theorists, today explain it as to mean that the relationship links (physical and logical) between the parts is itself a significant part and gives an additional value to the whole, which is not present in the other parts if simply summed up. The classical example of this thesis is the parts of the car, which being disassembled and laying on the floor do not mean the car as an object – they need to be assembled in specific sequence and order (Figure 2).

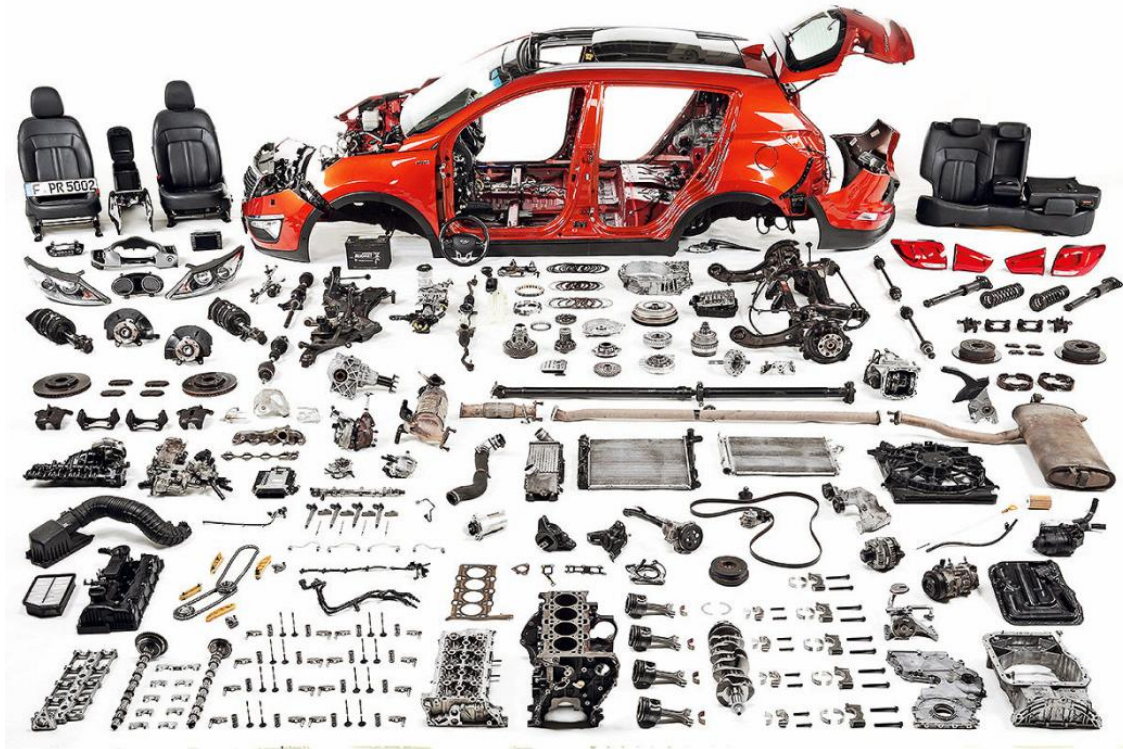


Figure 2: The whole gestalt objects, as an assembled car, have greater value, than the sum of its parts.

Finished gestalts are always integrities, and show overall integrity of human consciousness, which is a complete structure, consisting of members belonging to the whole, more or less distinct from each other. Speaking about psychology, interhuman relations and communication, outside the formed visual or virtual structure there are additional gestalt-qualities with deeper emotional content. Today, examining any kind of art we have to understand a gestalt like as a whole, integrating informational and emotional features of its parts and reaching a new level of expression. Gestalt models are created at the highest level of human consciousness. It is necessary to mention that this phenomena, first described during psychology studies, now is also used in a wide context of interpersonal relations and human behavior. The aim of both Gestalt applications in psychology and visual arts is finding some common features and insertion of structural order in chaotic, noisy atmosphere of human surrounding.

2. "CLASSICAL" METHODS OF GESTALTUNG

The aim of contemporary theory, created on the base of the German scientist's researches is to explain, how complex scenes can be reduced to more simple shapes. It also explains the ways, which people *unconsciously* use to connect and link design elements. There are 6 acknowledged basic principles of visual perception (Figure 3).

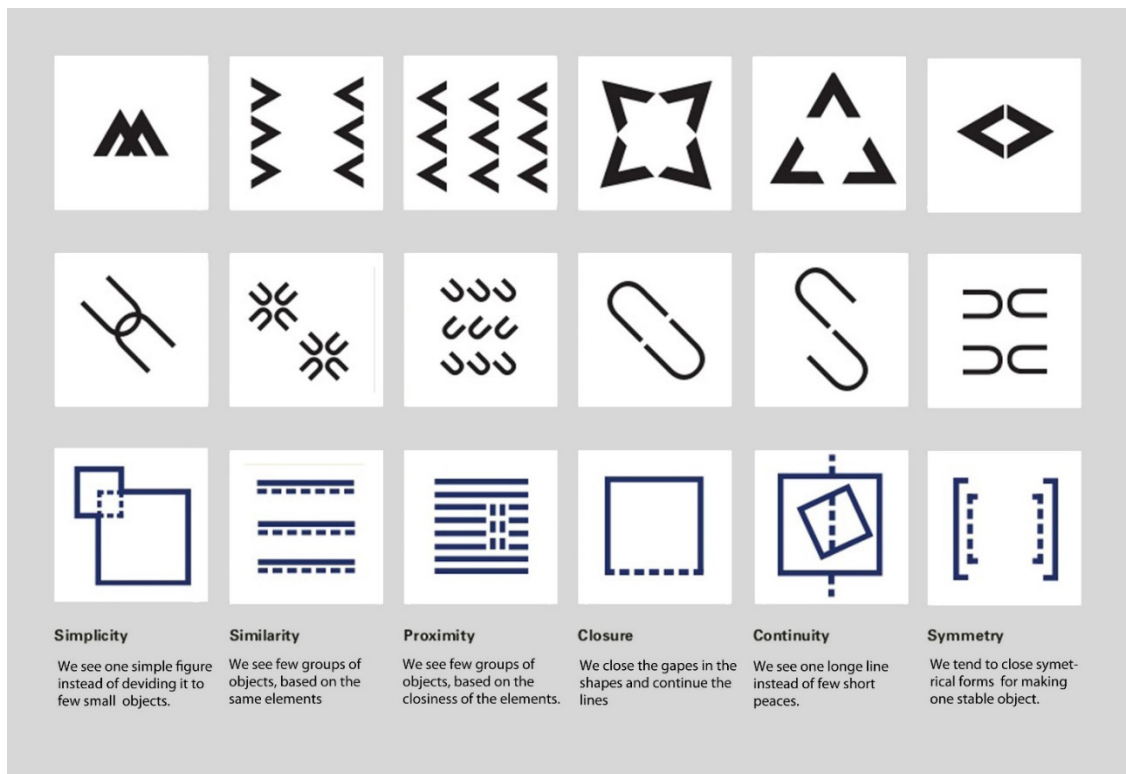


Figure 3: The basic principles of visual perception.

- **Figure/Ground** (or Simplicity): The human eye tries to isolate shapes from backgrounds and to describe the figures as simple and integrated as possible.
- **Similarity**. The human eye tends to build a relationship between similar elements within a design, building some kind of structure. Similarity can be achieved concentrating attention to basic composition elements such as shapes, colors, and size.
- **Proximity**: Simple shapes arranged together can create a more complex image
- **Closure**: We prefer to see complete shapes, which are easy to understand. If the visual elements are not complete, we can perceive a complete shape by unconscious using of imagination and filling in missing visual information (Figure 4)
- **Continuity**: The human eye follows the paths and lines of a design, and prefers to see a continuous flow of visual elements rather than separated objects. The effectiveness of this method depends on intermediate brakes or additional graphic elements.
- **Symmetry and balance**: The design should be balanced and complete; otherwise, the user will spend time and effort trying to perceive an overall picture.

Since the formulation of the "classic" gestalt principles, few decades passed by, and the amount of visual information, received every day has increased many times. Today, the methods of image recognition processes help to understand how a human mind transforms a huge stream of visual information into a meaningful and integrated image of the surrounding world. They also help to optimize ways of processing information, effectively exploiting the possibilities of human senses and consciousness.

On the other hand, information flow-makers are very interested in targeting and memorizing their messages, and therefore deliberately go beyond the established limits of information perception rules in order to attract users' attention and make them notice the incoming information.



Figure 4: *Uncomplete model of cube demands some spatial imagination*

3. CORRECTIONS AND TRANSFORMATIONS

Realizing the potential for applying Gestalt thinking helps artists and designers create really eye-catching works. They've got new insights and ways of approaching problems and challenges, which cause radical changes in the graphic design.

As a rule, new tendencies appear in the form of individual phenomena or singular artistic works. However, if fashion motifs or social movements stand for them, they soon turn into new means of expression in graphic design. Sometimes they get traits of uncomplicated gestalt, causing "visual irritation". Among the innovations related to changes in gestalt methods, the following factors could be noted:

- **Reverse of figure/ground contrast.** Sometimes the figure or some intensive eye-catching elements become a frame or a background for flat inactive foreground. This reverse usually is dedicated to create some visual misunderstanding or to convey secondary meaning (Figures 5 and 6)
- **Color similarity, destroying text structure.** Color can unify the pieces of printed or written text, displayed in unusual way or having large gaps, so being almost unreadable. If reader spend more time reading the text – he'll better understand and remember it in spite of poor readability. The play of the colors also brings some decorative effect (Figures 7 and 8)
- **Proximity of symbolic figures.** The small figures, forming one large gestalt object or brand logo, can have some narrative or symbolic meaning, communicating brand value and enriching the content (Figure 9)
- **Simplicity and symbolic meaning.** The simple shapes, containing symbolic meaning, have their roots in visual communication and religious iconography. The visual quests always attracts watcher's attention. (Figure 10)



Figure 5: Making background from foreground.
Des. FWIS

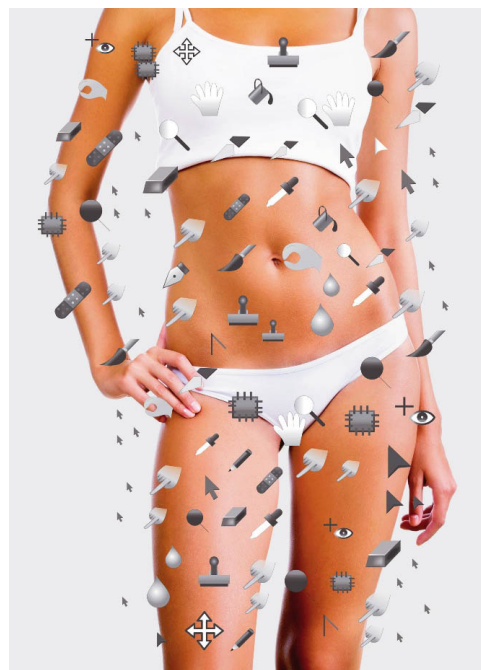


Figure 6: The human body as a background for
secondary elements. Des. Shiva Nallaperumal, MFA
(USA)



Figure 7: Art exhibition poster, des. Felix Wetzell
(Germany)



Figure 8: Book fair poster, des. Laura and Indre Klimaitė
(Lithuania)



5. CONCLUSIONS

- The principles of gestalt still are the basic principles of visual perception, helping the consumers to avoid visual overflow and to form an integrated vision of surrounding world.
- These principles, connected to psychology of perception, used to be flexibly adopted to contemporary aesthetic context.
- Transferring the principles of gestalt to the field of interpersonal relations can cause psychological problems and negative feelings in case of unfinished process.

6. REFERENCES

- [1] Kohler, W.: "The Task of Gestalt Psychology", (Princeton Legacy Library, New Jersey, 2015.)
- [2] Lupton, E., Philips, J.C.: "Graphic design. The New Basics", 2nd ed., (Princeton Architectural Press, New York, 2015.)



© 2018 Authors. Published by the University of Novi Sad, Faculty of Technical Sciences, Department of Graphic Engineering and Design. This article is an open access article distributed under the terms and conditions of the Creative Commons Attribution license 3.0 Serbia (<http://creativecommons.org/licenses/by/3.0/rs/>).

INTEGRATION OF THE VISUAL ELEMENTS OF ART AND PERSONALITY FACTORS IN PROCESS OF CHARACTER DESIGN

Nada Miketić , Ivan Pinčjer , Ana Lilić 

University of Novi Sad, Faculty of Technical Sciences,
Department of Graphic Engineering and Design, Novi Sad, Serbia

Abstract: Video game design is an extensive field of study and complex creation process which synthesizes various scientific areas such as information technologies, art and design, psychology, and other social sciences. During the time, character design evolved into a separate field of study. Character design process is constantly in front of new challenges, due to the changes in the digital era, and a considerable quantity of information that people are exposed to. The most attention is put on the visual appearance of the character during the creation process. There is a large number of influential factors on the visual representation of the character, some of them are: game genre, the target audience, platform. However, in the design stage, excellent knowledge of the visual elements of the art is required because they have the most influence on the visual representation of the character. Analogous to the real world and the real human characters, virtual characters have "personality" as well. In order to accent the specificity of the character, not only the art elements have to be considered, but personality characteristics. The paper will provide an overview of the elements of art and personality factors such as archetype, facial expression, view, body posture. The purpose of this paper is to emphasize the mutual connection of the art elements and personality factors and their final influence on the unique appearance of the character.

Key words: character design, the elements of art, virtual characters

1. INTRODUCTION

Character design for video games and movies have always been the most challenging process for creative industry workers. This paper explains design elements for "good" character visual and background knowledge that is essential for the creation of an iconic character. In the search for a deeper explanation of the character design process, the process itself will be analysed from two different aspects. The first is related to the creative process of thinking in which character is conceived. This aspect comprehends a psychological approach to the character, which involves the term archetype that has an important role in the process of creating a new character. The second aspect concerns the importance of basic elements of art, their practical use, and symbolism behind.

2. "BIRTH" OF THE CHARACTER

The first step in the process of character creation is doubtless the idea. Thus there is an idea for the particular character design, therefore a preliminary idea about the character nature. This initial idea about the character can be related to either their personality traits, their background story or both. The character is always in the service of the story (Tillman, 2011a). The basic principles of the character design are grounded in profound knowledge of archetypes. Thanks to archetypes people can recognize patterns that assemble personality and character traits, at first encounter with a particular character. Regardless the used medium – storytelling, more, television or video games – character design is based on the use of the universal categories which observer remember and based on these categories observer can easily identify new characters. According to this, the character design process, the use of archetypes as a guideline can enable the precise visual appearance of the character.

3. ARCHETYPES

There is a variety of archetypes that are established by Swiss psychologist and psychoanalytic Carl Gustav Jung. However, there will be analysed only relevant ones for this paper – ones that apply the storytelling and entertainment industry. Archetypes mentioned above are: *hero*, *shadow (villain)*, *fool*, *anima/animus*, *mentor*, and *trickster*.

Follows are presented these archetypes and their substantial traits, the ones that observer can immediately notice in the first encounter with the particular archetype. This also can serve as a directive during the character design process – the goal is to identify traits which are the most expressed at particular archetype, characteristics that are universally perceived as the same. If it is required to illustrate character which represents a hero then will be useful to become known with heroes structural elements. The archetype of the hero is defined throughout the following traits: very brave, unselfish and eager to help regardless of the consequences.

- The archetype of the villain, according to Jung, is defined as a shadow. The shadow character is closely related to animal instincts. He or she is described as ruthless, mysterious, unkind, unpleasant and evil.
- The archetype of the fool is present in the story in order to test the main character. The fool is optimistic, innocent and full of luck. The character that is represented as a fool makes unpredictable situations and in that way complicates relationships and make the story more interesting.
- Archetype animus is the female fellow, partner to the male character, whereas animus represents a male partner to the female character. This character has a role to please female and male drives and provides interest and possibility for the love in the story.
- The archetype of the mentor, which is present more in the movies than in video games (mentor in video games is commonly used to walkthrough player through tutorials). Mentor represents intellect and stability for the protagonist, wisdom, and support. He is wise and owns an enormous quantity of knowledge and has a mission to lead hero on his way heading to great doings. A mentor is often illustrated as an older male or female, because of the connection between old age and wisdom.
- The last archetype is the trickster. Trickster can be bowed both evil and good side of the story. Regardless of the supported side, trickster tends to turn the story for their own benefit.

Knowing the specific traits of the particular archetype is not enough for good design of the character. There is also required the knowledge of the basic elements of art and the way of using them in order to describe character traits of the specific archetype (Tillman, 2011b).

4. THE VISUAL APPEARANCE OF THE CHARACTER

4.1 The facial expression

The face is one of the most important channels of communication among humans. Facial expressions can reveal emotions which character is feeling, face reveals the identity of the character and across the face, the character can be "read". Accordingly, the face is the inevitable part which has to be analysed and paid special attention to it during the process of the character design.

In the communication process, the character can raise or lower brows, to frown, shrink or spread eyes and mouth. Although movement of the face can express particular emotions and define character, movement of the face can also emphasize the importance of the conversation or spoken words. For instance, raised brows to highlight an importance of something or can be understood as a sign to pay attention to something. Knowing various facial expressions and what they mean is necessary in order to present identity of the character that is essential for identification with the character. Since it is a large number of facial expressions, it is virtually impossible to distinguish all their meanings. During the design process of an animated character commonly used facial expressions and emotions which are the same as the majority of people and can be recognized easily (Isbister, 2006a). There are four basic emotions (Figure 1):

- anger,
- fear,
- happiness and
- sadness.

Since these emotions are common for all, they can be easily illustrated, because each of enlisted emotion is expressed the same to by all characters. It is certain that there is a "recipe" for illustration of basic emotions because they are usually expressed in the same way by the majority of the characters.

It is required that the facial expressions and emotions of the fictional character be as much as possible realistically presented – whether the character is very stylised or character very detailed and realistic –

because the aim of animated movie and video game is that the person consumes content as much as possible and to identify themselves with the character, a to induce emotional reaction to person (Isbister, 2006b).



Figure 1: Four basic emotions (Isbister, 2006)

4.2. The look

An inevitable part of the appearance of the character is the look. Similarly, with the face, the look has also a great indicator of the personality traits of the character and their emotions. The look can imply what character is interested in (if looking around environment), in that way person who is in the interaction with the character is paying attention to the same thing as the virtual character, regardless it is movie or video game character. Furthermore, the look can indicate whether the character is interesting or not. Importance of the look and eyes in the character design process can easily be conveyed with eye colour of additional effects for instance presence of magic in the eyes in form of smoke or fire (Isbister, 2006c).

4.3 Posture and shape of the body

As mentioned earlier, the same idea applies to the posture and shape of the body when identifying the character. Posture, the position of the body and movement (for animated characters), convey large quantity of the information related to characters personality, emotions and overall personality traits. For example, if it is required to design the hero character, it is common that construction of the body of the hero is muscular, athlete posture, nice - looking overall appearance and harmonious proportions of the body. There is no coincidence in the design of the heroes' body. Enlisted common characteristic of the appearance of the hero have to describe their ability for instance strength, fast movements can fight an opponent and easily overcome physical obstacles. On the other hand, villains can also be muscular, but their constitution of the body is different than heroes. Villains usually have a less harmonic body or less regular proportions than the hero character. They are often presented as extremely skinny or fat or muscular. Also, generally known common body positions which reveal the certain emotional state of the character and attention are: lowered shoulders (for the sad or disappointed character), spread hands and legs with slightly bended knees usually represent combat posture and attention to attacking. Knowing body language and position that character takes in particular situations, is essential for good character design (Isbister, 2006c).

5. IMPORTANCE OF THE BASIC ELEMENTS OF ART IN THE PROCESS OF CHARACTER DESIGN

Basic elements of art are in service of clear presentation the most characteristic traits of the particular character. They emphasize the archetype of the character. Basic elements of art can be described as the mirror of the personality traits of the character.

5.1 Line

The line is the simplest basic element of the art. Not only is it used to define the shape of the character, but also leads observers eye. It makes connections between shapes and communicates the direction of the body lines and movement. The first and most noticeable use of the line in the character design is outlined which defines the shape of the character. Regardless of the visual style in which character is presented, characteristic of the lines which enable visual representation of the character traits are line thickness, orientation, position and type (solid or dashed). Further, in the text, there is an explanation of each characteristic of the line and how they affect the visual appearance of the character.

- Line thickness – in essence, the line does not have thickness. It is a one – dimensional object. However, for the people to easily conceive lines, there has to be thickness. Different line thickness is differently perceived by the people. For instance, the thin line has loos effect, it is barely noticeable and soft. Whereas thick lines convey a completely opposite impression. When designing a character, if creating an honest, pure and serious character, the use of thin lines would be an appropriate choice. Opposite of that, when using thick lines the character appearance will be perceived as rough, heavy, strong and solid.
- Line orientation – this characteristic has also much influence on the presentation of the character traits. Horizontal lines can convey the sense of calmness, strength, and stability, whereas the use of vertical lines is the most appropriate for well balanced, self – confident and renowned character. Diagonal lines, as well as curved lines, suggest dynamic, movement in rising or fall.
- The position of the line – can refer to a contour line or structure line (the lines that define details of the character). Additionally, the position of the line also defines the relationship between elements of the character.
- Type of the line – straight lines as often perceived as stable and consistent, curved lines are dynamic, energized and natural (Solan, 2015a).

From this explanation of the different line characteristics, it is clear that the combination of the characteristics of the line and ways of using them determine the personality traits of the character.

5.2 Shape

The hope is in the close connection with the line, it cannot be detached from the line. The shape can be used for defining countries and details of the character. The most commonly used shapes in the character designing process are a circle, triangle, and square. A key technique in process of character design is to create a character from the basic shapes. Basic shapes enable easy understanding and recognition of the character by the observer. Interpretation of the basic shapes differs from each other for particular shapes. Circle – connotation of the circle are connected with the symbolism of its shape, which is common for the majority of people and cultures. Those are kindness, unity, peace, and whole. If the character consists mainly of circular shapes, the character will be in most cases perceived as positive, benevolent, merciful, well balanced, natural and fond of care for the community. Consequently, circular shapes are most commonly used in character design for children, younger audience or heroes with a high level of stylization. Triangle – dependence of its use, there are a variety of understandings of its symbolism. If the triangle is oriented with its peak on the top, it is usually described as stable, strong and restful shape. On the other hand, if the triangular shape is oriented with peek directing down than it symbolizes misbalance, instability, and sense of tension. Triangle can be analysed from two different perspectives: energy and temperament. Energy can mean dynamic, movement and speed, whereas temperament represents peoples character traits that can be described with a triangle shape. Those are aggression, hostility, dishonesty, passion, and sexuality. Square – square shapes and rectangular shapes are most commonly perceived as strong and the most stable shapes. Besides these understandings, rectangular and square shapes are often understood as certain, rational, strong, make and pure. Therefore, they are mainly used for the design of the hero character (Solan, 2015a).

5.3 Silhouette

This element of the art is the most responsible for creating the recognizable appearance of the character (Figure 2). Observing the character through silhouette enable the analogy of the line and shape at the same time. This technique is the most popular in the process of character design in the most renowned studios in the creative industry. Besides it represent a great way of the basic construction of the character, it is also

relevant for the reconstruction of the character, in the analysis of the existing characters. The most important feature that can be easily conveyed using silhouettes is character recognition. Silhouette can be analysed from two different aspects. First is static appearance which has to provide answers on the questions such as whether the character is different enough from existing ones, whether it has the interesting appearance, is it pleasant for observing. The second aspect is related to technical requirements. In this case, there are questions such as: is a silhouette of the character stands out enough from the background or environment, whether a person can in every moment recognize the character and follow them (Solan, 2015b).

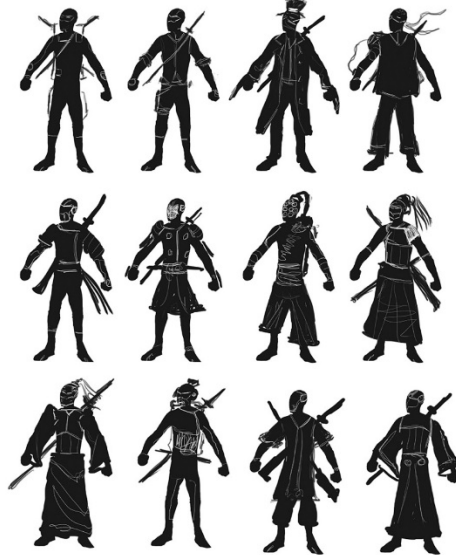


Figure 2: Silhouette of the character (Solan, 2015)

It is recommended to think about the functionality of the character during the silhouette phase. Regardless of the fictional nature of the character, they have to be functional. This also refers to the design of the body of the character – if the character is a monster with wings, the wings need to be strong enough to carry the monster safely. All additional parts and items on the character have to be in real relationship with the character – to convey a sense of real functional use.

5.4 Colour – analysis and importance of the colour in the process of the character design

The aim of the better representation of the character is to be easily understood by the observer and to fit in their mental models which are common to all people. In order to accomplish that, it is necessary to analyse and research colour, its use, and symbolism. It is known that the observer perceives the world and environment around mainly thanks to colour. During the time, different colours take the role of certain symbols which become widely accepted and established in mental models of people.

With the symbolism of the colours as guidelines, it is possible to connect colours with the personality traits of the character. In the visual culture, the most appropriate element for conveying the sense of good or bad is the colour. Characters in the animated movies of comic books have opposed appearance which is conveyed throughout colour. For example, good character opposed to bad character or hero opposed to a villain is presented with opposed colours in the colour spectrum. The most used opposed colour pairs are black – white and red – blue. The first pair, black – white, represents evil against good or negative character versus positive. Additionally, black colour represents a shadow character which cannot be presented as an evil character. The second colour pair, red – blue, is commonly used for the hero and villain design. The red colour is often used for villains, whereas blue is used for the appearance of the hero. When designing hero characters, for costume design are usually consisted of primary colours – red, blue, yellow or gold – whereas costumes for villains are usually designed utilizing secondary colours – green, purple and grey. The most known example for this is the Superman costume (which is a combination of the blue and red) and costume of his main opponent Joker, from the Batman saga, (who wears a combination of purple and green costume) (Tvtropes, 2017).

6. CHARACTER DESIGN CONCEPT

After the analysis of the most important influential factors on the character design process, the important phase to mention is character design concept phase. This phase is always at the beginning of the character design process. It is important to know that the previously described elements are defined in this phase. This is the first phase in the production pipeline and it is closely connected to the scenario and detailed textual description of the character. Archetypes, facial expression, look, shape and body posture are the usually defined in the game scenario where writer or scenarist create an initial idea of the character appearance. The main task for the concept artist is to make a visual representation of the character described in the written scenario (Figure 3). In the concept phase, it is recommended to define character precisely with all details and personality characteristic, with combining their inner and external characteristics (Vaughan, 2012).

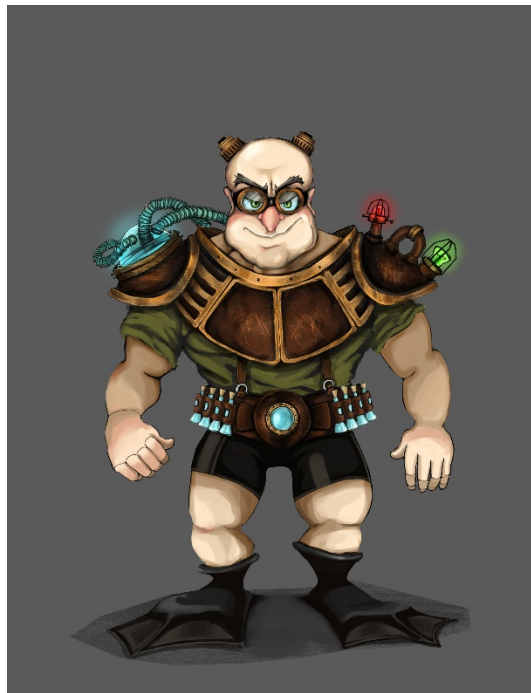


Figure 3: Concept of the character based on the scenario

7. CONCLUSION

Character design process is crucial segment because characters lead observer throughout the story. The primary goal of the character design process is a connection with the audience. Characters are an inevitable part of everyday life, they are present in every aspect of life both as virtual characters and physical characters. People commonly identify themselves with the characters, which is natural. Characters represent personalities which are in constant interaction with the people. Character designers have the power to define the type of the character for people to identify, as well as the target group for their product. The importance of the character can be seen from the definition of fun because characters are an integral part of the entertainment industry. "Fun represents the process which involves exploration of the relationships throughout simulations which enable persona to identify themselves with substitute persona (for example avatar) and in that way create subjective experience and relationships" (Solan, 2015b). Designers of the characters have to know precisely which part of the character has to be emphasized in order to create a recognizable character which is receptive for identification. Besides the detailed analysis of the character traits, the analysis of the references is required. Collecting and observing and analysing references is essential for finding answers to questions such as: "What part of the design is crucial for an appearance like this?" or "Why is the character good or bad?" or "Why is this character adored by the people?". Constant search and giving answers to these questions lead to successful character design.

8. ACKNOWLEDGMENTS

This work was supported by the Serbian Ministry of Science and Technological Development, Grant No.: 35027 "The development of software model for improvement of knowledge and production in graphic arts industry."


9. REFERENCES

- [1] Tillman, B.: "Creative Character Design", (Focal Press, Massachusetts, 2011a), page 5.
- [2] Tillman, B.: "Creative Character Design", (Focal Press, Massachusetts, 2011b), Chapter 2.
- [3] Isbister, K.: "Better game characters by design a psychological approach", (Morgan Kaufmann publications, San Francisco, 2006a), Chapter 5.
- [4] Isbister, K.: "Better game characters by design a psychological approach", (Morgan Kaufmann publications, San Francisco, 2006b), page 145.
- [5] Isbister, K.: "Better game characters by design a psychological approach", (Morgan Kaufmann publications, San Francisco, 2006c), Chapter 6.
- [6] Solan, R. J.S.: "Virtual character design for games and interactive media", (Taylor & Francis Group, Boca Raton, 2015a), page 26.
- [7] Solan, R. J.S.: "Virtual character design for games and interactive media", (Taylor & Francis Group, Boca Raton, 2015b), page 30.
- [8] Tvtropes, Good Colors, Evil Colors, Tvtropes, URL: <https://tvtropes.org/pmwiki/pmwiki.php/Main/GoodColorsEvilColors> (last request: 2018-10-05)
- [9] Vaughan, W.: "Digital modeling", (New Riders, 2012), Chapter 2.



© 2018 Authors. Published by the University of Novi Sad, Faculty of Technical Sciences, Department of Graphic Engineering and Design. This article is an open access article distributed under the terms and conditions of the Creative Commons Attribution license 3.0 Serbia (<http://creativecommons.org/licenses/by/3.0/rs/>).

REDESIGN OF KOZJANSKO REGIONAL PARK VISUAL IDENTITY THROUGH AN EYE TRACKING ANALYSIS OF THE CURRENT AND NEW SOLUTION

Elena Plahuta, Nace Pušnik 

University of Ljubljana, Faculty of Natural Sciences and Engineering,
Department of Textiles, Graphic Arts and Design, Ljubljana, Slovenia

Abstract: Nowadays, people are increasingly more aware of natural resources which enrich and shape our living space. The Kozjansko Regional Park boasts with rich cultural and natural heritage that is worth seeing in person. The visual identity of the park greatly influences the level of visits and awareness of these natural riches. Through its visual identity the park reflects its uniqueness, strategies, and vision, thus communicating with its current and potential visitors. The purpose of this study was to investigate and analyse the existing visual identity of the park through the colour combinations and typography of the existing logo. Additional aim of the study was the redesign of the existing printed material for the Kozjansko Regional Park's Gruska cave. In the study we have developed a redesigned solution of the existing graphic materials as a part of the park's visual identity.

Key words: brand colours, eye tracking, logo design, typography, visual identity

1. INTRODUCTION

Slovenia is widely known for its natural beauties and plenty possibilities for enjoyment of unspoiled nature. For this reason, parks are divided into three main groups: National, Regional and Landscape parks. Triglav National park is the biggest, followed by three regional parks (Kozjansko Regional Park, Škocjan Caves Regional Park, and Notranjska Regional Park) and around 40 Landscape parks. Over the years, there have been tries of connecting all regional parks under the same graphic outlook but somehow it was difficult to design the outlook which will capture all the essential information of three parks. For this reason, every park has its own graphic outlook (Figure 1).

Kozjansko Regional Park



Škocjan Caves Regional Park



Notranjska Regional Park



Figure 1: Visual identities of Slovenian regional parks

Our special interest was in graphic outlook of Kozjansko Regional Park. People responsible for park are trying to make it more known and for this reason they are trying to renovate its offer which pulls behind many other aspects of public communication.

Kozjansko Regional Park is positioned in eastern Slovenia. It has status of biosphere reserve and is under the UNESCO and Nature 2000 protection. Since park has rich natural and cultural inheritance, there are many possibilities for visitors to enjoy them. Here we bump into the problem of correct and appropriate advertising of different activities which are available within the park. Many activities such as hiking, cycling, Nordic walking, running, cultural events, science camps etc. should be properly advertised as part of the overall graphic image of Kozjansko Regional Park. Appropriate graphic outlook should communicate and attract visitors or random visitors. All these facts got our attention to make a research how well the existing corporate graphic identity works, what are their pros and cons and what kind of changes or adjustments could and should be made with the aim of better and more appropriate advertising (Adir et al, 2012; Airey, 2009).

2. METHODS

Two different approaches were used to investigate, how graphic outlook affects people (Butina et al, 2000; Dabner et al, 2011; Feng, 2009). First approach was online survey, which was mainly based on subjective responses of participants. Second method was more objective while participants were measured with an eye tracking device Tobii X120. In both methods participants had to look at some pictures, headlines/signs, search for certain information and answer questions about the presented content (Franken et al, 2015; Georg, 2018). The main difference was of course in gathered results. Eye tracking device provided gaze plots and heat maps based on which we could see if participants were honest about their answers and what attracted them the most.

First testing was as mentioned online survey. It was sent randomly through different communication channels. Participants were of different gender and age. Beside this, our interest was also in their education degree and region of residence. We believe that education and living environment can affect results gathered this way. 55 participants (N=55) have cooperated in the online survey. Data about their gender, age, education level and region of residence is shown in Table 1.

Table 1: Characteristics of online survey participants [%]

Gender		Age		Education level			Region of residence									
M	F	15-20	21-26	HSE	UE	HPE	1	2	3	4	5	6	7	8	9	10
20	80	10	90	75	20	5	27	20	15	12	7	7	5	3	2	2

M-male, F-female.

HSE-High School Education, UE-University Education, HPE-Higher Professional Education.

1-Savinjska, 2-Koroška, 3-Osrednjeslovenska, 4-Obalno-kraška, 5-Posavska, 6-Gorenjska, 7-Goriška, 8-Podravska, 9-Jugovzhodna, 10-Pomurska.

Second testing was performed in the laboratory conditions (Pušnik et al, 2016a; Pušnik et al, 2016b; Rayner, 1998). Environment of performed tests was in room that is equipped in line with standards suggesting optimal viewing conditions when performing tests on the screen ISO 9421 (International Organization for Standardization, 2009). As mentioned by standard, walls and ceiling should be in grey colour (RAL 7037) with specifications which are defined by ISO 3664 (International Organization for Standardization, 2008). Screen used in testing was 24-inch LCD screen (HP ZR24W) with resolution of 1920×1200 px. Similar to first testing, general data about the participants (N=55) was gathered at the beginning of each test and is shown in Table 2.

Table 2: Characteristics of eye tracking participants [%]

Gender		Age		Education level			Region of residence									
M	F	15-20	21-26	HSE	UE	HPE	1	2	3	4	5	6	7	8	9	10
18	82	35	65	62	27	11	24	22	16	7	9	7	5	4	4	2

M-male, F-female.

HSE-High School Education, UE-University Education, HPE-Higher Professional Education.

1-Savinjska, 2-Koroška, 3-Osrednjeslovenska, 4-Obalno-kraška, 5-Posavska, 6-Gorenjska, 7-Goriška, 8-Podravska, 9-Jugovzhodna, 10-Pomurska.

We would like to stress out that either test was performed with different participants (Rayner, 2001). Final number of participants combined in both tests was 110 and every result is from different person (nobody took same or the opposite test twice). In our opinion this is important while in this way we have avoided participants' accustoming to the displayed images and questions, thus limiting factors that could negatively affect the obtained results (Repovš, 1995).

3. RESULTS

Through the experimental part of the study we wanted to find out, what is the basic knowledge about different natural parks in Slovenia. First question was about difference between national, regional and landscape parks. More than 50% of all participants confirmed their knowledge about difference. Next question was about number of regional parks. A little less than 50% of participants answered correct number of regional parks which is 3.

When asking participants about their opinion if regional parks should be presented and advertised under the same brand, more than half of participants was not sure about it. Specificity of the regions is quite big so answers to this question are probably consequence of diversity.

Our next interest was in parks visits. Since we focused on regional parks, our question was about visits of regional parks. More than 50% of participants most often visits Škocjan Caves Regional Park. Quarter (approx. 25%) of participants already visited Kozjansko Regional Park. 20% of participants visited Notranjska Regional Park and around 5 % have not visited any of regional parks.

Before asking participants about appropriateness of logo variations we wanted to find out what is their opinion about visual identity of regional parks. The question was if visual corporate identity affects recognizability and consequently visits of Slovenian regional parks. More than 80% of participants opinion was that good visual corporate identity is important for recognizability and people's desire to visit the parks. For this reason, we asked participants, which graphic design affects the most recognizability. Table 3 presents answers to this question.

Table 3: The most influential part of graphic design [%]





















Logo	Marking boards	Web page	Colour selection	Leaflet	Business card	Ads	Typeface selection	Promotional vehicles
21	16	18	10	7	1	20	4	3

3.1 Online survey

Six series of logos (without typeface sign) were presented to participants (including the current one which is Logo 1 in 1st and Logo 3 in 5th series). Logos maintained the same layout; the differences were in the colour combinations. In each series from 1 to 4 (Table 4) participants had to choose one out of five presented logos while in series 5 and 6 (Table 5) their job was to select five out of ten. Tables 4 and 5 shows the percentage distribution of participants' choices/opinion.

In the 1st series Logo 1 was selected the most times. 57% of participants choose this version of logo. In 2nd series again the most times selected logo was under number 1. Logo 1 in 1st and 2nd series is actually inverted version (same red and green colour). When comparing 3rd and 4th series, the most participants choose Logo 2 (48% in 3rd series and 47% in 4th series). This is somehow logical while both logos are the same; differences were made in other presented logos.





















Table 4: Series of logos 1

Series	Logo 1	Logo 2	Logo 3	Logo 4	Logo 5
1 st					
Choice [%]	57	16	14	7	6
2 nd					
Choice [%]	36	32	20	7	5
3 rd					
Choice [%]	5	48	23	21	3
4 th					
Choice [%]	10	47	15	21	7

In 5th and 6th series (Table 5) participants had to choose five out of ten logos. Dispersion of results in this case is much higher. Table 5 shows undivided distribution of results (consequence of selecting five out of ten examples). Participants were more inclined to logos under the labels from 1 to 5. Four out of five logos achieved 12 or more percent participants choice. Background colour at logos from 1 to 5 was a bit darker


which could affect distribution of results. Similar is finding for 6th series. Percentage distribution is higher for logos from 1 to 5. At 6th series, background colour of logos remained the same while smaller part of the logo (inner part of letter P) differed in colour (saturation).

Table 5: Series of logos 2

Series	Logo 1	Logo 2	Logo 3	Logo 4	Logo 5
5 th					
Choice [%]	13	12	14	15	7
	Logo 6	Logo 7	Logo 8	Logo 9	Logo 10
					
Choice [%]	10	9	3	11	6
	Logo 1	Logo 2	Logo 3	Logo 4	Logo 5
6 th					
Choice [%]	15	11	13	15	6
	Logo 6	Logo 7	Logo 8	Logo 9	Logo 10
					
Choice [%]	12	7	5	13	3

Next task for participants was to select typeface, which (by their opinion) fits original logo the most (original logo was presented next to typefaces). Five different typefaces (among which the currently used was included; Typeface 5) were presented to participants. Table 6 shows percentage distribution for five different typefaces.

Table 6: Series of typefaces











Typeface			Choice [%]
1	Kozjanski park		26
2	<i>Kozjanski park</i>		25
3	Kozjanski park		21
4	Kozjanski park		15
5	Kozjanski park		13

1-Eagle Lake Regular, 2-Crimson Text Italic, 3-Montserrat Light, 4-Roboto Condensed Regular, 5-Anima Normal

Participants opinion was that the most suitable for current logo is typeface Eagle Lake Regular (Typeface 1), followed by Crimson Text Italic (Typeface 2). Both typefaces got similar percentage of answers. Surprising fact is that Anima Normal (Typeface 5) which is currently in use got the lowest percentage of answers.

The last task within the online survey was to select the most optimal combination of the logo and typeface (Table 7). Difference between 1st and 2nd series was in the colour saturation of the logo. In 1st series green colour was unsaturated while the 2nd series was saturated (green colour in 2nd series was the same as in the currently used logo). The allocation of typefaces (signs) under the logo was in all cases the same (the typeface used in the unsaturated and saturated colour combination was in the same place). Table 7 presents the percentage distribution of participants' choices/opinions.

Table 7: Series of logos and typefaces

Series	1	2	3	4	5
1 st	 Kozjanski park	 Kozjanski park	 Kozjanski park	 Kozjanski park	 Kozjanski park
Choice [%]	21	28	20	23	8
2 nd	 Kozjanski park	 Kozjanski park	 Kozjanski park	 Kozjanski park	 Kozjanski park
Choice [%]	13	16	31	33	7


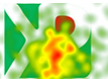


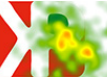
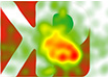
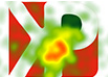









1-Eagle Lake Regular, 2-Crimson Text Italic, 3-Montserrat Light, 4-Roboto Condensed Regular, 5-Anima Normal

1st series of logo and typeface combined shows that participants were most favourable to the logo in combination with typeface Crimson Text Italic (28%). Second combination in 1st series (according to percent's) was combination logo and typeface Roboto Condensed Regular (23%). In 2nd series logo and typeface Roboto Condensed Regular achieved highest percentage (33%), followed by logo with typeface Montserrat Light (31%). Interesting observation is that currently used typeface (Anima Normal) in both series did not achieve highest percentage (1st series with 8% and 2nd series with 7%). Even though typeface Anima Normal is regular version of typeface, it has thin strokes, which could be of decisive influence of selecting/not selecting that combination.

3.2 Eye tracking testing

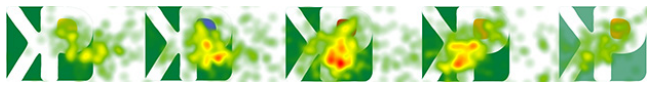
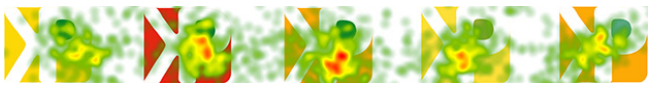
Tests with eye tracking device were performed after online survey. For this reason, we could eliminate logos, typefaces and combinations, which have not achieved the highest percentage through the online survey. Table 8 presents, what was participants choice about different variations of logo (when selecting one out of four). Compared to online survey, in this case participants had only four examples as an option. In 1st series most participants decided that Logo 2 is the most effective while 44% of them choose it. Based on average number of fixations we can notice that this logo also attracted the most attention (average number of fixations was 5.727). Similar finding is noticed in 2nd series; the highest percentage of participants choose Logo 2 (51%). Similar to 1st series, example with the highest percentage has the highest average fixation number (6.309). Winning cases of 1st and 2nd series are actually using the same colour combination but inverted. Similarly, the results of the 3rd and 4th series show highest percentage and average fixation number for Logo 2. In 3rd series 44% of participants choose Logo 2 (average fixation number 6.200) and in 4th series 42% (average fixation number 5.891). Comparison of heatmaps for all logos in all series shows that the maximum concentration of views is exactly in the cases described (Table 8).

Table 8: Series of logos 1 (eye tracker)

Series	Logo 1	Logo 2	Logo 3	Logo 4
1 st				
Fix. No. (avg.)	3.745	5.727	4.164	2.055
Choice [%]	22	44	27	7
2 nd				
Fix. No. (avg.)	3.800	6.309	4.836	2.582
Choice [%]	16	51	29	4
3 rd				
Fix. No. (avg.)	2.364	6.200	4.964	4.218
Choice [%]	9	44	35	13
4 th				
Fix. No. (avg.)	2.364	5.891	4.509	4.127
Choice [%]	11	42	36	11


Online survey (Table 5) helped us to eliminate logos that did not meet expectations about high choice. In 5th and 6th series (Table 9) is visible what was the percentage distribution if participants have less possibilities. 5th series shows that participants in most cases select logo 3 (34%); beside this average number of fixations (5.855) and heat map distribution shows that this logo was a favourite for the participants. Similarly, to 5th series, 6th shows that participants choose logo 3 the most times. Again, average number of fixations (4.927) and heat map distribution is in favour of this logo.

Table 9: Series of logos 2 (eye tracker)

Series	Logo 1	Logo 2	Logo 3	Logo 4	Logo 5
5 th					
Fix. No. (avg.)	1.855	3.800	5.855	4.582	2.600
Choice [%]	7	25	34	29	5
6 th					
Fix. No. (avg.)	2.273	4.164	4.927	3.564	3.436
Choice [%]	5	24	33	22	16

When comparing how suitable certain typeface is for logo (Table 10), participants equally (with 35%) selected two different typefaces (Crimson Text Italic and Montserrat Light). Even though distribution of percentage is the same, average number of fixations is higher at typeface Crimson Text Italic (5.563 : 4.545 in favour of typeface Crimson Text Italic). For this reason, we can assume that typeface Crimson Text Italic is more convenient to be combined with the logo.


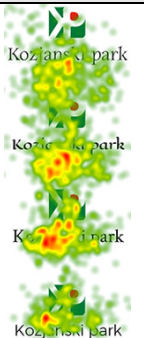






Table 10: Series of typefaces (eye tracker)

Typeface			Fix. No. (avg.)	Choice [%]
1	Koziański park		3.436	10
2	Koziański park		5.563	35
3	Koziański park		4.545	35
4	Koziański park		3.745	20

1-Eagle Lake Regular, 2-Crimson Text Italic, 3-Montserrat Light, 4-Roboto Condensed Regular, 5-Anima Normal

Next task for participants was to choose which typeface, logo and colour combination is by their opinion more suitable. When logo with lighter green colour was presented, almost half of participants decided that typeface Crimson Text Italic suits the most (47%). Confirming this results, average number of fixations is also the highest (7.690). When darker base of logo was presented with typefaces, participants opinion was the same (36% decided for typeface Crimson Text Italic). Typeface Eagle Lake Regular does not lag much with 35% but average number of fixations is in favour of typeface Crimson Text Italic.

Table 11: Series of logos and typefaces (eye tracker)

Logo & typeface 1		Fix. No. (avg.)	Choice [%]	Logo & typeface 2		Fix. No. (avg.)	Choice [%]
1		3.582	18	1		3.200	15
2		6.200	13	2		5.745	35
3		7.690	47	3		6.672	36
4		4.436	22	4		4.491	15

1-Anima Normal, 2-Eagle Lake Regular, 3-Crimson Text Italic, 4-Montserrat Light.

While tendency is to make all printing materials more attractive, renovation of an existing one was involved in our experiment. Two products were graphically renewed; brochure and poster for natural science camp. Since we wanted to find out if our solutions are better, the verification of the old and renewed product was inevitable. It would not make sense for participants just to stare in old and renewed brochure, so we actually gave them task to find certain information (same in both versions). In both examples' participants were asked to find data about number of different animal species that use Kozjansko regional park as their primary biosphere environment. Heat maps of observed pages are presented in Figure 2.

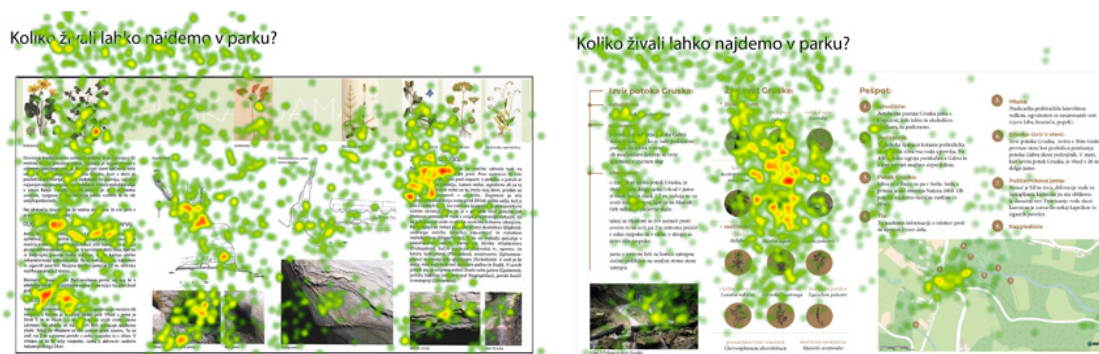


Figure 2: Example of old (left) and new (right) Kozjansko regional park brochure

Higher dispersion of fixations (combined in heatmaps) is noticed at the old brochure (Figure 2, left). Participants had difficulties (or did not find) to fixate on the part of the brochure where the data about number of species is. For this reason, number of correct answers was less than 50% (20 out of 55 participants answered correctly). When renewed version of brochure was presented to participants (Figure 2, right), we can see that main fixation area was at the part where the data about animal species is gathered. Since the data was visible and easy to find, 41 participants (out of 55) answered correctly.

Beside brochure, poster for natural science camp was renewed. Again both, old and new version of poster were presented to participants. In both cases, participants had to find data about submission deadline for camp. Old example of poster (Figure 3, left) shows two areas of participants interest. The lower area (red colour of the heat map) is the actual place where the data about submission deadline is positioned. At the renewed version of poster, fixations are gathered more together and in the upper part of the poster (Figure 3, right). Despite the fact that concentration of participants fixations is more together at the renewed version of poster, number of correct answers was higher for old version of poster (46 out of 55 correct answers for old poster and 45 out of 55 correct answers for renewed poster). It seems that new poster was too much graphical (colour and photography use) which was somehow distractive for participants. Focus was spread around the poster and this could be reason for less correct answers in comparison to old version of poster.



Figure 3: Example of old (left) and new (right) Kozjansko regional park poster for natural science camp

Renovation of printed matter was half-successful. If the brochure was obtained on the transparency of the data, we cannot claim same for the poster. Based on correct answers, it is welcome that brochure contains a lot of graphical material (different colours, photos, maps, etc.) while all this can be distractive if put on poster in too large amount. By changing the poster, we did not achieve a better effect on the participants. Information presented on poster should be clean and clear. For that, search of information is somehow easier.

4. DISCUSSION

More than 50% of participants new the difference between national, regional and landscape parks and the same number of participants new that there are three regional parks in Slovenia. Based on gathered data we can assume that participants had good general knowledge about the subject.

The ease of visiting parks is the following; most participants visited Škocjan Caves Regional Park, follows Kozjansko and Notranjsko Regional Park. Despite the fact that most participants of online survey and eye tracking testing visited at least two of mentioned parks, logos of three parks are not recognizable, more than half of participants did not recognize logos of parks they actually visited in the past.

Logo recognition was low but another interesting fact is that even though the most participants visited Škocjan Caves Regional Park, logo of mentioned park does not achieve significantly better recognition compared to the remaining two logos. In fact, the most recognized logo was Kozjansko Regional Park which can be consequence of the fact that many participants came from the area of Slovenia where the Kozjansko regional park is positioned.

Majority of participants agreed that visual image affects recognizability and visits of regional parks. The most important part of visual image by their opinion is logo. Online survey shows that a well-designed logo can create a good impression on visitors.

While testing colour combinations of logos and typefaces with online survey, deviations were small, however, the responses differed. Objective data about actual eye movement while observing certain combinations were missing. Nevertheless, analyse of data showed where are the weakness of presented logos, colour combinations and typefaces. For this reason, we could eliminate some examples and prepare examples of smaller scale for further testing. Investigation with the help of an eye tracking device guaranteed somehow more objective results.

Eye tracking testing included checking of two printed materials; old and restructured versions. The main goal of it was to rearrange data, add colours and photos which in our opinion could help to find certain information faster and with less effort. A lot of attention was paid to colour contrast of background colour and colour of typefaces. Connection of these two factors plays important role at visibility and legibility of presented information. Nevertheless, we set a limit not to use too many different colours and typefaces. Every printed matter was based on one dominant colour. Text data was emphasized by thoughtful introduction of colours, layout and size.

Brochure of Gruska cave had to be completely revised while the old version included some information which are old and had no special meaning for visitors. Text was somehow enriched with photos and

associated signatures which represented the combination for more favourable reading. Further extension included pictograms and maps.

Visibility of headlines and photo signatures was achieved with the introduction of brown colour on a white background; sans serif typeface was combined with that. Reverse colour combination was used on first and last page of brochure where background colour was dark brown and typeface colour was white. On these two pages photo of Gruska cave was used including two rectangles in dark brown colour. We have avoided placing text on a photo while this could have negative effect on contrast between background and typeface. Consequently, bad contrast could affect visibility and legibility; for this reason, text was placed into two rectangles. All this resulted in greater contrast and better visibility. Headlines were aligned centrally which represent universal alignment; words are evenly distant from one another.

Beside brochure, poster for natural science camp was changed. Compared to the poster which is in use, we added photos to the new one. Reason for this was to prove, how important role photo can have for certain products and that it can help get things closer to people. Central element of posters was photo of a girl in the field of dandelion flowers. The photo is also the part of main headline which is in white colour. This combination establishes enough of contrast between background (photo) and typeface. The main data was stressed with addition of green background (typeface remained in white colour). Area with registration information was divided from the rest of the information with dashed line.

Results gathered with an eye tracking device showed that redesign of printed materials were correct. Main role was in appropriate contrast between background and typeface colour. Transparency has been established with different hierarchy (compared to old printed materials). Another positive thing of redesign was introduction of photos. Especially testing of brochure showed that all implemented factors helped participants to find certain information faster and with less effort (this is concluded based on fixations and heat maps area coverage). Combination of text and photos, splitting a longer text into paragraphs, hierarchy and emphasis in the text has positive influence on attractiveness and sense of organization in printed materials.

Less successful was redesign of poster for natural science camp. There was small difference (answer correctness, number of fixations, heat maps distribution) between the poster which is in use and the poster we redesigned. Attractiveness of new poster is undoubtedly in good visibility of green letters on the white background. Opposite our opinion is that the frames which are in use at the older version of poster attract participants in the same amount as green letters of new poster, even though use of frames is more suggested for short texts and headlines.

Four typeface which turn out as the best in the online survey were tested with eye tracking device; calligraphic typeface Eagle Lake Regular, Serif Typefaces Crimson Text Italic and Anima Normal, sans serif typeface Montserrat Light. These typefaces differ in typographic style, thickness of strokes, use of serifs, etc. When observing results (heatmaps), it is noticeable that participants focused the most on letters j and z. We assume that these two letters were defining ones of attractiveness decision. Typeface which is in use (Anima Normal) was actually selected less times compared to other typefaces. We assume that reason for this can be in small contrast between typeface strokes (letters have extremely thin strokes) and background colour.

Testing logo and typeface together was compiled with four typefaces that were chosen the most times in online survey. Most of participants attention was the highest on the word Kozjanski (part of sign Kozjanski park). Logo colour combination did not have important role in this case which is noticeable through heatmaps. The latter were mostly spread across sign and not logo. Number of fixations was proportionate to the correctness of the answers; more fixations, more correct answers. Since sign was placed under logo, interesting further research could be how different placement of logo and sign could affect results.

5. CONCLUSIONS

The effectiveness of the redesigned solution was verified using the methods of online survey and eye tracking testing. The experiment included testing of the current visual identity, colour combinations of the logo and corresponding typography (with and without the logo). Through online survey, we acquired data on the general knowledge of people about regional parks and, in addition, subjective responses on colour combinations of logos and the corresponding typography. We have concluded that regional parks are well known and visited. The results of colour combinations of logos and the corresponding typography did not give us all the data we wanted and needed. Therefore, we made the check by an objective eye tracking method. The results from an eye tracking analysis showed some positive results for the redesigned visual identity and printed material. When testing typefaces without logo, participant's selection was based on

letters j and z (since those two letters draw high attention and had the biggest heat map area). The results of testing colour combination with the various typography showed that the colour of the logo does not influence the typography selection.

6. REFERENCES

- [1] Adir, V., Adir, G., Pascu, N.-E.: "How to design logo", *Procedia - Social and Behavioral Sciences* 122, 140-144, 2014. doi:10.1016/j.sbspro.2014.01.1316.
- [2] Airey, D.: "Logo design love: A guide to creating iconic brand identities", (New Riders, Berkeley, 2009), page 219.
- [3] Butina, M.: "Mala likovna teorija", (Debora, Ljubljana, 2000), page 174.
- [4] Dabner, D., Calvert, S., Casey, A.: "Grafično oblikovanje: Priročnik za grafične oblikovalce tiskanih, digitalnih in večpredstavnostnih medijev", (Tehniška založba Slovenije, Ljubljana, 2011), page 192.
- [5] Feng, G.: "Time course and hazard function: a distributional analysis of fixation duration in reading", *Journal of Eye Movement Research* 3 (2), 1-23, 2009. doi: 10.16910/jemr.3.2.3.
- [6] Franken, G., Podlesek, A., Možina, K.: "Eye-tracking study of reading speed from LCD displays: influence of type style and type size", *Journal of Eye Movement Research* 35 (6), 442-451, 2015. doi: 10.16910/jemr.8.1.3.
- [7] Georg, J., Color Theory 101, URL <https://www.sitepoint.com/color-theory-101-2/> (last request: 2018-02-25).
- [8] Pušnik, N., Možina, K., Podlesek, A.: "Effect of typeface, letter case and position on recognition of short words presented on-screen", *Behaviour & Information Technology* 8 (1), 1-8, 2016a. doi: 10.1080/0144929X.2016.1158318.
- [9] Pušnik, N., Podlesek, A., Možina, K.: "Typeface comparison – does the x-height of lower-case letters increased to the size of upper-case letters speed up recognition?" *International Journal of Industrial Ergonomics* 54, 164-169, 2016b. doi: 10.1016/j.ergon.2016.06.002.
- [10] Rayner, K.: "Eye movements in reading and information processing: 20 years of research", *Psychological Bulletin* 124 (3), 372-422, 1998.
- [11] International Organization for Standardization, ISO 9241-300:2008 - Ergonomics of human-system interaction-part 305: Optical laboratory test methods for electronic visual display, GENEVA: International Organization for Standardization, 2009.
- [12] International Organization for Standardization, ISO 3664:2009 – Graphic technology and photography: *Viewing conditions*, GENEVA: International Organization for Standardization, 2008.
- [13] Rayner, K., Foorman, B., Perfetti, C., Pesetsky, D., Seidenberg, M.: "How psychological science informs the teaching of reading", *Psychological science* 2 (2), 31-74, 2001. doi: 10.1111/1529-1006.00004.
- [14] Repovš, J.: "Kako nastaja in deluje učinkovita, tržno usmerjena celostna grafična podoba kot del simbolnega identitetnega Sistema", (Studi marketing, Ljubljana, 1995), page 191.



© 2018 Authors. Published by the University of Novi Sad, Faculty of Technical Sciences, Department of Graphic Engineering and Design. This article is an open access article distributed under the terms and conditions of the Creative Commons Attribution license 3.0 Serbia (<http://creativecommons.org/licenses/by/3.0/rs/>).

SCENTED CORPORATE VISUAL IDENTITY

Urška Stankovič Elesini , Tjaša Armič , Raša Urbas 
University of Ljubljana, Faculty of Natural Sciences and Engineering,
Department of Textiles, Graphic Arts and Design, Ljubljana, Slovenia

Abstract: *The aim of this research was to create a corporate identity and to enrich it with a coffee fragrance. To reach this goal, microcapsules with coffee essential oil were used. For testing, two types of samples were prepared: business cards, with designed and printed fragranced logotype, and samples with fully printed surface using printing ink enriched with the fragranced microcapsules. The microcapsules and the printed samples were analysed using selected testing methods, scanning electron microscope and sensory test. The sensory test was conducted in an odourless room, during afternoons, over a four-month period. During this pilot study, a questionnaire for respondents was prepared. Business cards were used for company customers, whose response on fragranced items was tested and analysed. From the results obtained during tests we established that the screen printing inks with added fragrant microcapsules emit a recognizable scent over a long period of time, and that their presence as a corporate identity attracts customers and produces positive effects.*

Key words: coffee essential oil, corporate identity, microcapsules, screen printing

1. INTRODUCTION

Fragrance can arouse memories related to previous experiences and emotions. Among all human senses, the scent is most strongly associated with a memorable emotion, and not with the facts. A scent can be associated with a pleasant experience, encouraging a system to refer to certain events and emotions (Ward et al, 2007; Michon et al, 2005). These memories influence the person's mood and can lead to mild changes in well-being, as was showed by Lindstrom (Lindstrom, 2011). He emphasized the importance of smell for the patients with dementia, Alzheimer's disease or amnesia caused by brain injuries in accidents. Lindstrom also emphasized that majority of our preferences for brands and products has been stamped up since the age of seven. Thus, many marketers try to manipulate our preferences also with the smell, which can be used in two ways (Ward et al, 2007): the first is related to the product attributes (e.g. the smell of the fragrant flower) and the other with the environment in which the products are sold (e.g. the smell of the baked bread in the shop). The scent recalls the memory on two stages: the first stage is associated with the recalling positive associations (e.g. the smell of the roasted bread or the boiled coffee), while the second stage recalls comfortable experiences and emotions during shopping (Ward et al, 2007). Bakeries, chocolatiers, florist shops and other specialized stores often have a noticeable smell of products in the sales area, however not all products emit smells, so these are added to the stores as, for example, artificially dispersed scents. Such a way of adding scents to the market environment encourages researchers to analyze and try to determine the psychological and the behavioral impact of the smell on the customer/s (Spangenberg et al, 2006).

Two interesting studies on the effect of the smell were presented in the Mattila and Wirtz studies (Mattila et al, 2001). In the first research, the test persons performed a catalogue purchase in a scented and unscented room. It was established that people in the scented room spent more time than in unscented room. In the second study, the test persons were tested in casinos. As it was concluded from the research, the people on slot machines consumed more money when the casino was pleasantly refined.

The idea for this research stemmed from a desire of Slovenian company, which deals with the coffee machines, to design a recognisable corporate identity, which should possess a suitable scent of fresh coffee that would pleasantly influence on customers. After an extensive literature research and suitable cooperation with the company, the aim of this research was to analyse the scent of coffee on printed products especially its intensity during determined period. For this purpose, the microcapsules with the coffee essential oil in the core were used in the process of printing, while the printed samples and designed business card were tested and analysed on general properties and by sensory test.

2. MATERIALS AND METHODS

2.1 Materials

2.1.1 Microcapsules

Single core microcapsules were synthesized by modified *in situ* polymerization. For the microcapsule shells, partially methylated trimethylolmelamine (Melamin, Slovenia) was used. Polyacrylic polymer was used as a modifying agent/poly-condensation initiator for the in-situ polymerization. Analytical grade sodium hydroxide (Kemika, Croatia) was used for the termination of the poly-condensation reaction and pH neutralization. To remove the formaldehyde released during the poly-condensation, ammonia (Kemika, Croatia) was added to the suspension of the microcapsules as the scavenger. As a core material, laboratory prepared coffee essential oil was used. The modified process of the *in situ* polymerization microencapsulation was performed in a 1-L laboratory reactor equipped with a turbine stirrer in the following stages: (1) preparation of an aqueous solution of the modifying agent; (2) emulsification of a core material at a room temperature with stirrer speed of 1500 rpm for 20 min; (3) addition of the partly methylated trimethylolmelamine amino-aldehyde prepolymer for the shell formation; (4) induction of the poly-condensation reaction by raising the temperature to 70–80°C; (5) poly-condensation process (approx. 1 hour) of microcapsules formation; (6) termination of the poly-condensation; (7) removal of the released formaldehyde by addition of an ammonia scavenger at 50°C; and (8) cooling to the room temperature.

2.1.2 Paper substrate

In research paper substrate Flora Avorio (manufacturer Gruppo Cordenon, Italy) was used. The paper was recycled, manufactured from primary wood-free cellulose (60 %), inkless wood-free cellulose (30%), and cotton fibres (10 %). The declared grammage of the paper substrate was 350 g/m² (Flora, 2017).

2.1.3 Sample preparation

Although the logotype was specially designed and printed for the company, additional samples were prepared for testing as follows. Microcapsules (suspended in an aqueous solution) in 20% mass conc. were mixed with printing ink (Elastil Compronte, Minerva, Italy) and pigments in 5% mass conc. Thus, prepared printing mixture was applied with screen printing to the surface of the paper substrate. The screen printing technique was performed manually. We have used a screen printing PET mesh with the thread density of 36 cm⁻¹ and monofilament diameter 80 µm, which was fixed to the aluminium frame at the thread angle 0° and the load tension of 15 N. All prints were made with one passage of the squeegee, and air-dried at 100°C. Unprinted samples were denoted as PS 350 and printed samples as PS 350S. With each PS 350-SP sample, side A was printed, and side B was unprinted.

2.2 Methods

2.2.1 Microcapsules

The appearance of the microcapsules was observed by scanning electron microscopy (SEM; JSM 6060 LV, Jeol, Spain). The microcapsule suspension was applied on a specimen stub and allowed to air-dry. The samples were covered with an ultra-thin coating of gold (with high vacuum evaporation). The size of the microcapsules was determined from the SEM images with the use of the ImageJ software and from the results, the size distribution curves were drawn. The release behaviour of microcapsules was performed by tests according to Hwang et al. (2006). For tests, the suspension of the microcapsules was added into the aluminium cups (5 × 7 cm in size), which were then placed into the drying oven. In the release test by Hwang et al. (8), the oven was heated first to 25°C and then to 40°C. The microcapsules were heated for both temperature ranges for 5 days. Each day, at the same time, the samples were weighed and placed back into the oven. With the use of Equation (1), the release rate of the tested microcapsules was calculated:

$$\text{Mass loss [\%]} = \frac{A_0 - A_n}{A_0} \cdot 100 \quad (1)$$

where A_n presents the weight (g) of the microcapsules after n days of the release test ($n = 1, \dots, 5$ days) and A_0 presents the weight (g) of the microcapsules suspension prior to the release test.

The first calculated mass loss after the first day corresponds to the water evaporation and the residual material corresponds to the dry mass/share of the microcapsules in an aqueous suspension. Subsequent drying in the 5 days period corresponds to the weight lost after every day due to the porosity of the shell.

2.2.2 Paper substrate

Before and after printing, the following properties were measured on the paper substrates: Grammage was measured according to the method described in the standard ISO EN 536:2012 (ISO 536:2012, 2012). Thickness was measured on a Mitutoyo apparatus, No: 2050 F–10, with a load of 500 cN·cm⁻² on the sample area of the measurement of 1 cm² and according to the standard ISO 534:2011 (ISO 534:2011, 2011). Roughness of the paper substrates was determined by the Bendtsen method, as described in the standard ISO 8791-2 (ISO 8791-2:2013, 2013). Air permeance was measured on a Bendtsen apparatus according to the method described in the standard ISO 5636-3 (ISO 5636-3:1992, 1992) Height of a capillary rise was measured in the machine direction (hereinafter MD) and cross-direction (hereinafter CD) by the Klemm method, according to the standard ISO 8787:1996 (ISO 8787:1996, 1996).

2.2.3 The sensory test

Before the sensory test and the samples were prepared, the preliminary test was conducted in the company. This test was performed with the intention to understand how the coffee fragrance influences the mood of employees. For this purpose, three open bags filled with the coffee were put at the main entrance hall of the company for 30 days. At first the employees were pleased with smelling the coffee when entering the company. However, after 14 days, they started to avoid the main entrance hall and entered the company through the back door. We have determined, that the smell was pleasant at the beginning, but after 14 days, the smell become annoying and employees start to avoid it. In contrary, customers that came to the company less frequently recognized the smell of coffee as pleasant each time they came to the main entrance hall of the company.

The sensory test was performed on the printed samples PS 350-SP. In the test 17 respondents participated (7 males and 10 females). For each respondent five samples of the PS 350-SP were prepared (S1 to S5). Testing was performed in the morning, always in the same ventilated room, without any other scents. Samples were stored separately for each respondent and together with their personal questionnaire.

Before starting, precise plan of the testing (shown in Table 1) was developed. Since each respondent rubbed the samples with their fingers, washing hands was compulsory before test. For this senseless soap Balea (Balea, Austria) was used. The rubbing of the samples was performed in the same manner each time (four rubs: left-right-left-right) with the use of only one finger. The scent was determined subjectively by each respondent and classified into one of five classes: scentless, barely perceptible scent, slight scent, strong scent and very strong scent. Testing was performed five times, starting in November 2017 and finishing in March 2018.

Table 1: Sensory test plan

Sample	Immediately after printing	After 1 months	After 2 months	After 3 months	After 4 months
S1	smell-rub-smell	smell-rub-smell	smell-rub-smell	smell-rub-smell	smell-rub-smell
S2	smell	smell-rub-smell	smell-rub-smell	smell-rub-smell	smell-rub-smell
S3	smell	smell	smell-rub-smell	smell-rub-smell	smell-rub-smell
S4	smell	smell	smell	smell-rub-smell	smell-rub-smell
S5	smell	smell	smell	smell	smell-rub-smell

At the same time as sensory test was performed, also a simple test was performed with the customers of the company. For them, business cards were designed and scented in the same way as in the case of samples PS 350-SP (by screen printing). These cards were given to the customers, when came to the company. They expressed their opinion about the scented business card after they got the card and after a period of one month, during which they carried it in their wallets.

3. RESULTS

3.1 Properties of the microcapsules

The size distribution of the synthesized microcapsules is presented in Figure 1. As it can be seen from the graph, the highest share of the microcapsules (74.7%) was in the interval from 0.7 to 11 μm . Smaller microcapsules are more resistant to the shear forces as bigger microcapsules and thus also to the shell rupture. Consequently, the smaller microcapsules longer retain material and fragrance in the core as the bigger microcapsules. Of course, the porosity of the wall of the microcapsules also has an influence on the release of the fragrance: the more porous is the wall, the shorter time the fragrance is released.

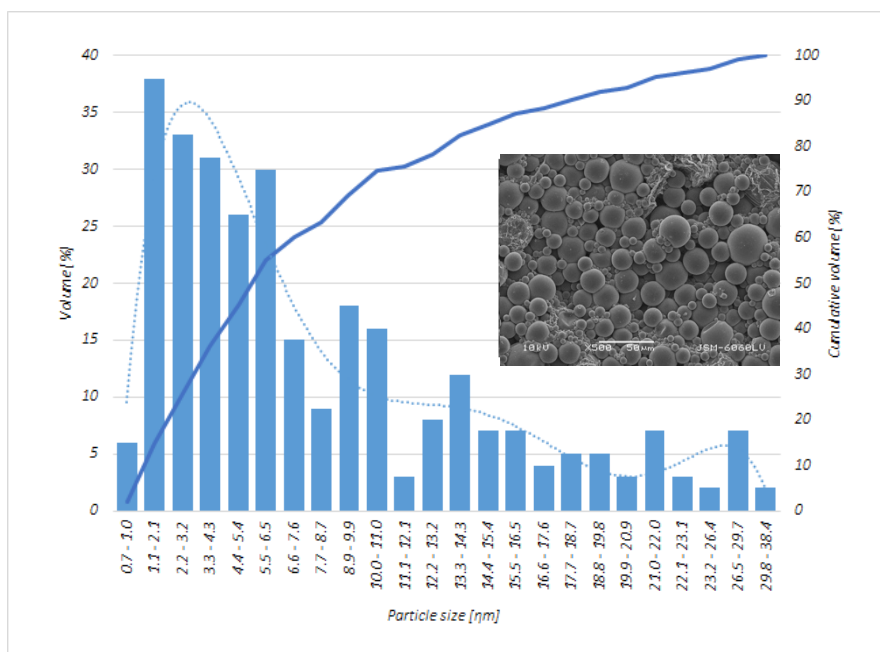


Figure 1: Size distribution and SEM image of the microcapsules with the essential oil of coffee in the core (SEM; 500 \times magnification)

According to the results in Figure 2, the microcapsules used in our research had a nonporous wall, since only 0.12% and 0.34% of the core material at 25 $^{\circ}\text{C}$ and 40 $^{\circ}\text{C}$, respectively, were released in 5 days. The drop of the mass loss shown in first day is due to the water evaporation.

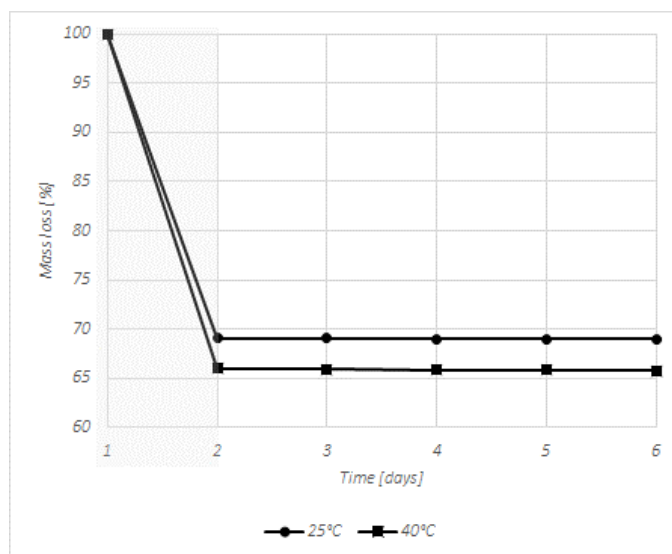


Figure 2: Proportion of the released core material through the microcapsule wall during 5 days, at 25 $^{\circ}\text{C}$ and 40 $^{\circ}\text{C}$

3.2 Properties of the paper substrate before and after printing

The measured properties of unprinted (PS 350) and printed (PS 350-SP) samples are shown in the Table 2. As it can be seen, the paper substrate possesses almost the same capillarity in both directions, MD and CD respectively. After printing the air permeability decreased significantly, while the roughness increased on printed side A and slightly decreased on unprinted side B.

Table 2: Properties of the samples PS 350 and PS 350-SP (A – printed side, B – unprinted side, MD – machine direction, CD – cross direction)

Property	PS 350	PS 350-SP
Grammage [g/m ²]	338.35	373.21
Thickness [mm]	0.48	0.51
Roughness (Bendtsen) [ml/min]	A = 1450 / B = 1350	A = 1845 / B = 1215
Air permeance (Bendtsen) [ml/min]	A = 439.00 / B = 450.00	A = 37.50 / B = 31.50
Height of capillary rise [mm]	MD = 16.60 / CD = 16.20	-

3.3 Results of the sensory test

In the sensory test, out of 17 involved respondents 82.4% of them drink coffee. The majority of the respondents (86.2%) believe that sight is the most important sense during the purchasing of products. 65.5% mean that the sound is also important, following with the smell (34.5%), touch and taste. Of course, the importance of each sense is changing according to the type of the product we are purchasing. 71.4% of respondents drink coffee two to four times per day, while 28.6% of respondents drink coffee two to five times per week. 35.3% of respondents recognised the scent of the coffee during smelling the samples, while 41.2% of respondents did not recognized the scent. Other respondents (23.5%) thought that the scent belonged to zirconia, garlic, herbs etc. As pleasant the scent was recognized by 17.7% of respondents, 29.4% thought it was interesting and 29.4% as annoying. Other respondents (23.5%) did not have any feelings about the scent. On the other hand, 41.4% of respondents replied that the smell of the coffee reminded them of the break at work, to the new beginnings, breakfast, childhood, parents, beautiful day and nice things.

Intensity of the scent before and after rubbing of the samples was followed for four months. As it can be seen from the Figure 3 (left), the samples were before rubbing scentless, barely or slightly scented after printing and even after four months. This implies, that the scent did not penetrate through the wall of the microcapsules, which coincides with the results of the release test (Figure 2). After the samples were rubbed, the scent was determined again, and the results are shown in the diagram in the Figure 3 (right).

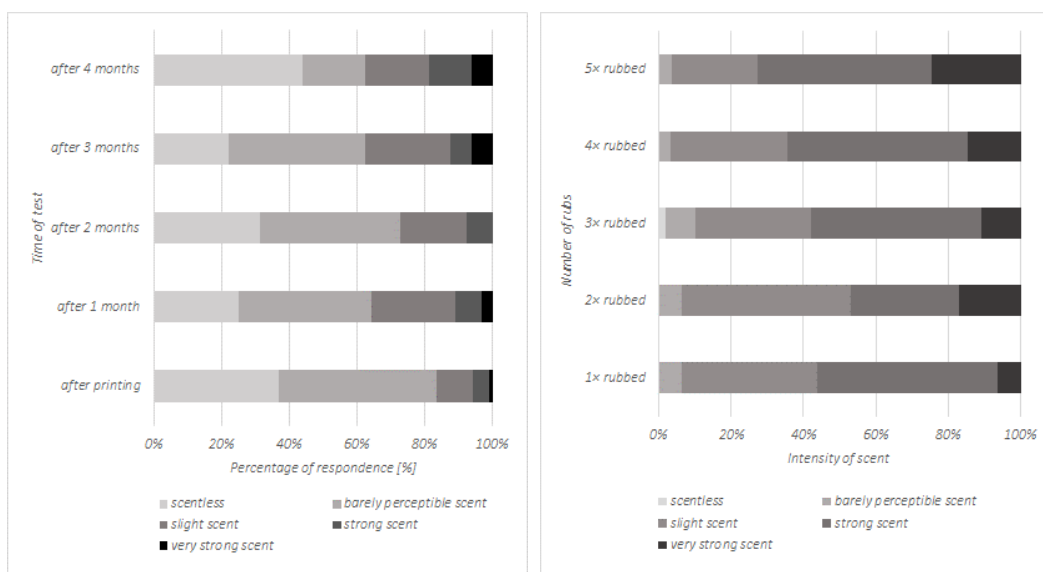


Figure 3: Intensity of the scent of the samples before (left) and after (right) rubbing

From the diagram it can be seen that the scent after rubbing is slight, strong and even very strong. The microcapsules, which were printed on the surface of paper substrate, were consequently trapped inside the layer of the printing ink. After rubbing some of them were ruptured and the coffee essential oil and also the scent was released from the core and detected during the test. Results show that also after 5x rubbing, the samples still emitted strong scent which implies, that the microcapsules in different sizes (Figure 1) prolong the emitting time of the scent, since some of the microcapsules can rupture earlier (especially bigger microcapsules) and some of them later (smaller microcapsules).

In our research, the second group of respondents were customers of the company. 13 customers participated in the research (4 males and 9 females). At their visit we gave them scented business cards, and all recognized the smell of coffee. According to the results, none of them have ever sign the scented contract, however 27.6% of them would certainly sign it and 48.3% would not although they loved the scented business card.

4. CONCLUSIONS

As was shown by the research,

- the pleasant smell is an important factor when purchasing a product or service,
- it is necessary to be careful of where and how the smell of i.e. coffee is used, since even the pleasant smell can become very annoying and thus distracting to the customers,
- the presence of the fragranced microcapsules involved in some elements of the corporate identity attract customers and gives positive effect on them,
- the fragrant microcapsules in different sizes emit a recognizable smell over a longer period even if they are immersed into the printing ink.

5. ACKNOWLEDGMENTS

The authors gratefully acknowledge dr. Boštjan Šumiga from the Faculty of Natural Sciences and Engineering, for the microcapsules prepared with the coffee essential oil.

6. REFERENCES

- [1] International Organization for Standardization, ISO EN 536:2012 Paper and board - Determination of grammage, International Organization for Standardization, 2012.
- [2] Flora, Recy & Tex, Gruppo Cordenons, URL: http://www.gruppocordenons.com/en/products/scheda-prodotto.html?id=2496&brand_id=38 (last request: 2017-12-01).
- [3] Hwang, J. S., Kim, J. N., Wee, Y. J., Yun, J. S., Jang, H. G., Kim, S.H. in Ryu, H.W.: "Preparation and characterization of melamine-formaldehyde resin microcapsules containing fragrant oil", *Biotechnology and Bioprocess Engineering* 11(4), 332-336, 2006. doi: 10.1007/BF03026249.
- [4] International Organization for Standardization, ISO 534:2011 Paper and Board – Determination of thickness, density and specific volume, International Organization for Standardization, 2011.
- [5] International Organization for Standardization, ISO 5636-3:1992 Paper and board – Determination of air permeance (medium range) – Part 3: Bendtsen method, International Organization for Standardization, 1992.
- [6] International Organization for Standardization, ISO 8787:1996 Paper and board – Determination of capillary rise - Klemm method, International Organization for Standardization, 1996.
- [7] International Organization for Standardization, ISO 8791-2:2013 Paper and board – Determination of roughness/smoothness (air leak methods) – Part 2: Bendtsen method, International Organization for Standardization, 2013.
- [8] Lindstrom, M.: "Brandwashed: Tricks Companies Use to Manipulate Our Minds and Persuade Us to Buy", (Crown Business, New York, 2011.), pages 21-23.
- [9] Mattila, A. S., Wirtz, J.: "Congruency of scent and music as a driver of in-store evaluations and behaviour", *Journal of Retailing* 77 (2), 273–289, 2001. doi:10.1016/S0022-4359(01)00042-2.

- [10] Michon, R., Chebat, J.C., Turley, L.W.: "Mall atmospherics : the interaction effects of the mall environment on shopping behaviour", *Journal of Business Research* 58(5), 576–583, 2005. doi: 10.1016/j.jbusres.2003.07.004.
- [11] Spangenberg, E. R., Sprott, D. E., Grohmann, B., Daniel, L., Tracy, D. L.: "Gender-congruent ambient scent influences on approach and avoidance behaviors in a retail store", *Journal of Business Research* 59, 1281-1287, 2006. doi: 10.1016/j.jbusres.2006.08.006.
- [12] Ward, P., Davies, B. D., Kooijman, D.: "Olfaction and the retail environment: examining the influence of ambient scent", *Service Business* 1(4), 295-316, 2007. doi:10.1007/s11628-006-0018-3.




© 2018 Authors. Published by the University of Novi Sad, Faculty of Technical Sciences, Department of Graphic Engineering and Design. This article is an open access article distributed under the terms and conditions of the Creative Commons Attribution license 3.0 Serbia (<http://creativecommons.org/licenses/by/3.0/rs/>).

DIGITAL MEDIA



LCD DISPLAY LEGIBILITY INFLUENCED BY TYPEFACES AND COLOUR CONTRASTS

Gregor Franken, Maruša Pangerc, Klementina Možina 
University of Ljubljana, Faculty of Natural Sciences and Engineering,
Department of Textiles, Graphic Arts and Design, Ljubljana, Slovenia

Abstract: *The evolution of high resolution displays, especially liquid crystal displays (LCD) that are among the most commonly used ones, has contributed to a larger circle of display readers. Despite high resolutions, problems in the legibility of typefaces still occur. Many typefaces may well be readable in print, but cause more difficulties when being read on displays. The aim of this study was to examine the influence of colour contrast on the legibility on LCDs to establish which type style is appropriate for a coloured text to be legible. Two different, specially designed typefaces for display use (one transitional, i.e. Georgia, and one sans-serif, i.e. Verdana) were tested in a satisfactory light-dark contrast of three different colour combinations involving five colours, i.e. dark grey (#1A1A1A) on white (FFFFFF), dark blue (#142451) on light grey (#D9D9D9) and red (#C62026) on light grey. The reading speed and fixations were analysed with an eye-tracking device Tobii 120X. Different texts in both typefaces at 12 pt (16 px), in 130% leading and all colour combinations were displayed on a 24-inch LCD display. The forty tested individuals were between 19 and 22 years old. The results showed that the selection of a particular colour combination and contrast greatly affects the speed of reading and legibility. Less visible colour combinations of text and background were read more slowly than the more contrasting or visible ones at both typefaces. At both typefaces, it was seen that at a slower reading speed, more fixations were needed and vice-versa. It might also be concluded that the transitional typeface Georgia is more legible than the sans-serif typeface Verdana. Nevertheless, it appears that different colour combinations had different reading speeds at different typefaces (transitional vs sans-serif). An appropriate contrast and colour combination can facilitate legibility on displays.*

Key words: colour contrast, eye-tracking technology, LCD display, legibility, reading, typography

1. INTRODUCTION

The evolution of high resolution displays, especially liquid crystal displays (LCD) that are among the most commonly used ones, has contributed to a larger circle of display readers. Despite high resolutions, problems in the legibility of typefaces still occur. Many typefaces may well be readable in print, but cause more difficulties when being read on displays.

The communication through a page or a display requires from the reader to translate symbols into meaning. Legibility refers to how easily this process is performed. To make reading possible, the text must be visible and recognisable; however, visibility and recognition are influenced by the typographical choice (Reynolds, 1988; Možina, 2001). Legibility and the reading process can be studied by tracking eye movement. Reading does not occur as a continuous movement of the eyes along the lines of a text, but rather as a sequence of rapid eye movements (saccades) and individual fixations. Fixations are short stops, which typically last between 200 and 250 ms (Abadi, 2006; Rayner et al, 2001) at individual words or groups of words that (within their duration) enable the brain to process information.

A large number of studies on legibility points to its importance. There are some typographic characteristics to be observed to make a text more legible. For a small type size, it is known that the differences in stroke weight and typographic tonal density (TTD) are significant (Možina et al, 2010; Rat et al, 2011), since they influence text legibility. Furthermore, a number of other typographic characteristics needs to be observed in order to make a text more legible, i.e. distinctive character features (counter shape), x-height, ascender, descender, serifs, contrast (stroke weight), set width, type size, leading (i.e. space between lines) etc (Franken et al, 2015; Možina, 2001; Reynolds, 1988; Tracy, 2003).

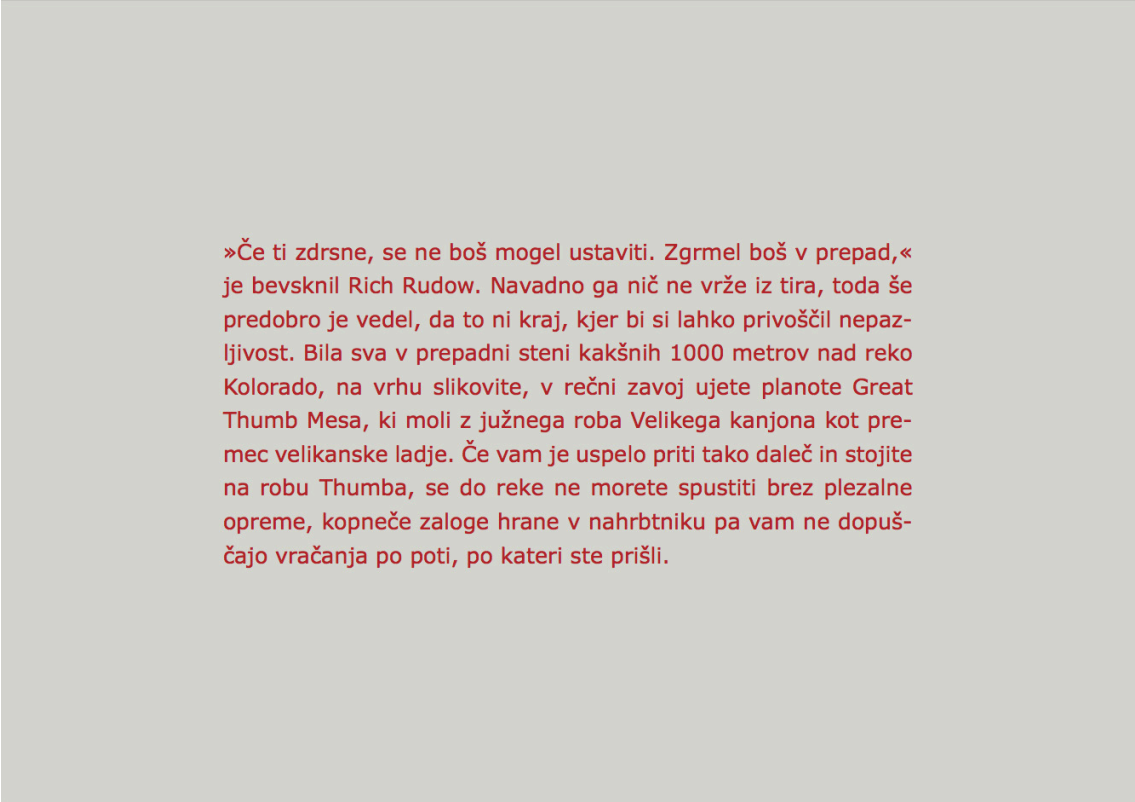
For better visibility of information, colour can be of use as well (White, 1996). Most typefaces are designed to be read as black letters on a white background and they in this manner achieve optimum legibility. When reading large amounts of type, the contrast of black and white is what readers are most accustomed to (Carter, 1997; Možina, 2001). To use colour for better typographic visibility, the contrast is poorer and we therefore have to take into consideration some recommendations (Carter, 1997; Možina, 2001; White, 1996). As type decreases in size, colour contrast has to increase in strength (Carter, 1997;

Možina, 2001). Letter and word spacing, and leading affect type colour (TTD). Similarly, when letter and word spacing and leading increase, TTD decreases (Carter, 1997; Keyes, 1993; Možina, 2001). Therefore, when colour is used to improve visibility, larger type size or black typefaces or sans-serif typefaces need to be used. Furthermore, larger leading should be applied when colour is used for typography or background or both (Carter, 1997; Možina, 2001). To attract the reader's attention, blue and red colours are often used with white background (Pušnik, 2016). The red colour is associated with danger, energy or warmth (Thussu, 2007). It can activate an avoidance motivation, and enhance performance and detail-oriented cognitive tasks (Mehta et al, 2009), and in turn, it can lead to greater attention. The blue colour, on the other hand, is supposed to represent trust, hope and serenity (Thussu, 2007). Despite the subdued tone, the combination of blue and white can affect the recipient and is a visible source of additional information (Thussu, 2007).

The legibility study (Franken et al, 2018) of different typefaces in different light-dark contrasts with different backgrounds displayed on an LCD display showed that a better contrast (however not maximum, i.e. black on white) increases the reading speed. Therefore, the aim of this study was to examine the influence of colour combination on the legibility on LCD displays to establish which type style is suitable for a coloured text to be legible.

2. EXPERIMENTAL

Two different, specially designed typefaces for display use – one transitional, i.e. Georgia, and one sans-serif, i.e. Verdana (McLean, 1996; Možina, 2003) – were tested in three different colour combinations involving five colours, i.e. dark grey (#1A1A1A) on white (FFFFFF) (Combination 1), dark blue (#142451) on light grey (#D9D9D9) (Combination 2) and red (#C62026) on light grey (#D9D9D9) (Combination 3). In controlled laboratory conditions (ISO 3664, 2009), the reading speed and fixations were analysed with an eye-tracking device Tobii 120X. The texts in both typefaces at 12 pt (16 px), in 130% leading and all colour combinations were displayed on a 24-inch LCD display with the resolution of 1900 × 1200 pixels at a 120 Hz refresh rate. In each typeface and each colour combination, a different text was presented to the tested individuals. We used six different texts from *National Geographic* (Slovenian edition) with the length of between 97 and 115 words, comprising between 10 and 13 lines (Figures 1 and 2).



»Če ti zdrsne, se ne boš mogel ustaviti. Zgrmel boš v prepad,« je bevsknil Rich Rudow. Navadno ga nič ne vrže iz tira, toda še predobro je vedel, da to ni kraj, kjer bi si lahko privoščil nepazljivost. Bila sva v prepadni steni kakšnih 1000 metrov nad reko Kolorado, na vrhu slikovite, v rečni zavoj ujete planote Great Thumb Mesa, ki moli z južnega roba Velikega kanjona kot premec velikanske ladje. Če vam je uspelo priti tako daleč in stojite na robu Thumb, se do reke ne morete spustiti brez plezalne opreme, kopneče zaloge hrane v nahrbtniku pa vam ne dopuščajo vračanja po poti, po kateri ste prišli.

Figure 1: Sample of text paragraph with Verdana typeface

Počepnem v travo, da bi si поблиže ogledala žival, ki se opoteka proti meni. Stara je približno štiri mesece, velika kot nogometna žoga, ima rahlo izbuljene oči in zagotovo je mehka in prijetnega vonja kot mlad kužek. Čutim neustavljivo željo, da bi jo dvignila in stisnila k sebi. Prav ta ljubkost je eden od razlogov, da je orjaški panda mednarodna znamenitost in hkrati kitajski kulturni simbol, gospodarska zlata jama in vir nacionalnega ponosa – Kitajska je namreč edina država, kjer še živijo ti azijski medvedi. Ves svet spremlja njena vztrajna prizadevanja, da bi se pande ohranili v naravnem okolju – v nekaterih pogledih je pri tem neverjetno uspešna.

Figure 2: Sample of text paragraph with Georgia typeface

The time required to read 600 characters (in seconds) and the number of fixations were calculated. Forty tested individuals were between 19 and 22 years old with normal or corrected-to-normal vision. In line with recommendations (ISO 9241, 2012), they were positioned 60 (+/- 1) cm from the display. The texts were set in a CSS style sheet and displayed as a HTML document. In this way, we ensured a precise display of texts in the chosen size. The texts were shown in the centre of the display. The display sequence varied using the Latin square design, which was used for counterbalancing the order of texts.

3. RESULTS AND DISCUSSION

Figure 3 shows the average influence of the used colour combinations on the speed of reading. Figure 4 shows the influence of the used typefaces and colour combinations on the speed of reading. Figure 5 shows the influence of used colour combinations on the number of fixations. Figure 6 shows the influence of the used typefaces and colour combinations on the number of fixations.

On average, the reading speed was the fastest at the combination of the red text on light grey background (Combination 3) (cf. Figure 3). The reading speed was the slowest at the blue text on light grey text (Combination 2) (cf. Figure 3), regardless of the used typeface (cf. Figure 4). At all examples, the texts prepared with Georgia were read the fastest (cf. Figure 4). On average, the texts prepared with the Verdana typeface were read the slowest, the only exception was dark grey text on white background (Combination 1). Verdana is a sans-serif typeface and should thus have better legibility than a transitional typeface. Obviously, at this type size (16 px), big counter size, wide letters and thick stroke width led to lower reading speed. The interaction between a greater number of fixations (cf. Figures 5 and 6) and slower reading was noticed, especially at the Verdana typeface. A larger counter size gave more fixations and consequently resulted in slower reading. On the other hand, the typeface Georgia, which was read faster, needed less fixations.

It was also interesting that the red text on light grey background (Combination 3) gave the fastest reading speed (cf. Figure 3) and the smallest number of fixations (cf. Figure 5), since this colour combination has the smallest light-dark contrast among the used colour combinations. Most likely, the unusual colour combination for a longer text (not only titles or a short text) held more attention by the readers. It was surprising that the blue and light grey colour combination (Combination 2) with a strong enough

light-dark contrast gave the worst legibility. Nevertheless, the reason is probably in the distribution of cones sensitive to short-wavelength light out of the fovea centralis, as there are more at the peripheral retina (Krauskopf, 1998). There should be no problem with larger objects in blue, while the typefaces with bigger counter sizes in smaller type sizes in blue obviously worsen legibility.

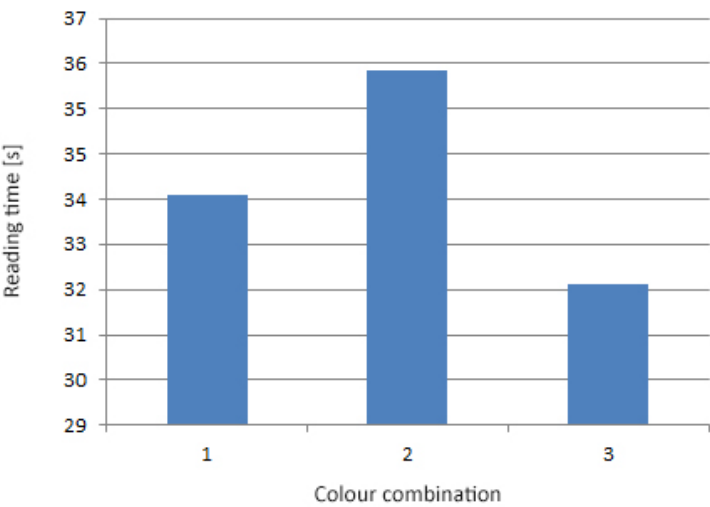


Figure 3: Average reading time [s] at used colour combinations

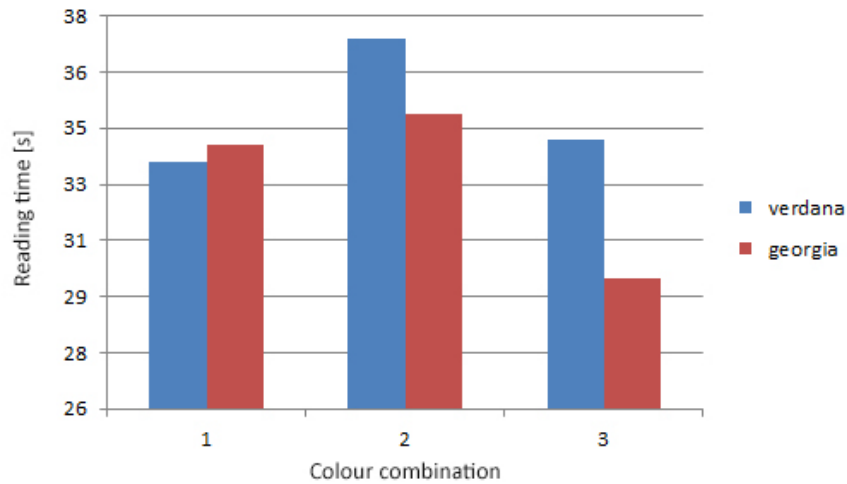


Figure 4: Reading time [s] at used typefaces in different colour combinations

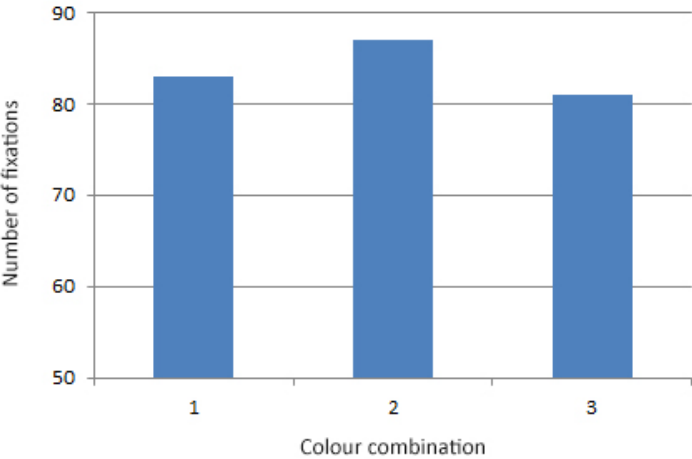


Figure 5: Number of fixations at used colour combinations

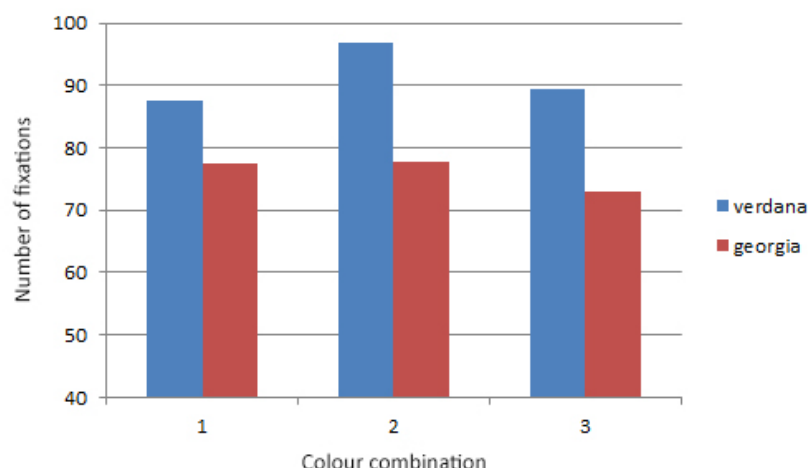


Figure 6: Number of fixations at used typefaces in different colour combinations

4. CONCLUSION

The results of the study showed that the selection of a particular colour combination and contrast greatly affects the speed of reading and legibility. Less contrasting or visible colour combinations of the text and background were read more slowly, i.e. blue and light grey, than the more contrasting or visible ones at both typefaces. At both typefaces, it was seen that at slower reading speed, more fixations were needed and vice-versa. It might also be concluded that the transitional typeface Georgia is more legible than the sans-serif typeface Verdana. Nevertheless, it appears that different colour combinations had different reading speeds at different typefaces (transitional vs sans-serif). Consequently, in order to be able to give an appropriate suggestion for usable display legibility, the study should be thought through with more diverse colour combinations and contrasts.

5. REFERENCES

- [1] Abadi, R. V.: "Vision and eye movements", Clinical and Experimental Optometry 89, 55–56, 2006. doi: 10.1111/j.1444-0938.2006.00026.x.
- [2] Carter, R.: "Working with computer type", (Rotovision, Crans, 1997), pages 30-37.
- [3] Franken, G., Podlesek, A., Možina, K.: "Eye-tracking Study of Reading Speed from LCD Displays: Influence of Type Style and Type Size", Journal of Eye Movement Research 8(1), 1-8, 2015.
- [4] Franken, G., Pangerc, M., Možina, K.: "Impact of Colour Combinations on LCD Display Legibility", Proceedings of AIC Lisboa 2018: colour & human comfort 2018, (AIC: Lisbon, 2018), page 6.
- [5] International Organization for Standardization, ISO 3664: Graphic technology and photography - Viewing conditions, International Organization for Standardization, 2009.
- [6] International Organization for Standardization, ISO 9241-303: Ergonomics of human-system interaction - Part 303: Requirements for electronic visual displays, International Organization for Standardization, 2012.
- [7] Keyes, E.: "Typography, color, and information structure", Technical Communication 4(4), 638-654, 1993.
- [8] Krauskopf, J.: "Color Vision: Color for Science, Art and Technology", (Elsevier, Amsterdam, 1998), pages 97-121.
- [9] McLean, R.: "The Manual of typography", (Thames and Hudson, London, 1996), page 60.
- [10] Mehta, R., Zhu, R. J.: "Blue or Red? Exploring the effect of color on cognitive task performances", Science, 323 (5918), 1226-1229, 2009. doi:10.1126/science.1169144.
- [11] Možina, K.: "Barva v tipografiji", Interdisciplinarnost barve, part 1, (Društvo koloristov Slovenije, Maribor, 2001), pages 341-364.
- [12] Možina, K.: "Knjižna tipografija", (University of Ljubljana Filozofska fakulteta, Oddelek za bibliotekarstvo in Naravoslovna fakulteta, Ljubljana, 2003), pages 109-212.

- [13] Možina, K., Medved, T., Rat, B., Bračko, S.: "Influence of Light on Typographic and Colorimetric Properties of Ink Jet Prints", *Journal of Imaging Sciences and Technology* 54 (6), 060403-1–060403-8, 2010. doi:10.2352/J.ImagingSci.Technol.2010.54.6.060403.
- [14] Pušnik, N.: "Vpliv barve in tipografije na hitrost zaznavanja napisov na konvencionalni in mobilni televiziji", PhD thesis, University of Ljubljana, Ljubljana, 2016.
- [15] Rat, B., Možina, K., Bračko, S., Podlesek, A.: "Influence of Temperature and Humidity on Typographic and Colorimetric Properties of Ink Jet Prints", *Journal of Imaging Sciences and Technology* 55(5), 050607-1–050607-8, 2011. doi: 10.2352/J.ImagingSci.Technol.2011.55.5.050607.
- [16] Rayner, K., Foorman, B., Perfetti, C., Pesetsky, D., Seidenberg, M.: "How Psychological Science Informs the Teaching of Reading", *Psychological Science in the Public Interest Monograph* 2, 31–74, 2001. doi: 10.1111/1529-1006.00004.
- [17] Reynolds, L.: "Legibility of Type", *Baseline* 10, 26-29, 1988.
- [18] Thussu, D. K.: "News as Entertainment: The rise of global infotainment", (Sage, London, 2007), pages 43-45.
- [19] Tracy, W.: "Letters of Credit: A View of Type Design", (David R., Boston, 2003), pages 30-32.
- [20] White, J. V.: "Color for impact", (Strathmoor Press, Berkeley, 1996), pages 3-22.



© 2018 Authors. Published by the University of Novi Sad, Faculty of Technical Sciences, Department of Graphic Engineering and Design. This article is an open access article distributed under the terms and conditions of the Creative Commons Attribution license 3.0 Serbia (<http://creativecommons.org/licenses/by/3.0/rs/>).

COMPRESSED SENSING AND SOME IMAGE PROCESSING APPLICATIONS

Aleš Hladnik¹ , Pavle Saksida² 

¹ University of Ljubljana, Faculty of Natural Sciences and Engineering,
Department of Textiles, Graphic Arts and Design, Ljubljana, Slovenia

² University of Ljubljana, Faculty of Mathematics and Physics, Ljubljana, Slovenia

Abstract: *We live in a digital media-overloaded world. An enormous number of images, sound and video files are continuously being created and either transmitted over the internet or stored on hard drives or portable storage devices. During their transmission or storage, however, such digital files are almost without an exception subjected to a process of discarding most of their original information, since e.g. fast opening of a web site image or a small audio file size are today of utmost importance. Loss in redundant or imperceptible information is therefore inevitable and incorporated in lossy compression algorithms such as JPEG, MPEG or MP3, but to record raw video or audio data only to be, in large part, soon discarded during the process of sending it to a receiver is obviously not an optimum approach. Compressed sensing is a signal processing technique that provides one solution to the above problem. Rather than performing acquisition followed by compression of a signal, it combines both steps in a single sensing – or sampling – operation. In other words, compressed sensing allows acquiring signals while taking only a few samples. One of the underlying assumptions of the signal is that it is sparse, i.e. it should be possible to represent it with a matrix, consisting of a large number of zero – or close to zero – coefficients. Images, when represented in a non-spatial domain, such as discrete cosine- or wavelet-domain, often comply with such a requirement.*

Theory behind the compressed sensing will be presented briefly together with several examples of successful implementation of this method in the field of signal – mainly image – processing.

Key words: compressed sensing, image acquisition, sparsity, signal processing

1. INTRODUCTION

The number of digital media files, such as still images, sound and video clips that are created every day is astonishing. For example, in 2017 every minute more than 400 hours of video were uploaded to YouTube, and 136,000 and 46,740 photos were uploaded on Facebook and Instagram, respectively (Schultz, 2017). However, the vast majority of this data is discarded during the process of its compression in order to secure its fast network transmission or a compact file storage on hard drives or portable storage devices. Loss in redundant or imperceptible information is therefore inevitable and incorporated in widely used lossy compression algorithms such as JPEG, MPEG or MP3. This traditional approach consisting of a raw data acquisition followed by its compression therefore seems wasteful; one can argue whether it would be possible to directly acquire just the useful part of a signal?

1.1 Compressed sensing

Compressed sensing (CS), also known as *compressive sensing/sampling* and *sparse sampling*, is a signal processing technique developed in years 2004-2006 (Candes et al, 2006) that attempts to solve this problem. In the conventional signal acquisition and compression scheme (Figure 1 left), a signal consisting of N samples (e.g. pixels in an image) is compressed producing a much smaller number of K elements (e.g. discrete Fourier transform (DFT), cosine transform (DCT) or wavelet transform (DWT) coefficients), which are transmitted from the sender to the receiver where a decompression – reconstruction – takes place, resulting in an approximation of the original signal, with a hopefully no significant perceptual difference to the original. In the CS workflow (Figure 1 right), on the other hand, signal acquisition and compression operations are merged – or rather substituted by – a single sensing (sampling) step. Here N samples are replaced by M measurements, which are then, similar to the conventional workflow, sent over the network and used to perform the reconstruction of the signal. Note that $K < M \ll N$. It can be shown (Candes et al., 2006) that the reconstruction is perfect (exact) as long as $M = O(K \cdot \log(N/K))$; see Figure 2. Two important prerequisites for CS to work are *sparsity* and *incoherence* and are discussed below.

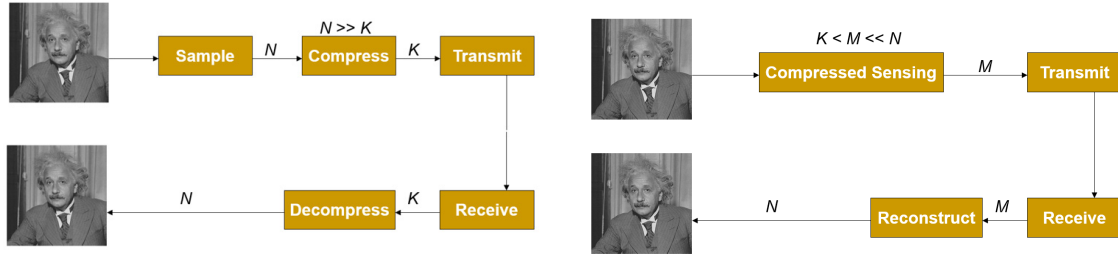


Figure 1: Conventional signal acquisition and compression scheme (left) and CS workflow (right) (Mancera, 2008).

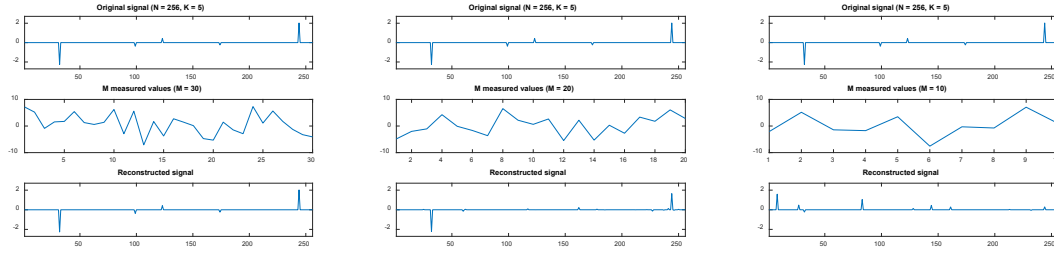


Figure 2: Original 1D signal has 5 non-zero values ($K = 5$). As the number of random measurements M decreases ($30 \rightarrow 20 \rightarrow 10$), signal reconstruction deteriorates and becomes suboptimal when $M < 20$. This is in agreement with the formula $M = O(K \cdot \log(N/K))$, since the computed value for M is 19.68.

1.2 Signal reconstruction

In principle, signal reconstruction is based on the idea of finding a solution to an underdetermined linear system $y = \Phi x$ (Figure 3 left) (Milliarde, 2016), where for the CS purposes y and x represent measurement and signal vectors, respectively, while Φ is a sampling/sensing matrix, also known as a *dictionary*. Such a system is characterized by having fewer equations than unknowns – $M < N$ – and generally has an infinite number of solutions. However, by imposing certain constraints to the system, the CS framework allows obtaining one particular solution. One such constraint is that the signal x is K -sparse, i.e., it must be possible to represent it with a vector, consisting of a large number of zero – or close to zero – coefficients and only K non-zero values. Digital images, when represented in a non-spatial, i.e. transform domain, such as discrete cosine- or wavelet-domain, often comply with such a requirement. If this is the case, the scheme shown in Figure 3 (right) applies. Here Ψ denotes a representation matrix corresponding to – when the signal is an image – DFT, DWT or DCT matrix coefficients. Φ is, as mentioned above, a dictionary consisting of randomly distributed values or, less often, of predetermined sequences, such as pseudo-random codes, binary codes, noiselets, etc. The second CS prerequisite is that the two orthonormal bases Φ and Ψ are incoherent, i.e. poorly correlated to each other.

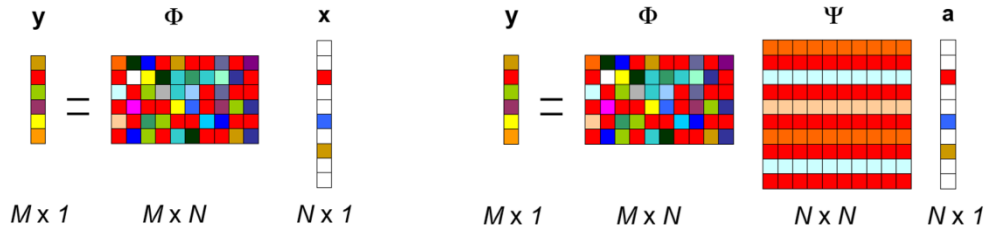


Figure 3: A general underdetermined linear system of equations $y = \Phi x$ having an infinite number of solutions (left) and a CS scheme $y = \Phi \Psi a$ where it is possible to obtain \hat{a} using numerical optimization routines (right).

From $y = \Phi \Psi a$ one can recover a , i.e. compute \hat{a} , by solving Eq. 1:

$$\hat{a} = \arg \min_a \{ \|a\|_0 \text{ s.t. } y = \Phi \Psi a \} \quad (1)$$

Since this is a computationally complex combinatorial (NP-hard) problem, various approximations using rather involved numerical non-linear optimization algorithms have been implemented (Adcock, 2015). Going into these techniques is beyond the scope of this introductory paper. One of the widely adopted approaches is the minimization of L_1 -norm (known as *Basis pursuit*), which leads to the sparsest solution. Vector \hat{a} obtained through this procedure has to be transformed back into the spatial domain, to obtain the conventional image representation.

2. RESULTS AND DISCUSSION

2.1 1D signal reconstruction

First, let's take a look at how we can reconstruct a 1D signal of length $N = 256$, such as a sound wave (Figure 4a) by means of CS. Unlike in Figure 2, the signal of interest is now in the frequency – DFT – domain (Figure 4b). It has six peaks, corresponding to the three frequencies ($K = 3$) contained in the original, time domain, signal: 31, 98 and 122. This is due to the fact that each real-valued sinusoid is equivalent to two complex sinusoids of frequency f and $-f$ and consequently has two peaks in the frequency domain. By performing 64 random measurements M (Figure 4c) it is possible to recover the signal in the frequency domain (Figure 4d) and – via inverse DFT – in the time domain (Figure 4e) perfectly. When the number of non-zero elements in the sparse representation of the same signal is raised to five ($K = 5$; frequencies: 21, 31, 39, 98, 122), however, the reconstruction with 64 measurements is no longer satisfactory (Figure 5) and M has to be increased as well to secure a perfect recovery.

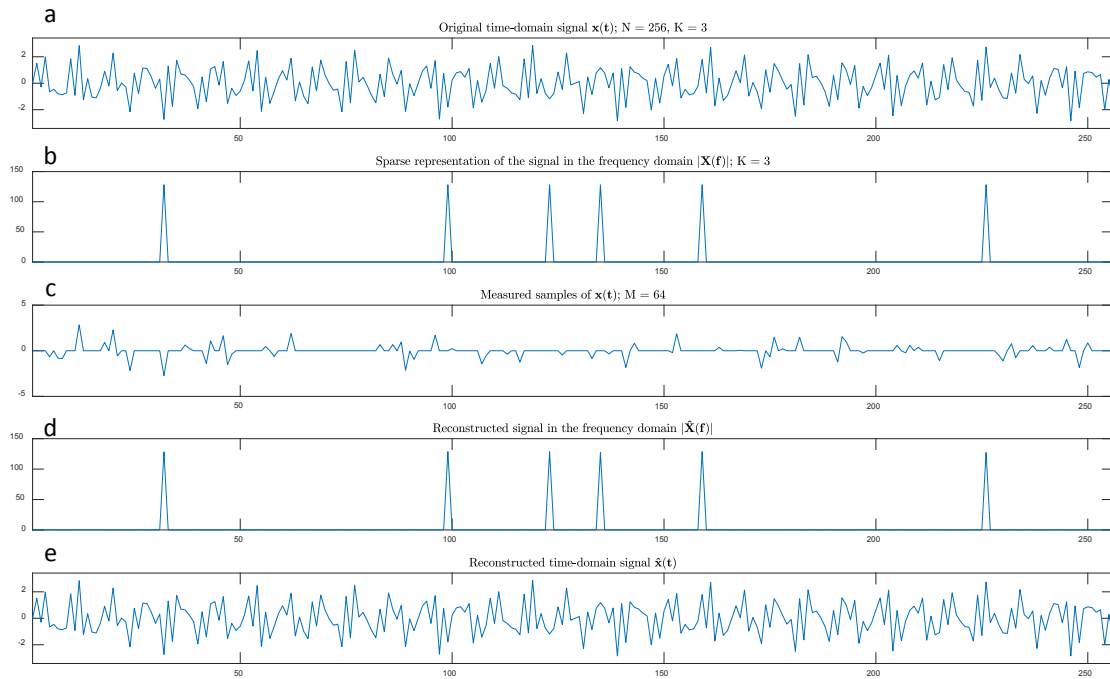


Figure 4: Perfect reconstruction of a 1D signal with $N = 256$, $M = 64$, $K = 3$.

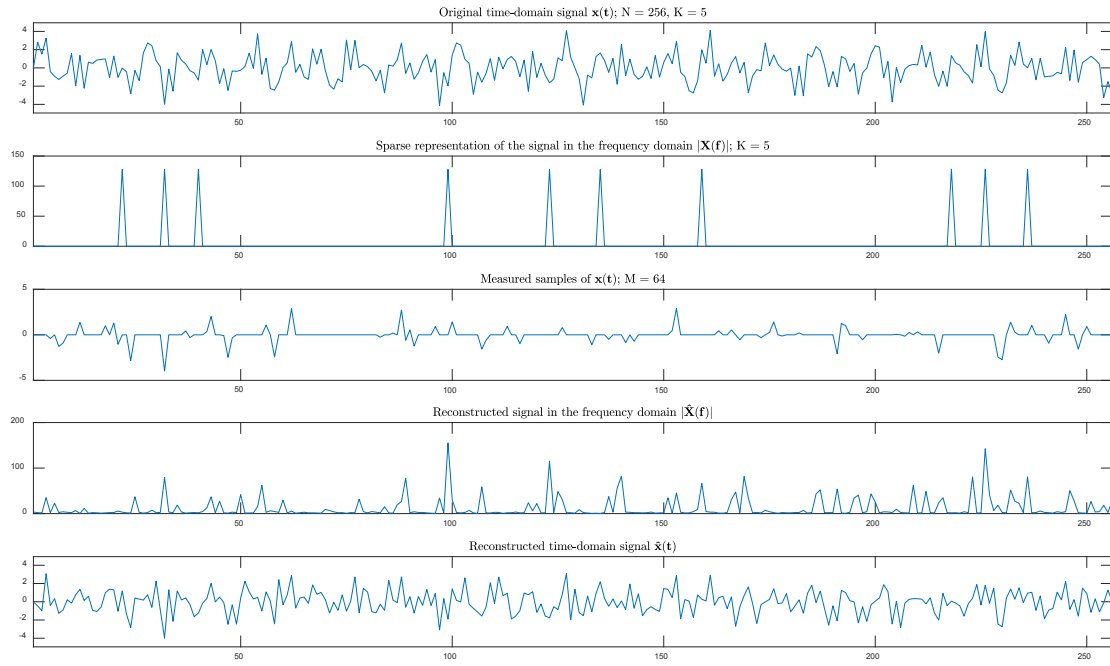


Figure 5: Approximate reconstruction of a 1D signal with $N = 256$, $M = 64$, $K = 5$.

2.2 2D signal reconstruction

The procedure for reconstructing a 2D spatial domain signal, such as a digital photograph, is in principle similar to the recovery of a 1D time domain signal shown above and is demonstrated here using a MATLAB code (Gibson, 2013) and a well known *cameraman* test image (Figure 6). For the sake of simplicity it is assumed that the image is sparse – strictly speaking, *compressible* – in the DCT domain (ψ is a DCT matrix); note that in general, it is more likely for a DWT-, rather than a DCT-, representation of a real-scene image that the assumption of sparsity is met. Dictionary Φ is a matrix of normally distributed random measurements. Due to certain computational issues, instead of reconstructing the whole image, only the two 50 x 50 px regions, i.e. subimages, were processed ($N = 2500$). The number of measurements M was $N/2$, $N/4$ and $N/6$, respectively. For obtaining \hat{a} , two approaches were adopted: L_1 -norm minimization (Basis pursuit; BP) and L_2 -norm minimization (Least squares solution; LS). Results are displayed in Figure 6.

It is evident that the Basis pursuit algorithm outperforms the Least squares approach by a large margin. Contrary to the latter one where even with $M = N/2 = 1250$ the reconstructed image is extremely noisy and of a poor quality, the application of the former one leads to an acceptable reconstruction of the image regions – especially where lower frequencies dominate, such as in the subimage displaying the man's coat – even with $M = N/4 = 625$. Of course, when the number of measurements M decreases too much, it becomes unlikely that the K -sparse signal will be recovered with a high precision.

With an additional mathematical effort it is possible to improve CS image reconstruction results even further. By implementing a more sophisticated numerical optimization algorithm OWL-QN (Galen et al, 2003) in Python, the author (Pyrunner, 2016) was able to quite successfully reconstruct the 1600 x 1200 px Escher-Wyss' image *Waterfall* by randomly taking only 10% of the samples (= measurements); see Figure 7 left. The image is recognizable even when starting from as little as 1% of the available data (Figure 7 right).

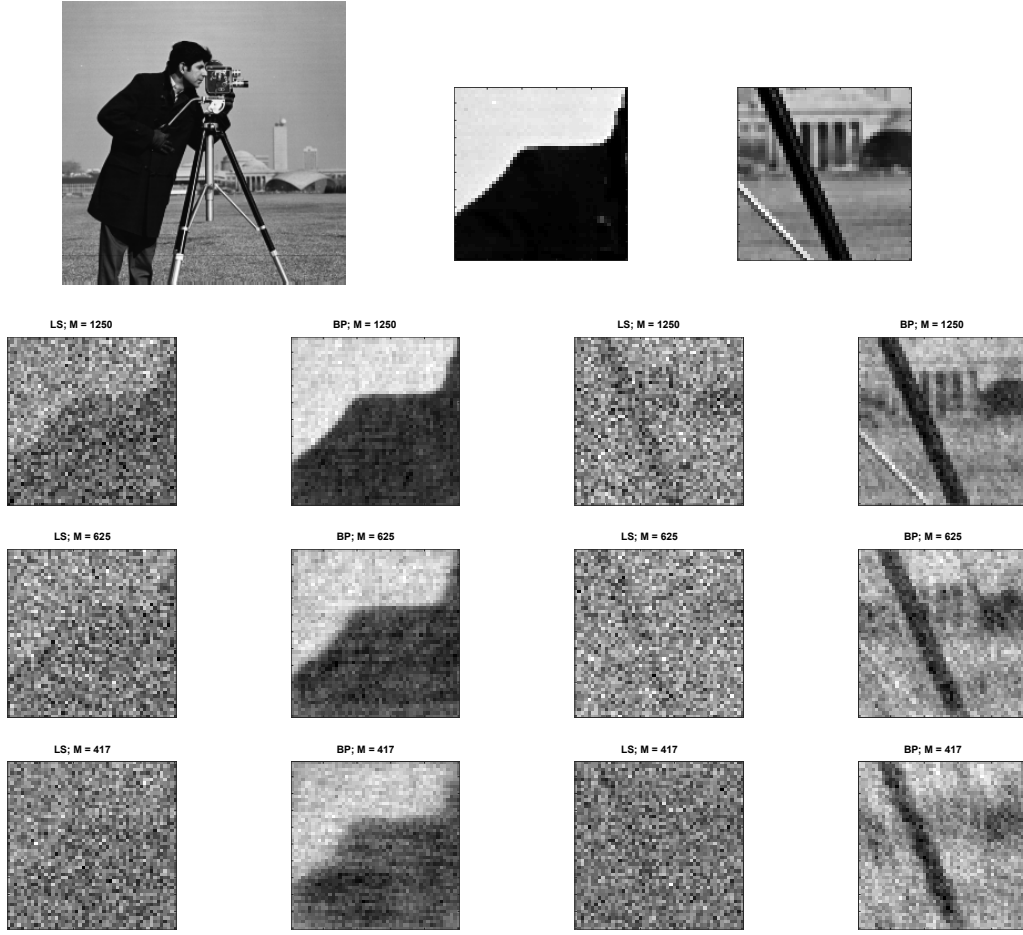


Figure 6: Image reconstruction results using minimization of L_1 -norm and L_2 -norm with $N = 2500$ and three different M values: $N/2$, $N/4$ and $N/6$.

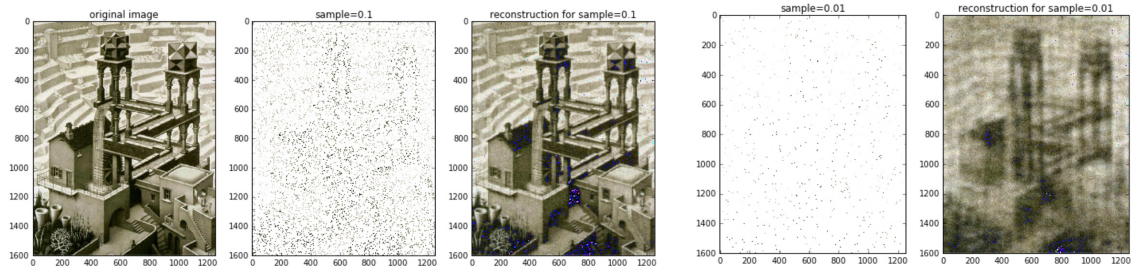


Figure 7: Image reconstruction results with advanced mathematical optimization: recovery from 10% (left) and 1% (right) of the original image data (Pyrunner, 2016).

As discussed above, one of the strengths of CS is that it allows acquiring signal a while taking only a few measurements y – see Figure 3b. This is especially beneficial and applicable in imaging techniques such as Magnetic resonance imaging (MRI). MRI uses magnetic fields to excite hydrogen atoms in the patient's body, resulting – after modelling – in measurements of the DFT of the image. Since the number of measurements is roughly proportional to the scan duration, longer scans are unpleasant for the patient, more prone to motion artifacts and consequently virtually impossible for certain moving body parts, e.g. lungs (Adcock, 2015). It is therefore highly desirable that the number of measurements – i.e. the scanning time – is as low as possible. Figure 8 shows an early example of a CS reconstruction (Mancera, 2008). The recovered image is clearly sharper and has less artifacts compared to the result obtained using the alternative – back-projection reconstruction – algorithm (Wikipedia, 2018).

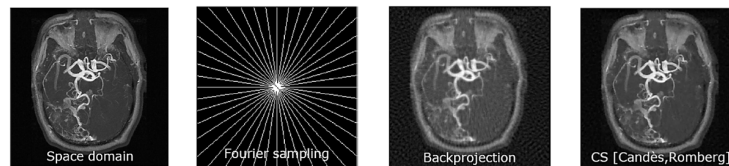


Figure 8: Magnetic resonance imaging – reconstruction results using backprojection- and CS approach.

3. CONCLUSIONS

CS is a signal processing technique that uses a sparse signal, which can be sampled at a rate less than the Nyquist-Shannon sampling rate, in order to reconstruct the signal via a constrained optimization method, such as L_1 -norm. It has during the last ten years developed into a rich research area of itself spanning a wide variety of applications, such as photography, computer tomography, transmission electron microscopy, radio interferometry, and many others. Developing new applications as well as new recovery algorithms remains an active field of research.

4. REFERENCES

- [1] Adcock, B.: "An introduction to compressed sensing", URL: <http://benadcock.org/wp-content/uploads/2015/11/AdcockBeijingTalk1.pdf> (last request: 2018-09-05).
- [2] Candès, E. J., Romberg, J. K., Tao, T.: "Stable signal recovery from incomplete and inaccurate measurements", Communications on Pure and Applied Mathematics, 59 (8), 1207–1223, 2006. doi: 10.1002/cpa.20124.
- [3] Galen, A.; Gao, J.: "Scalable training of L_1 -regularized log-linear models", Proceedings of the 24th international conference on Machine learning 2007, (ICML, Oregon, USA, 2007.)
- [4] Gibson, S.: "Simple Compressed sensing example", URL: <https://www.mathworks.com/matlabcentral/fileexchange/41792-simple-compressed-sensing-example> (last request: 2018-09-05).
- [5] Mancera, L.: "Compressed Sensing", URL: decsai.ugr.es/vip/files/presentations/20080701-CS.pps (last request: 2018-09-10).
- [6] Milliarde: "Compressed Sensing Intro & Tutorial w/ Matlab", URL: <https://www.codeproject.com/Articles/852910/Compressed-Sensing-Intro-Tutorial-w-Matlab> (last request: 2018-09-10).
- [7] Pyrunner: "Compressed Sensing in Python", URL: <http://www.pyrunner.com/weblog/2016/05/26/compressed-sensing-python/> (last request: 2018-09-10).
- [8] Schultz, J.: "How Much Data is Created on the Internet Each Day?", URL: <https://blog.microfocus.com/how-much-data-is-created-on-the-internet-each-day/> (last request: 2018-09-10).
- [9] Wikipedia: "Tomographic reconstruction", URL: [https://en.wikipedia.org/wiki/Tomographic_reconstruction#Back_Projection_Algorithm\[2\]](https://en.wikipedia.org/wiki/Tomographic_reconstruction#Back_Projection_Algorithm[2]) (last request: 2018-09-05).



GRADATION, COLOUR RANGE AND COLORIMETRIC ACCURACY OF DIGITAL PROJECTOR JVC DLA-RS 15

Iva Molek¹ , Dejana Javoršek² 

¹Multimedia and Graphic Technology Secondary School, Ljubljana, Slovenia

²University of Ljubljana, Faculty of Natural Sciences and Engineering, Ljubljana, Slovenia

Abstract: Nowadays, digital projectors are used for displaying static and dynamic content, while operating with a wide range of different projection technologies. Presentation methods are also used to present important colour reproductions where the colours should be displayed accurately. The purpose of our research was to improve the colour quality of presentation and to define display of colour in digital projection. For that purpose high quality digital projector JVC DLA-RS15 was used. According to standard ISO 12646: 2010, was researched the display of colours in digital projection. For the colorimetric analysis of the displayed colours, the spectrophotometer i1Pro and the spectroradiometer PR-650 were used. Since the vast majority of digital photographs is captured and displayed in the standardized sRGB colour space, we investigated how well the sRGB colour space is displayed using JVC DLA-RS15 digital projector and whether the standard could be achieved by profiling its modules. Based on the results of our research, it was found out that spectroradiometer PR-650 always shows the same results regardless of the measuring distance. However, in case of the spectrophotometer i1Pro, it proved best to perform measurements and profiling so that the measuring distance equals to the projection distance. The monitoring and the evaluation of digital projections based on chromaticity, gradation, channel and grey balance and colour range according to the standard ISO 12646:2010 is quite demanding and time-consuming. It has also been found that a large colour gamut of saturated primary colours at digital projector does not guarantee the quality of the displayed colours in the standard sRGB colour space.

Key words: digital projector, colorimetric analysis, profiling, colours

1. INTRODUCTION

Projectors have become an important part of every serious presentation. Nowadays digital projectors are used to project static and dynamic contents, and function with the help of a wide array of various projection technologies and modules respectively. With the aid of the digital projection modules we can choose from different pre-set options; some projectors can be geometrically calibrated (manual setting of contrast, brightness, correlated colour temperature) and characterized (Ashdown et al, 2018; Cooper, 2016; Matt, 2003; Wikipedia, 2018). In reference to the testing of digital projectors, only the source (Park & Park, 2010) is summarized. According to the ISF (Turk, 2018) specification for certification, the most precise rendering of six colours has been achieved so far with a colour difference of 1-3 with the default settings and a colour difference of 0.5 with the created profile (for all six re-produced colours) with the JVC DLA-RS25 digital projector. The source does not specify the details of the test methods, the method of measurement, or the calculation of the colour difference – the only information that is given is that the ISF calibrator is certified (Turk, 2018).

Experience and some sources (Matt, 2003) suggest that the calibration and profiling of a digital projector with visual evaluation can improve the display of colours. Other sources (Turk, 2018) indicate excellent results, but they probably only apply to the six basic colours, whereas there is no source that would deal with objective colorimetric evaluation of a digital projection based on the representation of real colours in different observation conditions.

The purpose of our research was to improve the colour quality of presentation and to define display of colour in digital projection. For that purpose high quality digital projector JVC DLA-RS15 was used.

The JVC DLA-RS15 belongs to the category of home theatre projectors (Turk, 2018; Feierman, 2018). It is based on liquid crystal technology on LCoS silicon. The rendering resolution of the projector is very high, up to 1920 × 1200 pixels, if such resolution is also supported by the computer. The projector has six modules for watching movies, i.e. Cinema 1, Cinema 2, Cinema 3, Natural, Stage and Dynamic. In the projector menu, a colour temperature of 5800 K, 6500 K, 7500 K, 9300 K, High Bright, Custom 1, 2, 3 (custom settings) can also be determined within the individual modules. The projector menu also includes gamma and grey (channel) balance settings. The JVC DLA-RS15 does not have full support for colour management (CMS); it only allows calibration of the channel (grey) level.

2. EXPERIMENTAL PART

For measurements of projected colours according to standard SIST ISO 12646:2010 (Feierman, 2018), was used: following equipment: digital projector JVC DLA-RS15, personal computer with Power Point, Reflecta projection, spectrophotometer i1Pro placed on a photographic tripod with applications i1Share and KeyWizard, spectroradiometer PR-650 placed on a photographic tripod and measurement charts according to standard. Standard ISO 12646:2010 (Graphic technology – Displays for colour proofing – Characteristics and viewing conditions) (Cooper, 2016) includes provisions for observing conditions in screen preview of printed material and soft proofing respectively. Because of the extensiveness of the standard, merely the measurements of gradation, colour range and colorimetric accuracy are focused on and performed a test of light conditions prior to measurements and profiling. Tests were performed in studio of Multimedia and Graphic Technology Secondary School.

First, the light conditions were tested. The white screen DPT-W315 was projected onto the projection screen. The brightness was measured in the middle of the projection, and on the left and the right for half the width of the projection outside the screen. The condition of the brightness (Lv) of the external field surrounding the screen was always fulfilled irrespective of the instrument, the measurement distance and the spatial conditions. With the already projected measuring plate (DPT-W315), we also measured the brightness (Lv) of the inner white field, i.e., the projection screen without projection. This condition was always fulfilled. Then the colour plate DPT-K315 was projected. The brightness was measured in the middle of the projection, and then the digital projector was turned off and measured the brightness again. With the JVC DLA-RS15, the standard was fully complied with.

After 45 minutes of heating the projector measurements of the unprofiled projection were performed. Calibration and profiling of the digital projector were performed using well-established applications i1Match 3.6 and basicColor display 4.1.22 in combination with spectrophotometer EyeOne Pro (i1Pro).

In the measurements, we focused on the default and reset projection modules of the selected projector:

- Natural Module: CCT: 6500 K, Gamma 1.0, Diaphragm 3
- Natural HB: Contrast: default, CCT: High Bright, Flash: 3, Bulb: High (200 W), Gamma: normal
- Natural 2.2: Contrast is default, CCT: 6500 K, Flash: 3, Bulb: High (200 W), Gamma: 2.2
- User1: Contrast: +50, CCT: High Bright, Flash: 3, Gamma: normal (Park et al, 2010)
- User-2: Contrast: -1 Brightness: 1 Saturation: -12 Hue: 0, CCT (gain R = 9, G = -7, B = -21; -1), Gamma: normal, Flash: 3, Bulb: High (200 W) (Park et al, 2010)

Prior to each measurement, the DPT-W315-T colour plate was projected on the projection screen, and instantly measured using the instrument with the target in the middle of the central field 5. We started with gradation measurements by projecting the colour plates (Figures 1a and 1b) of the centred grey fields (DPT-gamal (100-0) has 21 centred grey fields in the range R = G = B with values from 255 to 0) one by one to the projection screen. We measured the standardized colour values X, Y, Z, and calculated the gamma, which should be in the range of 1.8-2.4.

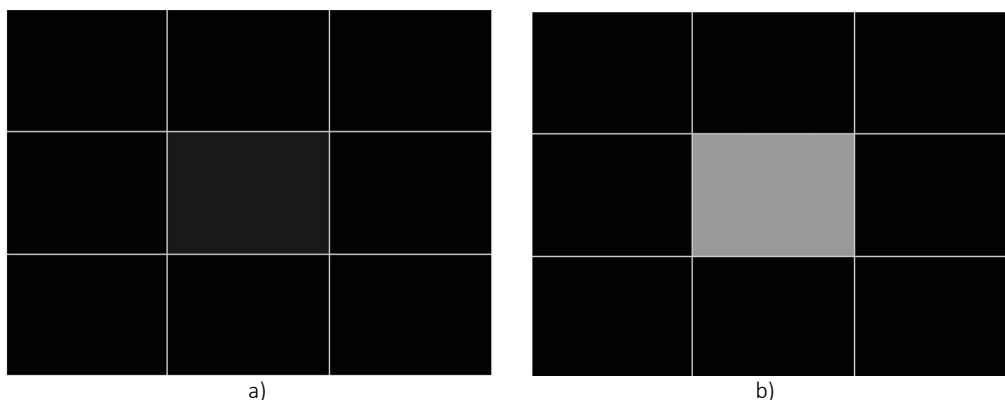


Figure 1: Colour chart for measuring gradations: a) DPT-gammaL (25) and b) DPT-gammaL (135)

For defining the colour range of the digital projector, the DPT-SPC colour charts (Fig. 2a and 2b) were projected one after the other (DPT-SPC colour plates have eight centred fields with primary R, G, B and secondary C, M, Y colours, including white colour W and black colour K. On each one, the standardized

colour values of X, Y, Z of the central field were measured. The chromatic coordinates x, y, and u', v' were calculated, so that the brightness of white colour is defined with $L^* = 100$.

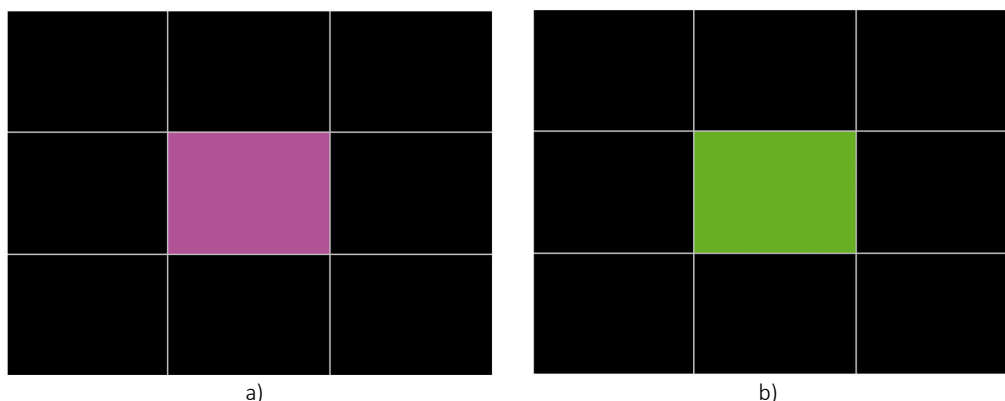


Figure 2: The colour charts for measuring the gamut: a) magenta and b) green.

The colorimetric accuracy of the digital projection was evaluated by using the 24 fields of the Colour Checker Classic colour chart. One after another, colour charts were projected to the screen (Figures 3a and 3b) and standardized colour values X, Y, Z of the central field were measured on each of them. Colour differences ΔE^*_{ab} between the displayed and reference values were calculated.

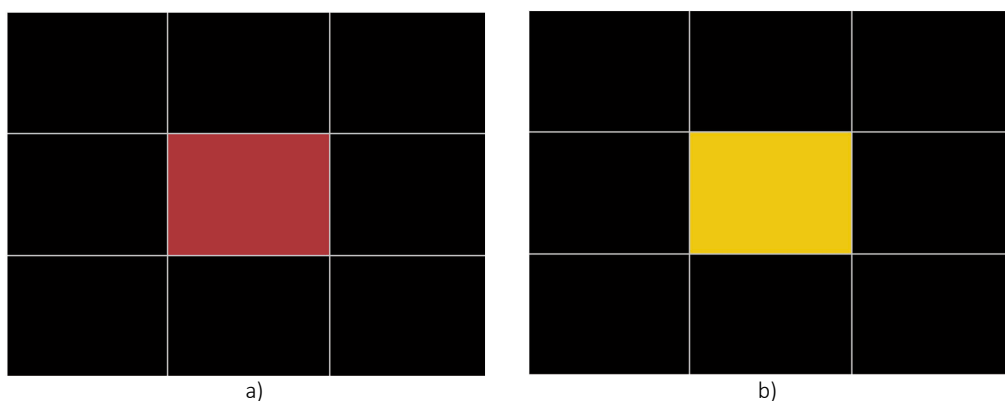


Figure 3: Colour Checker Classic colour charts a) Patch 15 Red and b) Patch 18 yellow

3. RESULTS AND DISCUSSION

3. 1 Gradation

In all projection modules, except in User-1, gamma is within the desired range, as can be seen in Figure 4. Since the projector settings also allow the gamma to be adjusted, an additional test with reset gamma 2.2 was performed, the Natural 2.2 module. It turned out that this setting had no effect neither on the value of the gamma nor on the display of tones, i.e., gradation. An essential change is noted in gradation in the User-1 module with the High Bright white tile reciprocal temperature and the increased contrast +50, which was set to ensure the highest possible brightness (L_v) of the white tile and thus approximate the requirements of the sRGB standard, however, such settings lead us to unwanted display of tones.

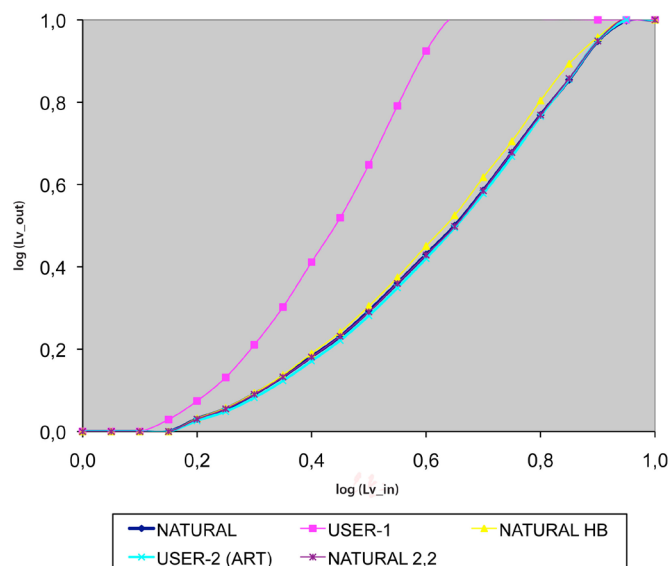


Figure 4: Gradation of the digital projector JVC DLA-RS15.

3.2 Colour gamut

It is clear from Figure 5 that all JVC DLA-RS15 digital projector modules feature exceptionally large colour scale, substantially larger than the standardized sRGB colour scale (sRGB: IEC mark). In Figure 6 in the diagram L^* (C^*uv) in yellow colour, we see that the colour is very saturated and almost as bright as white. All these are the consequences of the noticeably low brightness (L_v) of the JVC DLA-RS15 digital projector.

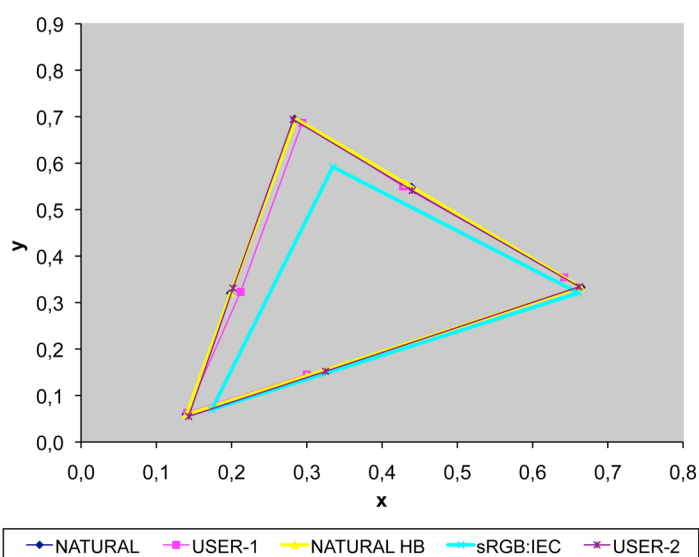


Figure 5: Colour gamut of the digital projector JVC DLA-RS15 presented CIE 1931 x,y chromatic diagram.

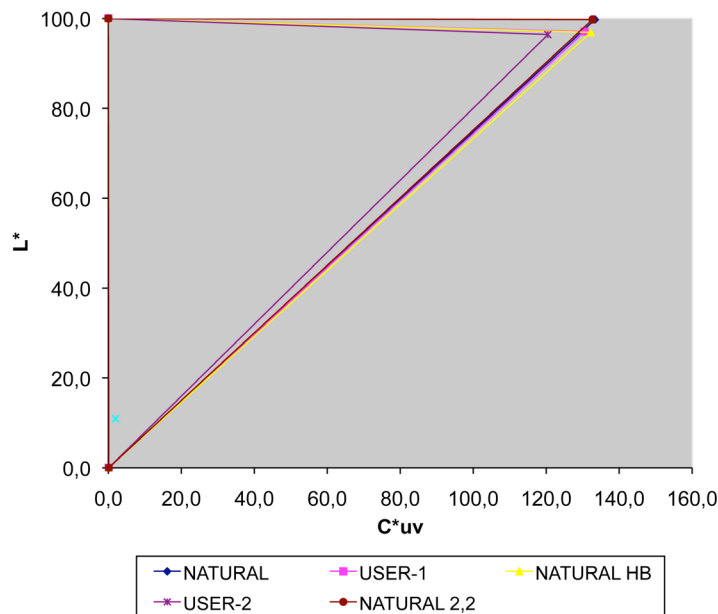


Figure 6: Brightness in relation to chrome for yellow of the digital projector JVC DLA-RS15.

3. 3 Colorimetric accuracy according to the ISO 12646:2010 Standard

Table 1 shows the results of the measurements using the spectroradiometer and the spectrophotometer. In measurements with the spectroradiometer, it was found that the colours were displayed best in the Natural module with an average dE^*ab 11.83 and a maximum dE^*ab 30.04. As expected, the colours were displayed worst in the User-1 module with an average dE^*ab 23.0 and the maximum dE^*ab 58.0. In the spectrophotometer measurements we found that Colour Checker Classic colours are best shown in User-2 module with an average dE^*ab 11.72 and a low maximum dE^*ab 17.58. They are followed by the default Natural module with an average dE^*ab 13.05 and the maximum dE^*ab 35.22, and the Natural HB module with an average dE^*ab 14.54 and the maximum dE^*ab 40.32.

This was followed by profiling the Natural HB module with different combinations of software and measurement technology. The Natural HB module was chosen to continue the tests, because it displays the tones somehow brighter than other modules. Measurements were performed with a spectroradiometer and spectrophotometer.

It is apparent from Table 2 that no combination of an application or a programme and a profiling instrument substantially improves the average colour deviation that, when measured with a spectroradiometer in the Natural HB module, comes to an average of dE^*ab 12.7 and a maximum of dE^*ab 41.09. It is slightly exceeded by the colour profile of basICC display 4.1.22 + i1Pro with an average dE^*ab 12.0 and a maximum dE^*ab 24.7, which is better compared to the maximum dE^*ab 41.1 without profile (Natural HB without profile). In both cases, the yellow colour in the field 16 with an average dE^*ab 41.09 without the profile and with an average dE^*ab 24.67 with the basICC display 4.1.22 + i1Pro profile deviates the most. The situation remains the same when measuring the displayed colours with the spectrophotometer. The results are shown in Table 3, except that the average dE^*ab values of the achieved colour differences are slightly higher: the colour profile basICC display 4.1.22 + i1Pro again performs best with an average dE^*ab 15.73 and a maximum dE^*ab 26.37.

Table 1: The colorimetric accuracy of digital projector JVC DLA-RS15 module, evaluated by Color Checker Classic chart, measured by PR-650 and i1Pro; yellow colour marks the dE^*ab values, lower than 5

Color Checker Classic	ΔE^*ab ; PR-650				ΔE^*ab ; i1Pro			
	Natural	User-1	Natural HB	User-2	User-1	Natural	User-2	Natural HB
Polje 1 (Dark skin)	7.47	12.39	4.03	7.42	8.89	8.44	7.38	11.36
Polje 2 (Light skin)	9.66	25.01	5.23	10.02	23.61	10.94	10.31	14.49
Polje 3 (Blue Sky)	8.48	21.48	9.90	9.03	18.69	9.54	10.93	10.11
Polje 4 (Olive Green)	9.07	22.96	9.44	8.71	19.19	10.32	9.83	11.69
Polje 5 (Violet)	8.19	19.95	8.99	9.51	18.34	9.30	11.91	10.43
Polje 6 (Bluish Green)	12.95	17.01	10.94	11.80	12.85	11.88	13.17	10.53
Polje 7 (Orange)	18.85	42.23	20.19	13.62	39.69	18.65	11.17	19.60
Polje 8 (Purplish Blue)	7.55	19.07	10.25	9.83	17.90	9.27	12.98	9.84
Polje 9 (Moderate Red)	6.53	18.29	7.51	9.80	18.21	8.79	9.11	13.40
Polje 10 (Purple)	9.29	25.07	13.38	7.68	20.41	11.20	8.86	13.86
Polje 11 (Yelow Green)	16.00	22.08	18.52	11.41	20.72	16.88	16.47	17.10
Polje 12 (Orange Yellow)	25.61	57.99	31.80	16.10	56.03	24.99	14.03	30.12
Polje 13 (Blue)	8.77	29.39	14.76	8.46	23.38	10.42	13.45	11.35
Polje 14 (Green)	11.83	32.48	13.97	10.59	27.19	11.93	13.43	12.30
Polje 15 (Red)	11.70	13.22	6.97	9.03	8.62	10.88	8.41	9.03
Polje 16 (Yelow)	30.04	40.76	41.09	38.09	39.99	35.22	17.58	40.23
Polje 17 (Magenta)	7.66	24.48	12.15	9.46	23.04	10.34	13.27	15.33
Polje 18 (Cyan)	5.52	24.30	6.64	8.74	20.63	5.30	11.46	13.56
Polje 19 (White)	20.97	15.16	15.86	18.67	18.45	20.12	16.10	20.10
Polje 20 (Neutral 8)	13.93	8.02	10.98	11.84	9.21	13.51	13.41	13.86
Polje 21 (Neutral 6,5)	10.55	18.70	10.22	9.37	16.51	10.60	11.37	12.07
Polje 22 (Neutral 5)	8.16	19.71	8.88	7.93	15.83	9.12	9.39	10.74
Polje 23 (Neutral 3,5)	6.83	15.25	6.79	7.94	12.60	8.97	8.08	11.07
Polje 24 (Black)	8.39	6.23	6.21	9.68	9.79	16.67	9.23	16.76
All colours								
Mx ¹ dE*ab	11.83	22.99	12.69	11.45	20.82	13.05	11.72	14.54
Max ² dE*ab	30.04	57.99	41.09	38.09	56.03	35.22	17.58	40.32
Tones only								
Mx ¹ dE*ab	11.47	13.84	9.82	10.91	13.72	13.17	11.26	14.10
Max ² dE*ab	20.97	19.71	15.86	18.67	18.45	20.12	16.10	20.10
¹ Mx - average value, dE*ab = 5.								
² Max - maximum value, dE*ab =10.								

Table 2: The colorimetric accuracy of the profiled module Natural HB of the JVC DLA-RS15 digital projector, evaluated with Color Checker Classic chart, measured with PR-650; yellow colour marks the dE^*ab values, lower than 5

Color Checker Classic	ΔE^*ab ; PR-650			
	Natural HB	Natural HB	Natural HB	Natural HB
	Without profile	i1ProBeamer	basIcCcolor display 4.1.22 + i1Pro	basIcCcolor display 4.1.22 + Spyder3)
Patch 1 (Dark skin)	4.03	8.32	7.03	7.43
Patch 2 (Light skin)	5.23	14.41	13.52	14.40
Patch 3 (Blue Sky)	9.90	11.45	10.12	10.60
Patch 4 (Olive Green)	9.44	10.00	8.49	9.00
Patch 5 (Violet)	8.99	12.54	11.08	11.68
Patch 6 (Bluish Green)	10.94	17.49	16.08	16.80
Patch 7 (Orange)	20.19	13.82	13.62	13.90
Patch 8 (Purplish Blue)	10.25	10.79	9.94	10.02
Patch 9 (Moderate Red)	7.51	11.43	10.23	11.03
Patch 10 (Purple)	13.38	7.13	5.79	6.42
Patch 11 (Yelow Green)	18.52	16.79	15.68	16.09
Patch 12 (Orange Yellow)	31.80	16.97	17.20	17.55
Patch 13 (Blue)	14.76	9.13	8.21	7.98
Patch 14 (Green)	13.97	13.36	11.85	12.47
Patch 15 (Red)	6.97	8.71	7.56	7.77
Patch 16 (Yelow)	41.09	30.64	24.67	27.36
Patch 17 (Magenta)	12.15	12.23	11.29	11.82
Patch 18 (Cyan)	6.64	10.60	9.42	9.69
Patch 19 (White)	15.86	23.69	22.93	22.85
Patch 20 (Neutral 8)	10.98	18.98	18.30	18.08
Patch 21 (Neutral 6,5)	10.22	14.72	13.83	13.94
Patch 22 (Neutral 5)	8.88	11.05	9.85	10.28
Patch 23 (Neutral 3,5)	6.79	8.44	6.67	6.95
Patch 234 (Black)	6.21	5.76	4.70	5.03
All colours				
Mx ¹ dE*ab	12.69	13.27	12.00	12.46
Max ² dE*ab	41.09	30.64	24.67	27.37
Tones only				
Mx ¹ dE*ab	9.82	13.77	12.72	12.85
Max ² dE*ab	15.86	23.69	22.93	22.85
¹ Mx - average value, $dE^*ab = 5$. ² Max - maximum value, $dE^*ab = 10$.				

Table 3: The colorimetric accuracy of the profiled module Natural HB of the JVC DLA-RS15 projector, evaluated with Color Checker Classic chart, measured by i1Pro.

Color Checker Classic	ΔE^*ab ; i1Pro					
	Natural	Natural HB	Natural HB	Natural HB	Natural HB	Natural HB
	Without profile	Without profile	i1ProBeamer	Spyder3Elite 4.0.2	basICColor display 4.1.22 + i1Pro	basICColor display 4.1.22 + Spyder3)
Patch 1 (Dark skin)	8.44	11.36	13.99	13.99	12.07	12.77
Patch 2 (Light skin)	10.94	14.49	17.96	19.44	17.15	18.06
Patch 3 (Blue Sky)	9.54	10.11	13.85	14.83	13.17	13.63
Patch 4 (Olive Green)	10.32	11.69	13.34	12.23	11.66	12.53
Patch 5 (Violet)	9.30	10.43	15.80	16.41	14.54	15.14
Patch 6 (Bluish Green)	11.88	10.53	18.96	19.95	18.56	19.26
Patch 7 (Orange)	18.65	19.60	17.15	17.11	17.05	17.39
Patch 8 (Purplish Blue)	9.27	9.84	16.57	18.26	14.88	14.95
Patch 9 (Moderate Red)	8.79	13.40	16.36	18.72	15.25	16.17
Patch 10 (Purple)	11.20	13.86	12.03	11.53	10.42	11.91
Patch 11 (Yellow Green)	16.88	17.10	19.39	21.02	19.08	19.38
Patch 12 (Orange Yellow)	24.99	30.12	19.65	20.59	19.71	20.16
Patch 13 (Blue)	10.42	11.35	15.52	17.19	14.05	13.43
Patch 14 (Green)	11.93	12.30	15.28	17.76	14.53	15.39
Patch 15 (Red)	10.88	9.03	14.13	16.53	12.25	13.20
Patch 16 (Yellow)	35.22	40.23	24.87	29.97	26.37	29.04
Patch 17 (Magenta)	10.34	15.33	16.72	19.21	16.31	16.79
Patch 18 (Cyan)	5.30	13.56	12.96	13.73	11.84	12.30
Patch 19 (White)	20.12	20.10	26.29	24.59	25.88	26.12
Patch 20 (Neutral 8)	13.51	13.86	21.8	21.57	22.18	21.38
Patch 21 (Neutral 6,5)	10.60	12.07	17.15	18.78	16.75	17.20
Patch 22 (Neutral 5)	9.12	10.74	14.64	13.80	12.87	13.54
Patch 23 (Neutral 3,5)	8.97	11.07	11.93	11.51	10.55	11.50
Patch 24 (Black)	16.67	16.76	22.26	18.87	11.32	14.84
All colours						
Mx ¹ dE*ab	13.05	14.54	17.02	17.84	15.73	16.50
Max ² dE*ab	35.22	40.32	26.29	29.97	26.37	29.04
Tones only						
Mx ¹ dE*ab	13.17	14.10	18.97	18.29	16.44	17.43
Max ² dE*ab	20.12	20.10	26.29	24.59	25.88	26.12
¹ Mx - average value, dE*ab = 5. ² Max - maximum value, dE*ab = 10.						

4. CONCLUSION

The control and evaluation of the projection, based on chromaticity, gradation, channel, grey balance, and colour gamut according to the ISO 12646:2010 standard is quite complicated and time-consuming. Choosing a suitable default module, whether for direct projection or for color management, is a major problem. Given that semi-professional and professional projectors are very expensive devices, the answer perhaps lies in colour management with hardware calibration and profiling - as is the case with better displays - and not in the set of (inappropriate) projection modules and/or settings with which we can experiment without achieving good results.

On the other hand, any colour management of digital projections will be effective and meaningful only if it will provide similar quality or colour differences as colour display on certified displays in accordance with ISO 12646: 2010 standard. A good channel balance and a very large colour range of saturated base colours do not yet provide a high-quality colour display in RGB colour spaces, in our case sRGB. The screen brightness (Lv) of the white tile, which defines a certain colour space, must be obtained by all means. With the existing equipment, colorimetric analysis and profiling studio projectors in the selected projection module and colour space are the only reasonable choice. It can be summarized that the digital projection in displaying the standardized sRGB colour space is not comparable to high-quality CRT or LCD computer displays.

By profiling of the JVC DLA-RS15 digital projection, we cannot achieve the desired colour differences between the displayed and the reference values, as they are on average about twice or approximately three times the size of the allowed ones. Nevertheless, with the profiling by using each combination of measuring and software equipment, a significant reduction in maximum deviations is achieved. That is precisely the reason why we do our best when profiling a digital projection in studio conditions.





5. REFERENCES

- [1] Ashdown M., Sato, Y.: "Steerable projector calibration", Computer Vision and Pattern Recognition - Workshops, 2005. doi: 10.1109/CVPR.2005.533.
- [2] Cooper, K.: "Northlight images", Northlight-images, URL: <http://www.northlight-images.co.uk/reviews/profiling/i1-beamer.html> (last request: 2018-05-09).
- [3] Feierman, A.: "JVC DLA-RS15 projector review", Projectorreviews, URL: <http://www.projectorreviews.com/jvc/dla-rs15/index.php> (last request: 2018-09-10).
- [4] Matt, S.: "Gut getroffen: Kalibrierung mit Eye-One Beamer", 86 – 88, 2003.
- [5] Park, S.Y., Park, G. G.: "Active calibration of camera-projector systems based on planar homography", 20th International Conference on Pattern Recognition, ICPR 2010, (IAPR, Istanbul, Turkey, 2010). doi: 10.1109/ICPR.2010.87
- [6] Turk, J.: "JVC dla-rs15 and rs25...a first look! jvc dla-rs15 projector", Avsforum, URL: <http://www.avsforum.com/avs-vb/showthread.php?t=1174409> (last request: 2018-05-01).
- [7] Wikipedia, Image projector, Wikipedia, URL: http://en.wikipedia.org/wiki/Image_projector (last request: 2018-09-09).



© 2018 Authors. Published by the University of Novi Sad, Faculty of Technical Sciences, Department of Graphic Engineering and Design. This article is an open access article distributed under the terms and conditions of the Creative Commons Attribution license 3.0 Serbia (<http://creativecommons.org/licenses/by/3.0/rs/>).

CONVERSION OF VIRTUAL REALITY INTO A MIXED REALITY

Ivan Pinčjer , Neda Milić , Irma Puškarević , Nada Miketić 

University of Novi Sad, Faculty of Technical Sciences,
Department of Graphic Engineering and Design, Novi Sad, Serbia

Abstract: Nowadays technology has developed a new form of appearance - virtual reality. This term currently exists in three different forms, virtual reality, augmented reality and mixed reality. Among these technologies, mixed reality has the most potential for use in everyday activities and education. This paper represents the overview of virtual reality technologies, their functioning and potential applications. When it comes to interaction, the mixed reality devices provide a completely new way of perception and understanding of the virtual space and objects. Since it is possible to interact with objects that exist in a virtual world in the same way as with objects that exist in the physical world, the high potential for the use of this technology for learning is evident. Utilizing advanced hardware components such as transparent displays and cameras simulating stereoscopic vision, in combination with advanced software technologies including spacial mapping, ambient lighting, ambient sound, identifying objects, movements from the real world and location, MR provides the closest HCI experience so far. Discussing the potential use of this technology, and current development phase in which it exists, the paper has the aim to induce questions and interest about further development of its use and application, such as multimedia learning (Mayer. 2009). The example of the use of MR technology on the HoloLens device is provided in this paper, in order to demonstrate the way of its use.

Key words: virtual reality, mixed reality, holograms, 3D modelling

1. INTRODUCTION

The moment we find ourselves irresistibly reminds us of the time when the first computers were created. Today we use them in ways that could not even be imagined. They were used exclusively for scientific purposes and to speed up the calculation. Their size was occupying the entire floors of the universities in which they were located. The borders that computers will reach are still not determined. The same situation can be recognized today in a "new" idea. Holograms are something that is part of science fiction, but also of everyday life. As a security measure, on the bills they became irreplaceable. However, the desire to record and reproduce the holographic animated image is still an unachievable goal. Nevertheless, the benefits of the holographic display can still be achieved with the help of high-end computing technology and the latest stereoscopic display that allows a virtual 3D projection.

As in the mid-20th century, computers were large and not easy to use, nowadays, holographic devices can be found that began their global conquest in the same way. Devices that allow the illusion of a holographic display is now made in the form of spectacles. Spectacles are, de facto, a whole computer with a plethora of different cameras and sensors, which in real-time maps the space around the users and put virtual models in it. As well as the first computers, these devices are waiting for improvement, fuelled by the versatility of the application.

Besides Microsoft, the world's largest corporations such as Apple, Google, Facebook, Disney, Amazon and many others are greatly developing their applications, to take advantage of this development of computer technology. It will not take much time until the virtual objects inserted into the real world become an everyday asset as e-mail or smartphones.

Since the digital world has become necessary, there is a great need to find ways to better interact with it. External devices such as mice and devices with touchscreen technology limit the interaction with the digital world to the 2D plane. Human-computer interaction is transmitted to a 3d real world, through virtual holograms. Of course, in the real world, we can use our own body to manipulate digital content.

In this mixed reality, the virtual space is replaced by the real world in which the user is aware of his real environment (not lost in space), which is a more natural environment for day-to-day tasks, such as work, learning or interacting with other people.

Mixed reality will enable digital content management in the same way as we manipulate real-world objects in a real environment. Finding the simplest solution for this kind of interaction with the digital world will show the path for further development of computer sciences.

As the big breakthroughs were made in the field of virtual reality (Tavanti et al, 2001), it would be a big step backwards if 3D models from VR could not be customized and used in an augmented or mixed reality. The way this transition can be done will be shown in this paper.

2. THE IMPORTANCE OF INTERACTION IN EDUCATION

Interactivity is the term emerged alongside new technologies and development of personal computers, and it is present in everyday life activities. Omnipresence of technologies in the everyday environment, including homes and schools, and its development aid people activities and different jobs. This led to the development of different habits and an increased necessity for interactivity with objects. Furthermore, interactivity is an essential characteristic, especially when it is utilized with learning new skills and acquiring new knowledge. Researchers who have studied learning problematic have identified interactivity as a key contributing factor to better learning. One of the first proposed theories by Bruner (1966), claims that learning is an active process and that learners construct their understanding of the subject when involved in the activity and build their knowledge based on existing knowledge and prior experience. According to Phil Race (2014), knowledge is just information for the student. The information becomes knowledge when something is done with it. This means that student has to apply, calculate, compare, analyse, interpret, integrate information in order to create individual knowledge. Creation of knowledge is an active process which educator facilitate through finding possibilities for learning. This opens an opportunity for combination of traditional approaches to education and interactive distance learning.

Additionally, it is important to emphasize that feedback is a key element of interaction (Oxland, 2004), whereas according to the constructivist theory of active learning interaction is a basic prerequisite for effective learning. Digital era and electronic devices ensured conditions for utilization these theories in their full potential. The form in which these theories found its use, is a new field of research called Human-Computer Interaction (HCI). HCI is an inevitable part of many scientific disciplines such as – computer sciences, graphic design, architectural planning, mechanical engineering et cetera. HCI can be considered as the tool designed to mediate between interaction human being and their environment. Concepts included in the HCI field of research are a presentation of information to the user, mental models, the possibility for the user to control the system, input devices, and user interface. Technology as an aid for performing various activities can be considered as a tool. The idea behind the tool as a mediator is that they along with humans form “functional organs”. Therefore, the combination of natural human abilities and capacities of external components – tools – provide conditions for performing a task or function much more efficiently. The analogy of this is that human eye aided with glasses form functional organ that provides better sight. Nowadays, there is a constant tendency for HCI to improve, to become as closest as possible to humans, immerse entirely in their lives and become insensible. Technologies that enable this are: VR, AR and, MR, which will be discussed follows.

3. NEW TECHNOLOGIES AND TYPE OF INTERACTION WHICH THEY PROVIDE (VR, AR, MR)

Technologies in which HCI is highlighted and provides an experience that erases barrier between virtual and physical world are:

- Virtual reality (VR)
- Augmented reality (AR)
- Mixed reality (MR)

Virtual reality – applies to a group of technologies that make the connection between the real and virtual world in “virtual continuum” that blends real environment with virtual. The main characteristic of VR technologies is that the observer is entirely immersed in a virtual world without the opportunity to see the real-world environment. The observer can have interaction with the virtual world in an approximately identical way as with the real world. Virtual reality emulates properties of the real world – laws of physics, time, space, mechanics, material properties – which is at the same time the main advantage of this technology. It was widely spread as a tool for educational purposes (Barracough et al, 1998), (Pinčjer et al, 2018).

Augmented reality – these technologies also connect virtual and real content. However, they retain the possibility of observing the real world environment and sense of it. AR technology enables that world becomes improved, refined with digital computer generated content, most commonly with a virtual object which covers real-world environment in the sense of additional digital layer. This technology enables interaction with a user as well.

Mixed reality – also integrates physical and virtual reality retaining the perception of the real-world environment. The main characteristic of MR is the representation of the virtual environment and objects in it conjoint on one display. MR technology exists between two ends of the virtual continuum – real-world environment and virtual reality.

4. MIXED REALITY

As it is previously explained, MR is created through the integration of real physical world and digital world, in the way that digital objects are entirely adapted and perceived as if they are the part of the physical world. MR bridges the gap between physical reality and virtual reality and makes that these two are perceived simultaneously as one world. The three components are required for MR experience to exist: human, computer and environment.

Digital objects are imported in the real world as a hologram using stereoscopic projection and addition of a light in front of the observer's eye. The more accurate term for holograms could be virtual holograms because they are not visible in the real world environment without special equipment – glasses. One of these special glasses for mixed reality perception is Microsoft HoloLens glasses.

HoloLens projects holograms onto transparent displays within glasses. With environment mapping, holograms are bound with real objects and positioned in the real world that is visible through display glasses. Each eye individually receives a stereoscopic image, adding the illusion of three-dimensionality to holograms. Virtual holograms are objects defined with light and sound. They can react on users look, body gestures and voice commands. Holograms can even have interaction with real-world objects and surfaces which encircles user, enabling them to transfer digital objects in the real world.

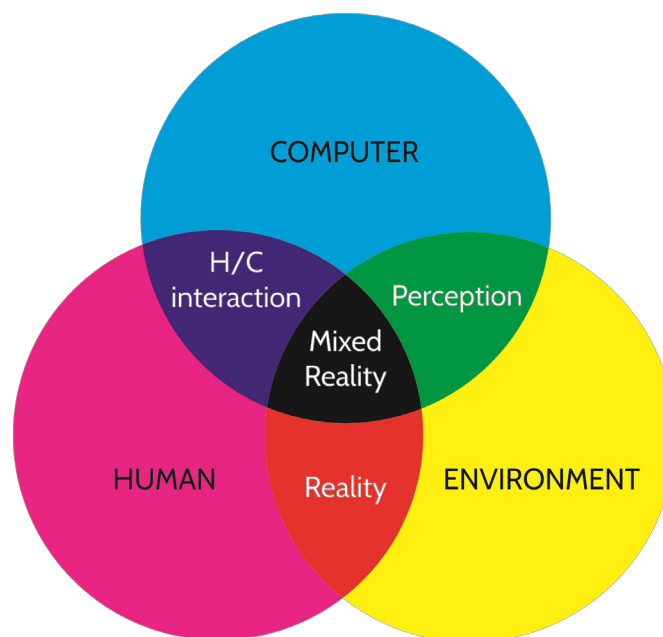


Figure 1: Mixed Reality binding Human, Environment and Computer (Bray, Zeller. 2018)

The realism of the hologram depends on its application. Games require holograms that will look like cartoon models, while simulations involve digital objects high level of realism. To make the digital world more realistic in real life, the Microsoft HoloLens use sound. Speakers are placed above the user's ears, allowing them to hear virtual digital objects that bounce off the real world surface or even hear objects behind them. This creates an illusion that virtual objects are really around the user. In this way, the

feeling of depth of space increases. As the speakers do not overlap the user's ears, they only add sound to the surrounding sound without blocking it.

Mixed reality devices with transparent displays show holograms by adding light to the real world. As the displays work on the additive system of colour mixing, where the black is obtained by the absence of light, it is clear that in the case of transparent displays, the absence of light will show the background, i.e. the environment. For this reason, the black pixels on the model will be completely transparent; they will not be displayed. This is an essential feature that must be taken into account when creating 3D models. Depending on the background even white pixels may be somewhat transparent.

In order to achieve the effect of depth, several techniques can be used. First one is to position the hologram to the places you would expect to find it in the real world. The realism of the mug hologram is much greater if the hologram is positioned on the table, where it would be expected to see mug, instead of floating somewhere in the air. In addition to mapping the surface on which a virtual hologram could stand, realism can also allow the setting of a shadow that would indicate that the object is in the real world. Adding a shadow is not as easy task, because if we remember, holograms work on the principle of adding a light to the world, and they cannot take it away to create a shadow. In order to achieve the shadow effect, it is necessary to do so call a negative shadow. It is achieved by first placing the mild halo effect around the virtual object in the form of the illuminated surface around the object. This illuminated surface is also a hologram and turning off the lighting in the appropriate places the shadow impression is obtained.

The holograms can be positioned, by the user, anywhere in the room. It is recommended that they are placed at approximately 2 meters from the users. The impact of the hologram's reality will be reduced as it gets closer to the user. Optimal area for placing the holograms is from 1 to 5 m.

The impression of reality is further achieved by the ability of holograms to go behind real world objects. For example, a holographic robot can find the door in the room and simply go through them, disappearing in the hallway. For the holographic devices to be successful in this type of tasks, they must be aware of their environment. It is this awareness that has enabled the use of virtual holograms in real space.

Several technologies are involved in the creation of MR. The MR device can detect environmental information using perception APIs (Application programming interface). The device can detect and receive information from an environment, such as a person's position in the area by monitoring head movements, spatial mapping, ambient lighting, ambient sound, identifying objects and location. A very important aspect of the MR technology application is the ability to translate movement from the physical world into the virtual in real time.

Mixed reality devices can distinguish different surfaces in the real world such as floor, walls, tables or chairs. This feature helps them set up virtual models at appropriate locations, creating constraints. Thus, virtual holograms can use these surfaces to move around or even sit on them.



Figure 2: Holograms using a real-world object, furniture
(Printscreen: https://www.youtube.com/watch?time_continue=17 [HYPERLINK](#))

Mapping of the environment is one of the first steps in the process of preparing the application for particular tasks. During the mapping, the user indicates the area in which the hologram will appear. Mapping begins by a user looking at the environment and passing through it. In this process, the topology of an area is created. The more time is spent in looking to the area; the area will be mapped with more details. Depending on the application's requirements, when the desired coverage is reached, the holograms can be placed in the mapped area. Mapping data can be saved and used on other occasions or even transferred to another device.

Based on data received from the sensor, the software determines the surface characteristics. The pathway taken by the camera during the scanning process is also taken into account, and the software can assume that the surface is a floor, etc. As devices for mixed reality are in the development phase, raw data can be taken from the sensors and used in the analysis and preparation of new applications.

5. CREATION OF VIRTUAL HOLOGRAM

Nowadays, technology (hardware and software) is available more than ever. The "ordinary" user is given the opportunity to deal with areas that, until recently, were considered unachievable for broad masses. This is also the case with software for creating a virtual hologram for mixed reality. However, in this technology, the hardware is still not present in people's homes, as is the case with personal computers. Independently of the hardware, with the appropriate software, it is possible to create a hologram that can be transferred later and used on the desired device.

6. REQUIRED STEPS FOR VIRTUAL HOLOGRAM CREATION

6.1 3D model

For enabling holograms to be seen in space, it is necessary to make them in digital form, as a 3D model. Regardless the model is an asset from the internet or created by the author it can be in the same way adapted for the use on the HoloLens device.

6.2 Unity software

Unity engine for creating video games, applications and interactive content generally, is necessary to use to adapt the model for the display on the HoloLens device. Unity also enables making the build of the app that needs to be deployed in the HoloLens device.

6.3 Visual Studio

For the creation of the app, for debugging and deployment on the device Visual Studio framework is required. In the Unity framework, it is possible to deploy the app on various devices such as computers, mobile phones, or any remote devices including HoloLens glasses. Also, the Visual studio provides a big advantage because it is possible to test and simulate the appearance and behaviour of the app on the chosen device.

7. TRANSFERRING 3D MODELS TO A VIRTUAL HOLOGRAM ON MICROSOFT HOLOLENS

An example illustrates the conversion of a virtual 3d model of a printing press Risograph – Riso EZ 570 to the virtual hologram on the Microsoft HoloLens MR device. A 3D model can be created in any 3D modelling software; an example model given here is created in the 3ds Max.

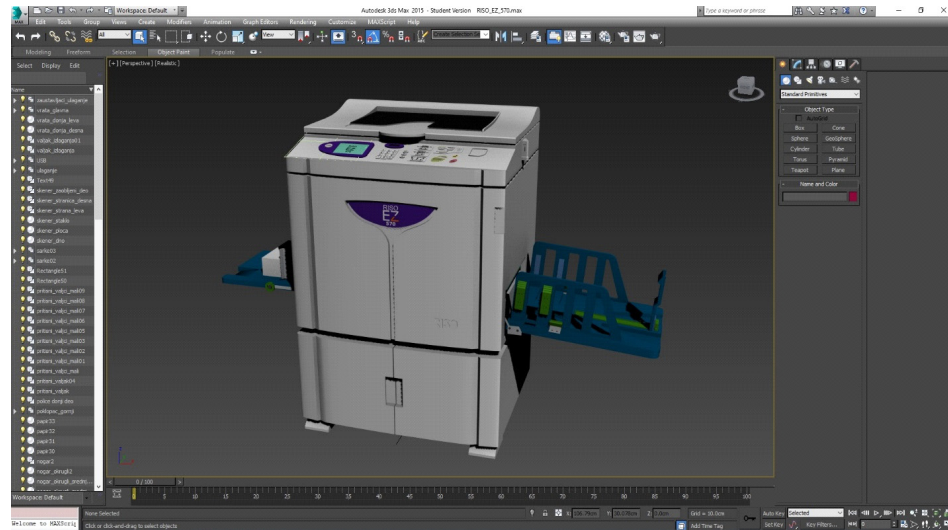


Figure 3: The virtual digital machine in 3ds Max

To import the model into Unity software, it is necessary to export it appropriately. This can be done in many ways, but the most convenient way is to export to the FBX exchange format. The reason for this is that this format keeps the full accuracy of the display and functionality of the object. This format stores information about all the parameters and elements that are present in the 3D scene: lights, textures, animations, object deformation, the position of normals, and more.

Therefore, the example object is saved as an FBX file.

Then it is necessary to make certain settings in Unity software so that the object can be adjusted to the display on the HoloLens device.

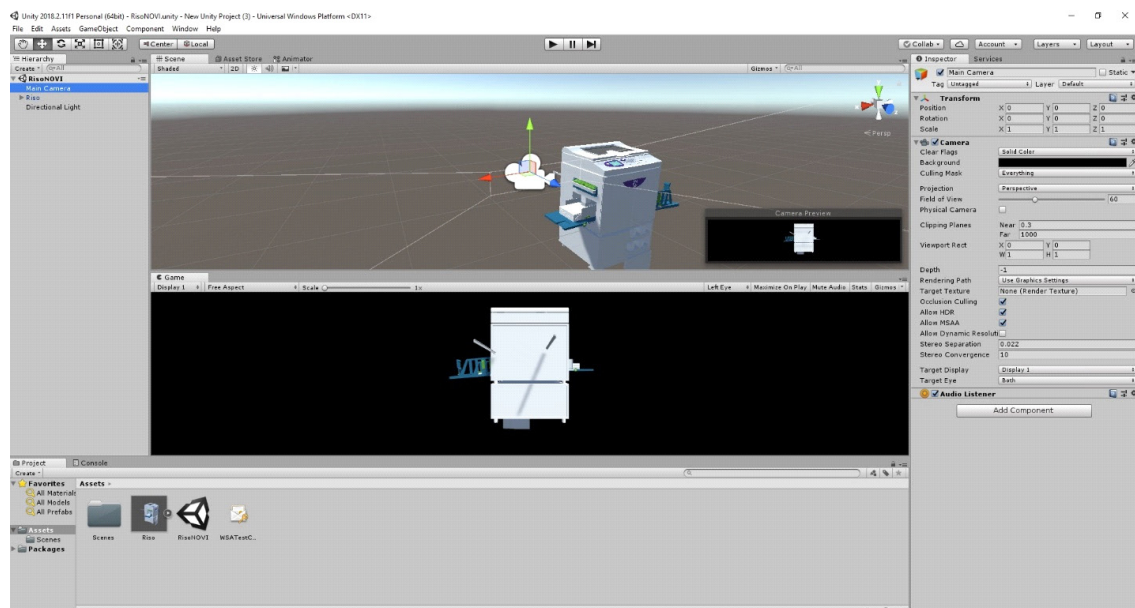


Figure 4: Virtual digital machine transferred to Unity where the camera is added

The settings that are executed are most related to the camera's position. A pre-defined Main Camera can be used, which is positioned at the $x = 0$, $y = 0$ and $z = 0$, while the object position is adjusted depending on the desired distance from the viewer. In the object's settings (when the object is selected), the value of the z position determines at what distance the observer will be located. In this case, a value of 2 is set, indicating that the viewer will have the feeling that the object is 2 meters away from it.

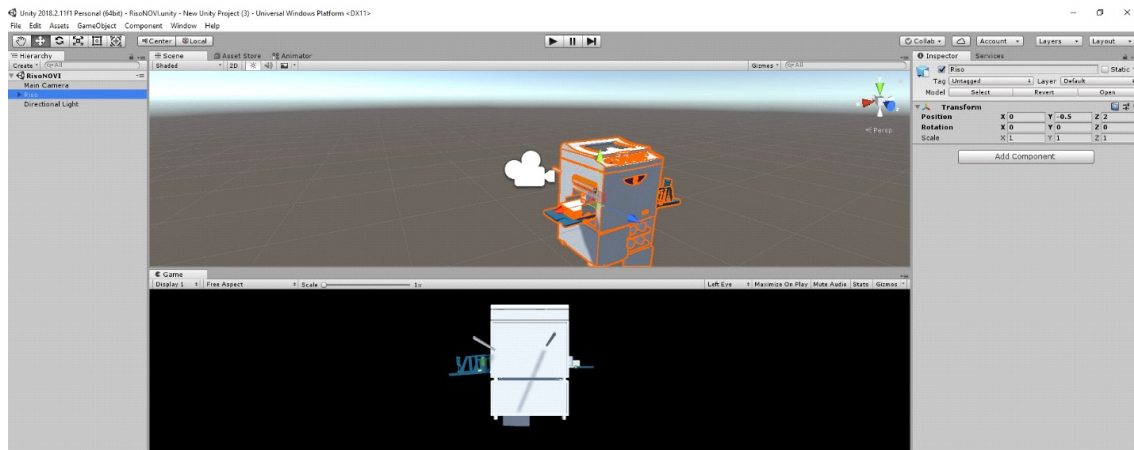


Figure 5: Positioning camera and the model at the right distance is crucial for optimal hologram viewing

After setting the object, it is necessary to create the Build scene and open it in Visual Studio software.

It is necessary to select the appropriate options for the Build scene:

- You need to choose the Windows Store platform, SDK Universal 10.
- For Target device it is necessary to choose Any device or HoloLens.
- UWP Build Type should be D3D
- UWP SDK should be selected Latest installed.
- Then, under the Debugging option, it is necessary to select Unity C # Projects.

After this, Build can be created by clicking on the button with the same name.

After executing settings in the Visual Studio software, it is possible to simulate the model within the emulator or upload the model to the HoloLens device.

8. CONCLUSION

Will wearing the entire computer on the head during the work day or after it comes into fashion? Definitely not. Is the connection between the digital and the real world opening up a new door to a better interaction between the computer and the user, and whether the user will have greater benefits in that interaction? Definitely yes. If the benefits of using such devices would be great enough to direct investment in the development of the technology of mixed reality, we can expect more, smaller and smarter devices that will become imperceptible at some point in the future.

Whether the benefits that such devices offer, in the field of education, will be sufficient to trigger their development or whether the game industry will have interest in a mixed reality to support evolutionary progress remains to be seen. Innovative ideas, software, new applications and its development of such devices no longer depend on one team. Research and development modules of the device and their open platform enable everyone to become part of the development team. Such an approach will certainly accelerate the development and application of mixed reality devices.

Researchers in educational institutions can contribute to the development of mixed reality devices by exploring the benefits of mixed reality on education and other real-world problems.

9. ACKNOWLEDGEMENT

The research is supported by the Ministry of Education, Science and Technology Development of the Republic of Serbia, project number: 35027 "Development of software model for scientific and production improvement in graphic industry".

10. REFERENCES

- [1] Barraclough, A., Guymer, I.: "*Virtual reality – A role in environmental engineering education?*", *Water Science & Technology*, 38 (11), 303–310, 1998. doi: 10.1016/S0273-1223(98)00668-4
- [2] Bray, B., Zeller, M.: "What is mixed reality", URL: <https://docs.microsoft.com/en-us/windows/mixed-reality> (last request: 2018-10-1)
- [3] Bruner, J. S.: "Toward a Theory of Instruction", (Oxford, Oxford University Press, 1966.)
- [4] Mayer, R. E.: "*Multimedia learning*", 2nd ed, (New York, Cambridge University Press, 2009.)
- [5] Oxland, K.: "*Gameplay and Design*" (Harlow, Addison-Wesley, 2004.)
- [6] Pinčjer, I., Tomić, I.: "Interactive Educational Tool for Digital Printing System", *Innovations in Publishing, Printing and Multimedia Technologies* (Kauno Kolegija, Kaunas, 2018), pages 106-112
- [7] Race, P.: "*Making Learning Happen*", 3rd ed, (London, Sage. 2014.)
- [8] Tavanti, M., Lind, M.: "2D vs 3D, implications on spatial memory", *Proceedings of IEEE Symposium on Information Visualization*, 2001. (INFOVIS 2001., San Diego, 2001), pages 139–145.



© 2018 Authors. Published by the University of Novi Sad, Faculty of Technical Sciences, Department of Graphic Engineering and Design. This article is an open access article distributed under the terms and conditions of the Creative Commons Attribution license 3.0 Serbia (<http://creativecommons.org/licenses/by/3.0/rs/>).

THE IMPLEMENTATION OF GAMIFICATION IN MOBILE APPLICATION

Anamarija Šišić, Lidija Mandić , Ana Agić , Ante Poljičak 
University of Zagreb Faculty of Graphic Arts, Zagreb, Croatia

Abstract: *The aim of this research was to design mobile application that engages and motivates the end user to be physically active by promoting healthy habits. More and more services and mobile applications have begun to implement game elements. Competing application analysis found that the implementation of gamification should be unobtrusive recurring task cycle. The application was designated for young people and the results shown that implementation of gamification motivated them to be more active.*

Key words: mobile application, gamification, user experience

1. INTRODUCTION

With the development of smartphone technology there is more competition on mobile application market. It is necessary to change design of application and adapt it to the needs of the end user. User experience (UX) is an interdisciplinary field of work, and it also includes the behaviors, attitudes and emotions that a user experiences when using a particular product, system, or service (Cao & Gremillion, 2015). Since user experience involves multiple methods and processes that change over time and often come up with new forms of solving problems that are mostly related to the development of technology In that process user experience (Cao & Ellis, 2015). One of the new methods for better UX in mobile application is implementation of gamification (Cao et al, 2015).

User-Centered Design (UCD) adapt user interface in a way that is consistent with the goals, tasks and needs of users. The main principles are: simplify the task structure to make actions intuitive, conceptual model need to be clear to the user, properly map the actions that leads to results and accept and take advantage of the limitations of the system. By applying these principles errors are reduced and users are more satisfy. This approach has disadvantage too due different view of how to solve the problem (Endsley & Johnes, 2004).

It is important to define target users and understand the context in which the users interact with product. The elementary phases of each research should be: competition analysis, target audience analysis, design, evaluation and implementation of design. It is important to know target user group who will use product or service, outline their most important needs and expectations, the way how they will use it, and functionality. Best practice has shown that for a particular project three or four personas create. It is important to determine the main faction of mobile app. Personas should usually include name, gender, occupation, age, short bio etc. Most often after defining personas, user scenario is created. It helps to identify the main functionalities of mobile application, help to understand user habits and how they interact with the system (Ilama, 2018).

After this preliminary research, benchmarking is followed. When analyzing competition it is important to find out where the disadvantages are and how to solve them. After this, the wireframe is made, mostly low-fidelity prototype. It is important to emphasize that colors in this stage are not used except gray shades that indicate a different level of information architecture. Moreover, such a simple structure allows the designer to experiment in designing functionality and solves potential problems with the information structure in the future. Cycle iterations, testing, and feedback from users are a useful way of addressing possible shortcomings until the best possible version of the product is obtained. Usability testing refers to product assessment (mobile applications) by testing through representative users. During the test, the participants will try to fulfill certain tasks. The goal is to identify usability issues, collect qualitative and quantitative data, and identify participant satisfaction when using mobile apps. Games and UX design are often intertwined because they both share a unique feature that separates them from other media and this is interactivity. The term gamification developed in the year 2000 when designers began to consider how positive emotions and feelings can be triggered through sound, graphics, etc. to increase the user experience in interactions with the software. So gamification is not a synonym for gaming, it's just how designers can affect user behavior and motivate them as "gamers" to make the expected actions through elements of the game like challenges and prizes (Uxplanet, 2018).

Gamification is based on human behavior, matched with natural learning and entertainment mechanisms. According to product design expert and famous author Nir Eyal, all user habits pass through four interconnected phases (Figure 1):

- Signs (or triggers) – visual data which encourage users to action
- Routines (or actions) - this is what the user actually plays in the game
- Awards - Include a move to the next level in the game and unlock achievements or items
- Investments - as players advance in the game, they become personally introduced into events and the final results of the game

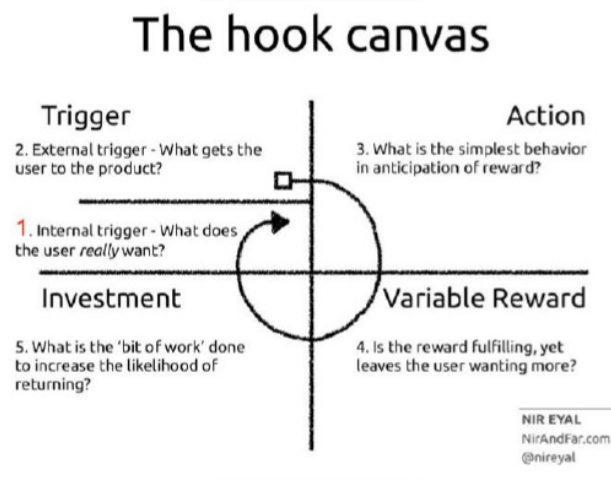


Figure 1: The process of integrating looping habits

2. RESEARCH AND DESIGN

The main goal of this research is the mobile application design for the Android operating system that engages and motivates the end user to be physically active by promoting healthy habits. From the beginning, part of the focus is on a system design that is easy to use and allows users to easily perform tasks, but more importantly, that the application, using game elements, is continually used. It was necessary to find what motivate users to use this app and what are the design strategies and gaming elements used in competing apps that motivate users to increase their physical activity. Three competitive applications were selected to study their functionality, motivation factors and possible usability problems: Nike+ Training Club, Zombies Run and Runkeeper.

From the above-mentioned analysis of competing applications it can be concluded that gaming implementation is a very complicated process, it must first be very subtle and unobtrusive. Also, it is important to realize the emotional connection of the user with the application because then the loop of habits begins to develop. What links all successful applications is a recurring task cycle - task execution - feedback - a new task. As far as the user interface is concerned, it would be desirable that it is easy, without too much information, because it should be borne in mind that the user will use the application when performing the task in different environments.

Following UCDF it is important to have good personas and design the user interface appropriate for a particular group of users. The survey referred to user habits regarding motivation and physical activity. The survey were conducted through an online survey, and based on the results obtained personas were created. The survey was done with 56 users, and the Google forms tool was used to create a survey. The participants were mostly students (19-25). The survey participants received 10 questions with the offered answers. According to results mostly participants used Android smartphones. The questions were:

1. What is your occupation?
2. Which operating system you are using?
3. How much do you spend daily on physical activity on average?
4. Do activities like jogging, walking, swimming, exercising over time become dull?
5. Favorite physical activity?

6. Do you play mobile games?
7. Do you use applications to increase productivity, track activity, weight and more?
8. Are you lacking motivation to keep your fitness goals?
9. If you had some reward for your ongoing activity, would you be more motivated then?
10. Would you use an app that rewards your ongoing activity and helps you move more?

Based on the results of the survey, three personas were created. Mostly participants answered that walking is their favorite activity. The application seeks to encourage users to enjoy their favorite activity, walking, in a fun way. The application "GOQUEST" has three functionalities that are related to the user's activity. The first functionality of the application is the so called "daily quest", which means a certain number of steps that the user passes on that day. The "daily search" functionality consists of a stylized map that the user can see on the home screen, this map indicates the way a user needs to pass that day. Additional maps, number of steps, miles, and time are provided with the map. When a user decides to overwrite a route that is the default on that day, he opens the map, the map shows the route that is generated from the user's location and ends near the user's initial location. The folder displays the points (3-5 points) that represent a certain character, or a badge that the user collects, these badges are actually a reward for a number of steps that a user makes on the road, for example, for 500 steps passed, the user wins one badge. The more steps you make or the more the badges accumulate over time the user is ranked higher in the ladder and for each level, the user is assigned one character and the name of that level, for example, "one level - a little monster".. The next functionality is to track user activity. When applying for a first registration, the user must enter some personal information such as weight and height information, then enter their goals, ie how many steps the daily minimum must (wants) to exceed. This functionality is divided into two parts, activities are primary while weight monitoring is secondary. The last feature is a table with the best results that changes each week and shows the best users, showing the number of steps past that week and the level that can be seen in the icon showing one of the main characters of the character (character). This functionality, though not primary, can motivate users to rank as much as possible on the ladder.

After the application's functionality is defined, the user interface sketch was made (Figure 2).

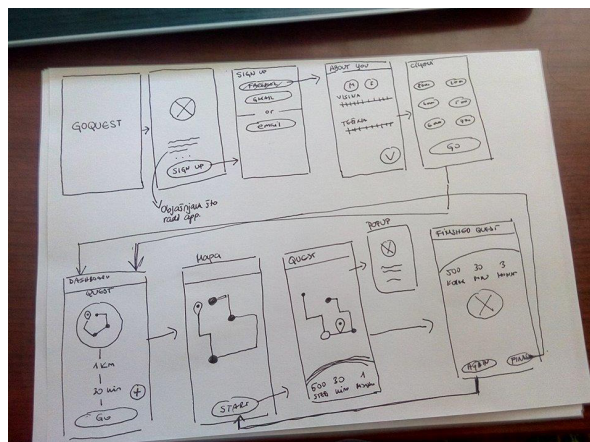


Figure 2: User interface layout

Prior to creating a prototype, the main app's apps have been defined. The main characters are small monsters that run through the application's functionality and their goal is to motivate users to perform activities. The main characters of the application are bright and saturated colors, so they have in some way defined the look of the rest of the interface, which is almost monochromatic and cleansed so that the user would not be overwhelmed with a lot of information and color. The application logo is made of the name of the application itself with a small eye detail inspired by the eyes of the main characters of this application. The eye is located inside the letter "Q", which looks like a magnifier with its appearance. This is to show the very essence of the app's own name, which is search, adventure, activity, and motivation. In Figure 3 are shown some screens of app.

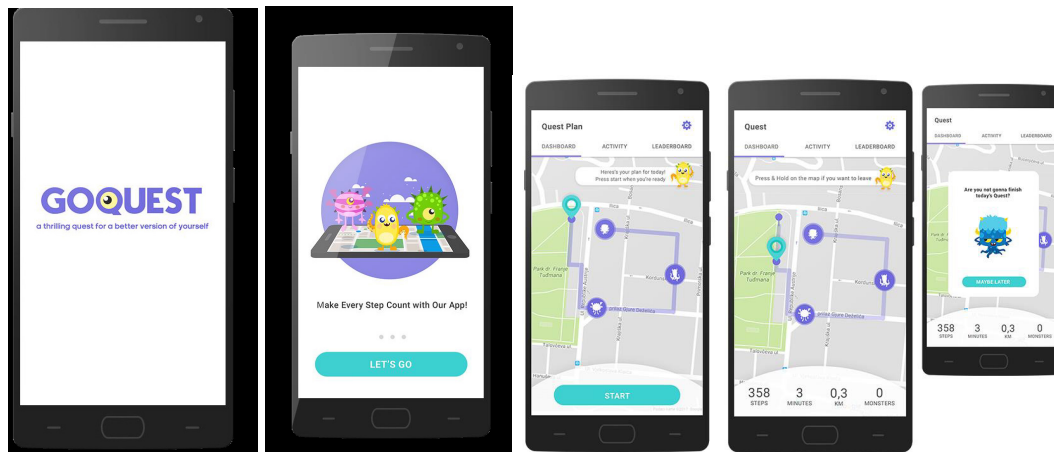


Figure 3: Splash screen, walk through, plan of activity, start, pop-up window

Participants are using a day prototype application via InVision prototype test site. Their task was to register through the application, set their own measures and go through the main functionality of the application. After the task was completed, participants answered questions about the application.

3. CONCLUSIONS

By analyzing the results of the survey conducted on the mobile application "GOQUEST", it comes to the conclusion that the functionality of the application is mostly clear to the respondents and easy to use. For example, showing the route on the map to most of the respondents (80%) was very understandable. Also, the survey confirmed that the graphic design of the application leaves a positive impression on the respondents. From this it can be concluded that the visual style of this application does not require any further changes. The level or slate allocation system was either user-friendly or intuitive, so in that case it would be better to present the user with a level-allocation system, for example by creating a screen where the user can see what level is now and how many badges should be collected) to the next level. In addition, questions about the motivational aspect of this app gave mostly positive answers, the vast majority of users would be able to show the activities and tables with the best results motivating them to move even further. Finally, most respondents gave a positive answer to the question of how fun their application is, so it can be concluded that the application of gamification in this app is successful. It can be concluded that the implementation of gamification in mobile applications definitely improves user experience.

4. REFERENCES

- [1] Cao, J., Gremillion, B.: "UX Design Process, Best Practices", Uxpin, URL: <https://www.uxpin.com/studio/ebooks/ux-design-process-documentation-best-practices/>, (last request: 2018-05-10)
- [2] Cao, J., Ellis, M.: "The elements of successful UX design", Uxpin, URL: <https://www.uxpin.com/studio/ebooks/ux-design-successful-elements-for-products/>, (last request: 2018-09-16)
- [3] Cao, J., Nouvel, S., Ellis, M.: "UX Gamification redefined", Uxpin, URL: <https://www.uxpin.com/studio/ebooks/ux-gamification-redefined/> (last request: 2018-07-07)
- [4] Endsley, M.R., Johnes, D.: "Designing for Situation Awareness, An Approach to User-Centered Design", 2nd ed, (CRC Press, Boca Raton, 2011).
- [5] Ilama, E.: "Creating Personas", Uxbooth, URL: <http://www.uxbooth.com/articles/creating-personas/> (last request: 2018-08-08).
- [6] Tubik Studio, Gamification in UX. Increasing User Engagement, Uxplanet, URL: <https://uxplanet.org/gamification-in-ux-increasing-user-engagement-6437cbf702aa> (last request: 2018-09-22).



© 2018 Authors. Published by the University of Novi Sad, Faculty of Technical Sciences, Department of Graphic Engineering and Design. This article is an open access article distributed under the terms and conditions of the Creative Commons Attribution license 3.0 Serbia (<http://creativecommons.org/licenses/by/3.0/rs/>).

WEB-BASED APPLICATION FOR INTERACTIVE SELECTION OF IMAGE PROMINENT COLOURS

Primož Weingerl , Dejana Javoršek 

University of Ljubljana, Faculty of Natural Sciences and Engineering,
Department of Textiles, Graphic Arts and Design, Ljubljana, Slovenia

Abstract: *An image can contain myriad different colours, but only a few of them are noticeable at first sight, hence in some way are defining the image. Therefore, the question arises which colours are prominent and what are the main factors that affect their prominence. In this paper, we present a web-based application that supports an interactive selection of colours and can be used to gather prominent colours for a set of images. The resulted database of images and their corresponding colours can be further used for investigating which image features or colour properties contribute to their prominence and for validating the models for automatic extraction of prominent colours from the images. First, the perception of prominent colours is addressed, and applied perspective of this knowledge is given. In the remainder of the paper, an overview of application architecture is presented, and a more detailed description of application's settings and usage is given. Although the main purpose of our application is to gather prominent colours of images based on the observer's opinion, the application could also be used for conducting other psychophysical experiments. The application supports three different modes for selecting the prominent colours: selection of basic hues, selection from ColorChecker Classic target and selection from custom defined patches.*

Key words: web application, colour scheme, prominent colours, colour selection

1. INTRODUCTION

Colour is a fundamental sensation, which helps us to interpret and understand the material world that surrounds us. It affects our emotions and visual attention (Ou et al, 2004; Kopacz, 2012), so we could use it to deliver the desired information to the end user. Consequently, image colours can convey different emotions (Liu et al, 2018) and therefore influence the information value of the image. However, from the technical aspect, an image can contain myriad different colours. This raises an interesting question of which colours are most prominent – noticeable at first sight, and what are the main factors that affect their prominence. This knowledge could be valuable for building algorithms for automatic extraction of image prominent colours, which have many different application values, e.g. they can be used for image categorisation, colour-based image retrieval or colour schemes extraction.

In the past, several techniques and methods for automatic colour extraction were presented, however, so far, little attention has been paid to develop an algorithm for extracting most prominent colours. Most techniques focus on extracting representative colours, which are not always the ones that are most prominent. Techniques for extracting colours from an image can be classified into three main categories: clustering-based methods, histogram-based methods and data-driven methods. Clustering-based algorithms categorised or grouped colours in the image – values of image pixels, based on specific criteria and use the centroid or mean value of each cluster as representative colours. A well-known clustering-based algorithm is k-mean, which goal is to group colours into a k number of clusters in order to minimise the within-cluster sum of squares – squared distances between each colour and the mean value of their corresponding cluster. While the k-mean algorithm assigns each pixel value to exactly one cluster, i.e. hard clustering, in fuzzy or c-means clustering, colours can belong to more than one cluster, i.e. soft clustering. Despite the popularity and convenience of the clustering-based algorithm, Lin and Hanrahan found out that people tend to select different colours in comparison to colours extracted with popular clustering methods, such as k-means and c-means (Lin, 2013). Few researchers have presented methods for extracting image representative colours based on histogram analysis. Based on the observation that people tend to select colours from distinctive regions of the image, Delon et al. developed an algorithm that finds peaks of one-dimensional histograms of hue, saturation and lightness, which according to their opinion, correspond well to spatial regions (Delon et al, 2007). Colours that represent histogram peaks can be used directly or as initial seeds for the clustering methods as mentioned above. Morse et al. proposed a similar histogram-based method, which also allows users to specify a maximum number of extracted colours and a minimum distance between them. The method strives to find peaks in the hue

histogram, which is weighted according to saturation and spatial coherence of each pixel in the image (Morse et al, 2007). With the increase in computational power that has enabled the recent breakthroughs in machine learning, the data-driven model has gained considerable research interest. Lin and Hanrahan presented a regression model for extracting colour schemes from images (Lin et al, 2013). The model is trained on user-generated colour schemes and uses more than a hundred features. In contrast to the algorithms that only consider the colour information when extracting colours, Liu and Luo presented a method that also considers users' emotion and feeling about the image (Liu et al, 2016). As discussed above, no previous study has focused on developing an algorithm for extracting image prominent colours. In order to be able to develop such an algorithm, extensive knowledge about the perception of image prominent colours and its influencing factors is needed. The application presented in this paper provides a simple and efficient way to create a database of image prominent colour, which is a basis for further studies.

2. APPLICATION OVERVIEW

This section starts with an overview of the application structure and then continues with a more detail description of application's settings and functionality.

2.1 Architecture overview

The application is developed based on a model–view–controller (MVC) architectural pattern, using popular Javascript library React (Reactjs, 2018). React was built by Facebook and is mainly used for developing single-page or mobile applications (progressive web applications). The main advantage of using React library lies in one-way data flow and virtual Document Object Model (DOM). The latter has a massive impact on the performance since the real DOM is only rendered when needed, while the one-way data flow allows robust and less-error-prone development. The overall structure of the application is shown in Figure 1. The processing in control and view part of the application is carried out directly in a client-side environment (browser). Consequently, each stage of application is loaded instantly and responds quickly to user interactions. To process data on the server-side and save results in a database, the PHP programming language and MYSQL database is used, respectively. The interface of the application was designed using Material Design design language and responsive web design (RWD) approach, which allows different page rendering on different devices and screen sizes, in order to optimise user experience. The main stage of the application, as it renders on desktop and tablet devices, is shown in Figure 2. At the moment, the application is not supported on devices with a width lower than 768px.

2.2 Input parameters

The application provides a number of settings that control its functionality and can be set through URL GET parameters. Bellows are the input parameters with their supported values and their corresponding data types:

- **num_img (integer)** sets the number of images that will be used in an experiment.
If this parameter is omitted all images in the set will be used.
- **colour_mode (string: hues | cc24 | custom)** sets the colour selection mode (see section 2.3).
By default cc24 (ColorChecker Classic target) mode is used.
- **min (int)** sets the minimum number of colours that need to be selected by the observer.
The default value is 3.
- **max (int)** sets the maximum number of colours that are allowed to be selected.
The default value is 7.
- **shuffle (boolean)** controls the order of presented colour patches. If set to true, the patches will be shuffled before being shown to the observer. Otherwise, they will be displayed as defined in a file. This parameter is active only in ColorChecker Classic and Custom colour modes.
- **sortable (boolean)** controls if selected colours can be sorted or not. The default value is true, which allows the observer to sort selected colours by drag and drop gesture.

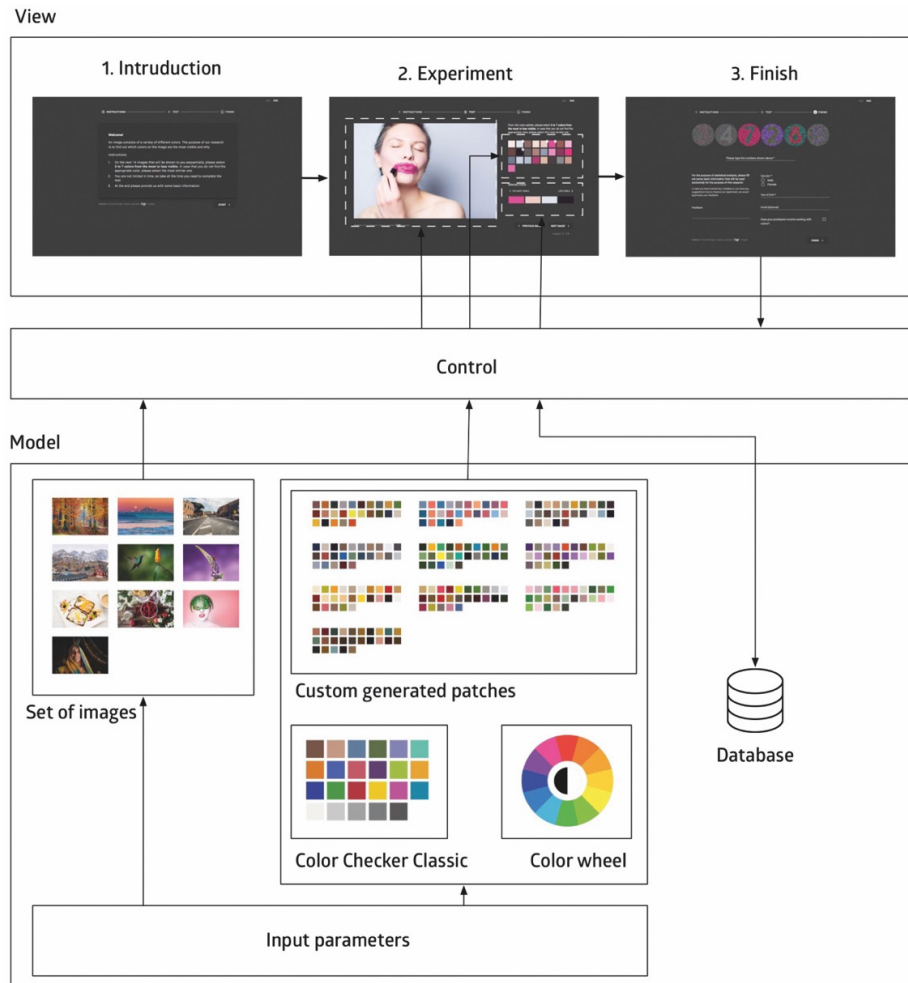


Figure 1: MVC architectural pattern of application.



Figure 2: Design of the application interface, as it renders on three different screen sizes.

2.3 Colour selection modes

An 8-bit RGB image can theoretically contain more than 16.7 millions colours. If the observer could select any colour from the image, we would obtain very precise sets of prominent colours. However, because some colours on the image can be quite similar and therefore indistinguishable for most observers, the variation between the observers – interobserver variability – will be considerable. Such results would be challenging to statistically analyse and provide little opportunity to make a further generalisation about the perception of prominent colours. In addition, selecting from the large set of colour patches can be frustrating for the observer and could decrease the usability of the application. Our application allows

the research administrator to balance between data precision and usability of the application, by supporting three different modes for selecting the colours. All three modes can be seen in Figure 3 and are explained below.

1. Prominent hues: this mode allows the observer to select only from the 12 basic hues: red, red-orange, orange, orange-yellow, yellow, yellow-green, green, cyan, cyan-blue, blue, purple and magenta. In addition, the observer can also select a black and white colour.

2. ColorChecker Classic: the observer can select from 24 patches of the ColorChecker Classic target. This target contains natural, chromatic, primary and grayscale colours, which represent natural objects, such as human skin, foliage and blue sky.

3. Custom: this mode allows the research administrator to define a custom set of colours for each image. The colours can be generated by using common extraction algorithms, such as K-means or K-fold. To import colours into the application, the colours must be defined inside the JSON file as a multidimensional array of objects, containing CIELAB and sRGB values.

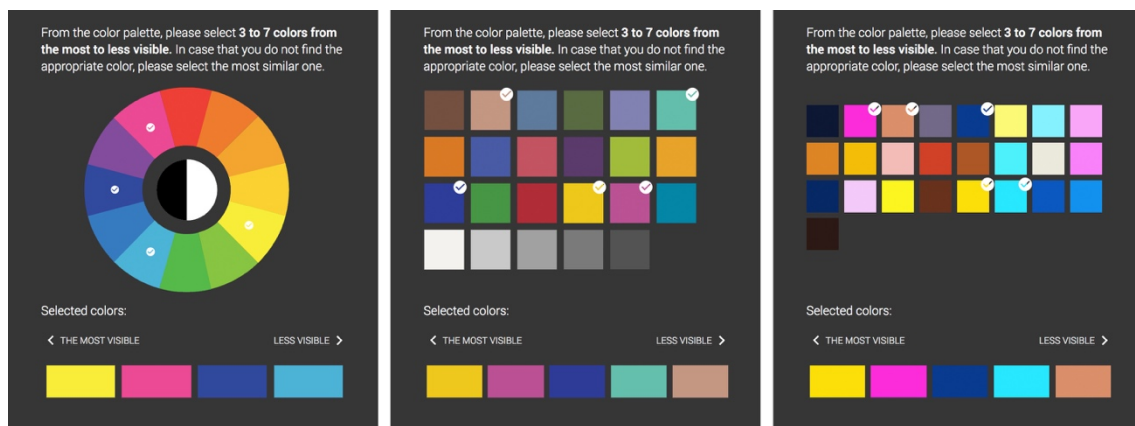


Figure 3: Colour selection modes of the application: Prominent hues (left), ColorChecker Classic patches (middle), Custom defined patches (right).

3. APPLICATION USAGE

Although the main purpose of our application is to gather prominent colours of images based on the observer's opinion, the application could also be used for other psychophysical experiments or purposes, e.g. if we want to find out which colours are harmonious on the image, or to get a colour scheme for a particular image without special restrictions. In the following, the detail description of how to use the application for collecting image prominent colours is given based on our case study.

3.1 Defining input parameters and images

In the presented case study we used 4 sets of 12 images. Participants in the study were asked to select 3 to 7 colours for each image, from the most to less prominent. They could select from 25 colours (custom colour selection mode), that were extracted from images in advance using the k-mean algorithm.

3.2 Collecting data

The process of collecting image prominent colours consists of three main parts: introduction, colour selection task and observer information task (Figure 4). In the first step, the introductory text, which explains the main task and the criteria that need to be taken into account when selecting colours, is shown. In the next step, images are sequentially displayed in pseudorandom order. For each image, the observer has to select colours that are most prominent in the image. If colour sorting is enabled (see section 2.2), the observer can also sort colours, based on their prominence, with drag and drop gesture. Otherwise, the colours are ordered based on their initial selection – from most prominent in the far right to the least prominent on the far left. In our case, the colour sorting was disabled. When the observer is satisfied with the selected colours and their order, he or she can continue to the next image. After all images have been displayed, the observer is redirected to the last step of the process, where he or she is asked to provide some personal information. In addition, the observer has to type numbers that

are visible in Ishihara colour test images, so that potential colour vision deficiencies of the observers can be determined when analysing results. At the end of the process, all collected data about selected colours and the observer are written to the database and observer is prompt to repeat the process with another set of images.

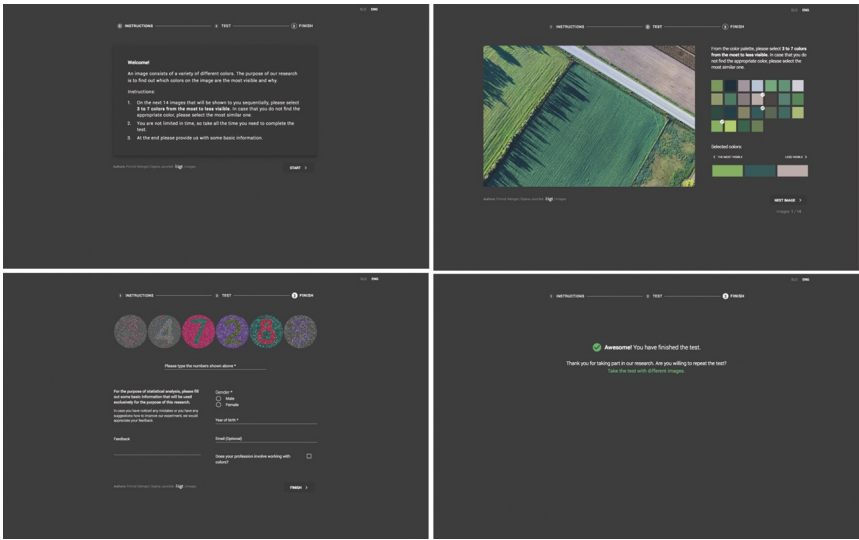


Figure 4: Three main steps for collecting data – introduction (top left), colour selection task (top right) and observer information task (bottom left) – and final notice at the end of the process (bottom right).

3.3 Viewing, editing and visualising data

For instant access to the results, while the research is still in process, we developed an interface, which allows the administrator an option to view, edit and visualise the collected data. In the top-left corner of the interface, the image and colours that were available for selection are displayed, just as it has been shown to the observers. The selected colours and personal data for each observer are displayed in a table at the right side of the interface. Each row represents data for each observer and can be edited or deleted if necessary. At the bottom, selected colours are visualised in a user-friendly manner. Each row represents the frequency of selecting a particular colour, whereas columns represent selected colours for each observer. Thus, the agreement between observers (interobserver reliability) and dispersion of selected colours can be easily discerned. In addition, the research administrator can export data in CSV or XLSX format for further analysis. The screenshot of the interface is shown in Figure 5.

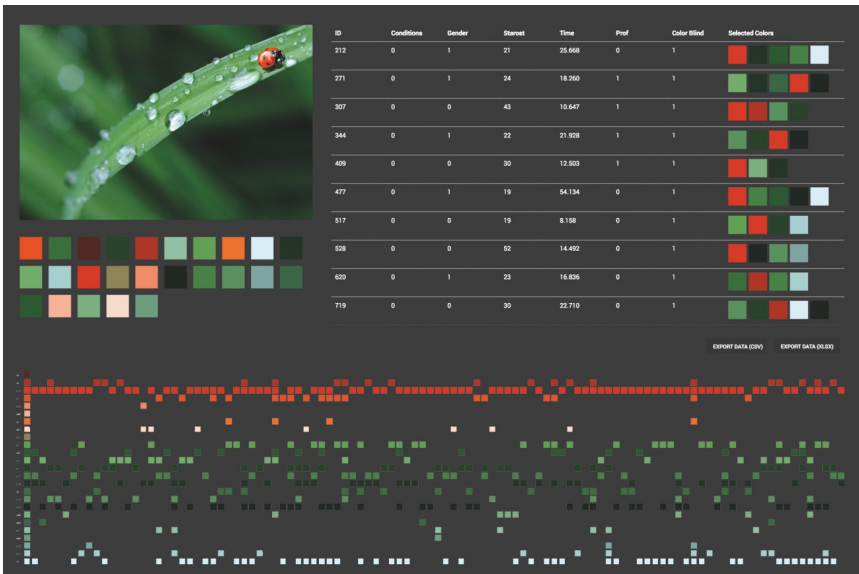


Figure 5: The interface for viewing, editing and visualising collected data

4. CONCLUSION

In this paper, the application for collecting image prominent colours, based on the observer's opinion has been presented. The application can also be used for conducting other psychophysical experiments, where observers have to select colours from the image according to specific criteria. The main advantages of our application are simplicity to use and effectiveness since colours are being selected interactively and data are collected automatically without any assistance from a research administrator.

5. REFERENCES

- [1] Delon, J., Desolneux, A., Lisani, J. L., Petro, A. B.: "Automatic color palette", *Inverse Problems and Imaging*, 2(2), 706-709, 2005. doi: 10.1109/ICIP.2005.1530153
- [2] Kopacz, J.: "Enhancing design using color", In book: *Colour Design*, 2012. doi: 10.1533/9780857095534.3.336
- [3] Liu, D., Jiang, Y. X., Pei, M., and Liu, S. G.: "Emotional image color transfer via deep learning", *Pattern Recognition Letters*, 110, 16-22, 2018. doi: 10.1016/j.patrec.2018.03.015
- [4] Lin, S., Hanrahan, P.: "Modeling how people extract color themes from images", *Proceedings of the SIGCHI Conference on Human Factors in Computing Systems*, 2013. doi: 10.1145/2470654.2466424
- [5] Liu, S., Luo, H.: "Hierarchical emotional color theme extraction", *Color Research & Application*, 41(5), 513-522, 2016. doi: 10.1002/col.21988
- [6] Morse, B. S., Thornton, D., Xia, Q., Uibel, J.: "Image-Based Color Schemes", *Image Processing*, 2007. *ICIP 2007. IEEE International Conference*, 2007. doi: 10.1109/ICIP.2007.4379355
- [7] Ou, L. C., Luo, M. R., Woodcock, A., Wright, A.: "A study of colour emotion and colour preference Part I: Colour emotions for single colours", *Color Research and Application*, 29(3), 232-240, 2004. doi: 10.1002/col.20010
- [8] React, A JavaScript library for building user interfaces, Reactjs, URL: <https://reactjs.org/> (last request: 2018-09-18).



© 2018 Authors. Published by the University of Novi Sad, Faculty of Technical Sciences, Department of Graphic Engineering and Design. This article is an open access article distributed under the terms and conditions of the Creative Commons Attribution license 3.0 Serbia (<http://creativecommons.org/licenses/by/3.0/rs/>).

TYPOGRAPHY



CHARACTERIZATION OF LETTERFORM COMPLEXITY

Irma Puškarević¹ , Uroš Nedeljković¹ , Nace Pušnik² 

¹University of Novi Sad, Faculty of Technical Sciences,

Department of Graphic Engineering and Design, Novi Sad, Serbia

²University of Ljubljana, Department of Textiles, Graphic Arts and Design, Ljubljana, Slovenia

Abstract: *The properties of typefaces are a prominent element in graphic communication. Over time, distinctive features of letterforms have evolved, influenced by the technological advancements. Today, letterforms are part of typeface units which serve as means of communication and are available in various styles. Research studies regarding the typeface legibility and the effects of semantic properties of typefaces have given a considerable insight into the effects of the distinctive features of typefaces. However, the construction of typographic stimuli design in previous research was unsystematic leading to inconsistent results and understanding of the typeface distinctive features effects. Therefore, the aim of this paper is to propose a systematic method for manipulation of the typographic stimuli in research studies. The design of the typographic test samples involved detection of the universal letterform structure and manipulation of the formal attributes of typefaces. The method of perimetric complexity was used to measure the complexity of the letterforms' formal attributes, as well as the complexity of the complete letterform. Due to diverse letterform properties, two metric systems for measuring perimetric complexity (Pelli's algorithm and morphological components function) were chosen. The analysis of the obtained results confirmed that particular formal attributes, singular or combined, are more complex than others, that is a gradient of letterform complexity was revealed. Also, the results of the letterform characterization using the second method provide slightly more conclusive results making it possible to infer which groups of formal attributes contribute to the increase of letterforms' complexity.*

Key words: typography, typeface properties, letterform, complexity of form, perimetric complexity

1. INTRODUCTION

The visual communication is an everyday human occurrence that is operating on both the conscious and subconscious level. The graphic communication, as a subordinate of visual communication, employs much of the verbal content, hence the properties of typefaces become a prominent element in this realm of communication. The technological advancements have left a mark on the formal structure of letterforms. For instance, at the beginning of mechanization of manuscripts, type forms have been merely a copy of scribes' calligraphic writings (Nedeljković et al, 2012; Highsmith, 2012). Gradually, the letterforms have evolved, going through several stages of reform over the centuries. After the industrial revolution, the major transformation in the design of type forms took place. Classical letterforms reached "astonishing height, width, and depth" (Lupton, 2004). Naturally, the effects of the new kinds of typography begun to interest academic circles. From a point of view of the typographic discipline, letterforms can be described by a limited set of elements. Dixon refers to these characteristics as formal attributes which she defines as "the basic individual units of description that refer to a typefaces' design and construction". In her descriptive typeface classification, these formal attributes are identified as construction, shape, proportion, modeling, weight, terminals, key characteristics, and decoration. Once these key characteristics of typeface design are defined, the greater is the opportunity to investigate effects of design properties.

Scholars in the field of human vision, cognitive and experimental psychology have been inquisitive about the letter identification process which is in a correlation with the design of letterforms (Rayner, 2009; Pelli et al, 2006). Research studies on the typeface legibility have vastly contributed to the pool of knowledge on letter identification and helped understand which distinctive features of letters aid reader in discerning visually similar letterforms. A study by Fiset et al. (Fiset et al, 2008), for example, confirms the crucial importance of terminations for letter identification. Another study by Beier and Larson (2013) uses stylization of the letter skeleton to determine and confirm that particular style characteristics are more legible than others. Nedeljković et al. (2017) set the grounds for their research on the two theoretical approaches – character differentiation and familiarity. Their findings confirm that familiarity with a typeface influences reading speed, but also that the ease with which we discern one character from another is affected by the congruency of a letterform with the universal letter skeleton. These and similar research studies on typeface legibility center around letterforms designed for longer passages of text where

variations of the letters' formal attributes are marginal. On the other hand, short passages of text (e.g. slogans, headings) are very often set in a display typeface where the form of a letter is embellished for the sake of the additional meaning production. A study by Beier et al. (2017) investigated the effects of the distinctive features of embellished letterforms and they found that embellished typefaces need to be designed in a way as to maintain the form of the common skeleton to sustain legibility. Namely, the findings of their study indicate that all the tested embellished letterforms hinder legibility. However, the particular letter features make a typeface less or more legible, hence a ranking of the distinctive features according to their legibility might be acquired.

Apart from the legibility concerns in a typeface design, additional interest of this process lies in the meaning production. Numerous studies investigated the communicative power of typefaces inferring that distinctive letter features can convey a mood, communicate attitude or attribute persona (Brumberger, 2003; Rowe, 1982; Childers et al, 2002). If one analyses the distinctive features of typefaces, one can set apart two sets of characteristics in the process of designing (Henderson et al, 2004). The first set of characteristics represent holistic descriptions that rely on perception and fall to a subjective evaluation (e.g. symmetry). The second set of characteristics are a graphic description of letterforms which can be evaluated objectively (e.g. short/tall). Along with Dixon's identifiers of formal attributes, these typeface characteristics contribute to both legibility and meaning production aspects. However, a method for a systematic manipulation of these characteristics has not been addressed. The lack of such method has resulted in the inconsistent treatment of the typographic stimuli design in the previous research and it was difficult to obtain consistent results and understanding about the effects of distinctive features. Even though the recent studies on the subject provide useful guidance (Beier et al, 2013; Nedeljković et al, 2017; Beier et al, 2017), there is still a need for a systematic method for manipulating typographic stimuli in research studies. Therefore, the aim of this paper is to propose a method for (i) resolving the issue of the inconsistent stimulus control in the research studies and (ii) formulating a list of distinctive letter features ranging between less complex to more complex forms.

2. METHODOLOGY

The design of the typographic test samples in this study involved detection of the universal letterform structure and manipulation of the formal attributes of typefaces.

For the purposes of detecting the universal structure, the model of the common letter skeleton was used (Frutiger, 1998). The core principle of this model is a neutral shape of a letter which can be isolated when stylistically different typefaces blend together. More precisely, when eight most commonly found typefaces (*Garamond*, *Baskerville*, *Bodoni*, *Excelsior*, *Times*, *Palatino*, *Optima*, *Helvetica*) are superimposed, the common skeleton is revealed. Software application Adobe Illustrator was selected as a tool to design test samples since it uses vector graphics to create shapes. Uppercase letter H was selected as a representative letterform. Once the universal structure was detected by superimposing the letter H of eight typefaces in Adobe Illustrator (Figure 1), an image (perceptual) metric was selected to quantitatively evaluate created universal structure as described by Nedeljković (Nedeljković, 2016).



Figure 1: Construction of the universal letterform structure in Adobe Illustrator

The structural similarity index (SSIM) was selected in the ImageJ program for a quantitative sample assessment using the option of the maximum intensity. The maximum intensity of the test samples was reached by superimposing the letter H of eight typefaces by overlapping each pixel of one letter sample with each pixel of another letter sample on an identical (x,y) position. The result of this process was an image of the letter H which was labelled as a referential image for the purposes of the similarity structure analysis with the previously detected universal structure. This referential structure was juxtaposed with each letter sample individually and then with the universal structure. Table 1 shows the results of the SSIM measurements where the value 1 means picture overlap 100%. As the structure similarity index shifts to the value 0, the difference between the two expands. The analysis of the results shows that the universal

structure is similar with the referential structure. Thus, the universal structure is taken as a base unit for the design of the typography test samples.

Table 1: The results of the SSIM index evaluation

Sample	Luminance	Contrast	Structure	MS-SSIM
1	0.99639	0.76683	0.83197	0.63567
2	0.99040	0.69327	0.81183	0.55741
3	0.98741	0.67588	0.81829	0.54611
4	0.99216	0.67697	0.80208	0.53873
5	0.99291	0.76016	0.85176	0.64288
6	0.99409	0.72212	0.81463	0.58478
7	0.99522	0.84861	0.87425	0.73835
8	0.99374	0.79764	0.83417	0.66120
Univ.struc.	0.99961	0.95720	0.94122	0.90059

The design of the typographic samples began by designing the formal attributes. The qualitative analysis of the formal attributes that Dixon introduces in her descriptive typeface classification (Dixon, 2008) revealed that particular attributes are less complex while others are more complex. Based on this analysis it is possible to distinguish particular formal attributes (parallel strokes, rounded terminals, skewed or dashed strokes, added shadow) according to their level of complexity. Therefore, two groups of test samples were defined. The former comprises of the constituent parts of the letterform with different levels of the form’s complexity (Figure 2) and the latter of the representative letter H constructed using the attributes from the first group (Figure 3). For the design of the test samples in both groups, the universal letterform structure was used as a reference for the starting point.

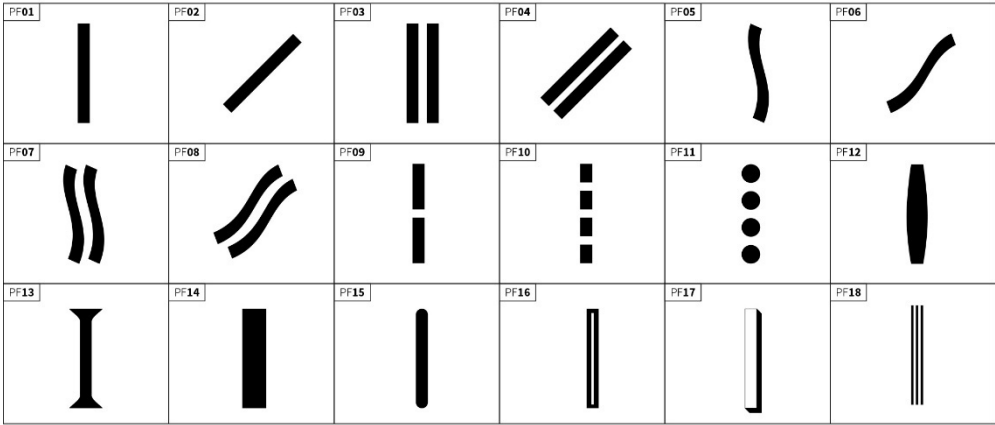


Figure 2: The formal attributes of letterforms of different complexity obtained with the qualitative assessment

The method of perimetric complexity was used to first measure the complexity of the constituent parts and then of the complete letterform. Due to diverse letterform properties, two metric systems which are different in its computational methods were chosen. Pelli’s algorithm (Pelli, 2006) and the morphological components function (Watson, 2012) are both metrics for determining the perimetric complexity of binary digital images and are integrated into the computing system of the Wolfram Mathematica software. First, it was necessary to define an input binary image for both methods. In the case of Pelli’s algorithm, the binary image is defined with values 0 and 1 where the value 0 represents foreground colour and value 1 background colour. The complexity of the perimeter is then defined by an average complexity value of the test samples. The morphological components function defines a binary image based on several separate regions which are label through integers.

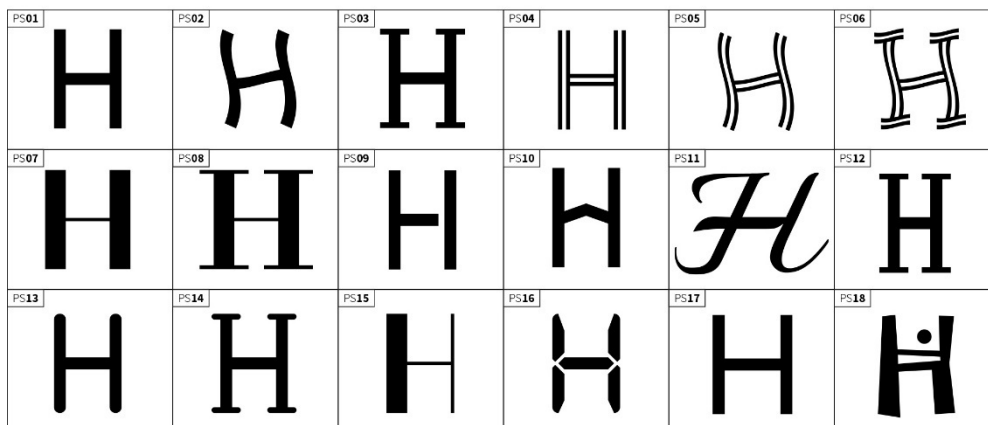


Figure 3: The formal attributes of letterforms of different complexity applied to the letterform H

3. RESULTS AND DISCUSSION

The letterform characterization was performed using two metric systems for evaluation of the perimetric complexity. The analysis of the obtained results confirmed that particular formal attributes, singular or combined, are more complex than others, that is a gradient of letterform complexity was revealed. The first analysis focused on evaluation of the perimetric complexity of the formal attributes. The results of the perimetric complexity evaluation using Pelli's algorithm show that formal attributes which are vertical and slash can be more or less complex i.e. no evident gradation of the form's complexity is presented (Figure 4). When a single vertical line is expanded horizontally, has rounded terminals, is slashed/dashed or wavy the complexity of the form is low and the difference in the complexity value between the forms is insignificant. When a single vertical line is upgraded with serifs and double lines (vertical or slash) the perimetric complexity is increased. Also, the complexity value between each sample has a slight increase. However, making a line within a line, adding shadow or scribbles increases the complexity of the form significantly. Additionally, it can be observed that the increase of the complexity is steady up to the OF07 sample when it abruptly expands.

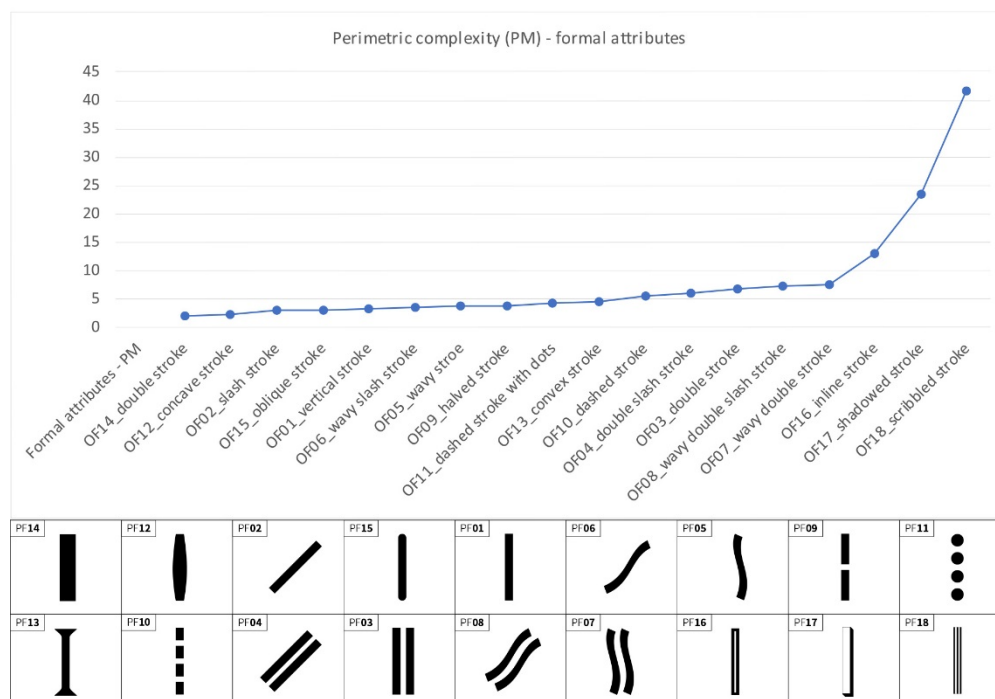


Figure 4: Graphic representation of the results of the perimetric complexity evaluation of the formal attributes using Pelli's algorithm

The results of the perimetric complexity evaluation using the morphological components function showed slightly different results. It was observed that singular vertical stroke is less complex, that is particular variations of the vertical stroke (e.g. horizontal expansion, oblique terminals, dashed stroke) increase the form's complexity gradually. Additionally, the results reveal that the complexity is increased when the stroke shifts angularly, is doubled or wavy (Figure 5).

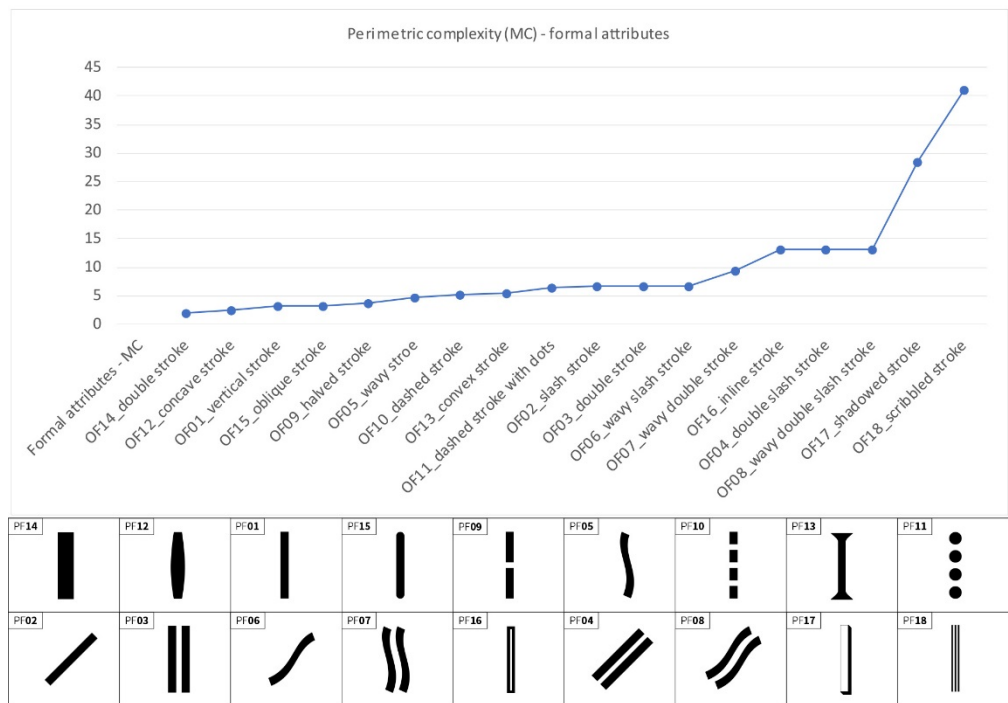


Figure 5: Graphic representation of the results of the perimetric complexity evaluation of the formal attributes using the morphological component function

In summary, it was observed that the morphological components function provides more conclusive results regarding the increase of the letterform perimetric complexity than Pelli's algorithm. Based on these results, it can be inferred that particular distinctive features i.e. formal attributes of letterforms are less or more complex. Also, the combination of particular attributes makes the form more complex where certain combinations expand the form's complexity drastically.

The second analysis focused on the evaluation of the perimetric complexity of the letterform H samples which were designed using the formal attributes from the first analysis. Figure 6 shows the results of the perimetric complexity using Pelli's algorithm. It can be observed that the complexity of the form is increased by combining the attributes. The attributes such as the letter contrast, proportions, oblique terminals, and irregular form have the less complex form while the letterform with serifs is more complex. A slight increase of the perimetric complexity is noticeable up to the OS08 sample, whereas a significant increase is noticeable from this sample onwards. With the obtained results using this method it is difficult to form a conclusive grouping of the letterform complexity.

Figure 7 shows the results of the perimetric complexity using the morphological components function. Similarly, to the analysis of the singular formal attributes, this method provides much better results in regards to a gradual representation of the letterform complexity. It can be observed that letterforms constructed with dominantly vertical strokes tend to be less complex regardless of the letterform's contrast, proportions or the obliqueness of the terminals. On the other hand, serifs, double strokes or references to tools (script letterforms) increase perimetric complexity. A slight increase of the perimetric complexity is noticeable up to the OS16 sample after which the complexity increases more rapidly. Nevertheless, this method provides the gradation of the perimetric complexity that is increasing more steadily than in the case of the results obtained with Pelli's algorithm.

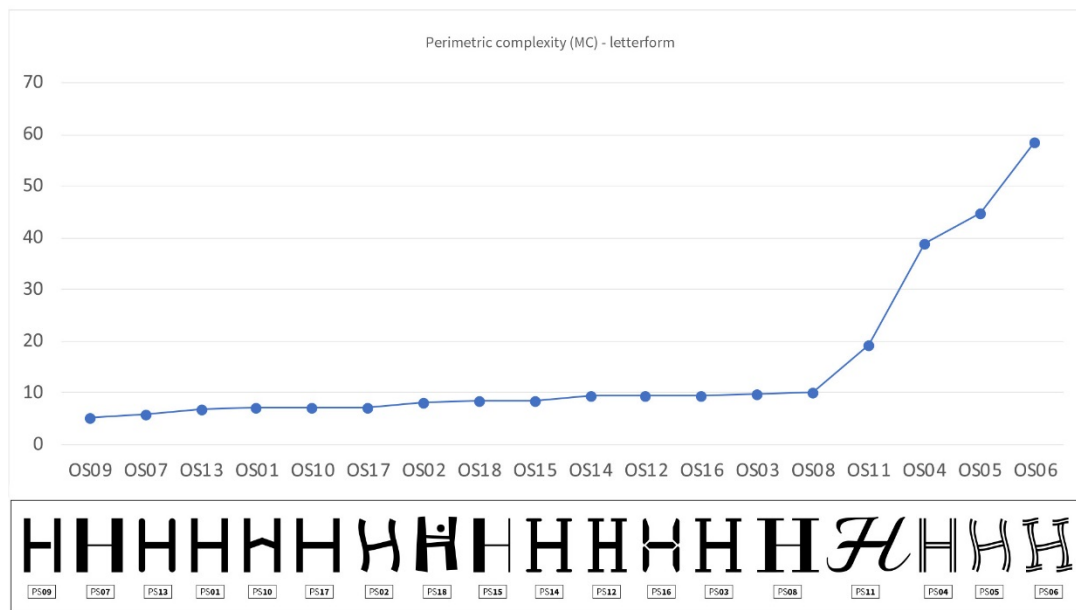


Figure 6: Graphic representation of the perimetric complexity evaluation for the letterform H using Pelli's algorithm

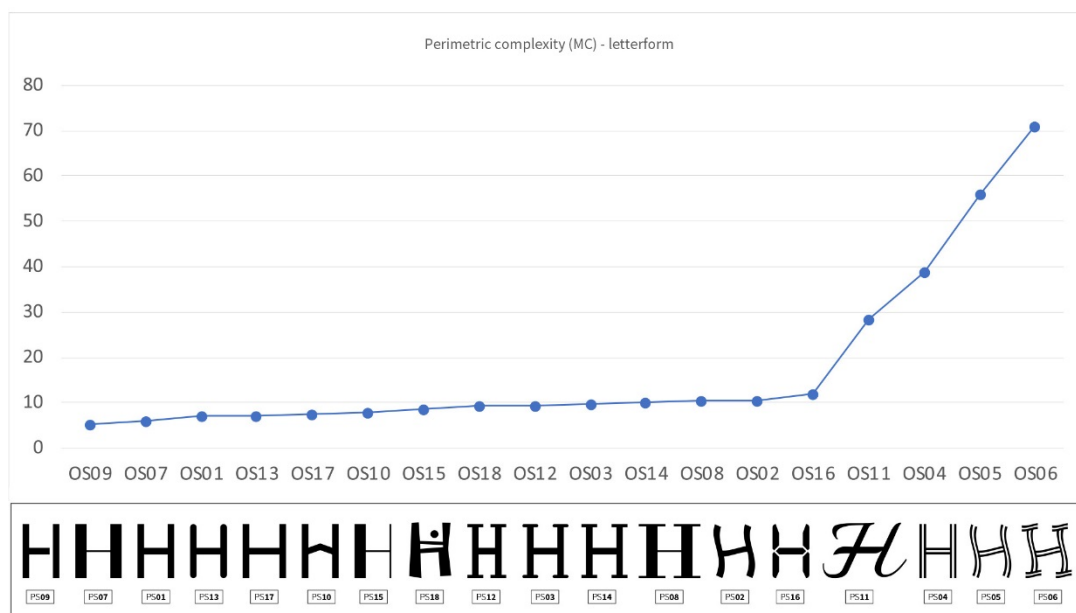


Figure 7: Graphic representation of the perimetric complexity evaluation for the letterform H using the morphological component function

4. CONCLUSION

The aim of this study was to propose a systematic method for manipulation of the typographic stimuli in research studies. The characterization of letterforms using the method of perimetric complexity has been proven functional and practical by the results of this study. Particularly, it was presented how the measurement of the letterform complexity, based on the quantitative analysis of the typeface formal attributes i.e. variations of the basic perceptual features successfully characterizes letterforms. Using the method of perimetric complexity, the results of the qualitative analysis were confirmed which revealed that combining the formal attributes in a single letterform provides a more complex structure. Additionally, the analysis in this study shows that one method of evaluating the perimetric complexity provides more conclusive results. The results of the letterform characterization using the morphological components function provide slightly more conclusive results where it was possible to observe that particular formal

attributes combinations such as irregular forms, slashed or double strokes increase the letterform's complexity. These findings are relevant for future research in the field of the effects of typeface legibility and embellished typefaces where the methodology presented in this study will help obtain more consistent results across research studies.

5. ACKNOWLEDGMENTS

This work was supported by the Serbian Ministry of Science and Technological Development, Grant No.: 35027 "The development of software model for improvement of knowledge and production in graphic arts industry."

6. REFERENCES

- [1] Beier, S., Larson, K.: "How does typeface familiarity affect reading performance and reader preference?", *Information Design Journal*, 20 (1), 16–31, 2013. doi: 10.1075/idj.20.1.02bei
- [2] Beier, S., Sand, K., Starrfelt, R.: "Legibility implications of embellished display typefaces", *Visible Language*, 51 (1), 112–133, 2017.
- [3] Brumberger, E.R.: "The Rhetoric of Typography: The Persona of Typeface and Text", *Technical Communication*, 50 (2), 206–223, 2003.
- [4] Childers, T.L., Jass, J.: "All Dressed Up With Something to Say: Effects of Typeface Semantic Associations on Brand Perceptions and Consumer Memory", *Journal of Consumer Psychology*, 12 (2), 93–106, 2002. doi: 10.1207/S15327663JCP1202_03
- [5] Dixon, C.: "Describing typeforms: a designer's response", *InfoDesign: Brazilian Journal of Information Design*, 5 (2), 21–35, 2008.
- [6] Fiset, D., Blais, C., Éthier-Majcher, C., Arguin, M., Bub, D., Gosselin, F.: "Features for uppercase and lowercase letter identification", *Psychological Science*, 19 (11), 1161–1168, 2008. doi: 10.1111/j.1467-9280.2008.02218.x
- [7] Frutiger, A.: *"Signs and symbols: their design and meaning"*, (Ebury Press, London, 1998).
- [8] Henderson, P.W., Giese, J.L., Cote, J.A.: "Impression management using typeface design", *Journal of Marketing*, 68 (4), 60–72, 2004. doi: 10.1509/jmkg.68.4.60.42736
- [9] Highsmith, C.: "Inside Paragraphs: Typographic Fundamentals", (The Font Bureau, Inc., Boston, 2012.)
- [10] Lupton, E.: "Thinking with type", (New York, Princeton Architectural Press, 2004).
- [11] Nedeljković, U.: "Univerzalno pismo modernistička utopija ili savremena komunikacijska potreba" PhD Thesis, University of Novi Sad, 2016.
- [12] Nedeljković, S., Nedeljković, U.: "Pismo i tipografija", (FTN Izdavaštvo, Novi Sad, 2012).
- [13] Nedeljković, U., Novaković, D., Pinčjer, I.: "Detecting universal structure and effects of typefaces", *Technical Gazette*, 24 (2), 557–564, 2017. doi: 10.17559/TV-20150831131738
- [14] Pelli, D.G., Burns, C.W., Farell, B., Moore-Page, D.C.: "Feature detection and letter identification", *Vision Research*, 46 (28), 4646–4674, 2006. doi: 10.1016/j.visres.2006.04.023
- [15] Rayner, K.: "Eye movements and attention in reading, scene perception, and visual search", *The Quarterly Journal of Experimental Psychology*, 62 (8), 1457–1506, 2009. doi: 10.1080/17470210902816461
- [16] Rowe, C.L.: "The connotative dimensions of selected display typefaces", *Information Design Journal*, 3 (1), 30–37, 1982. doi: 10.1075/idj.3.1.03row
- [17] Watson, A.B.: "Perimetric Complexity of Binary Digital Images", *The Mathematica Journal*, 14, 1–40, 2012. doi: 10.3888/tmj.14-5



© 2018 Authors. Published by the University of Novi Sad, Faculty of Technical Sciences, Department of Graphic Engineering and Design. This article is an open access article distributed under the terms and conditions of the Creative Commons Attribution license 3.0 Serbia (<http://creativecommons.org/licenses/by/3.0/rs/>).

AUTHOR INDEX – GRID 2018

A

Abram, T. // 469
Adamović, D. // 39
Adamović, S. // 39, 225, 435
Agić, A. // 591
Ahtik, J. // 375
Arman Kandirmaz, E. // 129, 189
Armič, T. // 551

B

Banić, D. // 237
Banjanin, B. // 197, 225, 243
Barbarić-Mikočević, Ž. // 121
Bates, I. // 121
Bečelić-Tomin, M. // 161, 169, 175
Beris, Y. // 499
Boadu, F. // 435
Boeva, R. // 291, 303
Böröcz, P. // 135
Bota, J. // 237
Bozhkova, T. // 71, 291
Brajković, R. // 469
Brunová, Z. // 213
Brozović, M. // 237, 261
Bushati, J. // 429

C

Cakić, S. // 281
Cichy, Ł. // 217
Cigula, T. // 45, 151, 357

D

Dalmacija, B. // 169
Dedijer, S. // 77, 197, 313
Delić, G. // 225, 243, 421
Dimovski, V. // 225
Dolić, J. // 267
Donevski, D. // 45
Držková, M. // 61

Đ

Đurđević, M. // 365
Đurđević, S. // 39, 421, 435

Dž

Džimbeg-Malčić, V. // 121

E

Erceg, T. // 281
Ermakov, A. // 455

F

Ferati, M. // 489
Fon, Ž. // 469
Franken, G. // 561

G

Gabrijelčič Tomc, H. // 383, 389, 469
Golob, M. // 143
Gómez-Robledo, L. // 77
Görgényi-Tóth, P. // 323
Gregor-Svetec, D. // 99
Grujić, D. // 205

H

Hajdek, K. // 555
Heđa, M. // 555
Hladnik, A. // 459, 567
Hoffman-Walbeck, T. // 445
Horvath, C. // 323, 397
Hozmanová, M. // 333
Hudika, T. // 45, 151
Huertas, R. // 77
Huzjak, J. // 357

I

Itrić, K. // 87
Ivanov, Z. // 291
Ivanova, Y. // 303

J

Jamnicky Hanzer, S. // 237
Jašúrek, B. // 213, 333
Javoršek, D. // 573, 597
Jevtić, M. // 383
Jurca, T. // 389
Jurič, I. // 51, 77, 313

K

Kailová, N. // 61
Karlovits, I. // 55, 99
Kašiković, N. // 181, 341, 365
Katić, M. // 411
Kavčič, U. // 253

Kecić, V. // 161, 175

Kerkez, Đ. // 161, 169, 175

Knific Košir, A. // 469

Kočevar, T. // 375, 389

Koltai, L. // 135

Končar, V. // 19

Konygina, T. // 455

Kordiċ, D. // 519

Kovačević, D. // 261

Kulčar, R. // 87

Kulić, A. // 169, 175

Kuščer, A. // 489

L

Lakićević, M. // 519

Lavrič, G. // 55, 99

Leovac Maćerak, A. // 161, 169

Lesha, V. // 429

Lilić, A. // 51, 341, 533

Lužanin, O. // 161

M

Malinauskas, J. // 525

Malnar, L. // 121

Mandić, L. // 267, 591

Mendizsa, A. // 99

Miketić, N. // 341, 533, 583

Milić, N. // 313, 583

Milošević, R. // 181, 421

Miljković, P. // 555

Minaeva, O. // 455

Molek, I. // 573

Možina, K. // 561

Muck, D. // 383

N

Nedeljković, U. // 605

Nikolić, Lj. // 281

Novaković, D. // 51, 421, 435

Novotny, E. // 347

O

Ozcan, A. // 129, 189

Ozomay, Z. // 129

Ö

Özden, Ö. // 103

P

Pál, M. // 197, 225, 313

Panáċ, O. // 61

Pangerc, M. // 561

Pasanec Preprotić, S. // 109

Pavlović, Ž. // 181, 197, 313

Petković, G. // 109

Pibernik, J. // 267

Pinčjer, I. // 39, 533, 583

Pivar, M. // 389

Plahuta, E. // 541

Plazonić, I. // 121

Pleša, T. // 99, 253

Politis, A. // 29, 475

Poljičak, A. // 151, 591

Porok, A. // 389

Prica, M. // 161, 169, 175

Prokai, P. // 397

Prša, M. // 357

Pucar Milidrag, G. // 175

Purg, P. // 405

Pušċarević, I. // 583, 605

Pušnik, N. // 541, 605

R

Rastovac, M. // 267

Ristić, I. // 281

Rodríguez Lezaca, A. // 435

Ropret, M. // 99

Rožić, M. // 87

Ružićić, B. // 205

S

Saksida, P. // 567

Selimović, A. // 459

Sesli, Y. // 129

Shterev, K. // 71

Simendić, B. // 281

Sönmez, S. // 103

Spiridonov, I. // 71, 291, 303

Stančić, M. // 181, 205

Stanković Elesini, U. // 489, 551

Strica, D. // 429

Szentgyörgyvölgyi, R. // 347

Š

Šafranj, J. // 411

Šišić, A. // 591

Škerjanc, A. // 389, 469

T

Teofilović, V. // 281

Todorova, D. // 275

Tomašegović, T. // 45, 151, 357

Tomašević Pilipović, D. // 161, 169

Tomić, I. // 51, 77, 313

Tóth, B. // 135

Trochoutsos, C. // 475

U

Urbas, R. // 181, 489, 551

V

Valdec, D. // 555

Vališ, J. // 213, 333

Vasić, J. // 197, 243, 365

Vladić, G. // 225, 243, 421

Vrabič Brodnjak, U. // 275

Vujčić, Đ. // 205

Vukić, N. // 281

Vukoje, M. // 87, 109

W

Weimert, M. // 347

Weingerl, P. // 597

Y

Yordanov, S. // 291

Z

Zeljковић, Ž. // 51, 435

Zorić, V. // 39

Ž

Żółtek-Tryznowska, Z. // 217

Ž

Žvab Rožič, P. // 469



9. INTERNATIONAL SYMPOSIUM
GRAPHIC ENGINEERING AND DESIGN
08-10. NOVEMBER 2018

GRID
2018

UNIVERSITY OF NOVI SAD
FACULTY OF TECHNICAL SCIENCES
DEPARTMENT OF GRAPHIC ENGINEERING AND DESIGN

<http://www.grid.uns.ac.rs/symposium>